Identifying attributable physical effects of contemporary climate change-driven sea-level rise on soft coastal landforms

by

Christopher Edwin Sharples

B.Sc. (Hons), M.Sc.

Geography and Spatial Sciences

School of Technology, Environments and Design,

College of Sciences and Engineering

Submitted in fulfilment of the requirements for the degree of Doctor of Philosophy

University of Tasmania

23rd November 2020

Declaration of originality

This thesis contains no material which has been accepted for a degree or diploma by the University or any other institution, except by way of background information and duly acknowledged in the thesis, and to the best of my knowledge and belief no material previously published or written by another person except where due acknowledgement is made in the text of the thesis, nor does the thesis contain any material that infringes copyright.

Christopher Sharples

8th August 2020

PhD Candidate

School of Technology, Environments and Design,

University of Tasmania

Authority of access

Three published peer-reviewed papers were produced during the preparation of this thesis. These papers have been reproduced in full in Appendix Two. All three are pertinent to this thesis, however only one was produced as a direct outcome of the research undertaken for this thesis (Sharples et al. 2020, for which a Statement of co-authorship is provided following). The other two published papers (Prahalad et al. 2015 and Thom et al. 2018) were produced as a result of other projects separate to this thesis. These latter papers provide supporting information relevant to this thesis, in which they are cited. For these reasons they have been reproduced in full in Appendix Two.

The publishers of these three papers as listed below hold copyright for that content, and access to the material should be sought from the respective journals:

Prahalad, V., Sharples, C., Kirkpatrick, J. & Mount, R., 2015. Is wind-wave fetch exposure related to soft shoreline change in swell-sheltered situations with low terrestrial sediment input? *Journal of Coastal Conservation*, vol. 19, pp.23-33. Publisher: © 2014 Springer

Thom, B.G., Eliot, I., Eliot, M., Harvey, N., Rissik, D., Sharples, C., Short, A.D. & Woodroffe, C.D., 2018. National sediment compartment framework for Australian coastal management, *Ocean & Coastal Management*, vol. 154, p. 103-120. Publisher: © 2018 Elsevier

Sharples, C., Walford, H., Watson, C., Ellison, J.C., Hua, Q., Bowden, N. & Bowman, D., 2020. Ocean Beach, Tasmania: A swell-dominated shoreline reaches climate-induced recessional tipping point? *Marine Geology*, vol. 419, 106081. Publisher: © 2019 Elsevier

The remaining un-published content of this thesis may be made available for loan and limited copying and communication in accordance with the *Copyright Act 1968*.

Christopher Sharples

8th August 2020

PhD Candidate

Statement of co-authorship

The following people and institutions contributed to the publication of work undertaken as part of this thesis. The published work (Sharples et al. 2020) is reproduced in full in Appendix Two and summarised in Chapter 5, Section 5.2.

Candidate: Chris Sharples, School of Technology, Environments and Design, University of Tasmania.

Author 1: Hannah Walford, University of Tasmania (Co-author)

Author 2: Christopher Watson, University of Tasmania (Primary Supervisor)

Author 3: Joanna Ellison, University of Tasmania (Co-author)

Author 4: Quan Hua, Australian Nuclear Science and Technology Organisation, N.S.W. (Co-author)

Author 5: Nick Bowden, Antarctic Climate and Ecosystems Co-operative Research Centre, Tasmania (Co-author)

Author 6: David Bowman, University of Tasmania (Co-author)

Author details and their roles:

Paper: Sharples, C., Walford, H., Watson, C., Ellison, J.C., Hua, Q., Bowden, N. & Bowman, D., 2020. Ocean Beach, Tasmania: A swell-dominated shoreline reaches climate-induced recessional tipping point? *Marine Geology*, vol. 419, 106081.

Author contributions: Sharples (65%), Walford (10%), Watson (10%), Ellison (5%), Hua (2.5%), Bowden (5%), Bowman (2.5%).

Chris Sharples was the primary author who developed the idea, carried out its execution and analysis, and was responsible for manuscript preparation; Hannah Walford undertook an earlier air photo analysis of Ocean Beach (with advice from Chris Sharples) whose results were not previously published and were incorporated into this paper; Christopher Watson assisted with analysis and interpretation of the results and critically reviewed the manuscript; Joanna Ellison supervised Hannah Walford's earlier honours work and critically reviewed the manuscript; Quan Hua analysed the peat samples and provided interpretation of their radiometric dates; Nick Bowden undertook repeated beach profile surveys and provided results and plots; David Bowman assisted with field work and provided discussion and interpretation of the peat dating findings; All authors helped refine the manuscript and gave final approval for publication.

We, the undersigned, endorse the above stated contributions of work undertaken for the published peer-reviewed paper contributing to this thesis:

Chris Sharples (7 Aug 2020)	Christopher Watson (7 Aug 2020)	Elaine Stratford (7 Aug 2020)
Candidate	Primary Supervisor	Head of School
School of Technology, Environments and Design	School of Technology, Environments and Design	School of Technology, Environments and Design

Table of contents

Abstract

Identifying attributable physical effects of contemporary climate change-driven sea-level rise on soft coastal landforms

By Chris Sharples

Changing climate has always been a fundamental driver of sea-level change. Changes in climate over the nineteenth and twentieth centuries have produced increased global sea-level rise which is expected to lead to increased erosion and progressive recession of many soft erodible coasts. However most swell-exposed sandy beaches have not yet shown such a response because other confounding processes such as beach erosion and recovery cycles are still commonly of larger scale and prevent the emergence of a detectable sea-level rise signal in beach behaviour. This thesis tests the hypothesis that there may nonetheless be some susceptible coastal landform types that are already responding to contemporary climate change-driven sea-level rise with an observable change in behaviour, for example a switch from shoreline stability to progressive recession, or an increase of previous shoreline retreat.

This study analyzed air photo and beach profile records for 35 coastal sites around Tasmania (Australia) over an approximately 70-year period to compile shoreline behaviour histories. Sites were selected from a range of geomorphic types hypothesised to be susceptible to early responses to sea-level rise. Twelve distinctive sites from four different coastal environments were analysed in some detail, with these results informing analysis of 23 other sites. For all 35 sites, a shoreline behaviour history was compiled using all suitable air photos to map shoreline position changes over time using the seaward vegetation line as a shoreline proxy. The sites include some that were known from previous work to have changed their behaviour during the air-photo period, and others whose histories were unknown at the outset. Sites influenced by local anthropogenic influences were mostly avoided, but in a few cases were used if the extent of artificial interference was clearly defined. Photogrammetric error margins were quantified for arguably the most important source of uncertainty, albeit more sophisticated uncertainty analyses are possible.

Some confounding factors which might prevent an early sea-level rise signal being detectable in shoreline behaviour are minimal on the Tasmanian coast, including vertical land movement and inter-annual sea-level variability associated with the El Nino Southern Oscillation. Present day relative sea-level rise around Tasmania is commensurate with the global average, implying that contemporary climate change-induced sea-level rise is the dominant component of local relative sea level rise. Variability in swell wave direction is another potentially confounding factor that is also minimal on Tasmania's western and southern coasts.

Study sites included 18 swell-exposed sandy beaches such as Ocean, Hope and Roches Beaches. However in order to explore shoreline responses in the absence of the swell-driven sand transport and shoreline recovery processes that may prevent detectable early sea-level rise signals, study sites were also selected at 11 sandy and sandy-saltmarsh shorelines in swell-sheltered tidal re-entrants such as Duck Bay and Cloudy Lagoon, and at 6 sites on soft-rock (cohesive clay) shorelines at Rokeby Beach and the Barilla shore in Pittwater estuary. All the sites are readily erodible and are expected to eventually recede in response to climate change-induced sea-level rise.

Of the 35 study sites, 10 exhibited a change of long-term shoreline behaviour over the air photo period. Sites showing a change from stability to long-term progressive recession include swell-exposed Ocean and Roches Beaches, with Nebraska and Prion Beaches showing similar but more recently emerging changes. A significant long-term increase of prior recession was found at several swell-sheltered sites at West Duck Bay and a swell-sheltered soft-rock shoreline at Barilla (Pittwater). The geomorphic and oceanographic conditions at each site were identified to frame multiple

hypotheses allowing assessment of whether an early response to rising sea-levels provides the best explanation for the observed changes, or whether other plausible explanations were available.

Sea-level rise and increasing onshore wind speeds emerged as the only identified drivers able to account for the observed changes at 8 of the 10 sites showing significant change. Both drivers are expected to result in storm waves more frequently running further landwards over deeper water and impacting higher on the shore profile, leading to increased shoreline erosion and recession. Both processes could drive such change at six of these sites, whereas sea-level rise is the only plausible driver identified at two sites (Roches Beach and South Barilla). At the other two sites (Stephens Bay South and Gordon), variability in sand supply and artificial interference are more likely to have driven the observed changes.

The 8 study sites exhibiting long term shoreline behaviour changes consistent with sea-level rise and/or increases in onshore wind speeds were in all cases characterised by (1) the presence of an active sediment sink capable of permanently sequestering increasing quantities of eroded sediment as shoreline erosion increases in response to more frequent higher wave attack, and (2) by a persistent (commonly unidirectional) sediment transport pathway capable of efficiently delivering eroded sediment to the sink with little or no return to the eroded shore. These two inter-related conditions exist for some but not all sandy swell-exposed beaches but are common (via differing mechanisms) for soft-rock coasts and for sandy shores within tidal swell-sheltered coastal re-entrants such as estuaries and lagoons. For swell-exposed sandy beaches where these critical conditions are present, the rapid permanent loss of eroded and mobile sand minimizes the effect of cross-shore and alongshore sediment exchanges that might otherwise prevent an early sea-level rise signal in shoreline behaviour, and instead allow a “tipping-point” style of switch from stability to recession to occur.

A range of other site conditions may also contribute to changing shoreline behaviour in certain process environments but are not always associated with long-term changes. However, a relatively high degree of local wind-wave exposure and fetch were found to also be critical conditions for changing shoreline behaviour within swell-sheltered tidal re-entrants such as Duck Bay, Cloudy Lagoon and Pittwater.

Of the 25 (out of 35) studied shorelines which have not yet shown any detectable long-term change of behaviour over the study period, 21 do not exhibit the critical conditions of having persistent sediment transport to sufficiently large active sediment sinks (e.g., Hope Beach, Cloudy Bay Beaches East and West), or in the case of swell-sheltered re-entrants these sites have only relatively limited wind-wave exposure and fetch. However, another four swell-exposed sandy beach sites did not exhibit any long-term behaviour change despite having the critical conditions of significant active sand sinks and persistent active sand transport pathways from the study shore to active sand sinks. In each of these cases, an actively gaining sand supply equal to or larger than the amount being permanently lost from increased erosion is inferred to be the key factor preventing an early change of behaviour by compensating for increasing sand losses attributable to climate change-induced drivers of shoreline change (e.g., at Mulcahy Bay Beach and Adventure Bay South Beach).

The range of differing site conditions and differing historic shoreline behaviours investigated in this study support the expectation that some coastal landform types will respond earlier than others to climate change-induced drivers including contemporary sea-level rise and increasing onshore winds. This study identifies some critical conditions differentiating early from late responders to coastal climate change-driven processes. This will improve capacity to plan adaptation to coastal climate change impacts by identifying shores susceptible to earlier changes under a continuing warming climate.

Glossary of Terms and Acronyms

The author of this thesis advocates appropriate and clear terminology as a key to good communication and the development of ideas (see for example: Eberhard & Sharples 2013). As far as possible, sea-level related terminology used in this thesis complies with the recent terminology provided by Gregory *et al.* (2019), or in the case of geomorphic terms with other recent widely published terminology. This glossary does not attempt to be a comprehensive list of terms related to sea-level rise and coastal geomorphology, but includes selected terms and acronyms used in this thesis, including several idiosyncratic terms which the writer has found useful for the purposes of this thesis (e.g. 'Bruun sink' and 'Early responder').

AAO	Antarctic Oscillation Index (a measure of the Southern Annular Mode SAM)
ABSLMP	Australian Baseline Sea Level Monitoring Project, a project of the Australian Bureau of Meteorology.
Accretion	Addition of material to a coast or shoreline (in the context of this thesis). Accretion may occur vertically and/or horizontally.
AHD	Australian Height Datum
Behaviour	The terms 'coastal behaviour' or 'shoreline behaviour' are used in this thesis to refer to a characteristic style of long-term changes (or stability) exhibited by a shoreline or coast. For example, a long-term progradation trend, a long-term recession trend or a long-term dynamic equilibrium or cyclic (cut and fill) style of changes would be three differing coastal behaviours. The term 'coastal behaviour' is compliant with the Wikipedia definition of behaviour, which allows for 'systems' (not merely humans or animals) to have 'behaviours': "**Behavior** (American English) or **behaviour** (Commonwealth English) is the range of actions and mannerisms made by individuals, organisms, systems or artificial entities in conjunction with themselves or their environment, which includes the other systems or organisms around as well as the (inanimate) physical environment." (accessed 2nd July 2019). The term has been widely used in the scientific coastal literature, for example see Cowell, Roy and Jones (1995).
BoM	The Australian Bureau of Meteorology. The Australian government agency responsible for collection of weather and climate data, and reputedly the only such agency to have retained the same name since it was founded(!)
BP	Before Present. Standard method of referring to past dates, usually in years BP.
Bruun sink	Term used in this thesis to refer to the lower beach-face (subtidal) sand sink that is created when sea-level rise drives increased coastal erosion and the eroded sand is moved offshore into new accommodation space (i.e., water depth) created by the rise of sea-level, as described by the Bruun Rule.
Contemporary climate change-driven sea-level rise	Refers to sea-level rise of global extent which commenced to be detectable at tide-gauges around the mid-1800s following millennia of relative mean global sea-level stability, and which is attributed to ocean thermal expansion and ice melting due to climatic changes.
DPIPWE	The Tasmanian Government Department of Primary Industries, Parks, Water and Environment; present-day (2020) Tasmanian state government agency responsible for capturing and archiving government-financed aerial photography. This

	department and its precursors going back to the former Lands & Surveys Department have been responsible for most systematic aerial photography in Tasmania since the 1940s.
Dynamic equilibrium	Term sometimes used to refer to minor or moderate variability about a constant average or median. Sometimes used in coastal geomorphology to refer to a stable beach which has some episodes of erosion and accretion, but no long-term trend to either recession or progradation.
Early Responder	In this thesis, a shoreline or coast exhibiting long-term physical changes in response to contemporary climate change-induced global sea-level rise earlier than the majority of soft erodible shorelines that are expected to eventually be susceptible to such changes.
Emerging	In this thesis, used in the sense of 'emerging behaviour change'. This refers to a shoreline which has changed its behaviour in a way that may become persistent, but the new behaviour has not yet persisted long enough to be regarded as 'long-term'.
ENSO	El Nino Southern Oscillation. A major quasi-cyclic mode of oceanographic variability which affects shoreline behaviour throughout the Pacific Ocean region and beyond.
Erosion	Removal of material from (in the context of this thesis) a coast or shoreline, typically by storm-driven waves and/or winds.
Exposure	In relation to waves, the aspect of a shoreline relative to waves reaching that shoreline. Thus 'high exposure' refers to wind waves arriving close to normal to a shoreline. Typically defined in respect of the dominant wind directions for a given coast.
Fetch	In relation to wind waves, the distance winds may blow across water and generate local wind waves before reaching a shoreline. Typically defined in respect of the dominant wind directions for a given coast.
Foredune	A shore-parallel sand ridge built of sand blown landwards from a beach or foreshore area and captured by backshore (dune) vegetation above the intertidal zone (paraphrase of Hesp 2002). May be an incipient (recently developed, ephemeral, temporary) or established (old, 'permanent') foredune. Note that certain dunes behind beaches or other shorelines that are sometimes referred to as "foredunes" may actually be other dune types such as the seawards sides of old (commonly vegetated) transgressive or parabolic blow-out dunes, and not foredunes in the sense of Hesp.
Frontal dune	Term often used in an ambiguous sense to refer to any dune (including foredunes) immediately backing a beach or other shoreline. Mainly used in this thesis to refer to dunes immediately backing a beach which are *not* foredunes in the sense of Hesp (2002), or whose mode of formation is uncertain.
GIA	Glacio-Isostatic Adjustment: Crustal response (by vertical movement) to the accumulation or melting of ice sheets.
GMSL	Global Mean Sea Level: globally averaged mean sea-level.
GMSLR	Global Mean Sea-Level Rise.
Holocene	The most recent geological period covering the current Interglacial climatic phase from 10,000 years BP to present. Note however that it has recently been suggested

	that the most recent part of the Holocene should be assigned as the beginning of a new geological period termed the Anthropocene.
Incipient	In this thesis, used in the sense of 'incipient foredune'. This refers to a recently - accreting shore-parallel dune on the seawards side of an established foredune, as defined by (Hesp 2002).
Late Responder	In this thesis, a shoreline or coast *not* exhibiting earlier long-term physical changes in response to contemporary climate change-induced global sea-level rise than the majority of soft erodible shorelines but expected to be susceptible to such changes in the longer term. Typically refers to shorelines not yet showing such changes, but likely to do so in future.
LIDAR	Light Imaging, Detection And Ranging; a high-resolution mapping technology using laser range finding technology, typically mounted on aerial platforms.
LIST	Land Information System Tasmania. The State Government mapping data service for Tasmania, located within DPIPWE.
Long-term	For the purposes of this thesis, "long-term" behaviour is that which is consistent over longer periods than the duration of average observed beach erosion and recovery cycles, and over longer periods than typical intervals between air photo dates. Approximately a decade (10 years) or less is typical for both measures in the shoreline histories analysed during this project, hence for the purposes of this thesis "long-term" trends are those which remain consistent on time scales of at least 10 years and ideally more than 20 years. For the purposes of this thesis 'long-term change' is also taken to mean a change of shoreline behaviour type or trend which persists long enough to rule out the most likely cyclic or episodic sources of variability as causes of the change. Examples are wave direction or sea-level variability related to ENSO cycles, or 'sand waves' moving along a coast that alternately deplete and supply sand to beaches. These processes typically cycle on inter-annual to inter-decadal time scales, hence behaviour changes persisting for at least 10 years and ideally more than 20 years are consistent with longer-term change trends. In comparison, *emerging* behaviour trends are those which so far have been consistent for less than 10 years but are continuing and may eventually become long-term behaviours.
Morpho-dynamic	Literally, refers to "shape-changing processes". Refers to the processes by which natural landforms change their shapes (forms), typically in response to geomorphic, oceanographic, meteorological, biological, and other processes.
NCCARF	National Climate Change Adaptation Research Facility. An Australian Commonwealth Government program which funded research into climate change adaptation issues.
Non-significant	A term frequently used loosely in this thesis to refer to shoreline position history plots with apparent linear shoreline trends (e.g., recession or progradation), but which yield low Pearson correlation coefficients (R^2) and/or whose air photo error margins are mostly greater than the net trend change.
Progradation	Progressive seawards accretion or growth of a shoreline by the addition of sediment (mainly sand). Episodic erosion events may occur but are insufficient to halt long-term seawards movement of the shoreline.

Recession	Progressive landwards retreat of a shoreline, typically as a result of multiple erosion events over long periods, with any shoreline recovery between events being insufficient to maintain a stable long-term shoreline position.
Re-entrant	Term used in this thesis to refer to coastal inlets which are not exposed to swell-waves (except close to their entrances) but which are tidal, permanently connected to the ocean, and subject to sea-level changes driven by sea-level variability on the adjacent open coast. Examples of re-entrants include tidal lagoons and estuaries.
RMSL	Relative Mean Sea Level: sea level and sea-level change at a particular location – which may be a function of a variety of drivers including isostatic crustal movement, global mean sea-level, climatically- or oceanographically-driven inter-annual variability (Southern Oscillation Index, Rossby Waves, etc.) or other causes.
RSLR, RMSLR	Relative Sea-Level Rise, Relative Mean Sea-Level Rise: a rise in sea-level relative to a local solid surface. May be the local expression of global mean sea-level rise or may be caused by local factors such as vertical land movement (e.g., subsidence).
SAM	Southern Annular Mode
Sediment Sink (or Sand Sink)	A place in which sand or other eroded sediment lost from a sediment cell is permanently stored (or sequestered) and/or a process by which sediment is permanently lost from a sediment cell (e.g., from a specific shoreline). This and related sediment budget concepts are discussed and defined by Komar (1996) and Rosati (2005).
SOI	Southern Oscillation Index (a measure of the El Nino Southern Oscillation ENSO)
SSH	Sea Surface Height (~ sea-level)
Stability	In the context of shoreline behaviour, "stability" refers to an essentially constant horizontal shoreline position, albeit this may exhibit some cyclic erosion and accretion around an equilibrium position (see for example Fig. 6.17 in Woodroffe 2003).
Swell storm	Swell waves of sufficient height to be classed as 'extreme' and thus storm waves.
ToE	Time of Emergence. The time when a signal of climate change (e.g., sea-level rise or increasing erosion due to sea-level rise) becomes obvious to most observers above the noise of other processes and the variability in the changing process itself.
TWWHA	Tasmanian Wilderness World Heritage Area
VLM	Vertical Land Movement (attributable to glacio-isostatic adjustments (GIA), tectonic movements, volcanic doming, anthropogenic fluid extraction, and other causes). Sometimes referred to as Vertical Land 'Motion'.
Wrack	Dead seagrass or seaweed washed onto shorelines including beaches. Abundant wrack may obscure *in situ* shoreline vegetation lines.

Acknowledgements

First and foremost I would like to thank my supervisors, who between them covered a very relevant background of geodesy with a focus on measuring sea level (my primary supervisor Dr Christopher Watson) and a very broad range of expertise in coastal geomorphology (my co-supervisor Professor Colin Woodroffe). My thanks to both supervisors for your insights and guidance. Amongst which I must include my thanks to Christopher Watson for making *Matlab*™ scripting look downright easy (actually it is not), and to Colin Woodroffe (amongst others) for regularly telling me since at least 2007 that I should do a PhD. Even back then, the research question on which this thesis is centred had been niggling away at me for at least 10 years, and in the end I realised that a PhD project was going to be the only practical means by which I would really be able to focus on it. So, I did.

I thank Peter Devine and Malcolm Crawford (Geodata Services, Tasmanian Department of Primary Industries, Parks, Water and Environment) for much assistance in obtaining scanned historical air photos from the large DPIPWE air photo archive, which was the primary source of data under-pinning my project. Matt Dell (consultant) gave much assistance with Landscape Mapper software, which I used to ortho-rectify air photos, and supplied recent original ortho-photos captured by himself for some beaches in Clarence and Kingborough Local Government areas. Several of the ortho-rectified photos used in this report were prepared during previous projects by Sarah Harries and Hannah Walford (as specifically recorded in Appendix One metadata).

Clarence City Council (Phil Watson and Karen Butler) supplied ortho-rectified air photos of Roches Beach at several dates free of charge to this thesis. High resolution ortho-rectified imagery of Roches Beach dated 15th May 2011 was supplied by Clarence City Council for this project and is used under Conditions of Use supplied by data owners, the Southern Tasmanian Councils Authority (STCA) and Southern Water (SW).

Jon Doole of Kingborough Council kindly supported this project by providing funding for the purchase of historic air photos of key coastal study sites within Kingborough Council area.

Dr Michael Lacey (Spatial Science Group, University of Tasmania) kindly and voluntarily wrote a Python script for ArcGIS (entitled '*Shoreline History'*) which greatly eased the process of extracting shoreline behaviour histories from raw shoreline position shapefiles plotted from ortho-rectified historic air photos. This constituted an automation of data extraction techniques previously developed for the ShoreWave Project by Sharples et al. (2012).

The Tasmanian Department of Primary Industries, Parks, Water and Environment (DPIPWE) provided support to this thesis in the context of the authors professional participation in a project managed by Rolan Eberhard to monitor the condition of six beaches in the Tasmanian Wilderness World Heritage Area (TWWHA). As in-kind support to this thesis, DPIPWE provided all historic air-photos of the six beaches, as well as providing helicopter transport to visit, examine and monitor the six beaches during Dec 2014, 2015 and 2016.

Nick Bowden repeatedly (over nearly a decade) provided convivial company on Tasmania's "wild west" coast as I assisted him to professionally survey beach profile data for Ocean Beach. Nick and Paul Boland also surveyed the six other south-west and south coast beaches studied during this project.

AMS ^{14}C dating of peat samples from Ocean Beach was supported by ANSTO Research Portal (grant #10649 to Professor David Bowman). The financial support from the Australian Government for the Centre for Accelerator Science at ANSTO through the National Collaborative Research Infrastructure Strategy (NCRIS) is acknowledged. Dr Quan Hua (ANSTO) carried out the AMS radiocarbon dating on peat samples and constructed the chronology for the peat profile.

Dr Neil White for provided data files for the Church and White (2011) SSH reconstruction. Dr Benjamin Hamlington kindly provided Dr. Christopher Watson with data files for the SSH reconstruction for the Australian region prepared by the method of Hamlington *et al.* (2011).

I also thank Peter Horton, Dr. John Hunter, Dr John Church, Dr Mark Hemer and Professor Bruce Thom for a range of other useful discussions and advice during this work.

Finally, and of course, I would also like to extend special thanks to my friend Vicki Lees and my sister Tricia Sharples, both of whom supported me in many ways on the home front as I became more and more focused on this project. This support became even more important in the final months of writing when plague stalked the globe and I suddenly found myself working entirely at home under conditions of social distancing and lockdown.

Chapter 1: Introduction

1.1 *Background*

This thesis asks whether any noticeable shoreline geomorphic behaviour changes can yet be attributed to contemporary climate change-driven changes in mean sea-level. Long-term tide gauge records, natural tide-level proxies and satellite altimetry show that following a multi-millennia period of relative stability, a global mean sea-level rise (GMSLR) of about 210 mm occurred between 1880 and 2009 (Church & White 2011). This is mainly attributed to climate change-driven thermal expansion of the ocean and ice melting from mountain glaciers and polar ice sheets. Long-term tide gauge records indicate this geologically-recent onset of sea-level rise began during the mid-1800s to early 1900s period (Gehrels & Woodworth 2013; Woodworth 1999), and is continuing with an increasing rate (Chen et al. 2017; Church & White 2006; Watson et al. 2015). In principle it could be expected that a rise of this magnitude would by now be causing noticeably increased erosion and recession of at least some erodible shorelines as described by the 'Bruun Rule of Erosion by Sea-Level Rise' (Bruun 1962, 1988).

However shoreline recession has been occurring for millennia on many soft coasts, and on some of these is at least partly[1] a response to local or regional relative sea-level rise (RSLR) caused by land subsidence (e.g., Pye & Blott 2006, 2015; Romine et al. 2013; Zhang, Douglas & Leatherman 2004). However, shoreline recession directly attributable to contemporary climate change-driven sea-level rise has not yet been clearly demonstrated on geologically stable coasts where local RSLR is comparable with the global average (GMSLR). This is despite about 210mm GMSLR since the 1800's and an observed Twentieth Century acceleration in global sea-level to recent rates of rise >3 mm yr^{-1} (Chen et al. 2017; Church & White 2006; Church & White 2011). These rates are comparable to or greater than the rates of RSLR associated with observed recession on some long-term subsiding coasts. For example, RSLR rates of as little as 0.6 up to 0.9 mm yr^{-1} (Shennan & Horton 2002) are probably a factor in the extensive recession of 'soft rock' coasts on the subsiding east coast of England which has been in progress for at least centuries (Pye & Blott 2006). In another well-studied example, long-term (multi-millennial) and ongoing recession of sandy shores on subsiding parts of the eastern USA coast are associated with Twentieth Century RSLR rates ranging from 2 mm yr^{-1} to 4 mm yr^{-1} (Zhang, Douglas & Leatherman 2004).

It has proven difficult to identify the effects of recent changes in sea level on shorelines of geologically stable (non-subsiding) coasts because of the influence of other processes that also cause shorelines to erode or accrete. The morpho-dynamic effects of these other processes are often large enough to mask or counter-act physical responses to recent change in global mean sea level (Le Cozannet et al. 2014). In some cases a shoreline response attributable to an underlying mean sea-level rise trend of geologically-recent onset might take centuries to unequivocally emerge from other sources of variability (e.g., Cowell et al. 1995; Davidson-Arnott 2005; Stive, Cowell & Nicholls 2009). In a common case, on swell-exposed sandy coasts the scale of coastal change that may result from interannual to interdecadal variability in wave climate, regional sea level or sand transport processes may be at least an order of magnitude greater than any changes induced by mean sea level change over the same periods (see Section 2.5.3). Processes such as wave climate variability are

[1] Note that some shorelines which are not capable of natural recovery after erosion will progressively recede even without any change in mean sea level. Cohesive clay, semi-lithified siltstones or limestones, and other soft-rock shores episodically erode in response to storm waves, but unlike unconsolidated sandy shores do not subsequently recover since natural processes do not return eroded materials such as clay, pebbles or cobbles to the eroded scarps to rebuild them. On longer timescales the same is true of most hard-rock shores. Sea-level rise may be expected to increase the rate at which such "non-recovering" shores recede but will not be the sole cause of their recession.

expected to dominate over and mask any coastal changes due to GMSL on many coasts for at least the next few decades (Mortlock & Goodwin 2015a).

The "Time of Emergence" (Hawkins & Sutton 2012) of noticeable physical coastal changes in response to the onset of geologically-recent sea-level rise is an issue of great consequence for coastal populations and infrastructure given the anticipated socio-economic and environmental impacts of the expected changes. The issue arises of whether any such attributable physical changes are detectable yet on geologically stable coasts, or whether some further sea-level rise must occur before geomorphic effects clearly attributable to sea-level rise will emerge on even the most susceptible coasts.

This thesis tests the proposition that shoreline changes attributable to contemporary climate change-driven sea-level rise may be already observable on some coasts where the geomorphic environment is most susceptible and confounding processes are minimal. The importance of investigating this proposition is that it may lead to improved ability to distinguish between shores having characteristics predisposing them to either earlier or later recessional responses to recent sea-level rise. Such information will enable better planning and adaptation to sea-level rise for that large proportion of human populations and their infrastructure that occupy coastal areas.

Key terms

A glossary of frequently used terms and acronyms is provided at the start of this thesis. Several terms are particularly significant in the context of this thesis, and are highlighted below:

This thesis is focused on asking whether the physical effects of global mean sea-level rise induced by changing climatic effects (ocean warming and ice melting) since the 1800s are yet identifiable in coastal landforms. This is as opposed to the effects of local or relative mean sea-level rise caused by land subsidence or other causes, typically occurring over longer periods into the past. In this thesis, the terms "Sea-Level Rise" (SLR), "Global Mean Sea Level Rise" (GMSLR) and "Relative Mean Sea Level Rise" (RMSLR) may refer to any sea-level rise irrespective of its cause(s). However, when the text is intended to refer explicitly to the sea-level rise process that is of specific interest to this thesis, then the term "*contemporary climate change-driven sea-level rise*" (or a variant thereof) is used. This refers to the renewed sea-level rise which commenced to register on tide gauge records from around the mid-1800s as a result of thermal expansion of the global ocean, and the addition of meltwater from mountain glaciers, polar ice caps and other lesser sources triggered by ongoing warming of the climate.

The terms "*shoreline behaviour*" or "*coastal behaviour*" are used here as a convenient way to refer broadly to styles or patterns of long-term (multi-decadal) coastal geomorphic change or lack thereof. Although these terms could be regarded as being somewhat anthropomorphic, there are precedents in the coastal science literature for similar usage, e.g. Cowell, Roy and Jones (1995).

The terms "*Early Responder*" and "*Late Responder*" have been coined by the writer to refer to shorelines (or more accurately, shoreline geomorphic process environments) which are respectively either highly susceptible to changing their behaviour (e.g., from stability to recession) in response to the onset of a relatively small amount of sea-level rise, or else are more resilient and not as susceptible to changing their behaviour. For the late-responder case, the expectation is still for a response, albeit later when more sea-level rise has occurred.

1.2 *Knowledge Gap*

The extent of the impact to date of contemporary climate change-driven sea-level rise on coastal landforms is presently poorly understood. The current scientific literature mostly supports the view that such impacts are yet to be clearly identified and are likely to be masked by the effects of other processes – for example wave climate variability (e.g., Mortlock & Goodwin 2015a) – for some

decades into the future. A review of this knowledge gap by Le Cozannet et al. (2014) concluded that the question of whether any shorelines were yet showing detectable responses to contemporary climate change-driven sea-level rise had not been unequivocally resolved (see literature review, Section 2.4). This thesis seeks to contribute to this knowledge-gap with an analysis of shorelines around the coast of Tasmania, Australia.

1.3 *Research Questions*

A proposition under-pinning this thesis is that *physical coastal behaviour changes attributable to contemporary climate change-driven sea-level rise may be already observable on some coasts where the geomorphic environment is most susceptible and confounding processes are minimal*. This proposition has been framed as two research questions to guide this thesis, namely:

RQ1: *What evidence may enable contemporary climate change-driven sea-level rise to be identified as a dominant factor driving changes in coastal landform behaviour?*

This research question is the essential pre-condition for being able to address the identified knowledge gap.

RQ2: *Are there some distinctive "early responder" shoreline types or coastal process environments which are responding to contemporary climate change-driven sea-level rise earlier than other "late responder" types?*

This research question seeks to confirm or refute a proposition underlying this thesis, namely that detectable responses to contemporary climate change-driven sea-level rise are to date only being seen in coastal environments that are most susceptible and most free of confounding processes; i.e., in "early responder" coastal morpho-dynamic environments.

The research framework adopted to investigate these questions is introduced below and more fully discussed in Chapter 3.

1.4 *Introduction to Research Framework*

This thesis has emerged from the writer's experience of over 20 years as a geologist specialising in coastal geomorphology in Tasmania (Australia). Tasmania presents a wide diversity of coastal landforms and differing exposure to marine conditions that make it an appropriate study region to test the research questions proposed above. Tasmania has over 6,500 kilometres of coastline at a 1:25,000 map scale (Mount 2001), including over 1000 swell-exposed sandy beaches (Short 2006b) and extensive erodible cohesive clay, soft-rock and salt-marsh shores. Tasmanian coastal wave climates range from swell-sheltered tidal re-entrants in many regions, to the west coast which has the highest wave energies of any Australian coast (Hemer, Simmonds & Keay 2008).

The study area for this project is restricted to Tasmania partly for reasons of cost and logistics, since it was important to be able to inspect all study sites in the field. Moreover, having considered the knowledge gap and research questions outlined above for some years, the writer was aware of a variety of coastal sites in Tasmania that warranted examination in greater detail to test the hypothesis that they were exhibiting a response to a recent (from the mid-1800s) onset of sea-level rise.

A further factor in the development of this thesis was the writers prior professional experience focussed on descriptive geomorphology rather than on numerical modelling approaches to coastal processes. The writers focus has primarily been on data collection and analysis of observed geomorphology and geomorphic processes. In particular, previous experience with coastal air photos suggested that these provided a useful source of objective information on coastal behaviour since circa 1945 whose potential to provide new insights into historical (multi-decadal) coastal behaviour has generally been under-utilised for Tasmanian coasts.

1.4.1 Guiding Principles

The physical responses of coastal landforms to sea-level rise are in many respects well understood and are the subject of an extensive scientific literature as reviewed in the following chapter. Shoreline erosion and progressive recession are fundamental morpho-dynamic responses to sea-level rise, although other more complex responses may occur, such as coastal barrier wash-over and "roll-back". Long-term progressive shoreline recession is common on erodible shores that have been subject to relative mean sea-level rise (RMSLR) for millennia as a result of land subsidence. However, shoreline erosion and recession may also occur for many reasons other than sea-level rise. Hence the identification of a shoreline response to contemporary climate change-driven sea-level rise on a stable coast is not as simple as identifying coastal recession approximately coincident with a new phase of sea-level rise.

Given these complexities, the approach to this thesis was based from the outset on four "Guiding Principles" as briefly outlined below[2]. These emerged from the writer's consideration of the research questions over a long period of professional coastal geomorphic practice prior to undertaking this thesis.

1. *Select sites distributed across a range of coastal geomorphic process environments hypothesised to be susceptible to early or to late responses to sea-level rise (SLR)*

A wide diversity of site types was selected to provide a better chance of sampling a range of early- or late-responder shorelines. These included several key sites already thought on the basis of their known historical or recent behaviour to be possibly showing an early response to sea-level (e.g. see Prahalad et al. 2015; Sharples 2010).

2. *As far as is practicable, utilise study sites from erodible coastal environments where other competing factors or processes ('noise') that might overwhelm or prevent a sea-level rise signal from being detected are absent or minimal.*

Sites with fewer confounding geomorphic processes and variables to consider are likely to make identification of sea-level rise signals (or lack thereof) simpler. Tasmanian sites in general have several advantages in this regard, having minimal or negligible vertical land movement and also minimal sea-level and wave-direction variability related to the El Nino Southern Oscillation (ENSO) compared to some other Australian coasts. Moreover, coastal sites in many parts of Tasmania – particularly the sparsely settled west and south coasts - have little or no local human interferences with coastal geomorphic processes. Where such factors are significant, they can complicate shoreline morpho-dynamics and may prevent or "mask" a sea-level rise signal. The inclusion of Tasmanian study sites on erodible cohesive clay shores and swell-sheltered but tidal (e.g., estuarine) sandy shores is also important in this respect since these are process environments in which the major complicating process of sandy shoreline recovery (accretion) after erosion events is minimal or absent.

3. *Identify sites exhibiting significant changes in the long-term (multi-decadal) behaviour of soft (erodible) shorelines, of types that would theoretically be expected to indicate the emergence of sea-level rise signals.*

As described in the literature review (Chapter 2), theoretical principles such as the Bruun Rule and observations of coasts subject to long-term RMSLR indicate the types of changes in soft shoreline behaviour that can be expected from of an onset of sea-level rise after a long period of negligible sea-level variability. The most characteristic changes expected on swell-exposed sandy shores are a long-term change[3] from stability or dynamic equilibrium (with erosion and accretion cycles around a stable mean shoreline position) to persistent shoreline erosion and progressive recession. For some shores

[2] These principles are discussed in more detail in chapter 3 Section 3.2.

[3] See glossary for the meaning of 'long-term' change in the context of this thesis.

that were historically receding for other reasons the dominant change may be an increase in the rate of recession.

Shores exhibiting such long-term changes that are identifiable in the historical aerial photo record have been sought to identify potential "fingerprints" of a sea-level rise response in shoreline behaviour. For Tasmanian sites generally, this record is available from circa 1945 to the present.

4. *Where suspected signals of contemporary climate change-driven sea-level rise (as long-term shoreline behaviour changes) are found in air photo time series, test this hypothesis by investigating whether the geomorphic processes and conditions at each such site can explain why that shoreline would show a physical response to contemporary climate change-driven global sea-level rise earlier than most. Also investigate whether known site processes and conditions can explain the observed change of behaviour without invoking contemporary climate change-driven sea-level rise as a cause.*

This is essentially the application of the classical scientific method to this project[4]. That is, having observed that some shorelines have changed their long-term behaviour during the Twentieth Century, a working hypothesis is that at least some of these are doing so in response to contemporary climate change-driven sea-level rise. The test of this hypothesis is to ask in each specific case whether there are geomorphic processes and conditions present which could drive an observable early response to sea-level rise of the sort observed (rather than masking or preventing such a response), and to also ask whether there are processes or conditions at each site which could explain the observed changes in other ways. A 'yes' to the first question and 'no' to the second would be the best evidence possible for a plausible identification of an 'early responder' shore.

1.5 Thesis Outline

The following outlines the structure of this thesis describing the purpose and content of each chapter or Appendix.

Chapter 1.0: Introduction
This chapter has introduced the research questions and provided a preliminary outline of the principles and methods to follow.

Chapter 2.0: Literature Review
Chapter 2 reviews the existing scientific literature to identify the state of current knowledge and relevant uncertainties regarding key issues addressed by this thesis.

Chapter 3.0: Project Methods
Chapter 3 further elucidates the principles guiding the research method. The workflow and methods used to collect and analyse data are provided, focussing in particular on the acquisition of shoreline

[4] A very large literature exists on the Scientific Method, however a useful summary is provided by Wikipedia (https://en.wikipedia.org/wiki/Scientific_method accessed 15th October 2019). Woodroffe (2003, section 9.1) also provides a discussion of the scientific method from a coastal geomorphic perspective. The scientific method is an empirical method of acquiring knowledge that requires creative thinking (to generate alternative hypotheses) and specific procedures that may vary from one field of study to another but is nonetheless underpinned by the same basic principles in all cases. These comprise making observations of some phenomena; formulating inductive hypotheses to explain the observations; making deductive predictions based on the hypotheses (i.e., predicting additional phenomena that should also be observable if a hypothesis is correct); and then testing those predictions by experimenting or making further observations. A scientific hypothesis must be falsifiable, meaning that it is possible to imagine an outcome of experiments or further observations which conflict with (disprove) the predictions of the hypothesis. On the other hand, no utterly final or 'absolute' proof of any scientific assertion is possible, however if a hypothesis continues to pass all valid tests then it may eventually be regarded as a sufficiently well-supported theory as to be beyond reasonable doubt.

behaviour histories from analysis of air photo time series. These are the primary data source upon which this thesis is based.

Chapter 4.0: Study Sites Selection
The fourth chapter describes the criteria applied in selecting study areas and sites within those areas. Lists the study sites selected against those criteria.

Chapter 5.0: Shoreline Behaviour Case Studies
Chapter 5 presents the key findings from detailed study of four case study areas (comprising 12 distinctive shoreline sites). These case studies identify processes likely to be driving the shoreline behaviours observed, and local geomorphic conditions inferred to be enabling observed changes to occur and to be observable.

Chapter 6.0: Shoreline Behaviour Analysis across all Study Sites
Assesses data from all (35) study sites to test the degree to which the findings from the previous chapter can explain the behaviour of other sites. The chapter summarises the key scientific findings of the thesis, including the identification amongst the full suite of sites of any additional drivers of shoreline behaviour that were not identified by the four detailed case studies.

Chapter 7.0: Discussion
Chapter 7 identifies the broader implications of the scientific findings, for coastal geomorphic studies of the Tasmanian coast generally, for understanding of shoreline responses to contemporary climate change and sea-level rise, and for improved identification and prediction of coastal hazards resulting from climate change. The discussion also identifies key limitations of the thesis and the implication these have for the research findings.

Chapter 8.0: Conclusions and Recommendations
Finally, Chapter 8 describes the degree to which the thesis findings respond to the knowledge gap and research questions identified in Chapter One. The Conclusions identify the key scientific findings of this thesis. Recommendation of useful directions for continuing research and data collection that arise from knowledge and data gaps are identified and discussed.

Bibliography
Provides the bibliographic details of all references cited in both the main text and appendices.

Appendix One: Shoreline Descriptions and Data
Appendix One contains descriptions, data and some of the data analyses compiled for each study site. This appendix includes information which is additional to the essential information reproduced in the main text and can be referred to for additional background information on most sites, including air photo metadata. Appendix One is the primary repository of the considerable amount of descriptive information and data analysis used or created during this thesis.

Note that some data used are only available in digital format but are listed in this appendix (ortho-rectified air photos, digitised shoreline shapefiles). Some analyses and plots derived from other third-party datasets - including Bureau of Meteorology wind data, CSIRO wave hindcasts, and sea-level reconstructions - are reproduced in the Appendix, however the original copyright data is cited but not reproduced.

Appendix Two: Published Refereed Papers
This appendix provides copies of three relevant refereed papers co-authored by the author which provide information relevant to this project. One of these papers is a direct outcome of this thesis (Sharples et al. 2020), whereas the other two (Prahalad et al. 2015; Thom et al. 2018) are outcomes of different projects but are relevant to this thesis. Further information about these papers is provided in the "Authority of Access statement" and the "Statement of co-authorship" at the front of this thesis.

Chapter 2: Literature Review

2.1 *Overview*

This chapter provides a review of available scientific literature relevant to four broad themes that are important issues for this thesis. These are:

1. *Sea-level rise as a driver of coastal erosion and recession*: A review of the reasons why sea-level rise is expected to typically (albeit not always) result in the onset or acceleration of shoreline recession on erodible coasts.
2. *Recent local and global sea-level rise:* A review of the evidence that sea-level rise is occurring, the distinction between local (or regional) and global sea-level rise, and a review of the rates and drivers of sea-level rise around Tasmania.
3. *Identifying contemporary climate change-driven sea-level rise as a cause of coastal change:* A review of issues and problems in determining whether climate change-driven sea-level rise is significantly influencing the observable physical behaviour of specific shorelines.
4. *How sea-level rise interacts with other coastal process drivers:* A review of the scientific literature regarding how sea-level rise affects key coastal processes and conditions so as to induce coastal landform changes including shoreline recession.

2.2 *Sea-level rise as a driver of coastal erosion and recession*

There are well-established theoretical and observational reasons to expect that a rise in sea level relative to an erodible coastal profile will generally (albeit not always) result in shoreline erosion and recession (or translation) of the shore profile landwards and upwards.

A seminal paper by the Danish-American coastal engineer Per Bruun is widely regarded as the first clear exposition of the principle that sea-level rise may drive coastal recession (Bruun 1962). The relationship identified by Bruun, later termed 'The Bruun Rule' (Schwartz 1967), used observations of receding swell-exposed sandy shores undergoing regional sea-level rise relative to subsiding coastal land (mainly east coast USA, especially Florida) to describe a relationship between the slope of a sandy swell-exposed coastal profile and the amount of horizontal shoreline recession that will occur in response to a given amount of sea-level rise.

The following review is focussed mainly on the Bruun Rule and its implications for swell-exposed sandy shores. However, many non-sandy and swell-sheltered shores are also susceptible to receding in response to sea-level rise, albeit at different rates and through partly differing processes. The response of non-sandy shores to sea-level rise is discussed further in Section 2.5.2 (Shoreline Substrate), and that of swell-sheltered sandy shores in Section 2.5.5 (Wave-Climate variability).

As noted by Zhang, Douglas and Leatherman (2004), sea-level rise does not cause coastal erosion by itself. Instead it acts as an enabler of increased erosion by allowing storm waves of any given size to more frequently reach further landwards over deepened water, and to higher levels on the shore profile, than previously. The Bruun Rule (Figure 1) is a 2-dimensional model which fundamentally describes how a rise in mean sea-level will allow wave action at higher levels on the shore profile than previously to transfer sand (via storm wave backwash) from the upper shore face (dune, upper beach or berm) to the lower shore face (subtidal area), resulting in translation of the shore profile upwards and landwards while preserving mass and original slope. That is, with reference to Figure 1, when mean sea level rises by height S then wave attack during storm events occurs higher on sandy shoreline profiles than previously, resulting in a volume of sand being eroded from the upper beach face (V_1) and deposited on the lower beach face (V_2), so translating the starting shore profile (1) landwards by a distance R (profile 2), and thus maintaining an equilibrium profile. The Bruun Rule

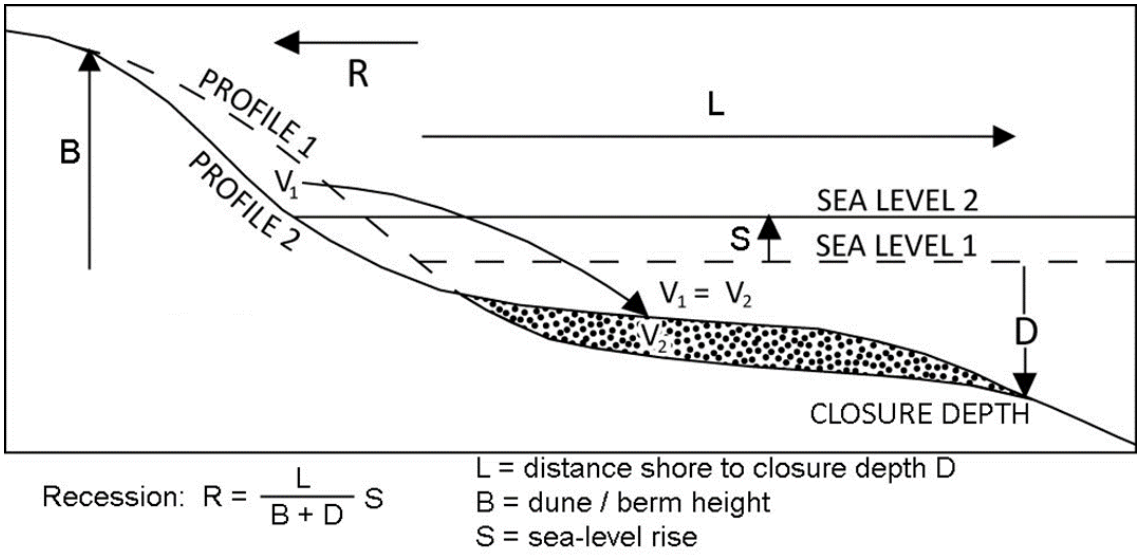

Figure 1: The basic concept expressed by the Bruun Rule in its simplest form (see text discussion). The Bruun Rule equation (Bruun 1962) given here is as cited by Mariani et al. (2012) and Davidson-Arnott (2005). Original figure drawn by Paul Donaldson.

equation (Figure 1) states that the recession distance R is a function of the steepness of the "active coastal slope" from the onshore dune or berm crest to the offshore "Closure Depth" (=L/(B+D) times the amount of sea-level rise (S). The term "Closure Depth" refers to the maximum depth to which sand is exchanged between the onshore and offshore parts of the shore profile and relates to the fact that the Bruun Rule models an idealised closed system.

This simple geometric relationship is predictive of the recession distance because a steeper cross-shore slope contains more sand mass per horizontal metre that a gentler slope, and so requires more wave energy to remove enough sand to recede the shoreline by a given horizontal distance. The increased wave energy is proportional to the amount of sea-level rise because a higher rise results in more frequent and higher upper beach wave attack. It is particularly important to note that the Bruun Rule in this most basic form considers only a closed two-dimensional coastal system in which nothing changes except sea-level. It does not allow for the effect of the many possible confounding factors in coastal geomorphic systems, such as changing wave climates and net gains or losses of sand from the simple closed system depicted in Figure 1, which can result in completely different outcomes under the same sea-level rise conditions (see further below).

Shoreline recession distances have been measured on portions of subsiding sandy coasts such as the eastern USA where confounding processes such as tidal currents are minimal (Zhang et al. 2004). For the most common range of sandy shore slopes, the amount of horizontal shoreline recession is about two orders of magnitude greater than sea-level rise and typically falls in the range of 50 – 100 times the vertical sea-level rise. This number is often referred to as the "Bruun Factor" for a shoreline.

The Bruun Rule in its simplest form (Figure 1) relies on several assumptions which are not always made explicit (Davidson-Arnott 2005; Mariani *et al.* 2012). These include:

1. that the shoreline (and backshore/offshore areas) is entirely unconsolidated sand (rocky or clay-rich shorelines behave very differently when eroding, with less transport of coarse eroded material and much more loss of very fine suspended clay and silt); and:
2. that the closure depth and dune or berm crest represent the limits of shore-normal sand movement in the coastal system and there is no cross-shore or alongshore transfer of sand into or out of the profile (in reality many coastal systems gain or lose sand to or from beyond these

limits, for example by littoral drift, offshore or onshore-directed currents, barrier-overwash and aeolian deflation processes); and:

3. that the shoreline is a swell-dominated one since an active fair-weather swell in-between erosion events is necessary to maintain the equilibrium shore profile and closure depth that is a key assumption of the Bruun Rule (in contrast, swell-sheltered sandy shores experience very little wave activity between wind-wave storm events but may be subject to daily tidal currents and arguably do not have a meaningful "closure depth" at all).

A great deal of observational evidence supports the fundamental principle of the Bruun Rule, namely that sea-level rise drives recession of soft erodible shores. Some of the strongest evidence is derived from field studies including long-term observations of shoreline recession on coasts which are experiencing substantial relative sea level rise because of land subsidence, (e.g., Mimura and Nobuoka (1995), Hands (1983), Zhang, Douglas and Leatherman (2004), Pye and Blott (2015); Romine et al. (2013)).

In addition, early experimental (wave tank) studies by Schwartz (1965) and recent laboratory simulations by Atkinson et al. (2018) have both supported the Bruun Rule as a realistic description of the response of open coast sandy beaches to sea-level rise (if most other processes are absent). Thus, the Bruun Rule is arguably a valid principle (under certain conditions) that should be a part of realistic coastal behaviour models provided that its assumptions are understood.

However sea-level rise is only one amongst many processes or environmental changes, both natural and artificial, that may influence the erosion and recession (or accretion and progradation) of coasts. For example, the substrate type - whether hard rock, soft rock, sand or heterogenous materials including artificial structures - influences susceptibility to erosion and the transportability of eroded materials. Since waves are the principal agent of shoreline erosion, wave climate variability including wave direction and storm magnitudes and frequencies also strongly determine shoreline behaviour, (e.g., Hemer 2009; Mortlock et al. 2017). On sandy coasts, sediment availability and transport processes such as onshore sand movement, alongshore (littoral) drift, tidal currents or aeolian sand deflation determine overall sand losses or gains (the 'sand budget') from the beach system (Komar 1996; Rosati 2005). These and other processes may have morpho-dynamic effects on sandy beaches that are several orders of magnitude greater than the effects of sea-level rise and so may dominate over or mask the effects of the latter (Cowell, Roy & Thom 1995; Stive, Cowell & Nicholls 2009). The Bruun Rule does not describe or model these other processes and so is not a complete model of shoreline behaviour.

There have been many attempts to augment the Bruun Rule by adding terms to account for other relevant coastal factors. For example, Hands (1983) modified the rule to allow for longshore drift of sand, and Davidson-Arnott (2005) proposed a modified formulation accounting for landwards movement of dune sands as an important aspect of sandy shore responses to sea-level rise. Dean and Maurmeyer (1983) recognised that the standard formulation of Bruun (1962) applies only to a very simple beach-dune configuration, and extended the rule to create a "Generalised Bruun Rule" also applicable to a barrier beach in which barrier roll-over into a backing lagoon or swamp may accompany sea-level rise as sand is moved landwards (by wash-over and aeolian transport) as well as offshore (Cowell et al. 2006). However, these and most other such proposals only incorporate a subset of the many processes and conditions driving shoreline behaviour and as such are only partial attempts at constructing complete coastal behaviour models around the Bruun Rule.

A number of authors have questioned the validity of the Bruun Rule, with some arguing it should be abandoned (e.g., Cooper and Pilkey 2004). However, although not always explicitly acknowledged, most objections have centred on the fact that the Bruun Rule is not in itself a complete coastal behaviour model since it does not incorporate the effects of all relevant concurrent processes other than sea-level rise. Thus, it is arguable that the Bruun Rule by itself can be considered valid, but *only* as a simple principle describing just one element of sandy shoreline behaviour (namely response to

sea-level rise). However, the use of the Bruun Rule by itself becomes invalid when it is used as though it were a complete coastal behaviour model.

It follows that a properly comprehensive coastal behaviour model must incorporate not only the Bruun Rule but also the full ensemble of all other known relevant conditions and processes such as substrate type (sand or otherwise), sediment transport and budgets, wave climate, storm climate, bedrock topography and so on. One example of a numerical coastal behaviour model more comprehensively incorporating other processes alongside the Bruun Rule is the Shoreface Translation Model (Cowell, Roy & Jones 1995; Cowell et al. 2006). However, such modelling is beyond the scope of this thesis and is not further discussed here.

Despite the limitations and caveats surrounding the use of the Bruun Rule as discussed above, the rule has informed this thesis in at least one important respect. The process which the Bruun Rule implicates as driving the recession of sandy shorelines under sea-level rise is that wave approach over deepened water allows wave erosion to occur higher and further landwards on the shore profile more frequently than previously. This process has been critical in the formulation of working and alternative hypotheses to test the notion that sea-level rise may explain the cases of changed long-term shoreline behaviour that have been the focus of this project (see chapter 5).

2.3 *Recent global and regional sea-level rise*

Global mean sea-level (GMSL) stood approximately 130 m below present levels during the Last Glacial Maximum (LGM) circa 20,000 years before the present (BP), but rose during the post-glacial marine transgression to reach approximately its present level by mid-Holocene time, circa 6000 - 7000 years BP (Lambeck & Chappell 2001; Lewis et al. 2013). For south-eastern mainland Australia, a relative sea-stand slightly above present levels during the mid-Holocene with a subsequent relative drop due to hydro-isostatic adjustment of the continental shelf is well-established (Lewis et al. 2013; Sloss, Murray-Wallace & Jones 2007). However models of glacio-isostatic adjustment (GIA) do not support a similar sea-level history for Tasmania (Lambeck & Nakada 1990). Proxy data including shells and saltmarsh sediment records indicate that relative sea-levels around Tasmania remained about 0.3 m below Twentieth Century levels for most of the period from circa 6000 yrs BP until AD 1880, when local relative mean sea-level rise (RSLR) commenced and has continued to the present (Gehrels et al. 2012). See Figure 2.

GMSL similarly commenced a significant renewed rise from the 1800s; Woodworth (1999) showed that several long-term (multi-century) European tide gauge records indicate an onset or acceleration of RSLR circa the mid-1800s, although a subsequent analysis of both tide gauge and proxy data by Gehrels and Woodworth (2013) suggested that global sea-level rates did not depart from background Holocene variability until as late as a 40-year period centred around 1925. The rate of this rise has increased over the Twentieth Century (Church & White 2006; Church & White 2011), albeit with some inter-decadal variability. By 2009, GMSL had risen 21 cm since 1880, and the average rate of global mean sea-level rise (GMSLR) over the whole Twentieth Century was 1.7 mm yr^{-1} (Church & White 2011). However, GMSL has continued to accelerate over the satellite altimetry era since 1993 (Watson et al. 2015), from 2.2 ± 0.3 mm yr^{-1} in 1993 to 3.3 ± 0.3 mm yr^{-1} in 2014 (Chen et al. 2017), supported by a recent study by Nerem et al. (2018).

The GMSLR that has occurred since the 1800s is attributed mainly to climatic factors, primarily ocean warming resulting in thermal expansion, as well as glacier and ice cap melting (Nicholls & Cazenave 2010). However atmospheric volcanic dust from major eruptions (e.g., Mt Pinatubo 1992) has had detectable cooling effects causing temporary GMSL falls on several occasions during the Twentieth Century (e.g., Nerem et al. 2018).

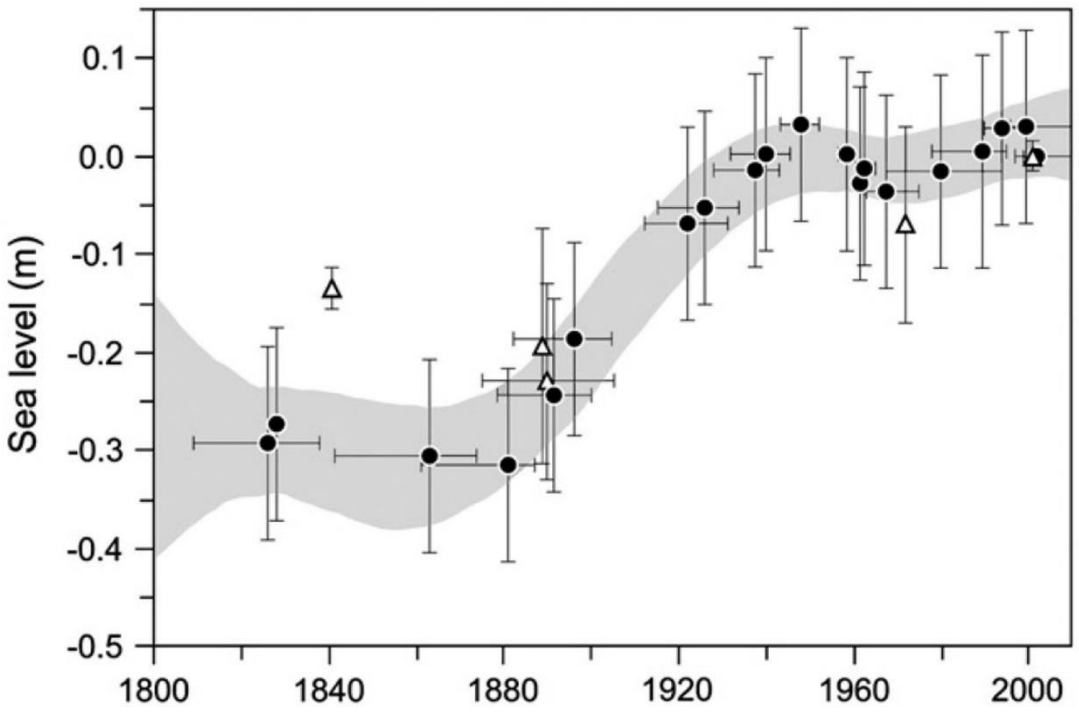

Figure 2: Sea-level curve for Tasmania since 1800, based on historical tide gauge data (triangles) and proxy data (mainly saltmarsh sediments). The grey envelope represents the 68% confidence limits. The onset of SLR circa 1880 with a rapid rise until circa 1920, and the slow-down circa 1950-1970 followed by renewed rise from circa 1990 are also seen in other long-term sea-level records both regionally and globally (see text). Reproduced from Gehrels et al. (2012, Fig. 5b).

Slangen et al. (2016) showed that anthropogenic (climate change) causes have dominantly determined the rate of global mean sea-level rise since the 1970s, and this remains true when natural perturbations such as those due to the El Nino Southern Oscillation (ENSO) and volcanic dust are considered (Nerem et al. 2018).

However, a range of other processes may contribute additional variability to relative sea-levels at regional and local scales. These include Vertical Land Motion (VLM) which may result from glacio- or hydro-isostatic adjustment, thermal (magmatic) doming, tectonic instability, or sediment compaction due to extraction of fluids. Regional sea level variability over various space and time scales also results from waves, tides, variable meteorological pressure systems, and larger climatic modes of variability of which ENSO is most significant for Australian coasts (see also Section 2.5.8).

Burgette et al. (2013) and White et al. (2014) analysed the 'noise' in tide gauge records around Australia, that is, sea-level variability unrelated to the local trend. White et al. (2014) found that with regional influences (most notably ENSO) removed and atmospheric pressure effects allowed for, Australian mean sea-level trends are close to global mean trends from 1966 to 2009, namely 2.0 ± 0.3 mm yr^{-1} for 1966 to 2009 and 3.4 ± 0.4 mm yr^{-1} for 1993 to 2009 (see Figure 3). This work also found that the sea level variability attributable to ENSO was less in Tasmanian waters than around much of the northern Australia coast (see Figure 3 and also Section 2.5.8 including Figure 10).

White et al. (2014) and Watson (2011) also found non-linear long-term sea level trends (not attributable to regional factors) in the longest Australian tide gauge records from Fremantle and Sydney, with both of these records showing larger rates of rise between 1920 and 1950, relatively stable sea levels between 1960 and 1990, and increased rates of rise again from the early 1990s onwards. These trends are also evident in both the local Tasmanian proxy sea-level record of Gehrels et al. (2012) (see Figure 2), and the global MSL reconstructions of Church and White (2011) and Hamlington et al. (2011).

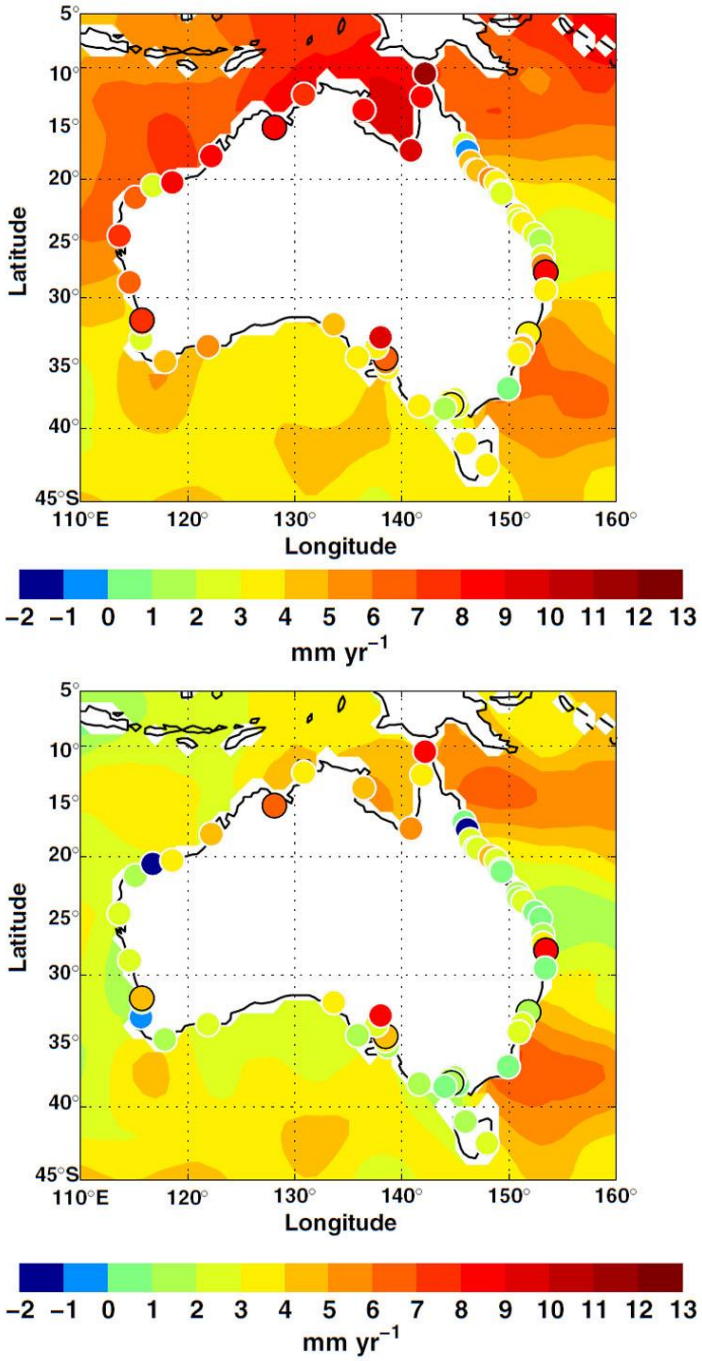

Figure 3: Sea-level trends around Australia from Jan 1993 to Dec 2010 from satellite altimeters (contours) and tide gauges (colour dots), expressed as Ocean Volume Mean Sea Level (White et al. 2014). Top shows trends prior to removal of ENSO signal, lower shows trends following removal of ENSO signal. Figure reproduced from White et al. (2014) with permission.

Although the amount of sea-level rise over the last century is comparatively small compared to the middle and upper range of sea-level rise projections for the next century (0.52 to 0.98 m above 1986-2005 levels by 2100 (IPCC 2013)), the rise of 0.21 m between 1880 and 2009 (Church & White 2011) is nonetheless a significant long-term rise from the perspective of coastal geomorphic processes. The Bruun Rule (Section 2.2) implies that sandy swell-exposed shorelines with no confounding influences might be expected to recede horizontally by as much as 10.5 to 21 metres in response to such a rise (assuming typical Bruun Factors between 50 and 100).

Tasmania is unusual in the southern hemisphere in having an early tide gauge record from 1841 to 1842 at Port Arthur in the south-east, which is tied into a known benchmark that has been surveyed into recent tide gauge measurements at the same site (Hunter, Coleman & Pugh 2003; Pugh et al. 2002). This work revealed a sea-level rise of 0.70 – 1.30 mm yr^{-1} over the period 1841 to 2002 (corrected for estimates of VLM), which is comparable to, but at the lower end of, GMSLR estimates for the whole Twentieth Century (see above). Finding no local or regional explanation for this rise (e.g., VLM), Hunter, Coleman and Pugh (2003) inferred that it commenced during the 1800's as part of the climatically-driven sea-level rise observed globally at long-term tide gauges in the northern hemisphere (Woodworth 1999). This is consistent with the sea-level proxy record for Tasmania over the last 200 years provided by Gehrels et al. (2012) based on saltmarsh sediment analysis (Figure 2). This saltmarsh record shows an onset of sea-level rise in eastern Tasmania circa 1880 following millennia of stable but slightly lower sea-levels.

Modern tide gauge records tied to a known datum are only available at 7 sites around Tasmania's coast. These include high-quality SEAFRAME stations in north-west Tasmania (Burnie) and south-east Tasmania (Spring Bay) that are part of the Australian Bureau of Meteorology (BoM) Australian Baseline Sea Level Monitoring Project (ABSLMP) network (see http://www.bom.gov.au). However, prior to 1985 Tasmanian tide gauge records are compromised by various data gaps and some unknown datum shifts (John Hunter *pers. comm.*, cited by Sharples (2006)). Thus, only the more recent decades of these tide gauge records are of use for comparing with air photo records of shoreline change. In the case of the Burnie and Hobart tide gauge records used for this thesis, only portions of those records after 1960 were reliable enough to use (see analyses provided in Chapter 5).

Given the paucity of high-quality and long-duration tide gauge data, this thesis has also used the sea-level change reconstructions for Tasmania by Church and White (2011) and Hamlington et al. (2011),. Both are global reconstructions (1° x 1° and 0.5° x 0.5° latitude-longitude grids respectively), which integrate long-term tide gauge records with satellite altimetry data from 1993 onwards, using variants of empirical orthogonal functions (EOFs). Linear fits to the Church & White and the Hamlington reconstructions for the grid cell closest to Ocean Beach (western Tasmania) yield SLR rates of 2.13 mm/$yr^{-1}$and 2.21 mm/yr^{-1} respectively over the period 1966 to 2009. These are comparable with the global-average rate of sea-level rise of 2.0 ± 0.3 mm yr^{-1} over the same period (White et al. 2014), providing confidence in the reconstruction data.

A key point emerging from the review above is that sea-level rise around Tasmania since the 1800s is comparable to climate change-induced global mean sea-level rise. The main source of interannual sea-level variability around Australia is related to ENSO and this is comparatively small around Tasmania (see further in Section 2.5.8 below). From this it can be inferred that the main driver of contemporary sea-level rise on Tasmanian coasts is the same climatic change processes that drive GMSLR (dominantly ocean thermal expansion and ice melting). This point is important in the consideration of alternative hypotheses for changing shoreline behaviours in Tasmania and is revisited by the case studies in Chapter 5.

2.4 *Identifying contemporary climate change-driven sea-level rise as a cause of coastal change*

Hawkins and Sutton (2012) state: "The time at which the signal of climate change emerges from the noise of natural climate variability (Time of Emergence, ToE) is a key variable for climate predictions and risk assessments." Contemporary global sea-level rise resulting from ocean thermal expansion and ice melting is an important climate signal whose Time of Emergence is expected to vary regionally because of regional differences in the non-climatic drivers of sea-level variability. Lyu et al. (2014) have calculated that the Time of Emergence for recent global climate change-driven sea-level rise may be as early as 2020 over more than 50% of the global ocean area and may be about 2030 for east coast Australia and 2040 for west coast Australia. Thus, sea-level rise may be clearly

obvious to non-experts in many human societies within a decade, however the question remains as to when the Time of Emergence of a sea-level rise signal (i.e., a physical response) in coastal landform behaviour may occur, and whether it may be sooner rather than later in at least some shoreline process environments.

There is a general acceptance amongst coastal geomorphologists that climate change-driven global sea-level rise will eventually become a dominant process driving widespread recession of soft coasts (e.g., Stive 2004). However, seasonal, inter-annual and inter-decadal variability in some oceanographic processes - especially elements of swell wave climate such as wave direction - drives considerable exchanges of sand between alongshore, offshore, and onshore coastal environments. Such processes are expected to prevent or hide any detectable physical response to sea-level rise for some possibly considerable period into the future (Davidson-Arnott 2005; Houston 2015; Le Cozannet et al. 2014; Mortlock & Goodwin 2015a; Stive 2004; Stive, Cowell & Nicholls 2009). Stive, Cowell and Nicholls (2009) and others imply that - at least on open coast swell-exposed shores - significantly more sea-level rise than has occurred to date, and/or a significant further increase in the rate of sea-level rise, will be needed before it will emerge as a dominant signal in coastal landform behaviour.

No signal of contemporary climate change-induced sea-level rise has yet been unequivocally demonstrated in the behaviour of swell-exposed sandy beaches (Le Cozannet et al. 2014). At many beaches, cross-shore sand exchange during erosion and accretion cycles continues to fully rebuild most beaches after erosion events, and a range of other processes move sand within and between coastal sediment cells for reasons unrelated to sea-level rise. For example, on sandy swell-exposed south-eastern African sandy beaches, Smith, Bundy and Cooper (2016) found no evidence in air photo records of systematic recession of shorelines attributable to sea-level rise since the 1930s. In other cases (e.g., Gratiot et al. 2008; Morton 2008) local coastal processes such as sand budget changes and long-term tidal cycles respectively caused changes that were too large for any longer-term sea-level rise signal to be detectable.

A well-studied process preventing the expression of sea-level rise signals in beach behaviour occurs on many embayed beaches of Australia's south-eastern coast. These beaches are subject to strong inter-annual beach rotation cycles causing physical changes of a magnitude greater than any theoretical response expected to sea-level to date. These cycles are driven by large episodic shifts in dominant swell wave directions related to ENSO, and result in alternating erosion and accretion phases at each end of the beaches (Barnard et al. 2015; Mortlock et al. 2017; Ranasinghe et al. 2004; Zhou et al. 2018).

Changes in wave climate variability due to climate change itself could also result in more shoreline variability on some beaches than sea-level rise alone would cause, at least for some time into the future. For instance, there is an emerging consensus amongst oceanographers that climate change will probably drive a pole-wards shift in extra-tropical cyclone tracks resulting in changes in the frequency and intensity of these storms at any given latitude (Masselink et al. 2016). Masselink et al. found that record extreme storm waves on the north-east Atlantic coast during the 2013/2014 winter – consistent with expected changes in storminess due to climate change – caused a degree of beach erosion significantly larger than any recessional signal that might be caused by sea-level rise alone. Similarly, Wahl and Plant (2015) found that since the 1980s variability in coastal erosion in the northern Gulf of Mexico has been driven at least as much by changes in wave climate as by regional sea-level rise, although they expect sea-level rise to become the dominating driver in future decades.

However, wave climate variability will not necessarily entirely or always mask the effects of sea-level rise. Under some conditions wave climate may simply be an additional factor which influences the degree to which shorelines show a response to sea-level rise. Thus in a part of the Solomon Islands where Albert et al. (2016) found that shoreline recession and destruction of a number of low-lying reef islands could be attributed to regionally-high rates of relative sea-level rise (RSLR), the rates of

shoreline recession varied between those island shores depending on their degree of exposure to wave energy.

Artificial coastal changes are also likely to mask or dominate over the effects of sea-level rise in many cases. For example, Aagaard and Sorensen (2013) found that a notable change of behaviour in a barrier spit on the Danish North Sea coast around 1970, from accreting to receding, was mainly attributable to channel dredging changing longshore sand transport processes, which dominated over any sea-level rise signal. Numerous other examples of anthropogenic influences on shoreline change have been documented world-wide.

Given factors such as those described above which tend to prevent the expression of sea-level rise signals in shoreline behaviour, the question of when those signals will emerge and begin to dominate is of great importance to coastal hazard assessment and coastal management planning. Le Cozannet et al. (2016) have undertaken a probabilistic Time of Emergence (ToE) study for swell-exposed gently sloping sandy beaches which assumes the Bruun Rule is valid for those beaches but incorporates other key factors additional to sea-level rise, including variable storminess, cross-shore and longshore sand transport processes. They found that under the higher-magnitude climate change scenarios defined by the IPCC (2013), a noticeable trend towards open coast sandy beach recession driven by climate change-induced processes, particularly GMSLR, is likely to emerge by the middle of the 21st Century. However they also found that a noticeable recession trend may not emerge at all on such shores during this time if future greenhouse gas emissions are lowered rapidly in accordance with the lower IPCC RCP 2.6 scenario, i.e., if GMSLR is limited to a median 0.4 m rise by 2081-2100 relative to 1986-2005 (IPCC 2013).

A recent review of research efforts to identify a signal of contemporary climate change-driven sea-level rise in coastal landform behaviour by Le Cozannet et al. (2014) concluded that no studies at that point in time have unequivocally demonstrated the emergence of such a shoreline response. Some studies have usefully identified a relationship between regionally-differing rates of relative sea-level rise (RSLR) and the degree of shoreline recession, for example Romine et al. (2013) in Hawaii and Zhang, Douglas and Leatherman (2004) on the eastern USA coast. Such studies convincingly demonstrate that relative sea level rise is a driver of shoreline recession. However, in both cases regionally variable vertical land motion (VLM) was the reason for the regional differences in rates of RSLR (caused by lithospheric flexure related to magmatic processes in Hawaii and glacio-isostatic adjustment in eastern USA). The RSLR demonstrated in these cases has been in progress for millennia, as has the shoreline recession driven by it. These studies did not attempt to differentiate shoreline changes attributable to long-term VLM - driven sea-level rise from any emerging changes attributable to contemporary (recent-onset) climate change driven sea-level rise.

However, one recent study presumably not available to Le Cozannet et al. (2014), namely a study of soft-rock cliff retreat along the Holderness coast (UK) by Pye and Blott (2015), does identify a significant acceleration since 1989 in the long-term shoreline retreat along this subsiding coast. These authors do not explicitly suggest that this may be a result of a new climate change-driven SLR signal emerging as an addition to the prior glacio-isostatic VLM that has driven regional relative sea-level rise along this coast for millennia. However, this possibility is consistent with their assertion that an increase in cliff retreat rates is to be expected in future as a response to ongoing acceleration of GMSL. This observation points towards a key methodological assumption that has been adopted in this thesis (see Section 3.2.3), namely that a shoreline response to GMSLR will manifest itself as a distinct change in long-term shoreline behaviour, which may be a switch from a mostly-stable to a receding shoreline, or an acceleration of recession on shores that were previously receding for other reasons.

Some claims of observed sea-level rise signatures seem equivocal on methodological grounds. For example an historic study of shoreline change on French Mediterranean pocket beaches from 1896 to 1998 using old surveys and aerial photography found an average shoreline retreat of 12.1 ± 3.5 m and

attributed this in part to sea-level rise (Brunel & Sabatier 2007, 2009). However, the feature mapped as the shoreline was described only as "the instantaneous limit of run-up". If this is a wetting or flotsam line visible on aerial photography then it is arguably a poor indicator of shoreline position since these can vary by metres horizontally on hourly to monthly time scales due to differing tidal stages, wave heights and onshore winds driving wave set-up (Boak & Turner 2005). None of these conditions can be easily controlled for with historic surveys or aerial photography. Hence this data seems unconvincing as a record of shoreline changes related to recent 20th Century sea-level rise.

Le Cozannet et al. (2014) identified two key limitations on existing studies that need to be addressed to improve capacity to identify SLR signals in coastal behaviour, namely a general lack of high-quality historical data describing variability in shoreline behaviour over the last century, as well as limited local sea-level change histories in many areas that lack nearby tide gauge records. This thesis addresses these two requirements through extraction of high quality shoreline behaviour histories from high-frequency ortho-rectified air photo time series for studied sites, and through the use of sea-level history reconstructions (Church & White 2011; Hamlington et al. 2011) in addition to Tasmania's spatially- and temporally-limited tide gauge records.

Additionally, Le Cozannet et al. (2014) distinguished between the use of model-based and empirical approaches to detecting sea-level rise signals in coastal behaviour, and suggested that problems with the accuracy of available coastal behaviour models are such that empirical (observation-based) approaches are more likely to be fruitful. This thesis supports this recommendation in that it is not based on attempting to model expected shoreline changes and then looking for those, but rather on *first* looking for observational evidence of long-term coastal behaviour changes and *then* testing the hypothesis that these may be a response to sea-level rise.

2.5 *Interaction of sea-level rise with other coastal process drivers*

2.5.1 Overview

The purpose of this section is to inform the selection and analysis of study sites in respect of how sea-level rise may affect coastal processes and conditions at those sites, and conversely how geological, geomorphic, climatic and oceanographic processes may influence the effects of sea-level rise at the study sites. The topics addressed in this section are those deduced most likely to be important for the Tasmanian coast based on general principles of coastal geomorphology.

2.5.2 Shoreline substrate

Coastal landform substrate type (composition) is a key factor in shoreline response to sea-level rise. Substrate type determines the erodibility of coastal landforms and is also a key factor in the capacity of some shorelines to accrete or recover from erosion. This thesis focusses on two main types of readily erodible shoreline substrates, namely sandy and soft-rock shores. These are discussed below, including the notable variant of saltmarsh shores associated with sandy substrates. Some other soft erodible shoreline substrates, for example shingle and muddy shores, are not discussed here because they have not been included amongst the study site types examined by this project.

Sand

Erodible shores on the Tasmanian coast are dominated by beaches of unconsolidated sand which are generally expected to recede in response to sea-level rise (see Section 2.2 above). Unconsolidated sand shores are probably the best-studied coastal substrate because of their very wide distribution and are consequently the subject of a very extensive scientific literature. No attempt is made here to thoroughly review this literature, rather this section identifies several characteristics of sand as a coastal substrate that are of particular relevance to this thesis.

Sand refers to sediment dominantly comprised of uncemented mineral (including shell) fragments in the grainsize range of 0.0625 - 2.0 mm (Pettijohn, Potter & Siever 1972). These grains are small enough to be readily mobilised by breaking waves but are also large enough to rapidly settle out if waves are not breaking (Short 2006b, p. 27). This allows sandy coastal beaches and dunes to exhibit characteristic cycles of storm erosion followed by fair-weather accretion and recovery (Woodroffe 2003, p. 290). See Figure 4. Sand landforms may be rapidly eroded if exposed to strong storm wave action with sufficiently energetic backwash to transport the eroded sand offshore. However, the eroded sand may not necessarily travel far offshore or alongshore unless exposed to strong currents such as energetic littoral drift and may instead settle out in nearshore areas close to the erosion site. From there the eroded sand may be gradually returned to the beach by fair-weather swell waves that have sufficient breaking wave energy to carry sand up the beach, but insufficient backwash energy to draw most of it back offshore again.

Figure 4: Examples of swell-exposed sandy beaches illustrating the recovery process typical of such sites following erosion events. In both cases an old foredune storm erosion scarp (LHS) is in the process of being buried by accreting incipient foredune sands (RHS) returned to the beach by fair weather swells after an erosion event, then blown landwards from the upper beach by onshore winds. It is plausible to expect that any shoreline recession tendency attributable to GMSLR will continue to be overwhelmed and prevented by this process until such time that GMSL has risen enough that wave erosion events penetrate far enough landwards to erode the foredune too frequently for full dune recovery to occur in-between such events. Top photo: Green Point Beach W. Tasmania (2010), bottom photo; Perkins Beach NW. Tasmania (2010). Photos by Chris Sharples.

However, in the absence of fair-weather swells sandy shores may not always exhibit such "two-way" cycles of erosion and recovery. Sandy shores are widespread within Tasmanian tidal re-entrants including estuaries and coastal lagoons permanently connected to the sea. Swell waves typically only refract short distances into these environments before becoming too attenuated to move sand, and instead the dominant process capable of moving sand under fair-weather conditions is tidal currents (Nordstrom 1992). Shoreline erosion in re-entrants mostly occurs during windstorms, when short steep locally generated wind waves can readily erode the sandy shores. However, under fair weather conditions there is typically only very weak wind-wave action, and the sand eroded during storms is more likely to be redistributed within the re-entrant by tidal currents than returned to rebuild the eroded shore. Whereas sandy shore recovery may occur under some circumstances within swell-sheltered re-entrants, there is little evidence of cyclic cross-shore sediment exchange of the sort seen on swell-exposed beaches (Jackson et al. 2002). Sandy shores within swell-sheltered re-entrants are commonly characterised by episodic erosion without recovery, leading to "one-way" progressive shoreline recession (Figure 5), rather than to shoreline recovery as is more characteristic of swell-exposed beaches.

Saltmarsh on sand

Sandy shore recovery after erosion may occur under some circumstances in swell-sheltered tidal re-entrants. One such circumstance that is relevant to this thesis can happen on sandy saltmarsh shores. Saltmarsh plants occur almost exclusively in swell-sheltered but tidal saline coastal environments and may grow on any shoreline substrate from mud to hard bedrock.

Saltmarsh shores on a sandy substrate are widespread in Tasmania (Prahalad et al. 2019). These are characteristically dominated by a suite of saltmarsh plant species which tend to capture sand, silt and organic debris to form a soft grey-brown peaty-sand-silt soil over the sand substrate (Figure 6). These saltmarsh shores are erodible if exposed to sufficiently energetic wind-waves reaching higher than their normal levels on the shore profile (Figure 6 top). However, sandy saltmarsh shores differ from other sandy swell-sheltered shores in that they can also vegetatively recover from erosion to accrete and prograde seawards (Figure 6 bottom), if the frequency or magnitude of erosion events decreases for long enough periods (Prahalad et al. 2015). This can occur because under reduced erosion stress the saltmarsh plants will re-establish and spread seawards, trapping sand, silt, and organic debris from the water column as they do so to accrete and re-establish a higher shore profile extending further offshore.

Soft rock

In coastal geomorphology, the term 'soft-rock' is widely applied to coastal bedrock substrates whose lithologies are more cohesive than loose shingle, sand, or mud, but still friable and able to be easily broken and crumbled by hand. See Tasmanian examples at Figure 7. Multiple factors influence the rate of erosion of rocky shores, e.g., wave energy, rock structure (jointing, bedding, etc) and others. However, a major factor is rock hardness, with softer rock types generally tending to exhibit faster erosion than harder lithologies (Emery & Kuhn 1982; Sunamura 1992; Trenhaile 1987). In Tasmania, the most common coastal soft rock types comprise semi-lithified cohesive clayey mudstones, sandstones, and conglomerates of mainly Palaeogene (Tertiary) or younger age. These are mostly fluvial, colluvial and lacustrine sediments that were deposited in a series of extensional basins (grabens) that developed in and around Tasmania and Bass Strait during the late stages of the breakup of the Gondwana super-continent, as Antarctica separated from Australia (Forsyth, Quilty & Calver 2014). On the Tasmanian coast most soft-rock substrates underlying swell-exposed coasts are today eroded down and mantled by sands. Soft rock substrates are instead mainly exposed on the shores of swell-sheltered coastal re-entrants. Nonetheless soft rocks in equivalent extensional basins on the coast of Victoria (mainland Australia) still commonly outcrop on swell-exposed open coasts, for example soft limestones near Port Campbell.

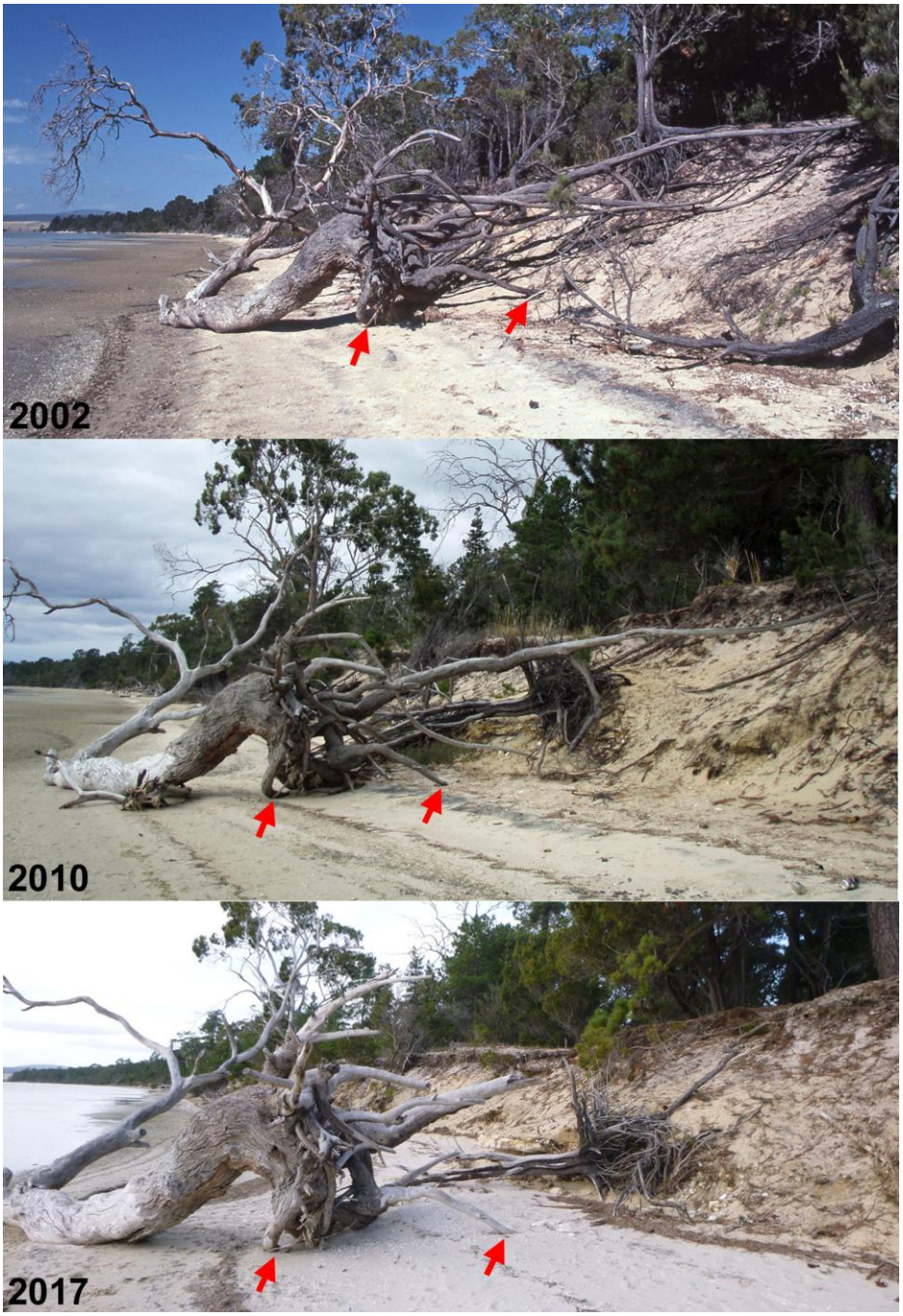

Figure 5: An example of slow but progressive recession of a swell-sheltered sandy shoreline at Five Mile Beach, Pittwater, in south-eastern Tasmania. Pittwater is a large estuarine lagoon with a permanently open tidal channel entrance, within which Five Mile Beach is the northern (swell-sheltered) side of the large Seven Mile Beach barrier spit. Studies by Oliver et al. (2017) infer that slow erosional recession of Five Mile Beach has been in progress for several millennia for reasons relating to landform evolution (but not necessarily to sea-level change). An air photo time series (Sharples et al. 2012) shows that a long stretch of Five Mile Beach receded an average of 7 metres (up to 12 metres in places) landwards during an unusually large erosion event or cluster of events between 1989 and 2002 (exact dates unknown). The above photo series taken at one Five Mile Beach location (147º 31' 37" E 42º 49' 42" S, WGS84) shows no subsequent shoreline recovery at all (e.g., by incipient dune accretion) from 2002 until at least 2017, with only some minor slumping of the large pre-2002 erosion scarp. Whilst no further large erosion events have occurred, there has however been a continuing slow and incremental retreat of this shoreline as indicated by comparison of fixed (arrowed) features in each photo, amounting to approximately 1.5 m retreat of the scarp toe between 2002 and 2017. This is mostly likely a continuation of the recession trend of the last few millennia, driven by occasional minor erosive onshore wind-wave events at high tide, but with no evidence yet available in this case of increased recession due to SLR. Photos by Werner Hennecke (2002) and Chris Sharples (2010, 2017).

Figure 6: Sandy saltmarsh shores in Boullanger Bay, north-west Tasmania (close to the West Duck Bay site studied during this thesis: see Section 5.4). These swell-sheltered shores comprise soft peaty-sand-silt soils trapped by saltmarsh vegetation growing over a sandy base (top photo). Prahalad et al. (2015) argued that when exposed to more frequent erosive wind-waves reaching higher on the shore profile over deepened water (e.g., because of rising sea-levels against a significantly wind-exposed shore) these shores may recede progressively as shown in the top photo. Conversely, saltmarsh may continue to grow and accrete peaty-sand soils on more wind-sheltered shores despite small amounts of sea-level rise. If the frequency or magnitude of erosive wind wave events decreases on an eroding saltmarsh shore (because of inter-annual or inter-decadal variability in local mean sea levels and/or wind climates) then saltmarsh shores can recover from erosion and return to an accreting mode as shown in the bottom photo, where recent *Sarcicornia* saltmarsh plant establishment is beginning to engulf an older erosion scarp. Photos by Chris Sharples (2010).

Two important characteristics of 'soft-rock' shores are that they are both more readily prone to erosion (e.g., by energetic wind waves) than hard lithologies (Emery & Kuhn 1982), but also have little if any capacity to naturally recover after erosion events like sandy shores may, so that each erosion event has a permanent effect and the shoreline persistently (if episodically) recedes. The eroded clay and silt fractions that form large proportions of soft-rock substrates are easily suspended and disperse widely in the water column so that they are permanently lost from the shore during erosion events. Coarser eroded materials such as pebbles and cobbles may form shingle berms immediately in front of the receded soft rock shoreline erosion scarp but cannot rebuild or reconstitute the original weakly cemented soft-rock shore profile so as to prograde the shoreline.

Figure 7: Actively receding soft rock shorelines in Palaeogene (Tertiary) age or younger cohesive clays and pebbly clays of lacustrine and fluvial origins (Forsyth 2002). The clays and coarse fractions released from these sediments by wave erosion cannot return to rebuild these shores, hence they only recede (with occasional slumping). Active recession of soft-rock shores therefore occurs under stable sea-levels but is expected to accelerate under rising sea-levels (Trenhaile 2011), which allow waves to reach higher and further to landwards on the shore profile over deepened water more frequently. Top photo: Barilla Bay, Pittwater, Tasmania, 2011 (swell-sheltered estuarine lagoon); bottom photo: Rokeby Beach, Ralphs Bay, Tasmania, 2010 (mostly swell-sheltered but exposed to refracted and attenuated swell under storm conditions). The undermined tree at Rokeby Beach has subsequently collapsed as shoreline recession has continued (see Appendix A1.5.2). Photos by Chris Sharples.

Soft rock shores are therefore a "one-way" shoreline substrate type which can erode but not recover, albeit occasional scarp slumps may give a temporary impression of shoreline progradation on air photos (e.g., Woodroffe 2003, p. 183-187). These shores are inferred to have typically been eroding and receding slowly and sporadically over much of the late Holocene, in response to occasional storm events, but are expected to recede more rapidly as sea levels rise (Pye & Blott 2015). Trenhaile (2011) attributes faster soft rock cliff recession with rising sea levels to the increase in water depth resulting in reduced wave attenuation. This allows erosive breaking waves to scarp the shore profile further to landwards than previously. Trenhaile (2011) has modelled soft rock cliff erosion under varying assumptions of sea-level rise rates and storm frequencies. He found that whereas storm frequency had only a minor effect on cliff recession rates, rising sea levels trigger significantly faster rates of shoreline recession. Trenhaile's modelling suggested that soft rock cliffs or scarps generally are

likely to respond to GMSLR by receding up to 1.5 to 2 times further in the next century than they have done in the last century.

2.5.3 Sediment budget

The concept of the "sediment budget" refers to the amount of mobile unconsolidated sediment moving into, through and out of coastal systems such as sediment cells or coastal compartments (Komar 1996; Rosati 2005). Thom et al. (2018) considered that sediment budget is likely to be the most important determinant of sensitivity to sea-level rise for open coast (swell-exposed) sandy beaches. The term "sediment budget" is mostly synonymous with "sand budget", however other grades of sediment are also relevant to some shoreline responses to sea-level rise, as noted below. Key elements of the sediment budget concept are outlined in following paragraphs, based mainly on the summary provided by Thom et al. (2018).

Following the pioneering work of Davies (1974), coasts may be considered as a hierarchy of compartments at differing scales from large regions down to individual beach cells (Thom et al. 2018). Such compartments provide a useful hierarchical framework in which to describe and analyse coastal sediment transport, gains, and losses. Sandy coast compartments in particular are highly dynamic environments which may be subject to either progressive or cyclic net gains (positive) or losses (negative) of sediment over time.

Compartments may gain sediment by onshore transport from continental shelf sources (Figure 8), from local biological sources (i.e., shell attrition), alongshore transport between "leaky" coastal compartments (including aeolian headland bypassing), or sometimes from other sources such as coastal rock erosion and river sediment input. Much of the coastal sands in northern, western and south-eastern Tasmania were probably initially supplied to the continental shelf as glacial outwash sands washed down rivers from Tasmania's glaciated mountain regions during multiple Pleistocene glacial low sea stands (Colhoun, Hannan & Kiernan 1996). In contrast, present-day (interglacial) Tasmanian rivers carry very little sand-grade sediment except where catchments are artificially disturbed (Nanson, Barbetti & Taylor 1995). However, national-scale shelf sediment mobility modelling by Harris et al. (2000) (see also Harris & Heap 2014) suggests that at the present time many open coast Tasmanian beaches are likely to be actively gaining the shelf-deposited sands as they are driven shoreward from the inner continental shelf by swell-generated bottom currents (Figure 8). This modelling is consistent with the continental-scale analysis of Short (2010) who identified strong Southern Ocean swells and winds as driving large volumes of shelf sediment onshore along much of the southern Australian continental margin including western Tasmania.

Conversely, beach sand may be lost offshore or by alongshore littoral current transport, by landwards aeolian transport in mobile transgressive dunes and deflation gullies, or by tidal current transport into accommodation space within estuaries, lagoons, and flood tide deltas. Fine clay- or silt-grade sediment derived from erosion of soft-rock or muddy shorelines may be suspended in the water column and disperse far away from the eroded shore via tidal or other currents. These and other means of permanent sediment loss or sequestration are referred to as sediment sinks.

New or re-activated sinks may be created in estuaries and tidal lagoons when sea-level rise raises the effective wave base and provides increased accommodation space (i.e., water depth) in which eroded and transported sediment can settle out and be permanently sequestered. For tidal lagoons this process is described by the *Flood-Tide Delta Aggradation Model* (Hennecke 2000; Hennecke & Cowell 2000). In a similar fashion, on swell-exposed sandy coasts the permanent movement of eroded beach and dune sand into the lower (subtidal) beach face zone as described by the Bruun Rule (Section 2.2, Figure 1) is an example of sand being lost into a sink that is created when sea-level rise creates new accommodation space (i.e., water depth) in the offshore or subtidal area. This particular type of sand sink is referred to in parts of this thesis as the "Bruun sink" because of its role in the process of shoreline recession due to sea-level rise as described by the Bruun Rule.

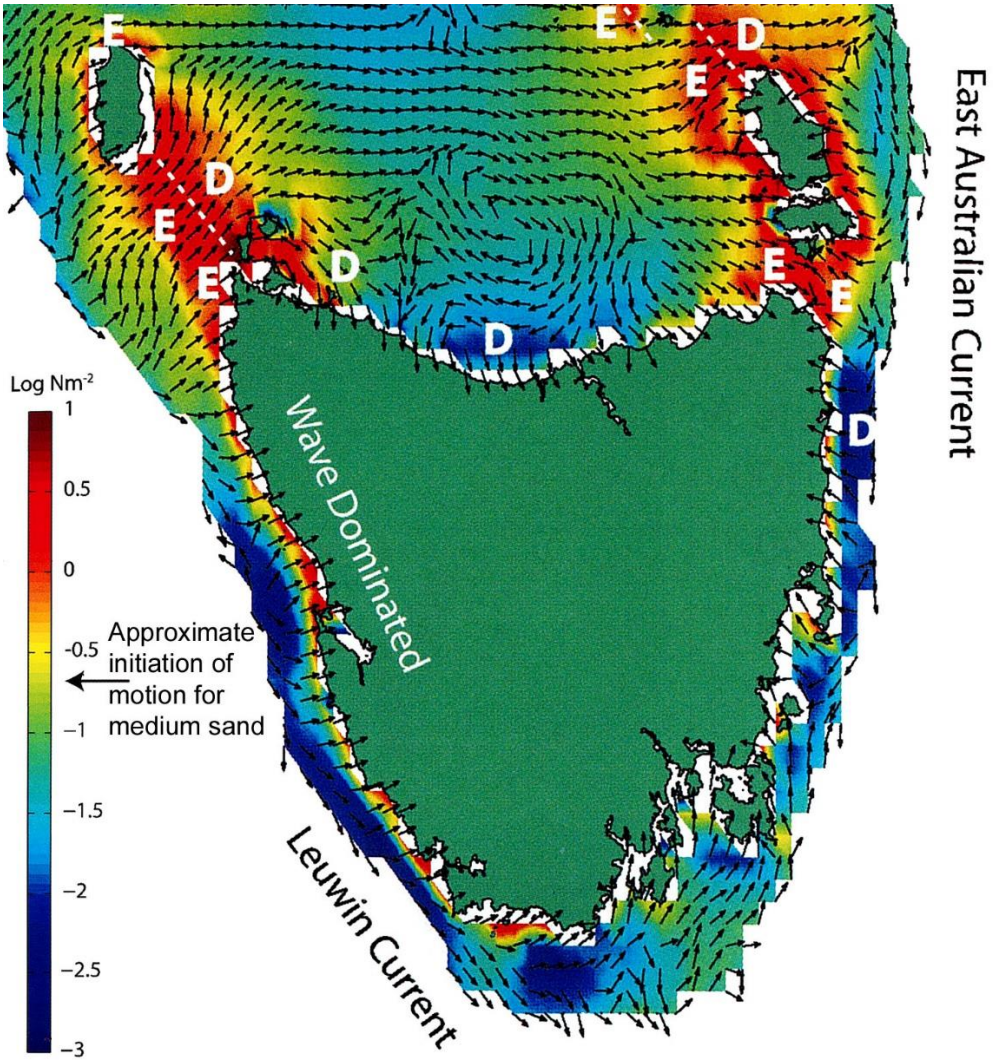

Figure 8: Modelled shelf sediment mobility for the Tasmanian coast, from the Geoscience Australia GEOMACs model (reproduced from Harris and Heap (2014), p. 538) based on wave, tidal and ocean currents. Colours depict mean magnitude of bed shear stress and arrows show mean current direction. This model indicates coastal areas that could be actively receiving sand from an offshore source *assuming* that unconsolidated sand is actually available in those areas. Notable areas of erosion ('E') and deposition ('D') are inferred based on currents increasing or decreasing along a transport pathway.

Some compartments (e.g. deeply embayed swash-aligned beaches) may have a dynamic but balanced cross-shore sand transport system which episodically moves sand offshore (during storms) and onshore (under normal fair-weather swells) within the compartment but neither gains nor loses sediment over time due to a lack of sediment transport processes capable of bypassing rocky headlands or permanently transporting significant quantities landwards or seawards (Woodroffe 2003, p. 290).

However, the sediment budget of many compartments is highly variable and can switch from positive to negative, either episodically or in response to a long-term change in conditions. An example of an episodic change in sand-budget on littoral drift-dominated coasts is the case of sand 'slugs' accumulating updrift of open coast headlands until they periodically get too large and are flushed around the headlands, This causes down-drift beaches to periodically switch from deficit to accretion and back again (Goodwin, Freeman & Blackmore 2013). Sea-level rise is expected to result in permanent switches to a more negative sediment budget as higher sea-levels result in more frequent erosion events at higher levels on the shore profile and/or make greater accommodation space

available for sand to be lost into sinks such as estuaries (Thom et al. 2018). However, there are few if any examples of such sea level rise-related switches described in the coastal literature.

It can also be expected that a shore with a stable or gaining sediment budget, or one which switches to gaining as increased erosion in one location increases the sand supply drifting alongshore to another, might resist receding in response to sea-level rise for longer than other shores, as suggested by Kinsela, Daley and Cowell (2016). This might be the case if the sand supply remains sufficient for full beach recovery despite the increasingly frequent erosion events at higher levels on the shoreface that result from a rising mean sea-level. Again however, there are few if any examples of such responses to sea-level rise in the literature.

Whereas sandy beach sediment budgets may be quite variable and may switch from losing to gaining or vice versa, another large category of soft erodible shores can only lose sediment and thus always has a negative sediment budget (Thom et al. 2018). These are weakly lithified shores which commonly have high silt and clay content, such as the soft-rock cohesive-clay shores found in many tidal embayments in Tasmania (see Section 2.5.2 above). Such shores are readily eroded by wave attack. Wave erosion events must become more frequent as sea-level rises and storms of any given magnitude and frequency reach further to landwards over deeper water and thus impact higher on the shore profile than previously. Much of the silt and clay liberated by such events is readily lost from the compartment, and there is not in any case a mechanism for such eroded sediment to rebuild the shore profile.

Sea-level rise is expected to cause some sandy sediment budgets to switch from stable to losing, however where a sediment budget is already negative it may be inferred that sea-level rise will increase the rate of sediment loss. Thus, it is a working hypothesis for this thesis that cohesive clay shores in Tasmania, which are normally receding at some (typically slow) rate and so have a persistently negative sediment budget, are likely to be an important category of shores showing early responses to sea level rise as their sediment budget simply becomes increasingly negative (see Section 2.5.2).

In principle, sediment budgets can be analysed and measured using carefully deployed tracer particles and/or sediment traps. However, such methods are typically expensive and time-consuming. In practice sediment budget analyses are generally qualitative and based on the interpretation of geomorphic indicators of sediment movement, such as deflected river mouths across sandy beaches, flood- and ebb-tide deltas, and subaqueous dune and ripple morphologies. These methods may be employed alongside modelling approaches to derive quantitative estimates of sand movements and budgets (see Shand & Carley 2011 for an example at Roches Beach, south-east Tasmania.).

2.5.4 Vertical land movement

Local sea-level change relative to the shoreline is in many places at least partly caused by vertical land movement (VLM), whose dominant drivers are glacio-isostatic adjustment (GIA), tectonic and magmatic processes, underground mining, compaction, and fluid extraction. Where the VLM results in land subsidence and thus relative local sea-level rise, it is commonly associated with shoreline recession. Well studied examples of this include south-east England (Pye & Blott 2006), the central-east USA coast (Zhang, Douglas & Leatherman 2004) and Hawaii (Romine et al. 2013). Sites where VLM is a significant cause of relative sea-level rise are assumed to also have a component of contemporary climate change-driven SLR, however in such cases it may be difficult to separate the effects of longer-term ongoing relative sea-level rise due to VLM from those of contemporary climate change-driven SLR. Hence an understanding of VLM is important in any attempts to discriminate between the effects of contemporary climate change-driven sea-level rise and other non-climate related processes on shoreline behaviour.

Australia mostly does not exhibit VLM on the scales seen in places such as eastern USA where long-term subsidence rates of up to 4.0 mm yr^{-1} observed on the North Carolina coast are associated with significant shoreline recession (Zhang, Douglas & Leatherman 2004). Nonetheless, subsiding soft-rock shorelines in parts of the south-east UK with estimated relative mean sea-level rise rates as low as -0.6 to -0.8 mm yr^{-1} over the last four millennia, have receded hundreds of metres on centennial time-scales (Pye & Blott 2006; Shennan & Horton 2002). Although it is unclear what portion of this recession would have occurred even in the absence of VLM[5], it is notable that the rate of RMSLR in this instance is comparable to or less than rates measured on some parts of the Australian coast.

Some limited stretches of the Australian coast are thought to exhibit sufficient VLM as to be problematic for identifying a climate change-driven sea-level rise signal in shoreline behaviour. For example, since the 1970s the long-running Fremantle (Western Australia) tide gauge record has been affected by land subsidence in the range of approximately -2 to -4 mm yr^{-1} (depending on dates and technique) associated with groundwater extraction (Featherstone et al. 2015). Watson (2011) also notes the Newcastle (NSW) tide gauge is sufficiently affected by localised land subsidence as to make its data problematical for sea-level variability measurements. Areas of far north-western Western Australia are also thought to be responding post-seismically in the vertical component to large earthquake events occurring in the far field throughout Sumatra after 2004 (Riddell et al.[6], submitted to Geophysical Journal international).

The geodetic evidence regarding VLM across the Australian continent over approximately the past two decades is mixed. In Tasmania, there are two long-running Global Navigation Satellite System (GNSS) sites, located in Hobart (HOB2) and Burnie (BUR2) respectively. Based on these, work by Burgette et al. (2013) and White et al. (2014) reported vertical land movement rates of 0.0 ± 0.5 mm yr^{-1} and -0.2 ± 0.8mm yr^{-1} for Hobart and Burnie respectively. However, Santamaria-Gomez et al. (2012) and King et al. (2012) estimated VLM between -0.5 and -1.0 mm yr^{-1} at Hobart suggesting marginal subsidence but still insignificant at the two-sigma level.

Most recently, Riddell, King and Watson (2020) investigated VLM across Australia and found disagreement between some of the GNSS-derived estimates of VLM and those from various geophysical models. Modelling of glacial isostatic adjustment (GIA) suggests low subsidence of Tasmania of approximately -0.2 mm yr^{-1} (Argus et al. 2014; Peltier, Argus & Drummond 2015); see also Riddell, King and Watson (2020). Modelling the crustal response to recent (post-1900) climate-induced ice mass loss also suggests a very small subsidence signal for Tasmania of the order of -0.1 mm yr^{-1} (Riva et al. 2017). This disparity between recent GNSS derived velocity estimates and those from various geophysical models remains an active area of investigation. It is possible that increased subsidence has occurred in Tasmania since 2004 as a post-seismic response to the Macquarie Ridge earthquake (Mw 8.1), occurring some ~1500 km to the south-east in December 2004 (Riddell et al.[6], submitted to Geophysical Journal International). However, for the purpose of this thesis – which focusses on the period from 1945 to present - there is no evidence to suggest that VLM is a significant signal in Tasmanian relative sea levels over that period.

[5] Soft-rock shorelines such as those on the south-east UK coast would normally recede at some detectable rate even in the absence of RMSLR (see Section 2.5.2 above), however it is reasonable to assume that RMSLR would cause some additional recession. This is because erosive storm waves of any given height must be approaching the shore over deepened water and thus losing less energy than previously (Trenhaile 2011). The greater wave energy thereby reaching the shoreline scarp is inferred to increase in the rate of shoreline/cliff-line retreat.

[6] Riddell, A.R., King, M.A. and Watson, C.S., 2020, Ongoing post-seismic vertical deformation of the Australian continent from far-field earthquakes. Submitted to Geophysical Journal International.

2.5.5 Swell wave climate variability

Tasmania's swell-wave climate is dominated by persistent south-westerly swells generated in the Southern Ocean by mid-latitude cyclonic weather systems associated with the Southern Annular Mode (Hemer, Simmonds & Keay 2008; Marshall 2003). These swells produce one of the world's highest-energy wave climates on Tasmania's west coast, but lose energy and height as they refract around the south-east and up the east coast of Tasmania (Short 2006b); see Figure 9. The east coast also receives intermittent swells generated by east coast cyclones in the Tasman Sea (Short 2006b). Hence whereas the west and south-west Tasmanian coasts receive relatively high swells (annual significant wave heights Hs ~3 m) with limited annual directional variability of mostly less than 20° (Durrant et al. 2013), the south-east and east coasts receive more variable but generally lower wave heights (typically annual Hs ~1.3m) over a much wider directional range between south and east (Durrant et al. 2013; Short 2006b). Moreover, whereas the south-westerly swells reach the roughly linear west coast mostly unimpeded by islands or complex coastal planforms, swells reaching south-east Tasmania are in many places refracted and attenuated by the complex headlands and deep embayments in the Storm Bay region (see Figure 17 in Section 4.2), before they reach the embayed beaches of that region (Short 2006b). Further information on the south-westerly swell wave climate is provided with the analysis of the west-coast Ocean Beach study site in Section 5.2 and appendix A1.3.8.

This section reviews three key elements of wave climate variability that are inferred to influence soft shoreline responses to sea-level rise, and which have informed the analyses documented in Chapters 5 and 6. These are: (1) the significantly differing morpho-dynamic process environments found in swell-exposed and swell-sheltered tidal coastal environments; (2) swell wave height variability; and (3) swell wave directional variability.

(1) Swell-exposed and swell-sheltered shores

Swell-sheltered tidal shores in coastal re-entrants such as estuaries and tidal lagoons have generally received less attention in the coastal science literature than swell-exposed open coasts, however reviews of coastal geomorphic processes in these environments are provided by Nordstrom (1992) and Jackson et al. (2002). These shores are just as exposed to sea-level variability as the open coast, are frequently composed of highly erodible substrates including sand, mud, and soft-rock, and are also commonly the site of extensive artificial coastal infrastructure potentially at risk from coastal recession. This section identifies some key differences in shoreline behaviour that are relevant to sea-level rise responses at swell-exposed and swell-sheltered erodible shores.

As noted in Section 2.5.2 above, on swell-exposed sandy coasts beach changes due to longshore sand drift, beach rotation processes and cross-shore sand transfers including storm erosion and recovery ('cut-and-fill') cycles can be of greater magnitude than expected shoreline responses to sea-level rise in the near future. The persistence of swell waves during the fair weather periods between storm events is a key factor driving these processes, any of which may mask or prevent the early emergence of a recessional coastal response to sea-level rise (Stive, Cowell & Nicholls 2009).

In contrast, there are little or no beach rotation or cross-shore (cut and fill) sand movement cycles on swell-sheltered tidal sandy shores such as those in estuaries or tidal lagoons (Jackson et al. 2002). River discharges (if present and significant), tidal currents and locally generated wind waves are the main sand transport processes in these environments. Short steep locally-generated wind-waves cause shoreline erosion in swell-sheltered waterways during wind-storms, but there is negligible wave action capable of moving sand during calm weather periods, when eroded sand is more likely to be moved into flood tide deltas or tidal flats by tidal currents than returned to the eroded shore (Nordstrom 1992; Thom et al. 2018). This means that erodible swell-sheltered shores may be easily and frequently eroded under certain circumstances, such as when sea-level rise is enabling increased

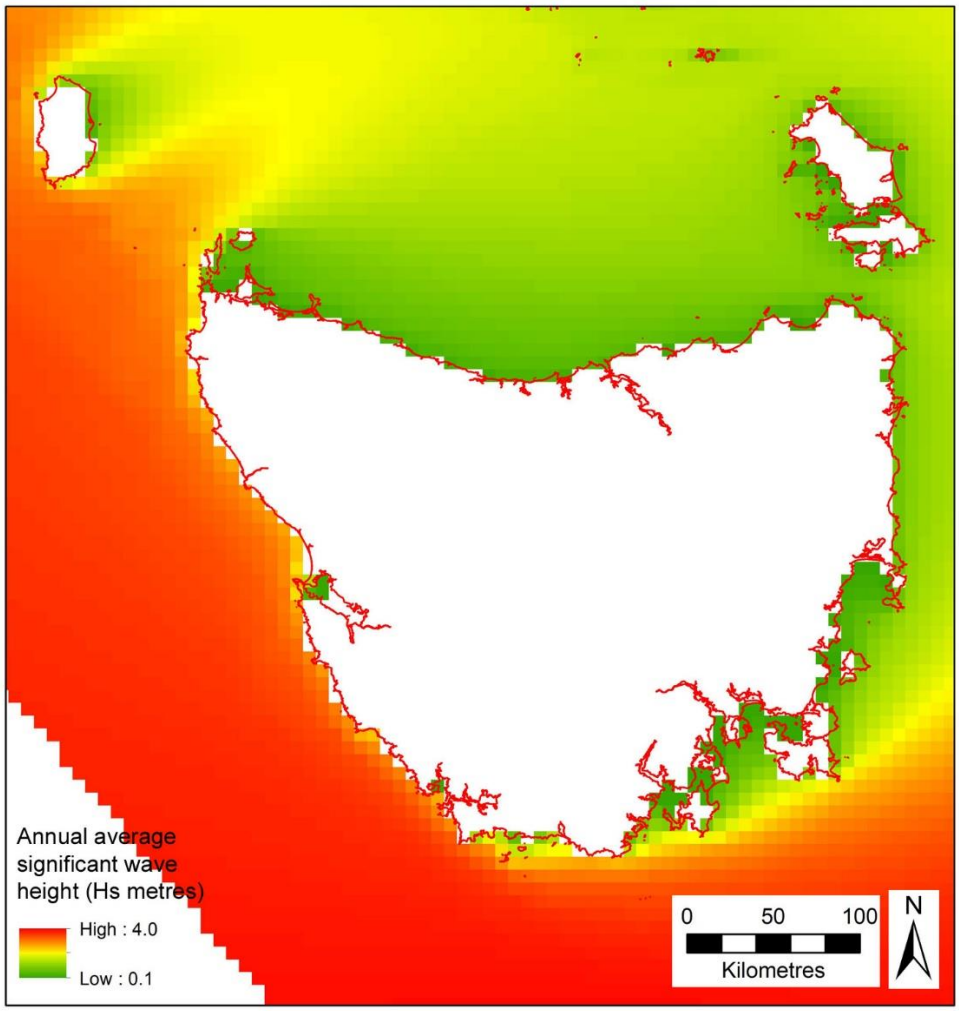

Figure 9: Annual average significant swell wave heights (Hs) for Tasmania, based on the 1979-2010 CAWCR hindcast (Durrant et al. 2013). Significant wave height is a standard measure of average swell wave climate.

landwards penetration of stormy locally generated wind-waves over deepened water. However, shoreline recovery will commonly be slow or absent due to a lack of onshore sand transport processes under fair weather conditions (see also discussion in Section 2.5.2, including Figure 5).

These conditions effectively mean that several significant sources of coastal process (sediment movement) 'noise' that may mask or prevent shoreline responses to sea-level rise on swell-exposed coasts are mostly absent from swell-sheltered tidal re-entrants. Under these conditions in which swell-sheltered shores progressively (if intermittently) lose sediment without recovery, the writer hypothesises that relatively early recessional shoreline responses to sea-level rise may be observable, potentially responding to sea-level rise with minimal lag times. In order to test this hypothesis, a number of swell-sheltered shoreline study sites were selected for this thesis.

(2) Swell wave height variability

From first principles, long-term changes in mean swell wave heights (e.g., Hs) are unlikely to affect the susceptibility of sandy beaches to sea-level rise, since each beach adopts a morpho-dynamic form in response to that mean wave height, as well as to tidal range and sand grainsize (Short 2006a). Thus, if mean wave heights change significantly, then (in the absence of other changes) the beach will simply transition to a new morpho-dynamic form in equilibrium with the new mean wave energy (Woodroffe 2003, pp. 284-287). For the same reason, from the perspective of mean wave height (and

thus energy) alone, there is no obvious reason to expect that a relatively higher energy swell-exposed coast (such as west coast Tasmania) would be more likely to show an earlier recessional response to sea-level rise than moderate or low-energy swell-exposed coasts such as those in eastern and south-east Tasmania.

Of more likely significance from the perspective of shoreline erosion and recessional responses to sea-level rise is the frequency and magnitude of extreme wave events, i.e., storm events. Most shoreline erosion is caused by extreme wave events, which here refers to that percentage of waves reaching an erodible shore that are large enough (high enough) to run up above the normal swash zone and High-Water Mark (HWM), so as to impact the upper beach and dune face with enough energy to erode and draw sand back down the beach in a reflected turbulent backwash. If the frequency of such erosional storm events is low enough, then the beach recovers between storms and the long-term shoreline position is stable. However, if either the actual frequency and magnitude of storms increases, or if rising sea levels allow storm waves of any given size to penetrate further landwards over deeper waters than previously and so cause erosion more frequently than before, then eventually storm erosion events may become too frequent for full shoreline recovery to occur. In this case the shoreline will begin receding in response to either one or both of these causes of increasing erosion event frequency (Thom et al. 2018). Either of these causes of increasingly frequent erosion may be driven by changing climates.

The only multi-decadal swell wave height record for any Tasmanian coast is that recorded by the Cape Sorell wave-rider buoy located over 10 km off the central west coast of Tasmania (see Figure 18 in Section 5.2). Since 1985 this buoy has recorded the stormiest wave climate (highest frequency and magnitude of extreme waves) for any Australian coast (Hemer 2010; Hemer, Simmonds & Keay 2008). However, as at 2010 the buoy had not recorded any significant long-term changes in storm frequencies and magnitudes at Cape Sorell (Hemer 2010).

One working hypothesis considered during this thesis was that coasts with higher storm frequencies and/or magnitudes might be more prone to early recessional responses to sea-level rise than less storm-dominated coasts. Even without considering climate change-driven increases in storm frequencies and magnitudes, on stormier coasts it would take less sea-level rise to increase the (already high) frequency of erosion events to a point where there is no longer time between erosion events for complete beach recovery to occur, than it would on less frequently stormy coasts. Although it has proved beyond the scope of this project to properly test this hypothesis it remains a possible contributing condition in case studies such as Ocean Beach (section 5.2).

(3) Swell wave directional variability

Swell-wave directional variability is one of the most important factors controlling sand transport along a coastline, because the primary driver of alongshore sand transport – littoral currents – are determined by nearshore wave directions (Komar 1996). Beach studies on the New South Wales (Australia) coast have shown that episodic large-scale redistribution of sand within embayments on that coast is related dominantly to differential cross-shore sand transport that may episodically change along beaches with exposure to waves and storms from differing directions (Harley et al. 2011). Inter-annual changes in swell wave direction related to the El Nino Southern Oscillation (ENSO) are a major cause of reversals of littoral current directions along the beaches, resulting in the phenomenon of 'beach rotation' as large quantities of sand episodically drift up then down the shore (Goodwin 2005; Ranasinghe et al. 2004; Short, Trembanis & Turner 2000). On the NSW-Queensland coasts swell direction variability may exceed 100° (Mortlock & Goodwin 2015a). These processes can cause beach accretion on scales that prevent the erosional effects expected from sea-level rise, but can also episodically deplete sandy beaches making them susceptible to erosion on scales larger than yet expected from sea-level rise (Mortlock et al. 2017). From the perspective of coastal responses to sea-

level rise, such 'noise' processes may prevent any sea-level rise signal in coastal landform behaviour from being detectable for some considerable time to come.

In contrast, some coasts are subject to significantly less swell wave directional variability and consequently are less susceptible to beach rotation or reversing littoral sand transport. This is the case for some southern Australian coasts including western and south-coast Tasmania, which are exposed to south-westerly swells whose annual directional variability is mostly less than 20° (Durrant et al. 2013). Less wave direction variability may increase the potential for a sea-level rise signal in shoreline behaviour to emerge by minimising one source of process noise that may overwhelm such signals, namely episodic or cyclic variability in alongshore sand transport.

However, beaches in eastern Tasmania receive both refracted south-westerly swells and also episodic easterly swells generated in the Tasman Sea, resulting in a large (but intermittent) overall swell wave direction variability from south to east (Short 2006b). Under these conditions it is possible that some open coast beaches on the east Tasmania coast are more susceptible to reversals of littoral drift than is likely to occur in western Tasmania. The effects of such changes in swell direction might overwhelm and prevent any beach change in response to sea-level rise. However, limited sampling of east coast Tasmanian beaches means that data collected during this project did not enable any such reversals at Tasmanian beaches to be identified.

Global climate change itself is also expected to result in longer-term changes in wave directions and directional variability on some coasts, and indeed this is already being observed. For example, a trend towards the positive phase of the SAM has been observed since the mid-1960s in the Southern Ocean (Hemer 2010; Hemer et al. 2008) and is resulting in an anti-clockwise rotation of wave directions along the southern Australian margin associated with a southwards movement and intensification of the Southern Ocean storm belt (Hemer, Church & Hunter 2010). In the Tasman and Coral Seas (east Australian margin), existing and projected polewards expansion of tropical systems is changing ENSO events and storm wave patterns to increase winter storm frequencies and intensities on the central NSW shelf with an anti-clockwise rotation of wave directions towards the east and southeast, generally reducing the efficiency of northwards longshore sand transport and headland bypassing while increasing onshore sand transport (Goodwin, Mortlock & Browning 2016; Mortlock & Goodwin 2015a, 2015b).

Hemer (2009) and Hemer et al. (2008) have pointed out that long-term swell wave directional change may be a significant factor in either increasing or decreasing coastal susceptibility to recession in response to sea-level rise, because of its effect on patterns of littoral sand transport. Leach et al. (2020) have provided a case study of potential coastal responses to changing swell directions and magnitudes at Port Fairy (Victoria). Depending on local coastal orientations and the degree of wave directional change, longshore sand transport fluxes and directions may change sufficiently to cause a switch to new patterns of accretion or depletion of sand in certain coastal areas. This could result in respectively a reduction or an increase in the susceptibility of certain coastal segments to the emergence of sea-level rise signals (e.g., shoreline recession) in shoreline behaviour.

2.5.6 Wind climate

Coastal winds drive locally generated wind-waves and may additionally contribute to near-shore water-level setup (Nordstrom 1992, p.50,53). On swell-exposed coasts these wind-driven 'seas' may both contribute to and modify the effects of swell waves in causing shoreline erosion and in driving littoral drift currents that transport sand alongshore (Woodroffe 2003, sect. 3.3). Within swell-sheltered coastal re-entrants, locally generated wind waves are the main agent of shoreline erosion (Nordstrom 1992, p. 50). Onshore to alongshore-directed winds may also cause landwards aeolian transport of sand from beaches and dunes via mobile transgressive dunes (Hesp 2002).

However, long-term changes to mean and extreme wind speeds and directions are also expected on at least some Tasmanian coasts in response to climate change (Grose et al. 2010). Where these occur, the resulting changes to shoreline erosion rates and magnitudes may result in shoreline position changes that are additional to or modify those driven by sea-level rise. Under such circumstances it may be difficult to distinguish between the contributions of sea-level rise and wind climate changes to long term shoreline behaviour changes.

Analyses of historical trends in measured wind speed records in the Australian region to date have generally been inconclusive (McVicar et al. 2008; Troccoli et al. 2012; Walsh et al. 2016). A national study (Troccoli et al. 2012) identified instrument variability as a major influence on apparent wind speed trends recorded, with higher (10 m) anemometers showed a mostly positive trend in wind speeds across Australia for the 1975 –2006 period, whereas lower (2 m) instruments showed a mainly negative trend. Several factors including sheltering, local topography and data continuity affect data quality, with sudden steps in data records being common and indicative of instrumentation changes rather than real wind changes (Troccoli et al. 2012).

Tasmania is dominated by a generally westerly air flow (Grose et al. 2010) related to the SAM (Marshall 2003). Winds reaching the west coast of Tasmania are the strongest and most persistent prevailing winds of any Australian coast (Grose et al. 2010), and vary between north-westerly and south-westerly as mid-latitude cyclones pass through the Southern Ocean (Short 2006b). As a result, the west coast beaches including Ocean Beach are exposed to the greatest frequency and magnitude of locally produced westerly wind-driven seas and storms in Tasmania (Davies 1973). Australian Bureau of Meteorology wind data from Cape Sorell (mid-west coast) analysed for this project recorded annual average onshore (westerly) synoptic wind speeds in the range 7.0 to 8.0 metres/second over the period 1992 – 2015.

The westerly winds are steered and rotated by topographic effects as they cross Tasmania's mountainous terrain and are steered through deep valleys (Short 2006b). In summer the coastal winds are also influenced by onshore sea breezes (Short 2006b). The result is complex directional variability across and around Tasmania but with an approximately westerly airflow mostly dominant.

Evidence from aeolian sediments show that the westerly wind flows associated with the Southern Ocean and SAM have varied in intensity on centennial and millennial time scales over at least the last 20,000 years, and that present-day westerly winds are as strong now as at any time in the last glacial climatic cycle (Fletcher et al. 2018; Shulmeister et al. 2004). Some regional studies of the SAM have indicated increased wind speeds over the Southern Ocean by about 20% since circa 1990 (Gillett, Kell & Jones 2006; Hemer, Church & Hunter 2010; Hurrell & Van Loon 1994; Thompson & Solomon 2002), with a southerly shift and strengthening associated with the positive SAM trend that is also affecting Southern Ocean wave climate (Fletcher et al. 2018; Marshall 2003). Robust global multi-platform satellite data since 1985 to 2018 has confirmed significant increases in both mean and extreme wind speeds over the Southern Ocean (Young & Ribal 2019).

Many of Tasmania's longest-term Bureau of Meteorology (BoM) wind records are compromised by the data problems identified by Troccoli et al. (2012), including large data gaps, sporadic changes in recording protocols and step-changes indictive of instrument changes or moves. Despite such flaws, a study by Kirkpatrick et al. (2017) interpreted Bureau of Meteorology wind records for Maatsuyker Island (on the south-western Tasmanian coast) as indicating an increase in western Tasmanian coastal winter wind speeds over the period 1970 – 2015. That study correlated this with variability in the SAM, reflected in a recent strengthening of the high-pressure zone to the north of Tasmania in winter and a decrease in pressures to the south. Similarly, Kole (2017) used BoM records to identify a zone of recently increasing wind speeds across Tasmania.

The wind record from Cape Grim (on the northern west coast of Tasmania) is largely free of the data management problems cited by Troccoli et al. (2012) because it has been carefully sited and

rigorously managed as part of the global Baseline Air Pollution Stations network by the World Meteorological Organisation with Australia's Bureau of Meteorology (BoM) and Commonwealth Scientific and Industrial Research Organisation (CSIRO). Analysis of the Cape Grim synoptic wind speed data during this thesis (see appendix A1.3.8) unequivocally demonstrates a multi-decadal trend of progressive increase in westerly wind speeds on the northern west coast of Tasmania since 1988 (R^2=0.6201), with interannual variability in the trend weakly correlated with the inverse of the Antarctic Oscillation (AAO) measure of SAM (R^2=0.26 after removal of first-order linear trends).

The observed strengthening of westerly winds over Tasmania, and particularly on the west coast, has informed hypotheses generated during this project to explain shoreline behaviour changes at least partly at some coastal study sites examined during this research (see chapters 5 and 6).

2.5.7 Other oceanographic processes

Tidal range

Tidal range is an important oceanographic variable which is one of the primary determinants of beach morpho-dynamic type (Short 2006a). Tidal range is likely to influence coastal responses to sea-level rise in at least two ways, namely:

1. Storm wave energies are distributed over a larger vertical range on shore profiles at sites with larger tidal ranges, but are concentrated on narrower coastal profile zones where tidal range is less (Nordstrom 1992, p. 50). Hence shoreline recession in response to sea-level rise is likely to be slower at sites with larger tidal ranges (disregarding other factors).
2. Conversely, tidal currents (which are the dominant transport mechanism for eroded sediments in swell-sheltered tidal re-entrants) are stronger (higher velocity) where tidal ranges are larger (Woodroffe 2003, p. 125). This may have consequences for rates of sediment loss from eroding and receding shores.

Spring tide ranges on the Tasmanian coast are mostly micro-tidal (<2 m), and are less than 1.5 m on the east, south-east, south and west coasts (Short 2006b, p.19). All but one of the study areas analysed for this thesis (West Duck Bay) are located on these micro-tidal coasts. Because of this small tidal range at most study sites, significant differences in coastal response to sea-level rise related to varying tidal range were not expected to be readily detectable in the data and have not been tested for. Such analysis might be fruitful if applied to larger datasets covering greater tidal range variability.

Meso-tidal ranges of around 3.0 m and greater occur on Tasmania's north (Bass Strait) coast. Meso-tidal ranges above 2.0 m have been measured in swell-sheltered coastal re-entrants close to the West Duck Bay study sites (Ch. 5.4) by Donaldson, Sharples and Anders (2012). This large (for Tasmania) tidal range is inferred to drive the strong tidal currents which are the main agent of eroded sediment transport at this site (see Ch. 5.4).

Inter-annual regional sea-level variability

In addition to relative sea-level variability induced by vertical land movement and inter-decadal global climatic changes, a range of tidal, meteorological, and oceanographic processes may also change local sea levels on daily, monthly, seasonal, inter-annual and decadal time scales. Such processes range from low pressure weather events causing barometric sea-level change (the "Inverse Barometer Effect") on hourly to daily time scales, through astronomical tidal cycles on monthly to decadal time scales, to ocean currents and larger – scale climate-mode related process such as the El Nino Southern Oscillation (ENSO). Any of these may contribute to local shoreline changes such as shoreline erosion if they cause locally elevated water levels coincident with storm events.

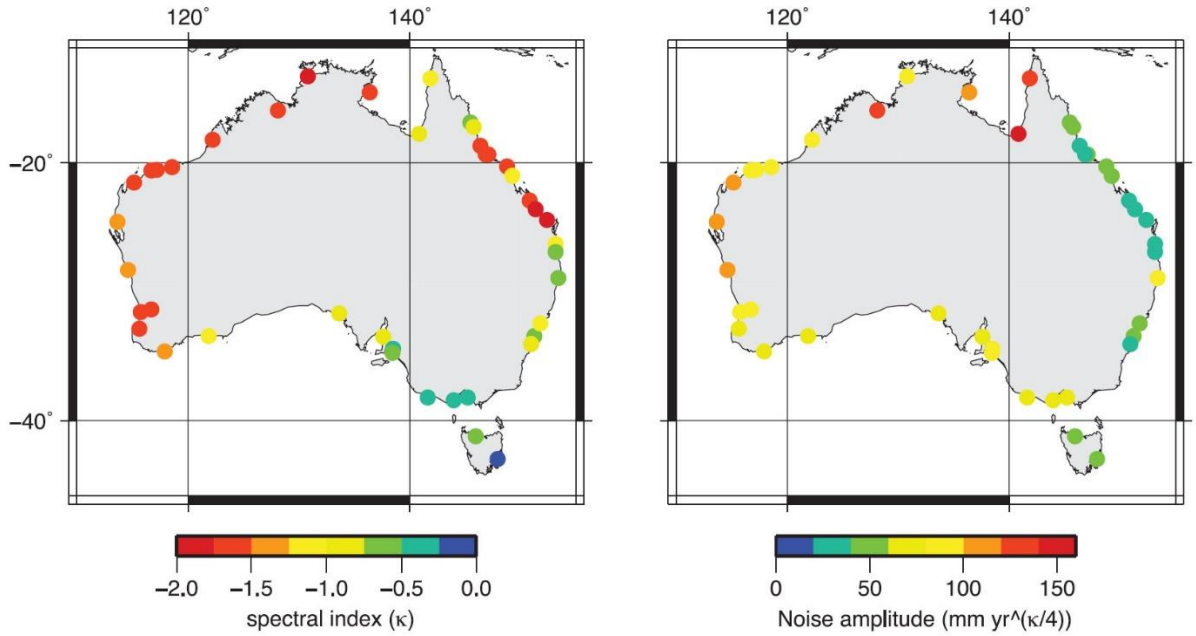

Figure 10: Sea-level 'noise' in tide gauge records around the Australian coast. The spectral index (LHS) indicates the variation between white noise (smaller (negative) or zero values = random variability) and time-correlated noise (larger (negative) values = cyclic oceanographic processes such as ENSO); the noise amplitude (RHS) refers to the strength of the noise. Thus, Tasmania's sea-level record exhibits mainly white noise (random variability) of relatively low amplitude, whereas many northern and western Australian sites exhibit time-correlated noise (i.e., the effects of cyclic oceanographic processes) of large amplitude, which are obscuring the contemporary climate change-driven sea-level rise signal more than is the case in Tasmania. Figure adapted with permission from Burgette et al. (2013, Fig. 5).

Burgette et al. (2013) and White et al. (2014) analysed sea levels around Australia. They found that seasonal sea-level variability (related to seasonal climatic and oceanographic processes) is greatest in northern Australia, whilst variability correlated with interannual and decadal processes - most significantly the El Nino Southern Oscillation (ENSO) - is greater in northern and western Australia. In each case, Tasmania is by contrast at the lower end of the 'noise' or variability scale (see Figure 3 in Section 2.3, and Figure 10 above), indicating comparatively low levels of annual and inter-annual sea level variability around the Tasmanian coast.

The consequences for this thesis are illustrated by data from the two Tasmanian tide gauges forming part of the Australian Baseline Sea-level Monitoring Array, at Burnie (north-west) and Spring Bay (south-east Tasmania). These respectively recorded sea-level rise rates of 3.1 and 3.6 mm/yr between Sep 1992 - July 2019 and May 1991- July 2019 (BOM 2019). These rates are commensurate with GMSLR (Chen et al. 2017), implying firstly that the main contributor to relative sea-level variability on Tasmanian coasts is contemporary climate change-driven SLR, and secondly that Tasmanian shoreline behaviour is likely to be less influenced by regional oceanographic processes such as ENSO over annual and interannual timescales than are most other Australian shores.

Barnard et al. (2015) showed that the variability in several oceanographic processes drives alternating phases of erosion and accretion on beaches around the Pacific Ocean basin by generating quasi-cyclic or episodic wave and sea-level anomalies. The ENSO was found to be most strongly associated with shoreline changes, as to a lesser extent were the Southern Annular Mode (SAM) and the Pacific Decadal Oscillation (PDO). Similarly Carvalho, Dalbosco and Guerra (2020) have demonstrated relationships between ENSO cycles and coastal erosion on Brazilian coasts. These modes of climatic and sea level variability drive changes in shoreline behaviour that can be large enough to overwhelm or prevent detectable responses to global mean sea-level rise in shoreline behaviour histories. Although the analysis of Barnard et al. (2015) did not include Tasmanian beaches, the lesser influence

of ENSO on Tasmanian sea-level variability suggests that effects of ENSO including quasi-cyclic coastal erosion are likely to be similarly reduced in Tasmanian waters.

These findings regarding sea-level variability are important to this thesis since it means that the relative mean sea level rise observed on Tasmanian coasts is close to the contemporary global climate change-driven mean sea-level rise (GMSLR) and is less influenced by other confounding factors (sea-level noise/variability) than are most other Australian coasts. This is inferred to increase the likelihood of a contemporary climate change - driven SLR signature being detectable in Tasmanian shoreline behaviour.

2.5.8 Local artificial disturbances

There are many ways in which localised artificial structures and activities may significantly modify coastal processes in ways that may overwhelm or prevent the effects of contemporary global mean sea-level rise from being expressed and detected. No attempt at a comprehensive discussion of artificial coastal process modification is made here. However, the following are selected examples from Tasmania, all of which illustrate a potential to complicate, mask or prevent detectable shoreline responses to sea-level rise:

- Deliberate stabilisation of naturally mobile or transgressive sand dunes, commonly with introduced dune-colonising grasses or pine trees (Hayes & Kirkpatrick 2012; Watt 1999). In addition to changing the form of coastal dunes by steepening them as sand accretes onto formerly mobile dunes, this may interrupt formerly active aeolian headland or barrier bypass sand transport processes, causing downwind coastal sand budget deficits. Such a deficit resulting from artificial stabilisation of formerly mobile transgressive dunes at Seven Mile Beach (Watt 1999) is a possible factor in apparently-increased shoreline erosion within the tidal channel entrance of Pittwater in south-east Tasmania (Sharples 2006).
- Construction of hard seawalls behind actively receding beaches is commonly undertaken to halt the recession so as to preserve coastal backshore spaces for human use but can also result in lowering and loss of beach faces in front of the walls. In some cases, the shoreline recession concerned may itself have been triggered as an early response to sea-level rise (e.g., at Roches Beach: Foster 1988; Sharples 2010).
- Construction of groynes to prevent or regulate longshore sand drift and to prevent sand loss from leaky coastal compartments. In a proposed example (not yet constructed) investigated by Shand and Carley (2011) for Roches Beach, the purpose of preventing the longshore drift is to prevent increasing sand losses whose onset may have been triggered by sea-level rise (Sharples 2010). See also Chapter 5.3.
- Significantly increased supply of sand to the coast near the mouth of the Ringarooma River in north-eastern Tasmania, as a result of tin mining during the last century which flushed large quantities of quartz sand into the river during the sluicing of tin-bearing weathered granite and derived alluvial deposits (Knighton 1991). The sand is currently continuing to work its way down the river in large point bars and will supply extra sand to the adjacent coastal environment for decades into the future at least. The potential exists for artificial beach sand gains of this sort to offset some local shoreline recession effects attributable to sea-level rise.

Because of the very wide diversity of artificial coastal disturbances that may occur, the potential implications (if any) of these for study sites having some artificial modifications that were analysed during this project are considered in a site-by-site basis in Chapters 5 and 6.

Chapter 3: Project Methods: Conceptual Framework and Procedures

3.1 *Research methods overview*

This thesis systematically investigates and extends observations made by the author over many years that were suggestive of changing coastal behaviour in a few (but not most) potentially erodible Tasmanian coastal environments.

A set of four principles guiding the methods used for this project were briefly presented in the Introduction (Section 1.4.1). This chapter describes the principles and the workflow used to implement them in more detail.

The method sets out to:

- categorise the long-term (multi-decadal) behaviour of erodible shorelines into broad trends of progradation, stability or recession (with or without some episodic variability);
- identify significant long-term (multi-decadal) changes in these behaviours, if any; and:
- test the hypothesis that some observed long-term behaviour changes may be driven by contemporary climate change-driven global sea-level rise, as well as testing as many plausible alternative hypotheses as can be identified.

Ortho-rectified historic aerial photography at every available date from the 1940s to recent is the primary source of data used to characterise shoreline behaviour during this approximately 70-year period, with recent beach profile surveys and other data sources as specified providing additional information in some cases.

3.2 *Guiding principles: description and implementation*

The four guiding principles for this thesis are described below.

3.2.1 Systematic selection of study sites

Select sites distributed across a range of coastal geomorphic process environments hypothesised to be susceptible to early or to late responses to sea-level rise (SLR)

The island of Tasmania includes a very wide diversity of readily erodible shoreline types (muddy, sandy, shingle, soft-rock) in a wide diversity of oceanographic and geomorphic environments ranging from one of the world's most high-energy swell-exposed coasts to extensive swell-sheltered tidal re-entrants.

As highlighted in the introduction (Section 1.1) and in the literature review (Section 2.4), it is notable that few shorelines globally have yet been unequivocally shown to be physically responding to contemporary climate change-driven sea-level rise. It appears from the literature that over the last few decades the larger proportion of research into coastal change and morpho-dynamics in Australia and elsewhere has been focussed on open-coast swell-exposed sandy beaches (e.g., Short 2006a; Thom & Short 2006). Many of the processes that are expected to mask or prevent shoreline responses to sea-level rise (see Ch. 2.5) are characteristic of this type of shoreline (e.g., Mortlock et al. 2017). These processes include large-scale episodic or cyclic cross-shore and alongshore sediment exchanges of significantly greater physical scale than any beach changes yet expected from contemporary climate change-driven sea-level rise (Le Cozannet et al. 2014).

It is therefore necessary to consider the possibility that one reason why little evidence of physical shoreline responses to SLR has yet been identified is that much of the research effort that might identify such responses has been focussed on a class of shorelines that is less likely to exhibit early

responses. The selection of study sites for this project has therefore included a range of shoreline types where the kind of swell-driven confounding sediment transport processes referred to above are absent or less significant, including cohesive clay soft-rock shores and swell-sheltered sandy re-entrant shores.

Nonetheless, swell-exposed sandy beaches are also well-represented in this thesis. This is partly to allow the characterisation and comparison of expected "late responders" to sea-level rise with any "early responder" shoreline types that may be identified, but also to investigate the possibility that some of these may indeed be showing early responses to SLR in situations where coastal geomorphic conditions are more susceptible owing to unusual local process environments.

The range of coastal landform types available in Tasmania is subject to several constraints, being essentially mid-latitude, temperate-climate, wave-dominated and mostly-microtidal coasts. However, within these constraints there is a wide range of shoreline types available for study. Amongst this coastal landform diversity, the considerations described in the Literature Review (Section 2.5) led to four broadly defined categories of Tasmanian shorelines being identified at the outset of this project as important to sample. These four categories are listed below, with the key reasons why they were considered important to this study. The study sites selected as representative of these categories are listed in Chapter 4.0.

1. ***Swell-sheltered tidal soft sandy shores***. These shores are subject to sea-level variability commensurate with open coast shores in the same regions but are not affected by certain processes such as cyclic cross-shore and alongshore sand exchanges which may prevent shoreline behaviour changes attributable to sea-level rise (see Sections 2.5.2 & 2.5.5). It was hypothesised that soft sandy erodible shores within swell-sheltered tidal re-entrants might be generally more prone to showing early physical responses to sea-level rise than those on the swell-exposed open coast. A significant portion of the study sites for this thesis were therefore deliberately selected from erodible sandy sites within tidal coastal re-entrants.

   Two categories of swell-sheltered sandy shores that are quite distinctive in their response to erosion have been used as study sites; these are:
   - *Non-saltmarsh sandy shores*. Readily erodible but in many cases not capable of shoreline accretion and recovery after erosion by locally generated wind-waves (see Sections 2.5.2 & 2.5.5).
   - *Sandy saltmarsh shores*. Readily erodible by locally generated wind-waves under changing conditions such as sea-level rise or increasing wind speeds, but also capable of vegetative recovery and sediment accretion if the frequency or magnitude of wind-wave erosion events reaching higher levels on the shore profile decrease (see Sections 2.5.2).

2. ***Very high energy storm-dominated swell-exposed sandy beaches***. It was speculated at the outset of this thesis that although swell-exposed sandy beaches were in general unlikely to show early responses to sea-level rise, some might exhibit such behaviour under unusual circumstances. The presence of bare deflating dunes backing most west and south-west Tasmanian beaches, and a known history of shoreline recession at one of these (Ocean Beach; see Section 5.2.2, Figure 19), suggested that very high-energy and storm-dominated sandy beaches might be exhibiting early responses to sea-level rise (see discussion in Section 2.5.5). The writer's participation in a south-west coast beach monitoring project conducted by the Tasmanian Department of Primary Industries, Parks, Water and Environment (DPIPWE) provided an opportunity to include a selection of these beaches in this thesis. The outcomes have proved somewhat different to the initial speculations and are discussed in Section 7.3.3.

3. ***Other swell-exposed sandy beaches***. Additional examples of swell-exposed sandy beaches were included in the selection of study sites chosen for this project for two reasons. The first was to include a number of such beaches thought not likely to be exhibiting an early response to sea-level rise in order to enable comparison between the characteristics and processes of such beaches and any coastal sites that might be found to exhibit early responses to sea-level rise. However a second reason was because at least two swell-exposed beaches (Ocean Beach and Roches Beach) were thought to be possibly showing an early response to SLR, and if this proved to be the case might point to unusual circumstances that allow early responses to occur on swell-exposed sandy beaches.

4. ***Soft rock 'one-way' shores***. The easy erodibility of soft rock shores, their inability to 'rebuild' after erosion in the manner a sandy shore may, and the expectation that they would show a detectable increased recession in response to sea-level rise all combine to make this shoreline type of high interest for studies aimed at identifying early responses to sea-level rise (see discussion in Section 2.5.2).

3.2.2 Utilise study sites with minimal confounding process 'noise'

As far as is practicable, utilise study sites from erodible coastal environments where other competing factors or processes ('noise') that might overwhelm or prevent a sea-level rise signal from being detected are absent or minimal.

The selection of sites in accordance with this principle partly overlaps with the preceding discussion of study site diversity but is highlighted as a principle in its own right because of its fundamental importance to the research approach adopted.

Study sites were selected with a view to minimising the amount of process 'noise' that might overwhelm or prevent any SLR signal from being expressed in coastal landform changes. The categories of process noise that are of most concern are:

- *local or regional relative sea-level variability at scales comparable to or greater than contemporary climate change-driven sea-level rise,* which make it problematical to distinguish shoreline behaviour changes driven by the latter from those driven by the former; and also:
- *sediment transport and budget processes which may cause long-term or cyclic shoreline change on scales comparable to or greater than that which sea-level rise would cause,* so that any sea-level rise signal that might be present is difficult or impossible to clearly distinguish.

The most important categories of 'minimal noise' shores encountered during this project are identified below.

The Tasmanian coast as a whole has two key noise-minimising conditions, namely:

- *Minimal vertical land movement (VLM)* resulting in negligible local relative sea-level change attributable to this cause (see details in Section 2.5.4).
- *Lesser regional inter-annual to inter-decadal sea-surface height variability caused by regional oceanographic processes (especially ENSO) than most other Australian coasts.* This similarly reduces the scale of local relative sea-level changes not attributable to climate-change-induced SLR (see details in Section 2.5.7).

Both of the above reduced-noise conditions may increase the possibility of a contemporary climate change - driven SLR signature being identifiable in Tasmanian shoreline behaviour. Whereas all coasts in Tasmania have these advantages, certain study sites within Tasmania are additionally free of some other types of local process 'noise' that may be problematical at some Tasmanian coastal sites. The main categories of shoreline environments identified that minimise local process noise likely to confound detection of sea-level rise signals were:

- *Swell-sheltered tidal re-entrant shores* where swell-driven sand movement processes such as beach erosion and accretion or beach rotation cycles, or other open coast sand movement processes, are mostly absent. On swell-exposed coasts, these processes typically cause beach variability on scales larger than expected beach responses to contemporary climate change-driven sea-level rise, and thus are likely to prevent any beach response to sea-level rise being detectable until significantly more sea-level rise has occurred (see Section 2.5.5).
- *Soft-rock shores* where the noise of cyclic shoreline recovery does not occur after erosion, and long-term shoreline change is persistently recessional. Although some shoreline recession is the norm for these shores irrespective of sea-level rise, any increase in recession driven by an onset of sea-level rise is likely to become apparent relatively quickly (see Section 2.5.2).
- *Shores with minimal local artificial disturbances.* Depending on type and scale, some artificial disturbances may cause shoreline morphology changes and modify sand budgets on scales significantly greater than any anticipated sea-level rise responses to date (see Section 2.5.8).
- *Shores with minimal swell direction variability.* Study sites on Tasmania's west and south-west coasts are subject to minimal annual swell direction variability (less than 20°), which on that relatively linear planform coast minimises the potential for significant changes in longshore sand drift flux or direction. This minimises the likelihood of another source of sandy beach morpho-dynamic noise which could potentially overwhelm any signal of contemporary climate change-induced sea-level rise response to date (see Section 2.5.5).

By default, all sites selected for analysis had the advantage of minimised sea-level variability resulting from VLM or ENSO (since all are Tasmanian sites). However, some sites were selected for investigation not primarily because of noise-minimisation criteria, but because of previously – known indications that they may have undergone a major long-term change of behaviour in recent decades. Most of these were largely free of the types of noise listed above, however in several cases (at Roches Beach, Gordon, and Nebraska Beach) significant artificial disturbances were present in parts of the sites. These sites were nonetheless analysed in order to better understand their known shoreline behaviour changes, and test these against a range of hypothetical explanations including sea-level rise and artificial disturbance.

With the above caveats, the selection of a proportion of additional sites in swell-sheltered re-entrants, on soft-rock coasts and in locations free of local artificial disturbances was a deliberate selection strategy aimed at facilitating testing for sea-level rise responses or lack thereof by eliminating as much process noise as possible. However, the selection of some sites subject to noise, in particular swell-exposed sandy beaches, was also deliberate and was intended to allow comparison of those sites with less 'noisy' sites. Shores selected in accordance with the criteria discussed here are described in Chapter 4.0 below.

3.2.3 Identify changes in shoreline behaviour using aerial photography

Identify sites exhibiting significant changes in the long-term (multi-decadal) behaviour of soft (erodible) shorelines, of types that would theoretically be expected to indicate the emergence of sea-level rise signals.

This thesis assumes that a shoreline response to sea-level rise will be expressed as an observable physical change in the long-term[7] behaviour of soft erodible shorelines. It is further assumed that the type of shoreline behaviour change that occurs will be a predictable response to sea-level rise for the shoreline type in question.

Based on these assumptions, the following are two important examples of long-term coastal landform behaviour change that might be indicative of a response to sea-level rise:

- A change from cyclic erosion and accretion around a mean or equilibrium shoreline position to a progressively receding shoreline, typically on swell-exposed sandy beaches. See Literature Review Section 2.2.
  or:
- A significant increase in the rate of a pre-existing long-term recession trend, for example on soft-rock shores or sandy shores in coastal tidal re-entrants. See Literature Review Sections 2.4 and 2.5.2.

Such changes could be evidence of a sea-level rise signal if they are found in coastal process environments where they are explainable as the response of known coastal geomorphic processes at the site to sea-level rise and are *not* equally or better explainable by other observed geomorphic drivers or processes at the site (see Section 3.2.4 below). A synopsis of the methods used in this thesis to identify long-term shoreline behaviour changes (or lack thereof) is provided below, with additional details of the workflow in Section 3.3.2 following.

Repeated vertical aerial photography since the late 1940s has been the primary source of shoreline behaviour data for this thesis. A time series comprising every available photo of adequate photogrammetric quality was used for each site (never just one early and one recent photo). All aerial photography used has been geo-referenced and ortho-rectified, mostly by the writer although existing ortho-photos have been used where available (details of all air photos used are provided in Appendix One). Photogrammetric position error margins for each ortho-rectified air photo were quantified by measuring and taking the average of the apparent displacement of 10 or more well-defined fixed reference features visible on each air photo in a time series from their positions on a selected reference photo (typically one of the more recent and higher-resolution ortho-rectified air photos for each study site).

On each ortho-photo, the seawards vegetation limit (or line) was digitised as the shoreline position proxy (Boak & Turner 2005) for that date (Figure 11). With a shoreline position digitised as a roughly shore-parallel line for each date, the landwards or seawards movement of the shoreline between consecutive air photo dates was interpolated along regular 100-metre-spaced shore-normal digital transects (Figure 12, LHS). Each transect plot was normalised for comparison between transects by plotting shoreline positions along each transect relative to the median shoreline position on that transect (Figure 12, upper RHS). Groups of transects showing coherent behaviour over time were

[7] For the purposes of this thesis, "long-term" behaviour is that which is consistent over longer periods than the duration of average observed beach erosion and recovery cycles, and over longer periods than typical intervals between air photo dates. Approximately a decade (10 years) or less is typical for both measures in the shoreline histories analysed during this project, hence for the purposes of this research "long-term" trends are those which remain consistent on time scales of at least 10 years and ideally more than 20 years. See also thesis glossary.

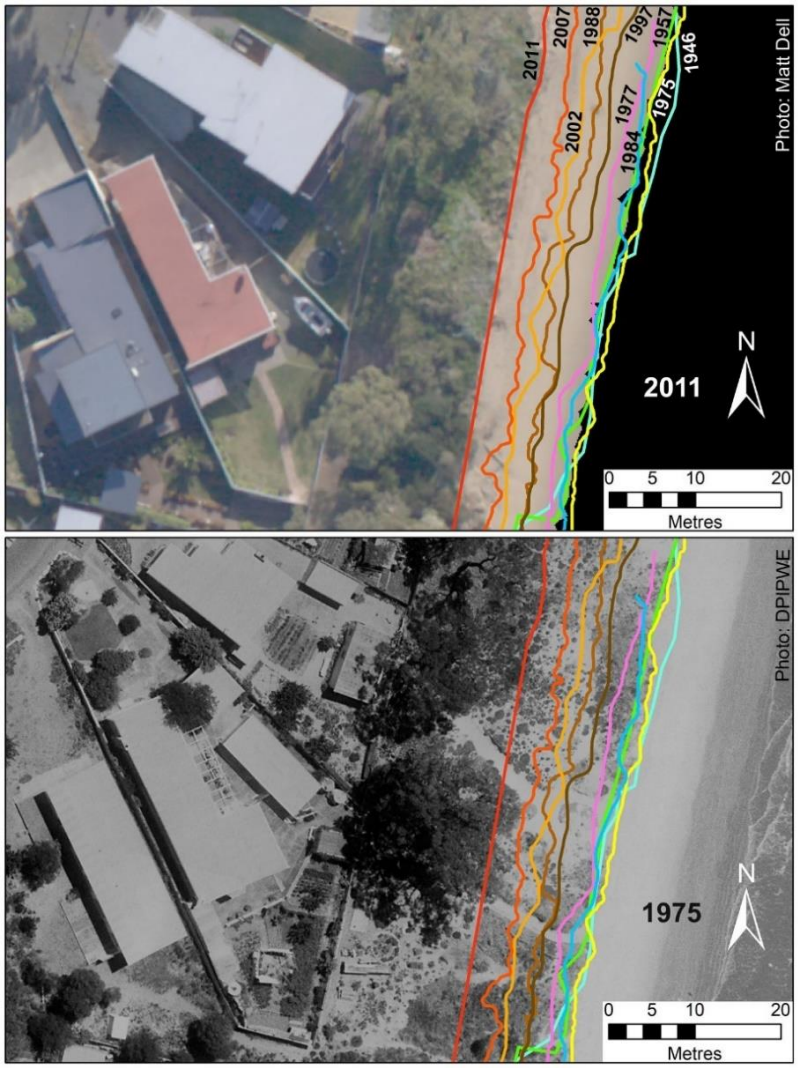

Figure 11: Example of a selected sequence of digitised shoreline positions at Roches Beach (Tasmania) from a time series of ortho-rectified air photos from 1946 to 2011, demonstrating how the vegetation line used as the shoreline proxy tracks shoreline change. The air photos used to digitise the 1975 and 2011 shorelines are shown to illustrate the shoreline position change between 1975 and 2011. Note that while the vegetation lines shown demonstrate an overall recession trend after 1984, they also demonstrate a shorter period of foredune accretion (shoreline progradation) within that period. More detail of shoreline position change is seen when all 32 air photo dates available for this section of shoreline are used (see Figure 13).

grouped into a single summary plot for each such shoreline section by plotting the medians of all transect shoreline positions at each air photo date (Figure 12, lower RHS; Figure 13).

The resulting shoreline history plots were analysed for long-term behaviour trends using a combination of visual inspection and linear regression analysis. Three simple types of long-term shoreline behaviour trend were identified in the data, namely linear shoreline position stability, progradation or recession trends. Some real and apparent variability around each linear trend was expected as a result of factors including short-term erosion and accretion cycles, erosion scarp slumping and air photo ortho-rectification errors.

Given the expected shoreline position variability and the limited frequency of air photos available for most sites, it was considered problematical to attempt to identify trends of greater complexity than linear, such as 2nd order polynomial trends. The measured air photo error margins were important to the analysis as 'reality checks' on identified shoreline behaviour trends and were used both for visual

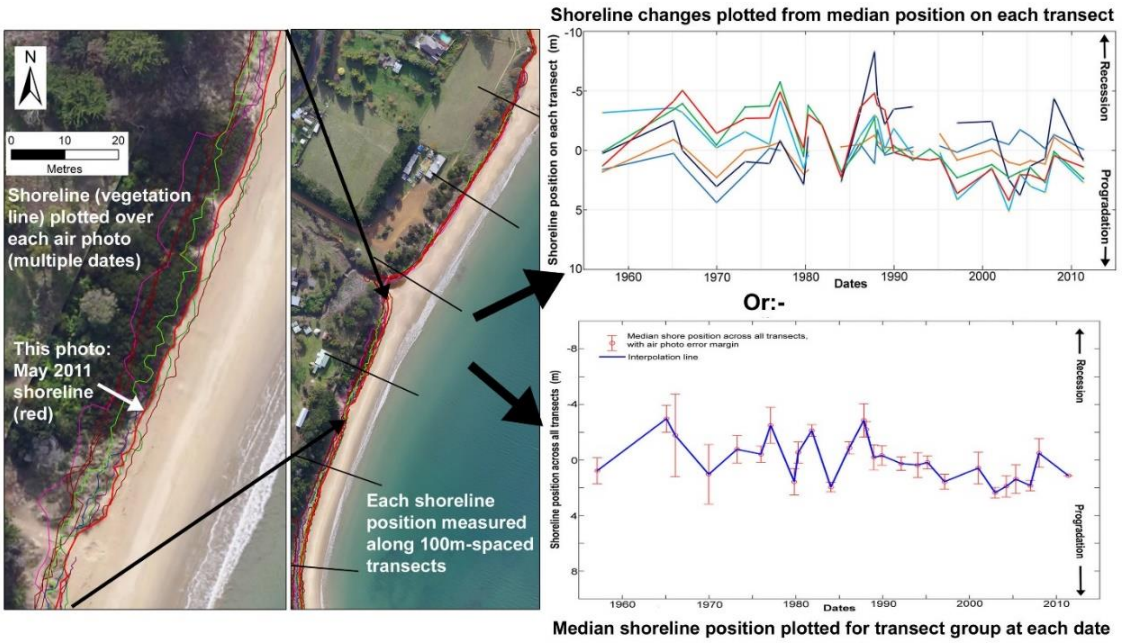

Figure 12: Figure illustrating the extraction of beach behaviour data from a time series of 27 aerial photo dates for northern Roches Beach (see also chapter Section 5.3). This figure shows two ways of plotting the shoreline behaviour of northern Roches Beach, which has undergone cyclic erosion and recovery events over a 50-year period with an essentially stable or slightly prograding underlying long-term trend. Shoreline position changes with time can be plotted along each transect within the beach section for individual comparison (top plot), or the median shoreline position at each date across all transects can be plotted to yield a summarised shoreline behaviour plot for the whole beach section (bottom plot).

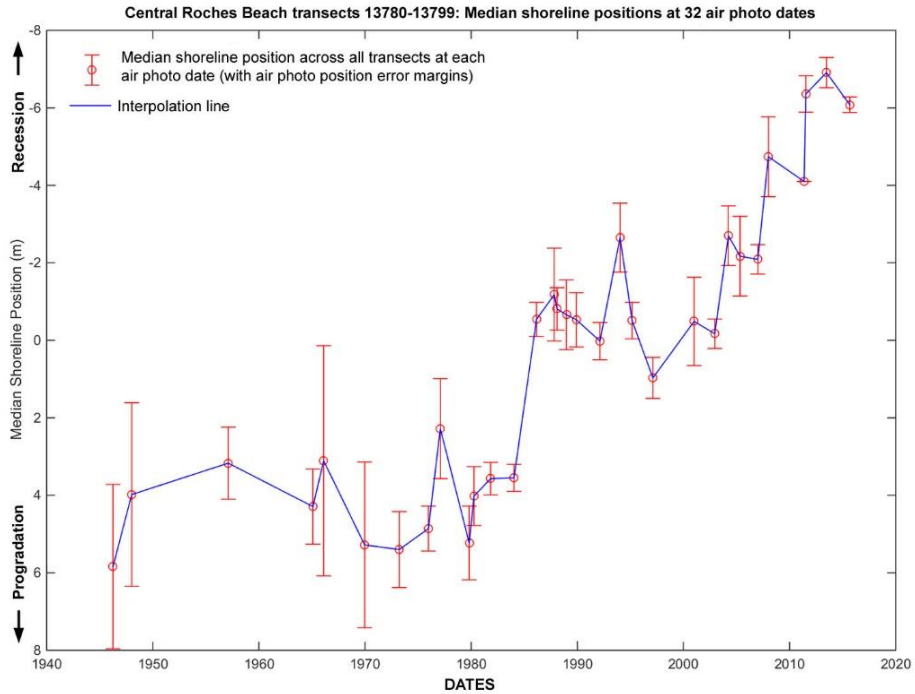

Figure 13: This summary plot of the median shoreline position at each of 32 air photo dates across 21 transects shows a marked long-term change of shoreline behaviour in the main central portion of Roches Beach (see also the same plot with piecewise linear fits at Figure 34 in Section 5.3.3). The beach was essentially stable for over 30 years prior to 1985, with some erosion and accretion episodes around a roughly stable shoreline position. After 1985, the beach showed a markedly changed behaviour trend for 26 years to 2011, comprising a dominant recession trend much larger than the air photo error margins, with some partial recovery episodes but never full recovery to the pre-1985 shoreline position. This behaviour trend ceased after a large erosion event during 2011 because the local government began artificially replenishing the dune and beach face, so that subsequent beach behaviour can no longer be considered as a natural geomorphic response.

evaluation of apparent trends and also in selected cases for numerical error-weighted linear trend analysis. For example, if an apparent long-term linear recession or progradation trend exhibits less overall shoreline position change (landwards or seawards) than the scale of most of the air photo error margins, then it is not demonstrated to be a real trend.

At most sites, a single linear shoreline behaviour trend was identified over the whole air photo period (circa 70 years). For example, the trend on Figure 12 (RHS) is a stable or possibly slightly prograding long-term linear trend over the whole air photo period, with inter-annual variability of greater amplitude than the majority of error margins and thus inferred to be real shoreline position variability. The short-term variability at this site is most likely mainly a result of episodic beach erosion and recovery cycles.

By contrast, visual inspection of the shoreline behaviour plot at Figure 13 is strongly suggestive of a switch circa 1985 from a long – term (multi-decadal) stable trend to a long-term receding trend. In this case, piecewise linear regression (before and after 1985) was used to verify the statistical significance (Pearson correlation co-efficient) of the two trends, together with an error-weighted piecewise regression to further verify the validity of the apparent switch in shoreline behaviour (additional details and plots for examples described here are provided in Section 5.3).

3.2.4 Test for alternative explanations

Where suspected signals of contemporary climate change-driven sea-level rise (as long-term shoreline behaviour changes) are found in air photo time series, test this hypothesis by investigating whether the geomorphic processes and conditions at each such site can explain why that shoreline would show a physical response to contemporary climate change-driven global sea-level rise earlier than most. Also investigate whether known site processes and conditions can explain the observed change of behaviour without invoking contemporary climate change-driven sea-level rise as a cause.

This principle follows from the observation that correlation does not necessarily imply causation. Where suspected sea-level rise signals (long-term changes of behaviour) are found in shoreline behaviour histories, it is necessary to test the possibility that the apparent response to contemporary climate change-driven sea-level rise might be better explained by other processes. This must include testing whether the rate of sea-level rise itself at the site is comparable to contemporary global climate change-driven sea-level rise or is dominated by other variables such as VLM, which might be the underlying driver of observed changes. There are two key elements in such testing, namely:

1. There must be a plausible process model available whereby known conditions and processes at each candidate site may be interacting with contemporary climate change-driven sea-level rise to produce the observed change of behaviour (rather than masking or over-whelming it).
   and:
2. It is also necessary to test whether the observed change of behaviour could plausibly be a response to processes or changes at the site which do not invoke contemporary climate change-driven sea-level rise as a contributing cause.

The best evidence for a plausible identification of an ‘early responder’ shore would be a positive outcome for point 1 of this test, and a negative outcome for point 2.

It is important to note that whereas it is always possible (and indeed useful) to propose a variety of speculative alternative explanations for any phenomenon, the only explanations of consequence are those for which credible evidence can be provided. Thus, plausible models require enough understanding of the geomorphic and oceanographic conditions and processes at the coastal sites in question to generate hypotheses about how sea-level rise might or might not be driving a distinctive shoreline response at those sites. These conditions and processes will include (but are not limited to)

shoreline substrate type(s) and topography, tidal conditions, wave and storm climates, wind climate, sediment transport processes, vertical land movement, artificial changes and others (Section 2.5 reviews the most important such factors for temperate mid-latitude coasts such as Tasmania).

The practical means of conducting this test will vary depending on the type and detail of the data available for a site. Given that only limited measured data on processes and shoreline behaviour is available for most Tasmanian sites, the tests applied in this thesis are qualitative assessments of broadly defined models based on observed but mostly not measured phenomena. However, for well-studied sites with good numerical data captured over significant periods, then the additional use of numerical coastal behaviour models to compare expected shoreline responses to sea-level rise against the observed changes will provide an additional level of confidence. It is hoped that numerical modelling will be undertaken as an extension and improvement on the research reported here when sufficient measured data is available on Tasmanian shoreline processes.

3.3 *Workflow*

In practical terms, the principles of the method in this thesis were applied to a workflow that comprised:

- Site selection.
- Data collection & preparation.
- Detailed case studies.
- Shoreline behaviour analysis across all sites.

These procedures are briefly explained as follows, with further details provided elsewhere as cross-referenced. Refer also to Figure 14 below which provides a flow-chart summary of the workflow.

3.3.1 Site selection

The selection of several study areas (and individual study sites within those areas) was based on them having been identified during work prior to this thesis as possible "early responders" to sea-level rise (these are the detailed case studies examined in Chapter 5). Nonetheless a systematic site selection process was undertaken alongside the initial selection of those sites to ensure that the final range of sites used were representative of as wide a range as possible of potentially relevant coastal geomorphic conditions and processes. The basis for the systematic site selection process is outlined in Sections 3.2.1 & 3.2.2 above and the final site selection is documented in Chapter 4 following.

3.3.2 Data collection & preparation

The most important data available that records long-term (multi-decadal) shoreline behaviour for Tasmania is vertical aerial photography, which for most areas is available from the late 1940s onwards. For most Tasmanian coastal areas, aerial photography has subsequently been repeated at increasingly frequent intervals, which in many locations has yielded photography at useful scales (1:40,000 or better) for 20 or more dates over the approximately 70-year period since the 1940s. As discussed in Section 2.3, contemporary climate change-driven global sea-level rise commenced during the mid-1800s and emerged from inter-annual to inter-decadal variability during a 40 year period centred around 1925 (Gehrels & Woodworth 2013; Woodworth 1999). Thus, aerial photography is available for at least the latter half of the period up to present during which putative early responders to contemporary climate change-driven sea-level rise might have begun to show a detectable change in shoreline behaviour. An assumption of this thesis is that such photography may enable detection

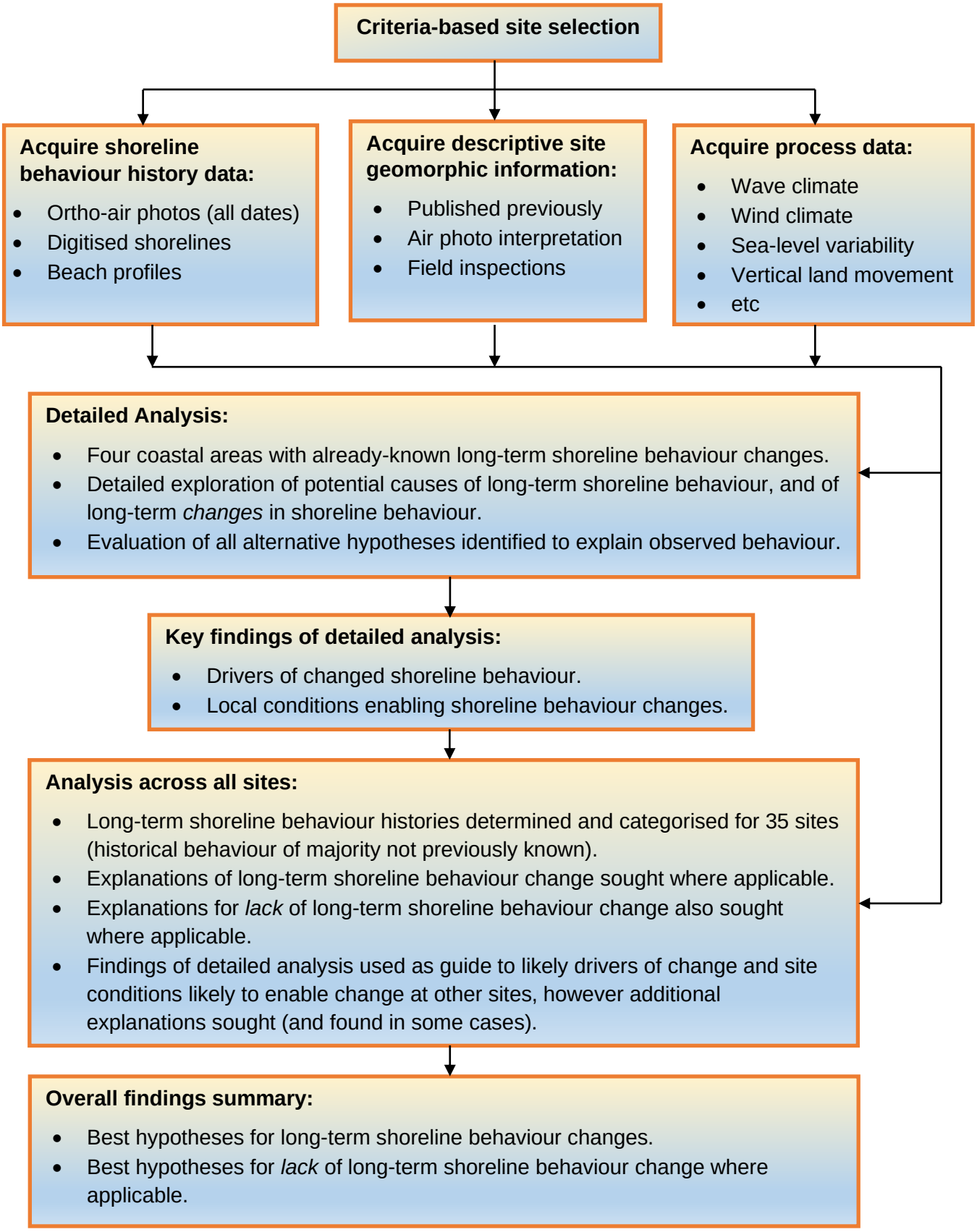

Figure 14: Workflow diagram for this thesis.

of shoreline behaviour change responses whose "Time of Emergence" has been during the mid- to late-20th Century. However aerial photography cannot identify any very early responses (during the Late 19th Century or early 20th Century) since if these have occurred, they will have become 'normal' shoreline behaviour by the time repeated aerial photography became available.

Surveyed beach profile data is also available for some Tasmanian beaches since 2005 or later and has been used for some study sites (see TASMARC beach profile data discussions below).

New types of high-resolution data enabling detection of shoreline behaviour change are becoming available but are mostly restricted to a much shorter recent period compared to conventional aerial photography. Satellite imagery of comparable resolution provides equivalent information - and one *Quickbird* satellite image has been used successfully in this thesis (for Roches Beach) but is only available for recent decades. Similarly, other recently-developed methods such as monitoring coastal topography using Unmanned Aerial Vehicles (UAVs or 'drones') with remote sensing technologies such as laser range-finding are beginning to provide very high-resolution records of physical shoreline changes, including the capacity to quantitatively compare coastal forms, volumes and positions at high resolution from one observation to the next. However, while these technologies will offer very high-quality shoreline change data in the future, the records available for Tasmanian coasts at the time of undertaking this thesis were too limited in location and duration to be useful in detecting long-term shoreline change for the purposes of this project.

Key datasets

The datasets listed below were identified as most relevant to the research questions. Some of these datasets were previously prepared and published by other workers as referenced in study site descriptions in Chapter 5 & 6, and Appendix One, particularly the oceanographic datasets. However very little air photo-derived data had previously been systematically compiled for coastal sites in Tasmania, hence this was the primary data collection focus of this project and is one of its major original contributions.

The key data acquired are:

- *Geological, geomorphic, and other process conditions at each site*. Mainly descriptive, qualitative information based on a wide variety of existing published mapping and other information, plus interpretation of features visible on aerial photography and field inspections by the writer at all sites. Includes information on local artificial disturbances at each site. This data allowed the generation of qualitative geomorphic process models for each site.
- *Ortho-rectified air photo time series for each study site.* The primary source of historic shoreline behaviour data used in this thesis. See additional details below.
- *Digitised shoreline positions for each air photo date at each study site*. Shoreline position data extracted from ortho-photos in a format ready for analysis. See additional details below.
- *TASMARC beach profile time series data for several but not all study sites.* Supplementary high-resolution shoreline behaviour history data for some sites (since 2005 or later). See additional details below.
- *Sea-level variability data.* Tide gauge data compiled by other workers as cited for Burnie (north coast) and Hobart (south-east coast) were used at several case study sites for which these were the closest records. Owing to a lack of any adequate tide gauge records on the (oceanographically distinctive) west coast of Tasmania, two reconstructed sea surface height histories for Ocean Beach (west coast) over the Twentieth Century to recent period have been used (Church & White 2011; Hamlington et al. 2011). Given good evidence of minimal VLM across Tasmania (see Section 2.5.4 above), the analysis of other Tasmanian shoreline sites was based on the reasonable assumption of sea-level rise commensurate with these local datasets (see also White et al. 2014).

- *Swell wave climate data.* The analysis of extreme (storm) wave data by Hemer (2010) from Tasmania's only long-term wave rider buoy record yielded important results pertinent to this thesis. Swell wave climate parameters for all open coast Tasmanian sites were derived from the CSIRO-BoM swell wave hindcast of Durrant et al. (2013).
- *Coastal wind records* Coastal winds generate local wind-waves which may be factors in shoreline erosion. Original Australian Bureau of Meteorology (BoM) synoptic and daily extreme wind records longer than circa 30 years for coastal stations were obtained and analysed by the writer for wind directions and for long-term wind speed averages and changes over time.
- *Other data* Additional data as required was obtained for some but not all sites as detailed in Appendix One site descriptions. Examples include historic records of storm events for Roches Beach (Appendix A1.4.2), littoral drift direction data interpreted from geomorphic indicators visible on aerial photography for Ocean Beach (Appendix A1.3.8) and radiometric (carbon 14) dating of inter-dune swamp peat deposits at Ocean Beach (Section 5.2 & Appendix A1.3.8)

Data preparation

Some of the datasets listed above were prepared and analysed by others as cited, and their published results were used as-is for this project (e.g., swell-wave data). In other cases, analyses of original data were undertaken as part of this thesis but are self-explanatory, for example original BoM wind observations were processed by the writer to yield wind direction roses, annual wind speed means and moving annual average wind speeds. The following brief descriptions of data preparation methods are focussed on those core datasets whose analysis was not routine and requires some explanation. These are the ortho-rectified air photo time series for each study site, the digitising of shoreline positions derived from the air photos, and the TASMARC beach profile data.

The standard methods adopted for initial preparation and analysis of these core datasets are summarised following the data preparation descriptions below.

Ortho-rectified air photo time series for each study site

Most air photos used in this project were obtained from the Tasmanian government Department of Primary Industries, Parks, Water and Environment (DPIPWE), following exhaustive searching of their air photo database by the writer. DPIPWE and its predecessor agencies have been responsible for the capture and archiving of most aerial photography undertaken in Tasmania since 1945. All air photos were obtained as scanned images (mostly at 2039 dpi), mostly unrectified but some recent images were already ortho-rectified by DPIPWE. Criteria applied to image selection included resolution and contrast sufficient to distinguish features 1.0 – 2.0 m diameter or less, minimal glare on water near study sites and a photo point approximately above or to seawards of the coastline (to avoid relief displacement on scarps or high dunes resulting in misleading shoreline positions). A few recent high resolution ortho-rectified air photos have been also obtained from other sources as detailed in Appendix One. The sourcing, metadata and ortho-rectification details for each air photo is detailed in Appendix One.

All available air photos of adequate photogrammetric quality were used for each of 35 distinctive shoreline study sites (listed in Chapter 4), which amounted to over 20 air photo dates at many sites and over 30 dates at a few sites. A total of 521 air photo frames were used for this thesis, of which 380 were individually ortho-rectified by the writer, and 141 were obtained already ortho-rectified by others (as specified in Appendix One metadata).

Geo-referencing and ortho-rectification of scanned air photos was performed by Chris Sharples using Landscape Mapper™ software pre-loaded with camera data and digital base maps for Tasmania. Field surveying of ground control points for all study sites was beyond the resources of this project,

however photo-to-photo ortho-rectification yielding relative instead of absolute error margins was considered appropriate for the purposes of this project.

For each study site, a reference photo of good resolution and recent date was selected first. In most cases this was an air photo already ortho-rectified by DPIPWE, but in a few cases the reference photo was georeferenced and ortho-rectified to well-defined ground control points selected from Land Information System Tasmania (LIST) 1:25,000 topographic mapping. All other photos for each study site were then ortho-rectified to the reference photo using ground control points visible on all photos (e.g., low-relief coastline rock outcrops, old well-defined structures at ground level and even features such as old trees and ponds where the trunk base or pond perimeter is well defined and obviously stable over time). Photogrammetric error margins for each photo were measured using well-defined reference features visible at all air photo dates, which were not also used as ground control points for the ortho-rectification process. The error margins were calculated as the average of the apparent displacements of as many reference features as possible (ideally 10 or more) from their positions on the reference image (which by definition had zero relative error). Error margins for each photo are listed in Appendix One. This method arguably captures the most important spatial uncertainty in the data used, although more sophisticated analyses of multiple sources of uncertainty are possible and may be useful in future work (e.g., Fletcher et al. 2011, p. 18).

Digitising shoreline positions for each air photo date at each study site

Changes in shoreline position over time is the fundamental information on which this thesis is based, hence it was important to select a shoreline position proxy which is both readily identifiable on aerial photography and also a credible indicator of changing shoreline behaviour. Amongst many possible shoreline position indicators or proxies (Boak & Turner 2005), the *in situ* (living) seawards vegetation line at the back of the beach or swash zone was judged most appropriate for this thesis (see example on Figure 11 in Section 3.2.3 above). This commonly used shoreline position indicator provides a strong visual contrast against bare sand and generally also contrasts adequately with bare hard- or soft-rock scarp faces. Vegetation limit is readily mappable from air photos of widely varying scale, pixel size and contrast limitations. This proxy may be mappable on older photos of poorer quality that may not support determination of some other shoreline proxies such as those based on specific contours or digital elevation models mapped from stereo air photos. The vegetation line may thus provide valid shoreline position data at more dates than some other methods can achieve.

The behaviour of an *in-situ* vegetation line mapped on multiple air photos over inter-annual to inter-decadal time scales at a given coastal site typically reflects the types of shoreline behaviour that this thesis has sought to identify, namely long-term trends of shoreline progradation, stability or recession. On most erodible shorelines (e.g., sand, or soft rock), an actively eroding or receding shoreline will be marked by an erosion scarp whose top is also the vegetation line. The vegetation line on a prograding beach will be an incipient foredune vegetation front to seawards of any older foredune scarping. A soft rock shore will only recede in the long term but may in the short term be characterised by a slumped and partly vegetated scarp that may give an impression of minor shoreline accretion in between erosion events. With experience such complications can usually be identified on air photos. However, because these situations can complicate the issue of defining a shoreline position, a number of conventions have been adhered to in digitising shoreline positions for the purposes of this thesis; these are illustrated on Figure 15.

The *in-situ* vegetation line as shoreline proxy was manually digitised as a line shapefile traced over the ortho-rectified air photos, using tools in Landscape Mapper™ and ArcGIS™ (see examples in Figure 11 and Figure 12). The digitising was performed zoomed in to the point where image pixilation was obvious but larger features still easily interpreted. Nearly all shorelines used in this project were digitised by Chris Sharples, however about half of the Ocean Beach shorelines were

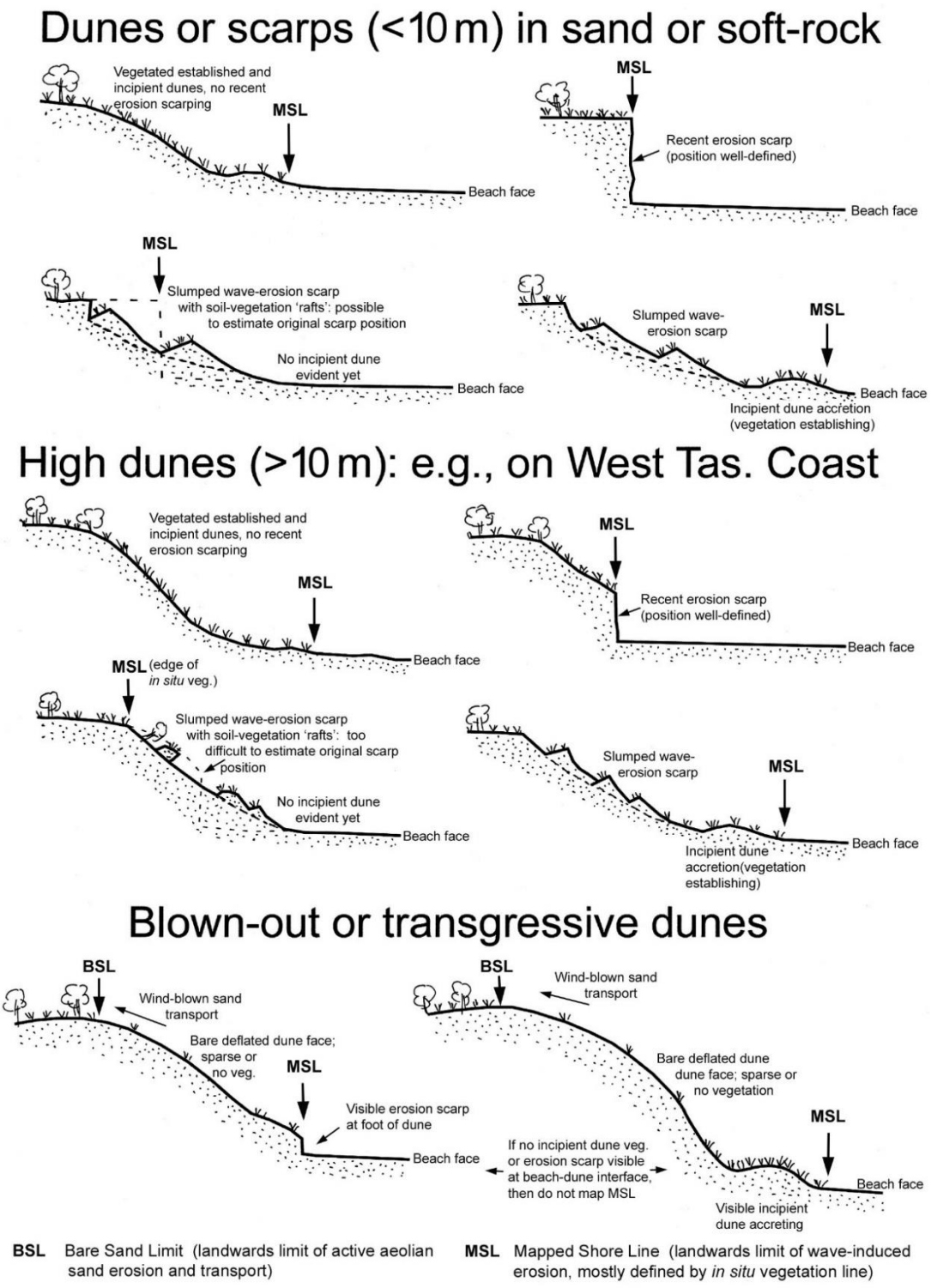

Figure 15: Shoreline mapping conventions adopted in this project for digitising shoreline positions on air photos (Mapped Shore Line: MSL). The shoreline position on both sandy and soft-rock shores is considered to be the *in situ* (living) vegetation margin; this is typically either the head line of a slumped dune scarp or the wave-exposed vegetation margin (typically either at a wave-eroded erosion scarp if the shoreline has recently eroded, an incipient dune front if a sandy shoreline is accreting, and at a vegetated established foredune margin if it is simply stable). This figure illustrates conventions adopted for mapping this shoreline proxy in simple cases and some more difficult cases including vegetation limits on very high eroded and slumped dunes. The figure also illustrates the adopted convention that a differently attributed line (shown here as the Bare Sand Limit: BSL) will be used to map coastal vegetation lines resulting from aeolian dune sand erosion ('deflation margin') and deposition (and not directly from wave erosion and consequent scarp slumping).

digitised by Hannah Walford and a few other shorelines previously digitised by Sarah Harries (for earlier projects) were also used (see metadata in Appendix One).

TASMARC beach profile time series data

Beach and frontal dune profiles surveyed at varied intervals for the TAsmanian Shoreline Monitoring and ARChiving project (TASMARC) project have been available for selected Tasmanian beaches since 2005 or later. TASMARC has been funded by the Antarctic Climate and Ecosystems Co-operative Research Centre at the University of Tasmania and co-ordinated by a professional surveyor, Nick Bowden. TASMARC is primarily a community science project involving volunteers who have been trained to survey beach and foredune profiles using a theodolite and staff at a variety of beaches around Tasmania where benchmarks have been installed and surveyed to ±50mm using differential GNSS. Their work has been supplemented with profiles measured by professional surveyors using Total Station methods.

Profiles measured at Ocean Beach and at 6 south-west and south coast sites by Nick Bowden, Paul Boland, Phil Cullen, and Matt Dell have been used in this project (see Appendix One). The profiles are valuable for determining recent beach behaviour at finer temporal and spatial resolution than the available aerial photography allows. However, the beach profile records are not yet long enough to confidently identify long-term trends and changes in beach behaviour, albeit they will undoubtedly become useful for this purpose when they provide longer-term records. The TASMARC website at www.tasmarc.info documents the beach profiling project and makes all the surveyed data – including that used in this thesis - publicly available for free download.

Initial analysis of shoreline behaviour history data

The following notes outline how the analysis of the shoreline behaviour history data is brought to the stage where insights can be inferred from the data and used to answer research questions.

Air photo data

Following the manual digitising of shoreline position lines as individual shapefiles for each air photo date as described above, the following steps were taken to complete the preparation and analysis of air photo derived shoreline behaviour data for each study site[8]:

1. The position of each digitised dated shoreline was measured along each of a series of 100 metre-spaced shore-normal digital transects (see Figure 12).
2. Shoreline positions on each transect were normalised by recalculating each as a distance landwards ('-') or seawards ('+') of the median shoreline position on each transect. This allows plotted shoreline position movements over time along different transects to be visually compared (see example in Section 3.2.3 Figure 12, top RHS). Multiple shoreline history plots across adjacent transects were compared to identify groups of transects with similar (coherent) shoreline histories.
3. Groups of coherent shoreline history plots were merged into single summary plots by plotting the median of the shoreline positions at each air photo date across the whole group of transects (see examples on Figure 12 lower RHS and Figure 13).
4. The summary plots were then analysed by calculating linear regression plots to test for long-term linear shoreline behaviour trends. Such trends were classified simply as progradation,

[8] The analysis methods used here are similar to some of those achievable using the *Digital Shoreline Analysis System* (DSAS) developed by the US Geological Survey as an ArcGIS™ plug-in. However, the methods used for this project were developed independently by the writer and colleagues at the University of Tasmania, including Dr Michael Lacey (who wrote the *Shoreline History* Python script to measure shoreline positions along multiple shore-normal transects) and Dr Christopher Watson (assistance with *Matlab*™ scripting).

stability or recession trends, and their significance or validity was assessed using Pearson correlation co-efficients, visual comparison against photogrammetric error margins and (in some cases) error-weighted linear regressions. Piecewise linear plots over different selected periods within a shoreline history plot were also used to test for long-term changes in behaviour trends.

TASMARC beach profile data

Surveyed TASMARC beach profile data has been plotted in two ways (Figure 16), namely as profile plots and "hinge point" plots.

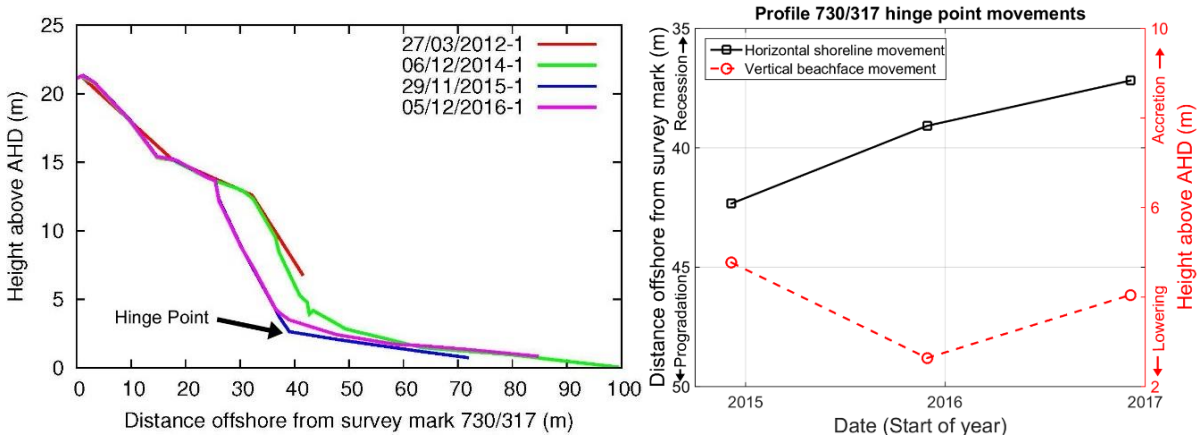

Figure 16: Example plots of TASMARC Prion Beach profile 730/317 survey data, as profile plots (LHS) and hinge point movement plots (RHS, 2014 – 2016 only). The plots demonstrate significant dune-front and beach-face erosion during 2015, with subsequent (vertical) beach-face accretion recovery but no (horizontal) dune-face recovery.

Profile plots are simple plots of the surveyed data showing a shore-normal topographic profile from the surveyed benchmark across the dune face and upper beach face. The profiles measured at each survey date can be stacked on top of each other to create a visual display of changes between each survey date. This type of data presentation is useful for comparing profiles over a relatively small number of survey dates but can become confusing if many profiles are being compared.

Hinge point plots[9] track the vertical movement of the (near flat or gently sloping) beachface and the horizontal movement of the (vertical or steeply angled) dune face between consecutive surveys. A 'hinge point' is identified on each profile plot which is the intersection of the beach face and the dune face (i.e., the back edge of the beach face and the seawards toe of the dune face). The hinge point may be obvious where a beach has been recently eroded (see Figure 16 LHS example) or a prograding incipient dune front is well developed, but may be obscured by slumping in some cases. In the latter case expert judgement is used the extrapolate the trends of the beach face and dune front to a hinge point that may be buried under slumped or wind-blown sand. The movement of the hinge points between each profile survey is plotted in both the vertical and horizontal planes as two separate line plots which can be visually interpreted as respectively the vertical movement of the beach face (accretion upwards or erosion downwards) and the horizontal movement of the dune front (landwards erosion or seawards accretion). See Figure 16 RHS example. Although hinge points are not quite as intuitively easy to interpret as profile plots they can provide a useful record of dune front and beachface changes over longer periods and more survey plots than is practical for profile plots.

Both profile and hinge point plots have mostly been analysed by simple visual interpretation for the purposes of this project where less than 10 years of consecutive plots have been available. A variety

[9] The hinge point plot format was suggested by Dr John Hunter (oceanographer, Hobart).

of options for numerical exploration of the profile data are available but have not been explored during this project.

3.3.3 Detailed case studies

Four coastal areas comprising 12 individual sites were selected as detailed case studies. Earlier initial studies of these areas by the writer and colleagues had indicated that long term changes of shoreline behaviour have occurred during the Twentieth Century. The areas – Ocean Beach (Walford 2011), Roches Beach (Sharples 2010), Barilla Bay (Sharples et al. 2012) and Western Duck Day (Prahalad et al. 2015) – cover a range of very different coastal process environments.

In each case assessment of these study areas for the present thesis utilised all available air photo dates (rather than only a selection of dates as in the initial studies cited above), and utilised consistent methods of shoreline behaviour history analysis, different to (albeit partly developed from) those employed in the earlier studies. These analyses tested the widest range of plausible alternative hypotheses that could be identified to explain the long-term behaviour changes identified in parts of these areas, and the lack of changes in other parts of them.

The four detailed case studies are documented in Chapter 5 and their key outcomes are summarised in Section 5.6. These studies identified a number of plausible drivers of the observed shoreline behaviour changes (including but not only sea-level rise), and also identified key local geomorphic conditions that were important in enabling the changes to occur.

3.3.4 Shoreline behaviour analysis across all study sites

Following the detailed analysis of selected study areas, broader analysis was conducted across all 35 individual study sites for which sufficient data was obtained. The aim was to test for significant relationships between shoreline behaviour histories and the processes and conditions at each site. This analysis was conducted more efficiently across a larger number of sites than the detailed analysis had been because the conclusions drawn from the latter provided guidance to the broader analysis.

The analysis is fully described in the Shoreline Behaviour Analysis Chapter 6. In summary, the analysis process comprised the following three steps:

1. *Classify each study site according to its style of historical behaviour.* Each study shoreline's long-term behaviour over the period of historic beach behaviour data (1940s to present) was determined. Shoreline behaviour was categorised as simple progradation, stability or recession trends (with or without short-term variability), and was also classified according to whether or not there were long-term changes in any of these, such as the onset of a long-term (multi-decadal) recession trend following decades of stability or progradation, or a significant acceleration of a prior long-term recession trend.
2. *Identify plausible explanations of shoreline behaviour.* For each shoreline behaviour category in turn, as many plausible hypothetical explanations for that behaviour at each relevant study site as could be identified were sought. These included the hypothesis that sea-level rise was a driver of long-term shoreline behaviour change where site history and conditions supported this possibility.
3. *Evaluation of alternative hypotheses.* For each site, all hypotheses generated to explain the shoreline behaviour and any changes of behaviour were evaluated against known site conditions and geomorphic processes. Drivers and conditions that explained shoreline behaviour in the detailed case studies were found to be informative for many of the broader range of sites in the Chapter 6 analysis, however some additional factors were also identified in the latter analysis.

The findings of the analyses detailed in Chapters 5 and 6 are summarised in Chapter Section 6.4. The following Discussion and Conclusions (Chapters 7 and 8) discuss the implications of the findings and identify answers to the research questions posed in this thesis.

Chapter 4: Study Sites Selection

4.1 *Introduction*

This chapter briefly describes the implementation of the first workflow element introduced in the previous chapter, namely site selection, and lists the final sites selected for study.

The site selection process was substantially informed by a co-incident systematic review of available geomorphic data for the entire Tasmanian coast (including the Bass Strait islands), which was undertaken by the author as part of a separate project. The author collaborated and co-authored with a group of Australian coastal geomorphologists co-ordinated by Professor Bruce Thom to develop a national sediment compartment framework for Australian coastal management, as documented by Thom et al. (2018). That paper is reproduced in Appendix 2 of this thesis. The compartment descriptions are on the *CoastAdapt* website (https://coastadapt.com.au/tools/coastadapt-datasets accessed 10th June 2020). This review provided the author with an up-to-date Tasmania-wide context for selecting appropriate coastal study sites for this thesis based on the most recent information available.

4.2 *Site selection*

Site selection was based on the first three of the four guiding principles for this thesis.

Principle 1: *Select sites distributed across a range of coastal geomorphic process environments hypothesised to be susceptible to early or to late responses to sea-level rise (SLR)*

Sites were selected from each of four geomorphic categories identified as likely to include both early and late responders to climate change-driven global mean sea-level. These categories are:

- Swell-sheltered tidal soft sandy shores (saltmarsh and non-saltmarsh varieties).
- Very high energy storm-dominated swell-exposed sandy beaches.
- Other swell-exposed sandy beaches.
- Soft rock 'one-way' shores.

Table 1 below lists all study sites selected, sub-divided amongst these four categories.

Principle 2: *As far as is practicable, utilise study sites from erodible coastal environments where other competing factors or processes ('noise') that might overwhelm or prevent a sea-level rise signal from being detected are absent or minimal.*

All Tasmanian coastal sites are subject to minimal vertical land movement, and to less sea-level variability related to regional oceanographic processes such as ENSO, than are many other coasts around mainland Australia (Section 3.2.2). These factors minimise several potential causes of local relative sea-level variability on all Tasmanian coasts which are problematical for identifying a contemporary climate change-related sea-level rise signal on some coasts elsewhere.

The selection of soft-rock shores and sandy shores within swell-sheltered tidal re-entrants was expected to be useful for this thesis since these sites are typically not subject to the noise of large-scale sand movement processes that can overwhelm sea-level rise signals on swell-exposed sandy beaches. The opportunity to include high-energy west-coast Tasmanian open coast sandy beaches in this study has had the advantage of providing study sites with minimal swell-wave directional variability. Such variability is a cause of large-scale sand transport variability on some coasts where it is likely to overwhelm any GMSLR signal in beach behaviour.

Many of the study sites for this project were also selected on the basis of having minimal known local artificial disturbances, which may be another source of process noise. The six high-energy south-west and south coast beaches from Mulcahy Bay to Prion Beach are good examples of this (Figure 17),

being located in the Tasmanian Wilderness World Heritage Area (TWWHA). However, a few sites were chosen despite the presence of some artificial disturbances because they were known or suspected to be showing long-term shoreline change behaviour of possible interest to this thesis. In these cases, it was considered that the effects of the disturbances were simple enough to be identified and accounted for. Examples include Gordon, Roches Beach and Nebraska Beach.

Principle 3: *Identify sites exhibiting significant changes in the long-term (multi-decadal) behaviour of soft (erodible) shorelines, of types that would theoretically be expected to indicate the emergence of sea-level rise signals.*

For the majority of study sites chosen, it was not known at the outset whether they had exhibited any long-term changes in behaviour over the air photo period since the 1940's. For most sites, this principle was intended as a possible outcome of the thesis; it was assumed that air photo time series analysis of most sites would not show a significant long-term behaviour change, but that some sites might do so.

However at least four study areas had been identified prior to this project as probably having changed their long-term behaviour in recent decades, namely Ocean Beach (Walford 2011), Roches Beach (Sharples 2010), Barilla Bay (Sharples et al. 2012) and Western Duck Day (Prahalad et al. 2015). These four areas (comprising 12 individual sites) were therefore selected for further detailed analysis as described in Chapter 5, since they were considered at the outset to be the most likely known sites to yield useful insights to guide investigation of the larger number of selected sites whose shoreline behaviour histories were completely unknown at the outset.

Beyond the criteria listed under the first two principles above, no attempt was made to select sites with an even spread of other geomorphic and oceanographic characteristics which preliminary speculation might suggest would drive a shoreline's susceptibility (or not) to sea-level rise[10]. This was partly on the grounds that to do so would pre-judge the findings of the thesis, and partly because the number of sites which could be analysed in the time available would be too limited to achieve a more useful diversity of site characteristics than already achieved by the selection criteria described above.

No attempt was made to ensure an even geographical spread of study sites around the Tasmanian coast, because simple geographic spread will not necessarily guarantee a good spread of site types. Instead the following practical criteria were the other main factors guiding site selection:

- Logistical support (including helicopter transport over three field seasons) was provided by DPIPWE for undertaking studies of remote south-west coast Tasmanian beaches (see also acknowledgements), hence these (usefully) figure more prominently in this work than would have otherwise been the case.
- Accessibility was a key consideration for all sites studied. It was considered important to inspect each site in the field as this may reveal relevant information not clearly identified by existing literature or data. All sites studied in this thesis have been inspected by Chris Sharples in the field, mostly during this project although in a few cases within a few years prior to it.
- The quality of the air photo record for each site was an important consideration. The frequency, duration and quality of available imagery was judged adequate for all sites selected.

[10] For example, differing sediment transport systems and sand budgets.

4.3 *Study sites selected*

Study sites selected as described above are listed in Table 1 following and located on map Figure 17 below. The table groups sites into the four type categories hypothesised to potentially include early responders, as described under *Guiding Principle 1*. Some geographically related shoreline areas comprise multiple similar sites exposed to different conditions. A separate shoreline behaviour history (based on an air photo time series) has been determined, plotted and analysed in Chapters 5 and 6 for each of the 35 distinctive shoreline sites tabulated in Table 1.

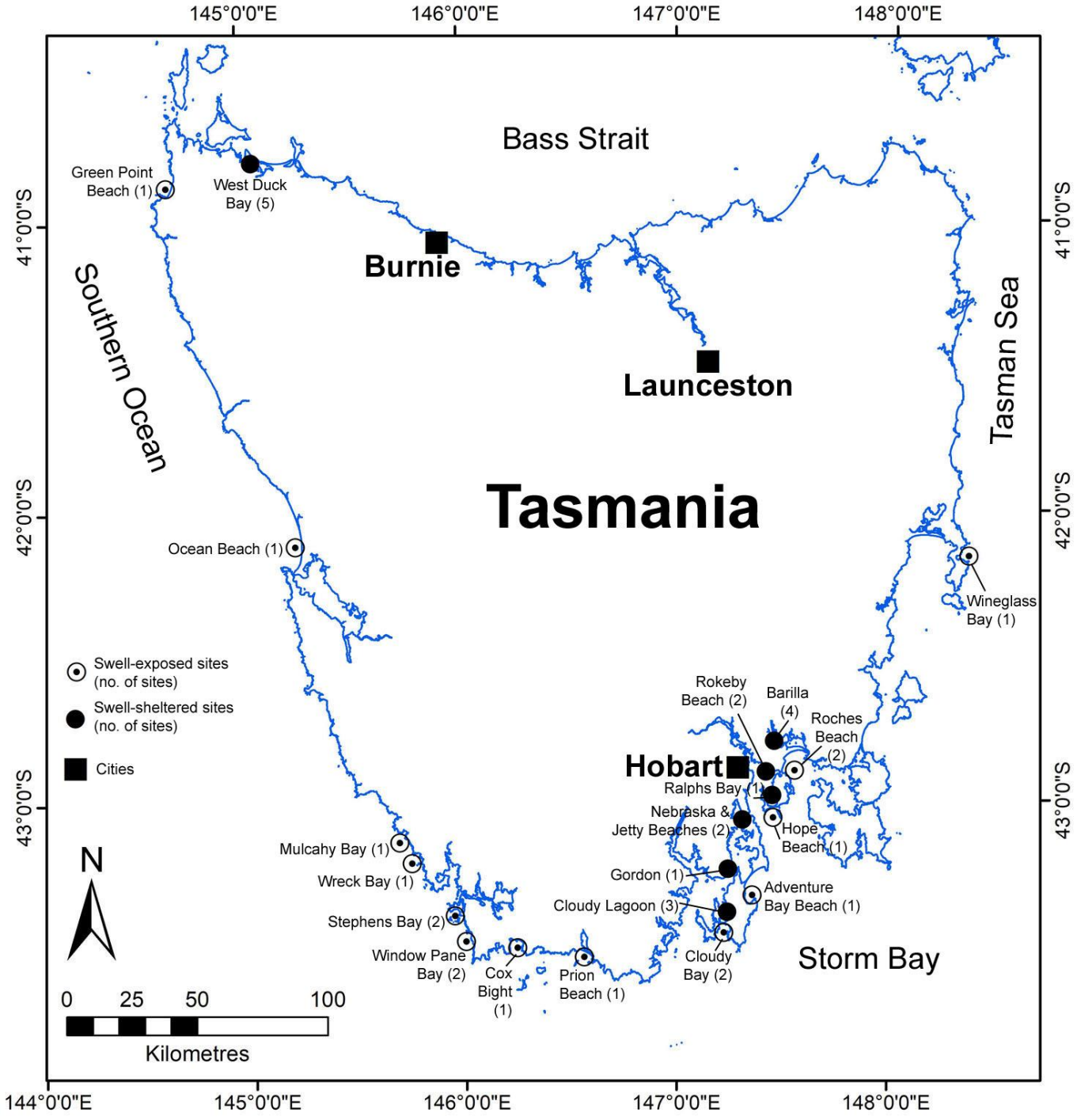

Figure 17: Locality map showing distribution of shoreline sites for which data was gathered and analysed during this thesis. See also Table 1.

Table 1: Coastal study sites for which a separate shoreline behaviour history has been determined in this study. Sites are first ordered by broad coastal geomorphic categories (see Section 3.2.1), then in order clockwise around the Tasmanian coast within each category (see map Figure 17). Note that some different sites are grouped together into areas as indicated by the site names.

Swell-sheltered tidal soft sandy shores			
Sandy swell-sheltered shores (non-saltmarsh)			
Number	**Site**	**Key site characteristics**	**Comments** (Including any indications of long-term shoreline change history)
1	Nebraska Beach (north Bruny Is.)	Receives some very refracted swell under normal conditions but dominated by generally westerly local wind-waves.	Likely coupled sand transport system with Nebraska Beach losing sand (early responder?) to Jetty Beach (gaining sand, late responder?).
2	Jetty Beach (north Bruny Is.)	Receives some very refracted swell under normal conditions but dominated by generally westerly local wind-waves.	
3	Gordon (D'Entrecasteaux Channel)	Receives very attenuated swell under normal conditions but dominated by local wind-waves. Nearby artificial shoreline protection.	Comparison of recent and 1947 High Water Mark surveys indicated 8 - 22m recession from 1947 to 2012
4	Cloudy Lagoon South (Bruny Island)	Swell-sheltered sandy shore backed by beach-ridge plain	Cloudy Lagoon is a tidal lagoon permanently connected to the ocean. The lagoon is a partly filled sand sink with capacity to sequester additional sand.
5	Cloudy Lagoon East (Bruny Island)	Swell-sheltered sandy shore	
6	Cloudy Lagoon North (Bruny Island)	Swell-sheltered sandy shore	
7	West Duck Bay North (eastern part)	Mostly swell-sheltered sandy (eroding beach ridge) shore	Prominent active (fresh) erosion scarp
Sandy saltmarsh shores (swell-sheltered)			
Number	**Site**	**Key site characteristics**	**Comments** (Including any indications of long-term shoreline change history)
8	Ralphs Bay shore (South Arm neck)	Sandy saltmarsh shore, swell-sheltered	Eroding in parts, very close to road, artificial boulder protection in parts
9	West Duck Bay North (western part)	Saltmarsh soils over Pleistocene sands, negative sand budget but shores also have capacity for vegetative recovery after active erosion (if erosion process stops)	Previous work by author and others indicated long-term shoreline recession and likely change of behaviour related to both wind and sea-level rise (Mount et al. 2010; Prahalad et al. 2015)
10	West Duck Bay North-West		
11	West Duck Bay South		
12	West Duck Bay South-east		
High-energy swell-exposed sandy beaches			
Number	**Site**	**Key site characteristics**	**Comments** (Including any indications of long-term shoreline change history)
13	Cloudy Bay Beach East (Bruny Island)	High foredune erosion scarp section frequently appears active (bare sand) in many historic air photos	Direct exposure to predominant south-westerly swells.
14	Prion Beach (South coast)	Long swell-exposed beach and vegetated foredune (long sand-spit without dune at eastern end of barrier was excluded from study).	Foredune seawards face anecdotally considered more eroded in last decade that previously.

15	Cox Bight (South coast)	Three adjacent swell-exposed sandy beaches treated as one site.	Some minor recent erosion apparent but mostly stable vegetated foredunes.
16	Window Pane Bay Beach North (South-west coast)	Very high frontal dune is eroded distal end of large former terrestrial transgressive dune (not a foredune). Medium swell exposure.	Very high eroding and slumping seawards dune face gives initial (misleading) impression of dramatic recession
17	Window Pane Bay Beach East (South-west coast)	Sandy and boulder beach backed by vegetated frontal dune. High swell exposure.	Mostly vegetated and stable frontal dune, with one long central section progressively eroding; looks like expanding erosion zone.
18	Stephens Bay Beach North (SW coast)	Sandy beach backed by partly bare deflating foredune. Moderate wind-exposure only	Mostly bare deflating foredune front.
19	Stephens Bay Beach South (SW coast)	Sandy beach backed by high bare deflating transgressive dune face. High wind-exposure.	Foredune developed in front of high deflating dunes, suggestive of shoreline progradation despite deflation.
20	Wreck Bay Beach (South-west coast)	Very high energy embayed beach, partly bare deflating dune fronts, some aeolian sand loss.	Partly deflating, partly stable vegetated frontal dune.
21	Mulcahy Bay Beach (South-west coast)	Very high energy embayed beach, partly bare deflating dune fronts, some aeolian sand loss.	Partly deflating, partly stable vegetated frontal dune.
22	Ocean Beach (West coast)	Long swell-exposed sandy beach barrier.	Wave eroded frontal dune has been receding for some decades, beach profile mostly low and wet with high tide lines very close to eroding foot of dune
23	Green Point Beach (far north-west coast)	High energy swell wave climate, embayed beach, showing recent strong recovery from erosion events.	

Other swell-exposed sandy beaches

Number	**Site**	**Key site characteristics**	**Comments** (Including any indications of long-term shoreline change history)
24	Wineglass Bay Beach (east coast)	Deeply embayed beach, receives mainly offshore winds and very refracted swell, no apparent sand sink.	Popular beach but free of any artificial interventions (walking track access only).
25	Roches Beach Main Central (SE Tas)	Long relatively narrow sandy beach with persistent active and receding foredune erosion scarp until 2011	Major erosion issues since circa 1980s; artificial interventions since 2011 to prevent further dune recession.
26	Roches Beach North (SE Tas.)	Stable sandy beach with low foredune.	No major historic erosion issues known
27	Hope Beach (South Arm neck)	Swell-exposed sandy beach embayed between rocky headlands	Major wave erosion events have been followed by full beach and dune recovery to date.
28	Adventure Bay South Beach (Bruny Island)	Sandy beach backed by low foredune, exposed to refracted swell.	Occasional erosion events but followed by full beach and dune recovery to date.
29	Cloudy Bay Beach West (Bruny Island)	Sandy swell-exposed beach but less directly swell exposed than Cloudy Bay East beach.	Adjoins permanently open tidal channel entrance to large lagoon (sand sink) but no morphological evidence of shoreline recession in progress.

Soft rock (semi-lithified sediment) "one-way" shores			
Number	**Site**	**Key site characteristics**	**Comments** (Including any indications of long-term shoreline change history)
30	South Barilla shore (Pittwater, SE Tas)	Scarped cohesive clay shoreline	Field evidence of fresh active erosion scarp, previous air photo evidence of acceleration (Sharples et al. 2012)
31	West Barilla shore (Pittwater, SE Tas)	Scarped cohesive clay shoreline	Erosion scarp present but mostly rounded and partly vegetated, not freshly active.
32	North-west Barilla shore (Pittwater, SE Tas.)		
33	North Barilla shore (Pittwater, SE Tas)		
34	Rokeby Beach West	Freshly actively eroding scarped cohesive clay shoreline. Relatively swell-sheltered but receives storm swells.	Wind-waves dominant but with only short fetches in dominant wind direction.
35	Rokeby Beach Central-East	Rounded and vegetated scarp in cohesive clay. Relatively swell-sheltered, less exposed to storm swells than west section.	Wind-waves dominant but with short fetches in dominant wind direction.

4.4 *Summary and context*

This chapter has briefly summarised the criteria used in selecting study sites for this thesis, which has drawn upon discussion and principles described in the first three chapters of this thesis. The process of site selection has established the basis for the analysis of shoreline behaviour histories which is the most important element of this thesis, and which is described in the following two chapters (Chapter 5 and Chapter 6).

Chapter 5: Shoreline Behaviour Case Studies

5.1 *Overview*

This chapter details investigations from four case study areas (comprising 12 distinctive coastal sites) at a level of detail sufficient to infer likely causes of their long-term shoreline behaviour. The study areas (Table 2) are each representative of one of the four broadly differing coastal geomorphic types identified in Section 3.2.1 as shoreline types that might exhibit early physical responses to contemporary climate change-induced sea-level rise. The four coastal areas were known from initial investigations prior to this thesis to have undergone long-term and continuing shoreline erosion and recession (Prahalad et al. 2015; Sharples 2010; Sharples et al. 2012; Walford 2011). The purpose of investigating these coasts was to quantitatively determine their shoreline behaviour histories for approximately the last 70 years from air photo time series data using an updated and consistent method. If long term shoreline behaviour changes were identified, then the aim was to use that information and other geomorphic and oceanographic data to test a working hypothesis that they are exhibiting early physical changes in response to sea-level rise.

Table 2: Case study areas and associated geomorphic type. Each case study area comprises 1 or more distinct shorelines within the same locality and geomorphic environment (as per the LH column).

Coastal geomorphic types (Section 3.2.1)	**Case study area**
1. Very high-energy storm-dominated swell-exposed sandy beaches (one large 15 km long site)	Ocean Beach (west coast); 1 distinct site
2. Other swell-exposed sandy beaches (two sites in adjoining 'leaky' embayments)	Roches Beach (south-east Tasmania); 2 distinct sites
3. Swell-sheltered tidal re-entrant 'low energy' soft sandy shores (four saltmarsh shores on sand and one receding sandy beach ridge shore, with widely varying wind-wave fetch and exposure)	West Duck Bay (north-west Tasmania); 5 distinct sites
4. Soft-rock (semi-lithified sediment) non-recovering ('one-way') shorelines in a swell-sheltered tidal re-entrant (four sites with widely varying wind-wave fetch and exposure)	Barilla shore (Pittwater, south-east Tasmania); 4 distinct sites

A standard format has been adopted for working through each of the four case studies in this chapter. Essential descriptive information and historical shoreline behaviour data is provided for each site, drawn from more detailed information that is not required in the body of this thesis but is provided in Appendix One. In either case the information provided is based on the authors own field observations, analysis of a time series of all available aerial photography for each site, beach profiling surveys if available, and analysis of available relevant published studies, geological and topographical mapping and other data. If the determination of the shoreline behaviour observed at each site identifies long-term changes in shoreline behaviour, then each case study evaluates the working hypothesis that sea-level rise is the dominant driver of change by asking two questions:

"*Are there geomorphic process conditions on this coast that would allow the observed change of behaviour to occur in response to sea-level rise, and to do so earlier than on most coasts?*";

and conversely:

"*Are there drivers other than sea-level rise on this coast that could have caused the observed change in behaviour?*"

These questions led the investigation through a process of proposing as many alternative hypotheses for the observed shoreline behaviour as could be identified by the author, followed by the elimination of any that are not consistent with available information.

The key findings from these four case studies are brought together at the end of this chapter (Section 5.6). Processes identified as likely drivers of any observed changes of behaviour are listed, as are the geomorphic conditions at each case study site that are inferred to have enabled the changes.

5.2 *Study Area 1: Ocean Beach*

5.2.1 Introduction

Ocean Beach is located on the central west coast of Tasmania near Strahan Township (Figure 18). The study area comprised the southern half of the beach (~19 kilometres length). Ocean Beach is an example of one of the four broad categories of coastal landform type from which study sites were selected for this thesis (namely "very high energy storm-dominated swell-exposed sandy beaches" as described in Section 3.2.1 and listed in Table 2 above).

This chapter section presents the essential data and findings of an investigation of shoreline behaviour at Ocean Beach since the 1940s. Additional supplementary data and information is provided in Appendix A1.3.8. These findings have also been published in the refereed paper Sharples et al. (2020), which is an outcome of this thesis (provided in Appendix 2).

5.2.2 Site description and processes

Geomorphic description

Ocean Beach (145° 15' 0" E 42° 10' 0" S) is the longest (32 km) sandy barrier beach on the mostly rocky west coast of Tasmania. The sandy barrier has developed across the mouth of the large deep structural trough of Macquarie Harbour (Forsyth, Quilty & Calver 2014), which has a permanently open tidal channel outlet at the southern end of the beach. The west-facing dissipative beach is classified as morpho-dynamically intermediate by Short (2006b), and is compartmentalised by long rocky headlands beyond its north and south ends (Davies 1973). The beach sand is quartz-dominant with only a minor carbonate fraction (Walford 2011) and is inferred to be of dominantly glacial outwash origin (Banks, Colhoun & Chick 1977). The Henty River which today discharges across Ocean Beach was a major outwash river supplying sand to the continental shelf from the nearby heavily glaciated quartzite-rich mountains of the West Coast Range during Pleistocene glacial low sea-stands (Banks, Colhoun & Chick 1977).

The surf zone is dominated by a double- to in places triple-bar system up to 600 metres wide cut by the largest rips of any Australian beach (Short 2006b). Most of the beach is today directly backed by vegetated dunes with actively eroding seawards scarps up to 30m high exposing palaeosols and some swamp peat lenses (Figure 21). The earliest (1947-49) air photos show extensive unvegetated transgressive dunes and deflation basins immediately behind parts of the Ocean Beach study area, however much of these have now stabilised through establishment of a vegetation cover including the introduced *Ammophila arenaria* ('marram grass'). However more extensive unvegetated transgressive dune fields still remain active behind the beach further north beyond the study area (Figure 18).

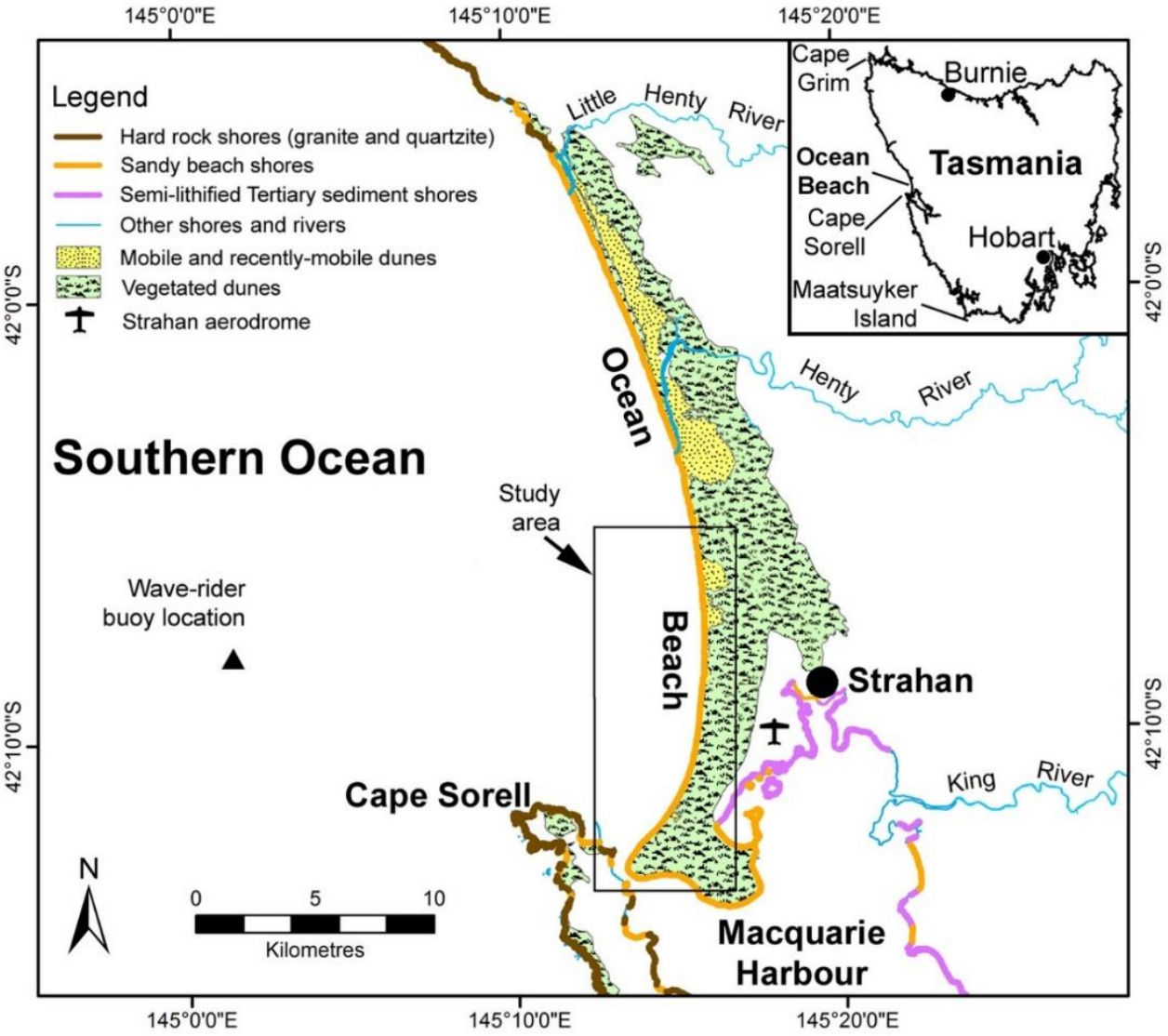

Figure 18: Ocean Beach locality map, showing regional location, key elements of coastal geology and local infrastructure including the nearest township (Strahan). Inset indicates the location of three west-coast Tasmania wind-recording stations mentioned in the text.

Sand transport and budget

Sand transport within the Ocean Beach embayment is dominated by a persistent mostly southwards littoral drift along the beach. This is demonstrated by a range of geomorphic indicators visible in air photos at most available dates, particularly the persistently southwards-deflected outlets of the Henty and Little Henty Rivers which cross the beach. A large flood-tide delta just inside the permanently-open tidal entrance of Macquarie Harbour is the final sink for the southwards-drifted sand (Figure 22). This sink is inferred to have been active throughout the air photo period, and considerable accommodation space remains available in the harbour to sequester additional sand.

The earliest available air photos (from 1947-48) show that sand was then also being transported permanently inland from the beach via aeolian transport in large bare mobile transgressive dunes, large parts of which have subsequently become vegetated and stable, partly through the establishment of the introduced marram grass *Ammophila arenaria* on seawards incipient foredunes (Cullen 1998). Thus, the amount of sand lost into this secondary sink has reduced since circa 1947.

Figure 19: View of Ocean Beach. View southwards over Ocean Beach from the dune crest near TASMARC transect 730/108 (see Figure 22), showing the very wide high-energy multi-bar breaker zone. Large slumps on recent high erosion scarps are visible along the distant dune front, and a lower scarp receding through a former inter-dune swale is active immediately below this viewpoint. Photo by Chris Sharples (2013).

In common with most western Tasmanian rivers, there is no evidence of a significant present-day supply of river sands to the beach (Nanson, Barbetti & Taylor 1995). The well-embayed location of the beach between long rocky coasts makes significant alongshore sand drift into or out of the embayment unlikely (Davies 1973), as do significant differences in sand granulometry and composition between Ocean Beach and other west coast beaches (Banks, Colhoun & Chick 1977). The only likely present-day sediment source for Ocean Beach is sand of originally Pleistocene glacial outwash provenance that is inferred to be actively driven onshore from the inner continental shelf by bottom currents associated with the large south-westerly swell, as implied by the shelf sediment mobility modelling of Harris et al. (2000); see also Harris and Heap (2014).

Swell wave climate

Ocean Beach is exposed to the most energetic and stormy wave climate of any Australian coast (Hemer 2010; Hemer, Simmonds & Keay 2008). The beach receives persistent westerly and south-westerly swells and winds with low annual directional variability that are associated with the Southern Annular Mode (SAM) (Marshall 2003). Annual mean swell wave directional variability about 5 km offshore from Ocean Beach is approximately 20° (227° - 246°T) based on the CAWCR wave hindcast (Durrant et al. 2013), but less (~5°) about 10 km offshore. A significant trend towards the positive phase of the SAM has been observed since the mid-1960s (Hemer 2010; Hemer, Simmonds & Keay 2008; Marshall 2003), resulting in a southwards movement and intensification of the Southern Ocean storm belt (Hemer, Church & Hunter 2010). However, data from the Cape Sorell wave rider buoy near Ocean Beach (Figure 18) that was analysed by Hemer (2010) showed no significant increase in swell wave height or storm frequency since 1985. This may be because the larger waves being generated further south lose more energy travelling the greater distance north to Tasmania (M. Hemer *pers. comm.*). The same southwards drift of SAM is also hypothesised to be resulting in swell waves reaching western Tasmania more frequently from more south-westerly and less westerly directions than previously, albeit confirmation of the degree of directional change at Ocean Beach is lacking because the nearby Cape Sorell wave-rider buoy does not measure wave direction.

Wind (wind-wave) climate

Westerly winds associated with SAM on the Tasmanian west coast are the strongest and most persistent prevailing winds of any Australian coast (Grose et al. 2010; Marshall 2003), exposing that

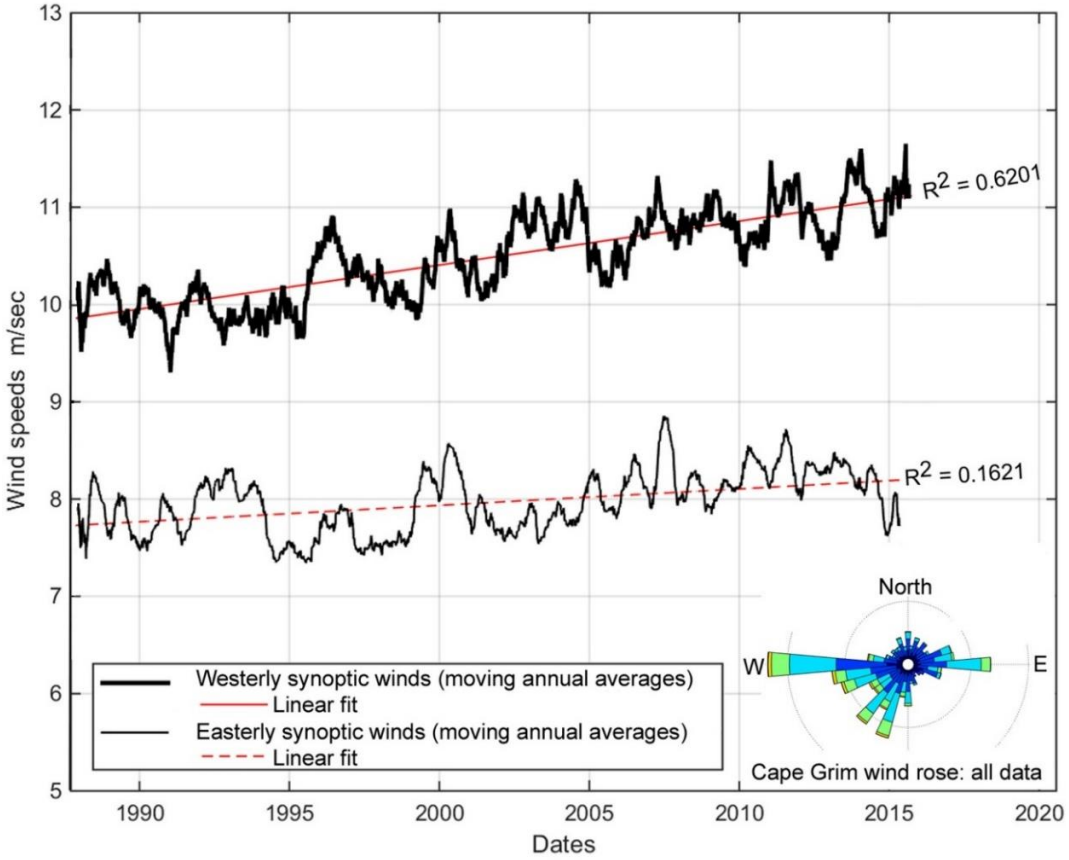

Figure 20: Moving annual averages on easterly and westerly synoptic wind speed records from Cape Grim. High quality synoptic (3-hourly) wind speed data from 1988 to 2015 shows progressive westerly wind speed increases since at least 1995, with dominantly seasonal (annual) variability in the easterly winds and longer inter-annual cycles showing significant correlation with SAM in the westerly winds (further details in appendix A1.3.8). Wind data from closer to Ocean Beach at Cape Sorell and Strahan Aerodrome (Figure 18) is suggestive of similar wind speed increases but is compromised by data gaps and step-changes presumably relating to equipment. However, it is reasonable to infer similar wind speed increases at Ocean Beach and Cape Grim since both are directly exposed to the same SAM-driven west-coast wind climate. Plots by Chris Sharples from original observational data supplied by the Australian Bureau of Meteorology (2016).

coast to strong waves and storms. Analysis of synoptic wind data from Bureau of Meteorology west coast weather stations at Cape Sorell, Strahan Aerodrome and Cape Grim for this project demonstrates a trend of increasing onshore wind speeds since at least 1995 (see Figure 20). This can be expected to have produced higher and more energetic locally generated wind-waves reaching the shore than previously and would also contribute to higher wave-setup and run-up at Ocean Beach.

Reconstructed sea-level data

Since there are no long-term tide gauge records for the west coast of Tasmania this project has used the regional sea surface height (SSH) reconstruction of Church and White (2011) and Hamlington et al. (2011) to compare reconstructed sea-level change (since ~1950) with shoreline change at Ocean Beach (Figure 26). The rates of sea-level rise determined from the closest grid cell to Ocean Beach in these reconstructions are comparable to GMSLR: linear fits to the Church & White and the Hamlington reconstructions yield SLR rates of 2.13 mm/yr^{-1}and 2.21 mm/yr^{-1} respectively over the period 1966-2009 (see Figure 181, Appendix A1.3.8). These are comparable with the global-average rise of 2.0 ± 0.3 mm yr^{-1} over the same period (White et al. 2014), providing confidence in the reconstruction data.

Figure 21: Dune-front erosion scarp at Ocean Beach. A typical recent wave-eroded dune scarp with some slumping (adjacent TASMARC transect 730/109: see Figure 22). The vegetation line at the top of the scarp (here in marram grass *Ammophila arenaria*) was digitised over air photos as the shoreline proxy, with care being taken to avoid confusing this with slumped vegetation clumps as seen here. The visible palaeosol horizon has not been dated, however the substantial period that it would have taken to form and be buried is the minimum period since this shoreline was last eroded back as far as it is now. Photo: Chris Sharples (2013).

Sea-levels around Tasmania are less influenced by seasonal and inter-annual variability related to the El Nino Southern Oscillation (ENSO) than are more northerly parts of Australia (Burgette et al. 2013), implying a reduced contribution from this driver to shoreline change at Ocean Beach compared with beaches elsewhere in Australia. Both of the SLR reconstructions used for Ocean Beach (above) show inter-annual to decadal sea surface height variability in the range of ~10-80 mm, consistent with sites having little exposure to larger modes of climate variability such as ENSO (White et al. 2014).

Vertical land movement

There are no nearby estimates of Vertical Land Movement (VLM) for Ocean Beach. Current and ongoing geodetic studies of Tasmania have yet to resolve disagreements between GNSS derived estimates of VLM at Burnie and Hobart ranging between 0.0 to -1.0 mm yr^{-1}, and geophysical models indicating subsidence in the range of -0.1 to -0.2 mm yr^{-1} (see details in Chapter 2 Section 2.5.4 above). However, for the purpose of this thesis, there is no evidence suggesting that VLM is a significant signal in Tasmanian relative sea levels. There is no anthropogenic extraction of sub-surface fluids or other known processes such as significant seismic activity likely to cause significant VLM at Ocean Beach.

Artificial disturbances

Ocean Beach is largely free of artificial disturbances that may affect geomorphic processes at the beach face and dune front. The main exception is the introduced dune-colonising grass *Ammophila arenaria* ('marram grass'), which is common in the dunes immediately backing the beach. This sand-trapping grass was deliberately planted from the 1950s to stabilise then-extensive active transgressive dunes (Cullen 1998), and may have accelerated foredune sand accretion and thus contributed to shoreline progradation prior to 1980 (Hayes & Kirkpatrick 2012); see Figure 22 & Figure 23. However, marram grass does not inhibit wave-erosion of dunes nor prevent shoreline recession.

5.2.3 Recent shoreline change history

Shoreline (vegetation line) positions for the Ocean Beach study area were digitised from ortho-rectified air photos taken at 21 dates from 1947/48 until 2010 (for exact dates see appendix A1.3.8). Shoreline position change histories were plotted along 188 shore-normal transects spaced 100 m apart, amounting to nearly 19 kilometres of beach shoreline. These were initially grouped into three areas of internally coherent histories as shown in Figure 22, and subsequently into two areas (with a small number of anomalous transects excluded as noted on Figure 22). The final two areas comprise the small south tip of the beach (which has episodically eroded and accreted but shown no long-

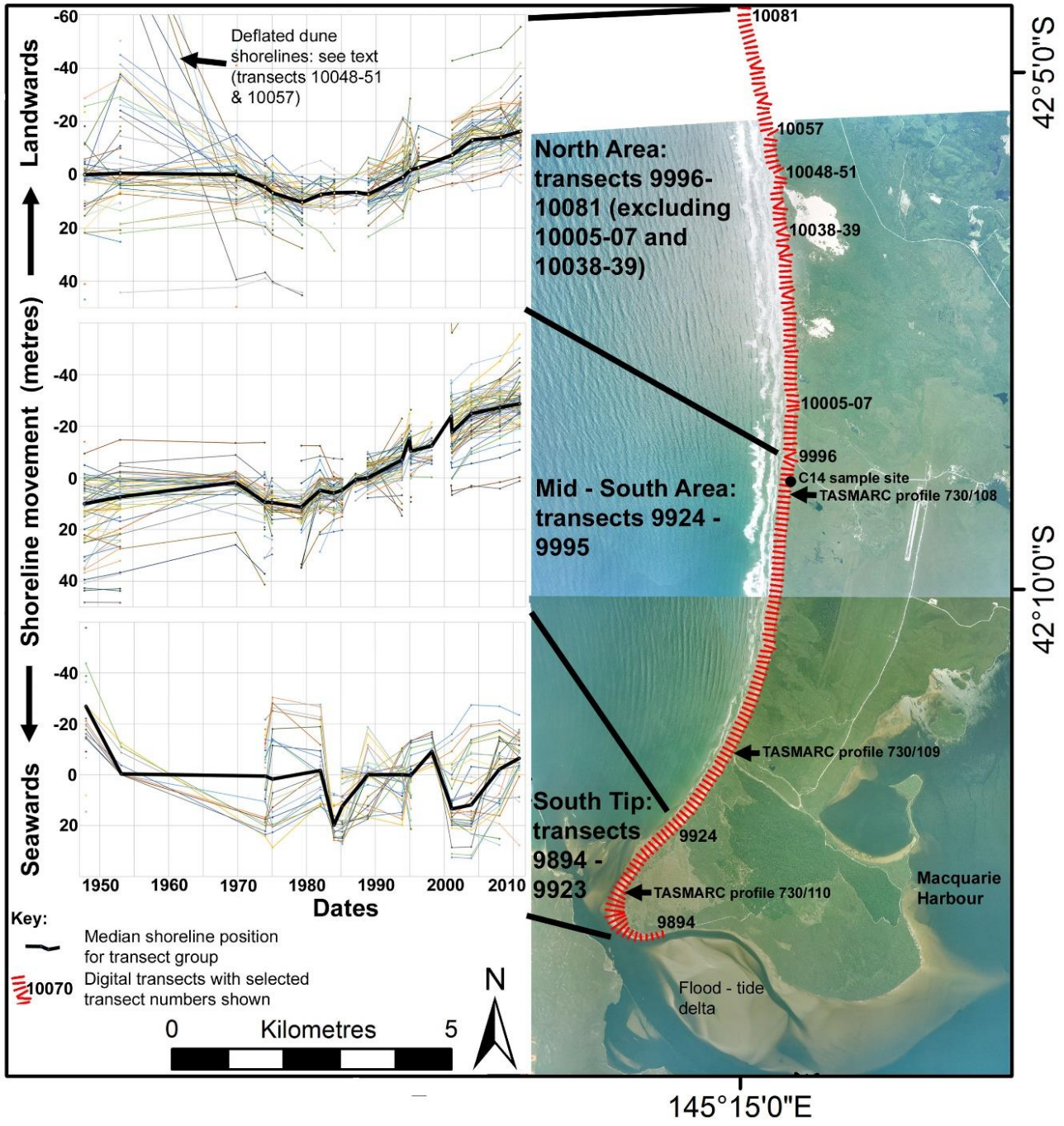

Figure 22: Air photo analysis results of shoreline horizontal movement for the whole Ocean Beach study area. Numbered digital transects (red lines) defining the study area are plotted over the 2008 air photo, and plots of all included transect shoreline movement histories are shown grouped into three areas. A few anomalous transects adjacent creek outlets and deflated areas as noted on this figure have been excluded from the analysis. Also shown are the three TASMARC beach profile locations and the peat site sampled for ^{14}C radiocarbon dating. Air photo © DPIPWE.

term trend towards either progradation or recession), and the large north to mid-south area (which has progressively and persistently receded since circa 1980). Figure 23 provides a plot of shoreline history summarised across the north to mid-south area.

The air photo analysis results (Figure 22 & Figure 23) demonstrate that from before 1947 until at least 1979 most of the study area shoreline (the north to mid-south area) was relatively stable with some erosion and accretion, including notable progradation between 1970 and 1979. This was the case despite persistent loss of sand into a large active sink as noted in the sand budget description above. Given the presence of an active sand sink, the only known explanation available for the observed shoreline stability is that the onshore sand movement from the shelf implied by the shelf sediment mobility modelling of Harris et al. (2000) was actually occurring and was sufficient to compensate for the loss of sand into sinks over this period. The increasing establishment of the introduced sand-trapping dune grass *Ammophila arenaria* probably accelerated sand capture and foredune accretion during the 1970s but did not explain the source of the sand.

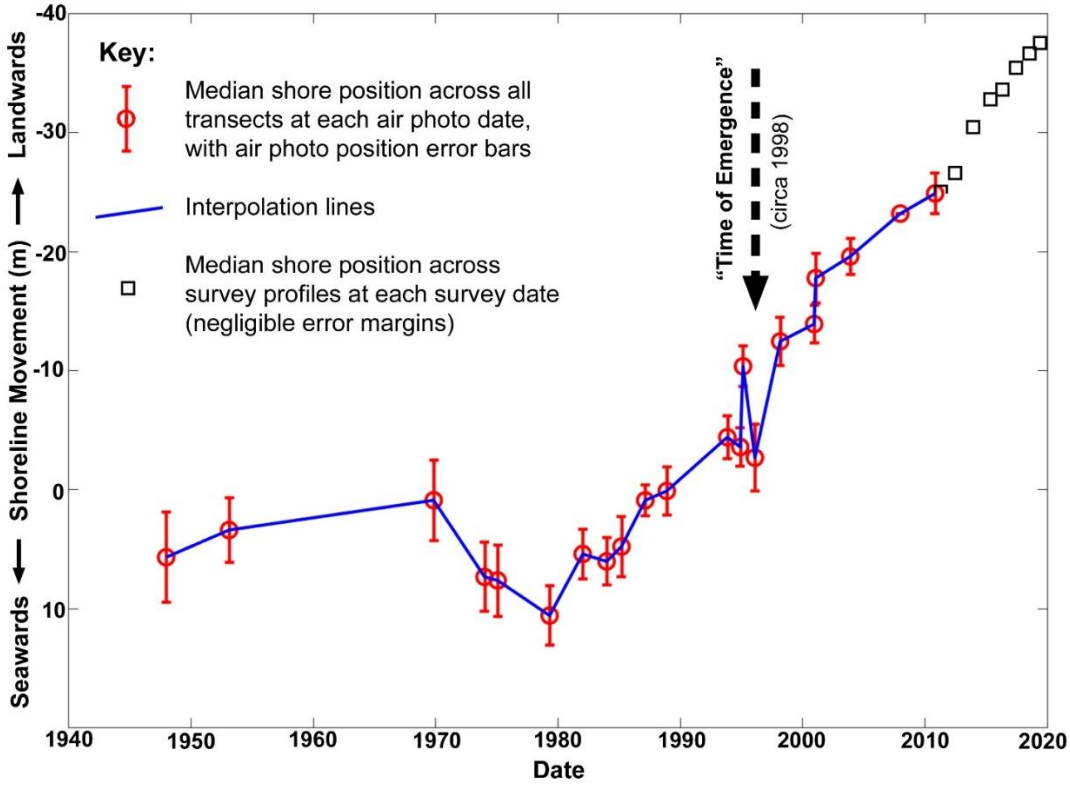

Figure 23: Summary plot of shoreline change history at the Ocean Beach study area. Circles with error bars identify the median horizontal shoreline position at each air photo date to 2010 across 153 normalised transects comprising the main (north plus mid-south) part of the study site but excluding the south tip of the beach. Squares identify the median shoreline positions across 2 beach profiles measured within the same area from 2011 to 2019 and plotted consistently with the air photo shoreline data (see details in Appendix A1.3.8).

However, at some time between the 5th May 1979 and 16th Jan 1982 air photos, Ocean Beach switched abruptly to a persistently receding shoreline which continues to recede without recovery as at 2019. The median progressive horizontal shoreline recession from circa 1980 until 2010 was approximately 35 metres (Figure 23), which is an order of magnitude larger than the mean measured air photo error margins of ±1.3 to 3.8m (Table 55), and therefore considered to be clearly significant. Although the beach underwent this marked change of long-term behaviour around 1980, the 'Time of Emergence' (Hawkins & Sutton 2012) indicated is circa 1998, this being when the recession trend signal exceeded the 'noise' of historic shoreline position variability (including error margins) and can be identified as a new long-term mode of shoreline behaviour for this beach (Figure 23).

Beach profile monitoring at two sites in the north to mid-south area demonstrates the recession trend has continued unabated from 2011 to 2019 at rates close to 1.0 m yr^{-1} on average (see Figure 24). Although direct measurements of shoreline position only extend back to 1947, ^{14}C dating of inferred back-dune swamp peats exposed in the receding shoreline scarp implies that the current degree of shoreline recession hasn't previously been reached in at least the last 1,800 years (see Figure 25). This indicates the shoreline recession since circa 1980 is of greater magnitude than any putative cyclic or episodic erosion processes affecting this beach on decadal to centennial time scales.

The southernmost tip of Ocean Beach has exhibited quite different behaviour throughout the air-photo period 1947-2010, with episodic shoreline erosion and accretion interpreted from the air photo record, but no overall trend towards either recession or progradation (Figure 22). The sand drifted south along the main part of the beach evidently accretes episodically at the southern tip prior to being permanently lost into the adjacent flood-tide delta sand sink. The TASMARC beach profile 730/110 within the southernmost tip area of the beach (Figure 24) shows the same alternating erosion-accretion pattern seen in the air photo history, continuing from 2011 to 2019.

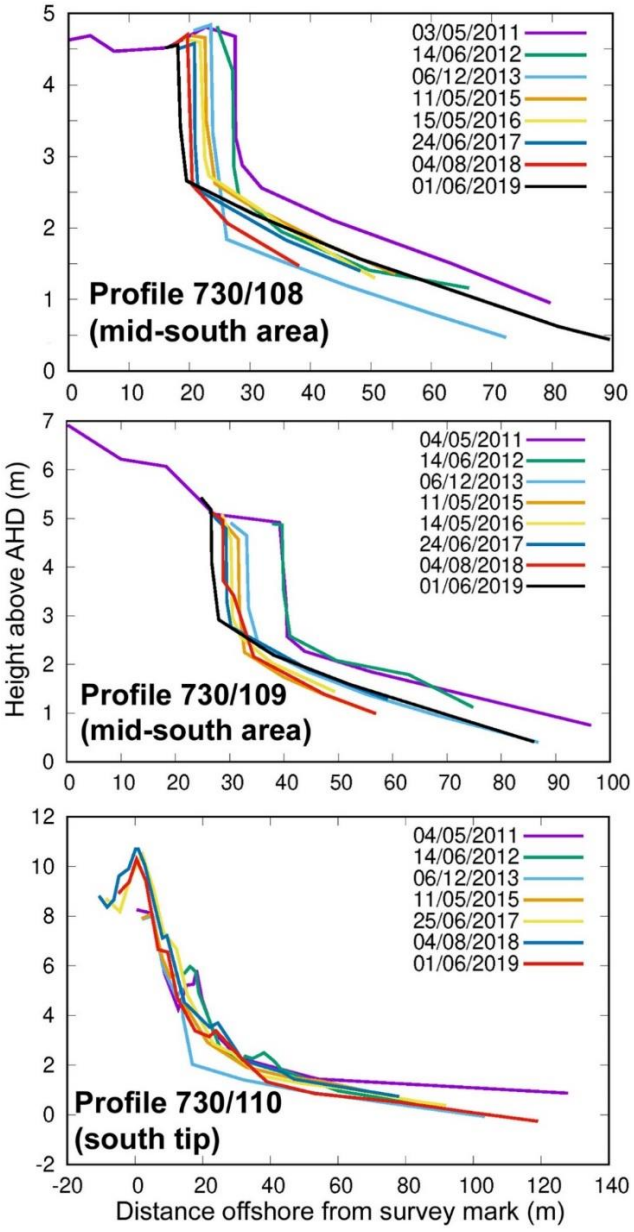

Figure 24: Simple profile plots for the three Ocean Beach TASMARC profiles (see Figure 22 for locations), showing the results of all profile surveys to 2019.

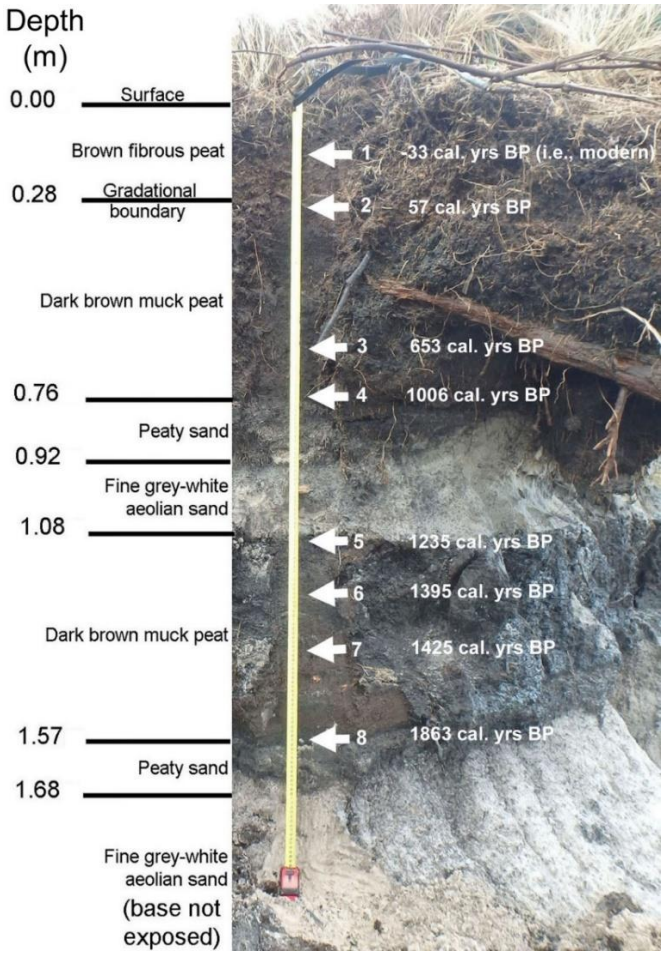

Figure 25: Peat sample profile. Sampled swamp peat profile in the active Ocean Beach erosion scarp at 42° 8.9' S 145° 15.8' E (near TASMARC transect 730/108: see Figure 22), showing facies variations with depth in metres, and location of samples 1 to 8 for which Carbon-14 dates were obtained. The median modelled calibrated age (years before present) is indicated beside each sample number. These dates imply the present extent of shoreline recession at this location is greater than has previously occurred during the last ~1800 years, otherwise the lowest now-exposed peat bed would have previously been eroded away at this position. Photo by C. Sharples.

5.2.4 Shoreline behaviour analysis: Ocean Beach

The observed switch from stability or progradation to persistent recession at Ocean Beach is comparable to that expected for sandy swell-exposed beaches in response to an onset of sea-level rise (Bruun 1962, 1988) in the absence of confounding factors. The hypothesis that the observed changes are driven by contemporary climate change-induced sea-level rise was tested by seeking and evaluating multiple alternative explanations as described under two questions in bold below.

Visual inspection and numerical analysis of relationships between the reconstructed Sea Surface Height (SSH) histories and shoreline changes at Ocean Beach (Figure 26) are consistent with a simple first-order causal relationship between sea-level rise and shoreline recession on inter-decadal time scales, as is expected from first principles (Bruun 1962). However, with first-order linear trends removed, there is no evidence of any significant correlation between SSH and shoreline position variability at shorter inter-annual time scales. In particular, the marked and rapid change in long-term shoreline behaviour which occurred between the air photo dates of 5th May 1979 and 16th Jan 1982 - from relatively stable or prograding, to continuously receding – does not correspond to any comparable variability in the SSH history. Any explanation of the marked change of shoreline behaviour at Ocean Beach that invokes sea-level rise as a cause needs to account for this.

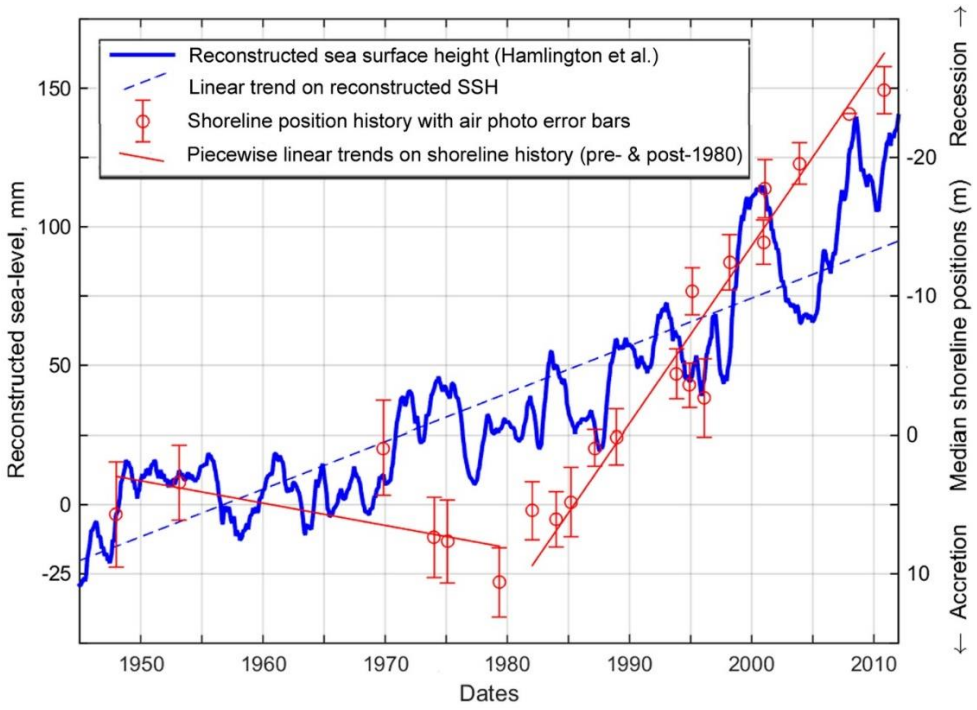

Figure 26: Shoreline position history at air photo dates and reconstructed SSH history. Error bars show the mean air photo position errors at each air photo date. A single linear trend line is fitted to the SSH history, and piecewise linear trends are fitted to the shoreline history pre- and post-1980. Further numerical analysis of this figure is provided in Appendix A1.3.8.

Are there geomorphic process conditions at Ocean Beach that would allow an earlier switch to recession in response to sea-level rise than on most open sandy coasts?

A simple hypothesis relying upon observations of the Ocean Beach process environment and supported by generalised models of geomorphic and oceanographic processes can explain the observed abrupt switch to an unprecedented degree and duration of recession at Ocean Beach as a response to sea-level rise. This hypothesis is described below and is diagrammatically illustrated in Figure 27. Other changing drivers which may be alternative or additional factors are considered in the following sub-section.

As noted in Section 5.2.2, dominantly southwards littoral drift is a major sand transport process at Ocean Beach which has evidently caused persistent and ongoing sand loss into the large active sand sink of the Macquarie Harbour flood-tide delta throughout the air photo period (Figure 22). Landwards loss of deflated sand in transgressive dunes is a secondary sink albeit it can be deduced from air photos that its capacity has reduced since 1947. However air photo evidence of shoreline stability or progradation prior to 1980 (Figure 22 & Figure 23) implies that loss of sand into these sinks must have been fully compensated for by an influx of sand from the only likely present-day sand source, namely sand actively driven onshore from the inner continental shelf by bottom currents associated with the large south-westerly swell (Harris & Heap 2014; Harris et al. 2000).

As mean sea level progressively rose at Ocean Beach during the Twentieth Century, storm wave events of any given magnitude must have more frequently reached higher and further landwards on the shore profile, over deepened water resulting from sea-level rise. Increased wave penetration would thus have eroded more sand from the upper beach and dune face than previously, with the backwash providing an increasing supply of sand to the nearshore southwards littoral drift current. This would have resulted in increasing rates of sand loss into the Macquarie Harbour sand sink. However, there is no evidence of an increased supply of sand to the beach from the shelf to compensate (for example, increased swell wave magnitudes could drive more sand onshore from the

shelf, however wave-rider buoy data show this has not occurred, at least between 1985 and 2010 (Hemer 2010); see Section 5.2.2).

With continuing sea-level rise gradually increasing the rate of net sand loss by this means, by circa 1980, Ocean Beach was probably close to losing more sand than it was gaining. A major storm or cluster of storms is inferred from air photo evidence showing approximately 5 metres of shoreline recession (erosion) between 5th May 1979 and 16th Jan 1982 (Figure 23). This could have tipped the beach into a recessional (net sand-losing) mode by removing a large mass of sand at a time when the sand budget was already close to negative. Shoreline recession has continued unabated after 1982 without any persisting shoreline or foredune recovery up to 2019 (Section 5.2.3). This reflects an ongoing and possibly still increasing sand deficit driven by ongoing SLR, further diminishing the capacity of the beach to recover between storm erosion events.

This "tipping-point" hypothesis is consistent with the finding noted above that shoreline recession and rising sea-levels at Ocean Beach are correlated trends on multi-decadal timescales (as expected from first principles), but not on shorter timescales (see Figure 26). That is to say, the observed abrupt shoreline change is unrelated to inter-annual SSH variability but is consistent with a gradually depleting sand budget (due to progressive mean sea-level rise) being tipped into a new (losing) state by a large erosion event.

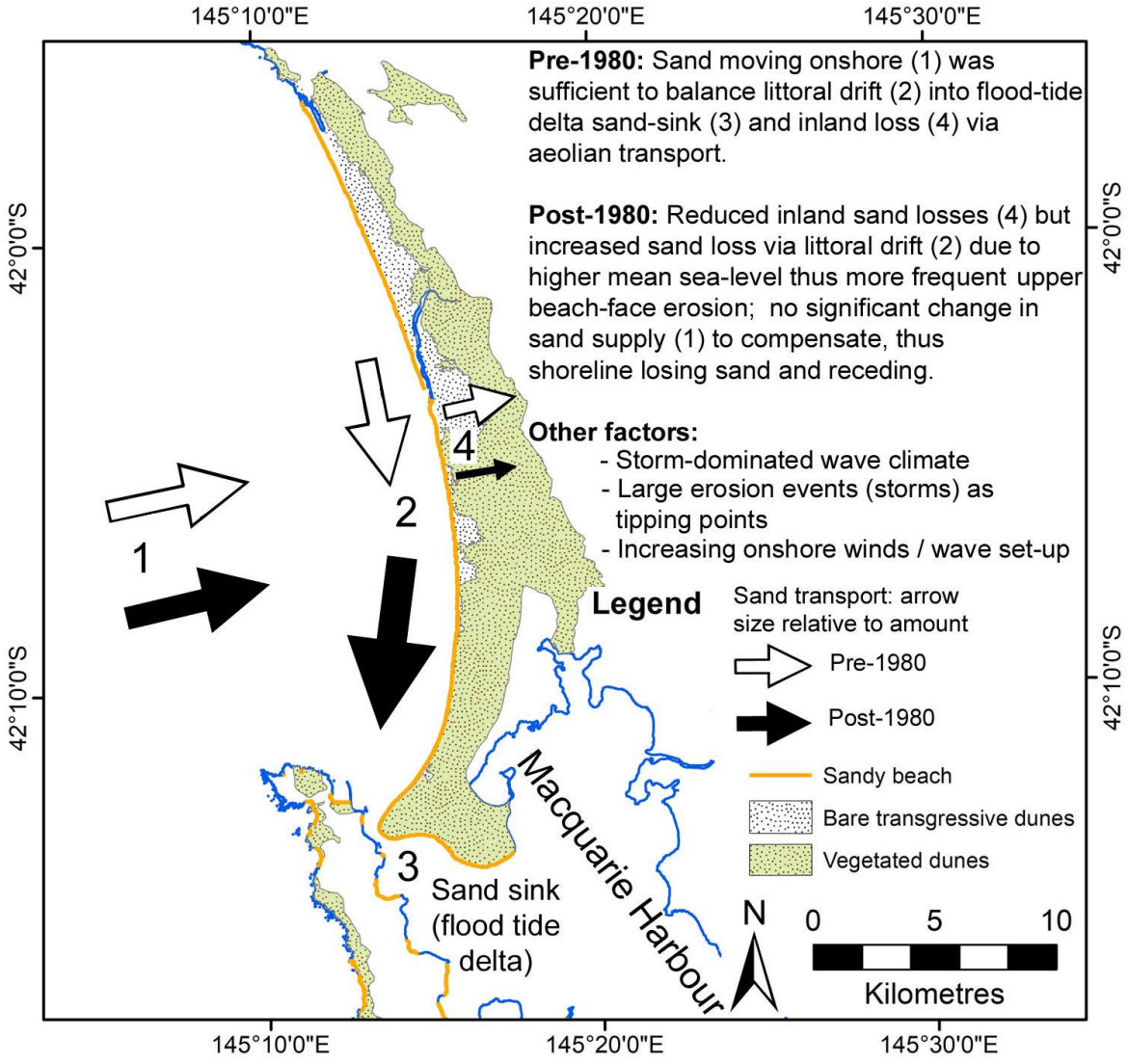

Figure 27: Shoreline change process model for Ocean Beach. See text for further explanation.

Are there drivers other than sea-level rise on this coast that could have caused the observed change in behaviour?

The alternative hypotheses listed in Table 3 have been considered and are evaluated below. No other potentially plausible explanations of the observed shoreline behaviour change have been identified.

Table 3: Alternative hypotheses investigated to explain observed changes.

Hypothesis	Evaluation (see following text)
A multidecadal variation in onshore supply of sand to the beach from the inner shelf	Not supported
Alternating sand surplus and depletion caused by sand waves or slugs moving laterally (alongshore) along the inner shelf or around headlands.	Not supported
Swell direction variability	Possible contributing factor but requires improved data and modelling to evaluate for the case of Ocean Beach.
Increased sand sink capacity	Not supported
Increased rate of southwards littoral drift into sand sink	Not supported
Increased frequency and/or magnitude of swell storms causing more erosion	Not supported
Vertical Land Movement (causing more RMSLR)	Not supported
Increased onshore winds (driving higher locally generated wind-waves)	Likely contributing factor (additional to sea-level rise)
Artificial changes	Not supported – could not cause observed shoreline changes

A multi-decadal variation in onshore supply of sand to the beach from the inner shelf would explain the observed shoreline history if it caused a marked reduction in sand supply circa 1980. Since the modelled sand supply (Harris & Heap 2014; Harris et al. 2000) is inferred to be a swell-driven process, changes in the SAM-driven swell wave climate would be the most likely explanation for any reduction. However there has been no significant change in swell wave magnitudes observed in recent decades (since 1985) at the nearby Cape Sorell wave-rider buoy which might alter rates of shelf sand mobility (Hemer 2010), and there is no known reason nor evidence available for a reduction in swell-wave magnitudes prior to 1985.

Alternatively, sand waves or 'slugs' moving laterally (alongshore) on the inner shelf or episodically around 'leaky' headlands might cause alternating sand surplus and depletion causing alternating beach accretion and erosion phases. For example, this occurs on the northern NSW coast (Goodwin, Freeman & Blackmore 2013). However, such episodes tend to recur on inter-annual to inter-decadal time scales, not in a one-time fashion as at Ocean Beach. Nor are longer-period (centennial to millennial-scale) sand-slugs a plausible explanation for the observed Ocean Beach recession, with inferences based on the dating of exposed peats (Section 5.2.3) indicating that the scale of the current erosion episode exceeds any during at least the last 1800 years. Moreover, sand slugs entering the Ocean Beach embayment would presumably need to be dominantly driven by the south-westerly swell northwards around Cape Sorell, however that headland is probably a major barrier to alongshore sand transport (as indicated by Davies 1973), rather than a 'leaky' barrier that could generate episodic sand slugs.

A lack of sand feeding alongshore into Ocean Beach from around Cape Sorell is also implied by significant differences in sand granulometry and composition between Ocean Beach and other west coast beaches noted by Banks, Colhoun and Chick (1977). The nature of shelf sand deposits off the Tasmanian west coast remain little studied beyond the inferred glacial origins of the dominantly quartz sands at Ocean Beach, and this does imply some uncertainty. Nonetheless available data does not suggest any reason to infer significant circa 1980 changes (especially reductions) in onshore or alongshore sand supply to Ocean Beach.

Swell direction variability can markedly change sand movement rates and directions causing beach rotation or new patterns of erosion and accretion on some coasts (Hemer 2009; Hemer, Church & Hunter 2010; Mortlock et al. 2017; Ranasinghe et al. 2004). However, swell wave direction

variability at Ocean Beach is very limited on both annual (seasonal) and inter-decadal time scales resulting in a mainly westerly to south-westerly swell direction (see Section 5.2.2 above). Given the relatively linear planform and roughly north-south orientation of the coastal region around Ocean Beach, the limited seasonal swell wave direction variability (which will be further reduced crossing the very wide multi-bar surf zone) is probably insufficient to cause reversals of alongshore sand movement. The expected anti-clockwise inter-decadal trend in swell directions (see Section 5.2.2) might be expected to have driven a more northerly or at least a reduced magnitude of southerly littoral sand transport through the study area since the 1970s, however this would counter-act rather than drive the observed long-term change in beach behaviour (by resulting in less sand loss into the Macquarie Harbour sand sink). Air photo time series evidence of the deflection of river mouths along Ocean Beach (see appendix A1.3.8, Table 54) shows no geomorphic evidence of any significant change in littoral drift around 1980 (or at other times).

However, there is no measured data on swell wave directions near Ocean Beach (see Section 5.2.2) and only very coarse-scale bathymetry available for the remote and largely unsettled west coast of Tasmania (100m contours mapped by Geoscience Australia: see appendix A1.3.8). This lack of base data for wave transformation modelling creates some uncertainty for estimating the degree to which swell wave direction variability may or may not change sand transport processes and shoreline positions at Ocean Beach. Nonetheless, the whole west coast of Tasmania is exposed to the same SAM-driven swell wave climate as Ocean Beach. Thus, if swell direction variability could explain the change in shoreline behaviour at Ocean Beach then similar changes should be seen on at least some of the other west coast Tasmanian beaches analysed during this thesis. However, equivalent evidence obtained during this thesis from four other similarly exposed and oriented west coast study site beaches beyond the Ocean Beach study area (see details in chapter 6 and appendix A1.3)[11] shows no comparable changes in shoreline behaviour over the same (1940s to recent) air photo period.

Another possible explanation of increased sand loss from Ocean Beach is that sea-level rise implies an increase in available sand accommodation space (water depth) in the Macquarie Harbour sand sink (flood tide delta). However, this would not have driven increased sand loss from the beach because the available space was already very large circa 1980 and not a limiting factor in the sinks capacity to sequester increasing amounts of sand. Similarly, an increasing magnitude of the southwards littoral drift currents themselves - which might explain shoreline recession as a result of increasing rates of sand loss following any erosion events – cannot be inferred from available data. This is because swell waves are inferred to be the main and most persistent driver of littoral drift at Ocean Beach, and there is no evidence of their magnitudes increasing there in recent decades, as noted in Section 5.2.2 above (Hemer 2010).

A further possible cause of a switch to increased shoreline recession would be an increasing frequency and/or magnitude of swell wave storms causing more erosion. However, a 2010 analysis of data from the Cape Sorell wave rider buoy directly offshore from Ocean Beach since 1985 found no significant change in storm frequencies or wave heights over that period (Hemer 2010; Hemer, Church & Hunter 2010). There is no known evidence for an earlier change circa 1980, and as already noted above, if such a driver of shoreline change were a key factor in the observed shoreline recession at Ocean Beach, then some similar long-term shoreline behaviour changes would be expected on other west coast study site beaches for which equivalent data is available. However, such changes have not been detected at those beaches (as described in chapter 6 and appendix A1.3).

Vertical Land Movement (VLM) can contribute significantly to regional differences in relative sea level change and hence to shoreline recession where VLM is negative (sinking). However, available evidence implies that VLM is not an explanation of the observed shoreline history at Ocean Beach.

[11] Greens Point Beach (Marrawah), Mulcahy Bay Beach, Wreck Bay Beach and Stephens Bay Beach.

Most VLM estimates for Tasmania are closer to 0.0 mm yr^{-1} than -1.0 mm yr^{-1} (Section 5.2.2). The absence of any anthropogenic influence on VLM in the Ocean Beach region (e.g., fluid extraction) further supports the conclusion that VLM is incapable of explaining the change at Ocean Beach, and particularly the abrupt onset of recession circa 1980.

Observational evidence (see Section 5.2.2) shows that onshore wind speeds on Tasmania's west coast have increased significantly since 1995 or earlier (see Figure 20). These winds would have more often than previously have produced higher locally generated onshore-directed wind waves. These would also likely contribute to higher wave set-up and run-up at the shore than previously. These factors could be expected to result in more frequent upper shoreface erosion than before. The working hypothesis proposed above for the observed shoreline behaviour change at Ocean Beach (Figure 27) assumes increasing upper shoreface erosion because waves of any given height will travel further landwards than previously over higher (deeper) water levels. Higher locally generated wind waves are an additional plausible driver of increased upper shoreface erosion.

Although some artificial influences are present at or near Ocean Beach, including exotic marram grass and pine infestations in the dunes and artificial training walls in the (permanently open) tidal entrance channel to Macquarie Harbour, there is no apparent mechanism by which any of these would have significantly modified shoreline sand erosion or transport processes at Ocean Beach. For example, although the exotic sand-trapping marram grass which has established at Ocean Beach is known to result in faster rates of foredune accretion (Hayes & Kirkpatrick 2012) it is not known to significantly modify dune erosion processes other than allowing higher erosion scarps to be produced.

5.2.5 Summary: Ocean Beach

An air photo time series for Ocean Beach has allowed determination of shoreline position changes between 21 dates from 1947/48 to 2010. The resulting shoreline history shows an abrupt change of long-term shoreline behaviour around 1980, from a stable or prograding shoreline for at least 30 years prior to an actively eroding and persistently receding shoreline afterwards. Surveyed annual beach profiles starting from 2011 demonstrate the recession was still continuing actively and unabated at 2019, nearly 40 years after the change. Dating of former back-dune swamp peats exposed in the receding erosion scarp yielded a radiometric Carbon-14 date older than 1800 years BP from the oldest (lowest) exposed peats. It can be inferred from this date that the current degree of landwards shoreline retreat is greater than during any previous recession cycles or episodes that have occurred within the last 1800 years, since otherwise the peat beds now exposed would have previously been destroyed by erosion.

This investigation has identified contemporary sea-level rise and increasing onshore winds as climate-related drivers either or both of which could explain the observed change of shoreline behaviour at Ocean Beach. Since both are actively changing processes at Ocean Beach, it is likely that both are contributing in some degree to the shoreline changes, however in the absence of good quality, high resolution data on some key parameters such as bathymetry to support quantitative analysis or numerical modelling, the relative contribution of each cannot be quantitatively determined.

The hypothesis proposed to explain the changing shoreline behaviour implies that several unusual conditions in the Ocean Beach geomorphic environment have enabled shoreline recession to occur in response to recent climate change-driven sea-level rise and wind speed increases without being masked or counter-acted by other normally-dominant processes, such as post-storm beach accretion and foredune recovery.

Arguably the most important of these conditions is the presence of the large active unfilled sand sink of the Macquarie Harbour flood-tide delta and an active sand transport pathway (persistent

southwards littoral drift) delivering increasing quantities of sand to that sink. As storm waves of any given size are enabled to reach further landwards over rising (deeper) water levels than before, sand is eroded from higher on the shoreface and lost into the persistent littoral current more frequently and in larger amounts than previously. This means that eroded sand is increasingly being lost from the beach system via mostly one-way littoral drift, faster than it can be returned to the beach following erosion events. Hence as the frequency and magnitude of erosion events increases due to higher sea-levels and thus higher storm wave levels, the rate of net sand loss will increase. This results in greater susceptibility to shoreface recession as an unchanging rate of onshore sand gain from the shelf becomes increasingly insufficient to compensate for sand losses. In other words, decreasing amounts of beach recovery that might mask physical beach responses to sea-level rise occur between increasingly frequent erosion events.

Ocean Beach is also exposed to a more highly energetic and storm-dominated wave climate than nearly all other beaches in Australia (Hemer 2010; Hemer, Simmonds & Keay 2008). Under conditions of frequent stormy or large-wave events, a relatively small rise in the mean sea level will trigger more frequent erosion events higher than before on the beachface than would occur under a less frequently stormy wave climate. Where an active sand sink is also present, eroded sand will feed into the sink faster than would occur under less stormy wave climates, reducing the capacity of beach recovery (sand accretion) processes to prevent shoreline recession.

These two factors are unusual in their degree and interaction at Ocean Beach and are inferred to be primary factors enabling an early morphological response to contemporary climate change-driven sea-level rise at this site. Ocean Beach is also exposed to relatively low inter-annual sea-level variability and to limited swell wave directional variability, both of which may be additional factors increasing that beach's susceptibility to exhibiting changes due to sea-level rise and/or increasing wind speeds

The amplitude of interannual variability in the Twentieth Century SSH reconstructions for Ocean Beach is ~10 to 80 mm (see Figure 26), which is low compared to interannual SSH variability typically in the range of 100 to 400 mm for Australian coasts having more exposure to dominant modes of climate variability, especially ENSO (see White et al. 2014, Fig.3). This means that ENSO makes less contribution to RMSL variability at Ocean Beach than it does on most other Australian coasts, mitigating it as a potential source of process noise which may mask or overwhelm the contemporary global climate change-driven sea-level rise signal.

Many coasts such as the mainland coast of eastern Australia are prone to seasonal and inter-annual swell wave direction changes of 100° or more (Mortlock & Goodwin 2015a; Mortlock et al. 2017). Swell direction variability on this scale can force alongshore sand transport reversals and large-scale beach rotation (Ranasinghe et al. 2004; Short, Trembanis & Turner 2000), resulting in episodic physical changes to sandy beaches that may be orders of magnitude greater than expected recent effects of sea-level rise (Stive, Cowell & Nicholls 2009). Consequently no sea-level rise signal is expected to be detectable in the physical behaviour of such beaches in the near future (Mortlock & Goodwin 2015a). In contrast, the much lesser swell direction variability on the Tasmanian west coast (approximately 20° annual variation at Ocean Beach: Durrant et al. 2013), combined with the relatively linear and dominantly north-south orientation of that coast, mean that alongshore sand transport reversals and beach rotation are unlikely in most locations and so less likely to obscure a sea-level rise signal in coastal behaviour.

5.3 *Study Area 2: Roches Beach*

5.3.1 Introduction

Roches Beach is located within the long broad south-opening coastal re-entrant of Frederick Henry Bay, on the eastern side of a low sandy isthmus linking South Arm peninsula to the mainland of south-eastern Tasmania, and about 14 km ESE of Hobart city (see Figure 17 & Figure 28). Roches Beach is an example of another of the four broad categories of coastal landform type from which study sites were selected for this thesis (namely "other swell-exposed sandy beaches" as described in Section 3.2.1 and listed in Table 2 above). This section follows the same structure as Section 5.2 above, presenting the essential data and findings of an investigation of shoreline behaviour at Roches Beach since the 1940s. Additional supplementary data and information about this site is provided in Appendix A1.4.2.

Much of the township of Lauderdale is situated on the lowest parts of the sandy isthmus behind Roches Beach and has historically been subject to both coastal erosion (at Roches Beach) and coastal flooding hazards (Sharples 2006). Numerous dwellings are situated on the foredune immediately behind the main 3.5 km long stretch of Roches Beach, making Lauderdale one of Tasmania's most at-risk coastal townships from a sea-level rise perspective. Shoreline erosion has been a concern for residents since the 1970's, and a boulder revetment currently protecting backshore areas behind the southern end of the beach was constructed in stages during the 1980s. The earliest major investigation of erosion at Roches Beach was conducted by Foster (1988), and the continuation of active shoreline recession from that time until 2011 resulted in a series of subsequent consulting reports including Byrne (2006), Cromer (2006), Sharples (2010) and Shand and Carley (2011).

Subsequent to a major erosion event at Roches Beach during July 2011, the local government (Clarence Council) has utilised beach scraping and sand replenishment to maintain the beach and foredune while investigating longer-term options to artificially protect the beach. As a result, this study only utilises beach change data up until July 2011 since subsequent changes have been dominantly driven by artificial interventions which have prevented the ongoing recession that otherwise might have continued to the present.

5.3.2 Site description and processes

Geomorphic description

Roches Beach (147° 29' 0" E 42° 54' 0" S) comprises several east-facing sandy beaches separated by small rocky outcrops. The longest of these is a 3.5 km long drift-aligned zeta-form beach beginning in the lee of rocky Mays Point at its southern end and running northwards to rocky Bambra Reef (see Figure 28). This study has divided Roches Beach into five distinctive sections based on differing long-term shoreline behaviour histories over approximately the last 70 years, as revealed by air photo time series analysis (see Figure 32). Attention is focussed primarily on two of these sections which contrast strongly in their behaviour, namely the long Roches Beach Main Central section which has changed its long-term behaviour from stable to receding, and the Roches Beach North section which has maintained its stable shoreline position (with small erosion and recovery cycles) throughout the air photo period (see Figure 32). The contrast in historical behaviour between these two sections reveals much about the sand budget and coastal processes at Roches Beach.

The main central 2.1 km length of Roches Beach is backed by a single 2 to 3 m high foredune which in turn fronts a low prograded beach-ridge plain with unconsolidated sands presumed to extend vertically to below present sea-level. There have been no detailed studies of the structure, age and

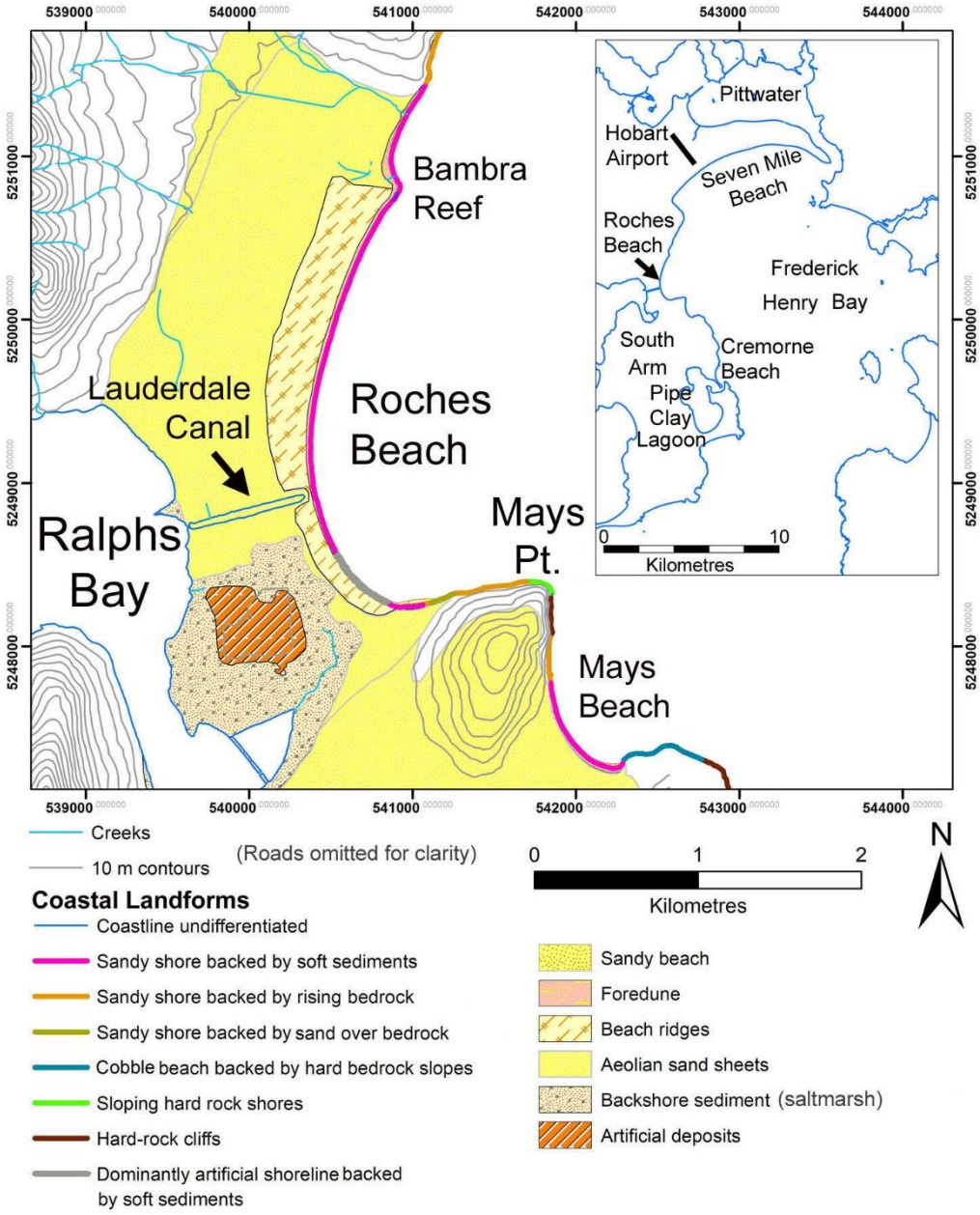

Figure 28: Geomorphic map of Roches Beach. Inset shows the context of Roches Beach within the large coastal re-entrant of Frederick Henry Bay, which opens southwards into the ocean-exposed region of Storm Bay. Shoreline landform mapping by Chris Sharples, soft-sediment polygons based on Davies (1959, 1961). Beach sections defined for the purposes of this analysis are shown on Figure 32 below.

origins of this beach; however, Davies (1959, 1961) inferred that it developed in mid- to late-Holocene times following the post-glacial marine transgression, with the development of a larger foredune at a currently undated time signalling the end of a phase of shoreline progradation and the onset of a period of relative shoreline stability.

Swell wave climate

Roches Beach receives refracted swell at its location approximately 15 km northwards inside Frederick Henry Bay from ocean-exposed Storm Bay (Figure 29). South-westerly swells from the Southern Ocean and south to south-easterly swells from the Tasman Sea (Carley et al. 2008) are attenuated and trained by the long northwards refraction pathway up the bay, exhibiting low average

Table 4: Key swell wave climate parameters for Roches Beach, from the Bureau of Meteorology Australia and CSIRO Australia CAWCR wave hindcast 1979-2010 (Durrant et al. 2013). These figures apply to the centre of the two closest inshore ~5km grid cells to the beach, which in both cases are approximately 4 km from the centre of the beach

	Annual	Summer (DJF)	Winter (JJA)
Average Significant wave height (m)	0.21 (0.16 – 0.26)	0.20 (0.16 – 0.24)	0.22 (0.17-0.27)
Average Maximum wave height (m)	0.62 (0.72-0.52)	0.56 (0.63-0.49)	0.65 (0.77-0.54)
Average Mean wave direction (ºT)	176 (175-178)	174 (173-175)	176 (174-179)

annual significant wave heights (<0.3 m) and very little directional variability by the time they reach Roches Beach (see Figure 29 & Table 4). The swell refracts around Mays Point (Figure 28) into the main drift-aligned zeta-form embayment of Roches Beach, driving a persistent northward littoral current into, through and out of the embayment (Shand & Carley 2011).

Wind (wind-wave) climate

There are no reliable long-term wind records from or directly pertinent to Roches Beach, with the nearest Bureau of Meteorology weather station at Hobart Airport being subject to very different low-level local wind patterns resulting from topographic steering effects (see Section 5.5.2 below). However other evidence indicates that Roches Beach dominantly receives north-westerly to south-westerly winds characteristic of the broader Hobart region: in particular the orientation of recently stabilised transgressive dunes in the eastern part of the Seven Mile Beach sandy barrier, approximately 10 km directly north-east of Roches Beach across Frederick Henry Bay (Figure 29), are indicative of dominantly westerly and south-westerly wind directions blowing across the bay from the area of Roches Beach (Donaldson 2010). Foster (1988) noted that wind directions measured at Hobart during known pre-1988 storm events at Roches Beach were mainly north-

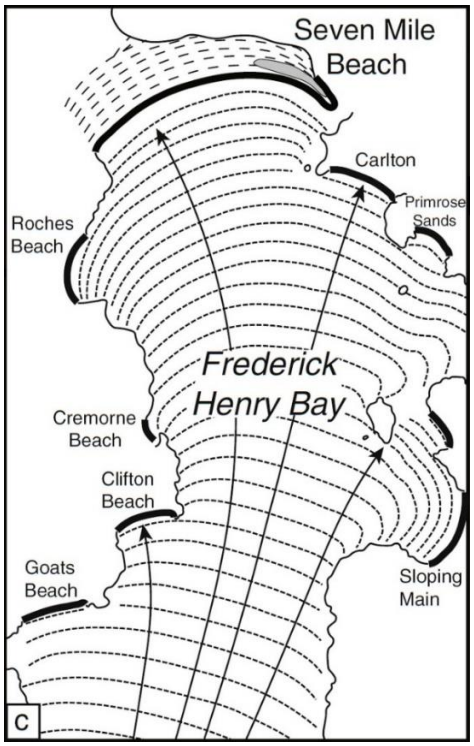

Figure 29: Swell wave refraction diagram for Frederick Henry Bay. This map demonstrates that most sandy beaches in Frederick Henry Bay are swash-aligned, with Roches Beach, the smaller Mays Beach (not shown) and Cremorne Beach being the most notable drift-aligned beaches. Grey stipple at the eastern tip of the Seven Mile beach barrier represents recently stabilised transgressive dunes. Reproduced from Oliver et al. (2017), based on original map by Davies (1958).

Figure 30: View north along the main part of Roches Beach several hundred metres north of the canal. This view taken 2010 shows the typical narrow beach face and scarped foredune front as it was over a period of direct observations by the author from 2001 until July 2011. Throughout this period the erosion scarp showed occasional slumping and minor indications of incipient dune recovery but was dominated by progressive retreat owing to numerous small erosion cuts. The incremental exposure of the tree stump visible in this photo was photo-monitored by the author between 2004 (when the tree was still growing, and its roots were just beginning to protrude from the scarp) until July 2011 when the root ball became completed undermined and separated from the scarp by a large erosion event. Photo by Chris Sharples, 6th March 2010.

westerly to south-westerly, as is typical given the prevailing westerly airflow across Tasmania (Grose et al. 2010). These winds would have been directed offshore at Roches Beach and hence resulting wind-waves would have had little or no effect on Roches Beach. The most common storm pattern at Roches Beach is evidently that large (erosive) swell storms are typically associated with south-westerly winds that are offshore-directed at Roches Beach, resulting in no effective wind-waves at the beach during the swell storms (see appendix A1.4.2,). Modelling by Shand and Carley (2011) also indicated that wind waves have little influence on littoral drift and sand movement through the embayment.

Erosion of Roches Beach by onshore-directed easterly to north-easterly wind-waves has been recorded or can be inferred on at least two occasions, but is evidently rare compared to erosion by swell-wave storms refracted northwards up Frederick Henry Bay (see Appendix A1.4.2, Table 64). No quantitative storm frequency and magnitude data is available for Roches Beach.

Sand transport and budget

Marine habitat mapping by the University of Tasmania's SEAMAP project (see Appendix A1.4.2, Figure 195) shows the low-gradient and mostly relatively shallow (<20 m) floor of Frederick Henry Bay is the likely source of sand that is driven northwards through Frederick Henry Bay by swell-driven currents, ultimately reaching Seven Mile Beach from where some of it was until recent decades transported across that beach barrier into Pittwater by aeolian processes in active transgressive dunes (Watt 1999).

On the western margin of Frederick Henry Bay, geomorphic evidence and littoral drift modelling by Shand and Carley (2011) indicate the dominant sand transport process at Roches Beach is a persistent northwards swell-driven littoral drift transporting sand around Mays Point into the drift-aligned embayment, across it and northwards along the shore, and then out of the embayment around

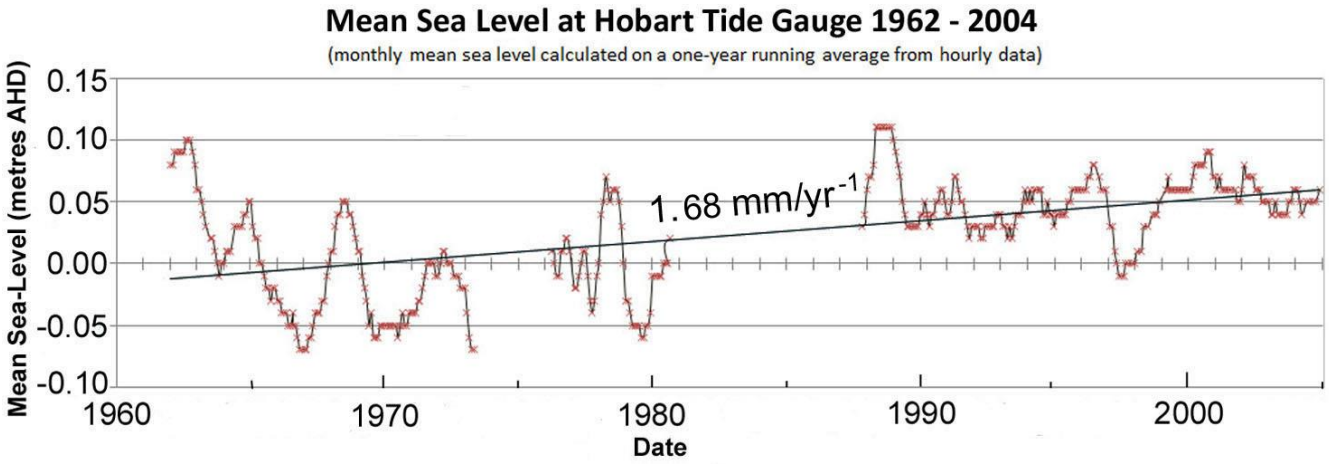

Figure 31: Mean sea level at the Hobart tide gauge, 1962 – 2004. A simple linear fit is shown plotted to the data, yielding a mean sea-level rise rate of 1.68 mm/yr^{-1} over the data period. This is the closest tide gauge record to Roches Beach. Although the Hobart tide gauge is over a century old, the data plotted here is the only reliable data up to 2004, owing to unsurveyed gauge and datum shifts. This data was processed and supplied by Dr John Hunter, from original tide gauge data.

Bambra Reef (Figure 28)[12]. In this way sand from the main central Roches Beach embayment is irreversibly lost northwards into an active sand sink with considerable capacity to continue accepting increased amounts of sand into the future.

Sea-level data

The nearest measured sea level data to Roches Beach is from the Hobart tide gauge record, located in the lower Derwent River estuary about 13km west of Roches Beach. Although Roches Beach is located in a different coastal embayment to the Hobart tide gauge it is reasonable to infer a similar sea-level history given these locations are in adjacent broad tidal swell-exposed embayments which both open to the ocean at nearby Storm Bay.

The rate of mean sea-level rise inferred from a calculated linear fit to the Hobart tide gauge record (Figure 31) is 1.68 mm/yr^{-1} over the period 1962-2004, which is comparable with the global-average rise of 2.0 ± 0.3 mm yr^{-1} over the 1966 – 2009 period (White et al. 2014). The rate at the Hobart tide gauge is similar to the rate observed at the climate quality gauge located at Burnie (1.4 mm/yr^{-1}, approximately 235 km away: see Section 5.4.2) and for Ocean Beach computed from reconstructed data (2.13 – 2.21 mm/yr^{-1}, approximately 190 km away: see Section 5.2.2) over approximately the same period. Additional information on the Hobart tide gauge record is provided in Appendix A1.4.2.

Vertical land movement

Current and ongoing geodetic studies of Tasmania have yet to resolve disagreements between GNSS derived estimates of VLM at Burnie and Hobart[13] ranging between 0.0 to -1.0 mm yr^{-1}, and geophysical models indicating subsidence in the range of -0.1 to -0.2 mm yr^{-1} (see details in Chapter 2 Section 2.5.4 above). However, for the purpose of this thesis, there is no evidence suggesting that VLM is a significant signal in Tasmanian relative sea levels. There is no anthropogenic extraction of

[12] The sand transport capacity of this littoral drift current is anecdotally illustrated by the fact that a failed shipping canal that was controversially excavated between Ralphs and Frederick Henry Bays during 1924 (Figure 28) was notoriously blocked at its eastern end by sand drifting along Roches Beach within days of its completion, and subsequent attempts to re-open it were again thwarted by the persistent sand drift (Alexander 2003, p. 161).

[13] The Hobart GNSS site is located at Mt. Pleasant, ~10 km north of Roches Beach

sub-surface fluids or other known processes such as significant seismic activity likely to cause VLM in the region of Roches Beach.

Artificial disturbances

Except for a boulder revetment wall constructed during the 1980s along a southern section of the main Roches Beach (see Figure 28), no other local artificial disturbances are known to have significantly affected sand movement associated with the beach and foredune front prior to July 2011 (further details provided in Appendix A1.4.2). However, following a major erosion event during July 2011, the local government (Clarence City Council) has implemented a policy of scraping and replenishing beach and dune sand at Roches Beach, hence as this study does not use shoreline data after that date.

5.3.3 Recent shoreline change history

Air photos taken at 30 dates from 4th April 1946 until 15th July 2011 have been used in this analysis (details in appendix A1.4.2, Table 65). The last photo was captured immediately after a large erosion event on the 9th – 10th July 2011. Shoreline positions (the seawards *in situ* vegetation line as outlined in Section 3.3.2) were digitised at each air photo date along approximately 5 kilometres of sandy shoreline excluding end sections backed by rising hard bedrock slopes. From these, shoreline change histories were plotted at 100 m – spaced transects. The shoreline transects were clustered into five beach sections based on visual comparison of transect histories. Each section displays a distinctive history (see Figure 32). Note that of the five beach sections described here, only two of these sections – Roches Beach North and Roches Beach Main Central – are listed in Chapter 4 and further analysed in Chapter 6 and elsewhere as the two key study sites in the Roches Beach Study Area.

Based on the air photo time series analysis whose results are illustrated in Figure 32 to Figure 34 following, the historic behaviour of each of the five beach sections is summarised as follows:

Roches Beach North This sandy beach is north of Bambra Reef and is backed by unconsolidated sands to below present sea-level. Figure 32 shows a stable shoreline position with repeated small erosion and recovery cycles but no long-term behaviour changes nor significant trend to either progradation or recession.

Bambra Reef Nearshore Intertidal bedrock reef with sandy beach and dune shore on landwards side, backed by unconsolidated sands to below present sea-level. Stable shoreline position with episodic erosion and recovery but no long-term behaviour changes nor significant trend to progradation or recession.

Roches Beach Main Central This major portion of the large zeta-form embayment between rocky Mays Point and Bambra Reef abruptly underwent a major long-term change of behaviour between the air photo dates in 1984 and 1986 (see Figure 33 and Figure 34). The earlier part of the air photo record shows a shoreline position history comprising at least 38+ years of approximately stable shoreline positions with small erosion and recovery episodes but no significant trend to either recession or progradation (uncertainty indicated on Figure 34 is approximately twice the slow recession rate indicated). There was then an apparent erosional step-change between 1984 and 1986, co-incident with at least two major shoreline erosion events listed and described by Foster (1988) as 'severe' (see Figure 33). This was followed by a progressively receding shoreline trend, most of which is beyond (further landwards than) the limits of pre-1985 shoreline positions (including error margins) and thus represents a significant change in long-term shoreline behaviour (see Figure 34). This recession trend continued in a progressive but stepwise fashion with some periods of partial

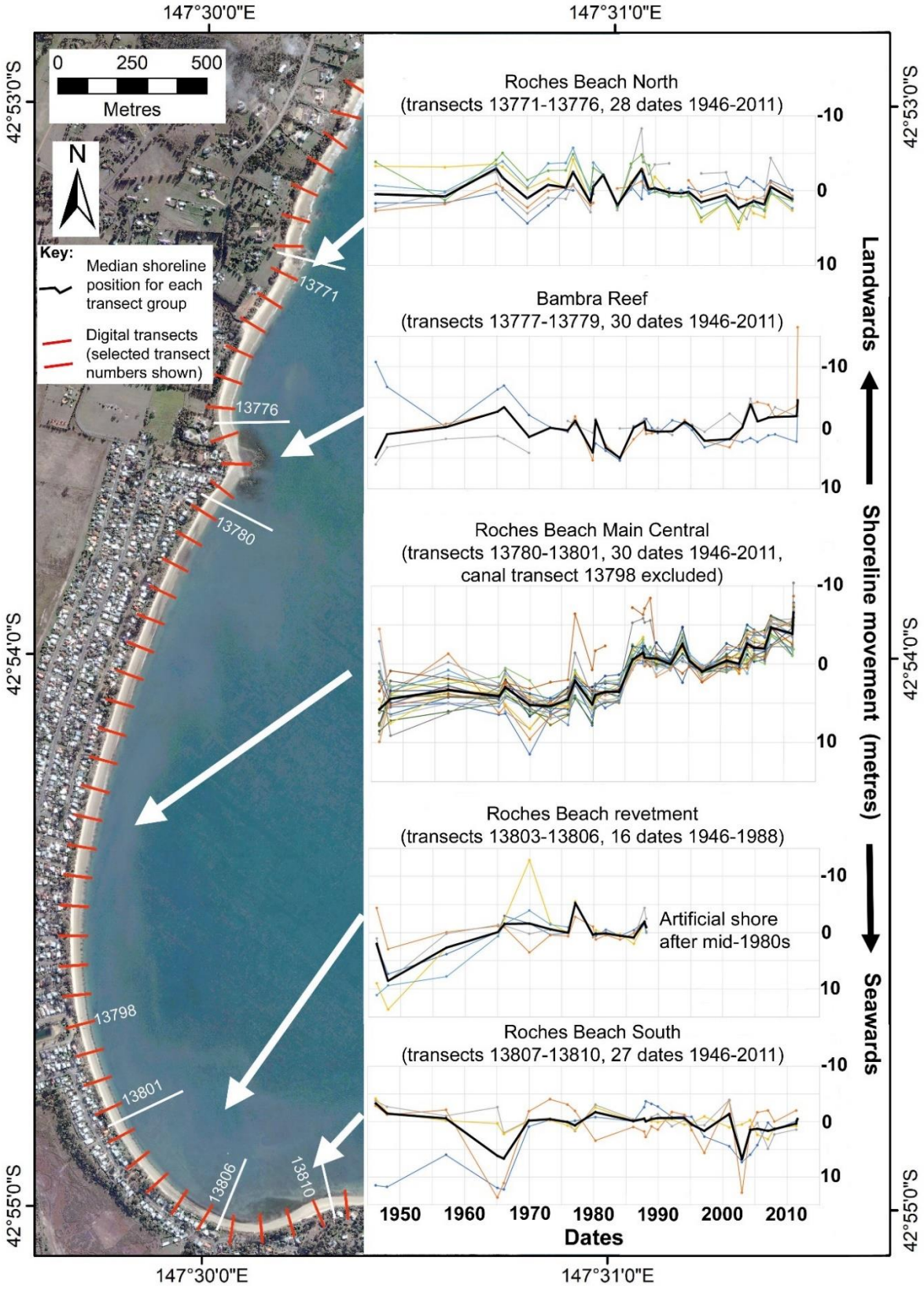

Figure 32: Plots of shoreline (vegetation line) movement histories along each digital transect (red plot lines) at Roches Beach at up to 30 air photo dates over the period 1946 to 2011 (plotted relative to the median shoreline position on each transect). Transects are plotted in five groups (bounded by white lines) which each exhibit distinctive shoreline behaviour. Some beach sections were not covered by air photos at all 30 dates (as indicated on the figure). The beach image is the May 2005 Quickbird satellite image.

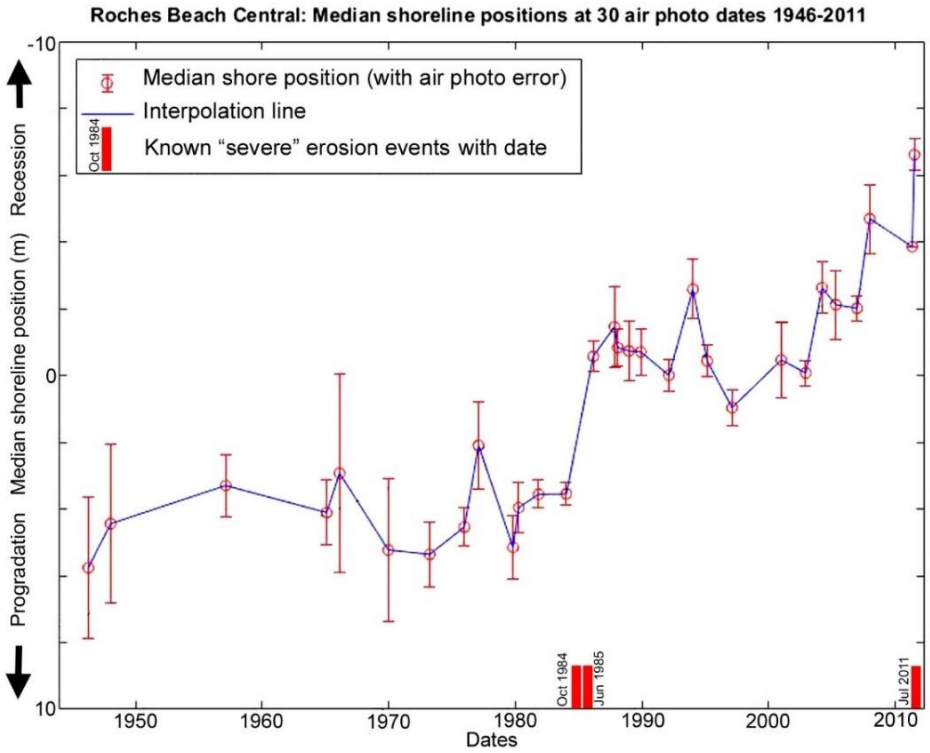

Figure 33: Summary plot of shoreline change history across all transects except 13798 (disturbed canal zone) in the main central area of Roches Beach (as shown on Figure 32) at 30 air photo dates from 1948 to 2011. These plot the median of the normalised shoreline positions measured across all included transects for each air photo date. Known erosion events independently characterised as 'severe' are indicated (from Table 64), and some other erosion events can be inferred from 'steps' in the shoreline position change record. However, this figure is not an exhaustive indication of all known erosion events (as listed in Table 64).

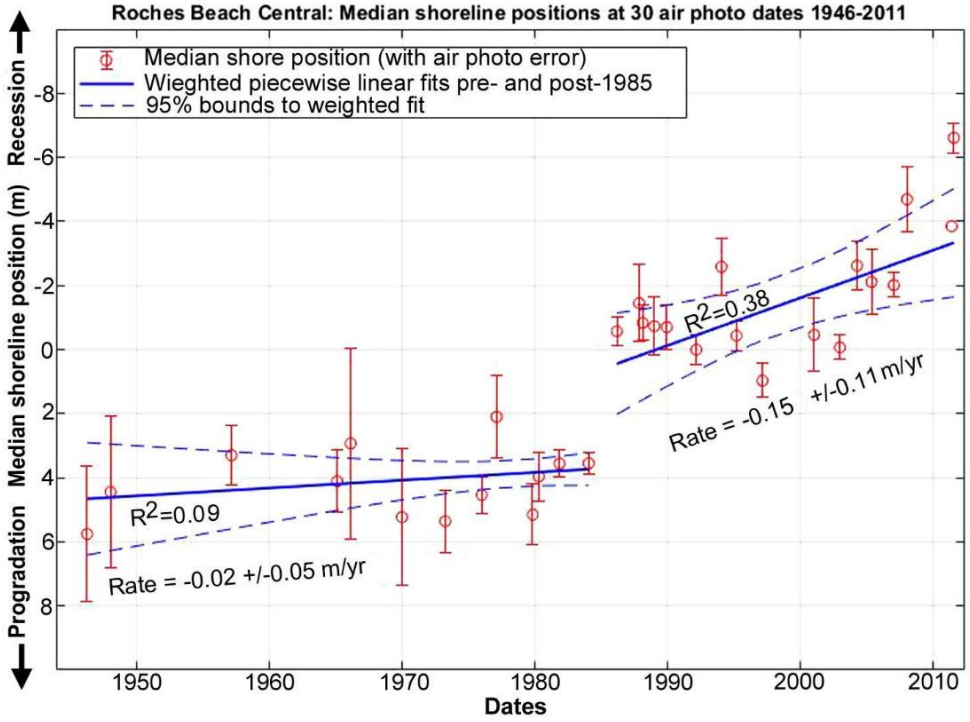

Figure 34: Error-weighted piecewise linear fits to shoreline position data for the main central part of Roches Beach pre- and post-1985. The shore position data shown comprises median shoreline positions at each air photo date across all central Roches Beach transects (except canal transect 13798) at 30 air photo dates from 1946 to 2011.

recovery for 25 years, before being artificially halted by beach replenishment and management works following the large erosion event during July 2011[14].

Roches Beach Revetment The southern part of Roches Beach just north of the "hook" of the main zeta-form embayment was subject to several significant erosion events prior to construction of a boulder revetment (seawall) during the 1980's (Foster 1988). See also appendix A1.4.2, Table 64. At least one of these events was likely driven by unusual north-easterly wind waves rather than swell waves. Nonetheless this shoreline section appears to have been mostly in a stable dynamic equilibrium prior to the revetment construction, and subsequently has been artificially stable except for lowering of the beach face in front of the revetment.

Roches Beach South The southern end of Roches Beach in the "hook" of the zeta-form embayment has episodically been a store or temporary sink for sand trapped after being driven into the lee of Mays Point by strongly refracted swell waves or moved southwards along the southern end of the main beach by littoral drift generated by occasional north-easterly wind-waves. A wide beach has been episodically present in this area but is occasionally scoured out (presumably during storm events), resulting in a shoreline history exhibiting episodic accretion and erosion, but no apparent long-term trend or change of trend towards either recession or progradation (Figure 32).

Summary The northern and southern ends of Roches Beach have been essentially stable over the air photo period since 1946, with some erosion and recovery (accretion) cycles but no long-term trends towards either progradation or recession, and no evident changes of long-term behaviour. In contrast the major central portion of Roches Beach which makes up the most swell-exposed section of this zeta-form embayment underwent a marked and abrupt change in long-term behaviour between 1984 and 1986, from a stable dynamic equilibrium before 1985 to a significant stepwise progressive recession trend from 1986 to 2011. After July 2011, artificial interventions halted the recession.

It is noteworthy that the main central part of Roches Beach is the only beach in Frederick Henry Bay known to have exhibited a long-term change in shoreline behaviour from stability to a near-continuously active erosion scarp undergoing progressive long-term (25 years+) recession, based on the authors observations of most of these beaches over the last 20 years approximately and air photo data for several beaches reported in Sharples et al. (2012) and Thom et al. (2018). Other beaches in Frederick Henry Bay have exhibited long-term shoreline position stability throughout the mid-twentieth century to recent period, with occasional erosion cuts followed by full shoreline recovery over a period of some years. This implies that the persistent recessional behaviour of Roches Beach (Main Central section) is at least partly dependent on processes or characteristics specific to that beach.

5.3.4 Shoreline behaviour analysis: Roches Beach

The observed switch from stability (or dynamic equilibrium) to persistent recession in the main central section of Roches Beach is comparable to changes expected for sandy swell-exposed beaches responding to an onset of sea-level rise in the absence of confounding factors (Bruun 1962, 1988). Since all of Roches Beach is subject to the same sea-level rise history, this implies that other factors sufficient to prevent a similar shoreline change strongly influence the other sections of Roches Beach that have not shown the same changes. The working hypothesis that the observed changes are

[14] A linear fit to the whole summary plot data series for Roches Beach Main Central (appendix A1.4.2, Figure 204) yields a better correlation co-efficient (R^2=0.71) than found for the piecewise "before" and "after" data series shown on Figure 34. Despite this, visual inspection and interpretation of the data series including consideration of error margins (Figure 33), together with piecewise analysis as shown on Figure 34, indicates that a distinct erosional step-change occurred between 1984 and 1986 separating different long-term shoreline behaviour trends.

driven by contemporary climate change-induced sea-level rise was tested by seeking and evaluating multiple alternative explanations under the two sub-headings below.

Are there geomorphic process conditions at Roches Beach that would allow an earlier switch to recession in response to sea-level rise than on most open sandy coasts?

This section proposes a working hypothesis which explains the abrupt change of shoreline behaviour apparent in the shoreline history of Roches Beach as being driven by contemporary climate change-induced sea-level rise. This hypothesis was originally proposed by Sharples (2010), and is illustrated diagrammatically on Figure 35.

The main sand transport processes at Roches Beach are cross-shore sand transport (offshore during erosive swell-storms, swell-driven onshore during fair weather), and a persistent swell-driven northwards littoral drift of sand into, through and out of the main embayment around Bambra Reef (Shand & Carley 2011; see section 5.3.2 above). Landwards or seawards movement of the shoreline position within this embayment may occur in response to a changing balance between the amounts of sand entering and leaving the embayment. Hence the essentially stable position of the shoreline (allowing for weighted air photo error margins: Figure 34) for at least the 38 years from 1946 until 1984 reflects a mostly stable balance between sand budget gains (positive) and losses (negative) over that period. Any short-term changes such as increased sand loss from the shore and the embayment during erosion events must have been fully compensated for on inter-annual time scales by subsequent drift of sand into the embayment and onshore, so that the shoreline position remained in an essentially stable dynamic equilibrium prior to 1984.

As sea-level progressively rose at Roches Beach during the Twentieth Century, this must have enabled storm wave events of any given magnitude to reach higher and further landward than previously on the shore profile, so that wave erosion of the upper beach and foredune face must have occurred more frequently than before (even without any increase in actual storm magnitudes and/or frequency). This implies that increasing quantities of eroded sand must have been more frequently moved offshore during storms, with a proportion of that eroded sand being transported northwards by the littoral drift around Bambra Reef and out of the embayment, rather than being returned to the beach.

Regarding the supply of sand into Roches Beach embayment, sand has probably also been increasingly eroded at the next comparably large and similarly-exposed swash-aligned beach to the south at Cremorne (Figure 28 & Figure 29) during simultaneous erosion events. However, that sand has evidently not been increasingly lost from the Cremorne embayment in recent decades to increase the littoral drift of sand northwards to Roches Beach, since there has been no comparable switch to progressive shoreline recession at Cremorne Beach[15]. This may be partly explainable by the steeper subtidal profile at Cremorne Beach than at Roches Beach (Carley et al. 2008), which I infer may result in less northwards shallow-water transport (loss) of eroded sand by swell-generated littoral currents (which are stronger in the narrower zone of shallow water close to the beach). The presence of the adjacent permanently open tidal (and largely sand-filled) Pipe Clay Lagoon is also likely to play a significant role in the Cremorne Beach sand budget as a sand store quite unlike any available at Roches Beach. Although some additional sand might be gained at Roches Beach from erosion of Mays Beach just to its south (Figure 28), this is a much smaller beach whose increased sand losses under sea-level rise could not substantially compensate for the increased sand deficit at the much longer main central part of Roches Beach.

[15] This statement is based on the authors sporadic observations of the (mostly stable) beach state at Cremorne since circa 2000, albeit no air photo time series analysis has been undertaken for that beach to date.

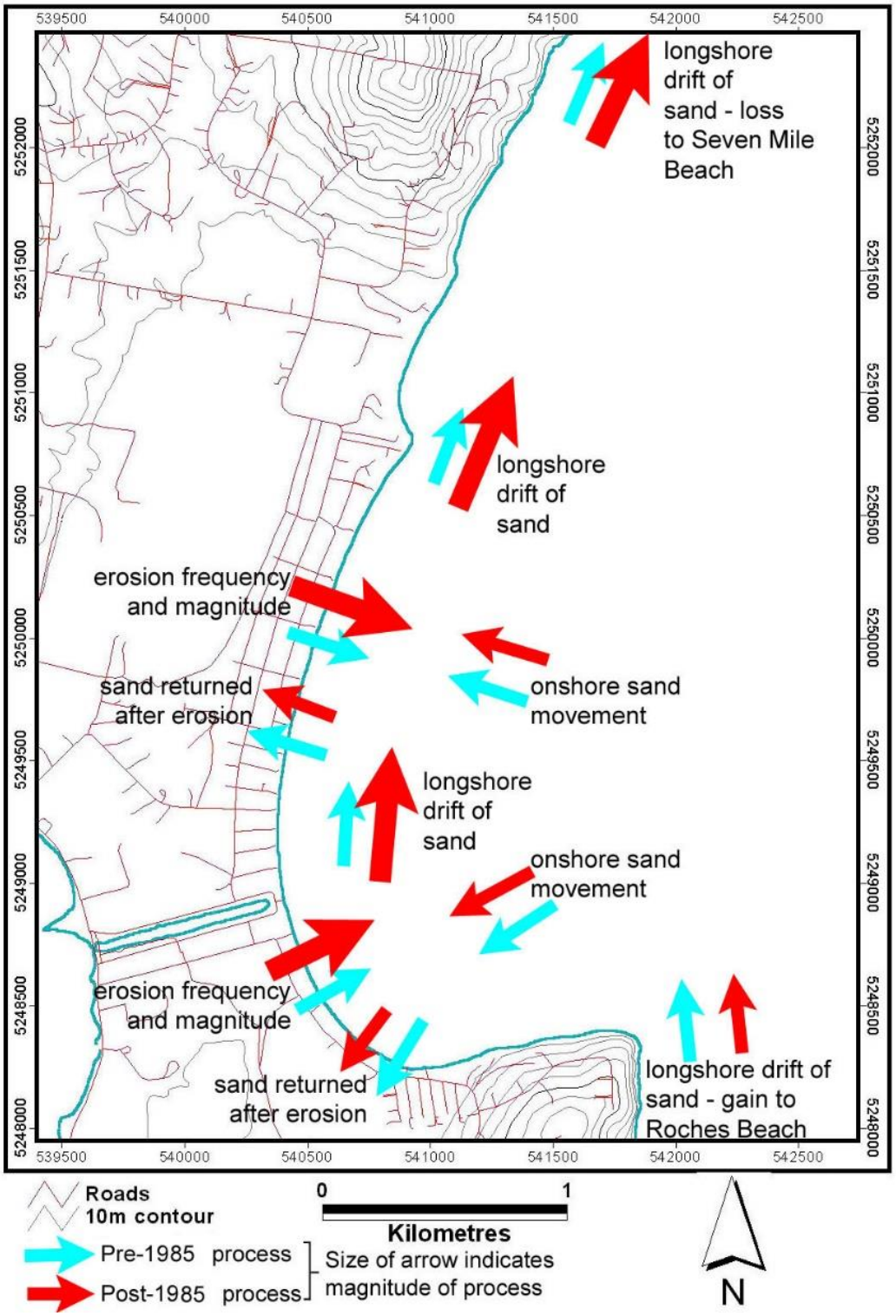

Figure 35: Model for Roches Beach response to sea-level rise. In summary, the sand budget at Roches Beach is dominated by a persistent and mostly unidirectional northwards swell-driven littoral drift of sand into, through and out of the embayment. As sea-level rise allows storm wave events of any given size to penetrate further landwards over deepened waster, the rate at which sand is eroded from the upper beach face increases. Because this results in increasing littoral drift transport of eroded sand out of the embayment, but there is no evidence of a commensurate increase in sand arriving from the south, the increasingly negative sand budget at Roches Beach results in progressive recession of the beach shoreline. See text for further discussion. Marginal co-ordinates are based on the Map Grid of Australia (Zone 55), GDA94 datum.

The effect of sea-level rise at Roches Beach must therefore have been to increase the rate of sand loss northwards from the embayment as storm wave events of any given magnitude more frequently had impacts higher on the upper beach profile, but without a compensating increase in sand gained to the embayment from the south. This would have resulted in a move away from a positive or balanced sand budget supplying enough sand to the beach to compensate for increasing losses, and towards a negative sand budget. However, up until 1984 there was evidently still enough surplus in the sand budget to compensate for increasing losses.

With sea-level rise resulting in erosion events more frequently reaching higher on the beach profile and episodically increasing the sand losses from the main Roches Beach embayment, by circa 1984 Roches Beach was probably close to losing more sand than it was gaining over inter-annual to decadal time scales. The largest erosional step-change in the air photo record (see Figure 33 & Figure 34) occurs between the 13th Jan 1984 and 26th Feb 1986 air photos and coincides with two known storms (during Oct. 1984 and June 1985) recorded as "severe" by (Foster 1988). This step-change arguably divides the shoreline history record into an earlier stable phase and a later progressively receding phase as shown by the data analysis on Figure 34 above, and is inferred to have resulted from at least the two known large storm erosion events noted above. These can be inferred to have tipped the beach into a dominantly recessional mode by removing a large mass of sand from the embayment at a time when the sand budget was already close to negative (i.e., net sand loss).

The air photo record (Figure 33), shows subsequent episodes of shoreline erosion between 1986 and 2011 with intervals of incomplete recovery resulting in step-wise but progressive shoreline recession until July 2011, after which the recession was halted by artificial intervention as noted in Section 5.3.3 above. This is consistent with the hypothesis of ongoing episodic and increasing sand losses attributable to sea-level rise during the 25 years after 1985 until 2011, further diminishing the capacity of the beach to recover between erosion events (and indeed probably continuing after that date but offset by artificial interventions).

Although the shorter section of 'Roches Beach North' to the north of Bambra Reef has undoubtedly been subject to increased erosion and sand loss for the same reasons as the main central beach, it has not shown a comparable change to progressive recession (Figure 32). This can be readily accounted for as a result of the increased sand lost from the main central beach providing additional sand gains to the northern beach. In contrast, the lack of any switch to a recessional trend in the southern 'sand trap' area is likely due to its location in the lee of Mays Point receiving less energetic wave action and less littoral drift during storms (Figure 32).

The hypothesis presented above implies that the relatively abrupt change in shoreline behaviour at Roches Beach between 1984 and 1986 is a 'tipping point' phenomenon resulting from an episodically decreasing sand budget surplus reaching a point beyond which the budget was more frequently negative and full recovery of the beach to its pre-1984 state no longer occurred. The record of known erosion events at Roches Beach (Appendix A1.4.2, Table 64) suggests that sand losses resulting from at least two 'severe' erosion events in 1984 and 1985 may have been large enough to tip the otherwise gradually and episodically changing sand budget sufficiently far into deficit as to be irreversible.

At drift-aligned Roches Beach the existence of an active large-capacity sand sink in the form of irreversible northwards sand losses, supplied by a persistent unidirectional (northerly) littoral drift driven by swell-wave refraction through Frederick Henry Bay, is deduced to be the critical factor that has permitted an early response to sea-level rise to occur. In contrast most other beaches in Frederick Henry Bay are swash-aligned (see Figure 29) and hence less likely to lose sand from their embayments, and are more prone to sand transport variability such as temporary reversals of littoral drift (e.g., in response to minor swell direction variations or occasional strong wind-wave events) which may mask sea-level rise effects.

Are there drivers other than sea-level rise on this coast that could have caused the observed change in behaviour?

The alternative hypotheses listed in Table 5 below have been considered and are evaluated in the text following. No other potentially plausible explanations of the observed shoreline behaviour change have been identified.

Table 5: Alternative hypotheses investigated to explain observed changes.

Hypothesis	Evaluation (see following text)
Vertical Land Movement	Not supported
Swell directional variability	Not supported
Increase in swell-storm magnitudes or frequencies	Not supported
Changes in onshore wind speeds	Not supported
Sand 'waves'	Not supported
Artificial structures	Not supported: existing artificial structures would not cause observed shoreline behaviour changes.

Vertical Land Movement (land subsidence) resulting in increased relative sea-level rise is unlikely to account for shoreline recession at Roches Beach. In part this is because GNSS-based measurements and GIA-based models indicate that vertical land movement (VLM) is negligible in the Hobart region (see Section 5.3.2 above). In any case, VLM is also unlikely to explain either the abrupt onset of shoreline recession between 1984 and 1986 or the restriction of recession effects in Frederick Henry Bay to only Roches Beach.

As discussed in Section 2.5.5, swell direction variability can markedly change shoreline exposure and sand movement directions resulting in changed patterns of erosion and accretion (Hemer 2009; Mortlock et al. 2017; Ranasinghe et al. 2004). However although both south-westerly and Tasman sea swells may enter Frederick Henry Bay (Carley et al. 2008), swell wave directional variability at Roches Beach is limited to just a couple of degrees (Table 4 & Figure 29). This small variability is a result of the long swell refraction pathway up Frederick Henry Bay which trains and attenuates swell as it approaches Roches Beach. This together with the north-south (drift-aligned) orientation of Roches Beach implies that the very limited directional variability of swell waves at Roches Beach makes significant change to shoreline erosion patterns or littoral drift rates and directions in response to swell direction variability unlikely.

A long-term increase in swell-storm magnitudes or frequencies could plausibly cause a switch from stable to recessional shoreline behaviour at swell-exposed beaches. However, this does not explain the changes at Roches Beach since other beaches exposed to the same swell wave climate and swell storms in Frederick Henry Bay have not shown comparable changes in behaviour[16]. See further below for discussion of wind-wave storms.

Although both Tasman Sea swells and south-westerly swells penetrate Frederick Henry Bay, the south-westerly swells are dominant (Carley et al. 2008). The only long-term (since 1985) record of south-westerly swell and storm-swell wave magnitudes for the Tasmanian region is that recorded by the Cape Sorell wave-rider buoy off Tasmania's west coast. Although distant from Frederick Henry Bay, any systematic change in the south-westerly (SAM-driven) swell wave magnitudes and storm frequencies recorded at the Cape Sorell buoy would likely be seen in the same south-westerly swells as they arrive at Storm Bay before refracting into Frederick Henry Bay towards Roches Beach (Hemer, Simmonds & Keay 2008). However, Hemer (2010) found no indication of increased swell wave magnitudes or storm frequencies since 1985 in the available record at the Cape Sorell buoy, and instead found a small non-significant decrease. It is therefore considered unlikely that increasing

[16] Based on the authors observations over the last 20 years approximately and air photo data for several beaches reported in Sharples et al. (2012) and Thom et al. (2018)

swell-wave magnitudes or swell-storm frequencies can account for the switch from stable to receding shoreline behaviour at Roches Beach.

Changes in onshore wind speeds (and thus in onshore wind-waves) may modify shoreline erosion processes (as inferred for Ocean Beach in Section 5.2.4 above). However, there is no clear evidence that wind speeds in the Hobart area have changed significantly in recent decades (see discussion in Section 5.5.2 below). In any case the question is largely moot since the predominant winds (north-westerly to south-westerly) at Roches Beach are directed offshore (Section 5.3.2 above), hence neither larger nor smaller wind-waves generated in the dominant wind directions would modify beach processes in any case.

Nonetheless onshore-directed wind-waves generated by north-east to easterly winds across 10 to 15 km fetches over Frederick Henry Bay have occasionally caused significant erosion at Roches Beach (Section 5.3.2). However, the nearby Hobart Airport wind record indicates that E to NE winds are very minor in the region (see Section 5.5.2 below), so that stormy winds from that direction are likely to be rare and therefore unlikely to cause and sustain the sort of major long-term shoreline behaviour change seen at Roches Beach.

The floor of Frederick Henry Bay is almost completely blanketed with unconsolidated sand in relatively shallow water of mostly <20 m depth (SEAMAP data, see appendix Figure 195), much of which is likely to be subject to northwards-directed bottom currents generated by the swell propagating up Frederick Henry Bay. On some coasts (e.g., northern New South Wales) large slugs or 'waves' (subaqueous dunes) of seafloor sand episodically move along the coast resulting in alternating accretion and depletion of sand on adjacent beaches as the mobile sand bedform moves past headlands (Goodwin, Freeman & Blackmore 2013). In principle such a process might cause the observed switch from shoreline stability to recession at Roches Beach, however, to produce alternating phases of shoreline stability and depletion on the multi-decadal time scale observed at Roches Beach would presumably require mobile sand bedforms of considerable wavelength and amplitude. No indications of such features in Frederick Henry Bay have been reported despite bathymetric and substrate mapping in Frederick Henry Bay by the SEAMAP marine habitat mapping project (University of Tasmania, see Figure 195).

Artificial structures and other changes (see appendix A1.4.2) are present at Roches Beach but have spatially restricted effects and do not appear to provide plausible explanations of the observed change of beach behaviour. The closed-off canal and the houses and roads on the back of the foredune have had no discernible effect on cross- or along-shore sand movements on the beachface. Although the mid-1980s construction of the boulder revetment (seawall) in the southern part of the beach is approximately coincident with the abrupt change in shoreline behaviour, this is presumably because the two large erosion events which are inferred to have tipped the beach into recession were also key factors in the decision to build the protective revetment. However, whereas the revetment only protects a short southern section of the backshore, the progressive recession which commenced circa 1985 has equally affected the whole ~3.5 km main central beach section. It is not plausible that "end effects" from the revetment would be effective for several kilometres beyond its northern end.

5.3.5 Summary: Roches Beach

An abrupt switch from long-term shoreline stability (for at least 38 years) to long-term progressive recession (for 25+ years) occurred at Roches Beach between the 1984 and 1986 air photos. The post-1985 recession trend is mostly beyond the range of pre-1985 shoreline position variability (including air photo error margins) and thus is a significant real change. No other beach in Frederick Henry Bay (exposed to similar wind, wave and tidal conditions) has shown a comparable change.

The above review of the geomorphic and oceanographic processes affecting Roches Beach that may influence sand erosion or accretion identified contemporary sea-level rise as the only available

driving process capable of forcing the observed change of shoreline behaviour. This is hypothesised to have occurred because of two key factors, namely:

1. the rise in sea-level has allowed storm wave events of any given magnitude to progressively reach higher on the shoreface and thus cause more erosion of the upper beach and dune face than previously; and:
2. a persistent swell-driven unidirectional northwards littoral drift has been efficiently moving the increasing amount of eroded sand out of the leaky Roches Beach embayment faster than it could be returned to the beach and dune face by fair-weather swell waves after each erosion event, or replenished by sand drifting into the embayment from the south. The sand continues north-wards to Seven Mile Beach which is in effect an active sand sink for Roches Beach.

As increasing amounts of sand were lost from the embayment without any compensating increase in the sand supply into the embayment, the sand budget in the main central embayment of Roches Beach would have been approaching a deficit. It is likely that the two severe erosion events recorded during the 1984 to 1986 interval removed a large volume of sand from the beach at a time when the sand budget was getting close to negative, thus 'tipping' the sand budget into dis-equilibrium and the beach into a recession trend from which it could no longer recover.

The first key factor above is likely to be occurring on all or most tidal sandy beaches, however the second factor is an unusual condition which has made Roches Beach a likely "early responder" to sea-level rise. At Roches Beach the persistent uni-directional littoral drift allows progressively increasing amounts of sand to be lost from the embayment as sea-level rise causes erosion more frequently higher on the shore profile. In contrast, many open coast sandy beaches – particularly those which are swash-aligned - are prone to episodic switches in wave and littoral drift directions within the embayment and less efficient sand loss from embayments. This results in more opportunities for beach recovery after erosion which tends to hide or overwhelm any response to sea-level rise.

No other explanation not requiring sea-level rise as a forcing factor has been identified which could explain the change in shoreline behaviour at Roches Beach.

5.4 *Study Area 3: West Duck Bay*

5.4.1 Introduction

The West Duck Bay study area comprises 5 distinct sites within an extensive region on the far north-west coast of Tasmania which is characterised by saltmarsh-dominated sandy shores and extensive inter-tidal sand-flats stretching from Boullanger Bay to Duck Bay (see Figure 17 & Figure 36). These are sheltered from the swell waves refracting through Bass Strait by Robbins Island and a series of Holocene sandy barriers. This study area is an example of another of the four broad categories of coastal landform type from which study sites were selected for this thesis (namely "swell-sheltered tidal soft sandy shores" as described in Section 3.2.1 and listed in Table 2 above). This section follows the same structure as the previous Sections 5.2 and 5.3 above, presenting the essential data and findings of an investigation of shoreline behaviour at West Duck Bay since the 1940s. Additional supplementary data and information on this case study area is provided in Appendix A1.2.5.

Areas landwards of the southern shore of the region (including west Duck Bay) are dominantly cleared for agriculture (mainly cattle grazing), however the saltmarsh areas remain mostly intact as a natural coastal buffer. Perkins Island, forming the northern shore of west Duck Bay, is an unsettled sandy barrier island with very little clearing of native vegetation. The largest town in the area is Smithton at the southern extremity of Duck Bay (Figure 36). The presence of extensive actively eroding saltmarsh shores in Duck Bay was previously reported by the author in (Mount et al. 2010) and Prahalad et al. (2015).

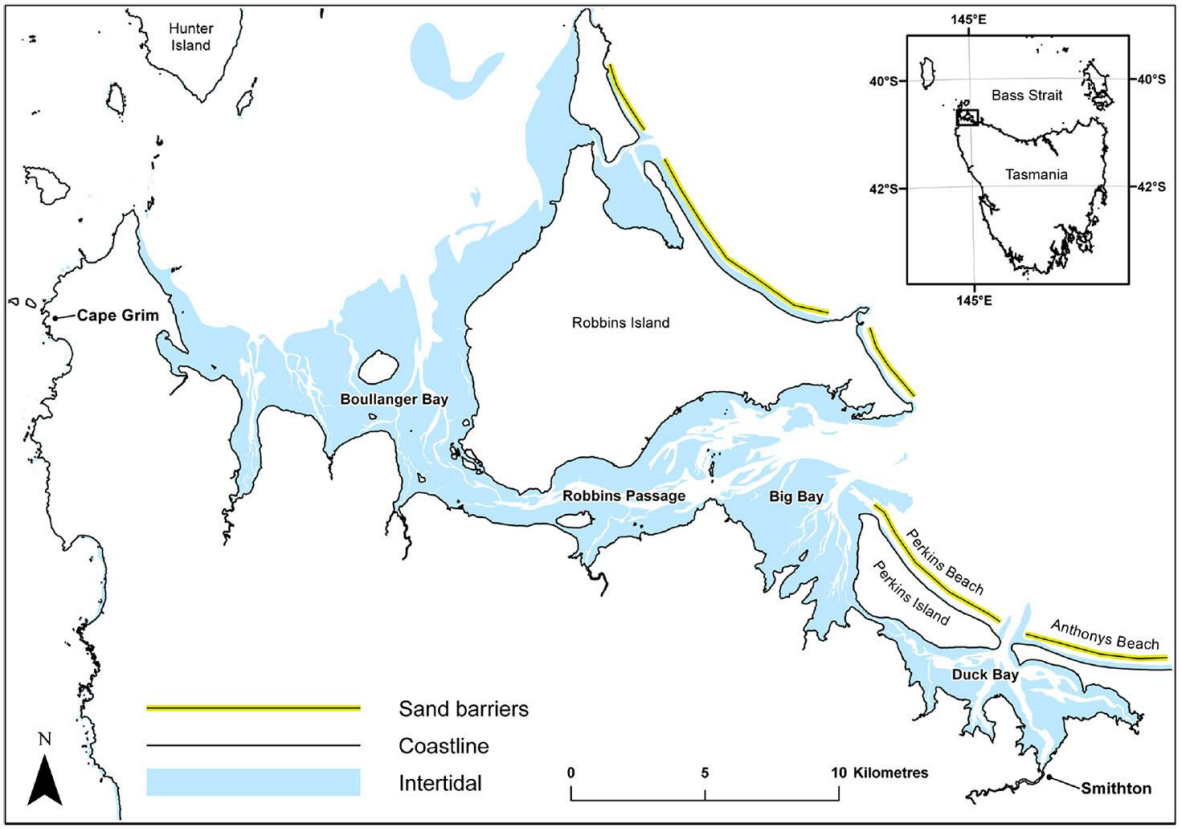

Figure 36: Locality map for Duck Bay and adjoining areas of far north-west Tasmania. Duck Bay (lower RHS of map) is located at the south-east end of a 30 km stretch of similar swell-sheltered meso-tidal embayments. The extensive 'intertidal' areas indicated in blue are sandflats of mostly eroding Pleistocene terrestrial sands that are extensively exposed daily at low tide. Deeper tidal channels cutting through the tidal flats are indicated by lack of colour. This figure is reproduced from Prahalad et al. (2015) with permission.

5.4.2 Site description and processes

The coastal geomorphology of the broader intertidal sand-flats region of which West Duck Bay is part has been field-mapped and reported on previously by the author (Mount et al. 2010; Prahalad et al. 2015). Five distinctive sites within the West Duck Bay portion of the earlier study area were re-examined for this project using air photos from additional dates and different analysis methods.

Geomorphic description

The geomorphology and shoreline character of the west Duck Bay case study area (centred around 145° 5' 0" E 40° 48' 0" S) is typical of the broader coast of far north-west Tasmania from Boullanger Bay to Duck Bay (as described by Mount et al. 2010); see Figure 36. Duck Bay is a tidal coastal re-entrant sheltered from the refracted swells entering Bass Strait by the Holocene-age sandy coastal barriers of Perkins Island and Anthony's Beach. To the south-west, backshore and hinterland areas comprise extensive low-relief plains thickly mantled by Pleistocene-age terrestrial aeolian sands. The extensive intertidal to sub-tidal sand flats in west Duck Bay are not Holocene coastal or marine sand deposits, but rather are the same Pleistocene aeolian sands as those onshore, which were inundated and stripped by marine erosion at the upper limit of the post-glacial marine transgression that ceased in the south-eastern Australian region circa 6,500 years BP (Lambeck & Chappell 2001). Along with thin (circa 0.5 m) patchy veneers of sand reworked by tidal currents and wind-waves, the intertidal sand flats also expose *in situ* interbedded dark cohesive peaty-sand beds and lenses which outcrop sporadically on the shoreline (Figure 37 top) and across the tidal flats. These have been identified as freshwater lacustrine beds, with samples from nearby Boullanger Bay yielding Pleistocene conventional radio-carbon dates of 26,720±180 yrs. BP and 36,930±400 yrs. BP (Morrison in: Mount et al. 2010). The intertidal exposure of these *in situ* peat beds implies that the tidal sandflats are currently dominantly stable or eroding rather than accreting sand.

The shoreline of west Duck Bay is mostly occupied by saltmarsh vegetation, typically with up to 0.5 m of soft grey clayey-sand marsh soil accreted over the Pleistocene sands (see Figure 6 in Section 2.5.2, Figure 37 (top) & Figure 38). Although saltmarsh vegetation has a degree of resistance to wave attack, a large proportion of the saltmarsh shoreline in west Duck Bay is actively eroding with fresh low scarps (Figure 37 (bottom) & Figure 38). However in some areas the saltmarsh vegetation edge is intact, actively growing and accreting a clayey-sand marsh soil as clay, silt, sand and organic debris in the water column is trapped by the vegetation (Figure 37, and see Figure 6 in Section 2.5.2). The main exception to saltmarsh shore in west Duck Bay is approximately 1.5 km of shoreline on the southern side of Perkins Island near the tidal entrance to Duck Bay, which is a sandy shore with an erosion scarp typically 1.5 to 2.0 m high cut in deep podzolic beach ridge sands.

Tidal range and processes

Duck Bay has a tidal range and bathymetry similar to the adjacent Big Bay to Robbins Passage to Boullanger Bay intertidal sandflats region (Figure 36). Mean spring tide ranges from 2.09 m up to 2.79 m have been measured at three sites in the latter region (Donaldson, Sharples & Anders 2012).

The intertidal sandflats indicated in blue on Figure 36 are inundated at high tide but are mostly exposed at low tide every day. Hence tidal currents flow off the exposed tidal flats and into the tidal channels that dissect the flats on every ebb tide. Although no attempt has been made to model or quantify tidal current flows in this region, the fact that cohesive Pleistocene peat beds interbedded with Pleistocene sands are exposed sporadically across the intertidal sandflats implies that the flats are at least partly scoured by tidal currents, which must be capable of removing loose surface sands during ebb tides into the only available sinks, namely the deep tidal channels incised into the intertidal flats (see Figure 36).

Tidal currents converging in the narrow shallow channel ("The Jam") at the western extremity of Duck Bay were inferred by (in Mount et al. (2010)) to have contributed to unusually rapid twentieth

century erosion of shorelines in that area (see Figure 39). However, no evidence has been identified of tidal currents being a direct agent of erosion elsewhere in Duck Bay (as opposed to a means of sediment transport).

Swell wave climate

With the exception of refracted and attenuated swells reaching short distances inside the mouth of Duck Bay between Perkins and Anthony Beaches (see Figure 36), Duck Bay is entirely sheltered from swell waves.

Wind (wind-wave) climate

The nearest available Bureau of Meteorology wind records pertinent to West Duck Bay are the high-quality record from Cape Grim (~30 km to the west) for 1987 onwards[17], and the longer but less reliable records from Smithton township and aerodrome, (~5 km east). See locations on map Figure 36 and wind roses on Figure 40 below. The dominant winds at Cape Grim are westerly to south-westerly and given the very low-profile country with minimal topographic steering between there and Duck Bay, similar dominant wind directions can be expected at Duck Bay. The much closer Smithton wind records support this, as well as exhibiting a sub-ordinate easterly wind flow that is also seen in the Cape Grim record.

The Cape Grim wind record shows a significant trend of ongoing westerly wind speed increases since at least 1995 (see Section 5.2.2, Figure 20). While this also might be expected to occur at Duck Bay, the closer Smithton wind speed records show no significant long-term increases. However, those records contain data step changes and a shift in location from Smithton Township to Smithton Aerodrome, hence their long-term wind speed records are suggestive of instrumentation and/or siting issues and are potentially problematic.

Locally generated wind-waves are the main agent of erosion on shorelines around West Duck Bay and have been observed by the author dislodging sediment from actively eroding saltmarsh scarps (see Figure 38). Wind-wave fetch modelling has previously been undertaken for West Duck Bay and surrounding swell-sheltered shorelines by Vishnu Prahalad in and Prahalad et al. (2015), using a cartographic wave exposure model developed by Pepper and Puotinen (2009). For Duck Bay the modelling used wind direction data from the Smithton weather stations to derive a dimensionless Wave Fetch Index (WFI) predictive of the degree of wind-wave erosion to be expected on shores of differing wind exposure and fetch relative to dominant wind directions. The WFI modelled for West Duck Bay is compared to the author's field mapping of shoreline erosion status (as at 2010) on Figure 39. Two key results are apparent from this figure, namely:

1. Larger and smaller WFI broadly correlate with distinctions between soft (mostly saltmarsh) shores that are respectively eroding, intermediate or accreting. The main exceptions to this pattern occur where wind-waves are not the dominant agent of erosion, which is the case at the swell-exposed mouth of Duck Bay and the narrow tidally dominated channel at the West end of Duck Bay.
2. WFI (and thus wind-wave capacity to erode) broadly increases from west to east across West Duck Bay, corresponding to dominantly westerly to south-westerly winds blowing across increasing fetches towards the east and north-east.

[17] The Cape Grim weather station is part of the global Baseline Air Pollution Stations network which is managed rigorously by the World Meteorological Organisation in association with the Australian Bureau of Meteorology and CSIRO.

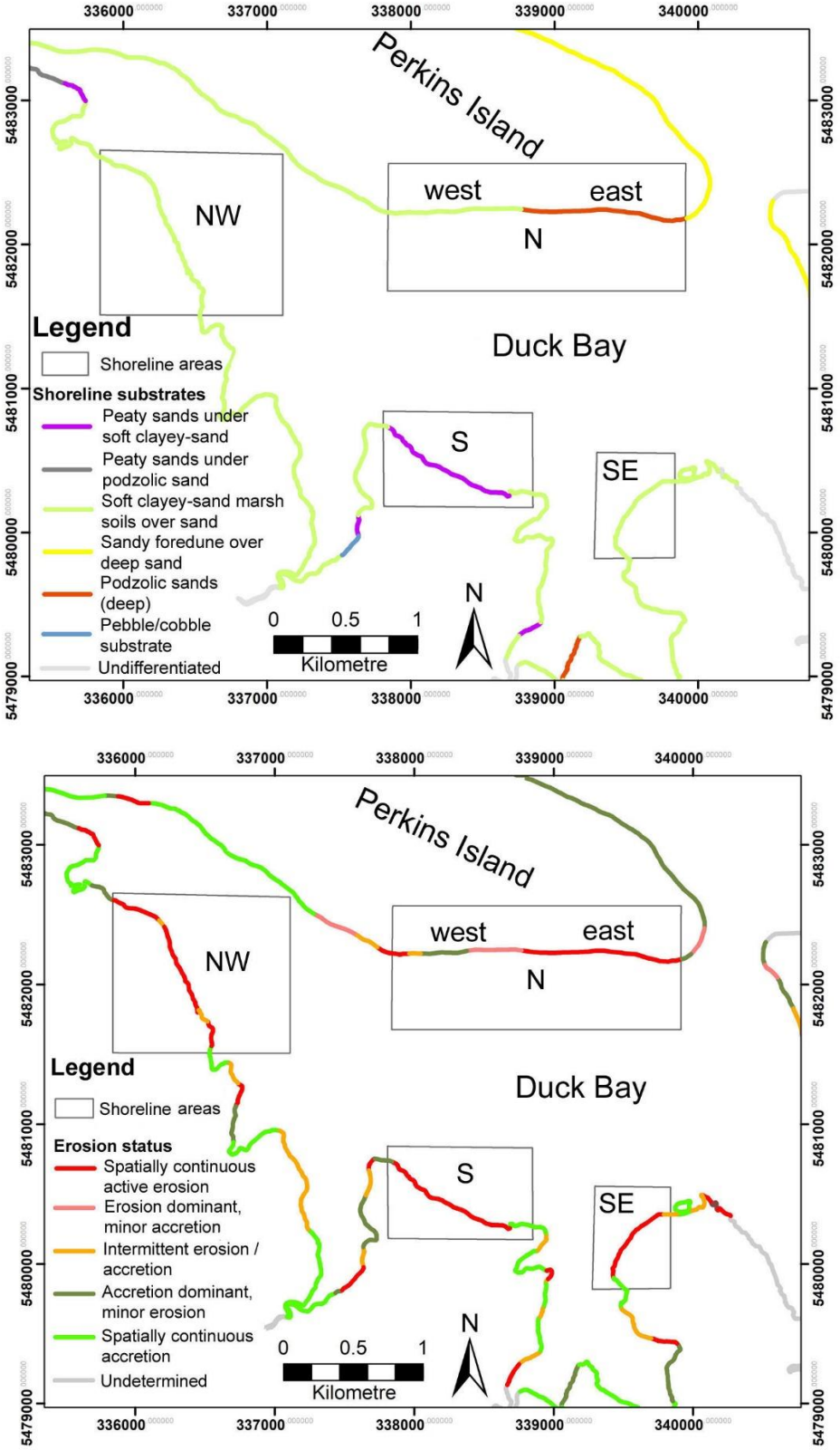

Figure 37: Shoreline substrate and erosion status at 2010 for western Duck Bay. Shoreline substrate (top) and shoreline erosion status as at 2010 (bottom) are both based on field mapping by Chris Sharples, as previously reported in Mount et al. (2010). The five most extensive stretches of actively eroding shoreline in this area (as at 2010) were selected for air photo time series investigation of historic shoreline behaviour and are indicated as Shoreline Areas NW, N (east & west sections), S, & SE. The map grid is Map Grid of Australia (MGA), Zone 55 (GDA94 datum).

Figure 38: A view of the West Duck Bay SE area shoreline (see Figure 37) taken close to high tide showing the actively eroding vegetation edge exposing dark clayey-sand saltmarsh soils immediately overlying pale-coloured intertidal sand flats which are extensively exposed at low tide. At the time of this inspection, the small locally generated wind waves were actively and visibly mobilising silt and clay from the eroding saltmarsh soil faces. Photo taken by Chris Sharples on 29th January 2010.

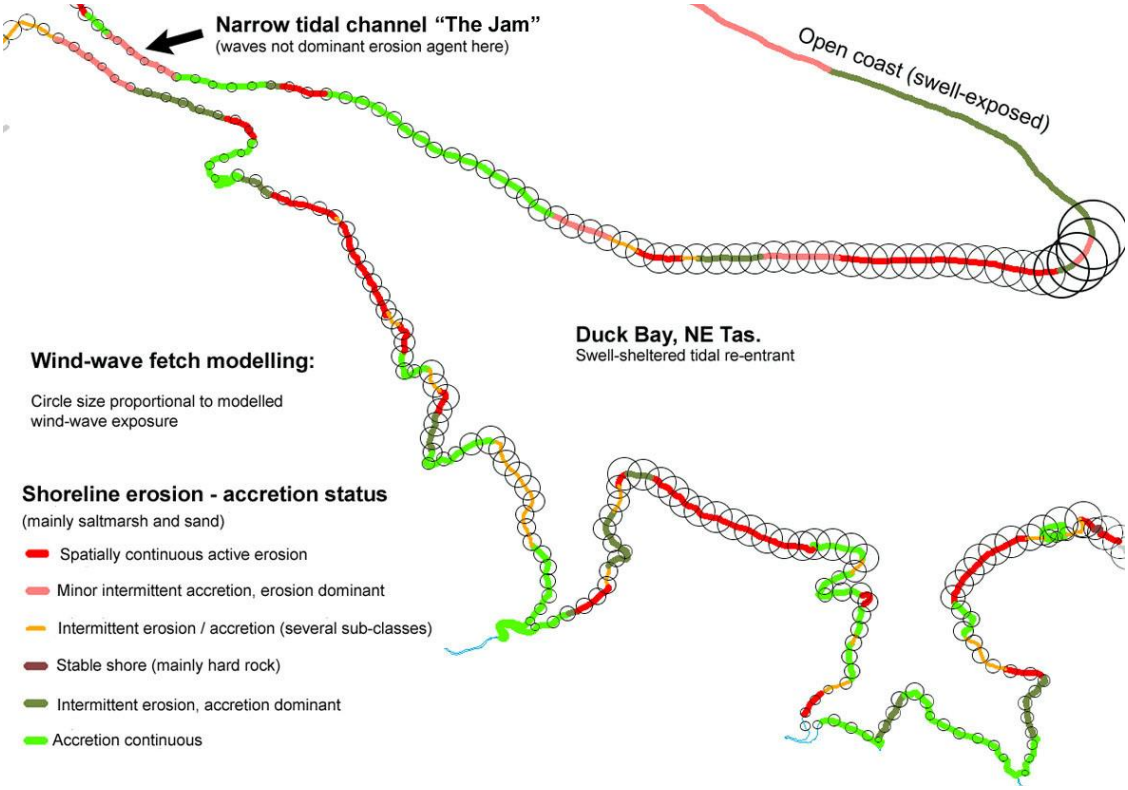

Figure 39: Wind-wave fetch exposure in western Duck Bay compared to shoreline erosion status as at 2010. Erosion status is based on comprehensive field mapping by Chris Sharples during 2010 (originally reported in Mount et al. (2010); see also Figure 37 bottom). The wind-Wave Fetch Index (WFI) is a dimensionless value calculated from fetch and wind direction frequency-magnitude distributions by Vishnu Prahalad (in: Mount et al. (2010) and Prahalad et al. (2015)) using the cartographic method of Pepper and Puotinen (2009). Higher WFI is represented by larger circles at each modelled shoreline point, and for Duck Bay was based on the Smithton wind records rather than the (higher quality but more distant) Cape Grim wind record.

Sand transport and budget

West Duck Bay has a negative sediment budget, with no significant sand gains and persistent losses of eroded sand via daily ebb-tide currents into deeper tidal channels and from these ultimately into the very large sink of Bass Strait.

As noted above, the extensive inter-tidal sandflats in Duck Bay are not recent or Holocene marine or coastal deposits, but rather are eroding terrestrial aeolian sands of Pleistocene age. Shoreline saltmarsh accretes grey clayey-sand soils over the sands, presumably by vegetative capture of sand, clays and organic matter moved by wind-waves and tidal currents in the nearshore water column. However, there is no evidence of sand being gained by the shorelines or intertidal flats from any external source (e.g., rivers or streams).

There is little or no accommodation space for sand eroded from shorelines to settle out into on the intertidal flats, since they are sub-aerially exposed and scoured by tidal currents during every tidal cycle. With continuing sea-level rise and deeper water depths, some accommodation space may eventually become available on parts of the tidal flats, however given the large tidal range in Duck Bay this is likely to occur only after considerable further (multi-metre) sea-level rise. Shoreline erosion is evidently freeing sand and finer sediments, some of which may be vegetatively recaptured by those saltmarsh shores that are still accreting (Figure 37 bottom), however ebb-tide currents can be expected to remove most loose sediment into the tidal channels incised across the intertidal sand flats (see Figure 36) where the sand fraction will settle out. It is unlikely that sand sinking into the deeper parts of these channels could be returned to the shallow tidal flat surfaces during flood tides. Indeed, Mount et al. (2010, p. 52) used a time series of LANDSAT imagery to track the movement of sand bedforms migrating along a large tidal channel into deeper offshore water in Bass Strait. The bedforms were tracked moving westwards through Robbins Passage and then northwards up the west side of Robbins Island over a 20-year period from 1990 to 2009. Similar sand transport probably occurs in other tidal channels across the region including those in Duck Bay.

Given that little sand is likely to be moved out of the deeper tidal channels back onto the (regularly exposed) intertidal flats by flood-tide currents, this sand transport process is effectively a uni-direction transport process that is persistently (with every tidal cycle) moving eroded shoreline and intertidal sands into the very large active sink of Bass Strait. Despite a superficial appearance of being a sheltered sand-filled depositional sand-trap, the extensive intertidal sandflats of the Duck Bay are in fact a persistently eroding area of exposed and eroding relict Pleistocene sands with an overall negative sand budget.

Sea-level data

The closest long sea level record to Duck Bay is the Burnie tide gauge record, 75 km south-east of Duck Bay. The Burnie tide gauge is part of ABSLMP, the climate quality Australian Baseline Sea Level Monitoring Project (http://www.bom.gov.au/oceanography/projects/abslmp/abslmp.shtml). Data from this tide gauge processed by Dr John Hunter and Vishnu Prahalad in 2010 shows a rise in mean sea-level between 1966 and 2006 of 5.4 cm at a mean rate of 1.4 mm yr^{-1} over that period (Mount et al. 2010). Data from http://www.bom.gov.au/ntc/IDO60201/IDO60201.202003.pdf (ABSLMP March 2020 report) shows a mean rate of 2.9 mm yr-1 at Burnie for 1993 to 2020. These are comparable to the global mean trend of 2.0 ± 0.3 mm yr^{-1} from 1966 to 2009, and 3.4 ± 0.4 mm yr^{-1} for 1993 to 2009 (White et al. 2014).

Since Duck Bay is a tidal marine environment, the mean sea level within the bay must have risen commensurately with rates measured at Burnie, and can reasonably be assumed to have been rising since the 1800s, as is the case for climate change-driven sea-level rise globally (see Section 2.3 including Figure 2).

Vertical land movement

Current and ongoing geodetic studies of Tasmania have yet to resolve disagreements between GNSS derived estimates of VLM at Burnie (75 km east of West Duck Bay) and Hobart which range between 0.0 to -1.0 mm yr^{-1}, and geophysical models indicating subsidence in the range of -0.1 to -0.2 mm yr^{-1} for Tasmania (see details in Chapter 2 Section 2.5.4 above). However, for the purpose of this thesis, there is no evidence suggesting that VLM is a significant signal in Tasmanian relative sea levels. There is no anthropogenic extraction of sub-surface fluids or other known processes such as significant seismic activity likely to cause VLM in the region of Duck Bay.

Artificial disturbances

The main artificial disturbance in the west Duck Bay area is land clearance for agriculture, however the study site shorelines remain physically buffered from cleared pastures by a fringe of saltmarsh and other vegetation. The proximity of cleared land may change nutrient and suspended sediment concentrations in Duck Bay, potentially affecting seagrass and marine fauna (Mount et al. 2010, pp. 147-148), but there is no apparent mechanism by which it may have significantly altered saltmarsh accretion or shoreline erosion behaviour in the study site shores over the air photo period.

An artificial levee and drainage channel has been constructed parallel to and between 20 and 50 m behind the present eroding shoreline in the southern two thirds of the NW study site, but do not appear to have significantly altered saltmarsh accretion or shoreline erosion behaviour in the NW study site over the air photo period. The shoreline histories along individual transects within this study site show no significant difference between the transects backed by the levee and channel, and those not so backed (see Appendix A1.2.5 Figure 94).

Rice grass (*Spartina anglica*) is an introduced invasive shoreline weed which in recent decades has become established in parts of Duck Bay (Mount et al. 2010, Section 6.2). A key impact of this weed is that it aggressively colonises shoreline fringes, in the process capturing silt-grade sediment suspended in the water column and creating erosion-resistant prograding muddy shores. Almost by definition therefore, this weed was not established on the eroding study area shores as at 2010 (when they were inspected by the author: see Figure 38), although their establishment after that date cannot be ruled out. However, rice grass was present at the southernmost end of the SE study site shore in 2010, which is probably explains (or is a factor in) the slight progradation of that end of the otherwise strongly receding shoreline (see Figure 41).

5.4.3 Recent shoreline change history

Shorelines (defined by the seawards saltmarsh vegetation line) were mapped (digitised) from ortho-rectified air photos taken at 16 dates from January 1945 to March 2012. Due to incomplete coverage at a few dates, only 14 or 15 air photo dates could be used at some sites. (see Appendix A1.2.5 for additional details of air photos used and the analysis summarised below).

Five sites were selected for analysis around the shores of west Duck Bay (Figure 40). All five were selected on the basis that the author had previously (during 2010) field-mapped them as actively eroding (Figure 37). The five sites vary significantly in wind-wave exposure and fetch with respect to the westerly to south-westerly winds inferred from available wind records to be dominant in Duck Bay (Figure 39 & Figure 40). Four of the sites are saltmarsh shores comprising sandy-clay saltmarsh soils over sand, and one (the N(E) site) is podzolized Holocene beach ridge sand (Figure 37).

Figure 40 provides a summary of the shoreline behaviour histories of the five distinct sites examined around West Duck Bay. Linear regression fits to the data indicate that the shorelines at all five sites have most likely been receding since at least the earliest (1945 or 1946) air photo dates, albeit some temporary episodes of accretion (recovery) on shorter timescales are possible but not confidently

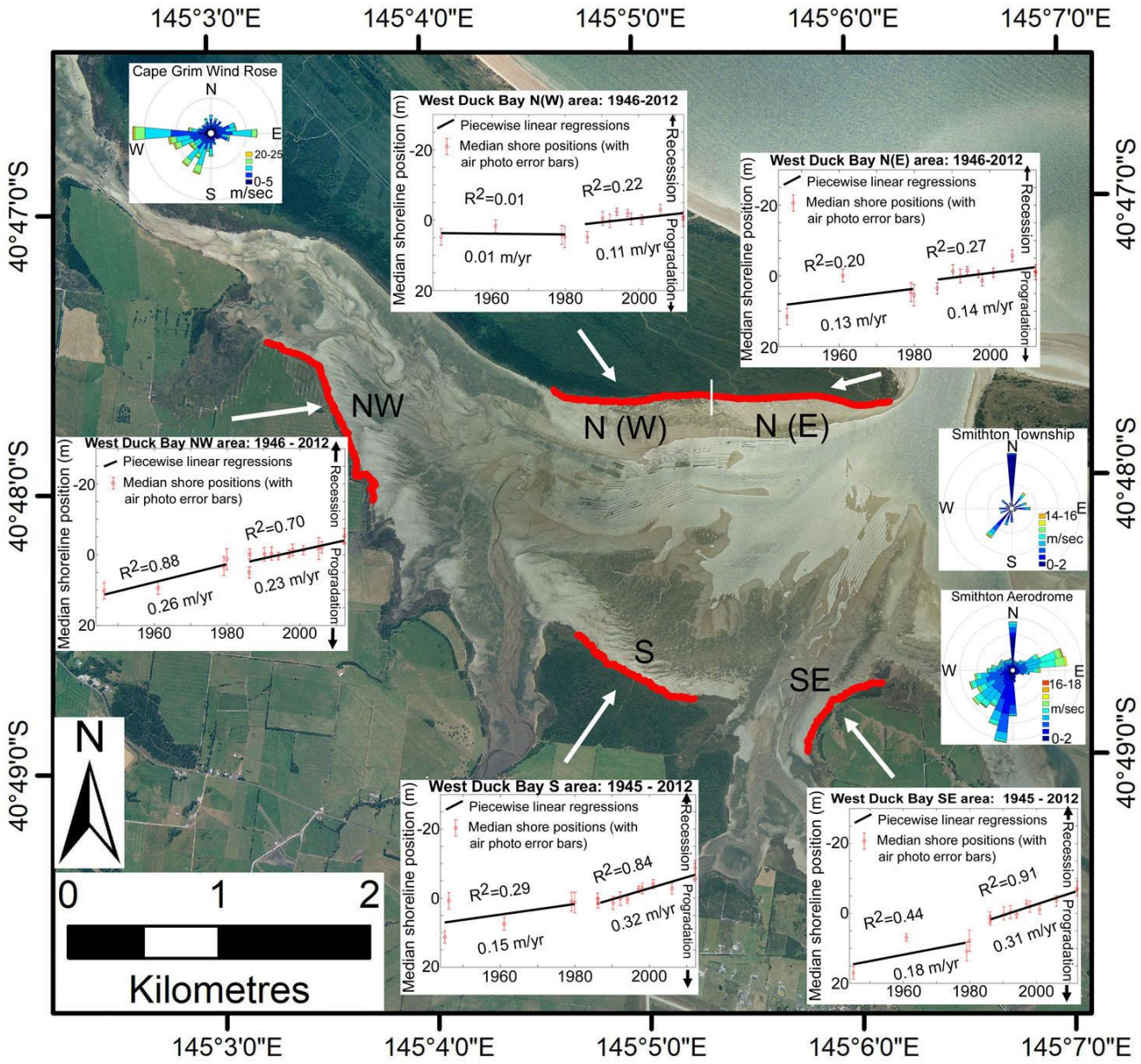

Figure 40: Summary plots of shoreline behaviour histories for Duck Bay. Piecewise linear regressions are shown fitted to each plot before and after 1980, in order to test for any increase in the rate of recession trends. Pearson correlation co-efficients and calculated linear recession rate are shown for each piecewise linear fit. Synoptic wind direction data is shown from the closest long-term Bureau of Meteorology weather stations, at Cape Grim (~30 km west) and Smithtown township & aerodrome (~5 km SE of Duck Bay). See locality map Figure 36. Air photo dated January 2006 © DPIPWE.

detectable in the air photo record. Piecewise linear fits were also used to test for different behaviour before and after the arbitrary date of 1980 at each site[18].

Based on the data summarised in Figure 40, three of the five study sites in West Duck Bay have probably been receding at approximately constant rates since at least the dates of the earliest air

[18] Note that whilst the summary piecewise plot for the N (W) site (Figure 93) suggests a stable shoreline prior to 1980, this fit has an insignificant correlation coefficient. A more likely interpretation of the data is a linear recession trend over the whole data period for this site, which yields a significant correlation coefficient of R^2=0.49 (see appendix Figure 92).

photos (1945 or 1946). These are the NW, N(W) and N(E) areas indicated on Figure 40, two of which are saltmarsh shores while the N(E) shore is an eroding podzolic Holocene sand shore.

The air photo data for the other two saltmarsh sites (S and SE) is similarly indicative of continuous recession since prior to the earliest (1945) air photos. However, these two sites also show a significant change in shoreline behaviour, with approximately doubled linear recession rates after 1980 which have very high Pearson correlation co-efficients (R^2=0.84 and R^2=0.91). See Figure 40.

5.4.4 Shoreline behaviour analysis: West Duck Bay

The working hypothesis that the observed shoreline behaviour histories (above) in parts of the West Duck Bay shore are driven by contemporary climate change-induced sea-level rise was tested by seeking and evaluating multiple alternative hypothetical explanations under the two sub-heading questions below.

Are there geomorphic process conditions at West Duck Bay that would allow an earlier recessional response to sea-level rise than on most coasts?

Eroded saltmarsh shorelines are capable of vegetative recovery and accretion to a stable or equilibrium shoreline position if drivers of erosion (such are greater wave magnitudes and/or wave attack at higher levels on the shore profile) stabilise at some level, allowing the shoreline position (vegetation line) to stabilise in response (see Figure 6 in Ch. 2.5.2). Thus, the observation that shoreline erosion and progressive recession has been continually active at the studied sites on the

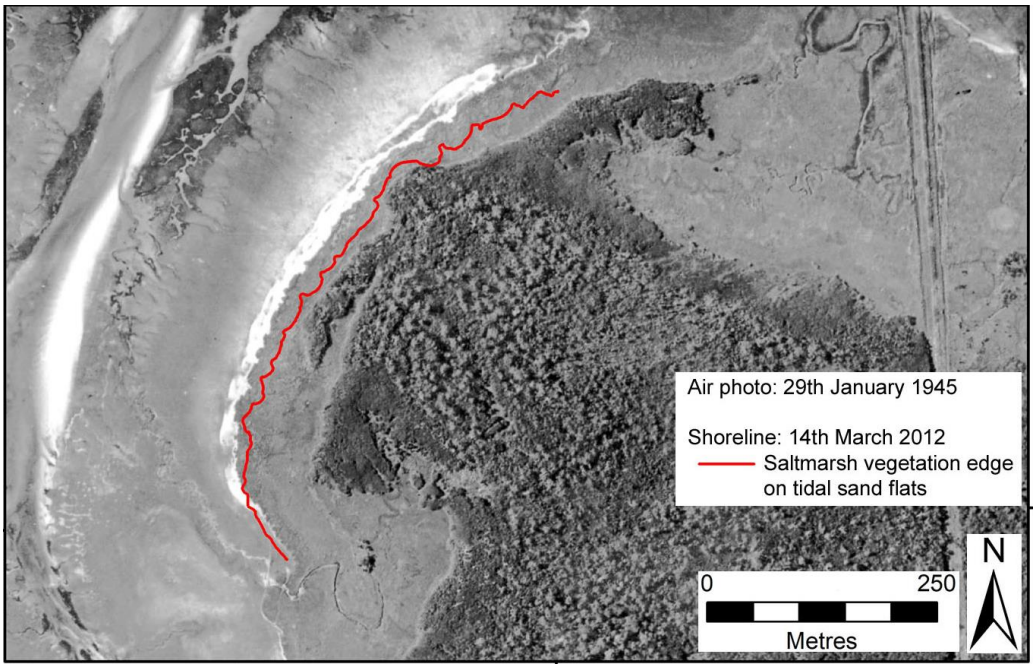

Figure 41: Comparison of shoreline positions in the West Duck Bay SE shoreline area from the earliest (29th January 1945) ortho-rectified air photo and the 2012 shoreline digitised from the 14th March 2012 ortho-photo. The mapped shoreline at both times was mostly a low saltmarsh vegetation margin contrasting strongly with the sandy tidal flats. The vegetation margin has receded significantly since 1945. In contrast, rice grass establishment over recent decades in the southernmost 100 metres of the digitised shoreline has resulted in stabilisation and some minor progradation of the shore in that area only.

West Duck Bay shore over at least the whole air photo period from 1945 onwards implies that the cause or causes of the erosion have also been active and increasing over the same period. The observed active shoreline recession can be explained as a response to sea-level rise by a simple working hypothesis that is consistent with observations of the West Duck Bay process environment

(described above) and is supported by generalised models of geomorphic and oceanographic processes. This hypothesis is set out in the following paragraphs. Other changing drivers which may be alternative or additional factors are considered in the following sub-section.

Apart from constricted tidal currents at the narrow western end of Duck Bay and limited swell-wave penetration near its northern entrance, locally generated wind waves are the only known agent of shoreline erosion in West Duck Bay. As mean sea-level progressively rose in Duck Bay since the 1800s, stormy wind-wave events of any given magnitude must have more frequently reached higher on the shore profile during high tides than previously. The higher water levels would allow increased landwards penetration of energetic (stormy) wind waves over greater water depth. These waves would thus retain the energy to erode saltmarsh further to landwards than previously, by dislodging vegetation and exposing the sandy substrate at higher levels than could previously occur. The overall negative sediment budget in Duck Bay - and especially the rapid loss of any eroded sediment from the shoreline area via the daily ebb-tide currents - would impede shoreline recovery by leaving less loose sediment available for saltmarsh vegetation to capture and accrete during the intervals available for shoreline recovery between erosion events.

If energetic wind-wave events only reach unusually high levels on the saltmarsh shore on rare occasions, then vegetative recovery and sediment accretion between erosion events will prevent any long-term recession of the saltmarsh shoreline. This may be the case if there is no long-term rise in mean sea-level, so that short-term sea level and/or wind speed variability result in only rare erosion events occurring. However, if sea-level is continuing to progressively rise on inter-decadal timescales, then the intervals between stormy erosion events impacting on those higher levels on the shore profile will decrease until there is insufficient time for shoreline recovery between erosion events. In this case the shoreline will continue to progressively recede on an active erosion scarp, as is observed at all five studied sites in the West Duck Bay study area (Figure 40).

It can be inferred that shoreline recession will follow a net rise in sea-level more rapidly on shores exposed to more frequent strong winds over longer wind-wave fetches (i.e., with higher WFI), because wave events energetic enough to erode saltmarsh will occur more frequently at the new higher sea-levels on those shores. In contrast less exposed shores with shorter fetches may still only receive energetic waves at higher levels too infrequently for net shoreline recession to occur and may even continue to keep up with sea-level rise by accreting. This is the broad pattern observed across West Duck Bay as a whole (Figure 39) (Prahalad et al. 2015).

The increase in the rate of shoreline recession after 1980 that is observed in the S and SE study sites could possibly be driven by the acceleration of sea-level rise that has been observed globally since the early 1990s (see Section 2.3). However, no statistically significant recent acceleration of sea-level rise since circa 1990 has yet been detected in individual Tasmanian tide gauge records including that at Burnie (C. Watson *pers. comm.*). An alternative or additional possibility is that increasing wind speeds – as recorded at nearby Cape Grim since at least 1995 (see Section 5.4.2 above) – may be at least partly driving the increased shoreline recession rate by generating more energetic wind waves in Duck Bay. This is further discussed in the following sub-section. In either case it is notable that - allowing for some topographic wind-steering along the length of West Duck Bay - the S and SE sites probably have longer fetches and more wind-wave exposure in westerly wind directions than the other studied sites (Figure 39, Figure 40). This would make those sites more likely to increase their rates of recession in response to either potential driver, because they are more frequently exposed to sufficiently high westerly wind-wave energies as to result in more frequent erosion in any case.

Irrespective of the increased recession rates at the S and SE sites, the observation that all the study site shores in West Duck Bay have been actively eroding and receding over the entire air photo data period since 1945 is significant. The capacity of the four saltmarsh sites (at least) to recover from erosion – and the fact they have not done so - implies that the cause or causes of the erosion have

also been active and increasing over the same period. Climate change-induced sea-level rise is the only potential driver of shoreline recession at Duck Bay that is known to have been changing (rising) from prior to 1945 until the present, hence is the most plausible explanation of active shoreline recession at Duck Bay since before that date. These shores could plausibly have started receding in response to sea-level rise quite soon after the commencement of the contemporary climate change driven phase of global sea-level rise during the 1800s and could have been continuing to actively recede in response to ongoing net sea-level rise up to the present.

Are there drivers other than sea-level rise on this coast that could have caused the observed change in behaviour?

The alternative hypotheses listed in Table 6 below have been considered and are evaluated in the text following. No other potentially plausible explanations of the observed shoreline behaviour change have been identified beyond these.

Table 6: Alternative hypotheses investigated to explain observed changes.

Hypothesis	Evaluation (see following text)
Swell wave climate variability	Not supported
Artificial shoreline disturbances	Not supported
Vertical Land Movement (subsidence)	Not supported
Increasing westerly wind speeds	Possible additional driver of shoreline recession

As noted in the previous discussion of Ocean Beach (Section 5.2.4), swell-wave climates and swell-driven sand transport processes may strongly influence shoreline behaviour in a variety of ways. However, the lack of swell-wave activity within West Duck Bay (apart from limited shoreline stretches close to the tidal entrance channel) mean these processes are unlikely to be plausible drivers of the observed shoreline behaviour in West Duck Bay.

Although artificial levees and associated drainage channels have been implicated in saltmarsh erosion processes in some situations within the north-western saltmarsh area (Mount et al. 2010, section 6.1 & Figs 6.1 & 6.2), this does not appear to be the case at the only West Duck Bay study site close to such structures. Approximately two thirds of the NW study site is backed to landwards (behind a saltmarsh buffer) by a levee and drainage channel constructed between March 1986 and March 1990. Although a short-term accretion anomaly is present in the air photo record at about this time, there is otherwise no significant difference in the overall linear shoreline recession trend between the part of the site backed by levees and that part not backed by them, nor between the long-term recession trends before and that after the levees were constructed (see details in appendix A1.2.5).

An introduced rice grass (*Spartina anglica*) infestation affects the study sites only at the southern extremity of the SE study site, where it is inferred to be responsible for the short stretch of otherwise-anomalous shoreline progradation observed at that location (Figure 41). Rice grass infestations typically stabilise shorelines and cause them to accrete, and this is not observed in any other part of the study sites, which as at 2010 were not infested by this weed.

Other artificial disturbances such as vehicle use on shoreline saltmarsh, excessive power-boat usage at high tide or artificial structures on the shoreline may damage saltmarsh shores and drive erosion (Mount et al. 2010). However, whilst some of these have impacted in other parts of Duck Bay, at the time of the authors field work in 2010 there was no known evidence of these or other artificial disturbances likely to cause erosion at or affecting the study sites.

Vertical Land Movement (land subsidence) resulting in additional relative sea-level rise is unlikely to account for any significant component of shoreline recession at West Duck Bay. In part this is because GNSS-based measurements at Burnie (75 km south-east of Duck Bay) and GIA-based models indicate that vertical land movement (VLM) only marginally suggests subsidence in the

northwest Tasmania region (see Section 5.4.2 above). Moreover, any VLM across Tasmania is likely to be linear over multi-decadal time scales, given the absence of earthquake-induced deformation in the vertical component[19] and of anthropogenic influences such as fluid extraction. VLM is moreover considered especially unlikely to explain the acceleration of shoreline recession after 1980 at the S and SE study sites but not at the other three sites in this study area.

Increasing wind speeds at West Duck Bay could cause active shoreline recession at West Duck Bay for a similar reason to rising sea-levels, namely by generating higher and more energetic wind-waves over the available fetches. More energetic wind-waves at high tide could reach higher on the shore profile than previously, thus eroding saltmarsh to higher levels and further landwards on the shore profile.

Increasing wind speeds at West Duck Bay are not clearly demonstrated by the nearest wind records, at Smithton. However, that wind record contains anomalies including step-changes in wind speeds (suggesting equipment differences) and is thus not reliable as a long-term wind speed record. In contrast the Cape Grim wind record (~30 km to the west) has been a high quality wind record since 1987, and demonstrates a significant linear increase in westerly wind speeds since at least 1995 (see Figure 20 in Section 5.2.2 above). Since the westerly winds recorded at Cape Grim blow towards West Duck Bay over predominantly very low-relief country, it is plausible that the same westerly wind speed increases could have affected Duck Bay since at least 1995.

The active long-term shoreline recession observed at West Duck Bay - and possibly its increased rate at more exposed sites in that bay - could be explained by the driver of sea-level rise alone as inferred above. However, if wind speeds have also increased at West Duck Bay – as appears likely since 1995 at least - this could be an additional factor contributing to the active shoreline recession, and in particular to its increase at two sites after 1980.

5.4.5 Summary: West Duck Bay

Only two changing processes capable of driving observed shoreline recession in West Duck Bay have been identified, namely contemporary sea-level rise and south-westerly to westerly wind speed increases, both of which can drive increasingly frequent erosion higher on the shore profile than previously, for the reasons described above. No other plausible explanations have been identified. A net rise in sea-level at West Duck Bay can be reasonably inferred based on the nearby Burnie tide gauge record which demonstrates a Twentieth Century to present rise commensurate with climate change-induced global mean sea-level rise (GMSLR) (Section 5.4.2). Sea-level rise reconstructions for western Tasmania by (Church & White 2011) and (Hamlington et al. 2011) similarly yield recent sea-level rise commensurate with GMSLR (see Section 5.2.2). The occurrence of increasing wind speeds at West Duck Bay since at least 1995 is not unequivocally demonstrated with available local data, but is a reasonable inference based on good-quality data from Cape Grim, ~30 km west of Duck Bay, and the low relief terrain between there and Duck Bay.

An important characteristic of the saltmarsh shores that characterise four of the five West Duck Bay study sites is that in the absence of actively increasing drivers of erosion (such as rising sea-levels or increasing wind speeds) these shores can vegetatively recover from any prior erosion and can be stable or even accrete sediment and prograde (see Section 2.5.2 and Figure 6).

Given the characteristic behaviour of saltmarsh shores, it is inferred from the available evidence (described above) that there have been two notable long-term changes of shoreline behaviour on the actively receding saltmarsh shores at West Duck Bay over the period since the 1800s when

[19] Riddell, A.R., King, M.A., and Watson, C.S., 2020, Ongoing post-seismic vertical deformation of the Australian continent from far-field earthquakes. Submitted to Geophysical Journal International.

contemporary climate change-driven sea-level rise is considered to have begun (see Section 2.3). These are:

1. A change from stable (vegetated) saltmarsh shores to an actively receding (scarped) shore. This occurred prior to the earliest (1945) air photos and potentially could have occurred as early as the 1800s; and:
2. An increase in the rate of active shoreline recession about or after 1980 at two of the most wind-wave exposed of the five analysed sites.

The air photo record is interpreted as showing that all four studied saltmarsh shoreline sites in West Duck Bay have shown a significant continuing erosion and recession trend since at least the 1940's. Given their capacity to vegetatively recover from erosion, this implies that they have been responding to a driver or drivers which have themselves been progressively increasing over most or all of that period (albeit potentially with some cyclic variability on shorter timescales, whose effects on shoreline behaviour are not detectable in the air photo record). Sea-level rise is the only driver inferred with high confidence to have shown a net increase (rise) over the whole air photo period at West Duck Bay, although wind speeds may have also been increasing at West Duck Bay since at least 1995 (based on the Cape Grim wind record). It is therefore likely that both drivers have been contributing to the observed shoreline recession at West Duck Bay, since at least 1945 (the start of the air photo period) in the case of sea-level rise, and at least since 1995 in the case of increasing wind speeds.

Two of the study sites (the S & SE sites) have shown a significant increase in their rate of shoreline recession after 1980 (Figure 40). Although sea-level rise acceleration has not yet been clearly demonstrated at the nearby Burnie tide gauge in isolation (see Section 5.4.4 above) an acceleration in global mean SLR since 1990 is well established (Chen et al. 2017; Watson et al. 2015). Increasing wind speeds since 1995 are only clearly demonstrated at the Cape Grim weather station but not at the closer and less reliable Smithton weather stations (Section 5.4.2). Nonetheless, either or both drivers are plausible explanations of the observed increase in shoreline retreat rates after 1980, and more-over no other likely explanations have been identified.

The other important observation arising from this analysis is that not all soft erodible shores at West Duck Bay have been receding; the authors shoreline field mapping (Figure 37) showed that as at 2010 - and despite areas of long-term active shoreline recession - other long stretches of the shoreline were accreting with no sign of previous erosion episodes. Some 'transitional' shores were evidently subject to intermittent phases of erosion and accretion (recovery). The spatial distribution of dominantly receding and dominantly accreting saltmarsh shorelines around West Duck Bay shows an obvious subjective correlation with respectively greater and lesser wind-wave fetch and exposure as measured by a Wave Fetch Index (WFI); see Figure 39. This observation is consistent with the previous findings of Prahalad et al. (2015) who used erosion mapping and WFI modelling over the broader Duck Bay to Boullanger Bay region (Figure 36) to quantify WFI thresholds between saltmarsh shores prone to erosion, stability and accretion.

The two (S and SE) shoreline areas which have shown an increase of shoreline retreat rates after 1980 are at the downwind end of Duck Bay in respect of the dominant westerly winds, and hence more exposed to generally westerly winds over a longer fetch than the more upwind NW shoreline area which has not shown an increased recession rate (Figure 40). The S and SE areas therefore can be expected to have responded earlier to increasing sea-level rise and wind speeds.

It is however a notable anomaly that the WFI modelling also indicates a similarly high wind fetch exposure for the N (W & E) study sites, yet these have not shown a comparable increase in shoreline recession rate to the S and SE areas. However, the Smithton wind record – on which the WFI modelling for Duck Bay is based – is known to be problematical in its wind- speed records as noted

above (Section 5.4.2), and similar scepticism over its directional wind record may also be reasonable. The Cape Grim wind record shows a strong direct westerly wind component not seen in the Smithton records (see Figure 40). It is possible that the North Duck Bay sites (W & E) could be more wind-sheltered with respect to more prevalent direct westerly winds in Duck Bay than a simple cartographic application of the wind rose data from the closer Smithton weather stations suggest. Further work to resolve this apparent anomaly would be useful.

5.5 *Study Area 4: Barilla Shore*

5.5.1 Introduction

As the final detailed case study area, the Barilla case comprises four sites in the upstream (western) part of Pittwater. Located at the head of Frederick Henry Bay in south-eastern Tasmania, Pittwater is a large tidal re-entrant protected from swell waves behind the Seven Mile Beach sandy barrier (see regional and local maps at Figure 17 & Figure 42). The permanently open tidal channel entrance to Pittwater is over 10 km eastwards from the Barilla sites (Figure 42). The backshore areas landwards of the study site shores are low-relief agricultural land cleared of native vegetation. Actively eroding shores in this area were previously noted by Sharples et al. (2012).

The Barilla study area is an example of another of the four broad categories of coastal landform type from which study sites were selected for this thesis (namely "soft-rock one-way shores" as described in Section 3.2.1 and listed in Table 2 above). This section follows the same structure as the previous Sections 5.2, 5.3 and 5.4 above, presenting the essential data and findings of an investigation of shoreline behaviour at upper Pittwater since the 1940s. Additional data and information on this case study area is provided in Appendix A1.5.1.

Figure 42: Locality map showing the Barilla case study area within Pittwater, south-eastern Tasmania. Pittwater is a tidal re-entrant sheltered from the swell-wave climate of Frederick Henry Bay behind the Seven Mile Beach barrier. The tidal channel is permanently open. The Coal River discharges into upper Pittwater adjacent the Barilla case study area. The four Barilla study sites are indicated in red. Satellite image dated 2019 © Google Earth.

5.5.2 Site description and processes

Geomorphic description

The Barilla case study area (147° 27’ 0” E 42° 48’ 0” S) comprises four stretches of scarped shoreline in the north-western part of Pittwater between Barilla Bay and the discharge point of the Coal River into upper Pittwater (see Figure 42). The four sites are characterised by shoreline erosion scarps ranging from less than one to about six metres high (Figure 43 & Figure 44), which are incised into fluvial and lacustrine semi-lithified sediments (‘soft rocks’) of Tertiary or Quaternary age. These are typically interbedded brown cohesive clays, silty clays, sandy clays, friable sandstones and minor pebble and gravel layers (Forsyth 2002). Slumped blocks of the soft-rock occur sporadically at scarp toes but are probably rapidly broken up and removed by wind-waves. Narrow flat intertidal zones at the scarp foot typically comprise exposures of the soft clayey bedrock with thin patchy veneers of sand and/or pebbles winnowed from the eroded bedrock (Figure 43 & Figure 44). Erosion scarps at the South Barilla study site are of mostly freshly incised appearance (Figure 43), whereas those in the study sites further north tend to frequently have a less active appearance characterised by rounded and vegetated scarp faces with some sporadic fresh slumps (Figure 44).

Nearby swell-exposed Seven Mile Beach (Figure 42) has approximate spring and neap tidal ranges of 1.2 m and 0.3 m respectively (based on Hobart tide gauge data: Short 2006b). These ranges are probably attenuated at the study area, however there are no tide gauge records within Pittwater.

The Coal River, which discharges into Pittwater close to the study sites (Figure 42) drains a dominantly cleared catchment with mainly agricultural land uses and a series of dams and weirs capturing a large proportion of the river flow for irrigation purposes. Consequently, river discharge rates are low with suspended clays and silts dominating the river’s small sediment load.

Figure 43: Typical low actively eroding cohesive clay scarp in the South Barilla study site, with thin patchy veneers of sand winnowed from the soft bedrock partly mantling exposed soft bedrock in the intertidal zone. Neither the planting of rows of trees as shown, nor the deployment of many car tyres along this shore in recent decades, has noticeably slowed the erosion of this scarp. Since these attempts to protect the shore were implemented circa 1992 (as indicated by air photos), scarp retreat has continued unabated and in one area near this location has accelerated (see Figure 46). Photo: Chris Sharples (2011).

Figure 44: Cohesive clay shore in the North-west Barilla study site, with a narrow pebbly intertidal zone. The shoreline and erosion scarps in this area are higher than at South Barilla but less active as evident here. This study has demonstrated very slow rates of shoreline recession at this site; however, some recent scarping and slumping is visible (probably partly triggered by tree collapses but with some wave impacts obvious at the scarp toe). Photo: Chris Sharples (2016).

Swell wave climate

Swell waves penetrate the tidal channel mouth of Pittwater adjacent Seven Mile Beach (Figure 42) but are rapidly attenuated and refracted inside the entrance. There is no effective swell wave activity at the Barilla study area.

Wind (wind wave) climate

The closest long-term wind record is located at Hobart Airport approximately five to ten kilometres south-east of the Barilla sites (see Figure 42). The directional wind record for Hobart Airport from 1958 to 2015 is shown on Figure 45. Both the synoptic and daily maximum wind records show a dominant north-westerly wind direction aligned with upper Pittwater and the general trend of the Coal River valley. This is inferred to be a result of the dominantly westerly air flows characteristic of the Hobart region (Grose et al. 2010) being topographically steered south-eastwards at low levels down the Coal River valley and towards the airport. Hence the dominant and also the most energetic wind-waves affecting the study sites will be generated by north-westerly winds across the long south-easterly fetch of upper Pittwater.

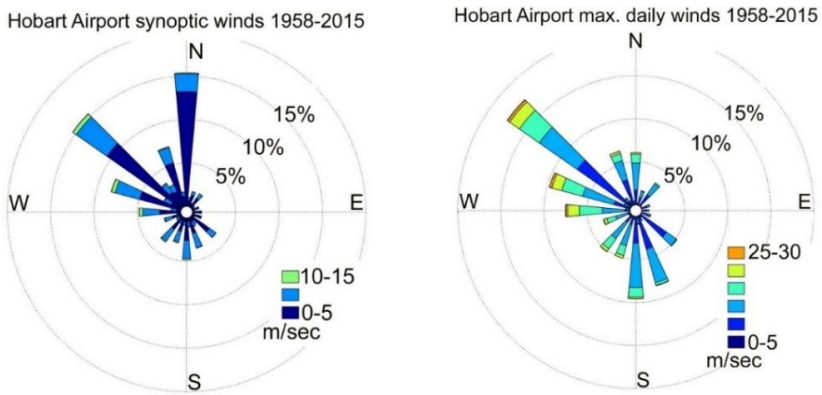

Figure 45: Wind direction data for Hobart Airport 1958-2015. Data plotted by Chris Sharples from original wind records supplied by the Australian Bureau of Meteorology.

The wind speed data for Hobart Airport appears to show a significant increase in mean synoptic winds speeds since 1990 (Appendix A1.5.1, Figure 224). However, this increase mainly occurs in two abrupt step-changes, which as noted by Troccoli et al. (2012) are likely to reflect instrumental changes rather than a real meteorological change, hence no clear evidence of a significant long-term wind speed change is seen in this data

Sediment transport and budget

The Barilla site shores are composed of clay-rich semi-lithified soft rock which cannot recover its previous form or mass after erosion (see Section 2.5.2). Energetic locally generated wind waves are the only apparent agent of coastal erosion on the Barilla shores. Immediately following any wind-wave erosion of the Barilla shores, it is inferred that the significant proportion of the eroded substrate that is clay- or silt-grade remains suspended and is dispersed in the water column by weak tidal, river discharge and wind wave-generated currents. Eventual slow deposition may occur in available (deeper water) accommodation space within Pittwater, or some of the suspended sediments may ultimately be dispersed through the permanently open tidal channel to the open coast. The coarser eroded sand and gravel fractions evidently settle out close to the erosion site (see Figure 43 & Figure 44) but as noted there is no mechanism by which this may rebuild the scarped shore. Such residual material is inferred to be occasionally redistributed within the intertidal zone and adjacent shallow waters by energetic wind-wave action.

Given that increasing accommodation space (i.e., water depth) for eroded sediment will become available within Pittwater due to ongoing sea-level rise, and with a proportion of the finer-grade eroded and suspended sediment probably being lost to the open coast, these conditions effectively constitute a permanently negative sediment budget resulting from a system of active sediment transport away from the eroded shoreline and into an active sediment sink (Pittwater and the open coast beyond) with capacity for increasing sequestration of eroded sediment as sea-level rise continues into the future.

Sea-level data

The nearest measured sea level data to the Barilla study area is from the Hobart tide gauge, measured in the lower Derwent River estuary about 15 km south-west of the Barilla sites. Although the Barilla sites are located in the upper reaches of a different coastal embayment to the Hobart tide gauge, both locations are in tidal marine environments permanently connected to the ocean at nearby Storm Bay. It is reasonable to infer a similar sea-level history to Hobart at the Barilla sites, albeit modulated by tidal hydrodynamics within Pittwater and possibly by the (relatively small) Coal River discharge near the Barilla sites.

The rate of mean sea-level rise inferred from a calculated linear fit to the Hobart tide gauge record (see Section 5.3.2: Figure 31) is 1.68 mm/yr^{-1} over the period 1962-2004, which is comparable with the global-average rise of 2.0 ± 0.3 mm yr^{-1} over the 1966 – 2009 period (White et al. 2014). The rate at the Hobart tide gauge is similar to the rate observed at the climate quality gauge located at Burnie approximately 235 km away (1.4 mm/yr^{-1}, see Section 5.4.2) and for Ocean Beach approximately 190 km away, computed from reconstructed data (2.13 – 2.21 mm/yr^{-1}, see Section 5.2.2) over approximately the same period. Additional information on the Hobart tide gauge record is provided in Appendix A1.4.2.

Vertical land movement

Current and ongoing geodetic studies of Tasmania have yet to resolve disagreements between GNSS derived estimates of VLM at Burnie and Hobart[20] that range between 0.0 to -1.0 mm yr^{-1}, and geophysical models indicating subsidence in the range of -0.1 to -0.2 mm yr^{-1} (see details in Chapter 2 Section 2.5.4 above). However, for the purpose of this thesis, there is no evidence suggesting that

[20] The Hobart GNSS site is located at Mt Pleasant which is just 2 km west of the West Barilla study site.

VLM is a significant signal in Tasmanian relative sea levels. There is no significant anthropogenic extraction of sub-surface fluids or other known processes such as seismic activity likely to cause significant VLM at the Barilla case study area.

Artificial interferences

The backshore areas have been largely cleared of native vegetation for agricultural purposes, beginning approximately 200 years ago. Vegetation clearance appears to have occurred to as close to the waterline as the top of the shoreline scarp in most areas. It is not obvious that this would have significantly affected shoreline erosion rates, however one consequence of the vegetation clearance has been the occurrence of soil tunnel erosion which has produced small soil pipes that in places are exposed in the shoreline scarp. These may contribute to scarp collapse but are sporadic features and hence probably only a minor influence on net scarp recession rates.

In common with many eastern Australian agricultural landscapes (Prosser & Winchester 1996), historic vegetation clearance in the Coal River catchment resulted in widespread gully erosion which supplied large volumes of silty sediment to the river. The landscape has subsequently largely stabilised, however this episode left a legacy of recent deltaic silt deposits in the Coal River estuary, and probably also resulted in silt filling some of the available sediment accommodation space in the upper Pittwater area near the Barilla sites.

As noted above, the construction of irrigation dams in the Coal River catchment during the twentieth century has resulted in smaller river discharges into Pittwater, which can be expected to have reduced water level variability unrelated to tides and sea-level change in upper Pittwater. This effect is not quantifiable with available information.

There have been numerous uncoordinated attempts to halt the erosion and recession of the scarped Barilla shorelines during recent decades. In the South Barilla area where shoreline recession has accelerated since circa 1990, unsuccessful attempts to stabilise the shores by planting trees and placing tyres have been made (Figure 43). Elsewhere, random dumping of rubbish in front of erosion scarps has occurred in a similarly quixotic effort to stop the erosion.

Oyster farms have been established in Pittwater since the 1980s, consisting of permanent, partly submerged parallel oyster racks typically 50 to 100 m long which are likely to absorb some wave energy during windy storm conditions. A large cluster of these racks has been established approximately 150 - 250 metres offshore and north of the South Barilla site since circa 1987 (based on air photo evidence). These may have somewhat reduced the impact of north-westerly wind waves on the South Barilla shore.

5.5.3 Recent shoreline change history

Shoreline position (defined as the vegetation line at the top of the shoreline scarp) at the Barilla study sites was digitised from ortho-rectified air photos taken at dates from 1946 to 2010. These are listed in appendix A1.5.1 Table 71. Due to incomplete air photo coverage at some dates, air photos from 39 dates were available at South Barilla, but only 37, 34 & 28 air photo dates were available at the West, North-west and North Barilla sites respectively. Nonetheless this time series is one of the most high-frequency multi-decadal air photo records available for any Tasmanian coastal areas. Figure 46 below summarises the shoreline behaviour history plots for each of the four Barilla case study sites.

The North, North-west and West Barilla sites all show similar shoreline position change histories suggesting a very slow shoreline recession over the air photo period of 1946 to 2010. Linear fits to these histories yield small recession trends that are within the uncertainty of the air photos. Shoreline change at these three sites is therefore considered negligible over the air photo period, albeit a very

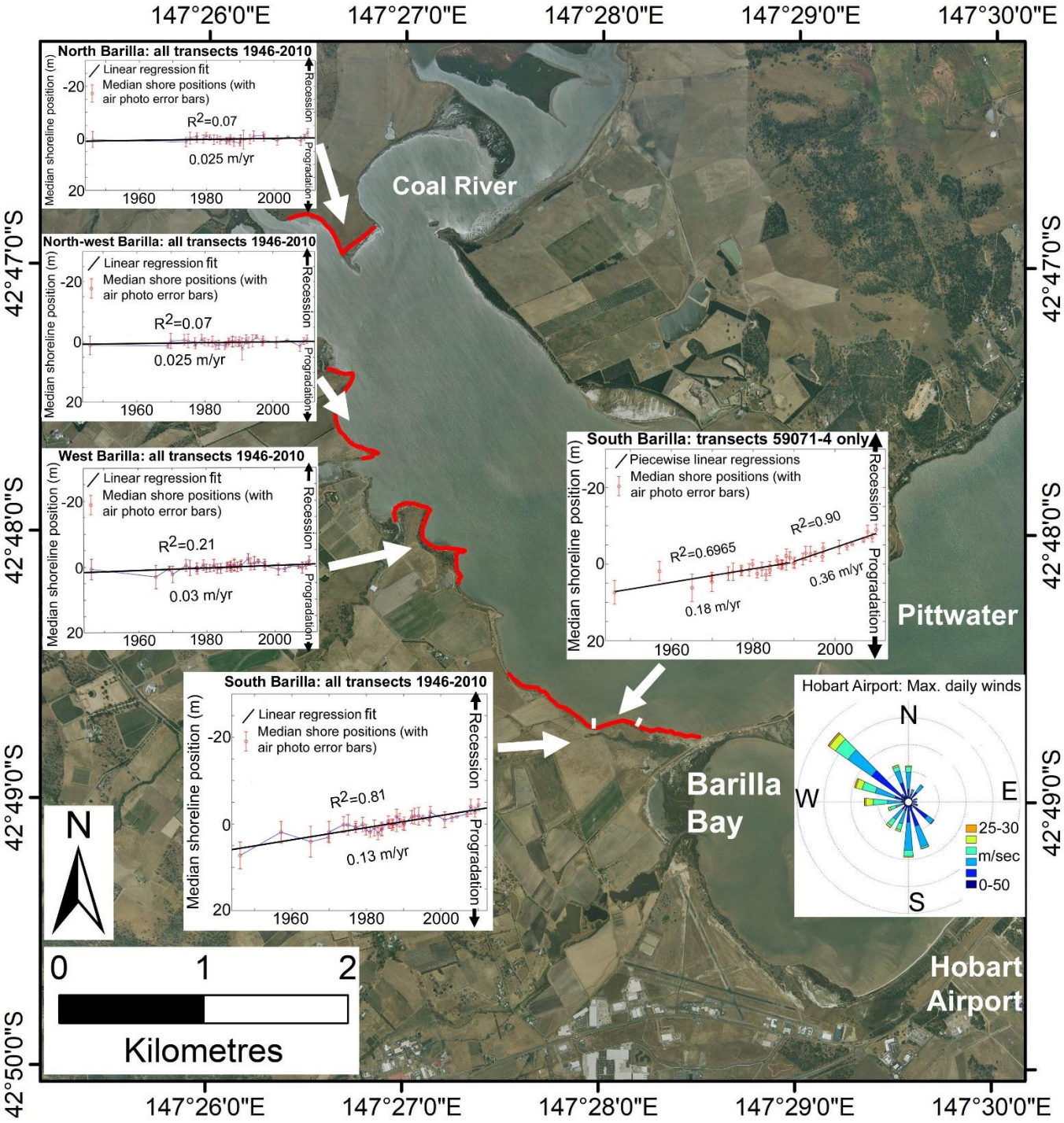

Figure 46: Summary shoreline history plots and maximum wind speeds record for the Barilla case study area over the air photo period from 1946 to 2010. For each of the four sites, a linear regression has been fitted to the median shoreline positions across all transects at all dates. Two plots are shown for the South Barilla Study site, one showing a single linear fit to the median shoreline positions at all dates, the other showing piecewise linear fits before and after 1990 on a cluster of four distinctive transects within this site that show a clear increase in the rate of their recession trend from about 1990 (see also Figure 47). The background image is the January 2010 air photo (© DPIPWE).

slow recession trend is suggested by the scarped (but partly rounded and vegetated) shorelines at each site (see Figure 44).

In contrast, the South Barilla site shows a significant shoreline linear recession trend which is larger than the air photo error margins over the whole air photo period, with a fresh active scarp retreating

at a linear rate of 0.13 metres per year over the period (see photo Figure 43 & map Figure 46). A portion of this site comprising four adjacent transects has shown a significant increase in its rate of recession after 1990, with a doubling of the linear recession rate from 0.18 m/yr^{-1} before 1990 to 0.36 m/yr^{-1} after 1990 (see Figure 46 & Figure 47).

It is noteworthy that the three sites showing negligible change all have shorter wind-wave fetches with respect to the dominant north-westerly wind direction across upper Pittwater than does South Barilla, and also have less direct exposure to the dominant wind waves, with the dominant wind blowing offshore at North Barilla, and parallel to the shore at West and North-west Barilla (see Figure 46).

In contrast, the South Barilla shore, which has shown significant recession since 1946, is more directly exposed to the dominant wind-wave direction across the longest available fetch in upper Pittwater. Moreover, the four transects within that site which have shown a significant increase in the rate of shoreline recession after 1990 are located on the part of the South Barilla shoreline most directly exposed to the dominant wind (and thus wind-wave) direction (Figure 47).

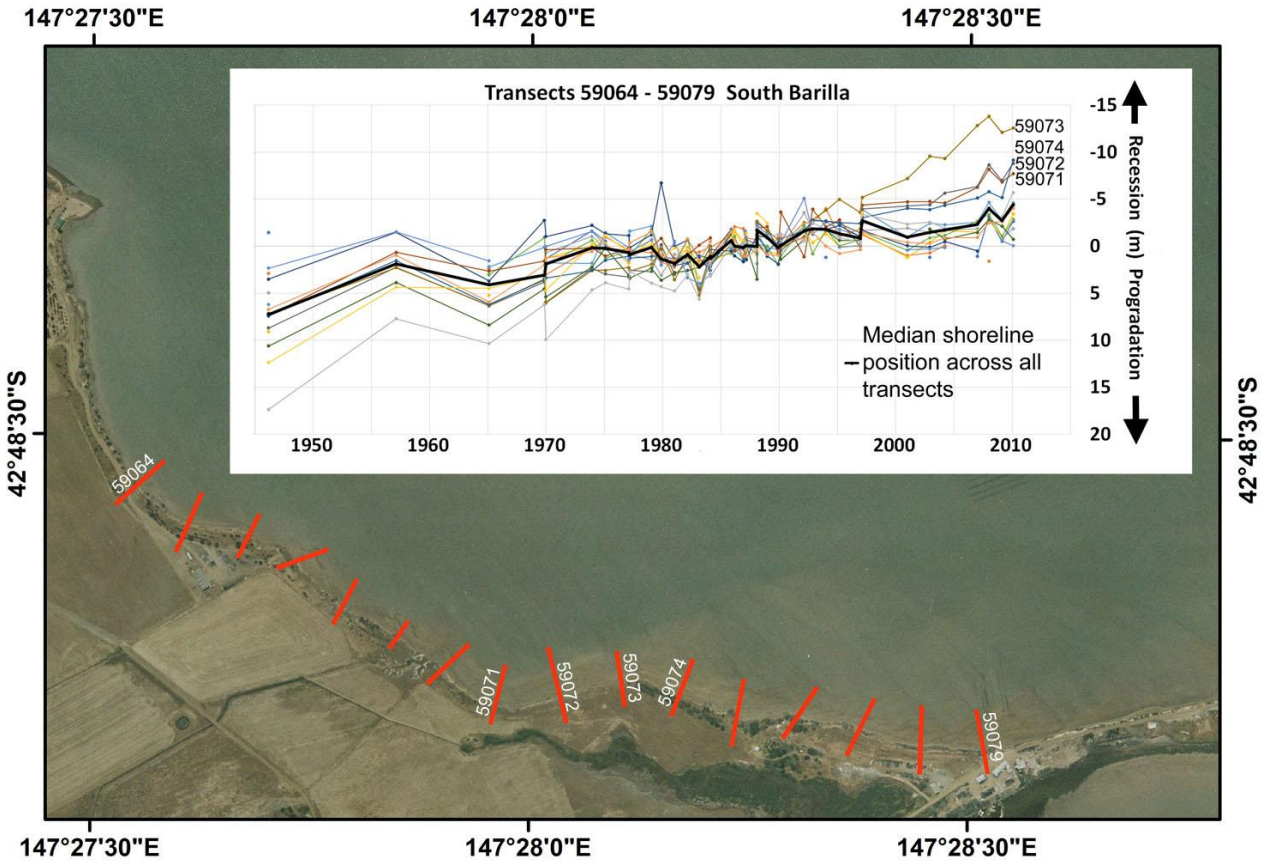

Figure 47: Shoreline position changes along all individual transects for the South Barilla shoreline, for 39 air photo dates from 1946 to 2010. A general linear recession trend is mostly coherent across all 100m spaced transects, however since circa 1990 four transects (59071-74, labelled) have exhibited notably increased rates of recession compared to the others. Background image is the 2010 air photo (© DPIPWE).

5.5.4 Shoreline behaviour analysis: Barilla Shore, Pittwater

Linear shoreline recession trends over the air photo period such as those observed over most of the South Barilla site, and inferred to be occurring at much slower rates at the West, North-west and North Barilla sites, require no special explanation beyond being the normal result of occasional stormy wind-wave attack on erodible cohesive clay substrates with no capacity for shoreline recovery after erosion impacts (see Section 2.5.2). Such shores can be expected to recede at some rate even in the absence of changing drivers such as sea-level rise. Given that locally generated

wind waves are the dominant agent of shoreline erosion in Pittwater, the relatively high rate of linear recession over most of the South Barilla shore is readily explained by that site being exposed to the dominant wind wave direction across the longest fetch available in upper Pittwater. Moreover the lower height of the erosion scarp in the South Barilla site would also facilitate faster shoreline recession than on the higher scarps found at the other three sites (compare Figure 43 & Figure 44), because of the lesser volume of material to be eroded for any given horizontal recession distance.

However, the observed increase in the rate of shoreline recession along a section of the South Barilla shoreline after circa 1990 requires some additional explanation. The hypothesis that the increase is an early response to sea-level rise was tested by seeking and evaluating multiple alternative explanations under the two sub-heading questions below.

Are there geomorphic process conditions at the South Barilla shore that would allow an earlier switch to recession in response to sea-level rise than on most coasts?

Contemporary climate change-induced sea-level rise is inferred to have occurred in Pittwater because a mean rise in sea-level commensurate with GMSLR has been measured on nearby swell-exposed coast at Hobart (see Section 5.5.2 above), and Pittwater is connected to the ocean via a permanently open tidal channel. Sea-level rise could plausibly cause the observed increase in the soft-rock shoreline recession rate because it allows the most energetic wind-waves generated by local windstorms to approach the shore over deeper water, thus impacting the shore profile higher and further to landwards than previously. This can occur without any change in the frequency and magnitude of wind wave storms. Less energetic but more frequent wind wave storms will similarly impact the profile to levels and distances landwards only previously reached by more energetic waves. The overall effect is a more rapid rate of shoreline recession due to wind-waves of any given magnitude eroding higher and further to landwards than previously. Other work has previously inferred that sea-level rise can be expected to drive increasing rates of recession of soft-rock coasts for this reason (Trenhaile 2011); see also Section 2.5.2.

It is notable that an significant increase in the rate of recession has been observed on only the most wind-wave exposed section of the South Barilla shoreline, which is itself the most wind-wave exposed of the four Barilla study sites, and has the longest fetch in the dominant wind direction (Figure 46 & Figure 47). This means that to date only the most extreme wind-wave events producing waves over the longest available fetch have been able to attack the soft rock scarps in the study area with sufficient energy and frequency as to result in a notable increase in the rate of shoreline recession.

The observed increase in the rate of the shoreline recession rate at the South Barilla study site has occurred over roughly the same period as the observed acceleration of contemporary climate change-induced global mean sea-level rise since circa 1990 (see Section 2.3). However, no statistically significant recent acceleration of sea-level rise since circa 1990 has yet been detected in individual Tasmanian tide gauge records including that at Hobart (C. Watson *pers. comm*.). Hence there is no local evidence to support the interpretation that observed increase of shoreline recession rate at the South Barilla site might be driven by an acceleration of contemporary climate change-induced sea-level rise.

It is more plausible that it is only in recent decades that any effects of sea-level rise at all have become sufficiently significant at the Barilla study area as to emerge above the ‘noise’ of the slow shoreline recession that is a normal long-term process on any soft rock shore. Thus, it is inferred that the observed increase of the recession rate is simply the first emergence of any change attributable to contemporary sea-level rise at the most susceptible site in the Barilla study area. The increase of the prior (normal) soft rock shoreline recession rate does not require any acceleration in that new driver of erosion (sea-level rise), only that some effect of the new driver emerge from the noise of prior recession rates that were not driven by sea-level rise.

Are there drivers other than sea-level rise on this coast that could have caused the observed change in behaviour?

The alternative hypotheses listed in Table 7 below have been considered and are evaluated in the text following. No other potentially plausible explanations of the observed shoreline behaviour change have been identified.

Table 7: Alternative hypotheses investigated to explain observed changes.

Hypothesis	Evaluation (see following text)
Shoreline morphology variations	Not supported
Wind speed increases	Not supported
Vertical land movement	Not supported
Artificial disturbances – land clearance and tunnel erosion	Not supported
Artificial disturbances – erosion scarp "protection" works	Not supported
Artificial disturbances – oyster farming	Not supported

The shoreline erosion scarp in the South Barilla area is notably lower (~1 m) than in the other study sites (~ 3 – 6 m high). Compare Figure 43 and Figure 44 above. This means that for a given amount of wave energy expended, the recession of the South Barilla shoreline scarp can be expected to be faster than at the other sites because of the lesser mass of material to be removed by erosion for a given amount of horizontal shoreline recession. Together with the longer available wind-wave fetch, this is probably a factor in the notably more rapid long-term linear recession rate across the whole South Barilla site compared to the other sites (Figure 46). However this explanation does not account for the recent increase of shoreline recession rate on the most exposed part of the South Barilla shore; this factor would only account for an increase if the height of the shoreline erosion scarp was decreasing as it is eroded further to landwards, which is not known or thought likely to have been the case (based on field (Figure 43) and air photo inspection).

Increasing wind speeds in the Barilla study area could cause an increase of shoreline recession rate at the South Barilla site for a similar reason to rising sea-levels, namely by more frequently generating higher and more energetic wind-waves over the available fetch which could run further landwards and erode higher on the shore profile more often than previously. However as noted in Section 5.5.2 above, the available wind record from nearby Hobart Airport does not clearly demonstrate increasing wind speeds in recent decades (see also appendix A1.5.1, Figure 224).

Vertical Land Movement (subsidence) resulting in locally increased relative sea-level rise is associated with shoreline recession in many places (see Section 2.5.4), but as discussed in Sections 2.5.4 & 5.5.2 above is probably negligible in the Barilla study area region. Moreover, VLM would in any case be unlikely to explain the acceleration of shoreline recession after 1990, and only at the South Barilla study site.

Artificial land clearance immediately landwards of the Barilla shorelines over the last 200 years has caused hydrological changes resulting in gully erosion and tunnel erosion, with some soil pipes opening in shoreline scarps. The exposed soil pipes may make the shoreline scarps slightly more susceptible to slumping in response to shoreline erosion and may thus have had some influence on overall shoreline recession during the last 200 years, however it is also likely that the rates of gully and tunnel erosion resulting from land clearance have reduced significantly over the Twentieth Century as the landscape adjusted to changing vegetation cover (Prosser & Winchester 1996). In particular, these landscape disturbances do not provide any explanation of the increase in the rate of shoreline recession in the South Barilla site after circa 1990.

A notable attempt to protect the South Barilla shoreline from coastal erosion was undertaken circa 1992 (based on air photo evidence), by planting trees and placing car tyres to protect the scarp from erosion (see Figure 43). This work has not slowed the continued recession of the shoreline, even though that was its intention. Conversely, the protection works do not provide any apparent

explanation for the observed increase of shoreline recession which has occurred along part of the shoreline where the protection attempts occurred.

Oyster racks constructed circa 1987 (based on air photo evidence) several hundred metres offshore and to the north of the South Barilla shore have probably absorbed some of the energy of north-westerly wind waves before they reach the South Barilla shore. If this effect were significant it would have reduced rather than increased the rate of shoreline recession at South Barilla. However the fact that the rate of shoreline recession in the most exposed part of the South Barilla has increased since circa 1990 implies that the degree to which the oyster farms have absorbed wave energy is less significant than the degree to which the driver of the increase – probably contemporary sea-level rise – has resulted in waves impacting higher and further landwards on the South Barilla shore profile.

5.5.5 Summary: Barilla shore, Pittwater

The 'soft-rock' cohesive clay shores in the Barilla study area have eroded and receded throughout the air photo period from 1946 to 2010. The observed recession rates range from a significant linear rate of 0.13 m/yr^{-1} (outside the uncertainty of the air photos) at the South Barilla site where shores are exposed to wind-waves over the longest available fetch, to very small recession rates of around 0.025m/yr^{-1} (within the uncertainty of the air photos) on the less exposed sites. This shoreline behaviour is characteristic of soft-rock shores subject to occasional wind-wave erosion events and is readily explained without recourse to additional drivers of change such as sea-level rise. Although sea-level rise could be a contributing factor in the observed recession, so long as the recession rate is roughly linear over the available record period, it is problematic to identify a component of this driven by contemporary sea-level rise.

However, the most wind-wave exposed shoreline section within the South Barilla site (which also has the longest fetch of the studied sites) has shown a significant increase of its recession rate after circa 1990. This requires some additional explanation, and the only hypothesis identified which plausibly explains it is an early response to contemporary climate change-induced sea-level rise (but not necessarily to any acceleration in the rate of that sea-level rise).

In contrast to Ocean Beach and probably West Duck Bay, there is no clear evidence that increasing wind speeds may be an additional driver of the shoreline recession rate increase at the Barilla study area. Nonetheless, in the swell-sheltered tidal environment of Pittwater wind-wave fetch and exposure plays a strong role in determining patterns of shoreline erosion and recession, with the fetch length and degree of exposure to the dominant wind wave direction correlating strongly with both faster rates of linear shoreline recession over the whole period investigated, and with recent increase of the recession rate on the most exposed shores.

5.6 *Chapter Summary*

5.6.1 Preamble

This summary section identifies key findings from the four case studies described in some detail throughout this chapter. These include the identification of several processes inferred to be causing or capable of causing the observed long-term shoreline behaviour changes (including but not limited to sea-level rise). These "drivers of change" are listed in Section 5.6.2 below.

The case study analyses also sought to identify geomorphic and oceanographic conditions at each site that may explain why the shoreline behaviour changes are being expressed as early physical responses that can already be observed at those sites. This is important given that in many coastal environments processes (or 'conditions') such as cross-shore and along-shore sand exchanges still

overwhelm or prevent observable responses to sea-level rise and other climate change-induced drivers (see Section 2.4). The identified "conditions enabling change" are summarised in Section 5.6.3 below.

Chapter 6 to follow builds on these findings by asking whether these identified drivers and conditions can explain changes in behaviour (or lack thereof) in the broader diversity of the 35 distinctive coastal sites for which this project has individually compiled approximately 70-year shoreline behaviour histories.

5.6.2 Drivers of change

Three 'drivers of change' are summarised below. These are the processes or 'drivers' identified as having the explanatory power to account for the long-term shoreline behaviour changes observed at the four case study areas. Two of these (sea-level rise and increasing onshore wind speeds) are likely to be active drivers of change in the case study areas, whereas the third (long-term swell-direction changes) is a possible albeit uncertain additional driver of change in one case (Ocean Beach). However, this driver may be more significant on some other Tasmanian coasts not examined in this project (as discussed further below).

A range of other natural and artificial drivers of change have been considered in the four case studies, for example, vertical land movement, aspects of swell wave climate variability, changes in alongshore and onshore sand movement and a range of artificial interferences with coastal processes. These and other processes are known to influence the long-term behaviour of many shorelines elsewhere (see Section 2.4), however the available evidence indicates their effects on observed shoreline behaviour changes in the case study areas examined here are probably negligible.

Sea-level rise

There is widely accepted evidence that sea-level rise is a driver of erosion and shoreline recession on soft shorelines including sand and soft-rock shores (see Section 2.2).

In each of the four case studies examined in this chapter, contemporary climate change-induced sea-level rise is a plausible driver of long-term changes of shoreline behaviour interpreted from the historical air photo record. In two cases (Roches Beach and Barilla) contemporary sea-level rise commensurate with GMSLR is the only driver identified as having the capacity to have caused the observed changes. However, the acceleration of GMSLR that has been observed since the 1990s (Section 2.3) has not yet been clearly demonstrated to have had observable effects on shoreline behaviour in Tasmania although it is a possible contributor to the changes at West Duck Bay.

Increasing onshore wind speeds (increasing wind-wave impacts)

A key finding from these case studies is that long-term increases in onshore wind speeds have occurred on at least Tasmania's west coast during recent decades. These increases in wind speed are attributed within the literature to climate change (Fletcher et al. 2018; Hemer, Church & Hunter 2010; Kirkpatrick et al. 2017; Marshall 2003) and have the potential to change long-term coastal behaviour in a fashion similar to sea-level rise, namely by driving an onset or increase in the rate of shoreline recession.

Analysis of long-term weather records (particularly the high-quality Cape Grim record from NW Tasmania: see Section 5.2.2 & Figure 20) shows that Ocean Beach and probably West Duck Bay have likely been exposed to progressively increasing westerly to south westerly winds since at least 1995 (see Sections 5.2 and 5.4). This change has been attributed to broader changes in the Southern Annular Mode (SAM) driven by contemporary climate change (Fletcher et al. 2018; Marshall 2003); see Section 2.5.6, also appendix A1.3.8 Figure 179.

Increasing onshore wind speeds can be expected to increase the magnitude of soft shoreline erosion for two reasons, firstly by more frequently generating higher and more energetic wind-waves, and

secondly because stronger onshore winds and those higher wind-waves will contribute to higher wave set-up at the shore. Both these effects increase shoreline erosion and recession rates for essentially the same reason that sea-level rise does, namely by enabling erosive waves to more frequently run further landwards and higher up the shore profile than previously.

A contribution from increasing wind-wave magnitudes to progressive shoreline recession at Ocean Beach and West Duck Bay is therefore likely, although this study has not quantified the relative effects of this compared to the sea-level rise contribution. Since locally-generated wind waves are sub-ordinate to swell waves at Ocean Beach (Hemer 2010), the contribution of this driver to shoreline recession is likely to be less significant at that location. In contrast, at West Duck Bay swell waves do not penetrate far into the bay, and local wind waves are the main agent of erosion, hence the effects of increasing wind-waves relative to those of sea-level rise are likely to be greater. On the other hand, since prevailing westerly winds are dominantly directed offshore at the Roches Beach site there is unlikely to be a significant contribution from any wind changes to the shoreline recession observed at that site (see Section 5.3.4).

For the Barilla case study area, the nearby Hobart Airport wind record does not provide good evidence of long-term wind speed increases. Outside of the high quality Cape Grim wind record, long-term wind speed increases are suggested in some Tasmanian west and south-west coast wind records such as those from Cape Sorell and Strahan Airport (appendix A1.3.8 Figure 175) and Maatsuyker Island (Kirkpatrick et al. 2017). However such increases are not clearly demonstrated in the records of other weather stations also exposed to the dominantly westerly air flows, such as Cape Bruny (see appendix Section A1.3.1), Hobart Airport (see appendix A1.5.1, Figure 224) and Hobart City (Ellerslie Road). In these latter records there is evidence of strong local topographic wind steering effects, together with large data gaps, changing recording protocols and obvious data step changes in some records, all of which make the identification of any trend in long-term wind speeds problematic.

However, given there is evidence that clearly-identifiable westerly wind speed increases on Tasmania's west coast are related to changes in the SAM driven by climate change (see above and Section 2.5.6), it is implicit that wind speeds may have increased on other Tasmanian coasts exposed to the same SAM-influenced westerly air flows. These are the dominant winds on both the western and southern coasts of Tasmania and are also important in the south-east (Storm Bay) region. Further careful analysis of additional wind records will be required to confirm or refute this (see Recommendations Section 8.3.3).

Swell wave direction changes

The direction from which swell waves approach a sandy shore can strongly affect the rate and direction of both alongshore and cross-shore sand movement on a beach. Hence seasonal or inter-annual variability in swell wave directions may result in cyclic or episodic sandy shoreline changes that may over-whelm and mask shoreline responses to sea-level rise to date on some coasts (Mortlock et al. 2017; Ranasinghe et al. 2004). However, long-term changes in swell-wave direction are also expected to result from contemporary climate change and are expected to change longer-term spatial patterns of alongshore sand transport and so of beach recession and progradation (e.g., Leach et al. 2020). Hemer et al. (2008) and (Hemer 2009) have argued that such changes will be a major mode of long-term climate change-driven shoreline change.

A long-term anticlockwise shift of wave directions in the SAM-driven south-westerly swell-wave climate that dominates western Tasmania's coast has been observed since the mid-1960s (Hemer 2010; Hemer, Church & Hunter 2010; Marshall 2003). The magnitude of the directional changes on Tasmania's west coast have not been measured but are likely of the order of a few tens of degrees or less (see Section 5.2.2). The relatively straight and north-south orientation of Ocean Beach, together with geomorphic evidence of a strong persistent southwards alongshore drift at that beach, suggests

that this shift has probably had little effect on sand transport rates or directions at Ocean Beach to date, albeit some residual uncertainty remains; see Section 5.2.4 and Sharples et al. (2020). Of the other case study areas, swell waves do not reach West Duck Bay and the Barilla shore. In the case of Roches Beach, the long swell refraction pathway through Frederick Henry Bay 'trains' the waves resulting in negligible directional variability at the beach irrespective of swell direction variability outside the bay (Section 5.3.2, Figure 29).

Long-term swell-wave directional change is therefore considered likely to have had negligible influence on shoreline behaviour change in the four case study areas examined in this chapter. However, the potential for some climate change-driven swell direction variability to cause shoreline behaviour changes on some Tasmanian beaches cannot be ruled out. As noted in Section 2.5.5, this potential source of shoreline behaviour change may be most effective on Tasmania's east coast beaches, which are exposed to the Tasman Sea wave climate which is already more directionally-variable that the SAM-driven swell wave climate of Tasmania's west and south coasts (Goodwin, Mortlock & Browning 2016; Hemer, Simmonds & Keay 2008). Because of other priorities in study site selection (Chapter 4), the suite of study sites selected for this project did not include east coast beaches most likely to be affected by Tasman Sea swell wave climate variability. However future research into these possibilities is recommended (see Section 8.3.4).

5.6.3 Conditions enabling change

The "conditions enabling change" as discussed here are not the processes driving shoreline behaviour changes (as discussed above), but rather are geological, geomorphic and oceanographic conditions at particular study sites that have enabled coastal behaviour changes in response to sea-level rise to be detectable (or, to emerge). These conditions contrast with those that cause changes in response to sea-level rise to be overwhelmed or prevented as is still the case at many coastal locations (see Section 2.4).

The conditions identified as enabling change in the four case studies examined in this chapter are listed and discussed below. These conditions are divided into two groups. *Critical conditions* are those associated with early shoreline behaviour changes in response to sea-level rise in all cases examined; these are inferred to be essential conditions for early responses to be manifest. In contrast *contributing conditions* are inferred to contribute to enabling the early emergence of such responses but were not identified as being indispensable for this to occur.

Critical conditions

Persistent (typically unidirectional) and permanent sediment transport away from eroding shores, and active sediment sinks with significant accommodation space

These two related conditions were factors in all working hypotheses that were found to have sufficient explanatory power to account for shoreline behaviour changes in the four case study areas.

Whereas a variety of active sediment sink types were identified across the four case study environments (see below), the critical factor in all cases was their ability to permanently sequester at least a significant proportion of sediment eroded from the shoreline so that it cannot return to rebuild the eroded shore. This is inferred to contribute to preventing full shoreline recovery between erosion events, particularly as sea-level rise results in erosion events occurring more frequently and higher on the shore profile than previously. The active sediment sinks identified in all four case studies also had the capacity to sequester increasing quantities of eroded sediment into the future, which will allow shoreline recession to continue and/or increase its rate.

Rapid and permanent transport of eroded material away from an eroded shoreline was also a critical factor identified at the case study areas, and may be more important than the existence of an 'ultimate' sink so long as it means the removed sediment is unable to return to the eroded site later and rebuild the eroded shore. It is inferred that a long-term change of behaviour towards shoreline recession will not occur if a shore is continuing to be able to recover fully after erosion. This is typically the case with well-embayed open coast swell-exposed sandy beaches undergoing the normal erosion and accretion cycle (Woodroffe 2003, p. 290) and lacking any mechanism that quickly removes eroded sand from the embayment.

Despite having the same ultimate effect on shoreline behaviour, the active sediment sinks and sediment transport mechanisms for each case study site were of quite varied geomorphic types, as summarised here (from the details in the preceding sub-sections of this chapter):

Ocean Beach (swell-exposed sandy beach):

- *Primary sink*: A flood-tide delta inside the permanently open tidal channel mouth of Macquarie Harbour is the most important active sediment sink. The harbour has a very large capacity (accommodation space) to continue sequestering increasing amounts of eroded sand in future.
- *Secondary sink*: Transgressive dunes transporting windblown sand inland from the beach are inferred to be aeolian sand sinks but of lesser capacity than the Macquarie Harbour flood tide delta. Gradual revegetation of formerly mobile transgressive dunes has made these sinks decreasingly important since the 1940s, particularly behind the southern half of the beach.
- *Eroded sediment transport*: Ocean Beach has a persistent and mostly unidirectional swell-driven littoral drift southwards through the main beach compartment to the permanently open tidal channel and into the sediment sink in Macquarie Harbour. Occasional wind-wave variability may cause littoral drift direction variability but that appears to be a minor variation.

Roches Beach (swell-exposed sandy beach):

- *Primary sink*: Littoral drift of sand northwards out of the main central embayment, around Bambra Reef into down-drift sediment cells and ultimately to Seven Mile Beach and its foredune constitutes an active sand sink with a very large capacity to continue sequestering sand eroded from the main Roches Beach embayment.
- *Eroded sediment transport*: Roches Beach has a persistent and mostly unidirectional swell-driven littoral drift northwards through the main central beach compartment and around Bambra Reef. Occasional wind-waves (e.g., from a north-easterly direction) may cause littoral drift direction variability, but it is inferred from the nearby Hobart Airport wind record that this is a minor and infrequent variation.

West Duck Bay (swell-sheltered sandy tidal re-entrant with largest tidal range in Tasmania):

- *Primary sink*: Ebb-tide currents that are active with every tidal cycle at the meso-tidal West Duck Bay study area are inferred to rapidly transport eroded shoreline sand and peaty-clay saltmarsh soil debris across the eroding intertidal sandflats, which are exposed daily at low tide. Although the tidal currents are bi-directional, eroded sand reaching the deeper tidal channels that cut through the intertidal flats are inferred to settle there during ebb tides, so that little sand returns to the intertidal flats on flood tides. These channels have been shown

to progressively move sand offshore into deep water in Bass Strait, which is therefore an active sediment sink with effectively unlimited capacity to sequester additional eroded sediment.

- *Eroded sediment transport*: The tidal currents are a strong and pervasive sediment transport mechanism within Duck Bay and adjoining swell-sheltered re-entrants with their very large (for Tasmania) meso-tidal range, which keep eroded saltmarsh soil debris suspended and sand mobilised on a daily (tidal cycle) basis until they are either captured by vegetative saltmarsh shoreline recovery processes (if these occur) or more commonly are transported offshore into deeper shelf waters via the major tidal channels.

Barilla shore, Pittwater (swell-sheltered cohesive clay 'soft-rock' shoreline):

- *Primary sink:* The significant proportion of the eroded soft-rock shoreline substrate that is of clay- or silt-grade remains suspended immediately following wind-wave erosion and is dispersed in the water column by tidal and wind wave-generated currents (albeit tidal range at Barilla is much smaller than at West Duck Bay, implying weaker tidal currents). Eventual slow deposition may occur in available (deeper water) accommodation space within Pittwater, or part of the suspended sediments may ultimately be dispersed through the permanently open tidal channel to the open coast. The coarser eroded sand and gravel fraction may settle out close to the erosion site but the lack of any mechanism to rebuild cohesive clay shores (in contrast to swell-exposed sandy shores) means that this is a permanent sink too. Some subsequent redistribution of the coarser fractions by wind wave activity in the nearshore zone is likely. With increasing accommodation space (i.e., water depth) for eroded sediment becoming available within Pittwater due to sea-level rise, and with a proportion of the finer-grade eroded sediment probably being lost to the open coast, these are active sediment sinks with capacity for increasing sequestration of eroded sediment as sea-level rise continues into the future.
- *Eroded sediment transport:* The transport and deposition of finer and coarser eroded shore substrate fractions as described above, together with the inability of a cohesive-clay soft-rock shore to "recover" or rebuild after erosion, in effect constitutes a system of active sediment transport away from the eroded shoreline and into an active sediment sink.

In principle, the lack of shoreline recovery capacity means that soft-rock shores such as Barilla should exhibit changes of shoreline behaviour resulting from an onset of climate change-driven erosion with little delay. However, scarp slumping and/or slower erosion rates due to lesser wind-wave exposure may slow or modulate this response in many cases.

High wind (wind-wave) exposure and fetch

High wind exposure and long wind-wave fetches are not shown to be indispensable conditions for an early response to sea-level rise to occur at swell-dominated sites. However, they are classed here as being "critical conditions" for enabling early responses to sea-level rise at swell-sheltered sites where wind-waves generated over available local fetches are the main agent of shoreline erosion and recession and thus of long-term shoreline behaviour change. The degree of wind-wave fetch and exposure were inferred to be the main factors explaining the distribution of shorelines showing differing degrees of response to sea-level in the two swell-sheltered case study areas of West Duck Bay and the Barilla shore at Pittwater (Sections 5.4 & 5.5).

At both areas all the shoreline sites analysed have been receding or at least exhibiting erosion scarps over the whole air photo period, however only those most exposed to the dominant wind direction over the longest fetches have exhibited a substantial increase of recession rate since circa 1980. This is inferred to be a signature effect of the increasing impact of climate change-related drivers (i.e., rising sea-levels and/or increasing wind speeds). These results indicate that an early response to climate-change driven sea-level rise and/or to wind-speed increases will most likely occur in swell-sheltered re-entrants where there is high exposure to sufficiently long wind-wave fetches (as was also found by Prahalad et al. (2015)). Albert et al. (2016) have identified a similar finding in the Solomon Islands, where shoreline recession attributed to regionally high RMSLR is greatest on shores most exposed to wave action.

In the case of Ocean Beach, which is highly exposed to both swell and locally generated wind-waves, there is insufficient relevant data to quantify or model the relative degree of control that each wave type exerts over shoreline erosion patterns or littoral drift directions and rates. However, the dominance of swell over wind-wave conditions inferred from the nearby Cape Sorell wave-rider buoy records (Hemer 2010) suggests that in this high-energy swell-exposed location local winds and wind-wave fetch and exposure are probably sub-ordinate controls on shoreline recession rates and patterns compared to the swell wave climate.

At the swell-exposed Roches Beach case study site, winds and wind-generated waves have not normally been a significant driver of the observed long-term shoreline behaviour changes because the dominant winds blow offshore (see Section 5.3.4), and for the same reason are not likely to be significant controls on littoral drift (as noted by Shand & Carley 2011) or erosion patterns.

Contributing conditions

The following geomorphic, geological, and oceanographic conditions were not identified by this thesis as being indispensable for an early shoreline behaviour response to sea-level rise to occur. However, they are inferred to contribute to enabling the emergence of such responses where they do occur, and to exert some control over the timing and nature of such responses. The following lists a range of contributing conditions that have been identified during this project, from both existing knowledge (literature review) and from the outcomes of this thesis. Key findings in regard to the latter are discussed below.

Active sediment source

An active sediment (sand) source was identified as being present in the two sandy swell-exposed case studies, namely Ocean Beach (swell-driven onshore sand supply from the shelf) and Roches Beach (swell-driven littoral drift of sand into and through leaky compartments). This condition was not identified as being a cause of shoreline behaviour change in response to climate change-induced drivers. Instead, in each case the incoming sand gains were interpreted as *preventing* a recessional response to increasing upper beach erosion driven by sea-level rise and increasing onshore winds *until such time* as the increasing sand losses due to increasing erosion driven by climate change-induced causes exceeded the capacity of the incoming sand gains to compensate for the losses.

It is implicit in this that an early shoreline behaviour change in response to the onset of climate change-induced drivers could most readily occur in cases where there is no gaining sediment supply, as is indeed the case at the other two case studies (West Duck Bay and the Barilla shore of Pittwater). However, where a sediment supply is active, the ratio between sediment gains and increasing sediment losses due to erosion is inferred to be a key factor or condition determining whether and when a change of shoreline behaviour occurs. In the two cases where a sand supply is a factor (Ocean Beach and Roches Beach), the eventual shoreline response is in the mode of a "tipping point" that occurs when the rate of sand loss increases to a degree which exceeds the available

sediment gains. In both cases it is inferred that a major erosive storm (or cluster of storms) was a trigger which tipped each beach quite abruptly into a new (recessional) behaviour mode.

Tidal range

Tidal range is mostly micro-tidal around Tasmania (with the exception of meso-tidal parts of the north coast including Duck Bay). Hence this study has in general been unable to assess whether significantly differing tidal ranges influence coastal behaviour in response to climate change-induced drivers. The discussion in the Literature Review (Section 2.5.7) identifies several ways in which tidal range differences might contribute to different shoreline responses to sea-level rise, however it is likely these are in general not major contributing conditions for Tasmanian coasts.

However, the West Duck Bay study area is subject to Tasmania's highest (meso-tidal) range, with measured mean spring tide ranges from 2.09 up to 2.79 m in similar nearby tidal environments (Donaldson, Sharples & Anders 2012). This large tidal range (for Tasmania) results in strong tidal currents within Duck Bay. These have been identified in Section 5.4 above as a persistent and effective transport pathway by which eroded shoreline sands are permanently removed to a sand sink. Hence the tidal conditions in Duck Bay do in turn result in one of the critical conditions identified as enabling an early coastal response to sea-level rise and/or increasing wind speeds, namely efficient transport of eroded sands to a sink.

It is also notable that the tidal dynamics in Duck Bay are strongly influenced by shallow water effects as the daily tidal cycles inundate and expose the sandy tidal flats. This raises the likelihood that ongoing sea-level rise may change the tidal dynamics in Duck Bay as water depths (especially at high tide) increase by significant proportions of their current depths. However further investigation of this issue was beyond the scope of this project.

Shoreline substrate type

The Literature Review (Section 2.5.2) identified a number of ways in which different shoreline substrate types are inferred to respond differently to sea-level rise. These included the markedly different responses of sandy shores on swell-exposed coasts and in swell-sheltered tidal embayments, as well as the very different ways in which soft-rock coastal landforms respond. The findings of the studies described in this chapter 5 are consistent with the discussion in Section 2.5.2, which is not repeated here. However, the results of the Chapter 5 case studies have also highlighted additional insights into the differing behaviour of these various substrates in response to sea-level rise which were not identified in the literature review. These are noted below.

Swell-exposed sandy beaches

The detailed case studies above have examined two swell-exposed sandy beaches (Ocean Beach and Roches Beach) that are inferred to have markedly changed their behaviour during the Twentieth Century in response to sea-level rise (Sections 5.2 and 5.3). In both cases the change of behaviour occurred abruptly (between two consecutive air photo dates), and probably in response to one or a cluster of large storm erosion events. In both cases the change in behaviour is inferred to have been a sudden sand budget switch from positive to negative following a long period of incrementally increasing net sand losses from each beach embayment.

This sort of change can be characterised as a "tipping point" change, and on the study results to date appears characteristic of swell-exposed sandy beaches with the critical sand sink and transport conditions discussed above, and the contributing condition of an active sand supply. This tipping point response to sea-level rise for swell-exposed sandy beaches is in notable contrast to swell-sheltered soft rock and sandy shores (see below), whose response to sea-level rise are indicated by case study results from West Duck Bay and the Barilla study area as being an increase in recession rates than an abrupt "tipping point" switch.

Soft rock shoreline behaviour

The Barilla case study has examined the response of a soft rock shoreline to sea-level rise within a swell-sheltered tidal re-entrant. Because these shores have no capacity for recovery (whether by vegetative recovery like saltmarsh shores or swell-driven recovery like open coast sandy beaches); any erosion is permanent (albeit scarp slumping can temporarily give an appearance of scarp recovery). As discussed in Section 2.5.2, soft rock shores (whether swell-sheltered or swell-exposed) will typically undergo shoreline recession at some rate even in the absence of any increasing drivers of erosion. The (normally slow) rate of shoreline recession will simply be a function of the frequency and magnitude of swell or wind-wave storms that is characteristic of the regional climate.

At most of the Barilla sites, such a continuous linear rate of recession was observed over the air photo period at nearly all sites (Section 5.5.3) and does not provide evidence of a response to an onset of sea-level rise for the reason described above. However, at the most wind-exposed site, a significant increase in the rate of recession was observed over recent decades. The only explanation identified for this is that it is a response to contemporary climate change-induced sea-level rise which has so far emerged above the "noise" of normal soft-rock recession at only the most highly wind-wave exposed site in the Barilla case study area. The increase in shoreline recession rate observed does not necessarily imply any acceleration of sea-level rise; instead it can be accounted for as simply the effects of a new driver of shoreline recession (sea-level rise) becoming observable (emerging) above the noise of a prior long-term soft rock shoreline recession process.

Hence the case study results suggest that – at least in one case – the observed soft-rock shoreline response to an onset of sea-level rise is an increase in prior recession rates. This is characteristically different from the "tipping point" response observed on (so far) two swell-exposed sandy beaches.

Sandy saltmarsh shores in swell-sheltered tidal re-entrants

An important characteristic of the sandy saltmarsh shores that characterise four of the five West Duck Bay study sites (Section 5.4 above) is that in the absence of actively increasing drivers of erosion (such as rising sea-levels or increasing wind speeds) these shores can vegetatively recover from any prior erosion and can be stable at some equilibrium position, or can even accrete sediment and prograde (see Section 3.2.1 and Figure 6). This is in contrast to soft-rock shores or non-saltmarsh sandy shores in swell-sheltered re-entrants, which are characterised by a lack of any shoreline recovery processes (see Section 2.5.2).

The air photo record demonstrates that all four of the studied West Duck Bay saltmarsh shorelines have been progressively receding since at least 1945 (albeit short episodes of stability and vegetative recovery cannot be ruled out given limited air photo frequency prior to circa 1980). This implies progressively increasing drivers of recession over the whole period, since if the drivers ceased to increase, the saltmarsh shores would revegetate and stabilise at some equilibrium position. The only known explanations available for this behaviour are responses to ongoing sea-level rise or wind speed increases (Section 5.4.4). Although increasing wind speeds in north-west Tasmania are only recorded from 1995 onwards (at Cape Grim: Figure 20), global climate change-driven sea-level rise is known to have been in progress since the 1800s (Section 2.3), hence on available information is the more probable driver of sandy saltmarsh shore recession in West Duck Bay since 1945 and earlier.

Hence the observed active recession of sandy saltmarsh shores in Duck Bay since at least 1945 implies that such saltmarsh shores may be particularly early and sensitive responders to sea-level rise on the Tasmanian coast, given that they have the capacity to vegetatively recover if drivers of erosion cease or diminish.

Other contributing conditions

A number of additional conditions have been inferred to be likely contributing factors enabling an early shoreline response to climate change-induced drivers in some of the case study sites analysed in this chapter. These conditions are listed below and their inferred contributions to enabling early shoreline responses to contemporary climate change-induced sea-level rise are summarised:

- *Swell-sheltered tidal environments* (Sections 2.5.2, 2.5.5 and 3.2.1); A lack of swell wave exposure results in less alongshore and cross-shore sand movement (which can mask or prevent early shoreline responses to sea-level rise).
- *Non-recovering (soft rock) shoreline substrates* (Sections 2.5.2 and 3.2.1); Lack of capacity for recovery after erosion events may allow relatively early increase in shoreline recession rates to emerge in response climate change-induced drivers (note substrate discussion above).
- *Storm-dominated swell-wave climate* (Section 2.5.5); A beach exposed to a storm-dominated wave climate may require less sea-level rise than other beaches in order for erosion events to become too frequent for beach recovery to occur in between, resulting in a switch to recession.
- *Minimal swell-wave directional variability* (Section 2.5.5); This minimises changes in alongshore sand transport directions and fluxes (which can result in episodic shoreline erosion and accretion "noise" masking the effects of longer-term GMSLR).
- *Minimal inter-annual sea level variability* (Section 2.5.7); Minimises regional sea-level variability on inter-annual to interdecadal time scales (which can result in episodic or cyclic shoreline erosion and accretion "noise" masking the effects of longer-term GMSLR).
- *Negligible or small vertical land movement* (VLM) (Section 2.5.4). Minimises local relative sea-level variability including progressive relative sea-level rise (which may result in shoreline erosion and recession "noise" masking the effects of longer-term GMSLR).

These conditions are inferred to be contributing factors in some cases but not essential enabling factors in all cases of early responses. For example, a storm-dominated wave climate and minimal swell-wave directional variability are both inferred to be factors contributing to an early response to climate change-induced sea-level rise at Ocean Beach, however a storm-dominated wave climate is not a factor at Roches Beach, and neither condition is a factor at West Duck Bay or Barilla Bay. The conditions listed above are not discussed further here since their enabling contributions have been inferred based on previous work as cited in the descriptive sections listed above, rather than being new insights derived from the research described in this chapter.

5.7 *Chapter findings in context*

This chapter 5 has examined four study areas (comprising 12 individual sites) in some detail. Each area has exhibited long-term changes in shoreline behaviour which have been best explained by one or more of several climate change-induced drivers, including sea-level rise in all cases. Site conditions have also been identified that were either critical or contributing factors enabling an early observable shoreline response to contemporary climate change-induced sea-level rise.

These conclusions provide the basis for the following Chapter 6, in which all 35 sites for which information was gathered during this project are examined in the light of the findings from the four Chapter 5 case studies. The analysis presented in Chapter 6 asks whether any drivers of change and the enabling geomorphic conditions identified in Chapter 5 can satisfactorily explain the behaviour of all 35 sites, or whether additional drivers and/or geomorphic conditions need to be invoked to explain some of these.

Chapter 6: Shoreline behaviour analysis across all study sites

6.1 *Introduction*

The previous Chapter 5 presented detailed analysis of coastal behaviour across four case studies, each with quite different coastal geomorphic settings. Between these, a total of 12 distinctive shoreline sites were systematically investigated using a combination of quantitative air photo analysis and geomorphic interpretation. Multiple hypotheses were investigated to explain observed long-term shoreline behaviour changes. In each case, climate change-induced drivers including not only sea-level rise, but also long-term wind speed increases and (in one case) possibly swell direction changes were found to be most probable. In order to assess potential factors that dictate an 'early response' to climate-driven change, the analysis also focused on what geomorphic conditions at each site *enabled* the response to these drivers, noting that many other shorelines are evidently less susceptible despite exposure to the same drivers. The Chapter 5 summary (Section 5.6) identifies these process drivers and geomorphic conditions inferred to be implicated in the observed changes of behaviour.

This Chapter 6 takes a broader view and considers a total of 35 coastal sites around Tasmania for which approximately 70-year air photo shoreline behaviour histories have been obtained. The analysis described aims to test whether the presence or absence of the same set of geomorphic conditions identified in Chapter 5 can explain observed air photo-derived shoreline behaviour histories of the additional coastal sites.

6.1.1 Approach

The shoreline behaviour analysis conducted for this chapter draws upon the quantitative evidence from air photo histories spanning 35 sites as detailed in Appendix One. The 12 sites examined in the detailed analysis presented in Chapter 5 are included to enable summaries of findings across all studied sites. Of the additional 23 sites, some form groups of related but distinct shorelines whereas others are single isolated shorelines. The approach taken for this chapter was as follows:

Each of the 35 study sites is categorised in Section 6.2 (Table 8) according to its long-term shoreline behaviour during the approximately 70-year air photo period between the mid-1940s and 2019. These categories were determined from the historic air photo time series and beach profile data (where available) which are recorded in Appendix One.

Two primary categories were defined according to whether or not each site has exhibited a long-term change[21] in its type of behaviour over the air photo period. Within these primary categories, each study site was classified depending on the type of long-term shoreline behaviour it has displayed over the whole air photo period, or else that it has changed from and to. For the purposes of this thesis, 'shoreline behaviour types' were broadly classed as *progradation*, *stability* or *recession* (as described in the glossary). Any of these may exhibit smaller-scale erosion and accretion cycles super-imposed on the dominant behaviour trend (see for example Fig. 6.17 in Woodroffe 2003). Note that shoreline behaviour categories were defined independently of substrate type (i.e., sand, soft rock) since substrate type is one amongst the variety of factors investigated to potentially explain shoreline behaviour.

The qualitative analysis is presented in Section 6.3. The analysis began by asking whether the long-term shoreline behaviour changes or lack thereof at each site can be best explained by either the presence or the absence of the "drivers of change" and "conditions enabling change" that were identified in the more detailed Chapter 5 case studies. Any other potentially plausible explanations were also sought and evaluated. The analysis was conducted for the smaller number of sites in each

[21] See glossary or Section 3.2.3 for the meaning of 'long-term', 'long-term change' and 'emerging change' as adopted for this project.

behaviour category in turn, with the results subsequently synthesised and summarised in the Section 6.4 summary.

6.2 *Classification of shores according to long-term historical behaviour*

Table 8 below categorises the type of observed long-term shoreline position variability ('behaviour') of the case study sites, as outlined in Section 6.1.1 above.

Table 8: Long-term shoreline behaviour categories as defined for the purpose of this study. See text (Section 6.1.1) for a brief explanation. Note that categories other than those listed are possible but were not encountered in this study.

Visual key: Recession -  Stability - Progradation - 

Shoreline behaviour type *(with numerical and visual key to types)*	***Study sites assigned to type categories***	***Appendix (Site data)***
Long-term or emerging behaviour change during air photo and beach profiles period:		
I. *Recession then significant long-term increase of recession rate* 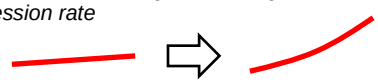	Gordon (D'Entrecasteaux) West Duck Bay S Area West Duck Bay SE Area South Barilla Shore	A1.2.3 A1.2.5 A1.2.5 A1.5.1
II. *Stability then long-term recession* 	Window Pane Bay Beach East Ocean Beach Roches Beach Main Central	A1.3.4 A1.3.8 A1.4.2
III. *Stability then emerging (<10 years) recession* 	Nebraska Beach	A1.2.2
IV. *Stability then long-term progradation* 	Stephens Bay Beach South (excludes 3 southernmost transects)	A1.3.5
V. *Stable or slightly prograding, then emerging (<10 years) recession* 	Prion Beach	A1.3.2
No significant long-term behaviour change during air photo and beach profiles period:		
VI. *Significant recession trend, no long-term change* 	Cloudy Lagoon East Cloudy Lagoon North West Duck Bay N Area (east) West Duck Bay N Area (west) West Duck Bay NW Area Mulcahy Bay Beach Rokeby Beach West	A1.2.4 A1.2.4 A1.2.5 A1.2.5 A1.2.5 A1.3.7 A1.5.2
VII. *Stability with small possible recession trend, no long-term change*	Ralphs Bay Shore (South Arm) Cloudy Lagoon South Cox Bight beaches (all) Wreck Bay West Barilla Shore	A1.2.1 A1.2.4 A1.3.3 A1.3.6 A1.5.1
VIII. *Stability, no long-term change*	Windowpane Bay Beach North Stephens Bay Beach North (after early recession) Roches Beach North Northwest Barilla shore North Barilla Shore Rokeby Beach Central-East	A1.3.4 A1.3.5 A1.4.2 A1.5.1 A1.5.1 A1.5.2
IX. *Stability, with small possible progradation trend, no long-term change*	Cloudy Bay Beach East Wineglass Bay Beach Hope Beach	A1.3.1 A1.4.1 A1.4.3
X. *Significant progradation trend, no long-term change* 	Jetty Beach Green Point Beach (Marrawah) Adventure Bay South Beach Cloudy Bay Beach West	A1.2.2 A1.3.9 A1.4.4 A1.4.5

6.3 *Shoreline behaviour analysis across all studied sites*

6.3.1 Introduction

The following sub-sections 6.3.2 and 6.3.3 provide a qualitative analysis of the causes of long-term changed or unchanged shoreline behaviour across the full ensemble of sites. Key data and descriptive information on which these analyses are based are briefly summarised in this chapter (and also in the preceding Chapter 5 for the case study areas). However, additional site geomorphic information, numerical data and discussions are provided for each site in Appendix One.

6.3.2 Analysis of shorelines with long-term changes in type of behaviour

This section qualitatively analyses the 10 (out of 35) studied sites exhibiting long-term or inferred emerging long-term changes in shoreline behaviour (as listed in Table 8 above). Five of these sites were part of the case studies analysed in detail in Chapter 5, however the other five are additional sites providing an opportunity to test the broader applicability of the findings presented in Chapter 5.

It was inferred in Chapter 5 (summary Section 5.6) that a rising mean sea level is likely to be a driver of the observed long-term changes in shoreline behaviour examined in that chapter. Increasing onshore wind speeds were also identified as a likely additional driver in some but not all of these cases, whilst changing swell directions may be a driver in some circumstances (but are yet to be conclusively demonstrated).

Chapter 5 concluded that at the sites studied the following geomorphic conditions were necessary to enable early changes of shoreline behaviour to occur in response to these climate change-driven coastal processes:

- a significant active sediment sink (the nature of which varies but in each case is a means by which sediment is permanently lost from and cannot be returned to the eroding shoreface); and:
- a persistently (generally unidirectional) active sediment transport path carrying any eroded sediment from the upper shoreface to that significant active sink.

Additionally, in the case of erodible swell-sheltered tidal re-entrant shores exhibiting potential early responses to climate change-induced drivers, all the sites showing changing behaviours have:

- relatively high wind-wave exposure and fetch for their respective re-entrants.

Some additional conditions were not inferred to be necessary for climate-related changes to occur but nonetheless are likely to contribute as enablers of changes in some cases; these include:

- Swell-sheltered tidal environments.
- Non-recovering (soft rock) shoreline substrates.
- Storm-dominated wave climates.
- Minimal swell-wave directional variability.
- Minimal inter-annual sea-level variability.
- Negligible or small vertical land movement.

The following analysis asks whether the climate change-induced drivers identified in Chapter 5 (as noted above) can explain the long-term or emerging long-term changes in shoreline behaviour type observed in all 10 sites showing a behaviour change, or whether other causes better explain the observed behaviour. For each shore, the analysis consisted of a qualitative geomorphic assessment. First, it was required to determine whether the necessary conditions for change as listed above are present, and second, whether the shore is most likely responding to climate change-induced drivers, or whether some other cause is more likely to be a dominant driver. The latter determination consists of inferring the likely sediment budget processes and drivers for change at the site from the observed

geomorphic conditions and shoreline behaviour history. Table 9 below summarises the shoreline behaviour types, and the site conditions found at each of the 10 study sites categorised as showing a long-term or emerging change of shoreline behaviour type during the air photo period.

Table 9: Site conditions for study site shores that <u>have</u> undergone long-term changes of behaviour types over the air photo period. The relevant site conditions "minimal inter-annual sea-level variability" and "small VLM" are not tabulated here since they are applicable to all Tasmanian coasts and thus to all the studied sites.

Shoreline behaviour categories	Site	Site conditions[2]							
		Active sediment sink[1]	Active sediment transport to sink	Active sediment source	Swell-sheltered tidal re-entrant	High re-entrant wind-wave exposure and fetch	Non-recoverable shore substrates ("soft-rock")	Storm-dominated swell-wave climate	Minimal swell-wave direction variability
I. *Recession then significant long-term increase of recession rate*	Gordon	L	Y	Y (reduced)	Y (attenuated swell)	-	-	-	-
	West Duck Bay S	O	Y	-	Y	Y	-	-	-
	West Duck Bay SE	O	Y	-	Y	Y	-	-	-
	South Barilla	R	Y	-	Y	Y	Y	-	-
II. *Stability then long-term recession*	Window Pane Bay East	O	Y	-	-	=	-	Y	Y
	Ocean Beach	R A	Y ?	Y	-	-	-	Y	Y
	Roches Beach (Main central)	L	Y	Y	-	-	-	-	Y
III. *Stability then emerging (<10 years) recession*	Nebraska Beach	L	Y	Y	Y (very refracted & attenuated swell)	Y	-	-	-
IV. *Stability then long-term progradation*	Stephens Bay Beach South	A	Y	Y	-	-	-	Y	Y
V. *Stable or slightly prograding, then emerging (<10 years) recession*	Prion Beach	R A	Y Y	Y	-	-	-	Y	Y

Notes: **1**. *Sediment sink types*: ***Littoral*** (L) longshore drift out of sediment cell; available accommodation space in ***Re-entrants*** (R) such as estuaries, tidal lagoons, etc; ***Aeolian*** (A) landwards sand loss via deflation gullies or mobile transgressive dunes; ***Offshore*** (O) sand loss via tidal or other currents, including sand loss from upper to lower beach face as described by Bruun Rule (here referred to as the 'Bruun sink').

2. *Site conditions* as described and discussed in Section 5.6.3: present (Y), not present ('-').

I. Steady recession then significantly increased rate of recession

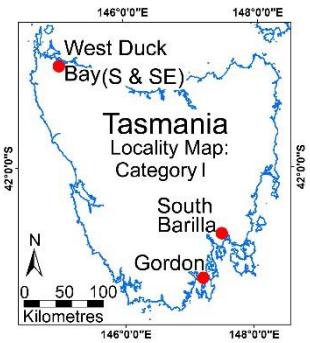

Three of the four sites assigned to this category are the *West Duck Bay (S* and *SE)* and *South Barilla* case study areas that were analysed in detail in Chapter 5 (Table 8 & Table 9; see locality map on RHS). As concluded in Sections 5.4.4 and 5.5.4, the most likely drivers of shoreline behaviour changes at these three sites were a combination of contemporary climate change-driven sea-level rise (at all sites) and wind speed increases (at the West Duck Bay sites). At all three sites, the geomorphic conditions identified as enabling that shoreline behaviour change to occur (Table 9) were:

- active sediment sinks.
- active (mainly tidal current) transport of eroded sediment to the sinks.
- swell-sheltered environments preventing swell-driven sand transport processes from masking the shoreline behaviour change.

- relatively high wind-wave exposure over long fetches.

Additionally, in the case of the Barilla (south) site a contributing condition is:

- A coastal substrate (cohesive clay 'soft-rocks') which cannot recover following erosion.

In contrast, the change of behaviour (significantly increased rate of shoreline recession) at the other site (*Gordon*, D'Entrecasteaux Channel: see Figure 48) is probably not primarily attributable to any of the climate-change-induced drivers identified in Chapter 5. This erodible sandy shoreline is subject to the two key conditions inferred to enable early physical responses to sea-level rise, namely an active sediment sink resulting from persistent unidirectional (northwards) sand transport. However, it can be inferred from local conditions that the most likely (or at least dominant) cause of the observed long-

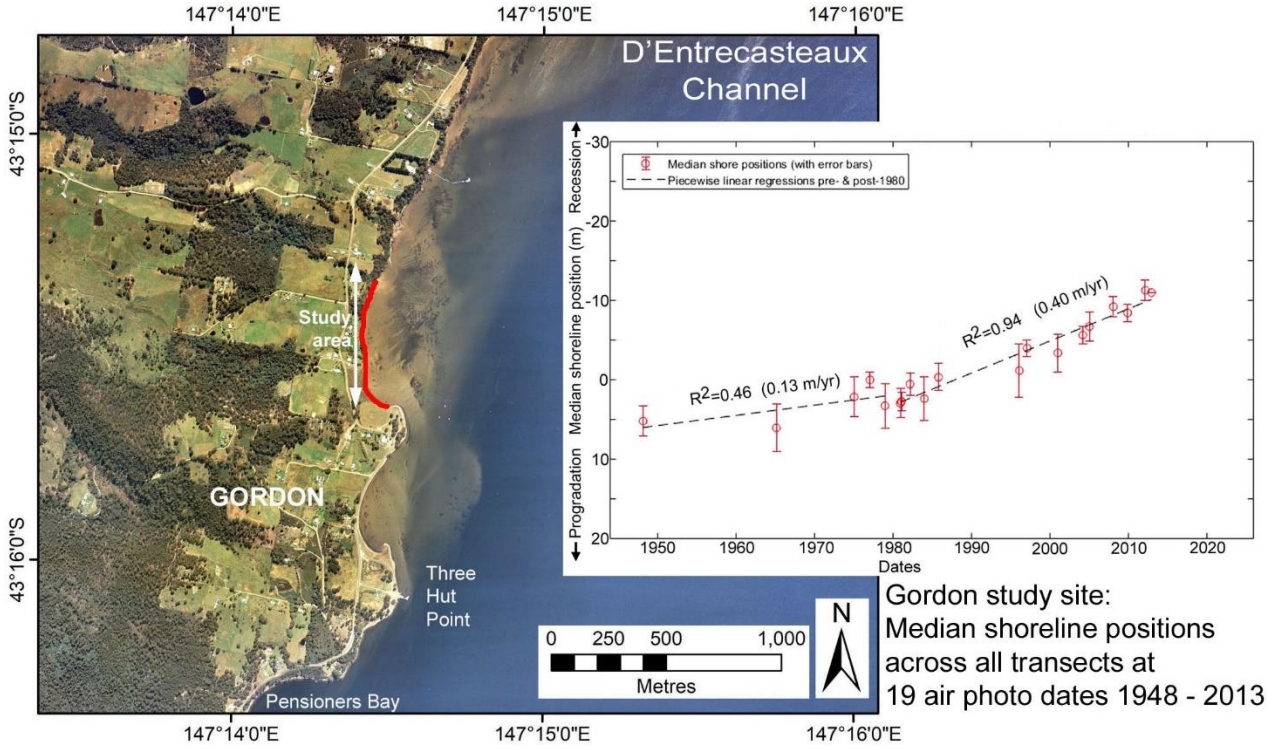

Figure 48: Gordon study site air photo and shoreline history summary plot with piecewise linear fits before and after 1980. Study site shoreline indicated in red. Air photo taken Feb. 1996 (© DPIPWE).

term behaviour change is the construction of local anthropogenic process interferences circa 1985. Sections of the shores of two formerly mobile updrift sandy spits (shown on Figure 48 and including 'Three Hut Point') have been artificially hardened to prevent sandy shoreline erosion. Since ongoing shoreline erosion of these sandy spits was the source of sand drifting northwards past the study site, the artificial shore protection works have resulted in a diminished supply of sand. This has created a sand budget deficit leading to increased shoreline recession at the study site. Whilst it is possible that this shore could additionally be responding to sea-level rise in some degree, any such effect is likely to be sub-ordinate to and problematic to distinguish from the obvious local anthropogenic process interferences. Further information on this site is provided in Appendix A1.2.3.

II. Stability then long-term recession

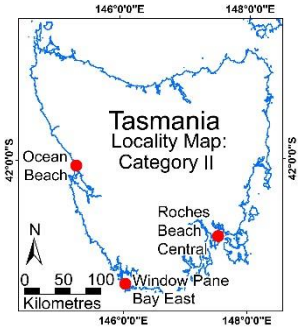

Two of the three sites in this changed behaviour category were analysed in Chapter 5 (*Ocean Beach* and *Roches Beach Central*). The most likely drivers of long-term shoreline behaviour change at Ocean Beach are a combination of contemporary climate change-driven sea-level rise and wind speed increases. Sea-level rise is the only likely change driver identified at Roches Beach. At these sites, the geomorphic conditions identified as enabling the shoreline behaviour change to occur were active sediment sinks and active transport of eroded sediment to the sinks (mainly by littoral drift).

At the third site in this category, *Window Pane Bay East*, a long sandy frontal dune is a relict (possibly Pleistocene terrestrial dune) landform which is fronted by a resilient boulder-beach (Figure 49) extending south-eastwards from the end of the sandy beach at the head of the Window Pane Bay embayment. The boulder beach and the dune have not been accreting sand under recent natural conditions (as indicated by the lack of incipient foredunes or beach sands over the boulders).

Figure 49: Actively eroding relict sand dune at Window Pane Bay East. This densely vegetated frontal dune exhibited no active erosion and showed no change from the earliest air photo (1948) until after 1961, however by 1975 a short section of the dune had started eroding and slumping. The actively eroding section of the dune has subsequently extended laterally along the dune front and further to landwards and was continuing to do so as at 2016. Both photos by Chris Sharples (Top: Dec. 2014; Bottom: Dec 2015). See also map and shoreline history plots on Figure 59 (further below).

A Twentieth Century change of behaviour at this site is interpreted from an air photo time series (see Figure 59). The entire length of the dune backing the east side of Window Pane Bay was stable and densely vegetated since prior to 1948, and most of it has remained stable to at least 2016. However active dune erosion and slumping commenced from part of the seawards foot of the dune between 1961 and 1975 and has continued to progressively expand alongshore and landwards until the present (see Figure 49 & Figure 59). This change is most plausibly explained by climate change-induced drivers identified in Chapter 5, namely sea-level rise and onshore wind speed increases causing more frequent higher wave attack on the dune than previously. No other plausible drivers of the changes observed have been identified. The following geomorphic conditions are present and would enable the observed change of behaviour in response to either or both of these drivers:

- active sediment sink (eroded dune sand is evidently transported elsewhere within embayment: the lack of a fronting sandy beach or incipient foredune implies that no swell-driven sand returns to the eroded dune across the bare boulder-beach shore in front of it).
- active transport of eroded dune sands to the sink (removal offshore by storm wave backwash).

The following additional conditions at the receding dune-face are not essential to explain the change in behaviour but are likely to be contributing factors:

- the eroding dune section is the part of the Window Pane Bay embayment most directly exposed to unrefracted south-westerly swell waves (see maps in appendix A1.3.4).
- storm-dominated swell-wave climate.
- minimal swell-wave directional variability.
- small VLM.

These conditions are consistent with those identified as enabling an early response to climate change-induced drivers at the case study sites analysed in Ch. 5. Additional information on this site is provided in Appendix A1.3.4.

III. Stability then emerging (<10 years) recession

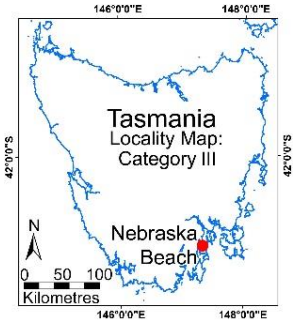

This category comprises a single site (*Nebraska Beach*, North Bruny Island), which has exhibited a change of behaviour comparable to those described above as 'stability then change to long-term recession', except that the changed behaviour has so far only been apparent for less than a decade and is to date notable mostly at the south-west end of the beach. The local conditions and shoreline histories are illustrated at Figure 50 below, and more information for this beach is provided in Appendix A1.2.2.

The shoreline of Nebraska Beach has historically exhibited long-term stability, whereas Jetty Beach to its north has historically exhibited long-term progradation (see Figure 50). Inferred wind wave-driven north-eastwards littoral drift of sand into and out of Nebraska Beach towards the sand-sink of Jetty Beach can account for this pattern. A recently (less than 10 years) emerging erosion trend at the south-west end of Nebraska Beach does not yet exceed past short-term shoreline variability at Nebraska Beach (in amplitude and extent), however the spatial pattern is suggestive of increasing north-eastwards sand losses outweighing south-westerly sand gains. This is consistent with sea-level rise as a plausible driver of the change (and possibly with increasing westerly (onshore) wind speeds, albeit these have not been demonstrated for this region of Tasmania). The following local geomorphic conditions could enable the observed change of behaviour in response to one or both of these drivers:

- active sediment sink (downdrift Jetty Beach embayment).
- active and persistent transport of eroded sand to the sink (dominantly south-west to north-east littoral drift driven by dominantly south-westerly to north-westerly wind-waves).

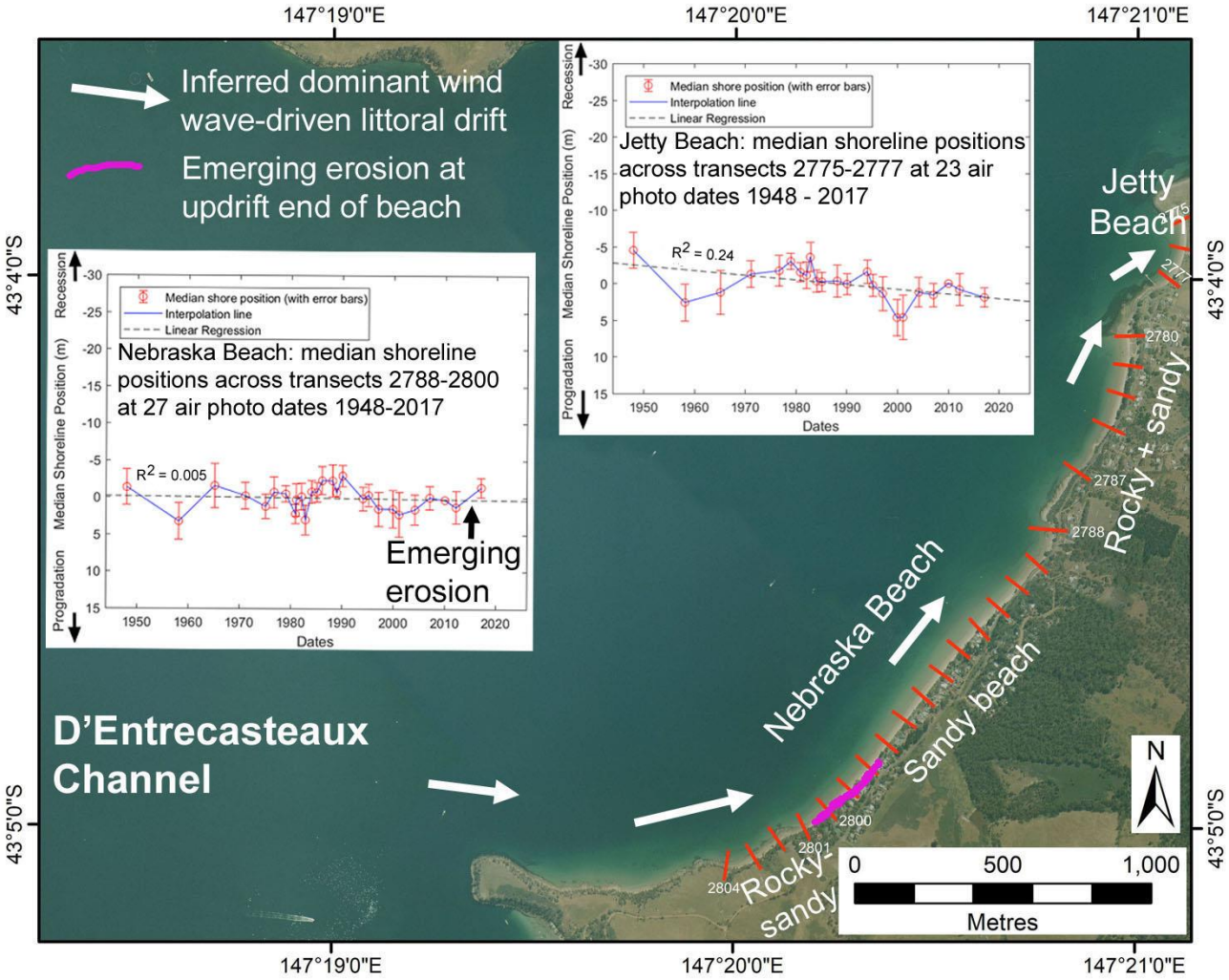

Figure 50: Summary history plots and inferred sand transport for Nebraska and Jetty Beaches, Bruny Island. Red lines indicate digital transects used for beach history analysis. Transects 2780-2787 and 2801-2804 are mixed rocky and sandy shores which are not included in the summary plots for Nebraska and Jetty Beaches. The air photo is dated 2010 (© DPIPWE).

- relatively high exposure to wind-waves over long fetches across D'Entrecasteaux Channel from the dominant westerly to north-westerly wind directions.
- mainly swell-sheltered environment which receives some refracted and attenuated swell. However locally generated wind-waves are probably dominant at this site (this condition minimises but does not fully prevent swell-driven sandy beach recovery processes that have tended to prevent shoreline behaviour change until recently).

These drivers and geomorphic conditions are similar to those driving long-term change at the 'stability then change to long-term recession' sites (above), which supports the hypothesis that Nebraska Beach is in the early stages of a long-term change from stability to recession. No other likely explanations of the changing behaviour of this beach have been identified.

However, it must be noted that this is not an ideal site for scientific analysis since nearly the whole beach is backed by residences constructed in the foredune, and the recent acceleration of erosion has led some residents to construct *ad hoc* seawall structures behind some (but not all) sections of the beach. In addition, the presence of some beach sections backed by older seawalls further north-eastwards along the beach introduce some uncertainties in the interpretation of historical beach behaviour, since it is

unclear whether these were constructed in response to particular erosion events or simply out of a desire for precautionary erosion protection by some landowners. Nonetheless, it is notable that the recent erosion and emerging recession has occurred mainly at the updrift (south-west) end of the beach where seawalls were not previously constructed, and which older seawalls further downdrift (to the NE) do not influence.

IV. Stability then long-term progradation

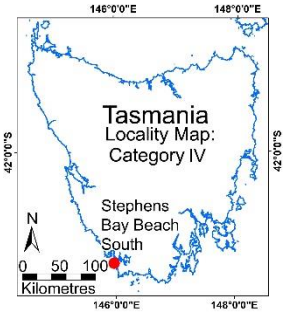

This changed behaviour category comprises a single site on the very high-energy south-west coast of Tasmania, namely *Stephens Bay Beach South* (see Figure 51 and Figure 60). This is a very distinctive site which over the air photo period has exhibited both increasing landwards sand losses via deflation, and also significant increasing sand gains from a combination of offshore shelf sources and south-eastwards (wind-wave influenced) littoral drift from the northern half of the embayment (see Figure 60). Although the site shares a number of geomorphic conditions associated with shoreline recession in response to climate change-induced drivers (see Table 9 and Section 5.6), at Stephens Bay Beach South the long-term change has been a shift from a deflating yet relatively stable shoreline position (both losing and gaining sand) towards progradation represented by the progressive growth of a foredune beginning only after 1980 (additional details are provided in appendix A1.3.5).

This shoreline behaviour change history is not obviously explained by a response to rising sea-level or increasing wind speeds. A more likely hypothesis is that it is part of a slow ongoing multi-decadal process of sandy barrier and sand budget adjustment in the aftermath of a major erosion event pre-dating the air photo record. It can be surmised that under the prevailing conditions of a very high-energy wind and swell-wave climate suppressing dune vegetation establishment and recovery, incipient foredune recovery is very slow with more aeolian sand mobility than would be the case on lower-energy shores. If this is correct, the observed change to progradation may be the long-delayed onset of effective foredune recovery following a large erosion event that triggered a multi-decadal phase of dune instability that is already evident on the earliest (1948) air photo for this site (see appendix A1.3.5, Figure 146) and is still active today albeit foredune recovery has also continued over recent decades.

Figure 51: View landwards from the southern half of Stephens Bay Beach. See also Figure 60. Landwards aeolian sand loss from the high dune in the background has increased since before 1948, when the front of the dune was already deflating but was still more vegetated in parts than it is now. Despite that ongoing deflation, the closer foredune began to accrete circa 1980, and has progressively grown larger and extended further along the back of the beach ever since. This behaviour (beach progradation with simultaneous deflation and continuing sand loss) is inferred to be part of a slow long-term recovery and shoreline progradation process occurring in a very high energy wind and wave environment, which is enabled by large continuing onshore and alongshore sand gains. Photo by Chris Sharples (2nd Dec. 2014).

V. Stable or slightly prograding, then emerging (<10 years) recession

This changing behaviour category comprises a single site, namely *Prion Beach* which is exposed to a relatively high-energy wave climate on Tasmania's unsettled south coast (see map to RHS). Prior to sometime between 2005 and 2009, this beach exhibited an overall long-term stable or slightly prograding trend with episodic erosion and recovery cycles of moderate scale (see Figure 52). However, since sometime between 2005 and 2009 until at least 2016, combined air photo and beach profiling data show the beach has undergone net recession on a scale that is now larger than observed previously in the air photo record, and with only minor temporary recovery phases (see Figure 52 below, additional information and data underpinning this discussion is available in appendix A1.3.2).

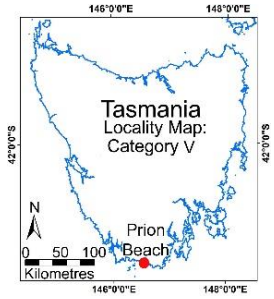

The most likely drivers of shoreline behaviour change identifiable at this site are a combination of contemporary climate change-driven sea-level rise and onshore wind speed increases. Long-term swell direction changes may also have affected beach processes but would more likely counter-act the observed change given the expected anti-clockwise swell rotation would reduce eastwards littoral drift and the loss of sand indicated below (see Section 2.5.5). No other potential drivers of the observed change have been identified. The geomorphic conditions identified as enabling a change to emerge in the observed shoreline behaviour (Table 9) are:

- Active sediment sinks (the large but close to sand-filled tidal lagoon behind the beach barrier is deduced to be gaining additional accommodation space in response to sea-level rise; there is also a minor aeolian sand sink in partly vegetated dunes beyond the eastern extremity of the beach).
- Persistent mostly uni-directional sand transport to sinks (dominantly eastwards littoral sand drift to a permanently open tidal channel and thence into lagoon; also, dominantly eastwards wind transport along beachface and across low sand spit into tidal channel and lagoon).

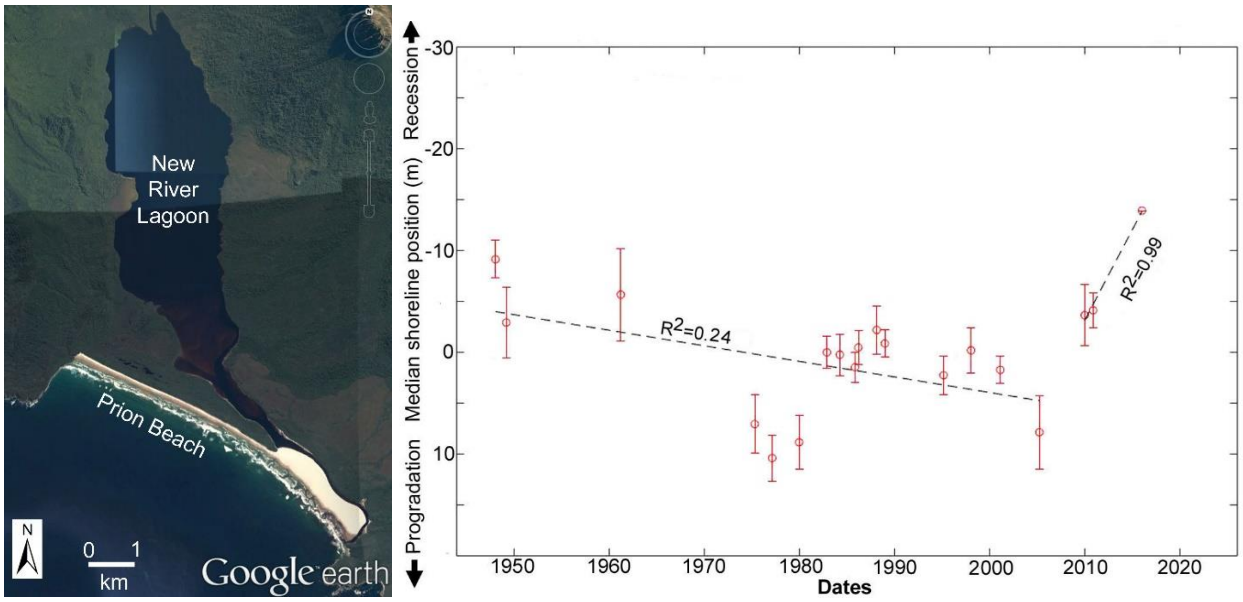

Figure 52: Prion Beach, south coast Tasmania. LHS: Satellite image showing Prion Beach backed by the extensive sand sink of New River Lagoon with its permanently open tidal channel entrance at the eastern extremity of the sand spit, and the direct exposure of the beach to south-westerly swells (Photo © Google Earth, 2017 image). RHS: Prion Beach shoreline history summary plot, showing median shoreline position across all transects at 19 air photo dates from 1948 to 2015, with air photo error margins indicated (the most recent shoreline position is based on the reference air photo used for ortho-rectification and hence has zero relative error margin by definition: see Methods Section 3.3.2). Piecewise linear regressions have been fitted to the data pre- and post-2006. From these a long prograding trend is inferred with some variability around erosion and recovery cycles until circa 2005. This is followed by an emerging recession trend starting with an abrupt erosion step-change between 2005 and 2009.

The following conditions (as noted in Section 5.6.3) affect this site and are deduced to contribute to or allow the shoreline behaviour and change of behaviour to emerge:

- active offshore (shelf) sand source (driving progradation trend prior to change).
- high wind-wave and swell exposure.
- storm-dominated swell-wave climate.
- minimal swell-wave directional variability.
- minimal VLM.

Although an emerging long-term shoreline behaviour change is inferred from the scale of recent net recession at Prion Beach, this changed behaviour has only been observed for circa 10 years to date (based on 3 air photo dates post-2005 until 2015, and 3 annual beach profile surveys along 7 field transects 2014 – 2016). Hence this beach warrants ongoing monitoring in order to determine whether the observed change does continue in the longer term.

6.3.3 Analysis of shorelines with unchanged types of long-term behaviour

This section analyses the 25 (out of 35) studied sites at which a long term (or likely emerging long-term) change in the type of shoreline behaviour has *not* been identified from the air photo record (these are listed on Table 10 below). Seven of these sites were part of the case study areas analysed in detail in Chapter 5, however the other eighteen are additional sites providing an opportunity to test the broader applicability of the conclusions reached in Chapter 5.

All sites present readily erodible shores that are exposed to climate change-induced drivers of shoreline change (sea-level rise and in some cases onshore wind speed increases) and so could in principle change their behaviour in response to these drivers. This analysis begins by testing the hypothesis that these shores have not yet responded to these drivers because they do *not* exhibit the geomorphic conditions identified in Chapter 5 as necessary ('critical') for this to occur.

That is, this section tests the prediction that shores *not* exhibiting early responses to climate change-induced drivers will:

- *not have* a significant active sediment sink; and/or will:
- *not have* a persistently (generally unidirectional) active sediment transport path to that significant active sink.

Additionally, in the case of erodible swell-sheltered tidal re-entrant shores not exhibiting early responses to climate change-induced drivers, these sites:

- *will have* relatively *low* wind-wave exposure and/or short fetches.

Other alternative or additional contributing explanations for the lack of change have also been sought, and one additional key factor (gaining sand budgets) is identified in Section 6.4.2 below.

This analysis proceeds by considering the unchanged sites in groups according to their long-term shoreline behaviour categories, as listed in Table 8 and Table 10. For each shore, the reasons for its lack of early response to climate change-induced drivers are inferred from the shoreline behaviour history and the observed geomorphic conditions including the likely sediment budget processes. The outcomes of these analyses are summarised in Section 6.4 (including Table 12).

Table 10: Site conditions for study site shores that have <u>not</u> undergone long-term changes of behaviour types over the air photo period. The relevant site conditions "minimal inter-annual sea-level variability" and "small VLM" are not tabulated here since they are applicable to all Tasmanian coasts and thus to all studied sites.

Shoreline behaviour category (over whole data period)	**Site**	**Site conditions[2]**							
		Active Sediment sink[1]	Active sediment transport to sink	Active sediment source	Swell-sheltered tidal re-entrant	High re-entrant wind-wave exposure and fetch	Non-recoverable shore substrates ("soft-rock")	Storm-dominated swell-wave climate	Minimal wave direction variability
VI. *Significant constant recession trend*	Cloudy Lagoon E	R	Y	-	Y	-	-	-	-
	Cloudy Lagoon N	R	Y	-	Y	-	-	-	-
	West Duck Bay N (E)	O	Y	-	Y	?	-	-	-
	West Duck Bay N (W)	O	Y	-	Y	?	-	-	-
	West Duck Bay NW	O	Y	-	Y	-	-	-	-
	Mulcahy Bay Beach	A	Y	Y	-	-	-	Y	Y
	Rokeby Beach W	R	Y	-	Y (some storm swell penetration)	-	Y	-	-
VII. *Stability with possible non-significant recession trend*	Ralphs Bay shore (S. Arm)	-	-	-	Y	-	-	-	-
	Cloudy Lagoon S	R	Y	-	Y	-	-	-	-
	Cox Bight Beaches (all)	-	-	Y	-	-	-	Y	Y
	Wreck Bay Beach	-	-	Y	-	-	-	Y	Y
	W. Barilla Shore	R	Y	-	Y	-	Y	-	-
VIII. *Stability*	Window Pane Bay Beach North	A	Y	Y	-	-	-	Y	Y
	Stephens Bay Beach North	A L	Y	Y	-	-	=	Y	Y
	Roches Beach N	L	Y	Y	--	-	-	-	-
	NW Barilla shore	R	Y	-	Y	-	Y	-	-
	N Barilla shore	R	Y	-	Y	-	Y	-	-
	Rokeby Beach Central-E	R	Y	-	Y	-	Y	-	-
IX. *Stability with possible non-significant progradation trend*	Cloudy Bay Beach East	-	-	Y	-	-	-	-	-
	Wineglass Bay Beach	-	-	Y(?)	-	-	-	-	-
	Hope Beach	-	-	Y	-	-	-	-	-
X. *Significant constant progradation trend*	Jetty Beach	-	-	Y	-	-	-	-	-
	Green Pt. Beach (Marrawah)	-	-	Y	-	-	-	Y	Y
	Adventure Bay S Beach	L	Y	Y	-	-	-	-	-
	Cloudy Bay Beach West	R	-	Y	-	-	-	-	-

Notes: **1**. *Sediment sink types*: ***Littoral*** (L) longshore drift out of sediment cell; Available accommodation space in ***Re-entrants*** (R) such as estuaries, tidal lagoons, etc; ***Aeolian*** (A) landwards sand loss in deflation gullies or mobile transgressive dunes; ***Offshore*** (O) sand loss via tidal or other currents, including sand loss from upper to lower beach face as described by Bruun Rule (here referred to as the 'Bruun sink').

2. *Site conditions* as described and discussed in Section 5.6.3: present (Y), some uncertainty (?), not present (-).

VI. Significant constant recession trend

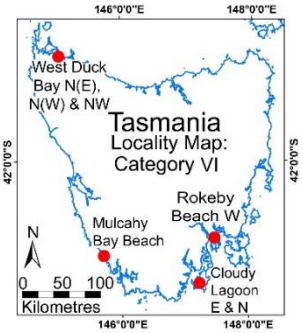

These sites have receded at a roughly linear rate over the whole air photo period, with no significant long-term change in the rate of recession but with some inter-annual variability. Five of the seven sites assigned to this category are located within the swell-sheltered tidal re-entrants of *West Duck Bay* (*N-E*, *N-W* and *NW*) and *Cloudy Lagoon* (*East* and *North*). Figure 53 below illustrates the summary shoreline history plots for the Cloudy Lagoon sites, and the West Duck Bay sites are described as part of a case study in Chapter 5 (Section 5.4.4).

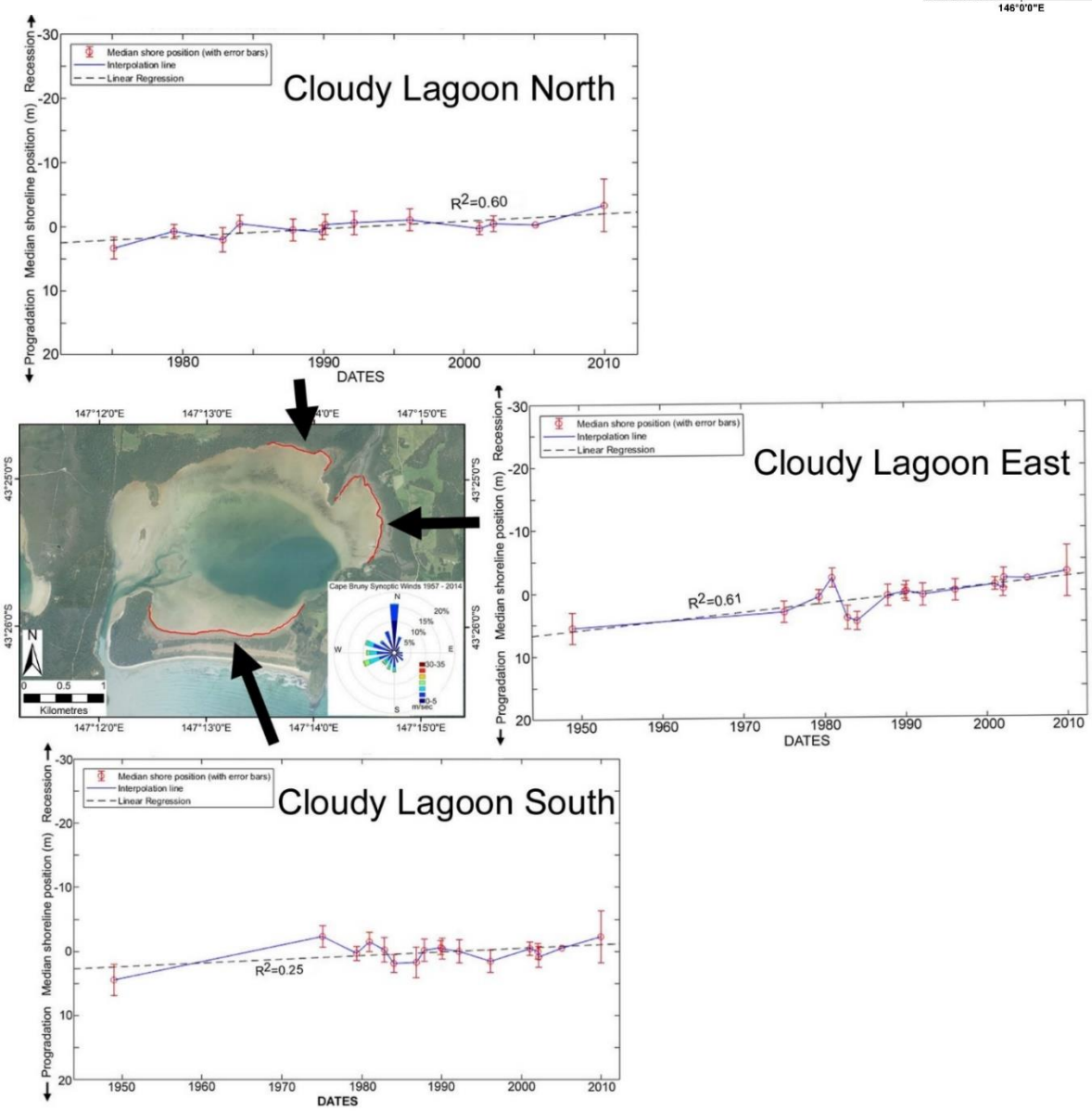

Figure 53: Cloudy Lagoon summary shoreline history plots. The lagoon is inferred to be an un-filled sand sink, whose accommodation space is increasing with ongoing sea-level rise. The North and East plots are interpreted as showing a slow but significant linear shoreline recession trend over the air photo period with only minor variability. The South plot shows a slower and less significant recession trend which is interpreted as a close to stable shoreline. The wind rose shows synoptic wind direction data for 1957 to 2014, from the nearest long-term Bureau of Meteorology weather station at Cape Bruny, 10 km to the south-west of Cloudy Lagoon. The fastest linear rate of recession is that for the eastern-most study site which has the longest fetch and most direct exposure in the dominant westerly wind direction (the anomalous northerly wind component may be a result of local topographic steering effects at Cape Bruny). The North study site plot is based on median shoreline positions at 13 air photo dates 1975 – 2009, the East plot shows data from16 air photo dates 1948 – 2009, and the South plot shows data from 17 air photo dates 1948 – 2009. Lagoon image is the 2009 air photo (© DPIPWE).

Additional information on these sites is provided in appendix Sections A1.2.4 and A1.2.5. All these sites are exposed to contemporary climate change-driven sea-level rise, and they may have been exposed to wind-speed increases in recent decades albeit some uncertainties remain. Hence all could change their behaviour in response to climate change-driven processes if enabling geomorphic conditions are present. However, whereas they have exhibited continual progressive shoreline recession they have not shown any long-term change of that recession rate (especially a significant increase) which might be a response to ongoing sea-level rise and/or wind speed increases over the last circa 70 years.

At these five re-entrant sites a sediment sink is available (Table 10), as is tidal current transport to the sinks for any eroded sediment. However, in all five cases local wind-wave fetch and exposure within each re-entrant is comparatively limited so that there is probably insufficient wind-wave energy to force a change of behaviour in response to the available climate change-induced drivers (albeit noting that some uncertainty exists in this regard for the West Duck Bay N (E & W) sites as noted in Section 5.4.5 above and Table 10). This inference is supported by the fact that in the West Duck Bay case, two similar nearby shoreline sites with probably higher wind-wave fetch exposures do indeed exhibit an acceleration of their prior recession trends.

In the case of the open coast swell exposed *Mulcahy Bay Beach*, deflation of the bare seawards-facing frontal dune face and several deflation gullies has resulted in slow but essentially constant shoreline recession over the air photo period (see Figure 54). This is inferred to be part of a very slow (50 year+) recovery process characteristic of a very high-energy wave and wind-exposed sandy coast after an inferred major (pre-1948) erosion event (as discussed in relation to Stephens Bay Beach South in Section 6.3.2 above). Further data and interpretation of the Mulcahy Bay shoreline history is provided in appendix A1.3.7.

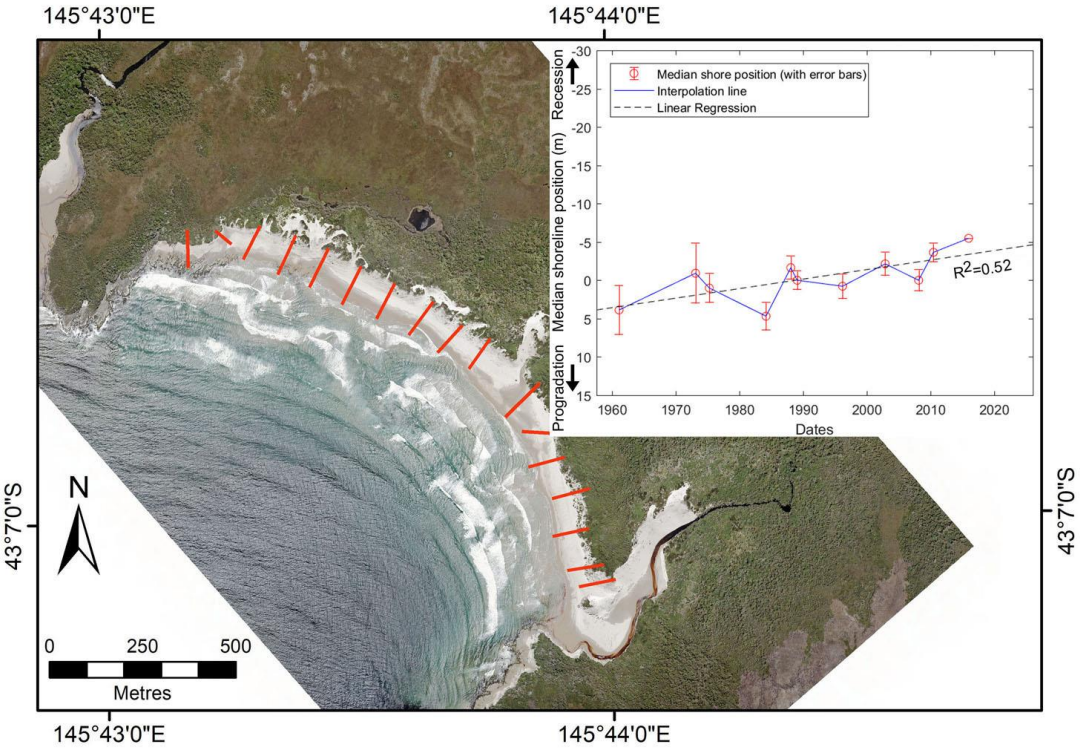

Figure 54: Mulcahy Bay Beach, south-west coast Tasmania. The summary shoreline history plot for Mulcahy Bay was compiled from the median shoreline position across all transects (red lines) at each of 11 air photo dates between 1961 and 2015. The plot is interpreted as demonstrating a slow but steady linear recession of the shoreline proxy (the dune-crest vegetation line) with short-term variability but no long-term change in the trend. The vegetation line recession is inferred to be driven mainly by aeolian dune deflation rather than wave attack, albeit some storm events are likely to have episodically scarped the dune face and caused some of the inter-annular variability seen in the summary plot. The beach image is the 2015 air photo (© DPIPWE).

It is particularly noteworthy that this site is exposed to two or possibly even three climate change-induced drivers of shoreline change, namely sea-level rise, increasing onshore wind speeds and possibly changing swell wave directions. The site also possesses both of the key geomorphic conditions identified in Chapter 5 as enabling an open coast sandy beach to respond early to climate change-induced drivers, namely an active (landwards aeolian) sand sink and a persistent (wind) sand transport process. However, despite these factors Mulcahy Bay Beach has not yet shown any significant increase of its long-term recession rate, nor any other obvious long-term shoreline behaviour change that might indicate a response to climate change-induced drivers over the air photo period.

The lack of any significant long-term behaviour change is inferred to be the result of a significant continuing onshore supply of sand to Mulcahy Bay from the continental shelf (as modelled by Harris and Heap (2014)), sufficient to nearly but not completely compensate for landwards aeolian losses from the beach and bare dune face. A continuing onshore sand gain can also be inferred from the relatively high and steep beach berm observed by the author at Mulcahy Bay on three visits during 2014 to 2016. The ongoing deflation of the beach and dune would otherwise result in a much lower and flatter beach profile. The air photo evidence indicates that the aeolian sand sink and landwards aeolian transport processes have been of relatively small scale, especially in comparison to sites such as Stephens Bay Beach on the same south-west coast. In the absence of other major sand sinks (such as littoral sand drift, which however is unlikely to leak from this deeply embayed beach site), it is likely that the modelled onshore sand gains have remained sufficient up to the present to mostly offset both a limited landwards aeolian sand loss as well as any increased offshore movement of sand resulting from increased beachface erosion driven by climate change-driven processes (as implied by the Bruun Rule: see Section 2.2). The result has been a slow ongoing but not significantly increasing shoreline recession rate.

The other site in this shoreline behaviour category is *Rokeby Beach West*, a scarped soft-rock (cohesive clay) non-recovering shoreline within the mostly[22] swell-sheltered tidal re-entrant of Ralphs Bay (see Figure 55). The site is exposed to the climate change-induced driver of sea-level rise (and possibly to increasing wind speeds). The shoreline scarp has been actively receding, albeit at an approximately constant rate over the whole air photo period, in contrast to a scarped but stable shoreline in the adjoining geologically similar central to eastern parts of the same beach. This greater rate of recession in the west part of the beach is inferred to be the result of occasional exposure to storm swells whose penetration into Ralphs Bay through a narrow entrance focusses mainly at the west end of Rokeby Beach.

Wind-wave erosion of the shore is limited by very short fetches and oblique exposure of the site to the dominant westerly to south-westerly winds at this site. Hence this site lacks the geomorphic condition identified in Chapter 5 as critical in enabling a (mostly) swell-sheltered re-entrant shoreline to show an early change in response to climate change-induced drivers, namely high wind-wave exposure, and fetch. It is implicit in the observed erosion status of the beach that whilst energetic storm swells penetrate Ralphs Bay often enough to keep the erosion scarp fresh and active on inter-annual to decadal time scales, they are not frequent enough to have yet notably increased the rate of recession in response to contemporary sea-level rise. Only very short fetches are available over which the dominant local winds can develop wind waves, and these are evidently insufficient to cause significant erosion at the study site. See appendix A1.5.2 for additional information about Rokeby Beach.

[22] The site sometimes receives storm swells through a very narrow entrance window into the Ralphs Bay re-entrant, however during fair weather only extremely attenuated swells reach this shoreline.

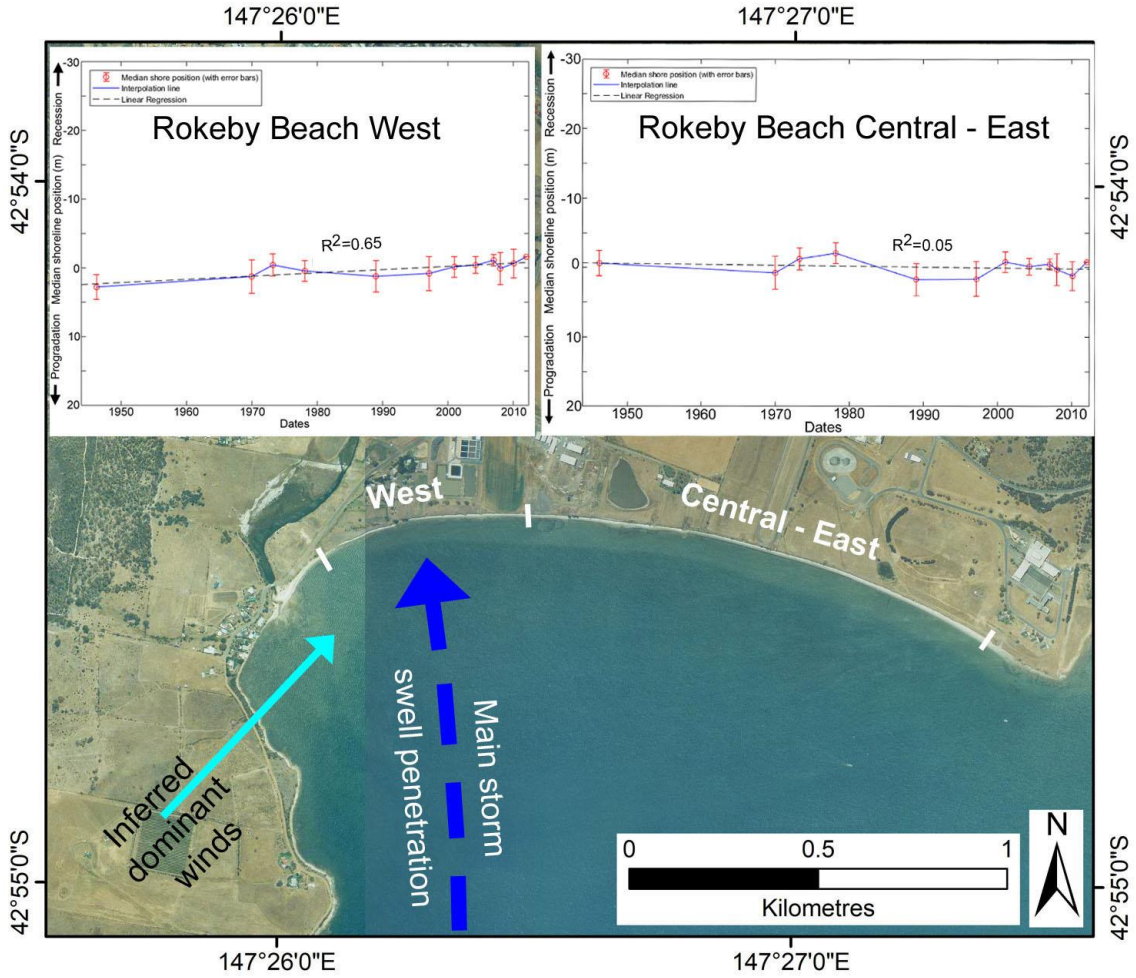

Figure 55: Rokeby Beach, south-east Tasmania. Shoreline history plots for the West and Central-East parts of Rokeby Beach are the median shoreline positions across all transects in each section at 12 air photo dates from 1946 to 2012. A linear regression fit has been plotted for each beach section. Inferred dominant wind-wave and swell directions shown (see appendix A1.5.2). Air photo taken Jan. 2001 (© DPIPWE).

VII. Stability with possible non-significant recession trend

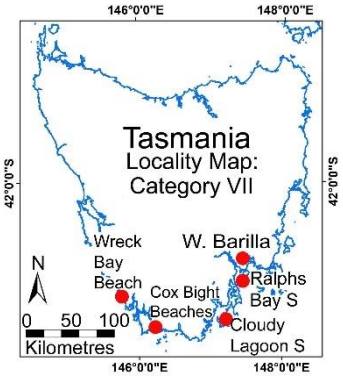

These sites have maintained an approximately stable or possibly slightly receding shoreline position over the whole air photo period, with some inter-annual variability. This category comprises two swell-exposed sandy beaches and three swell-sheltered re-entrant shores (see RHS locality map). Two of the latter are sandy and the other a cohesive clay soft-rock shore. All are exposed to contemporary sea-level rise driven by climate change, and the swell-exposed sandy beaches are exposed to increasing onshore wind speeds (see Table 12). Hence all these shores could in principle change their behaviour in response to climate change-driven processes if enabling geomorphic conditions are present.

The two swell-exposed sandy beach sites, *Wreck Bay Beach* (see Figure 56) and the three adjoining *Cox Bight Beaches* (treated as one site; see Figure 57), are both located deep within rocky embayments from which no sand gain or loss by littoral drift is likely, although both probably gain some sand directly onshore from the continental shelf as modelled by Harris and Heap (2014). Neither beach site exhibits any other significant active sand sink, with negligible landwards aeolian sand losses. The ostensible re-entrant of Freney Lagoon behind Cox Bight (Figure 57) is a permanently out-flowing freshwater lake

rather than a tidal lagoon, and thus not a potential sink for beach sands. At both beaches, any increasing offshore sand loss (into the "Bruun sink") due to increasing upper beachface erosion resulting from sea-level rise is probably offset by the likely onshore sand gains from the shelf. Hence these swell-exposed beaches do not have the necessary conditions of a significant active sand sink with a persistently active sand transport pathway to enable early responses to contemporary climate change-driven sea-level rise.

These conditions arguably account for these beaches unchanged behaviour to date. Non-significant recession trends identified at these beaches may be a simple artefact of minor shoreline variability and/or photogrammetric error margins in the air photo data or may represent a real but small imbalance

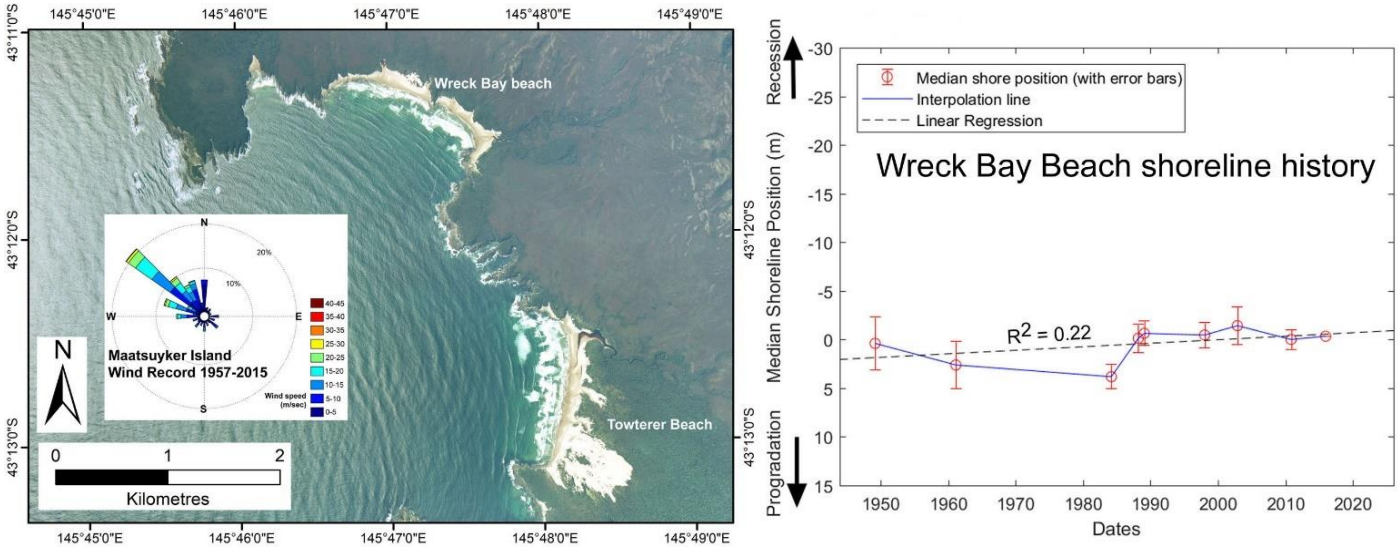

Figure 56: Wreck Bay Beach shoreline history plot. The plot is based on the median of shoreline positions across all transects at each of 9 air photo dates from 1949 to 2015. Although a small long-term linear recession trend can be inferred from the shoreline history data, this trend is smaller than most of the air photo error margins and is probably negligible. The air photo includes nearby Towterer Beach whose prominent active transgressive dune morphology confirms that the dominant wind directions recorded for the nearest long-term weather station at Maatsuyker Island (64 km to the SSE; wind rose shown) are also dominant in the Wreck Bay area. Due to the beach orientation, this limits the potential for landwards aeolian sand transport from Wreck Bay. Air photo image is the Nov. 2002 air photo (© DPIPWE).

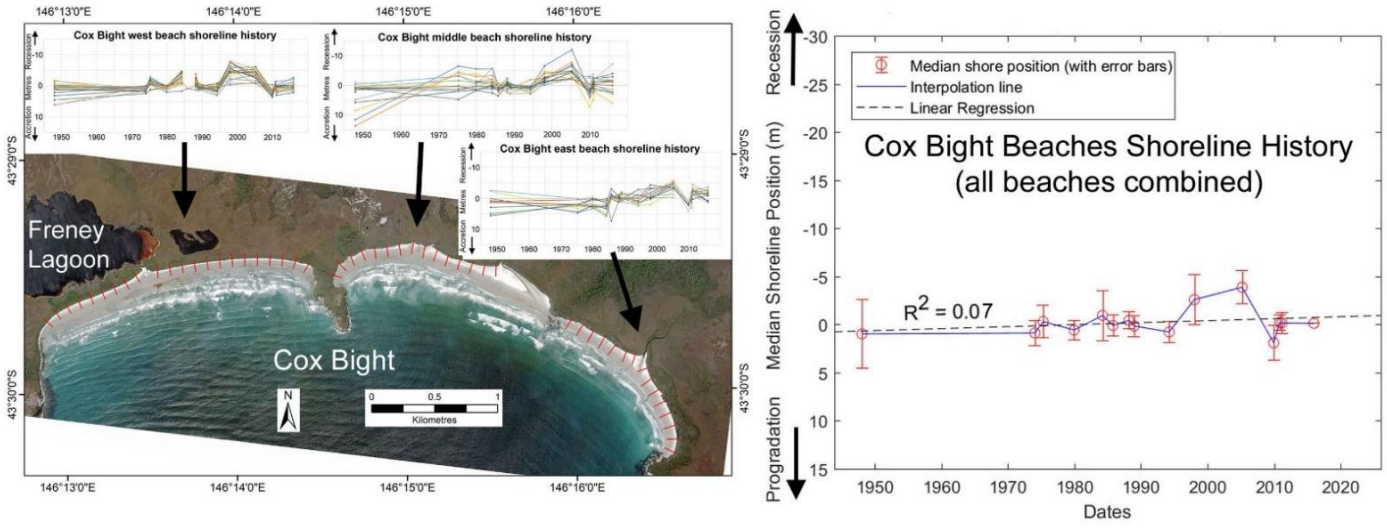

Figure 57: Cox Bight beaches shoreline history plots. Shoreline history plots for individual transects (shown in red) grouped by the three beaches (top) are sufficiently similar that they have been combined into a single summary shoreline history plot (below). The shoreline history is based on 15 air photo dates from 1948 to 2015. The eastern section of the middle beach was not used owing to frequent erosion caused by a large stream outflow. Although a small long-term linear recession trend can be inferred from the shoreline history data, this trend is smaller than most of the air photo error margins and is probably negligible. The air photo is dated Dec. 2015 (© DPIPWE).

in the near-stable sand budget of these beaches. Additional information on Cox Bight and Wreck Bay Beach is provided in appendices A1.3.3 & A1.3.6, respectively.

The sandy swell-sheltered *Ralphs Bay shore of South Arm* (Figure 58) lacks any significant active sand sink, with the bay seawards of this shore being so infilled with sand as to be exposed as tidal flats extending several hundred metres into Ralphs Bay for a significant part of each tidal cycle. With ongoing sea-level rise additional sand accommodation space will be created over these flats into which increasingly eroded upper beachface sands can be expected to be carried by tidal currents, however the degree of daily tidal flat exposure indicates that at the present time this sink has negligible capacity to sequester more sand. The prevailing winds at this site are westerly to south-westerly and thus directed alongshore to offshore, yielding no effective wind-wave fetch exposure at the upper beachface except under unusual onshore wind conditions at high tides. There is also little potential for wind wave-driven littoral drift of sand into or out of the very deep rocky embayment in which this shore sits.

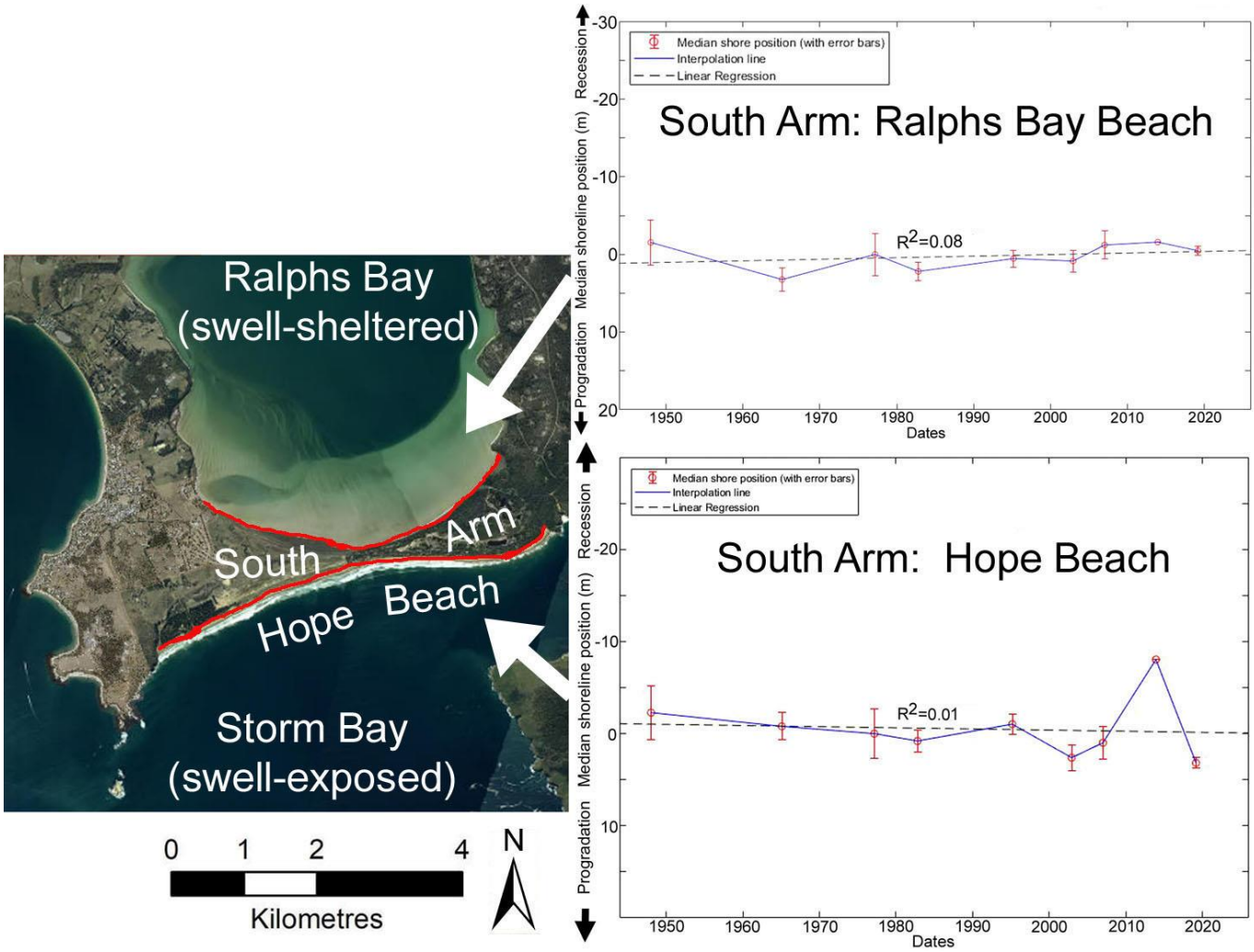

Figure 58: South Arm beaches shoreline history plots (south-east Tasmania). Both beach history plots are based on the median of shoreline positions across all transects at each of 9 air photo dates from 1948 to 2019. Beaches analysed are indicated in red. The shoreline history inferred for Ralphs Bay beach is one of long-term stability with a linear fit suggesting a very slight and non-significant recession trend. Hope Beach shows a slow non-significant progradation trend which is plausible given a likely onshore sand supply and no sand sinks. The large erosion and recovery event indicated by the data after 2010 was a real event monitored by the author (see also Figure 208 in appendix A1.4.3). Events of similar scale may have occurred previously on this ocean-facing beach or this event may be an indication of early response to sea-level rise which has not yet resulted in a long-term shoreline behaviour change. However, the relatively sparse air photo time series used does not enable these alternative possibilities to be tested. Background air photo © DPIPWE.

This site therefore lacks all three of the conditions summarised at the start of this Section 6.3.3 as necessary for an early recessional response to sea-level rise in swell-sheltered situations (namely an active sand sink, active sand transport to the sink, and high wind-wave exposure over long fetches). The shoreline history inferred from the air photo time series for this site (Figure 58 top) is that of a long-term stable shoreline with no significant change to date. A very small long-term shoreline recession trend can be inferred from a linear fit to the shoreline history data but is statistically non-significant.

With a stable sand budget (neither gaining or losing) and little potential for frequent upper beach erosion, the lack of shoreline behaviour changes over the air photo period is unsurprising. Further information about this site is provided in appendix A1.2.1.

The swell-sheltered tidal *Cloudy Lagoon South* shore (see Figure 53 above) is a prograded sandy beach ridge shore, however the stability of the shoreline position since 1948 as demonstrated by the air photo history implies that this shore is no longer prograding, and there is no evidence of any contemporary sand gains to this shore. Instead, the shore has two of the essential conditions for an early recessional change of shoreline behaviour in response to sea-level rise, namely the adjacent sand sink of Cloudy Lagoon which has significant accommodation space (i.e., water depth) available, and an efficient sand transport pathway into that sink via frequent tidal currents within the lagoon. However, this shore lacks the additional condition identified in Chapter 5 as needed for early recessional responses to sea-level rise in swell-sheltered tidal environments, namely relatively high wind-wave fetch exposure. In fact, the Cloudy Lagoon south shore is in a wind-sheltered situation behind the Cloudy Beach West barrier spit where the prevailing westerly and south-westerly winds mainly blow offshore so that wind-wave fetch exposure is very low at this site.

The lack of significant wind-wave fetch exposure at the shoreline (except in unusual north-easterly conditions) adequately explains the lack of any early recessional response to sea-level rise at this site. The apparent minor shoreline recession trend in the shoreline history data may not be real, but if it is then the most likely explanation is the early and minor beginnings of a sea-level response, with small quantities of shoreline sand eroded under infrequent unusual conditions being transported to the available sand sink by tidal currents.

The *West Barilla* shore (see Section 5.5) is an erodible soft rock (cohesive clay) shoreline that cannot recover from erosion, but which displays a mostly old or inactive erosion scarp with some rounding and slumping. This shore is located in the swell-sheltered tidal re-entrant of Pittwater and has two of the essential conditions identified in Chapter Five for an early response to sea-level rise, namely an effective active sediment sink and sediment transport pathway. However, this shore has exhibited little if any recession or other change over the air photo period. This shore has less wind-wave fetch in the dominant wind direction than the nearby South Barilla shore which has shown an accelerating active recession trend (see Section 6.3.2 above and Section 5.5). The West Barilla shore is also oriented parallel to the dominant local wind direction, in contrast to the South Barilla shore which directly faces the dominant winds. The lesser fetch and significantly less exposure of the West Barilla shore can therefore account for the lack of long-term behaviour change on this swell-sheltered shore. No alternative explanations for the lack of change have been identified. The apparent non-significant shoreline recession trend in the shoreline history data may be a simple artefact of photogrammetric error margins in the air photo data or might represent the real but very slow shoreline recession that may be expected from any non-recovering soft-rock shore irrespective of sea-level variability.

VIII. Stability

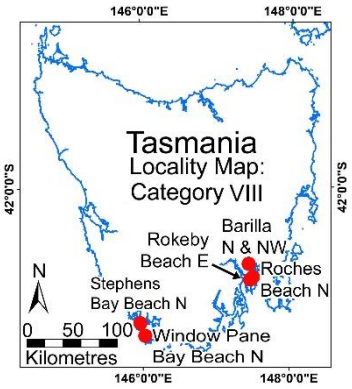

These sites have maintained an approximately stable shoreline position over the whole air photo period, with some inter-annual variability. This category comprises three swell-exposed sandy beaches and three soft-rock (cohesive clay) scarped shores. All of these are exposed to contemporary sea-level rise driven by climate change, all but one (Roches Beach N) are probably exposed to increasing onshore wind speeds, and the two south-west coast beaches (Window Pane Bay Beach North and Stephens Bay Beach North) are also potentially subject to changing swell directions (see Table 12). For these reasons, all could in principle change their behaviour in response to climate change-driven processes if the necessary geomorphic conditions are present.

One of the sandy beaches, the swell-exposed *Window Pane Bay Beach North* (see Figure 59) is deeply embayed between prominent rocky headlands and so unlikely to be losing sand by littoral drift. A formerly more active landwards aeolian sand sink (deflation gullies and transgressive dunes moving northwards in the early air photos, particularly at the east end of this beach section immediately north of the present creek outflow) is now very reduced and essentially negligible. A high (~50 m) bare dune scarp backing the north side of the bay (see Figure 59) is not an eroding coastal foredune but rather is the now wave-eroded leading edge of a stabilised terrestrial transgressive dune of Pleistocene or Early Holocene age. The head scarp position (*in situ* vegetation line) has not detectably changed over the air photo period (Figure 59), although some rafts of soil and vegetation have slid down the steep seawards' dune face. Any offshore sand loss (into the "Bruun sink") from increased upper beach face erosion resulting from sea-level rise is inferred to be offset by probable gains from the adjacent eroding Window Pane Bay Beach East (see Section 6.3.2 above) and from the continental shelf (as inferred from shelf sediment transport modelling by Harris and Heap (2014)). The lack of any significant active sand sink together with some probable sand gains provide adequate explanation of the stability of this beach (despite its ostensibly unstable dune appearance). Further information on Window Pane Bay is provided in appendix Section A1.3.4.

The other two sandy beaches in this shoreline behaviour category, namely *Roches Beach N* (see Chapter 5, Figure 32) and *Stephens Bay Beach North* (see Figure 60 below), are swell-exposed sandy beaches which both gain and lose sand in a sufficiently balanced fashion as to have maintained a mostly stable shoreline position with no significant long-term changes over the air photo period (except for an early recession phase which ceased by circa 1960 in the case of Stephens Bay Beach North).

The *Roches Beach N* sand budget is driven by a persistent south to north swell-driven littoral drift through a very leaky compartment. The sand source is the receding Roches Beach Central compartment to the south which has changed its long-term behaviour from stable to receding, thus supplying increasing quantities of sand to the Roches Beach N compartment (see Chapter 5 Section 5.3). However, the persistent littoral drift has evidently moved those increasing amounts quite efficiently through and out of the compartment so that the shoreline position has maintained its long-term stability. Thus, whilst Roches Beach N is exposed to sea-level rise and has an active sand sink with an active and persistent sand transport pathway, this has not resulted in changed shoreline behaviour because it has also been gaining increasing amounts of sand from the south, equivalent to any increasing losses into the sand sink, thereby maintaining a stable shoreline throughout the air photo period.

The *Stephens Bay Beach North* sand budget is more complex but is also a balanced sand budget (see Figure 60). Losses into active sand sinks driven by persistent uni-directional transport comprise minor active landwards aeolian sand transport from bare deflating seawards face of the frontal dune plus a significant inferred south-eastwards wind wave-driven littoral drift of beach sands to the prograding foredune area at Stephens Bay Beach South. Despite these active sand losses the shoreline position (vegetation line) backing Stephens Bay Beach North has remained stable over most of the air photo

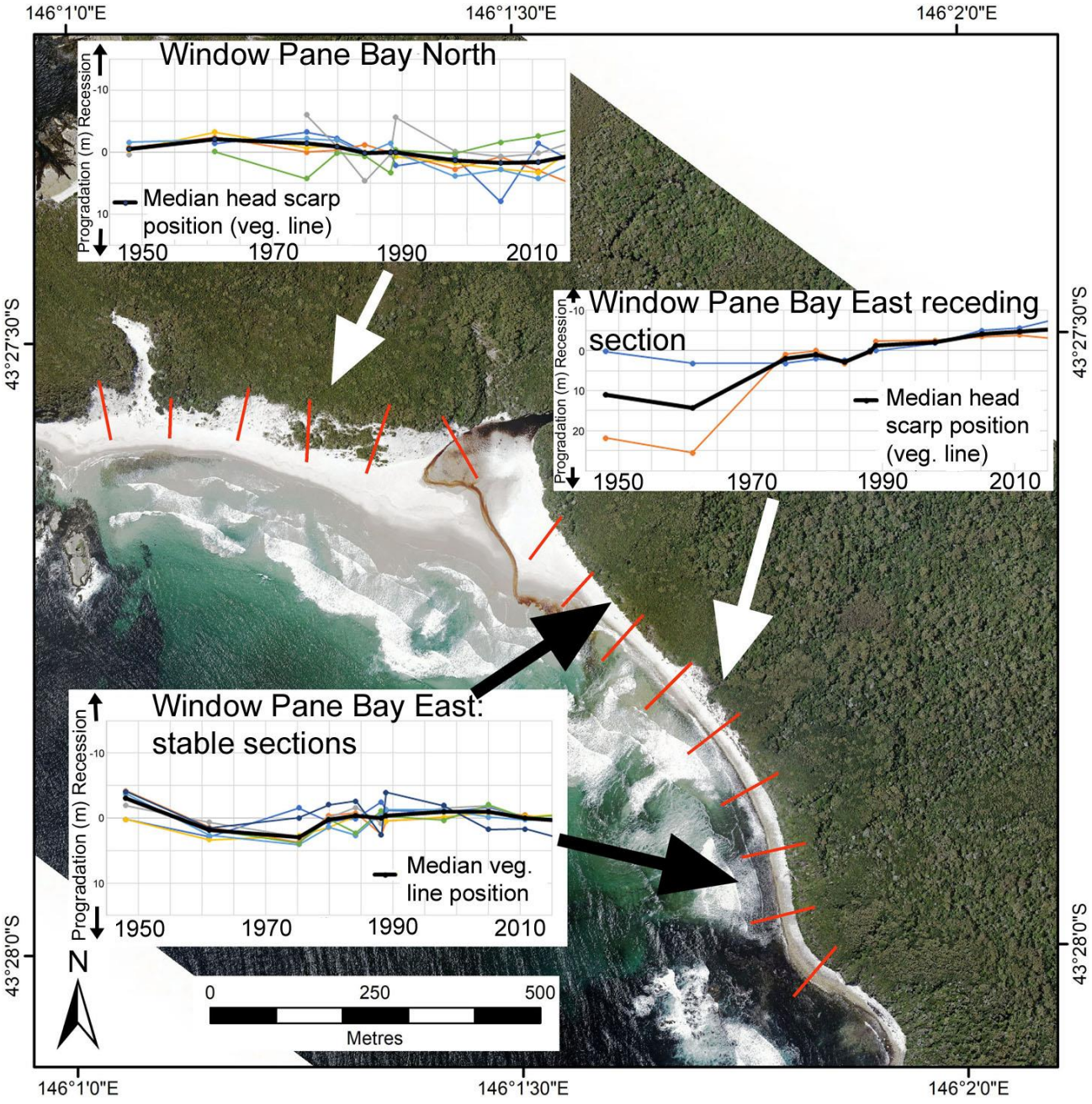

Figure 59: Window Pane Bay shoreline history plots. Plots of shoreline position (*in situ* vegetation line) change along each 100m-spaced digital transect (red lines) at 11 air photo dates during the period 1948 – 2015. The stream outflow separates two very different beach and dune types. A bare mobile dune transgressing northward from the creek outlet area is prominent on the 1948 air photo but has been fully stabilised and revegetated during recent decades. The base air photo is the 2015 air photo (© DPIPWE).

period (following an initial recession phase prior to 1960, inferred to be an initial response to a major erosion event pre-dating the air photo record; see appendix A1.3.5). The only available explanation for this long-term stability is swell-driven sand gains from the continental shelf to the beach and dune face, as modelled by Harris and Heap (2014), which must be roughly commensurate with the sand losses in order to explain the shoreline stability.). Further information on Stephens Bay Beach is available in appendix A1.3.5.

The three soft-rock (cohesive clay) shores in the unchanged stable shoreline category all present similar conditions. These are the *Northwest* and *North Barilla* shores (see Ch5 Section 5.5 and appendix

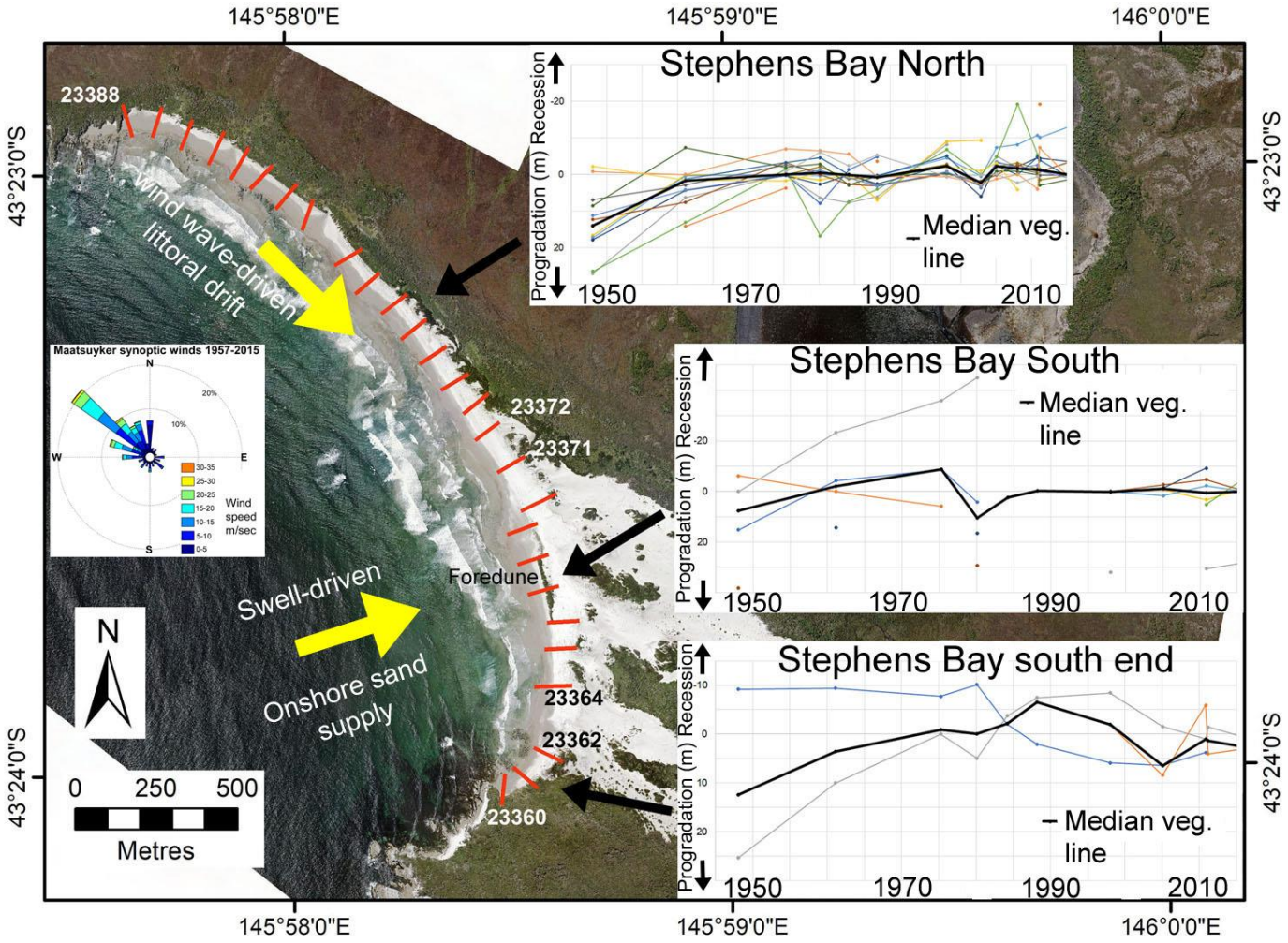

Figure 60: Stephens Bay shoreline history transect plots. Plots of shoreline position change along each 100m-spaced digital transect (red lines) at 13 air photo dates over the period 1948 – 2015. Shoreline positions are defined as seawards vegetation lines excluding creek-dominated and deflation hollow or windblown sand vegetation margins. Owing to extensive bare mobile sand areas in the southern area (transects 23364-23371), the time series plots for that area are of little value and interpretation of the shoreline history is based on visual interpretation of the air photo time series, noting in particular the foredune establishment that has occurred since circa 1980. The wind direction data from Maatsuyker Island (38 km to the SE) is inferred to be also applicable to this site based on the orientation of active deflation areas and transgressive dunes. Further information on Stephens Bay is provided in appendix Section A1.3.5. The background image is the 2015 air photo (© DPIPWE).

A1.5.1) and *Rokeby Beach Central-East* (see Figure 55 above, and information in appendix A1.5.2). The three are all located in swell-sheltered tidal re-entrants. Although all three have an effective active sediment sink and sediment transport pathway, these shores are also inactive, rounded and sometimes slumped erosion scarps which have exhibited little if any recession or other change over the air photo period. These similar shores all have much lesser wind-wave fetch and exposure than the related Barilla South shore which has shown an increasing recession trend (see Section 5.5). The limited fetch exposure adequately explains the lack of long-term behaviour change for these swell-sheltered shores. No alternative explanations for the lack of change have been identified.

IX. Stability with possible non-significant progradation trend

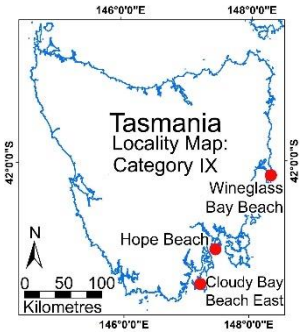

These sites have maintained an approximately stable or possibly slightly prograding shoreline position over the whole air photo period, with some inter-annual variability. Three potentially erodible open coast swell-exposed beaches are assigned to this category, namely *Hope Beach*, *Wineglass Bay Beach* and *Cloudy Bay Beach East*. See Figure 58 (above), Figure 61 and Figure 62 respectively (further information on these beaches is provided in appendices A1.4.3, A1.3.1 and A1.4.1). All three are exposed to contemporary sea-level rise, while Hope and Cloudy Bay East Beaches are possibly also exposed to increasing onshore wind speeds driven by climate change. Hence all could change their behaviour in response to climate change-driven processes if the necessary geomorphic conditions are present.

However, all three beaches are well-embayed between rocky headlands with negligible landwards aeolian sand transport and have no known significant sand losses into any alongshore sand sinks via littoral drift. In addition, shelf sediment mobility modelling (Harris & Heap 2014) suggests that all three beaches are likely to gain some sand from the continental shelf. This could explain their slight tendency towards progradation (albeit this may also be a simple artefact of minor shoreline variability and/or photogrammetric error margins in the air photo data) and would also compensate for any emerging offshore sand losses into the "Bruun sink" resulting from increased upper shoreface erosion driven by sea-level rise or increased onshore winds.

These sites therefore lack the geomorphic conditions identified in Chapter 5 as needed to enable a swell-exposed sandy beach to show an early response to sea-level rise, that is they do not have a significant active sand sink with persistent active transport of eroded sand to that sink. Although this condition is probably sufficient to explain the shoreline stability and lack of any long-term shoreline behaviour change at these beaches, the possible (albeit equivocal) progradation trends at all three beaches are suggestive that sand gains from offshore could be an additional contributing factor.

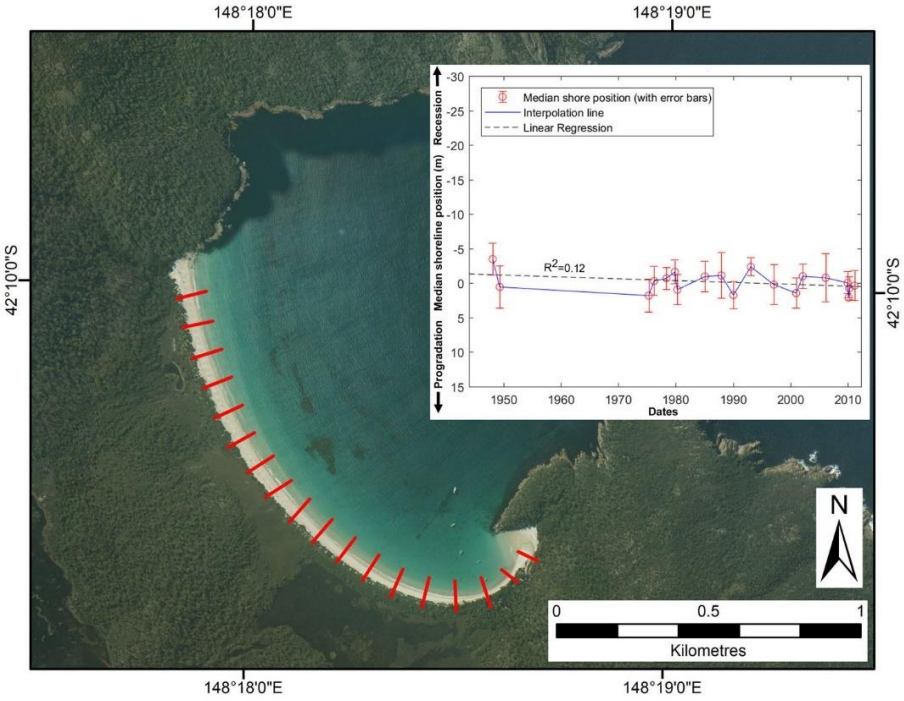

Figure 61: Wineglass Bay, eastern Tasmania: shoreline history summary plot. Median shoreline position across all transects (red lines) at each of 19 air photo dates from 1948 to 2011. A slow long-term progradation trend may be inferred from a linear fit to the data; however, the trend is smaller than the air photo margins and thus equivocal. Background air photo dated 2010 (© DPIPWE).

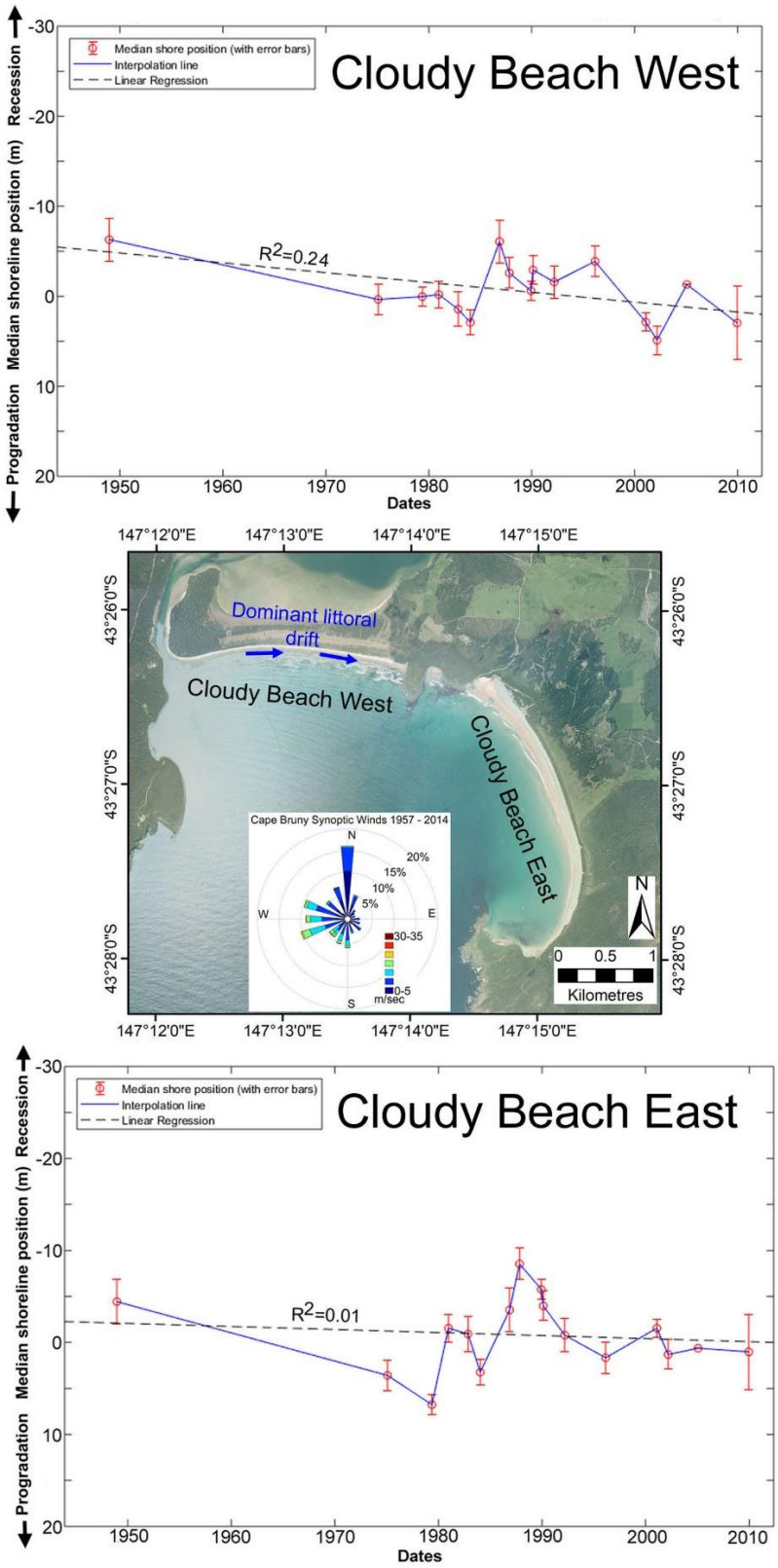

Figure 62: Cloudy Bay beaches summary shoreline history plots. The wind rose shows synoptic wind direction data for 1957 to 2014, from the nearest long-term Bureau of Meteorology weather station at Cape Bruny, ~10 km to the south-west of Cloudy Beach East (the anomalous northerly wind component may be a result of local topographic steering effects at Cape Bruny). The shoreline history plots are based on median shoreline positions across all 100 m – spaced transects at 16 air photo dates 1948 – 2009. Cloudy Bay image is the 2009 air photo (© DPIPWE).

X. Significant constant progradation trend

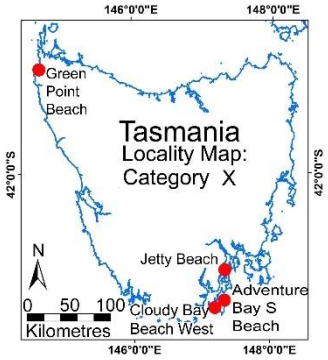

These sites have prograded at a roughly linear rate over the whole air photo period, with no significant long-term change in the rate of progradation but with some inter-annual variability. Four swell-exposed study sites have exhibited a significant progradation trend over the whole air photo period. In each case this trend is driven by a net gaining sand budget, although the reasons for the gains differ between study sites. All four sites are exposed to sea-level rise, and several are also probably exposed to increasing onshore wind speeds and possibly to changing swell-wave directions (see Table 12). Hence all could change their behaviour in response to climate change-driven processes if the necessary geomorphic conditions are present. Despite this there is not yet any indication of a significant response to these changing climate-driven processes in the form of changing shoreline behaviour over the 70-year air photo period.

In two of the four cases, the lack of any change in response to these drivers is likely attributable to a lack of the essential geomorphic conditions identified in Chapter Five: *Jetty Beach* (see Figure 50) and *Green Point Beach* (see Figure 63) are swell-exposed beaches with no significant active sand sinks and no active transport to sinks[23]. In both cases headlands prevent sand loss from the beach embayments

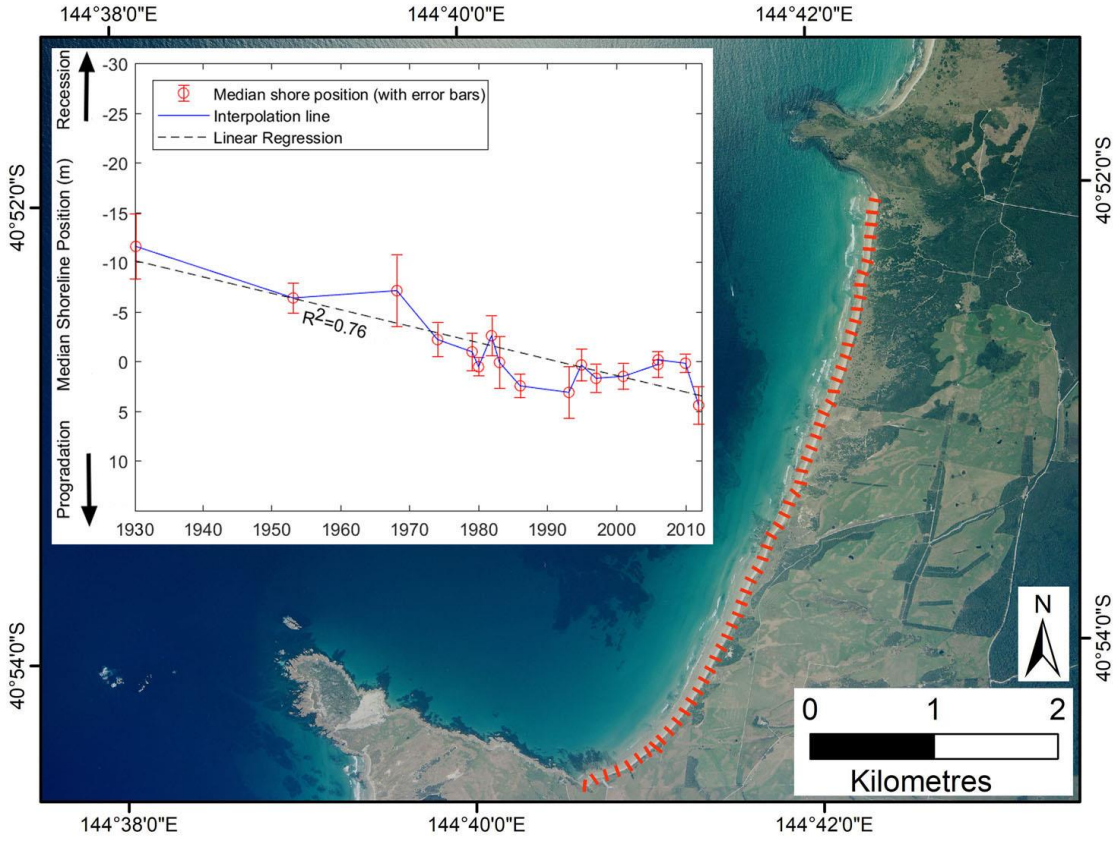

Figure 63: Green Point Beach summary shoreline history plot. The median shoreline position across all transects at each of 17 air photo dates from 1930 to 2011 is plotted, with air photo error margins and a linear regression fit to all data. A strong long-term progradation trend can be inferred from the air photo data. Background image is the 2006 air photo (© DPIPWE) with 100m-spaced digital transects shown in red. The 1930 air photo (used for the shoreline history plot) was one of the earliest air photos taken for mapping purposes in Tasmania.

[23] Jetty Beach is itself a sink for sand drifting from Nebraska Beach. However, there is currently no known sand transport out of Jetty Beach embayment to any other sink. Although the earliest (1948) air photos do indeed show aeolian sand loss from Jetty Beach via small unvegetated mobile headland-bypassing transgressive dunes, these have been stabilised by vegetation for some decades now.

by littoral drift, and also in both cases formerly active landwards aeolian sand sinks are now mostly stabilised with vegetation and inactive. Both receive a steady supply of sand (from the shelf offshore at Green Point Beach and by littoral drift from Nebraska Beach in the case of Jetty Beach) which has resulted in progradation and also offsets any offshore losses due to increasing beachface erosion under sea-level rise. Further information on these two beaches is provided in appendices A1.2.2 and A1.3.9.

In a third case, *Cloudy Bay Beach West* (see Figure 62 above), a large active sand sink is available in the form of the permanently open tidal re-entrant of Cloudy Lagoon, however the dominant littoral transport at adjacent Cloudy Bay Beach West is inferred from swell-wave patterns (see A1.4.5), to be persistently eastwards, drawing sand away from the tidal lagoon entrance rather than towards it. Since the beach is well-embayed between rocky headlands it is assumed there is some occasional re-distribution of sand along the beach under storm or south-easterly wind-wave conditions. This interpretation of the littoral drift combined with a modelled onshore gain of shelf sands (Harris & Heap 2014) can explain what otherwise appears to be an anomalous case of a beach immediately adjacent the permanently open tidal channel entrance to a large potential sand sink (Cloudy Lagoon) which not only shows no early recessional response to sea-level rise (as might be expected on the basis of the chapter 5 findings), but instead continues to prograde. Further information on Cloudy Bay Beach West is provided in appendix A1.4.5.

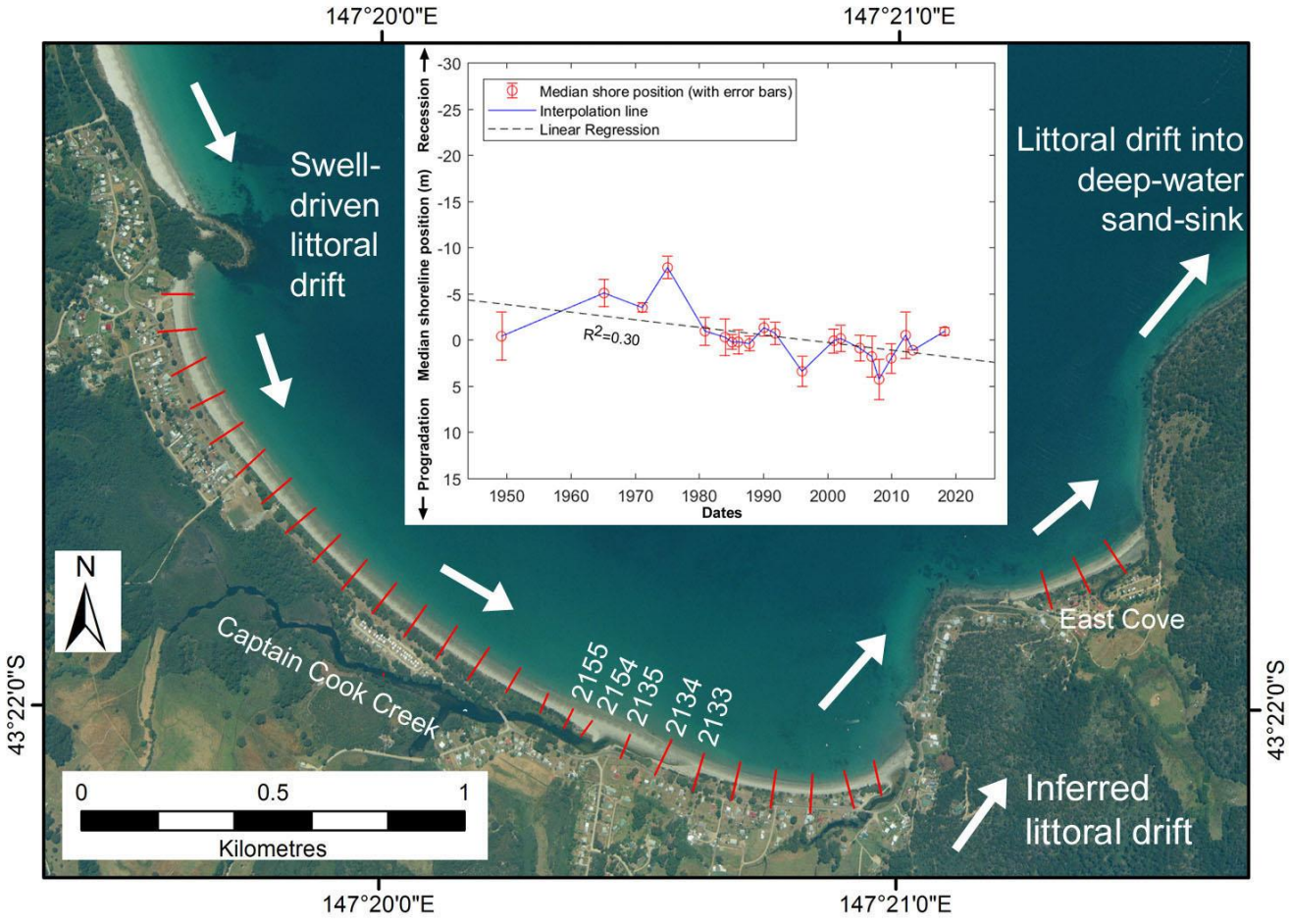

Figure 64: Adventure Bay South summary shoreline history plot. Digital transects shown in red. The median shoreline position across all used transects in the main Adventure Bay South embayment has been plotted at each of 21 air photo dates over the period 1949 to 2018. Shoreline movement at the main beach has been generally coherent across transects, except those affected by the shifting mouth of Captain Cook Creek (transects 2133, 2134, 2135, 2154 and 2155 as numbered on figure). These anomalous transects have been omitted from the summary plot, as have the spatially separate East Cove transects. The base image is the January 2005 air photo (© DPIPWE).

The fourth case is perhaps even more anomalous: swell-exposed *Adventure Bay South Beach* (see Figure 64) exhibits both an active sand sink and a persistent unidirectional swell-driven littoral drift of sand both into and out of its leaky embayment. Given that rising sea-level is expected to have been causing more frequent erosion events higher on the beachface than previously, an increasing loss of sand from the embayment compared to the (presumed unchanged) gains into the embayment should in theory result in an early switch to shoreline recession. This shoreline response model is similar to that proposed in Chapter 5 (Section 5.3) to explain the early response of Roches Beach to sea-level rise, however a significant difference at Adventure Bay Beach is the long term progradation trend (which was not present at Roches Beach prior to its change of behaviour). This suggests that (unlike Roches Beach) the rate at which Adventure Bay Beach has historically gained sand has been sufficiently large as to be still great enough to compensate for increasing rates of erosional sand loss due to sea-level rise.

It can be inferred that Adventure Bay South Beach is still likely to respond to sea-level rise with a relatively earlier change to recessional behaviour than beaches lacking the active sand sink and persistent sand transport pathway. However, this will depend on the degree to which its gaining sand budget is continuing to compensate for its increasing sand losses. With no quantitative data on this issue it is problematical to speculate how long this may take. Further information on Adventure Bay South Beach is provided in appendix A1.4.4).

6.4 *Summary Findings*

This summary draws together the key findings, both of the selected detailed shoreline behaviour studies described in Chapter 5, and of the broader analysis of all study sites described in Chapter 6. These summarised findings comprise the most important scientific findings of this thesis.

6.4.1 Findings for shores exhibiting long-term (or emerging long-term) changes in shoreline behaviour types

The four Chapter 5 case studies identified sites at which a long-term shoreline behaviour change on erodible shorelines is best explained as an early response to the climate change-induced process of sea-level rise (and possibly increased onshore wind speeds or changed long-term swell directions in some cases). For all of these, the following two geomorphic conditions were identified as being necessary explanatory factors (Section 5.6.3):

- an active sediment sink with significant accommodation space for eroded sediment; and
- a persistent (generally unidirectional) active sediment transport path to the sink.

Additionally, in the case of erodible shorelines within swell-sheltered tidal re-entrants, changes in shoreline behaviour probably attributable to early responses to climate change-induced drivers were only found on shorelines with the following local conditions:

- Relatively high wind-wave exposure and long wind-wave fetches in dominant wind directions.

Other geomorphic and oceanographic conditions may contribute to enabling shoreline behaviour changes at some sites in response to climate-induced drivers but were not identified as essential factors (see Section 5.6.3).

This chapter (Section 6.3.2) has analysed all study sites showing a significant long-term change in shoreline behaviour type over the air photo period. All these sites are exposed to contemporary climate change-driven sea-level rise. Some are additionally exposed to climate change-driven increasing onshore wind speeds and possibly to long-term swell direction changes in a few cases (Table 11). The purpose of the analysis was to determine whether the drivers and conditions found to explain shoreline behaviour changes in the four case study areas analysed in Chapter 5 can also explain the long-term changes observed at other study sites, or whether additional causes or conditions need to be invoked to explain any of these.

For the 10 (out of 35) sites exhibiting a long-term or likely emerging behaviour change, all had the two conditions identified as necessary for an early response to climate change-induced drivers (namely, active sediment sinks and persistent sediment transport pathways). Additionally, those changed shores within swell-sheltered tidal re-entrants were located on the most wind-exposed shores with the longest wind-wave fetches (see specific conditions on Table 9 and summary Table 11 below).

Nonetheless, the changes at two of these sites were found to be more plausibly attributable to different explanations, whose effects probably dominate over the effects of climate change-induced drivers given the conditions at these sites (*Gordon* and *Stephens Bay Beach South*; see Table 11).

Table 11: Summary of available explanations for long-term shoreline behaviour change at changed sites. The 'Drivers of Change' are the climate change-induced processes identified as plausible explanations of observed long-term shoreline behaviour changes. These explanations were initially identified through a process of comparing multiple hypotheses to explain Chapter 5 case studies, then further tested on additional sites in Chapter 6. The 'Conditions enabling Change' are those local geomorphic conditions inferred to be necessary for shores to show an early response to climate change-induced 'Drivers of Change'.

Shoreline behaviour category	Site	Drivers of change		Site geomorphic conditions enabling change	
		Climate change-induced drivers[1]	Other	Conditions enabling early response to climate change-induced drivers[2]	Other site conditions enabling change due to other drivers
Steady recession then acceleration of recession	Gordon	SL (only)	Local artificial interference (likely dominant driver)	AS, ST	Hardening of updrift sandy shores (= sand budget deficit)
	W. Duck Bay S	SL, WS(?)	-	AS, ST, HE	-
	W. Duck Bay SE	SL, WS(?)	-	AS, ST, HE	-
	S. Barilla	SL (only)	-	AS, ST, HE	-
Stability then long-term recession	Window Pane Bay East	SL, WS, SD(?)	-	AS, ST	-
	Ocean Beach	SL, WS, SD(?)	-	AS, ST	-
	Roches Beach Main Central	SL (only)	-	AS, ST	-
Stability then emerging (<10 years) recession	Nebraska Beach	SL, WS(?)	-	AS, ST	-
Stability then long-term progradation	Stephens Bay Beach South	SL, WS, SD(?) But changes not consistent with expected responses to climate-change-induced drivers	Ongoing long-term landform and sand budget adjustment following an inferred major erosion event preceding earliest air photo.	AS, ST	Very high energy wind & wave climate conditions (hindering rapid vegetation recovery and slowing foredune accretion after erosion).
Progradation then emerging (<10 years) recession	Prion Beach	SL WS SD(?)	-	AS, ST	-

Notes:

1. *Drivers*: Sea-level rise (SL), Onshore wind-speed increase (WS), Long-term swell direction change (SD).
2. *Enabling conditions*: Active sediment sink (AS), Persistent sediment transport to sink (ST), High wind-wave exposure and fetch if in swell-sheltered tidal re-entrants (HE).

The long-term behaviour changes at the remaining eight sites were inferred to be best explained as early responses to climate change-induced drivers. Of these, five were already part of the Chapter 5 analysis, thus only three are additional sites to test the broader applicability of the conclusions (above) from Chapter 5. These additional sites are *Window Pane Bay Beach East*, *Nebraska Beach* and *Prion Beach* (see Table 11). All eight sites conform with the Chapter 5 findings by exhibiting the necessary conditions (listed above) for an early response to contemporary climate change-induced drivers of coastal change. No additional geomorphic conditions are required to explain the changing shoreline behaviour of the additional three sites.

6.4.2 Findings for shores not exhibiting long-term changes in shoreline behaviour type

Table 12 below provides a tabular summary of the analysis of 25 coastal sites (out of 35) that *do not* exhibit a long term (or likely emerging long-term) change in shoreline behaviour over the air photo period. The discussion below elaborates the tabular summary.

All these sites are subject to rates of contemporary sea-level rise comparable to global mean climate change-induced sea-level rise. Some but not all sites are also exposed to onshore wind-speed increases inferred to be climate change-related, and a few may be exposed to swell wave direction changes resulting from climate change.

It was initially inferred that sites exposed to these drivers but not showing any changes in response to them would be sites lacking in the geomorphic conditions identified in Chapter 5 (Section 5.6.3) as necessary to enable an early response to climate change-induced drivers. These would be sites that:

- *do not* have a significant active sediment sink; and/or:
- *do not* have a persistent (generally unidirectional) active sediment transport path to a significant active sink.

Additionally, in the case of erodible swell-sheltered tidal re-entrant shores not exhibiting early responses to climate change-induced drivers, these sites:

- *will* have relatively low wind-wave exposure and short fetches in dominant wind directions (resulting in much slower or as yet undetected shoreline recession or acceleration of recession).

Other geomorphic and oceanographic conditions may contribute to enabling shoreline behaviour changes in response to climate-induced drivers but were not identified as essential factors (see Section 5.6.3). Hence their presence or absence was not considered to be a necessary condition of long-term change or lack of change, respectively.

The analysis presented in Section 6.3.3 (above) proceeded by determining whether or not an unchanged site lacked the necessary geomorphic conditions to enable long-term shoreline behaviour change. The analysis also considered whether there were any other conditions present which might prevent or mask any long-term changes of behaviour in response to climate change-driven processes.

In summary, the analysis found that of the 25 (out of 35) studied sites that *do not* exhibit a long term (or likely emerging long-term) change in shoreline behaviour over the air photo period:

- Nine (9) swell-exposed sites did not have significant active sand sinks and/or did not have a persistent active sand transport pathway from the study shore to the sand sink; and:
- Twelve (12) swell-sheltered re-entrant sites had relatively low (or negligible) wind-wave exposure and fetch.

These 21 sites fit the expectation of not having the essential geomorphic conditions (as identified in the Chapter 5 case studies) for an early response to climate change-induced drivers of shoreline change.

Table 12: Summary of available explanations for study site shores that have <u>not</u> shown long-term behaviour changes over the air photo period. The 'Drivers of Change' are the climate change-induced processes that are known or potentially active at each site causes identified as providing plausible explanations of observed long-term shoreline behaviour changes. These explanations were identified through a process of comparing multiple hypotheses in Chapter 5 and in relevant Appendix 1 sections.

Shoreline behaviour category	Site	Climate change-induced drivers active at site[1]	Conditions enabling early responses to climate change-induced drivers present at site[2]	Deduced explanations for lack of long-term behaviour change	
				Descriptive	Key factors[3]
Significant constant recession trend	Cloudy Lagoon East	SL WS(?)	AS ST	Receding sandy and saltmarsh shores in tidal swell-sheltered re-entrant. Active (tidal current) sand transport and sink available, however *wind-wave fetch and exposure insufficient to trigger early long-term significant increase of existing recession trend*.	**O**
	Cloudy Lagoon North				**O**
	West Duck Bay N (E)	SL WS(?)	AS ST	Receding sandy and saltmarsh shores in tidal swell-sheltered re-entrant. Active (tidal current) sand transport and sink available, however *wind-wave fetch and exposure insufficient to trigger early long-term significant increase of existing recession trend*.	**O**
	West Duck Bay N (W)				**O**
	West Duck Bay NW				**O**
	Mulcahy Bay Beach	SL WS SD(?)	AS ST	Beach embayed between rocky headlands, active but relatively minor landwards aeolian sand transport to inland sinks. *Sand gains from shelf offset any increased loss to aeolian sinks or offshore "Bruun sink".*	**+**
	Rokeby Beach West	SL WS(?)	AS ST	Soft rock (cohesive clay) shore in tidal re-entrant with normally very attenuated swell penetration.*;* Storm swell penetration triggers more erosion at west end of beach than central-east part (see below), but *neither occasional storm swell penetration nor dominant westerly wind-wave fetch and exposure are sufficient to trigger early long-term significant increase of existing recession trend.*	**O**
Stability with possible non-significant recession trend	Ralphs Bay shore (S. Arm)	SL	N	*Large sand sink effectively full, no significant active sink or sediment transport* (e.g., by tidal currents) until ongoing sea-level rise creates significant new accommodation space on tidal flats. Dominant winds blow offshore or alongshore, little alongshore drift sand transport potential.	**O**
	Cloudy Lagoon S	SL WS(?)	AS ST	Large sand sink available with weak tidal current transport for eroded sediments, however *very low wind-wave exposure and fetch (dominant winds mainly offshore) insufficient to trigger long-term change to recession trend.*	**O**
	Cox Bight Beaches	SL WS	N	Deeply embayed beaches between long rocky headlands, *no effective sand sinks or active sand transport to sinks*. Sand gains from shelf offset any loss to offshore "Bruun sink".	**x +**
	Wreck Bay Beach	SL WS SD(?)	N	Beach embayed between rocky headlands, *no effective sand sinks or active sand transport to sinks*. Sand gains from shelf offset any loss to offshore "Bruun sink".	**x +**
	West Barilla shore	SL	AS ST	Soft rock (cohesive clay) shores in tidal re-entrant with no swell penetration*; dominant north-westerly wind-wave fetch and exposure insufficient to trigger early significantly increased recession.*	**O**
Stability	Window Pane Bay Beach North	SL WS SD(?)	N	Minor ongoing sand loss via landwards aeolian transport, but this process much reduced since 1940s. *Sand gains from shelf and eroding east beach offset any loss to aeolian sink or offshore "Bruun sink*".	**x +**

	Stephens Bay Beach N	SL WS SD(?)	AS ST	Active landwards (aeolian) and significant alongshore (wind wave-driven) sand transport to active sinks, however *sand gains from shelf continue to offset losses*.	**+**
	Roches Beach N	SL	AS ST	Active longshore drift of sand into and out of compartment. *Increased sand gains from (eroding) updrift compartment offset losses to downdrift sink*.	**+**
	North-west Barilla shore	SL	AS ST	Soft rock (cohesive clay) shores in tidal re-entrant with no swell penetration*; dominant north-westerly wind-wave fetch and exposure insufficient to trigger early recessional acceleration response*.	**O**
	North Barilla Shore				**O**
	Rokeby Beach Central-East	SL WS(?)	AS ST	Soft rock (cohesive clay) shore in tidal re-entrant with very attenuated swell penetration*; dominant westerly wind-wave fetch and exposure insufficient to trigger early recession response*.	**O**
Stability with possible non-significant progradation trend	Cloudy Bay Beach east	SL WS(?) SD(?)	N	Beach embayed between rocky headlands, *no effective sand sinks or active sand transport to sinks*. Sand gains from shelf offset any loss to offshore "Bruun sink".	**x +**
	Wineglass Bay Beach	SL	N	Beach deeply embayed between rocky headlands, *no effective sand sinks or active sand transport to sinks*. Sand gains from shelf offset any loss to offshore "Bruun sink".	**x +**
	Hope Beach	SL WS(?)	N	Beach embayed between rocky headlands, *no effective sand sinks or active sand transport to sinks*. Sand gains from shelf offset any loss to offshore "Bruun sink".	**x +**
Significant constant progradation trend	Jetty Beach	SL WS(?)	N	*Inactive minor aeolian sand sink, currently no effective sand transport out of beach embayment*; Embayed beach is a sink gaining from updrift sand sources, with little potential for sand loss at present, hence ongoing progradation.	**x +**
	Green Point Beach (Marrawah)	SL WS SD(?)	N	Deep embayment between large rocky headlands with *no significant active sand loss pathway or sink*. Aeolian sand sink minor and diminished since 1940s. Sand gains from shelf more than offset any loss to offshore "Bruun sink", resulting in continuing net sand gains and progradation.	**x +**
	Adventure Bay South Beach	SL WS(?)	AS ST	Conditions for early response exist (*active sand sink and persistent transport to it*) but no change of behaviour identified yet. This is probably because *sand gains from updrift still enough to offset increasing downdrift losses*. It is likely that sand budget not yet at tipping point needed for recession response to begin.	**+**
	Cloudy Bay Beach west	SL WS(?) SD(?)	AS	Beach embayed between large rocky headlands. *Cloudy Lagoon is a potential sand sink, however there is no effective sand transport from beach to sink* (the dominant littoral drift within embayment moves sand away from the lagoon entrance). Sand gains from shelf probably offset any loss to offshore "Bruun sink".	**x +**

Notes:

1**.** *Drivers*: Sea-level rise (SL), Onshore wind-speed increase (WS), Long-term swell direction change (SD), None (N).

2. *Necessary geomorphic conditions enabling change (in all cases)*: None (N), Active significant sediment sink (AS), Persistent sediment transport to sink (ST); *Necessary geomorphic conditions for change <u>if</u> site located in swell-sheltered re-entrant*: High wind-wave exposure and fetch (HE).

3. *Key factors explaining lack of long-term behaviour change*: Lack of significant active sediment sink and/or persistent active sediment transport to the sink (**X)**; Relatively limited wind-wave exposure and fetch (**O**); Significantly gaining sand budget (**+**).

However, an additional four (4) unchanged swell-exposed sandy beach sites do indeed have significant active sand sinks and persistent active sand transport pathways from the study shore to the sand sink, and so might in principle be expected to show a long-term change of behaviour in response to changing climate change-induced driving processes. Each of these sites does however also have a gaining sand supply, and this is inferred to be the factor preventing a change of behaviour by compensating for any

increasing sand losses attributable to climate change-induced drivers of shoreline change. In two of these cases the inferred sand supply is a swell-driven sand supply moving onshore from the continental shelf (*Mulcahy Bay Beach* and *Stephens Bay Beach North*), while in the other two cases it is an incoming littoral drift of sand to the beach embayment equal to or larger than the amount of sand being lost from the beach embayment by littoral drift (*Roches Beach North* and *Adventure Bay South Beach*).

The other nine unchanged swell-exposed sandy beaches noted above - whose lack of long-term behaviour changes can be readily attributed to their lack of significant active sand sinks and/or effective sand transport pathways – are also gaining sand from an active source. Given that a positive (gaining) sand budget may be sufficient in itself to prevent any early behaviour changes in response to climate change-driven causes, the combination of this factor and the lack of the other necessary conditions for change must increase the resistance of these beaches to climate change-induced drivers of change over the time scales considered here.

However, it is also important to note that some beaches which *have* changed their behaviour in a fashion interpreted as a likely response to sea-level rise and onshore wind increases (e.g., *Ocean Beach* and *Prion Beach*; see Table 9) may have also been prograding in response to a gaining sand budget immediately prior to changing their behaviour to recession. No quantitative data is available regarding the rates of sand gains and losses at these beaches. However, it can reasonably be inferred that whether or not a beach with both an effective sand sink and an active sand source changes its behaviour will depend on the relative rates at which it gains and loses sand. That is, a very large and active sand sink such as that at Ocean Beach may be easily able to accept increasing quantities of eroding sand so that at a relatively early stage of increasing erosion the rate of sand loss from the beach exceeds its gains and it begins to recede. On the other hand, a gaining beach with only a smaller-capacity sand sink or a slower sand transport pathway may not change to recession for a long time, as its sand gains continue to exceed its sand losses.

This shoreline behaviour analysis has found that a lack of early shoreline behaviour response to sea-level rise or other climate-induced changes is correlated with an absence of the necessary conditions for change identified in Chapter 5 in many - but not all - cases. Table 12 above provides a summary of the mostly likely reasons for the lack of observed long-term shoreline behaviour change in each unchanged study site (two RH columns). In some cases, the conditions required for early response changes are present but still no response has been detected in the air photo or beach profiling record. In each of these cases an additional geomorphic process or condition likely to prevent an early response is identifiable at the sites in question, namely the presence of an *active sand source enabling the site to gain sufficient sand to counter-act the increased erosion and sand-loss effects of climate change-driven processes* so that no early changing response has occurred.

6.5 *Summary findings in context*

The summary findings in Section 6.4 above comprise the core scientific (geomorphic) findings of this thesis. Based on these findings, the following Chapter 7 "Discussion" identifies as far as possible some of the broader implications of these findings for understanding of Tasmanian coastal geomorphology generally, and for understanding of climate change impacts and hazards on coasts. Chapter 8 "Conclusions and Recommendations" evaluates the extent to which the thesis outcomes have filled the knowledge gap identified in the Introduction (Section 1.2), and identifies the answers that this project has arrived at to the Research Questions posed in Section 1.3.

Unsurprisingly, this thesis has identified a variety of data and knowledge gaps whose resolution would further improve scientific understanding of the research questions tackled by this project. Chapter 8 concludes by recommending a variety of knowledge gaps worthy of ongoing attention that are likely to lead to usefully improved understanding of coastal morpho-dynamics and sea-level rise responses in Tasmania as well as further afield.

Chapter 7: Discussion

7.1 *Introduction*

The previous chapter summarised the scientific findings of this thesis (in Section 6.4), drawing together analyses of the history of 35 individual shorelines over an approximately 70-year time period. This chapter now explores the implications of this work more broadly, both in terms of the applicability of the method presented, and for improved understanding of past and future soft shoreline behaviour in Tasmania and more generally.

7.2 *Aerial photography as a source of historic shoreline behaviour information*

The core data upon which this thesis is based were geo-referenced and ortho-rectified coastal aerial photographs obtained at multiple dates from 1945[24] until recently. From these, shoreline positions (defined as the seawardmost *in-situ* vegetation line) were digitised at each air photo date and were used to analyse shoreline changes over time. Photogrammetric error margins, measured on each air photo as apparent displacement of reference features from their positions on a reference photo, were utilised as a measure of data quality. All available air photos of adequate photogrammetric quality were used for each of 35 selected shorelines, which amounted to more than 20 air photo dates at many sites and over 30 dates at a few sites. A total of 521 air photo frames were used in this project, of which 380 were individually ortho-rectified by the author, and 141 were obtained already ortho-rectified by others (details in Appendix One). Other methods of analysing coastal changes from aerial photography are available (for example by generating digital terrain models (DTMs) at each date from air photo stereo-pairs). However, the method adopted yields the longest possible time series of shoreline position with approximately homogeneous uncertainty estimates (in contrast, old photographs are commonly not as reliable for DTM generation as they are for vegetation line identification).

Aerial photography provides the best available objective record of shoreline behaviour over roughly the latter (more recent) half of the period since the onset of global climate change-driven sea-level rise during the mid-1800s (see Section 2.3). This project has demonstrated the potential for aerial photography time series to yield useful insights into physical shoreline responses (or lack thereof) to that sea-level rise.

Although the length of time gaps in historical air photo records can impose limitations on the inferences that can be drawn from such data, the results of this thesis demonstrate that if all available photography is used so that time gaps are minimised as much as possible, then long term (multi-decadal) trends in shoreline behaviour, and long-term changes in such trends, can be inferred from the data with a high degree of confidence. This is most apparent where multiple consecutive air photos over multiple decades all demonstrate a consistent shoreline behaviour type (i.e., progradation, stability or recession). In addition, more frequent sampling with air photos can better constrain the timing and nature of long-term shoreline behaviour changes, and of storm events that are inferred to cause step-changes in shoreline behaviour (as seen in this study at Ocean, Roches, and Prion beaches for example (Sections 5.2, 5.3 and 6.3.2).

7.3 *Insights into broader Tasmanian coastal geomorphic processes*

The project described in this thesis has analysed the long-term shoreline behaviour of a significant number (35) of soft erodible Tasmanian shorelines using all available air photo data for each site.

[24] The earliest air photos at nearly all sites dated from 1945 or later. However, in one case the earliest available and usable air photo dated from 1930 (Green Point Beach).

This approach has yielded valuable new general insights into the behaviour of Tasmanian coasts during the last 70 years. Three important insights highlighted here are:

- Robust evidence is now available of the types and variability of long-term sandy and soft rock shoreline behaviour trends and changes of trends that have occurred on the Tasmanian coast during the last 70 years approximately. These include changes from stability to recession, or increased recession rates, in a moderate proportion of cases (Section 7.3.1).
- Amongst these trends, an unexpected result is that many Tasmanian sandy beaches have prograded over part or the whole of the study period, which in many cases is inferred to be the result of continuing sand movements from the inner continental shelf (Section 7.3.2).
- Sandy beaches on the Tasmanian west and south-west coast appear to be subject to a very slow and distinctive type of beach and dune recovery process following major erosion events. This is inferred to be related to the combination of a very high-energy wind and wave climate, and a large gaining sand supply (Section 7.3.3).

These points are elaborated below.

7.3.1 Long-term (multi-decadal) shoreline behaviour trends and changes in trends

All air photo-derived shoreline change histories obtained during this project exhibited some real or apparent shoreline position variability on inter-annual to decadal time scales. This short-term variability is typically due to a combination of beach storm erosion and recovery cycles, scarp slumping and small observational errors related to the photogrammetric method. This project has used simple linear regressions, including piecewise linear regressions on data for specific periods within a time series, to remove short-term variability and to estimate long-term (multi-decadal) trends and changes to these trends. For the purpose of this thesis, shoreline behaviour trends for both sandy and soft rock shores (with short term variability removed) have been classified into just three type categories, namely progradation, stability or recession. This was an optimum level of classification for this project since detection of more complex historic shoreline behaviours may be problematic given the frequency of air photo campaigns at most Tasmanian coastal sites (typically about 10-year air photo intervals at most sites over at least the first half of the air photo period).

Of the 35 coastal sites for which a shoreline behaviour history was compiled from air photo time series, 25 shores showed a steady linear trend over the whole circa 70-year air photo period (allowing for short-term variability as noted above). These were variously progradation at steady rates (7 sandy coast sites), stability (6 sites) or recession at steady rates (12 sites) as listed on Table 8 (Section 6.2). The inferred causes of these trends are discussed in Chapter 6 and summarised on Table 12 (Section 6.4.2). Although site selection was not random (see Chapter 4), the finding that a majority of shorelines studied have maintained an essentially linear trend (i.e., a single behaviour type, at a steady rate in the case of progradation or recession) over the latter half of the Twentieth Century up to the present is a new evidence-based finding about the behaviour of soft Tasmanian shores on inter-decadal to centennial timescales.

Conversely, a significant (but not dominant) proportion of Tasmanian shorelines (10 sites out of 35 studied) have exhibited a change in long-term (multi-decadal) behaviour, mostly from either stability or progradation to recession, or else a notable increase in the rate of a prior long-term recession trend. These are differentiated in Table 8 (Section 6.2) above, and the inferred causes of change are summarised on Table 11 (Section 6.4.1). In most cases (8) the only explanations found for this were climate change - induced drivers, namely sea-level rise and in a few cases increasing onshore wind speeds. This finding was not unexpected given the authors prior observations of some sites which prompted the research questions posed at the outset of this thesis. However, in one case (Gordon) the change was found to be more likely attributable to local artificial interferences, and in another

(Stephens Bay) to a long-term geomorphic process unrelated to climate change (see further discussion in Section 7.3.3 below).

7.3.2 Sandy coast progradation trends

Close to a third (9) of the swell-exposed sandy beaches studied have exhibited long-term (multi-decadal) progradation trends over all or else a significant part of the air photo record period. These are identified on Table 8 (Section 6.2). In some cases, the sand gained has been supplied by littoral drift (e.g., Jetty Beach and Adventure Bay Beach). However, for examples such as Green Point Beach, Stephens Bay Beach, Cloudy Bay Beach West & East, and Hope Beach, the only plausible sand source is continuing onshore movement of sand from the inner continental shelf. In most of these cases, the progradation trend has occurred over the entire air photo period and is still ongoing. However, in the case of Prion Beach, a long period of progradation (also inferred to be driven by shelf sands) preceded a switch to an emerging recession trend which this study has attributed to a response to sea-level rise.

Although the prevalence of prograding beaches on the Tasmanian coast was unexpected, it is consistent with previous regional-scale shelf sediment mobility modelling for Australia (Harris et al. 2000) and with the continental-scale Australian coastal sediment transport synthesis of Short (2010). Short stated that strong Southern Ocean swells and winds drive large volumes of shelf sediment onshore along much of the southern Australian continental margin including western Tasmania. However, although most of the sand moved onshore along the southern Australian margin is biogenic carbonate (Short 2010), much of the sand supplied to Tasmania's west and south coast beaches is quartz (Banks, Colhoun & Chick 1977; Harris & Heap 2014; Walford 2011). This is unsurprising given that large amounts of offshore quartz sand is derived from repeated Pleistocene glaciation of Tasmania's western and southern quartzose mountains, and was supplied by glacial outwash rivers from these to the continental shelf during glacial low sea-stands (Colhoun, Hannan & Kiernan 1996). During interglacial high sea-stands such as the present, bottom currents generated by very energetic swell waves are inferred to drive the sand onshore along the west and south coasts (Harris & Heap 2014). However, it is notable that the shoreline behaviour histories of some south-eastern and eastern Tasmanian beaches such as Hope and Wineglass Bay Beaches also exhibit some evidence (weak progradation) of continuing onshore supply of sand despite being less energetic coasts.

7.3.3 Very high-energy sandy coast morpho-dynamics

The behaviour of some south-west coast Tasmanian beaches, which are exposed to the highest-energy coastal wave and wind regimes in Australia (Grose et al. 2010; Hemer, Simmonds & Keay 2008), may reflect very long-term (multi-decadal to centennial) dune recovery processes following major beach and dune wave-erosion events prior to the earliest available air photos. These beaches include Ocean Beach, Mulcahy Bay Beach, Wreck Bay Beach and Stephens Bay Beach, as documented in Chapters 5 and 6, Appendix 1, and by Eberhard et al. (2015). The air photo and beach profile survey record is interpreted as showing these processes to involve long periods of aeolian deflation and landwards sand loss from bared seawards dune faces, which is however accompanied by little or no shoreline recession or beach lowering due to an abundant compensating onshore sand supply. Foredune vegetation recovery is evidently very slow at these beaches, which is inferred to be due to very high wind-exposure retarding foredune vegetation establishment. However although the extensive bare and deflating seawards dune faces backing much of these beaches are suggestive of active shoreline retreat, the findings of this project indicate this is a misleading impression since the beach and dune sands are kept replenished by an onshore sand supply. The only very high-energy beach studied which has been notably receding is Ocean Beach, and in that case only after an abrupt switch of behaviour related to the presence of a large sand sink of a sort not found at the other south-west beaches (see Section 5.2). The high-energy sandy coast morpho-dynamic process systems of the

south-west coast were not investigated in detail during this thesis but warrant further investigation as a little-studied very high-energy endmember of sandy coast morphodynamic processes.

7.4 *Insights into shoreline responses to global climate change processes*

Several findings of this thesis are important outcomes directly relevant to the research questions posed in Chapter 1 (Section 1.3), namely:

RQ1. *What evidence may enable contemporary climate change-driven sea-level rise to be identified as a dominant factor driving changes in coastal landform behaviour?*

and:

RQ2. *Are there some distinctive "early responder" shoreline types or coastal process environments which are responding to contemporary climate change-driven sea-level rise earlier than other "late responder" types?*

The project outcomes in regard to these questions are summarised in the concluding Chapter 8 (Section 8.2). However, it can be noted here that RQ1 is partly addressed by the general finding described in Section 7.3.1 above. That is, that long-term changes in Tasmanian shoreline behaviour have occurred during the last 70 years for which the method of identifying and examining multiple potential explanatory hypotheses has in 8 cases identified climate change-induced driving processes as the only plausible explanations found (see Section 6.4.1, Table 11).

In regard to RQ2, two findings identified below are particularly relevant, namely:

- The nature of the sediment budget has emerged from this study as the most consistently important condition governing the timing and style of a shoreline's early or later response to sea-level rise (Section 7.4.1).
- Sea-level rise is not the only climate change-induced driver of physical coastal changes, with onshore wind speed changes and long-term swell direction changes also being climate change-induced processes likely to contribute to early or late coastal responses (Section 7.4.2)

These points are elaborated below.

7.4.1 Sediment budgets: the critical condition governing the timing and style of shoreline responses to sea-level rise

The findings of this thesis (Section 6.4), indicate that the condition most consistently determining when a shoreline will begin exhibiting an attributable physical response to climate change-induced processes is the nature of its sediment budget. The amounts of sediment gained and/or lost by a coastal compartment - and changes in the balance between these as higher sea levels force increasing shoreline erosion and loss of sediment - is the factor which in all the relevant cases identified by this project (8 of 35 coastal sites) is most clearly linked to changes of long-term shoreline behaviour that are inferred to be responses to climate change-induced drivers including rising sea-levels and increasing onshore wind speeds. See discussion in Sections 5.6.2 and 6.4.

This is not only true for swell-exposed sandy shores whose sediment (sand) is capable of being either removed from or accreting to shorelines. It is also applicable to soft-rock shores, from which sediment removed by increasing impacts of wave erosion not only includes a sand fraction, but also both very fine (clay, silt) and coarse (pebble, cobble) fractions. Once eroded, neither of these can be returned to and accreted back onto the eroded soft rock shores. This makes them "one-way" shores capable only of change by eroding and receding in the long-term. These shores have what is in effect a persistently negative (losing) sediment budget and so will recede at some (typically slow) rate even in the absence of changing processes such as sea-level rise. However, their characteristically negative sediment

budget means that their rate of erosion and sediment loss will increase if they are exposed to increasing drivers of erosion such as higher sea-levels or more energetic onshore-directed wind waves (Section 2.5.3).

A wide variety of other factors may increase or decrease the susceptibility of erodible shores to show a response to climate change-driven processes. These include greater or lesser sea-level variability on inter-annual time scales (Section 2.5.8), a higher or lower frequency of storm events (Section 2.5.7) or vertical land movement (Section 2.5.4). Nonetheless, the results of this study indicate that it is the sediment budget which most consistently determines how quickly and to what degree a susceptible shoreline will actually show a physical response to a driver such as sea-level rise.

A related finding from this study is that the nature of the sediment budget is related to the style and timing of the change of behaviour in response to sea-level rise at a given shoreline. At swell-exposed sandy beaches which both gain and lose sand and are capable of beach and dune recovery following erosion ("two-way shores"), the switch from a prograding or stable to a persistently receding shoreline in response to ongoing sea-level rise has been observed in several cases to be an abrupt "*tipping point*" style of change. This is clearly evident at three swell-exposed sandy beaches inferred to have changed their behaviour in response to sea-level rise, namely Ocean Beach (Section 5.2), Roches Beach (Section 5.3) and Prion Beach (Section 6.3.2). In these cases, the observed change of behaviour from long-term stability or progradation to a persistent recession trend occurred abruptly between two consecutive air photo dates. This happened after a long period during which gradually increasing rates of sand loss into a permanent sand sink (due to increased erosion driven by sea-level rise) are inferred to have been masked and compensated for by continuing sand gains. In these cases, a large erosional storm or cluster of storms is inferred to have occurred when the overall sand budget was close to losing. The storm(s) are inferred to have rapidly and permanently removed a large enough mass of sand that the still-ongoing sand gains were no longer sufficient to allow full beach and dune recovery before the next erosive storms occurred, and so the beach switched to a new long-term recessional mode. The timing of such a switch or "tipping point" is inferred to depend on the relative rates of sand gains and increasing sand losses at each specific beach.

In contrast, examples of both soft rock and sandy shores in swell-sheltered tidal re-entrants that have changed their long-term shoreline behaviour in response to sea-level rise (and in some cases increased wind speeds) have done so in a less abrupt fashion. These lack gaining sediment supplies that may at first mask increasing sediment losses as happens on swell-exposed sandy shores. Consequently, the sites studied, including the South Barilla soft rock shore (Section 5.5) and the West Duck Bay S and SE sandy saltmarsh shores (Section 5.4), have increased their recession rates incrementally rather than abruptly[25]. As summarised in Section 6.4.1, wind wave fetch and exposure appear to be the critical condition determining how soon such swell-sheltered shores will show an increased rate of shoreline recession in response to climate change-induced drivers. However where such a response has emerged, the lack of masking sediment gains means that increasing rates of shoreline recession in response to increasing drivers such as sea-level rise are likely to occur in a roughly synchronous fashion, albeit subject to some lags related to variability in the drivers and in the frequency of sufficiently erosive wind-wave storms to actually erode the shores.

[25] See shoreline history plots in Sections 5.4 and 5.5. Although the use of piecewise linear fits to these plots may create the impression of abrupt changes, inspection of consecutive data points generally suggests more gradual rate increases, with significant differences being discernible between the longer time periods represented by the linear fits, but not so much on short-term time scales.

7.4.2 Climate change – induced drivers of physical coastal change not limited to sea-level rise

Many discussions of the impacts of climate change on coastal geomorphology are focussed on the effects of sea-level rise[26]. However, consideration of possible alternative explanations for observed coastal changes during this project has highlighted that physical coastal changes driven by global climate change will not necessarily be limited to the effects of sea-level rise.

Changing swell wave directions have been observed over recent decades in some regions such the Southern Ocean (Hemer, Church & Hunter 2010; Marshall 2003). Hemer (2009) has identified the potential for long-term shifts in swell-wave directions and directional variability as a result of climate change to result in substantial geomorphic changes on sandy coasts, resulting in new patterns of erosion, littoral drift and deposition causing changing spatial patterns of coastal recession and progradation. Given the wave direction changes over the Southern Ocean to date, it is possible that this could be or will eventually be a climate change-induced driver of long-term changes to beach behaviour on Tasmanian coasts. No examples of observed long-term shoreline behaviour changes for which swell wave direction change is a probable contributing cause have been identified in this project. However, this is a potentially fruitful direction for further investigation on some Tasmanian coasts.

Increasing wind speeds recorded on the south-west Tasmanian coast over recent decades have been attributed to climate change processes by Kirkpatrick et al. (2017), and were previously identified as probably contributing to shoreline change in north-west Tasmania by the author and colleagues as reported in Prahalad et al. (2015). The present study has collected additional evidence of increasing westerly wind speeds over Tasmania during recent decades (see Section 5.2.2) and has identified these as likely contributing to shoreline behaviour changes in addition to (but not instead of) sea-level rise. The inferred mechanism proposed in this project by which increasing onshore winds would cause changing shoreline behaviour (Section 5.2.4) is wind forcing higher local wind waves and driving increased wave set-up on the coast, with both effects resulting in more frequent wave attack higher on the shore profile and reaching further to landwards over deepened water than previously.

Hence, the evidence provided by this project indicates that sea-level rise is the principal climate change-induced driver of long-term shoreline behaviour on the coastal sites examined, however increasing onshore wind speed is a likely additional climate change-related contributing driver on some but not all shores. Long-term wave direction changes are also a potential additional contributing driver on Tasmanian coasts (depending on coastal orientation and the degree of wave direction change) but have not yet been demonstrated to be a contributing factor at any specific Tasmanian coastal site.

7.5 *Implications for coastal erosion hazard assessments*

There has been a growing awareness over recent decades that climate change and in particular sea-level rise will have considerable impacts on coastal areas, as a result of increased coastal flooding, erosion, and groundwater changes. A variety of methods have been developed to assess the likely scale, timing, and spatial variability of these impacts. In the case of shoreline erosion and recession, available methods range from simple deterministic Bruun Rule-based calculations which in many cases ignore critical geomorphic processes such as sediment budgets (see Section 2.2 discussion), to sophisticated coastal morpho-dynamic behaviour models using stochastic (probabilistic) methods to allow for the uncertainties in many of the relevant model parameters (e.g., the Shoreface Translation Model of Cowell et al. 2006).

[26] Chemical and thermal changes to coastal waters resulting from climate change may also impact on biophysical coastal and marine systems, however these are beyond the scope of this discussion.

However, methods of assessing likely shoreline responses to sea-level rise are in part constrained by the extent to which emerging physical coastal changes in response to sea-level rise or other climate change-induced processes have been shown or reasonably inferred to be related to specific geomorphic conditions and processes at particular sites. As noted in the review Section 2.4, there are few claims in the scientific literature that shoreline changes in response to contemporary (recent-onset) climate change-driven global sea-level rise are actually occurring at specific sites (as opposed to longer-term ongoing responses to relative sea-level changes attributable to VLM or other causes). This implies that coastal behaviour models used to predict the geomorphic effects of sea-level rise on soft shores have not been tested or trained on shorelines with a known recent history of physical response to contemporary global climate change-induced drivers of coastal change including sea-level rise.

It has been inferred from the evidence compiled by this thesis that such a response is observable at eight Tasmanian shoreline sites (out of 35 examined). In these cases, what is inferred to be a relatively early recessional response to climate change-induced coastal behaviour drivers such as sea-level rise is attributed to the presence of suitable enabling site conditions as described Section 6.4.1 (most critically the type of sediment budget and transport, and in some cases the degree of wind-wave exposure and fetch). Conversely, the majority of soft erodible coastal sites examined in this project are potentially susceptible to receding in response to sea-level rise but are not yet exhibiting any evidence of doing so. This thesis has shown that these sites are either lacking in one or more of the critical enabling conditions, or else simply have a sufficiently gaining sediment budget as to be still fully counter acting the recessional effects of sea-level rise (see Section 6.4.2). In other words, this thesis has identified several coastal geomorphic conditions inferred to either enable or retard an early physical response to contemporary global climate change-induced drivers of coastal change including sea-level rise.

It is anticipated that the insights and data that these findings provide will enable improved capacity to calibrate and train coastal behaviour models to identify shores of greater or lesser resilience or susceptibility to changing coastal behaviour drivers including sea-level rise. This outcome highlights the importance of site specific coastal geomorphic studies as indispensable input to informing and calibrating broader understanding and models of coastal geomorphic behaviour.

7.6 *Limitations and biases of the study*

Two main limitations or biases inherent in the methods adopted for this thesis have been identified. The consequences of these are considered in the following two subsections.

7.6.1 Restricted geographical scope of project

The sites examined for this thesis are geographically restricted to a single southern hemisphere mid-latitude island, namely Tasmania. Given the limited resources available to this project for purposes such as travel[27], this restriction was primarily dictated by the need to be able to visit and examine the geomorphic characteristics of each study site in the field. An advantage of this restriction was the practicality of also being able to obtain the majority of the required air photos from a single source, namely the Tasmanian Department of Primary Industries, Parks, Water and Environment (DPIPWE), which is the custodian of most historic Tasmanian air photos. The restriction of sites to Tasmania has permitted this project to focus on analysing the influence of a constrained range of geomorphic, oceanographic and meteorological conditions in greater depth than would have been feasible if sites were located over a broader geographical context with a wider range of conditions.

[27] Notwithstanding extensive use of helicopter transport to visit the remote south-west coast beaches repeatedly over three summer seasons! This was in-kind support provided by DPIPWE since the authors investigations also contributed to a separate DPIPWE project (see acknowledgements).

An additional advantage of geographically restricting sites to Tasmanian coasts is that these are less subject than many other coasts to a number of "noise" processes that have the potential to confound the detection of shoreline responses to sea level rise by preventing, counter-acting or masking them. Compared to many coasts elsewhere in Australia and other parts of the world, Tasmanian coasts are subject to small or negligible vertical land movement, a limited and mostly micro-tidal range, minimal ENSO-related interannual sea-level variability and minimal swell direction variability on western and southern Tasmania coasts. Sections 2.5 and 3.2.2 provide discussion of how these processes may confound identification of shoreline responses to contemporary climate change - induced drivers of coastal change such as sea-level rise. These "noise" limitations are a positive bias which improve the likelihood that any responses to sea-level that may be occurring on Tasmanian coasts will be more easily detectable.

Within the context of Tasmania, the study sites selected are not evenly distributed geographically, but are mostly limited to Tasmania's western, southern, and south-eastern coasts, with only one east coast site and no swell-exposed north coast (Bass Strait) locations. However, the focus in this project was on obtaining a usefully representative selection of soft coastal types rather than an even geographical spread (see Chapter 4). A result is that a number of potentially informative Tasmanian coastal types have not been included in this study, such as long swell-exposed drift-aligned east coast beaches. However, the results that have been obtained from the range of sites selected (see Section 6.4) show that the representation of Tasmanian soft coastal types that were studied has been useful, albeit a variety of other distinctive Tasmanian soft shoreline types remain to be similarly investigated in future.

7.6.2 Use of vegetation line as shoreline proxy

Boak and Turner (2005) identified at least 16 types of shoreline features that could be mapped as proxies for the shoreline position. This project has used one of these, the seawards *in situ* vegetation line, for two main reasons. As discussed in Section 3.3.2, these are:

1. The vegetation line is generally a reliable indication of shoreline recession or progradation because under most circumstances it moves seawards in response to coastal accretion and progradation and landwards in response to erosion and recession. Hence, changes in the position of the vegetation line over time provide the type of shoreline behaviour history information this thesis has required, namely information on long-term shoreline trends of recession, stability or progradation.
2. The vegetation line is generally a high-contrast feature which can be readily mapped even on photos of relatively poor resolution and contrast, which is often the case for older air photos. Hence using this proxy allows the usable air photo time series to be extended to the earliest dates possible. Moreover it is notable that whereas Boak and Turner (2005) only discuss the vegetation line in relation to sandy beaches and dunes, photogrammetric work for this project found it to be generally identifiable on soft rock shores as well.

The main limitation of using the vegetation line as a proxy for shoreline position change is that although it moves landwards in an effectively instantaneous manner during erosion events, there is generally a time lag before new vegetation establishes sufficiently to be visible on prograding shores (Boak & Turner 2005; Hanslow 2007). In addition, vegetation line position may be affected by other processes unrelated to sea-levels and wave erosion, including dune deflation and artificial disturbances (Hanslow 2007).

In regard to lag times in vegetation recovery and seawards growth, these are typically of the order of several months to several years. Given that the time gaps between air photos used in this study are commonly of a similar scale, and in addition that this study has been focussed on identifying long-

term trends (10 years +) rather than analysing short-term variability in beach behaviour (Section 7.3.1), the issue of vegetation growth lag times is unlikely to have significantly affected the main results obtained by this study (Section 6.4).

Use of the vegetation line as a shoreline position proxy is subject to uncertainties such as operator error in digitising the position of the line. This particular uncertainty was minimised by a single operator (Chris Sharples) digitising most shorelines used for this project. Beyond this, the use of a photogrammetric error margin described in methods chapter section 3.3.2 arguably captures the most important spatial uncertainty for the analyses undertaken, albeit more sophisticated uncertainty analyses can be applied (e.g., see Fletcher et al. 2011, p. 18).

The issue of vegetation line changes unrelated to wave action and drivers such as sea-level rise (which are the shoreline change drivers of interest in this project) has mostly been dealt with by not using sites subject to such influences. However, in one case - Stephens Bay Beach South (see Section 6.3.2) - long phases of shoreline stability and then a switch to progradation have been interpreted from indicators other that the main *in situ* vegetation line, which was displaced far inland by aeolian deflation and transgressive dune processes. In this case, the indicators of stability followed by progradation were the persistence of *in situ* dead trees on dunes and progressive incipient foredune growth.

Chapter 8: Conclusions & Recommendations

8.1 *Introduction*

This concluding chapter summarises the key findings and identifies the outcomes of this thesis with respect to the knowledge gap identified and the research questions posed in the introduction chapter of this thesis (Sections 1.2 & 1.3). These conclusions are followed by recommendations for ongoing research based on and responding to the findings of this thesis.

8.2 *Contributions to Knowledge*

8.2.1 Knowledge gap

The key knowledge gap which this thesis has sought to address was summarised in the introduction (Section 1.2) as: "*the extent of the impact to date of contemporary climate change-driven sea-level rise on coastal landforms is presently poorly understood*".

The data and inferences described in this thesis support a finding that significant long-term (multi-decadal) shoreline behaviour changes have been detected on some (but not a majority of) soft erodible shorelines in a coastal region (Tasmania) where contemporary climate change-induced sea-level rise is the dominant component of local relative sea level rise. In most of the cases identified, sea-level rise (with or without a contribution from increasing onshore wind speeds) is the most plausible or only available explanation of the observed changes.

These findings contribute to closing the knowledge gap, by significantly improving understanding of the impact to date of contemporary climate change-driven sea-level rise on coastal landforms in Tasmania.

8.2.2 Research questions

The outcomes for the two research questions posed in Chapter 1 are described below.

RQ1: How can we test for a sea-level rise fingerprint on erodible shorelines?

What evidence may enable contemporary climate change-driven sea-level rise to be identified as a dominant factor driving changes in coastal landform behaviour?

This thesis took as a starting point the proposition that certain types of changes in shoreline behaviour would be an indication that a shoreline might be responding to recent-onset or increasing sea-level rise (albeit in some cases it might turn out that other drivers were causing the change). This project has therefore sought to identify shores which have exhibited long-term shoreline behaviour change over the air photo record period. Such shores have then been tested to either confirm or discount such changes as being a response to sea-level rise.

The method of testing used in this project was an essentially qualitative one, albeit using quantitative data (from air photo time series) to first establish the long-term shoreline behaviour types, trends, and changes if any for each study site. The testing then used field and air photo observations along with previous published information about the landforms and geomorphic processes at each changing or changed study site to construct conceptual models of the geomorphic process systems governing shoreline behaviour at those sites (for examples see Figure 27 & Figure 35 in Sections 5.2.4 & 5.3.4 respectively). Consideration of such models allowed evaluation of which (if any) of a variety of alternative hypotheses to explain the changing shoreline behaviour are plausible given the site conditions. In each case a working hypothesis that sea-level rise is driving the change was evaluated

for its plausibility in the context of the geomorphic conditions at the site, as were all alternative hypotheses identified. Using this approach, 10 out of 35 shoreline sites examined were identified as exhibiting long-term or likely emerging long-term change over the air photo period; of these 8 were identified as most likely changing in response to sea-level rise (and possibly also increasing wind speeds in some cases), whereas 2 were identified as changing in response to other causes unrelated to climate change (see Section 6.4.1)[28].

Most available geomorphic information for Tasmanian coastal sites is of a qualitative nature, with such parameters as detailed bathymetry and accurate quantitative wave, wind and tidal data only being available for limited areas. Partly for this reason numerical models were not used to investigate morpho-dynamic processes in this project. However the more important reason for this is that consideration of conceptual models of shoreline behaviour was found in practice to be a sufficiently powerful method as to confidently eliminate implausible explanations for changing shoreline behaviour, leaving only one or a few possible explanations which might require more investigation to test further (see examples detailed in Chapter 5).

The conclusion drawn from this thesis is that the method adopted to distinguish between sea-level rise and other causes of long-term shoreline behaviour changes is a successful approach. Other more quantitative approaches to addressing this research question using numerical coastal behaviour modelling are also likely to yield fruitful results, however these methods were not pursued in this project.

RQ2: Are some erodible shores more susceptible to sea-level rise responses than others?

Are there some distinctive "early responder" shoreline types or coastal process environments which are responding to contemporary climate change-driven sea-level rise earlier than other "late responder" types?

The results of this project support a division of soft shores into differing types that will show physical shoreline behaviour changes earlier or later in response to contemporary climate change-induced sea-level rise. This division will depend on the local geomorphic conditions at each site (see Section 5.6.3).

The 35 distinct coastal study sites selected for this thesis are of types that are all expected (based on the scientific literature reviewed in Chapter 2) to eventually respond to sea-level rise with increased erosion and shoreline recession. However, whilst the results of this study support the interpretation that 8 of these sites do already show an established or emerging long-term shoreline behaviour change most likely attributable to contemporary (recent-onset) sea-level rise (and to increasing onshore winds in some cases), most of the sites studied have shown no long-term change as yet, or in two cases have changed for unrelated reasons.

Consideration of the geomorphic processes at the study sites which either have or have not changed their behaviour to date allows relatively simple explanations for these differences to be identified, which most consistently relate to sediment budgets and the balance between gained and lost sediment (as summarised in Section 6.4). In each case examined where a change of behaviour has not yet occurred it is reasonable to expect that continuing sea-level rise will result in progressively more frequent erosion events at increasingly higher levels on the shore profile, which at some future time will result in long-term shoreline recession commencing or significantly increasing. This will be true even for soft shores inferred to be relatively resilient "late responders" to sea-level rise, for example many open coast beaches with relatively large sand gains, or sheltered tidal re-entrant shores with only short wind-wave fetches (see Section 6.4.2). When sea-level reaches some sufficient height

[28] Note that the high proportion of changed sites whose changes were attributed to a response to sea-level rise is unsurprising given the fact that some of these were selected for study because of the authors previous preliminary observations suggesting this may be the case.

above present levels, it is expected that it will allow sufficiently frequent energetic wave attack so high on the shore profile that it will eventually overwhelm other processes tending to prevent recession, and will become the dominant driver of shoreline behaviour. In the meantime, however, only particularly susceptible sites such as those discussed in Section 6.4.1 are exhibiting early long-term changes, which justifies describing them as "Early Responders".

Hence, the findings of this project support a distinction between shorelines that are more susceptible to sea-level rise and will respond earlier to it than others, and some other shores which are more resilient to sea-level rise and will be intermediate or late responders to it. The key findings of this project in this respect are summarised in the following Section (8.2.3), and are discussed in more detail in Sections 5.6, 6.4 and 7.4.1. Given the implications that these differing response times have for coastal ecologies and for human use of coastal areas, there is clearly value in improved understanding of which shores are at earlier or later risk of beginning to recede in response to sea-level rise.

8.2.3 Key research findings

The most important findings and conclusions from the research undertaken on a selection of 35 soft erodible Tasmanian shorelines as described in this thesis are summarised below. These findings primarily relate to the two research questions discussed in the previous sub-section. However, they also include several other useful findings which are related to but not directly answering the research questions.

- Changes in long-term shoreline behaviour trends on eight of the 35 studied shorelines have been inferred to be driven by contemporary (since the 1800s) climate change-induced drivers including sea-level rise. These changes have been from either stability or progradation to recession (on swell-exposed sandy beaches), or from prior recession to a significantly increased rate of recession (on swell-sheltered sandy and soft-rock shores in tidal re-entrants). See Sections 6.2 & 6.4.1.
- Climate change – induced processes identified as the probable drivers of long-term shoreline behaviour change in the eight such cases identified by this study have included sea-level rise in all cases (allowing higher erosional wave attack reaching further to landwards than previously), and probably onshore wind speed increases in a few cases (generating larger locally-generated erosive wind-waves). Long-term swell wave direction changes were also identified as an additional possible driver of coastal change, however no cases where this was inferred to probably be a driver were found amongst the study sites examined. See Sections 5.6.2 & 6.4.1.
- In all eight cases where a long-term shoreline behaviour change during the last 70 years has been inferred to be a response to contemporary climate change-induced sea-level rise or increasing onshore wind speeds, a critical condition enabling the change to occur has been the presence of an active sediment sink and a persistent (mostly uni-directional) sediment transport process delivering increasing amounts of sediment eroded from the shoreline to the sink, and thus permanently removing sediment from the eroded shore. See Sections 5.6.3 & 6.4.1.
- Where a study site shoreline has been gaining sand as well as losing it, the changing balance between the amount of sand gained and the increasing amount of sand lost through increasing erosion driven by climate change-induced drivers is a key factor determining when the shore will change its long-term behaviour in response to sea-level rise. In some cases where sandy shorelines with an active sand sink have not yet changed their long-term behaviour in response to sea-level rise (e.g. Roches Beach N, Adventure Bay S), it is inferred that this is

because the gaining sand supply to the site is still large enough to compensate for the increasing amounts of sand lost from the site due to increased erosion related to sea-level rise. See Section 5.6.3 & 6.4.2.

- For soft swell-sheltered shorelines within tidal re-entrants, relatively early shoreline behaviour changes in response to climate change-induced drivers have been identified on shorelines having the longest fetches and highest exposure to dominant wind-wave directions (South Barilla and West Duck Bay S & SE). These locations are inferred to show the earliest responses because they are most frequently subject to wind waves of large enough magnitude to cause shoreline erosion. See Sections 5.6.3 & 6.4.1.
- Where swell-exposed sandy beaches have been identified as having undergone a change of long-term behaviour from long-term progradation or stability to long-term recession in response to sea-level rise, in most cases the change has occurred in an abrupt "tipping point" style. This is inferred to be due to gradually increasing loss of eroded sand having eventually reached a point at which the sediment budget has switched from gaining or balanced to losing. This style of change is most clearly seen in the air photo records for Ocean Beach, Roches Beach Main Central and Prion Beach, where an abrupt change has evidently been triggered by large erosion events that are inferred to have removed a large mass of sand at a time when the sediment budget was already close to switching to net loss. See Section 7.4.1.
- Where swell-sheltered sandy or soft rock shores in tidal re-entrants have been identified as having undergone a change of long-term behaviour in response to sea-level rise (South Barilla and West Duck Bay S & SE), the change has occurred in an incremental (but eventually significant) fashion as a previously slower net recession rate has increased in response to sea-level rise (and in some cases probably also to increased wind speeds). See Section 7.4.1.

8.3 *Recommendations*

During the course of this thesis, a number of potentially fruitful directions for further research into the ways in which susceptible shorelines may respond to contemporary climate change-induced processes including sea-level rise have emerged. These are listed and briefly discussed below.

8.3.1 Identification of shores approaching a long-term change of behaviour

This thesis has focussed on using historical data to identify shores which have already undergone a long-term change of behaviour in response to sea-level rise. However, the investigations undertaken have also suggested a number of possible indicators of sandy shorelines beginning to respond to higher sea-levels, but without yet having settled into a changed mode of long-term behaviour.

An example of this is beaches exhibiting larger storm bites (erosion events) than seen previously, but still subsequently showing full beach and foredune recovery to a prior long-term stable profile. Such behaviour is suggestive of storm waves beginning to erode higher and further landwards on the shore profile due to higher sea levels, but coupled with a sufficiently positive (gaining) sand budget as to still allow full recovery before the next (likely increasingly frequent) similar erosion event. This presents an indication of sea-level rise becoming a noticeable factor in beach behaviour, but without a long-term change in shoreline behaviour having yet occurred. The shoreline behaviour of Hope Beach is a good example of this which can be inferred from the historic air photo record obtained during this project (see Section 6.3.3, Figure 58 and Appendix A1.4.3).

Another likely indicator of increasingly frequent recent erosion at higher levels or further landwards than previously may be the exposure in foredune wave erosion scarps of parts of fragile features which cannot have previously been exposed to erosion, such as dune palaeosols, back-dune swamp

peats and middens. Given that such features are soft, easily-eroded and typically hundreds or thousands of years old, their exposure in foredune erosion scarps implies that the erosion event which exposed them is the largest such event since the features formed, otherwise the parts of them now exposed would have previously been destroyed by earlier erosion events. If foredune recovery to a prior long-term stable profile subsequently occurs, the temporary exposure of these features may also be suggestive of higher sea-levels allowing larger erosion events, but still without passing a tipping point at which the beach changes its long-term behaviour. The peat horizons exposed in the shoreline recession scarp at Ocean Beach are an example of this type of feature, although that beach has already changed its long-term behaviour (see Section 5.2, Figure 21 & Figure 25). However, similar palaeosols exposed in bare seawards dune faces at other south-west coast beaches such as at Mulcahy Bay and Wreck Bay provide examples of palaeosol exposure at sites not known to have yet changed their long-term behaviour.

Examples such as the above are suggestive of sites experiencing larger erosion events than previously in response to sea-level rise, but still having the capacity to fully recover to a former profile because of a sufficiently positive sand budget. Depending on the sand budget, some such sites may be approaching a "tipping point" at which shoreline recovery following a large erosion event may become inadequate to prevent a long-term change to a recession trend. This sort of tipping point change is seen in the historic record of shoreline change at Roches Beach. There, the change to a recession trend was characterised by continued erosion and recovery cycles, however the recovery phases were no longer sufficiently large or rapid enough to return the beach to its previous long-term stable profile before the next erosion event, as had occurred prior to the tipping point (see Section 5.3, Figure 33).

Further research into early indicators of shoreline behaviour change such as those noted above could lead to improved ability to predict the onset of shoreline recession at previously stable beaches.

8.3.2 Integration of beach history data with numerical modelling of shoreline behaviour

The discussion and conclusions (above) have alluded to the potential to improve numerical models of coastal behaviour[29] by applying improved data quantifying local geomorphic and oceanographic conditions at specific sites, and training them with quantitative data on observed historical shoreline behaviour and shoreline behaviour changes obtained from air photo time series. Given the importance of sediment budgets in determining the time and nature of shoreline responses to sea-level rise (Section 6.4), the development of improved capacity to characterise and quantify these at specific sites would be a particularly important element of improved numerical models.

If numerical models of shoreline behaviour can be improved by training them with data from specific shores that have either shown a change of long-term behaviour in response to sea-level rise, or that can be shown to have not done so yet, then this may also improve the capacity of numerical models to project future shoreline changes at other sites, especially those lacking good historical data.

8.3.3 Further analysis of wind speed records for Tasmania

One high-quality wind record for western Tasmania (Cape Grim) shows steadily increasing average and extreme wind speeds since at least 1995 (see Section 5.2.2). Increasing wind speeds can also be inferred from several other west coast wind records including Cape Sorell, Strahan Aerodrome (Appendix A1.3.8) and Maatsuyker Island (Kirkpatrick et al. 2017). However, these records include large data gaps, step changes suggestive of instrumentation issues, and changing recording protocols,

[29] This refers mainly to integrated models of shoreline behaviour incorporating multiple processes, such as the Shoreface Translation Model (Cowell et al. 2006), rather than models of component processes such as storm bite.

all of which result in less confidence in the data. Similarly in south-eastern Tasmania the Hobart Airport wind record ostensibly shows an increase in wind speeds over recent decades, however the increase is mainly in step changes (Appendix A1.5.1, Figure 224), which makes the attribution of changes to meteorological and climatological processes problematic.

Primarily on the basis of the high-quality Cape Grim record, which is exposed to the same SAM-driven wind climate as the whole west and southwest coast of Tasmania (see Section 2.5.6 & 5.2.2), there is a sound basis for inferring that shoreline behaviour at west and north-west coastal sites such as Ocean Beach and West Duck Bay have been influenced by changing wind climates as well as by sea-level rise (see Sections 5.2 & 5.4).

However, it remains unclear whether other areas of the Tasmania coast including the south-east are subject to increasing wind speeds. The ability to infer a greater or lesser contribution of long-term wind speed changes to shoreline behaviour changes in these coastal regions would improve confidence in assessing their risk of shoreline recession.

Hence it is recommended that more detailed analysis of Tasmanian wind records be undertaken, ideally alongside modelling and hind-casting, to improve the understanding of temporal and spatial variability in mean and extreme wind speeds and directions across Tasmania and its coastal areas.

8.3.4 Implications of changing swell directions for shoreline behaviour on Tasmanian coasts

Several discussions in this thesis have noted that long-term changes in swell wave direction variability related to global climate change have been observed in recent decades over both the Southern Ocean and the Tasman Sea (see section 2.5.5, including Goodwin, Mortlock & Browning 2016; Hemer, Church & Hunter 2010; Mortlock & Goodwin 2015b). These long-term changes have the potential to change previous littoral sand drift processes, resulting in new spatial patterns of shoreline accretion and erosion (Goodwin, Mortlock & Browning 2016; Hemer 2009; Hemer et al. 2008). This study has noted the consequent possibility that long-term wave direction changes may be a driver of long-term shoreline behaviour change on some Tasmanian coasts (e.g., Ocean Beach: see Section 5.2.4), in addition to sea-level rise and increasing onshore wind speeds.

However, this study has not identified any Tasmanian coastal study sites where wave direction change can be robustly identified as a driver of observed shoreline behaviour changes. This is partly a result of a lack of long-term observational data on wave directions in Tasmanian waters, and partly on a lack of capacity in this study to model the effects of changing wave directions on shoreline behaviour. The latter is in turn partly due to a lack of necessary base data in many areas, such as sufficiently high-resolution bathymetry. In contrast, as noted in Section 2.5.5, studies on the (more data-rich) NSW and Queensland coasts of eastern Australia have been able to identify changes in littoral and onshore sand transport patterns resulting from swell direction variability changes (Goodwin, Mortlock & Browning 2016; Mortlock & Goodwin 2015a, 2015b).

It is therefore recommended that future studies of Tasmanian coastal change in response to climate change processes should include:

- Collection of robust data on wave directions around Tasmania, including historical data if possible.
  and:
- Wave modelling (including acquisition of bathymetric data as necessary) to evaluate the effects of changing swell direction on soft Tasmanian coasts.

8.3.5 Investigation of long-term morpho-dynamics of very high energy beaches

Although the distinctive very high energy beaches of the south-west Tasmanian coast are remote from roads and generally difficult to access, they were considered priority study sites for this project due to their persistently eroding appearance (see Sections 2.5 & 3.2.1). Six of these beaches were included in this study through collaboration with a DPIPWE beach condition monitoring program using Tasmanian Wilderness World Heritage Area funding. This enabled the writer to visit these beaches repeatedly (using helicopter transport) over three summer seasons during the course of this PhD project. Prior to these visits there had been only one campaign of scientific examination of these beaches, which was documented by Cullen (1998) and Pemberton and Cullen (1999). The study documented in this thesis added considerable historic air photo data on these beaches which was not previously available. This has yielded new insights into the behaviour of these beaches over the last ~70 years.

The discussion chapter (Section 7.3) notes that despite a prevalence of bare deflating frontal dunes, the historical shoreline behaviour data shows that most south-west study site beaches are still gaining sand from offshore and have not as yet responded to sea-level rise with a change to recessional behaviour as could be inferred from their appearance (exceptions to this are Window Pane Beach East, and Ocean Beach further north). The south-west beaches are exposed to the most high-energy swell and wind climates of any Australian beaches and are amongst the highest-energy sandy coasts anywhere (Davies 1973; Hemer, Simmonds & Keay 2008). The behaviour of these beaches may simply be characteristic of very high energy beaches *per se*, rather than of beaches responding to sea-level rise or other climate change processes.

Quite apart from any significance these beaches may have from a climate change perspective, further studies of these beaches may yield useful new insights into a class of very high-energy beach morpho-dynamics which has been little examined to date.

Bibliography

Aagaard, T & Sorensen, P 2013, 'Sea level rise and the sediment budget of an eroding barrier on the Danish North Sea coast', *Journal of Coastal Research*, no. Special Issue 65, pp. 434-439.

Albert, S, Leon, JX, Grinham, AR, Church, JA, Gibbes, BR & Woodroffe, CD 2016, 'Interactions between sea-level rise and wave exposure on reef island dynamics in the Solomon Islands', *Environmental Research Letters*, vol. 11, no. 5, p. 054011.

Alexander, A 2003, *The Eastern Shore: A History of Clarence*, Clarence City Council, Rosny, Tasmania.

Argus, DF, Peltier, WR, Drummond, R & Moore, AW 2014, 'The Antarctica component of postglacial rebound model ICE-6G_C (VM5a) based on GPS positioning, exposure age dating of ice thicknesses, and relative sea level histories', *Geophysical Journal International*, vol. 198, no. 1, pp. 537-563.

Atkinson, AL, Baldock, TE, Birrien, F, Callaghan, DP, Nielsen, P, Beuzen, T, Turner, IL, Blenkinsopp, CE & Ranasinghe, R 2018, 'Laboratory investigation of the Bruun Rule and beach response to sea level rise', *Coastal Engineering*, vol. 136, pp. 183-202.

Banks, MR, Colhoun, EA & Chick, NK 1977, 'A Reconnaissance of the Geomorphology of Central Western Tasmania', in MR Banks & J Kirkpatrick (eds), *Landscape and Man*, Royal Society of Tasmania, Tasmania, pp. 28-54.

Barnard, PL, Short, AD, Harley, MD, Splinter, KD, Vitousek, S, Turner, IL, Allan, J, Banno, M, Bryan, KR, Doria, A, Hansen, JE, Kato, S, Kuriyama, Y, Randall-Goodwin, E, Ruggiero, P, Walker, IJ & Heathfield, DK 2015, 'Coastal vulnerability across the Pacific dominated by El Niño/Southern Oscillation', *Nature Geoscience*, vol. 8, no. 10, pp. 801-807.

Baynes, FJ 1990, *A Preliminary Survey of the Coastal Geomorphology of the World Heritage Area, South West Tasmania*, Department of Lands, Parks and Wildlife, Tasmania.

Boak, EH & Turner, IL 2005, 'Shoreline Definition and Detection: A Review', *Journal of Coastal Research*, vol. 21, no. 4, pp. 688-703.

BOM 2019, *Monthly Data Reports - Australian Baseline Sea Level Monitoring Project* Bureau of Meteorology, viewed 05/09/2019, <http://www.bom.gov.au/oceanography/projects/abslmp/reports.shtml >.

Booij, N, Ris, RC & Holthuijsen, LH 1999, 'A third-generation wave model for coastal regions; Part I, Model Description and Validation', *Journal of Geophysical Research*, vol. C4, no. 104, pp. 7649-7666.

Bronk Ramsey, C 2009, 'Bayesian analysis of radiocarbon dates', *Radiocarbon*, vol. 51, pp. 337-360.

Bronk Ramsey, C & Lee, S 2013, 'Recent and planned developmentsof the program OxCal.', *Radiocarbon*, vol. 55, pp. 720-730.

Brunel, C & Sabatier, F 2007, 'Pocket Beach Vulnerability to Sea-Level Rise', *Journal of Coastal Research*, vol. Special Issue 50, no. SI 50 (Proceedings of the 9th International Coastal Symposium), pp. 604-609.

—— 2009, 'Potential influence of sea-level rise in controlling shoreline position on the French Mediterranean Coast', *Geomorphology*, vol. 107, no. 1-2, pp. 47-57.

Bruun, P 1962, 'Sea-Level Rise as a Cause of Shore Erosion', *Journal of the Waterways and Harbors Division, Proceedings of the American Society of Civil Engineers*, vol. 88, pp. 117-130.

—— 1988, 'The Bruun Rule of Erosion by Sea-Level Rise: A Discussion of Large-Scale Two- and Three-Dimensional Usages', *Journal of Coastal Research*, vol. 4, pp. 627-648.

Burgette, RJ, Watson, C, Church, JA, White, NJ, Tregoning, P & Coleman, R 2013, 'Characterizing and minimizing the effects of noise in tide gauge time series: relative and geocentric sea level rise around Australia', *Geophysical Journal International*, vol. 194, no. 2, pp. 719-736.

Byrne, G 2006, *Roches Beach Lauderdale - Coastal Erosion Study*, Vantree Pty Ltd.

Carley, JT, Blacka, MJ, Timms, WA, Anderson, MS, Mariani, A, Rayner, DS, McArthur, J & Cox, RJ 2008, *Coastal Processes, Coastal Hazards, Climate Change and Adaptive Responses for Preparation of a Coastal Management Strategy for Clarence City, Tasmania*, Water Research Laboratory, University of New South Wales.

Carvalho, BC, Dalbosco, ALP & Guerra, JV 2020, 'Shoreline position change and the relationship to annual and interannual meteo-oceanographic conditions in Southeastern Brazil', *Estuarine, Coastal and Shelf Science*, vol. 235.

Chen, X, Zhang, X, Church, JA, Watson, C, King, MA, Monselesan, D, Legresy, B & Harig, C 2017, 'The increasing rate of global mean sea-level rise during 1993–2014', *Nature Climate Change*, vol. 7, no. 7, pp. 492-495.

Church, JA & White, NJ 2006, 'A 20th Century Acceleration in global sea-level rise', *Geophysical Research Letters*, vol. 33, p. 4.

Church, JA & White, NJ 2011, 'Sea-Level rise from the Late 19th to the Early 21st Century', *Surveys in Geophysics*, vol. 32, no. 4-5, pp. 585-602.

Colhoun, EA, Hannan, D & Kiernan, K 1996, 'Late Wisconsin Glaciation of Tasmania', *Papers and Proceedings of the Royal Society of Tasmania*, vol. 130, no. 2, pp. 33-45.

Cowell, PJ, Roy, PS & Jones, RA 1995, 'Simulation of large-scale coastal change iusing a morphological behaviour model', *Marine Geology*, vol. 126, no. 1, pp. 45-61.

Cowell, PJ, Roy, PS & Thom, B 1995, 'Effect of Barrier Size and Offshore Slope on Rates of Coastal Change Due to Sea Level Rise and Littoral Sand Loss', paper presented to Late Quaternary Coastal Records of Rapid Change: Application to Present and Future Conditions. 11th Annual Meeting, Antofagasta, Chile, 19-28 Nov. 1995.

Cowell, PJ, Roy, PS, Zeng, TK & Thom, B 1995, 'Practical Relationships for Predicting Coastal Geomorphic Impacts of Climate Change', in *Ocean and Atmosphere Pacific International Conferences*, Adelaide, pp. 1-5.

Cowell, PJ, Thom, B, Jones, RA, Everts, CH & Simanovic, D 2006, 'Management of uncertainty in predicting climate-change impacts on beaches', *Journal of Coastal Research*, vol. 22, no. 1, pp. 232-245.

Cromer, WC 2006, *Geotechnical Risk Assessment: Storm Surges causing Foredune Erosion and Flooding, Roches Beach, Lauderdale*, Clarence.

Cullen, P 1998, *Coastal Dune Systems of South-Western Tasmania: Their Morphology, Genesis, and Conservation*, Nature Conservation Report No. 98/1, Parks and Wildlife Service, Tasmania.

Cullen, P & Dell, M 2013, *Geomorphological evolution of the Prion Beach and New River Lagoon beach barrier system*, Nature Conservation Report Series 2013/03, Department of Primary Industries, Parks Water & Environment, Tasmania.

Davidson-Arnott, RGD 2005, 'Conceptual model of the effects of sea level rise on sandy coasts', *Journal of Coastal Research*, vol. 21, pp. 1166-1172.

Davies, JL 1958, 'Wave refraction and the evolution of shoreline curves', *Geographical studies*, vol. 5, pp. 1-14.

Davies, JL 1959, 'Sea level change and shoreline development in south-eastern Tasmania', *Papers and Proceedings of the Royal Society of Tasmania*, vol. 93, pp. 89-95.

—— 1961, 'Tasmanian Beach Ridge Systems in Relation to Sea Level Change', *Papers and Proceedings of the Royal Society of Tasmania*, vol. 95, pp. 35-40.

—— 1973, 'Sediment Movement on the Tasmanian Coast', in *1st Australian Conference on Coastal Engineering*, vol. Australia National Conference Publication No. 73/1, pp. 43-46.

Davies, JL 1974, 'The coastal sediment compartment', *Australian Geographical Studies*, vol. 12 pp. 139-151.

DCC 2009, *Climate Change Risks to Australia's Coast - A First Pass National Assessment*, Department of Climate Change, Canberra.

Dean, RG & Maurmeyer, EM 1983, 'Models of beach profile response', in PD Komar & JC Moore (eds), *CRC Handbook of Coastal Processes and Erosion*, Boca Raton, Florida, pp. 151-165.

Donaldson, P 2010, 'Facies Architecture and Radar Stratigraphy of the Seven Mile Beach Spit Complex, Tasmania', B.Sc. (Hons) thesis, University of Tasmania.

Donaldson, P, Sharples, C & Anders, RJ 2012, *The tidal characteristics and shallow-marine seagrass sedimentology of Robbins Passage and Boullanger Bay, far northwest Tasmania*, Blue Wren Group, School of Geography and Environmental Studies, University of Tasmania.

Durrant, T, Hemer, MA, Trenham, C & Greenslade, D 2013, *CAWCR Wave Hindcast 1979-2010 v.5*, CSIRO Data Collection; DOI: 10.4225/08/523168703DCC5, <http://doi.org/10.4225/08/523168703DCC5 >.

Eberhard, R & Sharples, C 2013, 'Appropriate terminology for karst-like phenomena: the problem with 'pseudokarst'', *International Journal of Speleology*, vol. 42, no. 2, pp. 109-113.

Eberhard, R, Sharples, C, Bowden, N & Comfort, M 2015, *Monitoring the Erosion Status of Oceanic Beaches in the Tasmanian Wilderness World Heritage Area: Establishment Report*, Nature Conservation Report Series 15/3, Department of Primary Industries, Parks Water & Environment, Tasmania, Hobart, Tasmania.

Emery, KO & Kuhn, GG 1982, 'Sea cliffs: their processes, profiles and classification', *Bulletin of the Geological Society of America*, no. 99, pp. 644-654.

Farmer, N & Forsyth, SM 1993, *Dover*, Geological Atlas 1:50,000 Series, Tasmania Department of Mines.

Featherstone, WE, Penna, NT, Filmer, MS & Williams, SDP 2015, 'Nonlinear subsidence at Fremantle, a long‐recording tide gauge in the Southern Hemisphere', *Journal of Geophysical Research: Oceans*, vol. 120, no. 10, pp. 7004-7014.

Fletcher, CH, Romine, BM, Genz, AS, Barbee, MM, Dyer, M, Anderson, TR, Lim, SC, Vitousek, S, Bochicchio, C & Richmond, BM 2011, *National Assessment of Shoreline Change: Historical Shoreline Change in the Hawaiian Islands*, U.S. Geological Survey, Reston, Virginia.

Fletcher, M-S, Benson, A, Bowman, DMJS, Gadd, PS, Heijnis, H, Mariani, M, Saunders, KM, Wolfe, BB & Zawadzki, A 2018, 'Centennial-scale trends in the Southern Annular Mode revealed by hemisphere-wide fire and hydroclimatic trends over the past 2400 years', *geology*, vol. 46, no. 4, pp. 363-366.

Forsyth, SM 2002, *Richmond, Sheet 5226*, Digital Geological Atlas 1:25,000 Scale Series, Mineral Resources Tasmania.

Forsyth, SM, Quilty, PG & Calver, CR 2014, 'Cenozoic Onshore Basins and Landscape Evolution', in KD Corbett, PG Quilty & CR Calver (eds), *Geological Evolution of Tasmania*, Geological Society of Australia, vol. Special Publication No. 24, pp. 437-450.

Foster, DN 1988, *Report on Coast Protection Study, Roches Beach, Lauderdale*, University of Sydney Pitt & Sherry Pty Ltd.

Gehrels, WR, Callard, SL, Moss, PT, Marshall, WA, Blaauw, M, Hunter, J, Milton, JA & Garnett, MH 2012, 'Nineteenth and twentieth century sea-level changes in Tasmania and New Zealand', *Earth and Planetary Science Letters*, vol. 315-316, pp. 94-102.

Gehrels, WR & Woodworth, PL 2013, 'When did modern rates of sea-level rise start?', *Global and Planetary Change*, vol. 100, pp. 263-277.

Gillett, NP, Kell, TD & Jones, PD 2006, 'Regional climate impacts of the Southern Annular Mode', *Geophysical Research Letters*, vol. 33, L23704.

Goodwin, ID 2005, 'A mid-shelf, mean wave direction climatology for southeastern Australia, and its relationship to the El Nino - Southern Oscillation since 1878 A.D.', *International Journal of Climatology*, vol. 25, pp. 1715-1729.

Goodwin, ID, Freeman, R & Blackmore, K 2013, 'An insight into headland sand bypassing and wave climate variability from shoreface bathymetric change at Byron Bay, New South Wales, Australia', *Marine Geology*, vol. 341, pp. 29-45.

Goodwin, ID, Mortlock, TR & Browning, S 2016, 'Tropical and extratropical-origin storm wave types and their influence on the East Australian longshore sand transport system under a changing climate', *Journal of Geophysical Research: Oceans*, vol. 121, no. 7, pp. 4833-4853.

Gratiot, N, Anthony, EJ, Gardel, A, Gaucherel, C, Proisy, C & Wells, JT 2008, 'Significant contribution of the 18.6 year tidal cycle to regional coastal changes', *Nature Geoscience*, vol. 1, no. 3, pp. 169-172.

Gregory, JM, Griffies, SM, Hughes, CW, Lowe, JA, Church, JA, Fukimori, I, Gomez, N, Kopp, RE, Landerer, F, Cozannet, GL, Ponte, RM, Stammer, D, Tamisiea, ME & van de Wal, RSW 2019, 'Concepts and Terminology for Sea Level: Mean, Variability and Change, Both Local and Global', *Surveys in Geophysics*.

Grose, MR, Barnes-Keoghan, I, Corney, SP, White, CJ, Holz, GK, Bennett, JB, Gaynor, SM & Bindoff, NL 2010, *Climate Futures for Tasmania Technical Report: General Climate Impacts*, Antarctic Climate and Ecosystems Co-operative Research Centre, Hobart.

Hamlington, BD, Leben, RR, Nerem, RS, Han, W & Kim, KY 2011, 'Reconstructing sea level using cyclostationary empirical orthogonal functions', *Journal of Geophysical Research-Oceans*, vol. 116.

Hands, EB 1983, 'The Great Lakes as a test model for profile response to sea level changes', in PD Komar (ed.), *Handbook of Coastal Processes and Erosion*, CRC Press, Boca Raton, Florida, pp. 176-189.

Hanslow, DJ 2007, 'Beach erosion trend measurement: A comparison of trend indicators', *Journal of Coastal Research*, vol. Proceedings of the 9th International Coastal Symposium, Gold Coast, Australia, no. Special Issue SI 50 pp. 588-593.

Harley, MD, Turner, IL, Short, AD & Ranasinghe, R 2011, 'A Re-evaluation of Coastal Embayment rotation in SE Australia: the dominance of cross-shore versus alongshore sediment transport processes', *Journal of Geophysical Research*, vol. 116, no. F4, p. 16.

Harris, PT & Heap, A 2014, 'Geomorphology and Holocene Sedimentology of the Tasmanian Continental Margin', in KD Corbett, PG Quilty & CR Calver (eds), *Geological Evolution of Tasmania*, Geological Society of Australia (Tasmania Division), pp. 530-539.

Harris, PT, Smith, R, Anderson, O, Coleman, R & Greenslade, D 2000, *GEOMAT - Modelling of Continental Shelf Sediment Mobility in Support of Australia's Regional Marine Planning Process*, AGSO Record 2000/41, Australian Geological Survey Organisation.

Hawkins, E & Sutton, R 2012, 'Time of emergence of climate signals', *Geophysical Research Letters*, vol. 39, no. L01702, p. 6.

Hayes, M & Kirkpatrick, JB 2012, 'Influence of Ammophila arenaria on half a century of vegetation change in eastern Tasmanian sand dune systems', *Australian Journal of Botany*, vol. 60, no. 5, p. 450.

Hemer, MA 2009, 'Identifying coasts susceptible to wave climate change', *Journal of Coastal Research*, no. Special Issue 56, pp. 228-232.

—— 2010, 'Historical trends in Southern Ocean storminess: Long-term variability of extreme wave heights at Cape Sorell, Tasmania', *Geophysical Research Letters*, vol. 37, no. L18601, p. 5.

Hemer, MA, Church, JA & Hunter, JR 2010, 'Variability and trends in the directional wave climate of the Southern Hemisphere', *International Journal of Climatology*, vol. 30, pp. 475-491.

Hemer, MA, McInnes, K, Church, JA, O'Grady, J & Hunter, JR 2008, *Variability and Trends in the Australian Wave Climate and Consequent Coastal Vulnerability*, CSIRO, Bureau of Meteorology and ACE-CRC, Hobart.

Hemer, MA, Simmonds, I & Keay, K 2008, 'A classification of wave generation characteristics during large wave events on the Southern Australian margin', *Continental Shelf Research*, vol. 28, pp. 634-652.

Hennecke, W 2000, 'GIS-Based Modelling of Potential Sea-Level Rise Impacts on Coastal Re-Entrants and Adjacent Shorelines', Doctor of Philosophy thesis, University of Sydney.

Hennecke, W & Cowell, P 2000, 'GIS Modelling of Impacts of an Accelerated Rate of Sea-Level Rise on Coastal Inlets and Deeply Embayed Shorelines', *Environmental Geosciences*, vol. 7, no. 3, pp. 137-148.

Hesp, P 2002, 'Foredunes and blowouts: initiation, geomorphology and dynamics', *Geomorphology*, vol. 48, pp. 245-268.

Hogg, AG, Hua, Q, Blackwell, PG, Niu, M, Buxck, CE, Guilderson, TP, Heaton, TJ, Palmer, JG, Reimer, PJ, Turney, CSM & Zimmerman, SRH 2013, 'SHCal13 Southern Hemisphere calibration, 0-50,000 cal. yr BP.', *Radiocarbon*, vol. 55, pp. 1889-1903.

Horton, BM, Rudman, T, Balmer, J & Houshold, I 2008, *Monitoring Dry Coastal Vegetation in the Tasmanian Wilderness World Heritage Area; Part 2: Appraisal of Method*.

Houshold, I, Chappell, J & Fifield, K 2006, 'Geomorphic response to intraplate neotectonics - Birch's Inlet, SW Tasmania', paper presented to 12th Conference of the Australian and New Zealand Geomorphology Group, Taipa Bay, New Zealand.

Houston, JR 2015, 'Shoreline Response to Sea-Level Rise on the Southwest Coast of Florida', *Journal of Coastal Research*, vol. 314, pp. 777-789.

Hua, Q, Barbetti, M & Rakowski, AZ 2013, 'Atmospheric radiocarbon for the period 1950-2010.', *Radiocarbon*, vol. 55, pp. 2059-2072.

Hunter, J, Coleman, R & Pugh, D 2003, 'The sea level at Port Arthur, Tasmania, from 1841 to the present', *Geophysical Research Letters*, vol. 30, no. 7, pp. 54-51 to 54-54.

Hurrell, JW & Van Loon, H 1994, 'A modulation of the atmospheric annual cycle in the Southern Hemisphere', *Tellus*, vol. 46A, pp. 325-338.

IPCC 2013, *Working Group 1 Contribution to the IPCC Fifth Assessment Report: Climate Change 2013: The Physical Science Basis, Summary for Policymakers*, Intergovernmental Panel on Climate Change.

Jackson, NL, Nordstrom, KF, Eliot, I & Masselink, G 2002, ''Low energy' sandy beaches in marine and estuarine environments: a review', *Geomorphology*, vol. 48, pp. 147-162.

Jevrejeva, S, Grinsted, A, Moore, JC & Holgate, S 2006, 'Non-linear trends and multi-year cycles in sea level records', *Journal of Geophysical Research*, vol. 111:C09012.

King, MA, Keshin, M, Whitehouse, PL, Thomas, ID, Milne, G & Riva, REM 2012, 'Regional biases in absolute sea-level estimates from tide gauge data due to residual unmodeled vertical land movement', *Geophysical Research Letters*, vol. 39, no. L14604, p. 5.

Kinsela, MA, Daley, MJA & Cowell, PJ 2016, 'Origins of Holocene coastal strandplains in Southeast Australia: Shoreface sand supply driven by disequilibrium morphology', *Marine Geology*, vol. 374, pp. 14-30.

Kirkpatrick, J, Nunez, M, Bridle, K, Parry, J & Gibson, N 2017, 'Causes and consequences of variation in snow incidence on the high mountains of Tasmania, 1983-2013', *Australian Journal of Botany*, vol. 65, pp. 214-224.

Knighton, AD 1991, 'Channel Bed Adjustment along Mine-Affected Rivers of Northeast Tasmania', *Geomorphology*, vol. 4, pp. 205-219.

Kole, A 2017, 'Observed zone of increasing wind speeds and tornado events in Tasmania, Australia', *The Bulletin of the Austral;ian Meteorological and Oceanographic Society*, vol. 30, no. 4, pp. 30-35.

Komar, PD 1996, 'The budget of littoral sediments: concepts and applications', *Shore Beach*, vol. 64, pp. 18-26.

Lambeck, K & Chappell, J 2001, 'Sea Level Change through the Last Glacial Cycle', *Science*, vol. 292, pp. 679-686.

Lambeck, K & Nakada, M 1990, 'Late Pleistocene and Holocene sea-level change along the Australian coast', *Palaeogeography, Palaeoclimatology, Palaeoecology*, vol. 89, pp. 143-176.

Le Cozannet, G, Garcin, M, Yates, M, Idier, D & Meyssignac, B 2014, 'Approaches to evaluate the recent impacts of sea-level rise on shoreline changes', *Earth-Science Reviews*, vol. 138, pp. 47-60.

Le Cozannet, G, Oliveros, C, Castelle, B, Garcin, M, Idier, D, Pedreros, R & Rohmer, J 2016, 'Uncertainties in sandy shorelines evolution under the Bruun rule assumption', *Frontiers in Marine Science*, vol. 3, no. 49.

Leach, C, Kennedy, DM, Carvalho, RC & Ierodiaconou, D 2020, 'Predicting Compartment-scale Climate Change Impacts Related to Southern Ocean Wave Forcing: Port Fairy, Victoria, Australia', *Journal of Coastal Research*, vol. 95, no. sp1.

Leaman, DE 1976, *Hobart Geological Survey Explanatory Report, Geological Atlas 1:50,000 Series, Sheet 8312S*, Tasmania Department of Mines.

Lewis, SE, Sloss, CR, Murray-Wallace, CV, Woodroffe, CD & Smithers, SG 2013, 'Post-glacial sea-level changes around the Australian margin: a review', *Quaternary Science Reviews*, vol. 74, pp. 115-138.

Lyu, KW, Zhang, XB, Church, JA, Slangen, ABA & Hu, JY 2014, 'Time of emergence for regional sea-level change', *Nature Climate Change*, vol. 4, no. 11, pp. 1006-1010.

Mariani, A, Shand, TD, Carley, JT, Goodwin, ID, Splinter, K, Davey, EK, Flocard, F & Turner, IL 2012, *Generic Design Erosion volumes and Setbacks for Australia*, WRL report no. 247, Water Research Laboratory, University of New South Wales Hobart.

Marshall, GJ 2003, 'Trends in the Southern Annular Mode from Observations and Reanalyses', *Journal of Climate*, vol. 16, pp. 4134-4143.

Masselink, G, Castelle, B, Scott, T, Dodet, G, Suanez, S, Jackson, D & Floc'h, F 2016, 'Extreme wave activity during 2013/2014 winter and morphological impacts along the Atlantic coast of Europe', *Geophysical Research Letters*, vol. 43, pp. 2135-2143.

McVicar, TR, Van Niel, TG, Li, LT, Roderick, ML, Rayner, DP, Ricciardulli, L & Donohue, RJ 2008, 'Wind speed climatology and trends for Australia, 1975-2006: Capturing the stilling phenomenon and comparison with near-surface reanalysis output', *Geophysics Research Letters*, vol. 35, L20403.

Mimura, N & Nobuoka, H 1995, 'Verification of Bruun Rule for the estimate of shoreline retreat caused by sea-level rise', paper presented to Coastal Dynamics 95, New York.

Mortlock, TR & Goodwin, ID 2015a, 'Directional wave climate and power variability along the Southeast Australian shelf', *Continental Shelf Research*, vol. 98, pp. 36-53.

—— 2015b, 'Wave Climate Change Associated with Enso Modoki and Tropical Expansion in Southeast Australia and Implications for Coastal Stability', paper presented to The Proceedings of the Coastal Sediments 2015, DOI 10.1142/9789814689977_0198.

Mortlock, TR, Goodwin, ID, McAneney, J & Roche, K 2017, 'The June 2016 Australian East Coast Low: Importance of Wave Direction for Coastal Erosion Assessment', *Water*, vol. 9, no. 2, p. 121.

Morton, RA 2008, 'Historical Changes in the Mississippi-Alabama Barrier-Island Chain and the Roles of Extreme Storms, Sea Level, and Human Activities', *Journal of Coastal Research*, vol. 24, no. 6, pp. 1587-1600.

Mount, R 2001, *Tasmania's Coastline and Coastal Waters*, Hobart.

Mount, R, Prahalad, V, Sharples, C, Tilden, J, Morrison, B, Lacey, M, Ellison, J, Helman, M & Newton, J 2010, *Circular Head Region Coastal Foreshore Habitats: Sea Level Rise Vulnerability Assessment*, Blue Wren Group, School of Geography and Environmental Studies, University of Tasmania, Hobart.

Nanson, GC, Barbetti, M & Taylor, G 1995, 'River stabilisation due to changing climate and vegetation during the late Quaternary in western Tasmania, Australia', *Geomorphology*, vol. 13, pp. 145-158.

Nerem, RS, Beckley, BD, Fasullo, JT, Hamlington, BD, Masters, D & Mitchum, GT 2018, 'Climate-change-driven accelerated sea-level rise detected in the altimeter era', *Proc Natl Acad Sci U S A*, vol. 115, no. 9, pp. 2022-2025.

Nicholls, RJ & Cazenave, A 2010, 'Sea-Level Rise and Its Impact on Coastal Zones', *Science*, vol. 328, no. 5985, pp. 1517-1520.

Nordstrom, KF 1992, *Estuarine Beaches*, Elsevier Applied Science.

Oliver, SN, Donaldson, P, Sharples, C, Roach, M & Woodroffe, CD 2017, 'Punctuated progradation of the Seven Mile Beach Holocene barrier system, southeastern Tasmania', *Marine Geology*, vol. 386, pp. 76-87.

Peltier, WR, Argus, DF & Drummond, R 2015, 'Space geodesy constrains ice age terminal deglaciation: The global ICE-6G_C (VM5a) model', *Journal of Geophysical Research-Solid Earth*, vol. 120, no. 1, pp. 450-487.

Pemberton, M & Cullen, P 1999, 'Soils, stratigraphy and shells; Coastal dune development in parts of western Tasmania', in J Hall & J McNiven (eds), *Australian Coastal Archaeology*, ANH Publications, Department of Archaeology and Natural History, The Australian National University, Canberra, vol. No. 31, pp. 271-277.

Pepper, AR & Puotinen, ML 2009, 'GREMO: a GIS-based generic model for estimating relative wave exposure', paper presented to 18th World IMACS Congress and MODSIM09 International Congress on Modelling and Simulation., Cairns, Queensland.

Pettijohn, FJ, Potter, PE & Siever, R 1972, *Sand and Sandstones*, Springer-Verlag, New York.

Prahalad, V, Kirkpatrick, JB, Aalders, J, Carver, S, Ellison, J, Harrison-Day, V, McQuillan, P, Morrison, B, Richardson, AMM & Woehler, E 2019, 'Conservation ecology of Tasmanian coastal saltmarshes, south-east Australia – a review', *Pacific Conservation Biology*.

Prahalad, V, Sharples, C, Kirkpatrick, J & Mount, R 2015, 'Is wind-wave fetch exposure related to soft shoreline change in swell-sheltered situations with low terrestrial sediment input?', *Journal of Coastal Conservation*, vol. 19, pp. 23-33

Prosser, IP & Winchester, SJ 1996, 'History and Processes of Gully Initiation and Development in Eastern Australia', *Zeitschrift fur Geomorphologie N.F.*, vol. 105, pp. 91-109.

Pugh, D, Hunter, J, Coleman, R & Watson, C 2002, 'A comparison of historical and recent sea level measurements at Port Arthur, Tasmania', *International Hydrographic Review*, vol. 3, pp. 27-46.

Pye, K & Blott, SJ 2006, 'Coastal processes and morphological change in the Dunwich-Sizewell area, Suffolk, UK', *Journal of Coastal Research*, vol. 22, no. 3, pp. 453-473.

—— 2015, 'Spatial and temporal variations in soft-cliff erosion along the Holderness Coast, East Riding of Yorkshire, UK', *Journal of Coastal Conservation*.

Ranasinghe, R, McLoughlin, R, Short, A & Symonds, G 2004, 'The Southern Oscillation Index, wave climate, and beach rotation', *Marine Geology*, vol. 204, pp. 273-287.

Riddell, AR, King, MA & Watson, CS 2020, 'Present‐Day Vertical Land Motion of Australia From GPS Observations and Geophysical Models', *Journal of Geophysical Research: Solid Earth*, vol. 125, no. 2.

Riva, REM, Frederikse, T, King, MA, Marzeion, B & van den Broeke, MR 2017, 'Brief communication: The global signature of post-1900 land ice wastage on vertical land motion', *The Cryosphere*, vol. 11, no. 3, pp. 1327-1332.

Romine, BM, Fletcher, CH, Barbee, MM, Anderson, TR & Frazer, LN 2013, 'Are beach erosion rates and sea-level rise related in Hawaii?', *Global and Planetary Change*, vol. 108, pp. 149-167.

Rosati, JD 2005, 'Concepts in sediment budgets', *Journal of Coastal Research*, vol. 21, pp. 307-322.

Santamaria-Gomez, A, Gravelle, M, Collilieux, X, Guichard, M, Miguez, BM, Tiphaneau, P & Woppelmann, G 2012, 'Mitigating the effects of vertical land motion in tide gauge records using a state-of-the-art GPS velocity field', *Global and Planetary Change*, vol. 98-99, pp. 6-17.

Schwartz, M 1965, 'Laboratory Study of Sea-Level Rise as a Cause of Shore Erosion', *Journal of Geology*, vol. 73, pp. 528-534.

—— 1967, 'The Bruun Theory of Sea-Level Rise as a Cause of Shore Erosion', *Journal of Geology*, vol. 75, pp. 76-92.

Shand, TD & Carley, J 2009, *Dune Building using beach scraping at Cremorne Ocean Beach and Roches Beach, Clarence City, Tasmania*, Technical report 2009/31 by Water Research Laboratory, University of New South Wales, for Clarence City Council.

—— 2011, *Investigation of Trial Groyne Structures for Roches Beach*, Water Research Laboratory, University of New South Wales.

Sharples, C 2006, *Indicative Mapping of Tasmanian Coastal Vulnerability to Climate Change and Sea-Level Rise: Explanatory Report. 2nd Edition*, Department of Primary Industries & Water, Tasmania, Hobart.

—— 2010, *Shoreline Change at Roches Beach, South-Eastern Tasmania, 1957-2010*, Antarctic Climate and Ecosystems Co-operative Research Centre, University of Tasmania, Hobart.

—— 2012, *A geomorphic risk assessment of shoreline erosion at Gordon, D'Entrecasteaux Channel, Tasmania*, Unpublished Report to private client.

—— 2017, *A Coastal Erosion Hazard Assessment for the Port Arthur and Coal Mines Historic Sites, Tasman Peninsula, Tasmania*, Port Arthur Historic Sites Management Authority.

Sharples, C, Mount, R, Hemer, MA, Puotinen, M, Dell, M, Lacey, M, Harries, S, Otera, K, Benjamin, J & Zheng, X 2012, *The ShoreWave Project: Development of a methodology for coastal erosion risk analysis under climate change, integrating geomorphic and wave climate data sets*, University of Tasmania, Hobart, Tasmania.

Sharples, C, Walford, H, Watson, C, Ellison, JC, Hua, Q, Bowden, N & Bowman, D 2020, 'Ocean Beach, Tasmania: A swell-dominated shoreline reaches climate-induced recessional tipping point?', *Marine Geology*, vol. 419.

Shennan, I & Horton, B 2002, 'Holocene land- and sea-level changes in Great Britain', *Journal of Quaternary Science*, vol. 17, no. 5-6, pp. 511-526.

Short, AD 2006a, 'Australian Beach systems - Nature and Distribution', *Journal of Coastal Research*, vol. 22, pp. 11-27.

—— 2006b, *Beaches of the Tasmanian Coast & Islands: A guide to their nature, characteristics, surf and safety*, Sydney University Press, Sydney.

—— 2010, 'Sediment Transport around Australia - Sources, Mechanisms, Rates, and Barrier Forms', *Journal of Coastal Research*, vol. 26, no. 3, pp. 395-402.

Short, AD, Trembanis, A & Turner, I 2000, 'Beach Oscillation, Rotation and the Southern Oscillation - Narrabeen Beach, Australia', in *International Conference on Coastal Engineering*, Sydney.

Shulmeister, J, Goodwin, I, Renwick, J, Harle, K, Armand, L, McGlone, MS, Cook, E, Dodson, J, Hesse, PP, Mayewski, P & Curran, M 2004, 'The Southern Hemisphere westerlies in the Australasian sector over the last glacial cycle: a synthesis', *Quaternary International*, vol. 118-119, pp. 23-53.

Slangen, ABA, Church, JA, Agosta, C, Fettweis, X, Marzeion, B & Richter, K 2016, 'Anthropogenic forcing dominates global mean sea-level rise since 1970', *Nature Climate Change*, vol. 6, no. 7, pp. 701-705.

Sloss, CR, Murray-Wallace, CV & Jones, BG 2007, 'Holocene sea-level change on the southeast coast of Australia: a review', *The Holocene*, vol. 17, no. 7, pp. 999-1014.

Smith, AM, Bundy, SC & Cooper, JAG 2016, 'Apparent dynamic stability of the southeast African coast despite sea level rise', *Earth Surface Processes and Landforms*.

Stive, M 2004, 'How Important is Global Warming for Coastal Erosion? - An Editorial Comment', *Climatic Change*, vol. 64, pp. 27-39.

Stive, M, Cowell, PJ & Nicholls, RJ 2009, 'Impacts of Global Environmental Change on Beaches, Cliffs and Deltas', in O Slaymaker, T Spencer & C Embleton-Hamann (eds), *Geomorphology and Global Environmental Change*, Cambridge University Press, Cambridge UK, pp. 158-179.

Sunamura, T 1992, *Geomorphology of Rocky Coasts*, John Wiley & Sons, Chichester.

Thom, B, Eliot, I, Eliot, M, Harvey, N, Rissik, D, Sharples, C, Short, AD & Woodroffe, CD 2018, 'National sediment compartment framework for Australian coastal management', *Ocean & Coastal Management*, vol. 154, pp. 103-120.

Thom, B & Short, AD 2006, 'Introduction: Australian Coastal Geomorphology,1984-2004', *Journal of Coastal Research*, vol. 22, pp. 1-10.

Thompson, DWJ & Solomon, S 2002, 'Interpretation of recent Southern Hemisphere climate change', *Science*, vol. 296, pp. 895-899.

Trenhaile, AS 1987, *The Geomorphology of Rock Coasts*, Oxford University Press.

—— 2011, 'Predicting the response of hard and soft rock coasts to changes in sea level and wave height', *Climatic Change*, vol. 109, pp. 599-615.

Troccoli, A, Muller, K, Coppin, P, Davy, R, Russell, C & Hirsch, AL 2012, 'Long-Term Wind Speed Trends over Australia', *Journal of Climate*, vol. 25, no. 1, pp. 170-183.

Wahl, T & Plant, NG 2015, 'Changes in erosion and flooding risk due to long-term and cyclic oceanographic trends', *Geophysical Research Letters*, vol. 42, pp. 2943-2950.

Walford, H 2011, 'Assessment of coastal erosion at Ocean Beach, Western Tasmania', Bachelor of Science (Honours) thesis, University of Tasmania.

Walsh, K, White, CJ, McInnes, K, Holmes, J, Schuster, S, Richter, H, Evans, JP, Di Luca, A & Warren, RA 2016, 'Natural hazards in Australia: storms, wind and hail', *Climatic Change*, vol. 139, no. 1, pp. 55-67.

Watson, C, White, NJ, Church, JA, King, MA, Burgette, RJ & Legresy, B 2015, 'Unabated global mean sea-level rise over the satellite altimeter era', *Nature Climate Change*, vol. 5, no. 6, pp. 565-568.

Watson, P 2011, 'Is there evidence yet of acceleration in mean sea level rise around mainland Australia?', *Journal of Coastal Research*, vol. 27, no. 2, pp. 368-377.

Watt, EJ 1999, 'The Morphology and Sediment Transport Dynamics of the Seven Mile Beach Spit', University of Tasmania.

White, NJ, Haigh, ID, Church, JA, Koen, T, Watson, C, Pritchard, TR, Watson, P, Burgette, RJ, McInnes, KL, You, Z-J, Zhang, X & Tregoning, P 2014, 'Australian sea-levels - Trends, regional variability and influencing factors', *Earth Science Reviews*, vol. 136, pp. 155-174.

Woodroffe, CD 2003, *Coasts: Form, Process and Evolution*, Cambridge University Press, United Kingdom.

Woodworth, PL 1999, 'High waters at Liverpool since 1768: the UK's longest sea level record', *Geophysical Research Letters*, vol. 26, no. 11, pp. 1589-1592.

Young, IR & Ribal, A 2019, 'Multiplatform evaluation of global trends in wind speed and wave height', *Science*.

Zhang, K, Douglas, BC & Leatherman, SP 2004, 'Global Warming and Coastal Erosion', *Climatic Change*, vol. 64, pp. 41-58.

Zhou, Y, Feng, X, Guan, W & Feng, W 2018, 'Characteristics of beach erosion in headland bays due to wave action: Taking the Narrabeen beach in Australia as an example', *Chinese Science Bulletin*, vol. 64, no. 2, pp. 223-233.

Appendix 1: Shoreline Descriptions and Data

A1.1 *Introduction*

This appendix records information compiled for the 35 distinct shoreline sites studied in this thesis. Although the descriptions and data for some geographically-related sites have been grouped in a single appendix section for convenience, in all cases a separate shoreline history has been determined, plotted and analysed as appropriate for each of the 35 distinctive coastal sites listed in Chapter 4 Table 1.

The information compiled in these appendices is more detailed for some sites than others, but in all cases includes metadata tables for all air photos used to analyse the shoreline behaviour history of each site. Also included is a list of the shapefiles digitised to record the shoreline positions digitised from the ortho-rectified air photos. These record the shoreline position for each site at each air photo date.

Other information provided in each appendix section includes variably detailed descriptive information for each site, and discussion of the shoreline behaviour history for each site. In most cases the appendices provide the opportunity for the reader to explore in more detail the background information supporting the (necessarily brief) site descriptions and analyses provided in the main text of this thesis.

Original Data

Original numerical data collected and analysed by the writer in the course of the thesis described in this thesis mainly comprises shoreline position data measured from historic aerial photographs (as described in Chapter 3), together with air photo error margin measurements. These original data (comprising extensive data tables) are not reproduced in this thesis but are stored in digital format as comma-separated values (.csv) files. Much of the analysis of these data was performed using Excel™ and Matlab™ software with resulting worksheets, tables and scripts also stored separately in digital format, however the resulting data and analysis plots are preproduced in this thesis, in Appendix 1 and elsewhere as required.

Other original copyright-protected data used in this research is not reproduced this thesis, however plots and other analyses of these datasets are provided in this thesis as relevant. The original datasets (not reproduced) include Bureau of Meteorology wind records, CSIRO wave hindcast data, tide gauge records and sea-level rise reconstructions as cited in this thesis.

A1.2 *Swell-sheltered soft sandy shores*

A1.2.1 Ralphs Bay shore, South Arm Neck (south-eastern Tasmania)

Geomorphic description

This site is a sandy saltmarsh shoreline which is the swell-sheltered north shore of the South Arm isthmus, a sand body extending to below present sea-level across most of its width and length. The shoreline behaviour history for this shore has been digitised from the same air photos used to digitise shoreline for Hope Beach; these are listed and described in Section A1.4.3 of these appendices.

The shore on the Ralphs Bay side of the neck is tidal and permanently connected to the sea but receives only very refracted and attenuated swell wave penetration. The tidal range is approximately 1.3 m (spring) to 0.3m (neap) ((Short 2006b). A relatively steep but very narrow reflective sandy shelly beach (Short 2006b) is fronted by very extensive flat intertidal sand flats which are exposed for over a kilometre northwards into Ralphs Bay at low tide (Figure 66). The narrow beach is immediately backed by low shelly sand beach ridges typically 0.2 – 0.3m high which extend tens of metres southwards (inland) until they are buried beneath vegetated transgressive sand dunes that have spread across the isthmus from the exposed Hope Beach side.

The western-central and easternmost sections of the sandy shore are mostly undisturbed with saltmarsh soils and vegetation occupying the beach ridges in the backshore area. However the South Arm road passes only a metre or two behind the shore along a stretch of several hundred metres in the central-eastern area, between transects 14546 to 14562 (see Figure 65 and Figure 67). Some artificial fill (gravel and in places boulders) has sporadically been placed along this shore section, however during 2015 this was in many places exposed in a low active erosion scarp along the shore immediately fronting the road (see Figure 65). The air photo record suggests that emplacement of artificial fill circa 1960s to protect the road resulted in apparent progradation of the shore along part of this shoreline stretch, however subsequent minor shoreline recession in the same areas indicates erosion of the fill (see Figure 67 and associated discussion). Numerous remnant ‘pedestals’ of saltmarsh soil and vegetation observed standing isolated on the sandy shore a metre or two in front of the main saltmarsh backshore during 2015 are interpreted to be remnants of earlier artificial fill that has subsequently eroded back (see Figure 65).

Figure 65: View east along central-eastern section of the Ralphs Bay shoreline on the north side of South Arm Neck. The main road has been located very close to this section of the shoreline since the earliest (1940s) photos and has been subject to occasional engineering and earthworks including placement of fill to protect the road. Location close to transect 14550 approx. (see Figure 67). Photo by C. Sharples.

Figure 66: View west along western-central section of the Ralphs Bay shoreline on the north side of South Arm Neck. The main road is 50 metres south of this shoreline, which has probably been little affected by artificial disturbances. Location near transect 14543 approx. (see Figure 67). Photo by C. Sharples.

Swell wave climate

Receives only very refracted and attenuated swells under normal conditions but would receive larger storm swells on rare occasions. However, swells can only reach shoreline briefly at high tide because of very broad intertidal sand flats

Wind (wind wave) climate

Dominant south-westerly wind directions blow offshore and wind-waves generated by these winds would not affect this shore. Wind waves would only reach this shore under unusual northerly wind conditions and only at high tide because of broad local sand flats. Hence wind-wave erosion events are likely to be rare events at this site.

Sand transport and budget

A small sand supply was evidently wind-blown across the South Arm neck from Hope Beach to Ralphs Bay by bare transgressive dunes during the mid-Twentieth Century (see 1948 and 1965 air photos and discussion in appendix A1.4.3 Hope Beach). Subsequent air photos show these former transgressive dunes gradually stabilised over the 2nd half of Twentieth Century, and they were mostly vegetated by the 1980s.

Extensive intertidal sand flats filling the south end of Ralphs Bay up to the shoreline are indicative of swell pushing sand into low-energy embayments within Ralphs Bay which became sand traps following the end of the last post-glacial marine transgression. It is possible that small amounts of sand are still being pushed into this sand-trapping area by swells entering Ralphs Bay from the Derwent estuary and Storm Bay, albeit this is only speculative.

The area of exposed intertidal sand flats at low tide today in southern Ralphs Bay implies that all available accommodation space for sand in the intertidal sand flat area was evidently filled well prior to modern times. There is little potential for littoral or tidal currents to transport significant amounts of sand out of this very deep embayment, which is a full sand trap or store. However contemporary climate change-driven renewed sea-level rise means that a slow increase in available sand accommodation space on the sand flats must be occurring as the mean water levels rise higher over the sand. This process is described by the Flood-tide delta Aggradation model used by Hennecke and Cowell (2000) and others, and will increasingly provide a sink for any sand eroded from the shoreline and moved across the sand flats by tidal currents at high tide.

This process has probably provided a very small sand sink during the air photo period and may be responsible for a putative very slow and non-significant recession trend in the Twentieth Century shoreline history (see Figure 67 and Figure 68). This sand sink will become more important in future as sea-level continues to rise enabling more frequent storm wave access to the shoreline and providing more accommodation space for sand eroded in such erosion events to sink into.

In summary, the sandy Ralphs Bay shoreline on the north side of South Arm neck has probably had only small and decreasing sand gains during the Twentieth Century. There has probably been little if any loss of sand out of the large infilled embayment but perhaps some small losses to the intertidal sand flats themselves as sea-level rise has created more accommodation space there. However, with contemporary sea-level rise continuing to increase the available accommodation space for sand to be sequestered on the intertidal sand flats, these are likely to become a more effective sand sink over time. With sea-level rise also increasing the frequency of any wave attack on the sandy beach, this is also likely to result in an increasing rate of shoreline recession in future.

Air photo analysis

Historic shoreline behaviour at on the Ralphs Bay (north) side of the South Arm neck was determined using ortho-rectified air photos from 9 dates between 1948 and 2019 (see Table 67 in appendix A1.4.3). These are not the full time series available for the neck area, however it is noteworthy that the nine air photos show a consistent shoreline behaviour trend with little variability (Figure 67 and Figure 68), which suggests that large departures from the apparent trend (perhaps hidden in time gaps between the used air photo dates) are unlikely.

Shore behaviour history from air photos

Shoreline variability has been relatively coherent between most transects along this shore over the air photo period (see Figure 67 inset) and shows little difference in historical behaviour between more and less disturbed parts of the shore. The western to central part of the shore is mostly well-separated

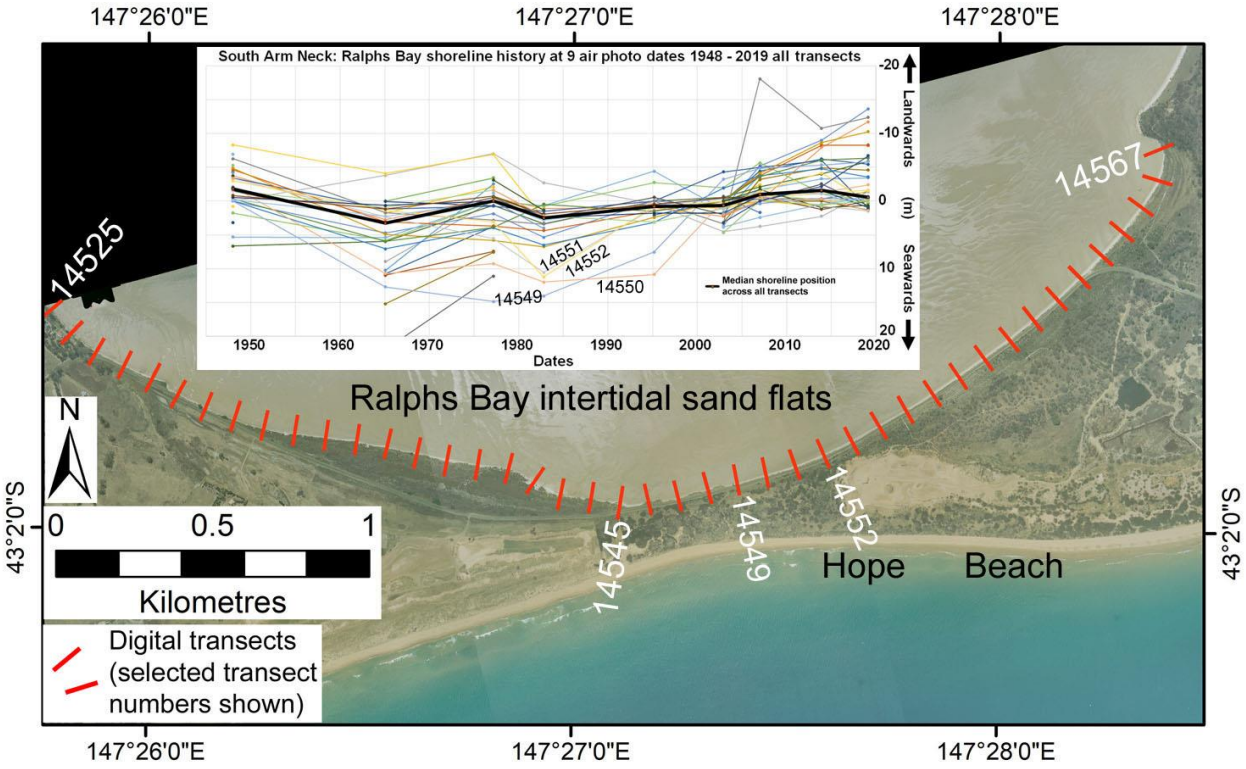

Figure 67: Plots of shoreline (*in situ* vegetation line) position movement on Ralphs Bay side of South Arm Neck. Shoreline movement histories shown for 9 air photo dates over the period 1948 to 2019 along all 100m-spaced digital transect lines used. The beach image is the January 2007 air photo. The anomalous transects 14549 to 14552 are labelled; these have been influenced by artificial fill placement – see text discussion.

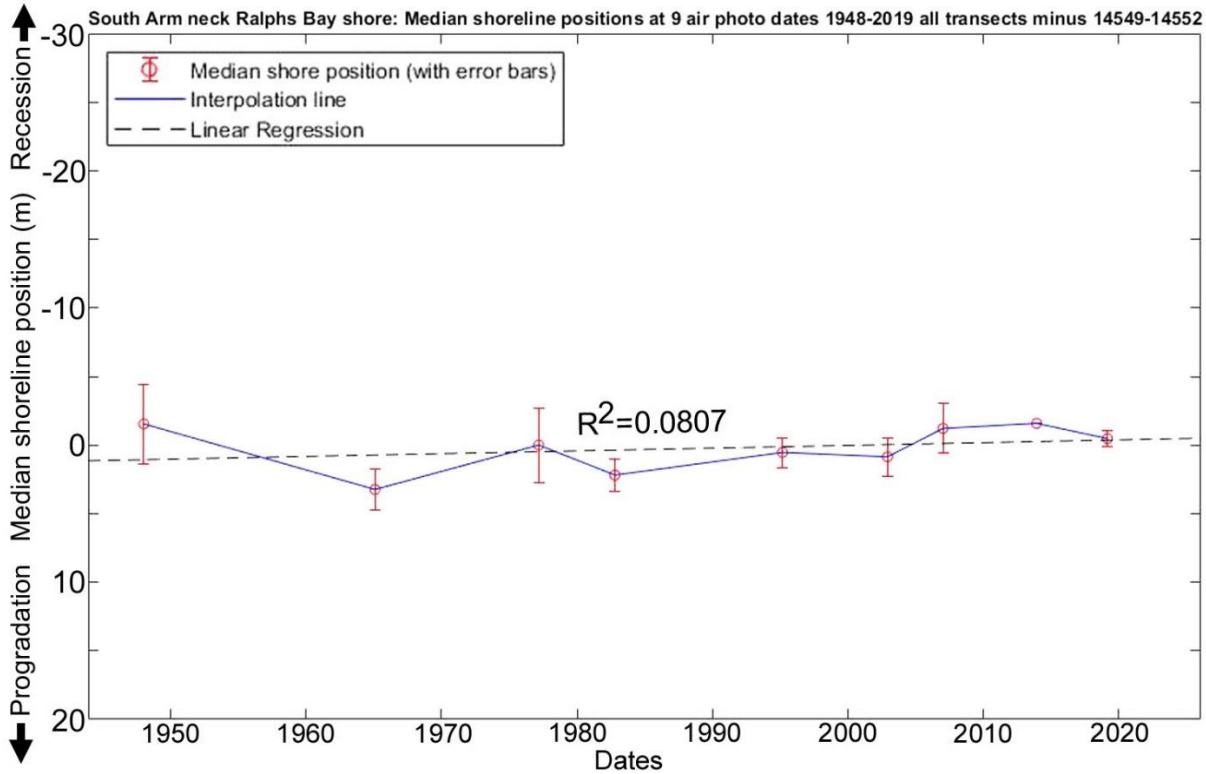

Figure 68: Summary plot of shoreline change history on the Ralphs Bay side of South Arm Neck (as shown on Figure 67) at 9 air photo dates from 1948 to 2019. These plot the median of the normalised shoreline positions at each date across all transects except the anomalous (disturbed) transects 14549-14552. A linear fit indicating a non-significant recession trend implies a stable or very slightly receding dynamic equilibrium shoreline position throughout the air photo period. There are no clear indications of a long-term change of behaviour at this beach.

from the nearby road and has been mostly un-affected by artificial disturbances over the air photo period. Most of the central to eastern part has been subject to minor placement of fill and boulders to protect the adjacent road, however the only part of this section exhibiting different behaviour is from transects 14549 to 14552. This stretch showed anomalously seawards shoreline positions during the 1960s to 1990s period and has subsequently receded anomalously since circa 2000 (see Figure 67). Artificial fill is evident in this stretch of shoreline, and the anomalous historical behaviour is interpreted to be the result of artificial fill being emplaced from the 1960s onwards to protect the adjacent road, and having begun to erode and recede in the last 20 years (as seen in Figure 65 above).

The summary plot shown in Figure 68 plots the median shoreline position across all transects except the anomalous transects 14549-14552; this plot is interpreted as the mostly coherent shoreline history of an essentially undisturbed shoreline, with the only section showing any apparent response to artificial interference having been excluded.

The history of the sandy saltmarsh shore on the north side of South Arm neck shows very little shoreline position variability beyond air photo error margins (Figure 68), and is most strongly suggestive of a very stable shoreline over the whole air photo period (1948 to 2019). The air photo record suggests a few small erosion and recovery cycles implying a dynamic equilibrium stability (Figure 67 and Figure 68), however these are mostly with the range of air photo error margins and may not be real. Similarly, a linear regression fit over the entire time series is suggestive of a slight trend towards shoreline recession, albeit the trend lies mostly within the air photo error range and has only a very small correlation co-efficient so may also not be real.

However, a small recession trend during the air photo period would not be surprising given that contemporary sea-level rise is expected to increase the sand accommodation space on the adjacent tidal sand flats (see *Sand budget* discussion above). See Hennecke and Cowell (2000). This will create additional capacity to sequester any sand eroded from the shoreline, resulting in a trend towards progressive shoreline recession without recover. Although such a trend is likely to become more noticeable with future increase and acceleration of sea-level rise, it is possible that an emerging process of this sort has been detected during the Twentieth Century by the air photo analysis, albeit not at a statistically significant level.

Air photo data tables

The air photos used for this analysis are the same ones used for Hope Beach, and these are listed and described in Section A1.4.3 of these appendices.

The following tables provide details of the shapefiles representing the Ralphs Bay shoreline position that were digitised from the ortho-photos.

Table 13: Digitised shoreline shapefiles produced for the Ralphs Bay shoreline of South Arm neck (using ortho-photos listed in Table 67 (Section A1.4.3).

Date of air photo(s)	Shapefile	Shoreline digitised by
8th Jan. 1948	Ralphs_MGA55_19480108.shp	Chris Sharples (2018)
2nd Feb. 1965	Ralphs_MGA55_19650202.shp	Chris Sharples (2018)
4th Mar. 1977	Ralphs_MGA55_19770304.shp	Chris Sharples (2018)
18th Oct. 1982	Ralphs_MGA55_19821018.shp	Chris Sharples (2018)
1st Mar. 1995	Ralphs_MGA55_19950301.shp	Chris Sharples (2018)
3rd Dec. 2002	Ralphs_MGA55_20021203.shp	Chris Sharples (2018)
4th Jan. 2007	Ralphs_MGA55_20070104.shp	Chris Sharples (2018)
1st Dec. 2013	Ralphs_MGA55_20131201.shp	Chris Sharples (2018)
24th Feb. 2019	Ralphs_MGA55_20190224.shp	Chris Sharples (2019)

A1.2.2 Nebraska and Jetty Beaches (Bruny Island)

Storm and Erosion history

Anecdotal information from Geoff Baxter (Tom Baxters dad, email dated 12th Jan 2018, Geoff & Val have a shack near the western end of Nebraska Beach):

"Hi Chris

Thanks for your help with and interest in dune erosion at Nebraska Beach. You are also right about the fallibility of our memories when recalling events of the past few years. We will have photos of the beach in the past but will have to search through them to see what use they are, so will undertake to send a further reply, with pictures, in the first half of February. (We are in Newcastle for the next 2 weeks) Since we purchased our property in 1984, there has always been erosion which takes sand from the beach, usually followed by its return variable periods later. In the last 6 to 8 years, our dune has retreated irrevocably, however. After significant change somewhere around 2012, some dune had reformed, with regrowth of grasses occurring, then several large storms between Dec 2015 and July 2016, I think, eroded to an extent that we lost 3 trees from the dune. Since then, so for all of 2017 really, sand has come and gone in its "usual" manner without further erosion of the main dune bank.

I'll see what photos, and written communications we have when we return in a couple of weeks and contact you further.

Regards

Geoff Baxter"

The above sounds like:

- Dynamic equilibrium from 1984 until last decade
- Major erosion event around 2012 (likely 13th July 2011 storm)
- Some recovery then further erosion events in 2015 and 2016 took shoreline back further than previously seen (3 large trees undermined: indicates unprecedented recession).
- Some recovery in 2017
- Remains to be seen if beach recovers to pre-2011 extent or continues to recede.

Air photo analysis

Based on shorelines (*in situ* vegetation lines) digitised over a time series of ortho-rectified air photos from 27 dates from 1948 to 2017, the history of shoreline behaviour and change at Nebraska Beach – Jetty Beach over the air photo period is summarised in the following figures.

Shore behaviour history from air photos

Results (see Figures):

Jetty Beach: slow but real progradation trend (beyond error margins) over whole period; likely long-term receiving sand from Nebraska Beach, not losing it via mobile dunes as it was in the 1940s and before. There are no seawalls at Jetty Beach

Nebraska Beach: Mostly no change – small cut and fills (mostly within error margin range) but no long-term recession or progradation trend. Likely sand budget balanced, both receiving sand from SW longshore drift and losing sand alongshore towards Jetty beach.

The most notable recent change at Nebraska is barely visible on air photo record: notable erosion in recent years at southwest extremity (visible on Figure 69 as a couple of transects (SW end ones) showing more recent recession that others). This could be a switch to long term recession (starting from updrift end of beach as might be expected), but is still within range of previous erosion phases and hasn't been going on long enough to say whether is a cyclic event or long term behaviour change

yet. (Nebraska has potential to be an early responder if sand supply constant, but loss rate increases with more erosion events on higher SL.)

Numerous artificial seawalls of differing ages complicates interpretation: they may be hiding effects of past erosion and may be precenting recession that would otherwise be seen. Need to redo analysis after first mapping the extent (and age if poss.) of protection structures along beach, and eliminating these from the data analysed (e.g., eliminated affected transects for dates affected and see how plots turn out).

Intervening areas: (Figure 69**):**

Area SW of Nebraska – very little change over whole period (not surprising with bedrock backshore).

Area between Nebraska and Jetty: Slow overall progradation, similar to Jetty (not surprising, catching some of the sand coming from Nebraska as is Jetty beach itself).

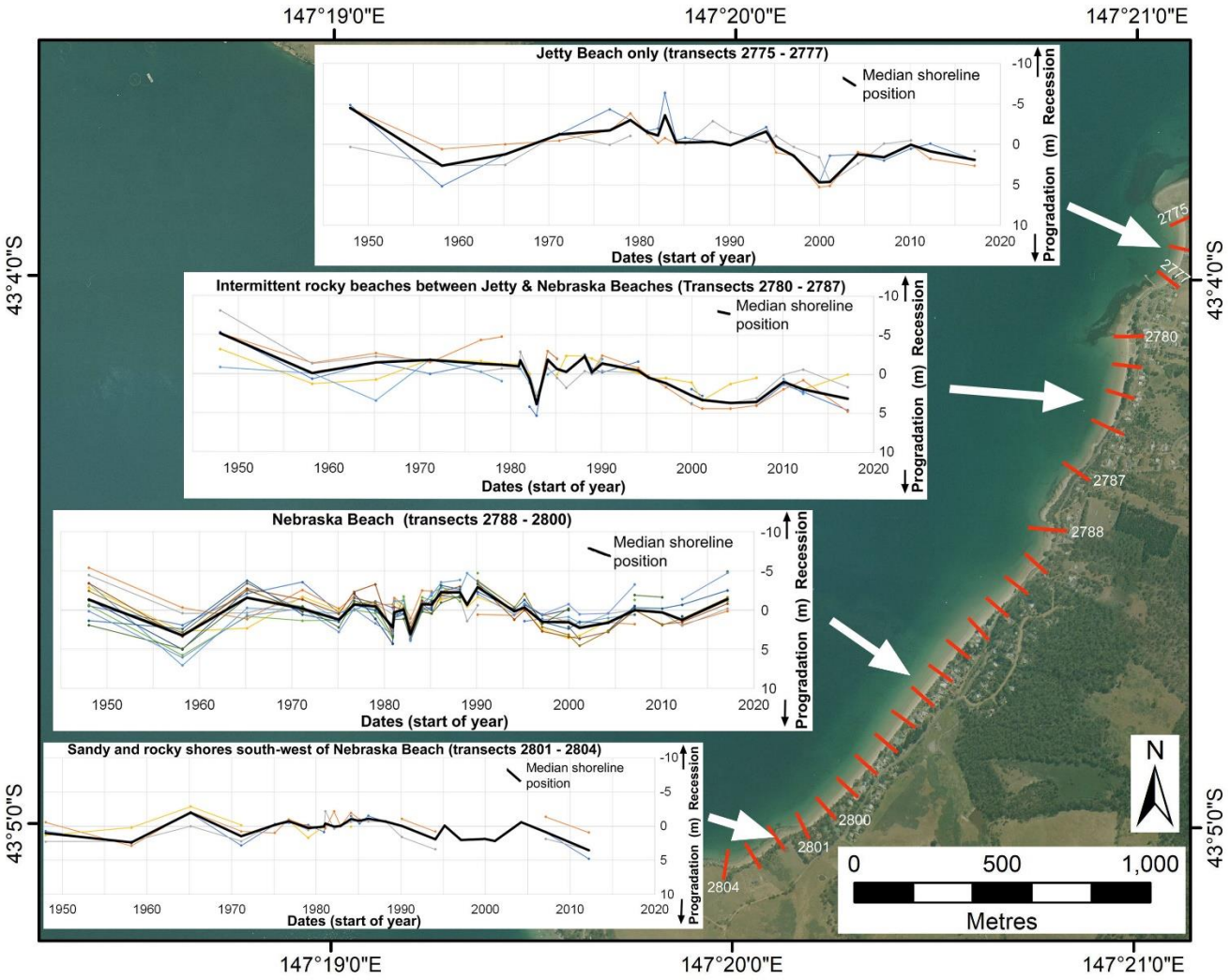

Figure 69: Plots of shoreline (vegetation line) position movement along each digital transect at Nebraska and Jetty beaches at up to 27 air photo dates (23 for Jetty Beach) over the period 1948 to 2017, plotted relative to the median shoreline position on each transect. Transect locations are indicated by red lines on the air photo, and each coloured line on the plots represents shoreline position changes over time along one transect (selected transects are numbered). The transects are plotted in four groups – one each for Jetty and Nebraska Beaches, and one each for intervening and adjacent rocky and sandy shorelines. The median history for each group is also shown as a heavier black line. The base image is the 2010 air photo.

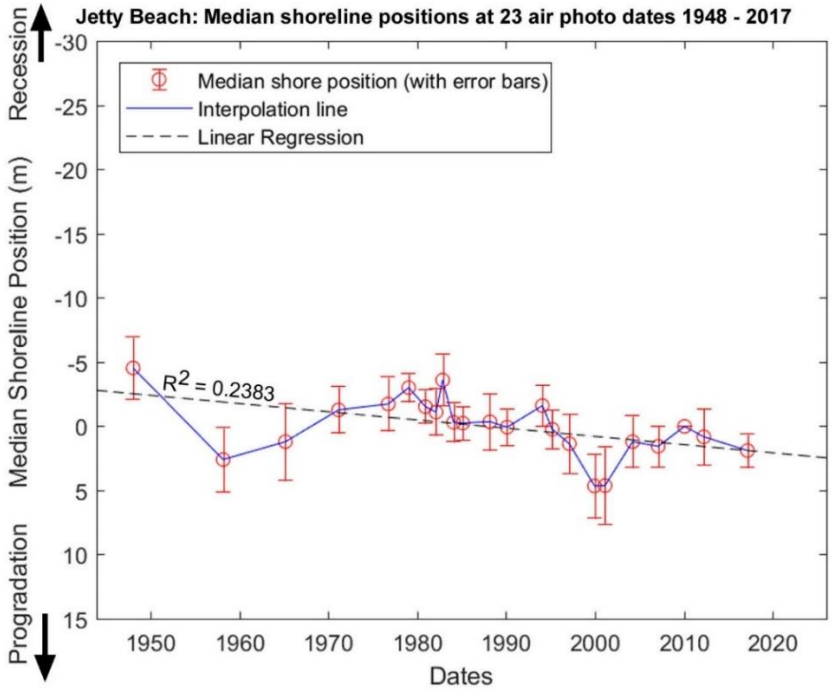

Figure 70: Summary plot of shoreline change history across the three transects at Jetty Beach (2775 – 2777: see Figure 69) for 23 air photo dates from 1948 to 2017. This plot shows the median of the shoreline positions measured across all transects (relative to the median position on each transect) at each air photo date. Figure shows shore positions at each air photo date with interpolation lines and linear fit (linear regression). For comparison purposes the Y-axis scale (shoreline position) is the same as for all other beach history plots in this project, emphasising the comparatively small horizontal shoreline movement detected over the air photo period for this beach.

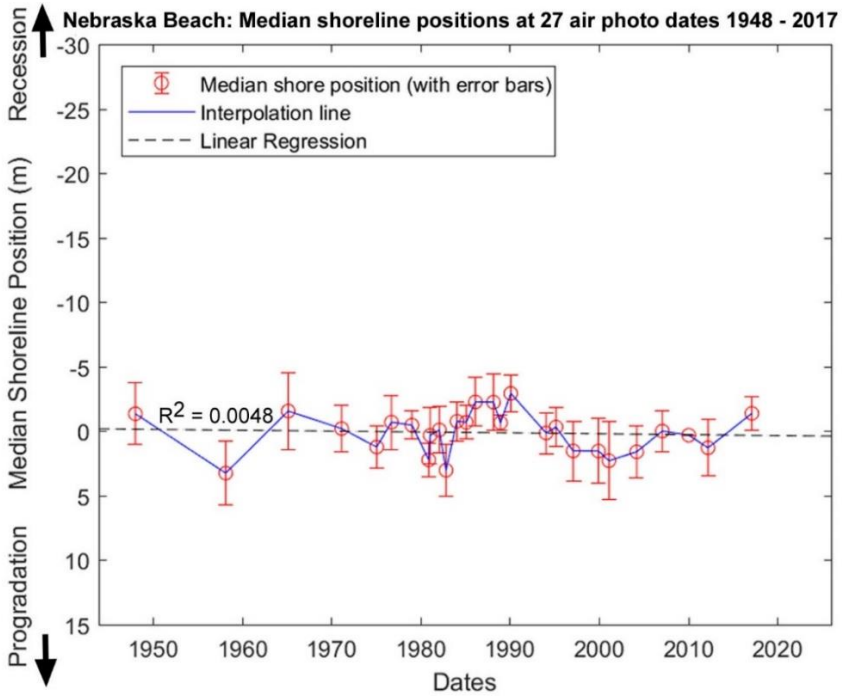

Figure 71: Summary plot of shoreline change history across transects 2788 to 2800 at Nebraska Beach (see Figure 69) for 27 air photo dates from 1948 to 2017. This plot shows the median of the shoreline positions measured across all transects (relative to the median position on each transect) at each air photo date. Figure shows shore positions at each air photo date with interpolation lines and linear fit (linear regression). For comparison purposes the Y-axis scale (shoreline position) is the same as for all other beach history plots in this project, emphasising the comparatively small horizontal shoreline movement detected over the air photo period for this beach.

Air Photo Data Tables

The following tables provide details of the air photos used, the resulting ortho-photos produced, and the shapefiles representing the shoreline position that were digitised from the ortho-photos.

Table 14: Original air photos and ortho-rectified air-photos produced for Nebraska - Jetty Beaches.

Photo Date	**Original DPIPWE air photos (film-frame) / Ortho-photo name**	**Final image resolution (original scan resolution if downsized) / pixel size of final ortho-photo**	**Original photo scale**	**Mean measured feature position error (± metres) for ortho-photo** [No. of measured feature position reference points]	**Comments**
9th Jan 1948	167-971 / *NebraskaJetty_Jan1948a_MGA55.tif/tfw*	600 dpi / 0.7 m pixel size	1:15,840	2.4 m [7]	Ortho-rectified by C. Sharples (Photo 167-970 overlaps, not used)
26th Feb 1958	331-23 / *NebraskaJetty_Feb1958_MGA55.tif/tfw*	1500 dpi (2039 dpi) / 0.6 m pixel size	1:31,680	2.5 m [8]	Ortho-rectified by C. Sharples
2nd Mar 1965	452-178 / *NebraskaJetty_Mar1965_MGA55.tif/tfw*	1500 dpi (2039 dpi) / 0.6 m pixel size	1:31,680	3.0 m [8]	Ortho-rectified by C. Sharples
16th Jan 1970	543-52 / *NebraskaJetty_Jan1970_MGA55.tif/tfw*	1500 dpi (2039 dpi) / 0.6 m pixel size	1:34,770	5.5 m [9]	Ortho-rectified by C. Sharples NOT USED: Poor accuracy but 2nd attempt was worse.
25th Feb 1971	567-238 567-240 / *NebraskaJetty_Feb1971a_MGA55.tif/tfw* *NebraskaJetty_Feb1971b_MGA55.tif/tfw*	1500 dpi (2039 dpi) / 0.22 m pixel size	1:10,000	1.8 m [7]	Ortho-rectified by C. Sharples
31st Jan 1975	670-7 / *NebraskaJetty_Jan1975_MGA55.tif/tfw*	1000 dpi (2039 dpi) / 0.55 m pixel size	1:20,000	1.6 m [4]	Ortho-rectified by C. Sharples Nebraska Beach only
27th Sep 1976	700-26 / *NebraskaJetty_Sep1976_MGA55.tif/tfw*	2039 dpi / 0.45 m pixel size	1:30,000	2.1 m [9]	Ortho-rectified by C. Sharples
15th Jan 1979	775-118 / *NebraskaJetty_Jan1979_MGA55.tif/tfw*	2039 dpi / 0.5 m pixel size	1:40,000	1.1 m [6]	Ortho-rectified by C. Sharples
1st Dec 1980	844-79 844-81 844-83 / *NebraskaJetty_Dec1980a_MGA55.tif/tfw* *NebraskaJetty_Dec1980b_MGA55.tif/tfw* *NebraskaJetty_Dec1980c_MGA55.tif/tfw*	2039 dpi / 0.1 m pixel size	1:6,000	1.3 m [7]	Ortho-rectified by C. Sharples
2nd Feb 1981	864-151 / *NebraskaJetty_Feb1981_MGA55.tif/tfw*	2039 dpi / 0.2 m pixel size	1:15,000	2.2 m [6]	Ortho-rectified by C. Sharples (excludes Jetty beach)
10th Feb 1982	906-96 /	2039 dpi / 0.56 m pixel size	1:42,000	1.8 m [9]	Ortho-rectified by C. Sharples

	NebraskaJetty_Feb1982_ MGA55.tif/tfw				Light levels adjusted; Jetty Beach 'washed out' when zoomed out, but veg. line visible zoomed in.
11th Nov 1982	931-84 / *NebraskaJetty_Nov1982_ MGA55.tif/tfw*	2039 dpi / 0.6 m pixel size	1:42,000	2.0 m [7]	Ortho-rectified by C. Sharples
5th Feb 1984	982-76 / *NebraskaJetty_Feb1984_ MGA55.tif/tfw*	2039 dpi / 0.26 m pixel size	1:20,000	1.5 m [8]	Ortho-rectified by C. Sharples
15th Feb 1985	1026-81 / *NebraskaJetty_Feb1985_ MGA55.tif/tfw*	2039 dpi / 0.2 m pixel size	1:15,000	1.3 m [9]	Ortho-rectified by C. Sharples
26th Feb 1986	1059-21 / *NebraskaJetty_Feb1986_ MGA55.tif/tfw*	1000 dpi (2039 dpi) / 0.3 m pixel size	1:12,500	1.9 m [6]	Ortho-rectified by C. Sharples
30th Oct 1986	1071-81 / *NebraskaJetty_Oct1986_ MGA55.tif/tfw*	2039 dpi / 0.5 m pixel size	1:42,000	1.5 m [9]	Ortho-rectified by C. Sharples NOT USED: Poor accuracy along Nebraska w.r.t. Feb. 1986 photo.
8th Mar 1988	1112-189 / *NebraskaJetty_Mar1988_ MGA55.tif/tfw*	1300 dpi (2039 dpi) / 0.7 m pixel size	1:23,000	2.2 m [10]	Ortho-rectified by C. Sharples
22nd Dec 1988	1125-1 / *NebraskaJetty_Dec1988_ MGA55.tif/tfw*	2039 dpi / 0.16 m pixel size	1:12,500	0.6 m [4]	Ortho-rectified by C. Sharples
14th Feb 1990	1150-224 / *NebraskaJetty_Feb1990_ MGA55.tif/tfw*	2039 dpi / 0.56 m pixel size	1:42,000	1.4 m [10]	Ortho-rectified by C. Sharples
31st Jan 1994	1217-85 / *NebraskaJetty_Jan1994_ MGA55.tif/tfw*	2039 dpi / 0.3 m pixel size	1:24,000	1.6 m [11]	Ortho-rectified by C. Sharples
11th Mar 1995	1234-112 / *NebraskaJetty_Mar1995_ MGA55.tif/tfw*	1000 dpi (2039 dpi) / 0.3 m pixel size	1:12,500	1.5 m [10]	Ortho-rectified by C. Sharples
15th Feb 1997	1269-148 / *NebraskaJetty_15thFeb19 97_MGA55.tif/tfw*	1000 dpi (2039 dpi) / 0.3 m pixel size	1:12,500	1.3 m [7]	Ortho-rectified by C. Sharples NOT USED: Very similar shoreline to 12th Feb image but less coverage
12th Feb 1997	1270-66 / *NebraskaJetty_12thFeb19 97_MGA55.tif/tfw*	1500 dpi (2039 dpi) / 0.4 m pixel size	1:24,000	2.3 m [11]	Ortho-rectified by C. Sharples
14th Dec 1999	1320-231 / *NebraskaJetty_Dec1999_ MGA55.tif/tfw*	1000 dpi (2039 dpi) / 0.6 m pixel size	1:20,000	2.5 m [11]	Ortho-rectified by C. Sharples
17th Feb 2001	1346-147 / *NebraskaJetty_Feb2001_ MGA55.ecw*	2039 dpi / 0.5 m pixel size	1:24,000	3.0 m [11] (quoted absolute accuracy ±2.5m)	Ortho-rectified by DPIPWE Original DPIPWE ortho file: 1346_147_op.ecw
28th Mar 2004	1382-256 / *NebraskaJetty_Mar2004_ MGA55.ecw*	2039 dpi / 0.5 m pixel size	1:24,000	2.0 m [11] (quoted absolute	Ortho-rectified by DPIPWE Original DPIPWE ortho file: 1382_256_op.ecw

				accuracy ±2.5m)	
25th Jan 2005	1390-146 / *NebraskaJetty_Jan2005_MGA55.tif/tfw*	1000 dpi (2039 dpi) / 1.18 m pixel size	1:42,000	2.0 m [11]	Ortho-rectified by C. Sharples NOT USED: Jetty Beach accuracy good but poor (~4m) errors along Nebraska Beach
13th Feb 2007	1422-127 / *NebraskaJetty_Feb2007_MGA55.ecw*	2039 dpi / 0.5 m pixel size	1:42,000	1.6 m [11] (quoted absolute accuracy ±15m)	Ortho-rectified by DPIPWE Original DPIPWE ortho file: 1422_127_op.ecw
3rd Jan 2008	1428-074 / *NebraskaJetty_Jan2008_MGA55.ecw*	2039 dpi / 0.5 m pixel size	1:24,000	1.6 m [11] (quoted absolute accuracy ±15m)	Ortho-rectified by DPIPWE Original DPIPWE ortho file: 1428_074_op.ecw NOT USED: Jetty Beach accuracy good but poor (~4m) errors along Nebraska Beach
30th Jan 2010	1443-075 / *NebraskaJetty_Jan2010_MGA55.ecw*	2039 dpi / 0.5 m pixel size	1:42,000	0.0 m [N/A] (quoted absolute accuracy ±15m)	REFERENCE IMAGE (zero relative feature position error by convention) Ortho-rectified by DPIPWE Original DPIPWE ortho file: 1443_075_op.ecw
30th Mar 2012	1471-206 / *NebraskaJetty_Mar2012_MGA55.tif/tfw*	1000 dpi (2039 dpi) / 0.7 m pixel size	1:24,000	2.2 m [11]	Ortho-rectified by C. Sharples
28th Feb 2017	Original digital ortho file: Dennes_Point_28-02-2017.ecw / *NebraskaJetty_Feb2017_MGA55.ecw*	? dpi / 0.1 m pixel size	1:400	1.3 m [7] (quoted absolute accuracy ±0.3m)	Original digital photo by DPIPWE, Ortho-rectified by DPIPWE
18th Mar 2017	Original digital ortho file: *JettyOnly_Mar2017_MGA55.jpg/jgw*	- / 0.06 m pixel size	-	1.6 m [6]	Captured and ortho-rectified by Matt Dell (as *Dennes_Ortho_2017.jpg/jgw*) NOT USED (Close in time to DPIPWE photo but covers smaller area)

Table 15: Digitised shoreline shapefiles produced for Nebraska-Jetty Beach (using ortho-photos listed in Table 14 above).

Date of air photo(s)	Shapefile	Shoreline digitised by	Comments
9th Jan 1948	NebraskaJetty_MGA55_19480109.shp	Chris Sharples (2018)	Low resolution. All beaches: veg line reasonably distinct to somewhat vague, looks a bit ragged (no recent erosion?).
26th Feb 1958	NebraskaJetty_MGA55_19580226.shp	Chris Sharples (2018)	Jetty Beach veg line distinct & straight – some recent erosion? Nebraska Beach veg line mostly distinct but somewhat ragged.

2nd Mar 1965	NebraskaJetty_MGA55_19650302.shp	Chris Sharples (2018)	Fair contrast (in Landscape Mapper) & resolution. Jetty Bch veg line distinct, fairly straight but a bit ragged. Nebraska Bch veg. line distinct and quite ragged – no recent erosion.
16th Jan 1970	NebraskaJetty_MGA55_19700116.shp	Chris Sharples (2018)	NOT USED: shoreline digitised but poor accuracy. Low res. Jetty & Nebraska Beaches veg lines distinct but ragged (No recent erosion)
25th Feb 1971	NebraskaJetty_MGA55_19710225.shp	Chris Sharples (2018)	Good high res image, shadowing allowed for. Jetty Bch veg line distinct but ragged (no recent erosion), wrack obvious on beach. Nebraska veg line distinct but also ragged (no recent erosion, likely some incipient dune grasses).
31st Jan 1975	NebraskaJetty_MGA55_19750131.shp	Chris Sharples (2018)	Nebraska Beach only; low res but veg line clear; Veg line mostly straight but res. not good enough to detect minor raggedness or incipient dune grasses.
27th Sep 1976	NebraskaJetty_MGA55_19760927.shp	Chris Sharples (2018)	Poor contrast, better in Landscape Mapper than ArcGIS. Jetty Beach - N end fairly straight veg line (recent erosion?), S end more ragged. Nebraska veg line generally fairly ragged – little recent erosion?
15th Jan 1979	NebraskaJetty_MGA55_19790115.shp	Chris Sharples (2018)	Poor contrast photo, but veg line mappable in Landscape Mapper. Jetty beach: ragged veg line with some dune blow-outs. Some likely wrack in front. Likely long time since dune erosion. Nebraska B. as for Jetty beach + some likely incipient dune grasses.
1st Dec 1980	NebraskaJetty_MGA55_19801201.shp	Chris Sharples (2018)	Prob. wrack on N end Jetty beach. Veg line ragged on most beaches– no recent erosion. Prob. some incipient dunes, unclear whether wrack in places.
2nd Feb 1981	NebraskaJetty_MGA55_19810202.shp	Chris Sharples (2018)	Excludes Jetty Beach. Shadowing makes veg line difficult to find in parts. Veg line ragged in parts (not recently eroded) but straight in S part of Nebraska Beach, but incipient dune

			grasses evident in most areas.
10th Feb 1982	NebraskaJetty_MGA55_19820210.shp	Chris Sharples (2018)	Poor photo contrast & resolution; best zoomed in Jetty beach veg line distinct, likely erosion scarp = recent erosion? Nebraska B. veg line straight – likely recent erosion?
11th Nov 1982	NebraskaJetty_MGA55_19821111.shp	Chris Sharples (2018)	Poor photo contrast and resolution; Jetty Beach veg line distinct but ragged & interrupted by blowout; some wrack on beach. Nebraska: Veg line ragged. (no recent wave erosion)
5th Feb 1984	NebraskaJetty_MGA55_19840205.shp	Chris Sharples (2018)	Jetty & Nebraska Beach veg lines distinct but ragged, likely some incipient dune grass (not recently eroded).
15th Feb 1985	NebraskaJetty_MGA55_19850215.shp	Chris Sharples (2018)	Both beaches: veg line ragged (not recently eroded), wrack line at N end Jetty Beach noted. Likely incipient dune grass present (hard to tell).
26th Feb 1986	NebraskaJetty_MGA55_19860226.shp	Chris Sharples (2018)	Nebraska Beach only: vegetation line straight and distinct in parts but not everywhere– possibly some recent scarping? Some shadowing obscures veg. line.
30th Oct 1986	NebraskaJetty_MGA55_19861030.shp	Chris Sharples (2018)	Shadows obscure veg line in parts; allowed for. Jetty beach veg line distinct & straight. Nebraska Beach veg line distinct in parts, seems ragged in parts. NOT USED: Poor accuracy along Nebraska w.r.t. Feb. 1986 photo.
8th Mar 1988	NebraskaJetty_MGA55_19880308.shp	Chris Sharples (2018)	Shadows obscure veg line in parts & allowed for. Jetty Beach – distinct straight veg line, no incip dunes evident: recent erosion? Nebraska B. reasonably distinct veg line but ragged in parts
22nd Dec 1988	NebraskaJetty_MGA55_19881222.shp	Chris Sharples (2018)	Shadows partly obscure veg line. Nebraska veg line well defined, straight, partly scarped: recent erosion?
14th Feb 1990	NebraskaJetty_MGA55_19900214.shp	Chris Sharples (2018)	Jetty B veg line well defined & straight, likely recent erosion scarp. Nebraska Beach as for

			Jetty B. No incipient dune veg identified
31st Jan 1994	NebraskaJetty_MGA55_19940131.shp	Chris Sharples (2018)	Jetty: Vegetation line somewhat ragged (no recent erosion) with probable incipient dune grasses. Nebraska: as for Jetty. Poor contrast in photo.
11th Mar 1995	NebraskaJetty_MGA55_19950311.shp	Chris Sharples (2018)	Jetty: Veg line is well-defined erosion scarp, incipient dunes not distinguishable. Nebraska: Shadowing allowed for. Vegetation line distinct, somewhat ragged.
12th Feb 1997	NebraskaJetty_MGA55_19970212.shp	Chris Sharples (2018)	Shadows make veg line hard to pick in places. Jetty B. veg line is prominent scarp, a bit ragged. Nebraska veg. line ragged, poss. some incipient dunes?
15th Feb 1997	NebraskaJetty_MGA55_19970215.shp	NOT USED:	Strong easterly shadows make veg line difficult to map in parts. Jetty & Nebraska veg line is prominent scarp; flotsam seen but prob. no incipient dunes? Significant erosion not recovered yet. NOT USED: Very similar shoreline to 12th Feb image but less coverage.
14th Dec 1999	NebraskaJetty_MGA55_19991214.shp	Chris Sharples (2018)	Jetty: ragged (slumped scarp?) veg line behind wrack lines. Nebraska: somewhat ragged veg line, likely includes incipient dunes; implies no recent erosion.
17th Feb 2001	NebraskaJetty_MGA55_20010217.shp	Chris Sharples (2018)	Jetty – Veg line distinct, much incipient dune growth evident. Nebraska – veg line distinct, prob. incipient dunes accreting.
28th Mar 2004	NebraskaJetty_MGA55_20040328.shp	Chris Sharples (2018)	Jetty - veg. line vague due to wrack but veg colour helps; incipient dune visible in front of older scarp line. Nebraska - more distinct scarped veg line, less evidence of wrack or incipient dunes
25th Jan 2005	NebraskaJetty_MGA55_20050125.shp	Chris Sharples (2018)	Vegetation line poorly defined due to poor resolution. Some morning shadowing allowed for. NOT USED: Poor (~4m) errors along Nebraska beach.

13th Feb 2007	NebraskaJetty_MGA55_20070213.shp	Chris Sharples (2018)	Whole beach. Vegetation line generally distinct but poor resolution. No incipient dunes identifiable. Overhanging trees allowed for.
3rd Jan 2008	NebraskaJetty_MGA55_20080103.shp	Chris Sharples (2018)	Whole Beach. Vegetation line distinct. Poor resolution. No incipient dunes identified. Overhanging trees allowed for. NOT USED: Jetty Beach accuracy good but poor (~4m) errors along Nebraska Beach
30th Jan 2010	NebraskaJetty_MGA55_20100130.shp	Chris Sharples (2018)	Whole beach. Vegetation line mainly sharp and distinct, likely mostly scarped? Numerous overhanging trees allowed for. Shadowing not apparent (overcast day?).
30th Mar 2012	NebraskaJetty_MGA55_20120330.shp	Chris Sharples (2018)	Whole beach. Distinct scarp + some incipient dunes on Jetty beach. Distinct scarp dominates Nebraska Bch, some incipient dunes. NE shadowing allowed for.
28th Feb 2017	NebraskaJetty_MGA55_20170228.shp	Chris Sharples (2018)	Whole Beach. Scarped veg line clear in many places but obscured by trees and shadows in parts. Wood / boulder wall mapped in parts – not always distinguishable from veg scarp.
18th Mar 2017	NebraskaJetty_MGA55_20170318.shp	Chris Sharples (2017)	Covers Jetty beach to north end Nebraska Beach only; Veg line fairly distinct scarp in parts but confused by flotsam in a few places. Significant incipient dune growth since 2012. North end Nebraska Beach veg line is mainly boulder wall. NOT USED: Close in time to Feb 2017 photo but covers smaller area

A1.2.3 Gordon (D'Entrecasteaux Channel)

Locality and general description

Study area is sandy shoreline immediately north of two sandy spits (Three Hut Point and another north of it). These have mostly artificially hardened shores, inferred to indicate they were eroding in the past. Date of hardening unclear and not obvious from air photos. Sandy bedforms moving northwards up coast are clearly visible in the shallow water adjacent study area. It is inferred the sandy spits were previously migrating northwards, and their hardening has both stopped this migration and reduced the sand supply for northwards drift, causing a sand deficit and shoreline erosion and recession at the study area.

In recent years the eroding study area shoreline has also been artificially hardened to prevent further shoreline recession. See unpublished consulting report by Sharples (2012) for further details of this site (noting that report was prepared prior to the air photo analysis undertaken for this thesis.

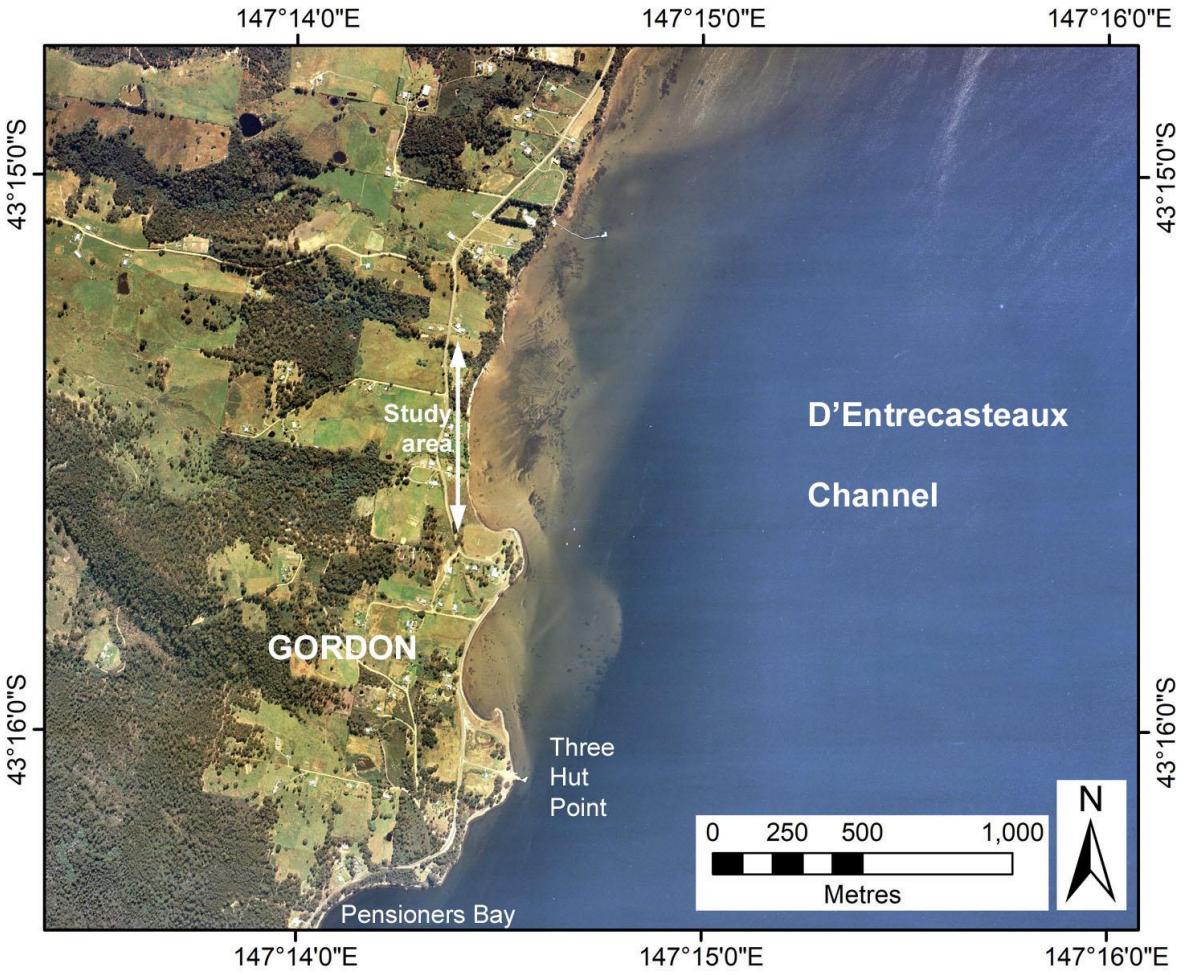

Figure 72: Gordon study area, showing the shallow mobile sand bars that are a key characteristic of this area. Oyster racks and dark patches inferred to be seagrass are visible. The two points immediately south of the study area (including Three Hut Point) are slightly recurved sand spits (Farmer & Forsyth 1993) which are inferred to have been supplying sand to the shallow offshore zone, where it was driven northwards alongshore by attenuated swells moving up D'Entrecasteaux Channel. The erosion and accretion of sand is inferred to have also been causing the sandy points themselves to slowly migrate northwards until they were stabilised with hardened shores. Air photo dated 23rd February 1996 (© DPIPWE).

Swell wave climate

An attenuated swell penetrates northwards to this site from the dominantly south-westerly swells entering the southern end of D'Entrecasteaux Channel and refracting northwards. Given that dominant wind directions at this site are mostly directed offshore (see below), the attenuated swell is

the most likely driver of storm waves reaching this site, and of nearshore northwards littoral currents driving sand past the study site (see Figure 72). However, whilst moderately energetic swell waves may erode the site during stormy conditions, during fair weather conditions the swell this far up D'Entrecasteaux Channel is weak and likely to be only a slow driver of sand to and along the site.

Wind (wind wave) climate

There is no nearby long-term wind record for the Gordon study site, however regional records such as that from Cape Bruny (see Figure 78) suggest dominantly westerly to south-westerly air-flows over the general area. From this it is reasonable to infer that the dominating winds at the east-facing Gordon study site shore would mainly blow offshore. Thus wind-waves generated by such winds in D'Entrecasteaux Channel would be directed offshore away from the site and would not normally drive either shoreline erosion or the northwards littoral drift at the site. Onshore directed wind-waves would only be expected during very infrequent easterly weather.

Sand transport and budget

Dominant northwards littoral sand drift into, along and out of the study site shore (see Figure 72). Clearly visible from sandy bedforms in shallow water adjacent shore.

Air photo analysis

The southern half of the study site mostly exhibits a clearly-defined vegetation line shoreline (which is certainly an erosion scarp in more recent photos and in many older photos), with only a few overhanging trees and shrubs obscuring the shoreline which can generally be confidently extrapolated beneath then. However, seagrass beds are evident in the sandy shallow subtidal zone, and seagrass wrack sometimes partly obscures the shoreline, although this is mostly recognisable and can be allowed for. The northern half of the study site shore is mostly obscured by tree canopies and shadowing at most air photo dates and has only been fully mapped at a few dates when camera angle or lighting conditions allow sections of the shoreline to be seen between and through the tree canopies.

Shore behaviour history from air photos

The shoreline history plots for the receded southern part of the study area (Figure 74, Figure 75) yield a good overall fit (R^2=0.8563) to a linear recession trend over the whole period. However, visual inspection suggests an inflection point in the plots circa 1980, with little net shoreline change before that date and a strong progressive recession trend thereafter. This was tested with piecewise linear regression fits to the south area summary history plot pre- and post-1980 (Figure 76). A slow recession trend prior to 1980 is suggested, however this trend is of lesser overall magnitude than the error margins of all but one of the relevant air photo data points, hence shoreline stability over this period is also quite likely. In contrast, a very strong linear recession trend is evident after 1980 (R^2=0.9442), of significantly greater magnitude than the relevant air photo margins, with an average rate of 0.40 m/yr recession.

Shoreline behaviour drivers and conditions

Portions of the two prominent sand-spits immediately south of the Gordon study site are hardened with boulders and rock revetments. Unfortunately, the construction date or dates for these shore protection works are unknown, and the revetments (or their absence) are difficult to distinguish on older air photos. Construction during the mid-Twentieth Century – possibly in stages – appears likely but is unconfirmed.

The distribution of shallow-water sand bars extending northwards from the two sand spits indicates these spits are the likely source of the sand being driven northwards along the study area shoreline

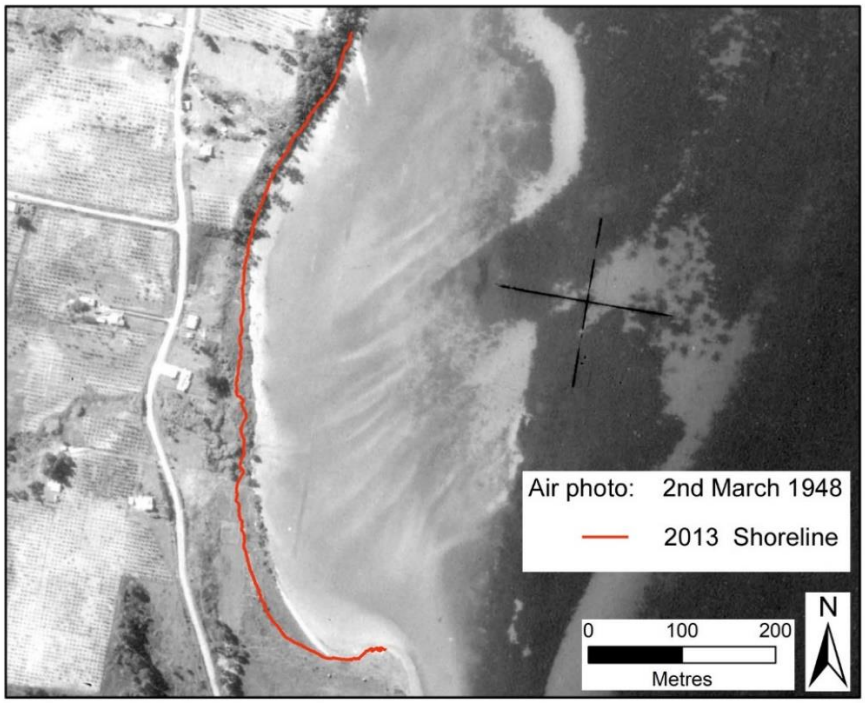

Figure 73: Comparison of 1948 (air photo) and 2013 (red line) shoreline positions at Gordon. The northern part of the study shoreline is immediately backed by exposed bedrock (Farmer & Forsyth 1993) and has shown negligible change over the air photo periods. The southern area – which has exhibited up to 20 metres of shoreline recession over the same period – is underlain and backed by a sand platform above High-Water Mark that extends inland to the foot of a short steep bedrock slope.

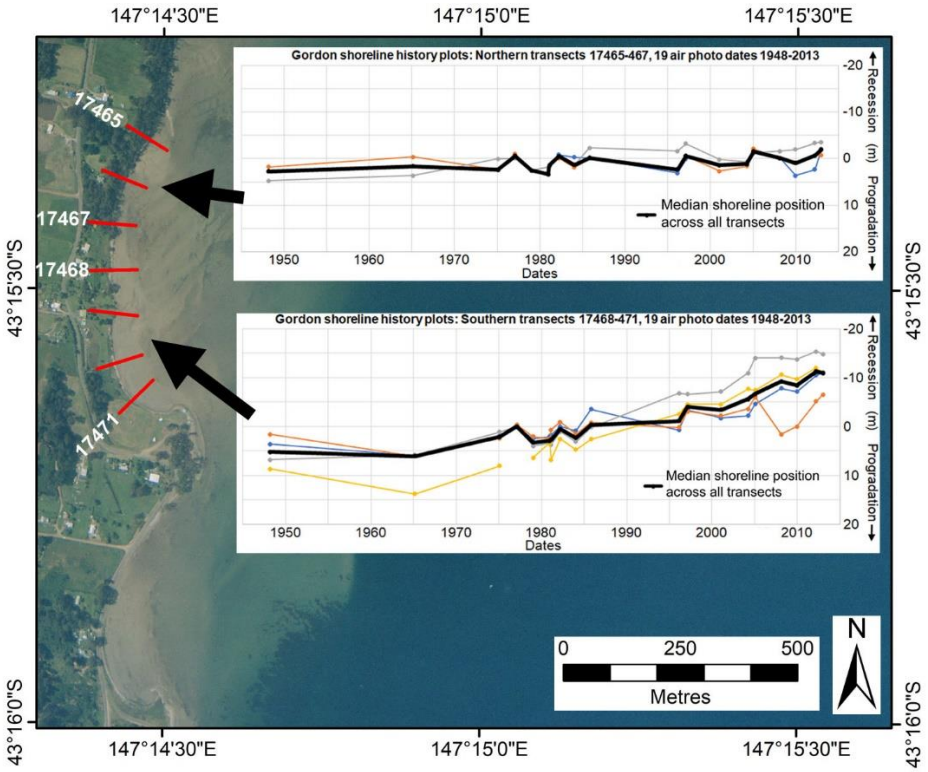

Figure 74: Shoreline position changes along all individual transects for Gordon shoreline, at 19 air photo dates from 1948 to 2013 as listed on Table 16 & Table 17. The plots are split into two groups demonstrating the markedly different historical behaviour between the northern (stable) and southern (receded) parts of the study area. The transects used are 100m – spaced red lines on the air photo, with selected transects numbered. See also summary plot Figure 75 below. The background image is the 2009 air photo (© DPIPWE).

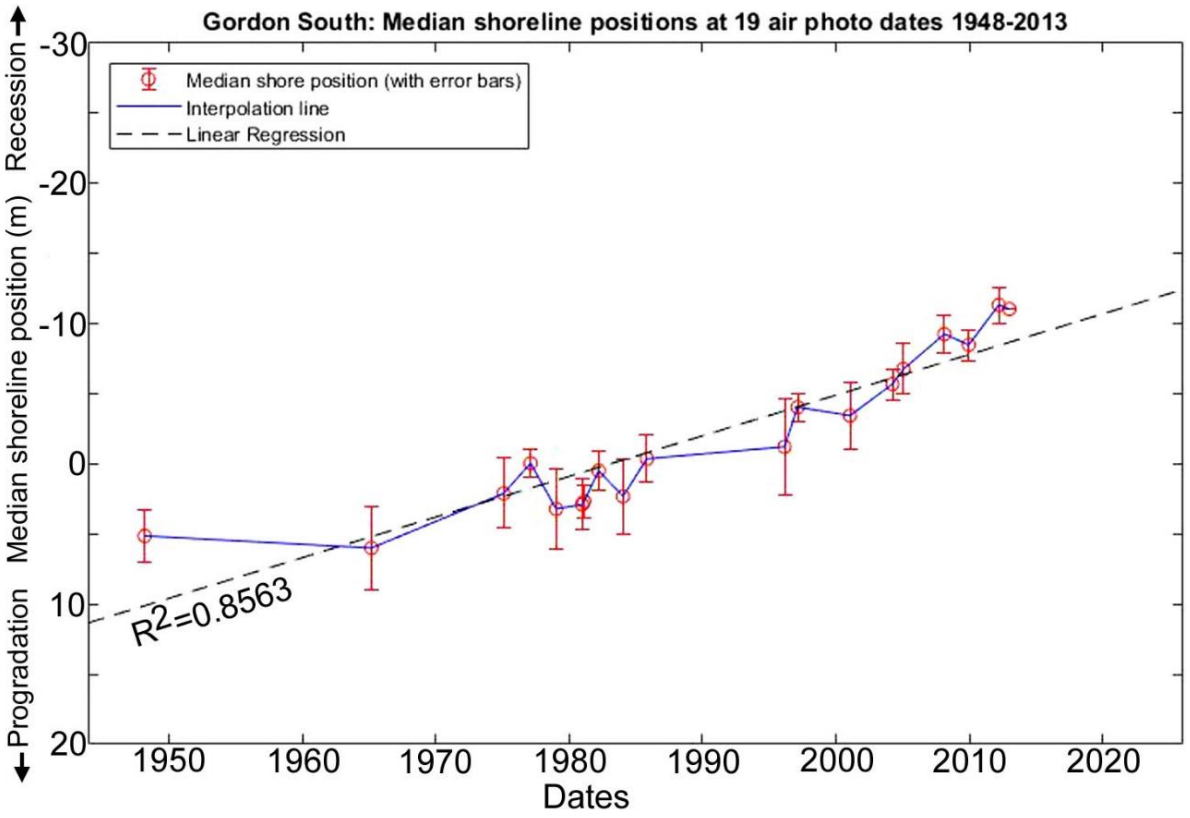

Figure 75: Summary plot of shoreline change history for the south (receded) part of the Gordon study area at 19 air photo dates from 1948 to 2013. This plots the median of the shoreline positions at each date across transects 17468-471 as shown in Figure 74, with a linear fit (first-order linear regression) over the whole air photo period.

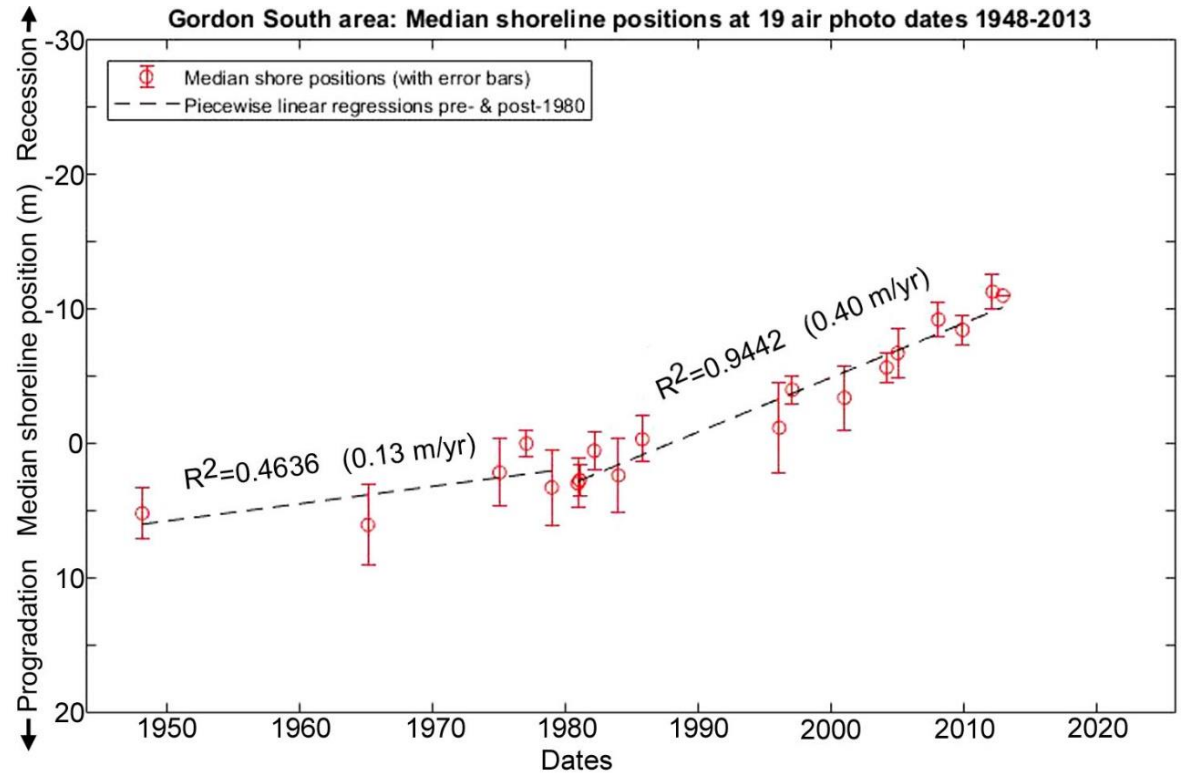

Figure 76: Summary plot of shoreline change history for the south (receded) part of the Gordon study area at 19 air photo dates from 1948 to 2013. Piecewise linear regression fits pre- and post-1980 demonstrate an equivocal slow recession trend (or stability?) prior to 1980 (see text), changing to a strong progressive recession trend after 1980.

(e.g., see Figure 72). The shoreline south of the two sand spits is a hard-rock shore which cannot be a sand source. It is reasonable to assume that the revetments were constructed to prevent shoreline erosion around the sand spits which were providing a source for the sand moving north, and that this would have significantly reduced the amount of sand drifting north to the study site, leading to a reduction in sand reaching this shore and compensating for sand eroded from it and drifted further north.

The summary shoreline history plots (Figure 75 & Figure 76) indicate a clear acceleration of shoreline retreat after the arbitrary date of 1980 chosen for the piecewise linear regression analysis shown in Figure 76, and it can be less confidently inferred from the interpolated plot lines on Figure 75 that a change from a stable to receding shoreline may have occurred between the air photo dates of 1965 and 1975.

In the absence of other plausible explanations, the acceleration of shoreline recession might plausibly be inferred to be a result of sea-level rise as has inferred for other sites examined in this project. However the construction of artificial hardening updrift from the study site can be expected to have caused a significant reduction in sand supply to that site resulting in a shift towards a more negative sand budget which begins to lose more sand during erosion events than it subsequent gains from the south, and so shifts towards more shoreline recession than previously. Although sea-level rise may be a contributing factor, given that the known artificial disturbance to the sand budget has been a likely driver of shoreline recession at the site since sometime during the Twentieth Century it is inferred that this is very likely to have been a driver of the observed change, and possibly the dominant driver.

Air photo data tables

The following tables provide details of the air photos used, the resulting ortho-photos produced, and the shapefiles representing the shoreline position that were digitised from the ortho-photos.

Table 16: Original air photos and ortho-rectified air photos produced for Gordon.

Photo Date	**Original DPIPWE air photos (film-frame) / Ortho-photo name**	**Final image resolution (original scan resolution if downsized) / pixel size of final ortho-photo**	**Original photo scale**	**Mean measured feature position error (± metres) for ortho-photo** [no. of measured feature position reference points]	**Comments**
2nd Mar 1948	182-3992 / *Gordon_Mar1948_MG A55.tif/tfw;*	600 dpi / 0.8 m pixel size	1:15,840	1.9 m [9]	Ortho-rectified by Chris Sharples
2nd Mar 1965	453-72 / *Gordon_Mar1965_MG A55.tif/tfw;*	2039 dpi / 0.4 m pixel size	1:31,680	3.0 m [9]	Ortho-rectified by Chris Sharples
31st Jan 1975	665-23 / *Gordon_Jan1975_MG A55.tif/tfw;*	2039 dpi / 0.6 m pixel size	1:40,000	2.5 m [10]	Ortho-rectified by Chris Sharples
7th Feb 1977	710-7 / *Gordon_Feb1977_MG A55.tif/tfw;*	2039 dpi / 0.1 m pixel size	1:6,400	1.0 m [7]	Ortho-rectified by Chris Sharples
6th Jan 1979	772-235 / *Gordon_Jan1979_MG A55.tif/tfw;*	2039 dpi / 0.5 m pixel size	1:40,000	2.8 m [9]	Ortho-rectified by Chris Sharples
21st Dec 1980	846-229 / *Gordon_Dec1980_MG A55.tif/tfw;*	2039 dpi / 0.25 m pixel size	1:15,000	1.8 m [10]	Ortho-rectified by Chris Sharples

13th Feb 1981	870-126 / *Gordon_Feb1981_MGA55.tif/tfw*	2039 dpi / 0.2 m pixel size	1:15,000	1.2 m [9]	Ortho-rectified by Chris Sharples
18th Mar 1982	917-207 / *Gordon_Mar1982_MGA55.tif/tfw*	1500 dpi (2039 dpi) / 0.5 m pixel size	1:30,000	1.4 m [10]	Ortho-rectified by Chris Sharples
14th Jan 1984	978-204 / *Gordon_Jan1984_MGA55.tif/tfw*	1500 dpi (2039 dpi) / 0.4 m pixel size	1:20,000	2.7 m [10]	Ortho-rectified by Chris Sharples
29th Oct 1985	1042-215 / *Gordon_Oct1985_MGA55.tif/tfw*	2039 dpi / 0.2 m pixel size	1:15,000	1.7 m [10]	Ortho-rectified by Chris Sharples
23rd Feb 1996	1249-153 / *Gordon_Feb1996_MGA55.tif/tfw*	1500 dpi (2039dpi) / 0.36 m pixel size	1:20,000	3.4 m [10]	Ortho-rectified by Chris Sharples
15th Feb 1997	1271-102 / *Gordon_Feb1997_MGA55.tif/tfw*	1500 dpi (2039dpi) / 0.2 m pixel size	1;12,500	1.0 m [8]	Ortho-rectified by Chris Sharples
21st Jan 2001	1344-117 / *Gordon_Jan2001_MGA55.ecw*	2039 dpi / 0.5m pixel size	1:24,000	2.4 m [9] (quoted absolute accuracy ±2.5m)	Ortho-rectified by DPIPWE Original DPIPWE ortho file: 1344_117_op.ecw (Secondary REFERENCE IMAGE for ortho-rectification)
28th Mar 2004	1382-196 / *Gordon_Mar2004_MGA55.ecw*	2039 dpi / 0.5 m pixel size	1:24,000	1.1 m [10] (quoted absolute accuracy ±2.5m)	Ortho-rectified by DPIPWE Original DPIPWE ortho file: 1382_196_op.ecw
25th Jan 2005	1390-236 / *Gordon_Jan2005_MGA55.ecw*	2039 dpi / 0.5 m pixel size	1:42,000	1.8 m [9] (quoted absolute accuracy ±15m)	Ortho-rectified by DPIPWE Original DPIPWE ortho file: 1390_236_op.ecw
18th Feb 2008	1433-033 / *Gordon_Feb2008_MGA55.ecw*	2039 dpi / 0.5m pixel size	1:24,000	1.3 m [9] (quoted absolute accuracy ±15m)	Ortho-rectified by DPIPWE Original DPIPWE ortho file: 1433_033_op.ecw
15th Dec 2009	1440-240 / *Gordon_Dec2009_MGA55.ecw*	2039 dpi / 0.5 m pixel size	1:42,000	1.1 m [10] (quoted absolute accuracy ±15m)	Ortho-rectified by DPIPWE Original DPIPWE ortho file: 1440_240_op.ecw
19th Mar 2012	1469-131 / *Gordon_Mar2012_MGA55.tif/tfw*	1500 dpi (2039 dpi) / 0.4 m pixel size	1:24,000	1.27 m [10]	Ortho-rectified by Chris Sharples
2013 (Specific date not supplied)	Original digital ortho files: Gordon_2013_2.ecw / *Gordon_2013_MGA55.ecw.*	- / 0.1 m pixel size	-	0.0 m N/A	REFERENCE IMAGE (zero relative feature position error by convention) Digital original photo. Captured and ortho-rectified by Matt Dell

Table 17: Digitised shoreline shapefiles produced for Gordon, (using ortho-photos listed in Table 16 above).

Date of air photo(s)	Shapefile	Shoreline digitised by	Comments
2nd Mar 1948	Gordon_MGA55_19480302.shp	Chris Sharples (2019)	Moderate resolution, good contrast. Vegetation line = mapped shoreline, mostly distinct against sandy intertidal zone, mostly visible (some tree canopies and shadows allowed for).
2nd Mar 1965	Gordon_MGA55_19650302.shp	Chris Sharples (2019)	Good resolution, moderate contrast. Vegetation line = shoreline. Shoreline well-defined in parts but obscured by likely wrack and veg. canopies in part. N. end too obscured to map.
31st Jan 1975	Gordon_MGA55_19750131.shp	Chris Sharples (2019)	Moderate resolution and contrast. Vegetation line = shoreline well defined. Some overhanging vegetation allowed for. N. end mostly obscured by tree canopies.
7th Feb 1977	Gordon_MGA55_19770207.shp	Chris Sharples (2019)	Good resolution and contrast. South end of study area missing. Vegetation line = shoreline well defined. Some overhanging vegetation allowed for.
6th Jan 1979	Gordon_MGA55_ 19790106.shp	Chris Sharples (2019)	Moderate resolution, moderate to poor contrast. Vegetation line =shoreline clear in parts, but poorly defined in some areas. Clearly scarped in part. Some overhanging vegetation allowed for.
21st Dec 1980	Gordon_MGA55_19801221.shp	Chris Sharples (2019)	Moderate resolution, moderate to poor contrast. Vegetation line =shoreline clear in parts, but poorly defined in some areas. Some overhanging vegetation allowed for.
13th Feb 1981	Gordon_MGA55_19810213.shp	Chris Sharples (2019)	Good resolution and contrast. Vegetation line = erosion scarp in parts = shoreline clearly defined in S half, mostly hidden by shadows and tree canopies in North half.
18th Mar 1982	Gordon_MGA55_19820318.shp	Chris Sharples (2019)	Moderate resolution, good contrast. Veg. line = erosion scarp = mapped shoreline. Shoreline mostly clearly distinguishable, some overhanging trees

			accounted for. Wrack clearly distinguishable.
14th Jan 1984	Gordon_MGA55_19840114.shp	Chris Sharples (2019)	Moderate resolution, good contrast. Veg. line = erosion scarp = mapped shoreline. Shoreline mostly clearly distinguishable, some overhanging trees accounted for.
29th Oct 1985	Gordon_MGA55_19851029.shp	Chris Sharples (2019)	Moderate resolution, moderate to poor contrast. Veg. line = erosion scarp = mapped shoreline. Shoreline vague in parts, some overhanging trees accounted for.
23rd Feb 1996	Gordon_MGA55_19960223.shp	Chris Sharples (2019)	Moderate resolution, good contrast. Veg. line = erosion scarp = mapped shoreline. Shoreline mostly clearly distinguishable, some overhanging trees accounted for.
15th Feb 1997	Gordon_MGA55_19970215.shp	Chris Sharples (2019)	Good resolution and contrast. Veg. line = erosion scarp = mapped shoreline. Shoreline mostly clearly distinguishable, some overhanging trees accounted for.
21st Jan 2001	Gordon_MGA55_20010121.shp	Chris Sharples (2019)	Moderate resolution and contrast. Veg. line = erosion scarp = mapped shoreline. Shoreline mostly clearly distinguishable, some overhanging trees accounted for.
28th Mar 2004	Gordon_MGA55_20040328.shp	Chris Sharples (2019)	Good resolution and contrast. Veg. line = erosion scarp = mapped shoreline. Shoreline mostly clearly distinguishable, some overhanging trees accounted for. North area too obscured, not mapped.
25th Jan 2005	Gordon_MGA55_20050125.shp	Chris Sharples (2019)	Coarse resolution, moderate contrast. Veg. line = erosion scarp = mapped shoreline. Shoreline poorly defined and partly obscured by overhanging trees etc, especially in north area, allowed for as necessary.
18th Feb 2008	Gordon_MGA55_20080218.shp	Chris Sharples (2019)	Coarse resolution, moderate contrast. Veg. line = erosion scarp = mapped shoreline. Shoreline partly obscured by overhanging trees etc, especially in north area,

			allowed for as necessary.
15th Dec 2009	Gordon_MGA55_20091215.shp	Chris Sharples (2019)	Moderate resolution and contrast only. Veg. line = erosion scarp = mapped shoreline. Shoreline is partly obscured by shadows and overhanging trees, esp. north end.
19th Mar 2012	Gordon_MGA55_20120319.shp	Chris Sharples (2019)	Good resolution. Veg. line = erosion scarp = mapped shoreline. Shoreline is partly obscured by shadows and overhanging trees.
DD MM 2013 (day-month date not supplied for ortho-photo)	Gordon_MGA55_20130101.shp	Chris Sharples (2019)	Very good resolution. Veg. line = erosion scarp = mapped shoreline. Shoreline is partly obscured by shadows and overhanging trees.

A1.2.4 Cloudy Lagoon (south Bruny Island)

Locality and general description

Three sections of the lagoon shoreline (north, east, and south) were selected for shoreline history studies (Figure 77). These sections exhibit mostly clearly defined vegetation-edge shorelines on high-contrast sandy shoreline sections and are free of obscuring overhanging tree canopies. Intervening shoreline sections omitted from this study are hard bedrock shore. Extensive fresh erosion scarps in semi-lithified sands along the north-western shore of Cloudy Bay Lagoon were also observed during fieldwork by the writer. These are inferred to be actively receding and ideally would have been mapped for this project using the air photo time series. However, this turned out to be impractical because of extensive overhanging tree canopies at most air photo dates which made collection of accurate shoreline change data very difficult or impossible.

Swell wave climate

Swell-sheltered tidal lagoon, locally generated wind waves only.

Wind (wind wave) climate

Dominantly westerly (NW to SW) winds at Cape Bruny (10km to SE). See Figure 78. The anomalous northerly wind component is unexplained but possibly a result of local topographic steering effects at Cape Bruny.

Sand transport and budget

All three lagoon sites demonstrate recession. The only available sink for sand lost from the receded lagoon shores is within the lagoon itself. Aerial photography suggests that the parts of the lagoon furthest from the entrance and closest to the receded shores do indeed still have more (deeper) accommodation space. Likely sand transport pathway following erosion is via tidal currents into deeper central parts of the lagoon. BUT likely very weak tidal currents (because at distal end of lagoon), thus not very efficient sand loss and some returns to shore likely.

Artificial disturbances

None identified that could affect shoreline

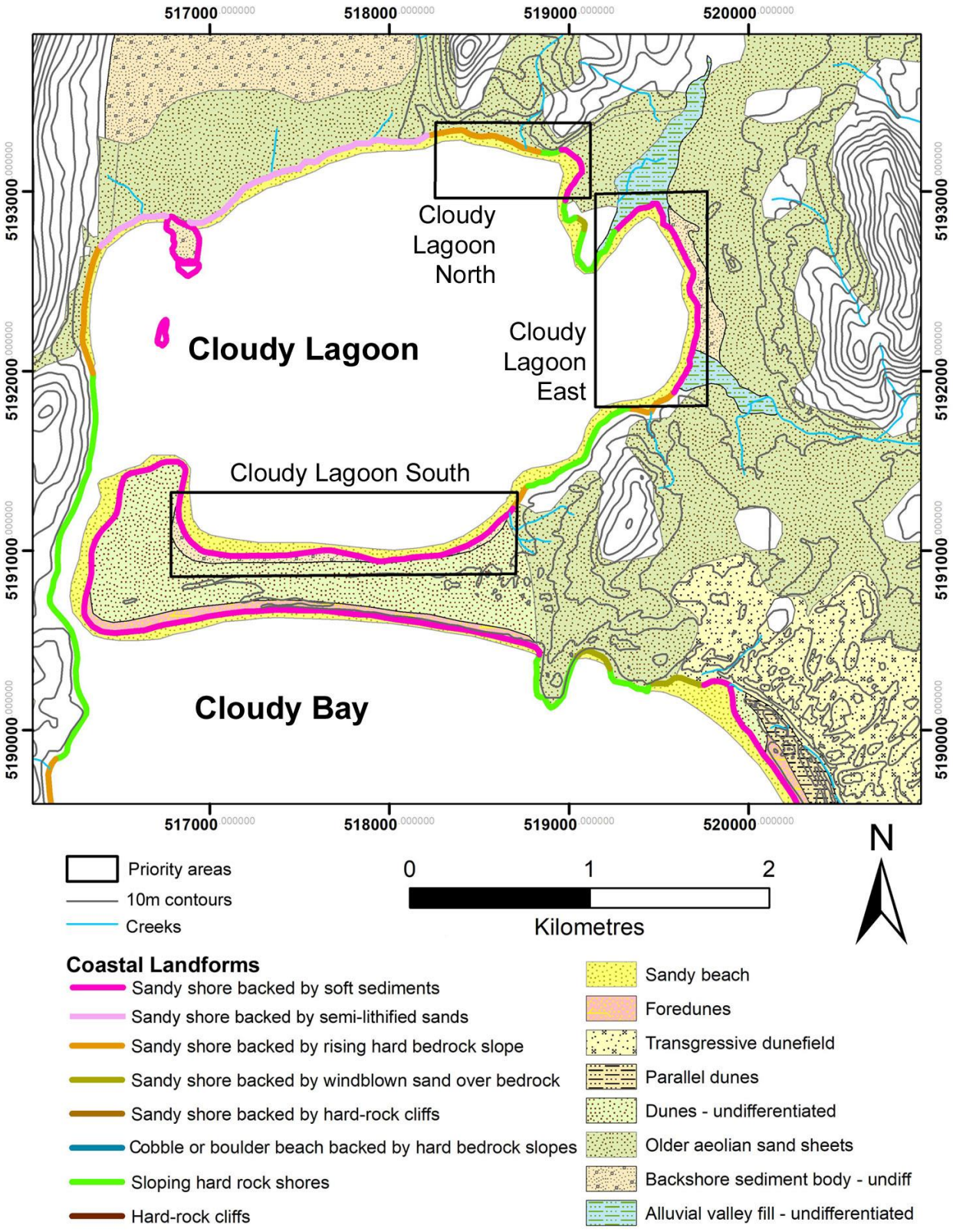

Figure 77: Coastal landforms at Cloudy Bay Lagoon, indicating the three priority areas selected for air photo history analysis. Coastal landform mapping is based on the 1:50,000 Dover Geological map sheet (Geological Survey of Tasmania), with additional field observations by C. Sharples. Co-ordinate system is Map Grid of Australia Zone 55 (GDA1994 datum).

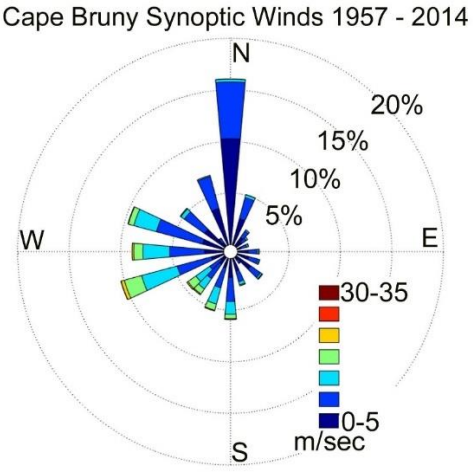

Figure 78: Cape Bruny synoptic wind directions 1957 – 2014. Cape Bruny, 10 km south-west of Cloudy Lagoon, is the nearest long-term weather station. Wind rose prepared by Chris Sharples, using original synoptic wind data from the Australian Bureau of Meteorology.

Air photo analysis

This analysis uses the same ortho-photos and digitised shoreline shapefiles as used for Cloudy Beaches East and West. See metadata in section A1.3.1.

At most air photo dates sea-grass meadows are notable in shallow waters within the lagoon. Wrack from these meadows is abundant along some lagoon shores at some air photo dates, although at some other dates (e.g., 31st Jan. 1975) the air photos show little of any shoreline wrack. The wrack is (in part) easily recognisable as dark parallel lines on sandy shores to seawards (lagoon-wards) of the *in situ* living vegetation line mapped as the shoreline. However, in some areas the distribution of wrack is more amorphous and not easy to distinguish from the living (terrestrial) vegetation line. In some cases, the vegetation line was indistinguishable in places and could not be mapped. Wrack was noted to be more abundant on west- or southwest-facing shores, and in the eastern half of the lagoon generally, reflecting the dominant role of westerly to south-westerly wind waves in wrack drift. The vegetation line shore tended to be most easily recognisable on shores sheltered from direct westerly or south-westerly wind-waves.

Cloudy Lagoon South

Low sandy beach ridges. Morphology suggests these prograded from the lagoon side rather than simply being the back side of the original sand spit. The position of this shoreline was mapped from air photos at 17 dates from 1948 to 2009 (unfortunately with a large temporal gap in available air photo coverage between 1948 and 1975). The shoreline (vegetation line) in this area was mostly clearly identifiable, with potentially confusing wrack lines being distinctive and mostly absent from the more sheltered western half of this area.

Shoreline change plots along individual transects (Figure 79) indicate a mostly stable shoreline over the air photo period, although in the more wind-exposed eastern part of this area there has evidently been a large shoreline erosion event between 1948 and 1975 followed by shoreline recovery prior to 1980. Plotting the median shoreline position across all transects at each air photo date (Figure 80) identifies the same erosion-recovery event as being of a magnitude exceeding air photo error margins and thus probably real. A linear fit to the data (Figure 80) suggests a small overall shoreline recession trend (Pearson correlation co-efficient r^2=0.2497), however pre-1980 this is overwhelmed by the erosion-recovery episode and post-1980 does not generally exceed air photo error margins, thus cannot be unequivocally demonstrated.

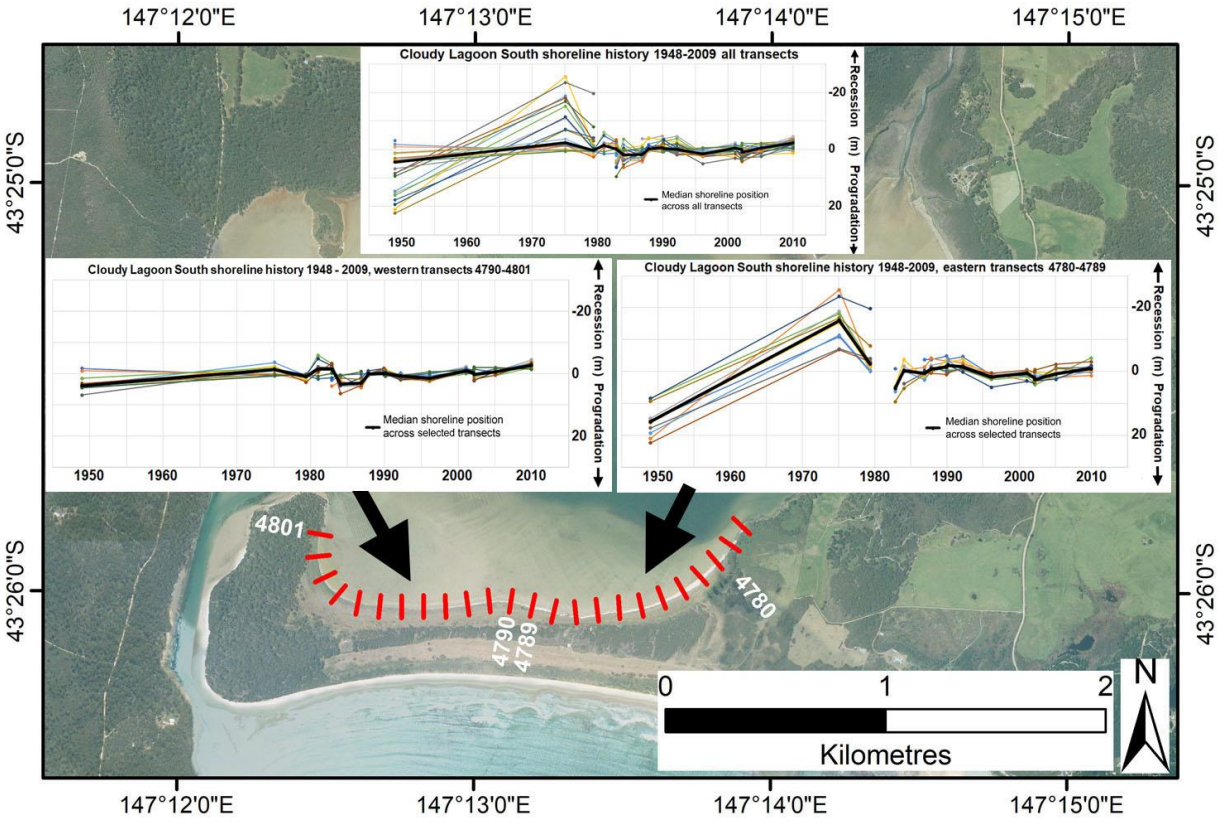

Figure 79: Shoreline position changes along all individual transects for Cloudy Lagoon South shoreline, for 17 air photo dates from 1948 to 2009 as listed on Table 20 & Table 21. The upper insert plot shows shoreline histories on all transects; these are split into two groups on the lower two insert plots. The transects used are 100m – spaced red lines on the air photo. See also summary plot Figure 80 below. The background image is the 2009 air photo (© DPIPWE).

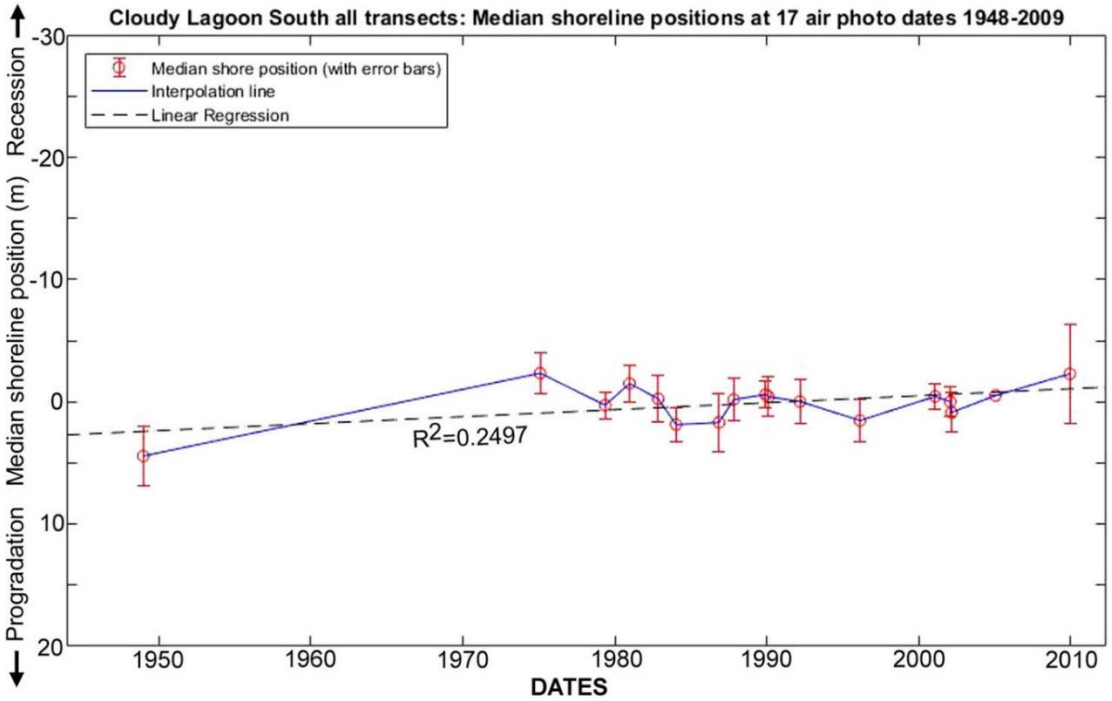

Figure 80: Summary plot of shoreline change history across all transects (as shown on Figure 79) at Cloudy Lagoon South shoreline for 17 air photo dates from 1948 to 2009, with air photo error bars and linear fit.

In summary, the sheltered lagoon shoreline in the Cloudy Lagoon South area has been essentially stable over the air photo period 1948 to 2009, with a possible non-significant trend towards recession but no long-term change of behaviour. Some erosion and recovery (dynamic equilibrium) has occurred, particularly in the more wind-exposed eastern part prior to 1980.

Cloudy Lagoon East

Changes in the position of this shoreline were mapped from air photos at 16 dates from 1948 to 2009 (see Table 20), along eighteen 100m – spaced transects. One available air photo date (for 14th Nov. 1986) did not cover this area. Large wrack accumulations are visible on this shore at most air photo dates, however the shoreline (living vegetation line) was mostly distinctive and mappable. This shoreline has the longest fetch across the lagoon from the south-west (dominant wind) direction and at some dates had the largest wrack accumulations seen in the Cloudy Lagoon air photos.

The dominant trend for this shoreline revealed by the air photo history is a simple progressive shoreline recession trend over the whole air photo period (1948 to 2009), with no apparent acceleration or change in the trend (Figure 81).

The recession trend is mostly linear over time on all transects, except for an anomalous period of apparent major erosion and progradation during the 1980 to 1985 period (Figure 81). Inspection of the air photos from that period, particularly around the transects having the most anomalous histories (4761 & 4756), suggests that the anomaly is more apparent than real: very large wrack accumulations occurred around the most anomalous transects during this period and may have obscured the actual *in situ* vegetation line resulting in misleading mapping of shoreline positions. That is, during the 1980 – 1985 period there seems to have been a major wrack accumulation event (but probably not a shoreline change event).

Summary Figure 82 shows the median shoreline position across all transects at each air photo date. Even with the 1980 – 1985 anomaly included, there is a significant linear shoreline recession trend (r^2 = 0.6095) over the whole air photo period, whose overall scale is beyond most air photo error margins and so undoubtedly real.

Cloudy Lagoon North

Changes in the position of this shoreline were mapped from air photos from 13 dates from 1975 to 2009 (available air photos (Table 20) for 15th Dec. 1948, 21st Dec. 1980, 14th Nov. 1986 and 5th Mar. 2002 did not cover this area). The shoreline (vegetation line) in this area was mostly clearly identifiable, with some potentially confusing wrack lines being distinctive and identifiable.

Some variability in apparent shoreline histories is evident along individual transects (see Figure 83), which is likely due to a combination of real variability and errors related to ortho-rectification and wrack obscuring in situ vegetation lines. However, across the whole site a small but statistically significant overall recession trend since prior to 1975 is evident (R^2=0.5994) as shown in Figure 84. Over the air photo period the recession trend appears linear with no suggestion of acceleration.

Air photo data

This analysis uses the same ortho-photos and digitised shoreline shapefiles as used for Cloudy Beaches East. See metadata in Section A1.3.1.

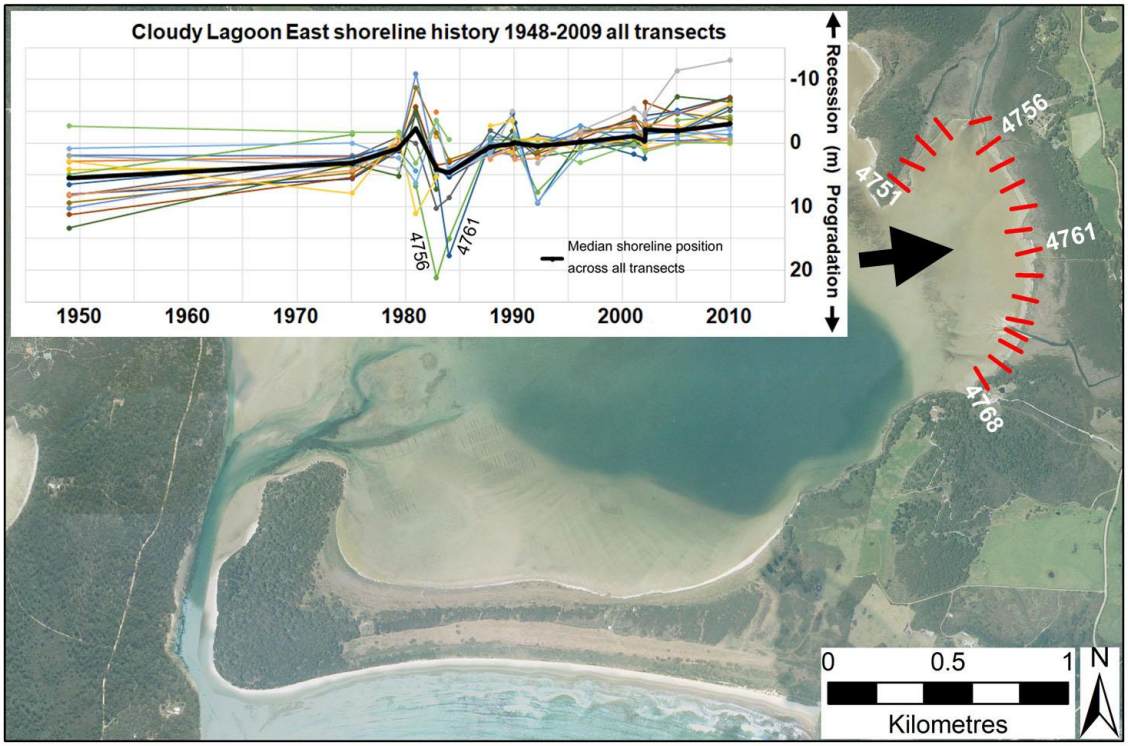

Figure 81: Shoreline position changes along all individual transects for Cloudy Lagoon East shoreline, for 16 air photo dates from 1948 to 2009 as listed on Table 20 & Table 21. The transects used are 100m – spaced red lines on the air photo, with selected transect numbers indicated. The background image is the 2009 air photo (© DPIPWE).

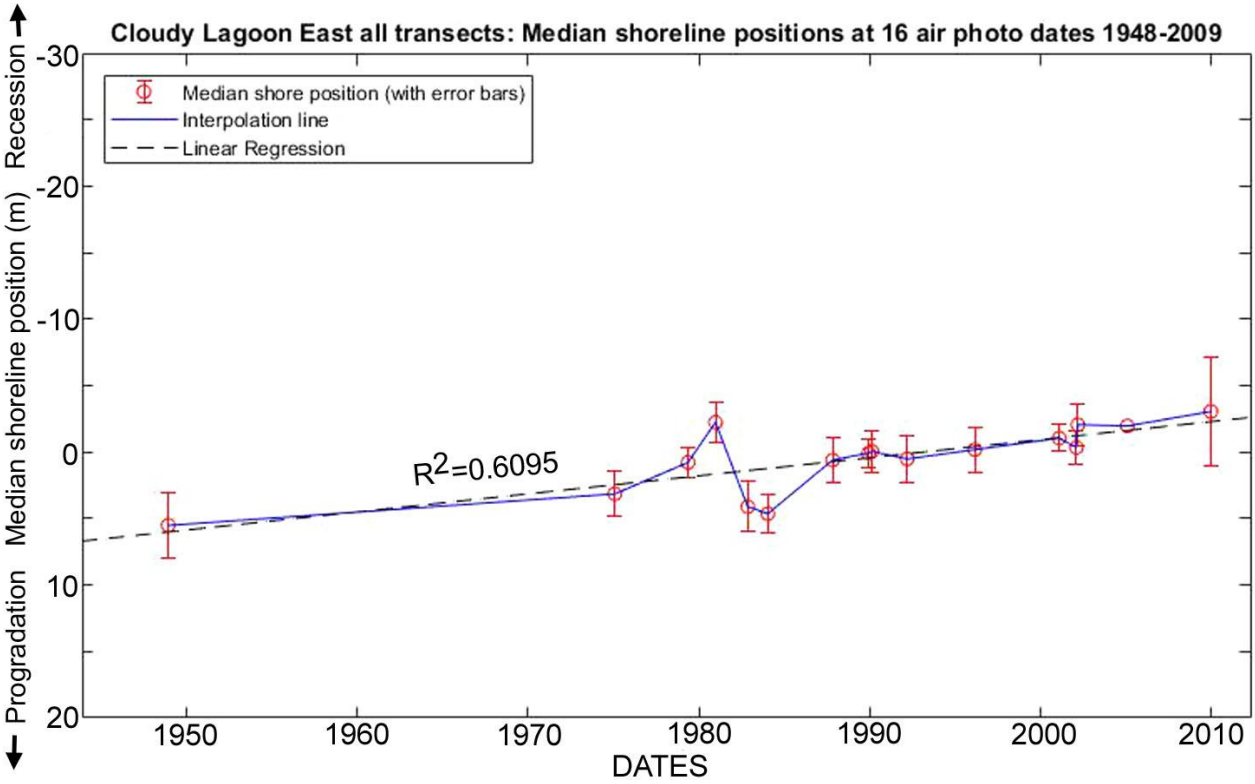

Figure 82: Summary plot of shoreline change history across all transects (as shown on Figure 81) at Cloudy Lagoon East shoreline for 16 air photo dates from 1948 to 2009, with air photo error bars and linear fit.

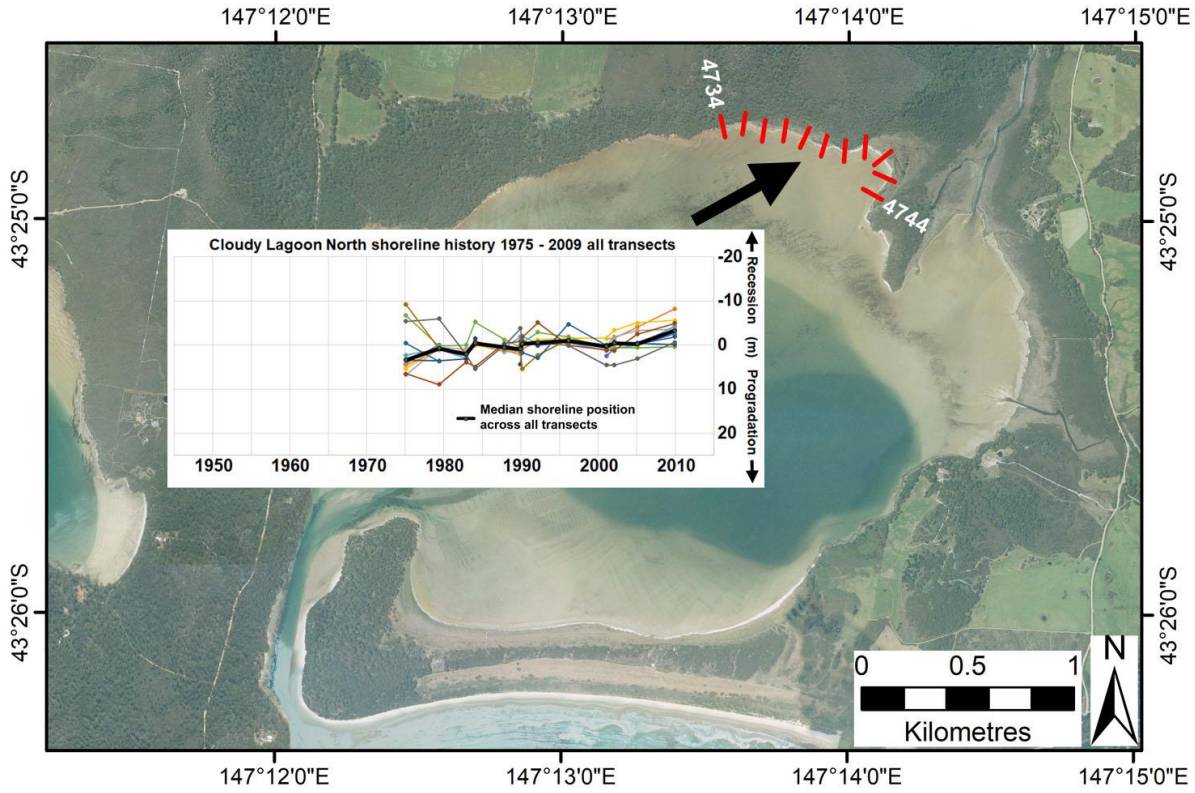

Figure 83: Shoreline position changes along all individual transects for Cloudy Lagoon North shoreline, for 13 air photo dates from 1975 to 2009 as listed on Table 20 & Table 21. The transects used are 100m – spaced red lines on the air photo. See also summary plot Figure 84 below. The background image is the 2009 air photo (© DPIPWE).

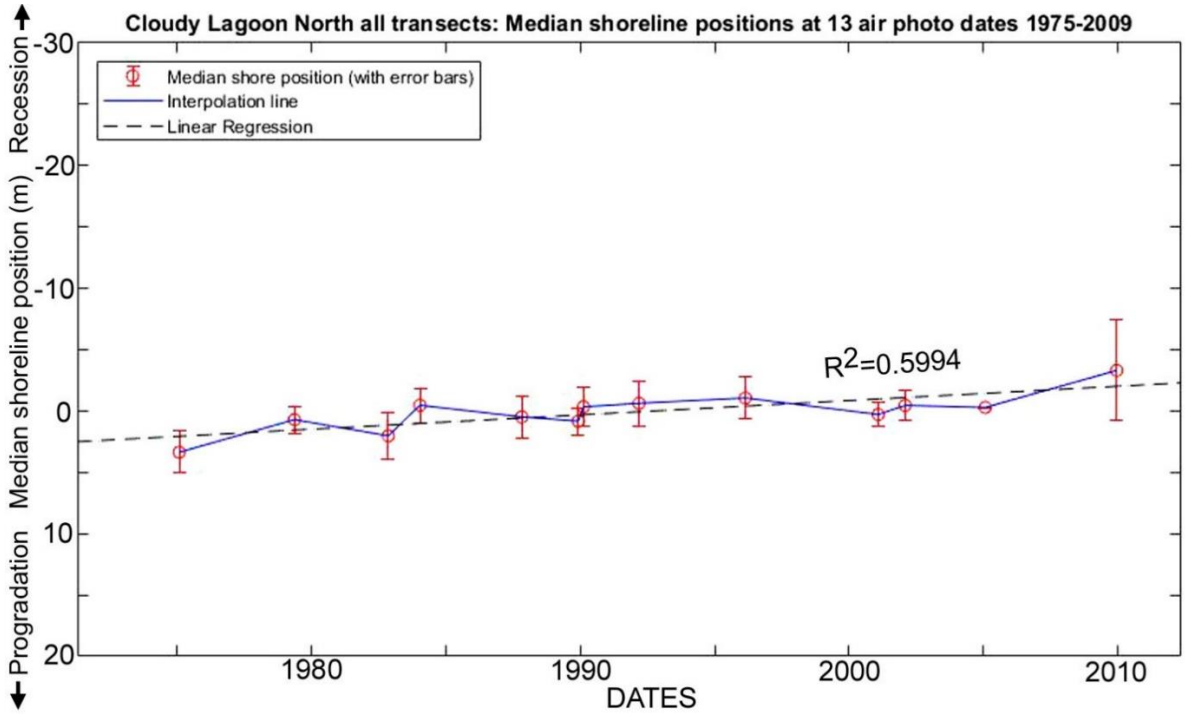

Figure 84: Summary plot of shoreline change history across all transects (as shown on Figure 83) at Cloudy Lagoon North shoreline for 13 air photo dates from 1975 to 2009, with air photo error bars and linear fit.

A1.2.5 West Duck Bay (far north-west Tasmania)

Locality and general description

The west Duck Bay study area is a portion of an extensive region on the far north-west coast of Tasmania which is characterised by saltmarsh-dominated shores and extensive inter-tidal sand-flats stretching from Boullanger Bay to Duck Bay, which are sheltered from the swell waves refracting through Bass Strait by Robbins Island and a series of Holocene sandy barriers. Areas landwards of the southern shore of the region (including west Duck Bay) are dominantly cleared for agriculture (mainly cattle grazing), however the saltmarsh areas remain mostly intact as a coastal buffer. Perkins Island, forming the northern shore of west Duck Bay, is an unsettled sandy barrier island with little or no clearing of native vegetation. The largest town in the area is Smithton at the southern extremity of Duck Bay.

Geomorphology and process environment

The coastal geomorphology of the broader intertidal sand-flats region of which west Duck Bay is a part has previously been field-mapped, studied and reported on by the author and colleagues (Mount et al. 2010; Prahalad et al. 2015). The West Duck Bay portion of the earlier study area was re-examined for this project using air photos from more dates and different analysis methods. The geomorphic information reported here is partly derived from the author's contributions to the previous publications except where otherwise cited. This study was restricted to the smaller area of west Duck Bay, in part because of the presence of substantial lengths of shoreline known to be actively eroding within a restricted area, and because it was thought that proximity to the more populated areas near Smithton township would result in more frequent air photo dates being available for analysis.

Geomorphic description

The geomorphology and shoreline character of the west Duck Bay case study area is typical of the broader coast of far north-west Tasmania from Boullanger Bay to Duck Bay as described by Mount et al. (2010). Duck Bay is a tidal coastal re-entrant sheltered from the refracted swells entering Bass Strait by the Holocene-age sandy coastal barriers of Perkins Island and Anthony's Beach. To the south-west, backshore and hinterland areas comprise extensive low-relief plains thickly mantled by Pleistocene-age terrestrial aeolian sands. The extensive intertidal to sub-tidal sand flats in west Duck Bay are not Holocene coastal or marine sand deposits, but rather are the same relict Pleistocene sands as those onshore, which were inundated and stripped by marine erosion at the upper limit of the post-glacial marine transgression that ceased in the south-eastern Australian region circa 6,500 years BP (Lambeck & Chappell 2001). Along with thin (circa 0.5 m) patchy veneers of sand reworked by tidal currents and wind-waves, the intertidal sand flats also expose *in situ* interbedded dark cohesive peaty-sand beds and lenses which outcrop sporadically on the shoreline and across the tidal flats. These have been identified as Pleistocene freshwater lacustrine beds (Mount et al. 2010). Radiocarbon dating of equivalent peats from nearby Boullanger Bay yielded Pleistocene conventional radio-carbon dates of 26,720±180 yrs. BP and 36,930±400 yrs. BP (Morrison in:Mount et al. 2010). The intertidal exposure of these *in situ* peat beds implies that the tidal sandflats are currently dominantly stable or eroding rather than accreting sand.

The shoreline of west Duck Bay is mostly occupied by saltmarsh vegetation, typically with up to 0.5 m of soft grey clayey-sand marsh soil accreted over the Pleistocene sands (see Figure 6 & Figure 85). A large proportion of the saltmarsh shoreline in west Duck Bay is actively eroding with fresh low scarps (Figure 85), however in some areas the saltmarsh vegetation edge is intact, actively growing and probably accreting clayey-sand marsh soil (see Figure 6 bottom). The main exception to saltmarsh shore in west Duck Bay is approximately 1.5 km of shoreline on the southern side of Perkins Island near the tidal entrance to Duck Bay, which is a scarped sandy shore typically 1.5 to 2.0 m high cut in deep podzolic beach ridge sands.

Tidal range and processes

The Robbins Passage to Boullanger Bay intertidal sandflats region has the highest measured tidal range on the Tasmanian coast, with mean spring tide ranges from 2.09 up to 2.79 m having been measured at three sites (Donaldson, Sharples & Anders 2012). Duck Bay probably has a similar tidal range, given its similar bathymetry and swell-sheltered environment only 10 km from the nearest tide gauge site used by Donaldson, Sharples and Anders (2012).

The intertidal sandflats are inundated at high tide but are mostly exposed at low tide every day. Hence tidal currents flow off the exposed tidal flats and into the tidal channels that dissect the flats on every ebb tide. Although no attempt has been made to model or quantify tidal current flows in this region, the fact that cohesive Pleistocene peat beds interbedded with Pleistocene sands are exposed sporadically across the intertidal sandflats implies that the flats are at least partly scoured by tidal currents, which must be capable of removing loose surface sands during ebb tides into the only available sinks, namely the deep tidal channels. It is unlikely that sand sinking into the deeper parts of these channels could be returned to the shallow tidal flat surfaces during flood tides. Indeed, Mount et al. (2010, p. 52) used LANDSAT imagery to track the movement of sand bedforms migrating along a large tidal channel into deeper offshore water in Bass Strait. The bedforms were tracked moving westwards through Robbins Passage and then northwards up the west side of Robbins Island over a 20-year period from 1990 to 2009.

Tidal currents converging in the narrow shallow channel at the western extremity of Duck Bay were inferred by Mount et al. (2010) to have contributed to unusually rapid twentieth century erosion of shorelines in that area (see Figure 87). However, no evidence has been identified of tidal currents being a direct agent of erosion elsewhere in Duck Bay (as opposed to a means of sediment transport).

Swell wave climate

With the exception of refracted and attenuated swells reaching short distances inside the mouth of Duck Bay between Perkins and Anthony Beach, Duck Bay is entirely sheltered from swell waves.

Wind (wind-wave) climate

The nearest available Bureau of Meteorology wind records pertinent to West Duck Bay are the high-quality record from Cape Grim (~30 km west) for 1987 onwards, and the longer record from Smithton township and aerodrome, (~5 km east). The dominant winds recorded at Cape Grim are westerly to south-westerly (Figure 86) and given the very low-profile country with minimal topographic steering between there and Duck Bay, similar dominant wind directions can be expected at Duck Bay. The much closer Smithton wind record (Figure 86) confirms this, as well as exhibiting a sub-ordinate easterly wind flow that is also seen in the Cape Grim record. Frequent but relatively low speed northerly winds at the Smithton sites are probably topographically steered south within the Duck River valley.

The Cape Grim wind record also shows a significant trend of ongoing wind speed increases since at least 1987 (see Figure 177 in Ocean Beach appendix A1.3.8 below)[30]. While this also might be expected to occur at Duck Bay, the closer Smithton wind speed record (not shown here) shows no significant increases. In fact, the Smithton wind record shows an apparent decrease in mean wind speeds associated with a step-change increase in data frequency, as well as being complicated by a shift in location from Smithton Township to Smithton Aerodrome. The more recent Smithton

[30] This is a credible record given the Cape Grim weather station is part of the global Baseline Air Pollution Stations network which is managed rigorously by the World Meteorological Organisation in association with the Australian Bureau of Meteorology and CSIRO. This management regime has required more rigorous data collection standards than have in the past been applied to many Australian wind records, as noted by Troccoli et al. (2012).

aerodrome wind record is of better quality than the older township record but has so far shown no clear indication of a trend towards either increasing or decreasing wind speeds.

Locally generated wind-waves are the main agent of erosion on shorelines around West Duck Bay and have been observed by the author dislodging sediment from actively eroding saltmarsh scarps (see Figure 85). Wind-wave fetch modelling has previously been undertaken for West Duck Bay and surrounding swell-sheltered shorelines by Vishnu Prahalad in Mount et al. (2010) and Prahalad et al. (2015), using a cartographic wave exposure model developed by Pepper and Puotinen (2009). The modelling used wind direction data from both Smithton and Cape Grim to derive a dimensionless Wave Fetch Index (WFI) predictive of the degree of wind-wave erosion to be expected on shores of differing wind exposure and fetch relative to dominant wind directions. The WFI modelled for West Duck Bay is compared to the author's field mapping of shoreline erosion status on Figure 87. Two key results are apparent, namely:

1. Larger and smaller WFI broadly correlate with distinctions between soft (mostly saltmarsh) shores that are respectively eroding, intermediate or accreting. The main exceptions to this pattern occur where wind-waves are not the dominant agent of erosion, which is the case at the swell-exposed mouth of Duck Bay and the narrow tidally dominated channel at the West end of Duck Bay.
2. WFI (and thus wind-wave capacity to erode) broadly increases from west to east across West Duck Bay, corresponding to dominantly westerly to south-westerly winds blowing across increasing fetches towards the east and north-east.

Figure 85: A view of the West Duck Bay SE area shoreline taken close to high tide but clearly showing the sharp distinction between the actively eroding vegetation edge exposing dark clayey-sand saltmarsh soils and the underlying pale-coloured intertidal sand flats which are extensively exposed at low tide. At the time of this inspection, the small locally generated wind waves were actively and visibly mobilising silt and clay from the eroding saltmarsh soil faces. Photo taken by Chris Sharples on 29th January 2010.

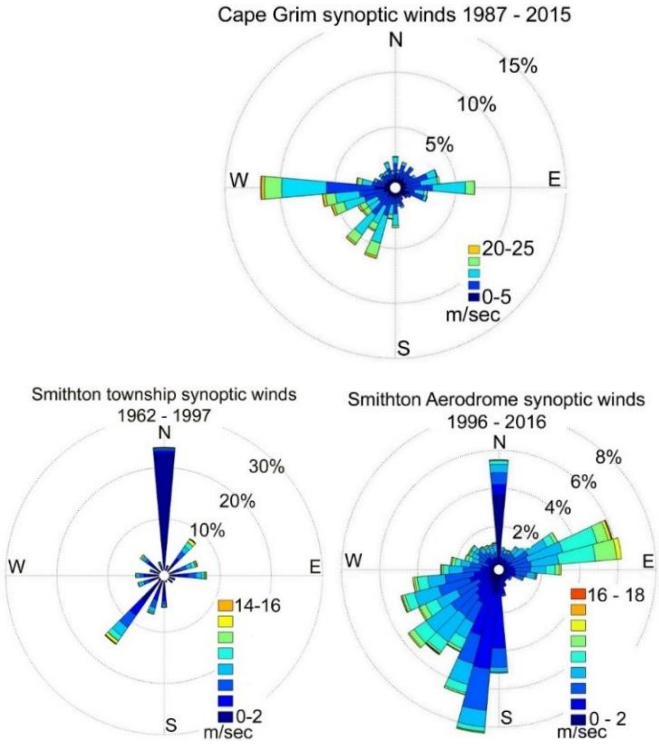

Figure 86: Synoptic wind direction records for the nearest Bureau of Meteorology weather stations. Cape Grim (top) is located ~30 km west and Smithtown township & aerodrome (bottom) are ~5 km SE of Duck Bay. South-westerly (southerly to westerly) winds dominate the records at all sites, with a subordinate easterly component of winds generated in Bass Strait. Wind roses plotted by Chris Sharples from original wind records supplied by the Australian Bureau of Meteorology. Wind speeds are plotted in metres per second as indicated by colour key.

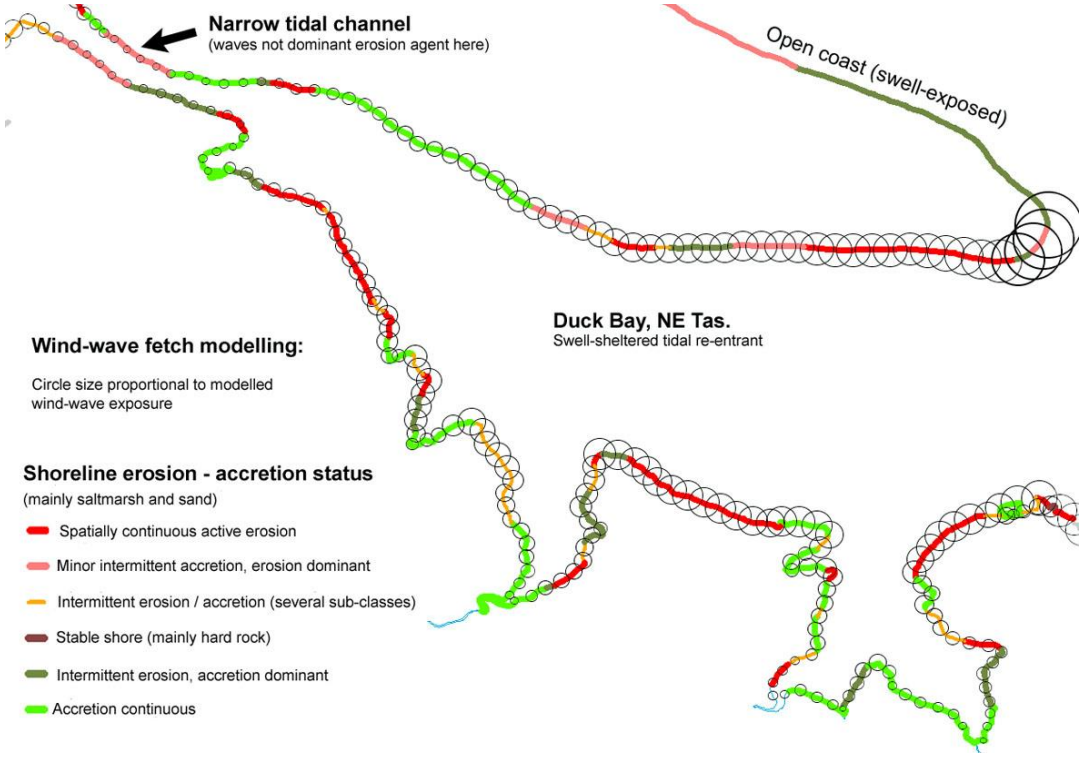

Figure 87: Wind-wave fetch in western Duck Bay as at 2010 compared to shoreline erosion status. Erosion status is based on comprehensive field mapping by Chris Sharples during 2010 (originally reported in Mount et al. (2010). The wind-Wave Fetch Index (WFI) is a dimensionless value calculated from fetch and wind direction frequency-magnitude distributions by Vishnu Prahalad (in: Mount et al. (2010) and Prahalad et al. (2015)) using the cartographic method of Pepper and Puotinen (2009). Higher WFI is represented by larger circles at each modelled shoreline point.

Sand transport and budget

As noted above, the extensive inter-tidal sandflats in Duck Bay are not marine or coastal deposits, but rather are relict sands of Pleistocene age which are eroding and losing sand permanently into tidal channels which dissect the sand flats. Shoreline saltmarsh accretes grey clayey-sand soils over the sands, probably by vegetative capture of sand, clays and organic matter moved by wind-waves and tidal currents in the nearshore water column. However, there is no evidence of sand being gained by the shorelines or intertidal flats from any source, with the main watercourses flowing into Duck Bay – the Duck River and Scopus Creek – showing no sign of active sand transport (e.g., sand point bars or deltaic deposits). Although these rivers drain a dominantly agricultural catchment which has been extensively cleared of native vegetation, they probably transport only small amounts of suspended clay and silt as is generally the case for rivers in western Tasmania under present-day conditions (Nanson, Barbetti & Taylor 1995).

There is little or no accommodation space for eroded sand to settle out into on the intertidal flats, since they are sub-aerially exposed and scoured by tidal currents during every tidal cycle. With continuing sea-level rise and deeper water depths, some accommodation space may eventually become available on parts of the tidal flats, however given the large tidal range in Duck Bay this is likely to occur only after considerable further sea-level rise. Shoreline erosion is evidently freeing sand and finer sediments, some of which may be vegetatively recaptured by those saltmarsh shores that are still accreting, however ebb-tide currents can be expected to remove most loose sediment into the tidal channels where the sand fraction will settle out and be gradually moved down the channels into the sand sink of Bass Strait as observed by Mount et al. (2010, p. 52). Given that little sand is likely to be moved out of the deeper tidal channels back onto the intertidal flats by flood-tide currents, this sand transport process is effectively a uni-direction transport process that is persistently (with every tidal cycle) moving eroded shoreline sands into the very large active sink of Bass Strait.

Despite a superficial appearance of being a sheltered sand-filled depositional sand-trap, the extensive intertidal sandflats of the Duck Bay are in fact a persistently eroding area of exposed and eroding relict Pleistocene sands with an overall negative sand budget.

Sea-level data

The closest long sea level record to Duck Bay is the Burnie tide gauge record, 75 km south-east of Duck Bay (Figure 88). The Burnie tide gauge is part of the climate quality Australian Baseline Sea Level Monitoring Project (http://www.bom.gov.au/oceanography/projects/abslmp/abslmp.shtml). Data from this tide gauge processed by Dr John Hunter and Vishnu Prahalad shows a rise in mean sea-level between 1966 and 2006 of 5.4 cm at a mean rate of 1.4 mm yr^{-1} over that period (Mount et al. 2010). Data from http://www.bom.gov.au/ntc/IDO60201/IDO60201.202003.pdf shows a mean rate of 2.9 mm yr-1 at Burnie for 1993 to 2020 (C. Watson *pers. comm.*). These are comparable to the global mean trend from 1966 to 2009 of 2.0 ± 0.3 mm yr^{-1} and 3.4 ± 0.4 mm yr^{-1} for 1993 to 2009 (White et al. 2014).

Vertical land movement

Current and ongoing geodetic studies of Tasmania have yet to resolve disagreements between GNSS derived estimates of VLM at Burnie (75 km east of West Duck Bay) and Hobart ranging between 0.0 to -1.0 mm yr^{-1}, and geophysical models indicating subsidence in the range of -0.1 to -0.2 mm yr^{-1} (see details in Chapter 2 Section 2.5.4 above). However, for the purpose of this thesis, there is no evidence suggesting that VLM is a significant signal in Tasmanian relative sea levels.

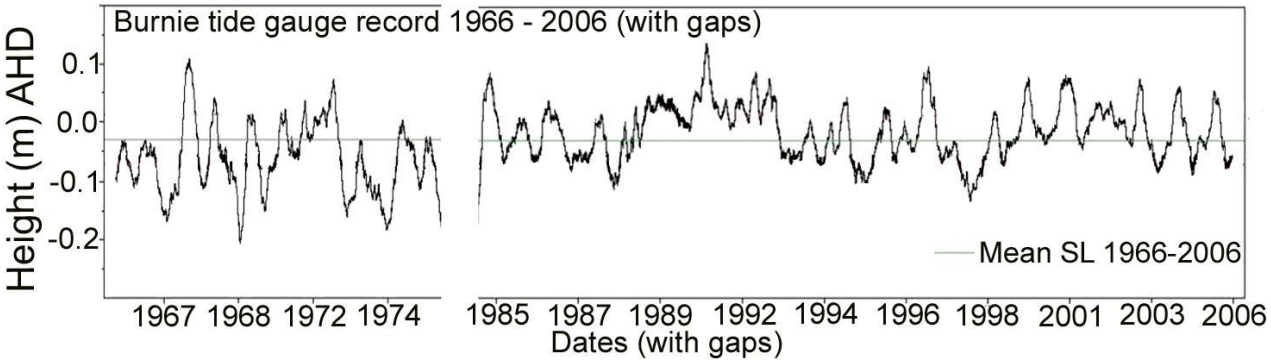

Figure 88: Burnie tide gauge record (1996 – 2006 with gaps). Data is smoothed with a moving average and shows a net rise in mean sea-level rise between 1966 and 2006 of 5.4 cm at a rate of 1.4 mm per year. Annual sea-level cycles are a dominant feature superimposed on the long-term trend. Data from the Australian National Tidal Facility was processed by John Hunter and Vishnu Prahalad, and this figure is copied from Mount et al. (2010) with diagrammatic modifications by C. Sharples.

Artificial disturbances

The main artificial disturbance in the west Duck Bay area is artificial land clearance for agriculture, however the study site shorelines remain physically buffered from cleared pastures by a fringe of saltmarsh and other vegetation. The N (E & W) and S study sites today remain separated from cleared areas by undisturbed native vegetation buffers at least 500m wide (see Figure 89 & Figure 97). The present shorelines in the NW and SE study sites are separated from cleared areas by saltmarsh buffers ranging from 20 m wide to mostly wider than 50m (see Figure 94 & Figure 101). The proximity of cleared land may change nutrient and suspended sediment concentrations in Duck Bay, potentially affecting seagrass and marine fauna (Mount et al. 2010, pp. 147-148), but there is no apparent mechanism by which it may have significantly altered saltmarsh accretion or shoreline erosion behaviour in the study site shores over the air photo period.

An artificial levee and drainage channel has been constructed parallel to and between 20 and 50 m behind the present eroding shoreline in the southern two thirds of the NW study site (visible on Figure 94). These structures were constructed behind portions of the Boullanger Bay to Duck Bay shoreline in an effort to protect low-lying pastureland from occasional inundation, and in some areas have been associated with significant saltmarsh loss on the seawards site of the levees (Mount et al. 2010, section 6.1 & Figs 6.1 & 6.2). However, they do not appear to have significantly altered saltmarsh accretion or shoreline erosion behaviour in the NW study site over the air photo period. The shoreline histories along individual transects within this study site show no significant difference between the transects backed by the levee and channel, and those not so backed (Figure 94). The air-photo time series shows that the levees and channel system behind the NW study site shore was constructed between March 1986 and March 1990. Although a small accretion-then-erosion anomaly appears in the air photo record during this interval (see Figure 94, Figure 95 & Figure 96), there is no significant long-term change in the overall shoreline behaviour trend, which is a slow shoreline recession trend both before and after the levee construction, and shows no long-term rate change throughout the air photo record.

Rice grass (*Spartina anglica*) is an introduced invasive shoreline weed which in recent decades has become established in parts of Duck Bay (Mount et al. 2010, Section 6.2). A key impact of this weed is that it aggressively colonises shoreline fringes, in the process capturing silt-grade sediment suspended in the water column and creating erosion-resistant prograding muddy shores. Almost by definition therefore, this weed was mostly not established on the eroding study area shores as at 2010 (when they were inspected by the author), although their establishment after that date cannot be ruled out. However, rice grass was present at the southernmost end of the SE study site shore in 2010,

which is probably the explanation of (or a factor in) the slight progradation of that end of the otherwise strongly receding shoreline (see Figure 100 & Figure 101).

Air photo analysis

Shorelines (defined by the seawards vegetation line) were mapped (digitised) from ortho-rectified air photos taken at 16 dates from January 1945 to March 2012. Due to incomplete coverage at a few dates, only 14 or 15 air photo dates could be used at some sites. Further air photos from an additional 8 dates were not be used due to quality issues precluding sufficiently accurate ortho-rectification. See air photo listing in Table 18 below.

Five sites were selected for analysis around the shores of west Duck Bay. All five were selected on the basis that the author had previously (during 2010) field-mapped them as actively eroding. The five sites vary significantly in wind-wave exposure and fetch with respect to the westerly to south-westerly winds inferred from available wind records to be dominant in Duck Bay (Figure 86 & Figure 87). Four of the sites are saltmarsh shores comprising sandy-clay saltmarsh soils over sand, and one (the N(east) site) is podzolized Holocene beach ridge sand.

Shore behaviour history from air photos

The following sections described the results of shoreline position change mapping from a 66 or 67-year air photo time series at each of the five analysed sites.

N Area (East and West)

This shoreline stretch comprises two distinct shoreline types which are therefore treated as separate sites:

The eastern half (transects 66236-66247) is an erosion scarp several metres high cut into podzolic beach ridge sands, which has shown varying degrees of slumping and vegetation cover over the air photo period. The mapped shoreline was the midway line on the slumped erosion scarp. An eastern-most transect (66235) exhibited markedly different shoreline behaviour to all the others, inferred to be due to its position exposed to swell waves at the tidal mouth of Duck Bay (Figure 89), and so was excluded from analysis.

The western half (transects 66248-66258) is a saltmarsh shoreline on clayey-peaty saltmarsh soils over sand. The mapped shoreline is the seawards vegetation line.

Shoreline histories on individual transects are plotted in two groups for these two shore types on Figure 89. Most shoreline histories on most transects within the two plotted groups are coherent implying parallel shoreline movements, however a difference in shoreline behaviour is evident between the two groups. Summary plots using a single linear fit and piecewise linear fits have been used to test for any significant differences in shoreline behaviour before or after 1980 (following figures).

The sandy scarp (eastern transect group) exhibits a statistically significant (R^2=0.5861) but slow overall recession (Figure 90) which does not show evidence of acceleration (Figure 91). In contrast the saltmarsh shoreline (western transect group) shows an apparent change in behaviour from a stable shoreline position (slight non-significant progradation trend) pre-1980 to a slow recession trend after 1980 (Figure 93). However given the limited data and poor correlation co-efficient on the pre-1980 linear fit (Figure 93), a more likely interpretation is that this site simply shows an overall approximately linear recession trend as indicated on Figure 92.

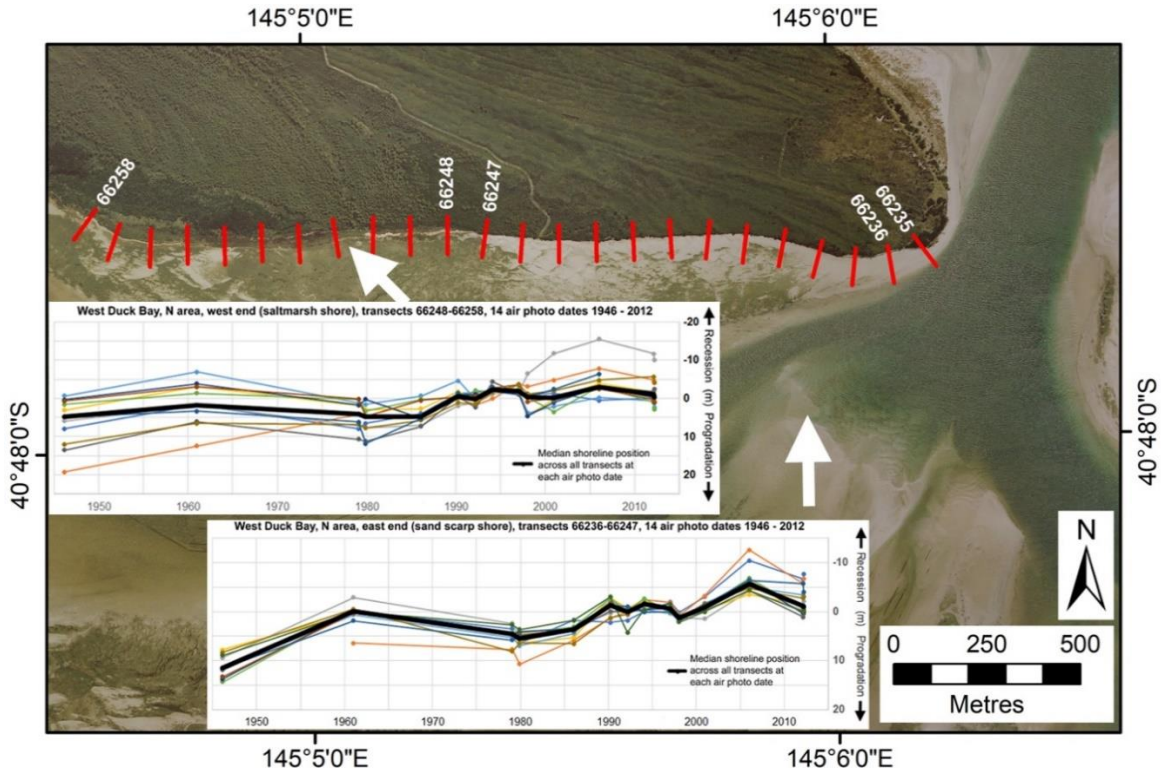

Figure 89: Plots of shoreline position change on each transect in the N study area at West Duck Bay at 14 dates over the period 1946 – 2012. Shoreline positions (seawards vegetation lines) are saltmarsh vegetation edges in the west (transects 66248-258) and the slumped beach ridge sand scarps in the eastern part (transects 66236-247). Separate plots are shown for these two distinctive shore types, with median shoreline positions for each shown as a heavy black line. The background image is the 2nd March 2012 air photo (© DPIPWE).

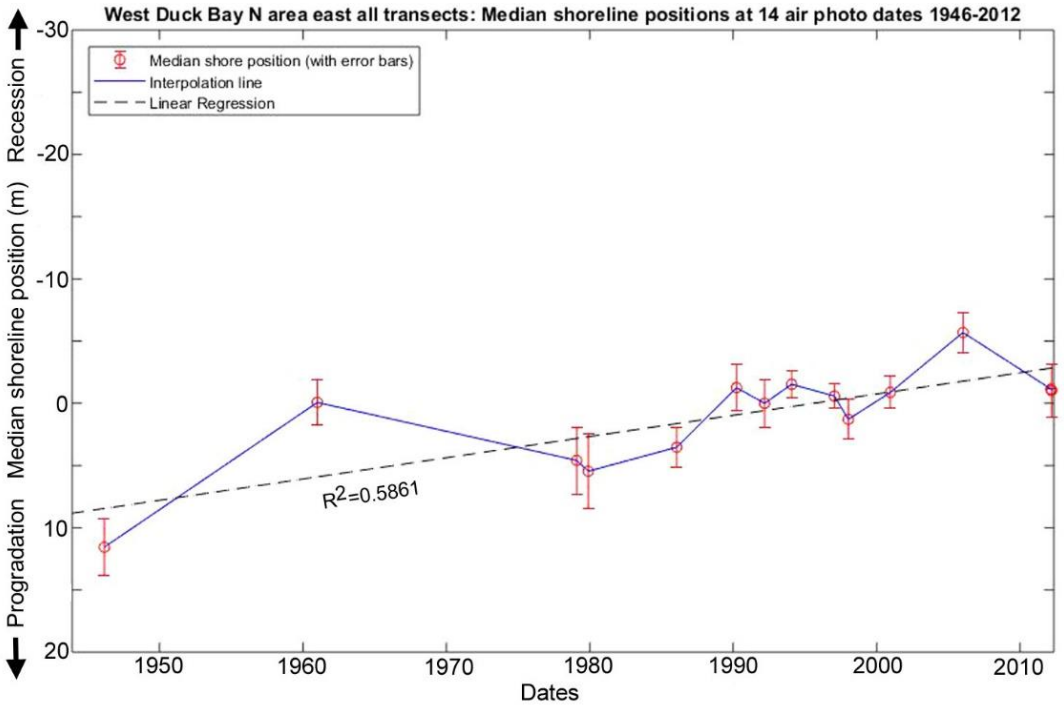

Figure 90: Summary plot of shoreline change history for West Duck Bay N area (eastern part) at 14 air photo dates from 1946 to 2012. This plots the median of the shoreline positions at each date across transects 66236-247 shown in Figure 89 , with a linear fit (first-order linear regression) over the whole air photo period.

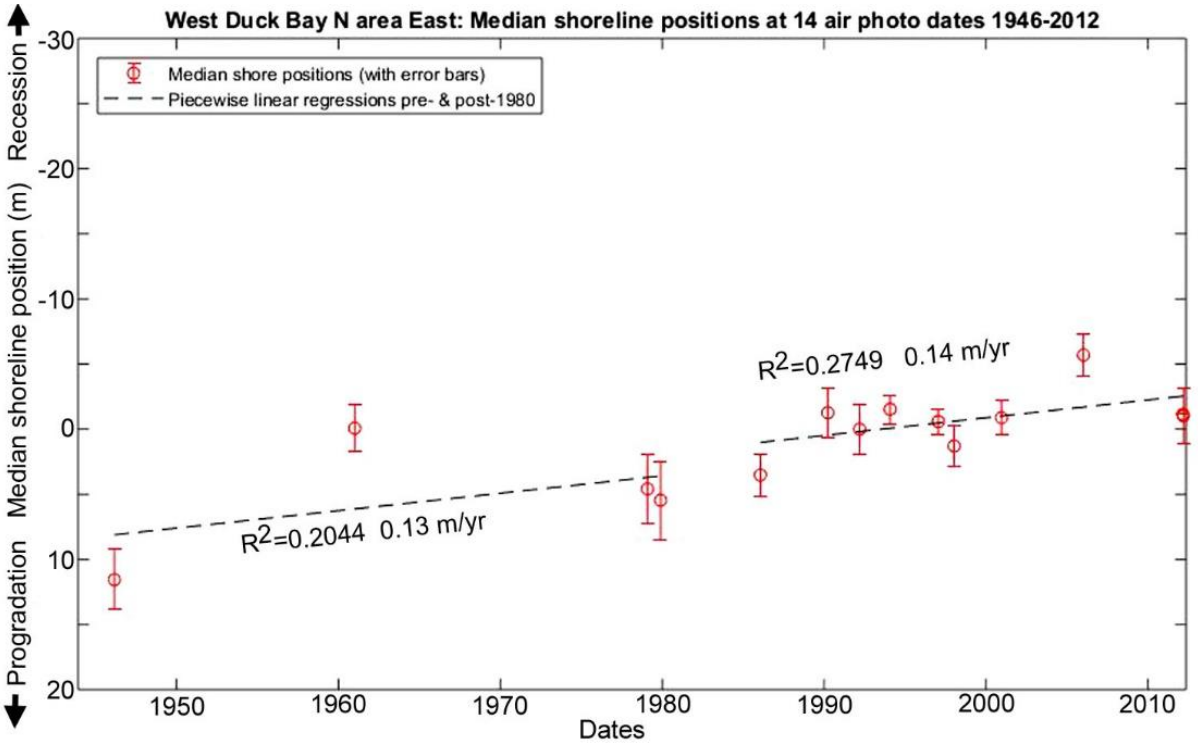

Figure 91: Summary plot of shoreline change history for West Duck Bay N area (eastern part) at 14 air photo dates from 1946 to 2012. Piecewise linear regression fits pre- and post-1980 demonstrate an overall recession trend both pre- and post-1980, with no significant change in the rate of recession.

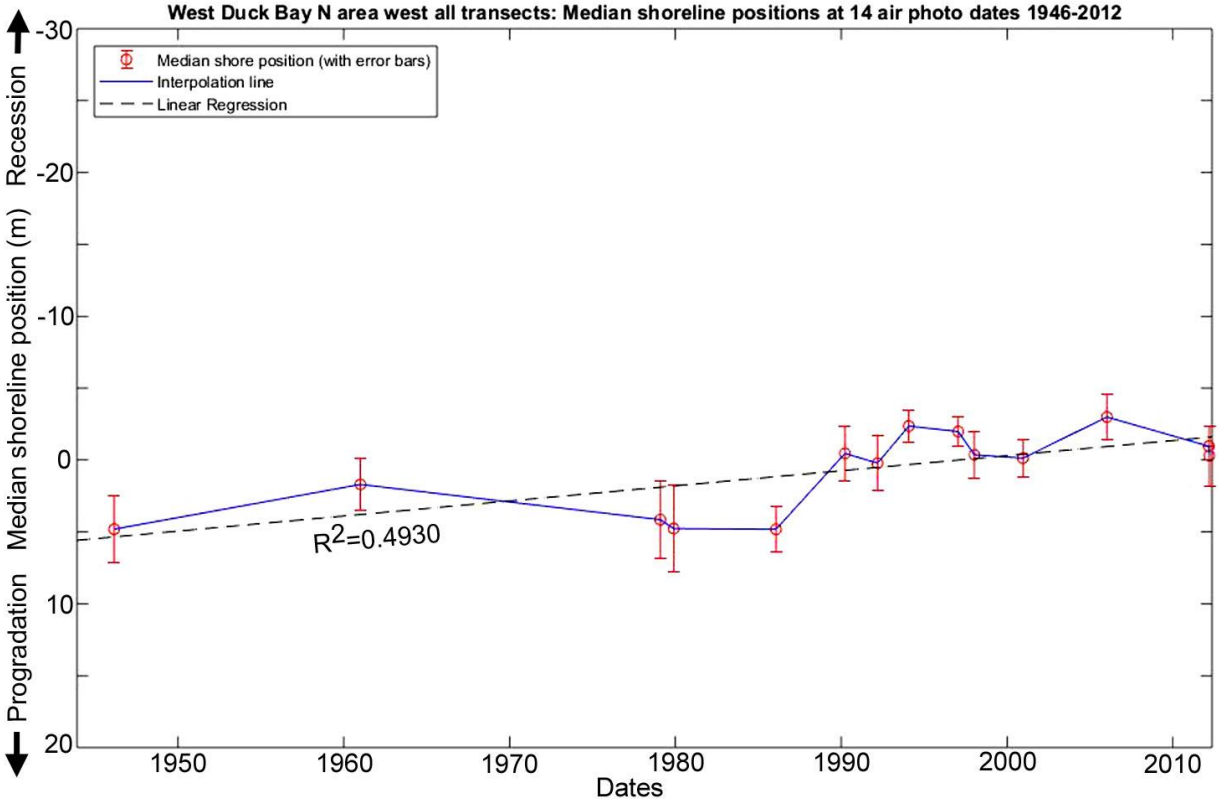

Figure 92: Summary plot of shoreline change history for West Duck Bay N area (western part) at 14 air photo dates from 1946 to 2012. This plots the median of the shoreline positions at each date across transects 66248-258 shown in Figure 89 , with a linear fit (first-order linear regression) over the whole air photo period.

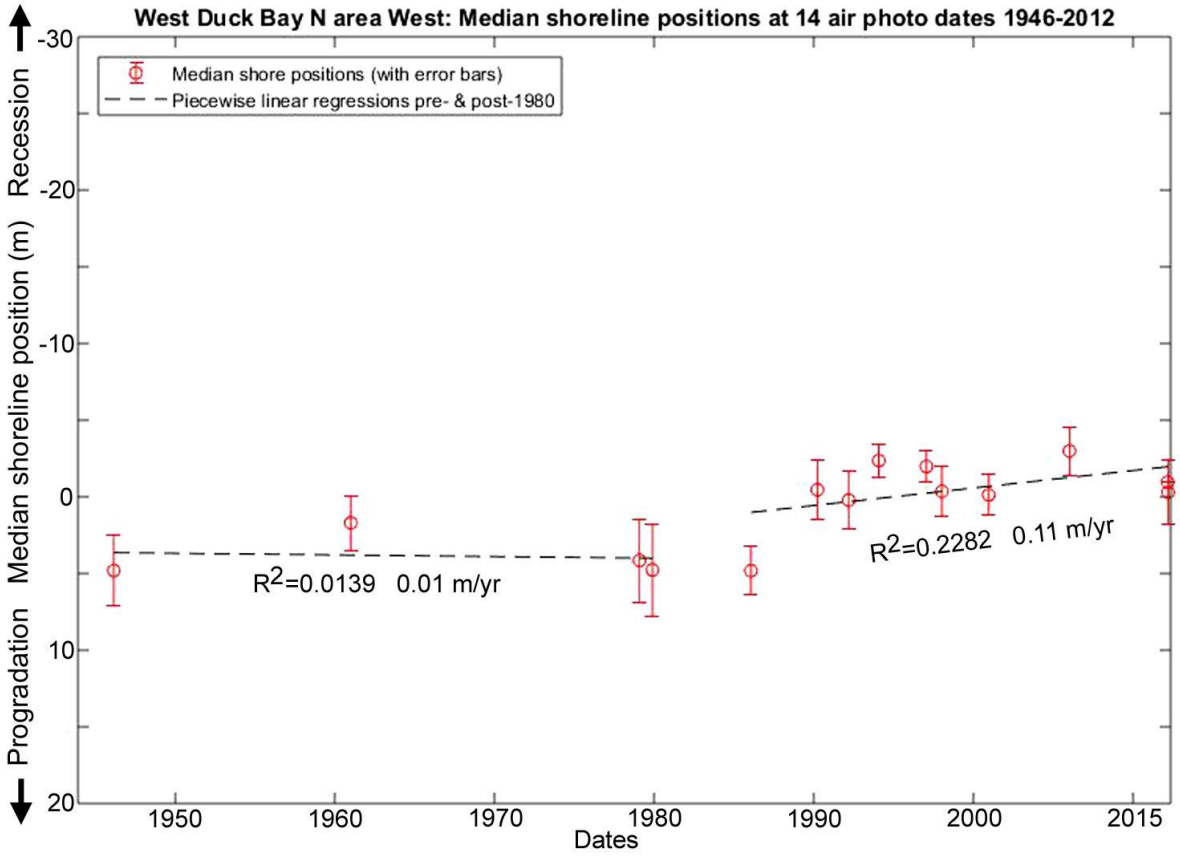

Figure 93: Summary plot of shoreline change history for West Duck Bay N area (western part) at 14 air photo dates from 1946 to 2012. Piecewise linear regression fits pre- and post-1980 suggest no overall recession prior to 1980 changing to a slow recession trend after 1980. However the very poor correlation co-efficient indicated for the pre-1980 fit implies that the single linear fit to the whole dataset shown on the preceding Figure 92 provides a more realistic interpretation of the data.

NW Area

This shoreline is a saltmarsh shoreline on clayey-peaty saltmarsh soils over sand. Shoreline histories on most transects are generally coherent, implying parallel shoreline movements along most of this coastal segment. Progressive shoreline retreat with only one notable apparent brief shoreline recovery episode (in the early 1980s) is seen in the air photo record from 1946 to 2012.

A linear regression fit to the data over the whole period (Figure 95) yields a good Pearson correlation co-efficient (R^2=0.8970). Piece-wise linear regression fits around an arbitrary date of 1980 (Figure 99) indicate very similar constant rates of shoreline retreat rates (averaging 0.24 m/yr) over the whole air photo period, with similar high Pearson correlation co-efficients before and after 1980.

The mostly constant retreat rate at this site is notable by comparison with West Duck Bay areas S and SE (described below) both of which demonstrate a doubling of retreat rates after 1980.

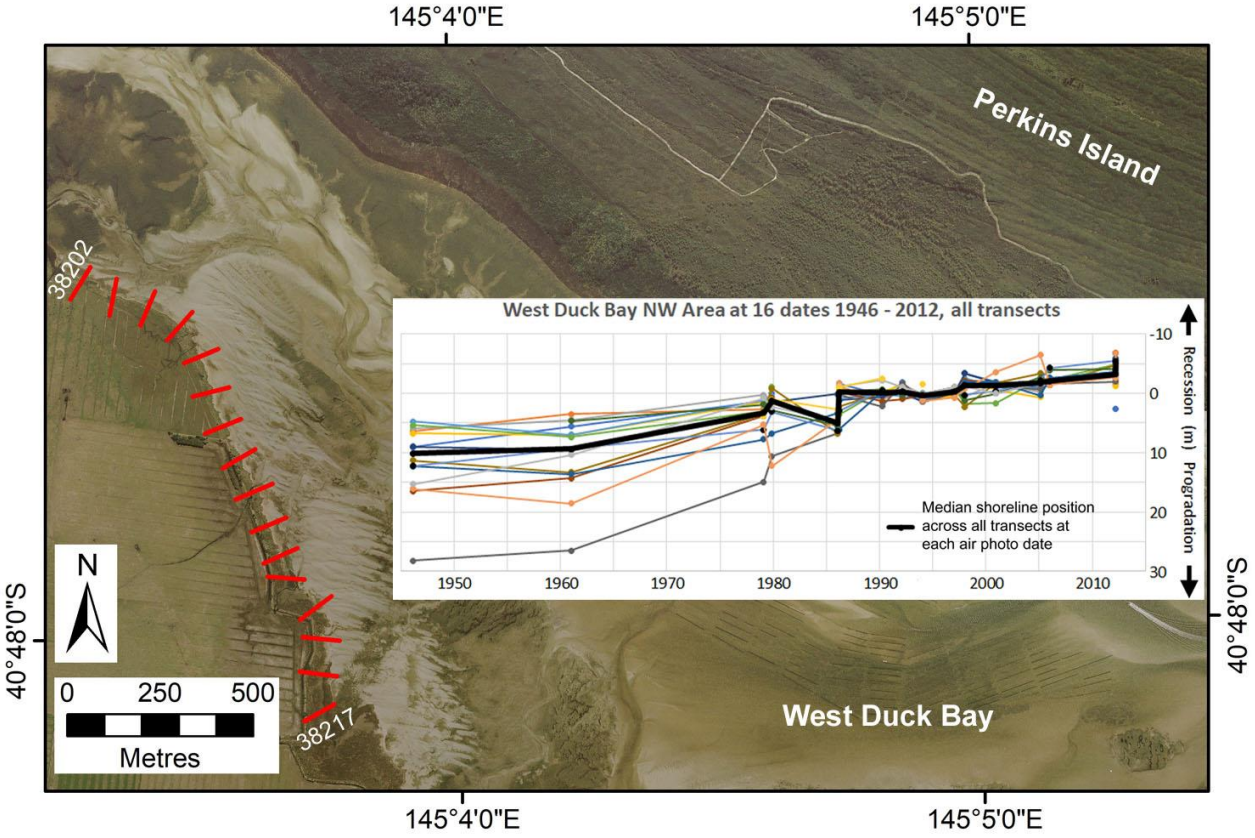

Figure 94: A plot of shoreline position change in the NW study area at West Duck Bay at 16 dates over the period 1946 – 2012. Shoreline position history along each 100m-spaced digital transect (red lines on map) is plotted relative to the median shoreline position on each transect. Shoreline positions are defined as seawards vegetation lines (saltmarsh edges where tidal sand flats are exposed). The median shoreline history across all 16 transects is shown by a heavy line. The background image is the 2nd March 2012 air photo (© DPIPWE).

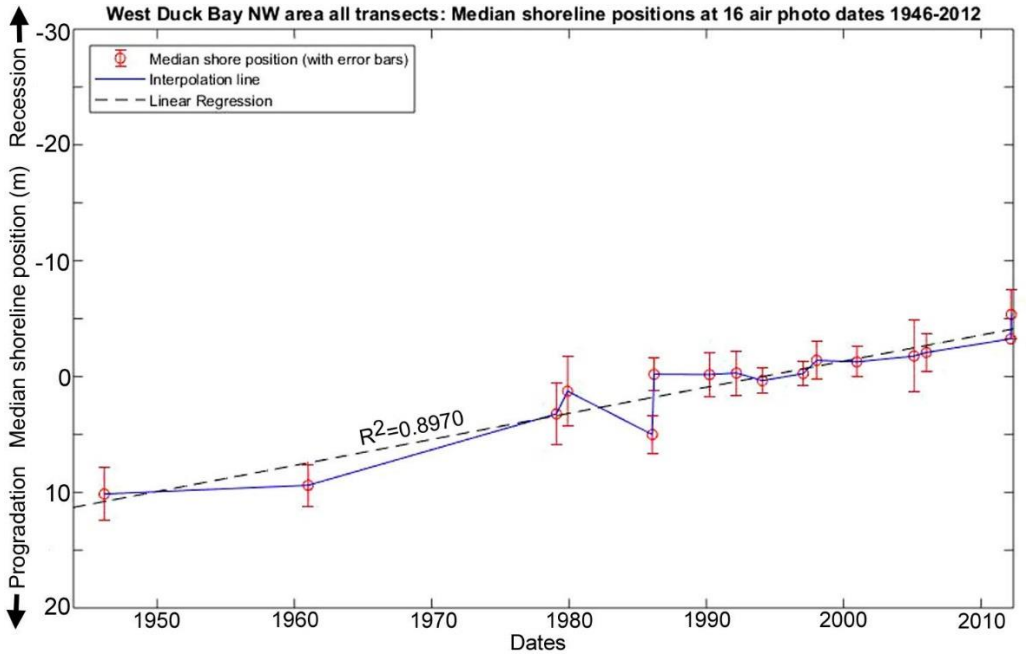

Figure 95: Summary plot of shoreline change history for West Duck Bay NW area at 16 air photo dates from 1946 to 2012. This plots the median of the shoreline positions at each date across all transects shown in Figure 94, with a linear fit (first-order linear regression) over the whole air photo period.

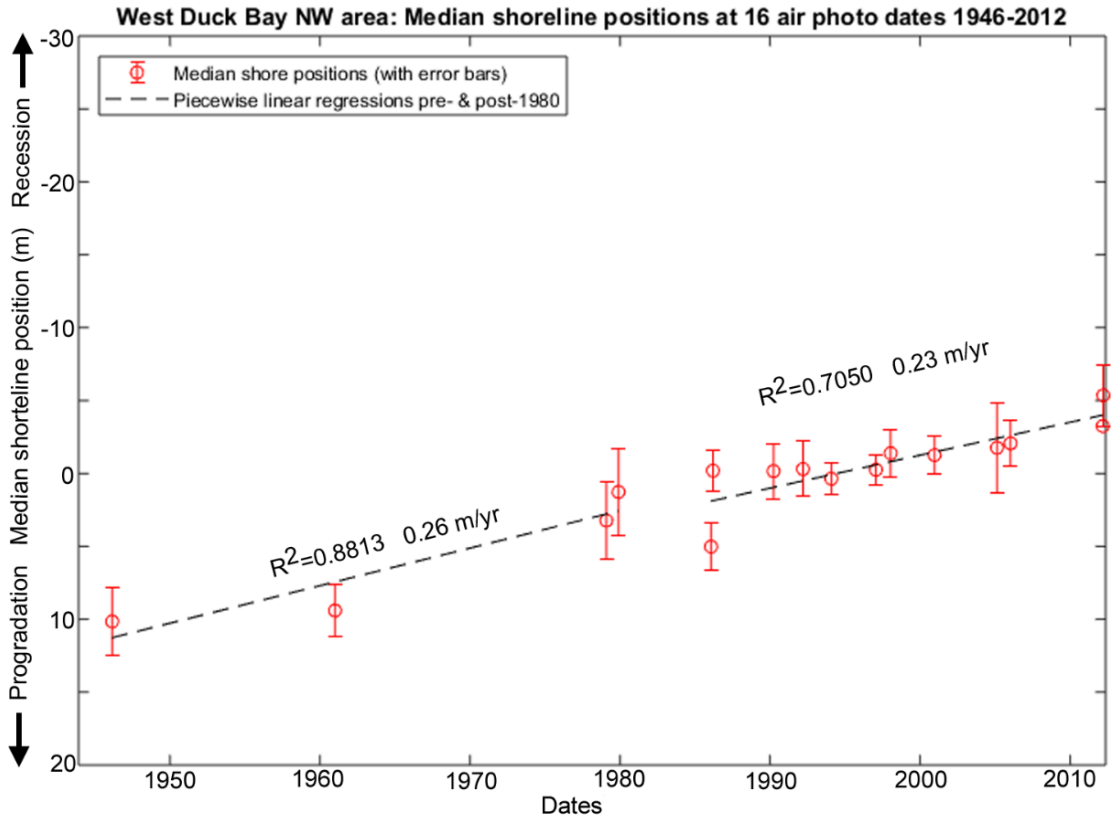

Figure 96: Summary plot of shoreline change history for West Duck Bay NW area at 16 air photo dates from 1946 to 2012. Piecewise linear regression fits pre- and post-1980 demonstrate that at this site shoreline recession has been nearly or entirely continuous but has not varied significantly in rate over the entire air photo period (with similar good Pearson correlation coefficients both pre- and post-1980).

S Area

This shoreline comprises a saltmarsh shoreline on clayey-peaty saltmarsh soils over sand with exposed interbedded Pleistocene freshwater peats.

Shoreline histories on most transects are generally coherent, implying mostly parallel shoreline retreat along most of this coastal segment. Progressive shoreline retreat with no significant shoreline recovery (progradation) is evident over most of the air photo period of 1945 – 2012. The exception is an apparent large erosion event circa 1946 followed by recovery, however the small number of air photos over this early period hinders confirmation of this interpretation.

A linear regression fit to the data over the whole period (Figure 98) yields a good Pearson correlation co-efficient (R^2=0.7148). However, piece-wise linear regression fits (Figure 99) indicate a near-doubling in the shoreline recession rate after 1980, with a higher Pearson correlation co-efficient of R^2=0.9146 for the post-1980 period. This indicates a probable acceleration in shoreline recession during the last 40 years.

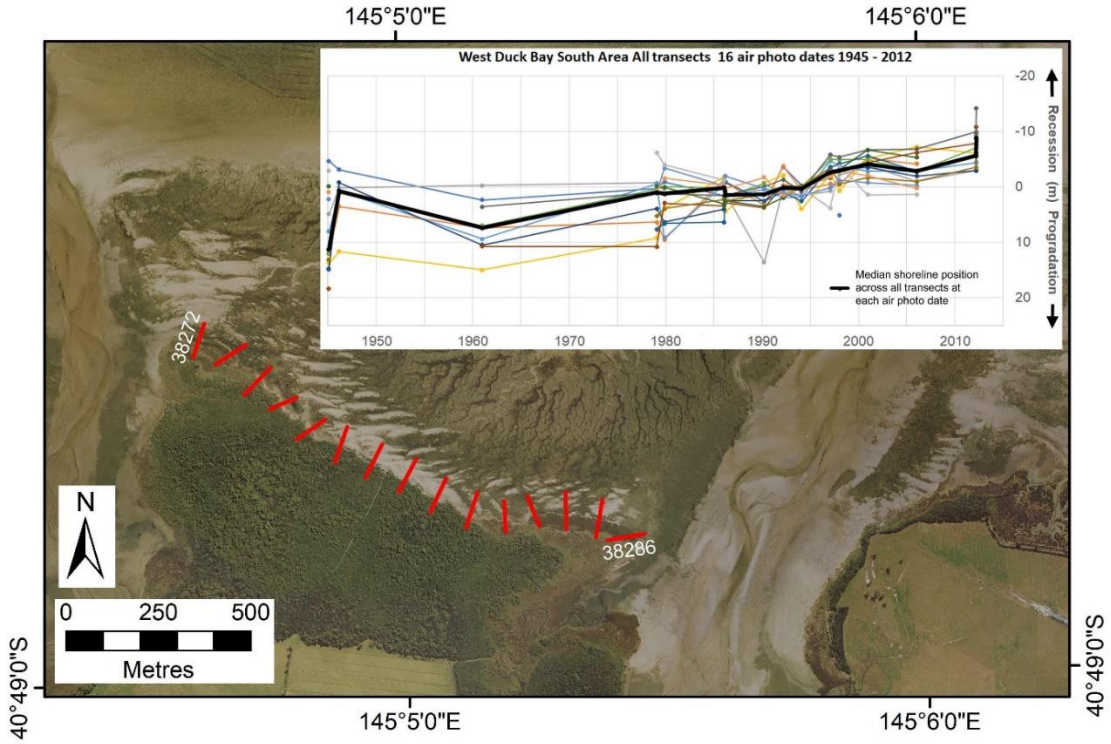

Figure 97: A plot of shoreline position change in the S study area at West Duck Bay at 16 dates over the period 1945 – 2012. Shoreline position history along each 100m-spaced digital transect (red lines on map) is plotted relative to the median shoreline position on each transect. Shoreline positions are defined as seawards vegetation lines (saltmarsh edges where tidal sand flats are exposed). The median shoreline history across all 15 transects is shown by a heavy line. The background image is the 2nd March 2012 air photo (© DPIPWE).

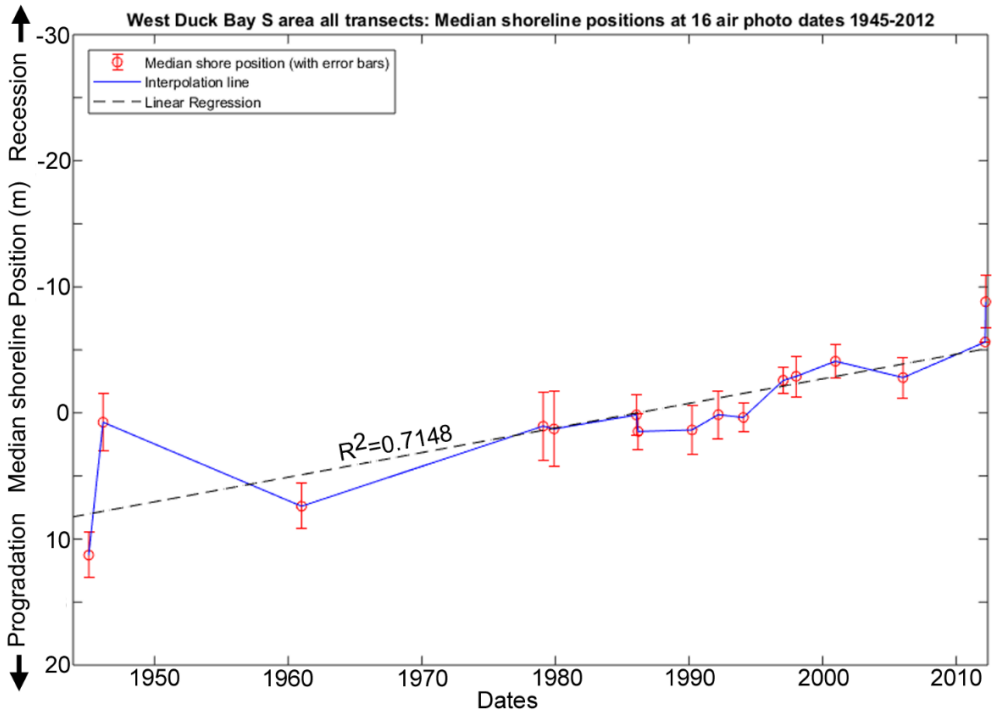

Figure 98: Summary plot of shoreline change history for West Duck Bay S area at 16 air photo dates from 1945 to 2012. This plots the median of the shoreline positions at each date across all transects shown in Figure 97, with a linear fit (first-order linear regression) over the whole air photo period.

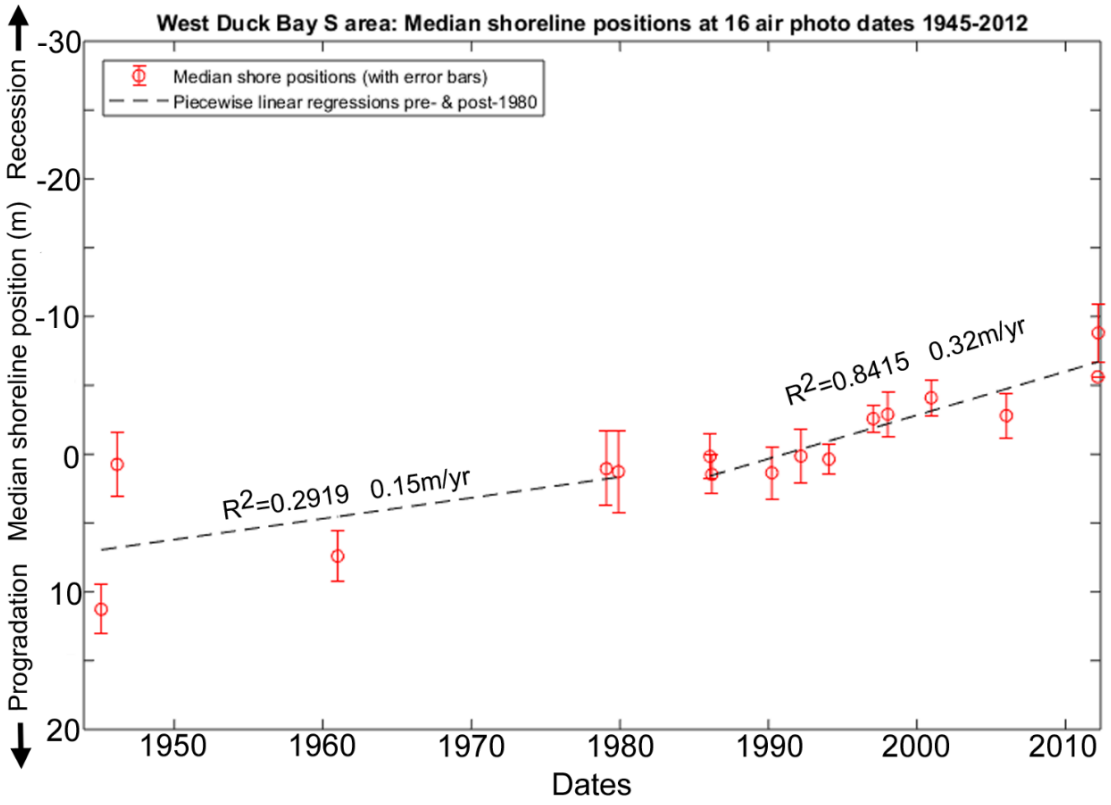

Figure 99: Summary plot of shoreline change history for West Duck Bay S area at 16 air photo dates from 1945 to 2012. Piecewise linear regression fits pre- and post-1980 demonstrate a doubling of shoreline recession rates after that date, albeit the number of photos and reduced error margins after 1980 also result in a significantly better post-1980 linear fit.

SE area

This shoreline is a saltmarsh shoreline on clayey-peaty saltmarsh soils over sand. See views of this shoreline in Figure 85. Shoreline histories on most transects are in Area SE are generally coherent, implying mostly parallel shoreline retreat along most of this coastal segment. Progressive shoreline retreat with no significant shoreline recovery is evident over most of the air photo period of 1945 – 2012, the exception being a phase of apparent progradation shortly prior to 1980 (Figure 102). A linear regression fit to the data over the whole period (Figure 102) yields a good Pearson correlation co-efficient (R^2=0.8794). However, piece-wise linear regression fits (Figure 103) indicate a near-doubling in the shoreline recession rate after 1980, with a higher Pearson correlation co-efficient of R^2=0.9146 for the post-1980 period.

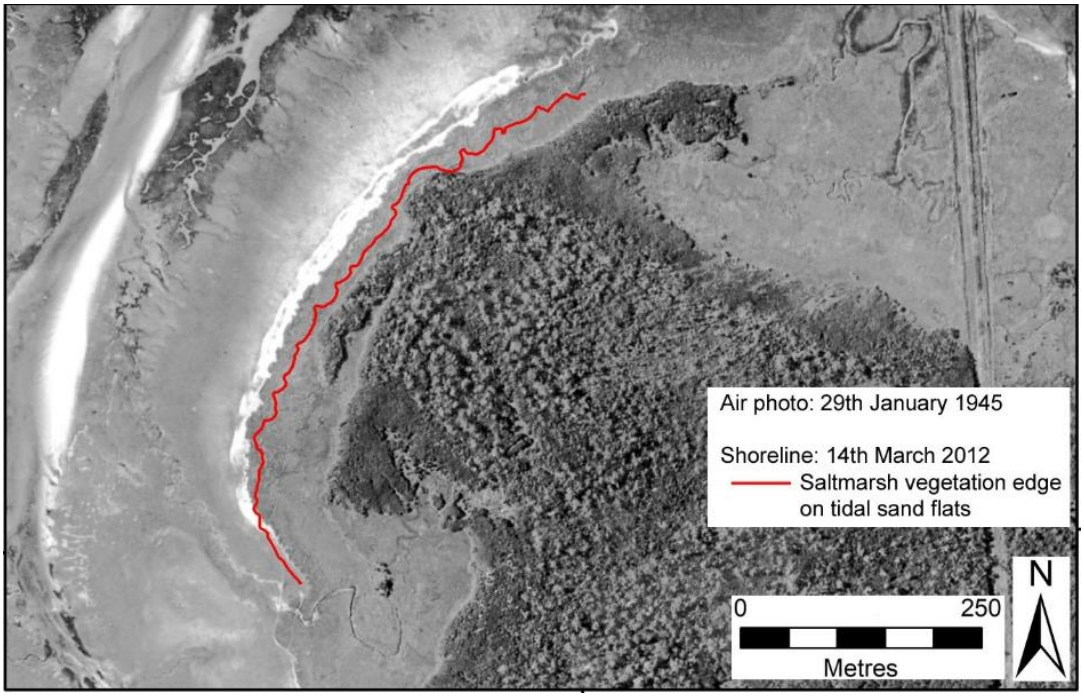

Figure 100: Comparison of shoreline positions in the West Duck Bay SE shoreline area from the earliest (29th January 1945) ortho-rectified air photo and the 2012 shoreline digitised from the 14th March 2012 ortho-photo. Compare Figure 101. The mapped shoreline in both cases was mostly a low saltmarsh vegetation margin contrasting strongly with the sandy tidal flats, except that the anomalously prograded southern end of this shoreline has been infested by the aggressive shoreline-colonising weed rice grass.

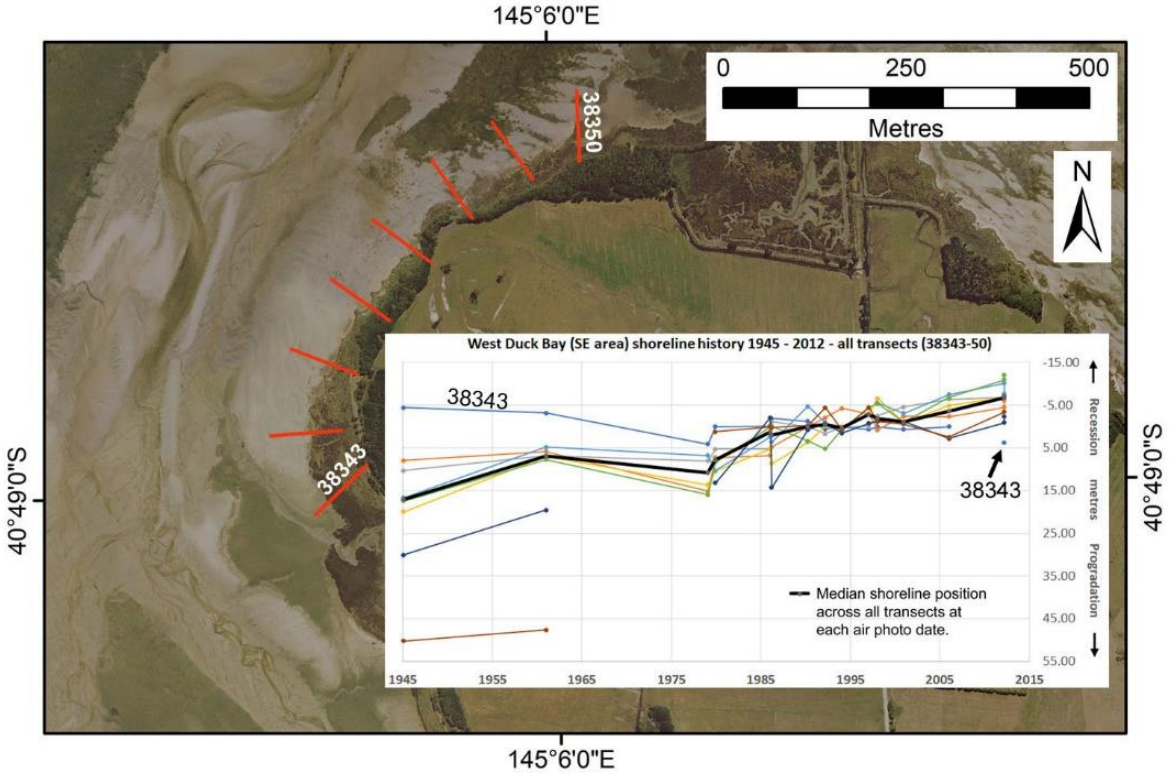

Figure 101: A plot of shoreline position change in the SE study area at West Duck Bay over the period 1945 – 2012. The anomalous prograded shoreline history on transect 38343 (indicated) is at least partly a result of rice grass infestation at the southern end (only) of this study site (see "Artificial disturbances"). The background image is the 2nd March 2012 air photo (© DPIPWE).

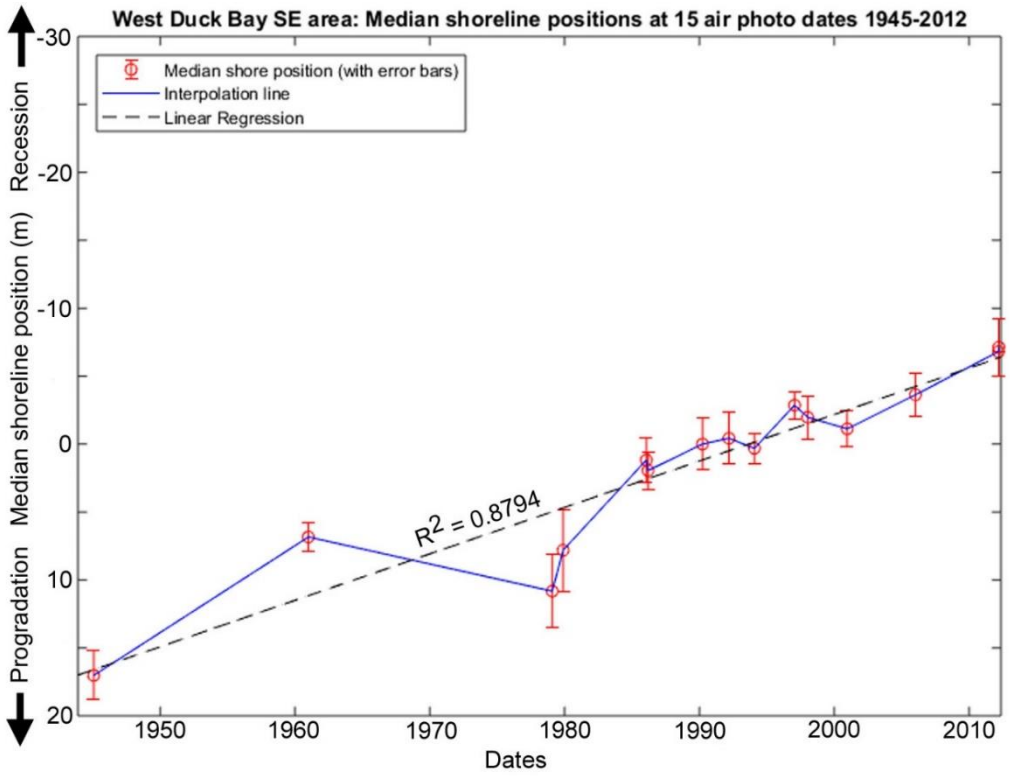

Figure 102: Summary plot of shoreline change history for West Duck Bay SE area at 15 air photo dates from 1945 to 2012. This plots the median of the shoreline positions at each date across all transects shown in Figure 101, with a linear fit (first-order linear regression) over the whole air photo period.

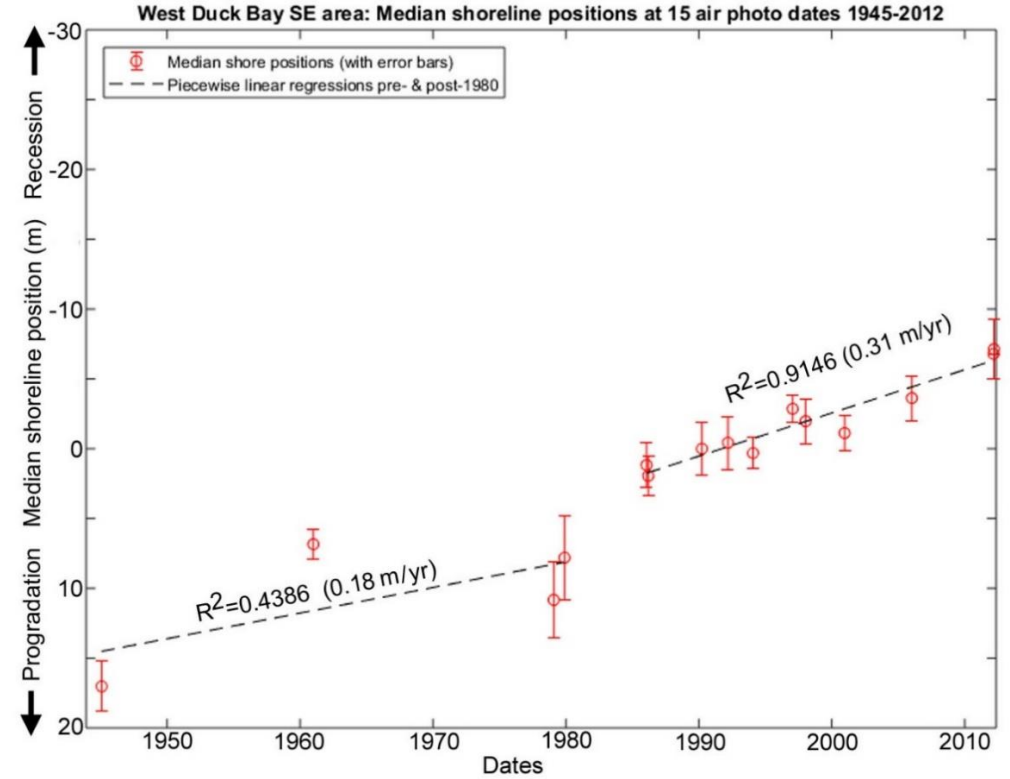

Figure 103: Summary plot of shoreline change history for West Duck Bay SE area at 15 air photo dates from 1945 to 2012. Piecewise linear regression fits pre- and post-1980 demonstrate a significant increase in shoreline recession rates after that date, albeit the number of photos and reduced error margins after 1980 also result in a better post-1980 fit.

Summary shoreline behaviour history and characterisation

Linear regression fits to the data indicate that the shorelines at all five sites have most likely been receding more-or-less continuously since at least the earliest (1945 or 1946) air photo dates. Piecewise linear fits were also used to test for different behaviour before and after the arbitrary date of 1980 at each site. Note that whilst the summary piecewise plot for the north (west) site suggests a stable shoreline prior to 1980, this fit has an insignificant correlation coefficient, and a more likely interpretation of the data is a roughly-constant recession trend over the whole data period for this site which yields a significant correlation coefficient of R^2=0.4930 (see Figure 92).

Three of the five study sites in West Duck Bay have probably been receding at approximately constant rates since at least the dates of the earliest air photos (1945 or 1946). These are the NW, N(W) and N(E) areas, two of which are saltmarsh shores while the N(E) shore is an eroding podzolic Holocene sand shore.

The air photo data for the other two saltmarsh sites (S and SE) is similarly indicative of continuous recession since prior to the earliest (1945) air photos. However in contrast these two sites also show a significant change in behaviour after 1980 compared to before that date, with approximately doubled linear recession rates after 1980 having very high Pearson correlation co-efficients (R^2=0.8415 and R^2=0.9146) after 1980 (see Figure 97 to Figure 103).

Air Photo Data Tables

The following tables provide details of the air photos used, the resulting ortho-photos produced, and the shapefiles representing the shoreline position that were digitised from the ortho-photos.

Table 18: Original air photos and ortho-rectified air photos produced for Western Duck Bay.

Photo Date	**Original DPIPWE air photos (film-frame) / *Ortho-photo name***	**Final image resolution (original scan resolution if downsized) / pixel size of final ortho-photo**	**Original photo scale**	**Mean measured feature position error for ortho-photo (± metres)** [No. of measured feature position reference points]	**Comments**
29th Jan 1945	1-3589 1-3629 1-3631 / *DuckBay_Jan1945a_MGA55.tif/tfw;* *DuckBay_Jan1945b_MGA55.tif/tfw;* *DuckBay_Jan1945c_MGA55.tif/tfw;*	600 dpi / 0.5 x 0.9 m stretched pixel size	1:15,840	1945a: 1.8 m [4] 1945b: 5.3 m [6] 1945c: 5.5 m [6]	Ortho-rectified by C. Sharples Photos appear stretched in image viewers but project correctly in GIS software Jan 1945a: Good accuracy - used (only 4 reference points but all close to priority shores) Jan 1945b: Poor accuracy - not used. Jan 1945c: Poor accuracy – not used
25th Feb 1946	4A-30323 4A-30324 / *DuckBay_Feb1946a_MGA55.tif/tfw;* *DuckBay_Feb1946b_MGA55.tif/tfw*	600 dpi / 0.8m pixel size	1:15,840	1946a: 4.3 m [10] 1946b: 2.3 m [7]	Ortho-rectified by C. Sharples Feb 1946a: Marginal accuracy - not used Feb1946b: Good accuracy - used
23rd Feb 1953	260-501 /	-	1:23,760	-	Not ortho-rectified – too damaged (damaged paper print scanned)

	Not ortho-rectified – photo too damaged				
1961 (day and month unknown)	377-74 377-76 377-77 377-87 / *DuckBay_1961a_MGA55.tif/tfw;* *DuckBay_1961b_MGA55.tif/tfw;* *DuckBay_1961c_MGA55.tif/tfw;* *DuckBay_1961d_MGA55.tif/tfw;*	2039 dpi / 0.2 m pixel size	1:15,840	1961a: 1.8 m [7] 1961b: 2.6 m [6] 1961c: 6.3 m [3] 1961d: 1.1 m [6]	Ortho-rectified by C. Sharples Used 1961a for Perkins Is. area and for southern two areas. Used 1961b for Western area. Used 1961d for southeast area 1961c is CRAP accuracy, not used
19th Feb 1968	505-21 505-22 / *DuckBay_Feb1968a_MGA55.tif/tfw;* *DuckBay_Feb1968b_MGA55.tif/tfw;;*	2039 dpi / 0.4 m pixel size	1:31,680	Feb1968a: 9.3 m [6] Feb1968b: 6.3 m [8] All (combined): 7.8 m [14]	Ortho-rectified by C. Sharples **Very poor accuracy - not used to digitise shoreline**
5th Feb 1970	548-66 548-67 / *DuckBay_Feb1970a_MGA55.tif/tfw;;* *DuckBay_Feb1970b_MGA55.tif/tfw;*	2039 dpi / 0.4 m pixel size	1:31,680	Feb1970a: 14.8 m [11] Feb1970b: 14.0 m [9] All (combined): 14.4 m [20]	Ortho-rectified by C. Sharples **Very poor accuracy - not used to digitise shoreline**
1st Feb 1979	790-13 / *DuckBay_Feb1979_MGA55.tif/tfw;*	2039 dpi / 0.6 m	1:40,000	2.7 m [14]	Ortho-rectified by C. Sharples
24th Nov 1979	808-8 808-30 / *DuckBay_Nov1979a_MGA55.tif/tfw;* *DuckBay_Nov1979b_MGA55.tif/tfw*	2039 dpi / 0.5 m pixel size	1:42,000	Nov1979a: 2.5 m [12] Nov1979b: 3.0 m [12] All (combined): 2.7 m [24]	Ortho-rectified by C. Sharples Both photos cover all priority areas; USED 1979a to map Perkins and westernmost priority shore, 1979b to map southern two (i.e., used both to map priority shorelines furthest from photo edges).
31st Jan 1983	952-1 / *DuckBay_Jan1983_MGA55.tif/tfw*	2039 dpi / 0.4 m pixel size	1:28,000	4.2 m [14]	Ortho-rectified by C. Sharples **Poor accuracy - not used to digitise shoreline**
24th Jan 1986	1053-89 1053-112 / *DuckBay_Jan1986a_MGA55.tif/tfw;* *DuckBay_Jan1986b_MGA55.tif/tfw*	1500 dpi (2039 dpi) / 0.3 m pixel size	1:20,000	Jan1986a: 3.8 m [5] Jan1986b: 1.6 m [8]	Ortho-rectified by C. Sharples Jan1986a: Marginal accuracy, not used. Jan1986b: Good accuracy, used.
14th Feb 1986	1058-61 / *DuckBay_Feb1986_MGA55.tif/tfw*	2039 dpi / 0.3 m	1:28,000	3.6 m [15]	Ortho-rectified by C. Sharples **Poor accuracy - not used to digitise shoreline** (very close in time to Jan & Mar air photos)
11th Mar 1986	1063-14 1063-15 1063-39 /	2039 dpi / 0.2 m pixel size	1:15,000	Mar1986a: 1.1 m [7] Mar1986b:	Ortho-rectified by C. Sharples

	DuckBay_Mar1986a_MGA55.tif/tfw *DuckBay_Mar1986b_MGA55.tif/tfw* *DuckBay_Mar1986c_MGA55.tif/tfw*			1.3 m [4] Mar1986c: 2.1 m [5] All (combined): 1.4 m [16]	
25th Mar 1990	1155-215 / *DuckBay_Mar1990_MGA55.tif/tfw*	2039 dpi / 0.6 m pixel size	1:42,000	1.9 m [16]	Ortho-rectified by C. Sharples
10th Mar 1992	1190-212 / *DuckBay_Mar1992_MGA55.tif/tfw*	2039 dpi / 0.6 m pixel size	1:42,000	1.9 m [16]	Ortho-rectified by C. Sharples
28th Jan 1994	1217-36 / *DuckBay_Jan1994_MGA55.tif/tfw*	2039 dpi / 0.3 m pixel size	1:24,000	1.1 m [16]	Ortho-rectified by C. Sharples
5th Dec 1994	1226-165 / *DuckBay_Dec1994_MGA55.tif/tfw*	2039 dpi / 0.56 m pixel size	1:42,000	4.3 m [15]	Ortho-rectified by C. Sharples **Poor accuracy - not used to digitise shoreline**
20th Jan 1997	1266-36 1266-59 / *DuckBay_Jan1997a_MGA55.tif/tfw;* *DuckBay_Jan1997b_MGA55.tif/tfw;*	1500 dpi (2039 dpi) / 0.35 m pixel size	1:20,000	Jan1997a: 2.7m [6] Jan1997b: 1.0 m [13]	Ortho-rectified by C. Sharples **Used Jan1997b only (Good accuracy, better coverage).**
11th Jan 1998	1285-80 / *DuckBay_Jan1998_MGA55.tif/tfw;*	2039 dpi / 0.3 m pixel size	1:24,000	1.6 m [15]	Ortho-rectified by C. Sharples 1285-79 overlaps - not used
16th Dec 2000	1335-36 / *DuckBay_Dec2000_MGA55.tif/tfw*	1500 dpi (2039 dpi) / 0.4 m pixel size	1:24,000	1.3 m [16]	Ortho-rectified by C. Sharples
1st Jan 2001	1340-228 / *DuckBay_Jan2001_MGA55.tif/tfw*	1500 dpi (2039 dpi) / 0.8 m pixel size	1:42,000	4.6 m [15]	Ortho-rectified by C. Sharples **Poor accuracy - not used to digitise shoreline**
13th Feb 2005	1392-64 / *DuckBay_Feb2005_MGA55.tif/tfw*	1500 dpi (2039 dpi) / 0.5 m pixel size	1:20,000	3.1 m [7]	Ortho-rectified by C. Sharples Covers west part of study area only.
8th Jan 2006	1403-102 / *DuckBay_Jan2006a_MGA55.tif/tfw*	1500 dpi (2039 dpi) / 0.3 m pixel size	1:20,000	1.6 m [13]	Ortho-rectified by C. Sharples
21st Jan 2006	1403-197 / *DuckBay_Jan2006b_MGA55.ecw*	2039 dpi / 0.5m pixel size	1:42,000	4.8 m [16] (quoted absolute accuracy ±15m)	Ortho-rectified by DPIPWE Original DPIPWE ortho file: *1403_197_op.ecw* **Poor accuracy - not used to digitise shoreline**
2nd Mar 2012	1468-004 / *DuckBay_Mar2012a_MGA55.ecw*	2039 dpi / 0.3m pixel size	1:24,000	0.0m [N/A] (quoted absolute accuracy ±5m)	REFERENCE LAYER Ortho-rectified by DPIPWE Original DPIPWE ortho file: *1468_004_op.ecw*
14th March 2012	1469-052 /	2039 dpi / 0.3m pixel size	1:24,000	2.1m [16]	Ortho-rectified by DPIPWE Original DPIPWE ortho file:

	DuckBay_Mar2012b_MGA55.ecw			(quoted absolute accuracy ±10m)	*1469_052_op.ecw*

Table 19: Digitised shoreline shapefiles produced for Western Duck Bay (using ortho-photos listed in Table 18 above).

Date of air photo(s)	Shapefile	Shoreline digitised by	Comments
29th Jan 1945	DuckBay_MGA55_19450129.shp	Chris Sharples (2019)	Poor resolution, medium contrast. Veg. line moderately distinct against sand flats
25th Feb 1946	DuckBay_MGA55_19460225.shp	Chris Sharples (2019)	Poor resolution but good contrast – veg. line distinct against sand flats. Slumped erosion scarp on Perkins Island not discernible.
1961 (day & month unknown – not in original records!!)	DuckBay_MGA55_19610101.shp	Chris Sharples (2019)	Good resolution, moderate to good contrast. Veg. line distinct where erosion-scarped or definable against sand flats, but vague in parts and on some photos. On Perkins Island mapped mid-line of recent slumped erosion scarp.
1st Feb 1979	DuckBay_MGA55_19790201.shp	Chris Sharples (2019)	Moderate resolution, poor contrast. Veg. line mostly definable against sand flats. On Perkins Island mapped mid-line of recent slumped erosion scarp.
24th Nov 1979	DuckBay_MGA55_19791124.shp	Chris Sharples (2019)	Moderate resolution and contrast. Veg. line mostly clearly defined against sand flats. On Perkins Island mapped mid-line of recent slumped erosion scarp.
24th Jan 1986	DuckBay_MGA55_19860124.shp	Chris Sharples (2019)	Moderate resolution and contrast. Veg. line mostly clearly defined against sand flats. On Perkins Island mapped mid-line of recent slumped erosion scarp.
11th Mar 1986	DuckBay_MGA55_19860311.shp	Chris Sharples (2019)	Resolution & contrast good. Veg. line mostly clearly defined against sand flats. Some low erosion scarps visible (mapped as veg. line).
25th Mar 1990	DuckBay_MGA55_19900325.shp	Chris Sharples (2019)	Resolution moderate contrast OK. Veg. line mostly clearly defined against sand flats.
10th Mar 1992	DuckBay_MGA55_19920310.shp	Chris Sharples (2019)	Moderate to poor resolution and contrast. Vegetation line clear

			against sand in parts. On Perkins Island mapped mid-line of recent slumped erosion scarp.
28th Jan 1994	DuckBay_MGA55_19940128.shp	Chris Sharples (2019)	Moderate resolution and contrast. Mapped veg. line mostly distinct against sand flats. On Perkins Island mapped mid-line of recent slumped erosion scarp.
20th Jan 1997	DuckBay_MGA55_19970120.shp	Chris Sharples (2019)	Moderate resolution and contrast. Perkins Is: mapped mid-line of recent slumped erosion scarp; Elsewhere vegetation line distinct but details poorly resolved.
11th Jan 1998	DuckBay_MGA55_19980111.shp	Chris Sharples (2019)	Poor resolution and contrast. Perkins Is: mapped mid-line of recent slumped erosion scarp; Elsewhere veg. line distinct in some areas, less so in others.
16th Dec 2000	DuckBay_MGA55_20001216.shp	Chris Sharples (2019)	Good resolution and contrast. Perkins Is: mapped mid-line of recent slumped erosion scarp; Elsewhere veg. line mapped, mainly clear against sand flats.
13th Feb 2005	DuckBay_MGA55_20050213.shp	Chris Sharples (2019)	Contrast moderate to poor, photo covers western part of study area only. Saltmarsh veg. edge well defined against sand flats.
8th Jan 2006	DuckBay_MGA55_20060108.shp	Chris Sharples (2019)	Good resolution and contrast. Erosional saltmarsh edge clearly defined against sand flats.
2nd March 2012	DuckBay_MGA55_20120302.shp (Reference Layer)	Chris Sharples (2019)	Good resolution and contrast. Erosional saltmarsh edge clearly defined against sand flats. Some shadows and overhanging trees allowed for on Perkins Island.
14th March 2012	DuckBay_MGA55_20120314.shp	Chris Sharples (2019)	Good resolution, moderate contrast. Veg line varies from well-defined to somewhat fuzzy in some areas.

A1.3 *Very high-energy swell-exposed sandy shores*

A1.3.1 Cloudy Bay Beach East (south Bruny Island)

Geomorphology and process environment

A swell exposed sandy beach, whose northern half is backed by a higher foredune than the southern half, and is more directly exposed to the dominant westerly winds and south-westerly swells than is the other swell-exposed beach in Cloudy Bay (Cloudy Bay Beach West).

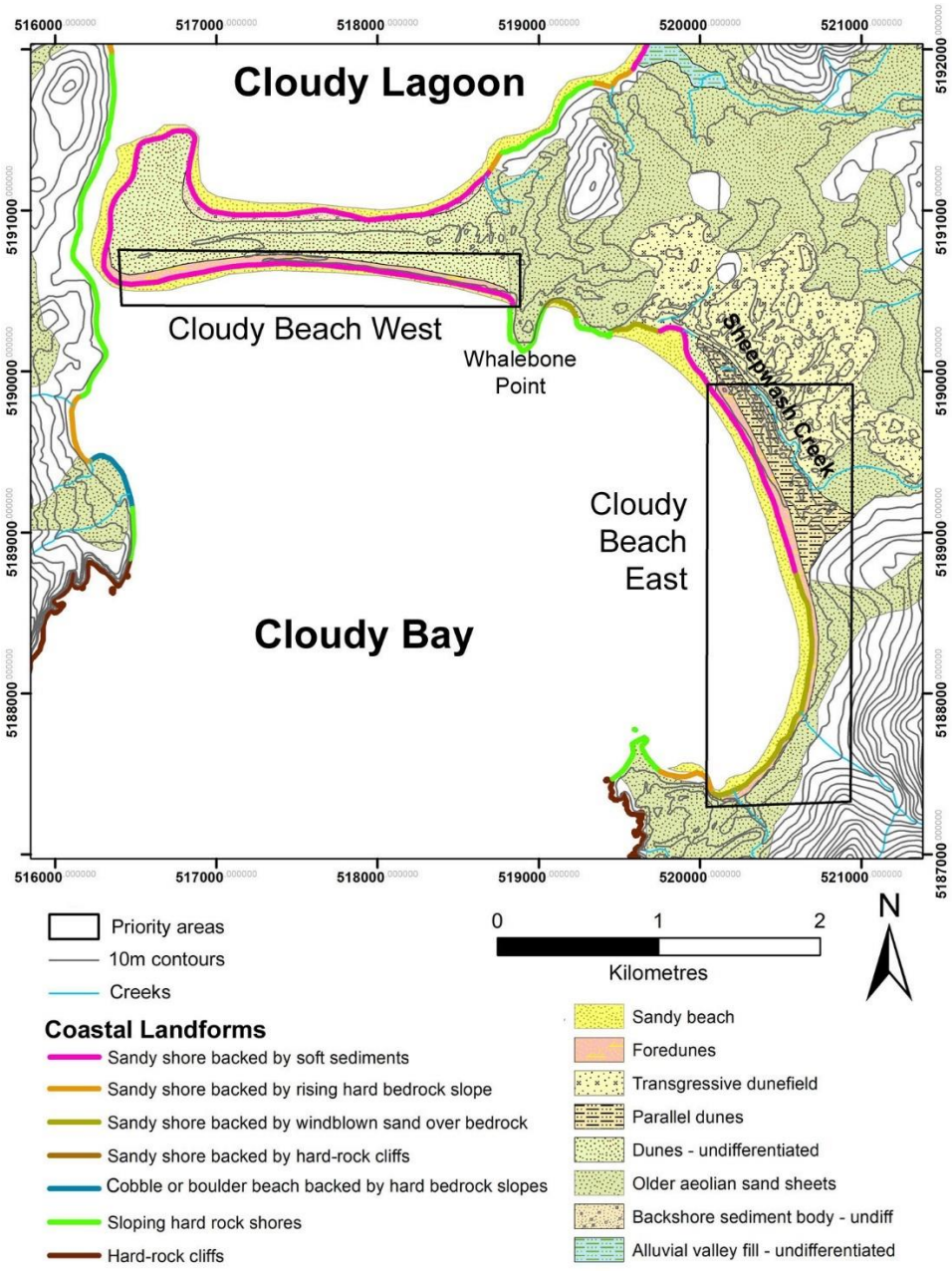

Figure 104: Coastal landforms at Cloudy Bay, south Bruny Island, indicating the more swell-exposed Cloudy Bay East priority area selected for air photo history analysis. The less exposed Cloudy Beach West analysis is described separately in Section A1.4.6. Coastal landform mapping is based on the 1:50,000 Dover Geological map sheet (Geological Survey of Tasmania), with additional field observations by C. Sharples. Co-ordinate system is Map Grid of Australia Zone 55 (GDA1994 datum).

Wind (wind-wave) climate

Likely similar to Cape Bruny wind record (10 km to SW), with dominantly north-west to south-west winds. The anomalous northerly wind component is unexplained but possibly a result of local topographic steering effects at Cape Bruny.

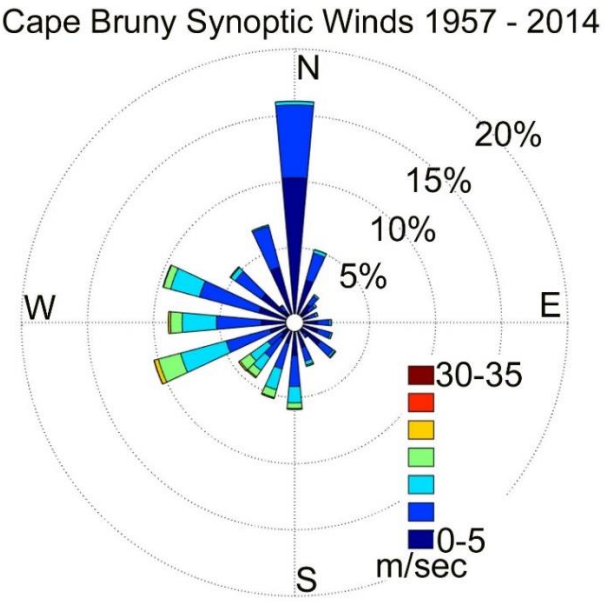

Figure 105: Cape Bruny synoptic wind directions 1957 – 2014. Cape Bruny, 10 km south-west of Cloudy Bay Beach east, is the nearest long-term weather station. Wind rose prepared by Chris Sharples, using original synoptic wind data from the Australian Bureau of Meteorology.

Sand transport and budget

The beach probably receives swell-driven onshore sand gains from the continental shelf (Harris & Heap 2014). The beach is well-embayed between rocky headlands with no likely alongshore sand losses or gains, and no other active sand sinks such as active transgressive dunes of significant estuaries or lagoons.

Air photo analysis

Air photos from 16 dates between 15th December 1948 and 15th December 2009 were used to analyse shoreline changes over time. Shorelines from the 2nd Feb 1965, 6th Feb. 1984 and 1st Feb. 2002 orthophotos were not used due to accuracy and quality issues (see Table 20 and Table 21 below). Shoreline history was measured along 28 100-metre spaced transects numbered 4862 to 4891, excluding transects 4877 and 4890 which were located respectively on a vehicular access track and a creek gully, which would have yielded highly anomalous results. A section of a few hundred metres length at the north-western end of East Cloudy Beach was excluded due to being of an entirely different nature, comprising unstable and largely unvegetated low hummocky dunes around the mouth of Sheepwash Creek instead of the high stable foredune backing the studied section of the beach. The shoreline history results are plotted below at Figure 106 & Figure 107.

Shore behaviour history from air photos

Shoreline change along all used transects was mainly coherent throughout the air photo period, with only minor shoreline position anomalies at most air photo dates. This means that shoreline movement landwards or seawards was roughly parallel along the whole section of beach studied. The plots (Figure 106 & Figure 107) show long-term shoreline stability with a suggestion of a non-significant progradation trend over the whole air photo period (~5.0 m seawards shoreline movement overall). This is less pronounced than the progradation trend seen at the adjacent less-exposed Cloudy Bay

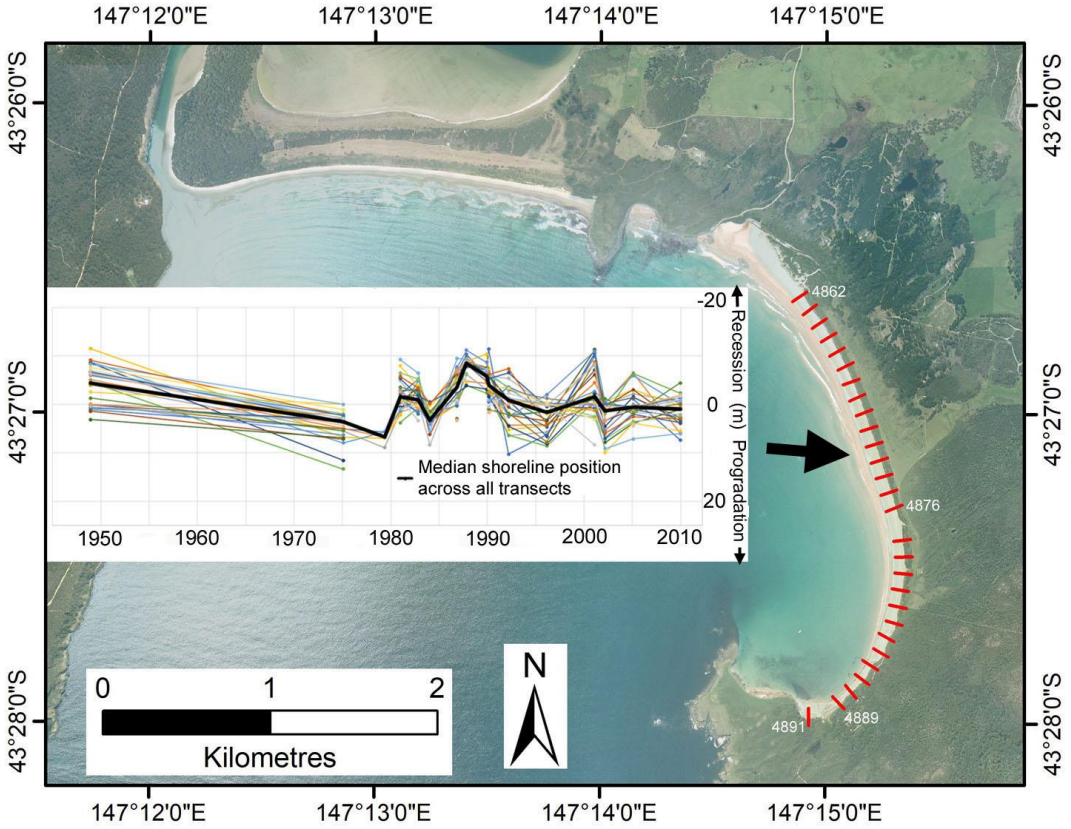

Figure 106: Shoreline position changes along all individual used transects for East Cloudy Beach shoreline, for 16 air photo dates from 1948 to 2009 as listed on Table 20 (omitting 2nd Feb 1965, 6th Feb. 1984 and 1st Feb. 2002 due to accuracy and quality issues with those photos). The used transects used are 100m – spaced red lines on the air photo with selected transect numbers indicated. This plot indicates that shoreline changes are coherent along the whole beach section studied and show long-term shoreline stability with a suggestion of a long-term non-significant progradation trend. Shorter erosion – accretion cycles (dynamic stability) are super-imposed. See also summary plot Figure 107 below. The background image is the 2009 air photo (© DPIPWE).

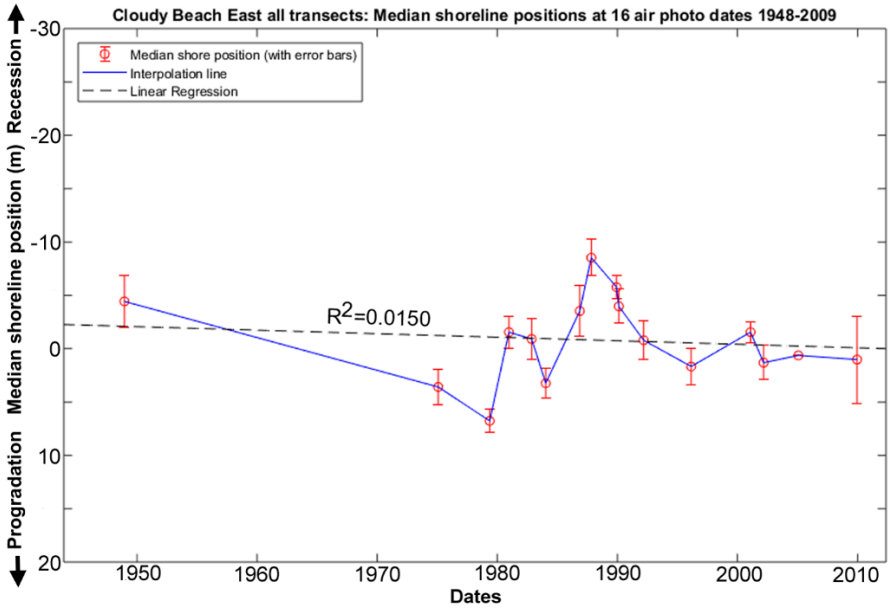

Figure 107: Summary plot of shoreline change history across all transects (as shown on Figure 106) at Cloudy Beach East shoreline for 16 air photo dates from 1948 to 2009, with air photo error bars. A linear regression fit indicates short-term variability but long-term shoreline stability with a suggestion of a small non-significant progradation trend.

Beach West (see Section A1.4.6, Figure 217). Shorter erosion – accretion (recovery) episodes of up to ~20 metres amplitude are super-imposed on the long term trend. The shoreline movement plots indicate (by landwards shoreline movement) that the most notable of these commenced with a major erosion event (or cluster of events) circa 1980 followed by a second major erosion event (or cluster of events) circa 1984-1986.

Air Photo Data Tables

The following tables provide details of the air photos used, the resulting ortho-photos produced, and the shapefiles representing the shoreline position that were digitised from the ortho-photos.

Table 20: Original air photos and ortho-rectified air photos produced for the Cloudy Bay beaches (east and west) and Cloudy Lagoon.

Photo Date	**Original DPIPWE air photos (film-frame) / Ortho-photo name**	**Final image resolution (original scan resolution if downsized) / pixel size of final ortho-photo**	**Original photo scale**	**Mean measured feature position error for ortho-photo (± metres)** [no. of measured feature position reference points]	**Comments**
15th Dec 1948	172-2260 172-2262 172-2247 172-2248 172-2213 172-2215 / *CloudyBay_Dec1948a_MGA55.tif/tfw;* *CloudyBay_Dec1948b_MGA55.tif/tfw;* *CloudyBay_Dec1948c_MGA55.tif/tfw;* *CloudyBay_Dec1948d_MGA55.tif/tfw;* *CloudyBay_Dec1948e_MGA55.tif/tfw;* *CloudyBay_Dec1948f_MGA55.tif/tfw*	600 dpi / 1.0 m E-W & 0.55 m N-S pixel size.	1:15,840	All photos: 2.4 m [16] (mean of all measurements except for Dec 1948f) Individual photos: Dec1948a: 2.4 m [3] Dec1948b: 2.5m [3] Dec1948c: 2.3m [3] Dec1948d: 2.3 m [4] Dec1948e: 2.6 m [3] Dec1948f: 5.9 m [3] Ortho Dec 1948f very poor accuracy – Not used	Ortho-rectified by Chris Sharples Pixels stretched in ortho process due to unusual camera orientation – photos appear stretched in Photoshop but display accurately in GIS software.
2nd Mar 1965	453-62 453-63 453-185 / *CloudyBay_Mar1965a_MGA55.tif/tfw;* *CloudyBay_Mar1965b_MGA55.tif/tfw;* *CloudyBay_Mar1965c_MGA55.tif/tfw*	2039 dpi / 0.45 m pixel size	1:31,680	14.0 m [13]	Ortho-rectified by Chris Sharples All poor to very poor ortho-rectification accuracy – not used. Suspect original photos distorted due to camera tilt?
31st Jan 1975	668-107 / *CloudyBay_Jan1975_MGA55.tif/tfw*	2039 dpi / 0.58 m pixel size	1:40,000	1.7 m [7]	Ortho-rectified by Chris Sharples
16th May 1979	799-123 799-124 / *CloudyBay_May1979a_MGA55.tif/tfw;* *CloudyBay_May1979b_MGA55.tif/tfw*	2039 dpi / 0.25 m pixel size	1:20,000	1.1 m [7]	Ortho-rectified by Chris Sharples
21st Dec 1980	846-274 846-341 846-343 / *CloudyBay_Dec1980a_MGA55.tif/tfw;* *CloudyBay_Dec1980b_MGA55.tif/tfw;*	2039 dpi / 0.25 m pixel size	1:15,000	1.5 m [9]	Ortho-rectified by Chris Sharples

	CloudyBay_Dec1980c_MGA55.tif/tfw				
11th Nov. 1982	931-177 / *CloudyBay_Nov1982_MGA55.tif/tfw*	2039 dpi / 0.65 m pixel size	1:42,000	1.9 m [10]	Ortho-rectified by Chris Sharples
14th Jan 1984	979-51 979-53 979-62 979-63 / *CloudyBay_Jan1984a_MGA55.tif/tfw; CloudyBay_Jan1984b_MGA55.tif/tfw; CloudyBay_Jan1984c_MGA55.tif/tfw; CloudyBay_Jan1984d_MGA55.tif/tfw*	2039 dpi / 0.19 m pixel size	1:15,000	1.4 m [11]	Ortho-rectified by Chris Sharples
6th Feb 1984	984-6 984-7 / *CloudyBay_Feb1984a_MGA55.tif/tfw; CloudyBay_Feb1984b_MGA55.tif/tfw.*	1500 dpi (2039 dpi) / 0.38 m pixel size	1:20,000	1.5 m [8]	Ortho-rectified by Chris Sharples NOT USED for shoreline mapping: close in time to Jan 1984 air photos and much poorer contrast and resolution.
14th Nov 1986	1076-98 / *CloudyBay_Nov1986_MGA55.tif/tfw*	2039 dpi / 0.58 m pixel size	1:42,000	2.4 m [7]	Ortho-rectified by Chris Sharples
30th Oct 1987	1092-174 / *CloudyBay_Oct1987_MGA55.tif/tfw;*	2039 dpi / 0.56 m pixel size	1:42,000	1.7 m [8]	Ortho-rectified by Chris Sharples
5th Dec 1989	1143-9 / *CloudyBay_Dec1989_MGA55.tif/tfw;*	1500 dpi (2039 dpi) / 0.75 m pixel size	1:42,000	1.1 m [8]	Ortho-rectified by Chris Sharples
14th Feb 1990	1150-154 1150-160 / *CloudyBay_Feb1990a_MGA55.tif/tfw*; *CloudyBay_Feb1990b_MGA55.tif/tfw*	2039 dpi / 0.55 m pixel size	1:42,000	1.6 m [15]	Ortho-rectified by Chris Sharples
9th Mar 1992	1190-34 1190-74 / *CloudyBay_Mar1992a_MGA55.tif/tfw; CloudyBay_Mar1992b_MGA55.tif/tfw*	2039 dpi / 0.56 m pixel size	1:42,000	1.8 m [15]	Ortho-rectified by Chris Sharples
23rd Feb 1996	1249-107 1249-119 1249-129 / *CloudyBay_Feb1996a_MGA55.tif/tfw; CloudyBay_Feb1996b_MGA55.tif/tfw; CloudyBay_Feb1996c_MGA55.tif/tfw*	1500 dpi (2039 dpi) / 0.37 m pixel size	1:20,000	1.7 m [10]	Ortho-rectified by Chris Sharples
1st Feb 2001	1345-168 1345-176 / *CloudyBay_Feb2001a_MGA55.tif/tfw; CloudyBay_Feb2001b_MGA55.tif/tfw*	1500 dpi (2039 dpi) / 0.75 m pixel size	1:42,000	1.0 m [17]	Ortho-rectified by Chris Sharples
1st Feb 2002	1352-204 1352-218 / *CloudyBay_Feb2002a_MGA55.tif/tfw*;	1500 dpi (2039 dpi) / 0.38 m pixel size	1:20,000	1.2 m [8]	Ortho-rectified by Chris Sharples

	CloudyBay_Feb2002b_MGA55.tif/tfw				
5th Mar 2002	1357-62 1357-63 / *CloudyBay_Mar2002a_MGA55.tif/tfw;* *CloudyBay_Mar2002b_MGA55.tif/tfw*	1500 dpi (2039 dpi) / 0.39 m pixel size	1:20,000	1.6 m [12]	Ortho-rectified by Chris Sharples
25th Jan 2005	1391-13 1391-90 / *CloudyBay_Jan2005a_MGA55.ecw;* *CloudyBay_Jan2005b_MGA55.ecw*	2039 dpi / 0.49 m pixel size	1:42,000	0.00 m [N/A]	REFERENCE IMAGE (zero relative feature position error by convention) Same resolution as 2009 ortho but better contrast) Ortho-rectified by DPIPWE Original DPIPWE ortho files: *1391_013_op.ecw* *1391_090_op.ecw*
15th Dec 2009	1439-76 1439-84 / *CloudyBay_Dec2009a_MGA55.ecw;* *CloudyBay_Dec2009b_MGA55.ecw*	2039 dpi / 0.50 m pixel size	1:42,000	4.1 m [11]	Ortho-rectified by DPIPWE Original DPIPWE ortho files: *1439_076_op.ecw* *1439_084_op.ecw* Marginal accuracy – but used since nothing better more recently
No DPIPWE air photo cover of main beach sections of interest from 2009 until 2017; some minor coverage of ends of beaches in 2010-2011 and 2011-2012 but not enough to be of use.					

Table 21: Digitised shoreline shapefiles produced for the Cloudy Bay beaches (east and west) and Cloudy Lagoon using ortho-photos listed in Table 20 above.

Date of air photo(s)	Shapefile	Shoreline digitised by	Comments
15th Dec 1948	CloudyShores_MGA55_19481215.shp	Chris Sharples (2019)	Moderate to poor resolution and contrast, but veg. line mappable. E. beach: Intact veg. line at toe of foredune mostly mapped, except in north third where veg. line at top of high slumping bare sand face mapped; W. beach: mapped scarped (slightly rounded) sandy dune front backed by sparse dune veg. and dune blowouts. Lagoon: Veg. line mapped, much of it clearly defined, not much wrack confusing shoreline position in this image.
31st Jan 1975	CloudyShores_MGA55_19750131.shp	Chris Sharples (2019)	Moderate resolution & contrast. E. beach: Incipient dune veg. line mapped at front of mainly bare high scarp face; W. beach: mapped scarped (slightly rounded) sandy dune front backed by sparse dune veg., likely some incipient dune veg. in front but sparse & difficult to see. Lagoon: Veg. line mapped, much of it clearly defined, not much wrack confusing

			shoreline position in this image. Shoreline better defined than in several subsequent photos.
16th May 1979	CloudyShores_MGA55_19790516.shp	Chris Sharples (2019)	Moderate resolution & contrast. Photo cover incomplete. E. beach: mapped seawards veg. line on dune, scarp largely revegetated, no incipient dune veg. visible; W. beach: mapped rounded sandy dune front (incipient dune?) backed by sparse dune veg., shadowing allowed for, broader incipient dune veg. zone at W. end. Lagoon: Veg. line mapped, but commonly difficult to differentiate from abundant wrack.
21st Dec 1980	CloudyShores_MGA55_19801221.shp	Chris Sharples (2019)	Moderate resolution, poor contrast. Photo cover incomplete. E. beach: mapped seawards veg. line on dune, scarp largely revegetated. Poss. some incipient dune veg. but unclear. W. beach: mapped rounded scarp at dune front backed by sparse dune veg., varying to incipient dune veg. front at west end. Lagoon: Veg. line mapped, but commonly difficult to differentiate from wrack.
11th Nov 1982	CloudyShores_MGA55_19821111.shp	Chris Sharples (2019)	Resolution and contrast poor to moderate; can't see if incipient dune veg present or not. E. beach: Mapped middle of slumped older veg. on high scarp. W. beach: mapped veg. line on old scarp+ incipient veg. line where visible at W. end of beach. Lagoon: Clear veg. line in parts; parts confused by wrack.
14th Jan 1984	CloudyShores_MGA55_19840114.shp	Chris Sharples (2019)	Good resolution and contrast. E. Beach: Incipient foredune veg. well-defined and front mapped as veg. line; high dune scarp behind revegetating; W. beach: mapped veg line at front of slumped scarp, mainly incipient dune front veg. Lagoon: Veg. line mapped, sometimes difficult to distinguish from wrack. NE lagoon shore wrack-dominated.

14th Nov 1986	CloudyShores_MGA55_19861114.shp	Chris Sharples (2019)	Moderate resolution and contrast. E. Beach: Old high scarp well vegetated, mostly mapped recent scarp top at foot of high dune; W. Beach: mapped top of recent partly-slumped dune, no incipient veg in front. Lagoon: Well-defined veg. edge.
30th Oct 1987	CloudyShores_MGA55_19871030.shp	Chris Sharples (2019)	Coarse - moderate resolution only. E. beach – high slumped dune scarp, not much detail visible, no incip. veg visible, mapped top of scarp; W. beach: Recent scarp mapped, no incip. veg. visible (but photo-qual. is mediocre): Lagoon: Veg line well defined where mapped.
5th Dec 1989	CloudyShores_MGA55_19891205.shp	Chris Sharples (2019)	Coarse resolution, moderate contrast; E. beach: recent steep high erosion scarp, some slumping & shadows, no incip. veg. visible, mapped top of scarp. W. beach: No recent erosion scarp evident; older slumped scarp with some clumpy incip veg visible in W. part (mapped veg. line incl. mid-slump line and incip. veg. line where visible). Lagoon: Priority areas only. Veg. line mapped, well defined. Wrack ignored.
14th Feb 1990	CloudyShores_MGA55_19900214.shp	Chris Sharples (2019)	Coarse resolution, moderate contrast, easterly shadowing. E. beach: recent steep (shadowed) erosion scarp along most of beach (scarp top mapped), no incipient veg. visible except W. end. W. Beach: Fairly recent to partly slumped scarp mapped, little incipient veg. visible. Lagoon: veg. line mapped where well defined, not mapped where difficult to pick. Wrack ignored where obvious.
9th Mar 1992	CloudyShores_MGA55_19920309.shp	Chris Sharples (2019)	Moderate contrast, coarse resolution. E. Beach: slumped scarp with incipient veg. in front in many parts - mapped as veg line where present. W. beach: slumped erosion scarp, not much incipient veg

			(some at W. end). Lagoon: Veg. line mostly well defined, wrack, shadows and overhanging trees allowed for.
23rd Feb 1996	CloudyShores_MGA55_19960223.shp	Chris Sharples (2019)	Moderate contrast & resolution. E. beach: incipient dune veg. in e. & w. parts, more recent scarp with less incip. veg. in middle; W. Beach: mostly recent slumped scarp, Incip veg. at w. end. Lagoon: veg. line distinct, some seagrass wrack present and allowed for (not shoreline). Northerly shadows allowed for in parts.
1st Feb 2001	CloudyShores_MGA55_20010201.shp	Chris Sharples (2019)	Moderate to shite resolution and contrast only (a bit 'fuzzy'). E. beach - mostly dominated by high (recent?) erosion scarp with slumping. W. beach – Slumped erosion scarp with some incipient veg in front (esp. at W. end). Lagoon veg line mostly distinct, but cannot discern details, e.g., scarps.
1st Feb 2002	CloudyShores_MGA55_20020201.shp Not used for open coast beaches where this shoreline yields anomalously "prograded" shoreline position relative to March 2002 photo (which is very close in time) and to other close dates. Used for lagoon shores: shoreline not anomalously displaced. Source of anomaly unclear.	Chris Sharples (2019)	Good resolution and contrast. E. beach – Incipient dune veg expanding along E half of foredune front, but little recovery in high eroded & slumped middle area. W. beach has old scarp with incipient dune veg spreading in front. Lagoon – mostly well-defined veg. line, overhanging trees allowed for.
5th March 2002	CloudyShores_MGA55_20020305.shp	Chris Sharples (2019)	Good resolution and medium contrast, veg. line clear in most places. E. beach foredune slumped with some incipient veg recovery in most parts. W. beach has slumped scarp and some incip. veg. recovery esp. towards W end. Lagoon veg. line mostly clear, overhanging trees & likely wrack allowed for.
25th January 2005	CloudyShores_MGA55_20050125.shp	Chris Sharples (2019)	Moderate resolution and good contrast, some shadowing allowed for. Veg line distinct, W. beach accreting in W. third (incip. dune veg),

			elsewhere scarped & slumping; E. beach midsection = high slumping scarp, incipient dunes accreting in east half. Lagoon veg. line distinct, overhanging trees & veg. allowed for. likely wrack on some shores is hard to distinguish.
15th December 2009	CloudyShores_MGA55_20091215.shp	Chris Sharples (2018)	Moderate resolution, good contrast, vegetation line well defined, some shadowing from NW. West beach mainly accreting incipient marram veg line with some dune face bare patches towards east. East beach veg line clear, includes high slumped section. Lagoon veg. line mostly well defined, allowed for some overhanging veg. and seagrass wrack obscuring in parts; need to distinguish some rocky shore platforms.

A1.3.2 Prion Beach (south coast)

Locality and general description

Prion Beach is a long high-energy swell-exposed sandy beach roughly halfway along the south coast of Tasmania in the South-west National Park and Western Tasmania Wilderness World Heritage Area (TWWHA). Apart from a mostly undeveloped bushwalking route and a rudimentary campsite, there are no significant local artificial disturbances at this beach (notably including an absence of the introduced dune-colonising marram grass *Ammophila arenaria*, which can promote faster and higher dune growth but does not prevent wave erosion). Access is by sea, air or walking only.

The beach was visited by Chris Sharples (with others) three times during this project, in November/December 2014, 2015 and 2016, as part of a DPIPWE-funded helicopter-based project to establish and survey beach profile transects. Chris Sharples has also visited Prion Beach on numerous other occasions beginning in 1976.

Geomorphology and process environment

Geomorphic description

Geomorphic aspects of Prion Beach have been described by Cullen (1998), Cullen and Dell (2013) and Short (2006b).

Prion Beach is highly exposed and swash-aligned to predominating south-westerly swells and Southern Ocean storms (Table 22 provides key swell wave climate parameters for Prion Beach based on the CAWCR wave hindcast 1979-2010 by the Bureau of Meteorology Australia and CSIRO Australia 2013). The beach is also exposed to apparently-dominant westerly winds driving both sand movement along the beach and local wind-waves (note there are no local wind records for Prion Beach, and the nearest (from Maatsuyker Island) are unlikely to be representative of this site owing to Maatsuyker's much greater exposure to westerly and north-westerly winds). The tidal range is approximately 1.2m (spring) to 0.2m (neap): Short (2006b)

Prion Beach lies within a broad embayment in a dominantly rocky and cliffed coast and faces south-southwest (aspect 205º T). The embayment is about 6 km wide and bounded by large steep rocky headlands at Point Cecil and Menzies Bluff (Figure 108). Prion Beach is the seawards side of a broad coastal barrier comprising dune and marine sands extending in depth to below present sea-level. The barrier spit extends across the mouth of the broad estuarine New River Lagoon; however, the eastern two kilometres of the beach is a 200-300 metre wide beach spit where no foredunes have established because the permanently-open tidal entrance channel episodically migrates across the spit (see Figure 109). The dominant pattern observed (intermittently) by the author since 1976 is that the tidal channel outlet shifts westwards to various locations along the low eastern section of the spit during occasional large storms or floods, but then progressively migrates back eastwards along the spit to its normal position hard against the rocky headland at the east end of the embayment (see Figure 108 & Figure 109). This implies the beach is dominated by an easterly longshore drift driven by the dominant south-westerly swell wave climate and mainly westerly wind-waves. The beach itself is a Transverse Bar and Rip (TBR) to Rhythmic Bar and Beach (RBB) morphodynamic type (Short 2006b) fronted by a 300 metre-wide rip-dominated surf zone.

The western two thirds of the beach is backed by a vegetated established foredune (Hesp 2002) which in turn is backed by several parallel dunes varying from about 4m to 25m high and interpreted by Cullen and Dell (2013) as representing a phase of Mid- to Late-Holocene shoreline progradation following the end of the last post-glacial marine transgression circa 7000 years ago. Erosion scarps in the seawards face of the main foredune expose only weakly developed palaeosols. The parallel dunes are backed by eastward-trending and now well-vegetated prograded curvi-linear dune ridges with some dune lakes in swales, forming the northern part of the barrier spit, which have yielded OSL

dates of 2.2 ±0.5 to 6.2 ±2.8 thousand years old (Cullen & Dell 2013). These represent an early phase in the Mid-Late Holocene accretion of the present barrier spit. Much older Pleistocene dunes dated to around the Last Interglacial phase (circa 125,000 years BP) have also been identified further inland on the eastern side of New River Lagoon and north of the New River tidal channel (Cullen & Dell 2013).

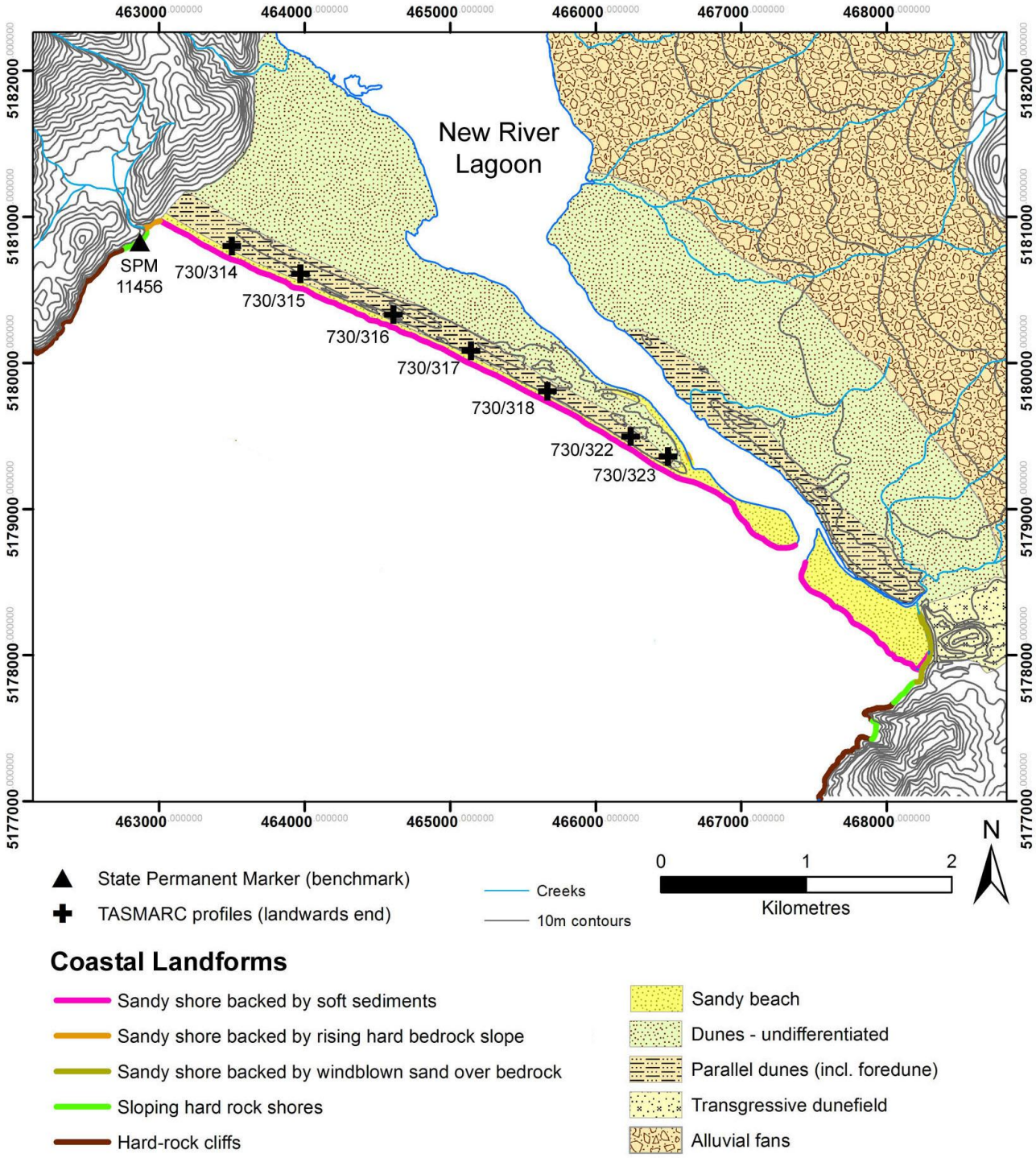

Figure 108: Coastal landforms at Prion Beach with TASMARC survey marks and permanent survey benchmark (SPM) indicated. Note the lagoon outlet channel is depicted at a temporary location but is mostly forced hard against the rocky shoreline at the eastern end of the beach. Coastal landform polygon mapping is based on Cullen (1998) and Cullen and Dell (2013); other shoreline landform mapping is by C. Sharples and Hannah Walford (polygon mapping). Surveyed TASMARC profiles run seawards from each survey mark. Co-ordinate system is Map Grid of Australia zone 55 (GDA94 datum).

Figure 109: View west along Prion Beach from the extensive unvegetated spit at its eastern end towards the beach and parallel-dune barrier backed by New River Lagoon (out of sight to the distant right). In this view, the New River outlet channel (foreground) is located against the rocky headland at the east end of the beach, however the channel outlet episodically migrates along the full length of the unvegetated spit in response to flood and storm events and subsequent eastwards migration of the outlet channel. Photo by C. Sharples (1978)

Figure 110: Eroded foredune scarp at Prion Beach on 5th December 2014, showing large erosion scarp with some beach face recovery and incipient dune accretion (to seawards of the scarp) since the last previous major erosion event (probably the July 2011 storm event). Subsequent TASMARC profile surveys show that these incipient foredunes were subsequently removed by further erosion events before full foredune recovery could occur (see further below). Photo by C. Sharples (2014), location about 220 metres west of TASMARC profile 730/316.

Swell wave climate

The hindcast swell wave parameters for Prion Beach are:

Table 22: Key swell wave climate parameters for Prion Beach, from the Bureau of Meteorology Australia and CSIRO Australia CAWCR wave hindcast 1979-2010 (Durrant et al. 2013). These figures apply to the closest inshore ~5km grid cell to the beach.

	Annual	Summer (DJF)	Winter (JJA)
Average Significant wave height (m)	1.55	1.37	1.61
Average Maximum wave height (m)	3.64	3.15	3.86
Average Mean wave direction (°T)	210	211	210

A notable feature of the swell wave climate is the low mean annual directional variability indicated by the CAWCR hindcast, which implies that there is likely to be little variability in swell-driven alongshore drift and sand transport at Prion Beach. Geomorphic indicators including the deflection of the permanent New River discharge channel against the rocky point at the end of the beach (to which it has historically returned after occasional flood break-outs over the sand spit further west) show that direction of sand transport along the beach is dominantly west to east, driven by the south-westerly swells.

Wind (wind wave) climate

There are no local wind records for Prion Beach, with the nearest records – for Maatsuyker Island to the west – unlikely to accurately represent the wind climate at Prion Beach owing to the latter's much greater sheltering from the north-westerly winds which dominate across open ocean reaches at Maatsuyker Island. Field observations at Prion Beach indicate that winds there are commonly westerly, however in the absence of local wind records the directional and speed variability of winds at Prion Beach is unknown.

In the absence of local wind data the contribution of local wind waves to beach behaviour at Prion Beach can only be evaluated in a broad qualitative way. However, given that winds there are probably dominated by westerly wind flows, the most common onshore-directed locally generated wind waves are likely to be generally south-westerly to westerly and thus similar in their effects to the south-westerly swells.

Sand transport and budget

The location of Prion Beach as a swash-aligned beach in an embayment between long rocky headlands means there is unlikely to be significant alongshore gain to or loss of sand from the embayment, however shelf sediment mobility modelling suggests than significant wave-driven sand may still be moving onshore from the shelf (Harris & Heap 2014; Harris et al. 2000).

Although small amounts of sand exposed in the seawards-facing foredune erosion scarp are being deflated and blown up the dune face to accrete as small transgressive sand lobes amongst vegetation immediately behind the dune crest in some places, no significant blowouts (deflation hollows) or transgressive dunes (active or inactive) are apparent along the foredune or behind it, and the morphology of the parallel dune ridges behind the beach indicates that landwards movement of windblown sand via transgressive dune transport is not and has not been a significant process at this beach (except at its far eastern end: see below).

At the eastern end of the foredune, persistent windblown sand forms indicate south-westerly winds transport beach sand over the low sand spit east of the dunes, both northwards into the lagoon and New River tidal channel, and eastwards along the sand spit. Behind the beach and barrier spit, the southern half of the tidal New River Lagoon is very shallow and infilled with sand, so that most sand blown into the lagoon or tidal channel cannot be accommodated and is probably returned to the

beach-face by river discharge and tidal currents through the permanently open lagoon mouth. However, with ongoing sea-level rise creating additional accommodation space in the lagoon, the lagoon may be transitioning towards being a more active sand sink than it was during the Twentieth Century.

The other known net loss of sand from Prion Beach occurs via wind-blown sand from the beach spit mobilising eastwards into transgressive dunes climbing the rocky slopes at the east end of the beach (Cullen & Dell 2013). See Figure 108. However, the vegetated character of these dunes suggests only small volumes of sand are currently being lost into them from the beach system.

A low recently active foredune erosion scarp with no incipient dune recovery over less than 100 m shorefront at the western extremity of Prion Beach is associated with a creek discharge zone and is probably mostly unrelated to wave erosion.

Artificial disturbances

Minimal -several rudimentary campsites and rough walking tracks only.

Air photo analysis

Ortho-rectified vertical air photos of Prion Beach at 19 dates from 1948 to 2015 (see Table 23) were used to determine and characterise the shoreline behaviour history of the beach and its foredune over that period. The *in situ* (living) vegetation line was mapped as the shoreline proxy at each air photo date (Table 24).

Shore behaviour history from air photos

The history of shoreline behaviour and change at Prion Beach over the air photo period is summarised in the following Figure 111 and Figure 112. These show shoreline changes on all individual transects and the overall median shoreline change history across all transects.

The shoreline history indicated by the air photo record is broadly one of overall shoreline progradation (especially in the western half of the beach) with large erosion and accretion cycles super-imposed during the period from before 1948 until at least 2004. This was followed between 2005 and 2009 by a change to progressive recession which was continuing as at December 2016[31].

Before the change, shoreline variability tended towards progradation in the more sheltered western half of the beach and more towards long-term shoreline position stability in the eastern half (Figure 111), with super-imposed cycles of beach and dune-front erosion and accretion. These shorter-term cycles were more variable and of larger magnitude towards the eastern part of the spit, but more coherent and of lesser magnitude towards the western end. This was probably a result of the western end of the beach being more sheltered from dominantly south-westerly storm swells. A large erosion event evidently impacted Prion Beach circa 1980 and another in the mid-1980's (Figure 111). However, the beach had mostly recovered from these by 2005, confirming that it was still in dynamic equilibrium around a gradually prograding shoreline position.

Starting with an (as yet undated) erosion event or events between March 2005 and December 2009, and continuing until the end of the currently available air photo record at 2015, several erosion events including a large July 2011 storm have caused progressive shoreline recession with only minor recovery at Prion Beach (Figure 112). It is possible that this still-relatively recent but continuing

[31] Although a single linear fit to all data points suggests a long-term stable shoreline up to 2015 with large erosion and accretion cycles (Figure 112 top), the fit is non-significant. Visual inspection of the same data suggests that a more plausible interpretation is a long period of progradation with large erosion and accretion cycles followed by a recent switch to progressive shoreline recession with only minor recovery episodes (Figure 112 bottom). This interpretation is supported by more significant correlation co-efficients on the piecewise linear fits applied before and after the interval between the putative prograding and receding beach behaviour phases.

recession phase could be the start of a long-term change from stability to progressive erosion at Prion Beach, since it (a) now represents a longer period of dominantly recessional shoreline behaviour than seen previously in the air photo record, and (b) the 2015 median shoreline position is now (slightly) more receded to landwards than the shoreline positions (including error margins) seen on any previous air photo. However, whilst it is tempting to suggest that the "Time of Emergence" of a new

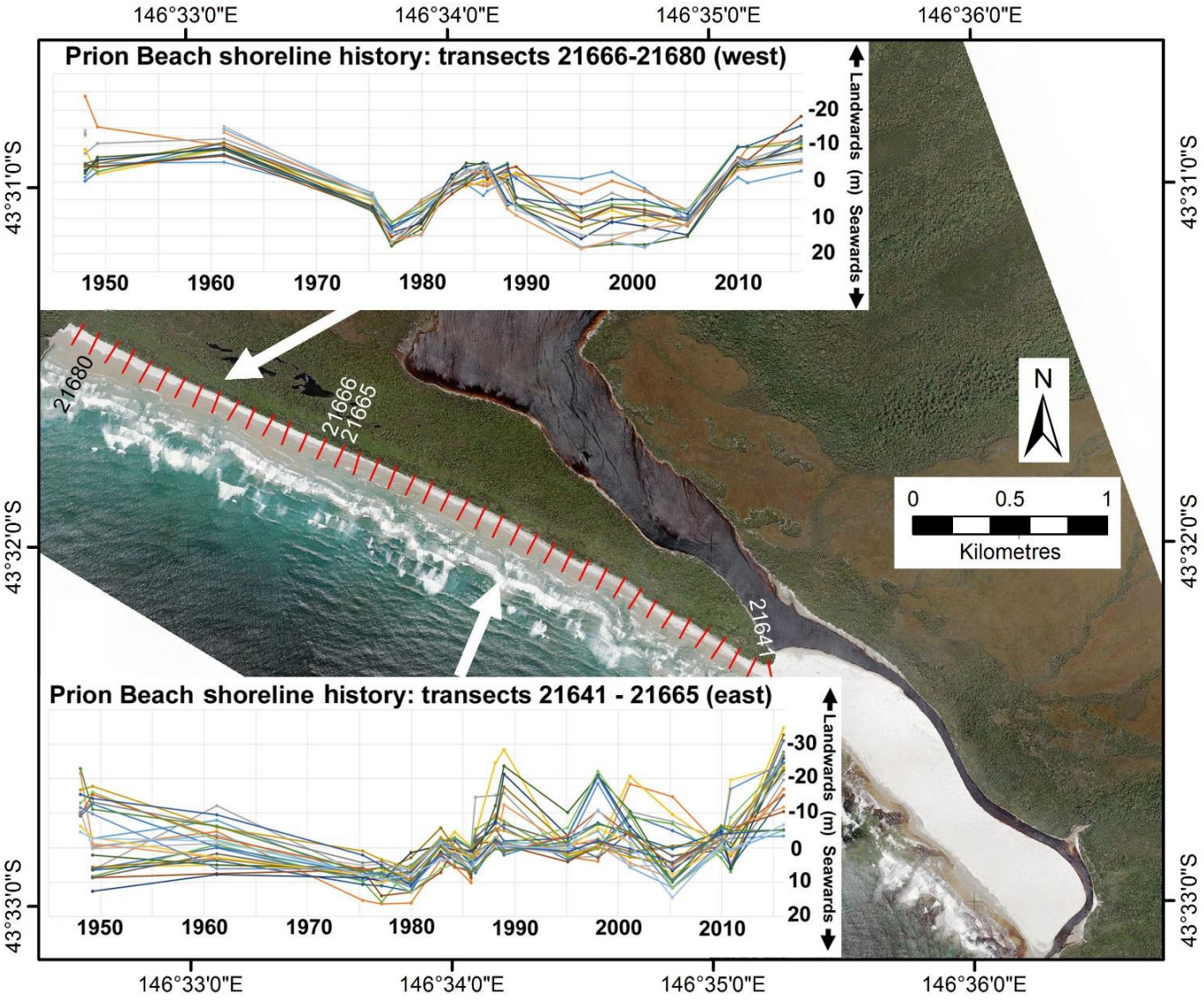

Figure 111: Plots of shoreline position (vegetation line) movement over the period 1948 to 2015 along each 100m-spaced digital transect at Prion Beach, plotted relative to the median shoreline position on each transect (except data from March 2011 excluded: see Table 23). The background image is the Dec. 2015 air photo. Transect locations are indicated by red lines on the air photo, and each coloured line on the plots represents shoreline position changes over time along one transect. Shoreline behaviour (phases of accretion or erosion) has been broadly similar along all transects, however transects are plotted in two groups whose shoreline movements have been notably more variable and of greater magnitude towards the east, compared to the more subdued and coherent shoreline movements in the western part of the beach.

shoreline recession trend has arrived at Prion Beach, this is still "only just" the case and it will require some additional years of continuing recession before it can be confidently stated that the shoreline has fundamentally changed to a new and long-term recession trend. Nonetheless, evidence from TASMARC beach profiles since late 2014 also provide additional evidence suggesting a switch to a predominantly receding mode since 2005. This is considered further below.

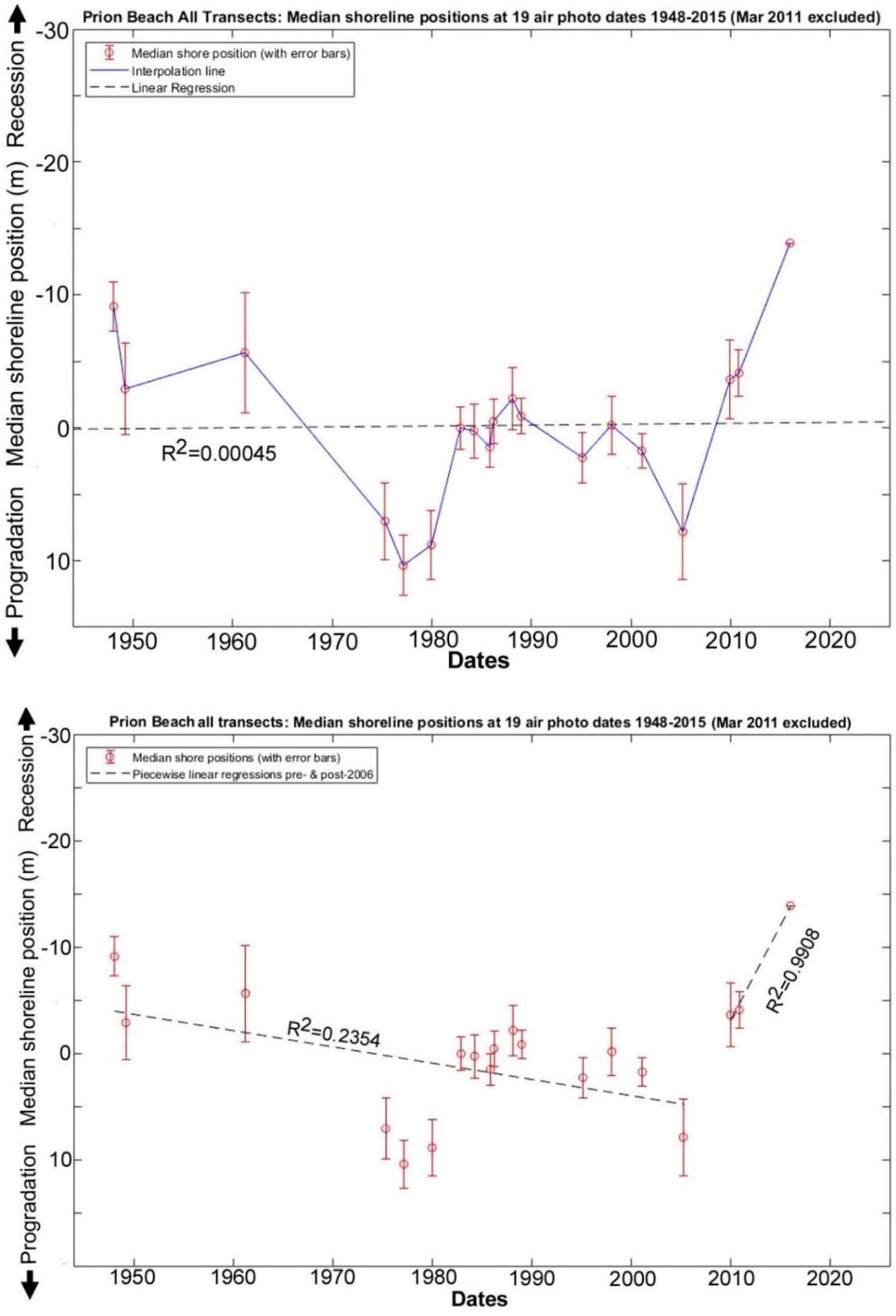

Figure 112: Summary plots of shoreline change history at Prion Beach at 19 air photo dates from 1948 to 2015 (March 2011 data excluded: see Table 23). Each data point is the median of the normalised shoreline positions across all transects at that air photo date, with position error bars for that air photo. Top: Data points with interpolation between points and with a single linear regression fitted to all data points; Bottom: data points only, with piecewise linear fits pre-and post-2006.

Surveyed shore profile analysis (TASMARC)

Cullen and Dell (2013) undertook a geomorphic investigation of Prion Beach funded by DPIPWE during 2012, as part of which they surveyed profile transects across the Prion Beach foredune at six locations along the beach. Subsequently these and an additional seventh profile transect were established with surveyed benchmarks during December 2014 as part of a DPIPWE World Heritage Area monitoring project managed by Rolan Eberhard in collaboration with the TASMARC project (Eberhard et al. 2015). The seven profiles were surveyed across both the foredune and beach face during November/December 2014, 2015 and 2016, using Differential GPS survey methods. Over these three field visits surveying was undertaken by Nick Bowden and Paul Boland, with assistance from Rolan Eberhard, Michael Comfort, Chris Sharples and others.

This section describes the results of the three annual profiles surveyed at all seven transects (2014-20160, and includes the earlier 2012 surveys by Cullen and Dell (2013) at the two central transects (numbered 730/316 and 730/317).

The TASMARC profiles are located on the western two-thirds of the beach backed by foredunes (see Table 26 and map Figure 108 for locations). Each profile extends normal to the shoreline from a survey mark on the landwards side of the established foredune or the next parallel dune behind, across the foredune and as far down the beach face as is reasonably accessible during each survey.

The results of all three TASMARC profile surveys (plus the earlier 2012 surveys where the data has been used) are plotted on Figure 113 to Figure 119 below in two forms, namely as profile plots and hinge point plots. These are:

- *Profile* plots depict the actual topographic profile surveyed along each transect at each survey date, plotted in a common scale to allow visual comparison of profile changes.
- *Hinge point* plots summarise the profile data by separately plotting the vertical and horizontal movement of the 'hinge point', which is the intersection between the base of the dune face and the back of the beach face. The two plots produced in this way summarise the horizontal movement of the dune front (the shoreline) and the vertical movement of the beach face over time.

It should be noted that in the case of the high slumping foredune at Prion Beach, the beach profiles do not identify the same shoreline feature as adopted for air photo analysis (the living vegetation line). Thus, each of these data sources has been analysed separately, however the results of both methods yield comparable data on the erosion / recovery status of the beach and dune.

The original processed survey data for each profile plot (provided as figures below) is available on the TASMARC website (www.tasmarc.info) and is not reproduced here. The hinge point data has been derived from the original profile data and is provided in tabular form on Table 27 further below (this data is not available on the website).

Shore behaviour history from profile surveys

As noted above, following an earlier large erosion event or events between 2005 and Dec 2009, during July 2011 a very large swell storm event caused major beach and dune erosion around large parts of the Tasmanian coast. The ortho-rectified air photos show that this storm caused further major beach and foredune erosion at Prion Beach (see discussions and Figure 112 above). During the full period of beach profile surveys at Prion Beach to date, from 2012 to 2016, the foredune has been dominated by a high slumped erosion scarp resulting from these previous erosion events.

Beach and dune behaviour indicated by profiling during the years 2012 to 2016 was different in different parts of the beach (compare plot figures below), as follows:

Western part of beach-dune shore (profiles 730/314 & 730/315):
See Figure 113 & Figure 114. Mostly no change: negligible erosion or accretion on dune face, minor storm-lowering of beach-face during 2015 followed by slight recovery.

Central part of beach-dune shore (profiles 730/316 & 730/317):
See Figure 115 & Figure 116. No further detectable erosion of the dune-face scarp occurred between 2012 and 2014, and there was notable accumulation of a new incipient foredune at the toe of the scarp, particularly on and near profile 730/316 (see photo Figure 110). During 2015 significant erosion of the dune scarp face (including destruction of the new incipient dune) occurred along with lowering of the beach face; this was followed by recovery (raising) of the beach face but no notable change to the dune face during 2016.

Central to eastern part of beach-dune shore (profiles 730/318 & 730/322):
See Figure 117 & Figure 118. No significant dune-face erosion and only minor incipient dune sand accumulation occurred over the period 2014 to late 2015. However, some beach-face recovery (accretion) occurred in this period (mainly on profile 730/318). Significant dune-face erosion occurred during 2016 on the more centrally located profile (730/318), but on the more easterly profile (730/322) the 2016 erosion only removed the small incipient dune from the toe of the dune face.

Eastern end of beach-dune shore (profile 730/323):
See Figure 119. Very little change to dune scarp-face or beach-face is detectable over the period 2014 – 2016, except for some minor accumulation of incipient dune sands at the toe of the dune scarp (back of the beach).

Other:
During fieldwork it was noted that in several places the recent (2014) scarp exposes fragments of anthropogenic (plastic) marine debris which were evidently buried within the seawards dune face during earlier phases of dune recovery following earlier erosion events. This implies what at least some parts of the recent foredune scarp have been eroded back further to landwards at previous times during the Twentieth century.

Beach Profile results Summary:
Over the period of beach profile monitoring (2012 to 2016) the scarped Prion Beach foredune face has shown no significant net recovery (accretion or progradation) from the multiple large erosion events that occurred after 2005, including the large July 2011 event. Although incipient dunes have briefly accreted on some but not all profiles, these were removed again by small erosion events during the period of monitoring. In contrast beach-face recovery (raising) has occurred following beach-face erosion (lowering) events on most profiles. During the period 2014 – 2016 there was no additional net erosion or recession of the dune face over the western and eastern ends of the beach-dune system, however some further net dune face erosion *has* occurred in the central part of the beach (most notably at profiles 730/317 during 2015 and 730/318 during 2016). The fact that these erosion events impacted mainly the central stretch of the beach indicates both that these were smaller events than the July 2011 erosion event (which air photo evidence indicates scarped the entire dune-front: see Figure 111 and Figure 112 above), and that the storm wave energies were focussed in the central part of the beach with the western end presumably being more sheltered by the rocky headland west of the beach. It is also notable that the differing erosion events that occurred were focussed on different parts of the beach (profiles 730/316 & 317 during 2015, and profiles 730/318 & 322 during 2016); this variability presumably reflects variability in storm swell wave and/or wind-wave directions between the events.

In sum, subsequent to the large erosion events that scarped the Prion Beach dune and beach between 2005 and July 2011, profile surveys show that no significant net recovery of the eroded dune face has occurred during the 5.5 years to the end of 2016, and that some additional net erosional recession of the dune face in the central part of the beach has occurred.

Summary shoreline behaviour history and characterisation

Combining the results from analysis of an air photo time series (1948 – 2015) and TASMARC shore profile survey results (2012 – 2016) as detailed above, the shoreline behaviour history of Prion Beach from 1948 to 2016 can be characterised as:

A long-term trend of net shoreline progradation with large-amplitude erosion and recovery cycles from at least 1948 until after 2005, followed by a change to progressive net shoreline recession until at least 2016. Although as at 2016 the recent recession phase slightly exceeded the scale and duration of previous erosional phases at Prion Beach, further data after 2016 will be necessary to determine whether the shoreline behaviour change to recession has become established as a new long-term trend.

The shoreline position in the most recent air photo (2015) is slightly further landwards than the previous most landwards shoreline position (1948), and the combined air photo and beach profiling record up to 2016 demonstrates a lack of any persistent shoreline (dune face) recovery following a large erosion event or events prior to Dec 2009. This period has included a further major erosion event in July 2011 and lesser erosion events during 2015 and 2016. This period of minimum 7 years with no persisting or net shoreline (dune-face) recovery is now unprecedented in the shoreline history record for this beach, with the longest prior duration without significant recovery being the maximum 7 years (probably less) of net shoreline recession from between Feb 1977 & Dec 1979 until between Dec 1979 & March 1984 (see Figure 112 & Table 25).

This behaviour is suggestive that Prion Beach may have switched from a previous long-term mode of progradation with full recovery from erosion events prior to Dec. 2009, to one of progressive erosional recession without full recovery (as is expected to occur in response to sea-level rise). However, given that the previous maximum scale of shoreline recession and recovery cycles at this beach have only recently been exceeded, it is not yet clear that a long – term change of behaviour has unequivocally occurred. Further monitoring of this beach over some years into the future will be essential to confirm whether Prion Beach has indeed changed its long-term behaviour subsequent to an erosion event or events between 2005 and 2009.

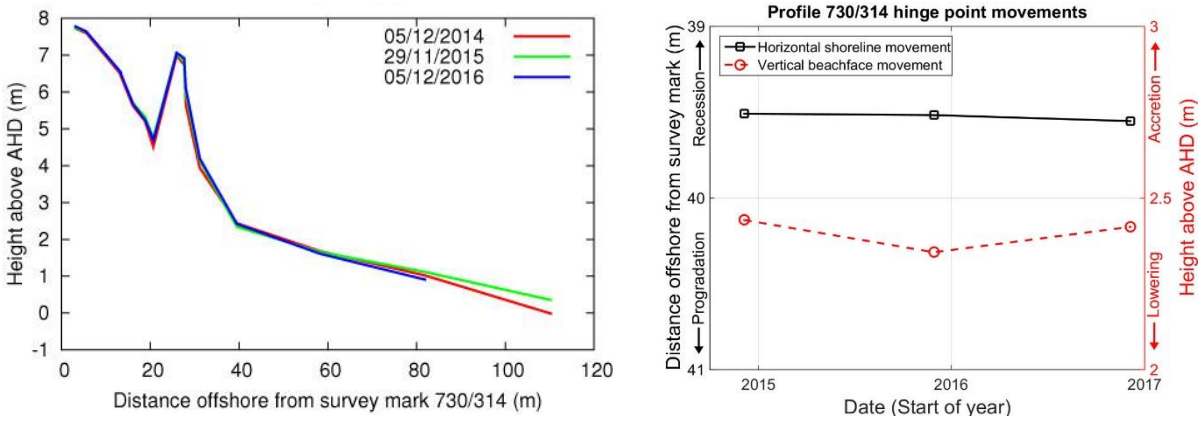

Figure 113: All surveys on TASMARC profile 730/314 to date, as profile plots (LHS) and hinge point movement plots (RHS). Both plots demonstrate very little beach and dune change at this transect over the period of beach profiling (2014 – 2016).

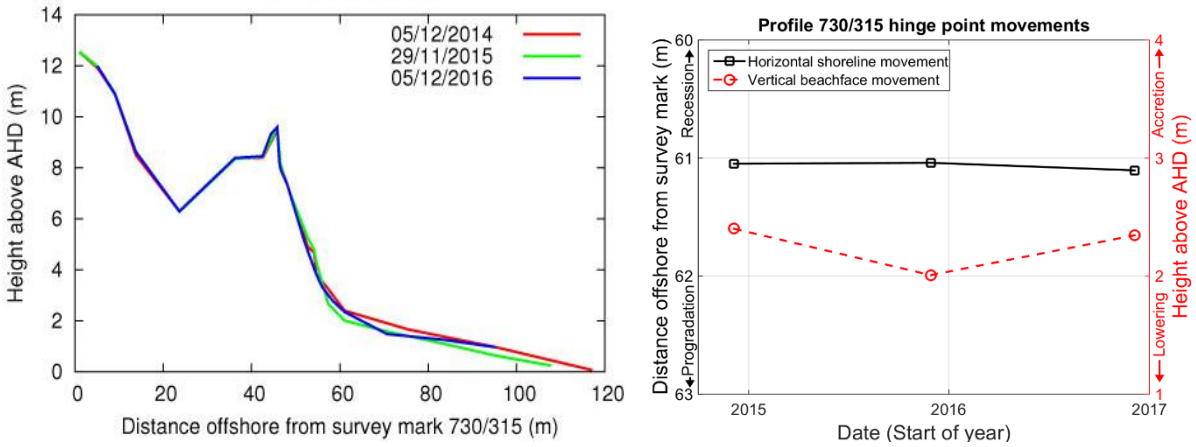

Figure 114: All surveys on TASMARC profile 730/315 to date, as profile plots (LHS) and hinge point movement plots (RHS). The plots demonstrate a mostly stable profile with minor erosion during 2015 which slightly lowered the beach face but had little effect on the dune face.

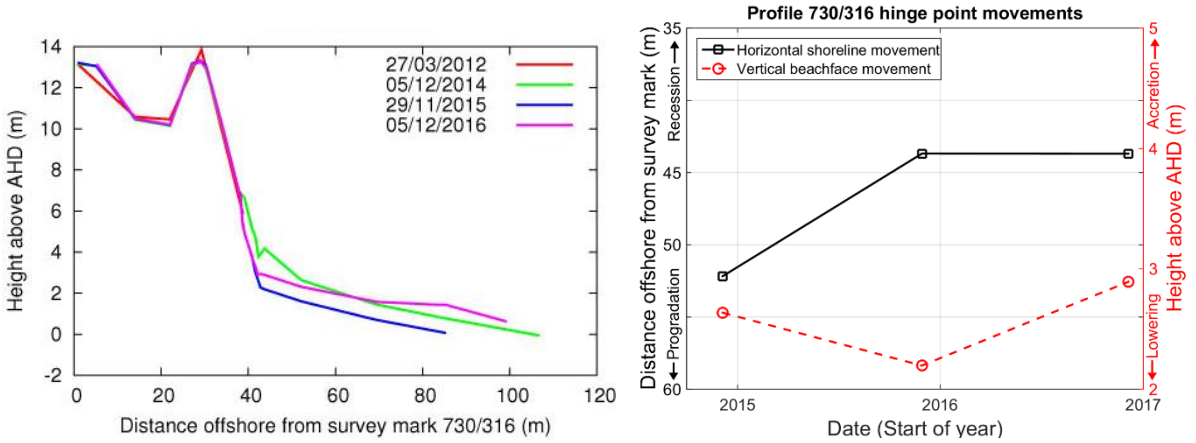

Figure 115: All surveys on TASMARC profile 730/316 to date, as profile plots (LHS) and hinge point movement plots (RHS, 2014-2016 only). The plots demonstrate erosion during 2015 of the beach-face and an incipient dune which had accreted at the foot of the dune scarp, followed by recovery of the beach face but little change to the dune face during 2016.

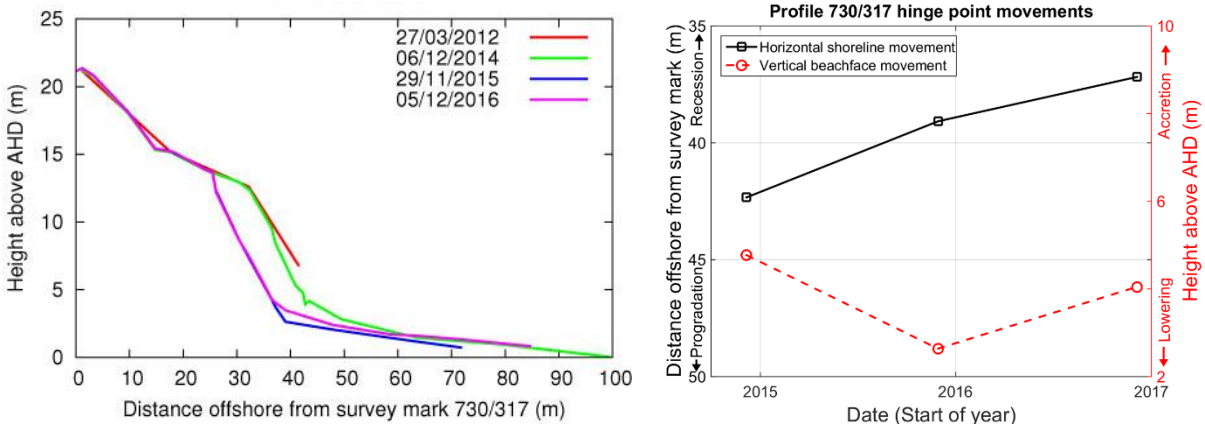

Figure 116: All surveys on TASMARC profile 730/317 to date, as profile plots (LHS) and hinge point movement plots (RHS, 2014 – 2016 only). The plots demonstrate significant dune-front and beach-face erosion during 2015, with subsequent beach-face recovery but little dune-face recovery.

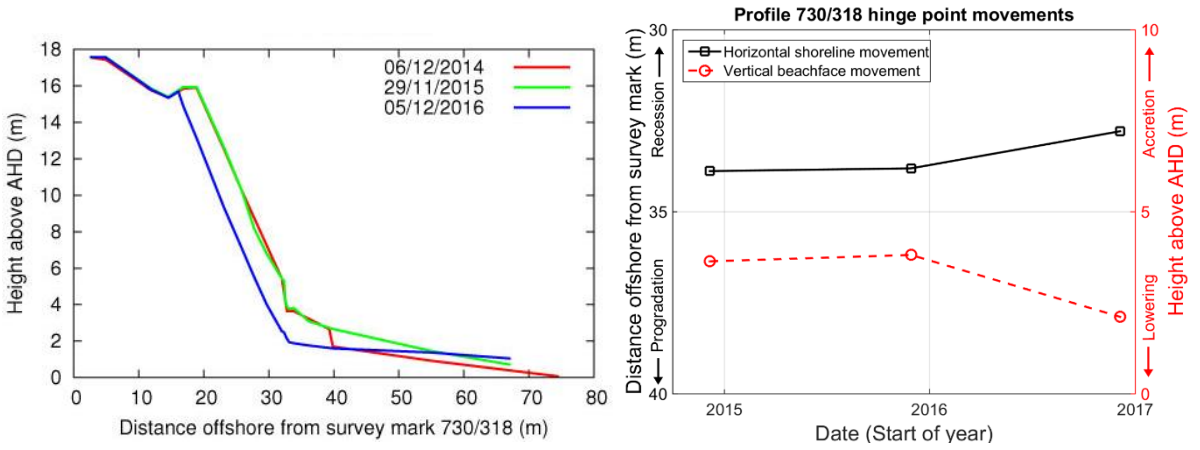

Figure 117: All surveys on TASMARC profile 730/318 to date, as profile plots (LHS) and hinge point movement plots (RHS). These plots demonstrate no significant erosion or dune recovery during 2015 at this location, but some dune erosion (recession) and beach-face erosion during 2016.

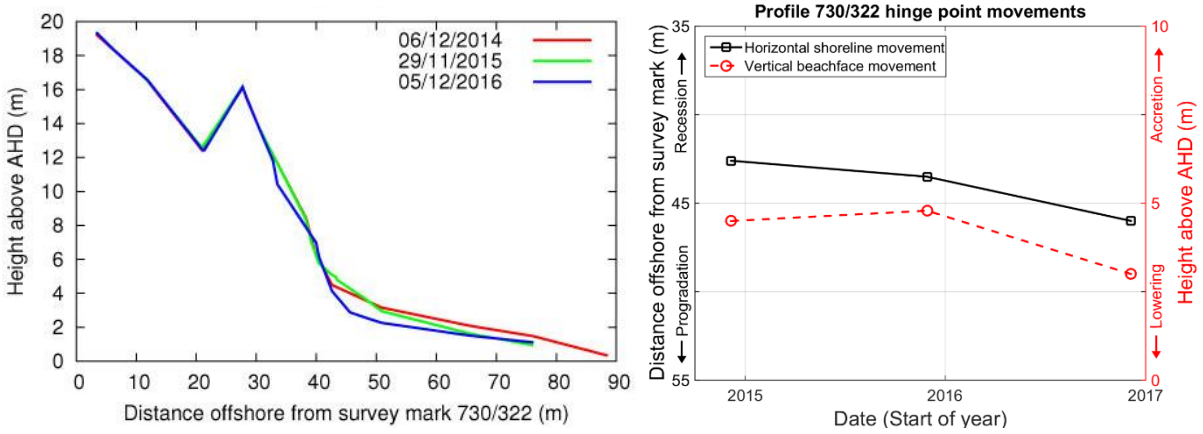

Figure 118: All surveys on TASMARC profile 730/322 to date, as profile plots (LHS) and hinge point movement plots (RHS). These plots demonstrate only minor dune and beach-face changes during 2015, followed by some erosion (lowering) of the beach face and the toe of the dune front during 2016.

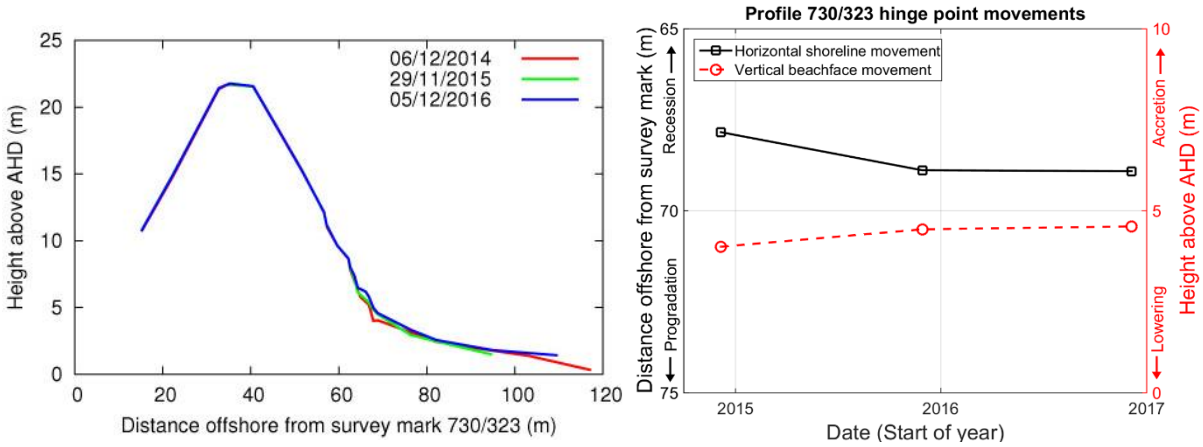

Figure 119: All surveys on TASMARC profile 730/323 to date, as profile plots (LHS) and hinge point movement plots (RHS). These plots demonstrate no significant erosion and some minor sand accumulation in the hinge-point area over the period 2014 – 2016, but overall little change at all.

Air photo data tables

The following tables provide details of the air photos used, the resulting ortho-photos produced, and the shapefiles representing the shoreline position that were digitised from the ortho-photos.

Table 23: Original air photos and ortho-rectified air-photos produced for Prion Beach.

Photo Date	**Original DPIPWE air photos (film-frame) / Final ortho-photo name**	**Final image resolution (original scan resolution if downsized) / pixel size of final ortho-photo**	**Original photo scale**	**Mean measured feature position error (± metres) for ortho-photo** [no. of measured feature position reference points]	**Comments**
17th Jan 1948	161-2819 / *PrionBeach_Jan1948_MGA55.tif/tfw*	600 dpi / 0.8 m pixel size	1:15,840	1.86 m [7]	Ortho-rectified by Chris Sharples
4th Mar 1949	182-4060 182-4061 / *PrionBeach_Mar1949a_MGA55.tif/tfw* *PrionBeach_Mar1949b_MGA55.tif/tfw*	600 dpi / 0.85 m pixel size	1:15,840	3.74 m [5] 3.17 m [7] **Mean: 3.45 m**	Ortho-rectified by Chris Sharples Each photo separately ortho-rectified
18th Mar 1961	365-21 / *PrionBeach_Mar1961_MGA55.tif/tfw*	1000 dpi (2039 dpi) / 1.03 m pixel size	1:35,640	4.53 m [12]	Ortho-rectified by Chris Sharples
15th April 1975	678-64 / *PrionBeach_Apr1975_MGA55.tif/tfw*	1000 dpi (2039 dpi) / 1.25 m pixel size	1:40,000	2.98 m [12]	Ortho-rectified by Chris Sharples
11th Feb 1977	714-27 714-28 / *PrionBeach_Feb1977_MGA55.tif/tfw*	1000 dpi (2039 dpi) / 0.47 m pixel size	1:15,000	2.26 m [11]	Ortho-rectified by Chris Sharples Mosaic produced using Landscape Mapper.
12th Dec 1979	808-153 / *PrionBeach_Dec1979_MGA55.tif/tfw*	2039 dpi / 0.61 m pixel size	1:45,000	2.63 m [12]	Ortho-rectified by Chris Sharples
12th Nov 1982	932-115 / *PrionBeach_Nov1982_MGA55.tif/tfw*	2039 dpi / 0.58 m pixel size	1:42,000	1.59 m [12]	Ortho-rectified by Chris Sharples
22nd Mar 1984	998-12 / *PrionBeach_Mar1984_MGA55.tif/tfw*	2039 dpi / 0.56 m pixel size	1:42,000	2.03 m [12]	Ortho-rectified by Chris Sharples
28th Oct 1985	1042-065 1042-066 1042-068 1042-070 1042-072 / *PrionBeach_Oct1985a_MGA55.tif/tfw* *PrionBeach_Oct1985b_MGA55.tif/tfw* *PrionBeach_Oct1985c_MGA55.tif/tfw* *PrionBeach_Oct1985d_MGA55.tif/tfw* *PrionBeach_Oct1985e_MGA55.tif/tfw*	1000 dpi (2039 dpi) / 0.17 m pixel size	1:5,000	All: 1.48 m [5] (up to max. 11m error in parts of 1985c)	Ortho-rectified by Chris Sharples Each photo separately ortho-rectified Photos 1985c very inaccurate in parts, used only by reference to 1986 photos to identify good accuracy areas

3rd Mar 1986	1061-56 / *PrionBeach_Mar1986 _MGA55.tif/tfw*	2039 dpi / 0.64 m pixel size	1:48,000	1.69 m [12]	Ortho-rectified by Chris Sharples
5th Feb 1988	1104-86 / *PrionBeach_Feb1988 _MGA55.tif*	1000 dpi (2039 dpi) / 0.74 m pixel size	1:25,000	2.36 m [11]	Ortho-rectified by Chris Sharples
15th Dec 1988	1124-150 / *PrionBeach_Dec1988 _MGA55.tif/tfw*	1000 dpi (2039 dpi) / 1.13 m pixel size	1:42,000	1.33 m [12]	Ortho-rectified by C. Sharples
13th Feb 1995	1229-132 / *PrionBeach_Feb1995 _MGA55.tif/tfw*	1000 dpi (2039 dpi) / 0.56 m pixel size	1:20,000	1.89 m [11]	Ortho-rectified by C. Sharples
8th Jan 1998	1283-159 / *PrionBeach_Jan1998_ MGA55.tif/tfw*	1000 dpi (2039 dpi) / 1.15 m pixel size	1:42,000	2.18 m [12]	Ortho-rectified by C. Sharples
1st Feb 2001	1345-198 / *PrionBeach_Feb2001 _MGA55.tif. /tfw*	1000 dpi (2039 dpi) / 1.14 m pixel size	1:42,000	1.32 m [12]	Ortho-rectified by C. Sharples
13th March 2005	1394-079 / *PrionBeach_March20 05_MGA55.ecw*	2039 dpi / 0.5 m pixel size	1:42,000	3.61 m [12] (quoted absolute accuracy ±15m)	Ortho-rectified by DPIPWE Original DPIPWE ortho file: 1394_079_op.ecw
15th Dec 2009	1439-043 1439-045 / *PrionBeach_Dec2009 a_MGA55.ecw PrionBeach_Dec2009 b_MGA55.ecw*	2039 dpi / 0.5 m pixel size	1:42,000	4.02 m [10] 1.96 m [7] **Mean: 2.99m** (quoted absolute accuracy ±15m)	Ortho-rectified by DPIPWE Original DPIPWE ortho files: 1439_043_op.ecw and 1439_045_op.ecw
5th Nov 2010	1449-104 / *PrionBeach_Nov2010 _MGA55.ecw*	2039 dpi / 0.3 m pixel size	1:24,000	1.72 m [11] (quoted absolute accuracy ±10m)	Ortho-rectified by DPIPWE Original DPIPWE ortho file: 1449_104_op.ecw
6th March 2011	1455-201 1455-199 1455-197 1455-195 1455-194 / MOSAIC *: PrionBeach_Mar2011 _MGA55.tif/tfw*	1000 dpi (2039 dpi) / 0.18 m pixel size	1:5,000	4.29 m [9] Poor error margins due to lack of good ground control features for eastern frames	Ortho-rectified by C. Sharples. Photos taken a few months before large erosive storm on 9th-10th July 2011. Quantitative data from this air photo NOT USED due to large error margin close in time to more accurate 2010 ortho-photo.
22nd Dec. 2015	Original DPIPWE digital ortho file: 24265A_Prion_Bay_D ec2015.ecw / *PrionBeach_Dec2015 _MGA55.ecw*	- / 0.1 m pixel size	-	0.0 m [N/A] (quoted absolute accuracy ±0.5m)	REFERENCE IMAGE (zero relative feature position error by convention) Digital original photo; ortho-rectified by DPIPWE

Table 24: Digitised shoreline shapefiles produced for Prion Beach (using ortho-photos listed in Table 23 above).

Date of air photo(s)	Shapefile	Shoreline digitised by	Comments
17th Jan 1948	PrionBeach_MGA55_19480117	Chris Sharples (2017)	Mostly vegetated foredune face with some smallish blow-outs and only sporadic signs of scarping or incipient dunes.
4th Mar 1949	PrionBeach_MGA55_19490304	Chris Sharples (2017)	Prominent slumped scarp on west – central established foredune face, in central east front of sparsely vegetated incipient dune scarped. Some small blowouts in dune face.
18th Mar 1961	PrionBeach_MGA55_19610318	Chris Sharples (2017)	Recent wave scarping along mostly vegetated fore-dune front (with some slumping & small blowouts), some lightly vegetated incipient dune scarping towards east.
15th April 1975	PrionBeach_MGA55_19750415	Chris Sharples (2017)	Recent erosion scarp truncating incipient dunes along full length of beach. Incipient dune veg difficult to discern (low res) but clearly present in some parts).
11th Feb 1977	PrionBeach_MGA55_19770211	Chris Sharples (2017)	Substantial lightly vegetated incipient dune accretion, mostly extending seawards of previous wave-erosion scarp. Recent wave scarping in central area.
12th Dec 1979	PrionBeach_MGA55_19791212	Chris Sharples (2017)	Substantial lightly vegetated incipient dune accretion, partly wave-scarped on seawards side esp. in central area of beach-foredune.
12th Nov 1982	PrionBeach_MGA55_19821112	Chris Sharples (2017)	West third: foredune face well vegetated with little evidence of recent scarping or slumping; central to east area: slumping at foot of foredune with wave erosion scarp at base mainly in central area. Some incipient dune veg detectable in east area.
22nd Mar 1984	PrionBeach_MGA55_19840322	Chris Sharples (2017)	Foredune face mostly well vegetated with low scarping and some bare slumped sand at foot of dune mainly behind centre of beach, incipient dune veg barely detectable in parts.
28th Oct 1985	PrionBeach_MGA55_19851028	Chris Sharples (2017)	Mostly recent to partly slumped scarp at foot of mostly well-vegetated foredune; no notable

			incipient dune seawards of scarp. Shoreline interpolated across several sections where air photo 1985c very inaccurate.
3rd Mar 1986	PrionBeach_MGA55_19860303	Chris Sharples (2017)	Seawards foredune face mainly vegetated, some scarping and slumping at foot of foredune (i.e. no recent major erosion events but some minor).
5th Feb 1988	PrionBeach_MGA55_19880205	Chris Sharples (2017)	Major erosion since Mar 1986; sparse incipient dune veg in front of slumped and partly revegetated foredune in west third, otherwise mainly old slumped & revegetating dune face with little incipient dune veg in front as yet.
15th Dec 1988	PrionBeach_MGA55_19881215	Chris Sharples (2017)	Some incipient dune development mainly in western part, elsewhere mainly slumped or vegetated dune face with little incipient dune growth.
13th Feb 1995	PrionBeach_MGA55_19950213	Chris Sharples (2017)	Good broad incipient dune and clumpy veg zone established along most of beach but especially in west half; some trimming of incipient dune front by wave scarping.
8th Jan 1998	PrionBeach_MGA55_19980108.shp	Chris Sharples (2017)	Little change since 1995; some incipient dune development in west part (seaward side scarped) and east end, elsewhere partly slumped erosion face with little incipient dune establishment.
1st Feb 2001	PrionBeach_MGA55_20010201.shp	Chris Sharples (2017)	Incipient dune veg establishing along much of beach, esp. west half. Shoreline mapped at edge of incipient dune veg.
13th March 2005	PrionBeach_MGA55_20050313.shp	Chris Sharples (2017)	Much incipient dune vegetation clumps evident, with mapped shoreline at recent low wave scarp truncating front of incipient dune.
15th Dec 2009	PrionBeach_MGA55_20091215.shp	Chris Sharples (2017)	Looks like mainly fairly fresh scarp in west half (minor slumping), with some incipient dune accretion evident mainly in east half.
5th Nov 2010	PrionBeach_MGA55_20101105.shp	Chris Sharples (2017)	Mainly just slumped scarp in west - central areas, but much incipient dune vegetation on slumped scarp in east third

6th March 2011	PrionBeach_MGA55_20110306.shp	Chris Sharples (2017)	Quantitative data from this shoreline not used due to large error margin in ortho-photo close in time to more accurate 2010 ortho-photo. Mainly slumped scarp in west-central areas, much incipient dune & veg establishment in east third.
22nd Dec 2015	PrionBeach_MGA55_20151222.shp	Chris Sharples (2017)	High slumped scarp with common soil-vegetation rafts below mapped vegetation line (mainly at the head-scarp).

Table 25: Summary shoreline history for Prion Beach. The left hand column of his table provide the medians of the shoreline positions measured on all transects (relative to the median position on each transect) at each air photo date, and the error margins for each air photo (from Table 23). This data was used to plot Figure 112 above, and is from the digital file *PrionBch_HistorySummary_1948_2015.csv* The right hand columns use the summary shoreline history data to record measurements needed to derive the quantitative measures of shoreline behaviour. Note: derived shoreline erosion and recovery figures are 'most likely" figures, ignoring error margins.

Year	Month	Day	Median Shoreline Position (metres)	Mean air photo error margin (metres)	Shoreline movement type since previous air photo date	Time since previous air photo date (decimal years)	Shoreline erosion since previous air photo date (landwards shoreline movement in metres)	Shoreline recovery (progradation) distance since previous air photo date (metres)	Minimum shoreline recovery rate (metres/year)
1948	1	17	-9.13	1.86	-	-	-	-	-
1949	3	4	-2.93	3.45	seawards (recovery)	1.13	-	6.2	5.45
1961	3	18	-5.66	4.53	landwards (erosion)	-	2.73	-	-
1975	4	15	7.03	2.89	seawards (recovery)	13.89	-	12.69	0.91
1977	2	11	10.36	2.26	seawards (recovery)	1.82	-	3.33	1.82
1979	12	12	8.81	2.63	landwards (erosion)	-	1.55	-	-
1982	11	12	0	1.59	landwards (erosion)	-	8.81	-	-
1984	3	22	0.23	2.03	seawards (recovery)	1.36	-	0.23	0.17
1985	10	28	1.45	1.48	seawards (recovery)	1.59	-	1.22	0.77
1986	3	3	-0.48	1.69	landwards (erosion)	-	1.93	-	-
1988	2	5	-2.2	2.36	landwards (erosion)	-	1.72	-	-
1988	12	15	-0.87	1.33	seawards (recovery)	0.85	-	1.33	1.56
1995	2	13	2.24	1.89	seawards	6.16	-	3.11	0.50

					(recovery)				
1998	1	8	-0.2	2.18	landwards (erosion)	-	2.44	-	-
2001	2	1	1.72	1.32	seawards (recovery)	3.88	-	1.92	0.49
2005	3	13	7.83	3.61	seawards (recovery)	4.11	-	6.11	1.45
2009	12	15	-3.64	2.99	landwards (erosion)	-	11.47	-	-
2010	11	5	-4.12	1.72	landwards (erosion)	-	0.48	-	-
2011	3	6	0.16	4.29	seawards (recovery)	0.33	-	4.28	12.96*
2015	12	22	-13.91	0	landwards (erosion)	-	9.79	-	-

* Note: Quantitative data from this air photo was not used since the derived shoreline recovery rate is a physically implausible extreme outlier and is likely to be a result of the large ortho-photo error margin in this case. As a result of uncertainty around the 2011 air photo, the 2015 erosion distance is also measured from the more reliable 2010 shoreline.

TASMARC shore profile data tables

Table 26: GPS-surveyed co-ordinates of each TASMARC transect survey mark at Prion Beach. The survey marks are located at the landwards end of each transect, which runs seawards normal to the shoreline from each mark. Latitude and Longitude are decimal degrees and eastings and northings are metric co-ordinates in the Map Grid of Australia Zone 55 (MGA55, GDA94 datum)

Transect	Longitude	Latitude	Easting	Northing
730/314	146.5483	-43.5249	463498.17	5180799.49
730/315	146.5541	-43.5266	463969.41	5180608.43
730/316	146.5620	-43.5291	464609.87	5180329.95
730/317	146.5686	-43.5314	465142.94	5180082.36
730/318	146.5751	-43.5339	465667.37	5179804.94
730/322	146.5821	-43.5367	466239.62	5179493.69
730/323	146.5853	-43.5380	466497.16	5179358.30

Table 27: Table of hinge points defined for each surveyed Prion Beach profile (derived from original TASMARC survey data).

TASMARC profile number	Survey date	Hinge point distance offshore from survey mark (metres)	Hinge point height above AHD (metres)
730/314	05/12/2014	39.509	2.436
730/314	29/11/2015	39.517	2.342
730/314	05/12/2016	39.552	2.416
730/315	05/12/2014	61.048	2.402
730/315	29/11/2015	61.04	2.009
730/315	05/12/2016	61.104	2.346
730/316	05/12/2014	52.173	2.636

730/316	29/11/2015	43.688	2.197
730/316	05/12/2016	43.697	2.893
730/317	06/12/2014	42.336	4.773
730/317	29/11/2015	39.08	2.639
730/317	05/12/2016	37.182	4.049
730/318	06/12/2014	33.881	3.64
730/318	29/11/2015	33.806	3.816
730/318	05/12/2016	32.787	2.116
730/322	06/12/2014	42.603	4.497
730/322	29/11/2015	43.506	.788
730/322	05/12/2016	46	3
730/323	06/12/2014	67.84	4.015
730/323	29/11/2015	68.885	4.493
730/323	05/12/2016	68.911	4.572

A1.3.3 Cox Bight Beach (south coast)

Locality and general description

Cox Bight on the south-southwest coast of Tasmania contains three high-energy swell-exposed sandy beach barriers separated by small rocky points. The beaches lie in the South-west National Park and Western Tasmania Wilderness World Heritage Area (TWWHA). The only local artificial disturbances at this beach are short walking tracks across the small rocky points, several undeveloped campsites behind the beach, and abandoned tin-mining excavations over 50 m inland of the middle beach. It is unlikely these have significantly influenced beach and dune geomorphic processes, and it is also notable that the introduced dune-colonising marram grass *Ammophila arenaria* – which can modify dune accretion processes – is absent. Access to Cox Bight is by sea, air or walking only.

The Cox Bight beaches were visited by Chris Sharples (and others) three times during this project, in November/December 2014, 2015 and 2016, as part of a DPIPWE-funded helicopter-based project to establish and survey TASMARC beach profile transects.

Geomorphology and process environment

Geomorphic description

Geomorphic aspects of the beaches have previously been described by Cullen (1998), Short (2006b)and Horton et al. (2008), with the latter also documenting an initial shoreline condition monitoring survey for Cox Bight.

Cox Bight is a 4.7 km deep and roughly 4.5 km wide south-facing embayment between prominent rocky headlands which allow little or no longshore drift of sand into or out of the embayment. The sandy beaches are located at the northern head of the embayment and are separated by Point Eric and a smaller rocky point to its east (Figure 120).

The 2.2 km long western beach faces south-southeast (aspect 170º T) and is a Transverse Bar and Rip (TBR) to Rhythmic Bar and Beach (RBB) morphodynamic type Short (2006b) fronted by a 150-200m wide surf zone with several rips. The beach is dominantly fine-medium grained sand with a cobble berm that is largest at the western end (Figure 121). The beach is backed by 2 prograded Holocene cobble beach ridges mantled by aeolian foredune sands (Cullen 1998, p. 41) and typically up to 2-5m high. The beach barrier is backed by an extensive plain of soft alluvial sediments extending in depth to below present sea-level, and impounds two large backshore freshwater lagoons, the larger of which (Freney Lagoon) has a permanently open channel discharging freshwater to the beach.

The middle beach extends 1.7 km eastwards from Point Eric and faces south-southwest (aspect 195º T). This is a dominantly fine-medium grained sand beach which is a Transverse Bar and Rip (TBR) morphodynamic type (Short 2006b) fronted by a 100m wide surf zone with several rips. The beach is backed by a foredune ranging from only 2-3m high in the west to 20-25m high in the most exposed central part of the beach (Figure 122), which in turn is backed by a soft sediment plain that probably extends in depth to below present sea-level for several hundred metres inland. A large creek discharge is deflected eastwards for 500m along the eastern end of the middle beach, and for that part of the beach is probably more important that wave action in determining the shoreline position (defined as the living *in situ* vegetation line).

The easternmost beach is about 1.4 km long and faces southwest (aspect 220º T). This is also a dominantly fine-medium grained sandy beach which is a Transverse Bar and Rip (TBR) morphodynamic type (Short 2006b) fronted by a 100m wide surf zone with several rips. The beach is backed by a foredune ranging 5 – 10m high in its northern to middle parts, and up to 20 – 30m high in its southern section where the dune caps a bedrock slope rising above sea-level behind the beach. The

northern to middle part of the foredune is in turn backed by a soft sediment plain that probably extends in depth to below present sea-level for several hundred metres inland, although the southern half of the beach is immediately backed by a rising bedrock slope. No evidence of dune blowouts or significant landwards transport of sand in wind-driven transgressive sand lobes or dunes was seen at any of the three beaches.

At the time of inspection, most of the foredunes behind each of the three beaches showed evidence of prior erosion scarps (except at the apparently more stable western end of the western beach), however these exhibited greater or lesser degrees of recent recovery through slumping and incipient dune accretion. The freshest erosion scarps seen during 2014 - 2016 were associated with creek outlets along the beaches and were probably a response to creek discharge erosion rather than to wave erosion. Considerable recovery following erosion was evident in the middle of the middle beach (Figure 122). However it is noteworthy that Cullen (1998), p. 41 reported extensive foredune scarping with exposure of one or two dune palaeosols behind the two beaches east of Point Eric at the time of his inspection. Any palaeosols were covered by slumping or incipient dune recovery by 2014-

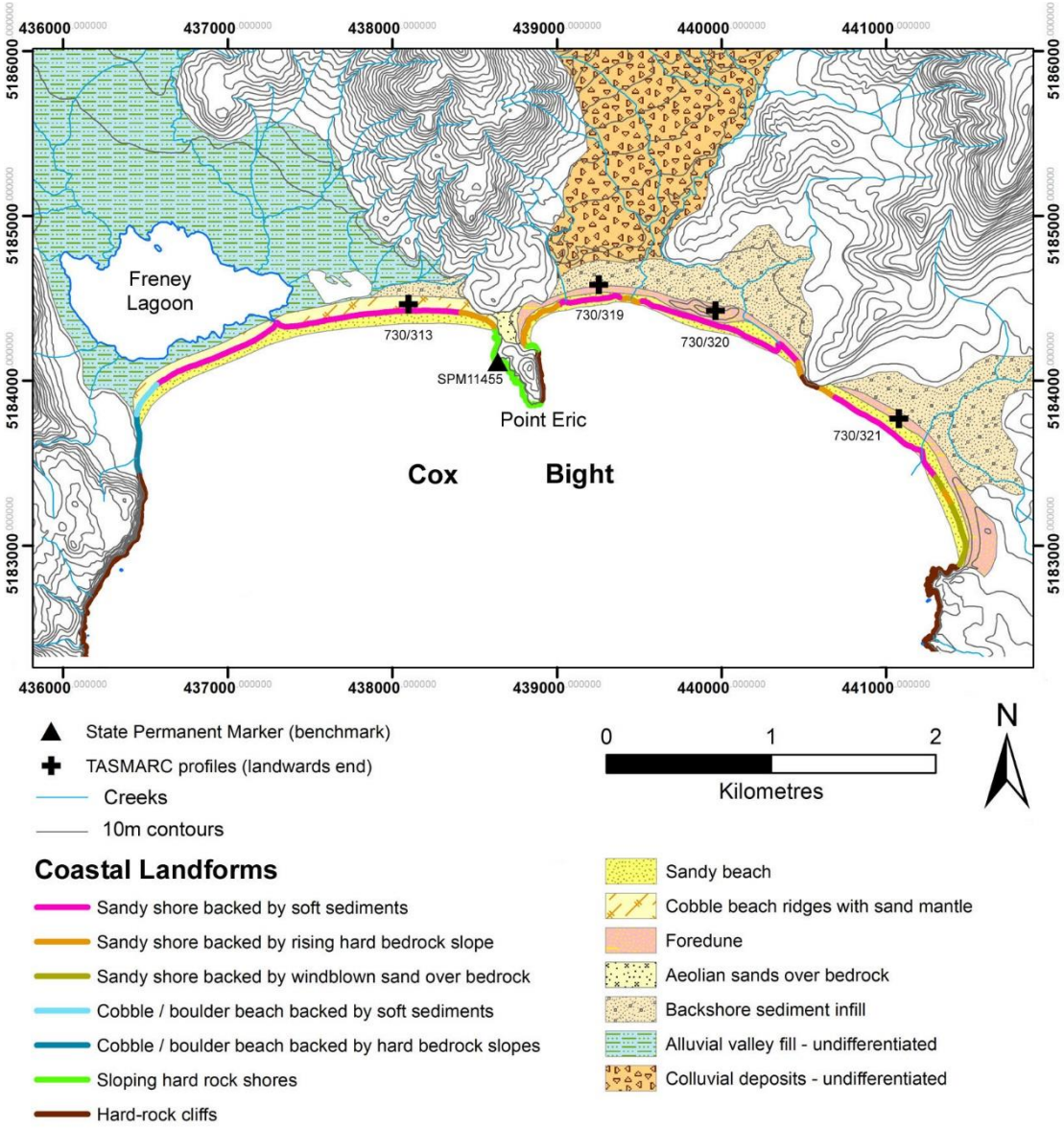

Figure 120: Coastal landforms at Cox Bight. Coastal landform mapping is based on Cullen (1998), with additional geomorphic mapping by C. Sharples. Permanent survey benchmark (SPM) and TASMARC survey profile locations and numbers are indicated. Co-ordinate system is Map Grid of Australia Zone 55 (GDA1994 datum).

Figure 121: View typical of the western Cox Bight beach, showing a sandy beach with a substantial cobble berm backed by foredune sands over cobble beach ridges. Foredune erosion scarps are notable along parts of west Cox Bight and some look fresh, however their age is unclear since no change occurred over the three years of beach monitoring. Some of the scarping seen between 2014 - 2017 may date back to erosion events suggested by the air photo record in the period between 1994 and 1998 (see Figure 125). Photo by C. Sharples (2014).

Figure 122: A high foredune backing a section of the middle beach of Cox Bight. Little evidence of prior scarping is discernible in this section, although strong westerly sand transport across the accreted seawards dune face appears to be preventing vegetation establishment on the lower seawards dune face in this windy location. Other parts of the Cox Bight beaches exhibit some exposed foredune wave erosion scarps with recovery through slumping and incipient foredune accumulation. Photo by C. Sharples (2014).

2017, however their exposure during 1998 does suggest a significant erosion event which the air photo record implies occurred between 1994 and 1998 (see Figure 125) (see also further discussion of shoreline behaviour below).

Swell wave climate

Cox Bight receives a persistent south-westerly swell generated by Southern Ocean winds strongly correlated with the Southern Annular Mode (Hemer, Church & Hunter 2010; Hemer, Simmonds & Keay 2008). Swell wave parameters for Cox Bight are given below.

Table 28: Key swell wave climate parameters for Cox Bight, from the Bureau of Meteorology Australia and CSIRO Australia CAWCR wave hindcast 1979-2010 (Durrant et al. 2013). These figures apply to the closest inshore ~5km grid cell to the beach.

	Annual	Summer (DJF)	Winter (JJA)
Average Significant wave height (m)	1.63	1.46	1.69
Average Maximum wave height (m)	3.6	3.15	3.8
Average Mean wave direction (°T)	228	228	228

The wave heights and directions apply to a 5 km grid square spanning most of the 4.7 km deep and 4.5 km wide Cox Bight embayment. Given the (lateral) depth of the embayment it is likely that wave heights near the beaches at the head of the bight are notably less than indicated by the CAWCR hindcast, because of wave energy lost through refraction and drag against the long rocky headlands bounding the bight (Davies 1973) in addition to the normal shoaling effects as the waves reach shallower depth. For the same reason some change in wave direction is likely as the swell refracts into Cox Bight, however the very limited swell directional variability indicated by the CAWCR hindcast is likely to be reinforced by refractional wave training within the Bight to yield very constant swell wave directions at the beaches themselves. It is likely that the south-westerly swell wave direction drives a generally easterly alongshore drift within the beaches (as seen in the deflection of the main creek at the middle beach towards the eastern end of the beach) and results in relative sheltering of the western end of the western beach.

Wind (wind wave) climate

A long-term (1957 – present) Australian Bureau of Meteorology wind record is available from Maatsuyker Island weather station, 17 kilometres south of and directly offshore from Cox Bight. Wind direction data from Maatsuyker Island is plotted in Figure 123 (below). This nearby wind record is likely to be broadly representative of winds at Cox Bight itself, albeit some differences due to local topographic wind-steering and sheltering effects are likely.

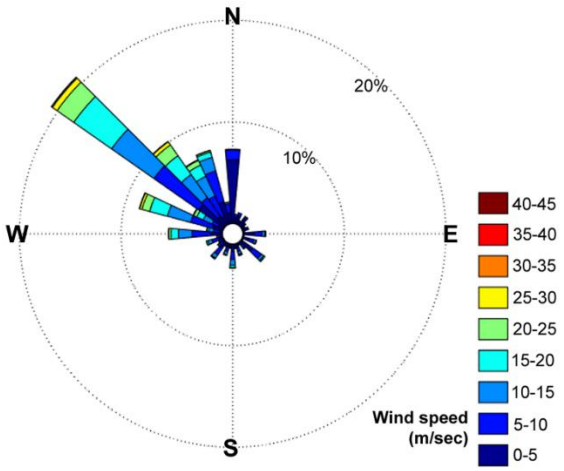

Figure 123: Wind directions for Maatsuyker Island, near Cox Bight. The figure was prepared in Matlab™ using all synoptic wind records for Maatsuyker Island from 1957 to 2015. Original data supplied by the Australian Bureau of Meteorology (2016).

A dominantly north-westerly wind flow is indicated, which would blow offshore from nearly all parts of Cox Bight beach except the eastern end of the easternmost beach. Hence strong locally generated wind waves at Cox Bight must almost always be generated and directed offshore and hence would not cause erosion except possibly at the eastern end of the eastern beach. Onshore winds are a very minor component of this wind record and thus are unlikely to be a significant cause of shoreline erosion.

Analysis of the Maatsuyker Island wind record by Kirkpatrick et al. (2017) indicated increased mean wind speeds over recent decades, at least in winter, and this has potential to produce increasingly energetic local wind waves which could cause increased erosion on shorelines. However, given that the dominant wind directions at Cox Bight are offshore, it is unlikely this has been a significant process at Cox Bight.

Since locally generated wind waves would only rarely be directed onshore at Cox Bight, south-westerly swell storms are likely to account for nearly all wave erosion occurring at the Cox Bight beaches.

Sand transport and budget

Shelf sediment mobility modelling suggests that some sand may still be moving onshore from the continental shelf into Cox Bight (Harris & Heap 2014; Harris et al. 2000), albeit there is no empirical data on this. However, given the deeply embayed nature of Cox Bight and the prominence of the bounding rocky points, it is unlikely that any nearshore sand is being transported either into or out of Cox Bight by longshore drift. A complete lack of deflation gullies or mobile sand dunes transgressing into backshore areas implies that no sand is currently being lost inland from the beaches or dunes by wind erosion and transport (which is to be expected given that the dominant local wind directions are offshore; see below). Although having a permanently open entrance, the main backshore lagoon at Freney Lagoon (Figure 120) is not tidal but rather freshwater, hence is not a sink for beach sand at current sea-levels.

In summary, with no significant mechanism of sand loss from the Cox Bight beaches or dunes apparent, and a possible continuing onshore movement of sand from the continental shelf, Cox Bight probably has a stable to gaining sand budget. Given the dominating south-westerly swell (see below) the dominant mode of sand movement within the bight is probably an easterly drift along the three beaches, with some likely leakage around the intervening small rocky points.

Artificial disturbances

Very minor backshore disturbance from walking tracks and rough campsites only.

Air photo analysis

Ortho-rectified vertical air photos of the Cox Bight beaches at 15 dates from 1948 to 2015 (see Table 29) were used to map and characterise the shoreline change history of the beaches and their foredunes over that period. Ortho photos for 3 additional dates (18th March 1961, 15th Dec 1988 and 25th Jan 2005) were not used because of poor ortho-rectification accuracies (> ±4 m); however, two of the excluded photos (from 1988 and 2005) were very close in time to more accurate photos that were used, hence 1961 is the only significant air photo date excluded. The *in situ* (living) vegetation line was mapped as the shoreline proxy at each air photo date (

Table 30), and in most parts of the three beaches corresponds to a low erosion scarp at the back of the beach and foot of the foredune (Figure 122 shows the main exception to this). Shoreline movement along the approximately 500-metre-long easternmost section of the middle beach was ignored for this analysis because the shoreline position (vegetation line) in that area is clearly influenced by the eastwards deflection of a major creek discharge and so is not necessarily reflective of responses to storm wave events or sea-level changes.

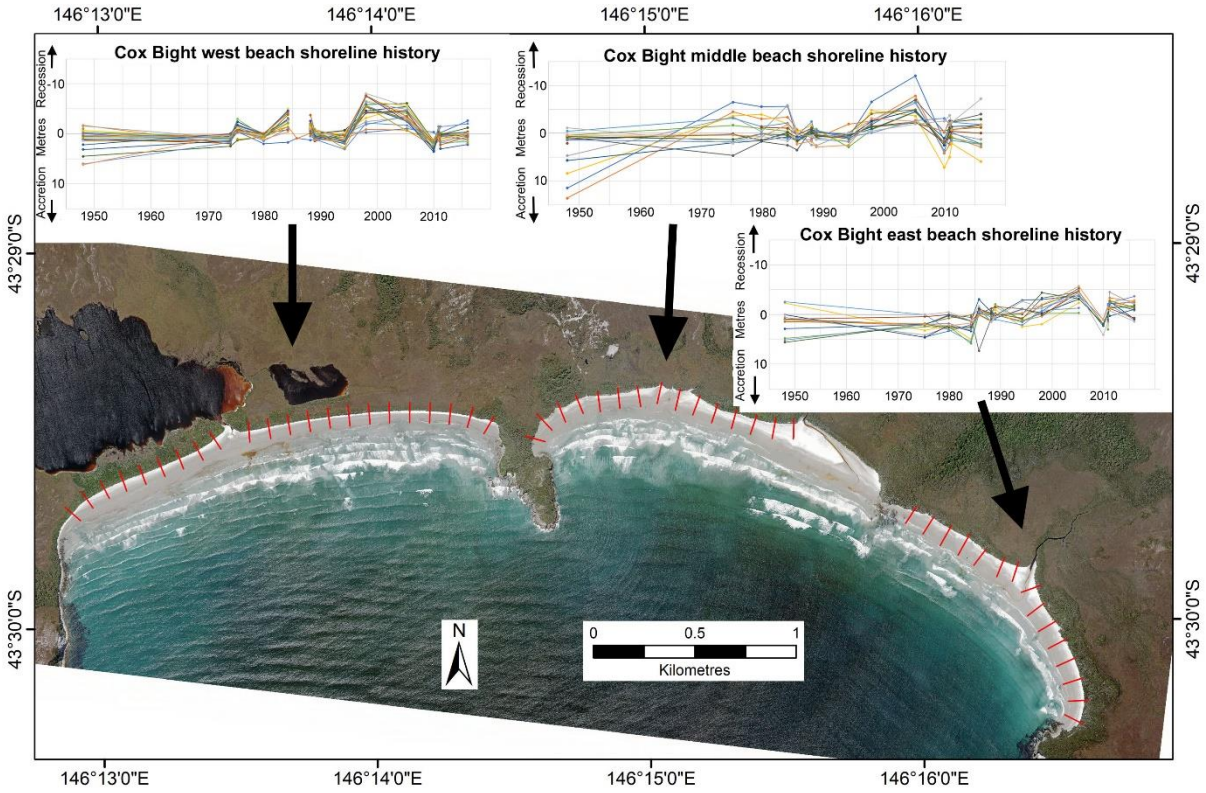

Figure 124: Plots of shoreline position (vegetation line) movement over the period 1948 to 2015 along each 100m-spaced digital transect used at Cox Bight beaches, plotted relative to the median shoreline position on each transect. The background image is the Dec. 2015 air photo. Transect locations are indicated by red lines on the air photo, and each coloured line on the plots represents shoreline position changes over time along one transects. Note that shoreline histories were not plotted for the eastern half of the middle beach where the 'shoreline' (vegetation line) behaviour is likely to be dominated by creek discharges rather than marine processes.

Shore behaviour history from air photos

Based on the ortho-rectified historic air photos listed in Table 29 and the shoreline positions digitised from these (

Table 30), Figure 124 shows horizontal shoreline movement from 1948 to 2015 along individual digital transects, plotted in three clusters corresponding to the three beaches in Cox Bight. The plots for all three beaches are similar, with only small amplitudes of apparent erosion and recovery events compared to Prion Beach further east on the south coast; see Figure 111. The largest erosion and recovery cycle is evident between 1994 and 2010 on all three beaches although the erosion phase appears to have been of largest magnitude on part of the middle beach; this probably reflects the exposure of this beach to less refracted and attenuated swell waves in the centre of Cox Bight than the two beaches to either side. At all three beaches, full recovery from the erosion event had occurred by 2010.

Given the similarity of the shoreline change histories at each Cox Bight beach, these records have been combined into a single plot summarising the overall shoreline history across all transects and indicating the air photo feature position error margins associated with each air photo date (Figure 125). The following key features of the Cox Bight beaches shoreline history are evident from the air photo data plots:

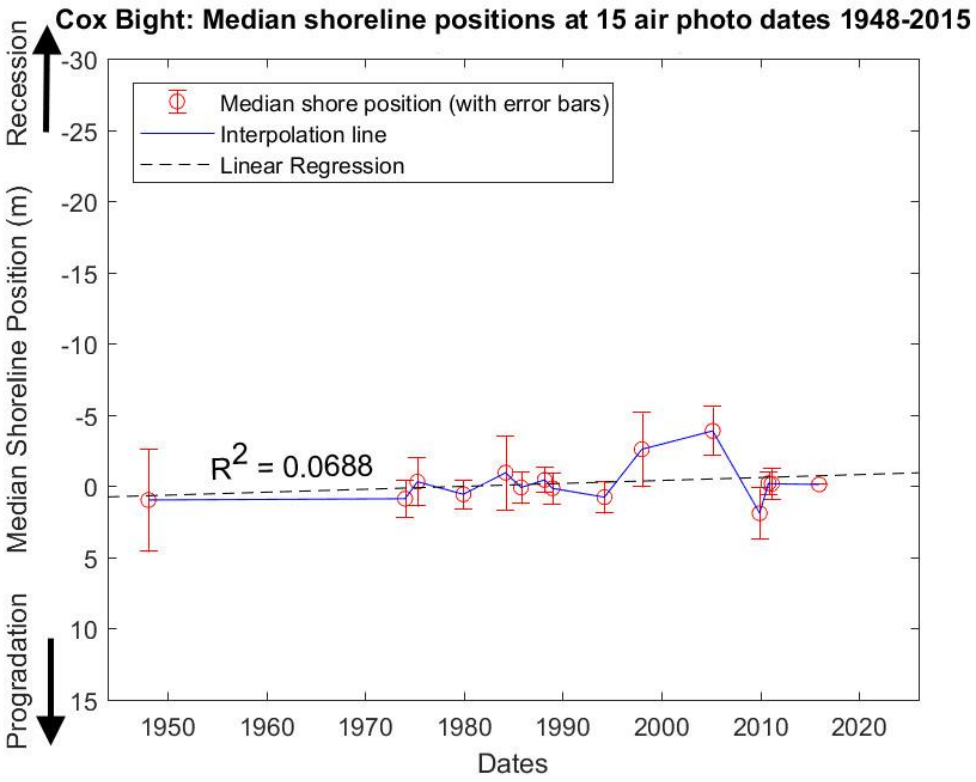

Figure 125: Summary plot of shoreline change history across all three beaches at Cox Bight at 15 air photo dates from 1948 to 2015. Error bars are the average measured feature position error margins relative to the 2015 air photo. Figure shows shore positions at each air photo date with interpolation lines and linear fit (linear regression). This plots the median of the shoreline positions measured on all used transects (relative to the median position on each transect) at each air photo date. For comparison purposes the Y-axis scale (shoreline position) is the same as for all other beach history plots in this project, emphasising the comparatively small horizontal shoreline movement detected over the air photo period for the Cox Bight beaches.

1. With one exception (see below), over most of the air photo record period there is no clear evidence of any shoreline change (recession or progradation), with mean air photo position error margins at most air photo dates overlapping. The overall shoreline trend for the 1948 to 2015 period is one of no significant change, with a linear regression fit showing only a very slight non-significant recession trend ($R^2 = 0.0688$).

2. The median shoreline position at 13th March 2005 is the only one which lies outside the error margins of earlier and later air photo shoreline positions and so must be the effect of a real erosion event or event cluster. This erosion event is evident in the air photo record of all three beaches (Figure 124), and the shoreline history depicted in Figure 125 indicates it probably occurred between the 24th March 1994 and 8th Jan 1998 air photo dates, although additional erosion may have occurred between the 1998 and 13th March 2005 air photo dates. Full shoreline recovery (by scarp slumping, revegetation, and incipient dune accretion) had evidently occurred by the 5th November 2010 air photo date.

Surveyed shore profile analysis (TASMARC)

Horton *et al.* (2008) have provided a one-time shore (beach and scarp) geomorphic condition survey for spot locations at Cox Bight. Subsequently four TASMARC beach profile survey marks were established at Cox Bight during December 2014 as part of a DPIPWE World Heritage Area

monitoring project managed by Rolan Eberhard in collaboration with the TASMARC project (Eberhard et al. 2015). The four profiles were surveyed across the foredune and beach face during December 2014, 2015 and 2016. Over these three field visits surveying was undertaken by Nick Bowden and Paul Boland, with assistance from Rolan Eberhard, Michael Comfort, Chris Sharples, and others.

The four TASMARC profiles cover all three beaches at the head of Cox Bight (See Figure 120 and Table 31 for profile locations). Each profile extends normal to the shoreline from a survey mark on the landwards side of the established foredune backing the beach, across the foredune and as far down the beach face towards the sea as was reasonably accessible during each visit.

The results of the TASMARC surveys are plotted on Figure 126 to Figure 129 below in two forms, namely as profile plots and hinge point plots. These are further explained in Section 3.3.2, but in brief profile plots depict the surveyed shoreline profile, whereas hinge point plots summarise the survey data by plotting the vertical and horizontal movement over time of the intersection between the top (back) of the beach face and the base (front) of the dune face. Thus, the hinge point plots show both the horizontal movement of the dune front (toe) and the vertical movement of the (back) beach face over time.

The original processed survey data for each profile plot (provided as figures below) is available on the TASMARC website (www.tasmarc.info) and is not reproduced here. The hinge point data has been derived from the original profile data and is provided in tabular form on Table 32 below. Photos showing the condition of each profile at the date of each survey are provided on the TASMARC website.

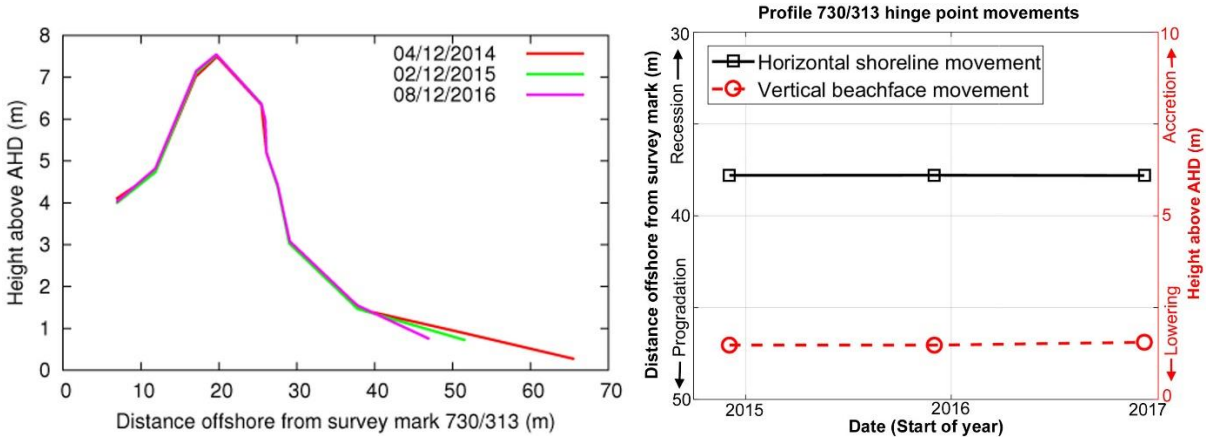

Figure 126: All surveys on TASMARC profile 730/313 (west beach) to date, as profile plots (LHS) and hinge point movement plots (RHS).

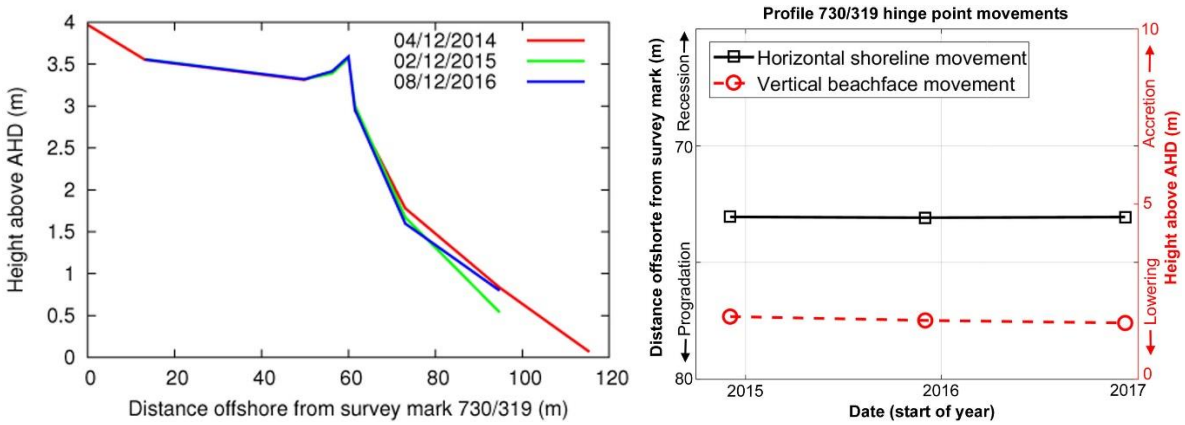

Figure 127: All surveys on TASMARC profile 730/319 (middle beach) to date, as profile plots (LHS) and hinge point movement plots (RHS).

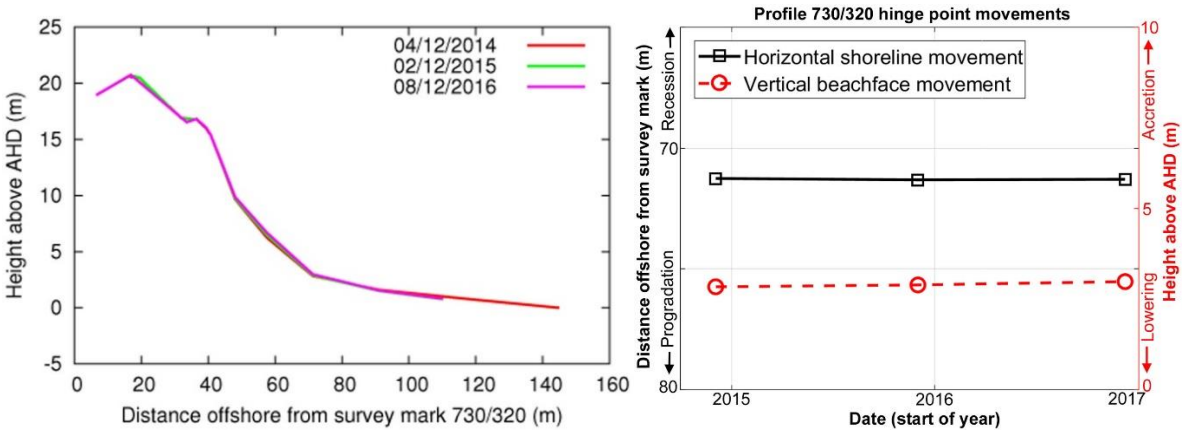

Figure 128: All surveys on TASMARC profile 730/320 (middle beach) to date, as profile plots (LHS) and hinge point movement plots (RHS).

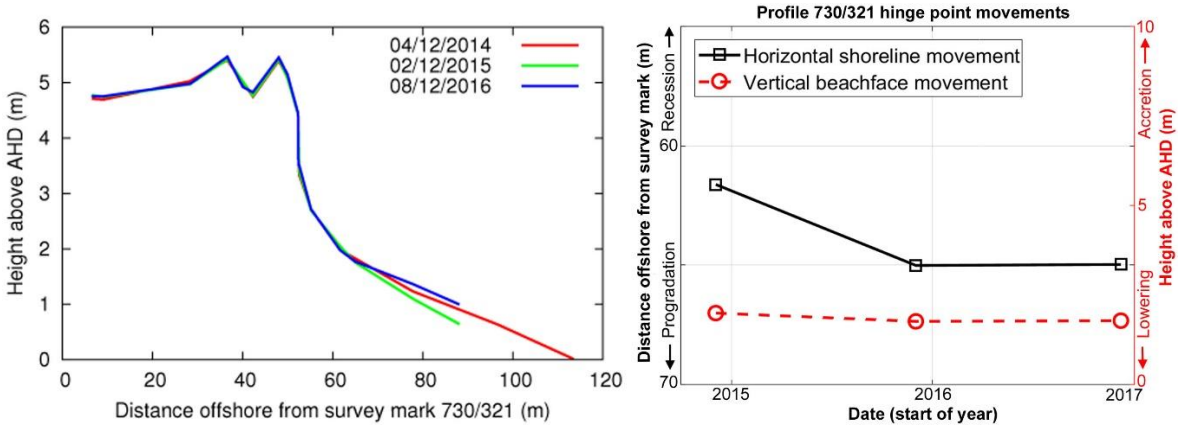

Figure 129: All surveys on TASMARC profile 730/321 (east beach) to date, as profile plots (LHS) and hinge point movement plots (RHS).

Shore behaviour history from profile surveys

All four profile records at all three beaches show very similar shoreline movement histories over the three years December 2014 to 2016, namely negligible dune face changes and only minor vertical beach face changes.

Except for profile 730/321 (Figure 129), no measurable horizontal movement (recession or progradation) of the dune face or shoreline was seen, as indicated by the horizontal shoreline movement plots in the hinge plots below. A small apparent seawards movement of the shoreline at profile 730/321 is likely to be the result of minor slumping at the base of the dune face.

Some measurable vertical movement of the beach face is evident in the profile plots and is a typical beach response to storm erosion followed by fair-weather swells returning the eroded sand to the beaches. However, these vertical beach face movements are virtually absent from the hinge point plots (which show negligible vertical hinge point movement), indicating that none of the beach-face erosion events over the profiling period were large enough to affect the hinge point at the back of the beach and foot of the foredune.

Summary shoreline behaviour history and characterisation

The available air photo history plus TASMARC profile record from January 1948 to December 2016 - comprising 15 air photo dates and three annual beach profiling dates – indicates that all three beach

shorelines at Cox Bight have been largely stable over that period. Only one shoreline erosion event is detectable (beyond error margins) during the 68-year period, and that was followed by full recovery so that to date there has been no significant shoreline movement trend – towards either recession or progradation - over the period. Other erosion events may have occurred in time gaps between air photos; however, the more recent air photos indicate recovery from any such events must have been complete.

The one significant erosion event (or cluster of events) known at the Cox Bight beaches probably occurred between the 24th March 1994 and 8th Jan 1998 air photo dates, although additional erosion events may have occurred before the 13th March 2005. Foredune erosion scarps from this event including exposed dune palaeosols were remarked upon by Cullen (1998), p. 41, however the air photo record shows that beach and foredune recovery (including scarp slumping and incipient foredune accretion) were virtually complete by the 5th November 2010 air photo date. As indicated by Figure 125, the median scale of shoreline retreat (and subsequent shoreline recovery) during this event was approximately 5 metres or less, which is a relatively small erosion event amplitude compared to the other south coast beach for which equivalent data is available, namely Prion Beach for which erosion events have caused median retreats of over 10 metres.

Beach and dune profiling have demonstrated that relatively frequent vertical beach lowering, and recovery occurs on the Cox Bight beaches in response to storms, but over the three-year profiling period no such storms were large enough to erode the foredune face. This contrasts notably with Prion Beach – also on the south coast – where storms over the same profiling period did significantly erode the foredune face on several occasions.

The most ostensibly recent scarps at Cox Bight appear to be those adjacent creek outlets (including short stretches near the outlet of Freney Lagoon and just east of Point Eric) and are probably related to creek discharges. Some foredune scarps are probably older features dating back to the 1990's erosion event and not yet slumped or obscured by incipient dune development.

The three Cox Bight beaches are evidently resilient and stable beaches which are unlikely to show early recessional responses to sea-level rise. The reasons for this resilience probably include the following:

- Cox Bight is likely to be continuing to receive a small (?) onshore gain of sand from the continental shelf.
- Cox Bight is unlikely to be losing sand eroded during storms because its deeply embayed character would not allow alongshore sand transport out of the Bight, and there is a lack of any other sand sinks such as tidal lagoons or onshore sand loss via transgressive dunes (Freney Lagoon is not a tidal lagoon and strong winds blow offshore, not onshore). Hence all sand moved offshore from the beach and dunes during erosion events is probably returned by fair weather swells.
- Although it is open to the dominant south-westerly swells and swell-storms, the deep rocky-bounded embayment of Cox Bight significantly attenuates swell wave energies before they reach the beaches, in contrast to more open south coast beaches such as Prion Beach. In addition, the limited directional variability of the swell waves, further reduced by refraction within the Bight, minimises variability in alongshore sand transport at the beaches.
- The highest frequency and strength of winds at Cox Bight blow offshore from the north-west, hence there are neither deflation gullies nor "sand blows" removing sand from the beach by landwards transport, nor are strong locally-generated wind waves likely to cause beach erosion since they dominantly propagate offshore (except possibly at the eastern end of the eastern Cox Bight beach).

Hence, the evident stability of the Cox Bight beaches (indicated by the air photo history and TASMARC beach profiling data) is probably the result of a stable to possibly slightly gaining sand budget, combined with a location within a deep embayment relatively sheltered from winds, swell waves and locally-generated wind waves.

Air Photo Data Tables

The following tables provide details of the air photos used, the resulting ortho-photos produced, and the shapefiles representing the shoreline position that were digitised from the ortho-photos.

Table 29: Original air photos and ortho-rectified air photos produced for Prion Beach

Photo Date	**Original DPIPWE air photos (film-frame) / Ortho-photo name**	**Final image resolution (original scan resolution if downsized) / pixel size of final ortho-photo**	**Original photo scale**	**Mean measured feature position error (± metres) for ortho-photo** [no. of measured feature position reference points]	**Comments**
17th Jan 1948	160-2753 160-2754 160-2755 160-2756 / *CoxBight_Jan1948a_MGA55.tif/tfw* *CoxBight_Jan1948b_MGA55.tif/tfw* *CoxBight_Jan1948c_MGA55.tif/tfw* *CoxBight_Jan1948d_MGA55.tif/tfw*	600 dpi / 0.75 m pixel size	1:15,840	3.6 m [10]	Ortho-rectified by C. Sharples
18th Mar 1961	365-62 / *CoxBight_Mar1961_MGA55.tif/tfw*	1000 dpi (2039 dpi) / 1.0 m pixel size	1:35,640	6.3 m [11]	Ortho-rectified by C. Sharples; Very poor accuracy despite repeat attempts. Excluded from final analysis.
18th Jan 1974	638-134 638-138 / *CoxBight_Jan1974a_MGA55.tif/tfw* *CoxBight_Jan1974b_MGA55.tif/tfw*	1000 dpi (2039 dpi) / 0.28 m pixel size	1:8000	1.3 m [5]	Ortho-rectified by C. Sharples Covers western beach only
15th April 1975	678-052 / *CoxBight_Apr1975_MGA55.tif/tfw*	1500 dpi (2039 dpi) / 0.66 m pixel size	1:40,000	1.7 m [11]	Ortho-rectified by C. Sharples
12th Dec 1979	808-171 / *CoxBight_Dec1979_MGA55.tif/tfw*	2039 dpi / 0.63 m pixel size	1:45,000	1.0 m [11]	Ortho-rectified by C. Sharples
22nd Mar 1984	998-006 / *CoxBight_Mar1984_MGA55.tif/tfw*	2039 dpi / 0.56 m pixel size	1:42,000	2.6 m [11]	Ortho-rectified by C. Sharples
15th Oct 1985	1040-58 1040-60 1040-61 1040-63 / *CoxBight_Oct1985a_MGA55.tif/tfw* *CoxBight_Oct1985b_MGA55.tif/tfw* *CoxBight_Oct1985c_MGA55.tif/tfw* *CoxBight_Oct1985d_MGA55.tif/tfw*	1000 dpi (2039 dpi) / 0.16 m pixel size	1:5,000	1.1 m [4]	Ortho-rectified by C. Sharples
8th Mar 1988	1114-75 / *CoxBight_Mar1988_MGA55.tif/tfw*	1000 dpi (2039 dpi) / 0.75 m pixel size	1:25,000	0.9 m [11]	Ortho-rectified by C. Sharples

15th Dec 1988	1124-121 / *CoxBight_Dec1988_15th_MGA55.tif/tfw*	1000 dpi (2039 dpi) / 1.14 m pixel size	1:42,000	2.0 m [11]	Ortho-rectified by C. Sharples. Excluded from final analysis since poorer accuracy than other 1988 air photos.
16th Dec 1988	1123-24 / *CoxBight_Dec1988_16th_MGA55.tif/tfw*	1000 dpi (2039 dpi) / 0.75 m pixel size	1:25,000	1.1 m [11]	Ortho-rectified by C. Sharples
24th Mar 1994	1221-100 / *CoxBight_Mar1994_MGA55.tif/tfw*	2039 dpi / 0.49 m pixel size	1:30,000	1.1 m [11]	Ortho-rectified by C. Sharples
8th Jan 1998	1283-152 / *CoxBight_Jan1998_MGA55.tif/tfw*	1000 dpi (2039 dpi) / 1.77 m pixel size	1:42,000	2.6 m [11]	Ortho-rectified by C. Sharples
25th Jan 2005	1391-67 / *CoxBight_Jan2005_MGA55.ecw*	2039 dpi / 0.5 m pixel size	1:42,000	4.2 m [10] (quoted absolute accuracy ±15m)	Ortho-rectified by DPIPWE Original DPIPWE ortho file: 1391_067_op.ecw Excluded from final analysis since poorer accuracy than other 2005 air photo.
13th Mar 2005	1394-86 / *CoxBight_Mar2005_MGA55.tif/tfw*	1000 dpi (2039 dpi) / 1.2 m pixel size	1:42,000	1.7 m [11]	Ortho-rectified by C. Sharples
15th Dec 2009	1439-53 / *CoxBight_2009_MGA55.ecw*	2039 dpi / 0.5m pixel size	1:42,000	1.8 m [8] (quoted absolute accuracy ±15m)	Ortho-rectified by DPIPWE Original DPIPWE ortho file: 1439_053_op.ecw
5th Nov 2010	1449-183 1449-184 / *CoxBightA_Nov2010_MGA55.ecw* *CoxBightB_Nov2010_MGA55.ecw*	2039 dpi / 0.3 m pixel size	1:24,000	0.8 m [11] (quoted absolute accuracy ±10m)	Ortho-rectified by DPIPWE Original DPIPWE ortho files: 1449_183_op.ecw 1449_184_op.ecw
6th March 2011	1455-218 1455-220 1455-222 1455-232 1455-234 1455-236 / *CoxBight_Mar2011a_MGA55.tif/tfw* *CoxBight_Mar2011b_MGA55.tif/tfw* *CoxBight_Mar2011c_MGA55.tif/tfw* *CoxBight_Mar2011d_MGA55.tif/tfw* *CoxBight_Mar2011e_MGA55.tif/tfw* *CoxBight_Mar2011f_MGA55.tif/tfw*	1000 dpi (2039 dpi) / 0.16 m pixel size	1:5000	1.1 m [9]	Ortho-rectified by C. Sharples Photos taken a few months before large erosive storm on 9th-10th July 2011 Final orthos marred by 'noise' (black pixels) but mainly usable.
22nd Dec. 2015	*Cox Bight_Dec2015_MGA55.ecw*	- / 0.1 m pixel size	-	0.0 m [N/A] (quoted absolute accuracy ±0.5m)	REFERENCE IMAGE (zero relative feature position error by convention) Digital original photo; Ortho-rectified by DPIPWE Original DPIPWE ortho file: 24265A_Cox_Bight_Dec2015.ecw

Table 30: Digitised shoreline shapefiles produced for Cox Bight (using ortho-photos listed in Table 29 above).

Date of air photo(s)	Shapefile	Shoreline digitised by	Comments
17th Jan 1948	CoxBight_MGA55_19480117.shp	Chris Sharples (2017)	Veg line sharp & distinct; poor photo resolution but prob. mainly a low scarp, no incipient dune seen. Higher slumped scarps common.
18th Mar 1961	CoxBight_MGA55_19610318.shp	Chris Sharples (2017)	Poor photo resolution, but veg line distinct, probably scarped in parts, some slumping of higher scarps identifiable. Shading allowed for, no incipient dunes identifiable. Excluded from final analysis because ortho-photo accuracy poor
18th Jan 1974	CoxBight_MGA55_19740118.shp	Chris Sharples (2017)	Western Beach only. Good photo resolution, veg line distinct scarp, no incipient dunes. Shadowing and overhanging trees allowed for.
15th April 1975	CoxBight_MGA55_19750415.shp	Chris Sharples (2017)	Distinct veg. line, minor slumping, no indication of incipient dunes evident. Strong northerly shadowing allowed for.
12th Dec 1979	CoxBight_MGA55_19791212.shp	Chris Sharples (2017)	Mainly a distinct sharp veg. line. Only minor slumping. No incipient dunes clearly visible, little shading evident.
22nd Mar 1984	CoxBight_MGA55_19840322.shp	Chris Sharples (2017)	Veg line sharp and well defined; no incipient dunes apparent. Northerly shadowing allowed for.
15th Oct 1985	CoxBight_MGA55_19851015.shp	Chris Sharples (2017)	Veg. line mostly distinct, commonly a low scarp. Slumping evident where scarp higher, minor incipient dunes in parts. Westerly shadowing and overhanging trees allowed for.
8th Mar 1988	CoxBight_MGA55_19880308.shp	Chris Sharples (2017)	Distinct sharp veg. line somewhat ragged with some slumping (not recently eroded?). Northerly shadowing allowed for. *Very close to 16th Dec 1988 shoreline*
15th Dec 1988	CoxBight_MGA55_19881215.shp	Chris Sharples (2017)	Distinct sharp vegetation line (little shadowing), some slumping, no indication of incipient dune.

			Excluded from final analysis since ortho-photo poorer accuracy than other 1988 air photos.
16th Dec 1988	CoxBight_MGA55_19881216.shp	Chris Sharples (2017)	Mostly distinct sharp veg line (but incipient veg, would be hard to discern given photo scale/res). Some shadowing from NE. allowed for. *Very close to Mar 1988 shoreline*
24th Mar 1994	CoxBight_MGA55_19940324.shp	Chris Sharples (2017)	Generally sharp distinct veg. line (some slumping on E beach dune-front); shadowing from NW & some overhanging foliage allowed for.
8th Jan 1998	CoxBight_MGA55_19980108.shp	Chris Sharples (2017)	Vegetation line distinct with some slumps obvious (E half of beaches) and some shadowing allowed for, but coarse resolution precludes seeing details.
25th Jan 2005	CoxBight_MGA55_20050125.shp	Chris Sharples (2017)	Vegetation line distinct but coarse resolution precludes seeing details. Some shadowing from the east allowed for. Excluded from final analysis since ortho-photo poorer accuracy than other 2005 air photo.
13th Mar 2005	CoxBight_MGA55_20050313.shp	Chris Sharples (2017)	Veg line difficult to pick in places owing to poor res and notable shadowing from N (allowed for) but tonal differences help.
15th Dec 2009	CoxBight_MGA55_20091215.shp	Chris Sharples (2017)	Veg line mostly distinct, prob. low scarp in many parts, no incipient dune veg seen.
5th Nov 2010	CoxBight_MGA55_20101105.shp	Chris Sharples (2017)	Veg line mostly distinct, scarp with some slumps. No incipient dune seen. Some shadowing and overhanging trees/bushes allowed for in defining shoreline.
6th Mar 2011	CoxBight_MGA55_20110306.shp	Chris Sharples (2017)	Long shadows in some areas. Veg line commonly sharp and distinct, in parts obviously slumped scarp; no incipient dune veg. seen.
22nd Dec 2015	CoxBight_MGA55_20151222.shp	Chris Sharples (2017)	Veg line well defined, typically clean scarp, no incipient dune veg. Some shadows and overhanging shrubs allowed for.

TASMARC shore profile data tables

Table 31: GPS-surveyed co-ordinates of each TASMARC transect survey mark at Cox Bight. The survey marks are located at the landwards end of each transect, which runs seawards normal to the shoreline from each mark. Latitude and Longitude are decimal degrees and eastings and northings are metric co-ordinates in the Map Grid of Australia Zone 55 (MGA55, GDA94 datum)

Transect	Longitude	Latitude	Easting	Northing
730/313	146.2344	-43.4902	438096.89	5184462.93
730/319	146.2487	-43.4892	439254.34	5184582.11
730/320	146.2575	-43.4907	439962.53	5184423.94
730/321	146.2712	-43.4967	441076.26	5183768.26

Table 32: Table of hinge points defined for each surveyed Cox Bight profile (derived from original TASMARC survey data).

TASMARC profile number	Survey date	Hinge point distance offshore from survey mark (metres)	Hinge point height above AHD (metres)
730-313	04/12/2014	37.815	1.468
730-313	02/12/2015	37.811	1.467
730-313	08/12/2016	37.825	1.546
730-319	04/12/2014	73.060	1.780
730-319	02/12/2015	73.092	1.671
730-319	08/12/2016	73.066	1.598
730-320	04/12/2014	71.271	2.830
730-320	02/12/2015	71.328	2.882
730-320	08/12/2016	71.306	2.974
730-321	04/12/2014	61.635	1.983
730-321	02/12/2015	65.029	1.752
730-321	08/12/2016	64.989	1.771

A1.3.4 Window Pane Bay Beach (south-west coast)

Locality and general description

Window Pane Bay beach is a high energy sandy and cobble beach exposed to south-westerly swells about 12 km north of South West Cape, making it the most southerly beach on the Tasmanian west coast (Figure 130). Introduced dune-colonising weeds capable of modifying beach and dune behaviour – such as marram grass *Ammophila arenaria* - have not established at Window Pane Bay.

Two distinctly different coastal sites are present at Window Pane Bay, separated by the main creek outflow. These are *Window Pane Bay Beach North* and *Window Pane Bay Beach East* (see Figure 130). The beach was visited by Chris Sharples (and others) in December 2014, 2015 and 2016, during a DPIPWE-funded helicopter-based project to establish and measure beach profile transects.

Geomorphology and process environment

Geomorphic description

Geomorphic aspects of Window Pane Bay beach have previously been described by Cullen (1998) and Short (2006b). The beach mostly faces southwest (aspect 210º True) and although strongly exposed to the south-westerly swells is located within a rocky embayment 1.7 km wide on a long mostly rocky and cliffed coastal section. The north-western end of the beach (*Window Pane Bay Beach North*) is somewhat sheltered behind the long rocky point of Flying Cloud Point which bounds the western side of the embayment. The 1.5km long fine to medium grained sand beach is a Transverse Bar and Rip (TBR) to Rhythmic Bar and Beach (RBB) morphodynamic type (Short 2006b) fronted by a 100m wide surf zone with several rips. At its south-eastern end the beach grades to a 600m long boulder beach (*Window Pane Bay Beach East*), whilst the more sheltered western end in the lee of Flying Cloud Point is a 100m long Reflective (R) morphodynamic beach type which sometimes includes an ephemeral tombolo connecting it to an offshore rock (Short 2006b). Window Pane Creek discharges across the broad middle of the beach in a meandering channel with a cobble bed load.

The north-western 700m of the beach (*Window Pane Bay Beach North*, west of the creek outlet) is backed by a very high steep eroding and slumped dune face up to 50 metres high (Figure 132). This is not a foredune in the sense of Hesp (2002) but rather is the wave-eroded distal (downwind) end of a large now-vegetated transgressive dune complex which Cullen (1998), p. 55 has interpreted (on the basis of NW-SE aligned dune ridges) to have accumulated in Late Pleistocene to Holocene times from sand blown south-eastwards from Island Bay into the Window Pane Bay embayment (Figure 131). It is likely that most of this dune complex mantles a bedrock surface above present sea-level. When inspected most of the seawards (southerly facing) dune face was bare slumping sand with rafts of organic soil and vegetation sliding down from the crest of the dune, however the dune crest and back dune area is well-vegetated and stable. No significant incipient dune accumulation was noted at the dune scarp toe. No palaeosols were noted in the slumped dune face, however at one or two locations a peat deposit with plant fragments is exposed at the base of the dune face. This appears different to the slumped peaty dune soil rafts and may represent an older swamp deposit underlying the dune sands. Some minor wind-driven deflation of the bare dune face is occurring with small active lobes of wind-blown sand transgressing into vegetation for a few metres on the lee (north) side of the dune crest, however there is also a large deflation gully at the western end of this high dune where wind is transporting sand northwards up and behind the dune-face for over 100 metres.

Window Pane Creek emerges through a 200m wide gap in the dunes onto the central part of the beach, which is backed by a broad low valley interpreted by Cullen (1998), p. 54 as a sediment infill basin (likely Holocene marine sediment infill) with some vegetated transgressive dunes. In this area the soft sediment infill is likely to extend in depth to below sea-level for some hundreds of metres

inland of the beach. Relatively fresh scarps at the dune toes on either side of the creek outlet are probably a result of fluvial (creek) erosion rather than wave erosion. Historic air photos show that large bare sand deflation areas and mobile sand lobes extended 200 hundred metres north of the creek outlet in 1948, but these progressively revegetated and stabilised over the latter half of the Twentieth Century (see further below).

Figure 130: Window Pane Bay from the southeast, showing the sandy beach backed by high scarped dunes in the distance (Window Pane Bay Beach North), and the boulder beach section backed by a sandy dune and vegetated transgressive dunes in the foreground (Window Pane Bay Beach East). Photo by C. Sharples Dec. 2014.

The south-eastern part of the beach (*Window Pane Bay Beach East*) is backed by a vegetated sandy dune rising 15 – 20 metres above the back of the beach, which also backs most of the boulder-beach further south-east of the sandy beach section (Figure 130). This dune may be partly a true foredune but is probably mainly a truncated seawards end of former Pleistocene/early Holocene terrestrial transgressive dunes. In either case it is clearly a fossil feature with no ongoing sand supply since (1) it was fully vegetated and had a well-developed stable organic soil horizon (prior to recent erosion) and (2) there is no present-day sand source for at least the southern half of the dune which is fronted by a boulder beach, not a sandy beach. A wave erosion scarp with some slumping but no incipient dune recovery was present along the dune toe behind this part of the beach at the time of inspection, and was mostly only 2 – 3 metres high but reached over 15 m high to the crest of the dune around the TASMARC profile 730/311 location (see Figure 130 & Figure 131). Historic air photos show this high scarp was not present in 1961 but that a small scarp had appeared by 1975 and has grown progressively higher and more laterally extensive along the dune front ever since, with no sign of dune recovery or incipient dune development. In 2014 – 2016 the dune erosion scarp continued south-eastwards behind the boulder beach to a little north of TASMARC profile 730/312, beyond which the foredune front is mostly stable and fully vegetated with no significant erosion scarp (see Figure 131).

No evidence of currently active dune deflation in the form of windblown sand accumulations in the lee of the dune crest were seen, nor were palaeosols exposed in the dune erosion scarp. This dune is in turn backed by stable vegetated transgressive dunes extending inland for 1.5km to the east and north-east, and up to 250 metres above sea-level. North-easterly trending dune ridges in this complex imply

previous sand transport and deposition by winds blowing from the south-west out of Window Pane Bay, in contrast to the north-westerly derivation inferred for the transgressive dunes backing the northwest part of Window Pane Bay beach. The depth to bedrock beneath the foredune is difficult to infer, however rising slopes close behind the dune and rocky reefs immediately offshore from the boulder beach section suggest the underlying bedrock surface rises above present sea-level beneath or close behind most of the foredune.

None of the slumping dune scarps at Window Pane Bay (backing the north-western beach section and the south-eastern section) showed either fresh wave-cut basal scarps or recent incipient dune growth. The persistence of these scarps over multi-decadal periods in the air photo record suggests that wave attack is frequent enough to prevent dune-front stabilisation and revegetation, yet infrequent enough that fresh scarps were not seen over the three-year period of TASMARC beach profile monitoring (see below).

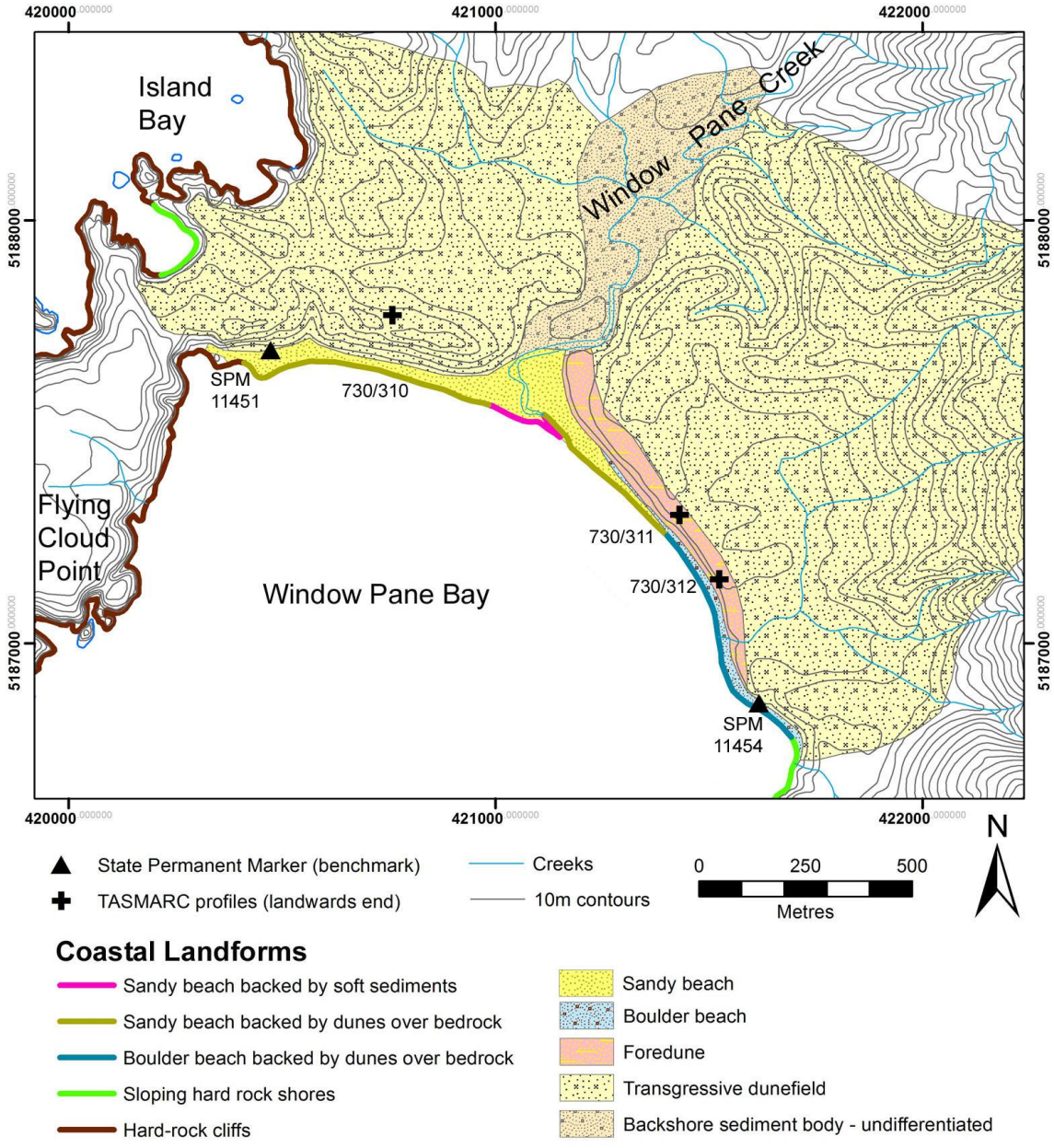

Figure 131: Coastal landforms at Window Pane Bay. Coastal landform mapping is based on Cullen (1998), with additional shoreline types mapping by C. Sharples. Permanent survey benchmark (SPM) and TASMARC survey profile locations and numbers are indicated. Co-ordinate system is Map Grid of Australia zone 55 (GDA1994 datum).

Figure 132: View looking northwards at the high slumping dune face backing the north-western end of Window Pane Bay beach (*Window Pane Bay Beach North* site). Much of the vegetation visible on the dune face is on rafts of peaty soil gradually sliding down the dune face. The well-vegetated area immediately behind the dune face is a transgressive dune complex of which the eroding face is probably the scarped distal end. Photo by C. Sharples Dec. 2014.

Figure 133: View of scarped and slumped 50m high dune face at the north-western end of Window Pane Bay close to TASMARC profile 730/310, showing rafts of soil and vegetation. The lack of either a recent wave scarp or of significant incipient dune growth at the toe of the slope is notable. Photo by C. Sharples Dec. 2014.

Swell wave climate

The north-western part of the beach (*Window Pane Bay Beach North*) is partly sheltered from the very high energy south-westerly swell and received partly refracted and attenuated swell. In contrast Window Pane Bay Beach East is directly exposed to the high energy south-westerly swells.

Wind (wind wave) climate

Strongly exposed to dominantly north-westerly wind, with some sheltering behind Flying Cloud Point.

Sand transport and budget

Shelf sediment mobility modelling suggests that persistent south-westerly swells may still be moving sand from the continental shelf directly onshore into Window Pane Bay (Harris & Heap 2014; Harris et al. 2000), albeit there is no empirical evidence for this.

Window Pane Bay is deeply embayed between prominent rocky points in a long high-energy rocky shore, and there seems little potential for sand to be moving alongshore into or out of the embayment. Currently bare slumped dune faces behind the western half of the beach and in the eroding dune behind the eastern half of the beach are not losing large amounts of sand to landwards, with only small lobes of windblown sand observed accumulating immediately behind the dune and scarp crest in each case (typical scale 0.5 – 1.0m wide and a few tens of centimetres deep). The large deflation gully behind the western end of the beach has shown no significant change between 1948 and 2015, with no evidence of expanding sand lobes being deposited at its distal (landwards) end (see Figure 134); this feature evidently functions simply as a wind gap through which very little sand is blown from the beach. In contrast, the large bare sand blow area that extended 200 metres inland behind Window Pane Creek in 1948 has gradually stabilised and revegetated since 1948 (Figure 134), so that previous losses of wind-blown sand from Window Pane Bay have reduced to negligible over the latter half of the Twentieth Century.

The dune backing Window Pane Bay Beach East which has commenced eroding circa 1980 was a fossil dune which was not actively gaining sand. Erosion is presumably due to more frequent higher wave attack (no other explanation apparent) which could be due to SLR and/or increased wind-wave setup due to stronger onshore winds. Sand eroded (backwash transport directly offshore during storms, and small amounts inland via deflation?) is being transported elsewhere within embayment (some lost into accommodation space in bay, some likely returning to north (sandy) shore of embayment and funnelled landwards in deflation gullies) and is not returning to rebuild dune (boulder beach in front of most of eroding section shows no sign of gaining sand and supplying it to rebuild dune face). Eroded sand is being lost from Window Pane Bay Beach East, and no sand is returning or being newly gained to replace it. Thus, the two early response conditions are satisfied – active sand sink, sand efficiently lost into it and not being returned to build dune face (which shows no morphological sign of rebuilding). No sign of gaining sand budget in section being eroded, since beach is still just boulders there (indicating no sand coming onshore). Sandy beach section further north is likely gaining offshore sand, however?

Whereas Window Pane Bay as a whole is probably gaining sand from the shelf, the boulder beach and lack of any incipient dune formation or scarp repair at Window Pane Bay Beach East indicates that the sand is not coming onshore and accreting onto the frontal dune (and has not since at least. However sand may possibly be coming onshore in northern part of bay and being funnelled landwards in deflation gullies, one of which is still active.)

In summary, the Window Pane Bay sand budget is stable to possibly slightly gaining (from the shelf), with former losses inland by wind transport evidently having reduced to negligible in recent decades.

Artificial disturbances

Minor campsite behind the creek outflow.

Air photo analysis

Ortho-rectified vertical air photos of Window Pane Bay at 11 dates from 1948 to 2015 (see Table 33) were used to map and characterise the shoreline change history of the beach and the backing dunes. An additional ortho photo from 1973 was not used owing to poor ortho-rectification accuracy (> ±4m), however this covers only the western end of the beach and is close in time to the 1975 air photo which gives full coverage. The *in situ* (living) vegetation line was mapped as the shoreline proxy at each air photo date (Table 34), however this line delineates three distinctive coastal feature types whose histories have been considered separately in this analysis. These three types are the seawards (wave-exposed) margin of the foredune backing the eastern half of the beach, the head if the slumping dune scarps backing most of the western half of the beach and (since 1975) a part of the foredune behind the eastern part of the beach, and the landwards margin of bare wind-blown deflation gullies and bare transgressive sand dunes (Figure 135 shows the extent of each type in 2015).

Shore behaviour history from air photos

Horizontal movement over time of the wave-exposed dune front and slumping dune head scarp vegetation lines have been measured along 100 metre-spaced digital transects, and are plotted in three groups on Figure 136. Movement of the bare deflated sand masses have simply been compared visually. The three types of mapped shoreline features have behaved differently over the air photo period and are described separately as follows:

Wave-exposed foredune vegetation line Except for a scarped central area described separately below, most of the vegetated seawards front of the sand foredune backing the eastern half of the sandy and cobble beach has shown negligible real change over the period from 1948 to 2015, with most apparent position change being within the range of ortho-photo error margins and thus likely not real (see lower plot on Figure 136). Although some small wave-eroded scarps are present at the seawards front of this dune, the air photo and TASMARC profile evidence indicates that these have been mostly stable features that have shown very little horizontal recession or recovery to date.

Head scarp of slumping foredune section Although most of the eastern foredune appears to have been a stable feature over the air photo period, progressive erosion and slumping has occurred in a central section of the foredune. From 1948 until 1961 the entire foredune front shows no change, however by 1975 a slumped section of dune had appeared along a 90-metre length in the middle of the foredune. This has subsequently extended progressively along the dune front and headwards towards the dune crest (see Figure 134). The head scarp plot (RHS plot on Figure 136) indicates a large initial slumping event between 1961 – 1975, which could have been triggered by a large wave erosion event at the foredune toe. This has been followed by slower but continuing progressive expansion of the slumped area (and its mapped head scarp) both laterally and vertically until at least 2015, when the slumped area reached up to the dune crest at one point and for 180 metres along the dune front. Although the seawards toe position of the slumped area (including slumped vegetation 'rafts') shows little detectable change, this has evidently resulted from progressive slumping of soil and vegetation rafts down the slump face followed by their ongoing destruction and dispersal by wave action at the toe of the slump.

Given the dominant direction and low directional variability of the south-westerly swell received by Window Pane Bay, the foredune slump area is probably the part of the bay that most frequently receives the highest swell (and swell-storm) wave energies, with the least energy loss through shoaling and refraction against the bounding rocky shores and some reefs within the bay. This is therefore the part of the beach that might be expected to be the first to receive topographically higher storm wave impacts as sea-level rises. This factor, together with the observed progressive expansion

of the foredune slump without any recovery in the 43+ years since it was initiated, is suggestive of a possible early response to renewed sea-level rise.

Head scarp of high slumping transgressive dune face The highest and most superficially-dramatic dune slump feature at Window Pane Bay is the 50-metre high slumping bare dune face backing the beach west of Window Pane Creek. As noted above this feature is the eroding distal end of a large formerly transgressive dune which must have accumulated by wind transport from the west under lower sea-levels than at present (i.e., pre-6,500 BP), hence it is likely this face has been eroding and slumping over most of the last circa 6,500 years since sea-level reached close to its present level at the end of the last post-glacial marine transgression. The air photo record shows little change in the horizontal position of the slump head scarp line between 1948 and 2015 (see Figure 135 and top plot in Figure 136). There is no systematic trend evident, and a substantial part of the variability exhibited is attributable to the air photo error margins and hence is likely not real.

The main change observed over the air photo period is the progressive sliding of two large soil and vegetation rafts down the slump face. A large western raft ("A" in Figure 134) had already detached from the head scarp and was sliding down the dune face in 1948; subsequent photos show this raft moving downslope and breaking up under wave action at the toe of the slump face (with most of the raft gone by 1988 but a few remnants still visible in 1998). Another large raft in several sections ("B" in Figure 134) is just beginning to separate from the head scarp in 1975 and has moved some tens of metres by 1988 but is still moving (with further additions from the head scarp) in 2015.

It is evident that wave action has been removing slumped debris (sand and soil/vegetation rafts) from the toe of the dune slump face over the air photo period, and that further rafts have been detaching from the head scarp over that period, but any progressive change in the head scarp position has been negligible over the period. This may in part be related to air photo position error margins, head scarp movement as rafts detach, and to ongoing vegetation growth obscuring the scarp margins. However, it also clearly implies little progressive overall change in the high slumping dune scarp over the air photo period.

In summary the high bare slumping transgressive dune face behind the western half of the beach is an old feature which is likely to have been initiated circa 6,500 years ago when sea-level reached close to its present level, and no change in its long-term behaviour is yet detectable from the air photo record since 1948.

Deflated wind-blown sand margins Two prominent features resulting from wind erosion and transport of sand are evident in the 1948 air photo, namely a prominent deflation gully above the western extremity of the beach, and an extensive area of bare deflation hollows and windblown sand deposits landwards of the mouth of Window Pane Creek, in the centre of the beach (see Figure 134 & Figure 135).

Of these, the western deflation gully barely changed its extent between 1948 and 2015 and has evidently not been a conduit for wind-blown sand as no detectable amounts have been deposited at the landwards end of the gully over the air photo period. Field inspection during the TASMARC profiling visits indicated the feature is essentially a stable wind-funnelling deflation gully with little evidence of significant recent sand erosion or deposition.

In contrast the unvegetated sand-blow area behind Window Pane Creek was at its maximum extent in 1948 and has progressively revegetated and stabilised over the whole air photo period, with near-complete vegetation cover by 2010. It is evident that this sand blow was triggered by some event or events prior to 1948 and has been recovering ever since. This blow is not exposed to dominant north-westerly wind direction (see Maatsuyker wind record) which have caused the biggest active and growing sand blows on the SW coast, e.g., Stephens Bay.

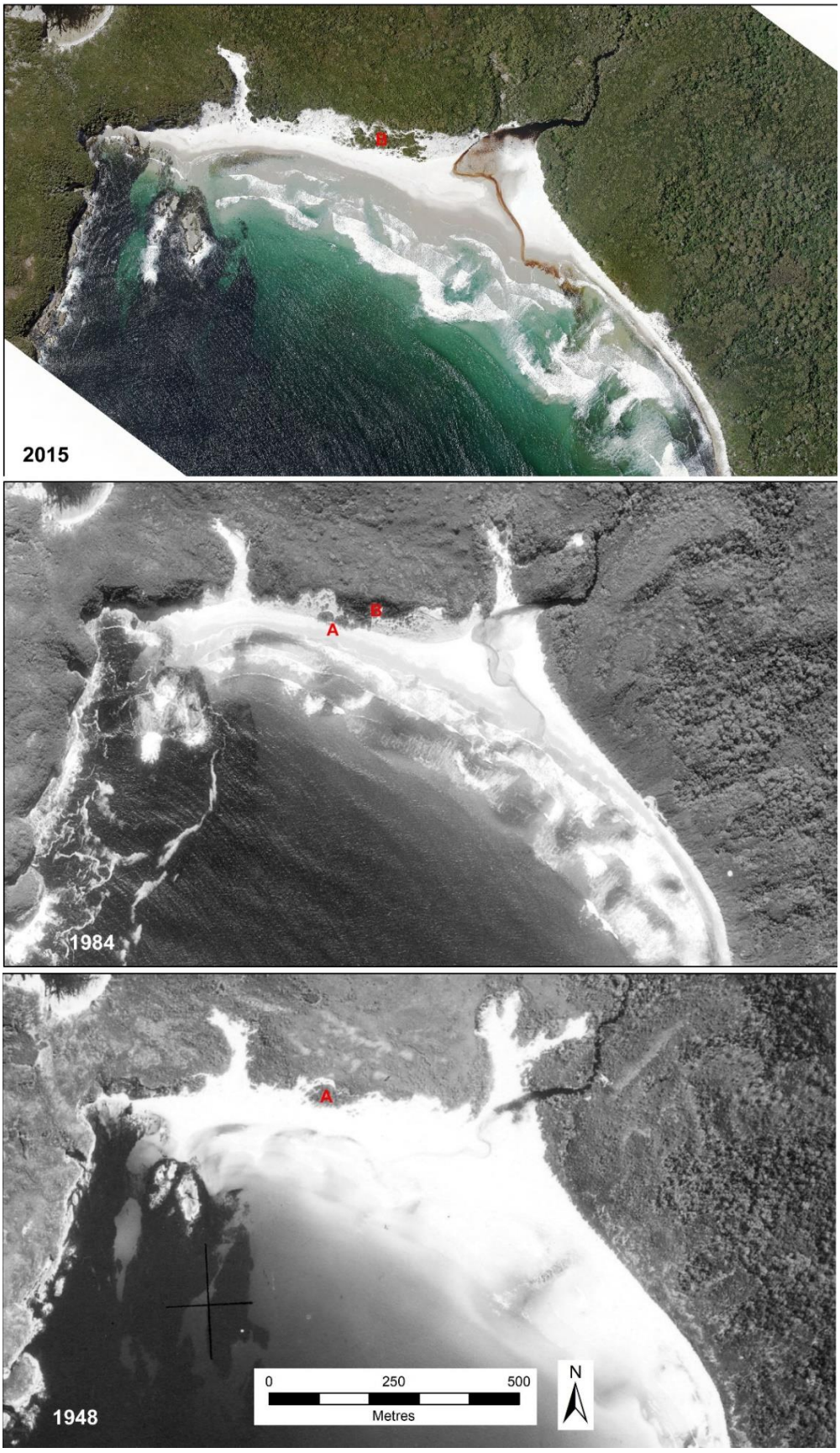

Figure 134: Comparison of ortho-rectified air photos of Window Pane Bay in 1948, 1984 and 2015.

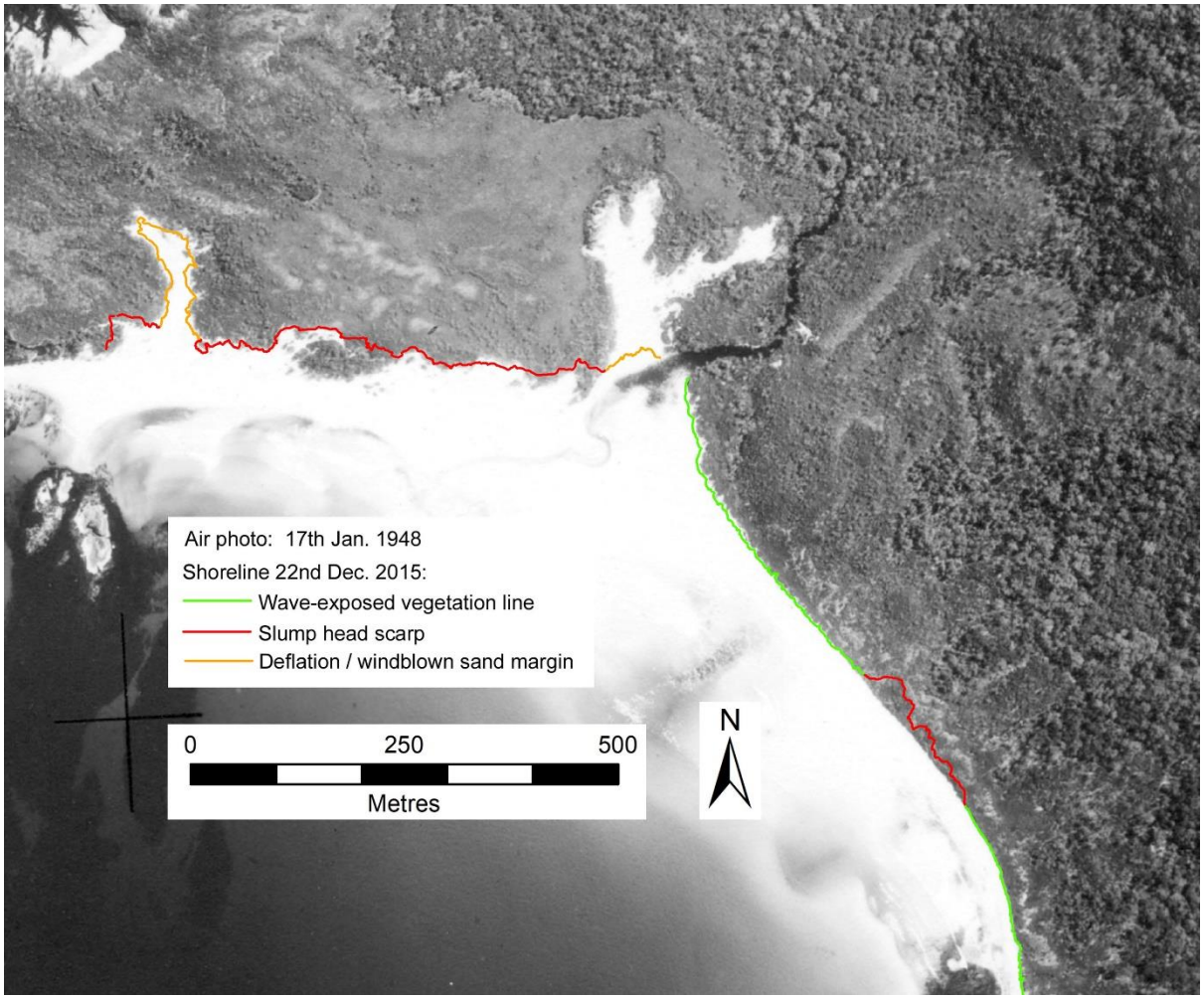

Figure 135: Comparison of shoreline positions at Window Pane Bay between 1948 (ortho-rectified photo) and 2015 (shoreline proxy and other features digitised from 2015 ortho-photo). Of particular note is that there has been negligible change in the position of the foredune vegetation line (eastern half of beach) except where a large slump has developed from 1975 onwards; and that the head scarp of the high dune-face slump backing the western half of the beach has shown negligible position change over the whole air photo period despite two very large vegetated soil rafts detaching and sliding down the slump face over that period. Similarly, the western deflation gully has changed little over the period, whereas the extensive mobile windblown sand lobes behind the main creek outlet have almost entirely revegetated. Air photo © DPIPWE.

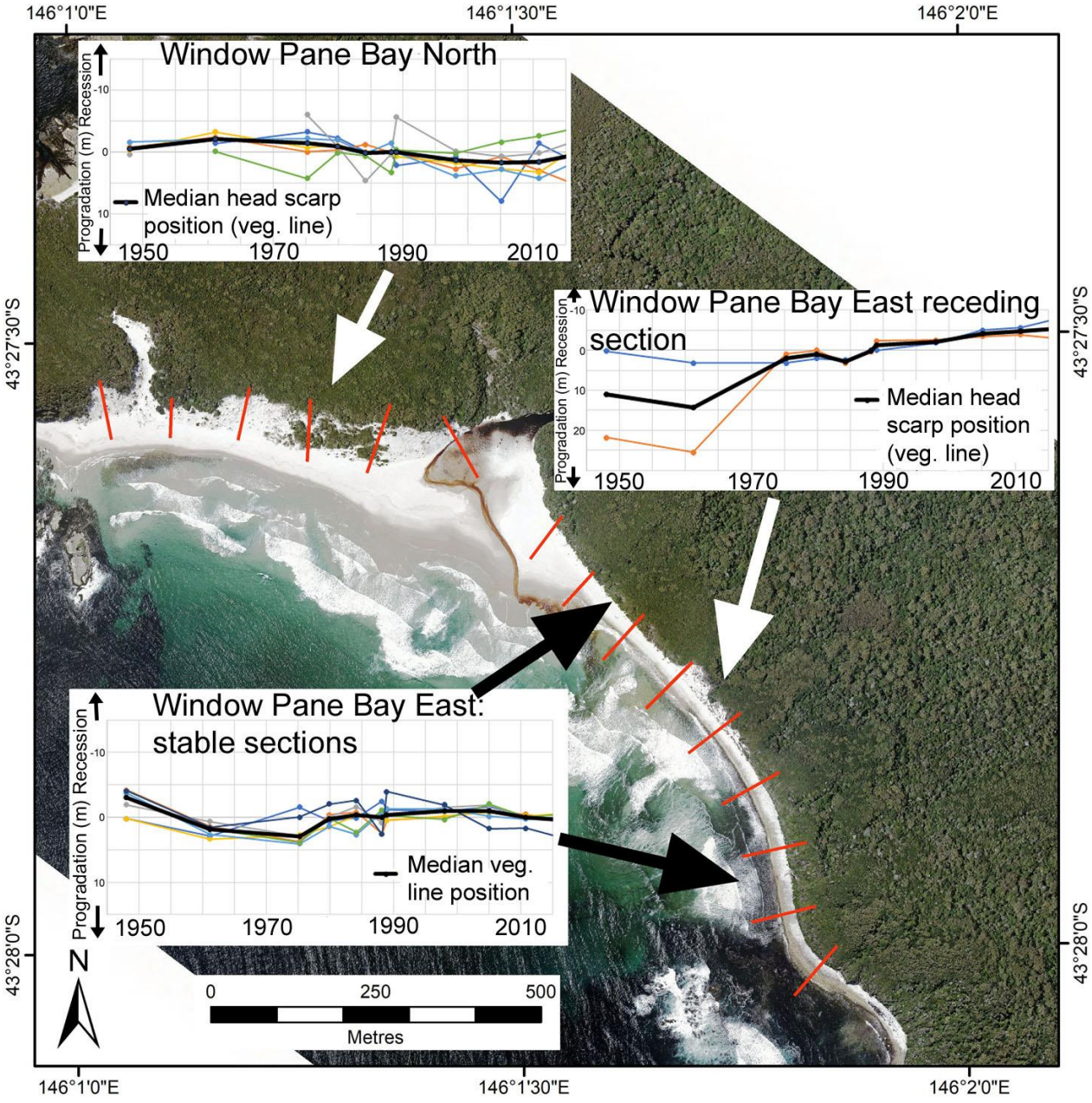

Figure 136: Plots of shoreline position (*in situ* vegetation line) movement within three key elements of the Window Pane Bay shoreline. Shoreline positions are plotted at 11 air photo dates over the period 1948 – 2015 along each 100m-spaced digital transect (red lines). Air photo error margins for each date are provided in Table 33. The base air photo is the 2015 photo (© DPIPWE).

Surveyed shore profile analysis (TASMARC)

Three TASMARC beach profile survey marks were established at Window Pane Bay during December 2014 as part of a DPIPWE World Heritage Area monitoring project managed by Rolan Eberhard in collaboration with the TASMARC project (Eberhard et al. 2015). Profile locations are shown on Figure 131 and listed in Table 35. The three profiles have been surveyed three times to date (in December 2014, 2015 & 2016), with surveying undertaken by Nick Bowden and Paul Boland, with assistance from Rolan Eberhard, Michael Comfort, Chris Sharples, and others. Each profile extends normal to the shoreline from a survey mark on the landwards side of the first dune, across that dune and as far down the beach face as was reasonably accessible on each visit.

The results of the surveys are plotted on Figure 137 to Figure 139 below in two forms, namely as profile plots and hinge point plots. Explanation in methods section. The original processed survey data for each profile plot (provided here as figures) is available on the TASMARC website (www.tasmarc.info) and is not reproduced here. The hinge point data has been derived from the original profile data and is provided here as Table 36 below. Photos showing the condition of each profile at the date of each survey are provided on the TASMARC website.

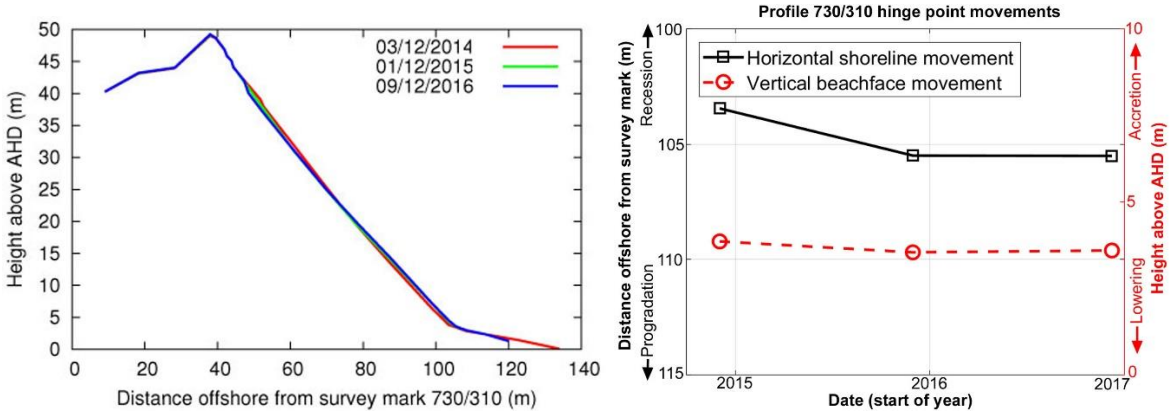

Figure 137: All surveys on TASMARC profile 730/310 (western half of beach) to date, as profile plots (LHS) and hinge point movement plots (RHS).

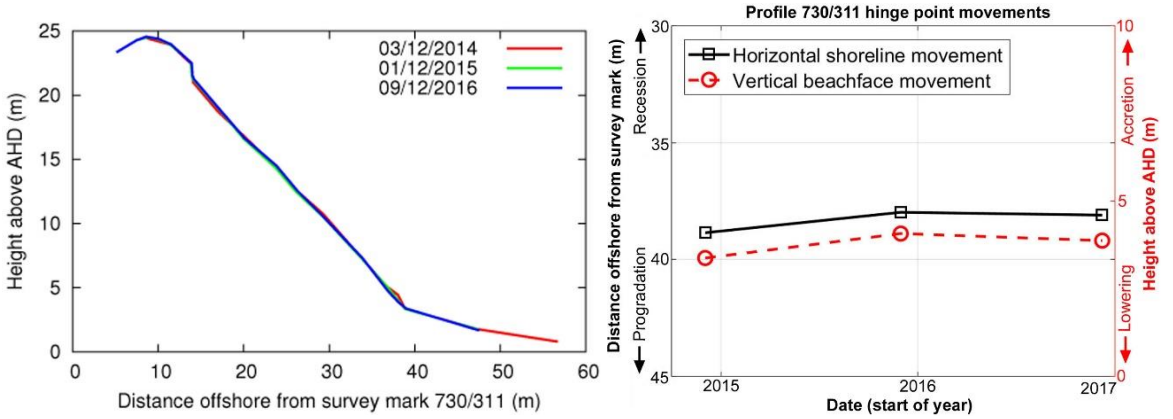

Figure 138: All surveys on TASMARC profile 730/311 (eastern half of beach) to date, as profile plots (LHS) and hinge point movement plots (RHS).

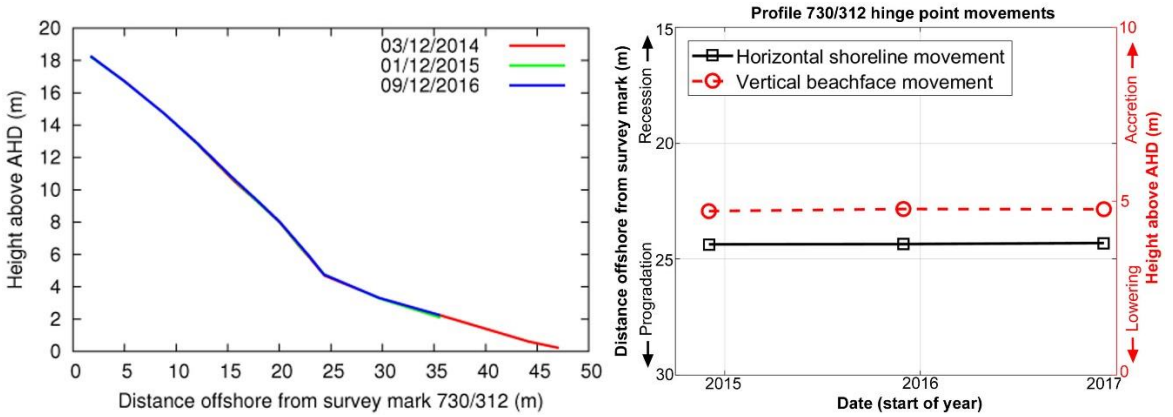

Figure 139: All surveys on TASMARC profile 730/312 (eastern half of beach) to date, as profile plots (LHS) and hinge point movement plots (RHS).

Shore behaviour history from profile surveys

The three TASMARC profiles at Window Pane Bay each sample one of the three key shoreline sections whose air photo-derived history is illustrated with plots in Figure 136 and discussed above. The TASMARC survey results for each are provided here:

Wave-exposed foredune vegetation line This shoreline type is sampled by TASMARC profile 730/312, whose plots (Figure 139) show no detectable moment of the dune face, hinge point or beach face. This result is consistent with the air photo history plots (Figure 136) which show no detectable change in the foredune seawards vegetation line position over the air photo period from 1948 to 2015.

Head scarp of slumping foredune section This shoreline type (the slumping section that has developed since 1961 on the eastern foredune) is sampled by TASMARC profile 730/311. The plots (Figure 138) show small (~ 1m) horizontal and vertical movements of the dune scarp face over the three yearly measurements that are consistent with the slow rate of ongoing scarp development slumping indicated since 1975 by the air photo history (see plot in Figure 136). The most notable change is a slight recession of the hinge point at the dune toe between Dec. 2014 and Dec. 2015, which probably represents removal of slumped sands by wave action at the back of the beach. This would result in maintenance of a constant position of the dune toe which the air photo history indicates has been the case since initiation of the slumping scarp after 1961.

Head scarp of high slumping transgressive dune face This high slumping dune face is sampled by TASMARC profile 730/310. Small scale (~1-2 m) horizontal and vertical movements of the slumping dune face were detected over the three yearly measurements, which are consistent with ongoing minor slumping of the dune face. Over the three yearly measurements, some removal of material from the upper slump face is evident in the profile plot, with some accumulation of material at the toe apparent in both the profile and hinge point plots. This behaviour is comparable with that inferred for this face over the whole air photo period, i.e., ongoing slumping of material down the slump face, with little change in the head scarp or dune toe (hinge point) positions.

Summary shoreline behaviour history and characterisation

The available air photo history plus TASMARC beach profiling record from January 1948 to December 2016 comprises 11 air photo dates and three annual beach profile dates. These data attest to a complex but mostly stable beach and dune history at Window Pane Bay. However, there are indications of recent-onset progressive instability in the most wave – exposed section of the bay, which is consistent with a possible early response to sea-level rise. Based on these data and other geomorphic observations, the shoreline history at Window Pane Bay is summarised below in terms of several distinctive sections of the bay:

Western half (Window Pane Bay Beach North): high slumping scarped dune The high (~50m) scarped dune face is incised into the distal (downwind) side of a Late Pleistocene or Early Holocene transgressive dune that must have developed at lower sea-levels than present when an exposed sand source was available to the west (see above). Major scarping and slumping of the Window Pane Bay face of this dune would have occurred circa 6,500 years ago when post-glacial sea-levels reached up to near their present level. It is possible that the dune face was subsequently stable and vegetated for some period in the Mid- to Late-Holocene following its initial adjustment to the Mid-Holocene high sea stand, however the air photo evidence shows it was actively slumping prior to 1948. This conceivably could be a relatively recent response to renewed global sea-level rise which commenced during the 1800s (Church & White 2011), however it is also possible that some slow dune face adjustment by slumping has been continuing up to the present since circa 6,500 years BP. Despite active slumping of the dune face since 1948, no progressive horizontal movement of either the toe or head scarp of the slump face has been detected over that period and any recent scarp recession is evidently slow. It may be expected that ongoing renewed global sea-level rise will eventually result

in some accelerated recession of this dune face but this is not evident in the data to date. Periodic future monitoring of the TASMARC profile (730/310) on this dune face is recommended to detect the onset of any such accelerated change.

Eastern half (Window Pane Bay Beach East): vegetated sandy frontal dune With the exception of the central slumped section described below, most of the vegetated sandy foredune backing the sand and cobble beach in the eastern half of Window Pane Bay has been very stable with no detectable progressive changes having occurred since at least 1948. This behaviour is consistent with the likely stable to possibly slightly gaining sand budget that is inferred for Window Pane Bay since at least 1948.

Centre of eastern half: progressively slumping central section of vegetated sandy frontal dune In contrast to the above, one central section of the vegetated eastern sandy dune has shown a significant change of behaviour since 1961, with a formerly stable vegetated part of the foredune having commenced slumping before 1975, presumably in response to a large wave erosion event at the seawards toe of the dune. This eroded and slumped dune section has not subsequently recovered from this event, but instead has continued to progressively expand vertically and laterally from 1975 up to at least 2016. This behaviour is suggestive of a long-term change in the behaviour of this dune, and it is notable that the change has commenced at the location within the bay most directly exposed to the highest swell-wave energies, and thus most likely to be sooner affected by increasingly frequent storm wave attack on a higher mean sea-level than elsewhere within the bay.

Deflation and bare mobile sand areas Geomorphic mapping has previously shown that windblown sands have been mobile and have formed dunes over large areas inland of the current beach and immediately backing dunes. These now-vegetated backshore dunes are likely to be of various ages ranging from Pleistocene to Holocene. However, since 1948 windblown sand mobility at Window Pane Bay has generally decreased, with one large sand blow becoming completely vegetated and stable between 1948 and 2010, and another large deflation gully showing no significant change over that period.

Air Photo Data Tables

The following tables provide details of the air photos used, the resulting ortho-photos produced, and the shapefiles representing the shoreline position that were digitised from the ortho-photos.

Table 33: Original air photos and ortho-rectified air-photos produced for Window Pane Bay beach.

Photo Date	**Original DPIPWE air photos (film-frame) / Ortho-photo name**	**Final image resolution (original scan resolution if downsized) / pixel size of final ortho-photo**	**Original photo scale**	**Mean measured feature position error for ortho-photo (± metres)** [No. of measured feature position reference points]	**Comments**
17th Jan 1948	160-690 / *Windowpane_Jan1948_MGA55.tif/tfw*	600 dpi / 0.8 m pixel size	1:15,840	2.5 m [7]	Ortho-rectified by Chris Sharples
18th Mar 1961	365-68 / *Windowpane_Mar1961_MGA55.tif/tfw*	1500 dpi (2039 dpi) / 0.7 m pixel size	1:35,640	3.5 m [10]	Ortho-rectified by Chris Sharples
19th Feb 1973	624-3 / *Windowpane_Feb1973_MGA55.tif/tfw*	1500 dpi (2039 dpi) / 0.6 m pixel size	1:30,000	7.7 m [5]	Ortho-rectified by Chris Sharples Crap accuracy, covers west part of beach only: but

					usable (frame 2 poss. better but not available as scan)
15th April 1975	678-43 / *Windowpane_Apr1975_MGA55.tif/tfw*	1400 dpi (2039 dpi) / 1.0 m pixel size	1:40,000	3.0 m [10]	Ortho-rectified by Chris Sharples
12th Dec 1979	808-167 / *Windowpane_Dec1979_MGA55.tif/tfw*	1500 dpi (2039 dpi) / 0.8 m pixel size	1:45,000	1.2 m [10]	Ortho-rectified by Chris Sharples
22nd Mar 1984	998-45 / *Windowpane_Mar1984_MGA55.tif/tfw*	1500 dpi (2039 dpi) / 0.7 m pixel size	1:42,000	1.2 m [9]	Ortho-rectified by Chris Sharples
8th Mar 1988	1114-65 / *Windowpane_Mar1988_MGA55.tif/tfw*	1000 dpi (2039 dpi) / 0.7 m pixel size	1:25,000	3.4 m [10]	Ortho-rectified by Chris Sharples
15th Dec 1988	1124-116 / *Windowpane_Dec1988_MGA55.tif/tfw*	1000 dpi (2039 dpi) / 1.1 m pixel size	1:42,000	1.8 m [10]	Ortho-rectified by Chris Sharples
8th Jan 1998	1283-144 / *Windowpane_Jan1998_MGA55.tif/tfw*	1000 dpi (2039 dpi) / 1.1 m pixel size	1:42,000	1.5 m [10]	Ortho-rectified by Chris Sharples
25th Jan 2005	1391-62 / *Windowpane_Jan2005_MGA55.ecw*	2039 dpi / 0.5 m pixel size	1: 42,000	1.4 m [10] (residual error; corrected for systematic 5.0m NW offset) (quoted absolute accuracy ±15 m)	Ortho-rectified by DPIPWE Original DPIPWE ortho file: 1391_062_op.ecw Ortho-photo has systematic 5.0m NW offset from reference 2015 ortho in Window Pane Bay area (corrected in digitised shoreline by offsetting it 5.0m to the SW, and in feature position errors by measuring reference feature positions with respect to reference image *after* offsetting each feature 5.0m SW).
5th Nov 2010	1449-142 / *Windowpane_Nov2010_MGA55.ecw*	2039 dpi / 0.3 m pixel size	1: 24,000	0.9 m [10] (quoted absolute accuracy ±10 m)	Ortho-rectified by DPIPWE Original DPIPWE ortho file: 1449_142_op.ecw
22nd Dec 2015	Original DPIPWE digital ortho file: *24265A_Window_Pane_Bay_Dec2015.ecw* / *Windowpane_Dec2015_MGA55.ecw*	- / 0.1 m pixel size	-	0.0 m [n/a] (quoted absolute accuracy ±0.5m)	Digital original photo; ortho-rectified by DPIPWE REFERENCE IMAGE (zero relative feature position error by convention)

Table 34: Digitised shoreline shapefiles produced for Window Pane Bay (using ortho-photos listed in Table 33 above).

Date of air photo(s)	Shapefile	Shoreline digitised by	Comments
17th Jan 1948	WindowPane_MGA55_19480117.shp	Chris Sharples (2018)	Coarse res, good contrast, veg line distinct, descriptions as for Dec 2015.
18th Mar 1961	WindowPane_MGA55_19610318.shp	Chris Sharples (2018)	Coarse res, poor contrast but long shadows allowed for; descriptions as for Dec 2015.
19th Feb 1973	WindowPane_MGA55_19730219.shp	Chris Sharples (2018)	West part of beach/dune only, low accuracy but worth using; descriptions as for Dec 2015.
15th April 1975	WindowPane_MGA55_19750415.shp	Chris Sharples (2018)	Coarse resolution, veg. line distinct, long shadows allowed for, descriptions as for Dec 2015.
12th Dec 1979	WindowPane_MGA55_19791212.shp	Chris Sharples (2018)	Moderate resolution, veg line distinct, descriptions as for Dec 2015.
22nd Mar 1984	WindowPane_MGA55_19840322.shp	Chris Sharples (2018)	Long (afternoon) shadows allowed for, moderate resolution, veg line distinct, descriptions as for Dec 2015.
8th Mar 1988	WindowPane_MGA55_19880308.shp	Chris Sharples (2018)	Shadows allowed for, veg line distinct, description as for Dec 2015
15th Dec 1988	WindowPane_MGA55_19881215.shp	Chris Sharples (2018)	Low res.; shadows allowed for, veg line distinct, description as for Dec 2015
8th Jan 1998	WindowPane_MGA55_19980108.shp	Chris Sharples (2018)	Veg line distinct but resolution coarse; description as for Dec 2015
25th Jan 2005	WindowPane_MGA55_20050125.shp	Chris Sharples (2018)	Veg. line distinct and description as for Dec 2015. WHOLE DIGITISED SHORELINE SHIFTED 5.0 m to SW to correct systematic ortho error (see ortho note above).
5th Nov 2010	WindowPane_MGA55_20101105.shp	Chris Sharples (2018)	Veg line distinct and description as for Dec 2015. Shadowing allowed for.
22nd Dec 2015	WindowPane_MGA55_20151222.shp	Chris Sharples (2018)	Margin of stable soil/veg mapped as veg line; includes dune slump-face head scarps and deflation gully margins. Large (mobile) vegetation rafts on dune slump face not mapped.

			Shadowing allowed for.

Notes:

1. The "vegetation line" is all cases is the margin of the undisturbed *in situ* soil + living vegetation cover. Vegetation lines mapped at Window Pane Bay include at least three sub-types:
    a. Wave-exposed vegetation lines behind sand or cobble/boulder beach.
    b. Vegetation line at head of slumping dune scarps ('slump head line')
    c. 'Deflation margin': aeolian deflation gully and unvegetated mobile sand dune margins.

    These three types are attributed accordingly for this beach's shoreline shapefiles. In all cases, the vegetation line mapped is the margin of *stable* soil/vegetation areas. For the purposes of the shoreline change analysis the deflation margins have been ignored and the 'wave-exposed vegetation lines' and 'slump head scarp' combined as the shoreline proxy.
2. Edges of large mobile vegetation rafts on slumping dune faces are *not* mapped as the vegetation line (two such rafts have moved down the main high slump face since 1948, one of which was still present and moving as at 2015).

TASMARC shore profile data tables

Table 35: GPS-surveyed co-ordinates of each TASMARC transect survey mark at Window Pane Bay. The survey marks are located at the landwards end of each transect, which runs seawards normal to the shoreline from each mark. Latitude and Longitude are decimal degrees and eastings and northings are metric co-ordinates in the Map Grid of Australia Zone 55 (MGA55, GDA94 datum).

Transect	Longitude	Latitude	Easting	Northing
730/310	146.0204907	-43.45873701	420758.111	5187775.265
730/311	TASMARC database gives same co-ords as 730/310 (one is wrong)	TASMARC database gives same co-ords as 730/310 (one is wrong)	421430.705	5187303.594
730/312	146.0298627	-43.46443837	421523.679	5187150.956

Table 36: Table of hinge points defined for each surveyed Window Pane Bay profile (derived from original TASMARC survey data).

TASMARC profile number	Survey date	Hinge point distance offshore from survey mark (metres)	Hinge point height above AHD (metres)
730/310	03/12/2014	103.464	3.846
730/310	01/12/2015	105.508	3.531
730/310	09/12/2016	105.523	3.584
730/311	03/12/2014	38.870	3.366
730/311	01/12/2015	37.993	4.064
730/311	09/12/2016	38.114	3.863
730/312	03/12/2014	24.378	4.704
730/312	01/12/2015	24.366	4.765
730/312	09/12/2016	24.323	4.759

A1.3.5 Stephens Bay Beach (south-west coast)

Locality and general description

Stephens Bay beach is a high energy sandy beach directly exposed to the south-westerly swells a few kilometres south of the entrance to Port Davey (Figure 140). The beach was visited by Chris Sharples during December 2014, 2015 and 2016 during a DPIPWE-funded helicopter-based project to establish and survey TASMARC beach profile transects. There have been no notable artificial beach or dune disturbances during the Twentieth Century to present period apart from a walking track which reaches the beach through the dunes at the northern end of the beach. However, an extensive Aboriginal midden has been exposed by dune deflation behind the southern part of the beach. Introduced dune-colonising weeds capable of modifying beach and dune behaviour – such as marram grass *Ammophila arenaria* - have not established at Stephens Bay.

Note that for the purposes of the analyses in Chapters 5 & 6 of this thesis, Stephens Bay Beach has been treated as two sites having distinctly different behaviours, name Stephens Bay Beach North (northern half of beach with minimal transgressive dune development) and Stephens Bay Beach South (central to southern area dominated by deflation, transgressive dune development and eventual foredune development). The southern 3 transects (as shown on Figure 148) at this beach have been ignored in the analyses.

Geomorphology and process environment

Geomorphic description

Geomorphic aspects of the beach have previously been described by Baynes (1990), Cullen (1998) and (Short 2006b).

Stephens Bay beach mostly faces southwest (aspect 240º True) and although strongly exposed to the south-westerly swells is located within a rocky embayment 2.3 km wide bounded by prominent rocky headlands. The beach is Transverse Bar and Rip (TBR) to Rhythmic Bar and Beach (RBB) morphodynamic type (Short 2006b) fronted by a 200m wide surf zone with several strong rips. The beach is backed by dunes ranging from about 6 metres high behind the north-western end of the beach up to about 50m high behind its southern end. With an exception described below, these dunes are mostly an old (Late Pleistocene or Holocene) transgressive dune complex with dominantly WNW to ESE oriented ridges (Cullen 1998) which has been wave-scarped on its seawards side, and are not foredunes in the sense of Hesp (2002). At the time of inspections (Dec 2014, 2015 and 2016) the seawards face of the dunes was mostly bare of living vegetation except behind the north-western end of the beach. However fresh wave erosion scarps were not apparent in the dune toes, and the bare dune faces were evidently partly slumped. There was little evidence of the accumulation of new incipient dunes at the toe of the bare dune faces, although a high sand berm abutting the dunes was apparent along much of the back of the beach. It is evident that the bare dune faces are deflating, with fresh lobes of windblown sand accumulating in the lee of the seaward dune crest. Although the backshore parts of the dune complex are mainly stable and vegetated behind the northern half of the beach, the degree of dune face deflation and the extent of currently actively mobile transgressive dunes blowing inland from the seawards dune faces in a south-easterly direction increases southwards along the beach. This difference is inferred to a be result of increasingly direct exposure to the dominant local wind direction towards the south end of the beach (see also below). Very extensive unvegetated and currently active transgressive dunes behind the southern half of the beach extend well over one kilometre south-eastwards and extend almost through to nearby Noyhener Beach (Figure 140) in part. At least one palaeosol is exposed in both the deflating seawards faces of the dunes and in deflation hollows within the active backshore transgressive dune complex (Figure 143). Behind the southern part of the beach the wind erosion (deflation) has also exposed extensive middens, as well as exposures of iron pans and peat deposits at the base of the dunes which may

represent earlier swamp deposits that were buried beneath the transgressive dunes as they initially formed.

A low established (vegetated) foredune a few metres high and about 400 metres long is present on the seawards side of the high deflating transgressive dunes behind the southern part of the beach (Figure 140, Figure 141). This feature exhibits a recently active wave erosion scarp on its seawards side, which exposes anthropogenic debris (plastics, wooden planks) in the foredune, supporting the historic air photo evidence (below) that this dune is of Late Twentieth Century age and origin. Further north in the middle (most wave exposed?) part of the bay, large beach scarps were observed in the high beach berm during field visits, although this scarping did not extend into the toe of the backing dune face itself (Figure 142).

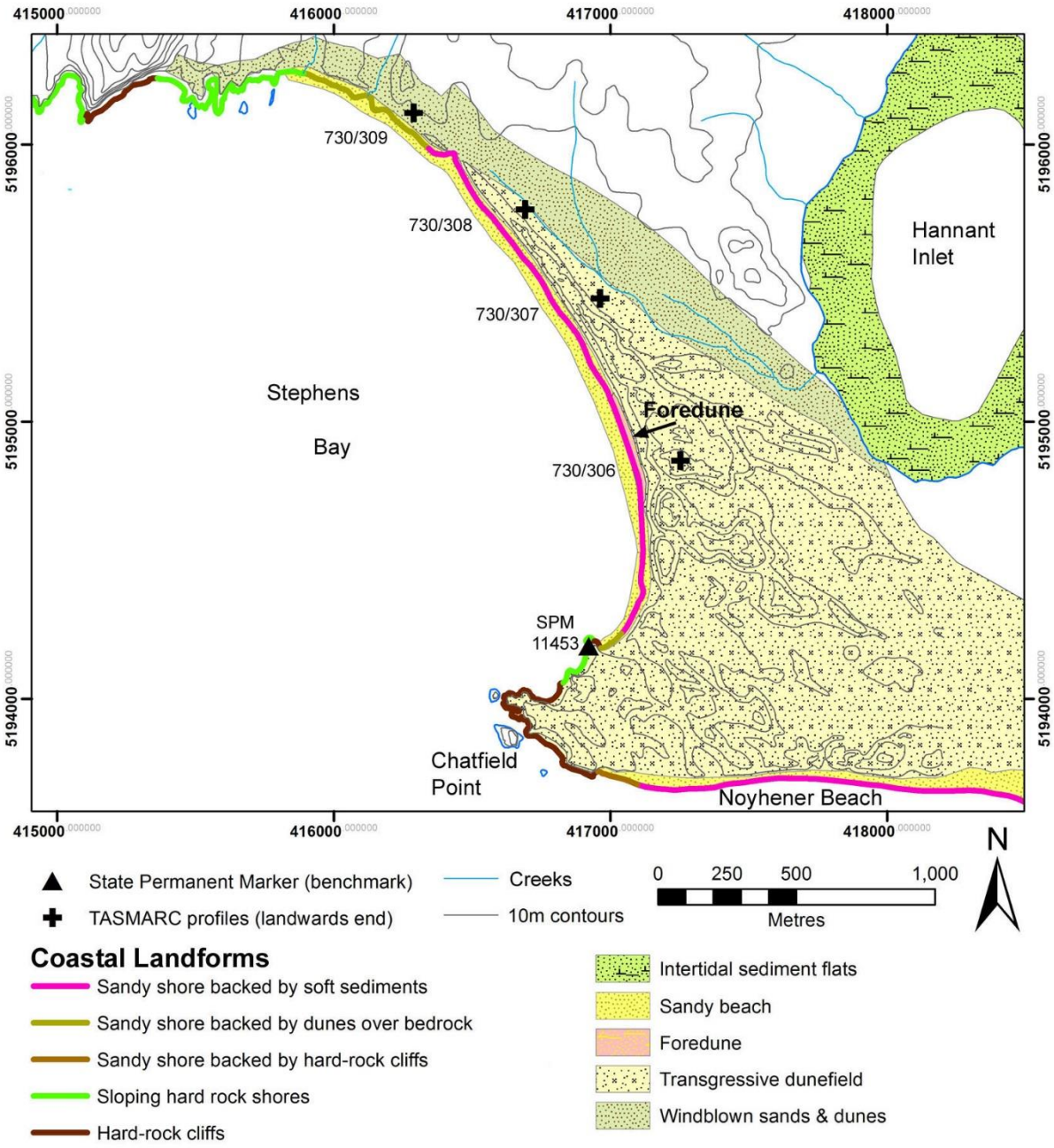

Figure 140: Coastal landforms at Stephens Bay; landform mapping is based on Cullen (1998), with additional geomorphic mapping by C. Sharples. Permanent survey benchmark (SPM) and TASMARC survey profile locations and numbers are indicated. Co-ordinate system is Map Grid of Australia Zone 55 (GDA1994 datum).

Figure 141: Northwards view along the recently wave-scarped foredune behind the southern part of Stephens Bay beach, showing strongly deflating high transgressive dunes behind. Photo by C. Sharples (2014).

Figure 142: View south from the middle part of Stephens Bay beach, showing a recent beach scarp cutting into the high beach berm below the deflating dune face. High deflating transgressive dunes fronted by the small vegetated foredune are visible in the distance towards the southern end of the beach. Photo by C. Sharples (2014).

Figure 143: A part of the high actively mobile transgressive dune complex behind the southern half of Stephens Bay, showing a palaeosol exposed in a deflation hollow on the dune crest. Photo by C. Sharples (2014).

Figure 144: View of the southern end of Stephens Bay showing the high bare deflating seawards side of an older transgressive dune with skeletons of former shrub cover still close to *in situ*, and the more recently accreted and vegetated foredune visible below. The dead shrubs were a living dune cover in the 1948 air photo, at which time the foredune did not exist. Photo by C. Sharples (2015).

Exposed palaeosols in the seawards dune faces behind most of Stephens Bay beach implies that those dune faces are currently more receded than at any time since the palaeosols formed, however their ongoing exposure seems to be mainly the result of wind erosion (deflation) of the dune faces removing sand landwards, rather than wave erosion removing sand offshore. Although it is likely that wave erosion has at some time triggered onset of dune deflation by exposing the seawards faces of the dunes, the presence of a large beach berm in front of the dunes along much of the beach together with the historic air evidence (below) suggests that significant wave erosion of the seawards dune faces has not occurred since at least prior to 1948. The exception to this is the small eroding foredune in front of the deflating dunes in the southern part of the beach, whose presence is itself indicative of a lack of wave erosion having reached the deflating dunes behind it for some decades at least. Whether – or when – wave erosion will cause significant shoreline recession at this beach is unclear, and ongoing monitoring of beach-dune profiles at Stephens Bay will be important in understanding how this beach is behaving and whether it is beginning to respond to sea-level rise.

Swell wave climate

Stephens Bay receives a persistent south-westerly swell generated by Southern Ocean winds strongly correlated with the Southern Annular Mode (Hemer, Church & Hunter 2010; Hemer, Simmonds & Keay 2008). Swell wave parameters for Stephens Bay are given below.

Table 37: Key swell wave climate parameters for Stephens Bay, from the Bureau of Meteorology Australia and CSIRO Australia CAWCR wave hindcast 1979-2010 (Durrant et al. 2013). These figures apply to the closest inshore ~5km grid cell to the beach.

	Annual	Summer (DJF)	Winter (JJA)
Average Significant wave height (m)	3.04	2.67	3.26
Average Maximum wave height (m)	6.32	5.61	6.73
Average Mean Wave direction (ºT)	242	240	245

The mean swell wave directions approaching Stephens Bay vary within about a 5º range and are close to directly onshore in the centre of the bay, hence are likely to generate only weak alongshore sand drifts in the nearshore zone, which probably vary frequently in alongshore direction resulting in little net alongshore sand drift within the bay from this cause (however see below).

Wind (wind-wave) climate

Maatsuyker Island weather station, 38 kilometres south-east of Stephens Bay, provides the nearest long-term (1957 – present) Australian Bureau of Meteorology wind record for a coastal site exposed to similar westerly SAM-dominated ocean fetch directions. Wind direction data from Maatsuyker Island is plotted in Figure 145 (below)and in view of the similar exposure is likely to be broadly representative of winds at Stephen Bay itself. This inference is supported by the strong similarity between the dominant north-westerly wind directions at Maatsuyker Island and the dominant direction of windblown sand propagation at Stephens Bay since 1948 (see Figure 147), albeit some differences due to local sheltering effects (e.g., at the northern end of Stephens Bay) are likely.

If north-westerly winds are dominant at Stephens Bay as they are at Maatsuyker Island, this has implications for both wind erosion and sand deposition processes, and for alongshore sand drift in the littoral zone. Whereas the swell wave climate is likely to drive relatively weak and frequently reversing alongshore sand drift within the bay (see above), in contrast locally-generated north-westerly wind-waves will drive dominantly south-directed alongshore sand drifts along the beach towards the southern end of the bay. Although the south end of the beach is not significantly wider than the northern half as might be expected from a dominantly unidirectional sand drift (see Figure 146), this is inferred to be a result of much of the sand delivered to the south end of the bay being subsequently moved inland by wind transport in the active transgressive dunes behind that end of the beach. The dominant southwards littoral drift of sand is probably also a factor in the growth of a new

foredune in the southern half of the beach since 1980 despite simultaneous ongoing landwards sand loss (see air photo history below).

As already noted the marked and ongoing expansion of south-easterly directed bare mobile transgressive dunes behind the southern half of the bay – and negligible development of active transgressive dunes behind the northern half of the bay – is consistent with the aspect of the southern half of the bay being directly towards the dominant north-westerly wind direction while the northern half of the beach is essentially parallel to and thus minimally exposed to the dominant winds.

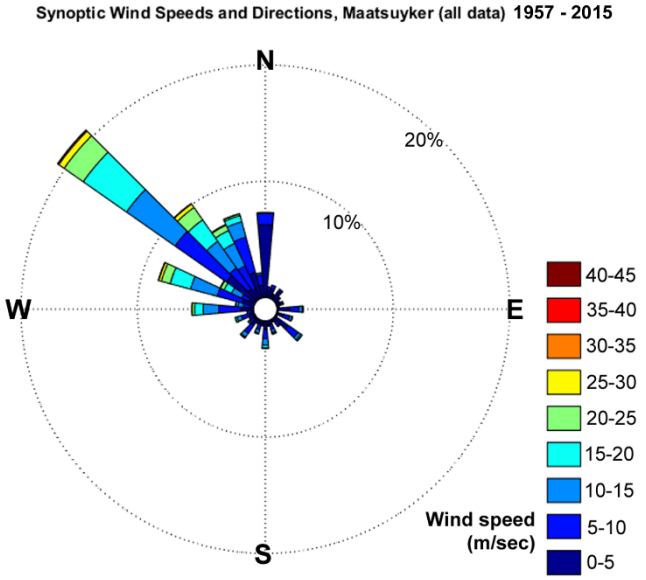

Figure 145: Wind directions for Maatsuyker Island, 38 km south-east of Stephens Bay. The figure was prepared in Matlab™ using all synoptic wind records for Maatsuyker Island from 1957 to 2015. Original data supplied by the Australian Bureau of Meteorology (2016).

Analysis of the Maatsuyker Island wind record by Kirkpatrick et al. (2017) indicated increased mean wind speeds in recent decades, at least in winter. Given the likelihood that this is also true for winds at Stephens Bay, some increases in both aeolian sand deflation and locally generated wind wave energies could be expected there in recent decades.

Sand transport and budget

Shelf sediment mobility modelling suggests that some swell-driven sand may be moving onshore from the continental shelf into Stephens Bay (Harris & Heap 2014; Harris et al. 2000). Although there is no empirical data on this it does appear to be the only available explanation for observed sand budget processes at the beach, particularly the growth of a new foredune concurrently with the loss of large quantities of sand to landwards in mobile transgressive dunes.

Stephens Bay is embayed between prominent rocky headlands oriented such that both swell and locally generated wind waves (see below) would be unlikely to move sediment alongshore into or out of the bay by littoral drift. The beach is sufficiently embayed that sand moved offshore during storms is unlikely to escape the bay alongshore and is probably mostly returned to the beach by fair-weather swells. However, field evidence and the air photo time series since 1948 (below) demonstrate that landwards deflation of seawards dune fronts has been ongoing throughout that period and has increased in the southern (more wind-exposed) part of the bay, where major extension of bare mobile transgressive dunes south-eastwards has also occurred over the whole period and is continuing. Although some of the deflated sand is probably reaching Noyhener Beach, most or all of it is being lost inland from Stephens Bay for the foreseeable future. This aeolian process is the only sand loss (sink) process known to be active at Stephens Bay.

No other sand sources or sinks are known to be active at Stephens Bay, and considering the beach and dune changes since 1948 (described below) it is likely that Stephens Bay has a balanced or even slightly gaining sand budget, with onshore sand gains from the shelf sufficiently exceeding landwards sand loss in mobile dunes as to allow the late Twentieth Century growth of a new foredune behind the southern half of the beach.

Air photo analysis

Ortho-rectified air photos of the Stephens Bay beach from 13 dates between 1948 and 2015 (see Table 38) were used to map and characterise the shoreline and dune change history of Stephens Bay over that period. An air photo for one additional date (1973) was not used due to poor ortho-rectification error margins but was close in time to the 1975 photo which was used.

The *in situ* (living) vegetation line was mapped as the shoreline feature which moves landwards or seawards as a shoreline recedes or progrades respectively. In most cases at Stephens Bay this comprised the scarped vegetation line at the top of bare slumped and deflating seawards dune faces, however in a few areas (most notably the recent foredune that has developed along the south half of the beach) it is the wave-exposed vegetation line at the seawards toe of the dune face. Extensive vegetation lines bounding deflation areas and mobile transgressive dunes behind Stephens Bay were not mapped as "shoreline". Their history from the air photo time series is also noted below.

Shore behaviour history from air photos

Visual inspection of the historic air photo time series and shoreline movement history plots (Figure 147 and Figure 148) demonstrate two main areas of the beach and backing dunes which have behaved in significantly different ways over the air photo period (1948 – 2015), namely the northern half of the beach (bare, slumped and deflating but persistent dune face with only minor deflation gullies and transgressive mobile dunes), and most of the southern half of the beach (high deflating dune faces fronted by a recently accreted low foredune and backed by extensive bare mobile transgressive dunes which have extended considerably to the south-east over the air photo period). Based on information from the air photo time series, the 1948-2015 geomorphic history of these two areas is described below.

1. *Mainly bare, scarped and deflating but persistent dune-face:* This mainly comprises the northern half of the beach and dunes (transects 23372-23388 excluding 23380 which was dominated by a creek outflow), however the southern-most end of the beach (transects 23360-62) also comprises dunes having similar character and history (see transect cluster plots on Figure 148). These two groups were initially considered together and Figure 149 is a plot summarising the shoreline movement history along all these transects over the air photo period. However, the southern 3 transects have subsequently been dis-regarded in the analyses described in Chapter 6.

   The northern half of the beach comprising most of the transects is directly exposed to the south-westerly swell but the backing dune faces are oriented roughly parallel to the dominant north-westerly wind direction and thus have relatively limited wind-exposure (see Figure 145). The summary plot of the air photo history (Figure 149) demonstrates an overall shoreline recession trend between 1948 and 2015 which is well beyond air photo error margins and yields a good Pearson correlation co-efficient of $R^2 = 0.5035$, thus is undoubtedly real. However, the summary plot also demonstrates that most of this recession occurred between 1948 and 1961, with subsequent shoreline recession being much slower and - since it is mostly within air photo error margins - possibly negligible. Nonetheless, inspection of air photos over the 1961 to 2015 period also shows that the seawards dune faces (seawards of the shoreline vegetation line as defined) have remained bare and deflating over that period, while their horizontal position has been stable or nearly so (i.e., 'persistent').

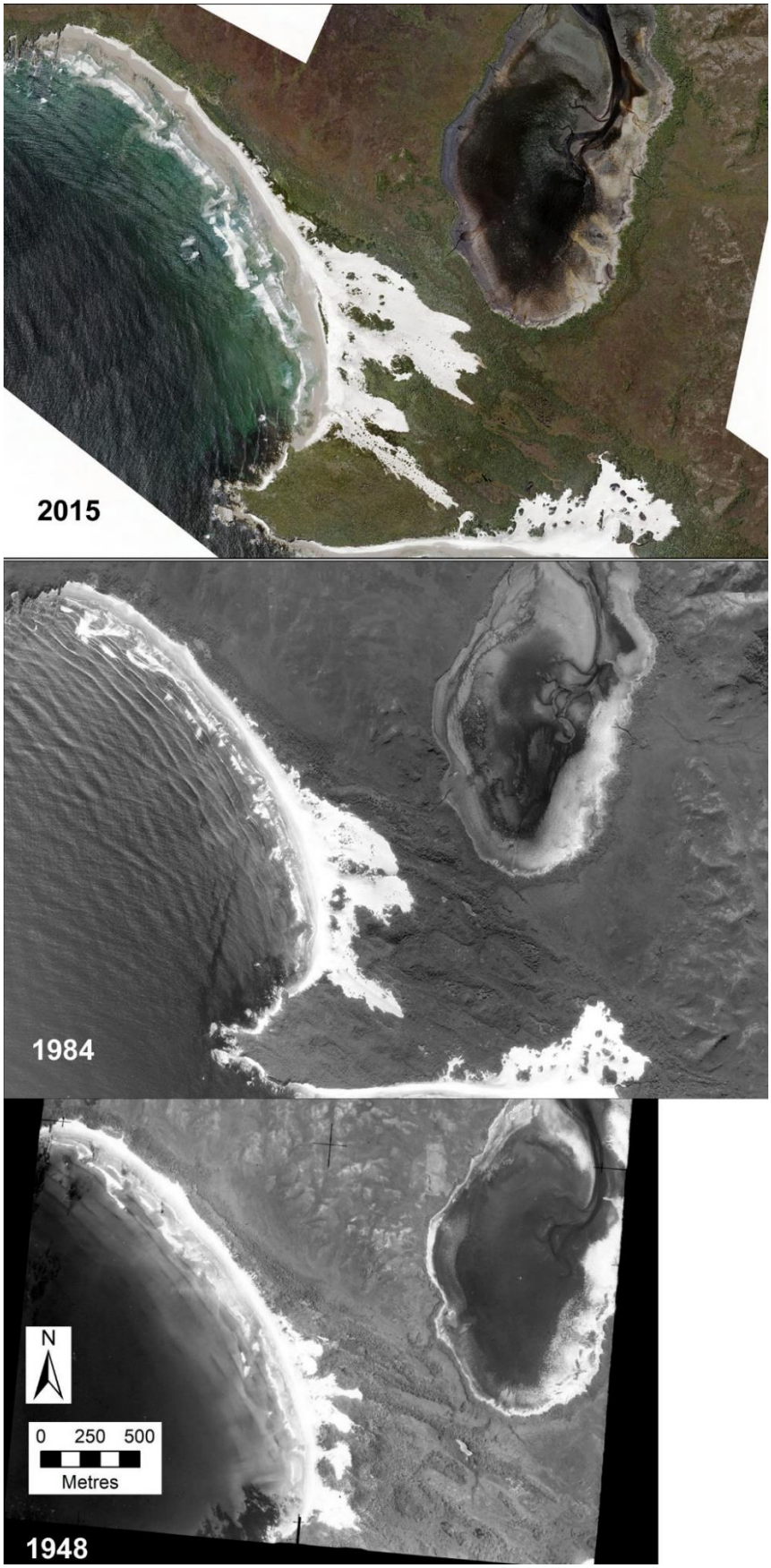

Figure 146: Comparison of ortho-rectified air photos of Stephens Bay in 1948, 1984 and 2015.

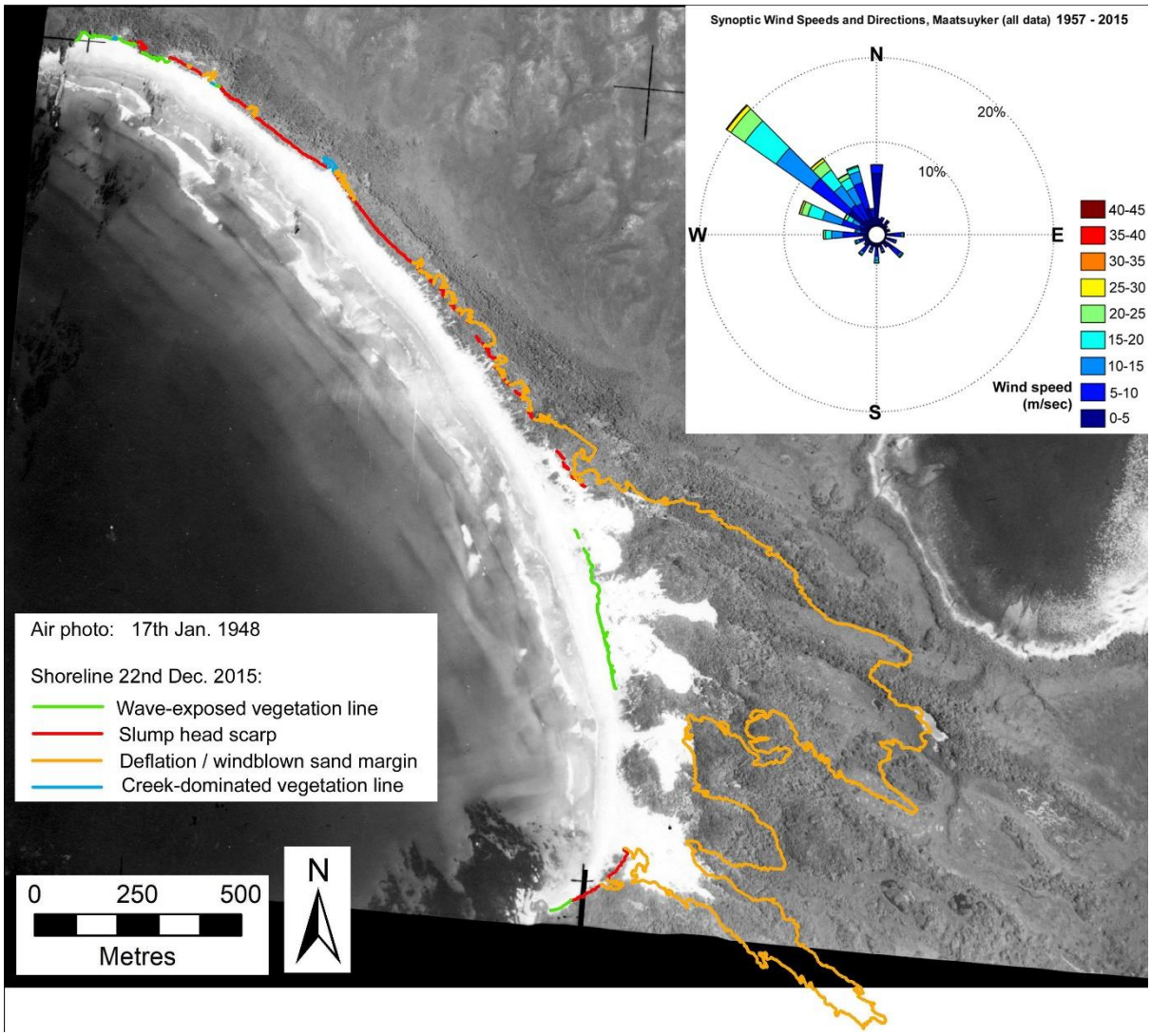

Figure 147: Comparison of shoreline positions at Stephens Bay from the earliest (1948) air photo (ortho-rectified) and the 2015 shoreline proxies and other features digitised from the 2015 ortho-photo. Comparison with the Maatsuyker Island wind direction data (top RH) demonstrates a strong similarity between the dominant wind directions at Maatsuyker and the direction of mobile sand propagation at Stephens Bay between 1948 and 2015. This implies Stephens Bay is subject to a similar wind climate as Maatsuyker, which is likely given the two locations are only 38 km apart and exposed to the same SAM-dominated ocean environment over similar westerly ocean fetches.

The overall history for this section of Stephens Bay appears to comprise an early phase of notable shoreline recession (possibly in response to a major storm event prior to 1948 which exposed the dune face paleosols and triggered dune face deflation?), followed by a marked reduction in shoreline recession rates by 1961, with only slow or possibly nil shoreline recession since. Dune face deflation has evidently continued, but with limited exposure of the dune faces to the dominant north-westerly wind there has been only limited landwards loss of dune face sand with only minor expansion of deflation gullies and transgressive dunes (see Figure 146 & Figure 147). It is likely that the limited landwards loss of sand has been fully compensated for by continuing swell-driven onshore supply of sand from the shelf. Large upper beach berms in this section (Figure 142) are indicative of an adequate sand supply to keep the beach stable despite landwards aeolian losses and net southwards alongshore drift of sand.

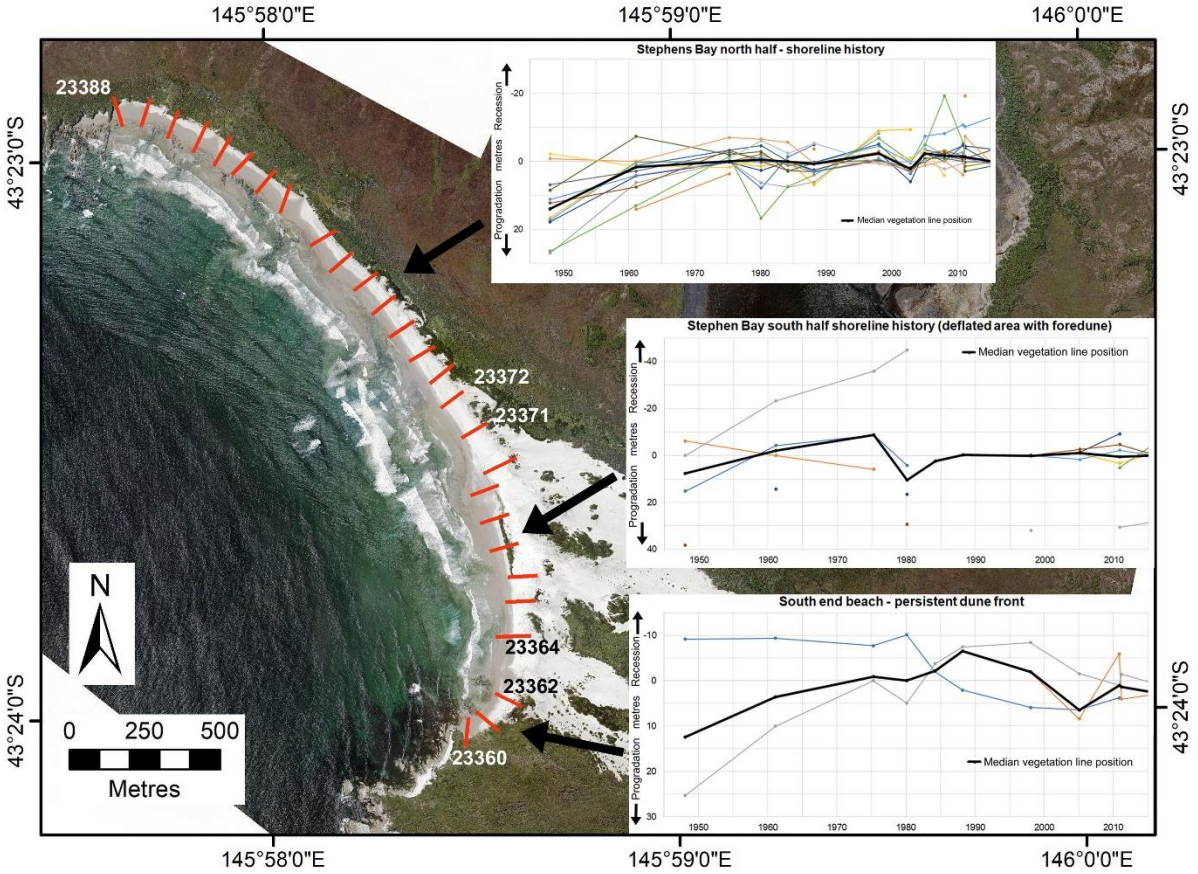

Figure 148: Plots of shoreline position at Stephens Bay over the period 1948 – 2015 along each 100m-spaced digital transect used at Stephens Bay, plotted relative to the median shoreline position on each transect. Shoreline positions are defined as seawards vegetation lines excluding creek-dominated and deflation hollow or windblown sand vegetation margins. Transect locations used are indicated by red lines on the air photo, and each coloured line on the plots represents shoreline position changes over time along one transect. The transect shoreline position histories are plotted in three broadly distinctive groups between the numbered transects as indicated, with the median shoreline history across each group shown by a heavy line. The background image is the 2015 air photo (© DPIPWE).

2. *Persistent southern high deflating dune faces with mobile transgressive dunes actively extending to landwards and a recently accreted frontal foredune to seawards:* The shoreline movement plots produced from the air photo time series for the southern half of Stephens Bay are very fragmentary (see Figure 148) due to extensive blown out areas with only short shoreline vegetation line sections (as defined for this work) in existence at most air photos dates. The interpretation of the beach and dune geomorphic history for this area from 1948 to 2015 is therefore essentially qualitative and based on visual inspection and comparison of the 13 air photos (see examples at Figure 146).

   The southern half of Stephens Bay is highly exposed to the dominant south-westerly swell wave climate (see above), and importantly is also directly exposed to the probable dominant local wind direction, in contrast to the less exposed northern half of the bay described above. In 1948 the high seawards dune faces backing the southern half of the bay exhibited large areas of bare wind-exposed sand and were cut by deflation gullies. These were backed by bare mobile transgressive sand dunes which were less extensive than seen in all subsequent air photos (Figure 147). The 1948 air photo also shows the seawards dune faces still had some patches of living vegetation (Figure 147), which today remain present *in situ* but only as dead skeletons (Figure 144). In the

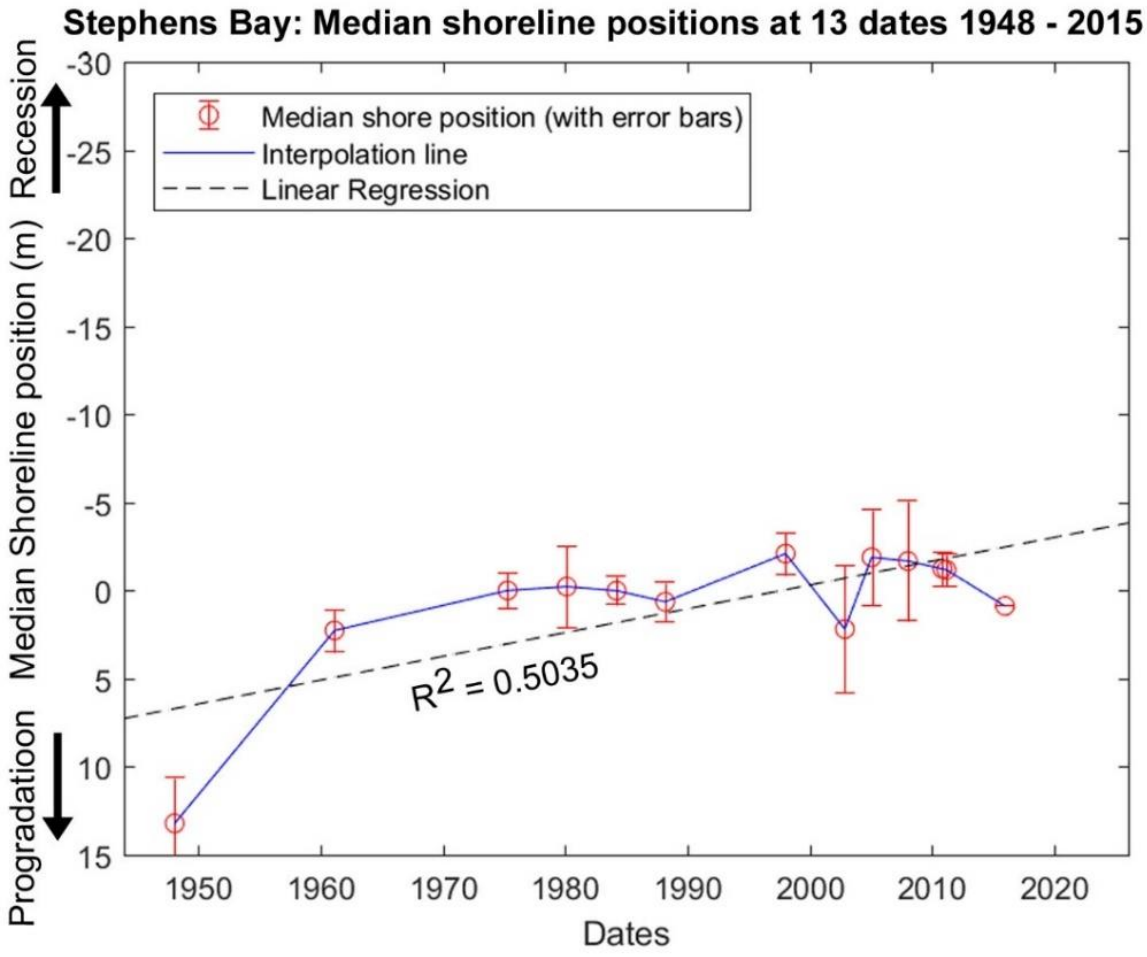

Figure 149: Summary median shoreline position history plot combining all transects used for the Stephens Bay sections backed by bare deflating but persistent dune faces. This plot combines data from the north half transects (23372 – 23388 excluding 23380) and the 3 southernmost transects (23360-23362) which cover similar features (vegetation line at crest of high slumped and deflating but persistent dune faces) with broadly similar shoreline movement histories as indicated by grouped plots on Figure 148. *Note these figures should be redone without the 3 southern transects (not really useful to include them).* Transects in the very differently behaved extensively deflated and mobile southern half of Stephens Bay (transects 23364-23371) as shown on Figure 148 are not included in this summary figure. This figure shows shore positions at each air photo date with air photo position error bars and interpolation lines and linear fit (linear regression). For comparison purposes the Y-axis scale (shoreline position) is the same as for all other beach history plots in this project, emphasising the comparatively small horizontal shoreline movement detected over the air photo period for Stephens Bay.

light of the subsequent rates of transgressive dune expansion (see Figure 146), it can be inferred that the observed dune mobility probably began not very long before the 1948 photo date. The most likely triggering mechanism would have been a large storm wave erosion event causing slumping of the dune front and exposure of bare sand to wind erosion. In 1948 there was no (true) foredune at the back of the beach in this area, and the fact one subsequently developed (below) suggests that the lack of one in 1948 is further evidence of a major erosion event not long before.

From 1948 to 2015 (and continuing) there was progressive expansion (or transgression) of deflation gullies and bare mobile transgressive dunes from the bare seawards dune faces in a south-easterly direction, reaching to about 800 – 900 metres inland by 2015 and continuing at the time of writing (see Figure 143, Figure 146, Figure 147). The areas of bare sand on the seawards dune faces increased (due to vegetation deaths) after 1948 (see Figure 144), but no attempt has

been made to identify any changes in the rate and volume of sand movement in the transgressive dunes. However it is particularly noteworthy that despite the major increase in the extent of active transgressive dunes moving inland since 1948 (and the volume of sand moving inland which this implies), the position of the high seawards dune front has nonetheless persisted with little or no horizontal recession, as indicated by the continued *in situ* presence of many shrub skeletons that covered the dune face as living shrubs in 1948 (Figure 144). This implies most of the sand blowing inland is not being eroded out of the seawards dune face, but rather is being supplied from the beach face and simply blown over the dune faces and onwards inland.

The other important change in the southern half of Stephens Bay during the air photo period is the appearance and growth of a substantial foredune *sensu stricto* (Hesp 2002) at the back of the beach and to seawards of the high bare dune faces discussed above. This feature was not present in the earliest air photos and is first apparent as a short sparsely vegetated incipient foredune in the 1984 air photo, after which later air photos depict it growing progressively longer (along the beach back) and wider up to 2015. Field observations in 2014, 2015 and 2016 showed a recent wave-eroded scarp at the front of the foredune (Figure 141), however there is so far no air photo or beach profile (see below) evidence of a foredune recession trend. Future observations will be necessary to determine whether the dune has ceased growing or is still accreting with some "cut and fill" cycle interruptions.

NOTE: The vegetation line shoreline proxy works poorly for south half of beach owing to very extensive blow-outs. Thus, no summary plot for South half has been produced, transect plot Figure 148 is of dubious value, and visual comparison of air photos is best source of info to reconstruct history. Plots for the North half make more sense and are more reliable.

Surveyed shore profile analysis (TASMARC)

Four TASMARC beach profile survey marks were established at Stephens Bay during December 2014 as part of a DPIPWE World Heritage Area monitoring project managed by Rolan Eberhard in collaboration with the TASMARC Project (Eberhard et al. 2015). One profile (730/306) samples the recent foredune and its high eroded backing transgressive dune face and bare mobile sand areas characteristic of the southern half of Stephens Bay (see above). The other three profiles (730/307,308,309) sample the high dunes with bare but persistent seawards faces characteristic of the northern half of Stephens Bay (see Figure 140 and Table 40). Each profile was measured from a survey mark inland of the seawards dune, over that dune and as far down the beach-face as practical on each occasion. The profiles were surveyed at annual intervals during November-December 2014, 2015 and 2016 by Nick Bowden and Paul Boland, with assistance from Rolan Eberhard, Michael Comfort, Chris Sharples and others.

The results of the three surveys are plotted on Figure 150 to Figure 153 below in two forms, namely as profile plots and hinge point plots. These are further explained in Chapter 3 Section 3.3.2, but in brief profile plots depict the surveyed shoreline in profile, whereas hinge-point plots summarise the survey data by plotting the vertical and horizontal movement over time of the intersection between the top (back) of the beach and the base (front) of the dune face. In this way the hinge point plots show both the horizontal movement of the dune front (toe) and the vertical movement of the (back) beach face over time.

The original processed survey data for each profile plot (provided as figures below) is available on the TASMARC website (www.tasmarc.info) and is not reproduced here. The hinge point data has been derived from the original profile data and is provided at Table 41 below.

Shoreline behaviour history from profile surveys

The beach and dune changes exhibited on the TASMARC profile lines over the period 2014-2016 are summarised here for the same southern and northern sections of Stephens Bay whose distinctive landform behaviour histories were summarised above from a 1948-2015 air photo time series:

1. *Southern half of Stephens Bay (TASMARC profile 730/306)* The small foredune immediately backing the beach-face has shown no discernible change over the three year period (as demonstrated by the hinge point movement plot (Figure 150) which represents the seawards toe of the small erosion scarp fronting this foredune (seen in Figure 141). This implies that the foredune face is probably not actively receding, however recovery of the dune face (by accretion of windblown beach sand) has been negligible during the 2014 – 2016 period.

   The high bare deflating dune face behind the foredune has shown some progressive horizontal retreat (of the order of a few metres) of its lower slopes over the 3-year period (profile plot Figure 150). However, the higher slopes have not receded and may have accreted sand deflated from the lower slopes. Given the longer-term history of stable persistence or only very slow recession of the position of this and adjacent bare seawards dune slopes since 1948 (see air photo discussion above), the recession observed in the TASMARC profiles could conceivably represent a recent onset or acceleration of dune retreat or may simply be part of a cyclic dune face deflation and accretion process. Given the longer-term history and the fact that only three years of apparent recession has yet been observed, a recent commencement of a new long-term recession trend cannot be demonstrated.

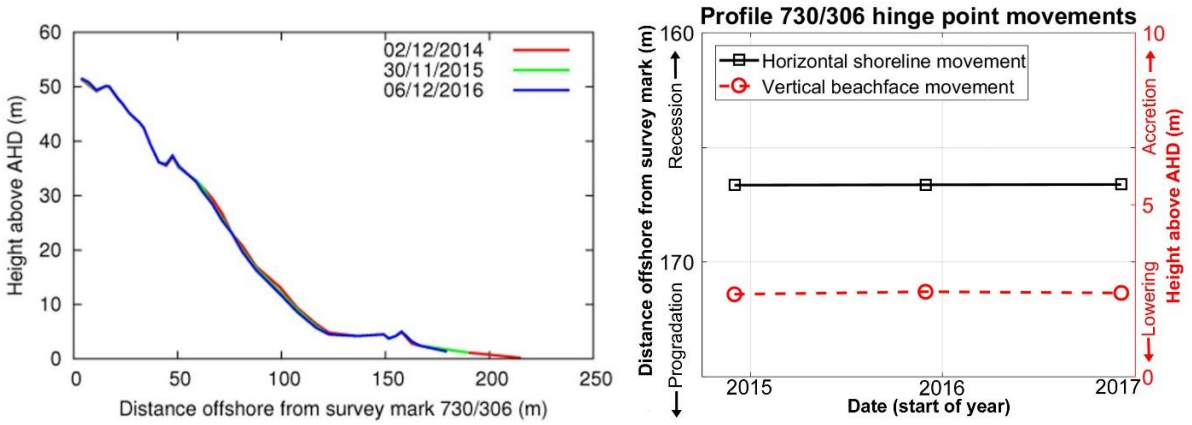

Figure 150: All surveys on TASMARC profile 730/306 to date. This is in the southern area of high bare deflating dune faces (profiled), with a recently-developed low frontal foredune to seawards (profiled) and extensive expanding mobile sand field to landwards (not profiled): see Figure 148. Presented as profile plots (LHS) and hinge point movement plots (RHS). The hinge point is the toe of the seawards side of the low foredune (representing the hinge between beach face and dune system) at about 166m from the survey mark.

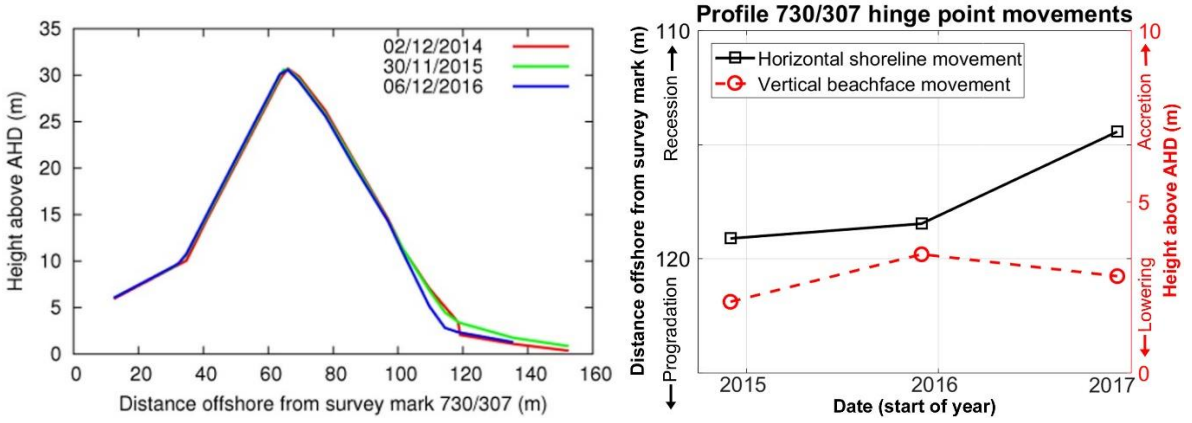

Figure 151: All surveys on TASMARC profile 730/307 to date. This is in the northern area of bare deflating but persistent (little-changing) dunes. Presented as profile plots (LHS) and hinge point movement plots (RHS). The hinge point is the clearly defined hinge between the toe of the seawards dune face and the back edge of the beach face at about 118m from the survey mark.

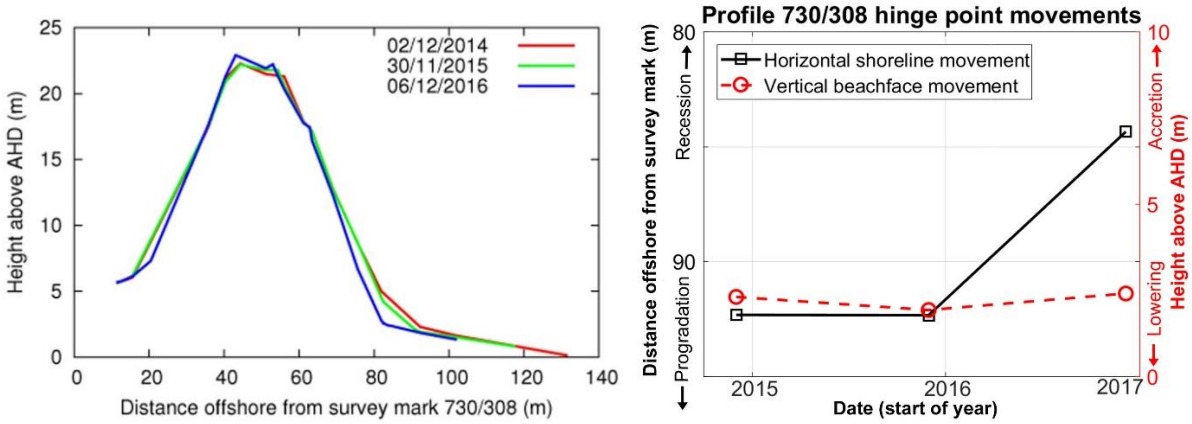

Figure 152: All surveys on TASMARC profile 730/308 to date. This is in the northern area of bare deflating but persistent (little-changing) dunes. Presented as profile plots (LHS) and hinge point movement plots (RHS). The hinge point is the clearly defined hinge between the toe of the seawards dune face and the back edge of the beach face at about 80 - 90m from the survey mark.

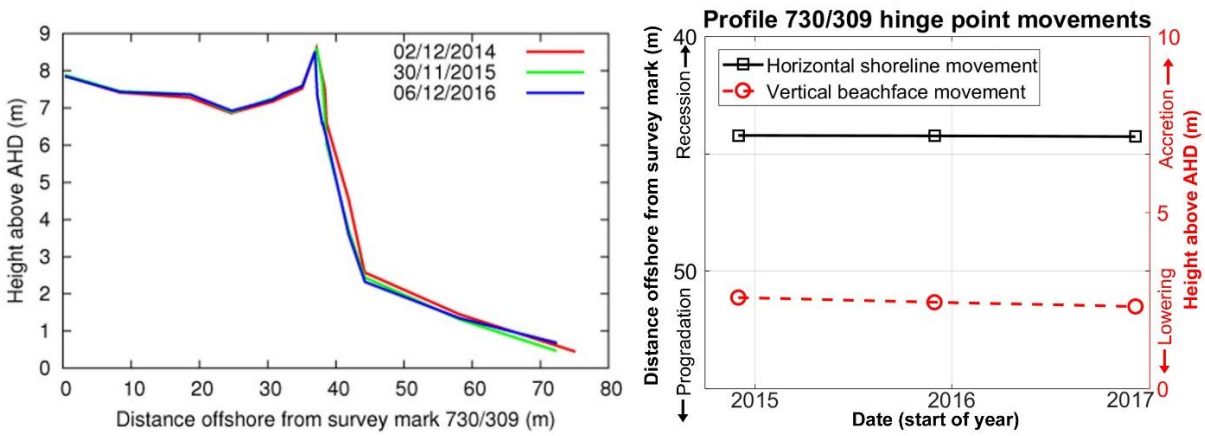

Figure 153: All surveys on TASMARC profile 730/309 to date. This is in the northern area of bare deflating but persistent (little-changing) dunes. Presented as profile plots (LHS) and hinge point movement plots (RHS). The hinge point is the clearly defined hinge between the toe of the seawards dune face and the back edge of the beach face at about 44m from the survey mark.

2. *Northern half of Stephens Bay (TASMARC profiles 730/307, 730/308, 730/309)* Over the three years of TASMARC data collection the three profiles distributed along the northern half of Stephens Bay all demonstrate both beach and seawards dune-face movements of the order of a few metres vertically and horizontally (see Figure 151 to Figure 153). On profiles 730/308 and 730/309 the observed changes comprise a lowering of the upper beach face and retreat of the lower seawards dune face, most probably in response to wave erosion of the upper beach (evident in Figure 142) and associated erosion and slumping of the dune toe. However, whilst behaving similarly, profile 730/307 does also show some recovery (sand accretion) on the upper beach face between 2014 and 2015.

   Given the longer-term history of stable persistence or only very slow recession of this and adjacent bare seawards dune slopes since 1961 (see air photo discussion above including Figure 149), the recession and beach lowering observed in the TASMARC profiles could conceivably represent a recent onset or acceleration of dune retreat. However, given the observed beach accretion on one of the profiles (730/307) it is likely the observed behaviour is simply part of a cyclic dune face deflation and accretion process. Given the longer-term history of stable dune face persistence and the fact that only three years of apparent recession has yet been observed, a recent commencement of a new long-term recession trend cannot be demonstrated.

   Profile 730/308 also notably shows some recession of the upper seawards dune face accompanied by accretion of sand on the dune crest over the three-year period. Based on field observations this is a result of wind deflation of the upper dune face with the sand being blown over the dune crest and deposited just in its lee. This is notable since it demonstrates the process of dune-face deflation and landwards movement of blown sand which is inferred to be an important process in beach and dune behaviour at Stephens Bay.

Summary shoreline behaviour history and characterisation

The Stephens Bay beach and dune system shows evidence of a likely major storm-wave erosion event prior to 1948 followed by a brief phase of dune-face recession which ended or slowed to a negligible rate prior to 1961. Despite this the seawards dune faces have remained bare, slumped and deflating from 1948 until at least 2016, with sand being blown inland from the deflating dune faces at rates varying from slow in the northern (less wind-exposed) part of the bay to much faster in the southern half of the bay which is most directly exposed to the dominant onshore wind direction. Continuous and ongoing expansion of bare mobile transgressive dunes to nearly a kilometre south-east of the southern half of the beach between 1948 and 2016 is indicative of large amounts of sand being lost inland from the beach and dune-face, and this is the main sand sink identified for Stephens Bay. The fact that this has occurred with only negligible dune-face retreat since before 1961 implies that more sand is continuing to be supplied to the beach from offshore by swell-driven transport, as is expected from Geoscience Australia shelf sand mobility modelling (Harris & Heap 2014; Harris et al. 2000). This sand must be moved up the beach by swash and onshore winds (forming large upper-beach berms), then be blown up and over the seawards dune face and into the backshore area. The fact that much larger quantities of sand have blown inland from the southern half of the beach since 1948 is a result of the greater exposure of that end of the beach to the dominant onshore wind direction, but is probably compensated for by the southern end of the beach receiving not only sand supplied from directly offshore but also sand supplied to the north end of the bay and then drifted southwards by the inferred dominant net alongshore drift within the bay. This greater supply of sand to the south half of the bay has not only permitted greater landwards loss of deflated sand to occur without notable retreat of the bare seawards dune faces but has also been sufficient as to allow the accretion of a new foredune at the back of the beach from 1984 to the present.

The 3-year TASMARC beach profile record (2014-2016) demonstrates some beach- and dune-face erosion, but also some sand accretion. Taken together with the air photo record of beach and dune behaviour since 1948 there is no evidence of a recent onset or acceleration of a long-term shoreline recession trend, with only very slow or negligible recession evident since 1961, and the erosion seen in the recent TASMARC record being indistinguishable from normal cyclic beach and dune erosion and accretion processes.

It is noteworthy that earlier Holocene (?) phases of south-eastwards transgressive dune mobility are evident as extensive vegetated inland dune ridges extending beyond but comparable to the presently active transgressive dune ridges which are they are progressively being engulfing by. These are clearly seen on air photos and were mapped by Cullen (1998) as stabilised Holocene transgressive and longitudinal dunes. The high deflating seawards dune faces behind Stephens Bay are the eroded seawards ends of these older dunes.

The evidence of at least one earlier phase of transgressive dune expansion behind Stephens Bay, which evidently ended with a phase of dune stabilisation and revegetation prior to the current phase of dune mobility, is suggestive that the present phase of bare deflating and transgressive dunes is an episodic phenomenon which has occurred before and is not necessarily related to sea-level rise. The evidence described in this chapter is suggestive of phases of dune mobility, each perhaps triggered by major wave erosion events removing dune face vegetation and exposing dune sands to wind erosion (deflation). A phase of bare mobile transgressive dune expansion follows, with re-vegetation of exposed dune faces inhibited by the very high energy wind climate of the south-west Tasmanian coast. The dunes may take decades or possibly centuries to stabilise but dune vegetation cover eventually returns, possibly in response to decadal-scale variations in wind climate or precipitation. The coastal dune system may then remain stable until another destabilising event such as a major storm triggers another phase of transgressive dune activity.

Recent climate change factors including sea-level rise and increasing wind speed are additional new process factors affecting Stephens Bay. It is possible that increasing wind speeds in recent decades may be accelerating the ongoing mobile dune activity at Stephens Bay, but no attempt has been made to test this hypothesis. In respect of sea-level rise, it is expected that most beaches will eventually respond with an onset or acceleration of landwards shoreline recession, however there is no evidence of this having yet commenced at Stephens Bay whose balanced or possibly gaining sand budget is probably making it a late responder to sea-level rise.

Air Photo Data Tables

The following tables provide details of the air photos used, the resulting ortho-photos produced, and the shapefiles representing the shoreline position that were digitised from the ortho-photos.

Table 38: Original air photos and ortho-rectified air-photos produced for Stephens Bay beach.

Photo Date	**Original DPIPWE air photos (film-frame) / Ortho-photo name**	**Final image resolution (original scan resolution if downsized) / pixel size of final ortho-photo**	**Original photo scale**	**Mean measured feature position error for ortho-photo (± metres)** [No. of measured feature position reference points]	**Comments**
17th Jan 1948	159-577 / *StephensBay_Jan1948_MGA55.tif/tfw*	600 dpi / 0.8 m pixel size	1:15,840	2.6 m [10] (one very anomalous large error (16.0m) distant from the beach omitted)	Ortho-rectified by Chris Sharples
16th Feb 1961	361-83 / *StephensBay_Feb1961_MGA55.tif/tfw*	2039 dpi / 0.5 m pixel size	1:35,640	1.2 m [11]	Ortho-rectified by Chris Sharples
19th Feb 1973	624-6 / *StephensBay_Feb1973_MGA55.tif/tfw*	2039 dpi / 0.4 m pixel size	1:30,000	7.5 m [11]	Ortho-rectified by Chris Sharples Poor accuracy – not used
15th Apr 1975	678-41 / *StephensBay_Apr1975_MGA55.tif/tfw*	2039 dpi / 0.7 m pixel size	1:40,000	1.0 m [11]	Ortho-rectified by Chris Sharples
14th Feb 1980	817-86 / *StephensBay_Feb1980_MGA55.tif/tfw*	2039 dpi / 0.6 m pixel size	1:45,000	2.3 m [11]	Ortho-rectified by Chris Sharples
10th Mar 1984	994-149 / *StephensBay_Mar1984_MGA55.tif/tfw*	2039 dpi / 0.55 m pixel size	1:42,000	0.8 m [11]	Ortho-rectified by Chris Sharples
8th Mar 1988	1114-25 / *StephensBay_Mar1988_MGA55.tif/tfw*	1000 dpi (2039 dpi) / 0.74 m pixel size	1:25,000	1.1 m [11]	Ortho-rectified by Chris Sharples
8th Jan 1998	1283-177 / *StephensBay_Jan1998_MGA55.tif/tfw*	1000 dpi (2039 dpi) / 1.1 m pixel size	1:42,000	1.2 m [11]	Ortho-rectified by Chris Sharples
16th Nov 2002	1360-216 / *StephensBay_Nov2002_MGA55.ecw*	2039 dpi / 1.0 m pixel size	1:42,000	3.6 m [7] (quoted absolute accuracy ±15m)	Ortho-rectified by DPIPWE Northern half of beach only Original DPIPWE ortho file: 1360_216_op.ecw

25th Jan 2005	1391-42 / *StephensBay_Jan2005_MGA55.ecw*	2039 dpi / 0.5 m pixel size	1:42,000	2.7 m [11] (quoted absolute accuracy ±15m)	Ortho-rectified by DPIPWE Original DPIPWE ortho file: 1391_042_op.ecw
10th Jan 2008	1429-196 / *StephensBay_Jan2008_MGA55.ecw*	2039 dpi / 0.5 m pixel size	1:42,000	3.4 m [7] (quoted absolute accuracy ±15 m)	Ortho-rectified by DPIPWE Northern half of beach only Original DPIPWE ortho file: 1429_196_op.ecw
5th Nov 2010	1449-170 / *StephensBay_Nov2010_MGA55.ecw*	2039 dpi / 0.3 m pixel size	1: 24,000	0.96 m [7] (quoted absolute accuracy ±10 m)	Ortho-rectified by DPIPWE Original DPIPWE ortho file: 1449_170_op.ecw
7th Mar 2011	1456-164 1456-165 1456-172 / *StephensBay_Mar2011a_MGA55.tif/tfw; StephensBay_Mar2011b_MGA55.tif/tfw; StephensBay_Mar2011c_MGA55.tif/tfw*	1000 dpi (2039 dpi) / 0.15 m pixel size	1:5,000	0.9 m [7]	Ortho-rectified by Chris Sharples Large proportion of black pixels produced by ortho-rectifying process (reason unknown) but photo still usable
22nd Dec 2015	Original DPIPWE digital ortho file: *Stephens_Bay_22-12-2015.ecw* / *StephensBay_Dec2015_MGA55.ecw*	- / 0.1 m pixel size	-	0.0 m [n/a] (quoted absolute accuracy ±0.3m)	Digital original photo; ortho-rectified by DPIPWE REFERENCE IMAGE (zero relative feature position error by convention)

Table 39: Digitised shoreline shapefiles produced for Stephens Bay (using ortho-photos listed in Table 38 above).

Date of air photo(s)	Shapefile	Shoreline digitised by	Comments*
17th Jan 1948	StephensBay_MGA55_19480117.shp	Chris Sharples (2018)	Coarse resolution, some easterly shadowing allowed for, veg line clearly defined.
16th Feb 1961	StephensBay_MGA55_19610216.shp	Chris Sharples (2018)	Moderate resolution, shadowing mostly minor but does obscure veg. line at north end beach, otherwise veg line mostly distinct.
19th Feb 1973	StephensBay_MGA55_19730219.shp	Chris Sharples (2018)	Not digitised; poor accuracy ortho.
15th Apr 1975	StephensBay_MGA55_19750415.shp	Chris Sharples (2018)	Moderate resolution, long shadows a problem in parts but allowed for, veg line generally distinct.
14th Feb 1980	StephensBay_MGA55_19800214.shp	Chris Sharples (2018)	Moderate resolution, long shadows a problem in parts but allowed for, veg line generally distinct.
10th Mar 1984	StephensBay_MGA55_19840310.shp	Chris Sharples (2018)	Moderate resolution, long shadows a problem in

			parts but allowed for, veg line generally distinct.
8th Mar 1988	StephensBay_MGA55_19880308.shp	Chris Sharples (2018)	Coarse resolution, shadowing allowed for, vegetation line fairly distinct.
8th Jan 1998	StephensBay_MGA55_19980108.shp	Chris Sharples (2018)	Coarse resolution, shadowing allowed for, vegetation line fairly distinct.
16th Nov 2002	StephensBay_MGA55_20021116.shp	Chris Sharples (2018)	Northern half of beach only, coarse res, not much shadowing, veg line fairly distinct.
25th Jan 2005	StephensBay_MGA55_20050125.shp	Chris Sharples (2018)	Moderate resolution, shadowing allowed for, veg line fairly distinct.
10th Jan 2008	StephensBay_MGA55_20080110.shp	Chris Sharples (2018)	North half of beach only, moderate resolution only, veg. line clearly defined, mostly no significant shadowing.
5th Nov 2010	StephensBay_MGA55_20101105.shp	Chris Sharples (2018)	High resolution, veg. line clearly defined, some shadowing allowed for.
7th Mar 2011	StephensBay_MGA55_20110307.shp	Chris Sharples (2018)	Black pixels partly obscure shoreline – some interpolation through black pixels used. High resolution, veg. line clearly defined, not much shadowing.
22nd Dec 2015	StephensBay_MGA55_20151222.shp	Chris Sharples (2018)	High resolution, veg. line clearly defined, minor shadowing and rocks allowed for.

*NOTE comments applicable to all air photo dates:

- Veg line is partly head scarp of slumped and deflating dune faces (remanent old veg. patches scattered over deflating slump faces ignored).
- Extensive devegetated and deflating seawards fronts of transgressive dunes, deflation gullies and mobile sand lobes are present.
- Northerly shadowing on steep dune faces creates some ambiguity in identifying vegetation line (head-scarp) position on sections of dunes in the northern third of the beach.

TASMARC shore profile data tables

Table 40: GPS-surveyed co-ordinates of each TASMARC transect survey mark at Stephens Bay (see also map Figure 140). The survey marks are located at the landwards end of each transect, which runs seawards normal to the shoreline from each mark. Longitude and Latitude are decimal degrees and eastings and northings are metric co-ordinates of the Map Grid of Australia Zone 55 (MGA55, GDA94 datum).

Transect	Longitude	Latitude	Easting	Northing
730/306	145.9782479	-43.39459028	417253.3194	5194858.192
730/307	145.9747392	-43.38928381	416961.924	5195444.025
730/308	145.9714536	-43.38636146	416691.8087	5195765.295
730/309	145.9665315	-43.38317555	416288.753	5196114.184

Table 41: Table of hinge points defined for each surveyed Stephens Bay profile (derived from original TASMARC survey data).

TASMARC profile number	Survey Date	Hinge Point distance offshore from survey mark	Hinge point height above AHD (metres)
730/306	02/12/2014	166.657	2.386
730/306	30/11/2015	166.643	2.461
730/306	06/12/2016	166.631	2.426
730/307	02/12/2014	119.121	2.069
730/307	30/11/2015	118.475	3.456
730/307	06/12/2016	114.442	2.818
730/308	02/12/2014	92.331	2.302
730/308	30/11/2015	92.344	1.922
730/308	06/12/2016	84.358	2.400
730/309	02/12/2014	44.229	2.578
730/309	30/11/2015	44.247	2.444
730/309	06/12/2016	44.275	2.324

A1.3.6 Wreck Bay Beach (south-west coast)

Locality and general description

Wreck Bay beach is a high energy swell-exposed sandy beach located on the far south-west coast of Tasmania about 16 kilometres north-west of Port Davey. The beach lies in the South-west National Park and Western Tasmania Wilderness World Heritage Area (TWWHA). The only artificial disturbances are several undeveloped campsites near the beach and the derelict steel ship hull (located at the low tide mark) from which the beach name is derived. It is unlikely these have significantly influenced beach and dune geomorphic processes. Although incipient infestations of coastal weeds including the introduced dune-colonising marram grass *Ammophila arenaria* have been found at Wreck Bay these have been removed by regular weed – control works.

Wreck Bay was visited by Chris Sharples (and others) three times during this project, in Nov/Dec 2014, 2015 and 2016, as part of a DPIPWE-funded helicopter-based project to establish and survey TASMARC beach profile survey transects.

Geomorphology and process environment

Geomorphic description

Geomorphic aspects of the beach have previously been investigated and described by Cullen (1998) and by Short (2006b).

Wreck Bay beach is about 1.5 km long facing southwest (aspect 200ºT) and embayed between protruding rocky headlands in a dominantly rocky coast (see Figure 156). The beach has a 250m wide double bar surf zone characterised as a Transverse Bar and Rip (TBR) inner bar with a high energy Rhythmic Bar and Beach (RBB) outer bar by Short (2006b). The intertidal beach face is composed of fine to medium-grained sand with hard quartzite bedrock outcrops sporadically protruding along the full length of the beach and at the base of the backing dune. The north-western third of the beach is dominated by a near-continuous rocky shore platform in the lower intertidal area, and a large rocky point near the middle of the beach divides it into two main compartments.

The beach is backed by partly-vegetated dunes 5 – 20 metres high which appear to mostly overlie bedrock that rises above present sea-level (inferred from the sporadic bedrock outcrops on the beach face and at the base of the dune-front). The central rocky point is also capped by vegetated windblown sand above storm wave swash levels, as is the rocky shore southwards of the southern end of the beach. Apart from minor development of small incipient foredunes (mainly in the more sheltered south-eastern parts of the bay: see Figure 154) and other poorly-defined patchy remnants of beach-derived sands blown onto the front of older dunes, the dunes are mostly not foredunes in the sense of Hesp (2002). Rather, they are mainly formerly mobile transgressive and longitudinal dunes inferred to be of Late Holocene age by Cullen (1998), p.70. These are currently partly devegetated exposing bare sand on their seawards faces, but are largely stable and vegetated in the back-dune areas where Cullen's mapping indicates a stable and vegetated but formerly-transgressive dune-field extending some hundreds of metres inland (Figure 154). The dune ridges trend in south-easterly directions but are much less extensive than at nearby Towterer Beach because the south-westerly aspect of Wreck Bay reduces exposure to the dominant (see Figure 156) north-westerly winds. Cullen noted the most extensive dunes occur behind the south-eastern end of the embayment where exposure to north-westerly winds is greatest, and include cliff top dunes above rocky shores beyond the end of the beach (see Figure 154). Cullen reported an auger hole 600m inland of the southern end of the beach encountering the shallow distal end of the windblown sands over river gravels.

During 2014 - 2016 large portions (but not all) of the seawards dune faces or scarps backing the beach were bare of vegetation (see Figure 155). Small fresh lobes of unvegetated windblown sand present immediately behind the crest of some of the dune-front scarps demonstrate those bare scarps are being

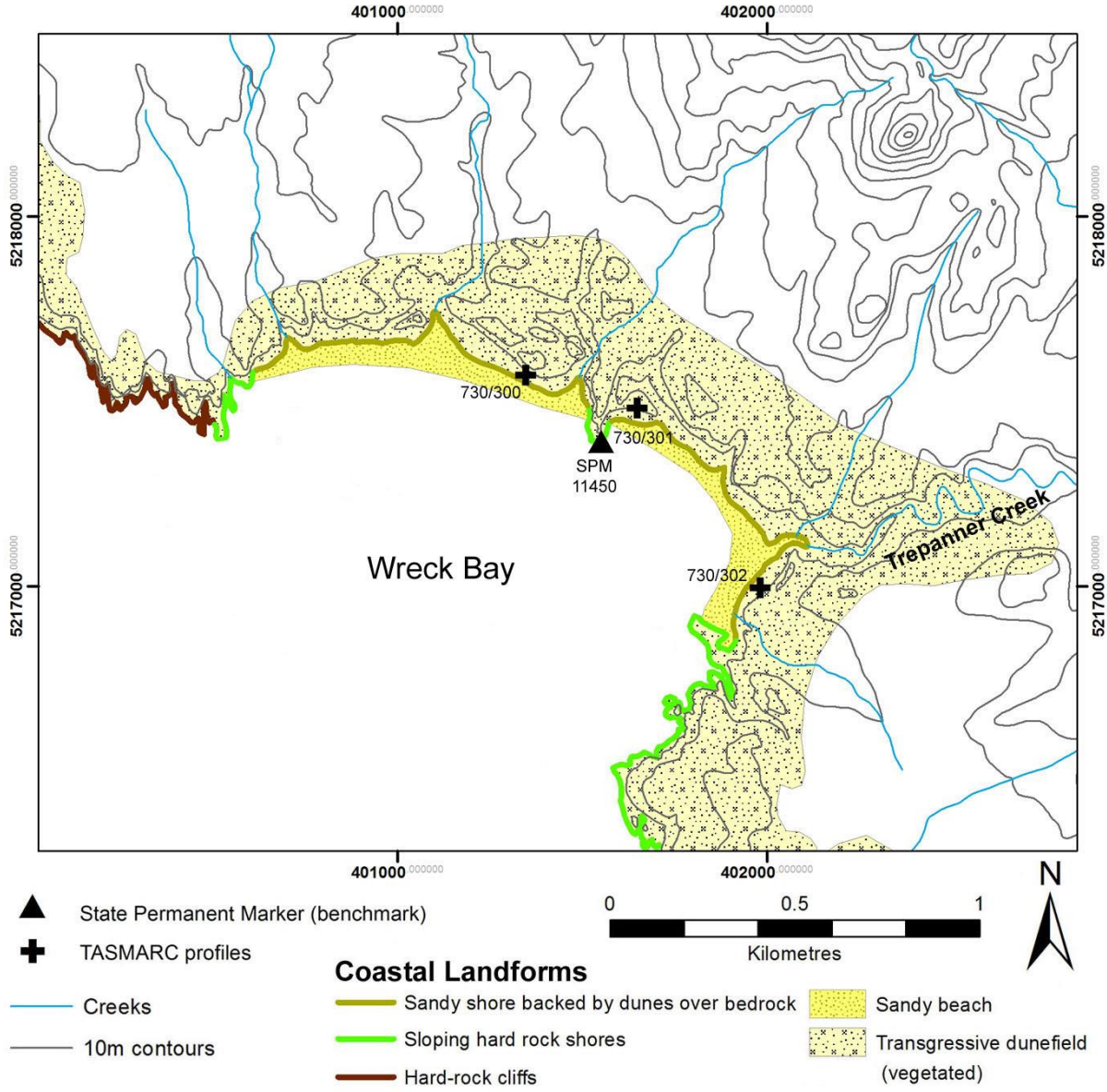

Figure 154: Coastal landforms at Wreck Bay. Coastal landform polygon mapping is based on Cullen (1998), other shoreline landform mapping by C. Sharples. Permanent survey benchmark (SPM) and TASMARC survey profile locations and numbers are indicated. Co-ordinate system is Map Grid of Australia Zone 55 (GDA94 datum).

actively deflated by onshore winds, although the amounts of sand being blown landwards are in most places currently too small to sustain actively mobile bare sand lobes extending more than a few metres landwards of the dune crests. The largest area of deflation hollows and 'sand blows' at Wreck Bay is a relatively small dune-crest region whose area has only slightly increased over the period of air photo records since 1949 (see Figure 157). Cullen (1998), p. 70 noted that active sand blows at Wreck Bay are small compared to other embayments in the region and attributed this to the relatively sheltering from the dominating north-westerly winds afforded by the southwest aspect of the embayment.

Stream discharges from Trepanner Creek in the south-east corner of the bay and from several other creeks along the beach appear to have contributed significantly to beach and dune changes immediately adjacent their mouths.

Figure 155: Aerial view south-eastwards along Wreck Bay beach, showing the prevalence of rocky outcrops on the beach and bare slumped and deflating seawards dune faces. The north-west compartment is closest to the camera, separated by the small rocky point from the distant south-east compartment. Photo by C. Sharples (2014).

Up to three palaeosols (buried soil horizons) are exposed in the scarped bare sand seawards dune faces, which implies that the bare deflating seawards dune faces are currently more receded (eroded to landwards) than at any time since the formation of the oldest exposed palaeosols (notwithstanding that the historical air photo results described below indicate that dune face recession has been very slow to negligible since at least 1949).

Cullen (1998, p. 70-71) illustrates dune soil profiles from Wreck Bay and notes the palaeosols have A-C profiles typical of coastal dunes in the region. Although no absolute dates are available for the palaeosols at Wreck Bay, Cullen infers them to be of equivalent ages to palaeosols at nearby Nye Bay, for which radiocarbon dating of contained charcoal have indicated ages ranging from 700 years BP to less than 200 years BP, with inferred dune ages of less than 1000 years being attributed to probable destruction of earlier dunes prior to 1000 years BP (Pemberton & Cullen 1999).

Swell wave climate

Wreck Bay receives a persistent south-westerly swell generated by Southern Ocean winds strongly correlated with the Southern Annular Mode (Hemer, Church & Hunter 2010; Hemer, Simmonds & Keay 2008). Swell wave parameters for Wreck Bay are given below.

Table 42: Key swell wave climate parameters for Wreck Bay, from the Bureau of Meteorology Australia and CSIRO Australia CAWCR wave hindcast 1979-2010 (Durrant et al. 2013). These figures apply to the closest inshore ~5km grid cell to the beach.

	Annual	Summer (DJF)	Winter (JJA)
Average Significant wave height (m)	3.08	2.70	3.30
Average Maximum wave height (m)	6.40	5.66	6.84
Average Mean wave direction (ºT)	239	238	243

The swell wave directions approaching Wreck Bay should in principle generate a south-eastwards littoral drift current at the beach, moving sand predominantly towards the south-eastern end of both beach compartments within the bay (note also swell wave patterns evident in Figure 156 air photo).

Although wave refraction within the bay probably minimises the magnitude of any littoral drift, inspection of air photos (e.g. see Figure 158) shows wider beaches in the south-east half of each beach compartment, supporting the inference of a south-eastwards littoral drift. The very limited directional variability of the swell (Table 42) is insufficient to cause regular (e.g., inter-annual) reversals of littoral drift within the bay leading to beach rotation, and any episodes of reverse littoral drift within Wreck Bay are probably rare events under unusual wind-wave conditions.

Wind (wind-wave) climate

The nearest long-term wind record for a south-west Tasmanian coastal site with ocean fetch exposures comparable to Wreck Bay is the Maatsuyker Island weather station, 64 kilometres to the south-south-east. A marked difference in active transgressive dune development behind Wreck Bay and nearby Towterer Beach (see Figure 156) is most simply explained by a dominating north-westerly wind direction driving transgressive dune activity at Towterer Beach (which directly faces north-west) but having less effect on Wreck Bay which faces south-west so that north-westerly winds blow along the beach rather than inland. This was also inferred by Cullen (1998). This implies that the recorded Maatsuyker Island wind directions are probably broadly applicable to Wreck Bay, which is a reasonable inference since both locations are exposed to the same Southern Ocean exposure and southwest coast climate.

Although present-day transgressive dune (bare mobile sand) activity is limited at Wreck Bay – probably for the reason noted above - the inferred dominant north-westerly winds do explain the south-eastwards elongation and extension of older now-vegetated transgressive dunes behind Wreck Bay, as previously noted by Cullen (1998). These older dunes may have developed under a stronger wind climate having similar directionality to the present day.

It can also be inferred that the dominantly north-westerly wind directions will generate dominantly north-westerly local wind waves at Wreck Bay, directed mainly south-eastwards along the beach face. These would drive a south-easterly littoral drift of sand along the Wreck Bay beaches, augmenting the likely south-easterly littoral drift generated by the swell (see above) so that any reversals of littoral drift direction at Wreck Bay would only occur under rare conditions of low swell and sub-ordinate wind directions. As noted above, inspection of air photos (e.g. see Figure 158) shows wider beaches in the south-east half of each beach compartment, supporting the inference of a dominantly south-eastwards littoral drift.

Analysis of the Maatsuyker Island wind record by Kirkpatrick et al. (2017) indicated increased mean wind speeds in recent decades, at least in winter. Given the likelihood that this is also true for winds at Wreck Bay, some increases in both aeolian sand deflation and locally generated wind wave energies could be expected there in recent decades.

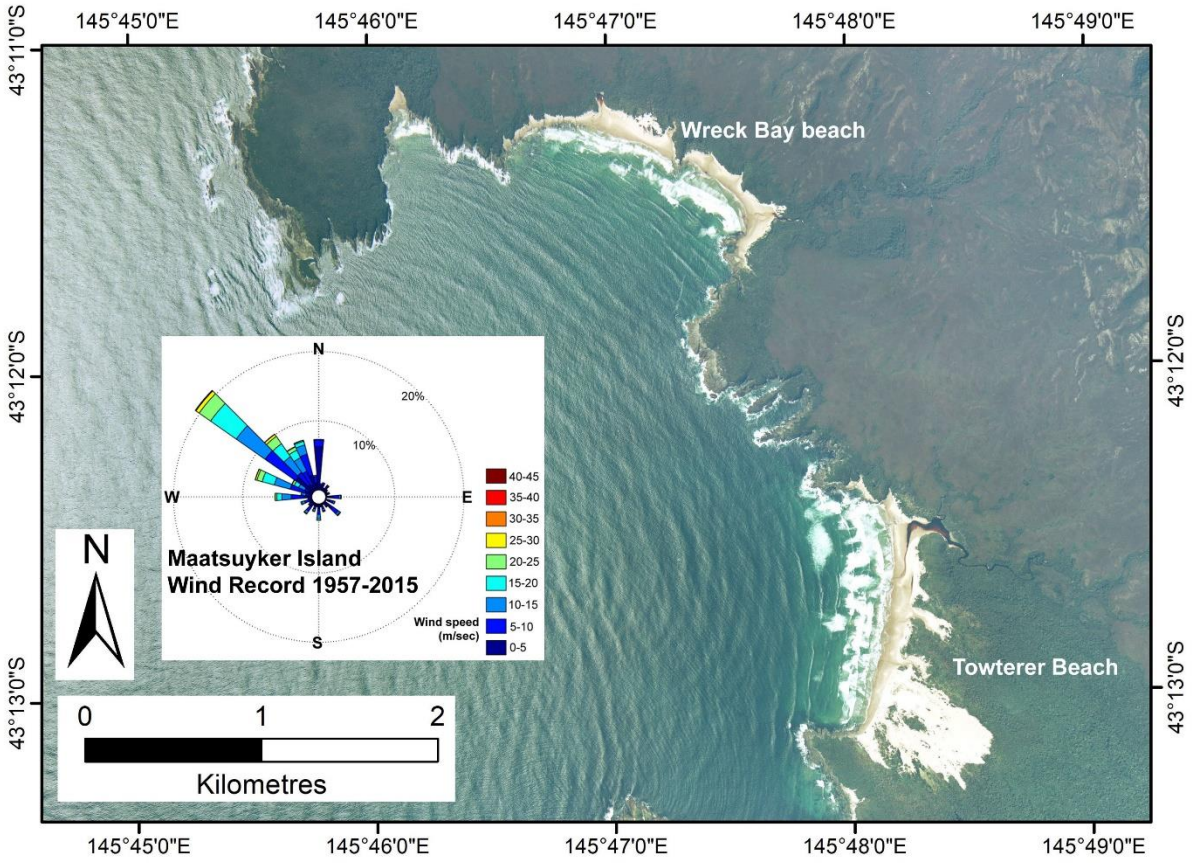

Figure 156: Wind directions for Maatsuyker Island (64 km SSE of Wreck Bay) superimposed on an air photo of Wreck Bay and the adjacent Towterer Beach. The notable development of active transgressive mobile sand dunes at Towterer Beach and relative lack of these at Wreck Bay can be explained in terms of beach orientation and wind exposure if the directional wind climate at Wreck / Towterer is like that measured at Maatsuyker Island. Background air photo image is the Nov. 2002 air photo (© DPIPWE). The wind rose figure was prepared in Matlab™ using all synoptic wind records for Maatsuyker Island from 1957 to 2015. Original data supplied by the Australian Bureau of Meteorology (2016).

Sand transport and budget

Shelf sediment mobility modelling suggests that some sand may still be moving onshore from the continental shelf into Wreck Bay (Harris & Heap 2014; Harris et al. 2000), albeit there is no empirical evidence for this. Given that Wreck Bay is embayed between long rocky headlands facing directly towards the dominant south-westerly swell direction, it is unlikely that significant sand is transported alongshore into or out of the embayment by littoral drift. The beach is sufficiently embayed that sand moved offshore during storms is unlikely to escape the bay and is probably mostly returned to the beach by fair-weather swells. Field evidence (above) and the air photo time series since 1949 (below) indicate that landwards deflation of seawards dune fronts has been an ongoing but relatively minor process over the last 70 years, with little expansion of bare mobile sand deposits in the backshore area implying that landwards aeolian sand transport rates have been insufficient to smother vegetation as occurs under high rates of windblown sand transport.

No other sand sources or sinks (e.g., tidal lagoons) are evident at Wreck Bay, and considering the limited beach and dune changes since 1949 (described below) it is likely that Wreck Bay has a stable (or balanced) sand budget, with likely slow landwards sand loss (by beach and dune deflation) being balanced by slow onshore gains from the shelf.

Air photo analysis

Ortho-rectified vertical air photos of the Wreck Bay beach at 9 dates from 1949 to 2015 (see Table 43) were used to map and characterise the shoreline and dune change history of Wreck Bay over that

period. Ortho-photos for 3 additional dates were not used, in one case (2008) because of poor ortho-rectification accuracies (> ± 4m), and in two other cases (1973 and 1975) because inscrutable difficulties with the ortho-rectification process precluded production of useful ortho-photos.

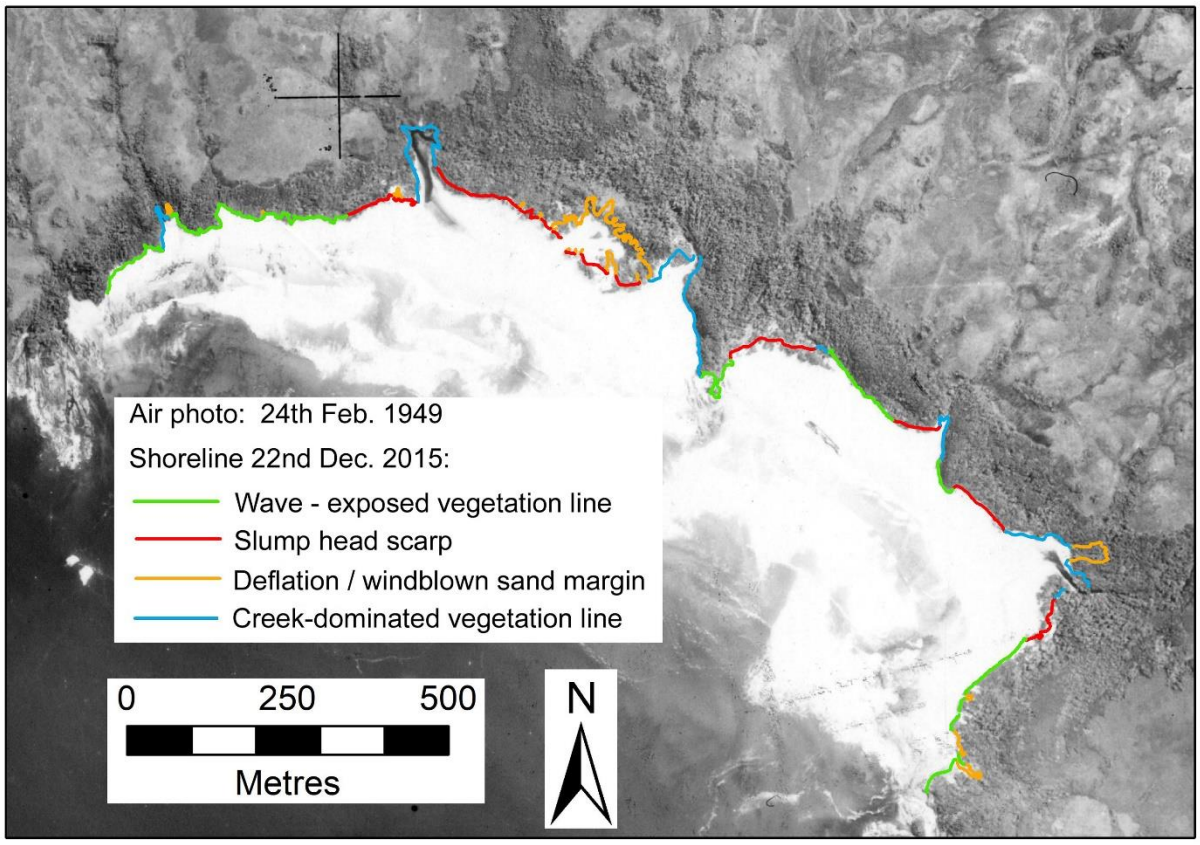

Figure 157: Comparison of shoreline positions at Wreck Bay between 1949 (ortho-rectified photo) and 2015 (shoreline proxy and other features digitised from 2015 ortho-photo). In most areas there has been little net change in the shoreline (vegetation line) position, with the most significant dune face (vegetation line) recession occurring adjacent TASMARC profiles 730/300 and 730/301 (see Figure 154**),** approximately 250 metres north-west and 150 metres east of the central rocky point respectively.

The *in situ* (living) vegetation line was mapped as the shoreline feature which moves landwards or seawards as a shoreline recedes or progrades respectively. In most cases this comprised either the wave-exposed vegetation margin at the seawards toe of the dune face or the scarped vegetation line at the top of bare slumped and deflating dune faces. However, two other vegetation line types were also mapped, namely vegetated dune margins shaped by adjacent creek discharges, and the margins of wind-eroded deflation gullies and transgressive wind-blown mobile sand masses (see Figure 157). These latter features were excluded from the shoreline change plots (below) as their changes are not direct responses to wave attack or sea-level changes.

Based on the ortho-rectified air photos listed in Table 43 and the positions of the included shoreline features specified above that were digitised from these (Table 44), Figure 158 depicts horizontal shoreline movement from 1949 to 2015 along individual digital transects. Several digital transects were not used because they intersected vegetation lines determined by deflation gullies, mobile windblown sand masses or creek discharges; these are not shown on Figure 158. The shoreline histories for each used transect have been plotted in three transect groups on Figure 158 showing the median history for each. The shoreline histories across each of the three groups are similar and mostly coherent albeit of somewhat differing movement scales, hence Figure 159 combines and summarises the shoreline history for the whole of the Wreck Bay beaches by plotting the median shoreline position across all used transects at each air photo date.

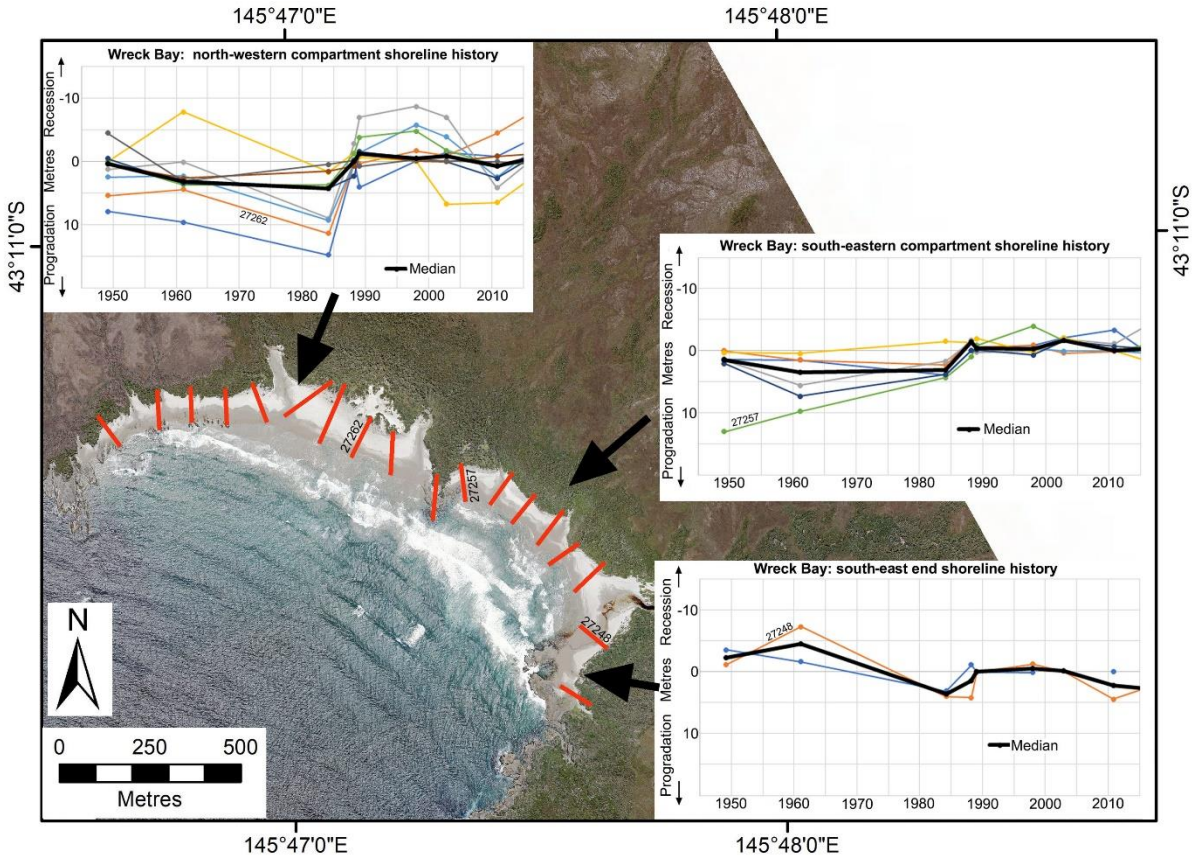

Figure 158: Plots of shoreline (*in situ* vegetation line) movement over the period 1949 to 2015 along each 100m-spaced used digital transect used at Wreck Bay, measured relative to the median shoreline position on each transect. These are plotted in three groups with the median shoreline positions at each date across each group also plotted. The background image is the December 2015 air photo. Transects intersecting only deflated sand gully margins, windblown mobile sand margins, or creek-affected shorelines were not used. Transect locations are indicated by red lines on the air photo, and each coloured line on the plots depicts shoreline position changes over time on one transect. The three transects adjacent the three TASMARC profiling sites (see Figure 154) are numbered on the transect map and the shoreline history plots.

Shore behaviour history from air photos

The following key features of the Wreck Bay beach and dune history are evident from the air photos and derived plots:

1. The shoreline history for Wreck Bay from 1949 to 2015 (Figure 158, Figure 159) shows the shoreline position (as defined above) has been stationary or nearly so over most of the period, with the main variability comprising a small progradation phase between 1961 and 1984 whose scale and error margins are outside subsequent air photo error margins and so probably real. A similar progradation phase between 1975 and 1984 at nearby Mulcahy Bay (see Section A1.3.2) implies that a real (but minor and short-lived) regional shoreline progradation phase did occur at these two beaches (at least) between 1975 and 1984.

   Otherwise, a linear regression fit to the summary shoreline history data (Figure 159) suggests a slight shoreline recession trend over the whole air photo period, however this trend has a low Pearson correlation co-efficient of $R^2 = 0.2215$. Given that the most recent air photo

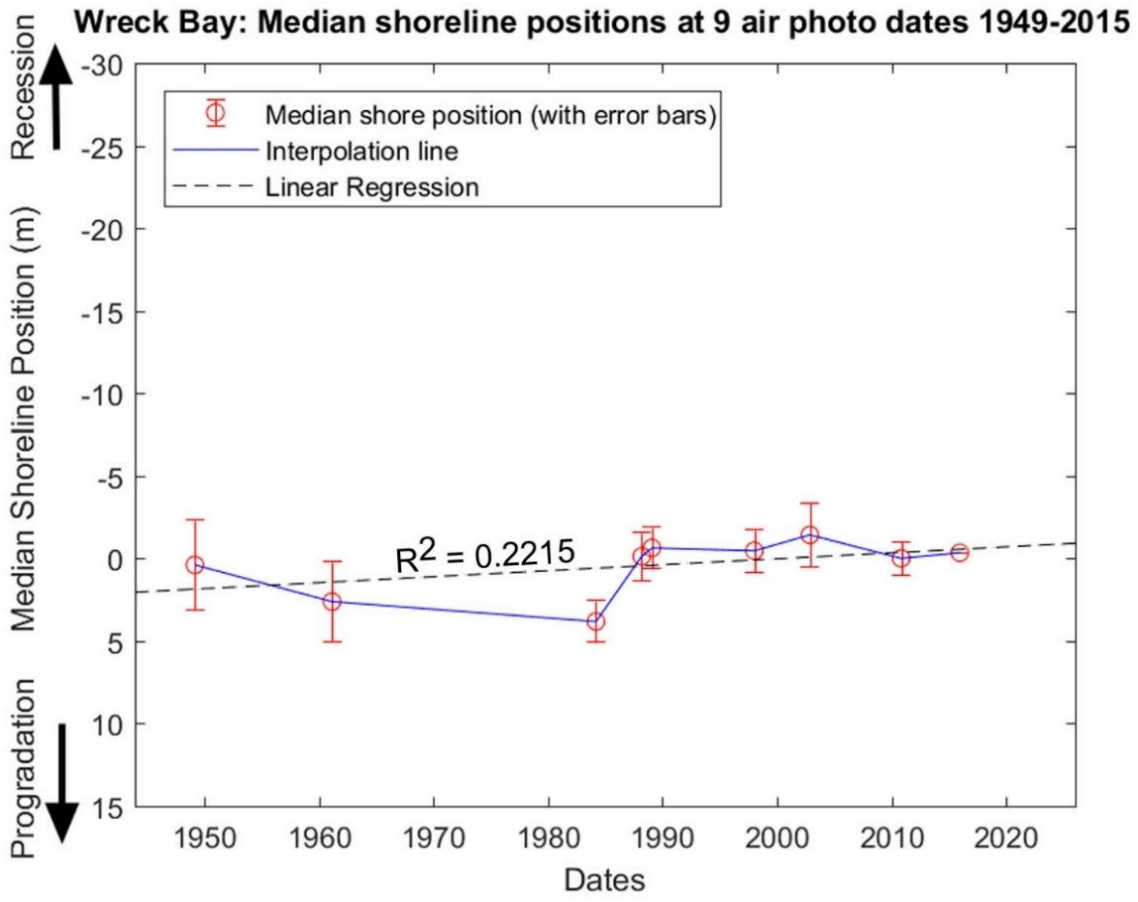

Figure 159: Summary plot of shoreline change history across all used transects (as shown in Figure 158) at Wreck Bay at 9 air photo dates from 1949 to 2015. This plot shows the median of the shoreline positions measured on all used transects (relative to the median position on each transect) at each air photo date. Error bars are the average measured feature position error margins relative to the 2015 air photo. Figure shows shore positions at each air photo date with interpolation lines and linear fit (linear regression). For comparison purposes the Y-axis scale (shoreline position) is the same as for all other beach history plots in this project, emphasising the comparatively small horizontal shoreline movement detected over the air photo period for the Wreck Bay beaches.

shoreline positions lie within the error margins of the earliest positions, and that shore positions since 1988 show no notable change at all, a recession trend cannot be demonstrated and the shoreline position has probably not changed measurably since 1949, apart from the small progradation event noted above.

2. Significant stretches of the seawards dune face at Wreck Bay have remained largely or partly vegetated throughout the air photo period while other stretches have presented mainly deflating bare sand seawards faces exposing palaeosols over the period (see Figure 157).

3. Development of wind-eroded deflation gullies and bare active mobile sand lobes or transgressive dunes in and behind the high deflating seawards dune face has been minor throughout the air photo period (see Figure 157); as noted above this is likely due to the relatively wind-sheltered aspect of the Wreck Bay beaches. Apart from the bare deflating seawards dune faces, the main areas of active dune sand mobility (deflation and accumulation) have been an area behind the middle of the beach and several areas at the south-eastern (most wind-exposed) end of the bay. Some minor expansion of deflation gullies and accumulating sand lobes is evident in these areas over the air photo period (Figure 157)

but is of small scale compared to bare sand transgressive dune expansion over the same period at the nearby more exposed Towterer Beach (Figure 156) and at Stephens Bay.

Surveyed shore profile analysis (TASMARC)

Three TASMARC beach profile survey marks were established at Wreck Bay during November-December 2014 as part of a DPIPWE World Heritage Area monitoring project managed by Rolan Eberhard in collaboration with the TASMARC project (Eberhard et al. 2015). The three profiles sample the two main beach sections (north and south of the central rocky point) and the more wind-exposed south-eastern end of the beaches (see Figure 154 & Table 45). Each profile was measured from a survey mark inland of the seaward dune, over that dune and as far down the beach-face as practical on each occasion. The profiles were surveyed at annual intervals during November-December 2014, 2015 and 2016 by Nick Bowden and Paul Boland, with assistance from Rolan Eberhard, Michael Comfort, Chris Sharples, and others.

The results of the three surveys are plotted on Figure 160 to Figure 162 below in two forms, namely as profile plots and hinge point plots. These are further explained in Chapter 3 Section 3.3.2, but in brief profile plots depict the surveyed shoreline in profile, whereas hinge-point plots summarise the survey data by plotting the vertical and horizontal movement over time of the intersection between the top (back) of the beach and the base (front) of the dune face. In this way the hinge point plots show both the horizontal movement of the dune front (toe) and the vertical movement of the (back) beach face over time.

The original processed survey data for each profile plot (provided as figures below) is available on the TASMARC website (www.tasmarc.info) and is not reproduced here. The hinge point data has been derived from the original profile data and is provided at Table 46 below.

Shoreline behaviour history from profile surveys

The three TASMARC beach-dune profile records show a vertical beach erosion and recovery cycle (most notably at profiles 730/301 and 730/302), with negligible dune face changes on two of the profiles, and a small horizontal recession at the toe of one dune face (profile 730/301) which was

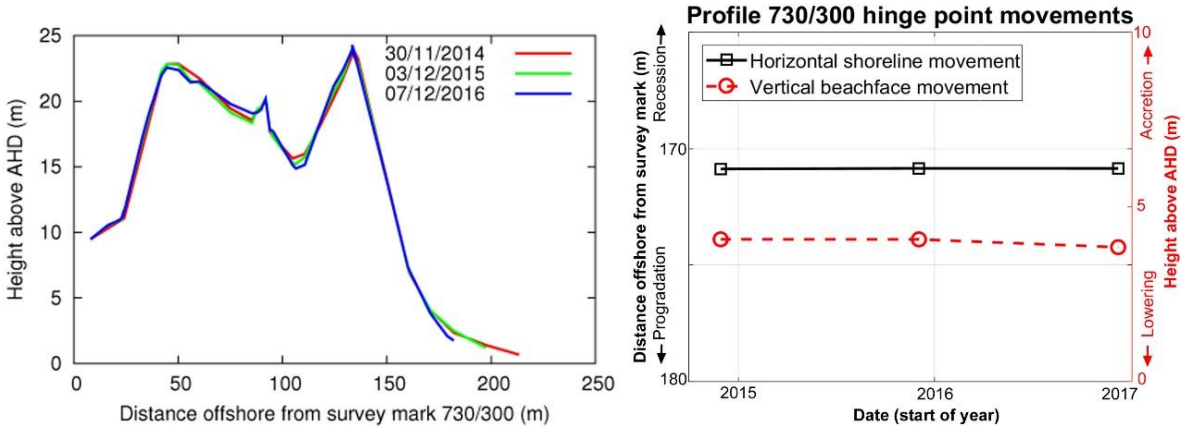

Figure 160: All surveys on TASMARC profile 730/300 (Wreck Bay north-west compartment) to date, as profile plots (LHS) and hinge point movement plots (RHS).

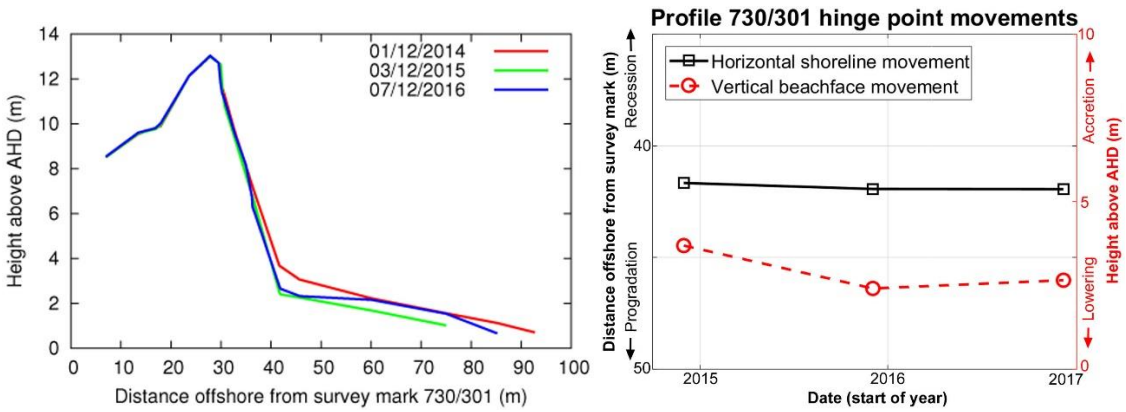

Figure 161: All surveys on TASMARC profile 730/301 (Wreck Bay south-east compartment) to date, as profile plots (LHS) and hinge point movement plots (RHS).

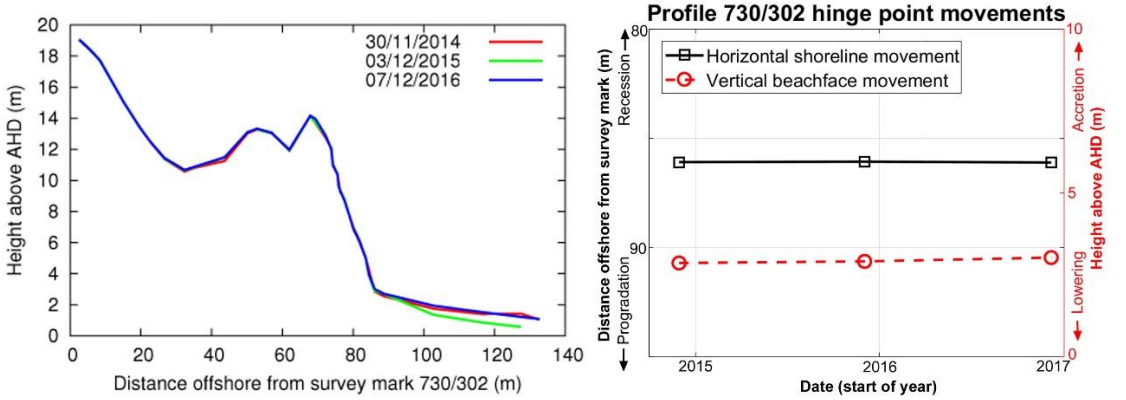

Figure 162: All surveys on TASMARC profile 730/302 (Wreck Bay south-east end) to date, as profile plots (LHS) and hinge point movement plots (RHS).

probably caused by slumping in response to the greater magnitude of beach lowering on that profile. Given that the air photo history (above) shows no detectable seawards dune face movement over several decades prior to 2014 (Figure 159), it is likely that movement of windblown sand from the recovering (accreting) beach face onto the dune face will have returned this dune profile to its 2014 condition within a year or so after the 2016 profile was measured, as must have occurred previously in response to similar events.

This beach and dune behaviour is characteristic of a beach and dune face in dynamic equilibrium, with frequent beach erosion and recovery events and less frequent dune toe erosion or slumping events followed by recovery, but no long-term progressive change indicated by the three-year TASMARC record.

Profile 730/300 (Figure 154) is of additional interest because it runs through the largest back-dune deflation hollow and mobile sand area that has persisted at Wreck Beach since 1949 (Figure 157). The TASMARC profiles of this back-dune area (Figure 160) show small areas of both sand deflation and accumulation (accretion) over the three-year period. This probably reflects the wind-driven movement of small mobile sand lobes across this back-dune area, which are likely to have been the main pattern of landform variability in that area since at least 1949 but do not appear to have resulted in significant modification of dune forms at any larger scale over that period.

Summary shoreline behaviour history and characterisation

The available beach and frontal dune behaviour history for Wreck Bay over the 67-year period between 1949 and 2016 has been one of cyclic wave-driven beach-face and dune-toe erosion and

recovery (Figure 160 to Figure 162), with ongoing slow aeolian deflation of some bare seawards dune faces, but little or no change to some other seawards dune faces that have remained vegetated throughout the data period. The shoreline movement history (as measured by the *in-situ* vegetation line on the frontal dune face) demonstrates a minor temporary progradation phase between 1961 and 1984 (also observed at nearby Mulcahy Bay), and overall is suggestive of a very slow landwards recession of deflating parts of the shoreline. However, this apparent recession lies within the air photo error margins (Figure 159) and therefore cannot be demonstrated, so that it is possible that no progressive shoreline change has occurred over the data period (1949-2016).

Overall, the shoreline position history for Wreck Bay from 1949 to 2016 can be characterised as stable (dynamic equilibrium) with a possible slow and non-significant recession trend, but no long-term change of behaviour.

Despite the very limited or negligible movement of the shoreline (dune face vegetation line) since 1949, the exposure of palaeosols in the bare seawards dune faces implies that those faces are currently in a more receded position than they have been at any time since the palaeosols were formed (which Cullen (1998) infers to be possibly centuries but not millennia ago). Given that many of the dune faces were bare and exposed in the earliest (1949) air photo, but that some other dune faces at Wreck Bay have remained mostly vegetated throughout the data period, the possibility arises that the bare dune faces were initially exposed by a major wave erosion event prior to 1949 (which evidently did not affect all sections of the dune front), and the eroded dune faces have subsequently been maintained in a bare state by ongoing dune face deflation, but with little or possibly no further dune face recession.

Throughout the data period bare seawards dune faces have remained mostly bare, have exhibited deflation gullies, and have been backed by accreting and mobile sand lobes (Figure 157), all of which imply the seawards faces have been actively deflating over the whole period. However, these features have changed little in size or distribution over the period, which implies that the rate of deflation of the dune front is too slow to allow major extensions of mobile transgressive dunes to develop as has occurred in more wind-exposed sites like nearby Towterer Beach and at Stephens Bay.

At the same time, the very slow (possibly nil) rate of recession of the seawards dune face despite ongoing deflation of sand into the backshore implies a continuing supply of sand to the beach sufficient to compensate for sand lost, or nearly so. Given that incoming alongshore sand supplies are unlikely at this well-embayed location, the only apparent source of a sand supply is a swell-driven movement of sand onshore from the shelf. This inference is supported by Geoscience Australia shelf sediment mobility modelling (Harris & Heap 2014; Harris et al. 2000).

Whether sea-level rise or increasing wind speeds are influencing beach and dune behaviour at Wreck Bay is not currently determinable since no potentially attributable change of behaviour such as a switch to or increase in rate of shoreline recession has been observed there to date. However, the beach history data gathered in this chapter provides a baseline against which any future shoreline behaviour changes will be detectable.

Air Photo Data Tables

The following tables provide details of the air photos used, the resulting ortho-photos produced, and the shapefiles representing the shoreline position that were digitised from the ortho-photos.

Table 43: Original air photos and ortho-rectified air photos produced for Wreck Bay.

Photo Date	**Original DPIPWE air photos (film-frame) / *Ortho-photo name***	**Final image resolution (original scan resolution if downsized) / pixel size of final ortho-photo**	**Original photo scale**	**Mean measured feature position error for ortho-photo (± metres)** [No. of measured feature position reference points]	**Comments**
24th Feb 1949	147-595 / *WreckBay_Feb1949_MGA55.tif/tfw*	2039 dpi / 0.45 m pixel size	1:15,840	2.72 m [10]	Ortho-rectified by Chris Sharples
16th Feb 1961	361-77 / *WreckBay_Feb1961_MGA55.tif/tfw*	2039 dpi / 0.50 m pixel size	1:35,640	2.43 m [10]	Ortho-rectified by Chris Sharples
19th Feb 1973	624-112 / *WreckBay_Feb1973_MGA55.tif/tfw*	2039 dpi / 0.41 m pixel size	1:30,000	8.5 m [10] Error margins ~20m at north end of beach	Ortho-rectified by Chris Sharples; **SHORELINE NOT DIGITISED DUE TO POOR ORTHO ACCURACY;** Error margins worst at north end of beach.
15th April 1975	678-34 / *No ortho*	2039 dpi / - m pixel size	1:40,000	- m [-]	**UNABLE TO ORTHO-RECTIFY DESPITE REPEATED ATTEMPTS (problem unclear)**
10th Mar 1984	994-38 / *WreckBay_Mar1984_MGA55.tif/tfw*	2039 dpi / 0.55 m pixel size	1:42,000	1.26 m [10]	Ortho-rectified by Chris Sharples
8th March 1988	1113-66 / *WreckBay_Mar1988_MGA55.tif/tfw*	1000 dpi (2039 dpi) / 0.74 m pixel size	1:25,000	1.44 m [10]	Ortho-rectified by Chris Sharples
25th Jan 1989	1128-133 / *WreckBay_Jan1989_MGA55.tif/tfw*	1000 dpi (2039 dpi) / 1.17 m pixel size	1:42,000	1.26 m [10]	Ortho-rectified by Chris Sharples
8th Jan 1998	1283-84 / *WreckBay_Jan1998_MGA55.tif/tfw*	1000 dpi (2039 dpi) / 1.2 m pixel size	1:42,000	1.28 m [10]	Ortho-rectified by Chris Sharples
16th Nov 2002	1360-178 / *WreckBay_Nov2002_MGA55.tif/tfw*	1000 dpi (2039 dpi) / 1.15 m pixel size	1:42,000	1.94 m [10]	Ortho-rectified by Chris Sharples
10th Jan 2008	1429-220 / *WreckBay_Jan2008_MGA55.ecw*	2039 dpi / 0.5m pixel size	1:42,000	4.41 m [10] (quoted absolute accuracy ±15m)	Ortho-rectified by DPIPWE (Secondary reference image for ortho-rectifying older photos) Original DPIPWE ortho file: *1429_220_op.ecw* Not used for analysis – marginal accuracy
6th Nov 2010	1450-17 / *WreckBay_Nov2010_MGA55.ecw*	2039 dpi / 0.3 m pixel size	1:24,000	1.01 m [10] (quoted absolute accuracy ±10m)	Ortho-rectified by DPIPWE Original DPIPWE ortho file: *1450_017_op.ecw*

22nd Dec 2015	Wreck_Bay_Alfhild_Bight_22-12-2015.ecw / *WreckBay_Dec2015_MGA55.ecw*	- / 0.1 m pixel size	-	0.0 m [N/A] (quoted absolute accuracy ±0.3m)	REFERENCE IMAGE (zero relative feature position error by convention) Digital original photo; Ortho-rectified by DPIPWE Original DPIPWE ortho file: *Wreck_Bay_Alfhild_Bight_22-12-2015.ecw*

Table 44: Digitised shoreline shapefiles produced for Wreck Bay (using ortho-photos listed in Table 43 above).

Date of air photo(s)	Shapefile	Shoreline digitised by	Comments*
24th Feb 1949	WreckBay_MGA55_19490224.shp	Chris Sharples (2018)	Medium resolution, veg line well defined, minimal shadows.
16th Feb 1961	WreckBay_MGA55_19610216.shp	Chris Sharples (2018)	Medium resolution, veg line well defined, no shadows.
19th Feb 1973	n/a	n/a	Shoreline not digitised due to very poor accuracy of ortho-photo.
15th April 1975	n/a	n/a	Shoreline not digitised because could not ortho-rectify air photo (reason inscrutable).
10th Mar 1984	WreckBay_MGA55_19840310.shp	Chris Sharples (2018)	Medium resolution, not much shadow, veg line well resolved.
8th Mar 1988	WreckBay_MGA55_19880308.shp	Chris Sharples (2018)	Medium resolution, shadowing allowed for, veg line mostly well defined.
25th Jan 1989	WreckBay_MGA55_19890125.shp	Chris Sharples (2018)	Shadowing allowed for, veg. line mostly defined within a metre or two.
8th Jan 1998	WreckBay_MGA55_19980108.shp	Chris Sharples (2018)	Quite a lot of shadowing allowed for, veg. line mostly defined within a metre or two.
16th Nov 2002	WreckBay_MGA55_20021116.shp	Chris Sharples (2018)	Some shadowing allowed for, veg. line clearly visible.
10th Jan 2008	WreckBay_MGA55_20080110.shp	Chris Sharples (2018)	Some shadowing allowed for, veg line clearly visible; digitised shoreline not used due to poor ortho-photo error margins.
6th Nov 2010	WreckBay_MGA55_20101106.shp	Chris Sharples (2018)	Minor shadowing allowed for, veg line clearly visible.
22nd Dec 2015	WreckBay_MGA55_20151222.shp	Chris Sharples (2018)	Veg line clearly visible.

*NOTE comments applicable to all air photo dates: Veg line is partly head scarp of slumped and deflating dune faces (remanent old veg. patches scattered over deflating slump faces ignored), partly wave-exposed veg lines over sandy + rocky shores. Deflating gullies and sand lobes present on small portion of dunes.

TASMARC shore profile data tables

Table 45: GPS-surveyed co-ordinates of each TASMARC transect survey mark at Wreck Bay. The survey marks are located at the landwards end of each transect, which runs seawards normal to the shoreline from each mark. Longitude and Latitude are decimal degrees and eastings and northings are metric co-ordinates of the Map Grid of Australia Zone 55 (MGA55, GDA94 datum).

Transect	Longitude	Latitude	Easting	Northing
730/300	145.786544	-43.18663755	401392.61	5217744.405
730/301	145.7898117	-43.18871369	401661.485	5217517.686
730/302	**145.786544** ***Duplicates 730/300; one or both are wrong***	-**43.18663755**	402057.364	5216942.151

Table 46: Table of hinge points defined for each surveyed Wreck Bay profile (derived from original TASMARC survey data).

TASMARC profile number	Survey Date	Hinge Point distance offshore from survey mark	Hinge point height above AHD (metres)
730/300	30/11/2014	170.885	4.062
730/300	3/12/2015	170.860	4.060
730/300	7/12/2016	170.863	3.836
730/301	1/12/2014	41.678	3.680
730/301	3/12/2015	41.947	2.400
730/301	7/12/2016	41.956	2.646
730/302	30/11/2014	86.103	2.851
730/302	3/12/2015	86.082	2.900
730/302	7/12/2016	86.121	3.017

A1.3.7 Mulcahy Bay Beach (south-west coast)

Locality and general description

Mulcahy Bay beach is a high energy sandy beach directly exposed to the south-westerly swells 26 kilometres north of the entrance to Port Davey (Figure 163). The beach was visited by Chris Sharples (with others) during December 2014, 2015 and 2016 as part of a DPIPWE-funded helicopter-based project to establish and monitor beach profile transects. Beach and dunes at Mulcahy Bay are effectively free of introduced species capable of modifying sandy geomorphic processes, including sea spurge and Marram Grass.

Geomorphology and process environment

Geomorphic description

Geomorphic aspects of Mulcahy Bay beach have previously been described by Pemberton and Cullen (1999), Cullen (1998) and Short (2006b).

Mulcahy Bay beach mostly faces southwest (aspect 220º True) and although strongly exposed to the south-westerly swells is located within a rocky embayment 1.5 km wide bounded by prominent rocky headlands which must absorb some of the swell wave energy before it reaches the beach. The beach is a Transverse Bar and Rip (TBR) to Rhythmic Bar and Beach (RBB) morphodynamic type Short (2006b), fronted by a 100m wide surf zone with several strong rips. The beach is immediately backed by 20m to 25 m high dune faces which are the eroded seawards edge of an extensive and now mostly vegetated Holocene transgressive dune complex described by Cullen (see Figure 163). Since Mulcahy Bay is relatively sheltered from the dominating north-westerly winds (see below), the vegetated transgressive dunes do not show the strong NW-SE dune ridge orientation found at more wind-exposed sites such as Towterer Beach and Stephens Bay, and for the same reason present day active deflation gullies and bare mobile transgressive dunes are minor (albeit notable) compared to sites such as Stephens Bay (Cullen 1998, p.72). The vegetated transgressive dune complex is itself partly backed by deep bleached white sands that Cullen interprets as possibly Pleistocene aeolian sand sheets.

Although it is likely that currently active wind deflation of the mostly bare seawards dune faces behind much of the beach was initiated by wave erosion exposing bare sand scarps, there was little evidence of recent wave-erosion during the period December 2014 – December 2016), apart from a large beach scarp close to the toe of the dune face behind the central-northern part of the beach during 2014-2015. The seawards dune faces were however mostly bare (Figure 165), and small to moderate-size actively accumulating lobes of windblown sand immediately in the lee of the dune crest indicate sand is actively (albeit slowly) being blown landwards from the dune faces. During 2014 – 2016 the beach and dune face exhibited significant beach berm accumulation at the seawards dune toe, with some revegetation of parts of the dune face (Figure 166), and lesser berm recovery with no incipient dune accumulation or vegetation recovery in other areas (Figure 167). Nonetheless several palaeosols (fossil buried soil horizons) are exposed in the bare dune faces, which suggest the dune face is in a state of net progressive recession, although the results of historic air photo analysis (see below) show that any net dune-face recession is currently very slow at this beach (see below).

Cullen (1998) notes the palaeosols have A-C profiles typical of coastal dunes in the region. Although no absolute dates are available for the palaeosols at Mulcahy Bay, Cullen infers them to be similar to palaeosols at nearby Nye Bay, for which radiocarbon dating of contained charcoal have indicated ages ranging from 700 years BP to less than 200 years BP, with inferred dune ages of less than 1000 years being attributed to probable destruction of earlier dunes prior to 1000 years (Pemberton & Cullen 1999).

Whereas the northern and southern ends of the beach are backed by dunes perched on partly exposed bedrock surfaces above present sea-level (Figure 163) which consequently have little potential for significant shoreline recession, the major central part of the beach is backed by soft sandy sediments that probably extend below present sea-level for several hundred metres landwards, and hence have considerable potential for shoreline recession.

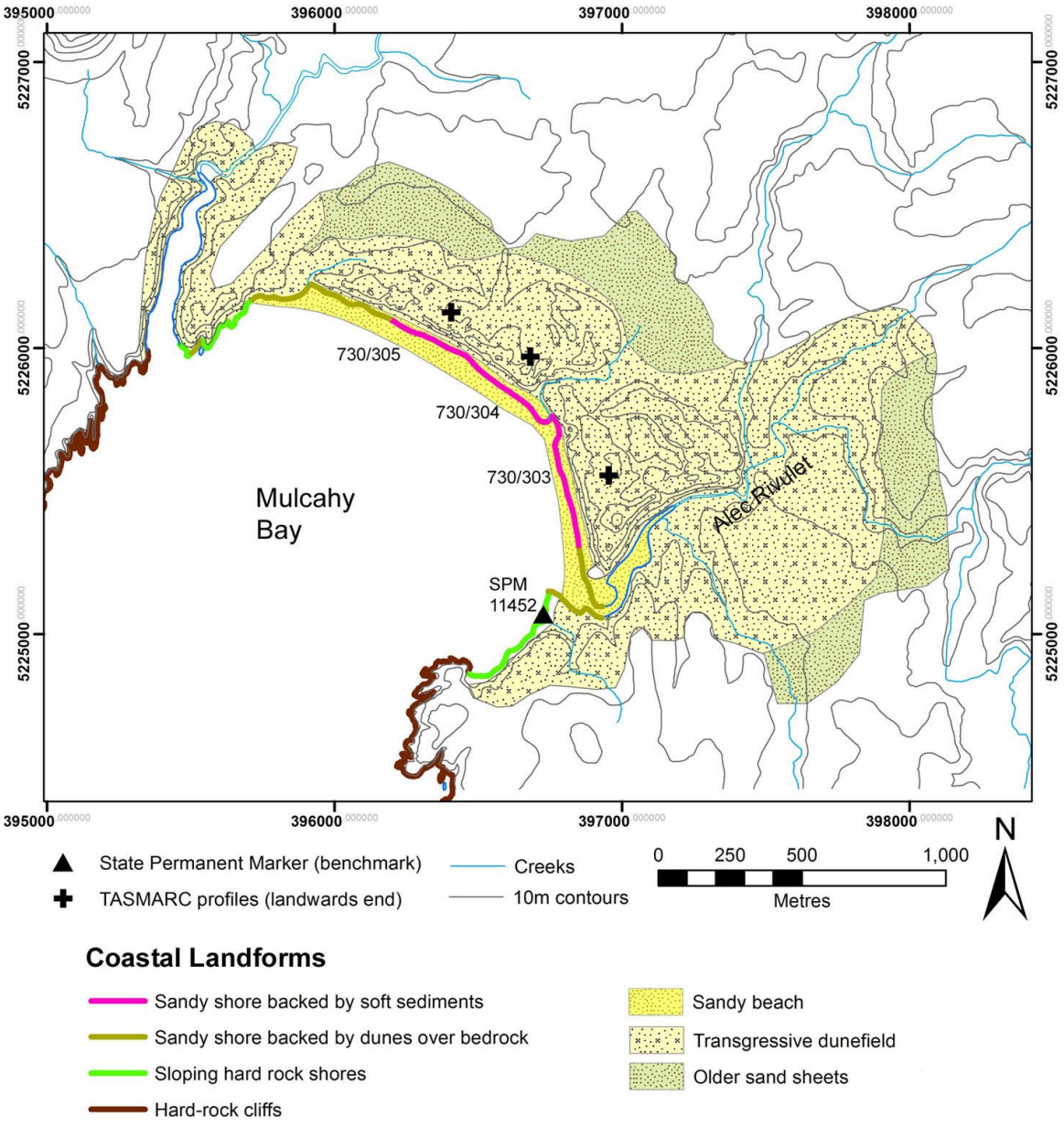

Figure 163: Coastal landforms at Mulcahy Bay. Coastal landform mapping is based on Cullen (1998), with additional shoreline type mapping by C. Sharples. Permanent survey benchmark (SPM) and TASMARC survey profile locations and numbers are indicated. Co-ordinate system is Map Grid of Australia zone 55 (GDA1994 datum).

Swell wave climate

Mulcahy Bay receives a persistent south-westerly swell generated by Southern Ocean winds strongly correlated with the Southern Annular Mode (Hemer, Church & Hunter 2010; Hemer, Simmonds & Keay 2008). Swell wave parameters for Mulcahy Bay are given below:

Key swell parameters:

Table 47: Key swell wave climate parameters for Mulcahy Bay, from the CAWCR wave hindcast 1979-2010 by the Australian Bureau of Meteorology and CSIRO Australia 2013 (Durrant et al. 2013). These figures apply to the closest inshore ~5km grid cell to the beach.

	Annual	Summer (DJF)	Winter (JJA)
Average Significant wave height (m)	3.11	2.73	3.33
Average Maximum wave height (m)	6.45	5.71	6.88
Average Mean wave direction (ºT)	239	237	243

These swell wave heights and directions apply to a grid cell just outside the Mulcahy Bay embayment headlands, about 2 – 3 km offshore from Mulcahy Bay beach. Given the (lateral) depth and the relatively narrow width of the embayment (see Figure 163) it is likely that wave heights near the beaches are notably less than indicated by the CAWCR hindcast, because of wave energy lost through refraction and drag against the bounding rocky headlands (Davies 1973) in addition to normal shoaling effects as the waves reach shallower water. The limited swell wave direction variability is also probably further reduced within the embayment as refractional wave training within the embayment yields less directional variability.

Considering the shoreline orientation at the beach, the swell wave directions indicated in Table 47 probably yield a small but persistent south-easterly longshore drift of sand along the northern half of the beach and possibly a frequent northerly drift along the southern part of the beach; however these interpreted drifts are probably significantly modified by interaction with locally generated wind waves (see below).

Wind (wind-wave) climate

The nearest long-term wind record for a south-west Tasmanian coastal site with ocean fetch exposures comparable to Mulcahy Bay is the Maatsuyker Island weather station, 74 kilometres to the south. However, a marked difference in active transgressive dune development behind two beaches only 12 kilometres south of Mulcahy Bay – northwest-facing Towterer Beach and southwest-facing Wreck Bay - is probably explained by a dominating north-westerly wind direction (see Wreck Bay section), as is also the case for Stephens Bay closer to Maatsuyker down the same coast. Since the Maatsuyker wind record indicates the same wind direction dominance (see Figure 164), it is reasonable to infer that this is probably true for a long stretch of the southwest coast extending from Maatsuyker northwards at least to Wreck Bay and likely to nearby Mulcahy Bay.

It is therefore inferred that the south-westerly aspect of Mulcahy Bay beach makes the bare dune faces less exposed to the dominant north-westerly winds and thus less prone to development of extensive active transgressive dunes as seen behind other north-west – facing beaches in the region.

However, it is also likely that the dominant north-westerly winds generate local wind-waves in Mulcahy Bay which would drive a south-eastwards littoral drift of sand down the beach, adding to the inferred bi-directional longshore drifts produced by swells (see above) to drive an overall south-eastwards drift of sand along the beach. This would explain the observed wider beach at the south-east end (Figure 168) and the forcing of the largest creek outlet crossing the beach (Alec Rivulet) hard up against the rocky shore at the south-east end of the beach.

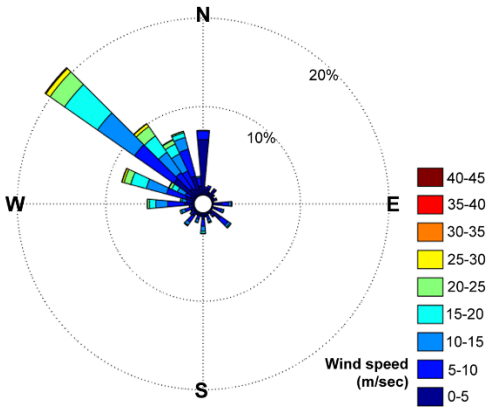

Figure 164: Wind directions for Maatsuyker Island, 74 km south of Mulcahy Bay but the nearest weather station exposed to a comparable south-westerly coastal wind climate. The figure was prepared in Matlab™ using all synoptic wind records for Maatsuyker Island from 1957 to 2015. Original data supplied by the Australian Bureau of Meteorology (2016).

Analysis of the Maatsuyker Island wind record by (Kirkpatrick et al. 2017) indicated increased mean wind speeds over recent decades, at least in winter. Given the likelihood that this is also true for winds at Mulcahy Bay, some increase in both aeolian sand deflation and locally generated wind wave energies can be expected at Mulcahy Bay in recent decades.

Sand transport and budget

Shelf sediment mobility modelling implies that some sand may still be moving onshore from the continental shelf into Mulcahy Bay (Harris & Heap 2014; Harris et al. 2000). Although there is no measured data on this, the direct exposure of the bay to the dominant south-westerly direction of the large swell that would drive onshore movement of shelf sands in this region makes some sand supply from this source plausible.

The coastal orientation with respect to dominant swell directions (see below) also means that the rocky headlands bounding Mulcahy Bay are sufficiently large and protruding as to make any significant alongshore movement of sand into or out of the embayment unlikely.

Field observations during 2014 to 2016 (see above) and interpretation of air photo time series since 1961 imply there has been some landwards wind-blown loss of sand from the beach and exposed seawards dune face over that whole period. However, the amounts lost have only been sufficient to build active mobile transgressive dunes of very limited but fluctuating extent (see Figure 168), and deflation of the dune fronts has only resulted in very limited dune face recession (see Figure 170 & discussion below).

As is true for most west coast rivers and streams, the creeks draining into Mulcahy Bay are unlikely to be supplying significant amounts of sand into the bay under recent and current climatic conditions.

No other sources or sinks of sand at Mulcahy Bay are evident. The likely existence of an onshore sand supply from the continental shelf, and a landwards aeolian sand sink, taken together with the air photo history suggesting only a slow dune face retreat since at least 1961 (see below), indicates that the bay likely has a balanced to slightly losing sand budget.

Figure 165: View northwards from near the southern end of Mulcahy Bay beach, showing the dominantly unvegetated and deflating seawards faces of the transgressive dune complex backing the beach. Exposed quartzite bedrock in the foreground underlies the southern end of the dunes above present sea-level. Photo by C. Sharples (2014).

Figure 166: Partly re-vegetated dune face near TASMARC profile 730/303, showing a high upper beach-face berm and notable incipient dune sand accumulation at the toe of the face, with advanced dune face revegetation reducing deflation of the face by wind. Photo by C. Sharples (2014).

Figure 167: View of bare dune face just north of TASMARC profile 730/304, showing at least one prominent palaeosol horizon exposed in the poorly recovering, deflating seawards dune face. Although beach berm recovery is substantial, there is little incipient dune accumulation at the foot of the eroded face, which remains largely unvegetated and deflating. Photo by C. Sharples (2014).

Air photo analysis

Ortho-rectified vertical air photos of Mulcahy Bay (beach and dunes) at 11 dates from 1961 to 2015 (see Table 48) were used to map and characterise shoreline change history over that period. The *in situ* (living) vegetation line was mapped as the shoreline proxy at each air photo date (Table 49). In most parts of the bay this line corresponds to the scarped vegetation line near the crest of high bare slumped and deflating seawards dune faces (as seen in the distance in Figure 165 and at the dune crest in Figure 167), although in some areas and at some times the seawards dune faces have more vegetation cover (e.g., Figure 166) and the mapped shoreline is a wave-exposed vegetation line near the seawards toe of the dune. Vegetation margins around deflation gullies and bare mobile wind-blown sand bodies in the immediate back-dune areas were not treated as 'shorelines' and their history was considered separately to the shoreline history at Mulcahy Bay. Figure 168 shows the distribution of these differing mapped vegetation line types as at 2015.

Shore behaviour history from air photos

Based on the ortho-rectified historic air photos listed in Table 48 and the shoreline positions digitised from these (Table 49), Figure 169 depicts horizontal shoreline movement from 1961 to 2015 along individual digital transects. One transect in the middle of the beach was not used as it fell on a deflation gully and did not cross a shoreline proxy as defined. Shoreline behaviour is similar and roughly coherent on all but two transects (27568 & 27569) which showed anomalous accretion (progradation) behaviour during the 1995-2010 period. These are near the south-eastern end of the beach and their behaviour might have resulted from an unusual degree of littoral sand drift and uninterrupted sand accretion at that time. It is also possible the apparent anomalous behaviour results from mapping errors since some of the air photos concerned have heavy shadowing which can make it difficult to accurately pick the vegetation line.

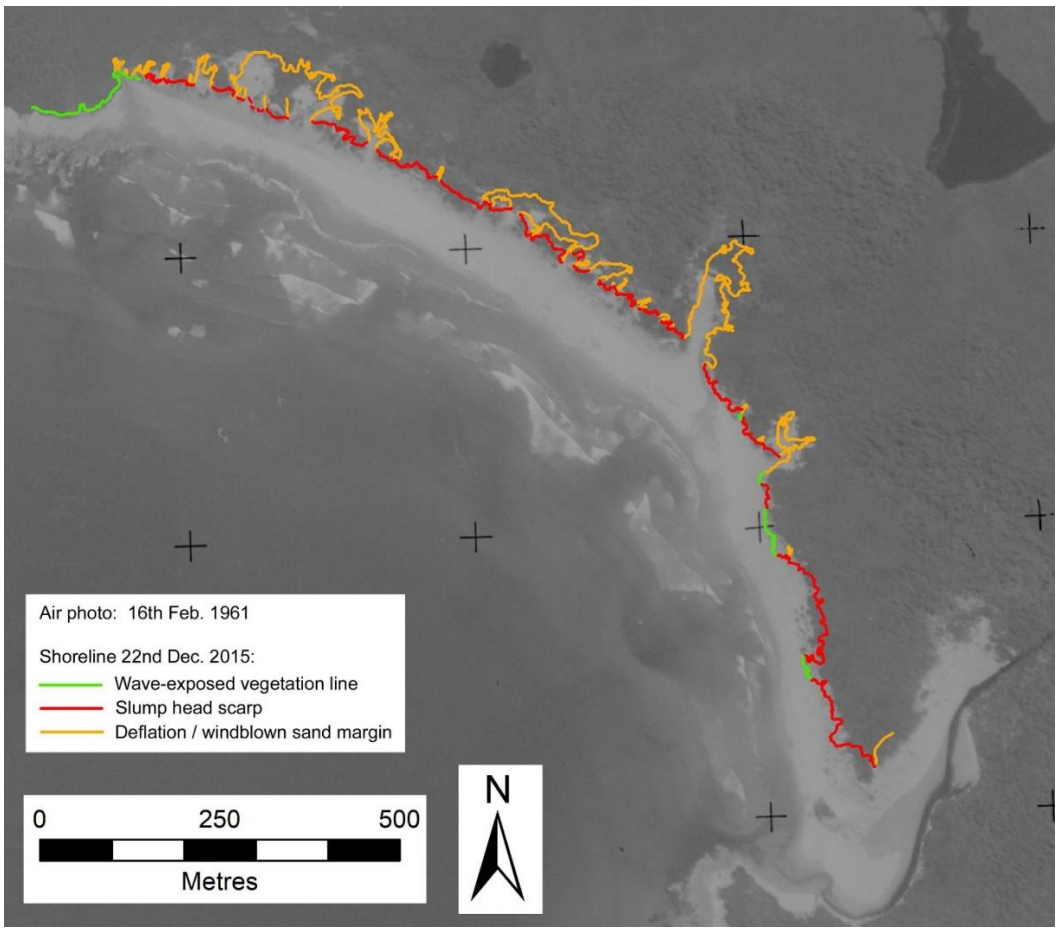

Figure 168: Comparison of shoreline positions at Mulcahy Bay from the earliest (1961) air photo (ortho-rectified) and the 2015 shoreline proxies and other features digitised from the 2015 ortho-photo.

Given the coherent shoreline history along all but two anomalous used transects, these records have been combined into a summary plot (Figure 170) showing the median of shoreline positions at each date across all used transects other than the two anomalous transects (27568 & 27569).

The following key features of the Mulcahy Bay beach and dune history are evident from the air photos and derived data plots:

1. The shoreline history for Mulcahy Bay from 1961 to 2015 is essentially a slow but continuing landwards recession of the mostly bare sand seawards dune face. Apparent prograding intervals (Figure 170) are of the order of a few metres horizontal movement only and apart from a notable progradation phase between 1975 and 1984 are largely within air photo error margins and so possibly not real. A similar progradation phase prior to 1984 at nearby Wreck Bay implies that a real (but minor and short-lived) shoreline progradation phase did occur at these two beaches (at least) between 1975 and1984. Otherwise, the overall recession trend exceeds error margins and is clearly real: a linear regression on this trend (see Figure 170) yields a significant Pearson correlation co-efficient of $R^2 = 0.5174$.

   Although wave erosion scarps in the beach berm and near the seawards dune toe were observed at Mulcahy Bay during the period 2014 – 2016, the air photo record is not

suggestive of major wave erosion events driving the historic recession of the shoreline proxy (which is mainly the vegetation line at the high crest of the seawards dune faces).

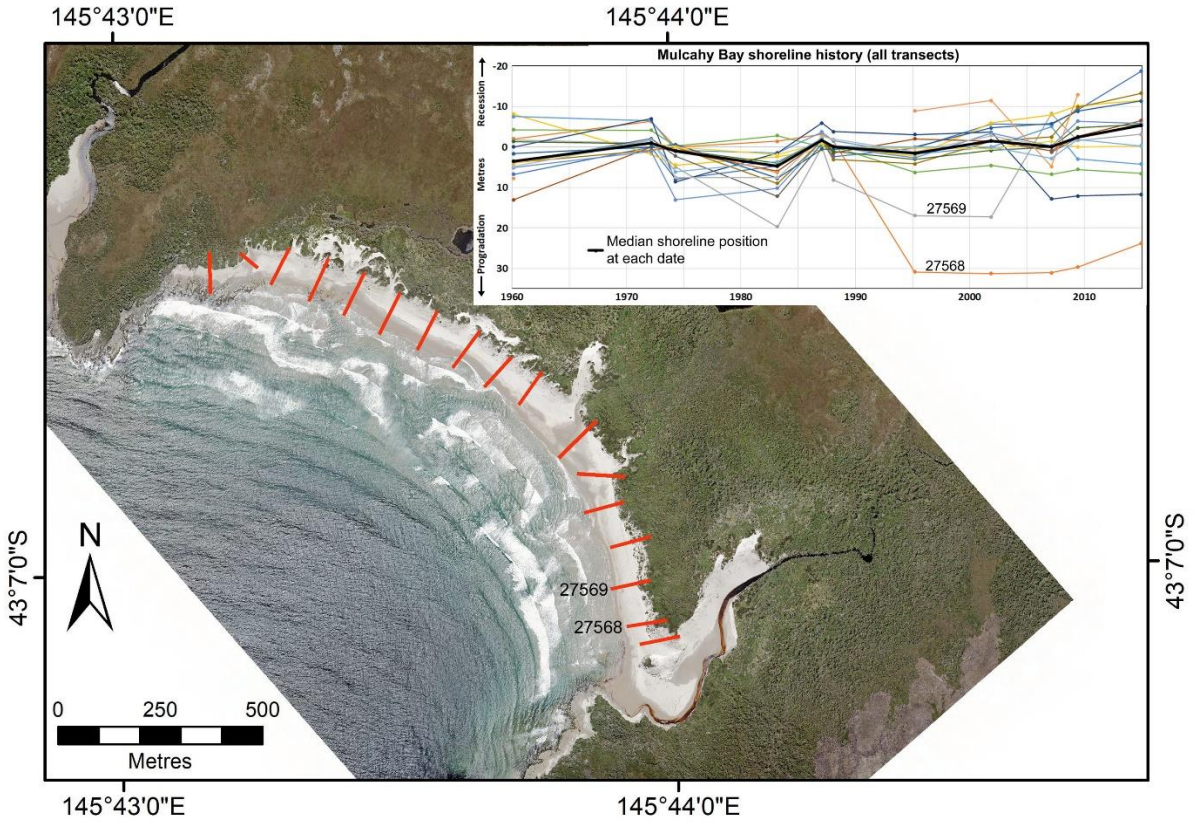

Figure 169: Plots of shoreline position at Mulcahy Bay over the period 1961 – 2015 along each 100m-spaced digital transect, plotted relative to the median shoreline position on each transect. Shoreline positions are defined as seawards vegetation lines excluding creek-dominated and deflation hollow or windblown sand vegetation margins. Transect locations used are indicated by red lines on the air photo, and each coloured line on the plots represents shoreline position changes over time along one transect. All transects used are shown, with the median shoreline history across all transects shown by a heavy black line. Two transects with somewhat anomalous shoreline histories (27568 & 27569) are indicated on the plot and map. One transect has been omitted because it crossed a deflation gully vegetation line, not a 'shoreline' as defined. The background image is the 2015 air photo (© DPIPWE).

Instead relatively slow deflation of the seawards dune face with landwards aeolian sand loss is more consistent with the slow progressive nature of the recession, the dune conditions observed in the field, and the air photo history of the bare mobile sand areas (see next below).

2. Numerous but mainly relatively small deflation gullies in the seawards dune face and bare accreting sand masses in the immediate back-dune area are present throughout the air photo period. Although these have somewhat changed their planform configuration over the period, significant landwards extension has only occurred at a couple of locations but is not the general rule (see Figure 168). This suggests that some sand has been deflating from the seawards dune face into the back-dune area throughout the air photo period (or the bare sand areas would have revegetated), but only at a limited rate which in most areas allows vegetation growth to keep pace on the landwards sides and prevent extension of bare sand masses further inland.

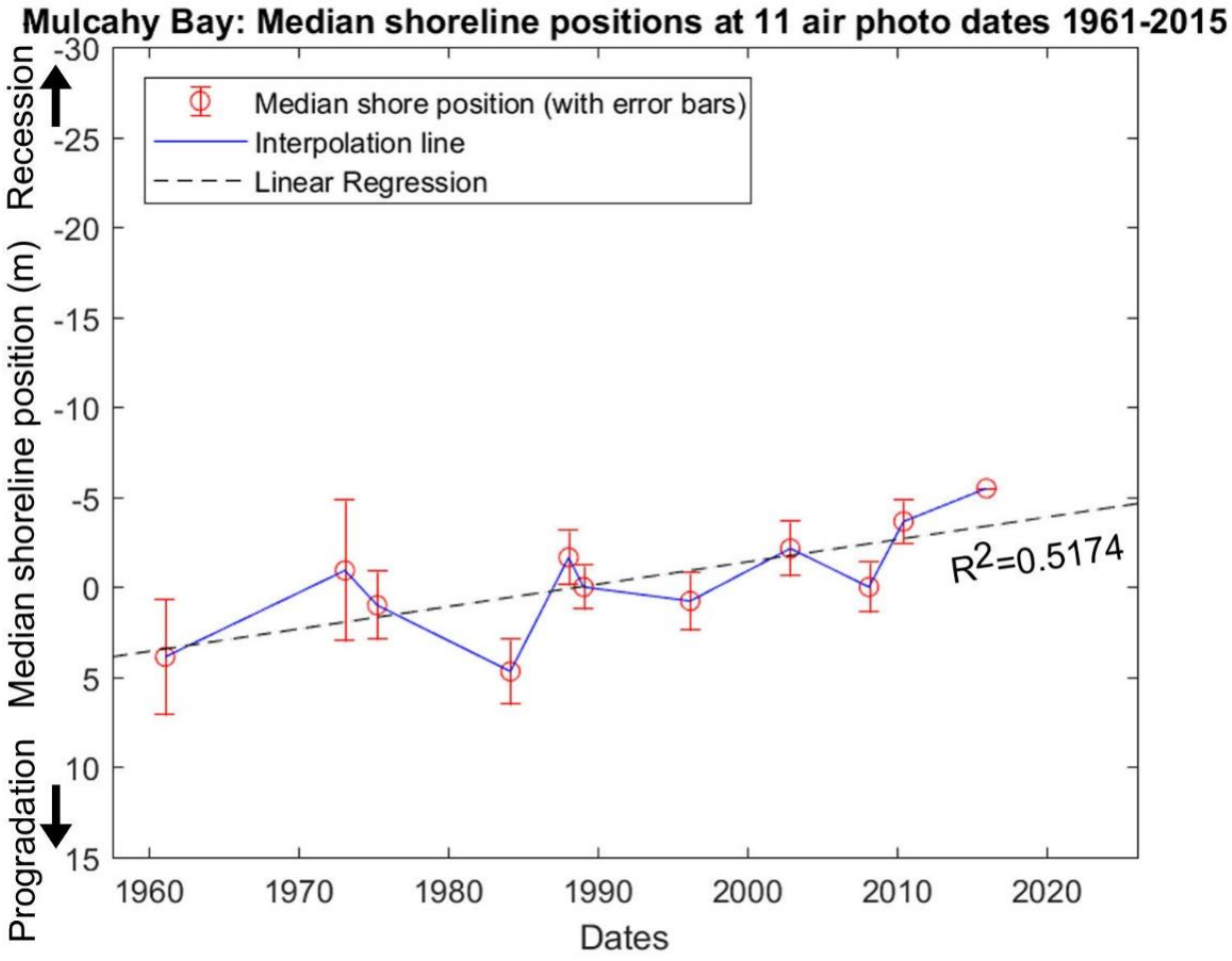

Figure 170: Summary plot of shoreline change history for Mulcahy Bay at 11 air photo dates from 1961 to 2015. This plots the median of the shoreline positions at each date across all transects shown in Figure 169 except transects 27568 & 27569 (as shown by Figure 169, all the transects show similar coherent shoreline histories except for 27568 & 27569 which exhibit anomalous shoreline accretion during the 1990s). Figure shows shore positions at each air photo date with interpolation lines and linear fit (linear regression). For comparison purposes the Y-axis scale (shoreline position) is the same as for all other beach history plots in this project, emphasising the comparatively small horizontal shoreline movement detected over the air photo period at Mulcahy Bay.

Surveyed shore profile analysis (TASMARC)

Three TASMARC beach profile survey marks were established at Mulcahy Bay during December 2014 as part of a DPIPWE World Heritage Area monitoring project managed by Rolan Eberhard in collaboration with the TASMARC project (Eberhard et al. 2015). The three profiles are evenly spaced along the beach (see Figure 163 and Table 50) and sample the same beach and dune areas whose longer-term air photo history is described and depicted in plots above (Figure 169 and Figure 170). Each profile was measured from a survey mark inland of the seawards dune, over that dune and down the beach face as far as was practical on each occasion. The profiles were surveyed at annual intervals during December 2014, 2015 and 2016 by Nick Bowden and Paul Boland, with assistance from Rolan Eberhard, Michael Comfort, Chris Sharples and others.

The results of the three surveys are plotted on Figure 171 to Figure 173 below in two forms, namely as profile plots and hinge point plots. Profile plots depict the surveyed shoreline in profile, whereas hinge-point plots summarise the survey data by plotting the vertical and horizontal movement over time of the intersection between the top (back) of the beach and the base (front) of the dune face. In

this way the hinge point plots show both the horizontal movement of the dune front (toe) and the vertical movement of the (back) beach face over time.

The original processed survey data for each profile plot (provided as figures below) is available on the TASMARC website (www.tasmarc.info) and is not reproduced here. The hinge point data has been derived from the original profile data and is provided at Table 51 below.

Shoreline behaviour history from profile surveys

The three TASMARC beach – dune profile records demonstrate mainly cyclic vertical beach face changes over the three years with notable (and probably cyclic) dune face change being measured at only 1 of the 3 sites. No measurable progressive (long-term) change to either the beach or dune faces is demonstrable from this 3-year profile record.

The middle profile 730/304 (Figure 172) shows no significant change at all to either the beach or dune faces from Dec 2014 to Dec 2016.

The south profile (730/303, Figure 171) shows beach scarping (wave erosion of the upper beach-face berm) but no measurable change to the dune face. Figure 166 shows the high beach-face at this location during Dec 2014, prior to its erosion between Dec 2015 and Dec 2016. Note that although the 730/303 hinge point plot appears to depict significant dune face recession, comparison with the profile plot shows this is not the case but is mostly an artefact of the choice of hinge point.

The north profile 730/305 (Figure 173) shows the greatest amount of change, with first beach face accretion (raising) and then erosion (lowering) over the three years, but no net (progressive) beach face change. However, this site does show a measurable horizontal recession of the lower half of the seawards dune face, which was probably caused by slumping of the lower dune face in response to the upper beach face being eroded by waves between Dec 2015 and Dec 2016. From the first two profile records it can be inferred that another phase of accretion (raising) of the upper beach face is likely to again cause partial or complete recovery of the lower dune face (as previously occurred between Dec 2014 and Dec 2015 when sand was returned to the beach face by waves and wind, and was moved up the dune face by wind).

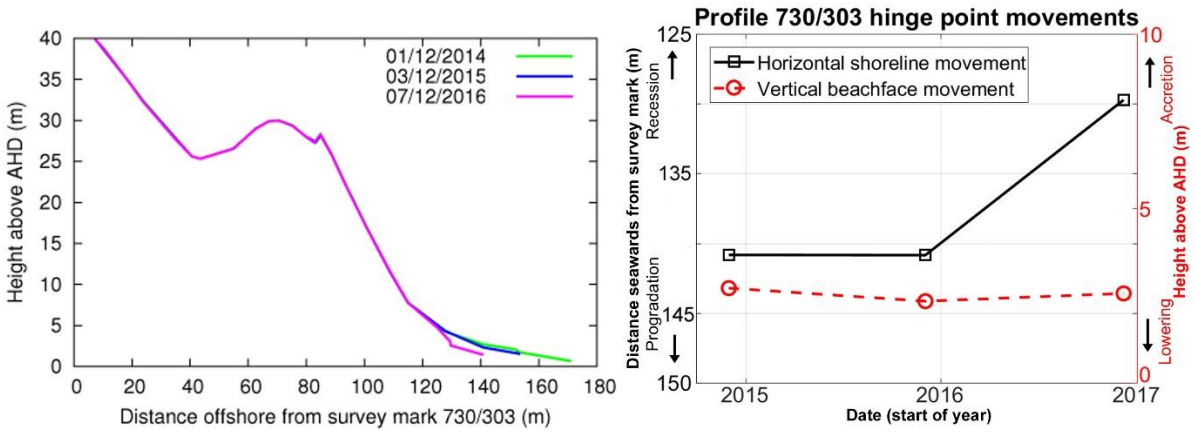

Figure 171: All surveys on TASMARC profile 730/303 (south) to date, as profile plots (LHS) and hinge point movement plots (RHS).

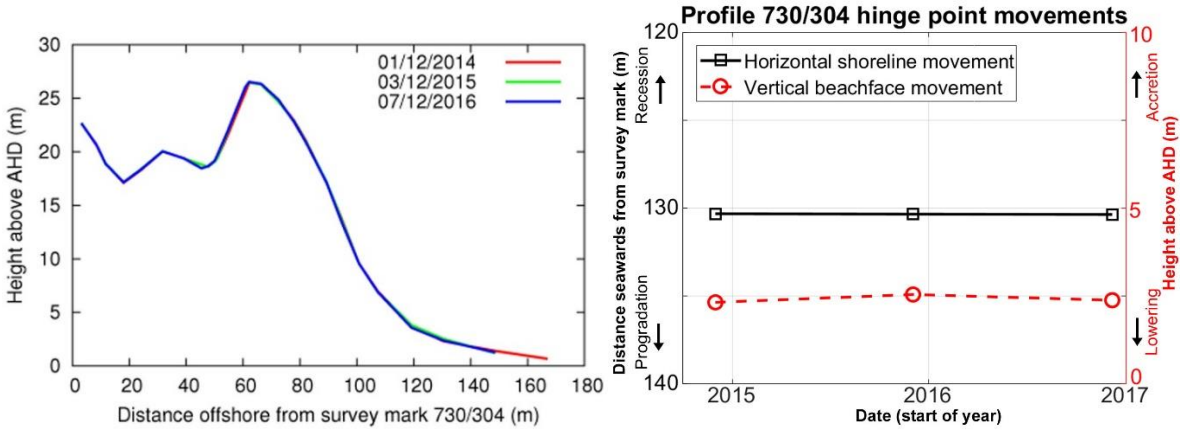

Figure 172: All surveys on TASMARC profile 730/304 (middle) to date, as profile plots (LHS) and hinge point movement plots (RHS).

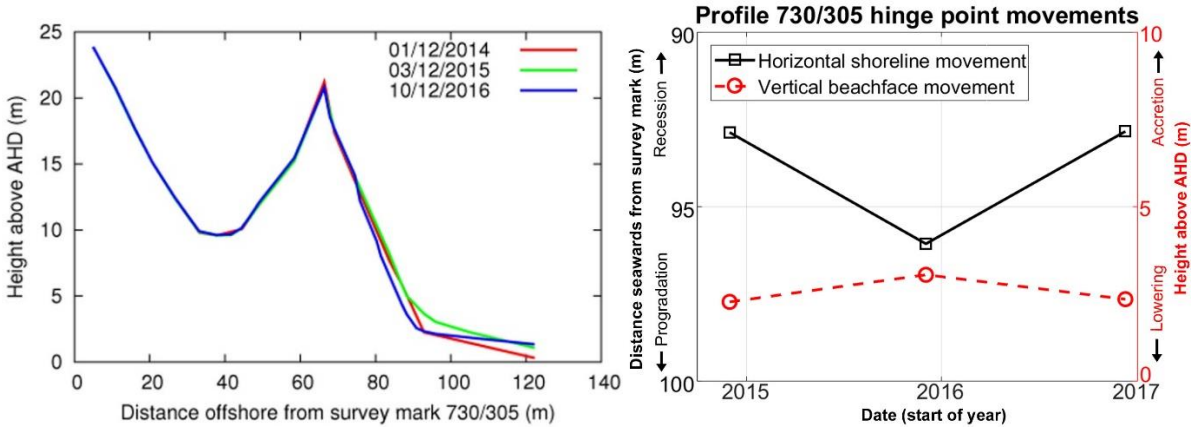

Figure 173: All surveys on TASMARC profile 730/305 (north) to date, as profile plots (LHS) and hinge point movement plots (RHS).

The overall result from 3 years beach profile monitoring at Mulcahy Bay is that whereas wave erosion of the beach face was significant it was also cyclic and resulted in no long-term change, while dune face changes likewise varied from negligible to minor slumping from which the dune face is likely to recover (through wind-blown sand accretion).

Summary shoreline behaviour history and characterisation

The available beach and frontal dune behaviour history for Mulcahy Bay over the 55-year period between 1961 and 2016 has been one of slow but progressive dune face retreat (detectable on decadal but not annual time scales), but with beach profiling and notably high upper beach face berms (e.g., Figure 166) providing no evidence of any progressive beach-face changes such as long-term lowering.

No significant (i.e., long term) change in this behaviour is detectable over the air photo and profiling period, and since it is also unknown when the current phase of slow dune face recession began it is difficult to identify triggering factors (such as increased erosion due to higher sea-level or increased deflation due to increasing wind speeds).

The mechanism of dune face retreat appears to be primarily wind deflation of bare exposed seawards faces (rather than wave erosion which seems to mainly affect the beach face in a cyclic fashion), and the air photo evidence indicates active landwards loss of windblown sand has occurred throughout the data period. However, whilst there is evidence of increasing south-west coast wind speeds in recent

decades, no acceleration of dune face deflation that might be expected to result from this has been detected in the data record

Sand has evidently been lost landwards from the beach and dune face throughout the data period, yet dune face retreat has been slow (with at least one phase of minor progradation (recovery) between 1975 and 1984) and high upper beach-face berms have been retained to the present (e.g., Figure 166). This implies there must be an ongoing supply of new sand to replenish beach and dune sand deflated inland, and the only apparent source for this is swell-driven movement of sand onshore from the shelf. This inference is supported by Geoscience Australia shelf sediment mobility modelling (Harris & Heap 2014; Harris et al. 2000).

Given the presence of some (minor) sections of seawards dune face with recovering vegetation cover at Mulcahy Bay (see Figure 166) and other sections with remanent shrub skeletons indicating a formerly more extensive shrubby vegetation cover (Figure 165 and Figure 167), it is reasonable to speculate that at some time prior to 1961- but probably less than centuries ago - the frontal dune at Mulcahy Bay had a more extensive vegetation cover than it does now. If that is so, it is evident that this cover was at some date severely compromised, perhaps by a very large storm wave erosion event which exposed the dune sands to wind deflation. The dunes have subsequently been kept mainly bare and deflating owing to the very windy south-west coast climate which inhibits revegetation of very wind-exposed dune faces (possibly exacerbated by increasing wind speeds in recent decades). Nonetheless recession of the bare exposed dune faces through wind erosion has been slow owing to a continuing swell-driven supply of sand to the beach and dune from the continental shelf.

Whether sea-level rise or increasing wind speeds are significant contributing factors in the ongoing slow dune face recession at Mulcahy Bay is not currently determinable since at this site there is yet no evidence of an acceleration of dune face recession or other change of shoreline behaviour which might be expected as these recent climate-change related factors become more important in the mix of geomorphic processes controlling beach behaviour. However, the beach history data gathered in this chapter provides a baseline against which any future shoreline behaviour changes at Mulcahy Bay will be able to be detected.

Air photo data tables

The following tables provide details of the air photos used, the resulting ortho-photos produced, and the shapefiles representing the shoreline position that were digitised from the ortho-photos.

Table 48: Original air photos and ortho-rectified air photos produced for Mulcahy Bay.

Photo Date	**Original DPIPWE air photos (film-frame) / Ortho-photo name**	**Final image resolution (original scan resolution if downsized) / pixel size of final ortho-photo**	**Original photo scale**	**Mean measured feature position error for ortho-photo (± metres)** [No. of measured feature position reference points]	**Comments**
16th Feb 1961	360-129 / *MulcahyBay_Feb1961_ MGA55.tif/tfw*	1000 dpi (2039 dpi) / 1.0 m pixel size	1:40,000	3.2 m [10]	Ortho-rectified by Chris Sharples
19th Feb 1973	624-145 / *MulcahyBay_Feb1973_ MGA55.tif/tfw*	2039 dpi / 0.4 m pixel size	1:30,000	3.9 m [10]	Ortho-rectified by Chris Sharples
15th April 1975	678-031 / *MulcahyBay_Apr1975_ MGA55.tif/tfw*	1000 dpi 2039 dpi) / 1.4 m pixel size	1:40,000	1.9 m [10]	Ortho-rectified by Chris Sharples
10th Mar 1984	994-033 / *MulcahyBay_Mar1984_ MGA55.tif/tfw*	2039 dpi / 0.57 m pixel size	1;42,000	1.8 m [10]	Ortho-rectified by Chris Sharples
28th Jan 1988	1104-033 / *MulcahyBay_Jan1988_ MGA55.tif/tfw*	1000 dpi (2039 dpi) / 0.79 m pixel size	1:25,000	1.5 m [10]	Ortho-rectified by Chris Sharples
25th Jan 1989	1128-071 / *MulcahyBay_Jan1989_ MGA55.tif/tfw*	1000 dpi (2039 dpi) / 1.14 m pixel size	1:42,000	1.2 m [10]	Ortho-rectified by Chris Sharples
11th Mar 1996	1252-025 / *MulcahyBay_Mar1996_ MGA55.tif/tfw*	1000 dpi (2039 dpi) / 1.23 m pixel size	1:42;000	1.6 m [10]	Ortho-rectified by Chris Sharples
16th Nov 2002	1360-137 / *MulcahyBay_Nov2002_ MGA55.tif/tfw*	1000 dpi (2039 dpi) / 1.14 m pixel size	1:42,000	1.5 m [10]	Ortho-rectified by Chris Sharples
19th Feb 2008	1431-224 / *MulcahyBay_Feb2008_ MGA55.ecw*	2039 dpi / 0.5m pixel size	1:42,000	1.4 m [10] (quoted absolute accuracy ±15m)	Ortho-rectified by DPIPWE Original DPIPWE ortho file: *1431_224_op.ecw* USED BY CS AS SECONDARY REFERENCE IMAGE FOR ORTHO-RECTIFYING AREAS BEYOND MULCAHY BAY ON COARSE-SCALE AIR PHOTOS.
11th June 2010	1450-033 / *MulcahyBay_June2010_ MGA55.ecw*	2039 dpi / 0.3m pixel size	1:24,000	1.2 m [10] (quoted absolute accuracy ±10m)	Ortho-rectified by DPIPWE Original DPIPWE ortho file: *1450_033_op.ecw*
22nd Dec 2015	24265A_Mulcahy_Bay_ Dec2015.ecw / *MulcahyBay_Dec2015_ MGA55.ecw*	- / 0.1 m pixel size	-	0.0 m [N/A] (quoted absolute accuracy ±0.5m)	REFERENCE IMAGE (zero relative feature position error by convention) USED FOR ORTHO-RECTIFYING MULCAHY BAY AREA ON ALL AIR – PHOTOS. Digital original photo; Ortho-rectified by DPIPWE

					Original DPIPWE ortho file: *24265A_Mulcahy_Bay_Dec2015 .ecw*

Table 49: Digitised shoreline shapefiles produced for Mulcahy Bay (using ortho-photos listed in Table 48 above).

Date of air photo(s)	Shapefile	Shoreline digitised by	Comments
16th Feb 1961	MulcahyBay_MGA55_19610216.shp	Chris Sharples (2018)	Low resolution, no shadows, veg line fairly distinct, Veg line is mainly head scarp of slumped and deflating dune faces. Minor remnant old veg. patches scattered over deflating slump faces ignored. Deflating gullies and sand lobes on dune widespread.
19th Feb 1973	MulcahyBay_MGA55_19730219.shp	Chris Sharples (2018)	Moderate resolution, veg. line mostly distinct, some westerly shadows obscure line in places. Veg line is mainly head scarp of slumped and deflating dune faces. Minor remnant old veg. patches scattered over deflating slump faces ignored. Deflating gullies and sand lobes on dune widespread.
15th April 1975	MulcahyBay_MGA55_19750415.shp	Chris Sharples (2018)	Low resolution, long shadows on dune face allowed for but veg line sometimes indistinct; veg line is mainly head scarp of slumped and deflating dune faces. Minor remnant old veg. patches scattered over deflating slump faces ignored. Deflating gullies and sand lobes on dune widespread.
10th Mar 1984	MulcahyBay_MGA55_19840310.shp	Chris Sharples (2018)	Moderate resolution, some shadowing allowed for; veg lines distinct, Veg line is mainly head scarp of slumped and deflating dune faces. Minor remnant old veg. patches scattered over deflating slump faces ignored. Deflating gullies and sand lobes on dune widespread.
28th Jan 1988	MulcahyBay_MGA55_19880128.shp	Chris Sharples (2018)	Coarse resolution, some shadowing allowed for; veg lines distinct, Veg line is mainly head scarp of slumped and deflating dune faces. Remnant old veg. patches scattered over deflating slump faces ignored. Deflating gullies and sand lobes on dune widespread.

25th Jan 1989	MulcahyBay_MGA55_19890125.shp	Chris Sharples (2018)	Coarse resolution, veg lines distinct. Veg line is mainly head scarp of slumped and deflating dune faces. Remnant old veg. patches scattered over deflating slump faces ignored. Deflating gullies and sand lobes on dune widespread.
11th Mar 1996	MulcahyBay_MGA55_19960311.shp	Chris Sharples (2018)	Coarse resolution, some shadowing allowed for; veg lines distinct, Veg line is mainly head scarp of slumped and deflating dune faces. Remnant old veg. patches scattered over deflating slump faces ignored. Deflating gullies and sand lobes on dune widespread.
16th Nov 2002	MulcahyBay_MGA55_20021116.shp	Chris Sharples (2018)	Moderate resolution, good contrast, veg. lines distinct. Veg line is mainly head scarp of slumped and deflating dune faces. Remnant old veg. patches scattered over deflating slump faces ignored. Deflating gullies and sand lobes on dune widespread.
19th Feb 2008	MulcahyBay_MGA55_20080219.shp	Chris Sharples (2018)	Moderate resolution, good contrast, veg. lines distinct, some strong shadowing allowed for. Veg line is mainly head scarp of slumped and deflating dune faces. Remnant old veg. patches scattered over deflating slump faces ignored. Deflating gullies and sand lobes on dune widespread.
11th June 2010	MulcahyBay_MGA55_20100611.shp	Chris Sharples (2018)	High res, good contrast. Veg line is mainly head scarp of slumped and deflating dune faces. Remnant old veg. patches scattered over deflating slump faces ignored. Deflating gullies and sand lobes on dune widespread.
22nd Dec 2015	MulcahyBay_MGA55_20151222.shp	Chris Sharples (2018)	High res, good contrast. Veg line is mainly head scarp of slumped and deflating dune faces. Remnant old veg. patches scattered over deflating slump faces ignored. Deflating gullies and sand lobes on dune widespread.

TASMARC shore profile data tables

Table 50: GPS-surveyed co-ordinates of each TASMARC transect survey mark at Mulcahy Bay (see also map Figure 163). The survey marks are located at the landwards end of each transect, which runs seawards normal to the shoreline from each mark. Longitude and Latitude are decimal degrees and eastings and northings are metric co-ordinates of the Map Grid of Australia Zone 55 (MGA55, GDA94 datum).

Transect	Longitude	Latitude	Easting	Northing
730/303	145.733388425	-43.115741558	396954.00172	5225553.63
730/304	145.730113783	-43.111961322	396681.228	5225969.403
730/305	145.7267603	-43.11053117	396405.970	5226124.086

Table 51: Table of hinge points defined for each surveyed Mulcahy Bay profile (derived from original TASMARC survey data).

TASMARC profile number	Survey Date	Hinge Point distance offshore from survey mark	Hinge point height above AHD (metres)
730/303	01/12/2014	140.837	2.712
730/303	03/12/2015	140.854	2.338
730/303	07/12/2016	129.730	2.560
730/304	01/12/2014	130.341	2.307
730/304	03/12/2015	130.362	2.530
730/304	07/12/2016	130.384	2.368
730/305	01/12/2014	92.881	2.260
730/305	03/12/2015	96.075	3.037
730/305	10/12/2016	92.852	2.337

A1.3.8 Ocean Beach (central west coast)

Ocean Beach was chosen as a study site because the author had been aware of persistent shoreline recession there dating from at least 1998. Partly as a result of this the author participated as an external co-advisor to Hannah Walford's 2011 honours study of Ocean Beach (Walford 2011). This subsequent Ph.D. project has nearly doubled the number of air photo dates used by Walford and has considerably extended her analysis.

Locality and general description

Ocean Beach is the longest and most accessible beach on the west coast of Tasmania, located less than 10 kilometres from the town of Strahan. The study area comprised the southern half of the beach (~18 kilometres length) because over much of the air photo period the northern half of the beach was dominantly backed by unvegetated transgressive dunes, so that at most air photo dates a shoreline position would not be identifiable by the method adopted for this study (see Section A2.1.3).

Geomorphology and process environment

Geomorphic description

Ocean Beach is the longest (32 km) sandy barrier beach on the mostly rocky west coast of Tasmania and is exposed to the most energetic and stormy wave climate of any Australian coast (Hemer 2010; Hemer, Simmonds & Keay 2008). The west-facing beach is strongly compartmentalised by large rocky headlands beyond its north and south ends (Davies 1973). The sandy barrier has developed across the mouth of the large deep structural trough of Macquarie Harbour (Forsyth, Quilty & Calver 2014), which has a permanently open tidal channel at the southern end of the beach. Macquarie Harbour receives several large rivers including the King and Gordon Rivers whose large discharges help keep the tidal channel at the southern end of the beach permanently open.

Ocean Beach is a high energy multi-bar wave-dominated beach classified as morpho-dynamically Intermediate by (Short 2006b). The surf zone is dominated by a double- to in places triple-bar system up to 600 metres wide cut by the largest rips of any Australian beach. Ocean Beach is micro-tidal, with a spring and neap tidal range of about 0.9 and 0.5 metres respectively (Short 2006b). At least since 2011 (when the writer began regular visits to this beach), much of the southern half of Ocean Beach except its accretionary southern-most tip has been a low, wet and eroded beach with a Mean High-Water line at or very close to the dune scarp backing the beach.

Most of the beach is directly backed by vegetated dunes with eroding seawards scarps up to 30m high exposing palaeosols and some peat lenses (see Figure 174). These dunes are not foredunes in the sense of Hesp (2002) but rather the actively receding fronts of old transgressive and parabolic dunes (Banks, Colhoun & Chick 1977), for which a Holocene age is indicated by limited soil profile development, well-preserved morphology, and radiometric dates for inter-bedded peat. At the time of writing (2019) established and incipient (accreting) foredunes are only present at the southern-most tip of the beach. The earliest (1947-9) air photos show extensive unvegetated transgressive dunes and deflation basins behind parts of the Ocean Beach study area, however much of these have now stabilised through establishment of a vegetation cover including the introduced *Ammophila arenaria* ('marram grass'). Unvegetated transgressive dune fields currently remain active further north beyond the study area. Palaeosols are commonly exposed in the scarped dune fronts (Figure 174) and their exposure is indicative of a degree of dune front recession unprecedented since at least the last phase of dune mobility that buried them (pre-1947 for most of the study area). Peats up to several metres thick exposed in the scarps at a few locations are interpreted as swamp or lake peats deposited in former back-dune swales.

Figure 174: Dune-front erosion scarp at Ocean Beach. A typical recent wave-eroded dune scarp with some slumping (adjacent TASMARC transect 730/109). The vegetation line at the top of the scarp was digitised over air photos as the shoreline whenever the shoreline was receding, with care being taken to avoid confounding this with slumped vegetation clumps as seen here. The visible palaeosol has not been dated, however the substantial period that it would have taken to form and be buried is the minimum period since this shoreline was last eroded back as far as it is. Photo: Chris Sharples (2013).

Swell wave climate

Ocean Beach is open to the Southern Ocean and thus receives persistent westerly and south-westerly winds and swells with low inter-annual variability attributed to the Southern Annular Mode (SAM; Marshall 2003). Monthly average significant wave heights (H_s) range between 2.6 m in November and 3.4 m in September recorded over a 20-year (1985-2006) period by a wave-rider situated in 100 m water depth at offshore at 42° 9.0' S, 145° 1.0' E, 15 km directly offshore from Ocean Beach (Hemer, Simmonds & Keay 2008). Short (2006) characterises typical wave heights in the near-shore surf zone at Ocean Beach as 3 – 5 metres high, and occasionally reaching 18 metres high further offshore at the wave-rider buoy.

Hemer (2010) and Hemer, Church and Hunter (2010); Hemer, Simmonds and Keay (2008) have described the swell wave climate reaching Ocean Beach, based on data from the adjacent Cape Sorell wave-rider buoy, satellite altimetry and global ocean wave models. The Cape Sorell wave-rider buoy is located about 15 km directly offshore from Ocean Beach and is Tasmania's only long term (since 1985) observational wave climate record, measuring combined swell and locally-generated wind wave heights, but not wave direction.

Key swell wave parameters for Ocean Beach are given below:

Table 52: Key swell wave climate parameters for Ocean Beach study area, from the CAWCR wave hindcast 1979-2010 by the Australian Bureau of Meteorology and CSIRO Australia 2013 (Durrant et al. 2013). These figures apply to the closest inshore ~5km grid cell to the beach, which is centred about 6.5 km offshore (west) from the middle of the Ocean Beach study area and receives slightly lower waves than adjacent more exposed hindcast cells, probably due to wave refraction and attenuation around Cape Sorell. Note that whereas the winter wave direction indicated is significantly more south-westerly than the summer wave directions, this is also anomalous compared to adjacent more exposed hindcast cells which receive more westerly winter wave directions as expected from the SAM influence on this coast. The anomalous more SW winter wave directionality may also be related to wave refraction effects around Cape Sorell.

	Annual	Summer (DJF)	Winter (JJA)
Average Significant wave height (m)	2.43	2.07	2.74
Average Maximum wave height (m)	5.33	4.62	5.89
Average Mean wave direction (ºT)	241	246	227

Ocean Beach receives a persistently south-westerly swell from the Southern Ocean where some of the largest waves of the global ocean are generated during extra-tropical cyclonic storms as far south as 55-60°S (Hemer, Simmonds and Keay (2008) record annual return significant wave heights (Hs) of 8.71 m at the Cape Sorell wave rider buoy). As nearly the most southerly point on the southern Australian continental margin, Ocean Beach (42°S) receives steeper waves, higher mean significant wave heights (peaking in September, after the southern winter) and more westerly wave directions than most other parts of that margin, indicative of closer proximity to the Southern Ocean wave-generation zone (Hemer, Simmonds & Keay 2008). Ocean Beach may receive the highest swell wave energy of any Australian beach, since all beaches to its south are much shorter and so lose more wave energy through refraction against their bounding rocky headlands (Davies 1973). Highly energetic extreme wave events and a predominance of swell over local wind sea states are a characteristic of the wave climate at Cape Sorell and Ocean Beach (Hemer, Simmonds & Keay 2008).

The primary mode of swell wave climate variability (in both wave height and direction) along the southern margin of Australia including western Tasmania is correlated with the Southern Annular Mode (SAM) (Hemer 2010) (Hemer, Simmonds & Keay 2008). Annual cycles in SAM result in the Southern Ocean storm belt moving south during the southern summer resulting in more south-westerly waves reaching western Tasmania, and north in winter with waves arriving from more westerly directions (Hemer, Simmonds & Keay 2008). Mean swell direction variability is limited to approximately 20º at Ocean Beach (Durrant et al. 2013) (Table 52), which greatly reduces the potential for beach rotation compared to eastern Australian beaches dominated by the El Nino Southern Oscillation (ENSO) e.g., Mortlock et al. (2017).

A significant trend towards the positive (higher index) phase of the SAM has been observed since the mid-1960s (Hemer 2010; Hemer, Simmonds & Keay 2008; Marshall 2003), resulting in an increase in wave heights (Hs) in the far Southern Ocean (south of ~48°S) and an anti-clockwise rotation of wave directions associated with a southwards movement and intensification of the Southern Ocean storm belt (Hemer, Church & Hunter 2010). Observational confirmation of this near Ocean Beach is lacking due to the Cape Sorell wave-rider buoy being incapable of measuring wave direction. However, 17 years of data from between 1985 to 2008 showed no increase in storm wave (extreme height) event frequency over that period and in fact show a non-significant decrease (Hemer 2010). Altimeter data also showed a non-significant negative trend in wave height (mean Hs) west of Tasmania over the same period (Hemer 2010; Hemer, Church & Hunter 2010). This may reflect the fact that whereas the southwards drift of SAM results in generation of higher waves, these lose more energy travelling the increased distance northwards to western Tasmania (M. Hemer *pers. comm*.).

These results indicate that increases in wave height (mean Hs) and storm wave event frequencies have so far been limited to latitudes south of 50°S and are unlikely to be drivers of changing shoreline behaviour to date at Ocean Beach. However, the same southwards drift of SAM is expected to have

resulted in swell-wave directions in western Tasmania becoming more frequently more south-westerly and less westerly than previously.

Swell-wave transformation at the shoreline

The transformation of the south-westerly swell waves as they approach the shoreline at Ocean Beach across the unusually-wide 600m wide multi-bar surf zone (Short 2006b) cannot be confidently modelled because of the lack of high-resolution offshore bathymetry for this remote coast (the best available bathymetry appears to be 100 metre contours compiled by Geoscience Australia). However, it is reasonable to expect that swell waves approaching from south-westerly to north-westerly directions would be significantly straightened and arrive mostly parallel to the shoreline. If this assumption is correct, it has at least two consequences, namely:

1. Wave direction variability of the order of 20° or more on annual to inter-decadal time scales is likely to result in little change to (mainly shore-parallel) swell wave directions at the shoreline.
2. Mostly shore-parallel swell wave directions at the shoreline mean that swell waves do not explain the persistent southwards longshore drift at Ocean Beach, nor would moderate changes in offshore wave direction significantly affect the longshore drift on annual to interdecadal time scales.

Wind (wind-wave) climate

Westerly winds associated with SAM on the Tasmanian west coast are the strongest and most persistent prevailing winds of any Australian coast (Grose et al. 2010), exposing that coast to strong locally-generated waves (seas) and storms. Long-term weather records are available from the Cape Sorell lighthouse 5 kilometres southwest of Ocean Beach and Strahan Airport 2 km inland. Australian Bureau of Meteorology wind data from nearby Cape Sorell recorded annual average onshore (westerly) wind speeds in the range 7.0 to 8.0 metres/second over the period 1992 – 2015 (Figure 175). The west coast beaches including Ocean Beach are exposed to the greatest frequency and magnitude of locally produced westerly wind-driven seas and storms in Tasmania (Davies 1973).

Changes in onshore wind speeds and directions could change the local wind-wave climate and wave setup against the shore and are also the key factor in aeolian sand transport in mobile transgressive dunes. Onshore wind data for Ocean Beach and some other west coast areas has been examined primarily as a proxy for locally-generated wind waves (or 'seas'), for which there is no direct measure at Ocean Beach (albeit they are a component of the waves measured by the Cape Sorell wave rider buoy).

For this study, synoptic (typically 3-hourly) and daily extreme wind data records up to 2015 were obtained from the Australian Bureau of Meteorology for coastal weather stations at Cape Sorell and Strahan Aerodrome close to Ocean Beach, Maatsuyker Island near Tasmania's south-western tip, and for Cape Grim in the north-western tip of Tasmania. This data was explored using *Matlab*™ software.

Wind climate drives locally generated wind-waves and near-shore wind-wave setup which may cause shoreline erosion, as well as landwards aeolian loss of sand in mobile transgressive dunes. Hence wind climate variability may result in shoreline position change. The west coast of Tasmania including Ocean Beach is dominated by westerly winds whose variability is related to the SAM (Marshall 2003). Evidence from aeolian sediments show that these westerly wind flows have varied in intensity on centennial and millennial time scales over at least the last 20,000 years, and that present-day westerly winds are as strong now as at any time in the last glacial climatic cycle (Shulmeister et al. 2004). Some regional studies of the SAM have indicated increased wind speeds over the Southern

Ocean by about 20% since circa 1990 (Gillett, Kell & Jones 2006; Hemer, Church & Hunter 2010; Hurrell & Van Loon 1994; Thompson & Solomon 2002).

Analyses of historical trends in measured wind speed records in the Australian region to date have generally been inconclusive (McVicar et al. 2008; Troccoli et al. 2012; Walsh et al. 2016), however a national study (Troccoli et al. 2012) identified instrument variability as a major influence on apparent wind speed trends recorded, with higher (10m) anemometers showed a mostly positive trend in wind speeds across Australia for the 1975 –2006 period, whereas lower (2m) instruments showed a mainly negative trend. Several other factors including sheltering, local topography and data continuity also affecting data quality, with sudden steps in data records being common and indicative of instrumentation changes rather than real wind changes.

Cape Sorell and Strahan Aerodrome weather stations are both within a few kilometres' seawards and landwards respectively of the Ocean Beach study area, however synoptic wind observations from these stations are subject to a 21-year data gap at Cape Sorell, with varying recording protocols and step changes in the data at both sites suggestive of instrument changes. The best quality data at both sites (1993 – 2015) is weakly suggestive of onshore (westerly) mean wind speed increase trends (Figure 175).

However, directional wind data is consistent across both weather stations and both observational periods at Cape Sorell. The strongest feature of the directional record is dominantly north-westerly to south-westerly winds (consistent with the Southern Annular Mode), however a notable secondary feature across the records is a strong northerly wind component of unknown cause (Figure 176). The dominant south-westerly to north-westerly winds can be inferred to drive dominantly onshore local wind waves at Ocean Beach, which will often be roughly co-incident with the south-westerly swells arriving at Ocean Beach and contributing additional wave setup. The strong northerly wind component will drive local wind-waves in a southerly alongshore direction, providing a possible explanation for the strong net southerly littoral drift of sand along Ocean Beach (see *Sand transport and budget* above).

Since the whole west coast of Tasmania is exposed to the same SAM-influenced wind climate as Ocean Beach, major trends in other credible wind records for the Tasmanian west coast may plausibly be inferred to be indicative of dominant wind trends at Ocean Beach. A study by Kirkpatrick et al. (2017) interpreted Bureau of Meteorology wind records for Maatsuyker Island (on the south-western Tasmanian coast) as indicating an increase in western Tasmanian coastal winter wind speeds over the period 1970 – 2015. That study correlated this with variability in the SAM, reflected in a recent strengthening of the high-pressure zone to the north of Tasmania in winter and a decrease in pressures to the south.

The weather station at Cape Grim (at the northern tip of the west coast) provides a high-quality west coast wind record from 1988 onwards since it is part of the global Baseline Air Pollution Stations network and is managed rigorously by the World Meteorological Organisation with Australia's Bureau of Meteorology (BoM) and Commonwealth Scientific and Industrial Research Organisation (CSIRO). The synoptic wind record from Cape Grim shows a dominant westerly to south-westerly directional component comparable to that at Cape Sorell and Strahan Aerodrome, with a sub-ordinate easterly component (Figure 177). These were plotted separately as approximately 1-year moving averages (Figure 177). The easterly wind speeds show a strong annual (seasonal) cycle with only a weak increasing linear trend. The westerly wind speeds show a less regular inter-annual cycle with sub-ordinate seasonal cycles, and a strong linear trend to higher wind speeds over the record period (R^2=0.6201). The same significant linear trend to higher wind speeds is also evident in the annual means of the synoptic westerly wind speeds at Cape Grim (Figure 178).

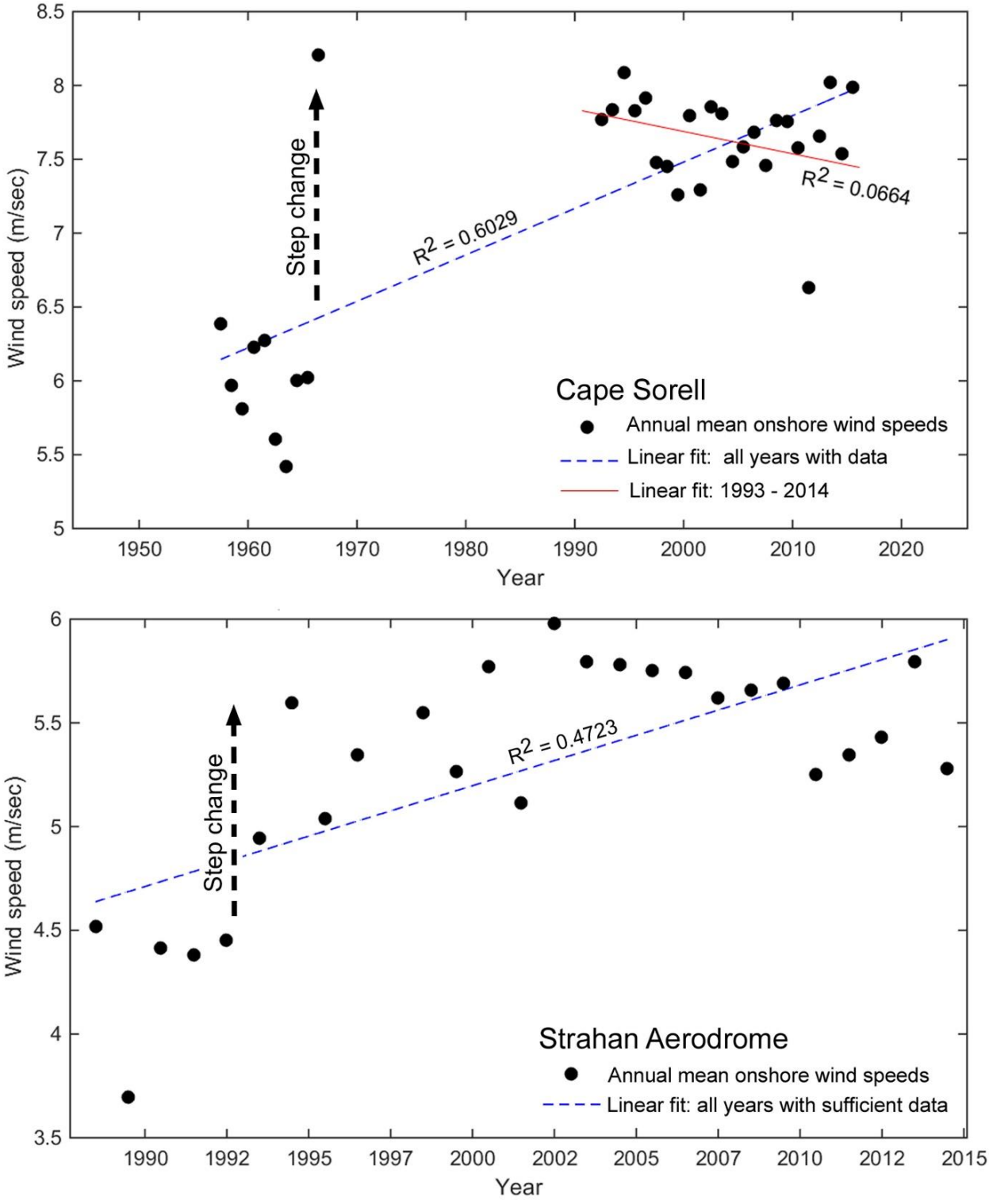

Figure 175: Annual means of synoptic onshore wind speed records from Cape Sorell and Strahan Aerodrome: Annual means were calculated from data records for onshore wind directions only (175° T to 20°T). These are the two wind records closest to Ocean Beach. Apparent wind speed increases over all available data are interrupted by step changes which as cautioned by (Troccoli et al. 2012) are suggestive of instrumentation changes, and by a long (21 year) data gap at Cape Sorell. The most recent data at both sites (1993-2015) is weakly suggestive of mean wind speed increases (if one year's anomalous data is ignored at Cape Sorell), hence is consistent with but does not clearly demonstrate increasing wind speeds over recent decades. Plotted from original observational data supplied by the Australian Bureau of Meteorology (2016).

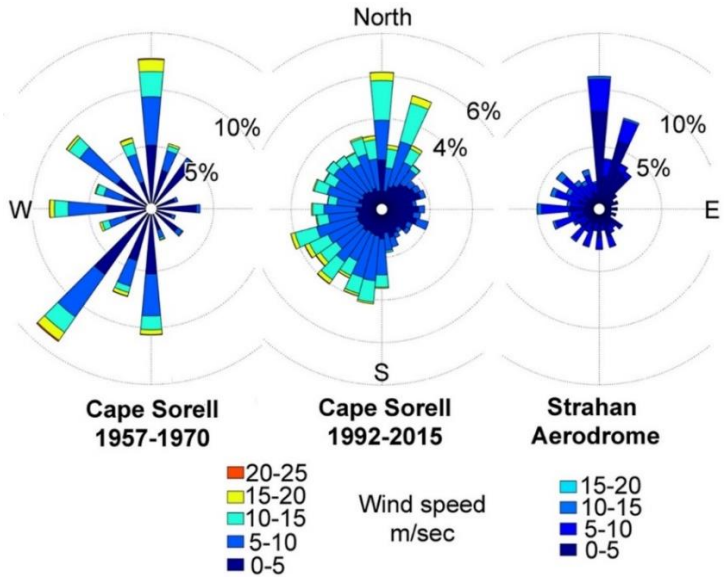

Figure 176: Synoptic wind roses – Cape Sorell & Strahan Aerodrome: Synoptic wind direction and speed data presented as wind roses for Strahan Aerodrome (all data 1975 – 2015) and Cape Sorell (plotted separately for early data 1957-1970 and later data 1992-2015). Wind directions are presented as True degrees, wind speeds are metres per second. Whereas the westerly and south-westerly wind components are predictable for western Tasmanian sites exposed to SAM-driven weather systems such as Ocean Beach, the strong northerly wind component in all three wind records is an unexpected but persistent feature of the Ocean Beach region. Plotted from original observational data supplied by the Australian Bureau of Meteorology (2016).

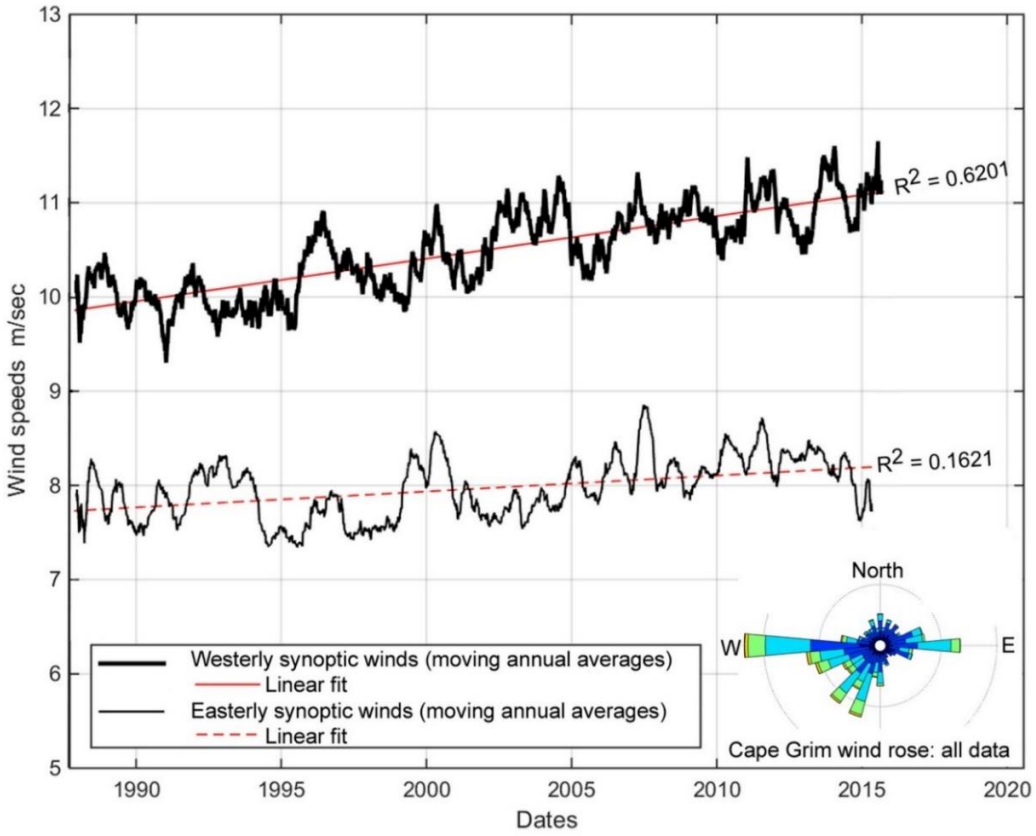

Figure 177: Moving annual averages on easterly and westerly synoptic wind speed records from Cape Grim. Synoptic (3-hourly) wind speed data from 1988 to 2015, showing dominant seasonal (annual) variability in the easterly winds, but also longer inter-annual cycles in the westerly winds. Original observational data from the Australian Bureau of Meteorology (2016).

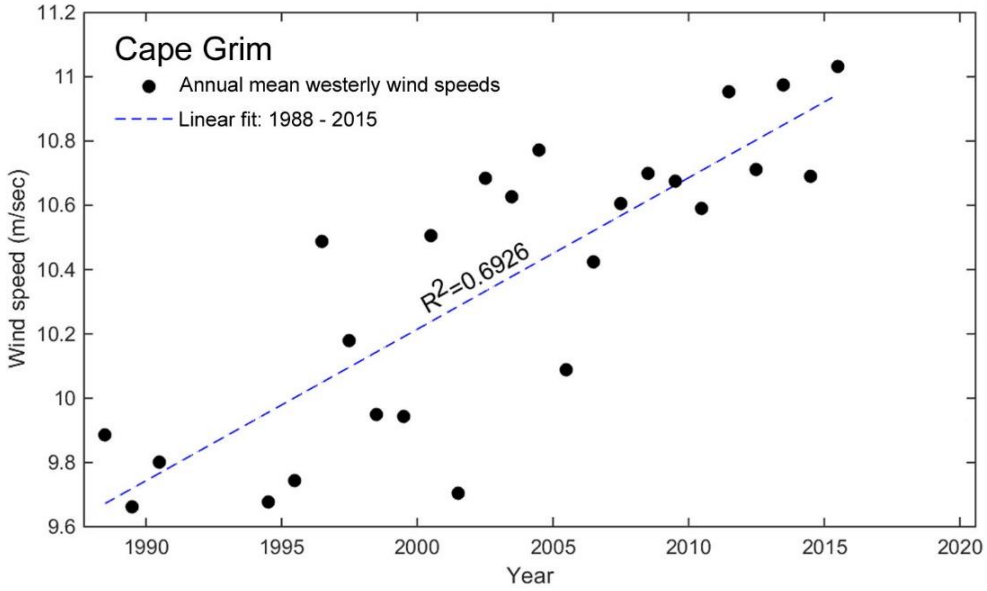

Figure 178: Annual means of synoptic westerly wind speed records from Cape Grim. Annual means were calculated only from data records for westerly wind directions equivalent to the onshore directions at Ocean Beach (175° T to 20°T). Means were calculated for all years with a minimum of 1500 onshore synoptic wind observations per year (1988-2015), excluding 1991-93 when higher wind speeds were not recorded. A trend of rising westerly wind speeds over the observational period appears strongly supported by this data. Plotted from original observational data supplied by the Australian Bureau of Meteorology (2016).

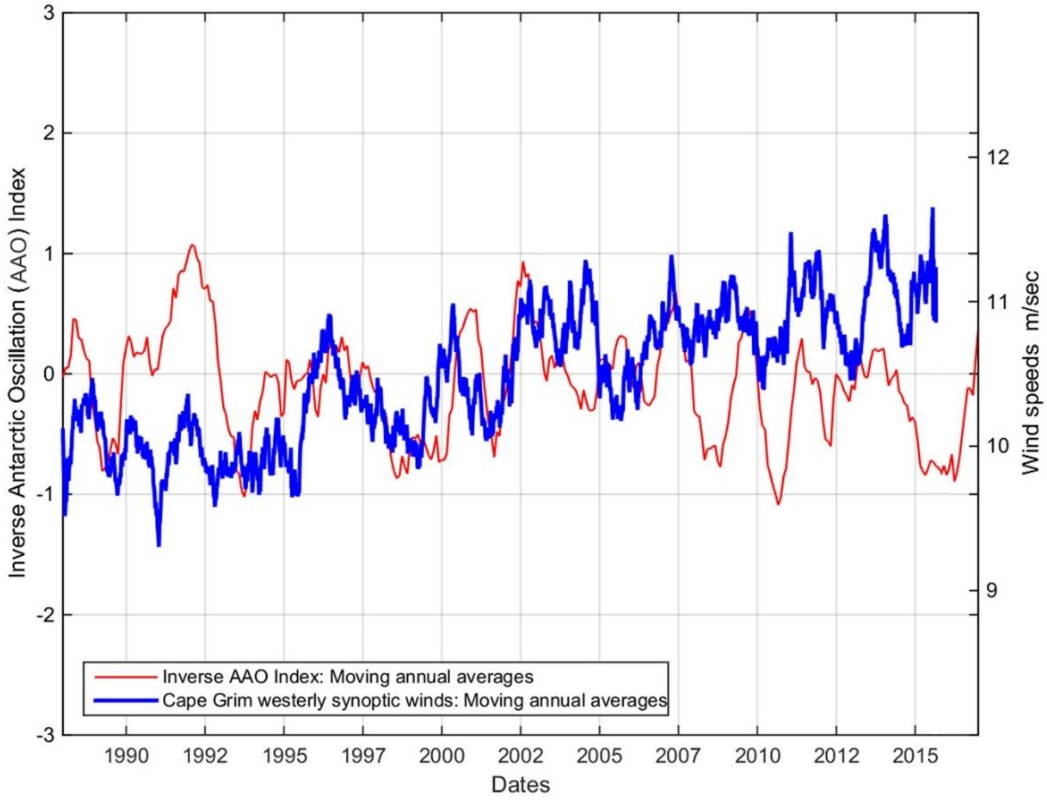

Figure 179: Moving annual averages on westerly synoptic wind speeds records for Cape Grim and the Inverse Antarctic Oscillation (AAO) Index. Visual inspection suggests some correlation between these datasets. With linear trends removed from both datasets a correlation co-efficient of R^2=0.26 was obtained. Original synoptic (3-hourly) wind data from Cape Grim was supplied by the Australian Bureau of Meteorology (BoM), and monthly AAO indices were obtained from the National Oceans and Atmospheric Administration (NOAA) website.

There is no significant correlation between the inter-annual variability in the westerly wind component and the Southern Oscillation Index (SOI), reflecting the limited influence of ENSO on Tasmanian coasts (Burgette et al. 2013). However, with linear trends removed, the westerly wind variability shows a weak correlation (R^2=0.26, 95% confidence 0.16-0.36, p<0.0001) with the inverse of the Antarctic Oscillation Index (AAO) measure of SAM (Figure 179). This could reflect some influence of SAM on the westerly winds.

The clear trend to increasing westerly wind speeds in the high-quality Cape Grim wind record over the last three decades supports the interpretation that the more equivocal Cape Sorell and Strahan Aerodrome records do indeed reflect an increasing westerly and south-westerly wind speed trend at Ocean Beach over a similar period, since these winds are responding to the same driving processes (the SAM) as the westerly Cape Grim winds.

Sand transport and budget

Understanding of sand sources, transport processes and sinks at Ocean Beach is inferred solely from visible geomorphic evidence and shelf sediment transport modelling only. No attempt has been made to quantify the sand budget, nor are detailed studies of the adjacent offshore shelf sedimentary environment or history available for this region.

The large quantity of siliceous and low-carbonate sand present in the Ocean Beach barrier was substantially derived from glacio-fluvial outwash during Pleistocene glacial phases, when the Henty, King and other rivers brought large quantities of quartzose sand down to the exposed continental shelf from the nearby heavily-glaciated West Coast Range (Banks, Colhoun & Chick 1977) p. 46. Large quantities of the glacial outwash sands are inferred to have been re-mobilised landwards from the exposed continental shelf by wind transport during glacial low sea stands, and by wave action during post-glacial marine transgressions.

Dominantly southwards littoral drift along the full length of Ocean Beach in the lower beach face and surf zone is demonstrated by geomorphic indicators including perched cliff-top dunes at the depleted north end of the beach (Banks, Colhoun & Chick 1977) p. 46, dominantly southwards deflection of the Henty and Little Henty River mouths as they cross Ocean Beach demonstrated by air photos from 1947 to 2011 (see Table 54), an accretionary beach and foredune zone receiving considerable quantities of sand at the southern tip of the beach only, and the forcing of the tidal channel mouth of Macquarie Harbour against a bedrock headland at the southern extremity of the beach. This is a major sand transport pathway at Ocean Beach and a large flood-tide delta just inside the permanently-open tidal entrance of Macquarie Harbour is the final sink for the southwards-drifted sand. Considerable accommodation space remains available in the harbour to sequester additional sand.

The very coarse bathymetry available for Ocean Beach (Geoscience Australia: 100m contour interval) currently precludes high resolution wave transformation studies to model causes of the littoral drift, however the dominantly southwards direction of that drift is its most critical characteristic for this study. The NNW – to SSE coastal orientation and the limited directional variability of the westerly to south-westerly swell (see below) should in principle drive a northwards littoral drift along most of Ocean Beach. However, this is not observed, and it is likely that the unusually wide (600 m) multi-bar surf zone trains swell waves to reach the shore oriented parallel to the shoreline (see *Swell wave climate* below). In this case the swell waves will not be significantly driving alongshore drift, leaving wind-waves generated by northerly winds as the only known mechanism at Ocean Beach that may be driving the observed southwards longshore drift. Northerly winds are a feature of the local wind climate (see Figure 176) and are sufficiently frequent and strong enough that wind-waves locally generated by these winds may drive the net southwards drift. Ocean currents are unlikely to affect sand transport in the littoral (surf) zone.

Landwards loss of deflated sand in transgressive dunes is a secondary sink albeit air photo evidence shows the active unvegetated transgressive dunes were considerably more extensive in the 1940s and

have subsequently become vegetated and stable over considerable areas. This is inferred to be largely owing to colonisation by introduced marram grass: Cullen (1998), so the volume of sand lost from the beach by landwards aeolian transport has probably decreased over the Twentieth Century.

Air photo evidence of shoreline stability or progradation prior to 1980 at Ocean Beach study area (Figure 183) implies that sand inferred to be continually lost into the known sinks via persistent southwards littoral drift must have been fully replaced from some source. However western Tasmanian rivers are not transporting significant amounts of sand-grade sediment today except where heavily disturbed by mining (Nanson, Barbetti & Taylor 1995), and there is no evidence of significant present-day supply of fluvial sands to Ocean Beach. The well-embayed location of the beach between long rocky coasts makes significant alongshore sand drift into or out of the embayment unlikely (Davies 1973). The only plausible known present-day sand source is sand actively driven onshore from the inner continental shelf by bottom currents associated with the large south-westerly swell (as indicated by shelf sand mobility modelling: Harris et al. (2000) in: Harris and Heap (2014), p. 538.

Reconstructed sea-level data

There are no long-term tide gauge records for the west coast of Tasmania, with the best record for the region being a fragmentary record for Granville Harbour (about 30 kilometres north of Ocean Beach) totalling only 4.2 years of actual records between 1974 and 1994 (Sharples 2006). Better tide gauge records exist for northern and south-eastern Tasmania, but those coasts are exposed to significantly different oceanographic environments hence their sea-level histories cannot be assumed to be comparable to Ocean Beach. Instead, the regional sea surface height (SSH) reconstruction of Church and White (2011), and that prepared by the method of Hamlington et al. (2011), were used to compare sea-level change with shoreline behaviour at Ocean Beach (Figure 180, Figure 181). Both reconstructions include the effects of drivers of sea-level variability other than GMSLR, including the El Nino Southern Oscillation (ENSO) which is an important factor in more northerly parts of Australia. However Tasmanian sea-levels are less influenced by seasonal and inter-annual variability related to ENSO than are more northerly parts of Australia (Burgette et al. 2013), hence there is less masking of GMSLR variability from this cause on Tasmanian coasts including Ocean Beach than elsewhere in Australia. The amplitude of the interannual signal in the Ocean Beach SSH reconstructions is ~10 to 80 mm (see Figure 180, Figure 182), consistent with sites having little exposure to larger modes of climate variability such as ENSO (White et al. 2014).

The Church & White reconstruction integrates long-term tide gauge and 1993-onwards satellite altimetry data using empirical orthogonal functions (EOFs) to represent regional patterns of variability on a 1° x 1° latitude-longitude grid. Their data reconstructed monthly SSH data without inverse barometer correction and with seasonal (annual) noise removed for the period 1950 to 2012 at the closest grid cell to Ocean Beach, centred at 42.5° S, 144.5° E.

The Hamlington *et al*. reconstruction uses cyclostationary empirical orthogonal functions (CSEOFs) to reconstruct SSH history for the period 1900-2013 on a 0.5° x 0.5° latitude-longitude grid. Their reconstructed monthly SSH data was used for the closest grid cell to Ocean Beach, centred at 42.25° S, 144.75° E. Seasonal noise was removed using annual moving averages.

The Church & White and Hamlington *et al.* SSH reconstructions were compared by plotting them against each other and comparing their power spectra (Figure 180). Visual comparison shows good coherence between the two reconstructions with seasonal noise removed, and the power spectra show that their variability is mostly coherent at inter-annual to decadal times scales but incoherent at time scales of a year or less (which is a consequence of the differing reconstruction methods).

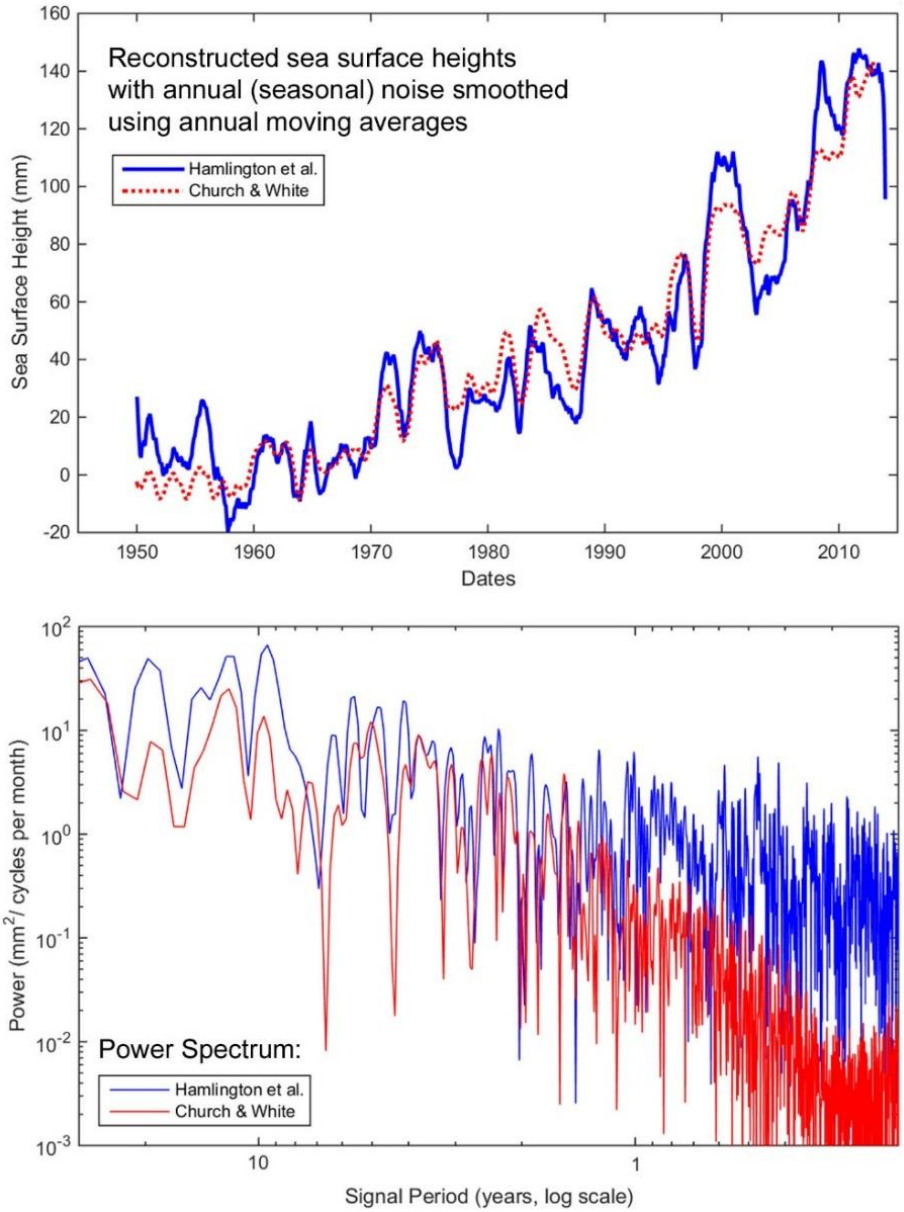

Figure 180: Comparison of Sea Surface Height (SSH) reconstructions for Ocean Beach. The top plot shows the similarity between the Hamlington et al and Church & White SSH reconstructions for the closest grid cells to Ocean Beach from 1950 onwards. Seasonal noise has been removed from both reconstructions using annual moving averages. The SSH's are arbitrarily zeroed for visual comparison, and the Hamlington et al. data has been interpolated onto the slightly different time intervals used by Church and White. The lower plot compares the power spectrum for each reconstruction, demonstrating two reconstructions are mostly coherent at inter-annual to decadal time scales but incoherent on annual and shorter time scales.

Given that the beach history data (aerial photography and beach profiling) is an inter-annual to decadal time series, and that the variability of both the Church & White and the Hamlington *et al.* reconstructions show good coherence at these time scales, further exploration of relationships between beach and sea-level history was conducted using the Hamlington *et al.* reconstruction because of its finer spatial resolution.

The rates of sea-level rise reconstructed for Ocean Beach by Church and White (2011) and by the method of Hamlington et al. (2011) are comparable to GMSLR: linear fits to the Church & White and Hamlington reconstructions over the period 1966-2009 yield SSH rises of 2.13 mm yr^{-1} and 2.21

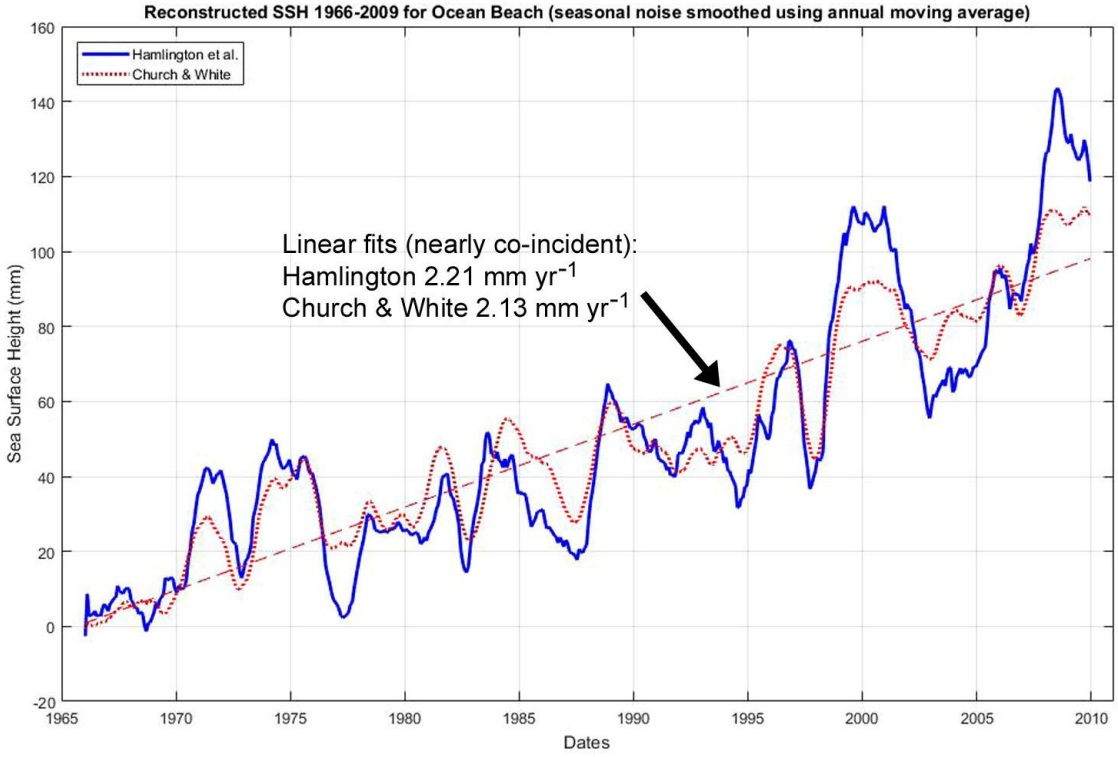

Figure 181: Comparison of reconstructed Sea Surface Height (SSH) histories for the closest grid cell to Ocean Beach from 1966 to 2009. The two reconstructions (Church & White 2011; Hamlington et al. 2011) have seasonal noise removed by plotting the annual moving average, and linear fits are plotted to the smoothed 1966 – 2009 reconstructions for comparison with the GMSLR linear rate of 2.0 ±0.3 mm yr^{-1} over the same period (White et al. 2014).

mm yr^{-1} respectively (Figure 181), which is comparable with the global-average rise of 2.0 ± 0.3 mm yr^{-1} over the same period (White et al. 2014). This is similar to rates measured from the oldest tide gauge record available for Tasmania (Hunter, Coleman & Pugh 2003), which used historic and modern tide gauge records to estimate that a mean rate of local relative sea-level rise between 0.70 mm/yr^{-1} and 1.30 mm/yr^{-1} has occurred at Port Arthur on the south-eastern Tasmanian coast between 1841 and 2002. Given the lack of a longer-term regional explanation for this rise (e.g., VLM), it is inferred (Hunter, Coleman & Pugh 2003) to have commenced during the 1800s as part of the recent sea-level rise observed at long-term Northern Hemisphere tide gauges. The same assumption is made for the recent sea-level rise reconstructed for Ocean Beach.

Figure 182 (below) plots the air photo-derived shoreline change history of the Ocean Beach study area (excluding southernmost tip) against the Hamlington *et al* reconstructed SSH history over the same period.

Visual comparison of the shoreline vs. SSH histories (Figure 182) yields the following observations:

1. The Ocean Beach SSH history is characterised by net progressive sea-level rise at decadal time scales prior to circa 1950 and after circa 1970, but no net rise over the two decades from 1950 to 1970. This period corresponds to the first two decades of the shoreline history record when shoreline position showed little change compared to later decades (with multiple shorter-term erosion and recovery episodes assumed to be masked by the limited air photo frequency). The Ocean Beach sea-level rise pause is consistent with Jevrejeva et al. (2006) and Church and White (2011) who previously reported a 1960s pause in GMSLR. Watson (2011), White et al. (2014) and Gehrels et al. (2012) also used regional Australian SSH records to demonstrate sea-level rise pauses after 1950 and before 1990, with some

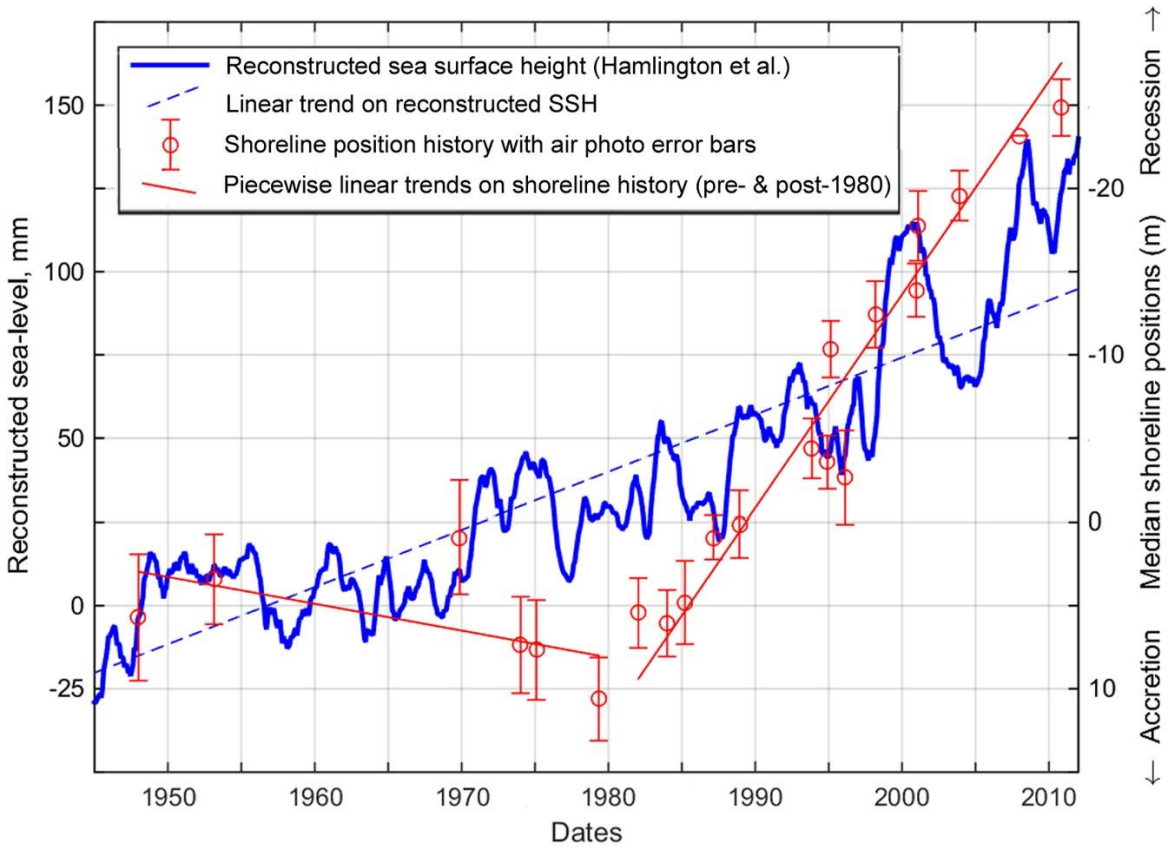

Figure 182: Shoreline position history at air photo dates and reconstructed SSH history. Error bars show the mean air photo position errors at each air photo date. A single trend line is fitted to the SSH history, and piecewise linear trends are fitted to the shoreline history pre- and post-1980.

differences in timing probably attributable to regional differences in oceanographic forcing (White et al. 2014).

2. The shoreline position prograded significantly during the decade 1970-1979 despite a net rise in sea-level over this period (which in principle might be expected to cause shoreline recession). A plausible explanation is that enhanced foredune sand trapping associated with marram grass expansion after its artificial introduction during the 1950s (Cullen 1998) dominated shoreline behaviour during this period, along with a presumed dearth of major erosive storms (in contrast to eastern Australia whose coast experienced several major erosion events during the same period).

3. The marked change in long-term shoreline behaviour which occurred between the air photo dates of 5th May 1979 and 16th Jan 1982 - from relatively stable or prograding to continuously receding at inter-decadal time scales – was a relatively rapid change that does not correspond to any apparent comparable variability in the SSH history (which shows a progressive rising trend for at least a decade prior to the change in shoreline behaviour). The most plausible explanation for the abrupt switch in shoreline behaviour is that it could have been triggered by a large storm erosion event or cluster of events (however long-term change from shoreline stability or progradation to persistent recession requires further explanation).

4. The period of nearly uninterrupted shoreline recession from 1982 until 2010 (and continuing to 2018: Figure 183) corresponds to a period of continuing progressive sea-level rise at the inter-decadal time scale.

Numerical data exploration of the shoreline vs. SSH histories (Figure 182) yields the following results:

The SSH and shoreline position histories show significant overall rising and receding trends (respectively) over the air photo record period, which yields a high Pearson correlation co-efficient between the two datasets; for raw monthly SSH, $r^2 = 0.84$ (95% confidence interval 0.64-0.93, p-value < 0.0001), and for yearly moving-averaged SSH, $r^2 = 0.83$ (95% confidence interval 0.62-0.93, p-value < 0.0001). The effect of air photo error margins on the un-detrended correlations was tested using random (Monte Carlo) resampling of shoreline positions at each air photo date within 1 standard deviation of the measured (mean) error margins; 5000 iterations yielded a strong peak in r^2 values between 0.80 and 0.85 implying the relatively small error margins have negligible effect on the correlation found.

The datasets were detrended by subtracting a single linear trend from the SSH, and piecewise linear trends from the shoreline history data pre- and post- the marked change of shoreline behaviour around 1980 (see linear trend lines on Figure 182). The detrended datasets yield only a low correlation co-efficient: for raw monthly SSH, $r^2 = 0.04$ (95% confidence interval -0.40-0.47, p-value = 0.8567), and for yearly moving-averaged SSH, $r^2 = -0.11$ (95% confidence interval -0.52-0.34, p-value = 0.6287).

These observations and correlations are consistent with a first-order causal relationship between sea-level rise and shoreline recession on inter-decadal time scales, as is expected from first principles (Bruun 1962). However, the detrended datasets provide no evidence of correlation between SSH and shoreline position variability at shorter inter-annual time scales. Notably, the marked and rapid change in long-term shoreline behaviour which occurred between the air photo dates of 5th May 1979 and 16th Jan 1982 - from relatively stable or prograding to continuously receding – does not correspond to any comparable variability in the SSH history.

Vertical land movement

There are no nearby estimates of Vertical Land Movement (VLM) for Ocean Beach. Well-preserved and cosmogenically-dated marine and river terraces at nearby Macquarie Harbour and in the Sorell River valley (c. 10 – 40 km south-east of Ocean Beach) record Pleistocene uplift rates averaging 0.1 m ka^{-1} (Houshold, Chappell & Fifield 2006). However, this evidence cannot be inferred to indicate contemporary VLM rates.

Current and ongoing geodetic studies of Tasmania have yet to resolve disagreements between GNSS derived estimates of VLM at Burnie and Hobart ranging between 0.0 to -1.0 mm yr^{-1}, and geophysical models indicating subsidence in the range of -0.1 to -0.2 mm yr^{-1} (see details in Chapter 2 Section 2.5.4 above). However, for the purpose of this thesis, there is no evidence suggesting that VLM is a significant signal in Tasmanian relative sea levels.

There is no anthropogenic extraction of sub-surface fluids or other known processes such as significant seismic activity likely to cause significant VLM at Ocean Beach, hence additional local subsidence is unlikely.

Artificial interferences

Ocean Beach is largely free of artificial disturbances that may affect geomorphic processes at the beach face and dune front. The backshore area is unsettled public land except at the southern and northernmost extremities where small settlements exist. There are no groynes, seawalls, or other artificial structures on or likely to affect the beach face. Vehicular access to the beach exists at only five points within the study area; at each of these points there is some vehicular erosion of the dune

face over distances of a few metres. Recreational four-wheel drive vehicles access the beach from the dunes at these points, but their use is mostly limited to the tidal beach face itself. The only major artificial infrastructure close to the study area are large training walls constructed on the rocky shore opposite the southern tip of Ocean Beach, which maintain a navigable tidal channel into Macquarie Harbour. A shack settlement comprising several dozen caravans and occupied huts with unsealed vehicular access is present some tens of metres behind the shoreline at the southernmost tip of Ocean Beach next to the tidal channel entrance to Macquarie Harbour.

Plantations of introduced Monterey Pine (*Pinus radiata*) were established more than 150 metres inland from the present beach and dune front from the 1980s on and are unlikely to affect beach processes. However, the introduced dune-colonising grass *Ammophila arenaria* ('marram grass') is common in the dunes immediately backing the beach, where it was deliberately planted from the 1950s onwards to stabilise the then-extensive active transgressive dunes (Cullen 1998). Marram is an aggressive dune coloniser and sand-binding grass (Hayes & Kirkpatrick 2012) and is likely to have facilitated more rapid fore-dune accretion and progradation prior to 1980 than might otherwise have occurred. However, marram grass does not prevent foredune erosion, and so can only enhance dune accretion under conditions where this would have been occurring anyway.

Cattle grazing, and firing have also historically occurred on parts of the stabilised dunes landwards of Ocean Beach (Banks, Colhoun & Chick 1977) but have not occurred in recent decades.

A number of artificial and natural process influences, and changes can be eliminated as explanations of the observed changes in shoreline history at Ocean Beach over the Twentieth Century.

Large training walls opposite the southern end of the beach at the tidal mouth of Macquarie Harbour maintain a navigable tidal channel but are unlikely to have affected the beach face or to have changed the capacity of the adjacent ebb- and flood-tide deltas to be active sinks for sand lost from the beach by erosion and longshore drift. It is unlikely that vehicle use on Ocean Beach has significantly influenced beach and dune processes, with direct impacts on the dune face being limited to about five restricted access points covering a few metres length of dune face, and most vehicle use on the beach occurring below the high-water mark (where sand is generally harder). The establishment of pine plantations and former cattle grazing that has occurred in backshore areas are everywhere at least a hundred metres behind the beach and there is no plausible mechanism apparent by which these may have modified beach and dune-front behaviour. Shack settlements at the north and south end of Ocean Beach are set back from the shoreline and frontal dune faces and are only relevant as a source of vehicular activity.

On the other hand, it is likely that the observed net seawards accretion of the dune-front vegetation line backing Ocean Beach between 1948 and 1979 – which accelerated notably in the decade prior to 1979 (see Figure 183) - was at least in part an effect of the establishment of introduced dune-colonising marram grass (*Ammophila arenaria*) from the 1950s onwards (Cullen 1998). This appears to have been most marked on previously-unvegetated transgressive dune fronts in the northern part of the study area. Establishment of this aggressive sand-binding grass accelerates foredune accretion and can reduce wind deflation of dunes (Hayes & Kirkpatrick 2012). However, it does not prevent wave erosion and scarping of dune fronts, as is frequently observed on many Tasmanian beaches such as Hope Beach (see Figure 208, appendix A1.4.3). Hence it can be inferred that some net dune accretion would have occurred between 1948 and 1979 even in the absence of marram (i.e., there must have been less frequent or smaller dune-front wave erosion events than subsequently in either case). Dune front recession after 1979 cannot be attributed to the grass but rather has occurred *despite* its presence.

Backshore peat sediment dating

Lenses of peat and sandy peat about 1.7m thick with inter-bedded inferred aeolian sands are exposed in the actively receding shoreline scarp at 42° 8.9' S 145° 15.8' E, about 225 metres north of the

surveyed beach profile 730/108. The approximately 2-metre-high active scarp at this location is not cut into a dune but is immediately backed by flat ground interpreted as a former inter-dune swale, extending 40 metres landwards to the foot of the first dune behind the beach at this location. The lenses are exposed in the scarp over about 250 metres north to south.

The author has observed after rainfall that groundwater actively flows out of the sampled erosion scarp. This together with the flat ground surface immediately landwards of the current scarp and the limited north-south extent of the exposed peat lenses supports an inference that the peats are swamp peats (not dune palaeosols) which accumulated in a back-dune swale that would have been water-logged when a former dune to seawards impeded the drainage. The aerial photography shows that a substantial dune about 20 metres wide was present to seawards of the sample site from at least 1947 until at least 1982, when the current phase of shoreline recession had started. The sample site was then a poorly drained back dune swale. By circa 1994 this dune was cut back to such a degree that the swamp would have become freely draining and relatively dry at the surface. This is consistent with the ^{14}C peat dates which indicate that the upper peats in the profile were still accumulating at very recent dates.

These peats were sampled for Carbon-14 dating on 15th May 2016 with a view to constraining the minimum time since the dune-front was last eroded back as far as it is now. Carbon-14 radiometric dating was conducted at the Australian Nuclear Science and Technology Organisation (ANSTO) by Dr Quan Hua.

The ^{14}C dating results (Table 53) indicate that the peats now exposed in an erosion scarp have accumulated from circa 1,800 years BP until modern times, with a hiatus circa 1,200 – 1,000 years BP. The existence of a dune to seawards of the sampled site since circa 1,800 years BP is necessary to have impeded drainage and allowed the peat to accumulate in a swampy environment. The sand-dominated hiatus between 1,200 – 1,000 years BP most likely represents a period when the former dune to seawards was eroding and deflating landwards so that aeolian sand temporarily buried the swamp, however the preservation of the lower peat lens demonstrates that the dune did not then erode back as far as the present-day scarp position. In sum, the evidence that the peats now exposed in an active erosion scarp accumulated in a back-dune swamp since circa 1,800 years BP demonstrates that the degree of horizontal shoreline recession at the sampled site at May 2016 (and later) exceeds any landwards erosion events or shoreline recession that have occurred during at least the last 1,800 years, since any greater previous recession would have previously destroyed the peats.

Table 53: Peat sample radiometric Carbon-14 dates. Age results (years Before Present or BP) for peat samples collected 15th May 2016 from Ocean Beach erosion scarp at 42° 8.9' S 145° 15.8' E. ^{14}C radiometric dating was conducted at the Australian Nuclear Science and Technology Organisation (ANSTO) by Quan Hua. Age calibration was performed using the OxCal v.4.2 program (Bronk Ramsey 2009)and the Bomb 14C data SH1-2 (Hua, Barbetti & Rakowski 2013) extended back in time using the SHCal13 data (Hogg et al. 2013). Modelled ages are based on P Sequence model with variable k values (Bronk Ramsey & Lee 2013).

Sample No.	Type	Sample depth (metres)	percent Modern C		Conventional ^{14}C age (years BP)		Modelled calibrated age (cal. years BP)	
			Mean	1σ	Mean	1σ	Median	2σ age range
1	Fibrous peat	0.10-0.12	123.50	0.26	Modern		-33	-34 to -11
2	Fibrous-muck peat	0.28-0.30	99.03	0.22	80	20	57	238 to -6
3	Muck peat	0.56-0.58	91.24	0.24	735	25	653	674-569
4	Muck peat	0.74-0.76	86.40	0.23	1175	25	1006	1060-965
5	Muck peat	1.08-1.10	84.58	0.21	1345	20	1235	1279-1184
6	Muck peat	1.24-1.26	81.91	0.26	1605	30	1395	1466-1359
7	Muck peat	1.40-1.42	82.32	0.18	1565	20	1425	1515-1380
8	Muck peat	1.56-1.58	78.02	0.68	1990	70	1863	2040-1704

Air photo analysis

Air photos of the Ocean Beach study area taken at 21 dates between Dec 1947 and Nov. 2010 were ortho-rectified and used to extract shoreline change data by the methods described in Appendix A2.1.

Shore behaviour history from air photos

Visual comparison of groups of transect histories allowed the total of 188 study site transects to be first grouped into three regions, namely:

1. A North area with significant portions dominated by large deflated and mobile dunes extending inland from the beach during the 1940s and 50s, but with strong foredune accretion in those parts after 1950, and a notable shoreline progradation trend on most transects from 1970 until 1979, followed by a notable switch to persistent and dominant progressive shoreline recession from 1982 until at least 2010.
2. A Mid – South area with less mobile dune areas during the 1940s and 1950s. This was also a dynamic equilibrium shoreline showing some erosion and some accretion prior to 1980, including a notable shoreline progradation trend on most transects from 1970 to 1979, but this also was followed by a strong switch to persistent and dominant progressive shoreline recession from 1982 until at least 2010.
3. The South Tip of the beach has shown very different behaviour over the whole air photo period, with periods of notable accretion and progradation interspersed with erosion events, but no long-term trend towards either recession or progradation over the last 60 years. The tip prograded about 150 metres between 1949 and 1975 but has subsequently fluctuated within a much smaller horizontal range of only 20 – 30 metres, suggestive of early recovery from a major erosion event prior to the air photo period.

Based on broadly similar historical shoreline behaviour in the North and Mid-South areas (despite greater early dune deflation and recovery in the northern area), the transect histories for these areas have been combined for further analysis, with the very distinctive South Tip area being considered separately.

The North to Mid-South region (153 used transects: 9924 to 10081) displayed consistent shoreline recession since after 1980, and the small South Tip region (30 transects: 9894-9923) displayed episodic progradation and erosion events throughout the air photo period but no long-term trend. Five transects (10005-07 & 10038-39) were excluded from analysis because air photo inspection shows them to be close to creek outlets whose discharge channels have repeatedly caused dune-front erosion unrelated to sea and wave exposure. Conversely a cluster of transects in the North area which show apparent anomalously receded shoreline (vegetation line) positions in the oldest photos, due to extensive dune deflation immediately backing the beach, have been retained in the data since they subsequently exhibited strong foredune recovery followed by progressive shoreline recession histories coherent with most of the beach after 1980 (transects 10048-51 & 10057).

For the final north to mid-south region, the median shoreline positions at each date across all used transects were plotted to provide a final quantitative shoreline movement history summary for further analysis (see Figure 183).

The analysis shows that the study area shoreline (excluding only the southernmost tip) has undergone a marked switch of long-term (multi-decadal) behaviour during the Twentieth Century, from dynamic equilibrium about a roughly stable or slightly prograding shoreline position, to persistent shoreline recession. For a period of at least 32 years since 1947 until at least 1979, the study area shoreline underwent both minor shoreline erosion (albeit of a lesser magnitude than the air photo error margins and thus equivocal) and notable shoreline progradation, especially from after 1969 until at least 1979 (of greater scale than the error margins and thus unequivocal). A small overall trend of shoreline progradation is apparent over the 1947 to 1979 period (Figure 183). However, during the 29 years

from 1982 until 2010 the air photo record shows a very persistent shoreline recession trend interrupted by only minor accretion intervals, some of which are of lesser scale than air photo error margins and thus possibly not real. The overall recession trend from 1982 is roughly an order of magnitude greater than the air photo error margins and represents a real switch in long-term beach behaviour after 1979. This change in behaviour was not gradual but occurred abruptly within an approximately 2.5-year interval (between air photos from 5th May 1979 and 16th Jan 1982).

In contrast, the air photo record for the southernmost tip of Ocean Beach demonstrates a history of episodic shoreline erosion and accretion throughout the air-photo period (1949 to 2010), but no overall trend towards either recession or progradation.

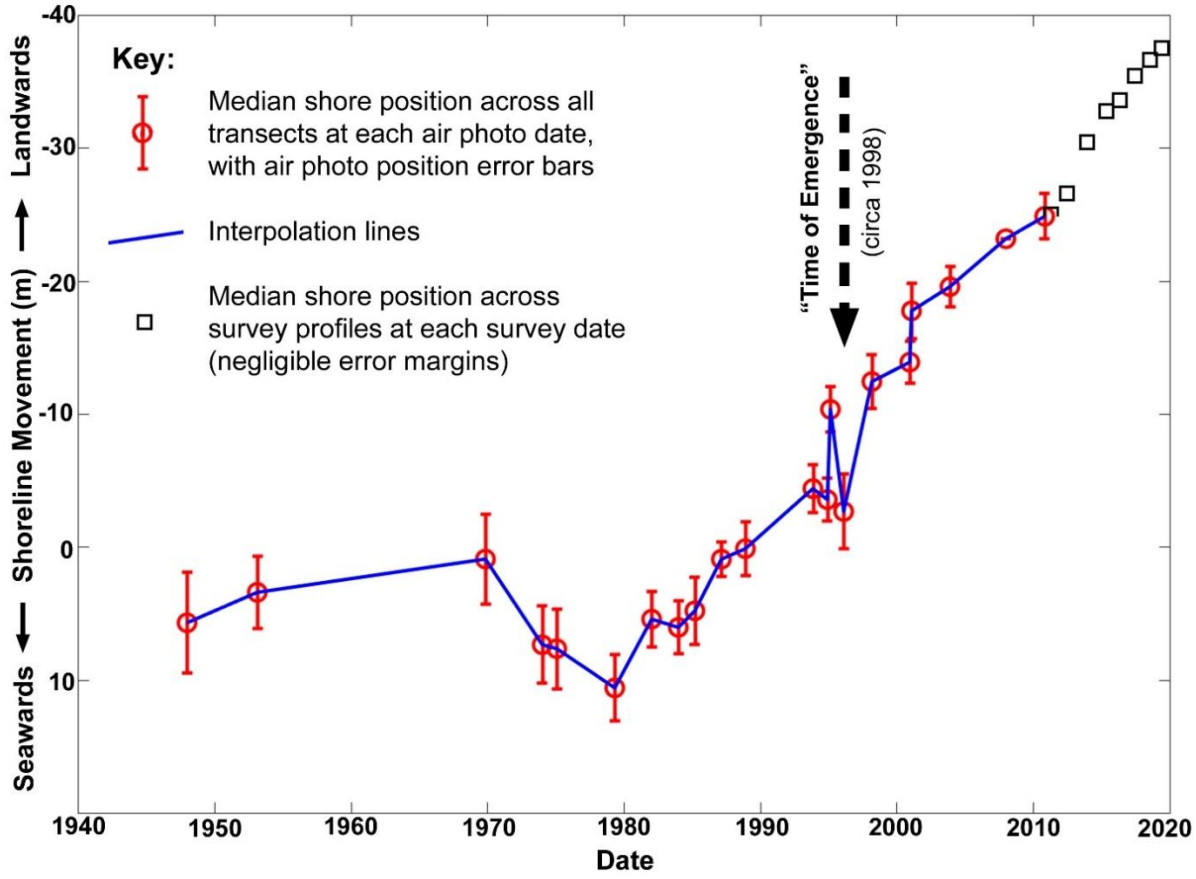

Figure 183: Summary plot of shoreline change history at the Ocean Beach study area. This plot shows the median horizontal shoreline position at each air photo date to 2010 across 153 normalised transects comprising the North and Mid-South parts of the study area, and the median shoreline positions across 2 beach profiles within the same area (TASMARC 730-108 & 730-109) surveyed at 8 more dates from 2011 to 2019. Although the beach underwent a marked change of long-term behaviour circa 1980, the "Time of Emergence" (Hawkins & Sutton 2012) indicated is the date (circa 1998) at which the subsequent persistent recession trend exceeded the limits of historic shoreline position variability (including error margins) and can be identified as a new mode of shoreline behaviour for this beach.

Qualitative data on longshore drift indicators

A persistent southward longshore (littoral) drift is a major sand transport process at Ocean Beach. This drift has not been quantitatively measured but is inferred from geomorphic indicators at several locations from the northern to the southern ends of the beach (see *Sand transport and budget* above). These include the mostly southwards deflection of the Henty River and Little Henty River discharge channels across Ocean Beach, which imply a dominantly southwards littoral current transporting sand alongshore through the lower beach and surf zone. Variability in the longshore drift has been qualitatively assessed by inspecting the form and deflection of these outlet channels in all available air photo dates from 1947 to 2011 (see Table 54). The Henty River is located mid-way along Ocean Beach and just north of the main study area, whereas the Little Henty River is near the northern end of

the beach, hence the photos covering these river mouths are not the same as those used for the shoreline history data although many were taken around the same dates (Table 55). While air photo inspection confirmed that the deflection of both outlets is mostly southwards, indicators of some variability include:

- Northwards deflection of the river channels across the beach. (Observed only for the Little Henty River, from 1988 to 1996 only: Channel pushed against rocky outcrops at north end of beach, possible storm aftermath, took nearly a decade to revert to normal channel again?)
- Mainly southwards channel deflection across the beach, but with a short final northward turn across the lower beach face (inferred to indicate dominantly southwards longshore drift but with a recent northwards drift episode).
- Southwards channel deflection along the beach with a final shoreline-normal outlet directly across the lower beach face (inferred to indicate recent storm erosion reworking outlet channels on the lower beach).

Table 54: Outflow channel configurations for the Little Henty and Henty Rivers at Ocean Beach. Qualitative data confirming dominantly southwards littoral drift at Ocean Beach but also indicating sub-ordinate variability. All air photos © DPIPWE.

Air photo date	Film - Frame	Henty River outlet channel	Little Henty River outlet channel
22nd Jan 1947	80-21549 (Zeehan)	-	Southwards along the beach.
27th Jan 1949	177-3284 (Strahan)	Southwards along the beach	-
22nd Feb 1953	302-115	Southwards along beach then short final turn north on lower beach	-
17th Feb 1956	316-2	-	Southwards along the beach.
26th Feb 1973	626-135	-	Southwards along beach then directly across beach.
26th Feb 1973	626-130	Southwards along the beach	-
9th Jan 1974	639-19	Southwards along the beach	-
24th Jan 1974	648-200	-	Southwards along beach then directly across beach.
3rd Feb 1975	668-162	-	Southwards along beach then directly across beach.
3rd Feb 1975	668-158	Southwards along beach	-
20th Feb 1979	793-105	-	Southwards along beach then short final turn to north on lower beach.
20th Feb 1979	793-111	Southwards along beach	-
18th Feb 1980	819-130	-	Southwards along the beach.
15th Jan 1982	897-178	-	Southwards along beach, then short final turn north on lower beach.
3rd Mar 1982	917-170	Southwards along the beach	-
7th Nov 1984	1010-055	-	Southwards along beach then directly across beach.
7th Nov 1984	1010-052	Southwards along beach then short final turn north on lower beach	-
18th Nov 1988	1119-134	-	Northwards along the beach.
14th Dec 1988	1121-124 1121-125	Southwards along the beach.	-
16th Nov 1993	1203-046	Southwards along the beach	-
2nd Dec 1994	1224-226	-	Northwards along the beach.
21st Dec 1994	1224-229	Southwards along the beach.	-
8th Nov 1996	1253-092	-	Northwards along the beach
13th Feb 2000	1323-131	-	Southwards along the beach with sub-ordinate channel directly across beach.
13th Feb 2000	1323-126	Southwards along the beach.	-
1st Feb 2001	1345-092	-	Southwards along the beach.
17th Dec 2000	1336-139	Southwards along the beach.	-
28th Nov 2003	1374-044	-	Southwards along the beach.
28th Nov 2003	1374-046	Southwards along the beach.	-
15th Nov 2007	1424-202	-	Southwards along the beach.
4th Jan 2008	1429-058	Southwards along the beach then directly across beach.	-
6th Nov. 2010	1450-135	Southwards along the beach.	-

6th Nov 2010	1450-145	-	Southwards along the beach.
5th Dec 2011	1464-001	-	Southwards along the beach then short final turn north on lower beach.

Surveyed shore profile analysis (TASMARC)

Three TASMARC beach monitoring survey marks were placed at Ocean Beach in 2011 and their positions established to ±50 mm accuracy using differential GNSS. A profile transect across the beach and backshore has been surveyed approximately annually up to 2018 from each survey mark, using total station survey methods (see profile and Hinge point plots Figure 185). These surveys have permitted the extension of the air photo-derived shoreline change record (to 2010) until 2019 at the three survey transect locations, at finer spatial and temporal scale than is provided by the air photo record.

The TASMARC ground surveys enable identification of the same features mapped from air photos as the shoreline position indicator, namely the seawards vegetation limit which at Ocean Beach also presents as either a scarp face or a change of slope between the beach and dune. Figure 184 plots the position of these equivalent shoreline indicators from 2011 to 2019 at each transect, with the preceding air photo shoreline movement history also measured along each TASMARC traverse and included on each plot. A small offset (variable 9.5 to 15.7m) between the air photo and ground survey co-ordinate frames has been manually adjusted to correctly locate the 2010 and 2011 shoreline positions relative to each other (the offsets result from the TASMARC shoreline positions being GNSS-surveyed to ±50 mm accuracy while the air-photo shoreline positions are measured relative to 1:25,000 LIST map co-ordinates with stated horizontal errors of less than ±12.5 metres for not less than 90% of well-defined details).

Note re combining air photo and TASMARC survey data on summary Figure 183:

Plotting shoreline positions measured from air photos required a manual adjustment to bring these in line with surveyed TASMARC shoreline positions because the air photos were geo-rectified to topographic mapping with a stated multi-metre error margin whilst the TASMARC surveys are accurate to ±50 mm in the same co-ordinate system. To incorporate the TASMARC data into a summary figure of the shoreline history for the whole main study area (the 'NSarea') the median of the shoreline position at each survey date was then calculated for the two TASMARC profiles located in the NSarea (730-108 and 730-109), together with the median of the 2010 air photo date shoreline positions measured on the same transects. To incorporate the medians of the TASMARC shoreline positions into Figure 183 consistent with the medians of all photo shoreline positions, each TASMARC median shoreline position was moved by the same distance needed to make the 2010 air photo median shoreline on the TASMARC profiles co-incide with the median 2010 air photo shoreline position across all 153 air photo transects (this involved subtracting 61.26m from each TASMARC transect measurement).

Shoreline behaviour history from profile surveys

Annual beach profile surveys from 2011 to 2019 at two transects in the main part of study area (TASMARC profiles 730/108 and 730/109) demonstrate un-interrupted continuation of the recession trends observed in the air photo record for those sites, amounting as at 2019 to at least 37 years of persistent recession with only minor interruptions since 1982 (see Figure 184). Although the TASMARC surveys could only be undertaken at roughly annual intervals, on each occasion the erosion scarps were fresh with some collapses but no indication of shoreline recovery such as incipient foredune accretion.

For TASMARC profile 730/110 at the southernmost tip of the beach, the 2011 – 2019 ground survey data shows a continuing pattern of alternating erosion and accretion comparable to that demonstrated

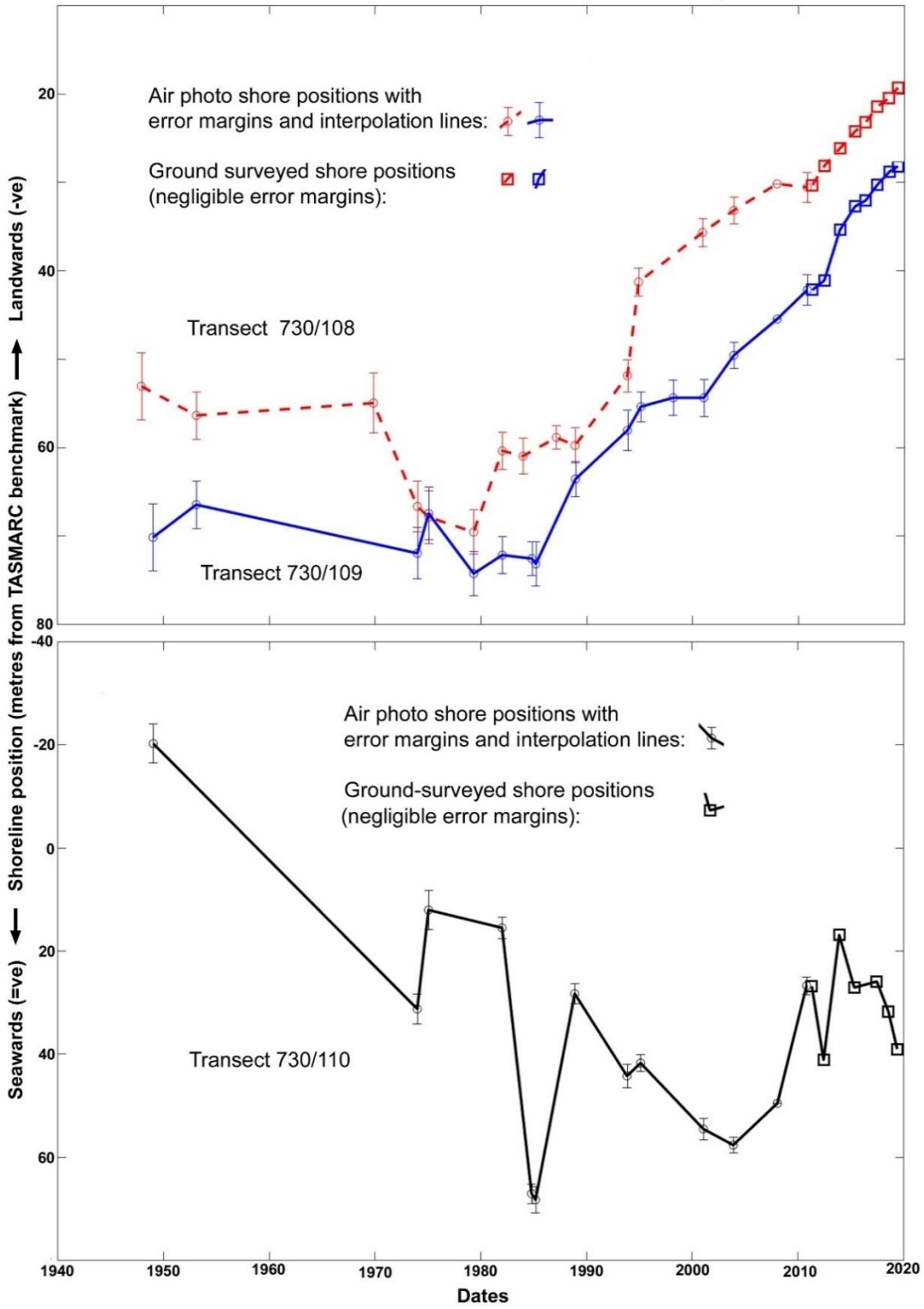

Figure 184: Shoreline movement history at three ground-surveyed transects. These plots depict the horizontal movement of the Ocean Beach shoreline at the three TASMARC beach profile transects at Ocean Beach, combining measurements from historic air photo time series for each site up to 2010, and the TASMARC ground surveys from 2011 to 2019. The top plot demonstrates that the shoreline recession which dominated the air photo record of the northern two transects (730/108 and 730/109) from circa 1980 until 2010 has continued unabated through the TASMARC survey period and was continuing at 2019. The bottom plot demonstrates that phases of accretion with no persistent recession erosion trend have characterised the southern-most transect (730/110) throughout the both the air photo and TASMARC survey period and were continuing as at 2019.

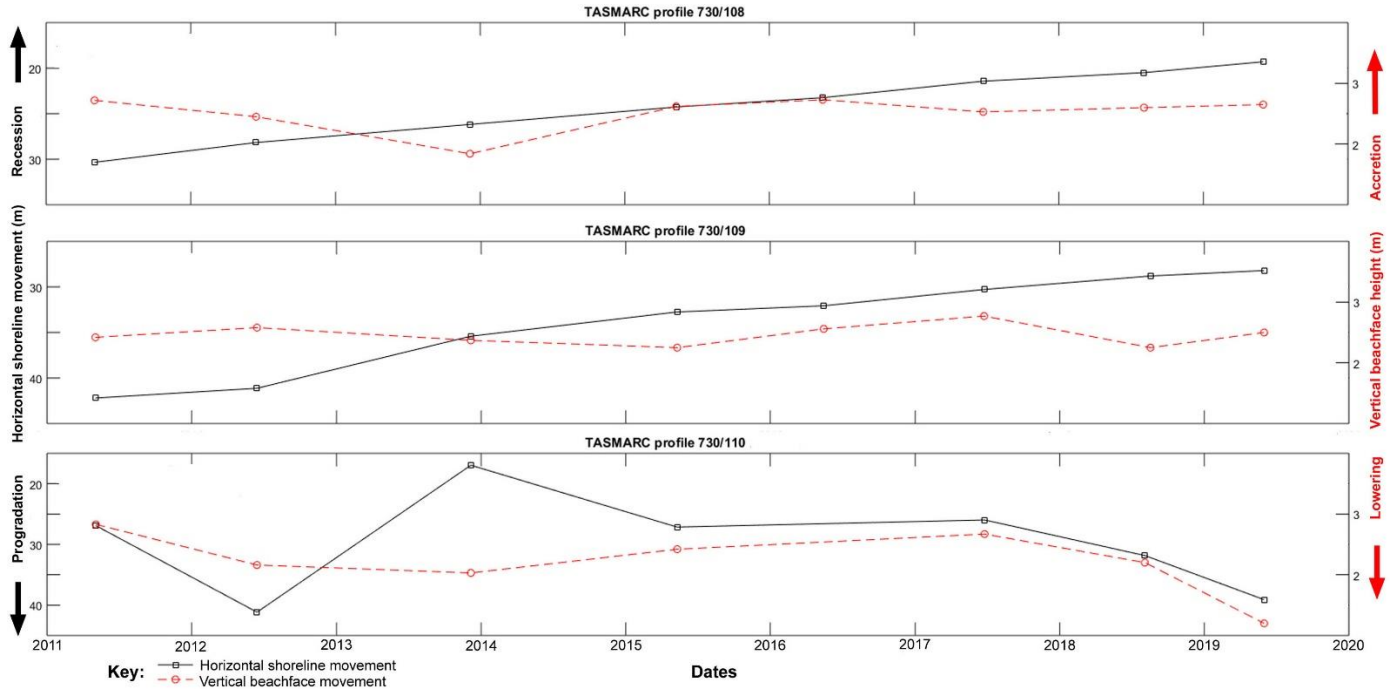

Figure 185: Hinge point plots for Ocean Beach TASMARC profiles. Profiles 730/108 & 730/109 show progressively receding shorelines with beach-face lowering and recovery, whereas Profile 730/110 shows shoreline erosion and recovery (and beach-face lowering and recovery) with no overall trend. See Section A2.2 for explanation of hinge point format. Horizontal distances relative to survey mark, vertical distances relative to AHD.

by the air photo record up to 2010 for the same location, with no significant long-term trend to either recession or progradation (Figure 184).

Summary shoreline behaviour history and characterisation

The air photo analysis results (Figure 183) demonstrate that about 1980 Ocean Beach switched abruptly from a multi-decadal history of relatively stable or prograding shoreline positions to a persistently receding shoreline which continues at present. Median progressive horizontal shoreline recession from circa 1980 until 2010 was approximately 35 m (Figure 183), which is well outside the mean measured air photo error margins of ±1.3 to 3.8m (Table 55). Although the beach underwent this marked change of long-term behaviour circa 1980, the "Time of Emergence" (Hawkins & Sutton 2012) indicated is the date (circa 1998) at which the subsequent persistent recession trend exceeded the limits of historic shoreline position variability (including error margins) and can be identified as a new mode of shoreline change for this beach (Figure 183). Beach profile monitoring at two sites demonstrates the recession trend has continued from 2011 to 2019 without abating. Although direct measurements of shoreline position only extend back to 1947, ^{14}C dating of inferred back-dune swamp peats exposed in the receding shoreline scarp & Table 53) imply the current receded shoreline position hasn't been reached in at least the last 1,800 years. It can be inferred from this that the current recession phase is of greater magnitude than any decadal- to centennial-scale cyclic or episodic processes affecting this beach.

Shoreline behaviour drivers and conditions

Hypotheses concerning the drivers of the observed historical shoreline behaviour at Ocean Beach and the local geomorphic conditions which have allowed the observed changes to occur are explored in Chapter 5 (Section 5.2.4). That discussion is not repeated here.

Air photo data tables

The following tables provide details of the air photos used, the resulting ortho-photos produced, and the shapefiles representing the shoreline position that were digitised from the ortho-photos. The original air photos were obtained as scanned images from the Tasmanian Department of Primary Industries, Parks Water and Environment (DPIPWE). Several other available photos at 1:40,000 scale were not used because they were close in time to better scale air photos which have been used.

The 2008 air photos (1431-22 & 1429-123) were ortho-rectified against LIST 1:25,000 mapping by Matt Dell and Hannah Walford using Landscape Mapper™ software. The ortho-rectified 2008 air photos were then used (by Hannah Walford and Chris Sharples as indicated below) as the Reference Layer for ortho-rectifying all other air photos with Landscape Mapper™, using features on the 2008 air photos as control points. The exceptions to this were the 2010 air photos (1450-124, 126, 128 & 137) which were obtained from DPIPWE as ortho-rectified images. The 2010 ortho-photos were found to have a systematic offset to the west-northwest relative to the 2008 ortho-photo's, averaging 6.98m. The 2010 shoreline was digitised over the DPIPWE ortho-photos, then the entire digitised shoreline was moved 6.98m to the ESE to bring it into the same reference frame as the 2008 reference ortho-photo. The average residual error margin for the 2010 shoreline position then became 1.70m (calculated by subtracting the average raw error (6.98m) from each individual feature position error measurement, ignoring the sign of the result, and averaging the results.)

Feature position errors for each ortho-photo were measured by comparing the position of stable features in each photo against the same features in the 2008 reference photos. Note that where photo frames overlap the positions of the same reference features may be measured for two different photo frames.

Table 55: Original air photos and ortho-photos produced for Ocean Beach.

Photo Date	**Original DPIPWE air photos (film-frame) / Ortho-photo file name**	**Final image resolution (original scan resolution if downsized) / pixel size of final ortho-photo**	**Original photo scale**	**Mean measured feature position error (± metres) for ortho-photo** [No. of measured feature position reference points]	**Comments**
19th Jan 1949 16th Dec 1947 16th Jan 1948 (all combined as "1948")	158-2369 158-2324 158-2315 131-787 131-834 158-2410 / OceanBeach_Stip_19th Jan1949_MGA55.tif/tfw OceanBeach_S_19thJa n1949_MGA55.tif/tfw OceanBeach_MidS_19t hJan1949_MGA55.tif/tfw OceanBeach_Mid_16th Dec1947_MGA55.tif/tfw	 All: 600 dpi / 0.78 m pixel size 0.76 m pixel size 0.77 m pixel size 0.87 m pixel size	 All: 1:15,840	 4.1 m [3] 4.2 m [4] 3.4 m [8] Combined Mean for 1949: 3.8 m [13] 2.5 m [4] 2.2 m [5]	Whole study area covered over 2 summer flying seasons (1947-49), combined as "1948"). Frame 168-838 (16th Dec 1947) missed – leaves small gap but mostly mobile dunes Ortho-rectified by Chris Sharples (excludes south end; 2 poor error margins)

	OceanBeach_MidN_16thDec1947_MGA55.tif/tfw OceanBeach_N_16thJan1948_MGA55.tif/tfw	0.83 m pixel size 0.85 m pixel size		2.9 m [3] Combined Mean for 1947-48: 3.3 m [12] **Final combined mean error margins for '1948' air photos:** **3.8 m [25]**	'N' photo errors measured relative to 1996 air-photos only (extends beyond 2008 reference photo); then mean 1996 error added to errors for 'N' air photo Taken as poorer of the combined means for 1947-48 and 1949
22nd Feb 1953 1st Feb 1953	301-98 (S. tip of beach) 302-36 305-54 / OceanBeach_22ndFeb1953_MGA55.tif/tfw (mosaic)	1000 dpi (2039 dpi) / 1.0m pixel size	1:35,640	2.7 m [26]	Whole study area Ortho-rectified by Hannah Walford and Chris Sharples
	OceanBeach_S_22ndFeb1953_MGA55.tif/tfw (S. tip of beach)	1.0m pixel size		12.5 m [6]	S. tip photo NOT USED due to poor ortho accuracy
27th Dec 1960	354-64 / OceanBeach_S_27Dec1960_MGA55.tif/tfw	1000 dpi (2039 dpi) / 1.3m pixel size	1:35,640	4.3 m [5]	South part of beach only Ortho-rectified by Chris Sharples NOT USED due to poor accuracy and limited coverage.
12th Nov 1969	536-78 536-80 536-92 536-94 /	2039 dpi 1000 dpi (2039 dpi) /	1:31,680		Whole study area Ortho-rectified by Chris Sharples
	OceanBeach_Nmid_12Nov1969_MGA55.tif/tfw	0.5m pixel size		7.7 m [13]	NOT USED due to poor accuracy
	OceanBeach_N_12Nov1969_MGA55.tif/tfw OceanBeach_Smid_12Nov1969_MGA55.tif/tfw	0.5m pixel size 1.0m pixel size		4.1 m [5] 3.0 m [7]	Used Used
	OceanBeach_S_12Nov1969_MGA55.tif/tfw	1.0m pixel size		9.0 m [13]	NOT USED due to poor accuracy
				Combined N & Smid: **3.4 m [12]**	
9th Jan 1974	638-184 638-224 / OceanBeach_9thJan1974_MGA55.tif/tfw (mosaic)	1000 dpi (2039 dpi) / 1.1m pixel size	1:40,000	2.9 m [38]	Whole study area Ortho-rectified by Hannah Walford

3rd Feb 1975	670-49 670-51 670-55 / OceanBeach_N_3rdFeb 1975_MGA55.tif/tfw; OceanBeach_Nmid_3rd Feb1975_MGA55.tif/tfw; OceanBeach_S_3rdFeb 1975_MGA55.tif/tfw	1000 dpi (2039 dpi) / 0.63m pixel size	1:20,000	 3.3 m [8] 1.9 m [10] 3.8 m [5] **Combined: 3.0 m [14]**	Most of study area with gap in south-middle area (scanned frame 670-53 failed to ortho-rectify in Landscape Mapper – unresolved problem) Ortho-rectified by Chris Sharples
5th May 1979	798-129 / OceanBeach_5thMay19 79_MGA55.tif/tfw	1000 dpi (2039 dpi) / 1.13m pixel size	1:45,000	 2.5 m [30]	North – middle area Ortho-rectified by Hannah Walford
16th Jan 1982	897-275 / OceanBeach_16thJan19 82_MGA55.tif/tfw 897-225 / OceanBeach_N_16thJa n1982_MGA55.tif/tfw	1000 dpi (2039 dpi) / 1.13m pixel size 2039 dpi (not down-sized) / 0.56 m pixel size	1:42,000	 2.1 m [20] 2.1 m [16] **Combined: 2.1m [30]**	Mid-south area Ortho-rectified by Hannah Walford North area Ortho-rectified by Chris Sharples (north & south ends warped and not used).
8th Nov 1984 31st Oct 1984	1009-25 1009-22 / OceanBeach_8thNov19 84_MGA55.tif/tfw (mosaic) 1007-206 / OceanBeach_31stOct19 84_MGA55.tif/tfw	1000 dpi (2039 dpi) / 0.565m pixel size 1000 dpi (2039 dpi) / 0.55 m pixel size	1:20,000	 2.0 m [20] 1.9 m [12] **Combined: 2.0 m [29]**	North area Mid area Ortho-rectified by Hannah Walford South area Ortho-rectified by Chris Sharples
19th Mar 1985	1030-155 / OceanBeach_19thMar1 985_MGA55.tif/tfw	1000 dpi (2039 dpi) / 1.13m pixel size	1:42,000	 2.5 m [24]	South area Ortho-rectified by Hannah Walford
26th Feb 1987	1088-41 / OceanBeach_26thFeb1 987_MGA55.tif/tfw	2039 dpi / 0.16m pixel size	1:12,500	 1.3 m [12]	Small part of middle area Ortho-rectified by Chris Sharples
14th & 16th Dec 1988	1123-141 1121-141 OceanBeach_Dec1988_ MGA55.tif/tfw (mosaic)	1000 dpi (2039 dpi) / 1.13m pixel size	1:42,000	 2.0 m [42]	Whole study area Ortho-rectified by Hannah Walford
10th Nov 1993	1203-70 /	1000 dpi (2039 dpi) / 1.2m pixel size	1:42,000	 2.3 m [26]	South area

	OceanBeach_10thNov1993_MGA55.tif/tfw 1203-66 / OceanBeach_N_10thNov1993_MGA55.tif/tfw	2039 dpi / 0.55m pixel size		1.7 m [27] **Combined: 1.8 m [43]**	Ortho-rectified by Hannah Walford North area Ortho-rectified by C. Sharples
2nd Dec 1994	1226-38 / OceanBeach_2ndDec1994_MGA55.tif/tfw	1000 dpi (2039 dpi) / 1.13m pixel size	1:42,000	1.6 m [26]	North area Ortho-rectified by Hannah Walford (Anomalous large-error area at south edge of photo not used).
23rd Feb 1995	1232-16 / OceanBeach_23rdFeb1995_MGA55.tif/tfw	2039 dpi / 0.60m pixel size	1:42,000	1.7 m [24]	South area Ortho-rectified by Chris Sharples (Completes beach coverage at similar time to Dec 1994 photo)
13th Feb 1996	1245-135 / OceanBeach_13thFeb1996_MGA55.tif/tfw	1000 dpi (2039 dpi) / 0.53m pixel size	1:15,000	2.8 m [5]	North area (part) Ortho-rectified by Chris Sharples
8th March 1998	1293-47 / OceanBeach_8thMar1998_MGA55.tif/tfw	1000 dpi (2039 dpi) / 0.53m pixel size	1:15,000	2.0 m [7]	South area (part) Ortho-rectified by Chris Sharples
17th Dec 2000	1336-142 / OceanBeach_17thDec2000_MGA55.tif/tfw	1000 dpi (2039 dpi) / 1.13m pixel size	1:42,000	1.6 m [28]	North-Middle area Ortho-rectified by Hannah Walford
1st Feb 2001	1345-121 / OceanBeach_1stFeb2001_MGA55.tif/tfw	1000 dpi (2039 dpi) / 1.13m pixel size	1:42,000	2.1 m [25]	Southern half of study area Ortho-rectified by Hannah Walford
28th Nov 2003	1374-116 1374-111 / OceanBeach_28thNov2003_MGA55.tif/tfw (mosaic)	2039 dpi / 0.56m pixel size	1:42,000	1.5 m [41]	Whole study area Ortho-rectified by Hannah Walford
15th Feb & 9th Jan 2008	Whole study area: 1431-22 1429-123 OceanBeach_JanFeb2008_MGA55.tif/tfw (mosaic)	2039 dpi / 0.56m pixel size	1:42,000	0.0 m [N/A]	Whole study area REFERENCE IMAGE (zero relative feature position error by convention) Ortho-rectified to LIST 1:25,000 mapping by Matt Dell and Hannah Walford
6th Nov 2010	Whole study area: 1450-124 1450-126 1450-128 1450-137 / OceanBeachA_6thNov2010_MGA55.ecw/eww	2039 dpi / 0.30m pixel size	1:24,000	1.7 m [20]	Whole study area

	OceanBeachB_6thNov2010_MGA55.ecw/eww OceanBeachC_6thNov2010_MGA55.ecw/eww OceanBeachD_6thNov2010_MGA55.ecw/eww				Ortho-rectified by DPIPWE (ecw / eww files renamed by C. Sharples) (Feature position error is residual average error after correcting systematic 6.98m (av.) WNW offset relative to 2008 reference image)

Table 56: Digitised shoreline shapefiles produced for Ocean Beach (using ortho-photos listed in Table 55 above).

Date of air photo(s)	Shapefile	Shoreline digitised by	Comments
16th Dec. 1947 & 16th Jan 1948	OceanBeach_MGA55_19471216.shp (file name based on earlier date)	Chris Sharples (2016)	North half of study area: Digitised together since photo dates only one month apart.
19th Jan. 1949	OceanBeach_MGA55_19490119.shp	Chris Sharples (2016)	South half of study area: Digitised separately to 1947-48 photos since photo date a year later, however results combined with 1947-1948 results as "1948" shoreline.
1st & 22nd Feb. 1953	OceanBeach_MGA55_19530222.shp	Hannah Walford (2011) (Chris Sharples (2016) checked Hannah's digitising and made minor edits)	HW digitised N & mid parts, S tip photo not used (poor error margins, small area). CS updated photo error margins using additional reference features. Beach appears recently cut back in northern area, no incipient dunes evident.
27th Dec. 1960	NOT USED	Chris Sharples (2016)	Not used due to poor error margins & limited coverage (S end of beach only).
12th Nov. 1969	OceanBeach_MGA55_19691112.shp	Chris Sharples (2016) Digitised N & Smid pic shores only (poor error margins for Nmid & S pics – not used).	New incipient dunes forming seawards of major erosion scarp.
9th Jan. 1974	OceanBeach_MGA55_19740109.shp	Hannah Walford (2011) (Chris Sharples (2016) checked Hannah's digitising and added several sections not previously digitised in the northern parts of study area).	CS updated photo error margins using additional reference features.
3rd Feb. 1975	OceanBeach_MGA55_19750203.shp	Chris Sharples (2016)	
5th May 1979	OceanBeach_MGA55_19790505.shp	Hannah Walford (2011) (Chris Sharples (2016) checked and (only) slightly edited previously digitised shoreline)	CS updated photo error margins using additional reference features.

16th Jan. 1982	OceanBeach_MGA55_19820116.shp	Hannah Walford (2011) & Chris Sharples (2016) (Chris Sharples (2016) checked and (only) slightly edited previously digitised shoreline)	HW digitised south-mid part; CS digitised additional north parts except at warped N & S ends of N photo. CS checked photo error margins using additional reference features.
31st Oct. & 8th Nov. 1984	OceanBeach_MGA55_19840000.shp	Hannah Walford (2011) & Chris Sharples (2016) (Chris Sharples (2016) checked and slightly edited previously digitised shoreline)	HW digitised north-mid parts; CS digitised south part. CS updated photo error margins using additional reference features.
19th Mar. 1985	OceanBeach_MGA55_19850319.shp	Hannah Walford (2011) (Chris Sharples (2016) checked and slightly edited digitised shoreline)	CS checked photo error margins using additional reference features.
26th Feb. 1987	OceanBeach_MGA55_19870226.shp	Chris Sharples (2016)	
14th & 16th Dec. 1988	OceanBeach_MGA55_19881200.shp	Hannah Walford (2011) (Chris Sharples (2016) checked and slightly edited digitised shoreline)	CS checked photo error margins using additional reference features.
10th Nov. 1993	OceanBeach_MGA55_19931110.shp	Hannah Walford (2011 – south part) & Chris Sharples (2016 – north part) (CS checked and made minor edits to south part of digitised shoreline)	CS checked photo error margins using additional reference features.
2nd Dec. 1994	OceanBeach_MGA55_19941202.shp	Hannah Walford (2011) (Chris Sharples (2016) checked and slightly edited digitised shoreline)	CS checked photo error margins using additional reference features. Deleted southern part of digitised shoreline overlapping with 1995 photo:- almost same date but error margin anomalously large at S edge of photo, & photo not as clear)
23rd Feb. 1995	OceanBeach_MGA55_19950223.shp	Chris Sharples (2016)	
13th Feb 1996	OceanBeach_MGA55_19960213.shp	Chris Sharples (2016)	
8th Mar. 1998	OceanBeach_MGA55_19980308.shp	Chris Sharples (2016)	
17th Dec. 2000	OceanBeach_MGA55_20001217.shp	Hannah Walford (2011) (Chris Sharples (2016) checked and slightly edited digitised shoreline)	CS checked photo error margins using additional reference features.

1st Feb. 2001	OceanBeach_MGA55_20010201.shp	Hannah Walford (2011) (Chris Sharples (2016) checked and slightly edited digitised shoreline)	CS checked photo error margins using additional reference features.
28th Nov. 2003	OceanBeach_MGA55_20031128.shp	Hannah Walford (2011) (Chris Sharples (2016) checked and slightly edited digitised shoreline)	CS checked photo error margins using additional reference features.
9th Jan. & 15th Feb. 2008	OceanBeach_MGA55_20080000.shp	Hannah Walford (2011) (Chris Sharples (2016) checked and slightly edited digitised shoreline)	Reference image: CS created more error margin reference features.
6th Nov. 2010	OceanBeach_MGA55_20101106.shp	Chris Sharples (2016)	Entire digitised shoreline shifted to eliminate consistent offset wrt. 2008 reference image (see Table 55 notes).

TASMARC shore profile data tables

Table 57: GPS-surveyed co-ordinates of each TASMARC transect survey mark at Ocean Beach (see map **Error! Reference source not found.**). The survey marks are located at the landwards end of each transect, which runs seawards normal to the shoreline from each mark. Longitude and Latitude are decimal degrees and eastings and northings are metric co-ordinates of the Map Grid of Australia Zone 55 (MGA55, GDA94 datum).

Transect	Longitude	Latitude	Easting	Northing
730/108	145.263183	-42.15089527	356499.049	5332009.988
730/109	145.2497888	-42.19216757	355486.3574	5327404.613
730/110	145.2254495	-42.21422634	353527.5887	5324913.718

Table 58: Table of hinge points defined for each surveyed Ocean Beach profile (derived from original TASMARC survey data).

TASMARC profile number	Survey Date	Hinge Point distance offshore from survey mark	Hinge point height above AHD (metres)
730/108	03/05/2011	30.34	2.72
730/108	14/06/2012	28.17	2.45
730/108	06/12/2013	26.18	1.84
730/108	11/05/2015	24.26	2.62
730/108	15/05/2016	23.24	2.73
730/108	24/06/2017	21.43	2.53
730/108	04/08/2018	20.49	2.60
730/108	01/06/2019	19.30	2.65
730/109	4/05/2011	42.2	2.42
730/109	14/06/2012	41.13	2.58
730/109	6/12/2013	35.41	2.37
730/109	11/05/2015	32.75	2.25
730/109	14/05/2016	32.07	2.56
730/109	24/06/2017	30.28	2.77
730/109	18/08/2018	28.8	2.25
730/109	01/06/2019	28.2	2.5
730/110	4/05/2011	26.91	2.83
730/110	14/06/2012	41.16	2.16
730/110	6/12/2013	16.96	2.03
730/110	11/05/2015	27.15	2.42
730/110	25/06/2017	25.97	2.67
730/110	4/08/2018	31.84	2.2
730/110	01/06/2019	39.1	1.2

A1.3.9 Green Point Beach (Marrawah, far north-west Tasmania)

Air photo analysis

17 air photo dates from May 1930 (almost the oldest known air photos of Tas; could not be ortho-rectified but georeferencing with "rubber-sheeting" in ArcMap gave comparable results - likely due to flat topography) to 2011.

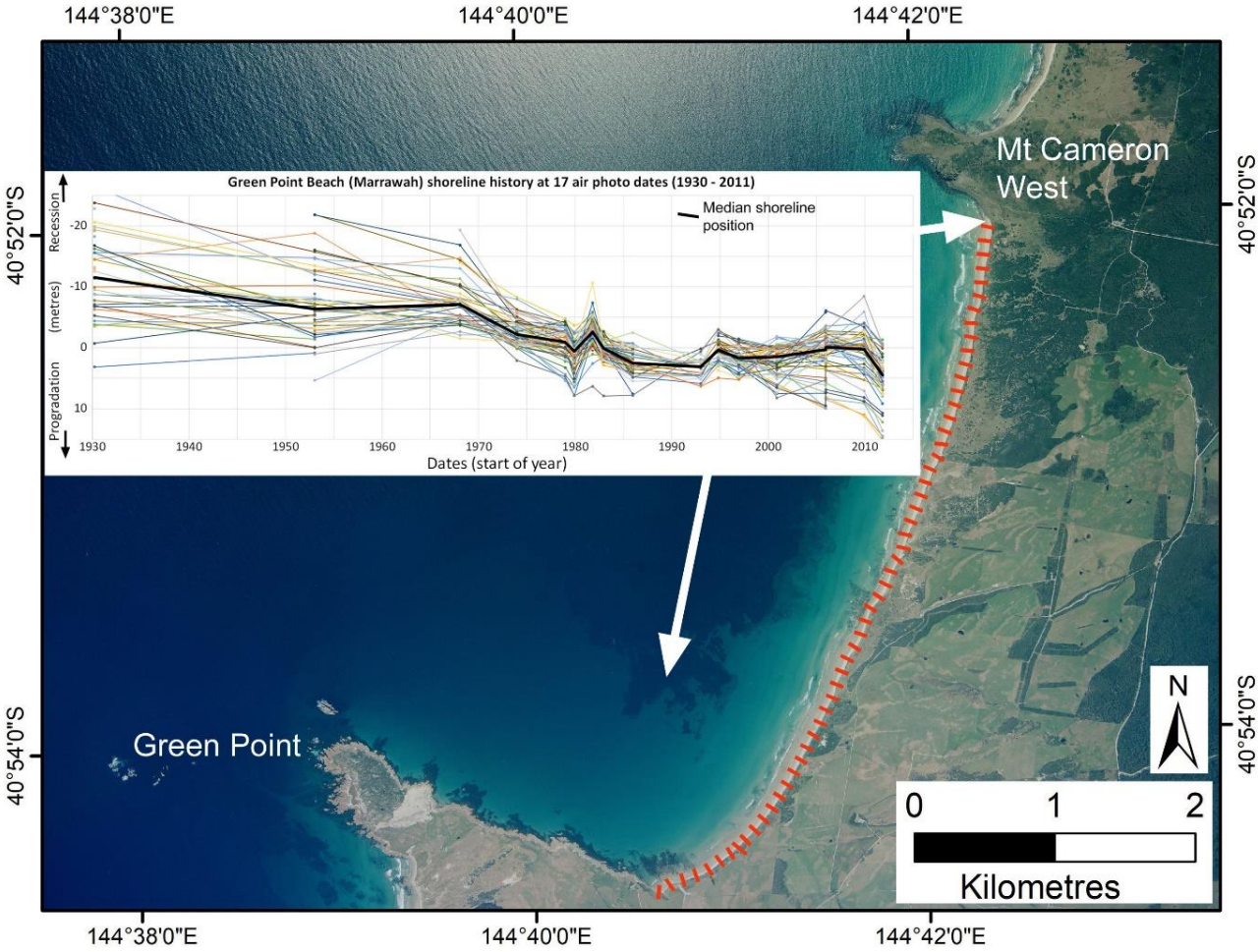

Figure 186: Plots of shoreline (*in situ* vegetation line) position movement over the period 1930 to 2011 along each 100m-spaced digital transect line used. The shoreline history is mostly coherent across all transects (i.e., along the full length of the beach) and hence all transect lines histories have been plotted together on this figure. The background image is the 21st January 2006 air photo, transect lines are indicated by red lines on the air photo, and each coloured line on the plot depicts shoreline position changes over time on one transect (measured relative to the median shoreline position on each transect.

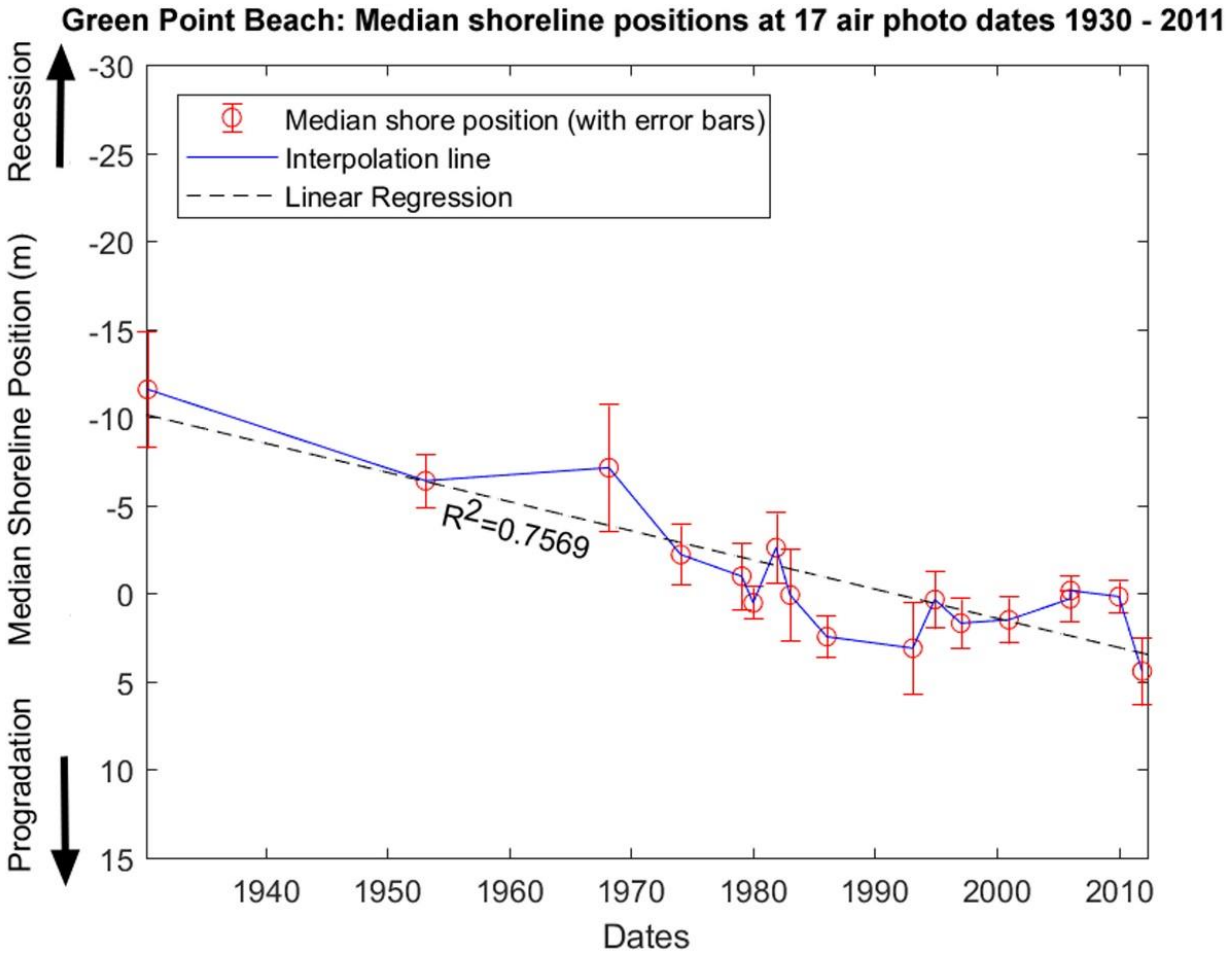

Figure 187: Summary plot of shoreline change history across all transects (as shown on Figure 186) at Green Point Beach at 17 air photo dates from 1930 to 2011. This plot shows the median of the shoreline positions measured on all transects (relative to the median position on each transect) at each air photo date. Error bars are the average measured feature position error margins relative to the 21st Jan 2006 air photo. Figure shows shore positions at each air photo date with interpolation lines and linear fit (linear regression). For comparison purposes the Y-axis scale (shoreline position) is the same as for all other beach history plots in this project.

Shore behaviour history from air photos

1. Early photos show extensive bare transgressive dunes extending inland in NE direction, mostly behind northern half of beach (most exposed? Check wind directions – is there a Marrawah wind record?). Fairly rapid early foredune accretion - can just see vegetation (incipient foredunes) beginning to establish across seawards end of transgressive dunes in 1930 pic, still large bare mobile sand blows in 1953 but by 1968 vegetated foredunes are well established and bare mobile dune sand areas much reduced (remnants mostly behind north end of beach). Some minor bare sand dune areas persist into 1980s and 1990s but only very minor, and virtually no bare areas by 2011. Basically, active deflation gullies and NE-trending bare mobile transgressive dunes behind north half beach in 1930s to 1950s, but thereafter progressively stabilised up to 2011 (largely due to marram grass establishment?)

2. Overall shoreline progradation trend from at least 1953 up to 1980 (at least partly driven by marram expansion?) (*same as at Ocean Beach*) then (*in contrast to Ocean Beach but with a change of behaviour around the same time – and for same reason, a big storm??*) a stable shoreline position with likely minor erosion/recovery events but no significant trend to either

progradation or recession between 1980 and 2011. (Overall progradation trend with good R^2= 0.7569 correlation, however inspection indicates progradation mainly up to 1980, then mainly stability with some recent progradation around 2010-2011)

Air photo data tables

The following tables provide details of the air photos used, the resulting ortho-photos produced, and the shapefiles representing the shoreline position that were digitised from the ortho-photos.

Table 59: Original air photos and ortho-rectified air photos produced for Green Point Beach, Marrawah

Photo Date	**Original DPIPWE air photos (film-frame) / Ortho-photo name**	**Final image resolution (original scan resolution if downsized) / pixel size of final ortho-photo**	**Original photo scale**	**Mean measured feature position error (± metres) for ortho-photo** [no. of measured feature position reference points]	**Comments**
3rd May 1930	1-861 1-862 / *GreenPointBeach_May1930a_MGA55.tif/tfw; GreenPointBeach_May1930b_MGA55.tif/tfw*	1000 dpi (both) / 0.6 m mean pixel size (1930a 0.56m, 1930b 0.64m)	1:20,000	3.3 [7]	Geo-referenced (not ortho-rectified) by C. Sharples from original scanned tiffs. [Georeferenced with ArcMap Geo-referencing tool using "Transformative projection" mode].
23rd Feb 1953	260-551 260-552 / *GreenPointBeach_Feb1953a_MGA55.tif/tfw ; GreenPointBeach_Feb1953b_MGA55.tif/tfw*	2039 dpi / 0.32 m pixel size	1:23,760	1953b (260-552): 1.48 [7]	Ortho-rectified by Chris Sharples NOTE: 260-551 and 260-552 both cover whole beach, but 260-552 used for shoreline mapping due to better contrast & smaller ortho-rec errors. However, 260-551 covers more of backshore active transgressive dunes.
8th Mar 1968	507-39 507-52 / *GreenPointBeach_Mar1968a_MGA55.tif/tfw;* *GreenPointBeach_Mar1968b_MGA55.tif/tfw*	2039 dpi / 0.4 m pixel size	1:31,680	 3.6 [4] 10.4 [5]	Ortho-rectified by Chris Sharples **NOTE:** USED Mar1968a (marginal accuracy, covers most of area) DID NOT USE Mar1968b (crap accuracy)
31st Jan 1974	654-21 / *GreenPointBeach_Jan1974_MGA55.tif/tfw*	2039 dpi / 0.68 m pixel size	1:40,000	1.7 [9]	Ortho-rectified by Chris Sharples
1st Feb 1979	790-34 / *GreenPointBeach_Feb1979_MGA55.tif/tfw*	2039 dpi / 0.51 m pixel size	1:40,000	1.9 [9]	Ortho-rectified by Chris Sharples
8th Jan 1980	810-91 / *GreenPointBeach_Jan1980_MGA55.tif/tfw*	2039 dpi / 0.52 m pixel size	1:40,000	0.9 [10]	Ortho-rectified by Chris Sharples
27th Nov 1981	891-104 / *GreenPointBeach_Nov1981_MGA55.tif/tfw*	2039 dpi / 0.56 m pixel size	1:42,000	2.0 [10]	Ortho-rectified by Chris Sharples
21st Jan 1983	945-75 / *GreenPointBeach_Jan1983_MGA55.tif/tfw*	2039 dpi / 0.53 m pixel size	1:42,000	2.6 [10]	Ortho-rectified by Chris Sharples
24th Jan 1986	1053-209 1053-212	1500 dpi (2039 dpi)	1:20,000	1.2 [9]	Ortho-rectified by Chris Sharples

	/ *GreenPointBeach_Jan 1986a_MGA55.tif/tfw; GreenPointBeach_Jan 1986b_MGA55.tif/tfw*	/ 0.35 m pixel size			
13th Feb 1993	1198-180 / *GreenPointBeach_Fe b1993_MGA55.tif/tfw*	1500 dpi (2039 dpi) / 0.36 m pixel size	1:20,000	2.6 [3]	Ortho-rectified by Chris Sharples North half of beach only
5th Dec 1994	1226-154 / *GreenPointBeach_De c1994_MGA55.tif/tfw*	2039 dpi / 0.56 m pixel size	1:42,000	1.6 [10]	Ortho-rectified by Chris Sharples
20th Jan 1997	1266-154 1266-159 / *GreenPointBeach_Jan 1997a_MGA55.tif/tfw; GreenPointBeach_Jan 1997b_MGA55.tif/tfw*	1500 dpi (2039 dpi) / 0.35 m pixel size	1:20,000	1.4 [9]	Ortho-rectified by Chris Sharples
1st Jan 2001	1340-138 / *GreenPointBeach_Jan 2001_MGA55.tif/tfw*	1500 dpi (2039 dpi) / 0.76 m pixel size	1:42,000	1.3 [10]	Ortho-rectified by Chris Sharples
8th Jan 2006	1402-238 1403-49 / *GreenPointBeach_8Ja n2006a_MGA55.tif/tfw ; GreenPointBeach_8Ja n2006b_MGA55.tif/tfw ;*	1500 dpi (2039 dpi) / 0.35 m pixel size	1:20,000	1.3 [10]	Ortho-rectified by Chris Sharples
21st Jan 2006	1403-226 / *GreenPointBeach_21J an2006_MGA55.ecw*	2039 dpi / 0.5 m pixel size	1:42,000	0.0 m [N/A] (quoted absolute accuracy ±15 m)	REFERENCE IMAGE (zero relative feature position error by convention) (Dec 2011 image not used as reference to ortho-rectify to since the ecw won't open properly in Landscape Mapper thus cannot ortho-rectify to it.) Ortho-rectified by DPIPWE Original DPIPWE ortho file: 1403_226_op.ecw
7th Jan 2010	1442-6 / *GreenPointBeach_Jan 2010_MGA55.tif/tfw*	1500 dpi (2039 dpi) / 0.8 m pixel size	1:42,000	0.9 [10]	Ortho-rectified by Chris Sharples
8th Dec 2011	1464-148 1464-149 / *GreenPointBeach_De c2011a_MGA55.ecw GreenPointBeach_De c2011b_MGA55.ecw*	2039 dpi / 0.3m pixel size	1:24,000	1.9 [10] (quoted absolute accuracy ±10 m)	Digital original photos; Ortho-rectified by DPIPWE Original DPIPWE ortho files: 1464_148_op.ecw 1464_149_op.ecw

Table 60: Digitised shoreline shapefiles produced for Green Point Beach, Marrawah (using ortho-photos listed in Table 59 above).

Date of air photo(s)	Shapefile	Shoreline digitised by	Comments
3rd May 1930	GreenPointBeach_MGA55_19300503.shp	Chris Sharples (2018)	Moderate resolution, vegetation line distinct. Difficult to discern differences between incipient and

			established foredunes, however large sand blowouts extending inland are present and obvious. Only wave-exposed veg lines mapped (not deflation margins).
23rd Feb 1953	GreenPointBeach_MGA55_19530223.shp	Chris Sharples (2018)	Used frame 260-552 only. Good resolution and contrast, no shadowing, veg. line distinct (mainly clumpy to sparse incipient dune veg establishing on beach side of extensive bare mobile sand blowouts). Large bare mobile transgressive dunes behind north half beach, distinct incipient dune line to seawards mapped.
8th Mar 1968	GreenPointBeach_MGA55_19680308.shp	Chris Sharples (2018)	Used frame 507-39 only. Moderate resolution, vegetation line a little fuzzy but mappable. However strong easterly shadowing obscures vegetation line in parts, needed to map zoomed out to pick line. Some incipient dune veg establishing at beach end of large blowouts.
31st Jan 1974	GreenPointBeach_MGA55_19740131.shp	Chris Sharples (2018)	Coarse resolution, no shadowing, vegetation line fuzzy but mappable. Veg. line mostly reasonably straight, with some faint incipient dune gasses mapped in north area. Some large bare deflating dune areas in backshore, especially behind north end of beach.
1st Feb 1979	GreenPointBeach_MGA55_19790201.shp	Chris Sharples (2018)	Coarse resolution, no shadowing, vegetation line fuzzy but mappable. Veg line ragged in northern area, likely includes clumpy incipient dune grasses. Some notably clumpy incipient dune veg. in south area.

			Some large bare deflation areas in backshore.
8th Jan 1980	GreenPointBeach_MGA55_19800108.shp	Chris Sharples (2018)	Coarse resolution, no shadowing, vegetation line fuzzy but mappable. Veg line ragged in northern area.
27th Nov 1981	GreenPointBeach_MGA55_19811127.shp	Chris Sharples (2018)	Coarse resolution, no shadowing, vegetation line fuzzy but mappable, less distinct veg in parts is likely incipient dune grasses. Veg. line ragged in northern area.
21st Jan 1983	GreenPointBeach_MGA55_19830121.shp	Chris Sharples (2018)	Moderate resolution, no shadowing, vegetation line fuzzy but mappable. Fairly ragged line in northern area, probably includes clumpy incipient dune veg. Smoother veg line in south area
24th Jan 1986	GreenPointBeach_MGA55_19860124.shp	Chris Sharples (2018)	Good resolution, veg line distinct, no shadowing. Veg line ragged in northern area, possibly part slumped, likely part clumpy incipient dune veg.
13th Feb 1993	GreenPointBeach_MGA55_19930213.shp	Chris Sharples (2018)	North half beach only, moderate to good resolution, good contrast, veg line distinct but some easterly shadowing obscures line in parts. Veg. line partly ragged, likely includes some incipient dune veg. Some older scarping behind ragged veg line evident.
5th Dec 1994	GreenPointBeach_MGA55_19941205.shp	Chris Sharples (2018)	Moderate resolution low contrast, no shadowing. Veg line a bit 'fuzzy' but mappable. Veg line ragged in north part, possibly includes clumpy incipient dune veg but hard to be sure.
20th Jan 1997	GreenPointBeach_MGA55_19970120.shp	Chris Sharples (2018)	Good resolution, veg line well defined, no shadowing. Veg line somewhat ragged in north half beach, less so in south. Likely includes clumpy incipient dune grasses (not certain).

1st Jan 2001	GreenPointBeach_MGA55_20010101.shp	Chris Sharples (2018)	Coarse resolution, no shadowing, veg line distinct, quite ragged in northern parts - no recent erosion, likely some incipient dune accretion but hard to identify clearly owing to coarse resolution.
8th Jan 2006	GreenPointBeach_MGA55_20060108.shp	Chris Sharples (2018)	Good resolution, no shadowing, veg line well defined looks somewhat ragged (no recent erosion?), possibly includes some clumpy incipient dune veg.
21st Jan 2006	GreenPointBeach_MGA55_20060121.shp	Chris Sharples (2018)	Moderate resolution, no shadowing, veg line well defined. Includes patchy incipient dune veg behind northern half of beach.
7th Jan 2010	GreenPointBeach_MGA55_20100107.shp	Chris Sharples (2018)	Coarse resolution, image somewhat contrasty but no apparent shadowing; veg line reasonably clear including clumpy incipient dune veg mapped as veg line.
8th Dec 2011	GreenPointBeach_MGA55_20111208.shp	Chris Sharples (2018)	Good resolution, veg. line clearly visible; mostly fairly ragged – not recently eroded, likely some incipient dune veg.

A1.4 *Other swell-exposed sandy shores*

A1.4.1 Wineglass Bay Beach (Freycinet Peninsula, mid-east Tasmania)

Figure 188: View looking south of the north-west part of Wineglass Bay beach and foredune during February 2011. This photo shows a small recent beach erosion scarp (foreground), however only traces of an old foredune erosion scarp are visible, with most of the foredune front colonised by patchy incipient foredune vegetation and no evidence of recent foredune erosion. Photo by C. Sharples.

Air photo analysis

A key limitation on interpretation of historic shoreline change at Wineglass Bay beach is that higher-resolution air photos mostly show diffuse or patchy incipient foredune vegetation to seawards of the denser established foredune vegetation, however on coarser resolution photos it is sometimes difficult to determine whether similar incipient vegetation is present or not. This has shoreline mapping implications since the adopted protocol for this project is to map the incipient vegetation front as the shoreline where present. This protocol has been followed, with the denser more established vegetation line to landwards being mapped as the shoreline where incipient vegetation to seawards cannot be discerned. However, this means that in some cases an apparent small retreat of the shoreline (on a coarse-resolution air photo) may not be real but rather an artefact of incipient vegetation being present but not discernible on the photo. Note that wrack or slumped vegetated dune scarp blocks are generally clearly recognisable as such on these air photos and are not mapped as incipient vegetation.

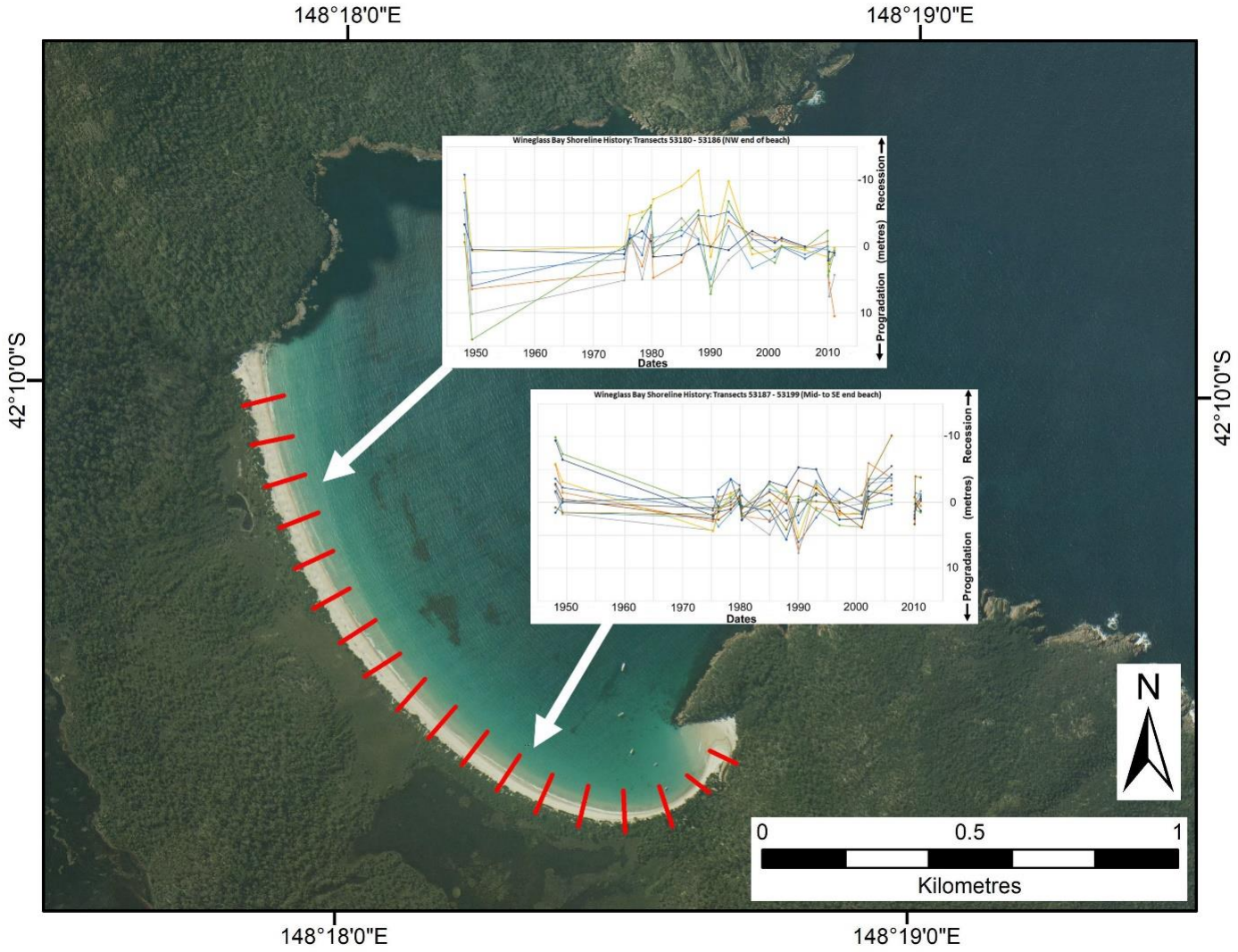

Figure 189: Plots of shoreline (vegetation line) movement along each digital transect at Wineglass Bay beach at 19 air photo dates over the period 1948 to 2011, plotted relative to the median shoreline position on each transect. Transect locations are indicated by red lines on the air photo, and each coloured line on the plots represents shoreline position changes over time along one transect. Transects are plotted in two groups, with the northern (more directly swell-exposed) group showing slightly less coherent transect plots with larger amplitudes of erosion and recovery. The base image is the Feb 2010 air photo.

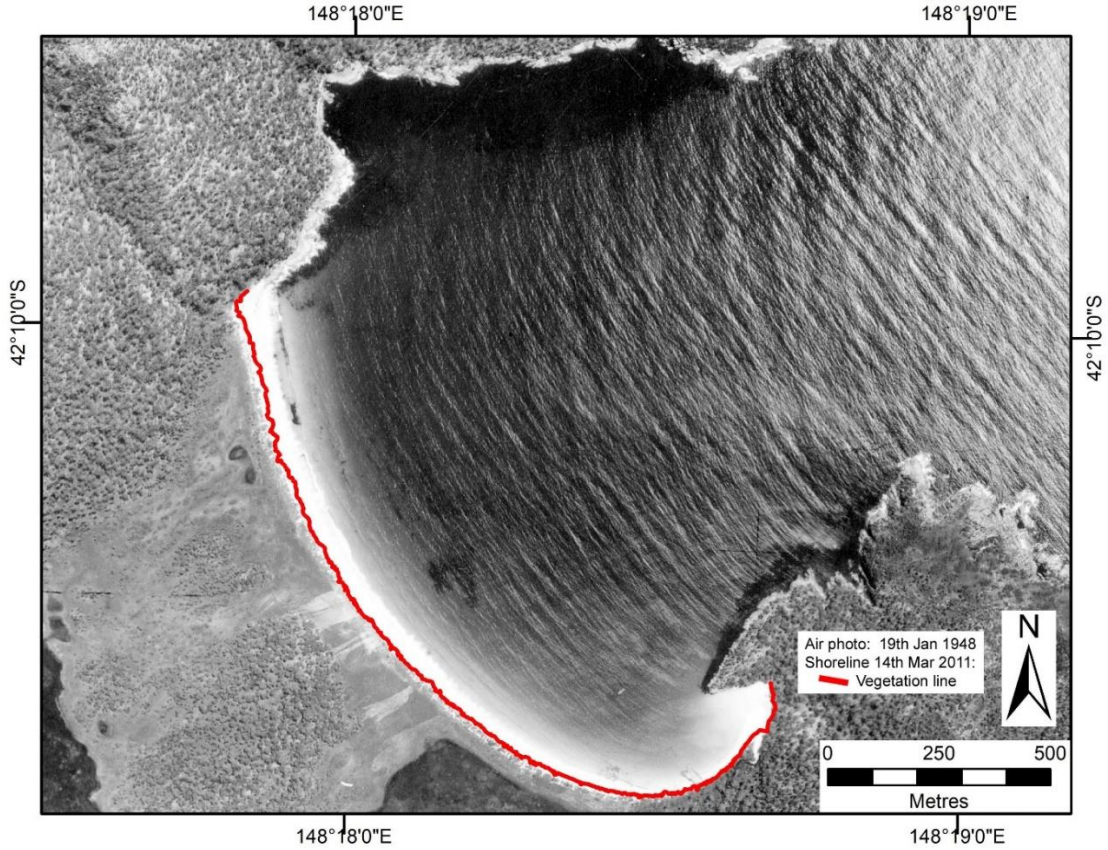

Figure 190: Comparison of shoreline positions at Wineglass Bay between 1948 (ortho-rectified photo) and 2011 (shoreline proxy digitised from 2011 ortho-photo). Very little difference (if any) between the shorelines 63 years apart is evident.

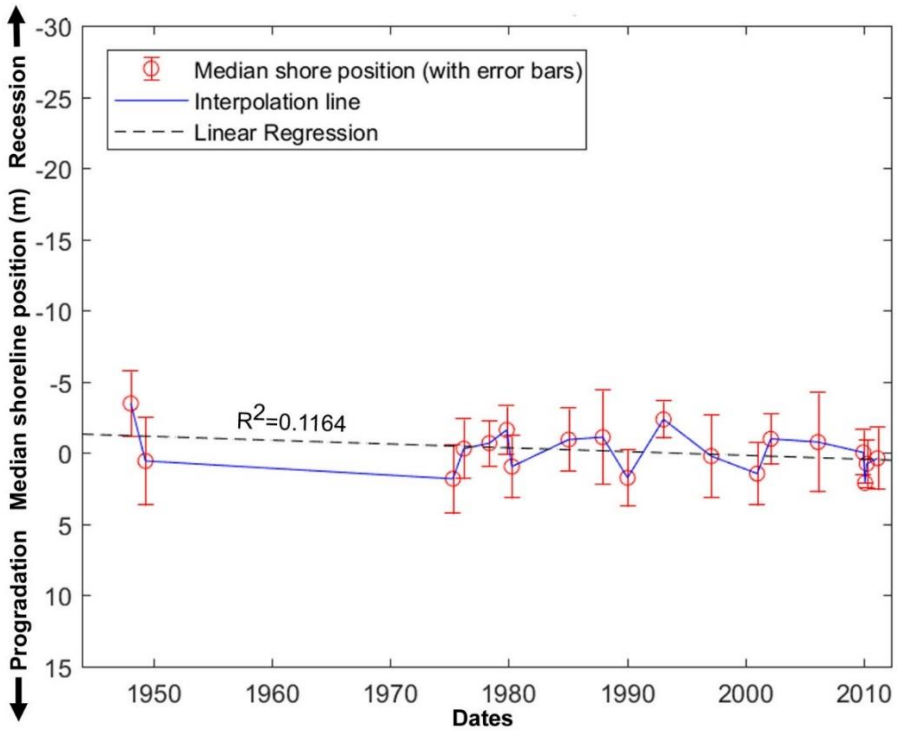

Figure 191: Summary plot of shoreline change history across all transects (as shown on Figure 189) at Wineglass Bay beach at 19 air photo dates from 1948 to 2011. This plots the median of the shoreline positions measured on all transects (relative to the median position on each transect) at each air photo date. Figure shows interpolation lines & linear regression plot.

Shore behaviour history from air photos

Essentially a very stable beach with a possible small long-term progradation trend (but equivocal; within error margins and low Pearson correlation co-efficient on linear regression line

More movement in NW half of beach throughout (indicating larger erosion events there throughout) – inferred due to more exposure to less refracted swell at North end of beach.

Some evidence of revegetated blow-outs in oldest photos, completely revegetated later – suggestive of pre-1948 mobile sand and transgressive dunes, but no activity during air photo period

Overall, the air photo record suggests that Wineglass Bay beach has been a very stable beach from pre-1948 up to at least 2011, with only small and mostly equivocal (less than error margin-scale) erosion events evident in the air photo record. Indeed, much of the apparent shoreline position variability may be an artefact of the incipient dune vegetation being more detectable – and thus mappable - in some photos than others. At most air photo dates there is no evidence of recent shoreline erosion at Wineglass Bay, with no scarps visible and incipient vegetation either clearly visible or suggested by tonal variations on coarser resolution photos. This is true of the air photos from 1948 until 1978, and from 1980 until the most recent air photo from 2011. The few apparent erosion events on the shoreline movement record for Wineglass Bay (Figure 191) are of lesser scale than the air photo error margins and are thus equivocal.

The only clear evidence of an erosion event at Wineglass Bay is the photographic evidence of a foredune erosion scarp, partly slumped with dune vegetation slump blocks, that is clearly visible backing the north-west half of the beach on the 6th November 1979 air photo. This implies a major erosion event since the previous air photo date of 15th May 1978, whose effects appear most marked in the NW half of the beach. Although the median shoreline position plot (Figure 191) shows only a small erosional movement in this interval and a larger one after 1980, these discrepancies fall within the air photo error margins and hence may not be real.

Whereas the longer times between air photos in the earlier part of the air photo record means that additional major undetected erosion events may have occurred prior to 1978, it is notable that no other evidence of large erosion events is seen in the later part of the air photo record despite much more frequent air photo dates, supporting the likelihood that this beach is only very rarely exposed to storm waves capable of causing foredune recession.

Air photo data tables

The following tables provide details of the air photos used, the resulting ortho-photos produced, and the shapefiles representing the shoreline position that were digitised from the ortho-photos.

Table 61: Original air photos and ortho-rectified air photos produced for Wineglass Bay Beach.

Photo Date	**Original DPIPWE air photos (film-frame) / Ortho-photo name**	**Final image resolution (original scan resolution if downsized) / pixel size of final ortho-photo**	**Original photo scale**	**Mean measured feature position error (± metres) for ortho-photo** [no. of measured feature position reference points]	**Comments**
19th Jan 1948	139-2904 / *WineglassBay_Jan1948 _MGA55.tif/tfw;*	600 dpi / 1.0 m pixel size	1:15,840	2.3 [9]	Ortho-rectified by C. Sharples (pixels stretched during ortho-rectification - result is good in GIS display)
16th April 1949	169-4629 / *WineglassBay_Apr1949 _MGA55.tif/tfw;*	600 dpi / 1.0 m pixel size	1:15,840	3.1 [10]	Ortho-rectified by C. Sharples (pixels stretched during ortho-rectification - result is good in GIS display)
18th April 1975	679-248 / *WineglassBay_Apr1975 _MGA55.tif/tfw;*	2039 dpi / 0.7 m pixel size	1:40,000	2.4 [9]	Ortho-rectified by C. Sharples
18th Mar 1976	695-99 / *WineglassBay_Mar1976 _MGA55.tif/tfw;*	2039 dpi / 0.5 m pixel size	1:40,000	2.1 [9]	Ortho-rectified by C. Sharples
15th May 1978	768-178 / *WineglassBay_May1978 _MGA55.tif/tfw;*	2039 dpi / 0.2 m pixel size	1:17,000	1.6 [8]	Ortho-rectified by C. Sharples
6th Nov 1979	804-62 / *WineglassBay_Nov1979 _MGA55.tif/tfw*	2039 dpi / 0.2 m pixel size	1:15,000	1.7 [9]	Ortho-rectified by C. Sharples
9th April 1980	832-60 / *WineglassBay_Apr1980 _MGA55.tif/tfw;*	1500 dpi (2039 dpi) / 0.8 m pixel size	1:42,000	2.2 [9]	Ortho-rectified by C. Sharples
29th Jan 1985	1023-57 / *WineglassBay_Jan1985 _MGA55.tif/tfw;*	2039 dpi / 0.6 m pixel size	1:42,000	2.2 [9]	Ortho-rectified by C. Sharples
17th Dec 1987	1094-12 / *WineglassBay_Dec1987 _MGA55.tif/tfw;*	1500 dpi (2039 dpi) / 0.8 m pixel size	1:42,000	3.3 [9]	Ortho-rectified by C. Sharples
22nd Jan 1990	1147-120 / *WineglassBay_Jan1990 _MGA55.tif/tfw;*	2039 dpi / 0.2 m pixel size	1:15,000	2.0 [9]	Ortho-rectified by C. Sharples
6th Feb 1993	1200-233 / *WineglassBay_Feb1993 _MGA55.tif/tfw;*	2039 dpi / 0.6 m pixel size	1:42,000	1.3 [10]	Ortho-rectified by C. Sharples
18th Feb 1997	1270-142 / *WineglassBay_Feb1997 _MGA55.tif/tfw;*	2039 dpi / 0.3 m pixel size	1:24,000	2.9 [10]	Ortho-rectified by C. Sharples
9th Jan 2001	1343-92 / *WineglassBay_Jan2001 _MGA55.tif/tfw;*	1500 dpi (2039 dpi) / 0.4 m pixel size	1:24,000	2.2 [10]	Ortho-rectified by C. Sharples

5th Mar 2002	1356-191 / *WineglassBay_Mar2002 _MGA55.tif/tfw;*	1500 dpi (2039 dpi) / 0.8 m pixel size	1:42,000	1.8 [10]	Ortho-rectified by C. Sharples
2nd Mar 2006	1407-22 / *WineglassBay_Mar2006 _MGA55.ecw*	2039 dpi / 0.5m pixel size	1:42,000	3.5 [10] (quoted absolute accuracy ±15 m)	Ortho-rectified by DPIPWE Original DPIPWE ortho: 1407-22_op.ecw
31st Dec 2009	1441-26 / *WineglassBay_Dec2009 _MGA55.tif*	1500dpi (2039 dpi) / 0.25 m pixel size	1:12,500	1.6 [4]	Ortho-rectified by Chris Sharples North half beach only
25th Feb 2010	1444-262 / *WineglassBay_Feb2010 _MGA55.ecw*	2039 dpi / 0.5 m pixel size	1:42,000	0.0 [N/A] (quoted absolute accuracy ±15 m)	REFERENCE IMAGE (zero relative feature position error by convention) Ortho-rectified by DPIPWE Original DPIPWE ortho: 1444-262_op.ecw
18th Apr 2010	1446-34 / *WineglassBay_Apr2010 _MGA55.tif*	1500 dpi (2039 dpi) / 0.25 m pixel size	1:11,00	1.7 [10]	Ortho-rectified by Chris Sharples
14th Mar 2011	1457-153 / *WineglassBay_Mar2011 _MGA55.ecw*	2039 dpi / 0.3 m pixel size	1:24,000	2.19 [10] (quoted absolute accuracy ±10 m)	Not used as reference image since does not display correctly in Landscape Mapper™. Ortho-rectified by DPIPWE Original DPIPWE ortho: 1457-153_op.ecw

Table 62: Digitised shoreline shapefiles produced for Wineglass Bay Beach, (using ortho-photos listed in Table 61 above).

Date of air photo(s)	Shapefile	Shoreline digitised by	Comments
19th Jan 1948	WineglassBay_MGA55_19480119.shp	Chris Sharples (2019)	Good contrast but very coarse resolution. Very little incipient veg. visible, established dune veg. front patchy/irregular but not blown out. Mapped irregular dune front veg. line including incipient veg where visible.
16th April 1949	WineglassBay_MGA55_19490416.shp	Chris Sharples (2019)	Coarse resolution, good contrast, abundant patchy incipient dune veg. in front of NW half of foredune. Mapped incipient veg. or if absent then established veg line. No erosion scarp visible. Northerly shadows allowed for.
18th April 1975	WineglassBay_MGA55_19750418.shp	Chris Sharples (2019)	Coarse resolution, moderate contrast only. No erosion scarp visible. Mapped established veg line and sporadic patchy incipient veg where visible. Northerly shadows allowed for.

18th Mar 1976	WineglassBay_MGA55_19760318.shp	Chris Sharples (2019)	Medium resolution, poor contrast, no erosion scarp visible. Mapped veg. line is minor patchy incipient veg where visible, elsewhere established veg line.
15th May 1978	WineglassBay_MGA55_19780515.shp	Chris Sharples (2019)	Good resolution but poor glary contrast. Can't identify any erosion scarp. Mapped patchy likely incipient veg. where present as shoreline, elsewhere established veg line. Strong northerly shadows allowed for.
6th Nov 1979	WineglassBay_MGA55_19791106.shp	Chris Sharples (2019)	Good resolution and contrast, *erosion scarp and recent slumped erosion scarp visible in NW half of beach*. Mapped fairly straight established veg edge, scarp and mid-slumped scarp as shoreline. Slumped veg. blocks common, only minor patches of incipient veg visible. Some tree shadows allowed for.
9th April 1980	WineglassBay_MGA55_19800409.shp	Chris Sharples (2019)	Coarse resolution, good contrast; incipient veg. barely visible but mapped as veg. line where visible, elsewhere established veg line mapped. *No scarp visible, but veg. line fairly straight – likely not long after large erosion event?* Some wrack ignored.
29th Jan 1985	WineglassBay_MGA55_19850129.shp	Chris Sharples (2019)	Moderate to coarse resolution, fair to poor contrast; patchy incipient veg. barely visible but mapped as veg. line where visible, elsewhere established veg line mapped. No scarps visible.
17th Dec 1987	WineglassBay_MGA55_19871217.shp	Chris Sharples (2019)	Good contrast but very coarse resolution; patchy incipient veg. barely visible but mapped as veg. line where visible, elsewhere established veg line mapped. No scarps visible.
22nd Jan 1990	WineglassBay_MGA55_19900122.shp	Chris Sharples (2019)	Good contrast and resolution, patchy incipient veg visible and mapped as veg. line where present, else established veg line mapped. No scarps visible.

6th Feb 1993	WineglassBay_MGA55_19930206.shp	Chris Sharples (2019)	Coarse resolution, good contrast but only clumpier incipient veg visible. Mapped established veg. line or incipient veg clumps where visible. No scarps identifiable.
18th Feb 1997	WineglassBay_MGA55_19970218.shp	Chris Sharples (2019)	Good contrast and resolution, patchy incipient veg visible and mapped as veg. line where present, else established veg line mapped. No scarps visible.
9th Jan 2001	WineglassBay_MGA55_20010109.shp	Chris Sharples (2019)	Moderate resolution, good contrast but only a little incipient veg. visible. Established veg line mapped plus incipient veg where visible, no scarps visible.
5th Mar 2002	WineglassBay_MGA55_20020305.shp	Chris Sharples (2019)	Coarse resolution, good contrast but only a little incipient veg. visible. Established veg line mapped plus incipient veg where visible, no scarps visible.
2nd Mar 2006	WineglassBay_MGA55_20060302.shp	Chris Sharples (2019)	Moderate resolution only, good contrast. Incipient veg. not visible but likely present; established veg line mapped; no scarps visible.
31st Dec 2009	WineglassBay_MGA55_20091231.shp	Chris Sharples (2019)	Good contrast and resolution; well established veg. Line with some incip. veg in front. No erosion scarp. Photo covers north half of beach only.
25th Feb 2010	WineglassBay_MGA55_20100225.shp	Chris Sharples (2019)	Contrast good, moderate resolution. No scarp visible, well defined vegetation line with some scattered incipient veg in front included in line.
18th Apr 2010	WineglassBay_MGA55_20100418.shp	Chris Sharples (2019)	Good contrast & resolution, well defined established veg. line with some scattered incipient veg. in front included in veg line. Minor upper beach

			scarp in parts but no dune erosion scarp.
14th Mar 2011	WineglassBay_MGA55_20110314.shp	Chris Sharples (2019)	Good resolution & contrast. No scarp visible, well defined vegetation line with some scattered incipient veg in front included in line.

A1.4.2 Roches Beach (south-eastern Tasmania)

Locality and general description

Roches Beach is located on the eastern side of a low sandy isthmus or neck linking South Arm peninsula to the mainland of south-eastern Tasmania, about 14 kilometres ESE of Hobart city (see Figure 192). Much of the township of Lauderdale is situated on the lowest parts of the sandy isthmus and has historically been subject to both coastal erosion at Roches Beach and to coastal flooding hazards from the opposite (Ralphs Bay) side of the isthmus (Sharples 2006). Numerous dwellings are situated on the foredune immediately behind a three-kilometre stretch of Roches Beach, making Lauderdale one of Tasmania's most at-risk townships because of expected increased flooding and erosion due to sea-level rise (DCC 2009). A failed shipping canal that was controversially constructed between Ralphs and Frederick Henry Bays during 1924 (Figure 192) was notoriously blocked at its eastern end by sand drifting along Roches Beach almost as soon as it was completed (Alexander 2003, p. 161). As a result, the canal and associated small ruined training walls do not significantly influence ongoing littoral drift and erosion processes at Roches Beach, although the flow pathway provided by the canal does make central parts of Lauderdale more vulnerable to storm surge floods moving onshore from Ralphs Bay to the west.

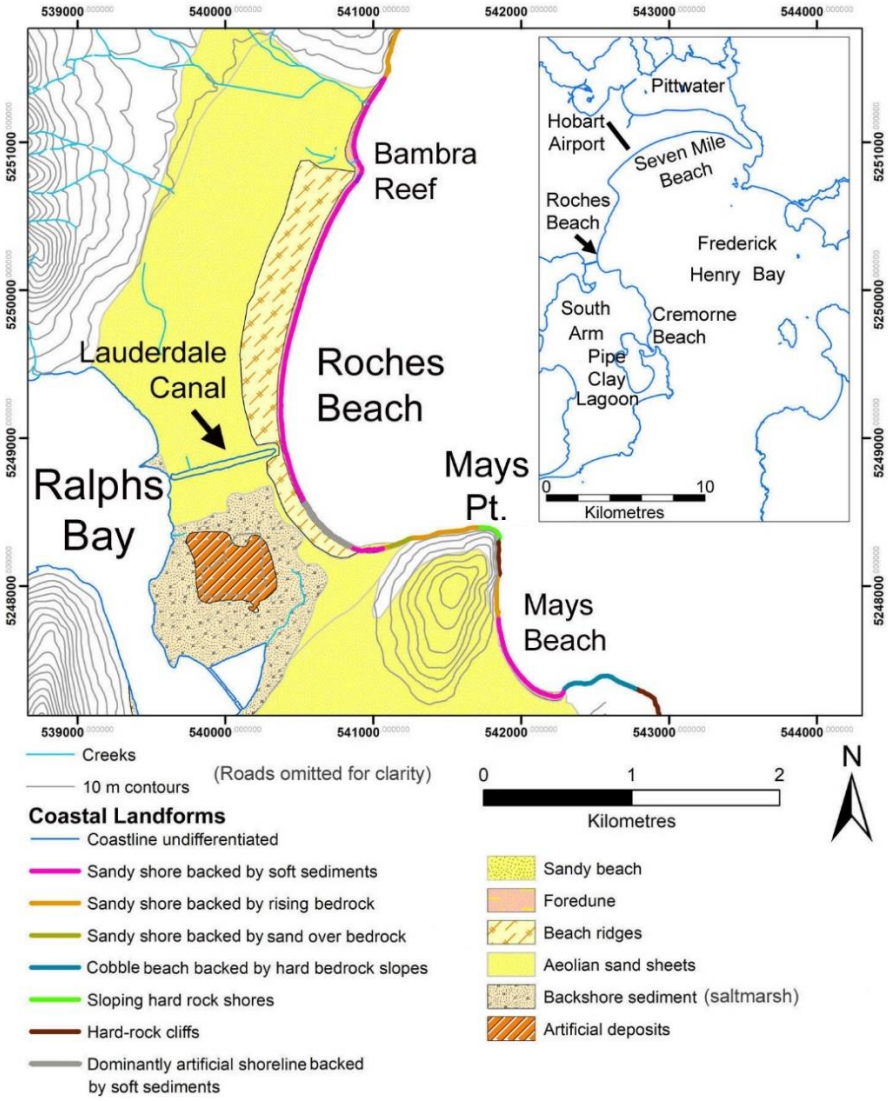

Figure 192: Locality and coastal landforms and substrates at Roches Beach, south-east Tasmania. Landform mapping is based on Davies (1961) with additional geomorphic mapping by C. Sharples. Co-ordinate system is Map Grid of Australia Zone 55 (GDA94 datum).

Figure 193: View north along the main part of Roches Beach several hundred metres north of the canal. This view shows the typical narrow beach face and scarped foredune front as it was over a period of repeated direct observations by the author from 2001 until July 2011. Throughout this period the erosion scarp showed occasional slumping and minor indications of incipient dune recovery but was dominated by progressive retreat owing to numerous small erosion events. The incremental exposure of the tree stump visible in this photo was photo-monitored by the author from 2004 (when the tree was still growing, and its roots were just beginning to protrude from the scarp) until July 2011 when the root ball was finally completed undermined and separated from the scarp by a large erosion event. Photo by Chris Sharples (6th March 2010).

Shoreline erosion has been a concern for residents at Roches Beach since at least the 1980's, when a boulder revetment currently protecting part of the southern end of the beach (Figure 202) was constructed in stages. The earliest major investigation of erosion at Roches Beach was conducted by Foster (1988), and the continuation of active shoreline recession from that time until 2011 has resulted in a series of subsequent consulting reports including Byrne (2006), Cromer (2006), Sharples (2010) and Shand and Carley (2011). Subsequent to a major swell-driven erosion event at Roches Beach during July 2011, the local government (Clarence Council) has utilised beach scraping and sand replenishment to maintain the beach and foredune while investigating longer-term options to artificially protect the beach. As a result, this study only utilises beach change data up until July 2011 since subsequent changes have been dominated by artificial interventions which have prevented the ongoing recession that would otherwise be expected to have continued to the present.

Geomorphology and process environment

Geomorphic description

Roches Beach comprises several low-energy wave-dominated beaches of fine to medium-grained sand separated by rocky outcrops, which Short (2006b) classifies as mostly an intermediate Low Tide Terrace (LTT) morpho-dynamic type. This study has divided Roches Beach into five distinctive sections based on differing long-term shoreline behaviour histories over approximately the last 70 years, as revealed by air photo time series analysis (see Figure 203). Attention is focussed primarily on two of these segments which contrast strongly in their behaviour, namely the long Roches Beach Main Central Section which has changed its long-term behaviour from stable to receding, and the Roches Beach North Section which has maintained its stable (dynamic equilibrium) shoreline position throughout the air photo period (see Figure 203). The contrast in historical behaviour between these two Sections reveals much about the sand budget and coastal processes at Roches Beach.

The main beach is located in a 3.5 km long drift-aligned zeta-form embayment (Figure 194, RHS), which extends from the bedrock control of the hard rocky (dolerite) Mays Point in the south (Figure 192), to the hard rocky dolerite salient of Bambra Reef in the north. The beach switches to a very low-

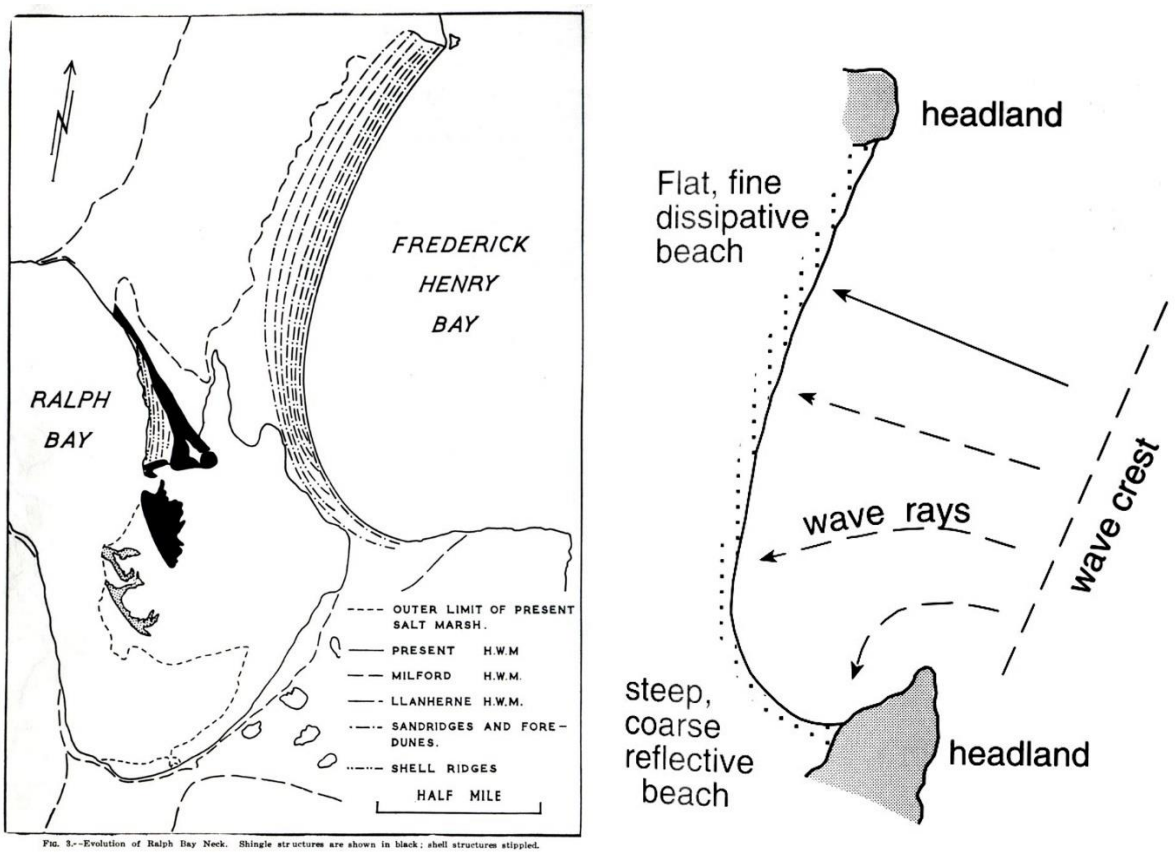

Figure 194: Development of the Ralphs Bay neck and Roches Beach. LHS: Figure reproduced from Davies (1961), showing development of Roches Beach on the eastern (Frederick Henry Bay) side of a series of prograded beach ridges which accreted as a spit across a former channel between South Arm peninsula (to the south) and the mainland (to the north) after sea-level reached approximately its present level circa 6500 years BP. RHS: Diagrammatic example of an embayed zeta-form beach showing wave refraction around a controlling headland. Figure reproduced from Woodroffe (2003, Fig. 6.5). Roches Beach is a characteristic example of such a beach, between the rocky headlands of Mays Beach to the south and Bambra Reef to the north.

energy reflective type in the southern 'hook' of the beach which is sheltered in the lee of Mays Point. The spring and neap tidal range is an approximately 1.2 to 0.3 m micro-tidal range (Short 2006b).

The main beach is backed by a single sandy foredune up to 3 m high above mean sea level (Cromer 2006), which in turn is backed by a series of lower but well-drained prograded sandy beach ridges whose surface forms have been subdued by urban development. The beach, dunes and beach ridges are underlain by unconsolidated sand to below present sea-level, which is turn is inferred to be underlain by semi-lithified Tertiary-age clayey bedrock at unknown depth (Leaman 1976, Fig. 10). Bambra Reef is an isolated hard bedrock high point of dolerite which is backed on the landwards side by beach and dune sands extending in depth to below present sea-level.

No dates (e.g., OSL determinations) are available for the dune and beach ridge sands backing Roches Beach, however these are assumed to have accreted following the last post-glacial marine transgression which end circa 6,500 years ago (Davies 1959, 1961). Davies considered the Lauderdale neck (or isthmus) was initially a channel which was closed by the growth across it of the sandy Roches Beach spit and another shelly spit on the Ralphs Bay side (Figure 194, LHS). At Roches Beach an early phase of progradation during which multiple beach ridges accumulated was following by a reduction in sand accumulation resulting in subsequent slower growth of a single higher but stable foredune.

Given the presence of active swell-driven littoral currents transporting sand northwards along through the Roches Beach embayment (see "Sand Budget" below), the beaches shoreline position represents a dynamic equilibrium determined by sand gains and losses from the embayment. As a zeta-form embayment (Figure 194, RHS) the position of the main Roches Beach shoreline is controlled by the swell refracting around rocky Mays Point and consequent littoral currents, but is free to recede or prograde along most of the embayment shoreline in response to losses or gains of sand.

The sandy floor of Frederick Henry Bay offshore from Roches Beach is very shallow (mostly shallower than 20 m, and less than 10 m depth for about 4 km offshore) and has a generally sandy and low-gradient bottom throughout (Figure 195). Carley et al. (2008) found that the transverse dune-beach-subtidal profile at Roches Beach was much flatter than for any other swell-exposed beach measured by them in the region (Clarence Municipality), and that it is flatter than the equilibrium profile that would be expected based on the Bruun Rule. In principle this should result in a net onshore swell-driven sand movement resulting in shoreline progradation, however the fact that this is not the case can be explained by the northwards longshore drift transporting sand out of the embayment faster than cross-shore swell-wave action can drive it onshore (Carley et al. 2008, p.61).

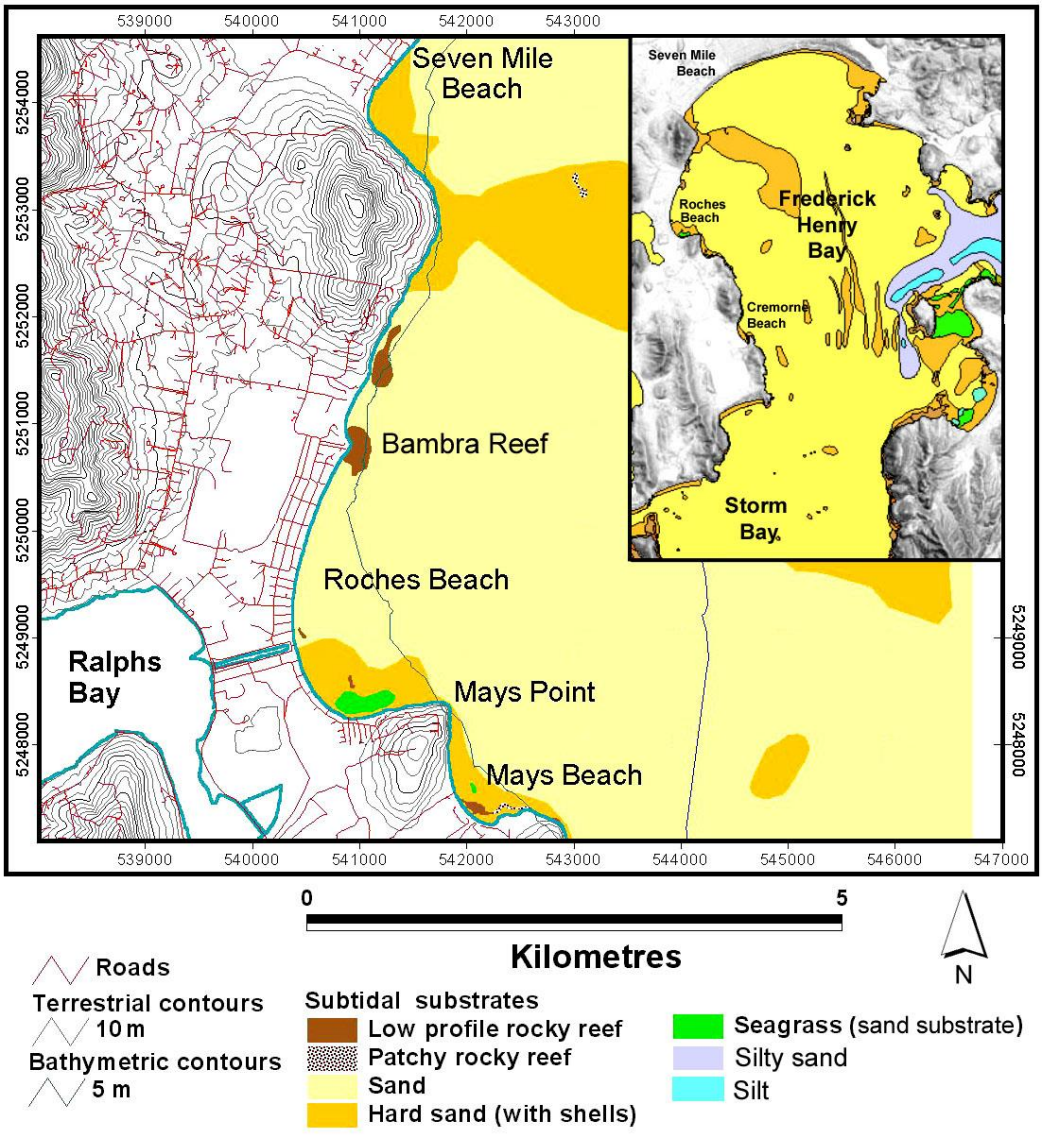

Figure 195: Bathymetry and bottom substrates of Frederick Henry Bay. Bathymetry and marine habitat (substrate) 1:25,000 scale mapping © SEAMAP Tasmania, University of Tasmania. Main figure shows detail adjacent Roches Beach, insert shows whole of Frederick Henry Bay. Map co-ordinate system is Map Grid of Australia (MGA) Zone 55, based on the GDA94 datum.

Swell wave climate

Roches Beach receives a persistent refracted swell at its location approximately 15 kilometres northwards up the broad coastal re-entrant of Frederick Henry Bay from the ocean-exposed waters of Storm Bay (Figure 196). Large south-westerly swells entering Frederick Henry Bay from the Southern Ocean and smaller south to south-easterly swells arriving from the Tasman Sea (Carley et al. 2008) are trained and attenuated by the long refraction pathway up the bay (Figure 196), and exhibit both low significant wave heights and very little directional variability by the time they are close to Roches Beach (see hindcast wave parameters in Table 63). Swell-wave modelling for Roches Beach by Shand and Carley (2011) using the SWAN wave model (Booij, Ris & Holthuijsen 1999) with nominal boundary conditions yielded wave heights comparable to those in Table 63 but increasing northwards along the beach. The modelled wave directions arrive from south of shore-normal which generates a northwards littoral drift along the beach (as seen in examples of actual storm and normal swell waves arriving in Figure 202 and Figure 198).

Table 63: Key swell wave climate parameters for Roches Beach, from the Bureau of Meteorology Australia and CSIRO Australia CAWCR wave hindcast 1979-2010 (Durrant et al. 2013). These figures apply to the centre of the two closest inshore ~5km grid cells to the beach, which in both cases are approximately 4 km from the centre of the beach

	Annual	Summer (DJF)	Winter (JJA)
Average Significant wave height (m)	0.21 (0.16 – 0.26)	0.20 (0.16 – 0.24)	0.22 (0.17-0.27)
Average Maximum wave height (m)	0.62 (0.72-0.52)	0.56 (0.63-0.49)	0.65 (0.77-0.54)
Average Mean wave direction (ºT)	176 (175-178)	174 (173-175)	176 (174-179)

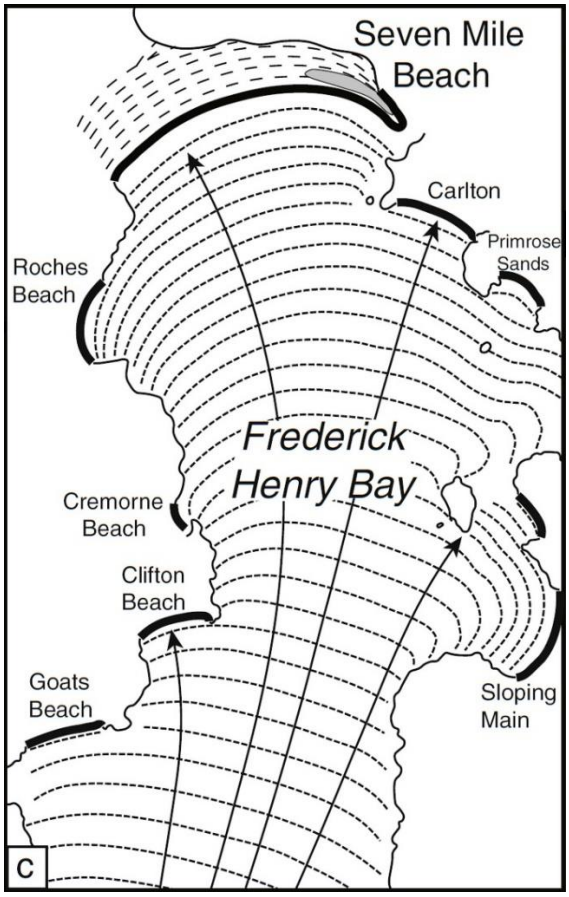

Figure 196: Swell wave refraction diagram for Frederick Henry Bay. This map demonstrates that most sandy beaches in Frederick Henry Bay are swash-aligned, with Roches Beach, the smaller Mays Beach (not shown) and Cremorne Beach being the most notable drift-aligned beaches. Reproduced from Oliver et al. (2017), based on original map by Davies (1958).

Wind (wind-wave) climate

The nearest long-term wind record to Roches Beach is at Hobart Airport, 5 kilometres north at the west end of the Seven Mile Beach barrier (see map Figure 192). However, the predominantly north-westerly winds recorded at that site are topographically steered down the Coal River valley further north (see Appendix Section A1.5.1) and are unlikely to be representative of dominant wind directions at Roches Beach. Instead, the orientation of recently-stabilised transgressive dunes in the eastern part of the Seven Mile Beach sandy barrier, approximately 10 km north-east of Roches Beach (Figure 192 & Figure 196), are indicative of dominantly westerly and south-westerly wind directions across Frederick Henry Bay (Donaldson 2010). Foster (1988) notes that recorded wind directions at Hobart City during known pre-1988 storm events at Roches Beach were mainly north-westerly to south-westerly, as is typical for the broader Hobart region. The Hobart City wind record is shown on Figure 197 below. These winds would have been directed offshore at Roches Beach and hence resulting wind-waves would have had little or no effect on Roches Beach. The most common storm pattern at Roches Beach is evidently that large (erosive) swell storms are typically associated with strong south-westerly winds that are offshore-directed at Roches Beach, resulting in no effective wind-waves at the beach during the storms.

Significant wind-waves can be directed onshore at Roches Beach by north-easterly to easterly winds blowing across the 10 to 15 km fetch of Frederick Henry Bay and the connecting Norfolk Bay (Shand & Carley 2011). However, the Hobart Airport wind record suggests that NE to E winds are rare in the Frederick Henry Bay region so that onshore-directed wind waves large enough to cause erosion at Roches Beach would be unusual. Nonetheless such winds evidently have driven at least two known erosion events. The air photo record demonstrates that one notable erosion event between the 22nd Dec 1975 and 4th Feb. 1977 caused significantly more erosion south of the canal than north of it (see also Sharples 2010, Fig. 37). This pattern implies erosion by north-easterly wind-waves to which the southern third of the beach is most directly exposed. In contrast observed swell erosion events (e.g., July 2011) have caused roughly similar amounts of shoreline retreat along most of Roches Beach. An observed easterly wind-wave event associated with an east coast low weather system on 5th-6th June 2016 also caused beach scarping at Roches Beach.

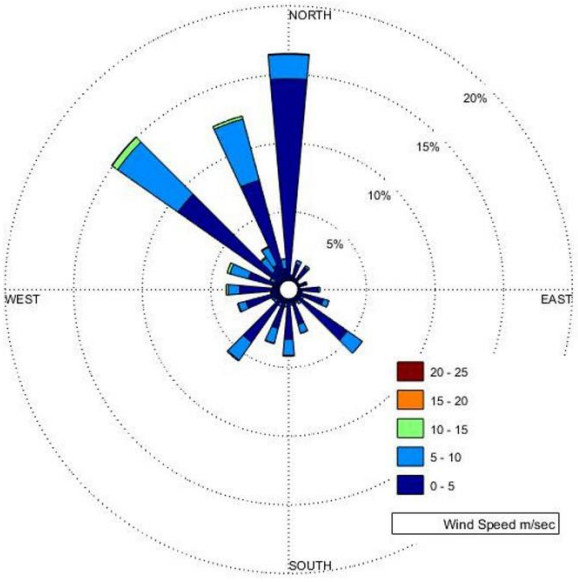

Figure 197: Synoptic wind rose for Hobart City (Ellerslie Road) Bureau of Meteorology weather station. The weather station is situated in the deep but broad valley of the lower Derwent River, hence the dominant northerly to north-westerly winds are inferred to be mainly topographically steered down the Derwent Valley at low levels. By comparison with other wind records for south-eastern Tasmania, the south-westerly (westerly to southerly) winds in this record are inferred to be the dominant regional winds and likely dominant at Roches Beach. The Figure uses all synoptic wind data for 1893 to 2015, plotted by Chris Sharples using data supplied by the Australian Bureau of Meteorology.

Storm Climate

Table 64 lists all storm events known to have caused erosion at Roches Beach, based on events observed by the author, those recorded by Foster (1988), Cromer (2006) and Sharples (2006), or those interpreted from the air photo history of shoreline position variability (Figure 204). The limitations of documentary histories and the arbitrary timing of aerial photography means that the list of erosion events compiled is not exhaustive, particularly in respect of smaller erosion events. No long-term wave records exist for the Hobart – Roches Beach region, and there is no exhaustive analysis of Hobart weather and tide gauge records available which might enable erosive storms to be identified and quantified in respect of frequencies and magnitudes. Nonetheless, with these caveats in mind the following observations can be made about the (erosional) storm climate at Roches Beach.

Most known shoreline erosion events at Roches Beach for which a wind direction was observed or is inferred from the Hobart weather station (Table 64) were associated with north-westerly to south-westerly winds that would have been blowing offshore at Roches Beach. These cannot have been wind-wave erosion events and are therefore inferred to have been swell-wave events. However, as detailed above two historical erosion events at Roches Beach are inferred (in one case) or known (in the other case) to have been driven by north-easterly or easterly wind-waves (associated with a large east coast low weather system in at least one of the two cases). However, the small proportion of E to NE winds recorded at the nearby Hobart airport weather station suggests that erosion events driven by E to NE wind-waves at Roches Beach are probably rare, and that most erosion events are swell-wave events as suggested by Table 64.

Figure 198: Large erosive swell storm wave arriving obliquely to Roches Beach during a major erosion event in July 2011. This view is looking south from south of the canal but north of the boulder revetment. Swell waves arriving at this angle drive northwards littoral drift, which was probably accelerated during this erosion event causing much of the sand eroded from the beach and dune to be quickly transported northwards and out of the embayment. Photo by C. Sharples (9th July 2011).

Given the low variability in swell-wave direction at Roches Beach (see above), it is probable that the spatial pattern of erosion during most swell-storms at Roches Beach is like that observed during the July 2011 event. That event resulted in a uniform retreat of the dune front by about 5 metres along most of Roches Beach between the rock revetment south of the canal to just south of Bambra Reef, and about 15 metres retreat of the sandy shoreline behind Bambra Reef itself, presumably as a result of the bathymetry refracting swell waves around the hard salient of Bambra Reef and focussing them on the adjacent sandy shore (Figure 199).

It should be noted that some storm surge events recorded in Table 64 are known to have caused flooding at Lauderdale but may not have caused erosion, since storm surges driven across Ralphs Bay into Lauderdale by westerly winds may cause flooding in the township (particularly along the canal) without resulting in erosion at east-facing Roches Beach on the far side of the isthmus.

Figure 199: Roches Beach erosion scarp near Bambra Reef following the large erosion event of 9th-10th July 2011. Approximately 15 metres of scarp retreat during the storm came close to undermining this house, whose proximity to the beach is typical of many at Roches Beach. Photo by C. Sharples (12th July 2011).

Table 64: Known and possible shoreline erosion events at Roches Beach (Lauderdale). This information is derived from previous reports and documentary records as cited, interpretation of the air photo record obtained by this project (particularly Figure 204), and in a few recent cases from personal observation. Wind directions noted at the Hobart weather station were determined by Foster (1988) as likely indicative of wind directions at Roches Beach (see also main text). Some storm surge events recorded here are known to have caused flooding at Lauderdale but may not have caused erosion (e.g., storm surges driven across Ralphs Bay into Lauderdale by westerly winds may cause flooding in the township without resulting in erosion at Roches Beach). Erosion events interpreted solely from the air photo record are only recorded if the scale of the inferred erosion is greater than the air photo error margins (several putative minor erosion events in the air photo record are omitted because their error margins are greater than the apparent shoreline retreat). Events which are known or likely to have caused erosion and shoreline retreat are noted in ***bold italics***.

Dates	Notes	Source
Nov 1967	Flooding of properties in South Terrace and Bayview Rd (Lauderdale) reported; not known whether accompanied by erosion.	Sharples (2006); *The Mercury* newspaper "Eastside News" 2nd Nov 1967 p. 4
4th – 6th Dec 1968	5m dune-front recession reported. ***Likely swell erosion*** (Hobart wind SSE – alongshore).	Foster (1988). No corresponding erosion event indicated by air photo record (Figure 204).
Oct-Nov 1970	Flooding of properties in South Terrace and Bayview Rd (Lauderdale) reported; not known whether accompanied by erosion.	Sharples (2006); *The Mercury* newspaper "Eastside News" 29th Oct 1970 p. 1; 5th Nov. 1970 p. 2.
3rd – 5th Aug 1974	***Likely swell erosion*** (Hobart wind SW - offshore)	Foster (1988)
Date between 22nd Dec 1975 and 4th Feb. 1977	***Likely north-easterly wind-wave erosion***: 5 to 13m shoreline retreat south of canal, only 5 metres or less retreat along beach north of canal. ***Unequivocal erosion event or events*** (scale greater than air photo error margins)	Air photo record interpretation (see Figure 204), not recorded by Foster (1988)

23rd – 25th April 1978	***Likely swell erosion*** (Hobart wind NNW – offshore)	Foster (1988)
1st – 3rd Dec 1979	***Likely swell erosion*** (Hobart wind W – offshore; however, this December was noted for "unseasonal strong winds" – likely associated with big SW swells)	Foster (1988)
18th – 20th July 1983	***Likely swell erosion*** (Hobart winds NW to SW – offshore, but likely associated with big SW swells).	Foster (1988)
15th – 18th Oct 1984	Erosion event described as 'severe'; ***likely swell erosion*** (Hobart winds NW to SW – offshore, but likely associated with big SW swells). ***Unequivocal erosion event.***	Three events recorded by Foster (1988). These fall within the 13th Jan. 1984 to 26th Feb. 1986 period indicated by the air photo record (Figure 204) as a large erosion event or series of events that caused greater than 10 metres shoreline retreat, and well outside air photo error margins.
2nd – 5th Mar 1985	***Likely swell erosion*** (Hobart winds gale force from SW – offshore but likely associated with big SW swells).	
3rd – 5th June 1985	Erosion event described as 'severe'; ***likely swell erosion*** (Hobart wind W to SSE – offshore to alongshore). ***Unequivocal erosion event.***	
Jan 1986	Storm surge reported, not known whether accompanied by erosion.	Cromer (2006)
25th July 1988	Storm surge flooding in Lauderdale, not known whether accompanied by erosion.	Sharples (2006); *The Mercury* newspaper 26th July 1988 p. 1
6th Aug 1991	Storm surge flooding in Lauderdale, not known whether accompanied by erosion.	Sharples (2006); The *Mercury* newspaper 7th Aug. 1991 p. 1-2
Date between 19th Feb. 1992 – 12th Jan. 1994	At least 5 metres shoreline retreat. ***Unequivocal erosion event or events*** (scale greater than air photo error margins)	Air photo record interpretation (see Figure 204).
26th May 1994	Storm surge flooding in Lauderdale, not known whether accompanied by erosion.	Sharples (2006)
Nov. 1994	Storm surge flooding, not known whether accompanied by erosion.	Cromer (2006)
Date between 14th Dec 2002 – 28th Mar. 2004.	At least 5 metres shoreline retreat. ***Unequivocal erosion event or events*** (scale greater than air photo error margins)	Air photo record interpretation (see Figure 204).
June 2005	Storm surge flooding, not known whether accompanied by erosion.	Cromer (2006)
Sept. 2005	Storm surge flooding, not known whether accompanied by erosion.	Cromer (2006)
Date between 4th Jan. 2007 & 3rd Jan. 2008	At least 5 metres shoreline retreat. ***Unequivocal erosion event or events*** (scale greater than air photo error margins)	Air photo record interpretation (see Figure 204).
26th – 27th Sept. 2009	Storm erosion of dune toe. ***Observed erosion event***. Storm type uncertain.	Nick Bowden *personal observation*, Shand and Carley (2009)
9th – 10th July 2011	Prolonged (2-day) south-westerly swell event caused erosion on west, south and south coast beaches. Swell refracted up Frederick Henry Bay with enough power to cause 5 metres shoreline recession along most of Roches Beach and 15m where swell refracted onto Bambra Reef. Winds at Roches on 9th July were light and westerly (offshore). This event was an ***observed severe and purely swell-driven erosion event.***	C. Sharples *personal observation*; *The Mercury* newspaper reports
5th-6th June 2016	Very large east coast low caused major (easterly) swell wave erosion on NSW beaches and on east coast Tas. beaches, but the swell did not penetrate to Roches Beach. However strong east-north-easterly winds generated wind waves across Frederick Henry Bay which caused beach scarping (but not dune scarping) at Roches Beach. The same wind-wave event also caused erosion at Coal Mines Beach from wind-waves generated across Norfolk Bay. ***Observed wind-wave erosion event.***	C. Sharples *personal observations*; Phil Watson (Clarence Council) *personal observations*. Sharples (2017)

Sand transport and budget

The current understanding of sand sources, sinks and transport at Roches Beach is based on available 1:25,000 marine substrate mapping (© SEAMAP, University of Tasmania; see Figure 195), interpretation of geomorphic and wave processes, and numerical modelling by Shand and Carley (2011). To date available resources have not permitted methods such as tracer-particle experiments or bedform analyses which might provide empirical data to support the inferences made here about sand transport processes at and near Roches Beach.

The relatively shallow (mostly less than 20 m), low-gradient and almost entirely sandy floor of Frederick Henry Bay (Figure 195) is the most likely source of most of the sand that has accumulated to form the Roches Beach barrier (Davies 1961), as well as the much of the larger Seven Mile Beach barrier (Oliver et al. 2017) and other embayed sandy beaches around Frederick Henry Bay[32]. Dating of beach ridges at Seven Mile Beach indicates continuous barrier progradation from ~3500 years ago until at least 500 years ago (Oliver et al. 2017), implying a continuous swell-driven supply of sand moving northwards through Frederick Henry Bay over that period. This sand supply would have been particularly mobile in the shallow waters along the eastern margin of Frederick Henry Bay so that sand would have been moved northwards into and out of the drift-aligned Roches Beach embayment *en route* to Seven Mile Beach. The authors own visual observation of a continuously sandy bottom immediately below the Low Water Mark along the entire rocky and sandy intertidal shoreline from Seven Mile Beach past Roches Beach to Cremorne Beach (Figure 195) demonstrates that Roches Beach embayment is leaky to alongshore sand drift, and attests that similar swell-driven northwards sand movement must be continuing at the present.

Beach ridge and foredune dates at Seven Mile Beach imply a hiatus in the progradation of the Seven Mile Beach barrier during the last 500 years (Oliver et al. 2017). However the presence of active transgressive dunes at the eastern end of the barrier during this more recent period demonstrates that swell-driven sand from Frederick Henry Bay was continuing to accrete on Seven Mile Beach before being transported by wind across the barrier and into Pittwater via the active transgressive dunes (Oliver et al. 2017). This implies that northwards sand transport through Frederick Henry Bay to Seven Mile Beach has not ceased although it evidently has been much reduced during the last 500 years[33].

The northwards swell in Frederick Henry Bay persistently drives intertidal and sub-tidal bottom sands northwards around Mays Point, across and through the Roches Beach embayment and out its northern end around Bambra Reef, which is not an effective barrier to sand movement (Shand & Carley 2011). Littoral drift modelling by Shand and Carley (2011) confirmed this to be the dominant sand transport pathway at Roches Beach (see Figure 200), with swell being the main driver of littoral currents and onshore (N to E) wind-waves contributing little to overall sand transport.

[32] Re-worked Pleistocene terrestrial dunes may have supplied some of the sand to build initial barriers at the end of the post-glacial marine transgression, however continued growth of the Seven Mile Beach barrier following apparent exhaustion of the *in situ* sands circa 6500 years BP requires another large sand source for which Frederick Henry Bay is the only available candidate (Oliver et al. 2017).

[33] With artificial stabilisation of the transgressive dunes by pine plantations and marram grass since the 1950s (Watt 1999) it is likely that the sand that was formerly transported across the barrier by wind is now accumulating in some very broad foredunes that LIDAR mapping shows behind parts of the eastern end of Seven Mile Beach.

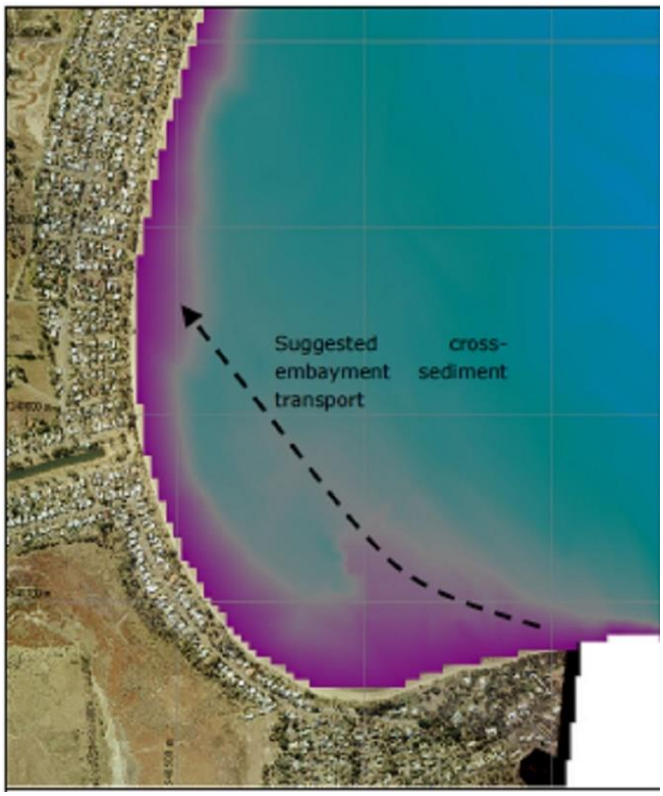

Figure 200: Modelled littoral drift at Roches Beach. Screenshot of Shand and Carley (2011) Figure 4-2. Offshore colours represent bathymetry (purple = shallower, blue = deeper). Littoral drift modelling by Shand and Carley (2011) indicates the main littoral current pushes sand around Mays Point and northwards, probably bypassing the southern 'hook' of the zeta-form embayment via a north-westwards-trending sand lobe indicated by the bathymetry. The air photo evidence confirms that the southern hook of the embayment has been a low-energy sand-trapping area throughout the air photo period (see below).

Modelled littoral drift rates increase northwards along the beach, which Shand and Carley (2011) attribute both to increasing exposure to wave energy and to waves occurring at a more oblique angle to the shoreline as the refractive influence of Mays Point diminishes. The modelling indicated a northwards gradient in rates of present-day littoral sand drift from around 2000 m^3/yr near the southern end of Roches Beach to a rate of 13,000 m^3/yr around Bambra Reef Shand and Carley (2011).

The modelling suggests that the main littoral drift of sand bypasses the southernmost 'hook' of the zeta-form embayment and produces a lobe of sand across the bay which is visible in the bathymetry (Figure 200). The hook is a low-energy area into which small amounts of sand leak and become trapped, as may be expected from the wave refraction patterns typically produced around a rocky headland controlling a zeta-form embayment on a drift aligned coast (Figure 194 RHS).

Sea-level data

The nearest measured sea level data to Roches Beach is from the Hobart tide gauge record, measured in the lower Derwent River estuary about 13 km west of the Roches Beach. Although this tide gauge has a long history, the record is compromised by data gaps and datum shifts. The record shown in Figure 201 is the useable portion of the data up to 2004 (data obtained and prepared by Dr John Hunter).

The mean rate of sea-level rise measured from a calculated linear fit to the Hobart tide gauge record is 1.68 mm/yr^{-1} over the period 1962-2004, which is comparable with the global-average rise of 2.0 ±

0.3 mm yr^{-1} over the 1966 – 2009 period (White et al. 2014)[34]. The amplitude of interannual variability in the sea level signal in the Hobart record is ~10 to 100 mm (see Figure 201), consistent with sites having little exposure to larger modes of climate variability such as ENSO (White et al. 2014).

Although Roches Beach is located in a different coastal embayment to the Hobart tide gauge it is reasonable to infer a similar sea-level history at Roches Beach given both sites are swell-exposed locations opening to the ocean at Storm Bay.

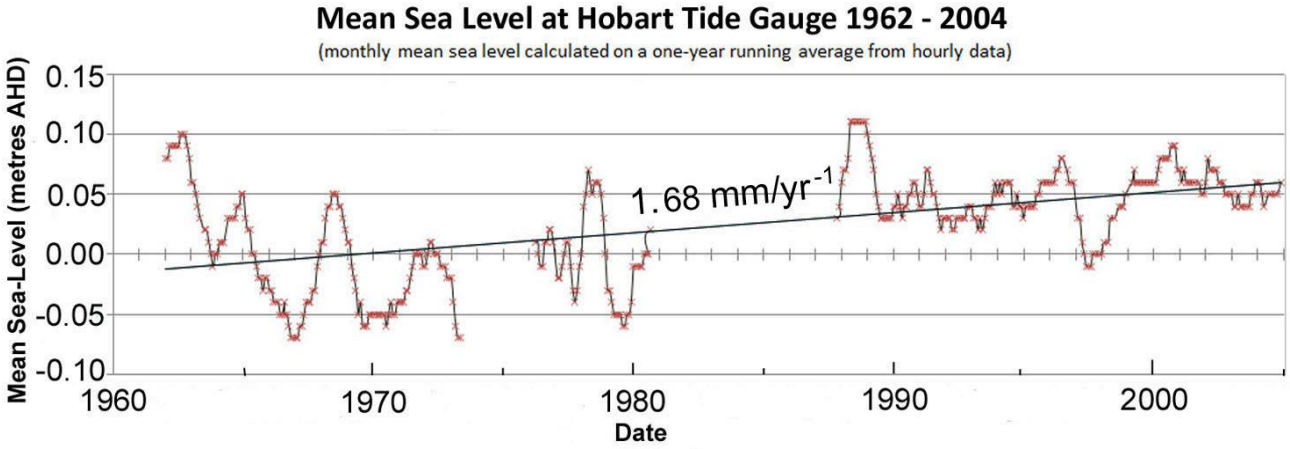

Figure 201: Mean sea level at the Hobart Tide gauge, 1962 – 2004. A simple linear fit is shown plotted to the data. This is the closest tide gauge record to Roches Beach. Although the Hobart tide gauge is over a century old, the data plotted here is the only reliable data up to 2004, owing to unsurveyed gauge and datum shifts. Mean sea-level heights shown in metres above the Australian Height Datum (AHD). This data was processed and supplied by Dr John Hunter, from original tide gauge data.

Vertical Land Movement

Current and ongoing geodetic studies of Tasmania have yet to resolve disagreements between GNSS derived estimates of VLM at Burnie and Hobart[35] ranging between 0.0 to -1.0 mm yr^{-1}, and geophysical models indicating subsidence in the range of -0.1 to -0.2 mm yr^{-1} (see details in Chapter 2 Section 2.5.4 above). However, for the purpose of this thesis, there is no evidence suggesting that VLM is a significant signal in Tasmanian relative sea levels. There is no significant anthropogenic extraction of sub-surface fluids or other known processes such as significant seismic activity likely to cause significant VLM at Roches Beach.

Artificial disturbances

Although the entire length of Roches Beach is backed by roads and houses, these are located on the foredune backslope or further inland and have negligible impact on sand movement processes on the beachface and foredune front. Similarly, the canal – which was cut through Roches Beach in 1924 but refilled with sand at the beach end within weeks (Alexander 2003) – has no significant impact on beach and foredune processes today. The associated derelict wooden training walls on Roches Beach were never completed and are very porous structures which are similarly unlikely to significantly modify beach processes including sand movement.

In contrast, the boulder revetment constructed during the 1980s south of the canal has had a significant local effect by preventing further shoreline recession. This has resulted in a major 'end effect' at the northern end of the revetment where the adjacent unprotected foredune had receded metres further back by 2011, and has also resulted in beach lowering and complete loss of dry beach

[34] This is a slightly greater rate than found at Burnie (1.4 mm/yr^{-1}: see A1.2.5) and less than Ocean Beach (2.13-2.21 mm/yr^{-1}: see A1.3.8) over approximately the same periods.
[35] The Hobart GNSS site is located at Mt Pleasant, about 10 km north of Roches Beach.

at high tide in front of the revetment (see Figure 202). Short sections of similar boulder protection were constructed behind Bambra Reef prior to 2011 but did not prevent major "end effect" erosion during the July 2011 erosion event and have now been extended.

Fabric fences constructed along the front of the eroding dune face circa the 1990s in order to encourage dune accretion were ineffective in halting incremental foredune erosion and were eventually removed circa 2005.

No other significant artificial disturbances to beach and dune processes at Roches Beach up to 2011 have been identified. However, following the July 2011 erosion event, the local government has implemented a policy of scraping and replenishing beach and dune sand at Roches Beach. As a result, further recession has been artificially prevented, and the scope of this research has been limited to the period ending at the July 2011 erosion event since subsequent beach change does not reflect the effects of natural morpho-dynamic processes at the site.

Figure 202: The boulder revetment at the southern end of Roches Beach, viewed from the north end of the revetment. This photo shows a typically low swell wave arriving obliquely to the shoreline under normal conditions two days after the major July 2011 erosion event. Lowering of the beach face in front of the revetment is evident, as is "end effect" foredune erosion beginning to extend behind the northern end of the revetment. Also evident is the typical proximity of houses to Roches Beach. Photo by C. Sharples (12th July 2011).

Air photo analysis

Digital (scanned) air photos covering all or part of Roches Beach were obtained from several sources as detailed in Table 65. Air photos from 30 dates have been used in this analysis, beginning 4th April 1946, and ending on the 15th July 2011 (air photo obtained immediately after a large erosion event on the 9th – 10th July 2011). Subsequent available air photos (24th June 2013 and 4th Sept 2015) have been excluded from this analysis because the beach and foredune have repeatedly been artificially managed by scraping and sand replenishment since the July 2011 storm. Hence, shoreline behaviour subsequent to July 2011 is not characteristic of natural morpho-dynamic processes and so is not relevant to this analysis.

Shore behaviour history from air photos

Inspection of shoreline history plots for individual and grouped transects reveals five shoreline areas with differing distinctive shoreline histories for the period 1946 to 2011 (Figure 203). These are summarised as below:

Roches Beach North (transects 13771-13776)

This section of sandy beach north of Bambra Reef has exhibited episodic erosion and accretion events around a roughly stable dynamic equilibrium shoreline position throughout the air photo period. There is no significant overall trend towards either recession or progradation, and no significant long-term (e.g., multi-decadal) change of shoreline behaviour.

Bambra Reef (transects 13777-13779)

The reef is an emergent bedrock (dolerite) high point forming a 'salient' in front of a beach and dune which are composed of sand to unknown depth below present sea-level. The July 2011 storm caused notably more erosion and retreat (15 m) of the beach and dune sands behind the reef than elsewhere in the main central section of Roches Beach (described below). This is inferred to be the result of waves being refracted and focussed onto the rocky salient. However there has historically been full shoreline recovery following erosion events at Bambra reef, albeit this may have in part been due to artificial shore protection works after storms, since some boulder revetment works of uncertain age were in place prior to the 2011 erosion event. Whether or not as a result, the history of the shoreline (beach and dune) immediately behind Bambra Reef has been one of episodic shoreline erosion and recovery events around a stable dynamic equilibrium position (Figure 203), with no significant trend to recession or progradation and no noticeable long-term change of shoreline behaviour over the air photo period.

Roches Beach Main Central (transects 13780-13801 excluding disturbed canal transect 13798)

Shoreline position change data for the main central part of Roches Beach (Figure 203) is plotted in summary formats on Figure 204 to Figure 206).

Although a single unweighted linear fit to all data points yields a higher Pearson correlation co-efficient (Figure 204 top), visual inspection suggests the data is better explained as two distinctively different shoreline change trends pre-and post-1985 (Figure 204 bottom and Figure 206). From at least 1946 until 1984 (38+ years), error-weighted linear regression yields a small low-significance recession trend (R^2=0.0860) whose error margins are greater than the apparent linear trend. The pre-1985 data is therefore best characterised as a dynamic equilibrium around a mostly stable shoreline position with erosion and accretion cycles of mostly less than ~4 m amplitude.

However, between the 13th Jan 1984 and 26th Feb 1986 air photo dates there is an abrupt switch to a significant (R^2=0.3841 error-weighted) linear recession trend from 1986 until 2011, which has a substantial recession rate (-0.15 m/yr) which is greater than its error margin. Foster (1988) lists two erosion events in the same 1984-1986 time gap which are the only ones his list characterises as 'severe' (Table 64) and which together co-incide with the largest recessional shoreline change visible between any two air photos in the record (4 to 5 metres: Figure 204).

The post-1985 shoreline change trend until July 2011 (~25 years) is mostly beyond the range of the pre-1985 shoreline position variability including error margins (see Figure 206) and thus represents a real change in long-term shoreline behaviour. The air photo record over this period is sufficiently detailed (17 air photo dates with error margins mostly smaller than associated shoreline movements) as to suggest that the recession trend was a step-wise succession of erosion events followed by partial (but never complete) shoreline recovery before the next erosion event (see Figure 204 bottom). Thus since 1986 the main central Roches Beach shoreline has never fully recovered to its pre-1985 position and was continuing to progressively recede further landwards until a large erosion event occurred on 9th-10th July 2011, which caused about 5 metres of further horizontal shoreline recession in one storm event.

Following this event, the beach and dune have been repeatedly scraped and the sand artificially replenished so that natural beach morpho-dynamic processes are no longer dominant. Hence this data set terminates at the 15th July 2011 air photo (which captures the July storm erosion results prior to artificial repair commencing).

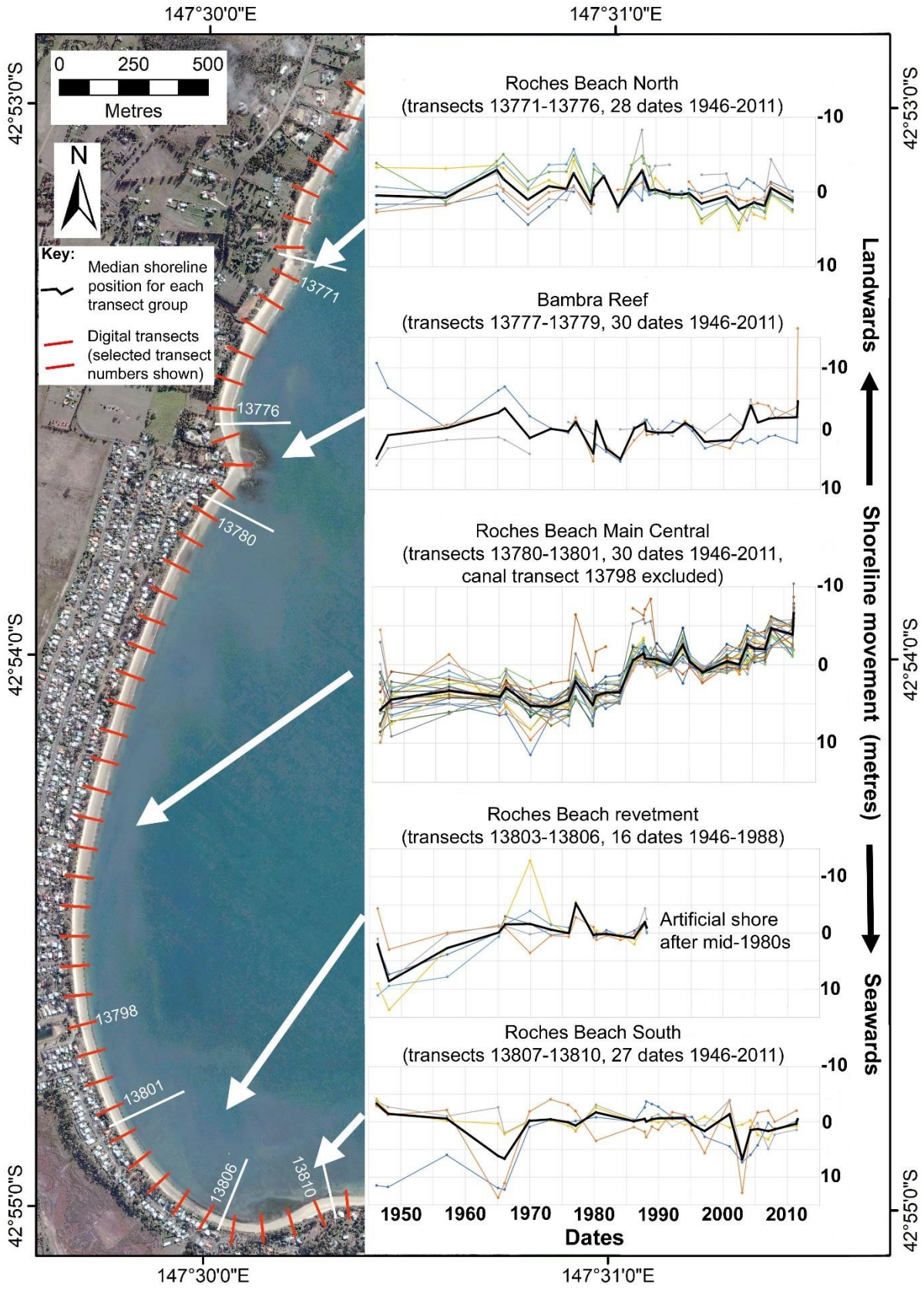

Figure 203: Plots of shoreline (vegetation line) movement histories along each digital transect (coloured plot lines) at Roches Beach at up to 30 air photo dates over the period 1946 to 2011, plotted relative to the median shoreline position on each transect. Transects are plotted in five groups (bounded by white lines). each exhibiting distinctive shoreline behaviour. The beach image is the May 2005 Quickbird satellite image.

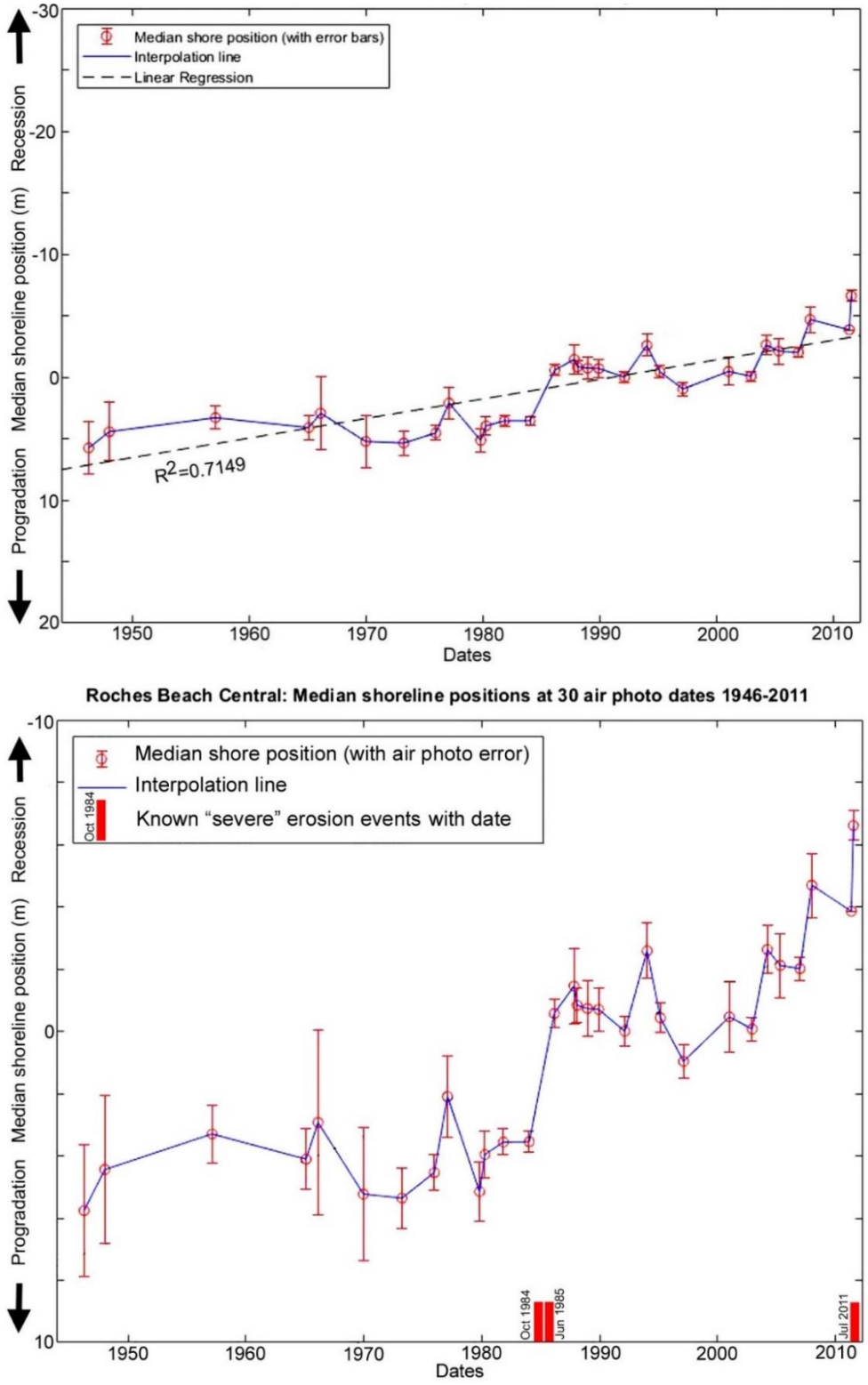

Figure 204: Summary plot of shoreline change history across all transects except 13798 (disturbed canal zone) in the main central area of Roches Beach (as shown on Figure 203) at 30 air photo dates from 1948 to 2011. These plot the median of the normalised shoreline positions measured across all included transects, with a single linear fit to all data points shown in top figure (same fit applies for lower figure but not shown). **Top**: Using standard Y-axis scale for comparison with other sites in this project; **Bottom**: using Y-axis scaled to shoreline position range. Known erosion events independently characterised as 'severe' are indicated (Foster 1988). Several other erosion events are known (see Table 64) but indications of their magnitude are only available where they have been captured by the air photo record itself (as a recession between consecutive air photos that is larger than the air photo error margins).

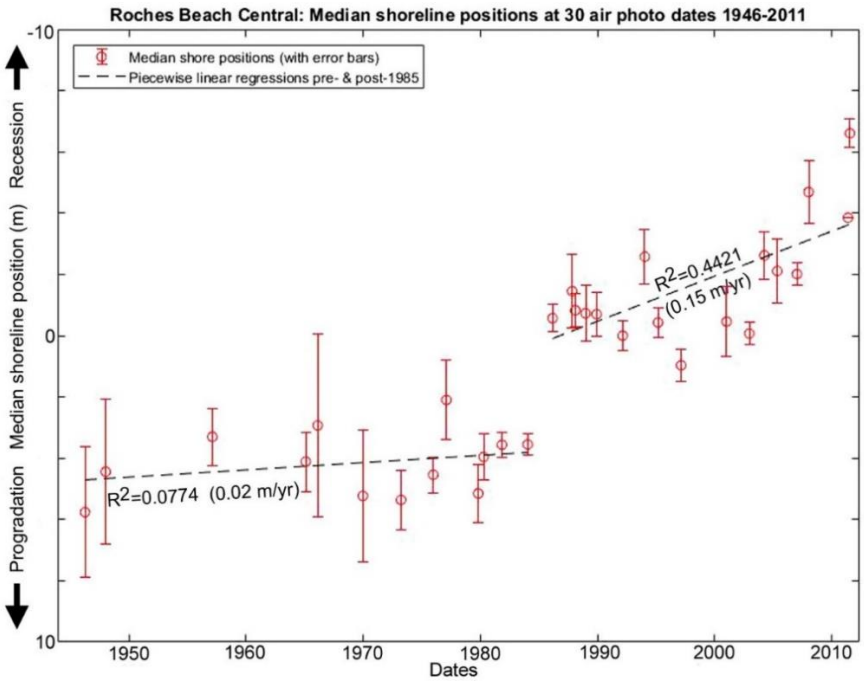

Figure 205: Piecewise linear fits to shoreline position data for central Roches Beach pre- and post-1985. The data shown comprises median shoreline positions across all central Roches Beach transects (except canal transect 13798) at 30 air photo dates from 1946 to 2011. From at least 1946 until 1984, linear regression yields a slow and low-significance receding trend that is probably better characterised as a dynamic equilibrium around a mostly stable shoreline position. Between 1984 and 1986 there is an abrupt switch to a significant (R^2=0.4421) linear recession trend (averaging 0.15 m/yr) from 1986 until 2011, which is mostly beyond the range of pre-1985 shoreline position variability (including error margins) and thus represents a real change in shoreline behaviour. Linear fits shown here have not been error-weighted.

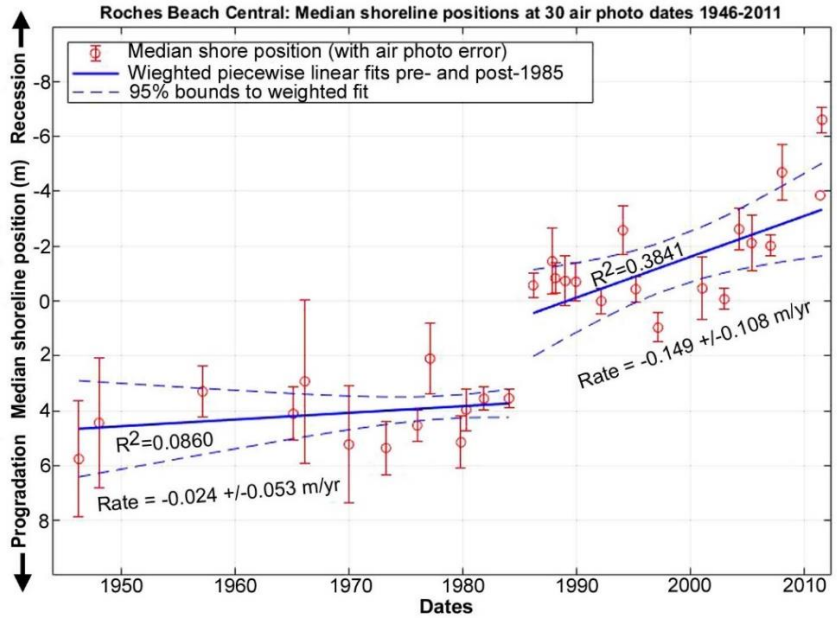

Figure 206 Error-weighted piecewise linear fits to shoreline position data for central Roches Beach pre- and post-1985. The shore position data shown comprises median shoreline positions at each air photo date across all central Roches Beach transects (except canal transect 13798) at 30 air photo dates from 1946 to 2011. The reference epoch for all shoreline positions is May 2011, since the May 2011 air photo was arbitrarily defined as error-free in the context of the error bars provided, and all other air photos were ortho-rectified to it. The median shoreline positions at each date (relative to the reference epoch) are arbitrarily shifted such that the median of all shoreline positions is located at zero on the y-axis. When undertaking regression analysis to the pre- and post-1985 data, the reference epoch was not included in the weighted regression since this would artificially bias regression parameters. To aid in qualitative assessment of the fit, the reference epoch is shown on Figure 206 without an error bar.

Roches Beach Revetment (transects 13802-13806)

The southern part of Roches Beach just north of the "hook" of the main zeta-form embayment has been protected by a large boulder revetment since the 1980s (Figure 202). As a result there has been negligible subsequent horizontal shoreline position change (albeit there has been significant lowering of the sandy beach face in front of the revetment: see Figure 202). The revetment was constructed in several stages during the 1980's, in response to erosion events during the 1970s and 1980's (Foster 1988). Hence this study has only mapped historic shoreline changes for this beach section prior to 1988, after which changes to the horizontal shoreline position have been artificially prevented.

The air photo record for this part of the beach indicates at a mostly stable shoreline since 1965 with least one notable erosion event between Dec. 1975 and Feb. 1977, which is also evident but mostly less significant in the central area (Figure 203)[36]. The spatial pattern of the latter event suggests it was the result of local wind-waves generated by unusual strong north-easterly winds across the ~10 km fetch of Frederick Henry Bay, since such waves would mainly impact the more directly-exposed southern area of the beach rather than the central area (which is more susceptible to refracted swell-wave storms such as the 2011 event). Full shoreline recovery subsequent to this erosion event is evident in the air photo record, however there is also evidence of later erosion related to the 'severe' storms noted by Foster (1988) in the 1984-1986 air photo time gap. These were followed by construction of the boulder revetment

The air photo history (Figure 203) is additionally suggestive that prior to about 1965 the shoreline in the area later protected by revetment was undergoing progressive recession which is not seen in the main central part of the beach further north. This is suggestive of a response to north-easterly wind wave events, which would have had less effect on the main central part of the beach. However, this trend is not apparent after 1965, and given the large error margins of the earlier air photos its reality must be considered doubtful in the absence of other supporting evidence.

Roches Beach South (transects 13807-13810)

The southern end of Roches Beach is in the "hook" of the zeta-form embayment and has been a temporary sink for sand trapped after being driven into the lee of Mays Point by strongly refracted swell waves (see Figure 194) or moved southwards along the southern end of the main beach by littoral drift generated by occasional north-easterly wind-waves. A wide beach is episodically present in this area but is occasionally scoured out (presumably during storm events), resulting in a shoreline history exhibiting episodic accretion and erosion, but no long-term trend or change of trend towards either recession or accretion (Figure 203).

Shoreline behaviour drivers and conditions

Hypotheses concerning the drivers of the observed historical shoreline behaviour at Roches Beach and the local geomorphic conditions which have allowed the observed changes to occur are explored in Chapter 5 (Section 5.3.4). That discussion is not repeated here.

[36] The air photo record also suggests a large erosion event circa 1970, however this is only indicated on two out of five transects and its nature and cause are unclear.

Air photo data tables

The following tables provide details of the air photos used, the resulting ortho-photos produced, and the shapefiles representing the shoreline position that were digitised from the ortho-photos.

Table 65: Original air photos and ortho-rectified air photos produced for Roches Beach.

Photo Date	**Original air photos (film-frame);** source DPIPWE unless otherwise stated **/ Ortho-photo name**	**Final image resolution (original scan resolution if downsized) / pixel size of final ortho-photo**	**Original photo scale**	**Mean measured feature position error (± metres) for ortho-photo** [no. of measured feature position reference points]	**Comments**
4th April 1946	31-11277 / *Roches_4thApril1946 MGA55.tif*	1000 dpi (2000 dpi) / 0.33 m	1:17,450	2.1 [6]	Ortho-rectified by Chris Sharples
8th Jan 1948	152-1654 (run 16) *Roches_8thJan1948_ MGA55.tif*	1000 dpi (1200 dpi) / 0.60 m	1:15,840	2.4 [6]	Ortho-rectified by Chris Sharples
12th Feb 1957	326-40 326-80 / *Roches_1957_326-40_MGA55.ecw* *Roches_1957_326-80_MGA55.ecw*	? / 0.50 m	1:14,000	0.9 [11]	Ortho-rectified by DPIPWE
2nd Feb 1965	433-156 / *Roches_2ndFeb1965_ MGA55.tif*	1500 dpi (2039 dpi) / 0.66 m	1:31,680	1.0 [10]	Ortho-rectified by Chris Sharples
8th Feb 1966	463-4 / *Roches-8thFeb1966_MGA55.tif*	1500 dpi (2039 dpi) / 0.65 m	1:31,680	3.0 [9]	Ortho-rectified by Chris Sharples
18th Dec 1969	538-(3 frames) or 542-(3 frames) / Roches_18thDec1969 _MGA55.ecw	? / 0.20 m	1:34,770	2.1 [11]	Ortho-rectified for Clarence City Council & supplied by CCC to Chris Sharples. (ecw supplied with incorrect 17th Feb date)
24th Mar 1973	627-86 627-87 627-88 / *Roches_24thMarch1973_MGA55_N.tif* *Roches_24thMarch1973_MGA55_Mid.tif* *Roches_24thMarch1973_MGA55_S.tif*	1000 dpi (2039 dpi) / 0.33m pixel size	1:12,500	1.0 [10] (Averaged across all 3 frames)	Each photo separately ortho-rectified by Chris Sharples
22nd Dec 1975	681-14:67 (selected frames) / *Orthomosaic_22-12-1975.ecw*	2039 dpi / 0.06 m	1:5,000	0.6 [10]	Ortho-mosaic supplied by Clarence City Council
4th Feb 1977	708-3 / *Roches_4thFeb1977_ MGA55.ecw*	? / 0.50 m	1:30,000	1.3 [9]	Ortho-rectified by DPIPWE
26th Oct 1979	801-58,60,62,64 / *Roches_26thOct1979 _MGA55.tif*	1000 dpi (2039 dpi) /	1:6,000	0.9 [7]	Ortho-rectified by Chris Sharples

		0.15 m pixel size			
9th April 1980	831-28, 831-65 / *Roches_9thApril 1980_MGA55.tif*	1000 dpi (2039 dpi) / 0.41 m	1:15,000	0.8 [11]	Ortho-rectified by Chris Sharples
1st Nov 1981	? / *Roches_1stNov1981_ MGA55.ecw*	? / 0.06 m	?	0.4 [5]	Ortho-rectified for Clarence City Council & supplied by CCC to Chris Sharples.
13th Jan 1984	977-? / *Roches_13thJan1984 _MGA55.ecw*	? / 0.06 m	1:5,000	0.35 [8]	Ortho-rectified for Clarence City Council & supplied by CCC to Chris Sharples
26th Feb 1986	? / *Roches_26thFeb1986 _MGA55.ecw*	? / 0.16 m	?	0.4 [9]	Ortho-rectified for Clarence City Council & supplied by CCC to Chris Sharples
30th Oct 1987	1092-240 / *Roches_30thOct1987 _MGA55.ecw*	? / 0.50 m	1:28,000	1.2 [7]	Ortho-rectified by DPIPWE
4th Feb 1988	? / *Roches_4thFeb1988_ MGA55.ecw*	? / 0.16 m	1:12,500	0.5 [9]	Ortho-rectified for Clarence City Council & supplied by CCC to Chris Sharples
22nd Dec 1988	1125-78,79,80 / *Roches_22ndDec198 8_MGA55.tif*	1000 dpi (2039 dpi) / 0.32 m	1:12,500	0.9 [10]	Photos ortho-rectified by Chris Sharples
1st Dec 1989	1142-61 1142-63 / *Roches_1stDec1989_ S_MGA55.tif Roches_1stDec1989_ N_MGA55.tif*	1000 dpi (2039 dpi) / 0.31 m	1:12,500	0.70 [10]	Photos individually ortho-rectified by Chris Sharples
19th Feb 1992	? / *Roches_19thFeb1992 _MGA55.ecw*	? / 0.16 m	?	0.5 [11]	Ortho-rectified for Clarence City Council & supplied by CCC to Chris Sharples
12th Jan 1994	1213-239 / *Roches_12thJan1994 _MGA55.tif*	1000 dpi (2039 dpi) / 0.60 m	1:24,000	0.9 [10]	Photo ortho-rectified by Chris Sharples
1st Mar 1995	1233-38 (S) 1233-40 (N) / *Roches_1stMar1995_ S_MGA55.tif Roches_1stMar1995_ N_MGA55.tif*	1000 dpi (2039 dpi) / 0.32 m	1:12,500	0.5 [11]	Photos individually ortho-rectified by Chris Sharples
15th Feb 1997	1272-141, 143 / *Roches_15thFeb1997 _MGA55.ecw*	? / 0.16 m	1:12,500	0.5 [10]	Ortho-rectified for Clarence City Council & supplied by CCC to Chris Sharples
4th Jan 2001	1342-46 1342-48 / *Roches_4thJan2001_ 1342-46_MGA55.ecw Roches_4thJan2001_ 1342-48_MGA55.ecw*	? / 0.50 m	1:24,000	1.1 [10]	Ortho-rectified by DPIPWE
14th Dec 2002	1362-197 1362-199 / *Roches_14thDec2002 _MGA55.ecw*	? / 0.12m	1:10,000	0.4 [9]	Ortho-rectified for Clarence City Council & supplied by CCC to Chris Sharples
28th Mar 2004	1383-53 /	1000 dpi (2039 dpi) /	1:24,000	0.8 [9]	Ortho-rectified by Chris Sharples

	Roches_28thMar2004_MGA55.tif	0.60m			
2nd May 2005	Quickbird satellite image / *Roches_2ndMay2005_qb_MGA55.tif*	? / 0.60m	?	1.0 [9]	Quickbird satellite image; ortho-rectified by Sinclair Knight Merz P/L (SKM), supplied by University of Tasmania to Chris Sharples (2010) for research purposes
4th Jan 2007	1418-257 1418-259 / *Roches_4thJan2007_MGA55.ecw*	? / 0.12m	1:12,500	0.4] [9]	Ortho-rectified for Clarence City Council & supplied by CCC to Chris Sharples
3rd Jan 2008	1428-16 / *Roches_3rdJan2008_MGA55.tif*	1000 dpi (2039 dpi) / 0.60m	1:24.000	1.0 [9]	Ortho-rectified by Chris Sharples
15th May 2011	*Clarence_2_69,78,79, 88,98,108, 109.ecw* (multiple frames)	NA / 0.1m	1:400	0.0 [N/A] REFERENCE PHOTO (nil error by convention)	Photos taken shortly before big July 2011 erosion event (storm). Flown & ortho-rectified by DPIPWE for Southern Tasmania Councils Authority and Southern Water; supplied by Clarence City Council.
15th July 2011	Matt Dell photography / *Roches_15thJuly2011_MGA55.tif*	N/A / 0.14 m	N/A	0.5 [5]	Photo taken just after 9th – 10th July erosion event, by Matt Dell for Clarence City Council; ortho-rectified and supplied by Matt Dell.
24th June 2013	Matt Dell photography / *Roches_24thJune2013_MGA55.ecw*	N/A / 0.12m	N/A	0.4 [7]	Photo taken and ortho-rectified for Clarence City Council by Matt Dell; supplied by Matt Dell.
4th Sept 2015	Matt Dell photography / *Roches_4thSept2015_MGA55.tif*	N/A / 0.11m	N/A	0.2 [8]	Geotiff photo taken and ortho-rectified for Clarence City Council by Matt Dell; supplied by Matt Dell.

Table 66: Digitised shoreline shapefiles produced for Roches Beach (using ortho-photos listed in Table 65 above). Note that shorelines digitised by Chris Sharples during 2010 were prepared for an earlier Roches Beach study (Sharples 2010); those digitised by Sarah Harries during 2011-2012 were prepared for a national study, and those digitised by Chris Sharples during 2015 were prepared specifically for this Ph. D. thesis (Sharples et al. 2012).

Date of air photo(s)	Shapefile	Shoreline digitised by	Comments
4th Apr 1946	Roches_MGA55_19460404.shp	Chris Sharples (2015)	
8th Jan 1948	Roches_MGA55_19480108.shp	Chris Sharples (2015)	
12th Feb 1957	Roches_MGA55_19570212.shp	Chris Sharples (2010)	
2nd Feb 1965	Roches_MGA55_19650202.shp	Chris Sharples (2015)	
8th Feb 1966	Roches_MGA55_19660208.shp	Chris Sharples (2015)	
18th Dec 1969	Roches_MGA55_19691218.shp	Sarah Harries (2011-12)	
24th Mar 1973	Roches_MGA55_19730324.shp	Chris Sharples (2015)	
22nd Dec 1975	Roches_MGA55_19751222.shp	Sarah Harries (2011-12)	
4th Feb 1977	Roches_MGA55_19770204.shp	Sarah Harries (2011-12)	
26th Oct 1979	Roches_MGA55_19791026.shp	Chris Sharples (2015)	
9th Apr 1980	Roches_MGA55_19800409.shp	Chris Sharples (2015)	
1st Nov 1981	Roches_MGA55_19811101.shp	Sarah Harries (2011-12)	
13th Jan 1984	Roches_MGA55_19840113.shp	Sarah Harries (2011-12)	
26th Feb 1986	Roches_MGA55_19860226.shp	Sarah Harries (2011-12)	
30th Oct 1987	Roches_MGA55_19871030.shp	Chris Sharples (2010)	
4th Feb 1988	Roches_MGA55_19880204.shp	Sarah Harries (2011-12)	
22nd Dec 1988	Roches_MGA55_19881222.shp	Chris Sharples (2015)	

1st Dec 1989	Roches_MGA55_19891201.shp	Chris Sharples (2015)	
19th Feb 1992	Roches_MGA55_19920219.shp	Sarah Harries (2011-12)	
12th Jan 1994	Roches_MGA55_19940112.shp	Chris Sharples (2015)	
1st Mar 1995	Roches_MGA55_19950301.shp	Chris Sharples (2015)	
15th Feb 1997	Roches_MGA55_19970215.shp	Sarah Harries (2011-12)	
4th Jan 2001	Roches_MGA55_20010104.shp	Chris Sharples (2010)	
14th Dec 2002	Roches_MGA55_20021214.shp	Sarah Harries (2011-12)	
28th Mar 2004	Roches_MGA55_20040328.shp	Chris Sharples (2015)	
2nd May 2005	Roches_MGA55_20050502.shp	Chris Sharples (2010)	
4th Jan 2007	Roches_MGA55_20070104.shp	Sarah Harries (2011-12)	
3rd Jan 2008	Roches_MGA55_20080103.shp	Chris Sharples (2015)	
15th May 2011	Roches_MGA55_20110515.shp	Chris Sharples (2015)	
15th Jul 2011	Roches_MGA55_20110715.shp	Sarah Harries (2011-12)	
24th Jun 2013	Roches_MGA55_20130624.shp	Chris Sharples (2015)	
4th Sep 2015	Roches_MGA55_20150904.shp	Chris Sharples (2015)	

A1.4.3 Hope Beach, South Arm Neck, south-eastern Tasmania

Locality and general description

This site is the swell-exposed seawards-facing south shore of the South Arm isthmus, which is a sand body extending to below present sea-level across most of its width and length. Note that a shoreline behaviour history has also been digitised from the same ortho-rectified air photos for the Ralphs Bay sandy saltmarsh shoreline which is located on the sheltered northern side of the same isthmus; these results are provided separately in Section A1.2.1 of these appendices.

Swell wave climate

Exposed to south-westerly and Tasman sea swells – likely some directional variability in Tasman swells but refraction around Betsey Island likely removes much of the variation by the time the swell reaches the beach.

Wind (wind wave) climate

South-west to north-east oriented active transgressive dunes in the 1948 and 1965 air photos (Table 67) are indicative of dominant south-westerly wind direction at Hope Beach.

Sand transport and budget

Hope Beach is an ocean-facing swell-exposed and swash-aligned beach. Although no quantitative data is available, shelf sediment transport modelling (see Figure 8) suggests there may be some continuing swell-driven onshore movement of sand from the continental shelf in the Storm Bay region (Harris & Heap 2014; Harris et al. 2000). This would account for the slight trend towards shoreline progradation observed in the beach history (see below).

Alongshore (littoral) drift of sand into or out of the Hope Beach embayment is unlikely to be significant. The strongly protruding rocky Cape Direction at its west end (Figure 207) is probably a major barrier to alongshore sand movement in or out. In contrast, inspection of swell refraction patterns around Betsey Island (visible in Figure 209) indicates that sand near the eastern end of Hope Beach will normally drift westwards further into the Hope Beach embayment, while the same refracted swell will prevent sand drifted from further east (Calvert's Beach) moving around Goat Bluff and into Hope Beach.

The historic air photos (Table 67) show that during the mid-Twentieth Century active transgressive dunes behind (north of) Hope Beach were transporting windblown sand out of the embayment and into Ralphs Bay to the north, albeit the quantities of sand lost by this means were probably small. However, by the 1980s vegetation establishment - particularly on the Hope Beach foredune – appears to have halted all or most of this wind-blown sand loss.

Several large sand mines subsequently established on lower ground behind the Hope Beach foredune have not breached the foredune or modified the beach, and as such are unlikely to have affected the Hope Beach sand budget since they have not changed sand transport patterns between the beach, foredune and surf zone / subtidal area.

In summary, Hope Beach has a stable to possibly slightly gaining sand budget, with no significant sand sinks (subsequent to the Twentieth Century stabilisation of former transgressive dunes).

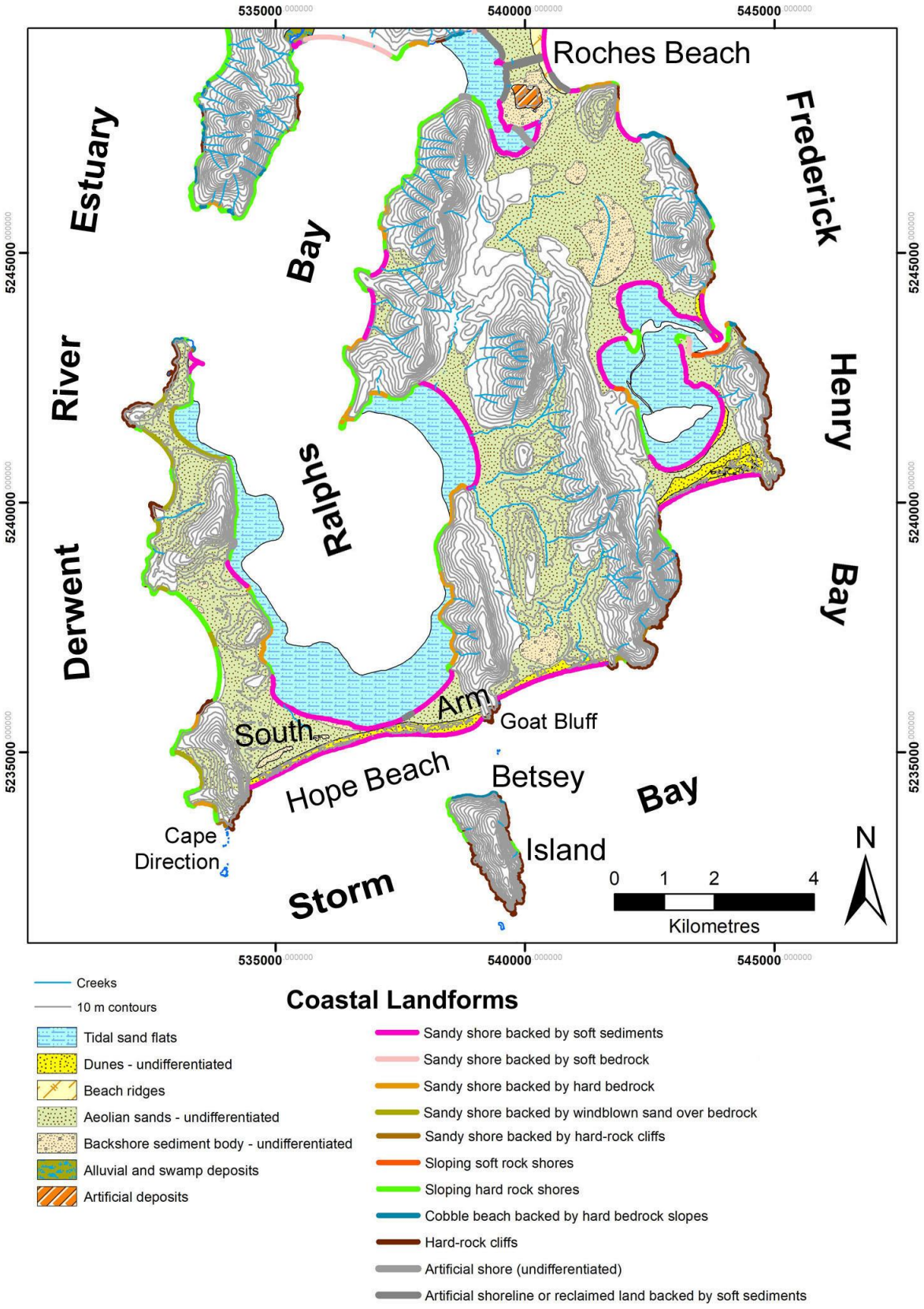

Figure 207: Coastal landforms at South Arm peninsula, south-east Tasmania. Coastal landform mapping is based on Tasmanian Geological Survey mapping (multiple 1:50,000 and 1:25,000 map sheets), with additional geomorphic mapping by C. Sharples. Co-ordinate system is Map Grid of Australia Zone 55 (GDA1994 datum).

Figure 208: View east on Central Hope Beach at three dates after a large swell storm event on 9th-10th July 2011. Views in 2014 and 2020 show progressive foredune recovery after the 2011 swell erosion event. Smaller erosion events occurred after 2011 but did not significantly impede dune recovery. The aggressive exotic sand-binging marram grass (*Ammophila arenaria*) dominates the accreting incipient dune in these photos but was also dominant on the seawards foredune face prior to the 2011 erosion event. By 2020 beach and dune recovery was nearly but not quite complete, with upper parts of the 2011 erosion scarp still visible. This was the largest erosion and recovery event in the air photo record examined for this project. There is some residual possibility that similar events previously may have occurred in time gaps between the air photos used, however examination of additional air photos would reduce this uncertainty. These views are all the same section of the beach near transect 14234.

Air photo analysis

Historic shoreline behaviour at Hope Beach was determined using ortho-rectified air photos from 9 dates between 1948 and 2019 (see Table 67). These are not the full time series available for Hope Beach, however it is noteworthy that the seven air photos prior to 2011 show a consistent shoreline behaviour trend with little variability (Figure 209 and Figure 210), which suggests that large departures from the apparent trend (hidden in time gaps between the used air photo dates) are unlikely.

Shore behaviour history from air photos

Several anomalously landwards shoreline positions on the 1948 air photo (see Figure 209 transect plots) are the result of bare mobile ('blowing out') transgressive dunes extending in places over 200 metres landwards (northwards) of the beach at that time, so that the digitised shoreline proxy (the vegetation line) was mapped a considerable distance landwards of the actual beach face on some transect lines (notably transects 14212, 14213 and 14232). Bare actively mobile transgressive sand dunes are evident behind much of the beach in the 1948 and 1965 air photos, with a SW to NE orientation indicative of the dominant wind direction. These almost entirely cross the South Arm isthmus at its narrowest point so that some wind-blown sand was evidently being lost from Hope Beach into Ralphs Bay at that time.

After 1948 the air photo time series shows a gradual stabilisation of the mobile transgressive dune areas by vegetation including trees, with the seawards face of the Hope Beach foredune being mostly vegetated by circa 1982. Given other indications of sand pits and farming areas being established on lower areas of the sandy isthmus behind the Hope Beach foredune over the same period, it is likely that the revegetation was partly a result of deliberate "land stabilisation" plantings and partly due to the spread of marram grass and other invasive species from nearby beach areas.

Apart from the changes in backshore transgressive dune behaviour noted above, from 1948 until 2020 the Hope Beach shoreline history has been one of erosion and accretion episodes oscillating around an essentially stable dynamic equilibrium position, with a non-significant suggestion of a slight prograding trend (see Figure 210). This history has been spatially coherent along the whole beach (see Figure 209).

The air photo history is also suggestive of a progressive increase in the amplitude of erosion-accretion cycles over the air photo history, with the most recent (2011 to 2020) erosion cut and subsequent recovery being the largest in the record and the cycle previous to that being the next largest (Figure 208, Figure 209). However, the limited number of air photos used in the analysis of this beach's behaviour makes the assertion of such an increasing trend problematical: ideally shorelines from additional air photo dates should be digitised as opportunity allows in order to test the reality of any such trend.

Artificial sand pits (mines) and farm pastures have been established in lower backshore areas behind the Hope Beach foredune since at least the 1960s. Although these have made substantial changes to backshore topography and vegetation patterns the foredune and beach face have not been subject to any significant modifications or artificial interventions apart from the establishment of the introduced marram grass on the foredune. This invasive sand-trapping dune grass may have at least in part contributed to the slight progradation trend evident in the shoreline history but would neither have caused nor prevented the large storm cuts also evident in the more recent parts of the air photo records as noted above.

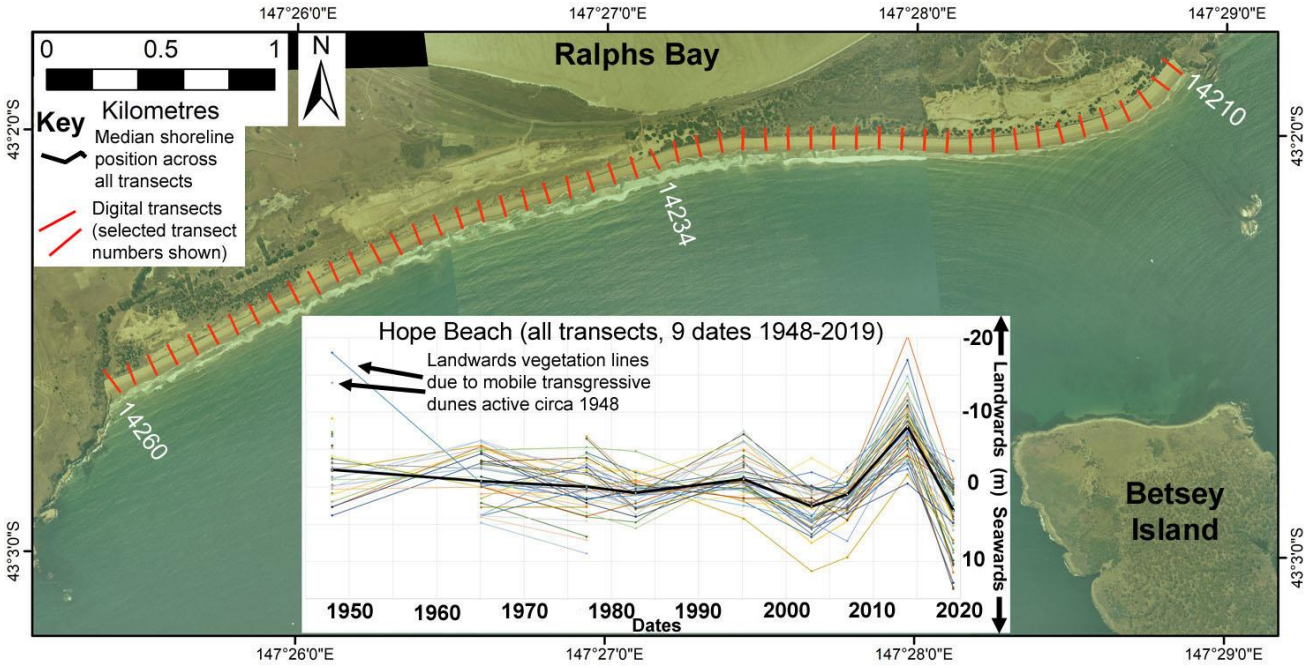

Figure 209: Plots of shoreline (*in situ* vegetation line) position movement at Hope Beach, over the period 1948 to 2019 along each 100m-spaced digital transect line used. The beach image is the March 1995 air photo.

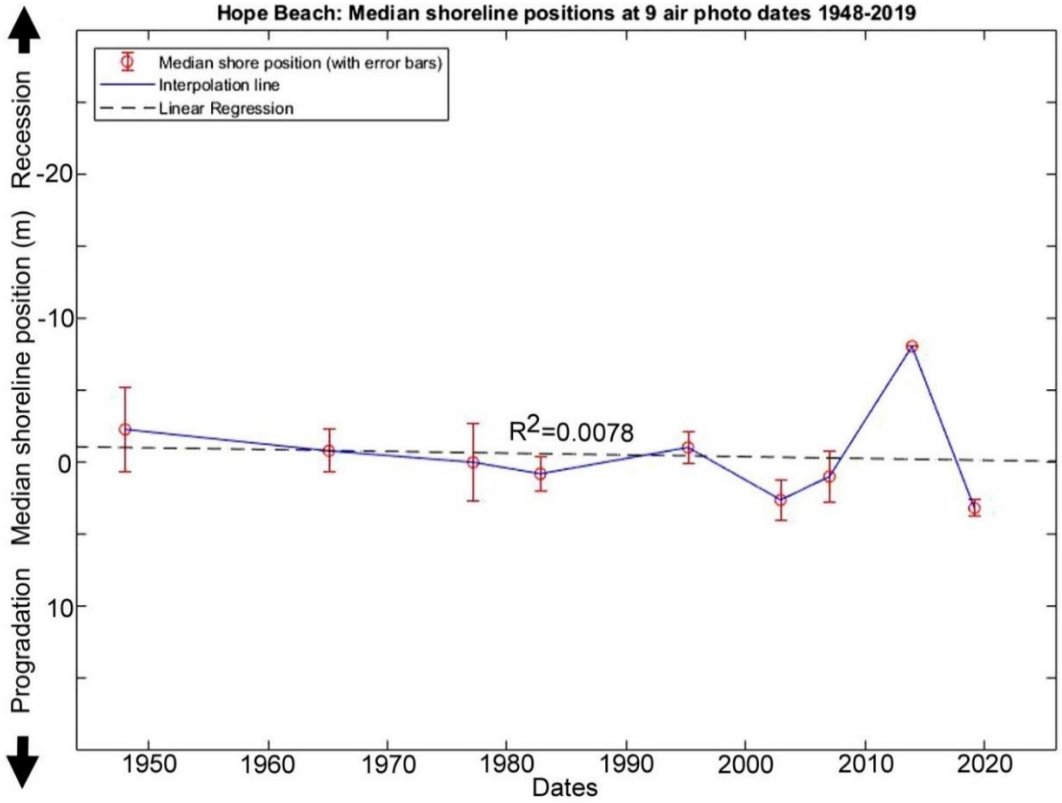

Figure 210: Summary plot of shoreline change history across all transects at Hope Beach (as shown on Figure 211), at 9 air photo dates from 1948 to 2019. These plot the median of the normalised shoreline positions across all transects at each date. A linear fit indicating a non-significant progradation trend implies a stable or very slightly prograding dynamic equilibrium shoreline position throughout the air photo period. Despite the July 2011 storm erosion event having caused a significantly larger storm bite (av. ~ 10 m horizontally) than any other seen in the air photo record for this beach, shoreline recovery was essentially complete by 2019. Hence there are still no clear indications of a long-term change of behaviour at this beach, whose initial response to sea-level rise will probably be a switch to progressive recession of the beach and foredune face leading to eventual breaching of the dune and subsequent wash overs and barrier roll-over.

Air photo data tables

The following tables provide details of the air photos used, the resulting ortho-photos produced, and the shapefiles representing the shoreline position that were digitised from the ortho-photos.

Table 67: Original air photos and ortho-rectified air photos produced for Hope Beach, South Arm, SE Tasmania.

Photo Date	**Original air photos, DPIPWE © unless otherwise stated (film-frame) / Ortho-photo name**	**Final image resolution (original scan resolution if downsized) / pixel size of final ortho-photo**	**Original photo scale**	**Mean measured feature position error (± metres) for ortho-photo** [no. of measured feature position reference points]	**Comments**
8th Jan 1948	82-1606 82-1607 / *Hope_1948_MGA55.tif*	? / 0.85 m	1:15,840	2.9 [9]	Ortho-rectified by Chris Sharples. 2 original photos joined to create mosaic.
2nd Feb. 1965	433-235 Hope_1965_MGA55.tif	? / 0.41 m	1:31,680	1.5 [10]	Ortho-rectified by Chris Sharples.
4th Mar. 1977	716-57 / *Hope_1977_MGA55.tif*	? / 0.50 m	1:30,000	2.7 [15]	Ortho-rectified by Chris Sharples.
18th Oct. 1982	928-174 to 928-181 / *Hope_1982_MGA55.ecw*	? / 0.14 m	1:5,000	1.2 [13]	Ortho-rectified by Matt Dell. 8 original photos joined to create mosaic.
1st Mar. 1995	1233-72 1233-77 1233-94 / *Hope_1995_MGA55.tif*	? / 0.33 m	1:12,500	1.1 [16]	Ortho-rectified by Chris Sharples. 3 original photos joined to create mosaic.
3rd Dec 2002	1362-106 1362-107 1362-108 / *Hope_2002_MGA55.tif*	? / 0.30 m	1:10,000	1.4 [15]	Ortho-rectified by Chris Sharples. 3 original photos joined to create mosaic.
4th Jan 2007	1419-90 1419-91 1419-93 / *Hope_2007_MGA55.tif*	? / 0.31 m	1:10,000	1.8 [19]	Ortho-rectified by Chris Sharples. 3 original photos joined to create mosaic.
1st Dec. 2013	Photographed by Matt Dell for Clarence City Council / *Hope-Calverts_2013_MGA55.ecw*	n/a / 0.10 m	n/a	0.0 [N/A] REFERENCE PHOTO Nil error by convention; absolute error ± 0.1 m cited by Matt Dell.	Ortho-rectified by Matt Dell for Clarence City Council using GPS-defined Ground Control Points visible on the air photo.
24th Feb. 2019	Photo-graphed by Matt Dell for Clarence City Council / *ClarenceWhole_25cm_2019_MattDell.ecw*	n/a / 0.25 m	n/a	0.6 [20]	Ortho-rectified by Matt Dell for Clarence City Council. Extensively slumped old dune scarp with considerable incipient foredune accretion in progress; shoreline = seawards veg. extent everywhere. Some dark shadowing at West end of beach prevents shoreline mapping.

Table 68: Digitised shoreline shapefiles produced for Hope Beach using ortho-photos listed in Table 67 above.

Date of air photo(s)	Shapefile	Shoreline digitised by	Comments
8th Jan 1948	Hope_MGA55_19480108.shp	Chris Sharples (2018)	
2nd Feb. 1965	Hope_MGA55_19650202.shp	Chris Sharples (2018)	
4th Mar. 1977	Hope_MGA55_19770304.shp	Chris Sharples (2018)	
18th Oct. 1982	Hope_MGA55_19821018.shp	Chris Sharples (2018)	
1st Mar. 1995	Hope_MGA55_19950301.shp	Chris Sharples (2018)	
3rd Dec 2002	Hope_MGA55_20021203.shp	Chris Sharples (2018)	
4th Jan 2007	Hope_MGA55_20070104.shp	Chris Sharples (2018)	
1st Dec. 2013	Hope_MGA55_20131201.shp	Chris Sharples (2018)	
24th Feb. 2019	Hope_MGA55_20190224.shp	Chris Sharples (2019)	

A1.4.4 Adventure Bay South Beach, Bruny Island

Sand transport and budget

The mouths of Captain Cook, Blighs and Dorloff Creeks are strongly deflected eastwards across the beach at most air photo dates, which is indicative of a swell-driven dominantly north-west to south-eastwards to eastwards alongshore drift and littoral sand transport pattern around the southern end of Adventure Bay under most conditions. This would result from the refraction of the south-westerly swell into the Bay. Further evidence that this is the dominant mode of littoral drift at this beach is provided by the historic air photos which mostly show clumpy incipient dune vegetation (marram grass) - indicating sand accretion - is often well developed on the upper beach immediately west (up-drift) of the mouths of each creek, even when little incipient dune accretion is evident elsewhere on the beach.

Air photo analysis

Based on the ortho-rectified air photos and digitised shorelines listed in Table 69 and Table 70 (and obtained according to the methods described in Appendix A2.1), the history of shoreline behaviour and change at Adventure Bay South over the air photo period (1949-2018) is summarised in the following Figure 211 and Figure 212, which depict, respectively, shoreline changes on all individual

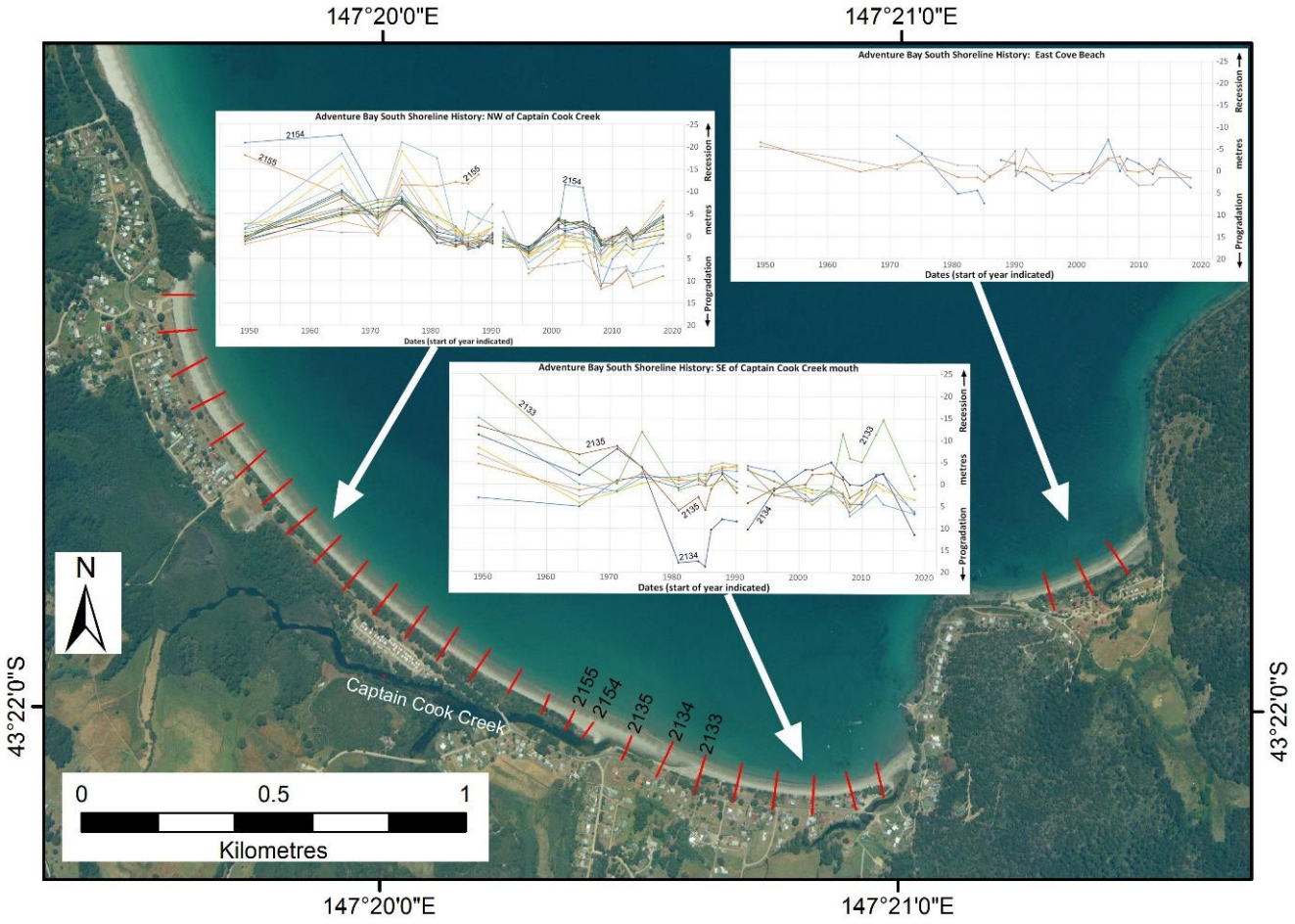

Figure 211: Plots of shoreline (vegetation line) movement along each digital transect at Adventure Bay South beaches at 21 air photo dates over the period 1949 to 2018 (22 for East Cove), plotted relative to the median shoreline position on each transect. Transect locations are indicated by red lines on the air photo, and each coloured line on the plots represents shoreline position changes over time along one transect. Transects are plotted in three groups separated by creek mouths and a stretch of rocky shore. It is notable that shoreline movement at the main beach has been generally coherent across transects, except those affected by the shifting mouth of Captain Cook Creek (transects 2133, 2134, 2135, 2154 and 2155). These anomalous transects are numbered on the figure. The base image is the January 2005 air photo (© DPIPWE).

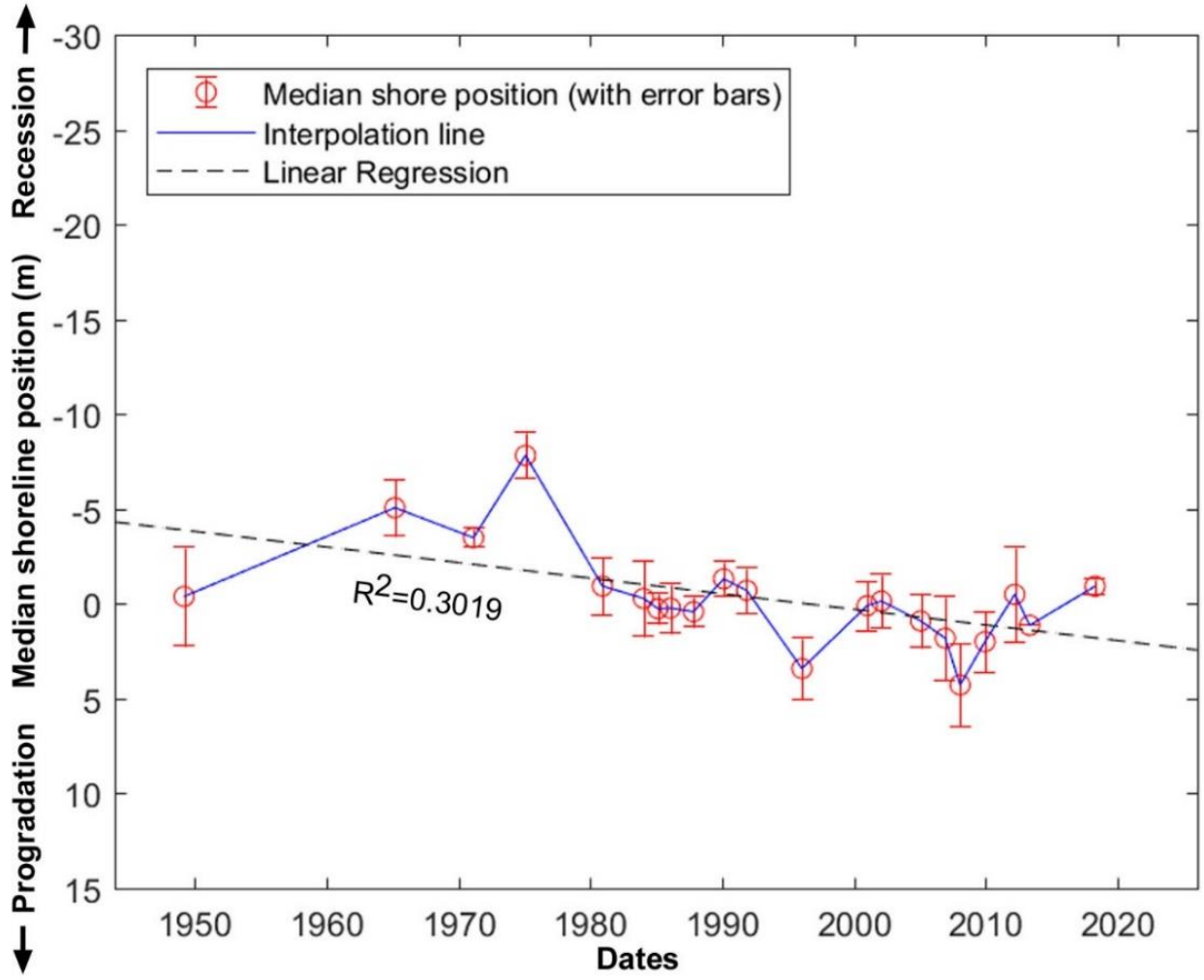

Figure 212: Summary plot of shoreline change history at the main Adventure Bay South beach (excluding East Cove beach and the anomalous transects 2133, 2134, 2135, 2154 and 2155 adjacent the mouth of Captain Cook Creek) at 21 air photo dates from 1949 to 2018. This plots the median of the shoreline positions measured on all transects (relative to the median position on each transect) at each air photo date. Figure shows interpolation lines & linear regression plotted.

transects at both Adventure Bay and East Cove beaches, and the overall median shoreline change history across all the transects not affected by creek discharge at the main Adventure Bay Beach.

Shore behaviour history from air photos

Except around the five transects closest to Captain Cook Creek, both the main beach (Adventure Bay Beach) and the nearby East Cove Beach have exhibited similar behaviour over the 69-year duration of the air photo record. Allowing for the air photo error margins (see Figure 212) and some variability between individual transects (Figure 211), the shoreline at both beaches has been relatively stable, with median shoreline erosion and recovery cycles involving around 5 metres or less horizontal shoreline movement, and full recovery of the prior shoreline positions within approximately 8 years or less. Super-imposed on the erosion-recovery cycles at both beaches has been a slow but significant trend towards long-term shoreline progradation (of the order of 5 metres seawards movement of the median shoreline position at both beaches over the period 1949 to 2018). A linear regression line fitted to the data yields a slow progradation trend with a correlation coefficient of $R^2 = 0.3019$ (Figure 212 bottom).

In contrast, shoreline behaviour has been much more variable on the five transects close to the mouth of Captain Cook Creek. Inspection of the air photo time series demonstrates this is a result of episodic

shifting of the creek discharge channel across the beach face. This has probably occurred as rapid channel shifts in response to occasional coastal and creek catchment floods, followed by gradual beach recovery after such events progressively moving the channel back eastwards in response to the normal NW – SE littoral drift currents at this beach.

A recent erosion event (or series of events) between 2013 and 2018 resulted in about 5 to (in places) 10 metres of shoreline recession in the north-western half of the main beach, with the eroded sand being transported south-east and causing the shoreline to prograde in the south-east (down-drift) part of the main beach (see Figure 213). Although this is significant, the historical record demonstrates that larger erosion (recession) events have occurred at this beach in the past (see Figure 212), hence the recent erosion does not constitute evidence of a change of shoreline behaviour (it will if the trend continues for some further years and recedes beyond the range of historical variability).

Overall, the air photo record demonstrates that Adventure Bay Beach and East Cove Beaches have been mostly stable to slowly growing (prograding) beaches over the 1949 to 2018 period (with sub-ordinate erosion-recovery cycles), indicating a slowly gaining sand budget over that time.

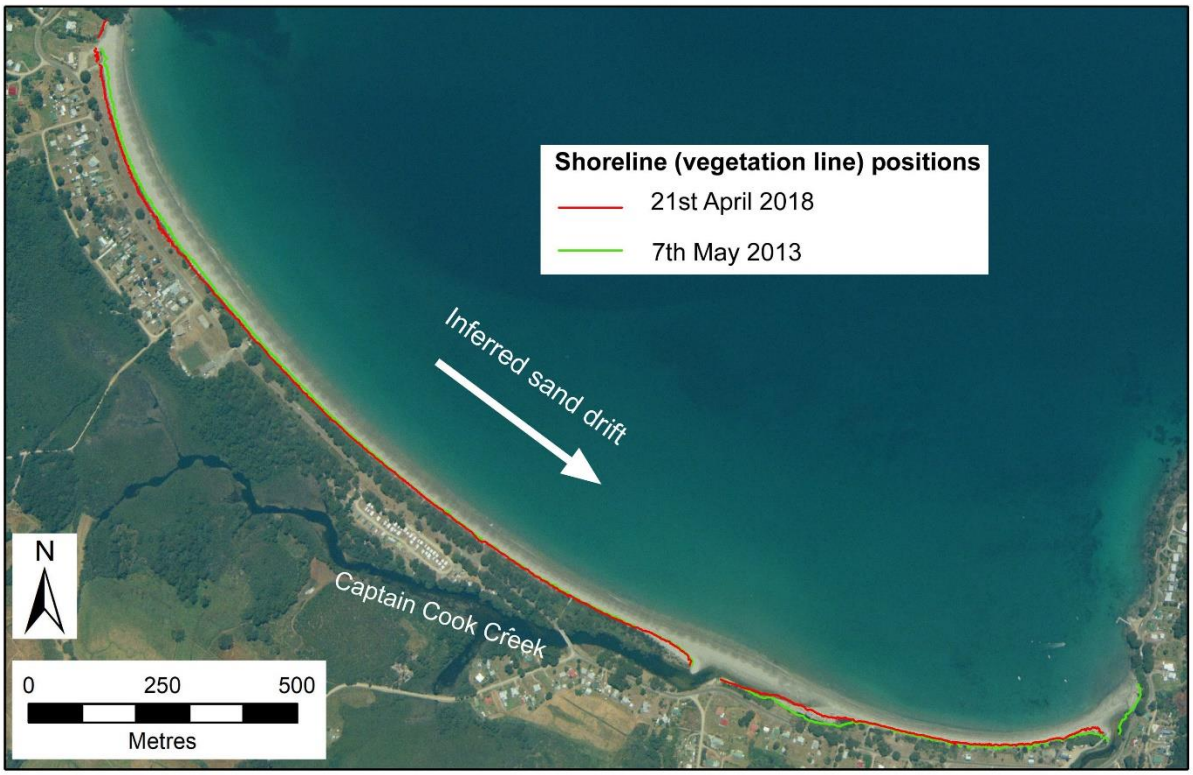

Figure 213: Shoreline position changes at the main Adventure Bay Beach south between May 2013 and April 2018. Significant shoreline recession has occurred north-west of Captain Cook Creek mouth, especially at the extreme north-west end of the beach, while notable shoreline growth (progradation) has occurred at the south-eastern end of the beach, particularly south-east of Captain Cook Creek mouth. This is as expected given the evidence for a dominantly south-eastwards alongshore drift through southern Adventure Bay and implies that the sand eroded from the north-west end of the beach has accumulated at the south-east end.

Air Photo Data Tables

The following tables provide details of the air photos used, the resulting ortho-photos produced, and the shapefiles representing the shoreline position that were digitised from the ortho-photos.

Table 69: Original air photos and ortho-photos produced for Adventure Bay South.

Photo Date	**Original DPIPWE air photos (film-frame) / Ortho-photo name**	**Final image resolution (**original scan resolution if downsized) **/ pixel size of final ortho-photo**	**Original photo scale**	**Mean measured feature position error for ortho-photo (± metres) /** [No. of measured feature position reference points]	**Comments**
2nd Mar 1949	182-949 182-964 / *AdventureBayS_Mar1949a_MGA55.tif/tfw* *AdventureBayS_Mar1949b_MGA55.tif/tfw*	600 dpi / 0.95 m pixel size	1:15,840	2.6 m [9]	Ortho-rectified by C. Sharples
2nd Mar 1965	452-164 / *AdventureBayS_Mar1965_MGA55.tif/tfw*	1500 dpi (2039 dpi) / 0.57m pixel size	1:31,680	1.5 m [8]	Ortho-rectified by C. Sharples
19th Feb 1971	567-44 567-46 / *AdventureBayS_Feb1971a_MGA55.tif/tfw;* *AdventureBayS_Feb1971b_MGA55.tif/tfw*	2039 dpi / 0.17 m pixel size	1:10,000	0.5 m [7]	Ortho-rectified by C. Sharples
31st Jan 1975	664-225 / *AdventureBayS_Jan1975_MGA55.tif/tfw*	2039 dpi / 0.6 m pixel size	1:40,000	1.2 m [7]	Ortho-rectified by C. Sharples
1st Dec 1980	844-47 844-50 844-53 / *AdventureBayS_Dec1980a_MGA55.tif/tfw;* *AdventureBayS_Dec1980b_MGA55.tif/tfw;* *AdventureBayS_Dec1980c_MGA55.tif/tfw*	1500 dpi (2039 dpi) / 0.11 m pixel size	1:6,000	1.5 m [7]	Ortho-rectified by C. Sharples
14th Jan 1984	980-76 / *AdventureBayS_Jan1984_MGA55.tif/tfw*	1000 dpi (2039 dpi) / 0.58 m pixel size	1:20,000	2.0 m [9]	Ortho-rectified by C. Sharples
15th Feb 1985	1026-57 / *AdventureBayS_Feb1985_MGA55.tif/tfw*	2039 dpi / 0.19 m pixel size	1:15,000	0.8 m [8]	Ortho-rectified by C. Sharples
28th Jan 1986	1056-58 / *AdventureBayS_Jan1986_MGA55.tif/tfw*	2039 dpi / 0.16 m pixel size	1:12,500	1.3 m [8]	Ortho-rectified by C. Sharples
30th Oct 1987	1092-168 / *AdventureBayS_Oct1987_MGA55.tif/tfw*	1300 dpi (2039 dpi) / 0.90 m pixel size	1:42,000	0.8 m [8]	Ortho-rectified by C. Sharples
14th Feb 1990	1150-177 / *AdventureBayS_Feb1990_MGA55.tif/tfw*	2039 dpi / 0.56 m pixel size	1:42,000	0.9 m [7]	Ortho-rectified by C. Sharples
16th Mar 1990	1152-143 / *AdventureBayS_Mar1990_MGA55.tif/tfw*	1000 dpi (2039 dpi) / 0.13 m pixel size	1:5,000	0.9 m [3]	Ortho-rectified by C. Sharples
14th Nov 1991	1173-54 /	2039 dpi / 0.60 m pixel size	1:42,000	1.2 m [8]	Ortho-rectified by C. Sharples

	AdventureBayS_Nov1991_MGA55.tif/tfw				
23rd Jan 1996	1245-96 / *AdventureBayS_Jan1996_MGA55.tif/tfw*	1000 dpi (2039 dpi) / 0.50 m pixel size	1:20,000	1.6 m [8]	Ortho-rectified by C. Sharples
1st Jan 2001	1345-147 / *AdventureBayS_Jan2001_MGA55.ecw*	2039 dpi / 1.00 m pixel size	1:42,000	1.3 m [9] (quoted absolute accuracy ±15m)	Ortho-rectified by DPIPWE Original DPIPWE ortho file: 1345_147_op.ecw
1st Feb 2002	1353-025 / *AdventureBayS_Feb2002_MGA55.tif/tfw*	1000 dpi (2039 dpi) / 0.60 m pixel size	1:20,000	1.4 m [9]	Ortho-rectified by C. Sharples
25th Jan 2005	1391-007 / *AdventureBayS_Jan2005_MGA55.ecw*	2039 dpi / 0.50 m pixel size	1:42,000	1.4 m [9] (quoted absolute accuracy ±15m)	Ortho-rectified by DPIPWE Original DPIPWE ortho file: 1391_007_op.ecw USED AS SECONDARY REFERENCE IMAGE FOR ORTHO-RECTIFYING
9th Dec 2006	1413-197 1413-199 / *AdventureBayS_Dec2006a_MGA55.ecw* *AdventureBayS_Dec2006b_MGA55.ecw*	2039 dpi / 0.50m pixel size	1:12,500	2.2 m [10] (quoted absolute accuracy ±15m)	Ortho-rectified by DPIPWE Original DPIPWE ortho files: 1413_197_op.ecw 1413_199_op.ecw
25th Jan 2008	1430-54 1430-56 / *AdventureBayS_Jan2008a_MGA55.ecw* *AdventureBayS_Jan2008b_MGA55.ecw*	2039 dpi / 0.50 m pixel size	1:24,000	2.2 m [10] (quoted absolute accuracy ±15m)	Ortho-rectified by DPIPWE Original DPIPWE ortho files: 1430_54_op.ecw 1430_56_op.ecw
15th Dec 2009	1439-133 / *AdventureBayS_Dec2009_MGA55.ecw*	2039 dpi / 0.50 m pixel size	1:42,000	1.6 m [9] (quoted absolute accuracy ±15m)	Ortho-rectified by DPIPWE Original DPIPWE ortho file: 1439_133_op.ecw
19th Mar 2012	1469-188 1469-213 / *AdventureBayS_Mar2012a_MGA55.tif/tfw* *AdventureBayS_Mar2012b_MGA55.tif/tfw*	1000 dpi (2039 dpi) / 0.65 m pixel size	1:24,000	2.5 m [10]	Ortho-rectified by C. Sharples
7th May 2013	Original digital ortho file: *AdventureBayS_May2013_MGA55.ecw*	- / 0.10 m pixel size	-	0.0 m [N/A]	REFERENCE IMAGE (zero relative feature position error by convention) Digital original photo; captured & ortho-rectified by Matt Dell as *AdventureBay_2013.ecw*
21st April 2018	Original digital ortho file: AdventureBayS_Apr2018_MGA55.tif	- / 0.06 m pixel size	-	0.40 m [9]	Air photo captured and ortho-rectified by Matt Dell

Table 70: Digitised shoreline shapefiles produced for Adventure Bay (using ortho-photos listed in Table 69 above).

Date of air photo(s)	Shapefile	Shoreline digitised by	Comments
2nd Mar 1949	AdventureBayS_MGA55_19490302.shp	Chris Sharples (2017)	Irregular veg line (established foredune front) with some scattered clumpy incipient dune veg. evident in front. No recent erosion.
2nd Mar 1965	AdventureBayS_MGA55_19650302.shp	Chris Sharples (2017)	Vegetation line mostly straight, with some scattered clumpy incipient dune veg in front.
19th Feb 1971	AdventureBayS_MGA55_19710219.shp	Chris Sharples (2017)	Clumpy incipient dune veg in front of established foredune veg; accretion occurring with no recent erosion. Some wrack at N end; some tree shadows on beach.
31st Jan 1975	AdventureBayS_MGA55_19750131.shp	Chris Sharples (2017)	Established foredune vegetation line somewhat irregular with scattered clumpy incipient foredune veg in front in places. No recent erosion.
1st Dec 1980	AdventureBayS_MGA55_19801201.shp	Chris Sharples (2017)	Extensive sparse clumpy incipient dune grass establishing in front of irregular established dune front (no recent erosion).
14th Jan 1984	AdventureBayS_MGA55_19840114.shp	Chris Sharples (2017)	Sparse clumpy incipient dune veg. evident seawards of established foredune veg. at NW end of beach. Established foredune veg line moderately irregular elsewhere (no recent erosion).
15th Feb 1985	AdventureBayS_MGA55_19850215.shp	Chris Sharples (2017)	Vegetation line somewhat irregular; clumpy incipient dune vegetation prominent in many areas seawards of established foredune veg (accreting beach).
28th Jan 1986	AdventureBayS_MGA55_19860128.shp	Chris Sharples (2017)	Vegetation line straight to somewhat irregular, with notable clumpy incipient dune vegetation in many places. (Not recently eroded)
30th Oct 1987	AdventureBayS_MGA55_19871030.shp	Chris Sharples (2017)	Vegetation line straight to fairly irregular. Common clumpy incipient dune vegetation. No recent erosion.
14th Feb 1990	AdventureBayS_MGA55_19900214.shp	Chris Sharples (2017)	Vegetation line somewhat irregular; no

			recent erosion. Only minor clumpy incipient dune veg visible.
16th Mar 1990	AdventureBayS_MGA55_19900316.shp	Chris Sharples (2017)	Mainly East Bay; vegetation line ragged with some clumpy incipient dune veg in front (no recent erosion).
14th Nov 1991	AdventureBayS_MGA55_19911114.shp	Chris Sharples (2017)	Poor photo contrast. Vegetation line slightly irregular, no incipient dune veg visible. Likely no recent erosion.
23rd Jan 1996	AdventureBayS_MGA55_19960123.shp	Chris Sharples (2017)	Vegetation line irregular with clumpy incipient dune veg common in front of older established dune veg (implying no recent erosion).
1st Jan 2001	AdventureBayS_MGA55_20010101.shp	Chris Sharples (2017)	Vegetation line – slightly irregular but little new (clumpy) incipient dune vegetation evident. Likely minor recent erosion only.
1st Feb 2002	AdventureBayS_MGA55_20020201.shp	Chris Sharples (2017)	Quite 'ragged' vegetation line (not recently eroded) but with only minor evidence of clumpy new incipient dune vegetation.
25th Jan 2005	AdventureBayS_MGA55_20050125.shp	Chris Sharples (2017)	Irregular vegetation line (old erosion scarp) but mostly little indication of recent incipient dune veg growth.
9th Dec 2006	AdventureBayS_MGA55_20061209.shp	Chris Sharples (2017)	Vegetation line somewhat irregular with sporadic patchy incipient dune vegetation on seawards side; likely beach accreting, no recent erosion.
25th Jan 2008	AdventureBayS_MGA55_20080125.shp	Chris Sharples (2017)	Vegetation line linear to slightly irregular, patchy incipient dune veg near N side Capt. Cook Ck. mouth only, but dune elsewhere not recently eroded.
15th Dec 2009	AdventureBayS_MGA55_20091215.shp	Chris Sharples (2017)	Vegetation line quite linear along most of main beach, no incipient dune evident, likely fairly recent erosion event.
19th Mar 2012	AdventureBayS_MGA55_20120319.shp	Chris Sharples (2017)	Shoreline is dominantly incipient dune veg with fairly straight edge: possibly recently scarped?

7th May 2013	AdventureBayS_MGA55_20130507.shp	Chris Sharples (2017)	No erosion scarp evident; shoreline is dominantly clumpy incipient dune veg line seawards of established foredune veg.
21st April 2018	AdventureBayS_MGA55_20180421.shp	Chris Sharples (2018)	Shoreline vegetation line well defined although beach a little over-exposed in some areas. Veg line mostly low erosion scarp at north end (near Quiet Corner, but some incipient dune vegetation present southwards near Captain Cook Creek.

A1.4.5 Cloudy Bay Beach West

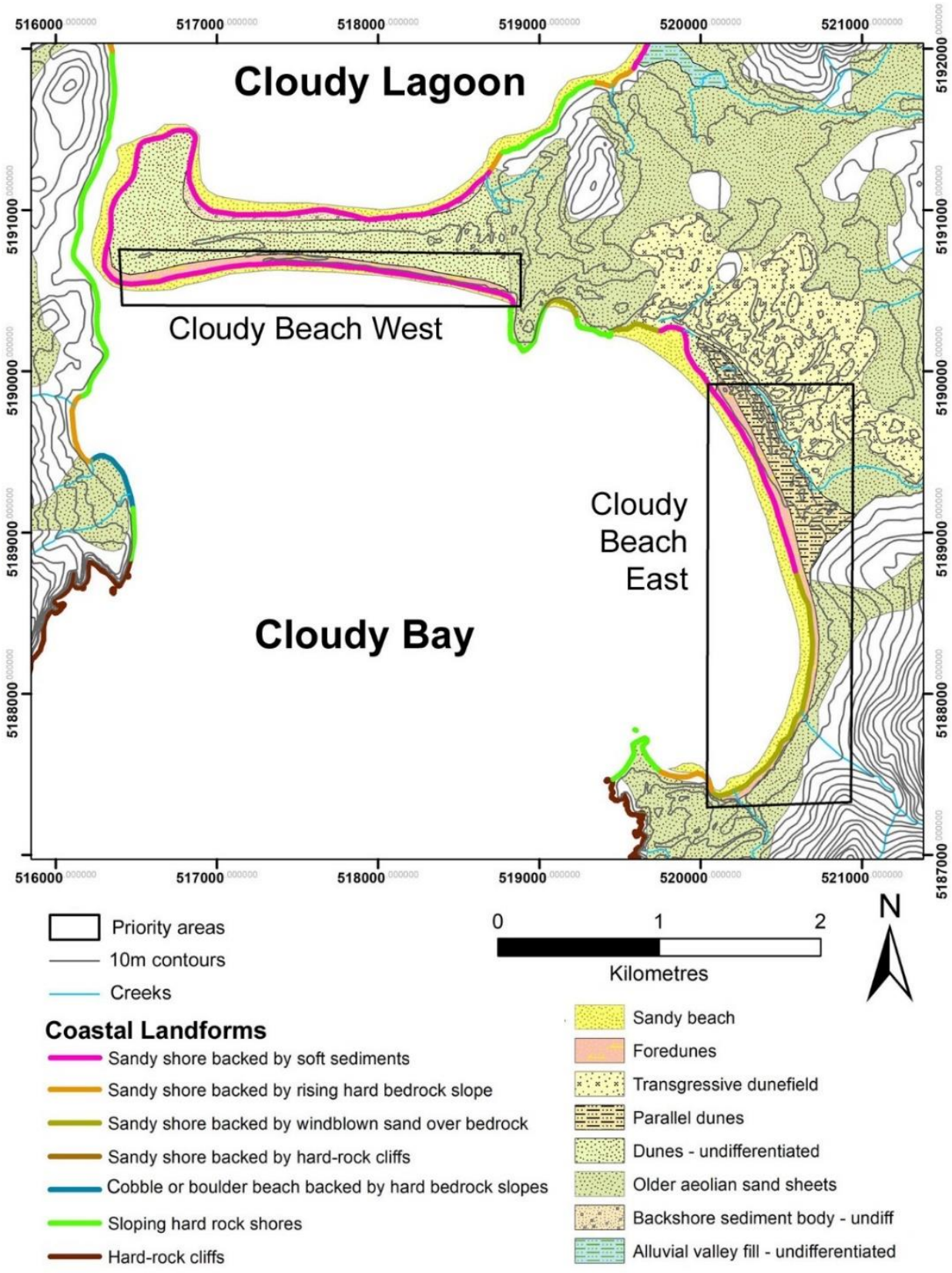

Figure 214: Coastal landforms at Cloudy Bay, indicating the Cloudy Beach West priority area selected for air photo history analysis as a less swell-exposed beach than the adjacent Cloudy Beach East (which is described in Section A1.3.1). Coastal landform mapping is based on the 1:50,000 Dover Geological map sheet (Geological Survey of Tasmania), with additional field observations by C. Sharples. Co-ordinate system is Map Grid of Australia Zone 55 (GDA1994 datum).

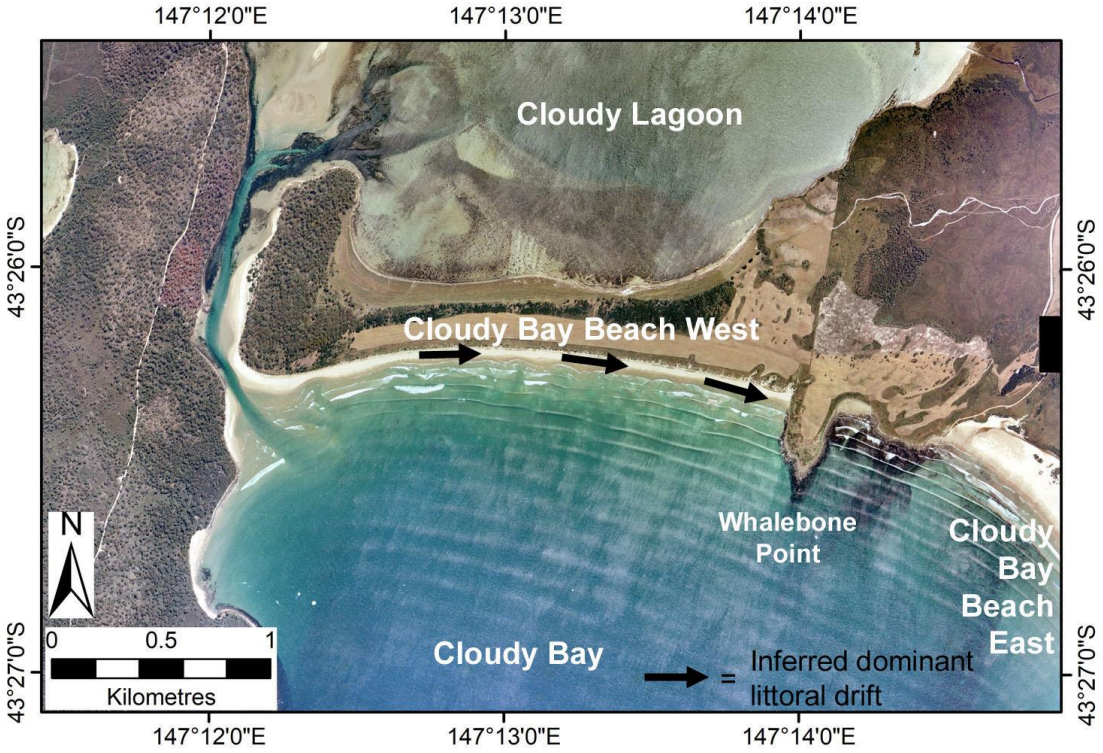

Figure 215: Typical swell wave pattern at Cloudy Bay Beach West. The visible pattern of swell waves arriving slightly oblique to the beach is interpreted as driving an easterly-directed littoral drift current along the central to eastern part of Cloudy Bay Beach West at the time of this photo. The photo date is 6th Feb. 1984 (photo © DPIPWE). A similar swell pattern is apparent on all other Cloudy Bay air photos in which the swell is visible.

Swell wave climate

Dominated by SAM-driven south-westerly swell; only limited swell-wave direction variability outside Cloudy Bay and swell wave direction variability further limited by refraction and training within Cloudy Bay (which is a fairly deep embayment). Exposed to slightly refracted south-westerly swells entering Cloudy Bay (not as directly exposed to swell as Cloudy Bay Beach East).

Wind (wind wave) climate

Cape Bruny BoM weather station 9 km to SW (see Figure 216, records dominantly westerly to south-westerly winds. Note SW-NE aligned deflation hollows at east end of beach indicate dominant wind direction. The anomalous northerly wind component is unexplained but possibly a result of local topographic steering effects at Cape Bruny.

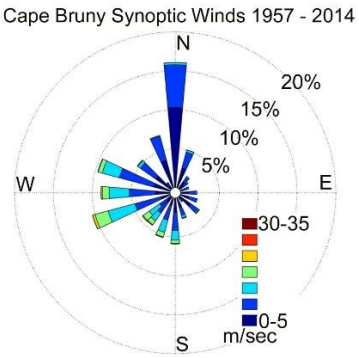

Figure 216: Cape Bruny synoptic wind directions 1957 – 2014. Cape Bruny, 9 km south-west of Cloudy Bay Beach west, is the nearest long-term weather station. Wind rose prepared by Chris Sharples, using original synoptic wind data from the Australian Bureau of Meteorology.

Sand transport and budget

There is no measured data on littoral drift currents at Cloudy Bay Beach West. However, interpretation of swell waves arriving slightly oblique to the beach - as visible on air photos (Figure 215) - implies that an eastwards sand drift is normally dominant along the central to eastern parts of the beach. Given the low variability in swell wave directions at this beach (see below) this is probably the dominant littoral drift direction and is likely reinforced by locally generated wind waves driven by the dominantly westerly to south-westerly winds at this site. The prominent rocky Whalebone Point (see Figure 215) is likely to allow only limited leakage of sand eastwards from this beach cell, and it is likely that some occasional westwards re-distribution of sand in the surf zone occurs under sub-ordinate south-easterly wind conditions and during storms.

Only a few small SW-NE aligned deflation hollows and transgressive mobile sand dunes are evident in the foredune at the most wind-exposed eastern end of the beach throughout the air photo record (see Figure 215). Hence landwards loss of sand via aeolian transport has been a persistent but only minor process at this beach.

Whereas tidal currents at the western end of the beach must move beach sands in and out of the permanently open tidal channel entrance to Cloudy Lagoon, the interpreted littoral drift currents (above) imply that sand eroded from most of the beach and foredune face during storm events will not drift west into the potential sand sink of Cloudy Lagoon. Instead any sand eroded from the central to eastern parts of the beach and foredune face will mostly be returned to the beach and foredune by subsequent fair-weather swells. Hence this beach could be expected to have a stable rather than losing sand budget, at least along its central to eastern parts, despite the proximity of the potential sand sink of Cloudy Lagoon.

The western end of the beach could however be expected to permanently lose sand into Cloudy Lagoon via tidal current transport, however there is no evidence of this occurring in the air photo record. One possible explanation is that the available sand accommodation space in Cloudy Lagoon is already largely full, so that sand has been mainly cycled by tidal currents between the beach and lagoon with little net loss during the air photo period. However, with continuing sea-level rise additional accommodation space (i.e., water depth) will become available in the lagoon, and this may eventually initiate some net sand loss from the west end of Cloudy Bay Beach West. However, an additional sand budget factor is that the beach has probably also been undergoing a net gain of sand as described below, which will probably further delay the onset of sand loss from this beach:

Interpreted littoral drift and tidal lagoon processes (as above) would imply a stable beach, however air photo data actually indicates progradation, implying the beach is receiving additional sand from an outside source. Most likely candidate is swell-driven sand transport from the shelf (Harris & Heap 2014).

Air photo analysis

Air photos from 16 dates between 15th December 1948 and 15th December 2009 were used to analyse shoreline changes over time. These ortho photos and the derived digital shorelines are the same as used for Cloudy Beach East and are listed in Table 20 and Table 21 in appendix Section A1.3.1. Shorelines from the 2nd Feb 1965, 6th Feb. 1984 and 1st Feb. 2002 orthophotos were not used due to accuracy and quality issues (see Table 20 and Table 21). Shoreline history was measured along 25 100-metre spaced transects numbered 4816 to 4840. The shoreline history results are plotted below at Figure 217 & Figure 218.

Shore behaviour history from air photos

Shoreline change along all used transects was mainly coherent throughout the air photo period, with only minor shoreline position anomalies at most air photo dates. This means that shoreline movement

landwards or seawards was roughly parallel along the whole section of beach studied. The plots (Figure 217 & Figure 218) show a small long-term progradation trend over the whole air photo period (~7m seawards shoreline movement overall), which is more pronounced than the smaller progradation trend seen at the adjacent more-exposed Cloudy Bay Beach East (see Section A1.3.1, Figure 106 & Figure 107). Shorter erosion – accretion (recovery) episodes of over 20 metres amplitude are super-imposed on this.

It is notable that an erosion event circa 1980 that is clearly evident (as a landwards shoreline movement) in the shoreline history for the nearby Cloudy Bay Beach East (see Figure 106 and Figure 107 in appendix Section A1.3.1) is not apparent in the shoreline history for Cloudy Bay Beach West (see Figure 217 & Figure 218). This may indicate that Cloudy Beach West was more sheltered than Cloudy Beach East from the storm or cluster of south-westerly swell storms that can be inferred to have caused this erosion. On the other hand, the same shoreline histories demonstrate that both beaches were eroded by a later erosion event or cluster of erosion events around 1985, perhaps indicating that this or these later storms arrived at Cloudy Bay from a more southerly direction than the circa 1980 storm, and so impacted both beaches more directly.

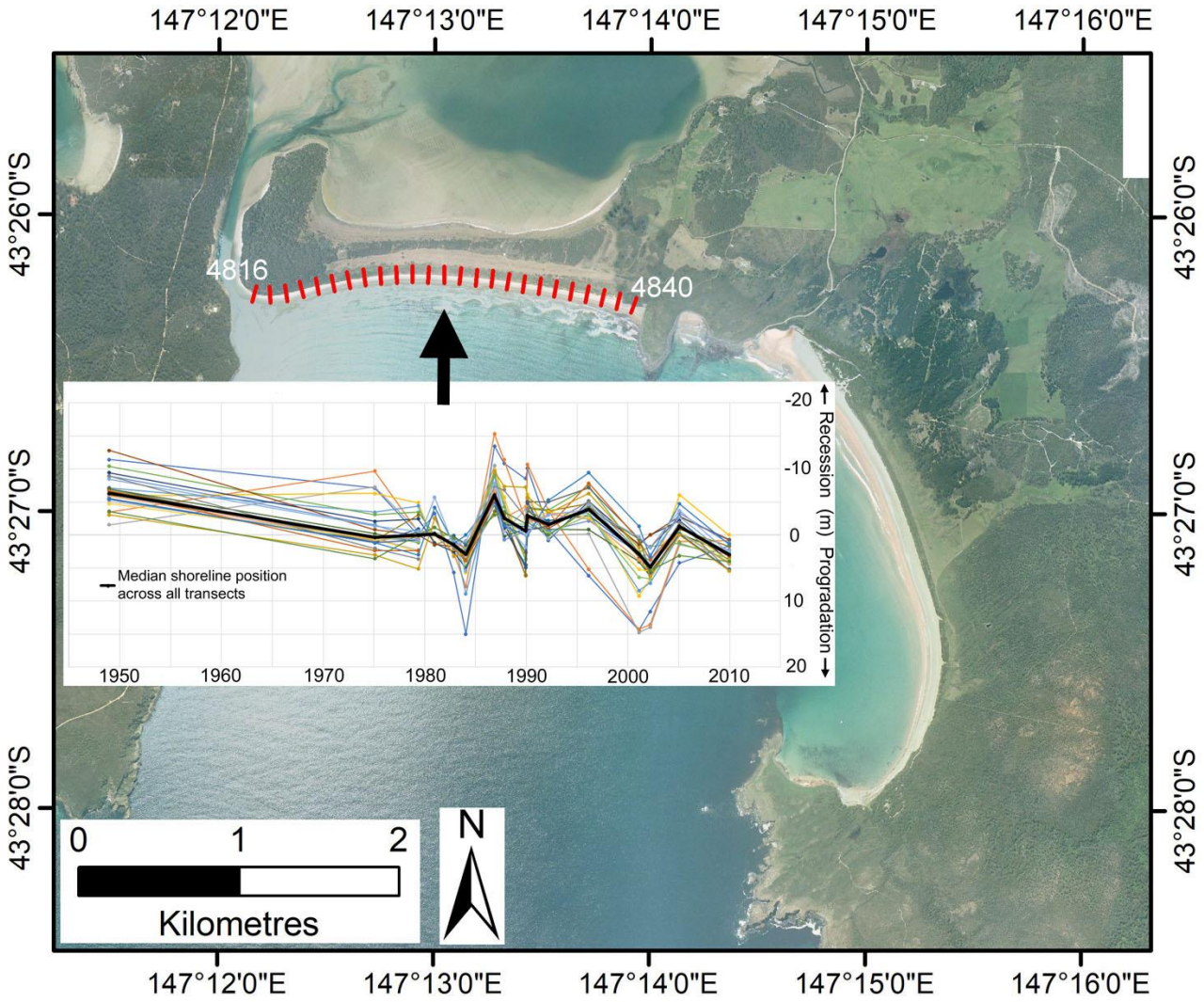

Figure 217: Shoreline position changes along all individual used transects for West Cloudy Beach shoreline, for 16 air photo dates from 1948 to 2009 (omitting 2nd Feb 1965, 6th Feb. 1984 and 1st Feb. 2002 due to accuracy and quality issues with those photos). The used transects used are 100m – spaced red lines on the air photo with selected transect numbers indicated. This plot indicates that shoreline changes are coherent along the whole beach section studied and comprise a slow long-term progradation trend with shorter erosion – accretion cycles super-imposed. See also summary plot Figure 218 below. The background image is the 2009 air photo (© DPIPWE).

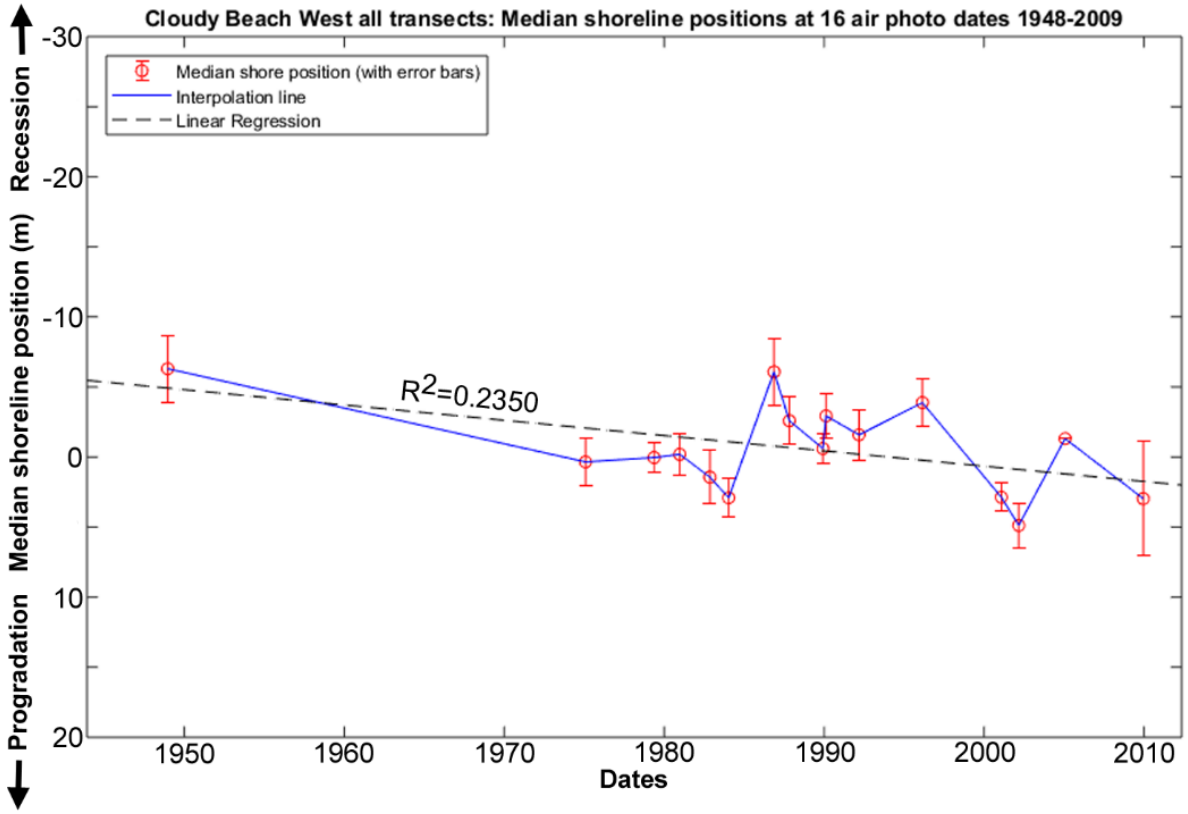

Figure 218: Summary plot of shoreline change history across all transects (as shown on Figure 217) at Cloudy Beach West shoreline for 16 air photo dates from 1948 to 2009, with air photo error bars. A linear fit (regression line) indicates a small overall progradation trend which is slightly more pronounced than the smaller progradation trend at Cloudy Bay Beach East (see Figure 106 & Figure 107) at Section A1.3.1).

Air photo data

This analysis uses the same ortho-photos and digitised shoreline shapefiles as used for Cloudy Beach East. See metadata in Section A1.3.1.

A1.5 *'One-way' (soft rock) shores*

A1.5.1 Barilla Shore (Pittwater, south-eastern Tasmania)

Locality and general description

The Barilla case study area comprises four sites in the upstream (western) part of Pittwater, which is a large tidal re-entrant protected from swell waves behind the Seven Mile Beach sandy barrier at the head of Frederick Henry Bay in south-eastern Tasmania. The permanently open tidal channel entrance to Pittwater is over 10 km eastwards from the Barilla sites and is adjacent Seven Mile Beach (see Figure 219). The sites are about 15 km north-east of the state capital of Hobart.

The backshore areas landwards of the study site shores are mainly low-relief agricultural land cleared of native vegetation. Patches of saltmarsh occur along the shoreline; however, these were deliberately excluded from the study sites which mostly comprise shoreline scarps eroded into cohesive clay 'soft-rock' substrate.

Figure 219: Locality map showing the Barilla case study area within Pittwater, south-eastern Tasmania. Pittwater is a tidal re-entrant sheltered from the swell-wave climate of Frederick Henry Bay behind the Seven Mile Beach barrier. The tidal channel is permanently open. The Coal River discharges into upper Pittwater adjacent the Barilla case study area. The four Barilla study sites are indicated in red. Satellite image dated 2019 © Google Earth.

Geomorphology and process environment

Geomorphic description

The Barilla case study area comprises four stretches of scarped shoreline in the north-western part of Pittwater between Barilla Bay and the discharge point of the Coal River into upper Pittwater (see Figure 219). The four sites are characterised by shoreline erosion scarps ranging from less than one to about six metres high (Figure 221 & Figure 222), which are incised into fluvial and lacustrine semi-lithified sediments ('soft rocks') of Cenozoic (Tertiary or Quaternary) age (Figure 220). These are typically interbedded brown cohesive clays, silty clays, sandy clays, friable sandstones and minor pebble and gravel layers (Forsyth 2002). Slumped blocks of the soft-rock occur sporadically at scarp toes but are probably rapidly broken up and removed by wind-waves. Narrow flat intertidal zones at

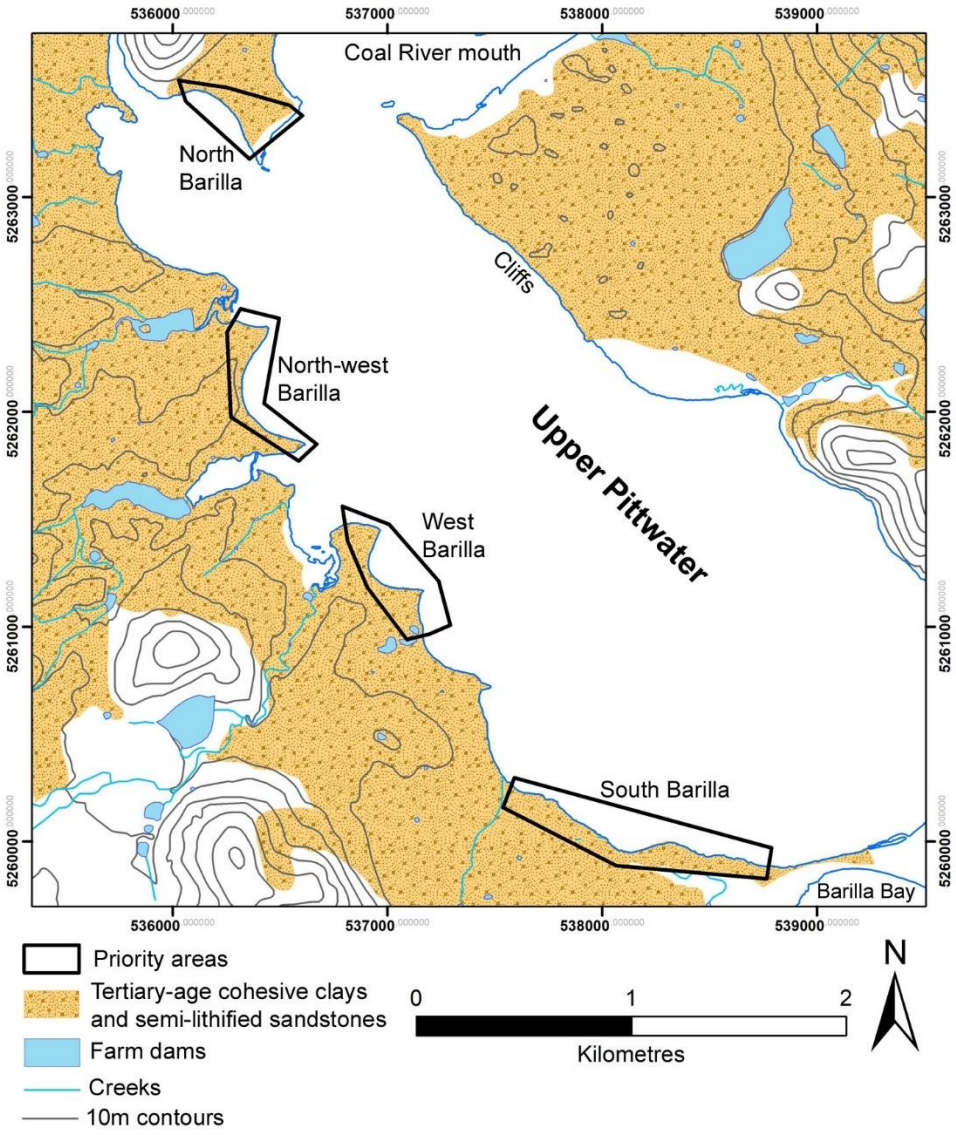

Figure 220: Barilla shore study sites, upper Pittwater, south-east Tasmania, indicating priority areas selected for historical shoreline change analysis. The distribution of Tertiary-age cohesive clays and semi-lithified sandstone is based on the Richmond and Hobart 1:25,000 map sheets of the Geological Survey of Tasmania (Forsyth 2002). Superficial veneers of Quaternary sediments and underlying hard lithified bedrock are not depicted on this map. Co-ordinate system is Map Grid of Australia Zone 55 (GDA1994 datum).

the scarp foot typically comprise exposures of the soft clayey bedrock with thin patchy veneers of sand and/or pebbles winnowed from the eroded bedrock (Figure 221 & Figure 222). Erosion scarps at the South Barilla study site are of mostly freshly incised appearance (Figure 221), whereas those in the study sites further north tend to frequently have a less active appearance characterised by more rounded and vegetated scarp faces with patchy slumps (Figure 222).

There is no tide gauge record available for Pittwater, however Seven Mile Beach has approximate spring and neap tidal ranges of 1.2 and 0.3 m respectively (Short 2006b). Given that the Barilla study site is over 10 km inside the tidal channel entrance of Pittwater, it is assumed that tidal ranges at the study area are smaller and tidal currents relatively weak, however no quantitative data or tidal modelling is available.

The Coal River, which discharges into Pittwater close to the study sites (Figure 219) drains a dominantly cleared catchment with mainly agricultural land uses and a series of dams and weirs

Figure 221: Typical low actively eroding cohesive clay scarp in the South Barilla priority area, with thin patchy veneers of sand winnowed from the soft bedrock partly mantling exposed soft bedrock in the intertidal zone. Neither the planting of rows of trees as shown, nor the deployment of many car tyres along this shore in recent decades, has had any noticeable slowing effect on the erosion of this scarp. Since these attempts to protect the shore were implemented circa 1992 (as indicated by air photos), scarp retreat has continued unabated and in one area has accelerated (Figure 229). Photo: Chris Sharples (2011).

Figure 222: Cohesive clay shore in the northern part of the North-west Barilla study site, with a narrow pebbly intertidal zone. The shoreline and erosion scarps in this area are higher than at South Barilla but less active as is evident in this scene. This study has demonstrated very slow rates of shoreline recession at this site, however some recent scarping and slumping is visible (probably partly triggered by tree collapses but with some wave impacts obvious too). Photo: Chris Sharples (2016).

Swell wave climate

Swell waves penetrate the tidal channel mouth of Pittwater adjacent Seven Mile Beach (Figure 219) but are rapidly attenuated and refracted inside the entrance. There is no effective swell wave activity at the Barilla study area.

Wind (wind wave) climate

The closest long-term wind record is located at Hobart Airport approximately ten kilometres south-east of the Barilla sites (see Figure 219). At least in terms of wind direction, this record appears to be a useful characterisation of the study area winds.

Wind directions

The directional wind record for Hobart Airport from 1958 to 2015 is shown on Figure 223. Both the synoptic and daily maximum wind records show a dominant north-westerly wind direction aligned with upper Pittwater and the general trend of the Coal River valley. This is interpreted as probably the result of the dominantly westerly winds characteristic of the Hobart region being topographically steered south-eastwards at low levels down the Coal River valley towards the airport. If this is correct, then the Barilla study sites (located in the drowned part of the Coal River valley) will be subject to the same dominantly north-westerly winds as the airport record shows. Hence the dominant and also the most energetic wind-waves affecting the study sites will be generated across the long south-easterly fetch of upper Pittwater.

The airport records show a moderate proportion of winds from other directions except that easterly and north-easterly winds are a very small proportion of the record (Figure 223). A strong northerly component of the synoptic wind record is not seen in the daily maximum wind record and is of uncertain origin. No attempt has been made to analyse the Hobart Airport wind record for any long-term wind direction changes.

Wind speeds

At first sight the wind speed data for Hobart Airport appears to show a significant increase in mean synoptic winds speeds since 1990 (Figure 224). However, this increase mainly occurs in two abrupt step-changes, which as noted by Troccoli et al. (2012) are likely to reflect instrument changes rather than a real meteorological change, hence no clear evidence of a significant long-term wind speed change is seen in this data.

Sediment transport and budget

The Barilla site shores are composed of clay-rich semi-lithified soft rock which does not recover its previous form or mass after erosion (see above and Section 2.5.2). Energetic locally generated wind waves driven by extreme wind conditions are the only apparent agent of coastal erosion on the Barilla shores. In this swell-sheltered environment with only very limited wind-wave activity in fair-weather conditions between storms, there is no mechanism available by which sediment could accrete onto the shoreline scarp.

Immediately following any wind-wave erosion of the Barilla shores, the significant proportion of the eroded substrate that is clay- or silt-grade probably remains suspended and is dispersed in the water column by weak tidal, river discharge and wind wave-generated currents. Eventual slow deposition may occur in available (deeper water) accommodation space within Pittwater, or some of the suspended sediments may be dispersed through the permanently open tidal channel to the open coast. The coarser eroded sand and gravel fraction evidently settles out close to the erosion site (see Figure 221 & Figure 222) but as noted there is no mechanism by which this may rebuild the scarped shore, and such residual material is probably redistributed from time to time within the intertidal zone and adjacent shallow waters by wind-wave action.

Given that increasing accommodation space (i.e., water depth) for eroded sediment will become available within Pittwater due to ongoing sea-level rise, and with a proportion of the finer-grade

eroded and suspended sediment probably being lost to the open coast, these conditions effectively constitute a system of active sediment transport away from the eroded shoreline and into an active sediment sink with capacity for increasing sequestration of eroded sediment as sea-level rise continues into the future.

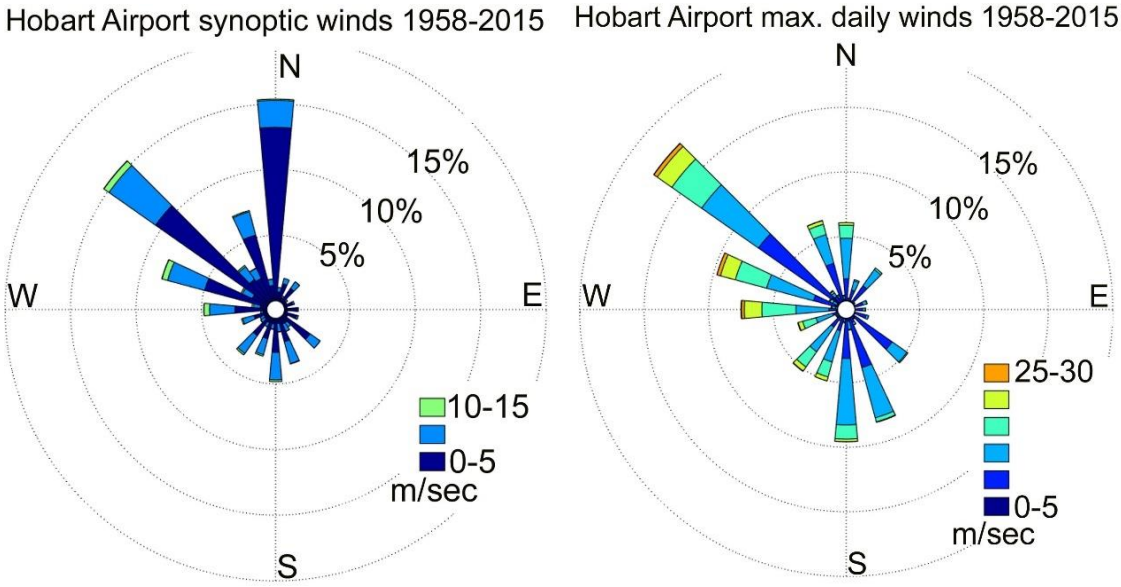

Figure 223: Wind direction data for Hobart Airport 1958-2015. Data plotted by Chris Sharples from original wind records supplied by the Australian Bureau of Meteorology.

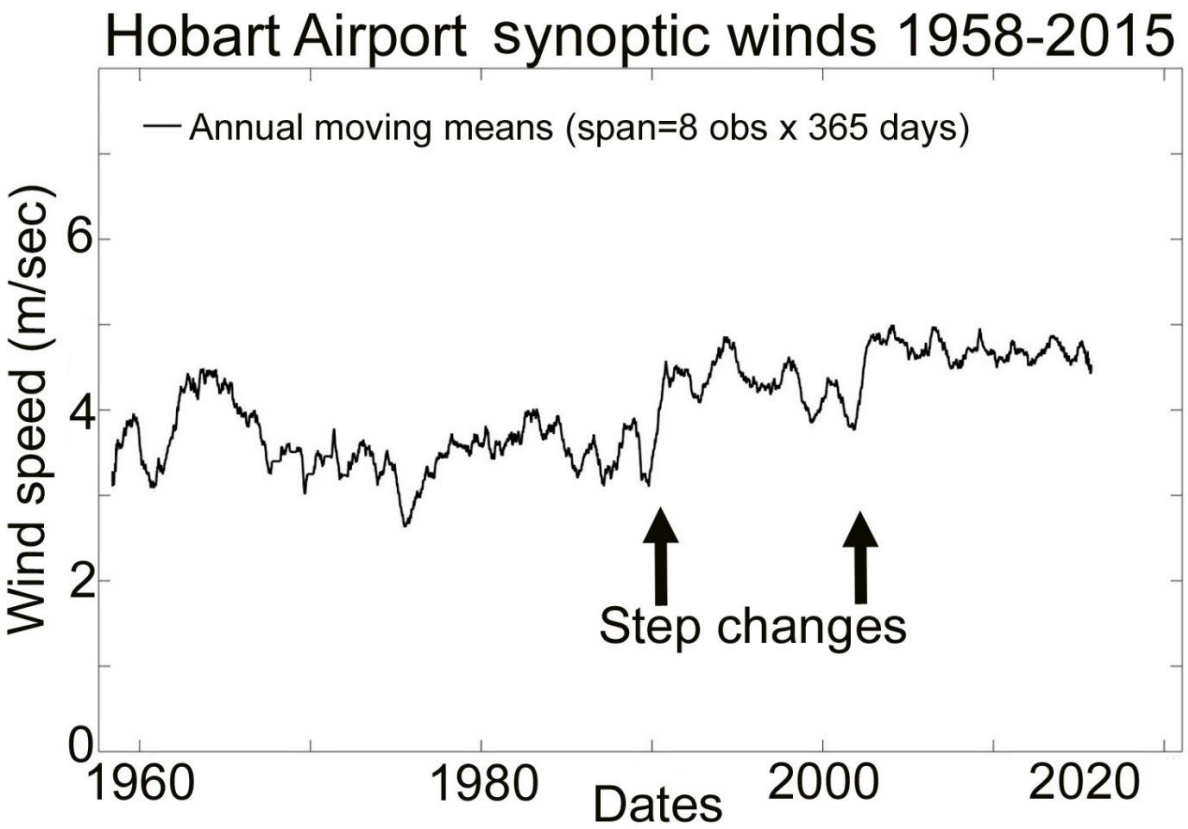

Figure 224: Moving annual means on synoptic wind data for Hobart Airport. A superficial impression of increasing wind speeds over time is largely created by two step-changes in the data (circa 1990 and 2003) which are likely to be artefacts of instrumentation changes. With these step changes allowed for, this data shows no clear trend of increasing wind speeds. Data plotted by Chris Sharples from original wind records supplied by the Australian Bureau of Meteorology.

Sea-level data

The nearest measured sea level data to the Barilla Study area is the Hobart tide gauge record, measured in the lower Derwent River estuary about 15 km south-west of the Barilla sites. Although this site has a long history, the record is compromised by data gaps and datum shifts. The record shown in Figure 225 is the useable portion of the data up to 2004 (data obtained and prepared by Dr John Hunter).

The mean rate of sea-level rise measured from a calculated linear fit to the Hobart tide gauge record is 1.68 mm/yr^{-1} over the period 1962-2004, which is comparable with the global-average rise of 2.0 ± 0.3 mm yr^{-1} over the 1966 – 2009 period (White et al. 2014)[37]. The amplitude of interannual variability in the sea level signal in the Hobart record is ~10 to 100 mm, consistent with sites having little exposure to larger modes of climate variability such as ENSO (White et al. 2014).

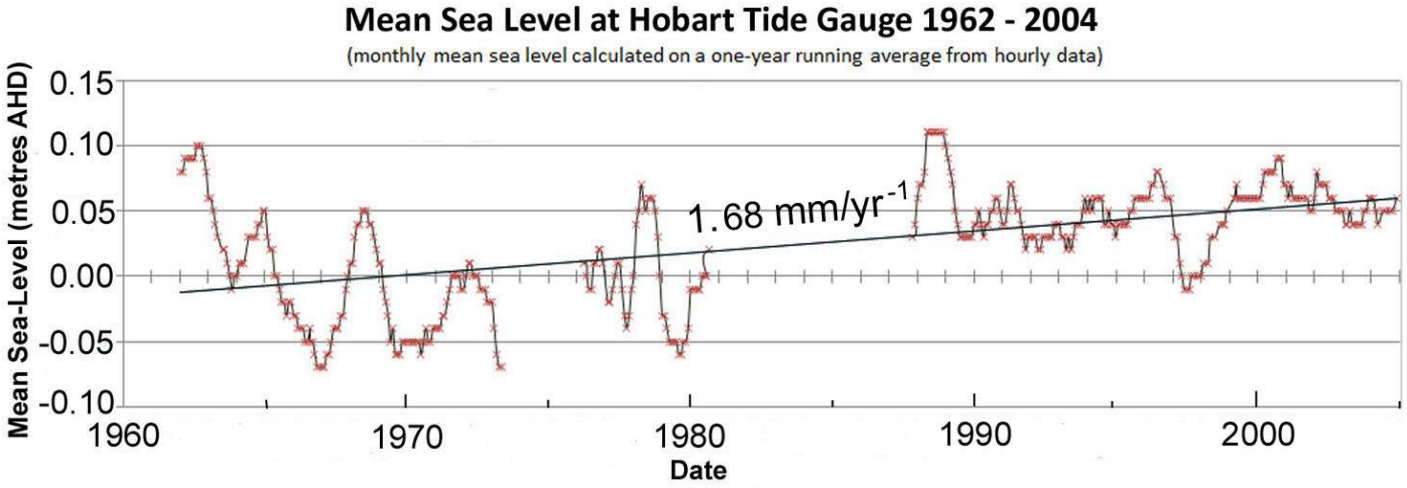

Figure 225: Mean sea level at the Hobart Tide gauge, 1962 – 2004. A simple linear fit is shown plotted to the data. This is the closest tide gauge record to the Barilla case study area. Although the Hobart tide gauge is over a century old, the data plotted here is the only reliable data up to 2004, owing to unsurveyed gauge and datum shifts. Mean sea-level heights shown in metres above the Australian Height Datum (AHD). This data was processed and supplied by Dr John Hunter, from original tide gauge data.

The Barilla sites are close to Hobart and are permanently tidal shores. It is reasonable to infer a similar sea-level history at those sites, albeit probably modulated by tidal hydrodynamics within Pittwater. Some influence on sea level at the Barilla sites is also possible as a result of discharges from the nearby Coal River, although those discharges are limited by the use of irrigation water for intensive agriculture in the catchment and probably have only a limited effect on water levels in Pittwater. However, no data is available to assess this issue with.

Vertical land movement

Current and ongoing geodetic studies of Tasmania have yet to resolve disagreements between GNSS derived estimates of VLM at Burnie and Hobart[38] ranging between 0.0 to -1.0 mm yr^{-1}, and geophysical models indicating subsidence in the range of -0.1 to -0.2 mm yr^{-1} (see details in Chapter 2 Section 2.5.4 above). However, for the purpose of this thesis, there is no evidence suggesting that VLM is a significant signal in Tasmanian relative sea levels. There is no significant anthropogenic extraction of sub-surface fluids or other known processes such as significant seismic activity likely to cause significant VLM at the Barilla case study area.

[37] This is a slightly greater rate than found at Burnie (tide gauge data: 1.4 mm/yr^{-1}: see A1.2.5) and less than Ocean Beach (reconstructed data: 2.13 – 2.21 mm/yr^{-1}: see A1.3.8) over approximately the same periods.
[38] The Hobart GNSS site is located at Mt Pleasant, which is only 2 km west of the west Barilla study site.

Artificial interferences

The backshore areas have been largely cleared of native vegetation for agricultural purposes, beginning approximately 200 years ago. Vegetation clearance appears to have occurred to as close to the waterline as the top of the shoreline scarp in most areas. It is not obvious that this would have affected shoreline erosion rates, however one consequence of the vegetation clearance has been the occurrence of tunnel erosion which has produced small soil pipes that in places are exposed in the shoreline scarp. These may contribute to scarp collapse but are sporadic features and hence probably only a minor influence on net scarp recession rates.

In common with many eastern Australian agricultural landscapes (Prosser & Winchester 1996), historic vegetation clearance in the Coal River catchment resulted in widespread gully erosion which supplied large volumes of silty sediment to the river. The landscape has subsequently largely stabilised, however this episode left a legacy of recent deltaic silt deposits in the Coal River estuary, and probably also resulted in silt filling some of the available sediment accommodation space in the upper Pittwater area near the Barilla sites.

As noted above, the construction of irrigation dams in the Coal River catchment during the twentieth century has resulted in smaller river discharges into Pittwater, which can be expected to have reduced water level variability unrelated to tides and sea-level change in upper Pittwater. This effect is not quantifiable with available information.

There have been numerous un-co-ordinated attempts to halt the erosion and recession of the scarped Barilla shorelines during recent decades. In the South Barilla area where shoreline recession has accelerated since circa 1990, unsuccessful attempts to stabilise the shores by planting trees and placing tyres have been made (Figure 221). Elsewhere, random dumping of rubbish in front of the scarp has occurred in a similarly quixotic effort to stop the erosion.

Oyster farms have been established in Pittwater since the 1980s, consisting of permanent, partly submerged parallel oyster racks which are likely to absorb some wave energy during windy storm conditions. A large cluster of these racks has been established approximately 150 - 250 metres offshore and north of the South Barilla site since circa 1987 (based on air photo evidence). These may have somewhat reduced the impact of north-westerly wind waves on the South Barilla shore.

Air photo analysis

Shoreline position at the Barilla study sites was digitised from ortho-rectified air photos taken at dates from 1946 to 2010. These are listed in Table 71. Due to incomplete air photo coverage at some dates, air photos from 39 dates were available at South Barilla, but only 37, 34 & 28 air photo dates were available at West, North-west and North Barilla, respectively. Nonetheless this time series is one of the most high-frequency air photo records available for any Tasmanian coastal sites since the 1940s.

The shoreline proxy (vegetation line) mapped for this study site is the (typically grassy) top of the ~0.5 to ~6.0 m high shoreline scarp eroded into cohesive clayey Tertiary sediments which comprises the studied shoreline. Four sections of the shoreline were selected for analysis (see Figure 219). Some other sections of shoreline were excluded since the chosen shoreline proxy proved very difficult to delineate and map because of complex slumping and obscuring vegetation. Different shoreline types present in parts - including complex creek mouth shores and saltmarsh shores - have also not been mapped since they are of a different geomorphic type. Bushes and trees overhanging the scarp have been allowed for where the scarp position is still obvious.

A high (~10-15m) soft-rock cliff-line immediately south of Coal River mouth (north-eastwards across Pittwater from the north-west site) was initially investigated as a study area, however the shoreline proxy (cliff-top vegetation line) proved to be problematical. The line was very difficult to identify in some photos due to overhanging tree canopies. Where the cliff top was discernible multi-metre relief

displacement errors which increase away from the photo nadir were commonly too large for the photo to be useful. The photogrammetric processing required to resolve such errors associated with high cliffs was beyond the scope of this project, hence this otherwise-ideal high scarped shoreline was not used in this analysis.

The following describes the shoreline position change results obtained from the four sites constituting the Barilla study area.

South Barilla

The South Barilla site shoreline history was analysed using shorelines digitised from 39 air photo dates from 1946 to 2010, excluding only 2 dates (2nd Jan 1991, 24th Jan 1969) whose air photo record did not cover the south area.

This north-facing mapped shoreline had the lowest (approx. 0.5 – 1.0 m) erosion scarp and consequently was easiest to map because the shoreline proxy – the scarp top vegetation edge - was most distinct due to lack of scarp slumps. The low scarp also resulted in minimal relief displacement error. Mapped scarp sections at other sites on the western shore of upper Pittwater were higher and in some photos the scarp-top/vegetation line was harder to pick owing to slumped and vegetated scarp slopes and larger parallax errors. Hence shoreline position mapping in the South Barilla study site is probably more accurate overall than at other sites, albeit still dependant on the primary error source, namely the accuracy of the ortho-rectification process itself.

A linear fit to the median shoreline positions across all transects at each air photo date (Figure 226) yields a significant recession trend of ~0.13 m/yr over the whole air photo period with a good Pearson correlation co-efficient of R^2=0.8087 (Figure 227). Over the whole air photo period, the shoreline recession distance exceeds most air photo position error bars hence is a real trend.

Although a linear recession trend provides the best fit to the overall recession trend on most transects, inspection of shoreline histories along individual transects identifies four adjoining transects (59071 – 59074) that show a significant acceleration of retreat rate compared to all other transects since circa 1990 (Figure 226). Shoreline histories and piecewise linear fits pre- and post-1990 for only these four transects confirm a doubling of recession rates since circa 1990 (Figure 226, Figure 228 & Figure 229). These four transects are located on the part of the South Barilla shoreline most directly exposed to the dominant north-westerly local wind direction in the Coal Valley.

West Barilla

The West Barilla site was covered by digitised shorelines from 37 air photo dates from 1946 to 2010, excluding 3 dates (12th Feb 1957, 4th Nov. 1969, 8th Feb 1984) whose air photo record did not cover the site, and 1 date (27th Feb. 1991) whose record covered only two of the 10 transects at that site, and yielded highly anomalous shoreline positions on those. The mapped vegetation line (scarp top) was difficult to pick in some photos but comparison between consecutive photos ensured the same feature was mapped in all cases and was clearly identifiable as the scarp top in many of the photos.

Plots of the West Barilla study site shoreline changes over the 1946 to 2010 period (Figure 230 & Figure 231) suggest a small trend towards recession (~0.03 m/yr), however this has a low Pearson correlation co-efficient (R^2 =0.2060) and is of similar or smaller scale than the air photo errors at most dates. Hence this shoreline has exhibited negligible clearly identifiable change over the air photo period, albeit a very slight overall recession tendency is suggested.

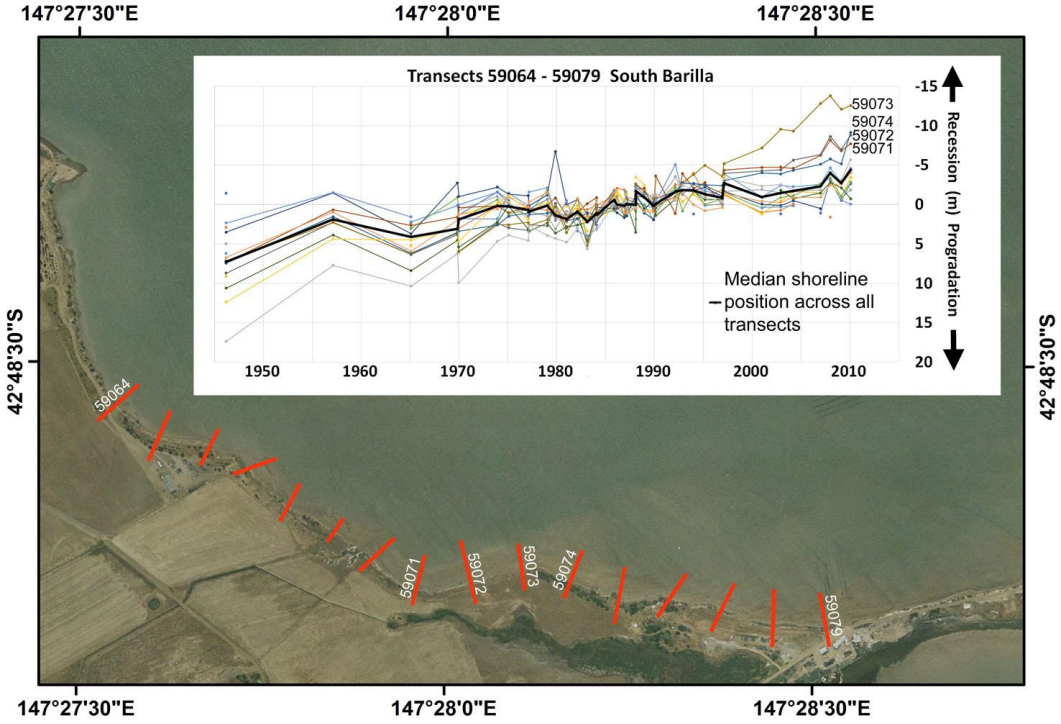

Figure 226: Shoreline position changes along all individual transects for South Barilla shoreline, for 39 air photo dates from 1946 to 2010. The transects used are 100m – spaced red lines on the air photo. A general linear recession trend is mostly coherent across all transects, however since circa 1990 four transects (59071-74, labelled) have exhibited notably accelerated rates of recession compared to the others. See also summary plot Figure 227 below. The background image is the 2010 air photo (© DPIPWE).

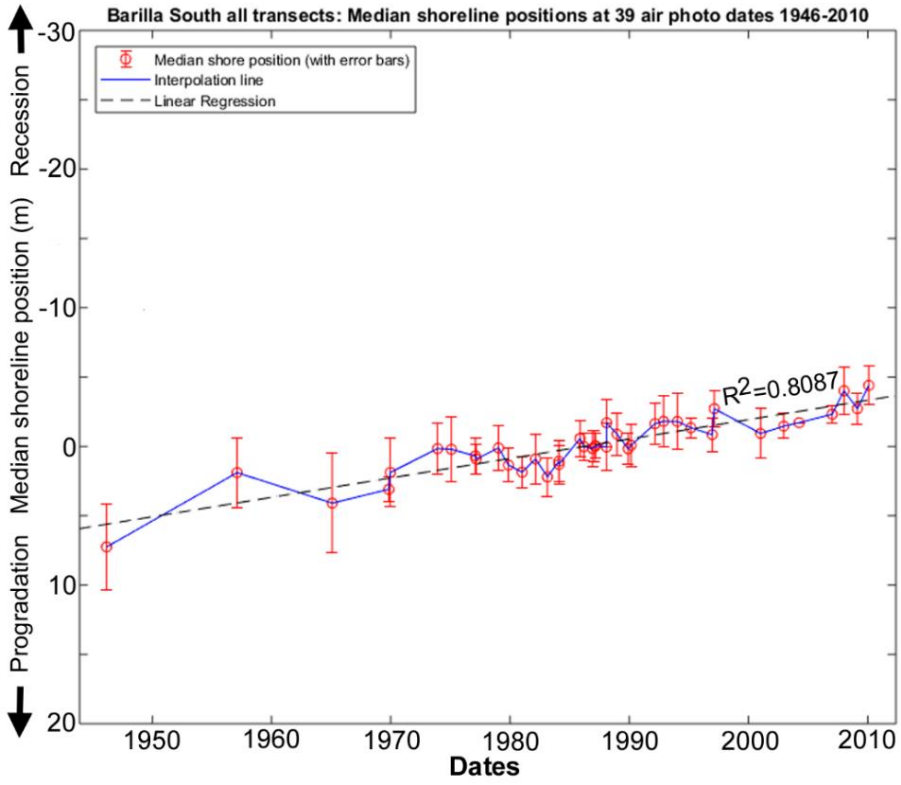

Figure 227: Summary plot of shoreline change history across all transects (as shown on Figure 226) at the South Barilla site for 39 air photo dates from 1946 to 2010. Median shoreline position at each air photo date is shown with air photo error bars and linear fit to all data shown with correlation co-efficient.

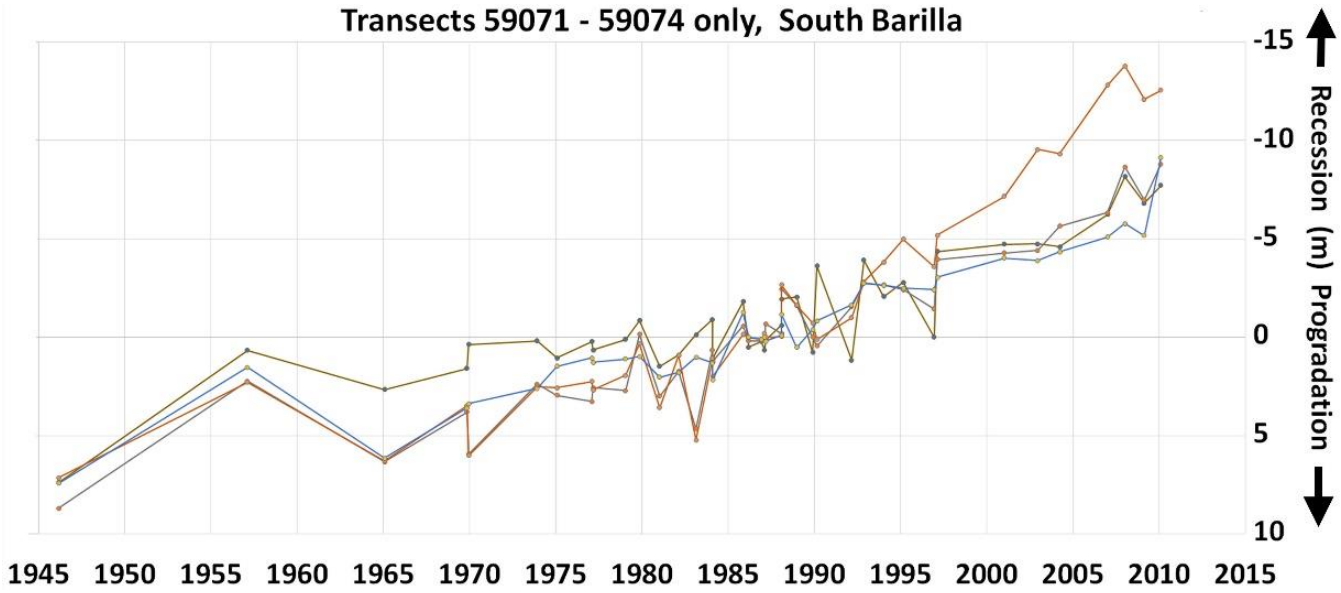

Figure 228: Shoreline position changes along only the cluster of transects 59071-74, which inspection of Figure 226 shows have a faster recession rate and more pronounced acceleration of recession since circa 1990 than is seen on other transects in the South Barilla study site.

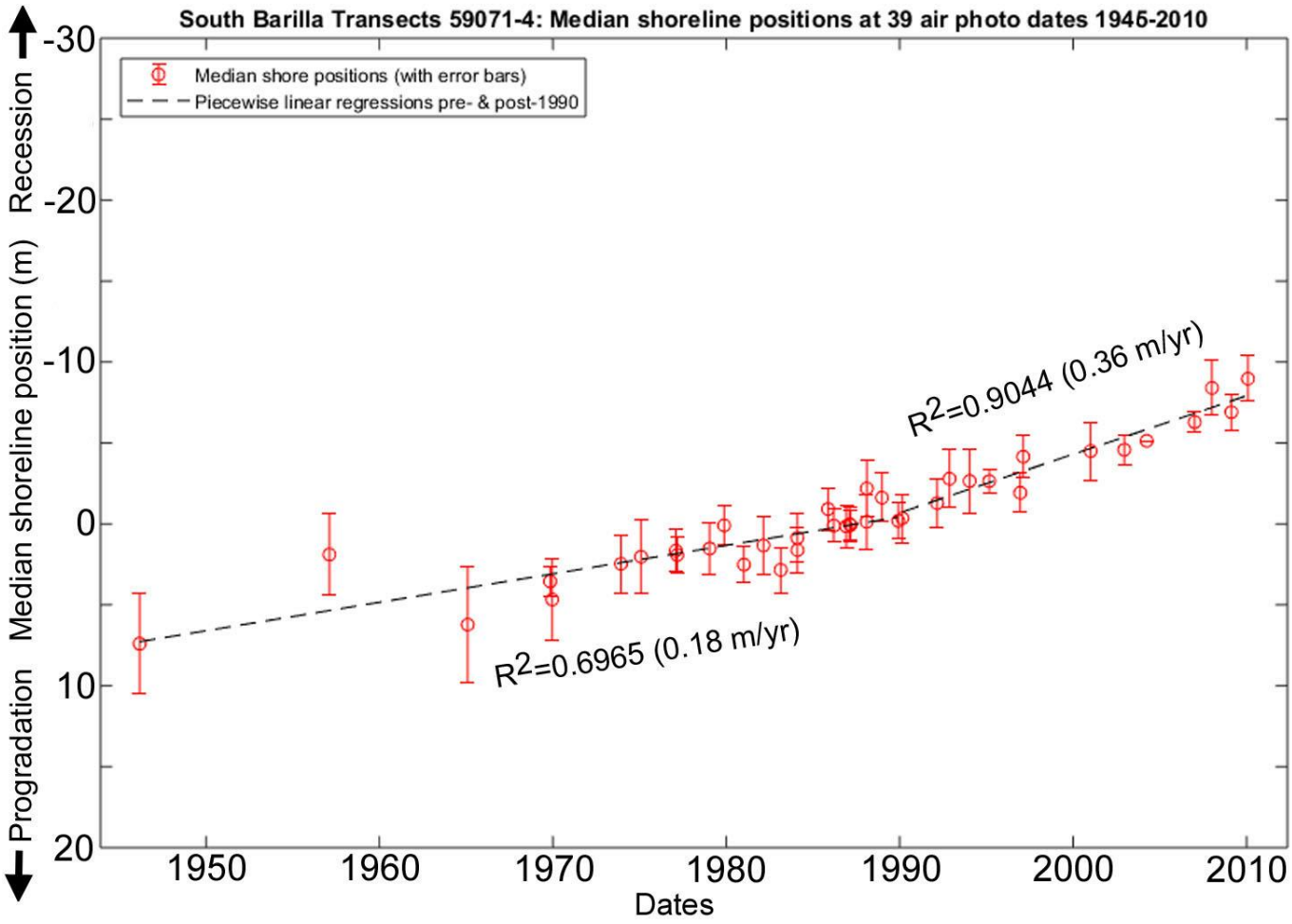

Figure 229: Summary plot of shoreline change history across the four transects 59071-74 (as shown on Figure 228) at South Barilla shoreline for 39 air photo dates from 1946 to 2010, with air photo error bars and piecewise linear fits pre- and post-1990.

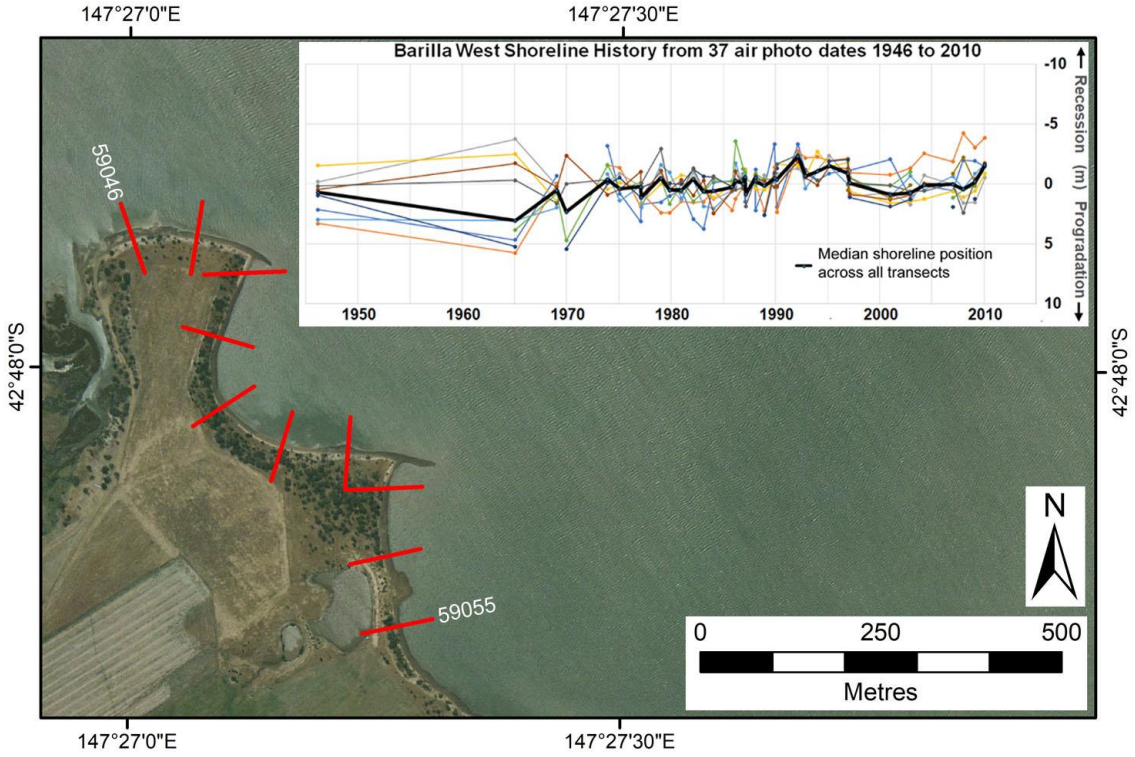

Figure 230: Shoreline position changes along all individual transects for West Barilla shoreline, for 37 air photo dates from 1946 to 2010. The transects used are 100m – spaced red lines on the air photo. See also summary plot Figure 231 below. The background image is the 2010 air photo (© DPIPWE).

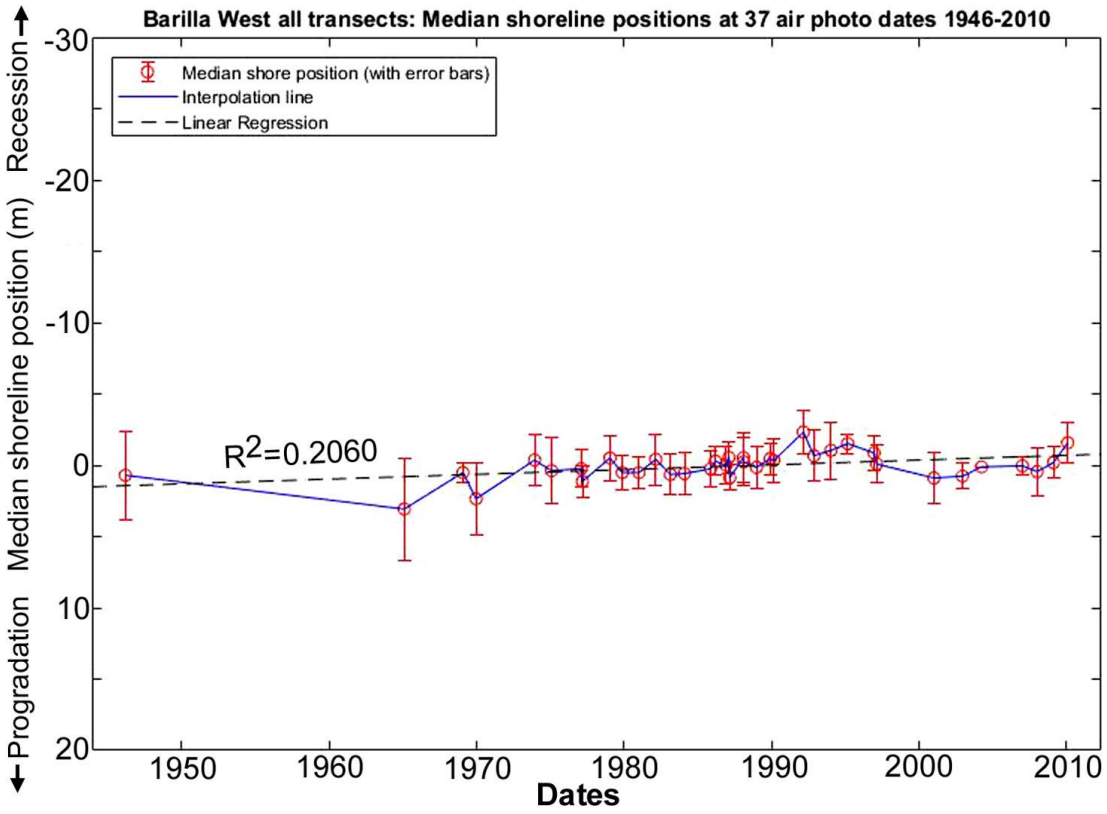

Figure 231: Summary plot of shoreline change history across all transects at the West Barilla shoreline for 37 air photo dates from 1946 to 2010, with air photo error bars and linear fit with correlation co-efficient.

North-west Barilla

The North-west Barilla area is covered by shorelines digitised for 34 air photo dates from 1946 to 2010, excluding 6 dates (12th Feb 1957, 4th Nov. 1969, 8th Feb 1984, 4th Mar 1987, 14th Dec 2002 & 4th Jan 2007) whose air photo record did not cover the site, and 1 date (2nd Feb 1965) which yielded an anomalously seawards shoreline compared to all others from an ortho photo known to have residual distortion in parts (see Table 71). The mapped vegetation line (scarp top) was difficult to pick in some photos but comparison between consecutive photos ensured the same feature was mapped in all cases and was clearly identifiable as the scarp top in many of the photos.

Plots of the North-West Barilla study area shoreline changes over the 1946 to 2010 period (Figure 232 & Figure 233) show a small but non-significant recession trend (~0.025 m/yr, R^2=0.0676) whose scale is smaller than the air photo position error bars at nearly all air photo dates. Hence this shoreline has exhibited negligible identifiable change over the air photo period and is best characterised as stable over that period.

North Barilla

The North Barilla area is covered by shorelines digitised for 28 air photo dates from 1946 to 2010, excluding 11 dates (12th Feb. 1957, 24th Jan. 1969, 4th Nov. 1969, 8th Feb. 1984, 4th Mar 1987, 4th Feb. 1988, 22nd Dec. 1988, 27th Feb. 1992, 1st Mar, 1995, 14th Dec., 2002 and 4th Jan. 2007) whose air photo record did not cover the site, and two dates (2nd Feb 1965 & 18th Dec 1969) which yielded anomalous shoreline positions compared to all others from air photos with large residual errors in some areas. The mapped vegetation line (mostly an erosion scarp top) was generally easy to identify and digitise in this area.

Plots of the North Barilla area shoreline history over the period 1946 to 2010 (Figure 234 & Figure 235) yield a very similar result to those for the North-west area, namely a small and non-significant recession trend (~0.025 m/yr, R^2=0.0737) whose magnitude is smaller than the air photo position error bars at nearly all air photo dates. This shoreline has exhibited no unequivocal change over the air photo period and is best characterised as stable.

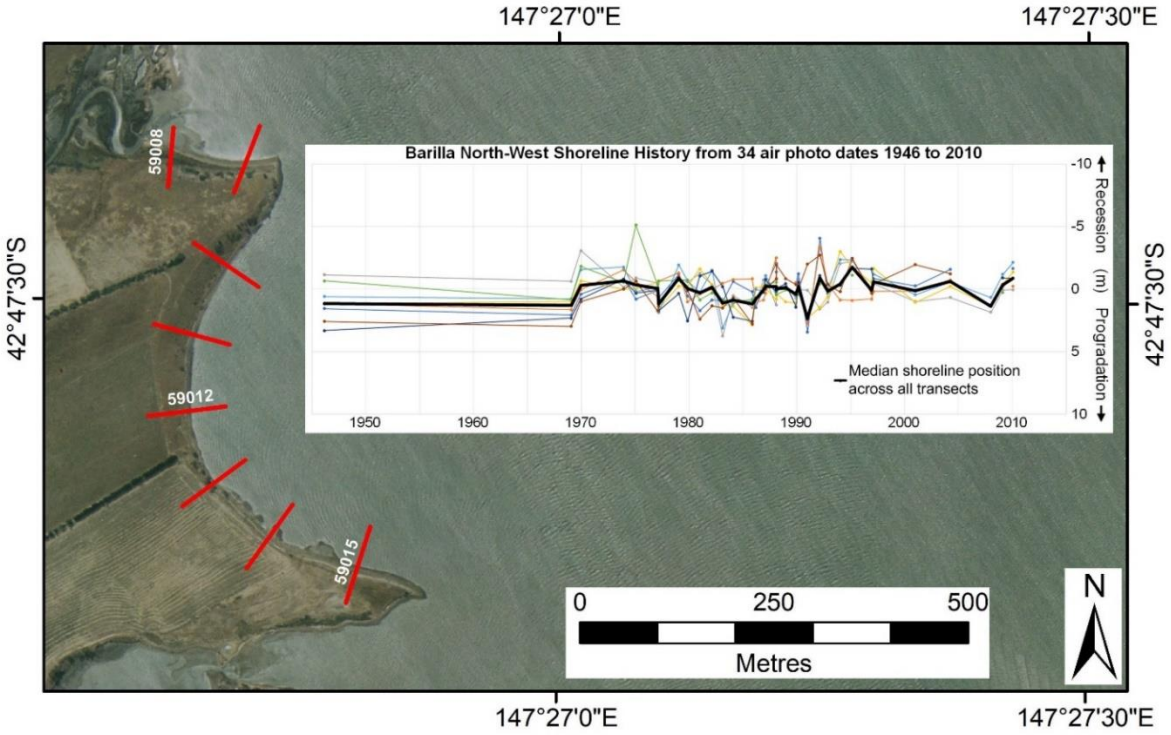

Figure 232: Shoreline position changes along all individual transects for Barilla North-West shoreline, for 34 air photo dates from 1946 to 2010. The transects used are 100m – spaced red lines on the air photo. See also summary plot Figure 233 below. The background image is the 2010 air photo (© DPIPWE).

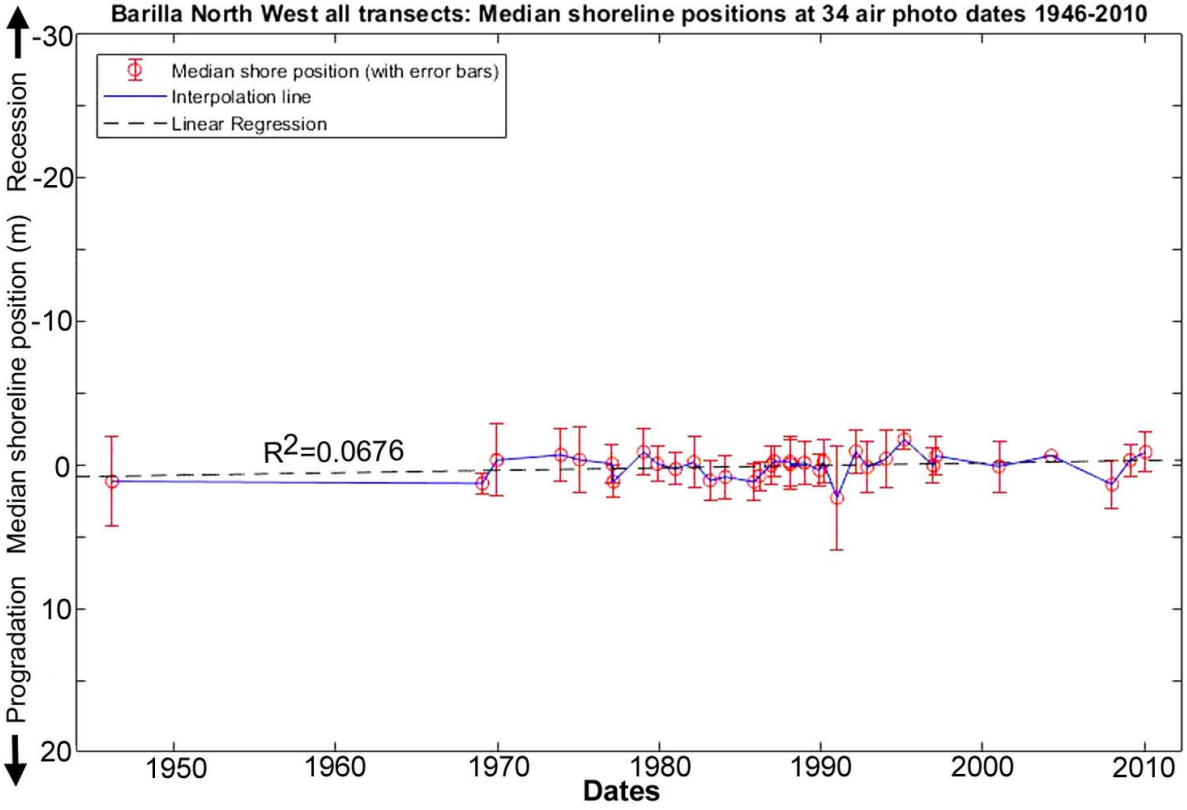

Figure 233: Summary plot of shoreline change history across all transects (as shown on Figure 232) at Barilla North-West shoreline for 34 air photo dates from 1946 to 2010, with air photo error bars and linear fit with correlation co-efficient.

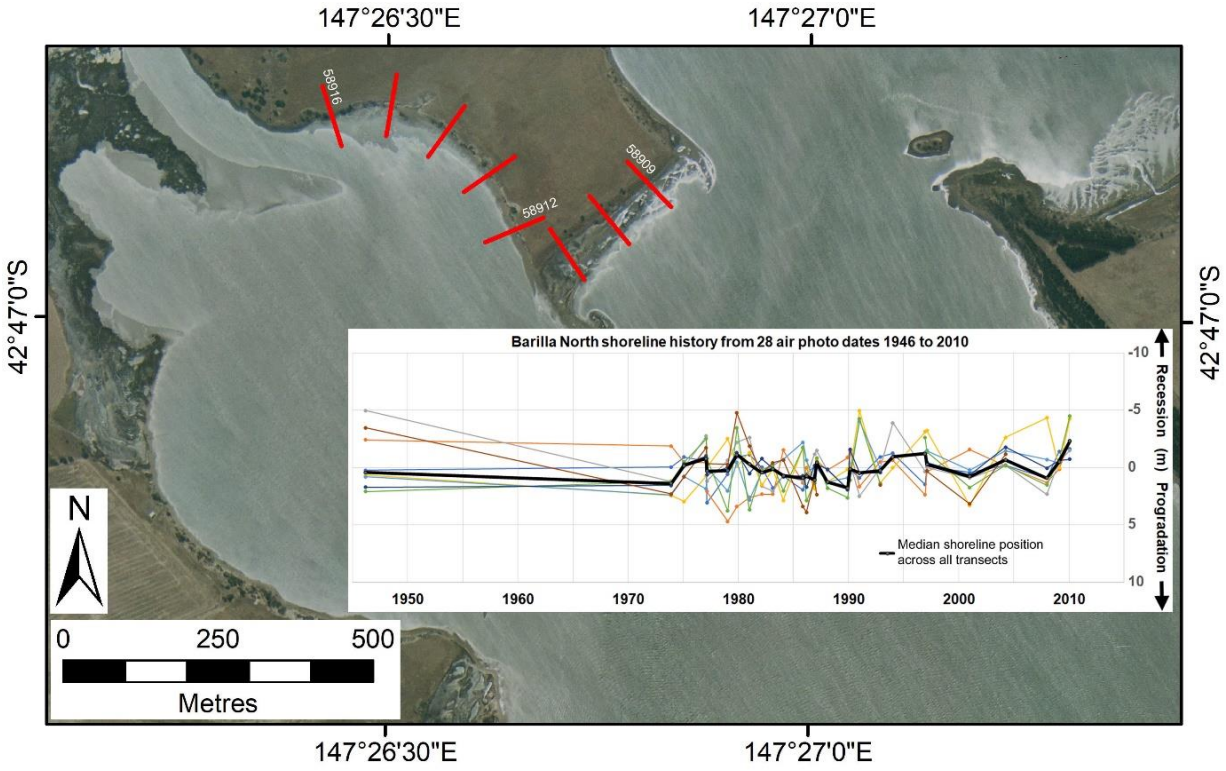

Figure 234: Shoreline position changes along all individual transects for Barilla North shoreline, for 28 air photo dates from 1946 to 2010. The transects used are 100m – spaced red lines on the air photo. See also summary plot Figure 235 below. The background image is the 2010 air photo (© DPIPWE).

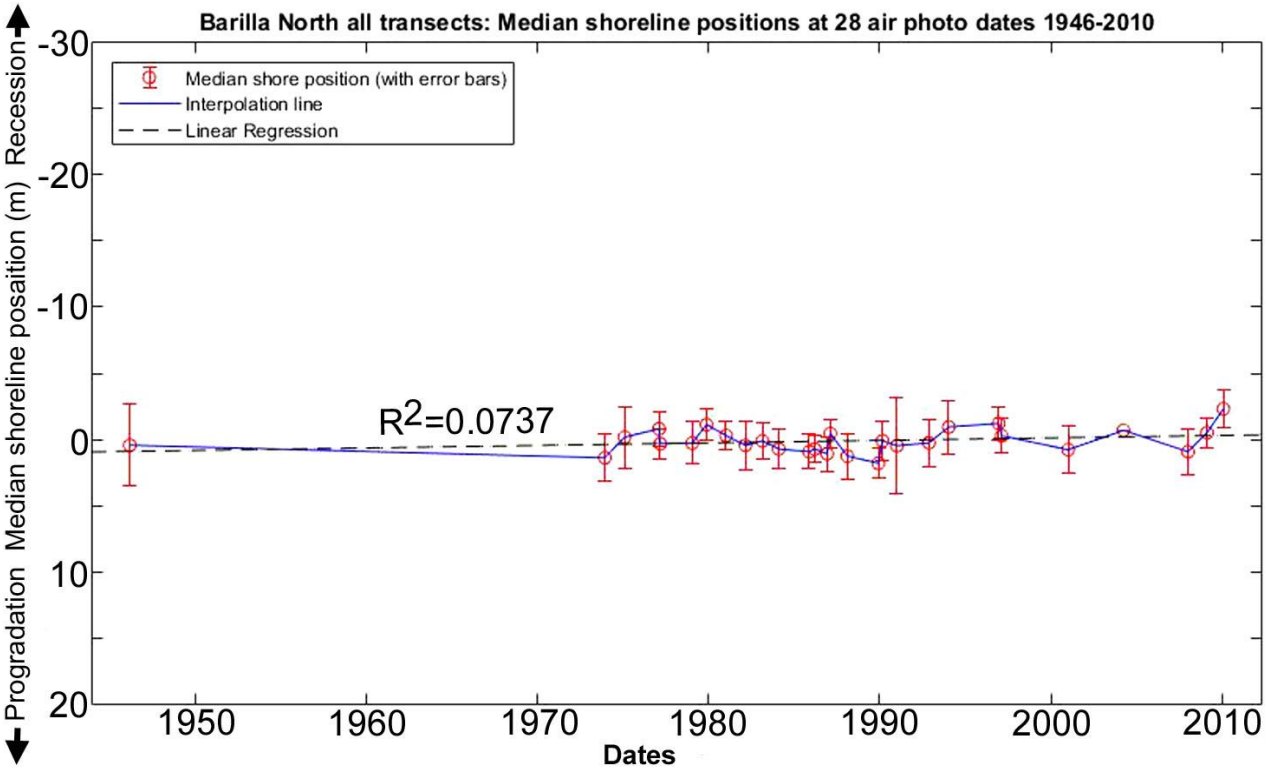

Figure 235: Summary plot of shoreline change history across all transects (as shown on Figure 234) at Barilla North shoreline for 28 air photo dates from 1946 to 2010, with air photo error bars and linear fit with correlation co-efficient.

Summary shoreline behaviour history and characterisation

The North, North-west and West Barilla sites all show similar histories suggestive of a very slow shoreline recession over the air photo period of 1946 to 2010. However linear fits to these histories yield poor correlation co-efficients, and the apparent linear recession trends are mostly of smaller scale than the air photo error margins. Hence shoreline change at these three sites has been negligible over the air photo period, albeit a very slow recession trend is suggested by the air photo histories and by the scarped (albeit somewhat rounded and vegetated) nature of the shorelines at each site.

In contrast, the South Barilla site shows a significant shoreline recession trend which is larger than the air photo error margins over the whole air photo period, with a fresh active scarp retreating at a linear rate of 0.13 m per year over the period. A portion of this site comprising four adjacent transects has shown a significant acceleration in its rate of recession around 1990, with a doubling of the linear recession rate from 0.18 m/yr before 1990 to 0.36 m/yr after 1990.

It is noteworthy that the three sites showing negligible change all have shorter wind-wave fetches with respect to the dominant north-westerly wind direction across upper Pittwater than does South Barilla, and also have less direct exposure to the dominant wind waves, with the dominant wind blowing offshore at North Barilla, and parallel to the shore at West and North-west Barilla .

In contrast, the South Barilla shore which has shown significant recession since 1946 is more directly exposed to the dominant wind-wave direction across the longest available fetch in upper Pittwater. Moreover, the four transects within that site which have shown a significant acceleration of shoreline recession after 1990 are located on the part of the South Barilla shoreline most directly exposed to the dominant wind (and thus wind-wave) direction.

Soft-rock shorelines such as the cohesive clay shores represented by the four Barilla case study sites do not recover after erosion events and will normally recede at some rate (dependant on storm wave exposure) even in the absence of changing drivers of erosion such as rising sea-levels or increasing wind speeds. Thus, neither the very slow to negligible shoreline recession at the West, North-west and North Barilla sites, nor the somewhat faster but still linear recession of most of the South Barilla shoreline provide evidence of any response to such changing drivers.

However, the accelerated recession of the most exposed portion of the South Barilla shore cannot be explained in the same way, but rather implies some changing condition or driver.

Air Photo Data Tables

The following tables provide details of the air photos used, the resulting ortho-photos produced, and the shapefiles representing the shoreline position that were digitised from the ortho-photos.

Table 71: Original air photos and ortho-rectified air photos produced for Barilla Bay.

Photo Date	**Original DPIPWE air photos (film-frame) / Ortho-photo name**	**Final image resolution (original scan resolution if downsized) / pixel size of final ortho-photo**	**Original photo scale**	**Mean measured feature position error for ortho-photo (± metres)** [No. of measured feature position reference points]	**Comments**
4th Mar 1946	29-9786 29-9787 29-9866 / *Barilla_Mar1946a_MGA55.tif/tfw;* *Barilla_Mar1946b_MGA55.tif/tfw;* *Barilla_Mar1946c_MGA55.tif/tfw*	600 dpi / 0.75 m pixel size	1:15,840	3.1 m [11]	Ortho-rectified by Chris Sharples
12th Feb 1957	326-83 / *Barilla_Feb1957_MGA55.tif/tfw*	1500 (2039) dpi / 0.33 m pixel size	1:14,000	2.5 m [3]	Ortho-rectified by Chris Sharples South Barilla only (small but high-exposure area)
2nd Feb 1965	433-162 433-220 / *Barilla_Feb1965a_MGA55.tif/tfw;* *Barilla_Feb1965b_MGA55.tif/tfw*	2039 dpi 1500 (2039) dpi / 0.44 m pixel size 0.60 m pixel size	1:31,680	3.6 m [18]	Ortho-rectified by Chris Sharples; Both photos have good accuracy in parts, large errors in other parts (original photo distorted??)
24th Jan 1969	511-182 / *Barilla_Jan1969_MGA55.tif/tfw*	2039 dpi / 0.2 m pixel size	1:14,400	0.7 m [2]	Ortho-rectified by Chris Sharples
4th Nov 1969	534-138 / *Barilla_Nov1969_MGA55.tif/tfw*	2039 dpi / 0.23 m pixel size	1:13,464	0.9 m [3] (good accuracy near study shoreline, error margin excludes one very anomalous 9.5 m error well south at aerodrome)	Ortho-rectified by Chris Sharples South Barilla – small area only
18th Dec 1969	538-218 / *Barilla_Dec1969b_MGA55.tif/tfw*	2039 dpi / 0.43 m pixel size	1:34,770	3.3 m [3] (includes one very anomalous error of 8.9m)	Ortho-rectified by Chris Sharples North Barilla only
18th Dec 1969	542-56 / *Barilla_Dec1969a_MGA55.tif/tfw*	~1000 dpi / 0.75 m pixel size	1:34,770	2.5 m [4]	Ortho-rectified by Sarah Harries (2011). Cropped version: south and west areas only. (refer to 534-138 for topographic information) Original scan obtained 2017 from DPIPWE corrupted; could not ortho-rectify after multiple attempts (NE area apparently distorted?).
5th Dec 1973	633-11 / *Barilla_Dec1973_MGA55.tif/tfw*	2039 dpi / 0.55 m pixel size	1:31,000	1.8 m [11]	Ortho-rectified by Chris Sharples

31st Jan 1975	664-208 / *Barilla_Jan1975_ MGA55.tif/tfw*	2039 dpi / 0.62 m pixel size	1:40,000	2.3 m [10]	Ortho-rectified by Chris Sharples
4th Feb 1977	708-14 / *Barilla_Feb1977_ MGA55.tif/tfw.*	2039 dpi / 0.37 m pixel size	1:30,000	1.3 m [11]	Ortho-rectified by Chris Sharples
4th Mar 1977	717-87 / *Barilla_Mar1977_ MGA55.tif/tfw.*	2039 dpi / 0.40 m pixel size	1:30,000	1.1 m [11]	Ortho-rectified by Chris Sharples
15th Jan 1979	775-160 / *Barilla_Jan1979_ MGA55.tif/tfw*	2039 dpi / 0.52 m pixel size	1:40,000	1.6 m [13]	Ortho-rectified by Chris Sharples
16th Nov 1979	799-94 / *Barilla_Nov1979_ MGA55.tif/tfw.*	2039 dpi / 0.57 m pixel size	1:42,000	1.2 m [13]	Ortho-rectified by Chris Sharples
6th Jan 1981	852-25 852-56 / *Barilla_Jan1981a_ MGA55.tif/tfw; Barilla_Jan1981b_ MGA55.tif/tfw*	2039 dpi / 0.20 m pixel size	1:15,000	1.1 m [13]	Ortho-rectified by Chris Sharples
22nd Feb 1982	912-142 / *Barilla_Feb1982_ MGA55.tif/tfw*	2039 dpi / 0.56 m pixel size	1:42,000	1.8 m [12]	Ortho-rectified by Chris Sharples
19th Feb 1983	958-68 / *Barilla_Feb1983_ MGA55.tif/tfw*	2039 dpi / 0.55 m pixel size	1:42,000	1.4 m [12]	Ortho-rectified by Chris Sharples
8th Feb 1984	983-177 983-178 / *Barilla_8thFeb1984a_MGA55.tif/tfw; Barilla_8thFeb1984b_MGA55.tif/tfw*	2039 dpi / 0.07 m pixel size	1:5,000	1.4 m [3]	Ortho-rectified by Chris Sharples Part only of area, higher resolution and effectively same date as full 1:20,000 coverage below.
5th Feb 1984; 11th Feb 1984	983-48; 986-16 / *Barilla_Feb1984a_MGA55.tif/tfw; Barilla_Feb1984b_MGA55.tif/tfw*	2039 dpi; 1000 dpi (2039 dpi). / 0.27 m pixel size; 0.53 m pixel size	1:20,000	1.5 m [15]	Ortho-rectified by Chris Sharples North part of area; South part of area (Different films but effectively one run)
13th Nov 1985	1044-91 / *Barilla_Nov1985_ MGA55.tif/tfw*	2039 dpi / 0.56 m pixel size	1:42,000	1.3 m [13]	Ortho-rectified by Chris Sharples Whole area
13th Mar 1986	1067-95 1067-142 / *Barilla_Mar1986a_MGA55.tif/tfw; Barilla_Mar1986b_MGA55.tif/tfw.*	2039 dpi / 0.20 m pixel size	1:15,000	1.0 m [12]	Ortho-rectified by Chris Sharples
2nd Dec 1986	1080-58 / *Barilla_Dec1986_ MGA55.tif/tfw*	2039 dpi / 0.41 m pixel size	1:31,000	1.3 m [13]	Ortho-rectified by Chris Sharples Whole area
9th Feb 1987	1087-8 1087-9 / *Barilla_Feb1987a_MGA55.tif/tfw; Barilla_Feb1987b_MGA55.tif/tfw*	1000 dpi (2039 dpi) / 0.45 m pixel size	1:15,000	1.1 m [13]	Ortho-rectified by Chris Sharples
4th Mar 1987	1088-63 1088-66	2039 dpi /	1:8,000	0.9 m [2]	South area only Ortho-rectified by Chris Sharples

	/ *Barilla_Mar1987a _MGA55.tif/tfw*; *Barilla_Mar1987b _MGA55.tif/tfw*	0.14 m pixel size			
4th Feb 1988	1105-131 1105-146 / *Barilla_4thFeb198 8a_MGA55.tif/tfw; Barilla_4thFeb198 8b_MGA55.tif/tfw*	2039 dpi / 0.16 m pixel size	1:12,500	1.7 m [10]	Ortho-rectified by Chris Sharples
8th Feb 1988	1120-24 / *Barilla_8thFeb198 8_MGA55.tif/tfw*	2039 dpi / 0.3 m pixel size	1:23,000	1.7 m [12]	Ortho-rectified by Chris Sharples
22nd Dec 1988	1125-66 1125-67 / *Barilla_Dec1988a _MGA55.tif/tfw; Barilla_Dec1988b _MGA55.tif/tfw*	2039 dpi / 0.16 m pixel size	1:12,500	1.5 m [10]	Ortho-rectified by Chris Sharples
1st Dec 1989	1142-21 1142-22 1142-23 1142-26 / *Barilla_Dec1989a _MGA55.tif/tfw; Barilla_Dec1989b _MGA55.tif/tfw; Barilla_Dec1989c _MGA55.tif/tfw; Barilla_Dec1989d _MGA55.tif/tfw*	2039 dpi / 0.16 m pixel size	1:12,500	1.1 m [16]	Ortho-rectified by Chris Sharples
25th Feb 1990	1154-67 / *Barilla_Feb1990_ MGA55.tif/tfw*	2039 dpi / 0.56 m pixel size	1:42,000	1.5 m [13]	Ortho-rectified by Chris Sharples
2nd Jan 1991	1162-189 / *Barilla_Jan1991_ MGA55.tif/tfw*	2039 dpi / 0.3 m pixel size	1:24,000	3.6 m [5]	Ortho-rectified by Chris Sharples
19th & 27th Feb 1992	1186-73 1187-171 / *Barilla_Feb1992a _MGA55.tif/tfw; Barilla_Feb1992b _MGA55.tif/tfw*	1000 dpi (2039 dpi) / 0.36 m pixel size	1;12,500	1.5 m [9]	Ortho-rectified by Chris Sharples
15th Nov 1992	1193-40 1193-76 / *Barilla_Nov1992a _MGA55.tif/tfw; Barilla_Nov1992b _MGA55.tif/tfw*	1000 dpi (2039 dpi) / 0.7 m pixel size	1:25,000	1.8 m [14]	Ortho-rectified by Chris Sharples
12th Jan 1994	1214-23 / *Barilla_Jan1994_ MGA55.tif/tfw*	2039 dpi / 0.3 m pixel size	1:24,000	2.0 m [13]	Ortho-rectified by Chris Sharples
1st Mar 1995	1233-51 / *Barilla_Mar1995c_ MGA55.tif/tfw*	1000 dpi (2039 dpi) / 0.3 m pixel size	1:12,500	0.7 m [4]	Ortho-rectified by Chris Sharples South area
11th Mar 1995	1234-195 1234-196 / *Barilla_Mar1995a _MGA55.tif/tfw; Barilla_Mar1995b _MGA55.tif/tfw*	1000 dpi (2039 dpi) / 0.3 m pixel size	1:12,500	1.6 m [13]	Ortho-rectified by Chris Sharples
13th Dec 1996	1256-100 /	1000 dpi (2039 dpi)	1:24,000	1.2 m [11]	Ortho-rectified by Chris Sharples

	Barilla_Dec1996_ MGA55.tif/tfw	/ 0.6 m pixel size			
15th Feb 1997	1272-102 1272-103 1272-127 / *Barilla_Feb1997a _MGA55.tif/tfw; Barilla_Feb1997b _MGA55.tif/tfw; Barilla_Feb1997c_ MGA55.tif/tfw*	1000 dpi (2039 dpi) / 0.3 m pixel size	1:12,500	1.3 m [13]	Ortho-rectified by Chris Sharples
4th Jan 2001	1342-71 / *Barilla_Jan2001_ MGA55.ecw*	2039 dpi / 0.5 m pixel size	1:24,000	1.8 m [13] (quoted absolute accuracy ±2.5m)	Ortho-rectified by DPIPWE Original DPIPWE ortho file: 1342_071_op.ecw
14th Dec 2002	1362-126 1362-248 / *Barilla_Dec2002a _MGA55.tif/tfw; Barilla_Dec2002b _MGA55.tif/tfw*	1000 dpi (2039 dpi) / 0.26 m pixel size	1:10,000	0.9 m [7]	Ortho-rectified by Chris Sharples
28th Mar 2004	1383-30 / *Barilla_Mar2004_ MGA55.ecw*	2039 dpi / 0.5 m pixel size	1:24,000	0.0 m [N/A] (quoted absolute accuracy ±2.5m)	REFERENCE IMAGE (zero relative feature position error by convention) Ortho-rectified by DPIPWE Original DPIPWE ortho file: 1383_030_op.ecw
4th Jan 2007	1419-34 1419-56 / *Barilla_Jan2007a_ MGA55.tif/tfw; Barilla_Jan2007b_ MGA55.tif/tfw*	1000 dpi (2039 dpi) / 0.26 m pixel size	1:10,000	0.6 m [7]	Ortho-rectified by Chris Sharples
3rd Jan 2008	1428-39 / *Barilla_Jan2008_ MGA55.ecw*	2039 dpi / 0.5 m pixel size	1:24,000	1.7 m [13] (quoted absolute accuracy ±15m)	Ortho-rectified by DPIPWE Original DPIPWE ortho file: 1428_039_op.ecw
14th Feb 2009	1437-11 / *Barilla_Feb2009_ MGA55.tif/tfw*	1000dpi (2039 dpi) / 0.6 m pixel size	1:24,000	1.1 m [13]	Ortho-rectified by Chris Sharples
30th Jan 2010	1443-240 / *Barilla_Jan2010_ MGA55.ecw*	2039 dpi / 0.5 m pixel size	1:42,000	1.4 m [13] (quoted absolute accuracy ±15m)	Ortho-rectified by DPIPWE Original DPIPWE ortho file: 1443_240_op.ecw

Table 72: Digitised shoreline shapefiles produced for Barilla Bay (using ortho-photos listed in Table 71 above).

Date of air photo(s)	Shapefile	Shoreline digitised by	Comments
4th Mar 1946	Barilla_MGA55_19460304.shp	Chris Sharples (2019)	Low resolution, moderate contrast. Erosion scarp top = vegetation line mapped at change in tone, but details not clear.
12th Feb 1957	Barilla_MGA55_19570212.shp	Chris Sharples (2019)	Moderate resolution, low contrast. Erosion scarp

			top = vegetation line mapped at change in tone, but details not clear.
2nd Feb 1965	Barilla_MGA55_19650202.shp	Chris Sharples (2019)	Low resolution, moderate contrast. Erosion scarp top = vegetation line mapped at change in tone, but details not clear.
24th Jan 1969	Barilla_MGA55_19690124.shp	Chris Sharples (2019)	East-facing western shores only. Good resolution and contrast. Erosion scarp top = vegetation line mapped
4th Nov 1969	Barilla_MGA55_19691104.shp	Chris Sharples (2019)	Southern (north-facing) shore only. Moderate resolution, good contrast. Erosion scarp top = vegetation line mapped.
18th Dec 1969	Barilla_MGA55_19691218.shp	Chris Sharples (2019).	Coarse resolution, moderate contrast. Erosion scarp top = vegetation line mapped at change in tone, but details not clear
5th Dec 1973	Barilla_MGA55_19731205.shp	Chris Sharples (2019)	Moderate resolution, good contrast. Erosion scarp top = vegetation line mapped at change in tone.
31st Jan 1975	Barilla_MGA55_19750131.shp	Chris Sharples (2019)	Coarse resolution, poor contrast. Erosion scarp top = vegetation line mapped at change in tone, but details not clear
4th Feb 1977	Barilla_MGA55_19770204.shp	Chris Sharples (2019)	Moderate resolution and contrast. Erosion scarp top = vegetation line mapped at change in tone, but details not clear.
4th Mar 1977	Barilla_MGA55_19770304.shp	Chris Sharples (2019)	Moderate resolution and contrast (better quality than Feb 1977 photo). Erosion scarp top = vegetation line mapped at change in tone, details clear in places, not all.
15th Jan 1979	Barilla_MGA55_19790115.shp	Chris Sharples (2019)	Low resolution, poor contrast. Erosion scarp top = vegetation line mapped at change in tone, but details not clear. Reasonable shoreline obtained.
16th Nov 1979	Barilla_MGA55_19791116.shp	Chris Sharples (2019)	Low resolution, poor contrast. Erosion scarp top = vegetation line mapped at change in tone, but details not clear.
6th Jan 1981	Barilla_MGA55_19810106.shp	Chris Sharples (2019)	Good photo: moderate resolution and contrast. Erosion scarp top = vegetation line mapped at change in tone. Scarp

			top clear in many sections – good shoreline mapped.
22nd Feb 1982	Barilla_MGA55_19820222.shp	Chris Sharples (2019)	Moderate resolution, poor contrast. Erosion scarp top = vegetation line mapped at change in tone, mappable but only just discernible in parts.
19th Feb 1983	Barilla_MGA55_19830219.shp	Chris Sharples (2019)	Low resolution, poor contrast. Erosion scarp top = vegetation line mapped at change in tone, but details not clear.
8th Feb 1984	Barilla_MGA55_19840208.shp	Chris Sharples (2019)	High resolution and contrast. Erosion scarp top = vegetation line mapped, clearly defined. GOOD ACCURATE SHORELINE
5th & 11th Feb 1984	Barilla_MGA55_19840205.shp	Chris Sharples (2019)	Coarse resolution, poor contrast. Erosion scarp top = vegetation line mapped at change in tone, but details not clear
13th Nov 1985	Barilla_MGA55_19851113.shp	Chris Sharples (2019)	Coarse resolution, moderate contrast. Erosion scarp top = vegetation line mapped at change in tone, but details not clear
13th Mar 1986	Barilla_MGA55_19860313.shp	Chris Sharples (2019)	Moderate resolution & contrast. Erosion scarp top = vegetation line mapped.
2nd Dec 1986	Barilla_MGA55_19861202.shp	Chris Sharples (2019)	Moderate resolution & contrast. Erosion scarp top = vegetation line mapped. Mostly poorly defined but mappable
9th Feb 1987	Barilla_MGA55_19870209.shp	Chris Sharples (2019)	Coarse resolution, moderate contrast. Erosion scarp top = vegetation line mapped. Mostly poorly defined but mappable.
4th Mar 1987	Barilla_MGA55_19870304.shp	Chris Sharples (2019)	Moderate resolution, mostly poor contrast. Erosion scarp top = vegetation line mapped. Mostly poorly defined but mappable.
4th Feb 1988	Barilla_MGA55_19880204.shp	Chris Sharples (2019)	Good resolution and moderate contrast. Erosion scarp top = vegetation line mapped. Well-defined in S area, less so on east shores of Pittwater.
8th Feb 1988	Barilla_MGA55_19880208.shp	Chris Sharples (2019)	Moderate resolution, poor contrast. Erosion scarp top = vegetation

			line mapped where clearly definable.
22nd Dec 1988	Barilla_MGA55_19881222.shp	Chris Sharples (2019)	Moderate contrast and resolution. Erosion scarp top = vegetation line mapped where clearly definable.
1st Dec 1989	Barilla_MGA55_19891201.shp	Chris Sharples (2019)	Poor to moderate resolution and contrast. Erosion scarp top = vegetation line mapped where clearly definable.
25th Feb 1990	Barilla_MGA55_19900225.shp	Chris Sharples (2019)	Poor to moderate resolution and contrast. Erosion scarp top = vegetation line mapped where clearly definable.
2nd Jan 1991	Barilla_MGA55_19910102.shp	Chris Sharples (2019)	Moderate resolution, poor to moderate contrast. Veg. line vague and difficult to pick in parts. Most accurate where recent shore scarp visible. Includes northern area only.
19th & 27th Feb 1992	Barilla_MGA55_19920227.shp	Chris Sharples (2019)	Moderate resolution and contrast, some shadowing allowed for on scarped shorelines.
15th Nov 1992	Barilla_MGA55_19921115.shp	Chris Sharples (2019)	Coarse resolution, moderate contrast. NE cliff-top mapped (that & some other sections of shoreline scarp well defined by shadowing)
12th Jan 1994	Barilla_MGA55_19940112.shp	Chris Sharples (2018)	Moderate resolution, contrast moderate only but some scarped sections well defined by shadows.; NE cliff-top very hard to pick, not mapped.
1st & 11th Mar 1995	Barilla_MGA55_19950300.shp	Chris Sharples (2018)	Used frames from 1st and 11th March 1995. Good resolution and contrast. NE cliff-top well defined and mappable.
13th Dec 1996	Barilla_MGA55_19961213.shp	Chris Sharples (2018)	Coarse resolution, good contrast, some erosion scarps clearly defined by shadows but veg line hard to define in parts.

15th Feb 1997	Barilla_MGA55_19970215.shp	Chris Sharples (2018)	Good resolution, medium contrast – some veg. lines a bit vague.
4th Jan 2001	Barilla_MGA55_20010104.shp	Chris Sharples (2018)	Coarse resolution, medium contrast - some veg. lines vague.
14th Dec 2002	Barilla_MGA55_20021214.shp	Chris Sharples (2018)	Good resolution and contrast. Erosion scarp very clearly delineated by shadowing in parts.
28th Mar 2004	Barilla_MGA55_20040328.shp	Chris Sharples (2018)	Good resolution & contrast.
4th Jan 2007	Barilla_MGA55_20070104.shp	Chris Sharples (2018)	Fine resolution, good contrast
3rd Jan 2008	Barilla_MGA55_20080103.shp	Chris Sharples (2018)	Coarse resolution, OK contrast, shoreline (veg. line) well-defined in parts, poorly-defined in others.
14th Feb 2009	Barilla_MGA55_20090214.shp	Chris Sharples (2018)	Coarse resolution, good contrast, shoreline (veg. line) reasonably well-defined.
30th Jan 2010	Barilla_MGA55_20100130.shp	Chris Sharples (2018)	Good resolution & contrast.

A1.5.2 Rokeby Beach (Ralphs Bay, south-eastern Tasmania)

Locality and general description

West Rokeby Beach and Central-East Rokeby Beach are treated as two sites because of very different historic behaviour.

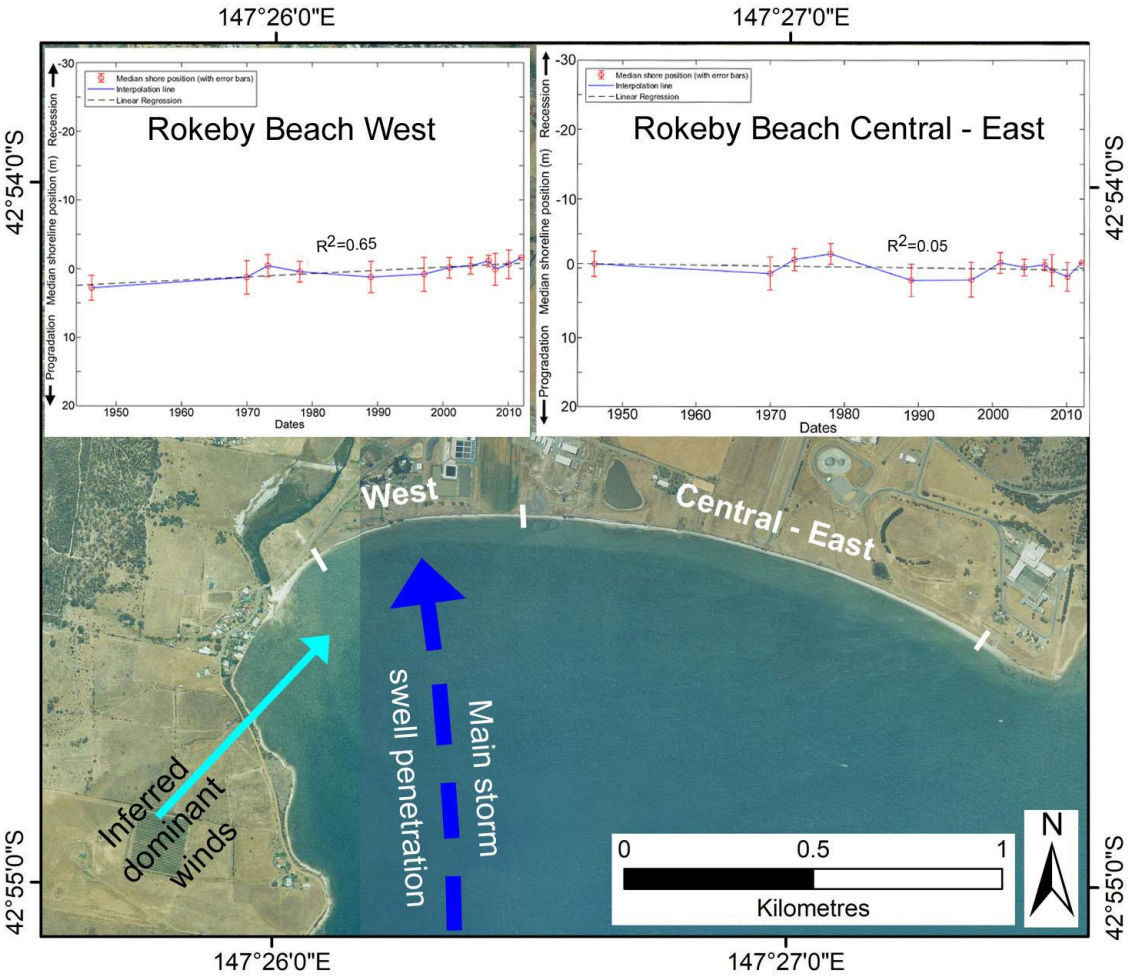

Figure 236: Rokeby Beach, south-east Tasmania. Shoreline history plots for the West and Central-East parts of Rokeby Beach are the median shoreline positions across all transects in each section at 12 air photo dates from 1946 to 2012. A linear regression fit has been plotted for each beach section. Inferred dominant wind-wave and swell directions shown. Air photo taken Jan. 2001 (© DPIPWE).

Figure 237: View west at the western end of Rokeby Beach (between transects 14873 and 124874; see Figure 241) showing narrow residual pebbly sand beach backed by the actively receding cohesive sandy/pebbly clay scarp ('soft rock'). Undermined trees and fences are typical evidence of active recession. Photo by Chris Sharples 1st May 2010.

Figure 238: View east near east end of Rokeby Beach showing less active erosion scarp in pebbly cohesive clay soft rock. Patches of establishing vegetation and more rounded-over scarps in the middle to eastern sections of the beach suggest less active erosion than at the western end. Photo by Chris Sharples 13th June 2011.

Figure 239: Storm swell waves attacking the western end of Rokeby Beach. This site normally receives only very refracted and attenuated swell waves through the narrow Ralphs Bay entrance and is mostly exposed to small short-fetch local wind waves. However large swell storms can penetrate Ralphs Bay with enough power to erode the western end of Rokeby Beach as shown here but are normally more attenuated at the eastern end of the beach (see also Figure 236). Photo by Chris Sharples 27th September 2009

Swell wave climate

Rokeby Beach is at northern end of Ralphs Bay. Swell refracted northwards up the Derwent estuary refracts into the Ralphs Bay entrance which is the Droughty Point – South Arm gap to the south of Rokeby Beach. Under normal conditions the swell is very attenuated and essentially negligible by the time it reaches Rokeby Beach. However, under storm swell conditions energetic storm swell waves may penetrate through narrow window at the Ralphs Bay entrance to focus narrowly on the west end of Rokeby Beach (as seen in Figure 236 & Figure 239) after refracting along the east coast of Droughty Point

Wind (wind wave) climate

No local wind records, however inferred that wind is similar to that over whole Hobart-lower Derwent estuary region (Figure 240): Dominant (prevailing) winds and wind-waves westerly / south-westerly.

- West Rokeby Beach (actively eroding) has moderate exposure over very short fetch (see Figure 236).

- Central-East Rokeby Beach has longer fetches but still quite short comparted to fetch needed to cause shoreline recession acceleration at Barilla.

Thus wind-waves not a strong agent of erosion – over longest fetches scarp shows inactive erosion and no change over 70 years; most active erosion is over shortest wind-wave fetches, suggesting wind waves are not the relevant agent of erosion (more likely storm swells).

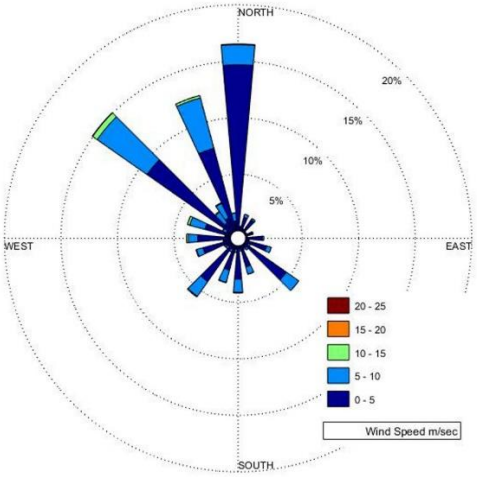

Figure 240: Synoptic wind rose for Hobart City (Ellerslie Road) Bureau of Meteorology weather station. The weather station is situated in the deep but broad valley of the lower Derwent River, hence the dominant northerly to north-westerly winds are inferred to be mainly topographically steered down the Derwent Valley at low levels. By comparison with other wind records for south-eastern Tasmania, the south-westerly (westerly to southerly) winds in this record are inferred to be the dominant regional winds and likely dominant at Rokeby Beach. The figure uses all synoptic wind data for 1893 to 2015, plotted by Chris Sharples using data supplied by the Australian Bureau of Meteorology.

Air photo analysis

Mapped scarp top = vegetation line. BUT:

Rokeby Beach is unusual amongst the shorelines studied for this project in the height (approximately 4 metres) of its erosion scarp. A significant source of shoreline position error for this site was encountered owing to relief displacement errors that caused the apparent position of the high erosion scarp top to shift by up to several metres depending on the camera position (photo centre point) relative to the scarp position. Since the scarp is oriented west-to-east, the most accurate scarp positions are obtained where the scarp position close to the centre of the photo in the north-south direction[39].

There is also considerable variation amongst air photos in the clarity or definition of the scarp top. If distinct shadowing from the north was present, this line was usually well-defined, however on some photos a combination of poor photo resolution and weak shadowing made some parts of the scarp top difficult to pick

The following three criteria were used to select air photos suitable for shoreline history analysis at Rokeby Beach (see Table 73):

Scarp position in photo: within central third of air photo in north-south direction.

Scarp top definition: clearly defined, usually by good shadowing band/or good resolution (pixel size).

Error margin: Less than ±3 metres (less than ±4m limit applied to most sites, given more difficult issues).

Based on these criteria, three ortho-photos and their derived digitised shorelines were not used, namely the 1957, 1977 and Feb. 2007 shorelines (see Table 73).

[39] Note that several other potential study sites for this project were rejected because of even greater relief displacement difficulties associated with even higher cliffed scarp shorelines (Tertiary-age sandstone and cohesive clay shores at D'Entrecasteaux Channel and Pittwater).

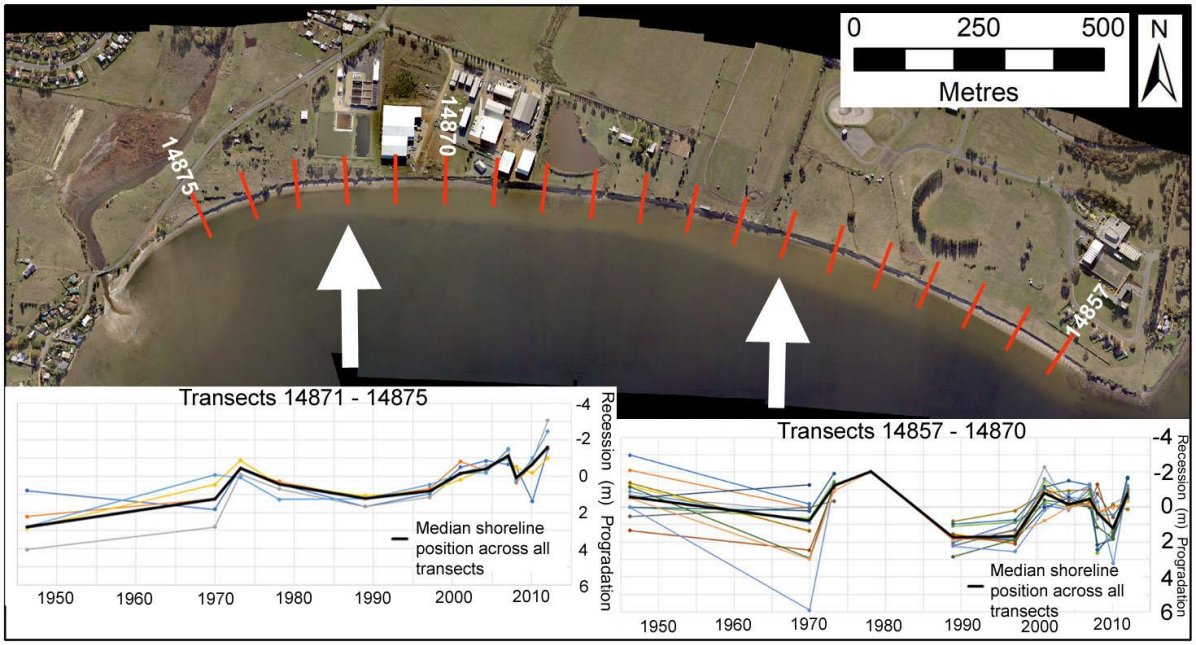

Figure 241: Shoreline position changes along individual transects for Rokeby Beach, at 12 air photo dates from 1946 to 2012. The transects used are 100m – spaced red lines on the air photo. Two notably different transect groups are plotted, a western group showing a small but significant recession trend since 1946 and the remaining (central-east) transects showing no significant change (see also summary plots Figure 242 & Figure 244. Shorter term variability in both plots is likely due to relief displacement and scarp slumping. The background image is the 2012 air photo (© Matt Dell).

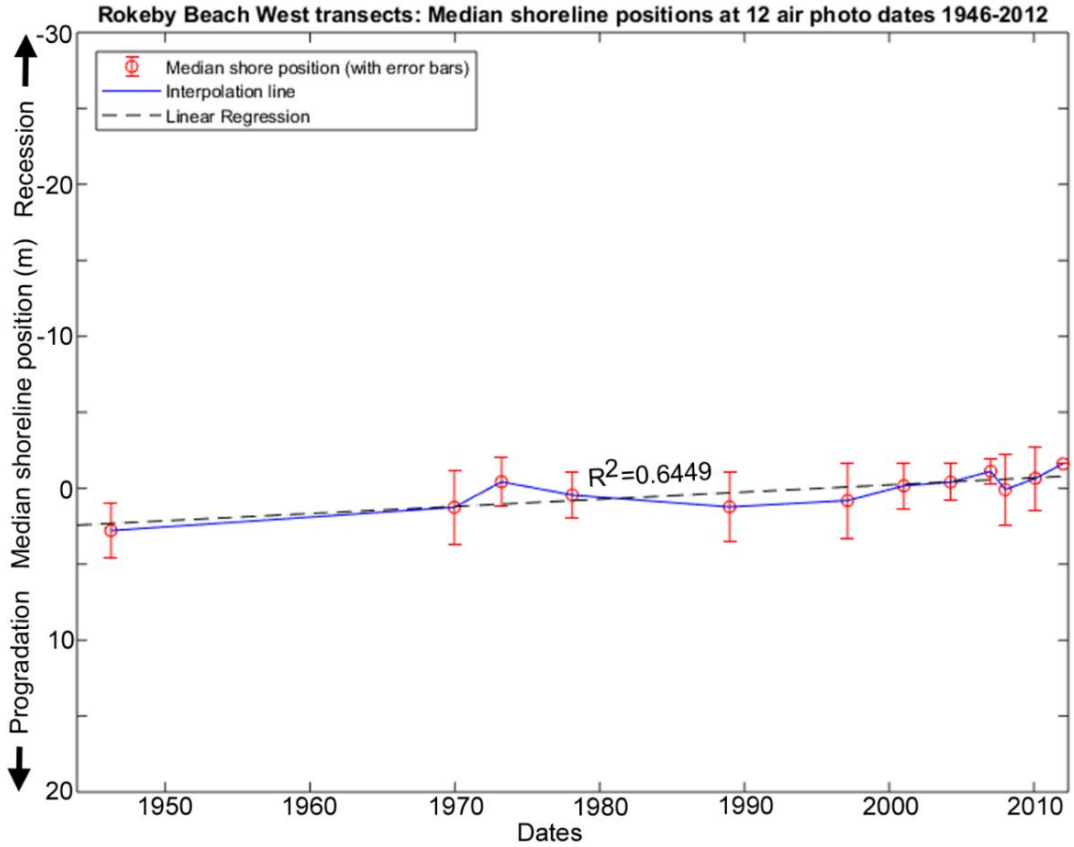

Figure 242: Summary plot of shoreline change history across the West Rokeby Beach site (the five westernmost transects as shown on Figure 241) at 12 air photo dates from 1946 to 2012, with air photo error bars and interpolation lines. A small but significant linear recession trend is evident.

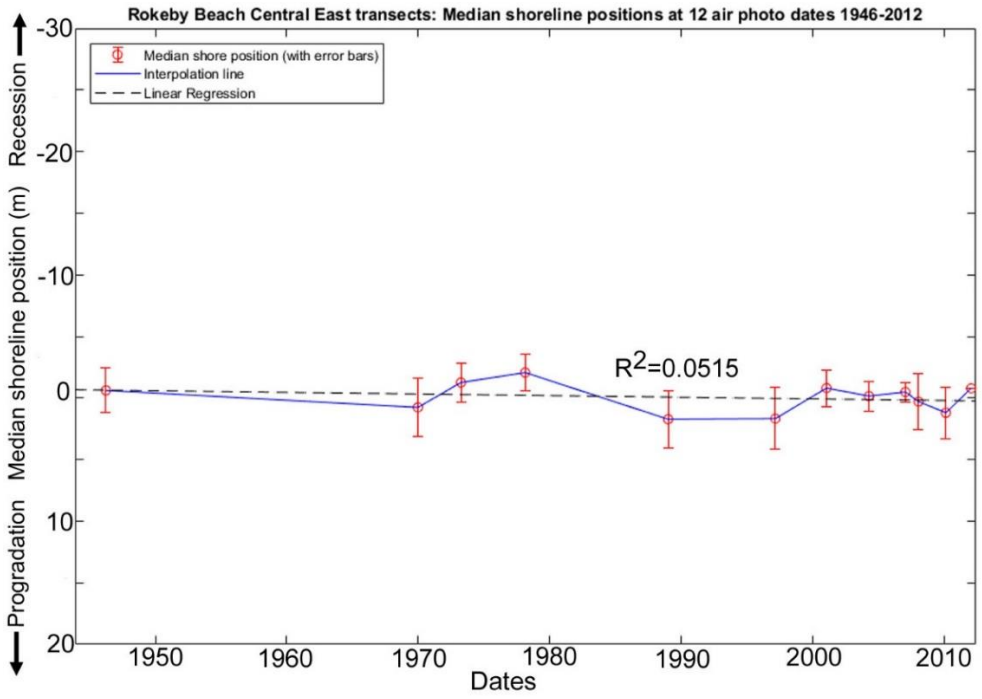

Figure 243: Summary plot of shoreline change history across the Central-East Rokeby Beach site (the central to eastern transects as shown on Figure 241) at Rokeby Beach at 12 air photo dates from 1946 to 2012, with air photo error bars and interpolation lines (bottom version). A very small and non-significant progradation trend falls within most air photo error bars and is probably not real. Allowing for minor slumping and air photo relief displacement, a stable shoreline position over the whole air photo period is the most likely interpretation of this plot.

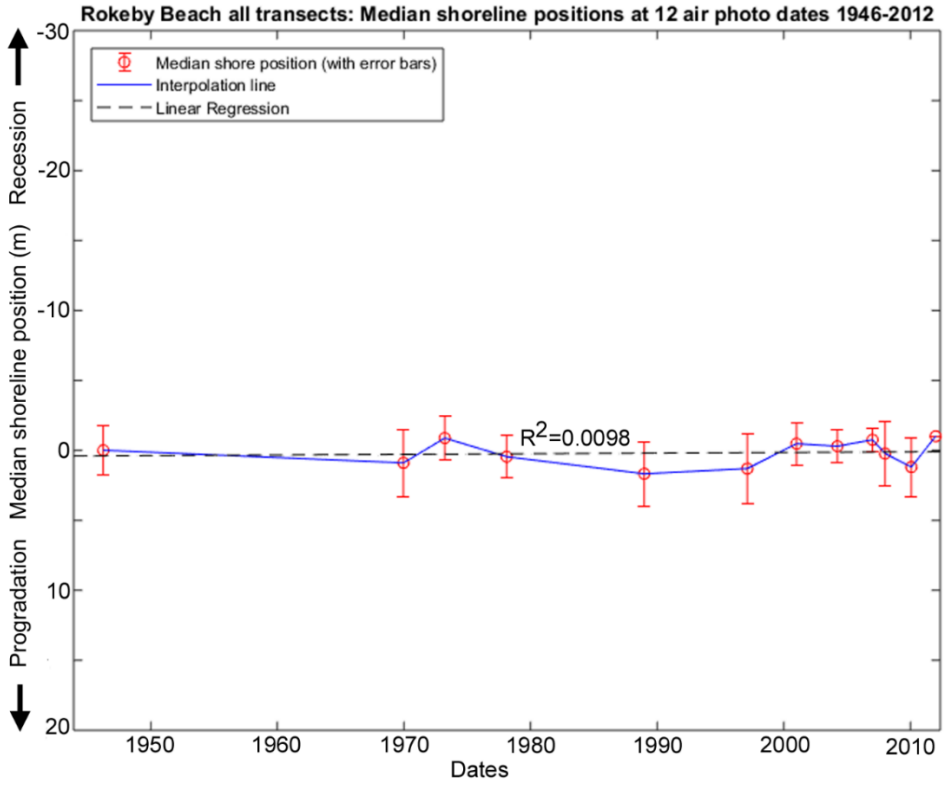

Figure 244: Summary plots of shoreline change history across all transects (as shown on Figure 241) at Rokeby Beach at 12 air photo dates from 1946 to 2012, with air photo error bars and interpolation lines (bottom version). With all transects included the recession trend in the western five transects is sub-ordinate to the lack of any overall trend in the remaining mid- to eastern transects.

Shore behaviour history from air photos

- Central – east parts of beach show stability (with some apparent short-term variability likely related to a combination of scarp-slumping and air photo error margins) and no trend over air photo period = negligible recession. Same appears true when medians taken across all transects, but when western 5 transects examined in isolation they do show a small but significant (R^2= 0.6449) linear recession trend at that end of the beach over the whole air photo period (but no unequivocal acceleration as yet); see Figure 241.
- Field inspection since 2005 has shown erosion fresher and more active at west 500m of beach than elsewhere (see Figure 237 & Figure 238). (West end = more swell-exposed - Figure 239).
- Two apparent erosion – recovery episodes (1973, 2001-2007) almost certainly an artefact of air-photo error margins and possibly some scarp slumping (true progradation not possible)

Shoreline behaviour drivers and conditions

Shoreline erosion scarp is inactive, rounded and slumped over the longest wind-wave fetches (Central-East area), but active, fresh and receding over shortest wind wave fetches (West area) – this implies wind-waves are not the primary agent of the observed active erosion and recession at the West site.

Narrowly focussed storm swell penetration is the only other available agent of erosion, and so is the most plausible cause of active erosion at West end (and lack of erosion in Central-East area)

But even at West site, recession shows no acceleration (compare Barilla site); most likely because the penetration of storm swells energetic enough to erode is unusual:- frequent enough to maintain a fresh and receding scarp, but not frequent enough to trigger accelerated recession in response to sea-level rise (more frequent wind-wave storm events over longer fetches than available would be needed for this to occur).

Air photo data tables

The following tables provide details of the air photos used, the resulting ortho-photos produced, and the shapefiles representing the shoreline position that were digitised from the ortho-photos.

Table 73: Original air photos and ortho-rectified air photos produced for Rokeby Beach. Due to relief displacement and other problems with interpreting the position of the approx. 4m high Rokeby Beach scarp top on air photos, the criteria of 'Scarp position in photo', 'Scarp top definition' and error margin are used in this table to select photos to be used in analysing shoreline change. See 'Air photo analysis' above for explanation.

Photo Date	**Original DPIPWE air photos (film-frame) / Ortho-photo name**	**Final image resolution (original scan resolution if downsized) / pixel size of final ortho-photo**	**Original photo scale**	**Mean measured feature position error (± metres) for ortho-photo** [no. of measured feature position reference points]	**Comments**
4th April 1946	31-11273 31-11274 / *RokebyBeach_Apr1946_MGA55.tif/tfw* (ortho-mosaic)	600 dpi / 0.7 m pixel size	1:17,540	1.8 [10]	Ortho-rectified by Sarah Harries *Scarp position in photo*: **OK** *Scarp top definition*: **Good** *Error margin*: **OK** **USED** *for shoreline history analysis*

12th Feb 1957	326-39 / *Rokeby Beach_Feb1957_MG A55.tif/tfw*	2039 dpi / 0.4 m pixel size	1:14,000	2.5 [7]	Ortho-rectified by Sarah Harries *Scarp position in photo*: **Not checked** *Scarp top definition*: **Poor** *Error margin*: **OK (marginal)** **NOT USED** *for shoreline history analysis*
18th Dec 1969	538-95 / *RokebyBeach_Dec19 69_MGA55.tif/tfw*	2039 dpi / 0.8 m pixel size	1:34,770	2.4 [10]	Ortho-rectified by Sarah Harries *Scarp position in photo*: **OK** *Scarp top definition*: **OK to Marginal** *Error margin*: **OK** **USED** *for shoreline history analysis*
24th Mar 1973	627-5 627-35 / *RokebyBeachMar197 3a_MGA55.tif/tfw; RokebyBeachMar197 3b_MGA55.tif/tfw*	2039 dpi / 0.16 m pixel size	1:12,500	1.6 [11]	Ortho-rectified by Chris Sharples For shoreline digitising, mainly used Mar1973b (best scarp location on N-S axis). *Scarp position in photo*: **Good** *Scarp top definition*: **Good** *Error margin*: **OK** **USED** for *shoreline history analysis*
14th Dec 1977	727-148 / *RokebyBeach_Dec19 77_MGA55.tif/tfw*	2039 dpi / 0.3 m pixel size	1:12,000	2.8 [11]	Ortho-rectified by Sarah Harries *Scarp position in photo*: **Marginal** *Scarp top definition*: **OK to marginal** *Error margin*: **OK (marginal)** **NOT USED** *for shoreline history analysis*
10th Feb 1978	741-221 / *RokebyBeach_Feb19 78_MGA55.tif/tfw;*	2039 dpi / 0.15 m pixel size	1:12,000	1.5 [8]	Ortho-rectified by Chris Sharples *Scarp position in photo*: **OK** *Scarp top definition*: OK *Error margin*: **OK** **USED** *for shoreline history analysis*
22nd Dec 1988	1125-52 1125-56 / *RokebyBeach_Dec19 88_MGA55.tif/tfw* (ortho-mosaic)	2039 dpi / 0.3 m pixel size	1:25,500	2.3 [11]	Ortho-rectified by Sarah Harries *Scarp position in photo*: **Uncertain** *Scarp top definition*: OK *Error margin*: **OK** **USED** *for shoreline history analysis*
15th Feb 1997	1272-113 / *RokebyBeach_Feb19 97_MGA55.tif/tfw*	2039 dpi / 0.3 m pixel size	1:12,500	2.5 [8]	Ortho-rectified by Sarah Harries *Scarp position in photo*: **Good** *Scarp top definition*: **OK** *Error margin*: **OK (marginal)** **USED** *for shoreline history analysis*
4th Jan 2001	1342-065 1342-092 / *RokebyBeach_Jan200 1a_MGA55.ecw, RokebyBeach_Jan200 1b_MGA55.ecw*	2039 dpi / 0.5 m pixel size	1:24,000	1.5 [11] (quoted absolute accuracy ±2.5m)	Ortho-rectified by DPIPWE Original DPIPWE ortho files: 1342_065_op.ecw, 1342_092_op.ecw *Scarp position in photo*: **OK** *Scarp top definition*: **OK** *Error margin*: **OK** **USED** *for shoreline history analysis*

28th Mar 2004	1383-010 1383-036 / *RokebyBeach_Mar2004a_MGA55.ecw* *RokebyBeach_Mar2004b_MGA55.ecw*	2039 dpi / 0.5 m pixel size	1:24,000	1.2 [11] (quoted absolute accuracy ±2.5m)	Ortho-rectified by DPIPWE Original DPIPWE ortho files: 1383_010_op.ecw 1383_036_op.ecw *Scarp position in photo*: **GOOD** *Scarp top definition*: **GOOD** *Error margin*: **OK** **USED** *for shoreline history analysis*
4th Jan 2007	1419-107 / *RokebyBeach_Jan2007_MGA55.tif/tfw*	1500 dpi (2039 dpi)	1:10,000	0.8 [10]	Ortho-rectified by Chris Sharples *Scarp position in photo*: **OK** (just within mid-one third) *Scarp top definition*: **GOOD** *Error margin*: **OK** **USED** *for shoreline history analysis*
13th Feb 2007	1422-090 / *RokebyBeach_Feb2007_MGA55.ecw*	2039 dpi / 0.5m pixel size	1:42,000	1.6 [11] (quoted absolute accuracy ±15m)	Ortho-rectified by DPIPWE Original DPIPWE ortho file: 1422_090_op.ecw *Scarp position in photo*: **POOR** *Scarp top definition*: **GOOD** *Error margin*: **OK** **NOT USED** *for shoreline history analysis*
3rd Jan 2008	1428_033 1428_060 / *RokebyBeach_Jan2008a_MGA55.ecw* *RokebyBeach_Jan2008b_MGA55.ecw*	2039 dpi / 0.5m pixel size	1:24,000	2.3 [9] (quoted absolute accuracy ±15m)	Ortho-rectified by DPIPWE Original DPIPWE ortho files: 1428_033_op.ecw 1428_060_op.ecw Used only 2008a to digitise shoreline (covers entire shore) *Scarp position in photo*: **OK** *Scarp top definition*: **POOR to OK** *Error margin*: **OK** **USED** *for shoreline history analysis*
30th Jan 2010	1443-157 / *RokebyBeach_Jan 2010_MGA55*	2039 dpi / 0.6 m pixel size	1:42,000	2.1 [11]	Ortho-rectified by Sarah Harries *Scarp position in photo*: **Marginal - just OK(?)** *Scarp top definition*: OK *Error margin*: **OK** **USED** *for shoreline history analysis*
DD MM not supplied 2012	Rokeby_Ortho_Medium_2012_v9.tif / *RokebyBeach_2012_MGA55.tif*	Undefined dpi / 0.14 m pixel size	-	0.0 [N/A]	REFERENCE IMAGE (Zero relative feature position error by convention) Original Geotiff captured and ortho-rectified by Matt Dell *Scarp position in photo*: **OK** *Scarp top definition*: **OK** *Error margin*: **OK** **USED** *for shoreline history analysis*

Table 74: Digitised shoreline shapefiles produced for Rokeby Beach, (using ortho-photos listed in Table 73 above):

Date of air photo(s)	Shapefile	Shoreline digitised by	Comments
4th April 1946	RokebyBeach_MGA55_19460404.shp	Sarah Harries (2011) Original shapefile: Rokeby_1946.shp	Moderate resolution but good contrast. Top of scarp veg line mapped. Shapefile checked by Chris Sharples 9th July 2019.
12th Feb 1957	RokebyBeach_MGA55_19570212.shp	Sarah Harries (2011); Original shapefile: Rokeby_1957.shp	Top of scarp veg line mapped. Several unclear sections deleted but still unclear in parts. Shoreline feature poorly defined in air photo, not used in final analysis (see Table 73).
18th Dec 1969	RokebyBeach_MGA55_19691218.shp	Sarah Harries (2011); Original shapefile: Rokeby_1969.shp	Poor resolution, poor contrast, top of scarp veg. line mapped but difficult to pick in parts. Most uncertain sections of veg/scarp line deleted. Shapefile checked by Chris Sharples 9th July 2019.
24th Mar 1973	RokebyBeach_MGA55_19730324.shp	Chris Sharples (2019)	Good resolution and contrast, scarp well centred on N-S axis. Top of scarp veg line well-defined by shadows, mapped.
14th Dec 1977	RokebyBeach_MGA55_19771214.shp	Sarah Harries (2011); Original shapefile: Rokeby_1977	Top of scarp veg line mapped. Ortho-photo marginal in key respects, not used in final analysis (see Table 73).
10th Feb 1978	RokebyBeach_MGA55_19780210.shp	Chris Sharples (2019)	Western third of beach only. Moderate resolution, moderate to poor contrast. Top of scarp veg line mapped, but difficult to pick in parts.
22nd Dec 1988	RokebyBeach_MGA55_19881222.shp	Sarah Harries (2011); Original shapefile: Rokeby_1988.shp	Top of scarp veg line mapped. Shapefile checked by Chris Sharples 9th July 2019; minor changes made.
15th Feb 1997	RokebyBeach_MGA55_19970215.shp	Sarah Harries (2011); Original shapefile:	Top of scarp veg line mapped.

		Rokeby_1997.shp	Shapefile checked by Chris Sharples 9th July 2019.
4th Jan 2001	RokebyBeach_MGA55_20010104.shp	Chris Sharples (2019)	Poor resolution, moderate contrast. Top of scarp veg line mapped.
28th Mar 2004	RokebyBeach_MGA55_20040328.shp	Chris Sharples (2019)	Moderate resolution, good contrast. Mapped scarp top – well defined by shadows
4th Jan 2007	RokebyBeach_MGA55_20070104.shp	Chris Sharples (2019)	Good resolution and contrast. Mapped scarp top – mostly defined by shadows, some vague sections.
13th Feb 2007	RokebyBeach_MGA55_20070213.shp	Chris Sharples (2019)	Moderate resolution and contrast. Mapped scarp top well defined by shadows, however not used in final analysis due to likely parallax errors (see Table 73).
3rd Jan 2008	RokebyBeach_MGA55_20080103.shp	Chris Sharples (2019)	Coarse resolution, good contrast. Top of veg. line scarp mapped. Scarp top poorly defined in parts due to coarse resolution.
30th Jan 2010	RokebyBeach_MGA55_20100130.shp	Sarah Harries (2011); Original shapefile: Rokeby_2010.shp	Top of scarp veg line mapped. Shapefile checked by Chris Sharples 5th July 2019.
2012 Unknown day/month	RokebyBeach_MGA55_20120101.shp	Chris Sharples (2019)	Good resolution, strong northerly shadowing. Top of scarp veg line mapped.

Appendix 2: Published Refereed Papers

This appendix reproduces the following previously - published refereed papers co-authored by Chris Sharples which contribute information or ideas relevant to this thesis.

Pages 476 – 486:

Prahalad, V., Sharples, C., Kirkpatrick, J. & Mount, R., 2015. Is wind-wave fetch exposure related to soft shoreline change in swell-sheltered situations with low terrestrial sediment input? *Journal of Coastal Conservation*, vol. 19, pp.23-33.

Pages 487 – 504:

Thom, B.G., Eliot, I., Eliot, M., Harvey, N., Rissik, D., Sharples, C., Short, A.D. & Woodroffe, C.D., 2018. National sediment compartment framework for Australian coastal management, *Ocean & Coastal Management*, vol. 154, p. 103-120.

Pages 505 – 518:

Sharples, C., Walford, H., Watson, C., Ellison, J.C., Hua, Q., Bowden, N. & Bowman, D., 2020. Ocean Beach, Tasmania: A swell-dominated shoreline reaches climate-induced recessional tipping point? *Marine Geology*, vol. 419, 106081

J Coast Conserv (2015) 19:23–33
DOI 10.1007/s11852-014-0352-x

Is wind-wave fetch exposure related to soft shoreline change in swell-sheltered situations with low terrestrial sediment input?

Vishnu Prahalad · Chris Sharples · Jamie Kirkpatrick · Richard Mount

Received: 5 October 2014 / Revised: 31 October 2014 / Accepted: 31 October 2014 / Published online: 30 November 2014

Abstract Rising sea levels and changing wind climates are widely expected to be associated with receding coastlines, creating a planning need for coastal change prediction, especially for soft shores like those associated with saltmarsh. We ask whether it is possible use a simple cartographic wind-wave fetch method to estimate the spatial pattern of progradation and recession of soft shores in swell-sheltered situations in which there is little or no input of new sediment from terrestrial sources. For points on an extensive embayment shoreline of this type we mapped change over 54 years from aerial photographs, recorded current shoreline morphology and calculated a wave fetch index (WFI). Morphological indication of strong progradation was associated with low WFI, but there was no statistically significant effect of variation in WFI on the degree of shoreline retreat. Saltmarsh shorelines averaged 14 cm per annum retreat between 1952 and 2006, a rate that did not vary significantly between air photo periods. We conclude that our geographic information system approach utilising WFI is likely to be useful as a planning tool in identifying those parts of sediment-poor saltmarsh shores where erosion is most likely or least likely to occur, but not particularly useful for predicting finer-scale variation in rates of shoreline recession within the particular substrate types in our study area. In the context of relative sea-level rise and increasing wind speeds, such modelling can help identify coastlines which are likely to support saltmarshes into the future.

Keywords Fetch wave exposure · Coastal erosion · Saltmarsh · Soft sediment · GIS · Tasmania

V. Prahalad (✉) · C. Sharples · J. Kirkpatrick · R. Mount
Discipline of Geography and Spatial Science, School of Land and Food, University of Tasmania, Private Bag 78, Hobart, Tasmania 7001, Australia
e-mail: vishnu.prahalad@utas.edu.au

Introduction

With the onset of accelerating global sea-level rise over the last century (Church and White 2006), coastal erosion has emerged as an increasingly significant issue in coastal conservation owing to the well-understood geomorphic principle that a rise in sea-level relative to an erodible shoreline will generally result in erosional recession of shorelines (e.g., Zhang et al. 2004; Stive et al. 2009). Given the consequences that shoreline recession may have for both ecosystems and human assets, there is an increasing need to improve our understanding of the relative susceptibility of coastlines to erosion (DCC 2009). Although shoreline substrate type is clearly the major influence on shoreline susceptibility to erosion (Benumof et al. 2000; Bezerra et al. 2011; Feagin et al. 2009; Cowart et al. 2010), it is also important to consider alongshore variability in the bio-physical processes which drive or inhibit erosion.

Waves are recognised to be the dominant mechanism of shoreline erosion in most coastal environments (Pethick 1993; Harris et al. 2002; FitzGerald et al. 2008; Fagherazzi and Wiberg 2009; Tonelli et al. 2010). They influence sea cliffs (Benumof et al. 2000; Bezerra et al. 2011), rocky reefs (Burrows et al. 2008; Hill et al. 2010), coral reefs (Chollett and Mumby 2012) and saltmarshes (Schwimmer 2001; van der Wal and Pye 2004; Marani et al. 2011). There is a need to identify relationships between variability in wave energy and shoreline type over large coastal areas, and consequent changes in ecology and geomorphology, including erosion, to inform holistic management of these areas. There is a good understanding of the erosional influence of wave action on open coasts but relatively little work has been undertaken on swell-sheltered tidal re-entrants, such as estuaries and embayments (e.g., Cowart et al. 2010, 2011). These coastal environments are sheltered from the open coast swell waves and support important ecosystems such as saltmarshes, which are

at the critical interface of threats from both global sea-level rise and local human impacts (van der Wal and Pye 2004; Prahalad et al. 2011; Saintilan and Rogers 2013).

Although saltmarshes occur where swell waves are absent, they are subject to wind waves that develop along available fetches within swell-sheltered tidal re-entrants. Wind waves are a primary mechanism of saltmarsh shoreline change, with sea level rise being an underlying driver. Despite the important role of wave energy in shaping saltmarsh shorelines (Allen 2000), the nature of this relationship has been studied to a much lesser extent compared to other bio-physical drivers of saltmarsh resilience (Marani et al. 2011; Stralberg et al. 2011; Mariotti and Fagherazzi 2013; Torio and Chmura 2013). The role of wave energy is particularly important in larger coastal areas where the availability of sediment is low in relation to relative sea level rise (Williams and Orr 2002; Mariotti and Fagherazzi 2013). This general lack of attention to the relative role of wave energy in studies of saltmarsh resilience is particularly acute in Australia (e.g., Saintilan 2009; Saintilan and Rogers 2013), where despite the considerable number of large estuaries and embayments (Heap et al. 2001) and their importance in the context of ecosystem services and human assets (DCC 2009), we could not locate a single study to this effect. Even where predictive models such as Sea Level Affecting Marshes Model (SLAMM) have been used, they consider wave energy within a limited context, omitting factors such as wind speed and direction, and rely on empirical data generated from Northern Hemisphere studies (Akumu et al. 2011). Our study aims to fill this gap and generate empirical data relating wave energy within a swell-sheltered tidal re-entrant environment in Australia to saltmarsh shoreline evolution. More generally, we seek to contribute to raising the profile of wave energy as an important mechanism of saltmarsh shoreline change, particularly where sedimentation is clearly not sufficient to compensate for the effects of relative sea level rise.

For a large study area in north-western Tasmania, Australia, we used wind-wave fetch derived from simple Geographical Information Systems (GIS) based cartographic wind-wave fetch exposure modelling to predict the spatial pattern of progradation and recession of soft shores in swell-sheltered situations in which there is little or no input of new sediment from terrestrial sources. Cartographic fetch modelling has emerged as an efficient method of quantifying wave exposure for coastal environments within GIS (e.g. Ekebom et al. 2003; Tolvanen and Suominen 2005). Wave exposure is strongly correlated with wave energy received and is primarily determined by fetch length (openness), near shore bathymetry, local wind conditions and offshore swell wave climate (Hill et al. 2010). For swell-sheltered coastal re-entrants such as estuaries and tidal lagoons, offshore swell waves are limited by barriers and can be excluded from wave exposure studies. Although more computationally intensive numerical models are available for modelling wave exposure (e.g., the SWAN model, Booij et al. 1999), simpler GIS based cartographic fetch-wave modelling using a point based approach has proven a robust and easy to use alternative in fetch-limited environments where swell waves are not significant (e.g., Cowart et al. 2010, 2011).

Study area

The study area is a large coastal tide-dominated re-entrant comprising over 100 km of dominantly soft low-profile, sandy and saltmarsh-colonised shores fronted by extensive intertidal to sub-tidal sand flats that are almost entirely sheltered from the swell-dominated wave climate of Bass Strait behind Robbins Island and the large prograded Holocene sandy barriers of Perkins Island and Anthonys Beach (Fig. 1). The shorelines are mostly backed by marshy low ground or slightly higher plains of windblown Pleistocene sand, sometimes mantling bedrock above sea-level but more generally extending in depth to below present sea-level. Native saltmarsh occurs extensively in the upper intertidal profile between the area just below the mean high tide mark and inland to the extent of storm tide with an elevation range of about 0.55 m (Mount et al. 2010). Within the re-entrant environment, the wave climate is characterised entirely by wind-waves generated locally across available fetches. The study area has the largest tidal range on the Tasmanian coast (a mesotidal range of up to 3.1 m: Donaldson et al. 2012), resulting in strong, partly channelized, tidal currents across the intertidal flats.

Apart from superficial Holocene reworking of sand by waves and tidal currents, the extensive intertidal to subtidal sand flats in the study area are not Holocene coastal or marine sediments but are mainly relict Pleistocene terrestrial aeolian, fluvial and lacustrine deposits that were partly inundated and stripped by marine erosion at the upper limit of the post-glacial marine transgression that ceased in the south-eastern Australia region circa 6,500 years BP (Lambeck and Chappell 2001). Whilst a thin (c 0.5 m) veneer of reworked sands mantles parts of the tidal flats, in many areas eroding Pleistocene freshwater peats are exposed on the tidal flat surface, both adjacent to the shoreline (Fig. 2b) and also in widely scattered patches across the intertidal flats. This implies that the flats are currently erosional rather than depositional environments (Mount et al. 2010). Rivers that flow into the sheltered waters, namely the Duck, Montagu, Harcus and Welcome, exhibit no evidence of active sand transport such as sandy point bars or recent deltaic deposits, and instead appear to be transporting only small amounts of clay and silt-grade sediment as is commonly the case for rivers in western Tasmania (e.g., Nanson et al. 1995). We therefore infer that there is a negative sand budget with little capacity for sandy

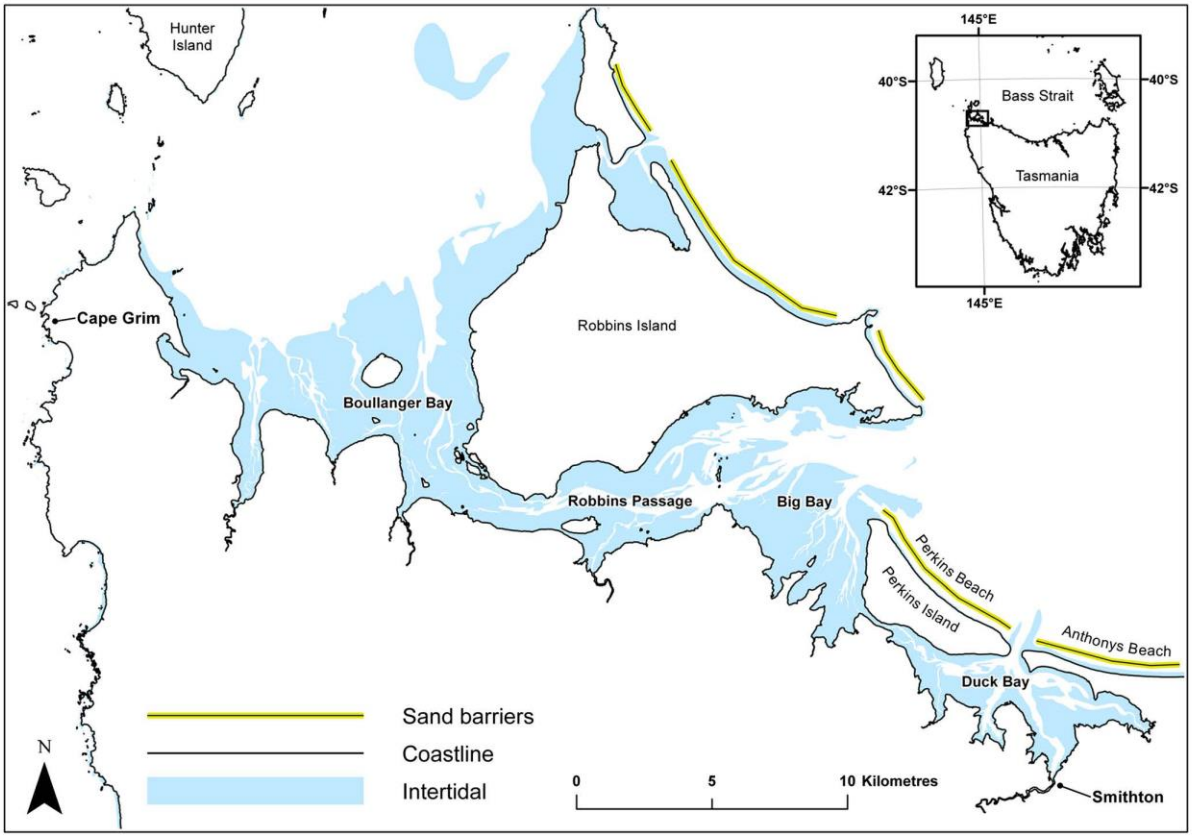

Fig. 1 Location map of the north-west Tasmania study area. The extensive intertidal areas shown are mostly sandflats that are exposed at low tide

sediment accumulation to be an influence on shoreline location.

Tide gauge data from Burnie, 70 km to the east of the study area shows a net rise in sea level between 1966 and 2010 of 5.4 cm at a steady 1.4 mm y^{-1} (Mount et al. 2010). This rate is consistent with the Australian average for the period 1920–2000, estimated to be 1.2 mm y^{-1} (Church et al. 2006). Wind speed data were available only from 1991 onwards for the study area. At the Cape Grim Bureau of Meteorology weather station to the immediate west of the study area there was a greater incidence of high wind speeds in the decade 2000–2010 than in the decade 1990–2000 (Mount et al. 2010). This observation is consistent with the longer term wind data for south-eastern Tasmania which shows that the decade before 2009 had higher annual mean wind speeds than the previous four decades (Prahalad et al. 2011).

The nearby land use is predominantly agricultural with extensive areas used for dairy and beef production, while intertidal parts of the study area (eastern sections) are used for marine aquaculture. The history of land use changes in the study area and their impacts on saltmarshes have been documented by Prahalad (2014). The main factors relevant to coastal erosion are the long tidal barriers (levees) constructed behind the saltmarsh shoreline and the presence of introduced rice grass (*Spartina anglica*). The rice grass competes with native saltmarsh vegetation communities in the lower tidal zone dominated by *Sarcocornia quinqueflora* (see Fig. 2d) and in places by *Juncus kraussii*, as well as extending to lower elevation than native saltmarsh.

Methods

Mapping of shorelines

In 2010, detailed field mapping was undertaken at a nominal scale of 1:10,000 or larger throughout the entire study area (Fig. 1). Mapping was based on field observations made by walking the entire shoreline length of the study area, with geographical positioning system (GPS) coordinates taken for all observations and transferred onto a vector line layer within the ArcGIS™ environment. Shorelines were classified into substrate type groups of similar fabric which might be expected to have similar responses to drivers of erosion (Table 1, Fig. 1). The soft sediment shorelines that are the subject of our paper were divided into those with saltmarsh (Fig. 2a, c, d)

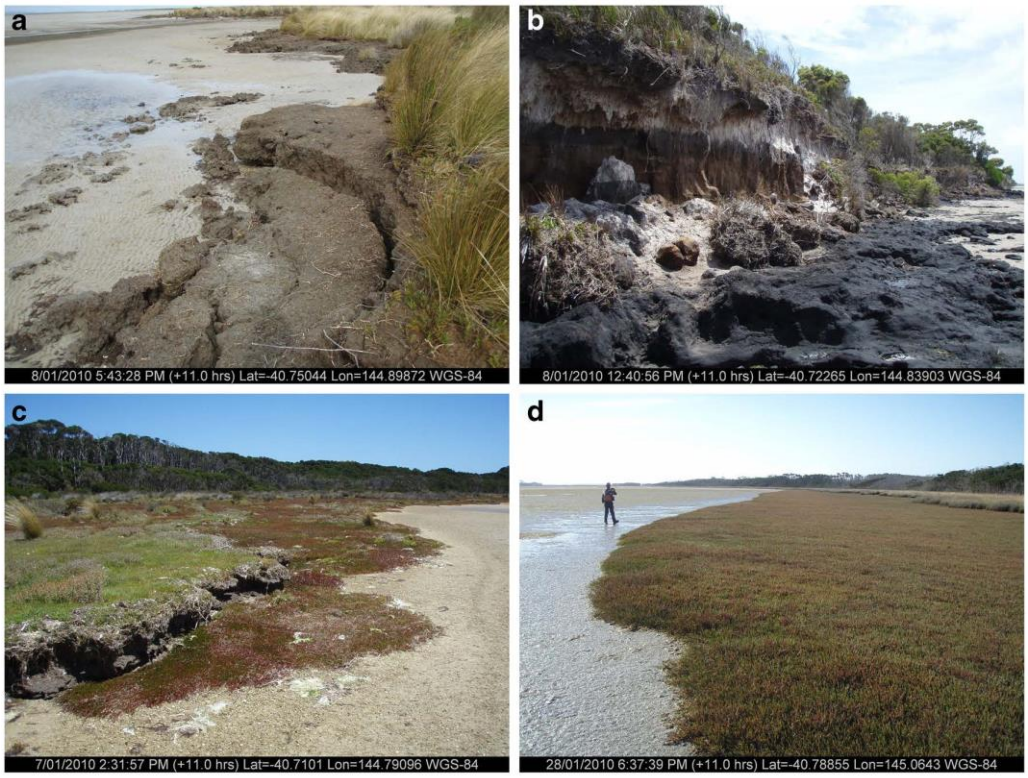

Fig. 2 Examples of fetch-dominated saltmarsh and non-saltmarsh shores in the study area. **a** A typical spatially-continuous, actively eroding soft saltmarsh shore within the study area where the low marsh dominated by *Sarcocornia quinqueflora* has been eroded back to the high marsh dominated by grasses and sedges (compare intact saltmarsh in **d**). This example comprises of sand, silt, clay and organic debris captured by saltmarsh plants, which has accumulated over a substrate of Pleistocene and superficially reworked Holocene sands. **b** A typical continuous, actively eroding soft non-saltmarsh shore within the study area. This example comprises well-podsolised Pleistocene terrestrial aeolian sands over a semi-indurated freshwater Pleistocene peat deposit which we infer to be a terrestrial swamp or lake deposit laid down in an inter-dune swale. **c** An example of temporally-intermittent saltmarsh erosion, with an old inactive erosion scarp in soft clayey-sand saltmarsh soil (over semi-indurated peaty sand) fronted by currently accreting secondary saltmarsh. **d** An example of spatially-continuous active saltmarsh accretion, with no evidence of scarp development along the marsh platform. This example is typical of an intact sequence of native saltmarsh with the low marsh dominated by *Sarcocornia quinqueflora* and the high marsh (to the back) dominated by grasses and sedges, with the backing *Melaleuca ericifolia* tree cover visible

and those sandy shores without saltmarsh (Fig. 2b). Shoreline stability status (Table 2) was also mapped. Our aim was to record current status without necessarily inferring whether erosion or accretion is progressive and non-reversing, or alternating (e.g., a cut-and-fill cycle). However, where clear evidence of episodic erosion and accretion was visible (e.g.,

Table 1 Grouped shoreline substrate type classes with their respective length and relative dominance within the study area (in terms of percent of the 107.2 km of shoreline mapped). Note that some of these groups lump together finer sub-divisions mapped in the field

Shoreline type group	Grouping for this study	Length (m)	Percent of the total shoreline
Erodible saltmarsh soil substrates over sand	Soft saltmarsh shores (swell-sheltered)	77,753	73
Soft erodible substrates over hard bedrock	Soft saltmarsh shores (swell-sheltered)	7,661	7
Other sands (including older Holocene podzolic beach ridge or Pleistocene aeolian sand sheet deposits)	Soft non-saltmarsh shores (swell-sheltered)	10,834	10
"Cut and fill" shorelines – foredunes and beach ridges	Cut and fill shores (swell-exposed and sheltered)	6,718	6
Dominantly hard stable bedrock shores	Hard shores (swell-exposed and sheltered)	4,254	4

Table 2 Grouped shoreline erosion type classes with their respective length and relative dominance observed during fieldwork within the study area (in terms of percent of the 107.2 km of shoreline mapped). Symbols shown are as used in subsequent figures. Note that some of these groups lump together finer sub-divisions mapped in the field. Except for hard bedrock shores, each substrate class in Table 1 may contain sections belonging to any of the stability classes listed here

Stability group	Symbol	Length (m)	Percent of the total shoreline
Actively eroding shores, continuous	AE	22,108	21
Dominantly actively eroding shores (with some sub-ordinate intermittent stability or accretion)	DE	7,884	7
Intermittently eroding shores (some spatially or temporally intermittent accretion, but accretion not dominant)	IE	23,557	22
Stable shores (i.e., mainly hard bedrock, or soft shores with no indication of accretion or erosion)	–	4,440	4
Dominantly accreting shores with some intermittent or prior erosion	DA	18,629	17
Accreting shores, no evidence of prior erosion	AA	30,601	29

old erosion scarps behind current accretion), then these were classified as having 'temporally intermittent erosion' (Fig. 2c). The heights of erosion scarps were recorded as another proxy measure for shoreline stability, on the assumption that higher scarps roughly reflect a greater degree of shoreline recession into the prior backshore terrain.

Historical aerial photograph analysis of shoreline change

Changes in the seaward boundary of saltmarsh were measured in parts of the study area for which there was a suitable time series of historical aerial imagery. Aerial photographs were available for parts of the study area for the years 1952, 1968, 1979, 2001 and 2006. The photos were all taken in summer months at unknown tidal levels. There was clear visibility of the saltmarsh-tidal flat interface owing to the distinctive colour and texture of saltmarsh vegetation. The aerial photographs (as 8 bit grey scale and 24 bit colour) were sourced from the Tasmanian Government TASMAP aerial photography database, scanned to a resolution of 1200 dpi and orthorectified using Landscape Mapper™ software. A LiDAR-derived digital elevation (DEM) model for the study area captured during May 2008 (with a vertical and horizontal accuracy of +/− 25 cm) and 1:25,000 cartographic vector layers sourced from Land Information Systems Tasmania (LIST) were used in the geo-rectification process (image to image geo-rectification with ground control points selected from the vector map layers). The average root mean square (RMS) error from the process was 6.8 m, with 2006 images having the lowest average RMS error of 3.1 m (with a range between 1.9 and 5.8 m). Hence, the 2006 images were used as the base layer to geo-rectify other older images further within the ArcGIS™ environment to reduce the relative positional error between the images to less than 5 m. Control points for this process included reliably identifiable creek lines and individual mature trees closer to the shorelines of interest to the study (cf. Cox et al. 2003; Prahalad et al. 2011).

For each time period, the shoreline position was digitised as the boundary of the vegetation and the tidal flat bare sand. Shorelines backed by artificial tidal barriers (mainly levees recorded during field work) were not included as the barriers are likely to have altered the natural shoreline response to climate change and sea level rise (Hood 2004; Prahalad 2014). The 2006 shoreline position was used as the 'reference shoreline' against which historic shoreline change were measured and analysed at 225 point locations spaced at 100 m intervals along the saltmarsh shoreline. Shoreline change was measured at each of these points as distance (m) of shoreline movement between two time periods and then annual rates calculated by dividing the distance by the number of years. The earlier series of photographs varied in their coverage of these points, hence only a subset of the 225 point locations was used for pairwise comparison between time periods.

Wind-wave fetch exposure modelling

Wind-wave fetch exposure modelling was conducted using the GIS-based cartographic wave exposure model called Generic Relative Wave Exposure Model ('GREMO', Pepper 2009; Pepper and Puotinen 2009). The model is based on the Wave Exposure Model (WEMo) developed by Malhotra and Fonseca (2007) for estuarine (swell-sheltered) environments and can incorporate bathymetric and wind speed/directional data. The model is implemented in the ESRI ArcMap™ software environment and readily customised to project needs (e.g., Hill et al. 2010). The data input for the model included: a point file of 1031 of the sampling points along the shoreline (spaced at 100 m intervals); a polygon file, which is the digitised coastline (nominal High Water Mark) of Tasmania; a 10×10 m digital bathymetric grid compiled to represent the bathymetry of the study area using the LiDAR DEM in the intertidal area and bathymetric contours below low water mark obtained from the Royal Australian Navy Hydrographers Chart; and wind speed/directional information (including storm winds), obtained for 16 compass directions

for two Bureau of Meteorology weather stations at Cape Grim and Smithton (station numbers 091245 and 091292 at the western and eastern ends of the study area respectively).

For each sampling point GREMO calculated the fetch length between the point (from the input point file) to the nearest potential wave blocking obstacle (input polygon file/coastline) at every 7.5° around the point (i.e., 48 fetch lines radiating from every point) to a distance of 30 km (to ensure differentiation between fetches open to Bass Strait and those more enclosed). The calculated fetch length was then weighted by overlaying the bathymetric grid data generated for the project to account for the attenuation effect of shallow bathymetry on waves. A distance of 2 km was set as the maximum distance for bathymetry interrogation. The resultant fetch-bathymetric values were further weighted by the wind speed and direction information and summed to calculate the relative aggregate fetch-wave exposure for each sampling point along the shoreline. The Cape Grim wind data were used for Boullanger Bay area while Smithton wind data were used for Robbins Passage, Big Bay and Duck Bay areas (see Fig. 1). No attempt was made to derive absolute wave energy estimates. Rather, the model produces a relative aggregate wave exposure as a dimensionless value that enables comparisons within the study area and is referred to as the Wave Fetch Index (WFI).

We identified and excluded from analysis shores where processes or environmental factors other than local fetch-dominated wave exposure were likely to be dominant influences on shoreline behaviour. We justify the exclusion of these data points as our aim is explicitly to examine the effect of wave exposure on shoreline behaviour, and not to compare that effect with other identifiable influences. Excluded shores comprise: shoreline sections associated with foredunes and beach ridges subject to swell waves and displaying 'cut-and-fill' behaviour (61 points); areas in front of artificial tidal barriers as they tend to amplify erosional loss (Prahalad 2014) (173 points); areas close to tidal channels and subject to tidal currents (34 points); mouths of estuaries subject to river discharge currents (73 points); areas invaded by *Spartina* which considerably alters native shoreline dynamics (Sheehan and Ellison 2014) (40 points); hard bedrock shores (43 points); and cartographic anomalies where the digitised shoreline vector layer in some places did not represent the actual current position or shape of shoreline as mapped on the ground (36 points). Of the remaining points, 502 were on saltmarsh shores and 69 were on non-saltmarsh shores.

Statistical analysis

WFI generated for each point on the shoreline for every 100 m was compared with the shoreline mapping data including substrate types, erosion status and scarp height. The Kruskal-Wallis H test was used to determine whether WFI differed between the substrate types including saltmarsh (502 data points), non-saltmarsh (69 data points) and cut and fill shores (61 data points). Analysis of variance with Tukey multiple comparison tests ($P<0.05$) was used to determine whether WFI varied between erosion classes (Table 2) and scarp height classes for each of saltmarsh and non-saltmarsh within swell-sheltered areas. Residuals were normally distributed in all cases. Scarp height observations were recorded against three classes for fetch-dominated saltmarsh shorelines: <0.2 m; 0.2–0.5 m; and no scarp. For the fetch-dominated non-saltmarsh shorelines, five of the six mapped scarp height classes were used: 0.2–0.5 m; 0.5–1 m; 1–2 m; 2–6 m; and no scarp. These height classes were chosen on the basis of an apparent clustering of scarp heights that became evident during field work.

Because there was considerable variation in aerial photograph coverage between years, the mean annual amount of shoreline change was calculated for 1952–2006, 1968–2006, 1979–2006, 1992–2006, 2001–2006, 1952–1968, 1968–1979, 1979–1992 and 1992–2001 time periods. The relationship of shoreline changes observed from aerial photo analysis with WFI were tested for all these periods using Pearson's product moment correlation coefficient, which was also used to test the relationships between the values for each of the time periods. Two sample t-tests were used to determine if mean annual shoreline change differed between each pair of 1952–1968, 1968–1979, 1979–1992, 1992–2001 and 2001–2006.

Results

Most of the coast in the study area consisted of soft, easily erodible sediments (Table 1). Half of the easily erodible coast in swell-sheltered areas exhibited evidence of recession, while 46 % showed evidence of accretion (Table 2). Of the saltmarsh shores, 33 % were actively accreting, while only 10 % of the non-saltmarsh shores were doing so. Forty-nine percent of the saltmarsh shore had evidence of erosion, much less than the 78 % for non-saltmarsh shorelines. The erosion status of the saltmarsh shorelines was related to WFI ($F_{4,497}=15.49$; $P<0.001$). The accreting shores with no evidence of prior erosion had lower wave exposure than the other three erosion status classes. There was however no significant difference in wave exposure between the other three erosion status classes. Erosion status for the non-saltmarsh shorelines was also related to WFI ($F_{4,64}=3.37$; $P=0.015$). Again, the accreting shores with no evidence of prior erosion had the lowest wave exposure, differing from the actively eroding and intermittently eroding shores, while the wave exposures of latter two erosion status classes were statistically indistinguishable.

The mean WFI for actively accreting saltmarsh shorelines was 65,515 (s.d.=44,784), while the equivalent figure for the actively accreting non-saltmarsh shorelines was 87,949 (s.d.=

50,596). The midpoint between the WFI means for the mild erosion and mild accretion classes could be considered a threshold and was 96,383 for saltmarsh and 159,978 for non-saltmarsh. Thus, the WFI threshold for erosion was much lower for saltmarsh shores than non-saltmarsh shores. Saltmarsh (median = 78,806), non-saltmarsh (median = 172,943) and cut and fill shores (median = 448,380) formed a sequence strongly related to WFI ($H_{2,\ 592}$=106.11, P<0.001), with the threshold WFI for a transition from saltmarsh to other types being approximately 110,000 (Fig. 3). In other words, a saltmarsh area subject to a WFI of above 110,000 is likely to erode continuously and be converted to non-saltmarsh shoreline types.

Thirty-nine percent of the saltmarsh points had no scarp, 21 % had a scarp shorter than 0.2 m in height and 40 % had a scarp between 0.2 and 0.5 m. In contrast, only 12 % of the non-saltmarsh points had no scarp, 26 % had a scarp shorter than 0.5 m and 62 % had a scarp taller than 0.5 m. For the saltmarsh shores, the non-scarped points had a lower mean WFI than the two scarped classes ($F_{4,\ 501}$=19.36, P<0.001). For the non-saltmarsh shores, points in classes containing scarps taller than 0.5 m were more exposed than classes with shorter or no scarps ($F_{4,\ 64}$=16.1, P<0.001).

In all of the 1952–1968, 1968–1979, 1979–1992, 1992–2001 and 2001–2006 time periods there was mean recession of saltmarsh coasts and some points on the coast where progradation was occurring (Fig. 4). The mean annual change did not differ significantly (P>0.05) between any of these time periods. The mean saltmarsh shoreline change between 1952 and 2006 was −14 cm per annum.

The strongest relationships between shoreline change measured from the aerial photographs and WFI was for the earliest time period (1952–1968, r=−0.590, d.f.=36, P<0.001) and for the full time period (1952–2006, r=−0.505, d.f.=77, P<0.001, total change (m)=3.26–0.000182*WFI). There were also significant relationships for 1979–2006 (r=−0.237, d.f.=102, P=0.016) and 1992–2006 (r=−0.142, d.f.=203, P=0.043). While changes in one time period were often reflected in another, there were several instances in which changes reversed between time periods. Change in 1952–68 was reflected in the periods 1992–2001 (r=0.407, d.f.=36, P=0.011) and 2001–2006 (r=0.365, d.f.=36, P=0.024). Change in 1968–1979 was inversely related to change in 1979–1992 (r=−0.443, d.f.=49, P=0.001) but was weakly reflected in change in 1992–2001 (r=0.408, d.f.=27, P=0.028). Changes in both 1979–1992 (r=−0.256, d.f.=60, P=0.045) and 1992–2001 (r=− 0.293, d.f.=121, P=0.001) were inversely related to change in 2001–2006.

Discussion

The simple relative wind-wave fetch exposure index (WFI) that we modelled proved to be useful in predicting sections of the shoreline which are most likely to be either accreting or eroding where other local processes or environmental factors apart from local wind-wave fetch exposure have little influence on shoreline behaviour. Some previous studies have largely attributed shoreline behaviour to shoreline composition, stating that the nature of the shoreline substrate determines the degree of erosion (open coast environments: Benumof et al. 2000; Bezerra et al. 2011; swell-sheltered environments: Feagin et al. 2009; Cowart et al. 2010). Our study similarly acknowledges the primary role of shoreline composition in determining susceptibility to erosion (e.g., hard stable bedrock shores vs soft saltmarsh shores), but particularly highlights the significance of wind-wave fetch exposure in explaining alongshore variability in shoreline change (erosion or accretion)

Fig. 3 The relationship between Wave-Fetch Index (WFI) and three different shoreline substrate types. The discontinuous lines represent WFI thresholds at which shoreline types changed. The boxes contain 50 % of the observations, the median is shown by a horizontal line, the whiskers show the range of values. Cut-and-fill shores are shown here for comparison but were not otherwise used in the analysis relating WFI to shoreline change

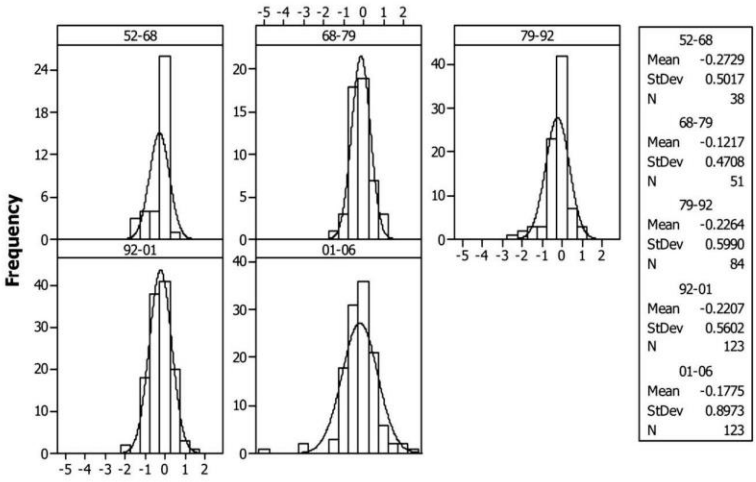

Fig. 4 Normal curves fitted to the distribution of shoreline change data (m, with negative values indicating retreat) for saltmarsh for the five aerial photo time periods, showing means, standard deviations (StDev) and the number of values (N)

within a given substrate type (in this case, within saltmarsh and sandy non-saltmarsh shore types).

The strong relationship we observed between shoreline change (erosion status) and wind-wave fetch exposure has been observed in other swell-sheltered coastal areas, such as in Venice Lagoon, Italy (Day et al. 1998; Marani et al. 2011), Westerschelde Estuary, Netherlands (Cox et al. 2003), Greater Thames area, U.K. (van der Wal and Pye 2004), and along the U.S. Atlantic Coast (Schwimmer 2001; Cowart et al. 2011; Mariotti and Fagherazzi 2013). Our modelling of WFI was most reliable in identifying parts of the shoreline in our study area where erosion is most likely or least likely to occur, but did not explain finer scales of shoreline change, as there was no strong correlation between increasing WFI and the sequence of the shoreline erosion classes (from intermittently eroding to actively eroding). More consequentially, we identified thresholds in the WFI (our proxy for wave energy) for shoreline change both within a particular substrate type (beyond which erosion was likely) and also between substrate types (at which shoreline substrate types changed) in our study area (Fig. 3).

The value of our modelling approach therefore lies in its ability to be used as a planning tool that reliably identifies distinctive sections of the shoreline based on their relative proclivity to shoreline change. This can contribute to saltmarsh conservation planning through identifying shoreline areas with local WFI thresholds below which saltmarshes continue to accrete (cf. Williams and Orr 2002). The WFI values could be used alongside shoreline inundation modelling to select priority areas for future saltmarsh conservation in response to sea level rise (Murdukhayeva et al. 2013; Torio and Chmura 2013). Even in areas where sediment inputs are considerable, WFI values can be integrated with existing models where applicable to better understand saltmarsh sustainability in the face of sea level rise (Stralberg et al. 2011).

The results from the shoreline stability classes were similar to those from the scarp classes, indicating that either could be used as an indicator of shoreline stability wherever it can be assumed that landscape gradients are similar before erosion occurs. A likely explanation for the strong relationship between erosion scarp height and WFI is that higher scarps indicate shores that are exposed to higher wave energy and thus have receded farther into the generally rising backshore terrain from a formerly stable or accreting shoreline position (Möller and Spencer 2002). The strong relationship between shoreline change measured from the aerial photographs for 1952–2006 and WFI is also most likely explained in the same way. That is, where shores have been dominantly experiencing erosional recession over multi-decadal time scales, in the absence of other local controlling factors, the shores with higher WFI are likely to have been eroded more frequently and more rapidly, and so are likely to have receded greater distances into the gently rising backshore, producing progressively higher erosion scarps (Marani et al. 2011). The concurrence between the direction of shoreline change measured from aerial photographs and the on-ground observations of erosion status suggests that either could be used to infer shoreline erosion susceptibility.

Evidence from air photo time series and observations of isolated remnant eroding saltmarsh soil 'pedestals' still standing on the tidal flats to seawards of many eroding shoreline scarps indicate ongoing net shoreline recession. Some of the analyses indicate that parts of the receding saltmarsh shores have prograded at times and receded at others (Fig. 4), possibly resulting from short and medium term variations in wind energy (e.g., individual storms), and sea level variations (e.g., long-term tidal cycles, El Nino, eustatic global sea level change). Our aerial photo intervals are too coarse to be able to meaningfully examine these variations and their effects on shoreline change. Of interest here, however, is the causal link between the long term net recession and relative sea level rise combined with an increasing incidence of strong winds. The strength of this link is unaffected by other known potential

causes as we excluded from sampling areas associated with tidal barriers, *Spartina* invasion and other local influences. Land subsidence, dredging and increased recreational boat use (boat wakes) are not relevant to erosion in our study area (cf. Cox et al. 2003; van der Wal and Pye 2004). In the case of saltmarshes, sediment availability (both allochthonous and autochthonous) has the potential to offset the effects of sea level rise by assisting saltmarshes to accrete vertically as they erode laterally (FitzGerald et al. 2008), and has been the central focus of modelling marsh sustainability with sea level rise (e.g., Stralberg et al. 2011). However for sediment-poor systems, as in the present case where allochthonous sediment input is negligible, irreversible shoreline erosion can happen through increased wind and thus wave energy even in the absence of sea level rise (Mariotti and Fagherazzi 2013).

With the strong relationship between shoreline erosion status and WFI, and in the context of increase in relative sea-level and higher speed winds, it is likely that many parts of the shoreline in our study area have become too frequently exposed to wave attack at higher levels, or have become too energetic (i.e., have crossed a wave energy threshold) for native saltmarsh vegetation to establish or re-establish in front of erosion scarps (compare Fig. 2a and c). Furthermore, our field observations suggest that saltmarsh shores in swell-sheltered tidal re-entrants may erode even under very mild wind-wave conditions (see Fig. 5). The onset of erosion may require an initial energetic storm event or some other mechanical disturbance to open a breach in the protective saltmarsh vegetation cover and expose previously-covered saltmarsh soils or sediments to wave action (van de Koppel et al. 2005). Where the initial erosion event occurs above normal high tide water levels on a high storm tide, saltmarsh regrowth may have sufficient time between such extreme events to re-establish in front of the erosion scarp and allow sediment accumulation and recovery to occur. However, if the storm erosion event is focussed at or below normal high tide levels, and exposes fine soft clayey, silty or peaty sediments, then very mild wave action amounting to little more than rippling may be all that is necessary to continue to remove some exposed sediment on each subsequent high tide, causing the scarp to actively recede even without storm erosion, and preventing regrowth of protective saltmarsh vegetation (Marani et al. 2011). Since even low wave energies are potentially erosive under these circumstances, it is reasonable to expect that this process is particularly effective at sites with higher wind-wave fetch exposure.

Fig. 5 This actively eroding saltmarsh shore at Duck Bay exhibited visible turbidity that is likely due in-part to fine sediment released into the water at high tide under the impact of the small wind waves visible here, which were generated across a short fetch under moderately breezy but not stormy conditions. It is indicative that this degree of regularly repeating erosion under non-stormy conditions is enough to prevent re-establishment of saltmarsh vegetation. Hence unless there is a drop in the local mean sea-level this shoreline can be expected to continue retreating landwards irrespective of storm event frequencies

Conclusion

Wind-wave fetch exposure modelling combined with either shoreline substrate mapping (geomorphic mapping) or historical aerial photo analysis can be a useful predictor of local and regional variation in shoreline erosion susceptibility where other agents or processes of geomorphic change are absent or insignificant. This means that, in order to use this technique effectively, it is necessary to also have some assessment of other processes that may be agents of shoreline instability in a region, and where these other processes may be locally dominant. Given that the main underlying drivers of shoreline erosion in the study area are thought to be relative sea-level rise and increasing wind speeds, such modelling can help identify areas which are more likely to support particular substrate types into the future. Saltmarshes are of particular interest given their ecological significance and vulnerability (Saintilan and Rogers 2013). Management can then focus on extending saltmarsh habitat range by promoting landward movement, particularly where this is currently prevented by artificial tidal barriers (Prahalad 2014). Indeed, given that similar conditions exist in other swell-sheltered environments in Australia and elsewhere, such modelling combined with geomorphic mapping can be integrated into existing tools for vulnerability assessment and planning holistic coastal area management.

Acknowledgments The data presented here were collected as part of a broader study of coastal ecosystem vulnerability to sea-level rise in far north-western Tasmania, funded by the Cradle Coast Natural Resource Management (NRM) Region and the Cradle Coast Authority. The full report on this broader study (Mount et al. 2010) is available at www.cradlecoastnrm.com/projects_coasts.html.We acknowledge Austin Pepper for allowing use of his wave-exposure modelling software (GREMO).

References

Akumu CE, Pathirana S, Baban S, Bucher D (2011) Examining the potential impacts of sea level rise on coastal wetlands in north-eastern NSW, Australia. J Coast Conserv 15:15–22

Allen JRL (2000) Morphodynamics of Holocene salt marshes: a review sketch from the Atlantic and Southern North Sea coasts of Europe. Quat Sci Rev 19:1155–1231

Benumof BT, Storlazzi CD, Seymour RJ, Griggs GB (2000) The relationship between incident wave energy and seacliff erosion rates: San Diego County, California. J Coast Res 16:1162–1178

Bezerra M, Moura D, Ferreira O, Taborda R (2011) Influence of wave action and lithology on sea cliff mass movements in Central Algarve Coast, Portugal. J Coast Res 27:162–171

Booij N, Ris RC, Holthuijsen LH (1999) A third generation wave model for coastal regions. 1. Model description and validation. J Geophys Res 104:7649–7666

Burrows M, Harvey R, Robb L (2008) Wave exposure indices from digital coastlines and the prediction of rocky shore community structure. Mar Ecol Prog Ser 353:1–12

Chollett I, Mumby PJ (2012) Predicting the distribution of *Montastraea* reefs using wave exposure. Coral Reefs 31:493–503

Church JA, White NJ (2006) A 20th century acceleration in global sea-level rise. Geophys Res Lett 33, L01602

Church JA, Hunter JR, McInnes KL, White NJ (2006) Sea-level rise around the Australian coastline and the changing frequency of extreme events. Aust Meteorol Oceanogr J 55:253–260

Cowart L, Walsh JP, Reide Corbett D (2010) Analyzing estuarine shoreline change: a case study of Cedar Island, North Carolina. J Coast Res 26:817–830

Cowart L, Reide Corbett D, Walsh JP (2011) Shoreline change along sheltered coastlines: insights from the Neuse River estuary, NC, USA. Remote Sens 3:1516–1534

Cox R, Wadsworth RA, Thomson AG (2003) Long-term changes in salt marsh extent affected by channel deepening in a modified estuary. Cont Shelf Res 23:1833–1846

Day JW Jr, Scarton F, Rismondo A, Are D (1998) Rapid deterioration of a salt marsh in Venice Lagoon, Italy. J Coast Res 14:583–590

DCC (2009) Climate change risks to Australia's Coast: a first pass national assessment. Department of Climate Change, Australian Government, 168 pp

Donaldson P, Sharples C, Anders RJ (2012) The tidal characteristics and shallow-marine seagrass sedimentology of Robbins Passage and Boullanger Bay, far northwest Tasmania. Report to Cradle Coast Natural Resource Management Region by the Blue Wren Group, School of Geography and Environmental Studies, University of Tasmania, 88 pp. Available for download at: www.cradlecoastnrm.com/projects_coasts.html

Ekebom J, Laihonen P, Suominen T (2003) A GIS-based step-wise procedure for assessing physical exposure in fragmented archipelagos. Estuar Coast Shelf Sci 57:887–898

Fagherazzi S, Wiberg PL (2009) Importance of wind conditions, fetch, and water levels on wave-generated shear stresses in shallow intertidal basins. J Geophys Res 114, F03022

Feagin R, Lozada-Bernard S, Ravens T, Moller I, Yeager K, Baird A (2009) Does vegetation prevent wave erosion of salt marsh edges? Proc Natl Acad Sci 106:10109–10113

FitzGerald DM, Fenster MS, Argow BA, Buynevich IV (2008) Coastal impacts due to sea-level rise. Annu Rev Earth Planet Sci 36:601–647

Harris PT, Heap AD, Bryce SM, Porter-Smith R, Ryan DA, Heggie DT (2002) Classification of Australian Clastic Coastal depositional environments based upon a quantitative analysis of wave, tidal, and river power. J Sediment Res 72:858–870

Heap A, Bryce S, Ryan D, Radke L, Smith C, Smith R, Harris P, Heggle D (2001) Australian estuaries and coastal waterways: a geoscience perspective for improved and integrated resource management. AGSO record 2001/07, Australian Geological Survey Organisation, 118 pp

Hill N, Pepper A, Puotinen M, Hughes M, Edgar G, Barrett N, StuartSmith R, Leaper R (2010) Quantifying wave exposure in shallow temperate reef systems: applicability of fetch models for predicting algal biodiversity. Mar Ecol Prog Ser 417:83–95

Hood GW (2004) Indirect environmental effects of dikes on estuarine tidal channels: thinking outside of the dike for habitat restoration and monitoring. Estuaries 27:273–282

Lambeck K, Chappell J (2001) Sea level change through the Last Glacial Cycle. Science 292:679–686

Malhotra A, Fonseca MS (2007) WEMo (Wave Exposure Model): formulation, procedures and validation. National Oceanic and Atmospheric Administration, Beaufort

Marani M, D'Alpaos A, Lanzoni S, Santalucia M (2011) Understanding and predicting wave erosion of marsh edges. Geophys Res Lett 38, L21401

Mariotti G, Fagherazzi S (2013) Critical width of tidal flats triggers marsh collapse in the absence of sea-level rise. Proc Natl Acad Sci 110: 5353–5356

Möller I, Spencer T (2002) Wave dissipation over macro-tidal saltmarshes: effects of marsh edge typology and vegetation change. J Coast Res 36:502–521

Mount R, Prahalad V, Sharples C, Tilden J, Morrison B, Lacey M, Ellison J, Helman M, Newton J (2010) Circular head region coastal foreshore habitats: sea level rise vulnerability assessment, Report to Cradle Coast Natural Resource Management Region and the Cradle Coast Authority, by the Blue Wren Group, School of Geography and Environmental Studies, University of Tasmania, 220 pp. Available for download at: www.cradlecoastnrm.com/projects_coasts.html

Murdukhayeva A, August P, Bradley M, LaBash C, Shaw N (2013) Assessment of inundation risk from sea level rise and storm surge in northeastern coastal national parks. J Coast Res 29:1–16

Nanson GC, Barbetti M, Taylor G (1995) River stabilisation due to changing climate and vegetation during the late Quaternary in western Tasmania, Australia. Geomorphology 13:145–158

Pepper A (2009) Extension, generalisation, and verification of a GIS-based relative wave exposure model. BSc Hons dissertation, University of Wollongong, NSW

Pepper A, Puotinen ML (2009) GREMO: a GIS-based generic model for estimating relative wave exposure. In: Anderssen RS, Braddock RD, Newham LTH (eds) 18th World IMACS Congress and MODSIM09 International Congress on Modelling and Simulation. Modelling and Simulation Society of Australia and New Zealand and International Association for Mathematics and Computers in Simulation, Cairns, p 1964–1970

Pethick JS (1993) Shoreline adjustments and coastal management: physical and biological processes under accelerated sea-level rise. Geogr J 159:162–168

Prahalad V (2014) Human impacts and saltmarsh loss in the Circular Head coast, north-west Tasmania, 1952–2006: implications for management. Pac Conserv Biol 20:272–285

Prahalad V, Kirkpatrick J, Mount R (2011) Tasmanian coastal salt marsh community transitions associated with climate change and relative sea level rise 1975–2009. Aust J Bot 59:741–748

Saintilan N (2009) Australian saltmarsh ecology. CSIRO Publishing, Melbourne

Saintilan N, Rogers K (2013) The significance and vulnerability of Australian saltmarshes: implications for management in a changing climate. Mar Freshw Res 64:66–79

Schwimmer RA (2001) Rates and processes of marsh shoreline erosion in Rehoboth Bay, Delaware, USA. J Coast Res 17:672–683

Sheehan RS, Ellison JC (2014) Intertidal morphology change following *Spartina anglica* introduction, Tamar Estuary, Tasmania. Estuar Coast Shelf Sci 149:24–27

Stive MJF, Cowell PJ, Nicolls RJ (2009) Beaches, cliffs and deltas. In: Slaymaker O, Spencer T, Embleton-Hamann C (eds) Geomorphology and global environmental change, Ch. 6. Cambridge University Press, New York, pp 158–179

Stralberg D, Brennan M, Callaway JC, Wood JK, Schile LM et al (2011) Evaluating tidal marsh sustainability in the face of sea-level rise: a hybrid modeling approach applied to San Francisco Bay. PLoS ONE 6(11):e27388

Tolvanen H, Suominen T (2005) Quantification of openness and wave activity in archipelago environments. Estuar Coast Shelf Sci 64: 436–446

Tonelli M, Fagherazzi S, Petti M (2010) Modeling wave impact on salt marsh boundaries. J Geophys Res 115, C09028

Torio DD, Chmura GL (2013) Assessing coastal squeeze of tidal wetlands. J Coast Res 29:1049–1061

van de Koppel J, Van der Wal D, Bakker JP, Herman PMJ (2005) Self-organization and vegetation collapse in salt marsh ecosystems. Am Nat 165:E1–E12

van der Wal D, Pye K (2004) Patterns, rates and possible causes of saltmarsh erosion in the Greater Thames area (UK). Geomorphology 61:373–391

Williams PB, Orr MK (2002) Physical evolution of restored breached levee salt marshes in the San Francisco bay estuary. Restor Ecol 10: 527–542

Zhang K, Douglas BC, Leatherman SP (2004) Global warming and coastal erosion. Clim Chang 64:41–58

Ocean and Coastal Management 154 (2018) 103–120

Contents lists available at ScienceDirect

Ocean and Coastal Management

journal homepage: www.elsevier.com/locate/ocecoaman

National sediment compartment framework for Australian coastal management

B.G. Thom[a,f,g], I. Eliot[b], M. Eliot[b], N. Harvey[c,h], D. Rissik[d], C. Sharples[e], A.D. Short[f,g], C.D. Woodroffe[g,*]

[a] Wentworth Group of Concerned Scientists, Sydney, NSW 2000, Australia
[b] Damara WA Pty Ltd, 2/19 Wotan St, Innaloo, WA 6019, Australia
[c] Department of Geography, Environment and Population, University of Adelaide, Adelaide, SA 5005, Australia
[d] National Climate Change Adaptation Research Facility, Griffith University, Gold Coast, Queensland 4222, Australia
[e] School of Land and Food (Discipline of Geography & Spatial Science), University of Tasmania, Hobart, Tasmania 7001, Australia
[f] School of Geosciences, University of Sydney, Sydney, NSW 2006, Australia
[g] School of Earth and Environmental Sciences, University of Wollongong, NSW 2522, Australia
[h] College of Marine and Environmental Sciences, James Cook University, QLD 4811, Australia

ARTICLE INFO

Keywords:
Sediment compartment
Cell
Longshore transport
Coastal planning
Australia

ABSTRACT

The concept of coastal sediment compartments was first used in the 1960s in the United States. It has since been recognised as appropriate for defining sections of the Australian coast, but had not been uniformly adopted around the nation in the way that has underpinned management, as in other countries. In 2012, the Australian Government supported a project to better understand coastal sediment dynamics using the sediment compartment approach as a framework within which to consider future shoreline behaviour and the impacts of climate change, including rising sea level, changing wave climates and sediment budgets. This paper outlines the sediment compartment project and uses case studies to demonstrate its application. The project consisted of three steps. The first step involved delineation of a hierarchy of coastal sediment compartments following a nationally agreed set of criteria, integrating the onshore/offshore geologic framework with known patterns of sediment movement and those inferred from surface landforms. This identified more than 100 primary compartments bounded by major structural features such as headlands or changes of shoreline orientation. At a finer scale, approximately 350 secondary compartments were identified, many of which encompass smaller scale structural features that define tertiary scale compartments or cells. For verification of this sediment compartments approach to coastal planning and management, the second step of the study comprised case studies of contrasting compartments with different patterns of sediment supply, transport and deposition. The third step, involved embedding all secondary compartments around the continental coast into the Shoreline Explorer, within the *CoastAdapt* toolbox (National Climate Change Adaption Research Facility). Information regarding the sensitivity of shorelines to change was compiled at the compartment scale, based upon evidence such as substrate, sediment transport attributes and oceanographic forcing, including waves, tides and storm processes. Presentation of information through *CoastAdapt* within the compartments framework provides a resource to facilitate improved coastal planning and management over different implementation levels, from national strategy scale down to local policy scale. Case studies from several contrasting settings around the Australian coast demonstrated the potential and feasible application of the sediment compartment approach at different spatial and temporal scales.

1. Introduction

A sediment compartment approach has been used in a number of countries as a means to improve coastal management at a range of spatial scales, through a better understanding of sediment mobility and transport within and between each compartment. The concept was first outlined in the United States (Inman and Chamberlain, 1960; Bowen and Inman, 1966), where it was incorporated into beach management by Komar (1976). Sediment cells, also called littoral drift cells, were delineated for much of the coast of the United Kingdom, based on

* Corresponding author.
E-mail address: colin@uow.edu.au (C.D. Woodroffe).

https://doi.org/10.1016/j.ocecoaman.2018.01.001
Received 13 July 2017; Received in revised form 22 December 2017; Accepted 2 January 2018

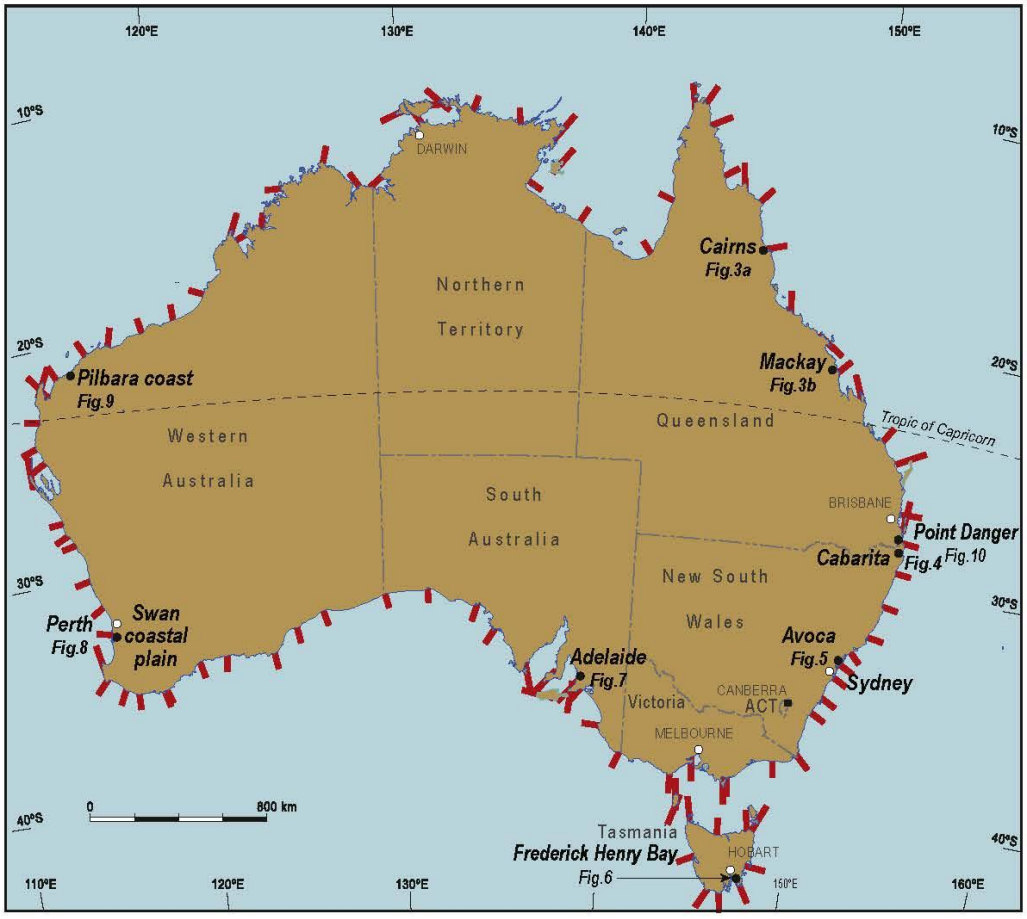

Fig. 1. Boundary points of primary sediment compartments around the Australian coast (from McPherson et al., 2015), and the location of pilot and case study sites.

perceived interruptions to movement of sand and shingle along beaches (Motyka and Brampton, 1993; Bray et al., 1995). These cells form the basis for shoreline management plans in England and Wales (Cooper et al., 2001, 2002; Cooper and Pontee, 2006; Nicholls et al., 2013).

In Australia, the concept of the coastal sediment compartment was introduced by Davies (1974). He recognised the nature of sediment compartments and a hierarchical structure of these around the Australian coast (Davies, 1977, 1980), where significant quantities of sand are transported northwards along both west and east coasts (Short, 2010). Efforts were made to understand the sediment budget for the Gold Coast (Chapman, 1981), and these concepts were applied along New South Wales (NSW) in a monograph focused on coastal management (Chapman et al., 1982). Searle and Semeniuk (1985) proposed a natural sectors approach that guided overall management of large-scale coastal works in southern Western Australia.

As indicated above, there is no standard usage nor definition of the terms cell and compartment, with littoral or sediment cell, coastal cell, sediment compartment and coastal compartment all utilised to define a section of coast (Cowell et al., 2003; McGlashan et al., 2005; Woodroffe et al., 2012; Eliot, 2013; George et al., 2015; Tecchiato et al., 2016). The terms are sometimes used interchangeably and at other times may mean somewhat different things. Despite the use of the term sediment cell in the UK and USA, general Australian usage prefers the term cell employed at a smaller spatial scale than compartment. In Western Australia, both cell and compartment terms and concepts have been used, with the smaller cells nested with larger compartments. For instance, Eliot et al. (2011) focus on compartments defined by broad scale structural elements. This contrasts with more recent reports by Stul et al. (2012, 2015) which place emphasis on transport processes at a finer scale and use the concept of cell to reflect connectivity of mobile sedimentary features. Much depends on the purpose of the investigation. In this study undertaken at a continental scale, it was agreed to use the term sediment compartment within a much broader hierarchical classification.·

In 2012, the Australian Government supported a project to better understand coastal dynamics for the entire continent including consideration of potential climate change impacts. The project was seen as providing a method for assessing present and future natural hazards and impacts to coastal assets at risk from extreme events and climate change. The approach is based on an understanding of Australia's coastal geomorphology and sediment pathways using geologic frameworks for understanding movements of sediments and shorelines at present-day and future time scales. The approach and definition of the hierarchal coastal sediment compartments are provided in section 3 and section 5.2 identifies some key compartment characteristics relevant to assessing hazards.

The project built on previous recent work supported by the Australian Government, which assessed climate change risks to Australia's coasts (Harvey and Woodroffe, 2008; DCC, 2009; Harvey and Caton, 2010). It involved a *First Pass National Assessment* and incorporated a detailed shoreline classification termed *Smartline* (Sharples et al., 2009). In 2011, the Australian Government agreed that steps should be undertaken to assess risk through the application of the nationwide sediment compartment approach, especially given its initial

successful application in Western Australia (WA) in relation to coastal planning (Stul et al., 2007; Eliot et al., 2011). This has led to the stepwise evolution of the *Coastal Sediment Compartment Project* (Thom, 2015), which was initially supported by Geoscience Australia (GA) and subsequently by the National Climate Change Adaptation Research Facility (NCCARF) as part of the Shoreline Explorer tool within *CoastAdapt* (https://coastadapt.com.au/).

The project comprised three steps. The **first step** consisted of a national hierarchical classification of the entire 30,000 km long Australian coast identifying boundary points for provinces, divisions, regions and primary and secondary compartments each defined by orientation, geologic and topographic characteristics (Hazelwood et al., 2013; McPherson et al., 2015). Sitting within the secondary compartments are smaller tertiary compartments or cells with identifiable pathways of sediment movement driven by waves and currents. The dynamics and connectivity of sediment transfers from sources to sinks within these compartments, operating over differing time scales, indicate areas of potential vulnerability to the impacts of extreme events and climate change.

The **second step** was to undertake two pilot studies: one at two sites in WA on the west coast (the Swan and Pilbara regions, Eliot, 2013), and the other in NSW on the east coast at two sites (Avoca Beach in central NSW, and Cabarita Beach in northern NSW, Mariani et al., 2013) (see Fig. 1 for locations). These studies examined ways to assess complex geomorphological relationships between the underlying geology and coastal sediments, including the direction and magnitude of sediment transport, the sediment budget and the vulnerability of the shoreline and assets to extreme events and scenarios of climate change.

The **third step** was developed as part of *CoastAdapt*, a NCCARF phase-2 project to support coastal stakeholders and communities in Australia manage risks associated with a changing climate, funded by the Australian Government through the Department of Environment (changed in 2016 to Department of Environment and Energy). It was agreed in 2015 that a team of coastal scientists with expertise in coastal geomorphology should pool their knowledge to examine characteristics of compartments around the Australian coast at three spatial scales, primary, secondary and tertiary. The emphasis was on the secondary scale, of which there are around 350 mainland compartments. The emphasis has been on providing preliminary information on the nature of and potential impacts in each compartment, in a user-friendly format, in order that users would be better equipped to make use of the compartment approach in adaptation planning.

Use of this multi-scale sediment compartment approach, in which sediment movement is linked to geological frameworks and coastal processes, better accounts for the varying coastal conditions around the Australian coast. It offers a powerful tool that can be used to make robust and consistent assessments of sea-level rise and changes to other forces associated with regional variations in the impacts of climate change. Recent advances in technology and coastal science have improved the nation's capacity to use the approach, including capture of the fine-scale form of seabed texture and structures through remotely-sensed techniques. Interest has already been shown by state governments in the potential for application of the approach at state and regional levels. There is recognition that more information on sources and movements of sediments, especially offshore, will give potential users a greater capacity to make decisions on use of coastal lands than exists at present.

2. Background

2.1. Concept of coastal sediment compartment

Coastal sediments move along a number of pathways over time as they are transported by various processes into temporary or permanent coastal sinks. Sources of beach material, their modes of transport across and beyond the surf zone, and their longshore transport, were described by Cuchlaine King in her synthesis of beach processes (King, 1972). She recognised the pioneering work of Californian researchers in developing the sediment cell concept. This concept goes back at least to Inman and Chamberlain (1960) and Inman et al. (1963) who developed the littoral compartment/cell concept for southern Californian and Kauai respectively. Inman and Frautschy (1966) then identified four littoral sediment compartments along the central California coast, whereas Bowen and Inman (1966) identified positive and negative contributions to a littoral sediment budget. Komar (1976) in reviewing the California research went on to examine the various sources of coastal sediments, their means of transport and losses, and Rosati (2005) described approaches to determining a sediment budget. Sediment cells also underpin management of much of the coast of Great Britain (Motyka and Brampton, 1993; Cooper and Pontee, 2006; Nicholls et al., 2013), forming the framework for shoreline management plans.

In Australia, Davies discussed coastal sediment transport systems, including sediment sources, transport, and sinks, putting these factors together to present the concept of a coastal sediment compartment, with its inputs, outputs and store (Davies, 1974). In 1977, he applied this concept to his overview of the Australian coast which he divided into four segments (Davies, 1977): warm temperate humid, warm temperate arid, tropical arid and tropical humid. Chapman et al. (1982) used the sediment budget approach to assess both the evolution and present stability of coastal compartments along the NSW coast. The northern NSW coast is dominated by longshore transport of sand to the north, as discussed below; whereas the southern NSW coast is more embayed with prominent headlands that interrupt longshore sand transport. Chapman et al. (1982) mapped all major compartments discriminating whether their boundaries were closed or leaky to longshore transport.

Recently, several studies have diagrammatically and quantitatively depicted some of the different ways sediment systems operate on the Australian coast (Woodroffe et al., 2012; Eliot, 2013; Mariani et al., 2013), following the concepts introduced by Davies (1974). These studies show how coastal investigations can capture the relative importance of sediment processes in relation to shoreline behaviour. The power of such studies is their ability to determine changes in sediment volume along vulnerable shorelines where natural and built assets are at risk from erosion or inundation under different sea-level and wave conditions.

Building on earlier work by authors such as Searle and Semeniuk (1985), recent reports in Western Australia on coastal compartments (Eliot et al., 2011) and sediment cells (Stul et al., 2012, 2015) provide separate physical frameworks for marine and coastal planning. In the 2011 report, available descriptions of geologic features and large landforms were used to identify compartments at strategic, regional and local scales currently used for coastal planning and management. The more recent work of Stul et al. (2015) focusses at a local government and site scale. In WA, these multi-scale frameworks facilitate comparison and analyses of environmental data across and within each compartment as well as between different levels in the hierarchy (Eliot et al., 2011). Critically, they are seen as steps in coastal risk analysis that will ensure more efficient allocation of resources. They also address issues of present sustainability and adaptation to climate change, the latter including both sea-level rise and potentially disastrous impacts of more extreme events on the economy and society.

It is recognised that investigations at the tertiary sediment compartment scale are most useful to define and analyse active geomorphic processes that move sediments into, along, and out of, a section of coast. Calculation of a sediment budget within a tertiary compartment can be extended to the secondary scale if appropriate. Essentially there is a “store” of sediment within a tertiary compartment comprising landform units, such as beaches, barriers and dunes, which are capable of being mobilised under different process conditions of varying magnitude and frequency. The nature of those processes could change over

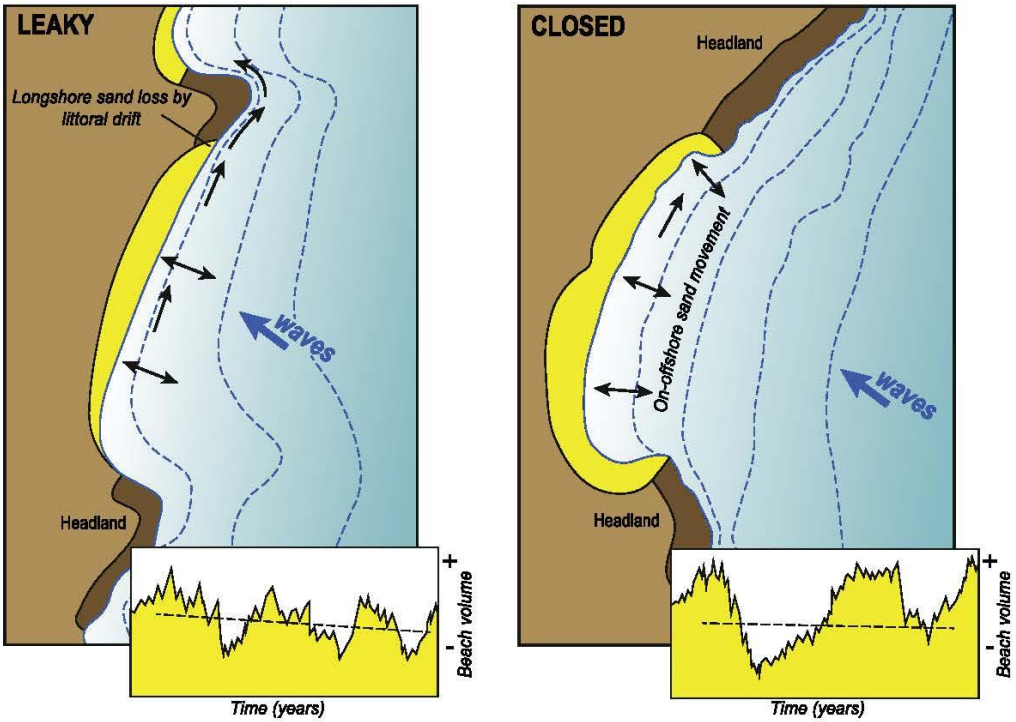

Fig. 2. The concept of 'leaky and 'closed' sediment compartments, expanding on depiction by Thom (1989). Black arrows indicate sediment pathways, and the compartment are typical examples at the tertiary scale.

time, especially as sea level rises and wave climate changes.

The concept of the 'closed' coastal sediment compartment was applied to the southeast Australian coast by Davies (1974). The concept was expanded in this region by Chapman et al. (1982), who showed how differences in the supply of marine sand over the last 6000 years have led to the evolution of different types of coastal barriers (see also Thom, 1974; Roy et al., 1994; Woodroffe et al., 2012). Thom (1989) simplified the concept into two types: 'closed' and 'leaky', and this contrast is illustrated in Fig. 2. Recently it has been shown how consideration of headland characteristics can be used to infer the extent to which longshore transport along the coast of California is impeded (George et al., 2015). As noted by Woodroffe et al. (2012), this approach in NSW has been considered a useful tool in the estimation of sediment budgets, following procedures outlined in the NSW Coastline Management Manual (1990).

2.2. The national need for the sediment compartment approach

In its report to the Minister for Climate Change and Energy Efficiency in 2011, the then Coasts and Climate Change Council recommended that the Australian Government establish a science-based program that would develop and deliver consistent information on climate change risk. Such a program should involve centralised access to information on the physical effects of climate change, including the use of regional modelling, in order to assist with hazard assessment and coastal management planning and decision making. In the view of the Council, state agencies and local governments would benefit from access to such information. Intergovernmental collaboration was suggested as part of the program as this would minimise duplication and make for more efficient use of funds and technical resources. Although this Council ceased to exist in 2012, the incoming Minister for Environment in the Australian Government, agreed that there was a need for a national analysis of risk to coastal local governments in managing impacts from climate change and supported the recommendation for further work on the sediment compartment approach.

The need for information on Australia's many coastal regions, and more coordination between levels of government with coastal management responsibilities, was identified in the report of the Standing Committee on Environment to the House of Representatives in 2009 (HORSCCCWEA, 2009), the DCC Coastal First Pass Risks report (DCC, 2009), and the Baker and McKenzie legal liability study commissioned for Australian Local Government Association (Baker and McKenzie, 2011). This need follows past recommendations to the Australian Government through national inquiries as far back as 1979 advocating a stronger role for the Australian Government in coastal management similar to that in other federated nations. In Australia, coastal planning and management is largely the responsibility of state and territory governments with varying levels of delegation to local governments. There is a very limited role for the Australian Government (Harvey and Caton, 2010). Stakeholder engagement prior to the development of *CoastAdapt* indicated that stakeholders wanted more information about the most appropriate scales for climate adaptation planning, access to better information and guidance on sediment and coastal dynamics, as well as on the susceptibility of the coast to climate change effects. All these interests are addressed by the sediment compartments approach, with the secondary compartment chosen in this study to provide a regional assessment of the sediment behaviour and budget, while acknowledging at an operational level the tertiary compartment and its behaviour is the key to both understanding present conditions as well as predicting future impacts at a more local level.

The scientific basis for adopting a national approach to assessing hazard impacts and consequent risk to built and natural assets emerged from the *First Pass National Assessment* (DCC, 2009). Differences in geology, climate, geomorphic processes, ecological conditions, and projections of impacts of climate change drivers on sections of the

Australian coast highlighted the need to develop methods that would capture the direction and rate of present and future coastal change needed in decision making. These geographic differences have been well established in national reviews of coastal Australia including the work of Bird (1971, 1993), Davies (1974), Galloway et al. (1984), Thom (1989), and Short and Woodroffe (2009). However, it was the work of DCC (2009) in highlighting the huge cost to the Australian taxpayer of impacts of climate change, in particular sea-level rise, which drove home the future requirement for a national, coordinated approach. Successive federal governments have resisted the opportunity to take a clear leadership role leaving state and local governments to address issues with their own resources. Nevertheless, the federal government did recognise that NCCARF, a university-based facility, should be supported at least until 2017 to assist in providing improved tools, such as *CoastAdapt*, for state and local governments to use in addressing climate change problems. To this end the sediment compartment approach has been tested by integrating the coastal and seabed geology with known patterns of sediment movement and those inferred from depositional landforms. Sediment compartments can be applied at different spatial and temporal scales and information made available as a resource to facilitate improved coastal planning and management. While the spatial scale is defined by the compartment boundaries, the temporal scale will consider the contemporary compartment behaviour, as well as predicting future behaviour based on relevant climate scenarios.

3. The national hierarchical classification

As a way to achieve a consistent approach to understanding changes to coastal conditions in the future, a decision was taken at the national level to adopt a hierarchical geographic classification. Within this classification secondary compartments, the focus of this study, are located.

Geoscience Australia (GA) coordinated the development of this hierarchical division of the Australian coast into compartments. The approach was based on previous multi-scale work in WA (Eliot et al., 2011). This provided a framework for the national classification undertaken by a group of experts working initially with GA. Expert judgements were used to define compartment boundaries down to the secondary scale and to establish boundary points based on the criteria outlined below. The results were quality checked by others including representatives of state governments and are now available on the GA website (https://data.gov.au/dataset/primary-and-secondary-coastal-sediment-compartment-maps).

The following indicates the hierarchical classification adopted in this project:

- **Provinces (2):** Based primarily on climate and divided roughly along the Tropic of Capricorn (between North West Cape 21°45′S and Sandy Cape 24°40′S) into the northern *tropical* coastal province and southern *temperate* coastal province In other countries climate, orientation and other major delineations may be involved.
- **Divisions (7):** Based on *province*, then primarily coastal orientation (NW, NE, SE, S and SW), apart from the Gulf of Carpentaria.
- **Regions (23):** Based on *division*, then geology, with some contribution from coastal orientation/configuration, as in Tasmania, an island with three distinctive coasts, and the irregular South Australian gulfs.
- **Primary compartments (102):** Based on *regions*, which are then subdivided at major physical coastal boundaries into primary compartments. Primary coastal compartments are sections of the coast that are bounded by major, usually distinctive, structural features such as rocky headlands or major changes in orientation of the coast.
- **Secondary compartments (> 350):** Based on *primary compartments*, with subdivisions into secondary compartments recognising secondary coastal boundaries. Secondary compartments are also formed by structural elements within which there may be sediment exchange. Secondary boundary points are identified at scales between 1:1,00,000 and 1: 25,000.
- **Tertiary compartments (> 1000):** Based on *secondary compartments*, which are sub-divided at obstructions (usually headlands) into tertiary compartments, some as small as an individual beach. Tertiary compartments may act as self-contained sediment compartments or be linked to adjoining compartments. These typically occur at scales less than 1: 25,000.

In order to obtain a national overview of coastal behaviour now and into the future, the decision was made to focus on the secondary compartment scale (Fig. 1). At this scale it was considered by the authors that sufficient information was available to provide a national understanding of the sensitivity of shoreline change building on earlier national scale work by Sharples et al. (2009) using the *Smartline* method (which provides a linear segmentation of the Australian shoreline based on characteristics of form and fabric). To this end, ~350 secondary compartments have been identified; several further compartments may be added when outlying islands are considered in more detail (for example, Torres Strait). In some cases the relevance of information will be increased by studies focused at the tertiary scale that have been, or should be, undertaken to better inform decision makers. Pilot studies were undertaken at a tertiary level to demonstrate the influence of compartment structures on coastal dynamics at this scale.

4. Pilot studies

The aim of Step 2 was quite specific: to use pilot studies to investigate the potential application of the sediment compartment approach in characterising how specific sections of coast would respond under present and future conditions. This involved two projects on either side of the continent to examine geologic and landform characteristics, oceanic and sediment transport processes, and sediment budgets at four locations to test the applicability of the approach. In Western Australia, the project was undertaken by Damara Pty Ltd which has experience in working with WA state agencies in applying similar concepts. The company selected contrasting sites in microtidal wave-dominated Swan coastal plain in the southwest and arid, macrotidal Pilbara in the northwest (see Eliot, 2013). In New South Wales, the Water Research Laboratory (WRL) of the University of New South Wales studied two sites, the embayed Avoca Beach in central NSW and longer more open Cabarita Beach in northern NSW (Mariani et al., 2013).

The **Damara** project investigated two Western Australian sites and, using late Holocene coastal landforms in very different coastal environments, demonstrated that a compartment hierarchy supports improved representation of long-term coastal dynamics. The project provided examples of geomorphic and geologic setting influence on coastal response to sea-level rise. For the southwest site, significance of discrete pathways for shelf-shore sediment exchange through coastal reef systems was identified, influencing the spatial distribution of expected response within larger scale coastal compartments. For the northwest site, the roles of episodic sediment supply from rivers and the wide area of coastal floodplain were examined through landforms and available sediment budget evidence. This suggested that the coastal floodplain response to sea-level rise is likely to change systematically along a coastal compartment, reflecting the relative availability of sediment and its ability to be transferred across the floodplain. The contrast between the geomorphic features defining the active compartment between the southwest and northwest sites suggested there may be a need to identify compartments in different ways according to their setting.

The **WRL** sites represent contrasting closed and leaky tertiary scale compartments. This project examined shoreline response to extreme events and climate change at both sites and tested the applicability of

deterministic and probabilistic approaches for the assessment of coastal change. Sediment budgets were inferred with consideration of present day and future climate change scenarios out to 2100. Probabilistic modelling was seen as a method for evaluation of long-term shoreline responses that would most assist planning and management decisions.

In all four study areas, the inherited character of landforms of late Quaternary age, including but not confined to deposits emplaced during the last 6000 years, offered investigators a sediment exchange history that can be shown to influence shoreline change at both multi-decadal and short-term storm impact scales.

Some of the **key lessons** learnt from the pilot studies in **Step 2** include:

- There is a fundamental need for high quality bathymetric data. Often areas of concern around the Australian coast lack such data from low tide to depths of expected sediment movement on the inner continental shelf, so-called "closure depth". These depths will vary with compartment type, sediment type and energy conditions (e.g. 10–60 m water depth). However, modelling studies require good bathymetric control which is usually available on land but less so below sea level.
- Coupled with bathymetry is the need for data on surface sediment texture from the beach-beach to the inner continental shelf (10's of metres depth), which is essential for modelling. Sediment data can be obtained through mapping of sediment bedforms and rock features (for instance, by using marine LiDAR or other forms of bottom and sub-bottom mapping and profiling); and, by coring and dating the sediment sequence at shallow depths to measure the depth of reworking and evaluate the shoreface evolution over the past several hundred years.
- Barrier and preferably shoreface chronology is desirable to set the present coast within its evolutionary framework. Knowledge of barrier evolution provides data on rates of sand supply and impacts of longer term changes in drivers such as wave climate and sediment budget. Work by Goodwin et al. (2006) in northern NSW and Oliver et al. (2017a, 2017b) in southern NSW has been able to reconstruct Holocene sediment budget and its variation though time in response to changing climate, sediment supply and/or degree of embayment infilling. On a regional scale, Short (2010) used the volume of Australia's barrier systems to calculate rates of onshore Holocene sand supply around the coast.
- Large sections of northern Australia, like the Pilbara, experience high tidal ranges and low waves, and have a mix of sand and muddy sediments, often interacting with mangrove communities. Sediment movements in such locations require careful mapping and understanding of processes of sediment exchange, often developed through fine-scale transitions and interactions between wave and tidal current forcing. These regions also have low-lying coastal plains that experience cyclone-driven river floods, extreme waves and marine inundation. In such locations, coastal change can be the result of episodic state-changing events, followed by lower energy wind, wave and tidal conditions. These can produce sequential, ephemeral and relict landforms. Assessment of potential climate change impacts requires an understanding of these complexities at different scales.
- Another highly desirable data set should come from long-term monitoring nearshore, beach/intertidal and backshore environments. The WRL report (Mariani et al., 2013) concludes that high quality topographic surveys, preferably in concomitance with wave data, will allow validation of models of shoreline change including capacity of beaches and dunes to recover from the impact of erosion events. Surveys of beaches influenced by the presence of intertidal rock surfaces (such as the different types of "perched" beaches described in the Damara report, Eliot, 2013) require special attention due to inherent difficulties in applying standard modelling techniques.
- Modelling of shoreline change using the sediment compartment approach involves consideration of complexities beyond those normally invoked in standard numerical modelling approaches such as the Bruun Rule (see Woodroffe et al., 2012, section 3.4 for a review of the issues in using the Bruun Rule for coastal planning and management). Eliot (2013, p. 33) cautions against reliance on a tool that gives a fixed allowance for a setback suggesting that the method used in WA under the State Coastal Planning Policy has "partly stifled sub-regional assessment of the threat provided by sea-level rise". Both pilot studies examined the need to understand geomorphic and sediment transport factors in any model of shoreline response to extreme events and to sea-level rise.
- Pilot studies offered support for a close examination of the drivers of sediment movement and how models should best incorporate that knowledge in assessing shoreline change, inundation and risk to assets. They highlight the need for both maintaining and indeed expanding wave and tide recording systems as a spatial network around the Australian coast.
- Both the WRL study (Mariani et al., 2013) and the Damara report (Eliot, 2013) showed how the sediment compartment approach at both tertiary and secondary scales can assist in determining rates of alongshore/littoral transport. The rates vary over time as well as between different sites highlighting the need to consider time scales. This point is made in the Damara 2013 report in their evaluation of how carbonate sand moves through and along different calcarenite reefs on the inner continental shelf. It is also an issue along the NSW coast where there is uncertainty over the connection between so-called relict offshore sand bodies and the nearshore.

5. NCCARF national coastal compartment project

5.1. Framework and method

The team of coastal experts that divided the Australian coast into provinces, divisions, regions, primary compartments, and secondary compartments made an assessment of the ~350 secondary compartments in relation to the sensitivity of its shorelines to change over time. This is the **third step** in the evolution of the Australian approach to using the coastal sediment compartment concept.

Access to this information can be obtained from the NCCARF website under the heading of *Shoreline Explorer* in *CoastAdapt*. This shows boundaries of each compartment, an attribute table describing location, general geomorphology, and sensitivity to change. The table also contains a pdf link to more information for that compartment including in some cases specific details on selected tertiary compartments or cells. The scale of such compartments, in general, makes them convenient on a national scale to assess present-day changes in shoreline position and hence potential for modification under changed climate conditions. It was assumed that present-day exposure and vulnerability of assets are reasonable guides to where problems are likely to arise as a result of ongoing sea-level rise and therefore where adaptation efforts may be needed.

5.2. Assessment of sensitivity of compartments to change

One of the key objectives of the project at a national scale was to assess the sensitivity of different shoreline types to change over time. While no specific time frame was defined, it was assumed that the drivers for change in any given secondary compartment would interact with available sediment and landform conditions at both a regional and local morphodynamic level (following principles outlined in Wright and Thom, 1977; Cowell and Thom, 1994; Wright, 1995). Accordingly, information is provided for each secondary compartment on sensitivity to future change, including sea-level rise. A sensitivity rating was assigned to each compartment to which is also attached a confidence rating.

5.2.1. Sensitivity

A key purpose for which the sediment compartments project was undertaken was to provide information on the sensitivity of coastal landforms to climate change. Sensitivity was assessed using expert opinion based on available information in the geographic area. This is focused primarily on their morphodynamic behaviour in response to sea-level rise over coming decades, but includes potential impacts through changing wave climate (height, direction), including increasing mid-latitude mean and extreme wind speeds generating increased local wind-waves, altered cyclone intensity, duration and tracks, and more subtle adjustments to tidal amplitude, sea-surface temperature, or changes in terrigenous sediment delivery as a result of changes in rainfall and runoff. The sensitivity of unconsolidated sandy and muddy coasts as well as weakly lithified rocky shores within each secondary compartment has been ranked according to the following scale (see https://coastadapt.com.au/sites/default/files/factsheets/Datasets_guidance_1_present.pdf):

1. Shorelines that are presently accreting and are likely to continue or accelerate their accretion as sea-level rise continues (as a result of increased supply of sand from an alongshore source or from river/tidal channel sources).
2. Shorelines that are currently stable but are likely to start accreting as sea-level rise continues (includes shorelines that periodically grow seaward but may be subject to episodes of erosion).
3. Relatively stable shorelines which may be subject to periodic erosion followed by recovery (accretion), but no long-term recession expected in the next few decades since the sediment budget remains sufficiently balanced over time from offshore, alongshore or terrestrial sources.
4. Shorelines that currently do not show evidence of long-term recession but are likely to begin receding with continuing sea-level rise (based on sediment availability onshore and offshore).
5. Shoreline recession is occurring now (typically documented by historical shifts in shoreline position) and the shoreline is likely to continue to recede as sea level rises (possibly at a faster rate depending on local conditions).

Sensitivity scores in many heterogeneous secondary compartments vary from one tertiary compartment to another, indicating the importance of focusing at the appropriate scale when making coastal management decisions. The significance of the principal factors influencing the sensitivity scores is outlined below.

Sediment budget is typically the most important determinant of landform sensitivity to sea-level rise for open coast (swell-exposed) sandy beaches (Komar, 1996; Rosati, 2005). Sandy coasts are highly dynamic environments, which may be subject to net gains (positive) or losses (negative) of sediment over time. Sand may be supplied to the compartment by onshore transport from shelf sources, from alongshore transport into compartments including headland bypassing, or from sources such as river input, cliff erosion, or dune headland overpassing. Sand may be lost through offshore transport, by alongshore transport, by landwards transport into mobile dunes, or via tidal current transport into estuaries and flood tide deltas. Some compartments (e.g. deeply embayed beaches) may have a dynamic but balanced sand volume which neither gains nor loses sediment over time. The sediment budget of many compartments is highly variable and can switch from positive to negative, either episodically or in response to a long term change in conditions. In particular, sea-level rise may result in a switch to a more negative budget as higher sea levels result in more frequent erosion events or make greater accommodation space available for sand to be lost into sinks such as estuaries. The periodic storm cut, and recovery, typical of many Australian beaches, can transition into a system which undergoes long-term recession, depending on factors such as the recurrence frequency of storms and the availability of a sediment supply. Whereas the sediment budget on a beach may be quite variable, weakly lithified shores (such as Tertiary-age cohesive clays in southeastern Tasmania, or shores abutting the lateritic soils in the Pilbara in WA, or weakly lithified dune-rock calcarenite across southern Australia) can be considered as always losing. These settings can only lose sediment through erosion, especially their clay and silt fractions, and cannot subsequently recover. Such shorelines may exhibit a relatively early acceleration of prior rates of shoreline retreat in response to sea-level rise (Trenhaile, 2011).

Substrate or composition of coastal landforms determines erodibility and also the capacity to accrete or recover from erosion. Erodible coastal landforms on the Australian coast are dominated by unconsolidated sandy shores, muddy coasts and semi-lithified 'soft-rock' coasts and are potentially sensitive to sea-level rise. Depending on other conditions, some of these shores, most notably sandy beaches, but also some saltmarsh or mangrove shores, may accrete and recover following erosion, and so may be relatively resilient in the face of sea-level rise.

Wave climate due to both swell waves and locally generated wind waves provides a driving force on open coasts. Waves can cause cross-shore sediment movement in either direction, typically occurring as cycles of storm erosion and recovery. On a high energy beach system, this process may support the coastal adjustment to sea-level rise, by causing a net transfer of sediment from offshore towards the beach. In contrast, sandy shores within tidal but swell-sheltered locations, such as estuaries and tidal lagoons, commonly experience a less balanced erosion-recovery cycle, with increased tendency for horizontal deposition during the recovery phase. This discrepancy in the pattern of erosion-recovery means that lower energy shores can potentially be more susceptible to progressive recession under rising sea levels. Changes in wave climate, particularly in wave height and direction, can have dramatic impacts on sandy shores as they erode and/or realign and change their rates of longshore sand transport.

Extreme events refer to the frequency and intensity of waves exceeding a certain level (e.g. > 3 m) which leads to general beach erosion. High energy wave-dominated beaches (such as those across southern Australia) are likely to begin receding relatively early in response to sea-level rise. This occurs because relatively small rises in sea level enable storm waves to begin eroding the upper beach too frequently for full beach recovery to occur between erosion events. On soft-rock coasts which do not in any case recover from erosion, a higher frequency of erosive storm wave events (including locally-generated wind-wave events) may be expected to result in a greater acceleration of prior retreat rates compared to less stormy shores. In a changing wave climate any increase in the frequency and/or intensity of extreme events will not only erode the beaches but could accelerate shoreline recession.

5.2.2. Confidence

Detailed studies of some tertiary compartments, including their sediment budget and Holocene evolution, have been undertaken in NSW and WA (for example those studies noted above in Step 2). However, for the greater part of the Australian coast, relevant information on geomorphic, geological and meteorological and oceanographic conditions is only available at regional scales. In order to provide a characterisation of the sensitivity of secondary compartments to sea-level rise for the entire Australian coast, it has therefore been necessary in many cases to infer potential for change from expert judgement of the relative susceptibility of one landform compared to another. Processes are inferred from what is known about each landform type and its known capacity to change over short, medium and long time scales.

In order to clarify the degree to which the differing sensitivities have been applied to each compartment on the basis of detailed studies as opposed to simply expert judgement based on limited information, a 'Confidence' ranking has been applied to the description and sensitivity ratings provided for each compartment (e.g. Rissik et al., 2005; Maxwell et al., 2015), as follows:

Low	There is limited or no information describing landforms or coastal landform change over the historical period.
Medium	Some information is available on changes to landforms; it may come from multiple sources which may include recent landform change from site descriptions and occasional aerial photographs over past decades.
High	Detailed information is available identifying changes to coastal landforms spanning the historical period, and includes regular remotely-sensed information over the past 30 years or more.

5.3. How to use Shoreline Explorer for coastal compartments

The following are recommended steps to assist users of *CoastAdapt Shoreline Explorer* to access coastal compartment information for application in coastal management and adaptation (see https://coastadapt.com.au/sites/default/files/factsheets/Datasets_guidance_1_present.pdf).

1. Start by looking at the coastal compartments information and identify the level of sensitivity for the compartments that relate to a local government area or location of interest. The sensitivity rating is on a scale of 1–5, with higher numbers indicating a greater sensitivity to erosion, and lower numbers a greater likelihood of accretion.
2. If the sensitivity to change is medium to high, for example 4 or 5, a brief indication of the reason is provided in the *Shoreline Explorer* attributes and attached descriptions, however it is useful to get further expert advice on the cause of the erosion risk. For example, this may be needed to understand whether the sensitivity is due to high volumes of longshore sediment transport, or a deficient offshore sand supply. Limited offshore sources of sand are often revealed at beaches where recovery from storm erosion is slow or incomplete. Additionally, a high level of sensitivity suggests that planning may need to consider adjacent compartments.
3. Consider the scale of planned development in the area adjoining a coastal sediment compartment. If a large or high value development is planned, for example a hospital, it is useful to consider the implications of that development at all compartment scales. Detailed impact modelling using local data will also be needed for large developments or for critical infrastructure. For many smaller decisions, it is appropriate to consider implications at a more detailed scale than the scale of secondary compartments.
4. If a planned development is near a sediment compartment boundary, or where a boundary is shared by adjoining local government agencies it is useful to consider the adjoining sediment compartments, as well as for the adjoining councils to consult in planning, assessment and decision-making (see metropolitan case study, section 6.4, and NSW *Coastal Management Act* (2016) section 16 (1) (b) (i)).

Other sources of information will also be required for effective coastal planning and management, particularly where the compartment sensitivity rating is high. For example, designing effective coastal protection measures requires an understanding of the location, nature, volume and transport of local sediment sources. The following section makes use of the compartment approach from a number of Australian cases to show how an understanding of sediment movements over time will be important for planning and management purposes.

6. Application of the Australian approach: case studies

It has been possible from this national review of Australian sediment compartments to select a set of locations that clearly illustrate the type of change occurring around the coast, together with an understanding of pathways of sediment movements and estimates of sediment budgets that bring about these changes. Based on these and other cases in Australia, this approach clearly helps explain spatial variation of coastal landforms subject to change as a result of sea-level rise and other effects of climate change, and offers a valuable tool in any assessment of impacts of such changes. There is an increasing emphasis on using a variety of methods to determine rates and directions of sediment movements in and out of compartments at different spatial and time scales. While it is not yet possible to offer any more than initial estimates of the magnitude and direction of such processes, it is a matter of growing interest from government agencies in all states to improve the national capacity to provide both resilient and adaptive actions to protect natural and built assets at risk in locations close to the shore.

Six case studies have been selected. These case studies were selected to cover different climate and environmental conditions and, ranging from tropical to temperate to arid, river-dominated to wave and/or tide-dominated, quartz and carbonate rich, and one metropolitan. Each case is underpinned by a large range of investigations, with some of the relevant papers listed in the pdf file noted in the attribute table in *Shoreline Explorer*, and a subset of references contained herein to highlight the nature of work undertaken to date. Each study makes some indication of potential risk associated with likely future shoreline change is possible based on our interpretation of sensitivity, level of confidence in the information available, and what are considered to be impacts under climate change.

6.1. River-dominated coast

The northern tropical humid coast of Australia has numerous river systems that have built deltas at their mouths. On the northeast coast these are exposed to southeast trade wind and waves, coupled with meso to marco tides which flood to the north, all resulting in predominantly northerly transport of river derived sand. Two examples of river deltaic systems from north Queensland, a tropical humid region with episodic fluvial sediment supply to the coast, are shown in Fig. 3. The area associated with the Barron River delta, between Trinity Inlet and Buchan Point, includes the low-lying city of Cairns, its airport and urban residential and cane-farming lands to the north. It is characterised by tradewind and tide driven longshore transport, including headland bypassing, and exposure to tropical cyclones. Large tracts of coastal land here are vulnerable to river flooding and storm surges accompanying tropical cyclones and sea-level rise (Nott, 2005). The Barron River supplies ~5000 m^3/yr; however, northerly longshore transport exceeds this amount (Fig. 3a) leading to a negative sediment budget and ongoing shoreline recession, requiring that the shoreline is protected by armouring. In addition the river channels switch and tend to deliver variable pulses of flood-borne sediment all of which leads to a dynamic and eroding shoreline (BPA, 1984). Future sea-level rise will exacerbate these present trends, and when combined with inundation from river flooding, along with storm surges during projected more intense cyclones, will require considerable planning and investment in infrastructure to ensure the urban and rural areas minimise risk. Sediment moved alongshore accumulates in sinks which should continue to accrete in the future.

The Pioneer River, in the vicinity of the city of Mackay, discharges ~44,000 m^3/yr of sand to the coast. The tidal range is ~6 m and there is bi-directional flow of sediment at the mouth as shown in Fig. 3b (EPA, 2004). Most sand however is transported ~30 km north by tradewind driven longshore sand transport and headland bypassing into a sink at Sand Bay while Far Beach immediately to the south receives considerably less and is slowly accreting. These processes will most likely continue into the future. Much of Mackay, however, is built on the low-lying Pioneer River floodplain and has a history of inundation from storm surges and river flooding. In this area vulnerability under climate change will largely be an extension of the inundation threats

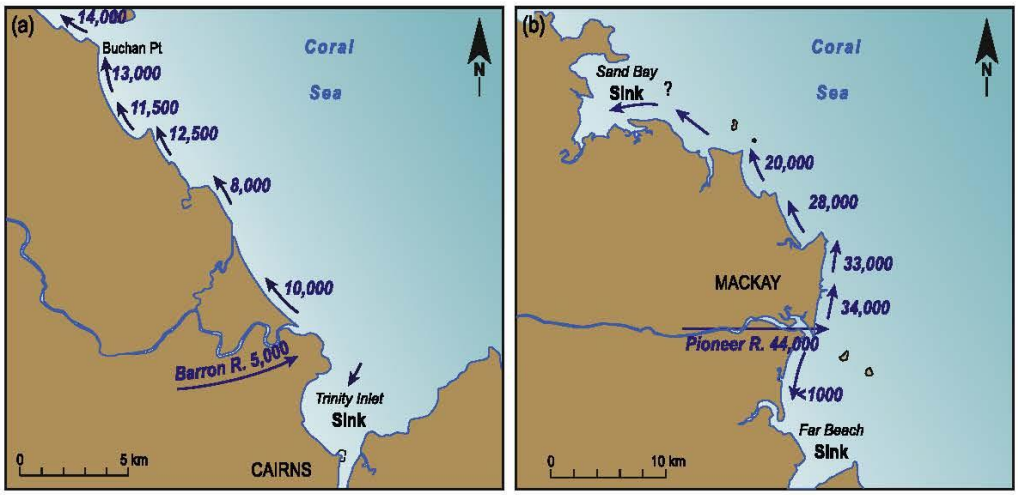

Fig. 3. Conceptual sediment transport pathways (longshore sand transport in cubic metres per year) associated with a) the mouth of Barron River and delta near Cairns. (based on BPA, 1984), and b) the mouth of the Pioneer River near Mackay (after Jones, 1987). Both are mesotidal and exposed to southeast trade winds and waves, with long headland-bound beaches. The deficiency in river-derived sediment at Cairns is resulting in ongoing shoreline recession, while longshore variation is rates is a result of both changing shoreline orientation and degree of headland bypassing. Both are examples at the secondary compartment level.

posed since settlement in the 19th century.

6.2. Wave-dominated coast

Compartments along the southeast coast of Australia fall into two basic types, closed and leaky (Fig. 2). The latter are mainly in the northern part of NSW especially at both secondary and tertiary scales. Closed compartments occur at tertiary scales; they dominate the central and southern part of this state with limited or zero leakage of sand around prominent rocky headlands. Overall the coast is wave-dominated and microtidal and contains numerous headland-embayed beaches rich in quartz sand derived from long periods of reworking terrestrial material on the continental shelf during the Cainozoic (Roy and Thom, 1981). Most of the rivers draining the Eastern Highlands have delivered no sand to the open coast in the Holocene. Sand forming dunes, beaches, flood-tide deltas and nearshore deposits has been transported into the present embayments through onshore and alongshore transport processes during this period.

One of the best known sediment transport systems in NSW was the subject of an early study by Gordon and colleagues in the 1970s (PWD, 1978). They identified sediment budgets and erosional events especially in the vicinity of Cape Byron. Since then several studies have examined sediment transport in this open compartment extending from the Clarence River in the south to, and along, the Gold Coast in Queensland (see summaries in Mariani et al., 2013; Patterson, 2013). Sand pulses around headlands have been shown to be a mechanism of longshore transport generating large migratory updrift rips that erode the beach and expose the backshore-dunes and infrastructure to wave erosion followed by sand wave accretion (Short, 1999, Fig. 9.13d).

Longshore sand transport to the north is considered to be a major factor in the sand budget and shoreline changes in northern NSW (Fig. 4). As shown by Mariani et al. (2013) in the WRL pilot study and Patterson (2013, Figs. 3–26), transport rates have been the subject of numerous, and at times conflicting, estimates both within and between leaky tertiary compartments. However, it is still uncertain as to how much sand is also currently coming onshore, and can continue to come onshore from the inner shelf even as sea level rises, to sustain beach/dune systems along this stretch of coast (Cowell et al., 2000; Daley and Cowell, 2012; Mariani et al., 2013, Table 11). Clearly more work remains to determine net transport along this stretch of coast, and whether there is any net onshore addition to the sand budgets to these leaky compartments, in order to evaluate the behaviour of shorelines and risk to built assets under climate change conditions.

In central and southern NSW, each of the secondary compartments can be conveniently sub-divided into tertiary compartments as defined by prominent rock headlands that restrict longshore sediment transport (Chapman et al., 1982). The sediment transport system is dominated by onshore-offshore sand exchange following storms and periods of post-storm recovery such as captured by the long-term measurements at Moruya in a tertiary compartment on the NSW south coast (Thom and Hall, 1991; McLean et al., 2010). Rivers play a minor role in supplying sediment to the coast (for example, the Shoalhaven River in southern NSW, see Carvalho and Woodroffe, 2017). Work by Roy, Cowell, Kinsela and others near Forster highlights products of sediment exchange over time within a compartment that has served as a major sand sink during late Pleistocene interglacial and Holocene rising and high sea level intervals (see Kinsela et al., 2016). Where accommodation space is more limited, shorelines undergoing recession today in all likelihood will continue to recede as sea level rises.

Fig. 5 shows part of a secondary compartment on the central coast of NSW (Hudson, 1999). The Avoca tertiary compartment, studied by Mariani et al. (2013) as part of the WRL pilot study, sits within this section of coast. The confined occurrence of beach and nearshore sand by rock reefs is clearly shown. Further offshore are shelf sand bodies at water depths greater than 20 m that along this section of coast have been defined by side-scan sonar, seismic and drilling investigations (Field and Roy, 1985; Gordon and Hoffman, 1986; Roy and Hudson, 1988; Hudson, 1999). These may offer a source of nourishment sand if beach sand supplies become depleted as sea level rises. It is not entirely clear whether these deeper sand sources on the inner shelf are connected to the confined shoreface and beach system. In all likelihood they are not, but further field studies are required if the beach is to be nourished from an offshore source. However, Mariani et al. (2013, Table 11) in their probabilistic estimates of recession to 2100 involving a sea-level rise of 1.1 m, assumed no net onshore drift.

6.3. Deeply embayed coast

The deeply embayed secondary compartment of Frederick Henry Bay, southeast Tasmania, offers an opportunity to review interconnected sediment systems (Fig. 6). This is a south-opening coastal embayment into which Southern Ocean swell penetrates and is

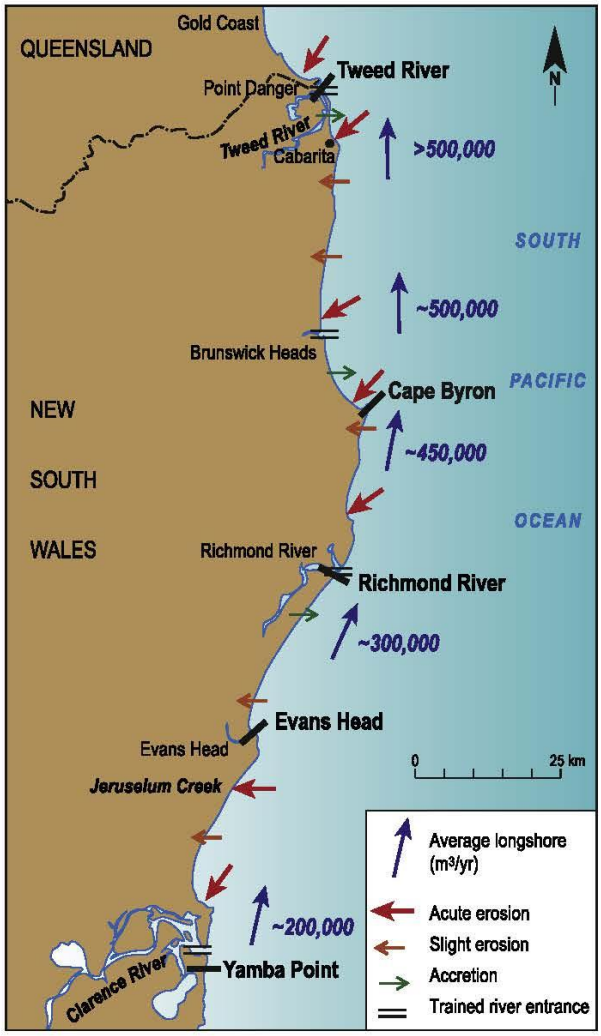

Fig. 4. The primary compartment in northern NSW from the Queensland border south to the Clarence River, exposed to mesotides and predominantly southerly swell, comprising four secondary compartments, showing volumes of sediment estimated to be moved north by longshore processes (adapted from Patterson, 2013). Cabarita Beach within the northernmost secondary compartment was the tertiary compartment examined in the WRL pilot study.

refracted with little directional variability once within the bay. The bay is broad (10 km wide) and relatively shallow (mostly less than 20 m deep), with a sandy floor. There is negligible river sand supply, although modelling suggests there may be some ongoing transport from the inner shelf into the bay (Harris and Heap, 2014). Present-day sand transport processes in the bay are inferred to be mainly swell-driven towards the north with ongoing alongshore transport through several leaky tertiary compartments. Two sheltered tidal lagoons, Pittwater and Pipeclay Lagoon, serve as sand sinks; shoreline recession of the most wind-wave exposed soft-rock (cohesive clay) shores in swell-sheltered Barilla Bay appears have accelerated since the 1940s, perhaps as a response to either sea-level rise and/or increased wind speeds driving local wind-waves. Sand is also trapped within several swash-aligned tertiary beach compartments inferred to be closed. The much larger Norfolk Bay is also a sand sink although swell-driven sand transport into the bay is probably weak.

Sediment budget and transport pathways for Frederick Henry Bay are largely inferred from geomorphic evidence. Seven Mile Beach, at the head of the bay, is a prograded barrier (Davies, 1961). A preliminary estimate inferred that ~60,000 m^3/yr of sand had been supplied from offshore since circa 7000 years BP to build this feature (Byrne, 2006). However, the sedimentary history of successive beach ridges records the accumulation of sand from both locally reworked and offshore sources, with at least one long hiatus, and a rate of accretion that appears to have slowed during the past 500 years (Oliver et al., 2017c). Detailed studies of erosional events and shoreline behaviour extending back 70 years have been undertaken at Roches Beach (Sharples, 2010; Sharples et al., 2012, and work in progress; Carley et al., 2008). A time-series of 32 aerial photographs from 1947 to 2015 shows a marked long-term (multi-decadal) change in shoreline behaviour around 1980, from stable (with cut-and-fill cycles) to persistently receding, which in this leaky tertiary compartment could be a response to increasing alongshore loss of sand related to more frequent erosion of the upper shoreface under sea-level rise (Sharples, 2010; Sharples et al., 2012; work in progress). Modelling studies coupled with historical air photo analysis have been used to assess long-term risk from sea-level rise for Clarence local council (Carley et al., 2008; Shand and Carley, 2011; Dell and Sharples, 2012). All these studies point to vulnerability of local residential areas in some tertiary compartments as sea level rises (sensitivity 5), given limited onshore sand transport to compensate for net offshore and alongshore sand loss, although beaches in some other (closed) tertiary compartments are inferred to be currently stable (sensitivity 3).

6.4. Metropolitan coast

A highly modified secondary compartment forms the metropolitan Adelaide coast. Located in Gulf St Vincent, South Australia, the coast is exposed to westerly wind waves and occasional southerly swell, which drive a net northerly longshore sand transport. Beaches have been sustained from a predominantly relict Holocene sand source with minimal new sediment entering the system. There are no major rivers and no significant sediment supply from the southern section of coast. A 29-km stretch of sandy coast, from Kingston Park to Outer Harbour is shown in Fig. 7. Originally backed by Holocene dune and foredune ridges, sediments have been continually transported northward since the end of the postglacial marine transgression resulting in accretion of LeFevre Peninsula, which has acted as a sediment sink for this section of the coast (Bowman and Harvey, 1986; Harvey and Bowman, 1987). There is a net northerly sediment transport of ~75,000 m^3/yr in the south, decreasing to the north (Department of Environment and Heritage [DEH], 2005). Extensive coverage of the seabed by seagrass means there is a lack of a natural offshore sand supply; historic seagrass dieback released ~80,000 m^3/yr to the beach system.

Urban development has progressively removed and/or isolated sediments from the active beach zone thus blocking any natural source of onshore sand replenishment; the deficit for this section of coast therefore requires ongoing beach recycling-nourishment. Periodic dredging of offshore sand deposits provided large volumes of temporary sand nourishment but viable offshore deposits have now been exhausted so that geologically older inland-based sand deposits have been used to offset the deficit.

Natural sediment movement is counteracted by a highly managed system of coastal protection with rock armouring on over half of the coast and an ongoing sand recycling and nourishment program (DEH, 2005; Short, 2012). Early management practice trucked sand from natural sand sinks to erosion zones. Today there is a combined system of pumping in the south supplemented by trucking further north (Fig. 7). It is clear that an understanding of the dynamics of future shoreline change and sediment budget for this compartment is going to require more investment in resolving the balance between beach amenity and coastal protection works. Sea-level rise will only exacerbate the existing deficit of coastal sediment requiring further demand

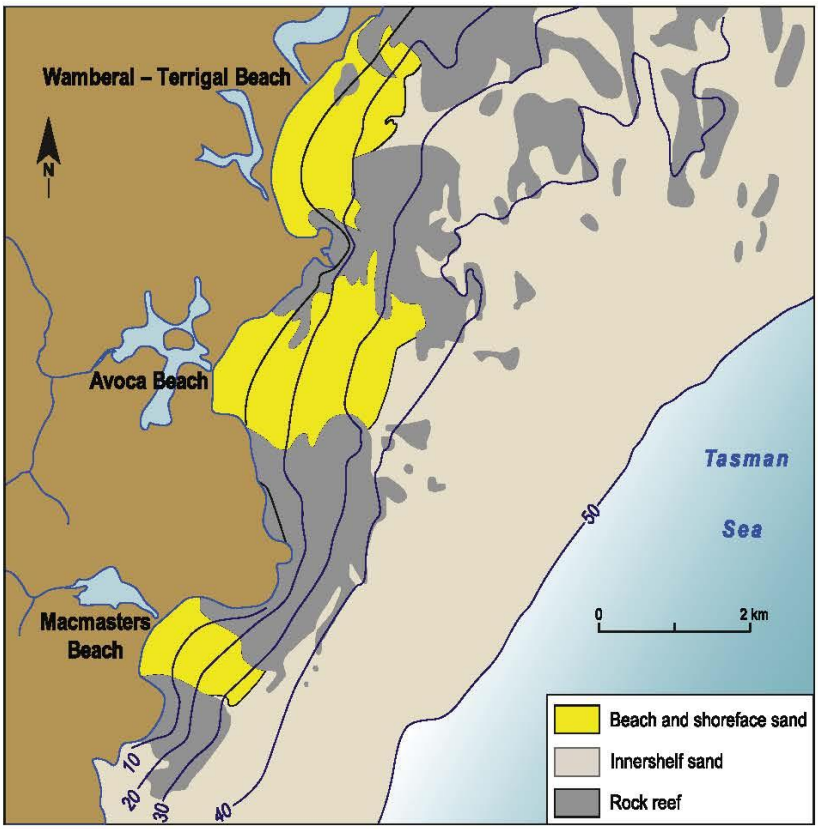

Fig. 5. Closed compartments in the area adjacent to Avoca Beach in central NSW showing the extensive rocky outcrops on the seafloor constraining availability of sand from offshore and restricting longshore transport or sediment exchange between compartments (adapted from Hudson, 1999). These three beach systems are tertiary compartments within the broader secondary compartment; Avoca Beach was the tertiary compartment examined in the WRL pilot study.

on relict sand sources or mining of sandy seagrass beds. At least Adelaide has an institutional structure and a 40-year continuous record of detailed beach profiling data that places it in a position to sustain ongoing cooperation between the three local councils and state agencies in planning for the future.

6.5. Wave-dominated carbonate coast

Secondary sediment compartments between Cape Naturaliste and Cape Peron, in southwestern WA, including the southern part of the Swan Coastal Plain, provide a case study on a high energy carbonate sediment coast. Lithified carbonate features provide a complex geological framework for this coast, including platform and ramp structures across much of the shelf, and multiple chains of reefs and islands that mark previous ancient shorelines. The energetic offshore wave climate, with prevailing southwest swell, provides impetus for south to north coastal sediment transport. However, inside the reef chains, alongshore littoral sediment transport is highly modified by wave sheltering and rock exposed in the nearshore, creating locations of reduced, or even reversed, transport. Rates of alongshore transport in the order of 85,000–100,000 m^3/yr have been identified at Mandurah and Dawesville, where mechanical sand bypassing is used to offset the adverse trapping by navigational channels. For more sheltered locations, alongshore transport can be negligible, and in locations of discontinuous reef, substantial discrete onshore sediment feeds can occur. The consequent alongshore variability in transport, including a mixture of alongshore and cross-shore dynamics, develops source-sink patterns of sediment transfer, with substantial dune barriers that have been active over the late Holocene.

The spatial connectivity of sediment exchange along this coast has previously been identified (Searle and Semeniuk, 1985) and the need to integrate coastal management across jurisdictional boundaries has been acknowledged. For this reason, nine local councils have joined into a partnership to develop adaptation strategies to meet the challenges of climate change. The area includes Geographe Bay, which was subject to the first Australian assessment of potential impacts of climate change on the coast (Kay et al., 1992). It has been the subject of several unpublished consultancy reports, as well as the Damara pilot study (Eliot, 2013).

Application of the compartment approach in southwest WA benefited from access to a large data base of onshore and offshore geomorphology and sediment movements. In particular, a combination of marine LiDAR and multibeam sonar bathymetric surveys offered an opportunity to examine in detail topographic features at a range of scales. In offshore waters it was possible to show details of sediment availability and pathways that are rarely accessible to this degree elsewhere in Australia (for example see Stul et al., 2012, 2015). Much of the land can be shown, using airborne LiDAR surveys, to be low-lying and subject to inundation by future sea-level rise. The framework provided by the sediment compartment approach, underpinned by knowledge of geological structures, is seen as a way of assessing thresholds of change across different time scales by considering both susceptibility (long term) and instability (short term) (Eliot et al., 2011 and Eliot, 2013).

This coast is representative of extensive sections of southern and western coasts of Australia, dominated by calcareous beach and dune sediments. Lithification, particularly of Pleistocene barrier deposits into beach and dune calcarenite, has major ramifications for all Holocene shores and sediment compartments along these coasts. Offshore features at both secondary and tertiary scale in the vicinity of Mandurah are depicted in Fig. 8. Also shown are the principal pathways for sediment movement at these scales along this calcarenite-dominated

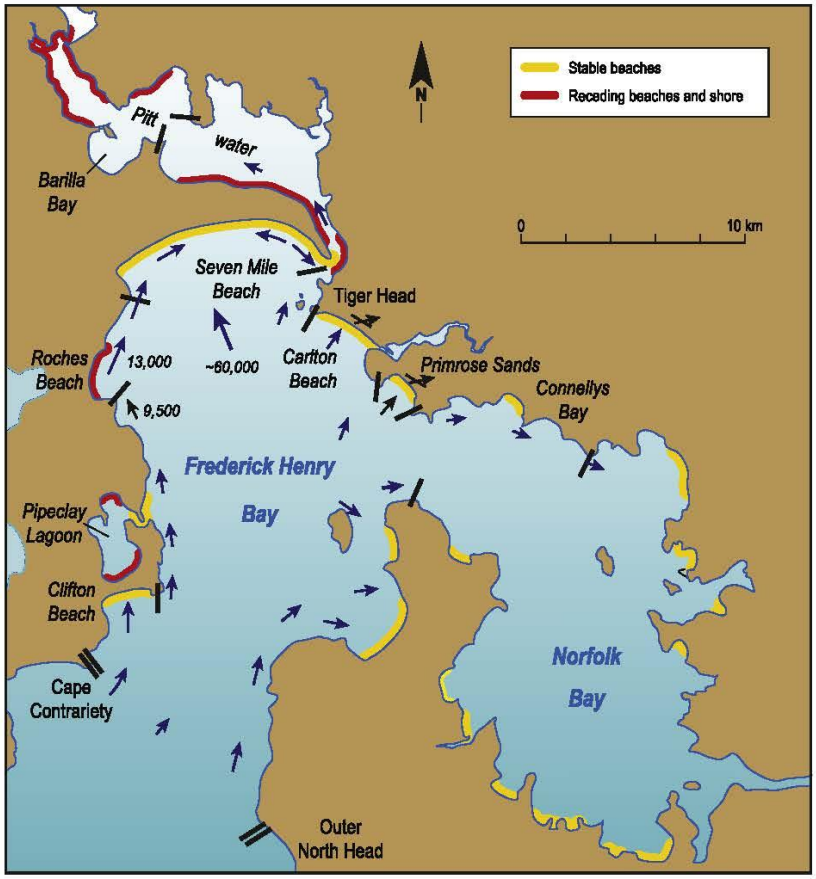

Fig. 6. Inferred dominant ongoing sand transport pathways (arrowed) in Frederick Henry Bay, southeast Tasmania. Estimates of sand transport (in cubic metres per year) from Byrne (2006) and Shand and Carley (2011). Tertiary compartment boundaries (leaky and closed) indicated by black lines; double lines indicate boundaries to secondary compartment; black arrows indicate sediment pathways.

coast. Calcareous and quartzose sands mobilised in the late Quaternary have been cemented at present and lower sea levels to form linear ridges, seabed pavements and submarine platforms. Offshore these ridges are undergoing progressive wave, current and biogenic destruction, thus providing some mobile sand for transport, in places across cemented calcarenite pavements. Temperate algae supported by the reefs and seagrass banks on sand sheets between them are bioproductive and contribute a significant amount of calcareous sand to sediment budgets in this region (for example, see Semeniuk and Searle. 1986; Collins, 1988; and Tecchiato et al., 2016). The importance of landform scale is highlighted by a progressive shift in dominant landform characteristics when considered at finer scales, implying a change from swell-dominated longshore transport to more local-scale fluctuations in sandbar formation that are more influenced by cross-shore transport (Eliot, 2013).

6.6. Mixed-energy sub-tropical coast

The compartment approach has been applied on the arid, sub-tropical Pilbara coast of northwest WA. This is a broad and extensive coastal floodplain with a complex geologic and sedimentary structure (Semeniuk, 1993). This region is episodically subject to storm surge inundation during tropical cyclones. It experiences highly variable fluvial input with numerous intermittent streams and rivers discharging either directly into the ocean or into shallow basins on the coastal lowlands. Some rivers, such as the Ashburton and De Grey, have a capacity to deliver large volumes of sediment in single flood events. Most of the sediment is dispersed on the inner continental shelf where it is reworked by tidal currents and wave action. Coastal processes operate in a complex interacting way across the inner shelf, with the role of wave energy increasing towards the shore. Tidal currents, associated with a general tidal range of 2–3 m, larger in some locations, change in direction and increase in velocity offshore to a tidal breakpoint, with localised areas of focusing where rock features provide constriction (Eliot, 2013). Connection between the shelf and inshore zones occurs intermittently through sand sheets or more extensive tidal ridges. However, the spatial extent and speed of currents varies over time giving rise to a range of wind, wave and tidally formed sedimentary structures (Eliot and Eliot, 2013; Eliot et al., 2013).

For much of the Pilbara, coastal deposits occur as sand ribbons on the seaward side of limestone ridges, with extensive, flat sandy deposits in the nearshore. The low elevation and distribution of these features, often over-topped by surges during cyclones, and very high tides, indicates that wave transport from the nearshore is limited by sand dispersion from tidal currents at variable delivery rates. This suggests that sediment supply is not determined so much by nearshore processes, but is controlled further offshore with the seabed assuming a structure that matches the supply rate. Also to consider is the exchange of sediments between the coast and landward networks of lagoons and tidal creeks in areas not drained by major rivers. This can constitute a “coastal” plain extending 10–20 km to landward of the shore. Rapid switching can occur between erosion and accretion within these networks leading to either import or release of sediments to coastal wave/current processes and hence changes in shoreline position (Eliot, 2013). Estimates of net sediment transport rates in the vicinity of Onslow are shown in Fig. 9. This information on sediment dynamics has a range of purposes: in the short term it is important in assisting the management of dredged material from shipping channels; it also offers an understanding of

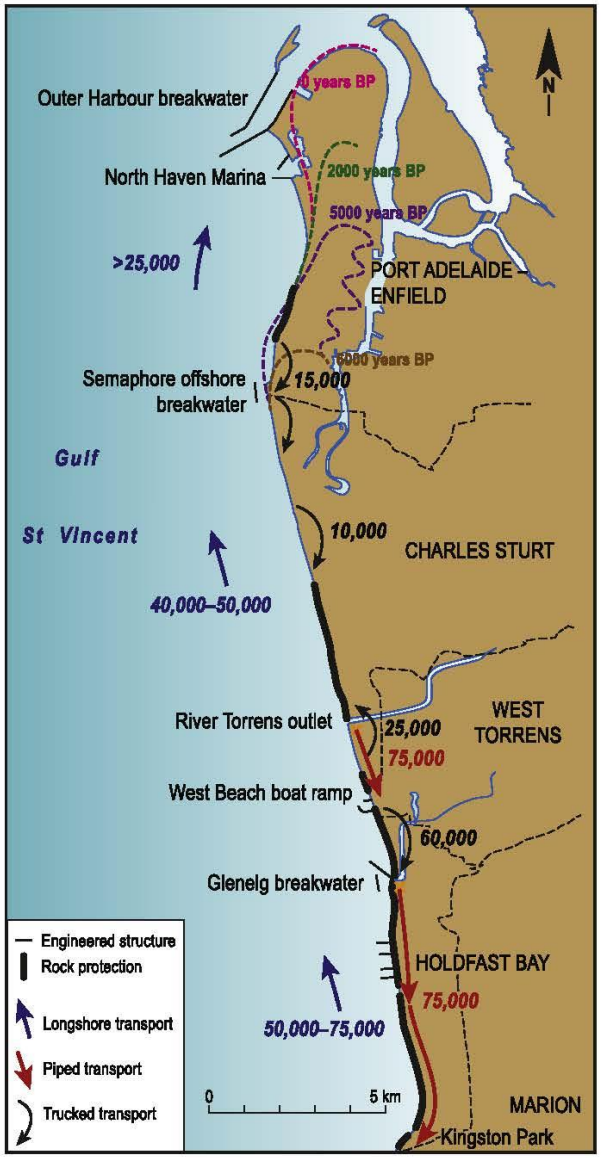

Fig. 7. The metropolitan coast of Adelaide, which is the northern half of a secondary compartment, showing estimates of northward sediment transport in the nearshore (blue arrows), shoreline hard-rock protective measures, and sand transfer by trucking (red) and pipeline (black arrows) for this section of coast between Outer Harbour and Kingston Park. Several local government areas are represented. Holocene evolution of the shoreline position north of the Semaphore breakwater is recorded based on radiocarbon dating in Harvey and Bowman (1987). (For interpretation of the references to colour in this figure legend, the reader is referred to the Web version of this article.)

pathways for sediment transport and shoreline position which are most likely to keep pace with sea-level rise, or experience drowning leading to future growth of tidal lagoons where there are now tidal flats.

7. Sediment compartment approach and coastal planning

The above six case studies illustrate some of the considerable variation in coastal settings and processes on a continental scale. They also illustrate the need to understand the morphodynamics of each sediment compartment, its geology, geomorphology, oceanographic processes and in particular its sediment dynamics. Only with this understanding can useful models of compartment behaviour be developed. This in turn will allow management plans to be based on realistic scenarios of shoreline behaviour incorporating the complexity of interacting processes including the interconnectivity of impacts as expressed in a nationally accepted spatial framework.

To be useful, the sediment compartment approach must be relevant to regional (and local) land use planning and to development assessment. In the report on *Climate Change Risks to the Australia's Coast* (DCC, 2009; augmented in a supplementary report by DCCEE in 2011), it was clear that many settled areas of the coast have built assets at risk to future changes of shoreline position and inundation from sea-level rise. These assets include private residential property and businesses, and public infrastructure and amenity facilities. There is exposure today to coastal hazards and these reports highlight the probable extent to which risks are increased as a result of climate change.

Continuous pressure to build and rebuild in coastal areas may place more assets in harm's way. The short and long-term social, economic and environmental costs of such activities must be weighed against the benefits. Risk assessments should be informed by the best available methods for understanding the complexity of coastal processes likely to impact adversely on those assets over their lifetime. A method developed in this study involves application of the multi-scale sediment compartment approach, which takes into consideration the sensitivity of compartment shorelines to change over time. Such an approach recognises that some parts of the shoreline will be fast responders, while others will be relatively slow, or hardly change at all until a tipping point is reached in relation to sediment supply required to sustain shoreline position.

Investment in the application of the sediment compartment approach is particularly important in locations deemed to be erosion "hot spots" in order to manage present and future risk. There is a temptation to use less expensive, simplified methods that do not identify sources and sinks of sediments, but rather apply 'rule of thumb' tools to determine future shoreline positions. However, limitations of these less rigorous methods have been made clear in the case studies accompanying this work (Eliot, 2013; Mariani et al., 2013; see also Woodroffe et al., 2012). Unless there is an understanding of sediment pathways over a range of time and space scales, decision makers will be forced to make assessments of hazards and risks to assets without having the benefits of an approach which these case studies demonstrate can enhance the level of certainty in planning and development assessments. These benefits are already apparent in the application of the approach in the UK and California, and initial work in Western Australia. Reform of the planning system in NSW offers potential for further application of the approach at different scales.

As noted above, the UK provides an example of how the sediment compartment approach can inform coastal planning and management at the regional (county) scale. There *Shoreline Management Plans* (SMPs) are built around knowledge of sediment pathways. They have recently been expanded to look at the implications for three climate change scenarios. That work highlights both present and future risk and enables local governments in conjunction with agencies of the UK government to reach decisions on what and where to protect or permit the sea to invade the land (Nicholls et al., 2013).

In Western Australia, the Department of Transport commissioned Damara to report on the coastal compartment and sediment cell approaches to assist coastal planning (Damara, 2012; see also Damara report 2011 to Departments of Environment and Conservation, Planning and Transport). In so doing it was acknowledged inherited topographies, particularly the geologic framework, play a major role in how sediments are moved and impact on the use of the coastal zone through landform development (see Eliot, 2013). Although not a novel appreciation, incorporation of this understanding, coupled with information on onshore and offshore sources of sediment in decision-making provides decision-makers in WA with a powerful tool to address management and risk issues, including impacts of extreme events and sea-level

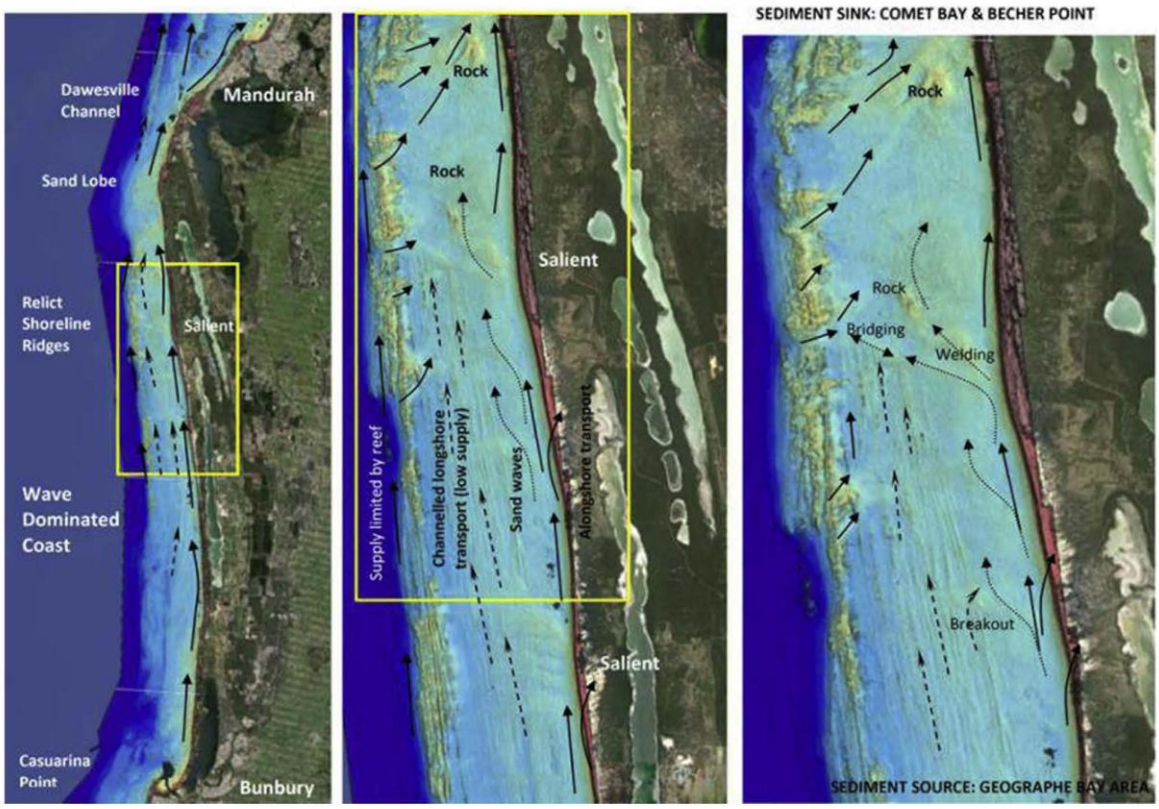

Fig. 8. Interpretation of LADS bathymetry near Binningup, south of Mandurah in Western Australia (from Eliot, 2013).

rise at local and regional scales.

Coastal reform in NSW, including the passage through Parliament in 2016 of the new *Coastal Management Act*, indicates a way for state and local authorities to develop a new generation of Coastal Management Programs incorporating the sediment compartment approach. Secondary compartments are listed by name in a schedule attached to the Act. This will open the opportunity for local councils and state agencies to be better informed on the nature of coastal hazards at present and in the future. Current approaches based on council and state boundaries do not provide sufficient information on sediment pathways along stretches of coast subjected to common processes. If all the states and the Northern Territory adopt a multi-scale compartment approach similar to that envisaged in WA and NSW, it will be possible to provide a more consistent and rigorous method of assessing shoreline

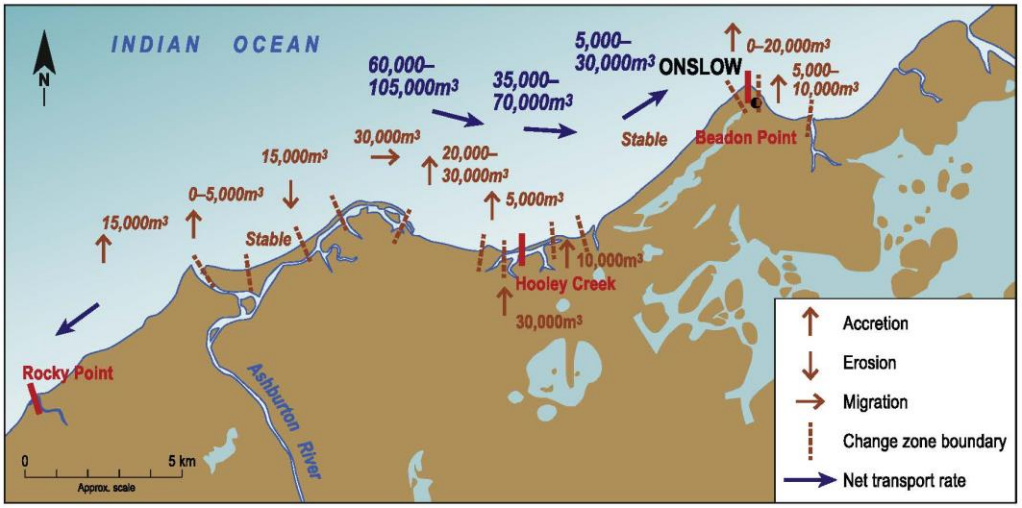

Fig. 9. Conceptual sediment budget (cubic metres per year) derived from surface features for a section of the secondary sediment compartment near Onslow on the Pilbara coast, where the Ashburton River delivers sediment episodically (from Eliot, 2013; Eliot and Eliot, 2013).

a)

b)

Fig. 10. a) A view of Point Danger which forms the 'leaky' sediment compartment boundary between northern NSW (background) and southern Queensland (photograph A. Short). b) an overview of longshore drift (yellow arrows) and the pumping required (orange arrows) to restore sediment bypassing required as a result of breakwaters that train the Tweed River entrance, trapping longshore sand transport (http://ci.wrl.unsw.edu.au/current-projects/tweed-river-sand-bypassing-project/).

change and inundation risk than exists at present. This multi-scale compartment framework is also the approach recommended in the guidelines of Engineers Australia on adapting to climate change (Harper, 2012), and will be further expanded in the revised *NSW Coastal Management Manual* (2017).

8. Conclusions

There is scope in Australia for the application of a national approach to coastal management based on sediment compartments involving collaboration between agencies at different levels of government. Experience in the UK is worth considering where the Environment Agency has a lead role in working with council groups divided up into regions, the boundaries of which are defined by sediment compartments or cells. Preliminary work in Western Australia by the Department of Transport shows an interest in this approach by an operational state agency. The fact that NSW has incorporated the compartment concept into legislation is another step in this direction. In that state the Office of Environment and Heritage has commenced offshore surveys using the compartment approach as a framework for management to assist local councils in the development of new Coastal Management Programs as required under the new legislation (*Coastal Management Act*, 2016). In Victoria, the state government is also initiating studies based on the compartment approach. There is now potential for all three levels of government in Australia to commit to a nationally agreed method of assessing coastal hazard and climate change impacts by implementing the sediment compartment approach. Experience in the UK (Cooper and Pontee, 2006) and the USA (Wright et al., 2016) indicates that there will be a permanent need to incorporate new information, new science and new policy arrangements as the new climate change era unfolds.

Current institutional arrangements suggest that there could be a role for federal agencies to provide guidance, thus providing a building block for applying a consistent nationwide approach. Management of national coastal and marine data should be seen as a federal responsibility. Compartment descriptions, as in *CoastAdapt*, will need to be updated and sensitivities reassessed over time; maintaining expertise in this area will require attention. However, given current responsibilities, it is apparent that state governments in conjunction with local councils will play the major role in the application of the compartment approach to coastal planning and management.

Local governments, with few exceptions lack the resources to apply the compartment approach. Also, compartment units frequently overlap council boundaries (see Fig. 7). However growing interest in regional hazard assessment and land use planning should encourage increased collaboration between councils and hence demand for more joint technical support to address these issues. The possibility therefore exists for the federal, state and local governments to share information on future risk based on the compartment approach, and in collaboration develop mechanisms to ensure coastal regions are better prepared to meet future challenges driven by the forces of climate change. This can help avoid the "one size fits all" approach towards coastal assessment.

Any agreement to establish a nationally consistent approach must appreciate the cost as well as benefits. Given current responsibilities, it will especially require continued investment by state governments. For the sediment compartment approach to add value to decision making there must be continued investment in collection of data on both land and in offshore conditions: wind and wave climates, bathymetry, as well as sediment type, age and structures. Technologies have been developed for this information to be collected. It is important that mechanisms exist so that experiences in applying these technologies and the data they generate are shared.

There will be opportunities in the future for all levels of government to work in collaboration. An example would be an updated agreement to manage assets at risk in Tweed and Gold Coast which straddles both local and state government boundaries (Fig. 10a). At present an agreement exists between NSW and Queensland on the Tweed River sand bypass project (Fig. 10b). This multi-decadal agreement ensures that the sand trapping by river breakwaters on the NSW border does not adversely impact on beaches downdrift located in Queensland (see Patterson et al., 2011, and www.tweedsandbypass.nsw.gov.au). Continuation of the agreement may depend on assessment of future sediment flows under climate change conditions for this section of coast. This could involve participation of the federal government given its interest in the economy of southeast Queensland including the operation of the low-lying Coolangatta international airport.

What is clear from this national assessment of all secondary coastal sediment compartments around the vast coast of this continent, supported by pilot and case studies, is that the compartment approach greatly assists in building capacity of governments to manage changes to coastal conditions. By incorporating geomorphic diversity into the evaluation of coastal dynamics at different scales, it offers a framework for assessing sediment exchanges between adjacent landforms both onshore and offshore. As sediment moves from one place to another, a different response to an external driver, such as sea-level rise, may occur. In this way the link becomes more apparent between sediment compartments and source-pathway-sink behaviour. The compartments, primary, secondary or tertiary, provides a spatial reference for behavioural changes that occur due to proximity to sinks or sources. No simple rule of thumb answer is of much value in such circumstances. As sea level rises or wave climate changes, the nature of sediment movement along the pathway or pathways may increase or slow down so that responses at the source or in the sink will change over time. The compartment approach will improve understanding of possible changes in degrees of stability or resilience of coastal features and hence provide managers with more realistic scenarios for purposes of long-term planning.

Acknowledgements

We wish to thank Geoscience Australia, in particular, Martyn Hazelwood, for providing the original sediment compartment data layers. This study forms part of *CoastAdapt* which was developed by the National Climate Change Adaptation Research Facility (NCCARF) with funding from the Australian Government through the Department of the Environment and Energy. We gratefully acknowledge Oiyu Yeung, Steve Webb, Leonard O'Sullivan and Shereen Sharma for their support in the delivery of the sediment compartment layer and descriptions. Tanya Stul and Bob Gozzard were of great assistance in the work on the Western Australian coast. Scott Smithers assisted with north Queensland and Doug Fotheringham with South Australia.

References

Baker, McKenzie, 2011. Local Council Risk of Liability in the Face of Climate Change –Resolving Uncertainties, a Report Commissioned by Australian Local Government Association. 22nd July 2011, Sydney.

Bird, E.C.F., 1971. The origin of beach sediments on the North Queensland coast. Earth Sci. J. 5, 95–105.

Bird, E.C.F., 1993. The Coast of Victoria. Melbourne University Press, Melbourne.

Bowen, A.J., Inman, D.L., 1966. Budget of littoral sands in the vicinity of Point Arguello, California. US Army Coast. Eng. Res. Center Tech. Mem. 19, 1–56.

Bowman, G.M., Harvey, N., 1986. Geomorphic evolution of a Holocene beach ridge complex, LeFevre Peninsula, South Australia. J. Coast. Res. 2, 345–362.

BPA, 1984. Mulgrave Shire Northern Beaches. Beach Protection Authority, Brisbane 366 pp.

Bray, M.J., Carter, D.J., Hooke, J.M., 1995. Littoral cell definition and budgets for central south England. J. Coast. Res. 11, 381–400.

Byrne, G., 2006. Roches Beach Lauderdale – Coastal Erosion Study. Report to Clarence City Council by Vantree Pty Ltd. .

Carley, J.T., Blacka, M.J., Timms, W.A., Anderson, M.S., Mariani, A., Rayner, D.S., McArthur, J., Cox, R.J., 2008. Coastal Processes, Coastal Hazards, Climate Change and Adaptive Responses for Preparation of a Coastal Management Strategy for Clarence City, Tasmania. Report by Water Research Laboratory. University of New South Wales.

Carvalho, R.C., Woodroffe, C.D., 2017. Modifications to the Shoalhaven estuary and the coastal sediment budget over the past 40 years. In: Proceedings of Coasts and Ports,

June 2017, Cairns.
Chapman, D.M., 1981. Coastal erosion and the sediment budget, with special reference to the Gold Coast, Australia. Coast. Eng. 4, 207–227.
Chapman, D.M., Geary, M., Roy, P.S., Thom, B.G., 1982. Coastal Evolution and Coastal Erosion in New South Wales. Coastal Council of New South Wales, Sydney 341 pp.
Collins, L.B., 1988. Sediments and history of the Rottnest Shelf, southwest Australia: a swell-dominated, non-tropical carbonate margin. Sediment. Geol. 60, 15–49.
Cooper, N.J., Barber, P.C., Bray, M.J., Carter, D.J., 2002. Shoreline management plans: a national review and engineering perspective. Proc. Inst. Civil Eng. Water Marit. Eng. 154, 221–228.
Cooper, N.J., Hooke, J.M., Bray, M.J., 2001. Predicting coastal evolution using a sediment budget approach: a case study from southern England. Ocean Coast. Manag. 44, 711–728.
Cooper, N.J., Pontee, N.I., 2006. Appraisal and evolution of the littoral 'sediment cell' concept in applied coastal management: experiences from England and Wales. Ocean Coast. Manag. 49, 498–510.
Cowell, P.J., Thom, B.G., 1994. Morphodynamics of coastal evolution. In: Carter, R.W.G., Woodroffe, C.D. (Eds.), Coastal Evolution, Late Quaternary Shoreline Morphodynamics. Cambridge University Press, pp. 33–86.
Cowell, P.J., Stive, M., Roy, P.S., Kaminsky, G.M., Buijsman, M.C., Thom, B.G., Wright, L.D., 2000. Shoreface sand supply to beaches. In: Proceedings 27th International Conference on Coastal Engineering. ASCE, pp. 2496–2508.
Cowell, P.J., Stive, M.J.F., Niedoroda, A.W., de Vriend, H.J., Swift, D.J.P., Kaminsky, G.M., Capobianco, M., 2003. The coastal-tract (part 1): a conceptual approach to aggregated modeling of low-order coastal change. J. Coast. Res. 19, 812–827.
Daley, M., Cowell, P.J., 2012. Long-term shoreface response to disequilibrium stress: a conundrum for climate change. In: Proceedings of the NSW Coastal Conference, Kiama.
Damara, W.A., the Geological Survey of Western Australia, 2011. Dongara to Cape Burney, Western Australia: Coastal Geomorphology. Prepared for the Department of Planning, Department of Transport and the City of Geraldton-Greenough.
Damara, W.A., 2012. Coastal Hazard Mapping for Economic Analysis of Climate Change Adaptation in the Peron-Naturaliste Region. Prepared for the Peron-Naturaliste Partnership Coastal Adaptation Decision Pathways (PNP-CAPS) project, Report 169–01.
Davies, J.L., 1961. Tasmanian beach ridge systems in relation to sea level change. Pap. Proc. R. Soc. Tasmania 95, 35–41.
Davies, J.L., 1974. The coastal sediment compartment. Aust. Geogr. Stud. 12, 139–151.
Davies, J.L., 1977. The coast. In: Jeans, D.N. (Ed.), Australia – a Geography. Sydney University Press, pp. 134–151.
Davies, J.L., 1980. Geographical Variation in Coastal Development, second ed. Longman, London.
Dell, M., Sharples, C., 2012. Clarence City Council Shoreline Monitoring Program; Report to Clarence City Council by Blue Wren Group. School of Geography & Environmental Studies, University of Tasmania.
Department of Climate Change, 2009. Climate Change Risks to Australia's Coast: a First Pass National Assessment. Australian Government, Canberra.
Department of Environment and Heritage, 2005. Adelaide's Living Beaches: a Strategy for 2005–2025. Technical report. Department of Environment and Heritage, Adelaide 206 pp.
Eliot, I., Nutt, C., Gozzard, B., Higgins, M., Buckley, E., Bowyer, J., 2011. Coastal Compartments of Western Australia. A Physical Framework for Marine Coastal Planning. 75pp.
Eliot, I., Gozzard, B., Eliot, M., Stul, T., McCormack, G., 2013. Geology, Geomorphology & Vulnerability of the Pilbara Coast, in the Shires of Ashburton, East Pilbara and Roebourne, and the Town of Port Hedland, Western Australia. Damara WA Pty Ltd and Geological Survey of Western Australia, Innaloo, Western Australia.
Eliot, M., 2013. Application of Geomorphic Frameworks to Sea-Level Rise Impact Assessment. Damara WA Pty Ltd.
Eliot, M., Eliot, I., 2013. Interpreting estuarine change in northern Australia: physical responses to changing conditions. Hydrobiologia 708, 3–21.
EPA, 2004. Mackay Coast Study. Environment Protection Agency, Brisbane 113 pp.
Field, M., Roy, P.S., 1985. Offshore transport and sand-body formation: evidence from a steep, high-energy, shoreface, southeastern Australia. J. Sediment. Petrol. 54, 1292–1302.
Galloway, R.W., Story, R., Cooper, R., Yapp, G.A., 1984. Coastal Lands of Australia. Institute of Biological Resources, Commonwealth Scientific and Industrial Research Organization.
George, D.A., Largier, J.L., Storlazzi, C.D., Barnard, P.L., 2015. Classification of rocky headlands in California with relevance to littoral cell boundary definition. Mar. Geol. 369, 137–152.
Goodwin, I.D., Stables, M.A., Olley, J.M., 2006. Wave climate, sand budget and shoreline alignment evolution of the Iluka-Woody Bay sand barrier, northern New South Wales, Australia, since 3000 yr BP. Mar. Geol. 226, 127–144.
Gordon, A.D., Hoffman, J.G., 1986. Sediment features and processes of the Sydney continental shelf. In: Frankel, E., Keene, J.B., Waltho, A.E. (Eds.), Recent Sediments in Eastern Australia- Marine through Terrestrial. Geol Soc Aust, Spec Pub, pp. 29–51.
Harper, B.A., 2012. Guidelines for Responding to the Effects of Climate Change in Coastal and Ocean Engineering, third ed. Engineers Australia, Crows Nest, NSW.
Harris, P.T., Heap, A., 2014. Geomorphology and Holocene sedimentology of the tasmanian continental margin. In: Corbett, K.D., Quilty, P.G., Calver, C.R. (Eds.), Geological Evolution of Tasmania. Geological Society of Australia (Tasmania Division), pp. 530–539.
Harvey, N., Bowman, G.M., 1987. Coastal management implications of a Holocene sediment budget: Le Fevre Peninsula, South Australia. J. Shorel. Manag. 3, 77–93.
Harvey, N., Caton, B., 2010. Coastal Management in Australia. University of Adelaide Presshttp://dx.doi.org/10.1017/UPO9780980723038.
Harvey, N., Woodroffe, C.D., 2008. Australian approaches to coastal vulnerability assessment. Sustain. Sci. 3, 67–87.
Hazelwood, M., Nicholas, W.A., Woolf, M., 2013. National Coastal Geomorphology Information Framework Implementation: Discovery and Distribution. Geoscience Australia Record 2013/35.
HORSCCCWEA, 2009. Managing our coastal zone in a changing climate. The time to act is now. In: House of Representatives Standing Committee on Climate Change, Water, Environment and the Arts, 368 pp.
Hudson, J.P., 1999. Gosford City Beach Nourishment Feasibility Study. Report prepared for Manly Hydraulics Laboratory. NSW Department of Public Works.
Inman, D.L., Chamberlain, T.K., 1960. Littoral sand budget along the southern California coast (abstract). In: Report 21st International Geological Congress, Copenhagen, pp. 245–246.
Inman, D.L., Gayman, W.R., Cox, D.C., 1963. Littoral sedimentary processes on Kauai, a subtropical high island. Pac. Sci. 17, 106–130.
Inman, D.L., Frautschy, J.D., 1966. Littoral processes and the development of shoreline. In: Proc. Coast. Eng. Speciality Conf. ASCE, Santa Barbara, pp. 511–536.
Jones, M.R., 1987. Nearshore Sediments and Distribution Patterns, Mackay Coast. Geological Survey of Queensland Record, 1987/25, 16 pp. plus figures.
Kay, R.C., Eliot, I.G., Klem, G., 1992. Analysis of the IPCC Sea-Level Rise Vulnerability Assessment Methodology Using Geographe Bay, SW Western Australia as a Case Study. Department of Arts, Sports, Environment and Territories, Canberra.
King, C.A.M., 1972. Beaches and Coasts, second ed. St Martin's Press, New York 570 pp.
Kinsela, M.A., Daley, M.J.A., Cowell, P.J., 2016. Origins of Holocene coastal strandplains in southeast Australia: shoreface sand supply driven by disequilibrium morphology. Mar. Geol. 374, 14–30.
Komar, P.D., 1976. Beach Processes and Sedimentation. Prentice-Hall, New Jersey 429 pp.
Komar, P.D., 1996. The budget of littoral sediments: concepts and applications. Shore Beach 64, 18–26.
Mariani, A., Flocard, F., Carley, J.T., Drummond, C., Guerry, N., Gordon, A.D., Cox, R.J., Turner, I.L., 2013. East Coast Study Project - National Geomorphic Framework for the Management and Prediction of Coastal Erosion, Water Research Laboratory. WRL Research Report. School of Civil and Environmental Engineering, UNSW Australia, Manly Vale, NSW.
Maxwell, P.S., Pitt, K.A., Olds, A.D., Rissik, D., Connolly, R.M., 2015. Identifying habitats at risk: simple models can reveal complex ecosystem dynamics. Ecol. Appl. 25, 573–587.
McGlashan, D.J., Duck, R.W., Reid, C.T., 2005. Defining the foreshore: coastal geomorphology and British laws. Estuar. Coast. Shelf Sci. 62, 183–192.
McLean, R., Shen, J.-S., Thom, B.G., 2010. Beach change at Bengello Beach, Eurobodalla Shire, New South Wales: 1972–2010. NSW Coastal Conference, Batemans Bay, Australia.
McPherson, A., Hazelwood, M., Moore, D., Owen, K., Nichol, S., Howard, F., 2015. The Australian Coastal Sediment Compartments Project: Methodology and Product Development. Geoscience Australia Record 2015/25.
Motyka, J., Brampton, A., 1993. Coastal Management: Mapping of Littoral Cells. HR Wallingford.
Nicholls, R.J., Townend, I.H., Bradbury, A.P., Ramsbottom, D., Day, S.A., 2013. Planning for long-term coastal change: experiences from England and Wales. Ocean Eng. 71, 3–16.
Nott, J., 2005. Letter to the editor: comment on the paper 'Quantifying storm tide risk in Cairns' by Ken Granger. Nat. Hazards 34, 375–379.
NSW Government, 1990. Coastline Management Manual, Public Works Department. NSW Government Printer.
Oliver, T.S.N., Tamura, T., Hudson, J.P., Woodroffe, C.D., 2017a. Integrating millennial and interdecadal shoreline changes: morpho-sedimentary investigation of two prograded barriers in southeastern Australia. Geomorphology 288, 129–147.
Oliver, T.S.N., Tamura, T., Short, A.D., Woodroffe, C.D., 2017b. Changing rates of sand deposition at Pedro Beach, southeastern Australia: implications for compartment-based management. In: Proceedings NSW Coastal Conference, Port Stephens.
Oliver, T.S.N., Donaldson, P., Sharples, C., Roach, M., Woodroffe, C.D., 2017c. Punctuated progradation of the Seven Mile Beach Holocene barrier system, southeastern Tasmania. Mar. Geol. 386, 76–87.
Patterson, D.C., 2013. Modelling as an Aid to Understand the Evolution of Australia's Central East Coast in Response to Late Pleistocene-holocene and Future Sea-Level Change. PhD thesis. University of Queensland.
Patterson, D.C., Elias, G., Boswood, P., 2011. Tweed River sand bypassing long term average sand transport rate. In: Proceedings of the 20th NSW Coastal Conference, Tweed Heads, NSW.
PWD, 1978. Byron Bay – Hastings Point Erosion Study, NSW Dept. Public Works, Coastal Engineering Branch Report, PWD 78026.
Rissik, D., Cox, M., Moss, A., Rose, D., Scheltinga, D., Newham, L.T.H., Andrews, A., Baker-Finch, S.C., 2005. VPSIRR (Vulnerability - Pressure - State - Impact - Risk and Response): an Approach to determine the condition of estuaries and to assess where management responses are required. In: Zerger, A., Argent, R.M. (Eds.), MODSIM 2005 International Congress on Modelling and Simulation, Melbourne, Australia, pp. 170–176.
Rosati, J.D., 2005. Concepts in sediment budgets. J. Coast. Res. 21, 307–322.
Roy, P.S., Cowell, P.J., Ferland, M.A., Thom, B.G., 1994. Wave-dominated coasts. In: Carter, R.W.G., Woodroffe, C.D. (Eds.), Coastal Evolution: Late Quaternary Shoreline Morphodynamics. Cambridge University Press, pp. 121–186.
Roy, P.S., Hudson, J.P., 1988. Surface Sediment Samples from the Inner Continental Shelf between MacMasters and Foresters Beaches on the NSW Central Coast: Interpolation and Correlation with PWD Side Scan Sonar Data. Report prepared for NSW Public

Works Department.
Roy, P.S., Thom, B.G., 1981. Late quaternary marine deposition in New South Wales and southern Queensland: an evolutionary model. J. Geol. Soc. Aust. 28, 471–489.
Searle, D.J., Semeniuk, V., 1985. The natural sectors of the inner Rottnest Shelf coast adjoining the Swan Coastal Plain. J. R. Soc. West Aust. 67, 116–136.
Semeniuk, V., 1993. The Pilbara Coast: a riverine coastal plain in a tropical arid setting, northwestern Australia. Sediment. Geol. 83, 235–256.
Semeniuk, V., Searle, D.J., 1986. Variability of Holocene sea-level history along the southwestern coast of Australia: evidence for the effect of significant local tectonism. Mar. Geol. 72, 47–58.
Shand, T.D., Carley, J., 2011. Investigation of Trial Groyne Structures for Roches Beach, Report to Clarence City Council by Water Research Laboratory. University of New South Wales.
Sharples, C., 2010. Shoreline Change at Roches Beach, South-Eastern Tasmania, 1957–2010. Report to Antarctic Climate and Ecosystems Co-operative Research Centre. University of Tasmania, Hobart.
Sharples, C., Mount, R., Pedersen, T., 2009. The Australian Coastal Smartline Geomorphic and Stability Map Version 1: Manual and Data Dictionary v1.1. Report for Geoscience Australia and the Department of Climate Change, by School of Geography & Environmental Studies. University of Tasmania, pp. 178.
Sharples, C., Mount, R., Hemer, M.A., Puotinen, M., Dell, M., Lacey, M., Harries, S., Otera, K., Benjamin, J., Zheng, X., 2012. The ShoreWave Project: Development of a Methodology for Coastal Erosion Risk Analysis under Climate Change, Integrating Geomorphic and Wave Climate Data Sets. Report to the Commonwealth Department of Climate Change and Energy Efficiency. University of Tasmania, Hobart.
Short, A.D., 1999. Handbook of Beach and Shoreface Morphodynamics. Wiley, Chichester 379 pp.
Short, A.D., 2010. Sediment transport around Australia - sources, mechanisms, rates and barrier forms. J. Coast. Res. 26, 395–402.
Short, A.D., 2012. Adelaide beach management 1836–2025. In: Cooper, J.A.G., Pilkey, O.H. (Eds.), Pitfalls of Shoreline Stabilization: Selected 15 Case Studies. Springer, pp. 15–36.
Short, A.D., Woodroffe, C.D., 2009. The Coast of Australia. Cambridge University Press 288 pp.
Stul, T., Eliot, I., Pattiaratchi, C., 2007. Sediment cells along the perth metropolitan coast. In: Proceedings of Coasts and Ports Australasian Conference. Engineers Australia, Melbourne.
Stul, T., Gozzard, J.R., Eliot, I.G., Eliot, M.J., 2012. Coastal sediment cells between Cape Naturaliste and the Moore River, Western Australia. In: Damara WA Pty Ltd and Geological Survey of Western Australia for the Western Australian Department of Transport, Fremantle.
Stul, T., Gozzard, J.R., Eliot, I.G., Eliot, M.J., 2015. Coastal sediment cells for the Vlamingh region between Cape Naturaliste and Moore River, Western Australia. In: Report Prepared by Seashore Engineering Pty Ltd and Geological Survey of Western Australia for the Western Australian Department of Transport, Fremantle.
Tecchiato, S., Collins, L., Stevens, A., Soldati, M., Pevzner, R., 2016. Carbonate sediment dynamics and compartmentalisation of a highly modified coast: Geraldton, Western Australia. Geomorphology 254, 57–72.
Thom, B.G., 1974. Coastal erosion in eastern Australia. Search 5, 198–209.
Thom, B.G., 1989. Global Climatic Change: Issues for the Australian Coastal Zone. Prime Minister's Science Council. Australian Government Printing Service Press, Canberra 6 October 1989.
Thom, B.G., 2015. Coastal Compartments Project: Summary for Policy Makers. http://www.environment.gov.au/system/files/resources/4f288459-423f-43bb-8c20-87f91adc3e8e/files/coastal-compartments-project.pdf.
Thom, B.G., Hall, W., 1991. Behaviour of beach profiles during accretion and erosion dominated phases. Earth Surf. Proc. Land 16, 113–127.
Trenhaile, A.S., 2011. Predicting the response of hard and soft rock coasts to changes in sea level and wave height. Clim. Change 109, 599–615.
Woodroffe, C.D., Cowell, P.J., Callaghan, D.P., Ranasinghe, R., Jongejan, R., Wainwright, D.J., Barry, S.J., Rogers, K., Dougherty, A.J., 2012. Approaches to risk assessment on Australian coasts: a model framework for assessing risk and adaptation to climate change on Australian coasts. In: National Climate Change Adaptation Research Facility, Gold Coast, 203 pp.
Wright, L.D., 1995. Morphodynanamics of Inner Continental Shelves. CRC Press, Boca Raton.
Wright, L.D., Nichols, C.R., Cosby, A.G., D'Elia, C.F., 2016. Collaboration to enhance coastal resilience. EOS 97, https://doi.org/10.1029/2016EO057981.
Wright, L.D., Thom, B.G., 1977. Coastal depositional landforms: a morphodynamic approach. Prog. Phys. Geogr. 1, 412–459.

Marine Geology 419 (2020) 106081

Contents lists available at ScienceDirect

Marine Geology

journal homepage: www.elsevier.com/locate/margo

Ocean Beach, Tasmania: A swell-dominated shoreline reaches climate-induced recessional tipping point?

Chris Sharples[a,*], Hannah Walford[a], Christopher Watson[a], Joanna C. Ellison[b], Quan Hua[c], Nick Bowden[d], David Bowman[e]

[a] School of Technology, Environments and Design, University of Tasmania, Private bag 78, Hobart, 7001 Tasmania, Australia
[b] School of Technology, Environments and Design, University of Tasmania, Locked bag 1370, Launceston, 7250 Tasmania, Australia
[c] Australian Nuclear Science and Technology Organisation, Locked bag 2001, Kirrawee DC, New South Wales 2232, Australia
[d] Antarctic Climate and Ecosystems Co-operative Research Centre, Private bag 80, Hobart, 7001 Tasmania, Australia
[e] School of Natural Sciences, University of Tasmania, Private bag 55, Hobart, 7001 Tasmania, Australia

ARTICLE INFO

Editor: Edward Anthony

Keywords:
Beach processes
Sea level change
Australia and New Zealand
Spatial analysis
Erosion
Recession

ABSTRACT

Global sea-level rise since the Nineteenth Century is expected to eventually cause recession of many shores, however most swell-exposed sandy beaches have not yet shown such response. This study analysed a 70-year air photo and beach profile record for swell-dominated Ocean Beach (western Tasmania) to show an abrupt change of long-term shoreline position variability circa 1980, from episodic erosion and accretion since at least 1947 to persistent recession with no recovery up to the present. Dating of back-dune peats exposed in the dune scarp showed that recent shoreline recession exceeds any in the last 1800 years. Investigation of potential causes identified recent-onset sea-level rise (SLR) on a tectonically-stable coast and increasing winds driving increased wave-setup as drivers with sufficient explanatory power to account for the observed changes, although data limitations and residual uncertainties mean additional contributing factors such as interdecadal wave direction changes cannot be ruled out. We hypothesise that Ocean Beach has experienced earlier recession in response to SLR and other climate change effects than many other beaches owing to exposure to a very high-energy storm-dominated wave climate, littoral drift efficiently delivering eroded sand to a large-capacity active sand sink, and low variability in swell-wave directions and inter-annual sea-levels. We hypothesise that sea-level rise with higher onshore wind speeds generating increased wave setup at Ocean Beach since before the 1980s has increased upper beach erosion event frequency until the formerly stable or gaining sand budget reversed to deficit. A major storm or storm cluster abruptly tipped the beach into its current recessional mode when its sand budget was close to deficit. Factors causing an early shoreline response to sea-level rise at this site are applicable more widely as potential indicators of beaches likely to respond earlier than others to climate-induced changes including not only SLR but also wind climate changes.

1. Introduction

Long tide gauge records and satellite altimetry show that following a long period of relative stability, a global mean sea-level (GMSL) rise of about 210 mm occurred between 1880 and 2009 (Church and White, 2011). This is mainly attributed to climatically-driven thermal ocean expansion and ice melting and is continuing with an increasing rate (Watson et al., 2015; Chen et al., 2017). A rise of this magnitude would in principle be causing noticeable recession of at least some erodible shorelines as predicted by the 'Bruun Rule of Erosion by Sea-Level Rise' (Bruun, 1962, 1988).

Progressive shoreline recession has been occurring for millennia on coasts with higher than average local relative SLR caused by regional land subsidence (e.g., Pye and Blott, 2006, 2015; Zhang et al., 2004; Romine et al., 2013). However progressive recession has not yet been clearly demonstrated on tectonically-stable coasts where local sea-level rise is comparable with the global average. This is despite a rise of about 210 mm in GMSL since the 1800's with an acceleration to recent rates of $> 3\,\text{mm year}^{-1}$ (Church and White, 2011; Chen et al., 2017), which is comparable to the rates of local sea-level rise causing observed recession on subsiding coasts.

It has proven difficult to identify shoreline changes attributable to recent GMSL change on tectonically-stable coasts because many other processes are active, such as cyclic or episodic wave climate, sea-level

* Corresponding author.
E-mail address: Chris.Sharples@utas.edu.au (C. Sharples).

https://doi.org/10.1016/j.margeo.2019.106081
Received 1 May 2019; Received in revised form 5 November 2019; Accepted 5 November 2019
Available online 06 November 2019
0025-3227/

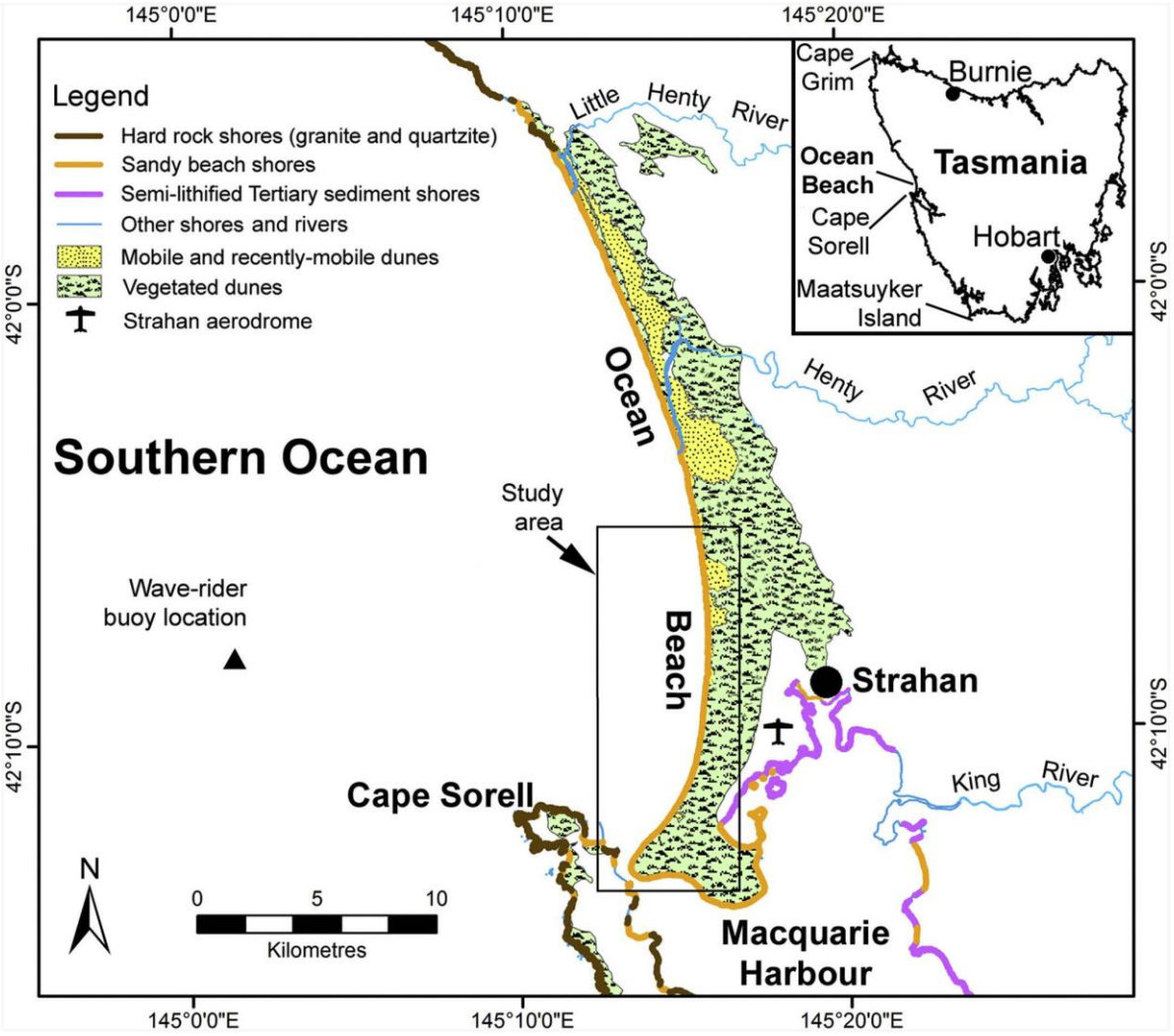

Fig. 1. Ocean Beach locality map. Key elements of coastal geology and local infrastructure including the nearest township (Strahan) are shown. Inset indicates the location of three west coast wind-recording stations mentioned in the text.

or sediment transport variability (Le Cozannet et al., 2014). For some locations it might take centuries for the recession signal associated with GMSL rise to unequivocally emerge from the noise of other processes (Cowell et al., 1995; Stive et al., 2009).

The "Time of Emergence" (Hawkins and Sutton, 2012) of noticeable physical coastal changes in response to recent GMSL rise is an issue of great consequence for coastal populations, ecosystems and infrastructure. Confirmed observation of such attributable changes, or whether it will require some further sea-level rise before the physical effects of recent GMSL rise emerge on tectonically-stable coasts, remains unclear.

This study tests the proposition that shoreline recession attributable to SLR of comparable magnitude as GMSL change may be already observable on some tectonically-stable coasts where the geomorphic environment is particularly susceptible and confounding processes are minimal. The study site is at Ocean Beach on the west coast of Tasmania (Fig. 1), where recent local sea-level rise is commensurate with GMSL rise over recent decades (see below). Ocean Beach is subject to few artificial disturbances, probably-negligible vertical land movement, low swell wave directional variability, low sea-level variability in response to major climate modes such as the El Niño Southern Oscillation (ENSO), and no significant change in swell wave magnitudes or storm frequencies in recent decades (Hemer, 2010). Since only limited quantitative coastal data exists for this relatively remote site (e.g., very coarse bathymetry, no local Global Navigation Satellite System (GNSS) stations), this study relies mainly on qualitative interpretation of geomorphic processes (based on previous work as cited, our field observations and analysis of the air photo record).

Analysis included spatial analysis of the last 70 years of shoreline change at Ocean Beach, based on all usable historic air photos (21 dates), beach profiles at three locations surveyed annually from 2011 to 2018, radiometric ^{14}C dating of peaty sediments exposed in a dune erosion scarp to identify the age of sediments now eroding, and investigation of coastal processes active at Ocean Beach that may drive early landform change in response to sea-level rise and wind climate changes, or else may cause the observed shoreline changes without invoking these.

This paper is structured as follows: Section 1 (this introduction)

identifies the problem we seek to address. Section 2 (Coastal setting) describes existing data about the study site which was selected because of its anomalous recent behaviour. Section 3 (Methods and data acquisition) describes the new shoreline behaviour data collected for this analysis, and the sources of additional data used in our analysis. Section 4 (Results) describes the outcome of these data analyses, identifying that an unprecedented change of behaviour has occurred at Ocean Beach. Section 5 (Discussion) considers possible alternative explanations of the change, and Section 6 (Conclusions) concludes that sea-level rise can explain the observed change but is probably not the only contributing factor. A short final Section 7 (Recommendations) identifies some additional data analyses which cannot be undertaken at present due to lack of adequate-resolution bathymetric data but would when possible provide a test of our explanatory model and no doubt further insights into the study site.

2. Coastal setting

Ocean Beach (145° 15′ E 42° 10′ S) is the longest (32 km) sandy barrier beach on the mostly rocky west coast of Tasmania (Fig. 1) and is exposed to the most energetic and stormy wave climate of any Australian coast (Hemer et al., 2008; Hemer, 2010). The west-facing beach is compartmentalised by long rocky headlands beyond its north and south ends (Davies, 1973). Other shorter more embayed beaches on the west coast probably receive less wave energy at the shore because of refraction against their bounding rocky headlands (Davies, 1973). Significant differences in sand granulometry and composition between Ocean Beach and other west coast beaches implies little alongshore transport of sand into or out of the Ocean Beach embayment (Banks et al., 1977).

The sand is quartz-dominant with only a minor carbonate fraction (Walford, 2011) and is inferred to be of dominantly glacial outwash origin (Banks et al., 1977), with the Henty River that today discharges at Ocean Beach having been a major outwash river delivering sand from the nearby heavily glaciated West Coast Range to the continental shelf during Pleistocene glacial low sea-stands. The sandy barrier has developed across the mouth of the large deep structural trough of Macquarie Harbour (Forsyth et al., 2014), which has a permanently open tidal channel at the southern end of the beach. The beach is today directly backed by mostly vegetated dunes with eroding seawards scarps up to 30 m high exposing palaeosols and some peat lenses.

Ocean Beach faces the Southern Ocean hence receives persistent westerly and south-westerly winds and swells with low inter-annual variability attributed predominantly to the Southern Annular Mode (SAM) (Marshall, 2003). Monthly average significant wave heights (H_s) range between 2.6 m in November and 3.4 m in September recorded by the Cape Sorell wave-rider buoy situated in 100 m water depth 15 km directly offshore from Ocean Beach (Hemer et al., 2008). Westerly winds associated with SAM on the Tasmanian west coast are the strongest and most persistent prevailing winds of any Australian coast (Grose et al., 2010), exposing that coast to strong waves and storms. Waves approach Ocean Beach across a very wide (~600 m) multi-bar surf zone (Short, 2006).

Sand transport within the Ocean Beach embayment is dominated by a mostly southwards littoral drift along the beach which is demonstrated by geomorphic indicators including perched cliff-top dunes indicating beach and dune depletion at the north end of the beach, two large river mouths deflected south along the beach at most air photo dates (see Supplementary information Table S3), an accretionary beach and foredune zone receiving considerable quantities of sand at the southern tip of the beach only (Fig. 2), and the forcing of the tidal channel mouth of Macquarie Harbour against a bedrock headland at the southern extremity of the beach. The very coarse bathymetry available for Ocean Beach (Geoscience Australia: 100 m contour interval) precludes high resolution wave transformation studies to model causes of the littoral drift, however the observed dominantly southwards direction of that drift is its most critical characteristic for this study. A large flood-tide delta just inside the permanently-open tidal entrance of Macquarie Harbour is the final sink for the southwards-drifted sand (Fig. 2), and considerable accommodation space remains available in the harbour to sequester additional sand. There is no evidence of significant present-day supply of river sands to the beach today (Nanson et al., 1995) and the well-embayed location of the beach between long rocky coasts makes significant alongshore sand drift into or out of the embayment unlikely (Davies, 1973).

White et al. (2014) showed that sea-level change around Tasmania has been close to GMSL trends since at least the mid-Twentieth Century, after removal of the effects of ENSO. Sea-levels around Tasmania are less influenced by seasonal and inter-annual variability related to the ENSO than are more northerly parts of Australia (Burgette et al., 2013), implying a reduced contribution from this driver to shoreline change at Ocean Beach compared with beaches elsewhere in Australia.

There are no nearby estimates of Vertical Land Movement (VLM) for Ocean Beach, however recent GNSS data and GIA model-based estimates imply vertical land stability or only slight subsidence between 0.0 and $-1.0\,mm\,year^{-1}$ for northwest and southeast Tasmanian coastal sites, with most estimates closer to $0.0\,mm\,year^{-1}$ (King et al., 2012; Santamaria-Gomez et al., 2012; Burgette et al., 2013; Argus et al., 2014; White et al., 2014; Peltier et al., 2015). There is no anthropogenic extraction of sub-surface fluids or other known processes such as significant seismic activity likely to cause significant local VLM at Ocean Beach, and in particular no significant groundwater extraction for utility purposes in this region (the average annual rainfall to 1999 recorded at the closest weather station to Ocean Beach (Strahan Airport) was $1493\,mm\,year^{-1}$, indicative of the generally high precipitation in western Tasmania: Australian Bureau of Meteorology data). However, whilst there are no known local processes likely to cause VLM at Ocean Beach, the lack of GNSS data from the immediate vicinity of Ocean Beach implies a residual uncertainty over the possibility of local VLM rates sufficient to influence coastal processes.

Ocean Beach is largely free of artificial disturbances that may affect geomorphic processes at the beach face and dune front. The backshore area is unsettled public land except at the southern and northernmost extremities where small settlements exist. There are no groynes, seawalls or other artificial structures on or likely to affect the beach face. Training walls along the rocky south shore of the mouth of Macquarie Harbour are unlikely to have changed the capacity of the adjacent ebb- and flood-tide deltas to be sand sinks. Vehicular access to the beach exists at five points in the study area; at each there is some vehicular erosion of the dune face over distances of a few metres. Recreational four-wheel drive vehicles access the beach from the dunes at these points, but their use is mostly limited to the tidal beach face.

Plantations of introduced pines (*Pinus radiata*) were established over 150 m inland from the present beach and dune front from the 1980s on and are unlikely to affect beach processes. However, the introduced dune-colonising grass *Ammophila arenaria* ('marram grass') is common in the dunes immediately backing the beach, where it was deliberately planted from the 1950s to stabilise the then-extensive active transgressive dunes (Cullen, 1998) and may have contributed to shoreline progradation prior to 1980 (see Section 4.1). Cattle grazing, and fires have also historically occurred on parts of the stabilised dunes landwards of Ocean Beach (Banks et al., 1977) but have not occurred in recent decades.

3. Methods and data acquisition

Initial studies undertaken as detailed in Section 3.1 below demonstrated a major change of shoreline behaviour at Ocean Beach and that the degree of this change was unprecedented in over 1800 years (as described in Section 4.1). Subsequently, data on possible drivers of this change were obtained as described in Section 3.2 (these are explored in Section 4.2).

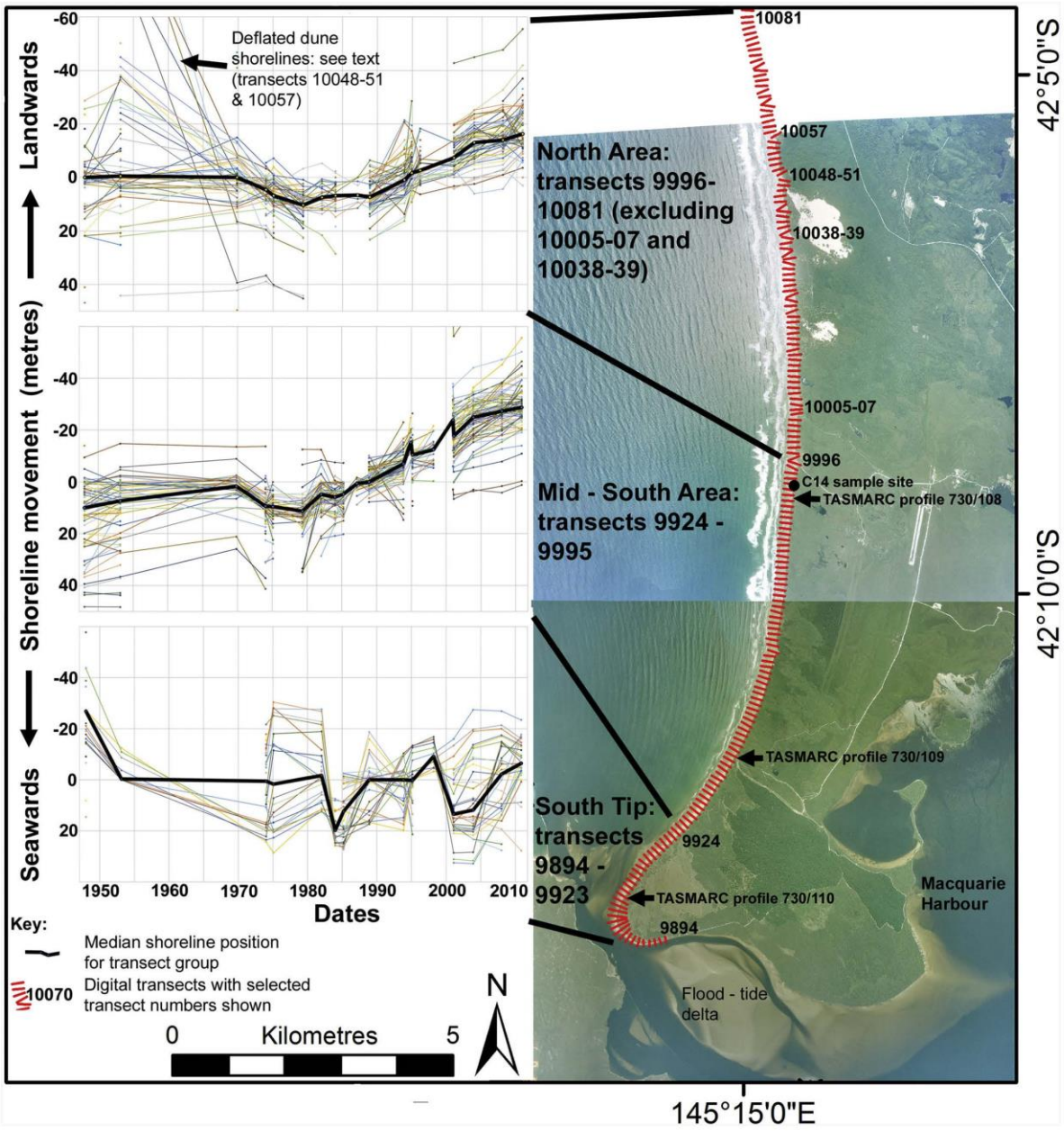

Fig. 2. Air photo spatial analysis results of shoreline horizontal movement for the whole Ocean Beach study area (see text). Numbered digital transects (shore-normal lines) defining the Ocean Beach study area are plotted over the 2008 air photo, and plots of all included transect shoreline movement histories are shown grouped into three areas (see also Supplementary information). Also shown are beach profile survey (TASMARC) locations and peat site sampled for ^{14}C radiocarbon dating.

3.1. Data on shoreline change

3.1.1. Air photo history (1947–2010)

Aerial photography is available for Ocean Beach from 1947 until 2010. The study area comprises the southern half of Ocean Beach, an approximate length of 18 km, because over much of the air photo period the northern half of the beach was dominantly backed by unvegetated transgressive dunes so that at most air photo dates a shoreline position would not be identifiable by the methods adopted for this study.

Historic air photos were obtained from the Tasmanian Department of Primary Industries, Parks, Water and Environment (DPIPWE), comprising air photos taken at 21 dates between Dec. 1947 and Nov. 2010 at scales ranging from 1:15,840 to 1:45,000 (see Supplementary information Table S1). The 2008 air photo was ortho-rectified using control points from 1:25,000 topographic mapping, and was then used as the control image against which to ortho-rectify remaining photos and to provide reference features to measure error margins in all ortho-

photos.

The shoreline proxy used was the vegetation line at the back of the beach (Boak and Turner, 2005), which is readily mappable from air photos at all dates used despite varying photo scale and contrast limitations that may rule out the use of some other shoreline proxies requiring determination of shoreline elevations from stereo-photos. This line is a reliable indicator of erosion and recession (indicated on photography by the vegetated top of a dune erosion scarp) or accretion and progradation (by a vegetated incipient foredune front). This shoreline feature was manually digitised for each air photo date in a homogeneous process by only two operators (CS and HW).

Shoreline change was measured as horizontal movement of the digitised shoreline position over time along each of ≈180 shore-normal transects spaced 100 m apart. Visual inspection of shoreline history plots initially grouped into 3 three areas identified two regions with different broadly coherent histories, namely a small episodically accreting south tip area and a much longer north to mid-south section whose history is the focus of this study (see Fig. 2). For this section, the median of the shoreline positions at each date across all used transects (153) were plotted to provide a final quantitative shoreline movement history summary for further analysis, with average shoreline position error margins at each air photo date based on reference feature displacements compared to the 2008 air photo (see Supplementary information for more details of air photos used and analysis).

3.1.2. Shore profile surveys (2011–2018)

No pre-2011 shore profile surveys for Ocean Beach are known to us. As part of the Tasmanian Shoreline Monitoring and Archiving Project (TASMARC) three survey marks were placed at Ocean Beach during 2011 and their positions established to ± 50 mm using differential GNSS. A profile transect across the beach and backshore has been surveyed approximately annually up to 2018 from each survey mark, using conventional total station survey methods (TASMARC, 2019). These surveys have allowed the extension of the air photo-derived shoreline change record (up to 2010) until 2018 at the three survey transect locations, at finer spatial and temporal scale than is provided by the air photo record.

3.1.3. Backshore peat sediment dating

Peats exposed in a 2 m high eroding shoreline scarp interpreted as a former interdune swale were sampled for radiocarbon (^{14}C) dating, to identify the minimum time since the dune-front was last eroded back as far as it is now (see also Supplementary information). Samples were obtained from the dune face by manually sampling a cleaned vertical section at regular intervals; samples were sealed in plastic bags on site. Radiocarbon dating by accelerator mass spectrometry (AMS) was conducted at the Australian Nuclear Science and Technology Organisation (ANSTO) (Hua et al., 2001; Fink et al., 2004). Chronology of the peat profile was constructed using the SH zone1–2 bomb ^{14}C data (Hua et al., 2013) extended back in time by the SHCal13 data (Hogg et al., 2013), and the OxCal P_sequence with variable accumulation rate k (Bronk Ramsey and Lee, 2013).

3.2. Data on potential drivers of shoreline change

Data on possible drivers of shoreline changes were acquired and analysed as described below.

3.2.1. Geomorphic processes

Apart from limited sand sampling and granulometry (Banks et al., 1977; Short, 2006), quantitative or detailed geomorphic process studies relevant to shoreline change at Ocean Beach have not previously been undertaken. Discussion of geomorphic or morpho-dynamic processes provided here is based on interpretation of available data as cited, air photo interpretation, and multiple site visits by the first two authors.

3.2.2. Sea-level history

There are no long-term tide gauge records for the west coast of Tasmania, with the best record for the region being a fragmentary record for Granville Harbour (about 30 km north of Ocean Beach) totalling only 4.2 years of actual records between 1974 and 1994 (Sharples, 2006). More comprehensive tide gauge records exist for northern and south-eastern Tasmania (approximately 125 to 200 km away), yet the useful records remain limited in time to 1992 onwards. Here we use the regional sea surface height (SSH) reconstruction of Church and White (2011), and that prepared by the method of Hamlington et al. (2011), to compare reconstructed sea-level change (since ~1950) with shoreline change at Ocean Beach. Both reconstructions show close agreement to the Tasmanian tide gauge record (where available) and hence present a valuable data source for this study. Carson et al. (2017) have demonstrated some significant residual uncertainties for pre-1992 reconstructions at some locations (e.g., Sydney), however Fig. 7 of the same analysis indicates low interdecadal variability deviation for the Ocean Beach region. See also the Supplementary information including Fig. S1.

3.2.3. Swell wave climate

This project has relied on previous studies in evaluating the influence of swell wave climate on shoreline behaviour at Ocean Beach. Quantitative swell wave parameters for Ocean Beach are derived from the 1979–2010 CAWCR wave hindcast (Durrant et al., 2013, which includes metadata) and are summarised in Table 1. Hemer (2010) and Hemer et al. (2008, 2010) have described the swell wave climate reaching Ocean Beach, based on data from the adjacent Cape Sorell wave-rider buoy, satellite altimetry and global ocean wave models. The Cape Sorell wave-rider buoy is located about 15 km directly offshore from Ocean Beach and is Tasmania's only long term (since 1985) observational wave climate record, measuring combined swell and locally-generated wind wave heights. Wave direction is not quantified in this record.

3.2.4. Wind data

Historical variability in onshore winds at Ocean Beach and some other west coast areas has been explored because changes in wind speeds and directions may affect shoreline processes as noted in Section

Table 1
Swell wave climate characteristics at Ocean Beach. Notably the winter wave direction is more south-westerly than the summer wave directions, which is anomalous compared to adjacent more exposed hindcast cells which receive more westerly winter wave directions as expected from the SAM influence on this coast. The anomalous more SW winter wave directionality may be related to local wave refraction effects around Cape Sorell.
Data from the CAWCR hindcast (Durrant et al., 2013).

	Significant wave height (Hs) m	Maximum wave height (max) m	Mean wave period (Tm) s	Mean wave direction (Dm) ° T
Annual average value	2.43	5.33	8.36	241
Average summer value (DJF)	2.07	4.62	7.94	246
Average autumn value (MAM)	2.35	5.30	8.52	245
Average winter value (JJA)	2.74	5.89	8.65	227
Average spring value (SON)	2.56	5.53	8.33	245

4.2.3.

For this study, synoptic (typically 3-hourly) and daily extreme wind data records from 1957 until 2015 were obtained from the Australian Bureau of Meteorology for coastal weather stations at Cape Sorell and Strahan Aerodrome close to Ocean Beach, Maatsuyker Island near Tasmania's south-western tip, and for Cape Grim in the north-western tip of Tasmania (see Fig. 1).

4. Results

4.1. Beach shoreline change

Results from the air-photo time series of 21 dates from 1947 to 2010 showed that most of the study area shoreline (north and mid-south plot groups in Fig. 2) has undergone a marked change of long-term (multi-decadal) behaviour during the Twentieth Century, from dynamic equilibrium about a roughly stable or slightly prograding shoreline position, to persistent and still-continuing shoreline recession. This change occurred abruptly circa 1980, within a 2.5-year interval between the air photo dates 5th May 1979 and 16th Jan 1982. Median progressive horizontal shoreline recession from after 1979 until 2010 was approximately 35 m, which is about an order of magnitude greater than the mean measured air photo error margins of ± 1.3 to ± 3.8 m (Supplementary information Table S1), and hence represents a real change in long-term beach behaviour after 1979. There is no evidence in the air photo record of dune recovery during this period, and beach profiling (see immediately below) shows the same trend continuing without recovery to the present.

The southern tip of Ocean Beach shows quite different behaviour throughout the air-photo period, of episodic shoreline erosion and accretion but no overall trend towards either recession or progradation (Fig. 2).

Approximately annual beach profile surveys from 2011 to 2018 at TASMARC profiles 730/108 and 730/109 (Fig. 3) showed un-interrupted continuation of the erosion and recession trends observed in the air photo record for those sites, at rates averaging close to 1 m per year, along with lowering of the beach face. At each survey, the erosion scarps were fresh with some collapses but no indication of shoreline recovery such as incipient foredune accretion. The TASMARC profile 730/110 at the southernmost tip of the beach (Fig. 3) shows a continuing pattern of alternating erosion and accretion during 2011 to 2018 as seen in the prior air photo record for that area.

Lenses of peat and sandy peat about 1.7 m deep with inter-bedded inferred aeolian sands were found in the actively receding shoreline scarp at 42° 8.9′ S 145° 15.8′ E, about 225 m north of the surveyed beach profile 730/108 (see Fig. 4). Radiometric ^{14}C dating of 8 peat samples from the scarp yielded ages grading from modern at the surface to a median modelled and calibrated age of 1863 cal. years BP at the base of the peat lens (see details in Supplementary information Table S2). The approximately 2 m high active scarp at this location is backed by flat ground interpreted as a former inter-dune swale, extending 40 m landwards to the foot of the first dune behind the beach at this location. The peat lenses are interpreted as inter-dune swamp deposits. The lenses are exposed in the scarp over an alongshore distance of about 250 m north to south. The aerial photography shows that a substantial foredune about 20 m wide was present to seawards of the sample site from before 1947 until at least 1982, when the current phase of shoreline recession started. The sample site was then a poorly-drained back dune swale. By circa 1994 this dune had eroded back to such a degree that the swamp would have been freely draining and relatively dry at the surface. This is consistent with the ^{14}C peat dates which indicate that peat accumulation in the upper lens continued until modern times.

4.2. Potential drivers of beach change

Coastal processes investigated for potential influence on the observed shoreline change history are described below.

4.2.1. Local sea-level history in relation to beach behaviour history

The rates of sea-level rise reconstructed for Ocean Beach by Church and White (2011) and by the method of Hamlington et al. (2011) are comparable to GMSL (White et al., 2014) and to rates measured from the longest tide gauge record available for Tasmania (Hunter et al., 2003), of 0.70–1.30 mm year^{-1} between 1841 and 2002 in south-east Tasmania. Given the lack of a likely regional explanation for this rise (e.g., VLM), Hunter et al. (2003) inferred it commenced during the 1800s as part of the recent global sea-level rise observed at long-term tide gauges elsewhere.

Fig. 5 plots the median air-photo derived shoreline change history for the Ocean Beach study area (excluding southernmost tip) against the monthly Hamlington et al. reconstructed Sea Surface Height (SSH) history smoothed with a 1-year moving average to remove annual (seasonal) noise and zeroed arbitrarily. The SSH and shoreline position histories show significant overall rising and receding trends (respectively) over the air photo record period. Unsurprisingly, these series yield a high Pearson correlation co-efficient between the two datasets; for raw monthly SSH, $r^2 = 0.84$ (95% confidence interval 0.64–0.93, $p < 0.0001$), and for yearly moving-averaged SSH, $r^2 = 0.83$ (95% confidence interval 0.62–0.93, $p < 0.0001$). The effect of air photo error margins on the correlations was tested using random (Monte Carlo) resampling of shoreline positions at each air photo date within 1 standard deviation of the measured (mean) error margins; 5000 iterations yielded a strong peak in r^2 values between 0.80 and 0.85 implying the relatively small error margins have negligible effect on the correlation found.

To assess correlation with inter-annual and higher frequency signals within the data, a single linear trend was subtracted from the SSH record, and piecewise linear trends removed from the shoreline history data pre- and post- the marked change of shoreline behaviour around 1980 (see linear trend lines in Fig. 5). The detrended datasets yield only a low correlation co-efficient: for raw monthly SSH, $r^2 = 0.04$ (95% confidence interval − 0.40-0.47, p-value = 0.8567), and for yearly moving-averaged SSH, $r^2 = -0.11$ (95% confidence interval − 0.52-0.34, p-value = 0.6287). The amplitude of the interannual signal in the SSH record was ~10 to 80 mm, consistent with sites having little exposure to larger modes of climate variability such as ENSO (White et al., 2014).

4.2.2. Swell wave climate and storminess

Waves are the primary agent of shoreline erosion, and variation in both swell wave energies or direction may drive shoreline position changes. This work has relied on previous wave climate studies as cited below, which should be referred to for additional information. Ocean Beach receives a persistently south-westerly swell from the Southern Ocean where some of the largest waves of the global ocean are generated during extra-tropical cyclonic storms as far south as 55–60° S (Hemer et al., 2008). Highly energetic extreme wave events and a predominance of swell over local wind sea states are a characteristic of the wave climate at Ocean Beach (Hemer et al., 2008).

Table 1 shows wave climate parameters offshore from Ocean Beach, derived from the closest cell of the 1979–2010 CAWCR wave hindcast (Durrant et al., 2013), which is centred about 6.5 km offshore from the middle of the Ocean Beach study area, and receives slightly lower waves than adjacent more exposed hindcast cells.

The primary mode of swell wave climate variability (in both wave height and direction) along the southern margin of Australia including western Tasmania is correlated with the SAM (Hemer, 2010; Hemer et al., 2008). Annual cycles in SAM result in the Southern Ocean storm belt moving south during the southern summer resulting in more south-

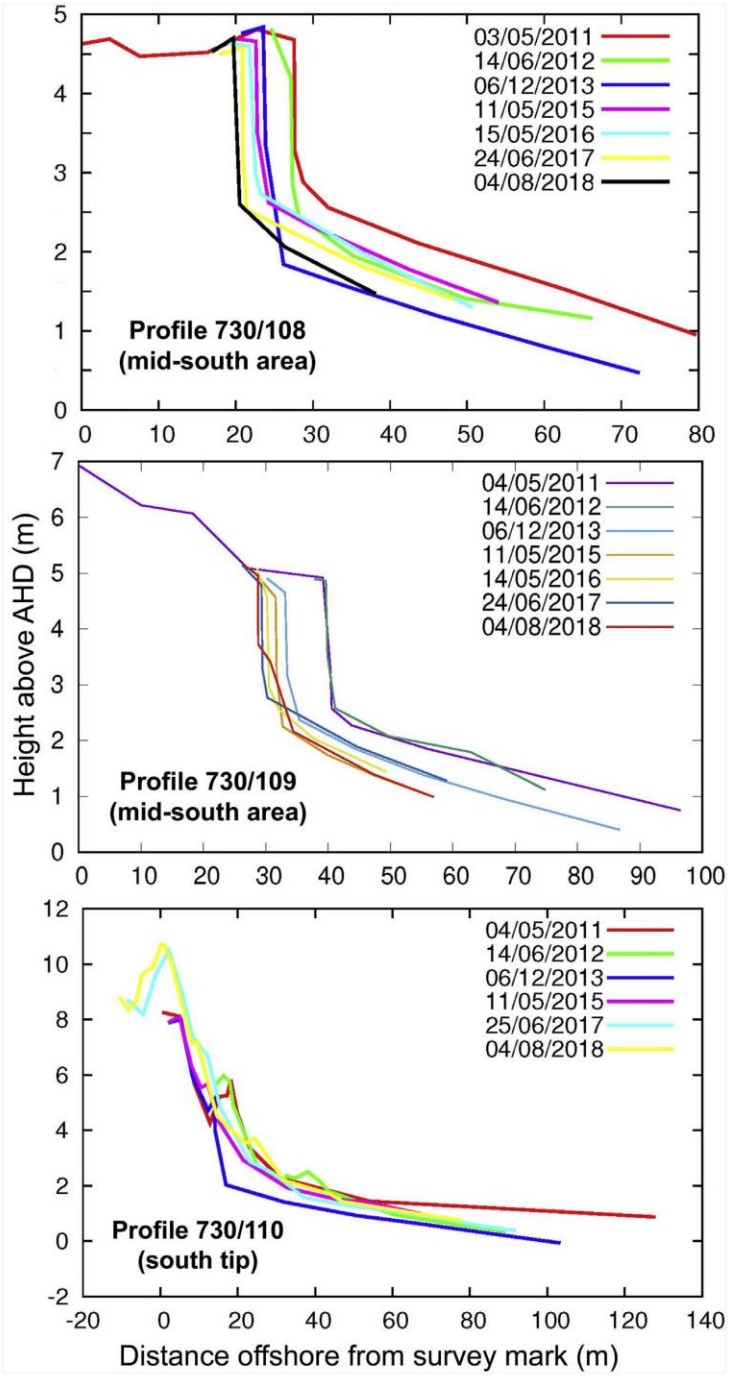

Fig. 3. Ocean Beach TASMARC beach profile results (TASMARC, 2019). See Fig. 2 for profile locations. 'AHD' is the Australian Height Datum.

westerly waves reaching western Tasmania, and north in winter with waves arriving from more westerly directions (Hemer et al., 2008). Mean swell direction variability is limited to approximately 20° at Ocean Beach (Table 1), which greatly reduces the potential for sand transport reversals and beach rotation compared to eastern Australian beaches dominated by variation attributed to the ENSO (e.g., Ranasinghe et al., 2004; Mortlock et al., 2017).

A significant trend towards the positive (higher index) phase of the SAM has been observed since the mid-1960s (Hemer, 2010; Hemer et al., 2008; Marshall, 2003), resulting in an increase in wave heights in the far Southern Ocean (south of ~48°S) and an anti-clockwise rotation of wave directions associated with a southwards movement and

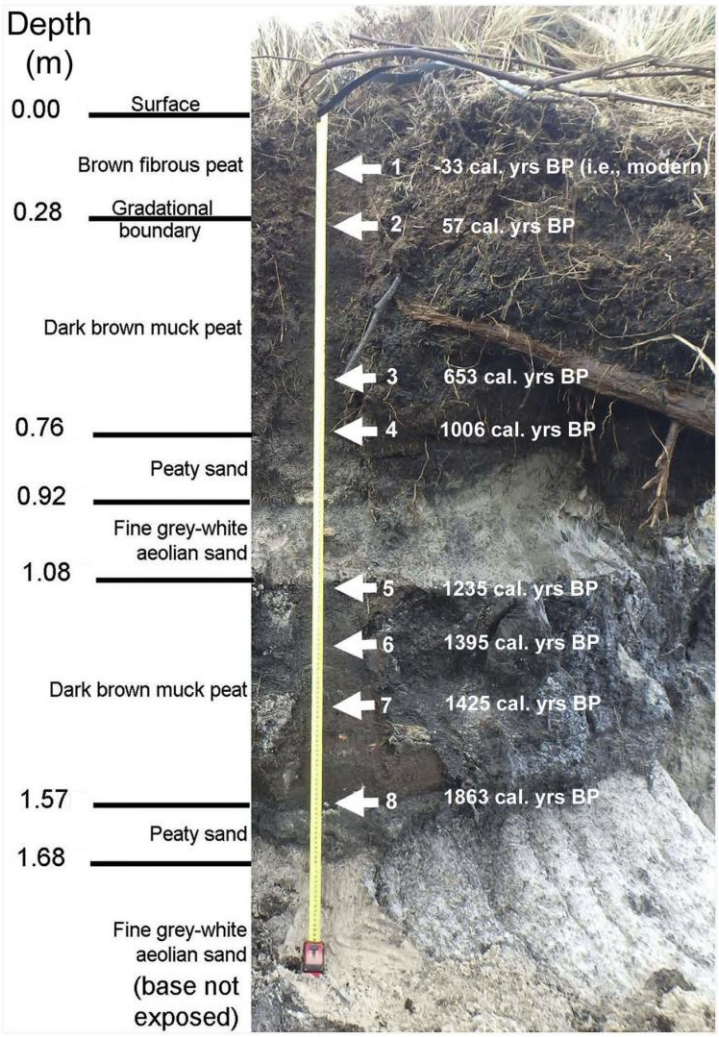

Fig. 4. Sampled Ocean Beach erosion scarp peat profile, showing facies variations with depth in metres, and location of samples 1 to 8 for which Carbon-14 dates were obtained (see details in Supplementary information Table S2). The median modelled calibrated age (cal. years BP) is indicated beside each sample number.

intensification of the Southern Ocean storm belt (Hemer et al., 2010). However, 17 years of data from the Cape Sorell wave-rider buoy between 1985 and 2008 showed no increase in storm wave (extreme height) event frequency over that period and in fact show a non-significant decrease (Hemer, 2010). Satellite altimeter data also showed a non-significant negative trend in wave height (mean Hs) west of Tasmania over the same period (Hemer, 2010; Hemer et al., 2010). This may reflect the fact that whereas the southwards drift of SAM results in generation of higher waves, these lose more energy travelling the increased distance northwards to western Tasmania (M. Hemer, pers. comm.).

These results indicate that increases in wave height (mean Hs) and storm wave event frequencies have so far been limited to latitudes south of 50° S and are unlikely to be drivers of changing shoreline behaviour to date at Ocean Beach. However, the same southwards drift of SAM is expected to have resulted in swell-wave directions in western Tasmania becoming more frequently more south-westerly and less westerly than previously, albeit observation of the latter near Ocean Beach is lacking due to the Cape Sorell wave-rider buoy being incapable of measuring wave direction.

4.2.3. *Wind trends*

Wind climate drives locally-generated wind-waves and near-shore wave setup which may contribute to shoreline change through erosion, as well as landwards aeolian loss of sand in dunes. Evidence from aeolian sediments show that the westerly winds that dominate western Tasmania have varied in intensity on centennial and millennial time scales over at least the last 20,000 years, and that present-day westerly winds are as strong now as at any time in the last glacial climatic cycle (Shulmeister et al., 2004). Regional studies of the SAM have indicated increased wind speeds over the Southern Ocean by about 20% since circa 1990 (Hurrell and van Loon, 1994; Thompson and Solomon, 2002; Gillett et al., 2006; Hemer et al., 2010).

Analyses of historical trends in measured wind speed records in the Australian region to date have been inconclusive (McVicar et al., 2008; Troccoli et al., 2012; Walsh et al., 2016). A national study by Troccoli et al. (2012) identified instrument variability (especially height) as a major influence on apparent wind speed trends recorded, with

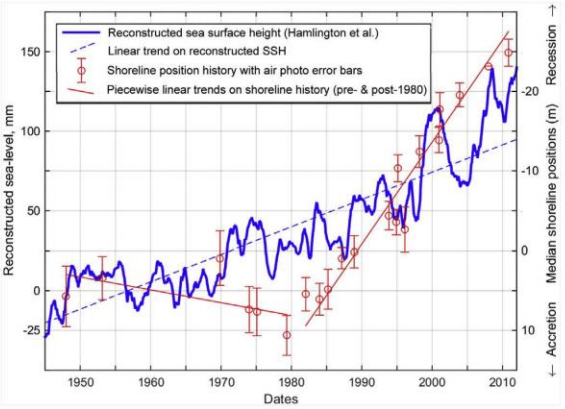

Fig. 5. Shoreline position history at air photo dates and reconstructed sea surface height history with linear trend lines. Error bars show the mean air photo position errors at each air photo date. A single linear trend line is fitted to the SSH history, and piecewise linear trends are fitted to the shoreline position history pre- and post-1980.

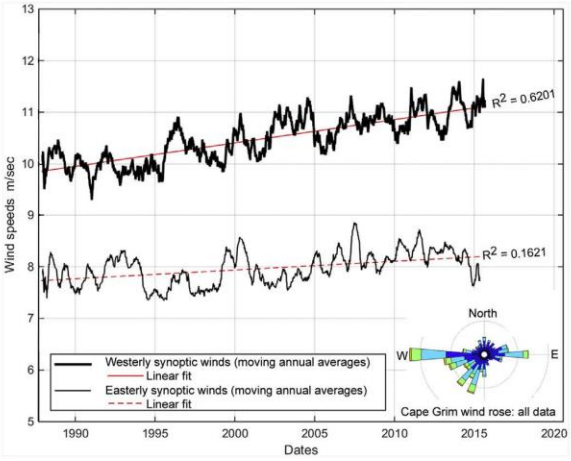

Fig. 6. Moving annual averages on easterly and westerly synoptic wind speed records from Cape Grim: Synoptic (3-hourly) wind speed data from 1988 to 2015, showing dominantly seasonal (annual) variability in the easterly winds, but also longer inter-annual cycles in the westerly winds.
Original observational data from the Australian Bureau of Meteorology (2016).

sheltering, local topography and data continuity also affecting data quality.

Cape Sorell and Strahan Aerodrome weather stations are close to the Ocean Beach study area (Fig. 1), however synoptic wind observations from these stations are subject to a 21-year data gap at Cape Sorell, with varying recording protocols and step changes in the data at both sites suggestive of local changes, e.g. instrumentation. The best quality data at both sites (1993 to 2014/15) is weakly suggestive of onshore (westerly) mean wind speed increase trends (see Supplementary information Fig. S2).

Directional wind data is consistent from both weather stations (Supplementary information Fig. S3) showing dominantly north-westerly to south-westerly winds consistent with the SAM. These may drive onshore local wind waves at Ocean Beach, which would be roughly coincident with the south-westerly swells arriving at Ocean Beach and contributing additional wave setup. A notable secondary feature across the records is a strong northerly wind component which would drive local wind-waves in a southerly alongshore direction at some times.

As the whole west coast of Tasmania including Ocean Beach is exposed to the same SAM-influenced wind climate, major trends in other wind records for the Tasmanian west coast may plausibly be inferred to be indicative of dominant wind trends at Ocean Beach. Kirkpatrick et al. (2017) interpreted Bureau of Meteorology wind records for Maatsuyker Island (on the south-western Tasmanian coast, see Fig. 1) as indicating an increase in winter wind speeds over the period 1970–2015. That study correlated this finding with variability in the SAM, reflected in a recent strengthening of the high-pressure zone to the north of Tasmania in winter and a decrease in pressures to the south.

The weather station at Cape Grim, 150 km north of Ocean Beach and exposed to the same westerly airstream, provides a high-quality west coast wind record from 1988. Cape Grim synoptic wind records show a dominant westerly to south-westerly directional component comparable to that at Cape Sorell and Strahan Aerodrome, with a subordinate easterly component. We have plotted these separately as approximately 1-year moving averages (Fig. 6). The easterly wind speeds show a strong annual (seasonal) cycle with only a weak increasing linear trend. The westerly wind speeds show a less regular inter-annual cycle with sub-ordinate seasonal cycles, and a strong linear trend to higher wind speeds over the record period ($R^2 = 0.6201$). The same significant linear trend to higher wind speeds is also evident in the annual means of the synoptic westerly wind speeds at Cape Grim.

There was no significant correlation found between the inter-annual variability in the Cape Grim westerly wind component and the Southern Oscillation Index (SOI), reflecting the limited influence of ENSO on the Tasmanian west coast. However, with linear trends removed, the westerly wind variability shows a weak correlation ($R^2 = 0.26$, $p < 0.0001$) with the inverse of the Antarctic Oscillation Index (AAO) measure of SAM (see Supplementary information Fig. S4), reflecting the influence of SAM on the westerly winds. The clear trend to increasing westerly wind speeds in the Cape Grim wind record over the last three decades supports the interpretation that the more equivocal Cape Sorell and Strahan Aerodrome records do indeed reflect an increasing westerly and south-westerly wind speed trend at Ocean Beach over a similar period, since these winds are responding to the same driving processes (the SAM) as the westerly Cape Grim winds.

5. Discussion

5.1. A long-term change of behaviour

The air photo analysis results (Figs. 2, 5 and 7) demonstrate that about 1980 Ocean Beach switched abruptly from a multi-decadal history of relatively stable or prograding shoreline positions to a persistently receding shoreline which continues without any evidence of dune or shoreline recovery up to at least 2018. Median progressive horizontal shoreline recession from circa 1980 until 2010 was approximately 35 m (Fig. 7), which is well outside the mean measured air photo error margins of ± 1.3 to 3.8 m (Supplementary information Table S1). Although the beach underwent this marked change of long-term behaviour circa 1980, the "Time of Emergence" (Hawkins and Sutton, 2012) indicated is the date (circa 1998) at which the subsequent persistent recession trend exceeded the limits of historic shoreline position variability (including error margins) and can be identified as a new mode of shoreline change for this beach. Beach profile monitoring at two sites demonstrates the recession trend has continued from 2011 to 2018 without abating (Figs. 3 and 7). Although direct measurements of shoreline position only extend back to 1947, ^{14}C dating of inferred back-dune swamp peats exposed in the receding shoreline scarp (Fig. 4 and Supplementary information Table S2) imply the current receded shoreline position hasn't been reached in at least the last 1800 years, since any recession of this extent would have previously destroyed the basal peat layer. It can be inferred from this that the current recession

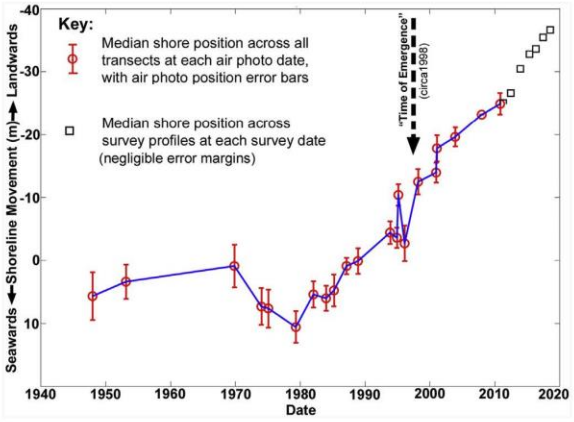

Fig. 7. Summary plot of shoreline change history at the Ocean Beach study area, showing the median horizontal shoreline position at each air photo date to 2010 across 153 normalised transects comprising the North plus Mid-south study site sections (see also Fig. 2), and the median shoreline positions across 2 beach profiles measured within the same area from 2011 to 2018 (see also Fig. 3). The Supplementary information provides further details on the construction of this figure.

phase is of greater magnitude than any decadal- to centennial-scale cyclic or episodic processes affecting this beach. The duration and magnitude of this changed behaviour is unprecedented for Tasmanian beaches including other west coast beaches, based on both anecdotal and published data sources.

The observed switch from stability or progradation to persistent recession at Ocean Beach is comparable to that expected for sandy swell-exposed beaches in response to an onset of sea-level rise after a period of negligible rise, in the absence of confounding factors (Bruun, 1962, 1988). However, many swell-exposed sandy beaches have not yet shown a comparable change despite a similar recent SLR history. To test the hypothesis that Ocean Beach is responding to sea-level rise we ask two questions below, namely: "Are there geomorphic process conditions at Ocean Beach that would allow an earlier switch to recession in response to sea-level rise than on most open sandy coasts?" (Section 5.2); and conversely "Are there factors other than sea-level rise at Ocean Beach that could have caused the observed change in behaviour?" (Section 5.3).

5.2. A model for an early response to sea-level rise at Ocean Beach

We propose a simple hypothesis relying upon observations and supported by generalised models of geomorphic and oceanographic processes (as described in this paper) which can explain the switch to an unprecedented degree and duration of recession at Ocean Beach as a response to recent-onset sea-level rise (Fig. 8). We note other changing drivers which may be additional factors in the following Section 5.3.

As noted in Section 2, dominantly southwards littoral drift is a major sand transport process at Ocean Beach which has caused persistent and ongoing sand loss into the large active sand sink of the Macquarie Harbour flood-tide delta (Fig. 2). Landwards loss of deflated sand in transgressive dunes is a secondary sink albeit air photos show its capacity has reduced since 1947. However air photo evidence of shoreline stability or progradation prior to 1980 (Figs. 2 and 7) implies that loss of sand into these sinks must have been fully compensated for by the only likely present-day sand source, namely sand actively driven onshore from the inner continental shelf by bottom currents associated with the large south-westerly swell (as modelled by Harris et al., 2000 in: Harris and Heap, 2014).

As local mean sea-level progressively rose during the Twentieth Century (Fig. 5), storm wave events of any given magnitude must have more frequently reached higher on the shore profile and eroded more sand from the upper beach and dune face than previously, providing an increasing supply of sand to the nearshore southwards littoral drift current. This would have resulted in increasing rates of sand loss into the Macquarie Harbour sand sink. However, we have no evidence of an increased supply of sand to the beach from the shelf to compensate, for example by increased swell wave magnitudes driving more sand onshore from the shelf (Hemer, 2010; Hemer et al., 2010).

With continuing sea-level rise gradually increasing the rate of net sand loss by this means, by circa 1980 Ocean Beach was probably close to a state of dis-equilibrium, i.e. losing more sand than it was gaining. A major storm or cluster of storms is implied by air photo evidence of shoreline erosion circa 1980, and this could have 'tipped' the beach into recessional mode by removing a large mass of sand at a time when the sand budget was already close to net sand loss. Continued shoreline recession without shoreline or foredune recovery up to 2018 reflects an ongoing and probably still increasing sand deficit driven by ongoing SLR, further diminishing the capacity of the beach to recover between storm erosion events.

This model (see Fig. 8) is consistent with the finding (Section 4.2.1) that shoreline recession and rising sea-levels trends at Ocean Beach are strongly correlated on multi-decadal time-scales (as expected from first principles), but not on shorter time-scales. The observed abrupt shoreline change is unrelated to inter-annual SSH variability but is consistent with a gradually depleting sand budget being tipped into a new state by a large erosion event.

5.3. Can other factors explain the observed change of shoreline behaviour?

A multi-decadal variation in onshore supply of sand to the beach from the inner shelf would explain the observed shoreline history if it caused a marked reduction in sand supply circa 1980. Since the modelled sand supply (Harris et al., 2000 in: Harris and Heap, 2014) is inferred to be a swell-driven process, changes in the SAM-driven swell wave climate would be necessary to explain any reduction. However there has been no observed significant change in swell wave magnitudes in recent decades at the nearby Cape Sorell wave-rider buoy which might alter rates of shelf sand mobility (Hemer, 2010; see Section 4.2.2). Alternatively, sand waves moving laterally along the inner shelf might cause periodic sand depletion, however available data does not support this explanation: Davies (1973) noted the adjacent Cape Sorell is probably a major barrier to such lateral shelf sand transport, and this is also implied by significant differences in sand granulometry and composition between Ocean Beach and other west coast beaches noted by Banks et al. (1977). Whilst the nature of shelf sand deposits off the Tasmanian west coast remains little studied beyond the glacial origins of the sands adjacent Ocean Beach (see Section 2), the limited available data does not support circa 1980 changes in onshore sand supply to Ocean Beach.

Swell direction variability can markedly change sand movement directions causing beach rotation (involving new patterns of erosion and accretion) on some coasts (Ranasinghe et al., 2004; Hemer, 2009; Hemer et al., 2010; Mortlock et al., 2017). However, swell wave direction variability at Ocean Beach is very limited on both annual and inter-decadal time scales (since at least the 1960s) resulting in a mainly south-westerly swell direction (Section 4.2.2, Table 1). Given the linear and roughly north-south orientation of the Ocean Beach coast, the limited swell wave direction variability (which will be further reduced crossing the very wide multi-bar surf zone) would not explain reversals of alongshore sand movement directions, and air photo time series of the deflection of river mouths across the beach (referred to in Section 2 above) shows no geomorphic evidence of any significant change in littoral drift around 1980. Nor is it obvious that limited wave direction variability would cause a major reduction in rates of onshore sand supply. Indeed, the expected anti-clockwise inter-decadal trend in swell

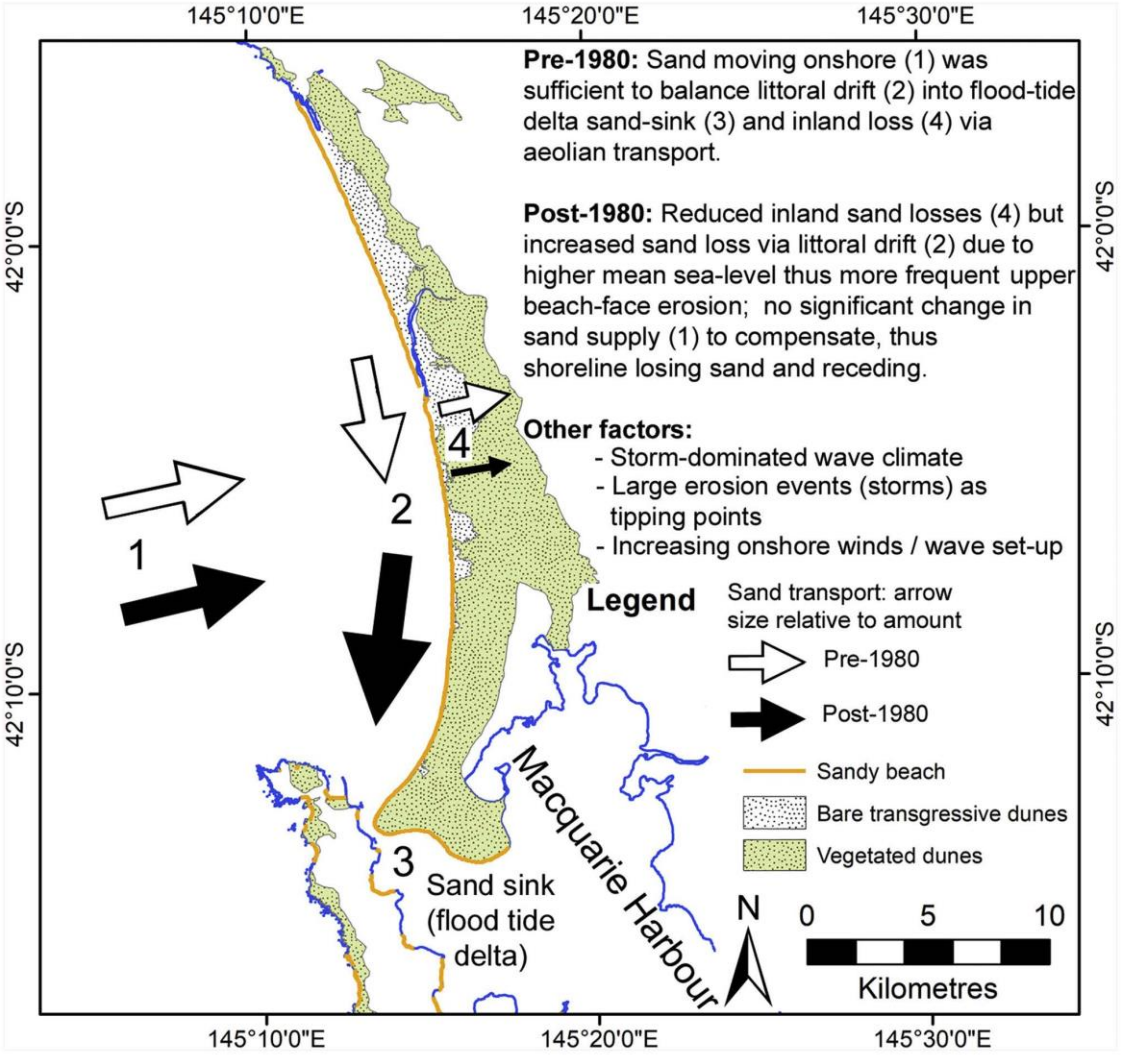

Fig. 8. Shoreline change process model for Ocean Beach.

directions (Section 4.2.2) should in principle have resulted in a more northerly or at least a reduced magnitude of southerly littoral sand transport through the study area since the 1970s, which would have counter-acted rather than have driven the observed long-term change in beach behaviour. However given the lack of measured data on mean inter-decadal swell wave direction changes near Ocean Beach (Section 3.2.3) and the lack of suitable base data (e.g., bathymetry) for wave transformation modelling at this remote site (see Section 7), there are uncertainties over the degree to which swell wave direction variability may or may not change sand transport processes and shoreline position at Ocean Beach. Hence this changing process is a potentially contributing factor.

On the other side of the sand budget, available data does not suggest either an increasing sand sink capacity, or an increasing rate of southwards littoral drift into the main sink, which might otherwise explain shoreline recession.

Another possible cause of a switch to increased shoreline recession would be an increasing frequency and/or magnitude of swell storms causing more erosion. However, a 2010 analysis of data from the Cape Sorell wave rider buoy directly offshore from Ocean Beach since 1985 found no significant change in storm frequencies or wave heights over that period (Hemer, 2010; Hemer et al., 2010).

Although Vertical Land Movement (VLM) can contribute significantly to regional differences in relative sea level change and hence to shoreline recession, available evidence implies that VLM in Tasmania is not an explanation of the observed shoreline history, with most estimates well below $-1.0\,\mathrm{mm\,year^{-1}}$ (see Section 2) and with this mechanism in any case incapable of explaining the abrupt onset of recession circa 1980.

Observational evidence (Section 4.2.3, Fig. 6) shows that onshore wind speeds on Tasmania's west coast have increased since the 1980s or earlier. These winds would have more often produced larger wind waves and higher wave set-up at the shore than previously, which can be expected to result in increased run-up and so more frequent upper shoreface erosion. Since the model proposed for the observed shoreline behaviour change at Ocean Beach (Fig. 8) depends upon increasing upper shoreface erosion, greater locally-generated wind wave magnitudes and frequencies are a plausible additional driver of this.

The proposed explanation for the major change in shoreline behaviour at Ocean Beach (Section 5.2, Fig. 8) is a hypothesis relying upon observations and supported by generalised models (e.g., Harris et al., 2000) of geomorphic and oceanographic processes. Our hypothesis is limited to the extent that additional factors such as potential interdecadal changes to wave direction are poorly understood in this region. Changes to wave direction may be a contributing factor; however, this as an alternative hypothesis alone is not well supported by the qualitative data obtained from the site. Quantitative modelling to further understand these dynamic processes would require significant in situ observations (e.g., bathymetry, currents, wave spectra, sediment transport, etc.) that are not currently available.

6. Conclusions

Three key findings have emerged from this study investigating the changed behaviour of Ocean Beach, Tasmania.

Firstly, historic air photos from 1947 to 2010 and beach profile surveys from 2011 to 2018 demonstrate that an abrupt change in long-term shoreline behaviour occurred between 1979 and 1982, from dynamic equilibrium since at least 1947 about a roughly stable or slightly prograding shoreline position (32+ years) to persistent shoreline recession continuing as at 2018 (36+ years) without any shoreline recovery. This change is unprecedented for Tasmanian beaches in recent decades, and evidence from dated peats exposed in the shoreline erosion scarp demonstrate the horizontal shoreline recession since 1982 exceeds any previous erosion or recession events at the same site for at least the last 1800 years.

Second, the observed shoreline behaviour change is consistent with known changes in climate-driven processes at the study site, namely sea-level rise and increasing onshore wind speeds. Interdecadal wave direction variability (also related to climate trends) is limited on this coast but may also play some role in the observed changes depending on the scale and local effects of this process, which are uncertain but with improved bathymetric data could be further investigated. No evidence supporting other alternative explanations has been identified albeit residual uncertainties remain. In the context of Ocean Beach's geomorphic environment, the recent rise in sea-level and increase in onshore wind speeds and thus wind-wave set-up at Ocean Beach during the Twentieth Century to recent period can each plausibly explain the observed multi-decadal change of shoreline behaviour. Either changing process would result in more frequent wave erosion higher on the shore face releasing sand at faster rates than previously, to be transported southwards by littoral drift and lost into the large active sand sink of Macquarie Harbour. Both are likely to be factors in the observed change in shoreline behaviour, with uncertain relative contributions.

Third, an earlier morpho-dynamic response to climate change at Ocean Beach compared to other swell-exposed sandy beaches implies unusual local geomorphic conditions. Most swell-exposed beaches have not yet shown physical changes attributable to longer term climate change, but rather are dominated by other processes with morpho-dynamic effects orders of magnitude greater than any expected effects of recent trends in sea-level rise or increasing local wind wave activity (Cowell et al., 1995; Stive et al., 2009; Mortlock et al., 2017). Our model of changing shoreline behaviour (Fig. 8) suggests several aspects of the Ocean Beach geomorphic environment as likely key factors in the apparent unusually early response of this beach to recent sea-level rise and wind speed increases.

Probably most important is the presence of the large unfilled sand sink of the Macquarie Harbour flood-tide delta and a persistent active sand transport pathway (southwards littoral drift) delivering increasing quantities of sand to that sink as increased wave erosion removes more sand from the beach face. This results in susceptibility to shoreface recession with sea-level rise and onshore wind increase. In addition, Ocean Beach is also exposed to a more highly energetic and storm-dominated wave climate than nearly all other beaches in Australia (Hemer et al., 2008; Hemer, 2010). Under conditions of frequent stormy or large-wave events, a relatively small rise in the mean sea-level may trigger more frequent erosion events higher on the shore face than would occur under a less stormy wave climate. These two factors are unusual in their degree and interaction at Ocean Beach, and we infer that this unusual combination has driven an early morphological response to recent sea-level rise at this site.

The ability to distinguish between beaches having characteristics predisposing them to earlier or later recessional responses to recent sea-level rise or onshore wind increases is of critical importance in planning adaptation to sea-level rise for that large proportion of human populations and their infrastructure that occupy coastal areas globally. This Ocean Beach case study suggests potential to identify distinctive coastal geomorphic types that are 'early responders' to climate change effects including sea-level rise, and to use them as indicators of which other shorelines can be expected to show early physical responses including progressive shoreline recession.

7. Recommendations

This study has noted that the dominantly southwards littoral drift at Ocean Beach that is demonstrated by multiple geomorphic indicators is a critical sand transport mechanism for the model of shoreline change proposed in this study, as is increased wave run-up and erosion associated with rising sea-levels and local wind-wave setup. The geomorphic evidence cited in this study supports the model proposed, however we note there remain uncertainties as to the variability in littoral sand transport rates and directions consequent on wave and wind climate variabilities identified in Section 4.2 above. It is not currently possible to produce high resolution wave transformation and wave run-up modelling for Ocean Beach since the available bathymetry for this (remote and only sparsely inhabited) coast is limited to coarse 100 metre contours (Geoscience Australia bathymetry). When higher resolution bathymetry becomes available for the Ocean Beach region, we recommend such modelling be undertaken in order to both test models and to improve understanding of the unusual coastal behaviour described here.

Author contributions

This work originated as a study of beach erosion undertaken during 2011 as a B.Sc. (Honours) project at the University of Tasmania by Hannah Walford (2011), with supervision from Dr. Joanna Ellison and advice from Chris Sharples.

Chris Sharples expanded on Hannah Walford's original study by spatial analysis of additional air photos, field work, data analysis and interpretation, and preparation of this paper.

Hannah Walford undertook fieldwork at the site, ortho-rectified and digitised shorelines from over half the air photos used in this subsequent study and provided an initial analysis of the results.

Dr. Christopher Watson undertook data exploration and analysis including Matlab™ scripting, participated in interpretation of results and provided input to and review of this paper.

Dr. Joanna Ellison supervised Hannah Walford's original project including review and discussion of analysis methods and interpretation of results. She participated significantly in the writing and review of this subsequent paper.

Dr. Quan Hua carried out AMS radiocarbon dating on peat samples and constructed the chronology for the peat profile.

Nick Bowden surveyed the three beach profiles annually from 2011 to 2018 and provided analysis and interpretation of the results.

Professor David Bowman assisted with peat profile sampling and beach profile surveying at Ocean Beach, provided discussion and interpretation of the peat dating findings, and reviewed a draft of this paper.

None of the co-authors have any conflicts of interest associated with

the research reported here.

Declaration of competing interest

None of the co-authors have any conflicts of interest associated with the research reported here.

Acknowledgements

Much of the research reported here was undertaken by Chris Sharples with post-graduate research funding provided by the University of Tasmania, Australia. Most of the air photos used were supplied without charge for research purposes by the Tasmanian Department of Primary Industries, Parks, Water & Environment (DPIPWE). We thank Peter Devine and Malcolm Crawford (DPIPWE) for their assistance in accessing historic air photos.

Matt Dell and Dr. Michael Lacey helped with advice on ortho-rectification of air photos and extraction of shoreline movement histories from digitised shorelines, respectively. A Python™ script for ArcGIS written by Michael Lacey was used for analysis of digitised shoreline changes throughout this work.

We thank Dr. Neil White for providing the data files for the Church and White (2011) SSH reconstruction. Dr. Benjamin Hamlington kindly provided Dr. Christopher Watson with data files for the SSH reconstruction for the Australian region prepared by the method of Hamlington et al. (2011).

Annual surveys (2011 to 2018) of the three TASMARC beach profile transects were supported by funding provided by the Antarctic Climate and Ecosystems Cooperative Research Centre (ACE-CRC) at the University of Tasmania, Australia.

AMS ^{14}C dating of peat samples was supported by ANSTO Research Portal (grant #10649 to Professor David Bowman). We acknowledge the financial support from the Australian Government for the Centre for Accelerator Science at ANSTO (Australia) through the National Collaborative Research Infrastructure Strategy (NCRIS).

We also thank Dr. John Hunter, Dr. John Church, Dr. Mark Hemer and Professors Colin Woodroffe and Bruce Thom for discussions and advice during this work.

We also acknowledge that our manuscript was notably improved in response to useful comments by two anonymous referees.

Appendix A. Supplementary data

Supplementary data to this article can be found online at https://doi.org/10.1016/j.margeo.2019.106081.

References

Argus, D.F., Peltier, W.R., Drummond, R., Moore, A.W., 2014. The Antarctica component of postglacial rebound model ICE-6G_C (VM5a) based upon GPS positioning, exposure age dating of ice thicknesses, and relative sea level histories. Geophys. J. Int. 198 (1), 537–563. https://doi.org/10.1093/gji/ggu140.

Banks, M.R., Colhoun, E.A., Chick, N.K., 1977. A reconnaissance of the geomorphology of central western Tasmania. In: Banks, M.R., Kirkpatrick, J.B. (Eds.), Landscape and Man: The Interaction Between Man and Environment in Western Tasmania. Royal Society of Tasmania, pp. 29–54.

Boak, E.H., Turner, I.L., 2005. Shoreline definition and detection: a review. J. Coast. Res. 21 (4), 688–703.

Bronk Ramsey, C., Lee, S., 2013. Recent and planned developments of the program OxCal. Radiocarbon 55, 720–730.

Bruun, P., 1962. Sea-level rise as a cause of shore erosion. Journal of the Waterways and Harbors Division, American Society of Civil Engineers, 88, 117–130.

Bruun, P., 1988. The Bruun rule of erosion by sea-level rise: a discussion of large-scale two- and three-dimensional usages. J. Coast. Res. 4, 627–648.

Burgette, R.J., Watson, C.S., Church, J.A., White, N.J., Tregoning, P., Coleman, R., 2013. Characterizing and minimizing the effects of noise in tide gauge time series: relative and geocentric sea level rise around Australia. Geophys. J. Int. 194 (2), 719–736. https://doi.org/10.1093/gji/ggt131.

Carson, M., Köhl, A., Stammer, D., Meyssignac, B., Church, j, Schröter, J., Wenzel, M., Hamlington, B., 2017. Regional sea level variability and trends, 1960–2007: a comparison of sea-level reconstructions and ocean syntheses. Journal of Geophysical Research: Oceans 122 (11), 9068–9091.

Chen, X., Zhang, X., Church, J.A., Watson, C.S., King, M.A., Monselesan, D., Legresy, B., Harig, C., 2017. The increasing rate of global mean sea-level rise during 1993–2014. Nat. Clim. Chang. 7 (7), 492–495.

Church, J.A., White, N.J., 2011. Sea-level rise from the late 19th to the early 21st century. Surv. Geophys. 32 (4–5), 585–602. https://doi.org/10.1007/s10712-011-9119-1.

Cowell, P.J., Roy, P.S., Thom, B.G., 1995. Effect of barrier size and offshore slope on rates of coastal change due to sea level rise and littoral sand loss. In: Late Quaternary Coastal Records of Rapid Change: Application to Present and Future Conditions. Abstract Volume, 11th Annual Meeting, International Geological Correlation Program Project 367, pp. 23–24.

Cullen, P., 1998. Ammophila Arenaria and Euphorbia paralias: Serious Threats to the Integrity of the South West Tasmanian Coastline. Unpublished report. Parks and Wildlife Service, Tasmania.

Davies, J.L., 1973. Sediment movement on the Tasmanian coast. In: Proceedings of the 1st Australian Conference on Coastal Engineering. Australian National Conference Publication 73/1. Canberra, Institution of Engineers Australia, pp. 43–46.

Durrant, T., Hemer, M., Trenham, C., Greenslade, D., 2013. CAWCR Wave Hindcast 1979–2010. v5. Centre for Australian Weather and Climate Research (Commonwealth Scientific and Industrial Organisation and Bureau of Meteorology) https://doi.org/10.4225/08/523168703DCC5. Data Collection.

Fink, D., Hotchkis, M., Hua, Q., Jacobsen, G., Smith, A.M., Zoppi, U., Child, D., Mifsud, C., van der Gaast, H., Williams, A., Williams, M., 2004. The ANTARES AMS facility at ANSTO. Nucl. Inst. Methods Phys. Res. B 223–224, 109–115.

Forsyth, S.M., Quilty, P.G., Calver, C.R., 2014. Cenozoic onshore basins and landscape evolution. In: Corbett, K.D., Quilty, P.G., Calver, C.R. (Eds.), Geological Evolution of Tasmania. Geological Society of Australia Special Publication 24. pp. 437–450.

Gillett, N.P., Kell, T.D., Jones, P.D., 2006. Regional climate impacts of the Southern Annular Mode. Geophys. Res. Lett. 33, L23704. https://doi.org/10.1029/2006GL027721.

Grose, M.R., Barnes-Keoghan, I., Corney, S.P., White, C.J., Holz, G.K., Bennett, J.B., Gaynor, S.M., Bindoff, N.L., 2010. General climate impacts. In: Climate Futures for Tasmania Technical Report. Antarctic Climate and Ecosystems Co-operative Research Centre, Hobart.

Hamlington, B.D., Leben, R.R., Nerem, R.S., Han, W., Kim, K.-Y., 2011. Reconstructing sea level using cyclostationary empirical orthogonal functions. J. Geophys. Res. 116, C12015. https://doi.org/10.1029/2011JC007529.

Harris, P.T., Heap, A., 2014. Geomorphology and Holocene sedimentology of the Tasmanian continental margin. In: Corbett, K.D., Quilty, P.G., Calver, C.R. (Eds.), Geological Evolution of Tasmania. 24. Geological Society of Australia Special Publication, pp. 538.

Harris, P.T., Smith, R., Anderson, O., Coleman, R., Greenslade, D., 2000. GEOMAT – Modelling of Continental Shelf Sediment Mobility in Support of Australia's Regional Marine Planning Process. Australian Geological Survey Organisation (Record 2000/41).

Hawkins, E., Sutton, R., 2012. Time of emergence of climate signals. Geophys. Res. Lett. 39 (L01702), 6.

Hemer, M.A., 2009: Identifying coasts susceptible to wave climate change. J. Coast. Res., Special issue no. 56.

Hemer, M.A., 2010. Historical trends in Southern Ocean storminess: long-term variability of extreme wave heights at Cape Sorell, Tasmania. Geophys. Res. Lett. 37, L18601. https://doi.org/10.1029/2010GL044595.

Hemer, M.A., Simmonds, I., Keay, K., 2008. A classification of wave generation characteristics during large wave events on the Southern Australian margin. Cont. Shelf Res. 28, 634–652.

Hemer, M.A., Church, J.A., Hunter, J.R., 2010. Variability and trends in the directional wave climate of the Southern Hemisphere. Int. J. Climatol. 30, 475–491.

Hogg, A.G., Hua, Q., Blackwell, P.G., Niu, M., Buck, C.E., Guilderson, T.P., Heaton, T.J., Palmer, J.G., Reimer, P.J., Reimer, R.W., Turney, C.S.M., Zimmerman, S.R.H., 2013. SHCal13 Southern Hemisphere calibration, 0-50,000 cal yr BP. Radiocarbon 55, 1889–1903.

Hua, Q., Jacobsen, G.E., Zoppi, U., Lawson, E.M., Williams, A.A., Smith, A.M., McGann, M.J., 2001. Progress in radiocarbon target preparation at the ANTARES AMS Centre. Radiocarbon 43, 275–282.

Hua, Q., Barbetti, M., Rakowski, A.Z., 2013. Atmospheric radiocarbon for the period 1950–2010. Radiocarbon 55, 2059–2072.

Hunter, J., Coleman, R., Pugh, D., 2003. The sea level at Port Arthur, Tasmania, from 1841 to the present. Geophys. Res. Lett. 30 (7). https://doi.org/10.1029/2002GL016813.

Hurrell, J.W., van Loon, H., 1994. A modulation of the atmospheric annual cycle in the Southern Hemisphere. Tellus 46A, 325–338.

King, M.A., Keshin, M., Whitehouse, P.L., Thomas, I.D., Milne, G., Riva, R.E.M., 2012. Regional biases in absolute sea-level estimates from tide gauge data due to residual unmodeled vertical land movement (Fig. 1a). Geophys. Res. Lett. 39. https://doi.org/10.1029/2012GL052348.

Kirkpatrick, J.B., Nunez, M., Bridle, K.L., Parry, J., Gibson, N., 2017. Causes and consequences of variation in snow incidence on the high mountains of Tasmania, 1983–2013. Aust. J. Bot. 65, 214–224. https://doi.org/10.1071/BT16179.

Le Cozannet, G., Garcin, M., Yates, M., Idier, D., Meyssignac, B., 2014. Approaches to evaluate the recent impacts of sea-level rise on shoreline changes. Earth-Sci. Rev. 138, 47–60.

Marshall, G.J., 2003. Trends in the Southern Annular Mode from observations and reanalyses. J. Clim. 16 (24), 4134–4143.

McVicar, T.R., Van Niel, T.G., Li, L.T., Roderick, M.L., Rayner, D.P., Ricciardulli, L., Donohue, R.J., 2008. Wind speed climatology and trends for Australia, 1975–2006: capturing the stilling phenomenon and comparison with near-surface reanalysis

output. Geophysics Research Letters 35, L20403. https://doi.org/10.1029/2008GL035627.
Mortlock, T., Goodwin, I., McAneney, J., Roche, K., 2017. The June 2016 Australian East Coast Low: importance of wave direction for coastal erosion assessment. Water 9 (2), 121.
Nanson, G.C., Barbetti, M., Taylor, G., 1995. River stabilisation due to changing climate and vegetation during the late Quaternary in western Tasmania, Australia. Geomorphology 13, 145–158.
Peltier, W.R., Argus, D.F., Drummond, R., 2015. Space geodesy constrains ice-age terminal deglaciation: the global ICE-6G_C (VM5a) model. Journal of Geophysical Research Solid Earth 120, 450–487. https://doi.org/10.1002/2014JB011176.
Pye, K., Blott, S.J., 2006. Coastal processes and morphological change in the Dunwich-Sizewell area, Suffolk, UK. J. Coast. Res. 22 (3), 453–473.
Pye, K., Blott, S.J., 2015. Spatial and temporal variations in soft-cliff erosion along the Holderness coast, East Riding of Yorkshire, UK. J. Coast. Conserv. https://doi.org/10.1007/s11852-015-0378-8.
Ranasinghe, R., McLoughlin, R., Short, A., Symonds, G., 2004. The Southern Oscillation Index, wave climate, and beach rotation. Mar. Geol. 204, 273–287.
Romine, B.M., Fletcher, C.H., Barbee, M.M., Anderson, T.R., Frazer, L.N., 2013. Are beach erosion rates and sea-level rise related in Hawaii? Glob. Planet. Chang. 108, 149–167.
Santamaría-Gómez, A., Gravelle, M., Collilieux, X., Guichard, M., Míguez, B.M., Tiphaneau, P., Woppelmann, G., 2012. Mitigating the effects of vertical land motion in tide gauge records using a state-of-the-art GPS velocity field. Glob. Planet. Chang. 98–99, 6–17.
Sharples, C., 2006. Indicative Mapping of Tasmanian Coastal Vulnerability to Climate Change and Sea-level Rise: Explanatory Report, 2nd edition. Unpublished Report to Department of Primary Industries and Water, Tasmania, pp. 83 173p.
Short, A., 2006. Beaches of the Tasmanian Coast and Islands: A Guide to their Nature, Characteristics, Surf and Safety. Sydney University Press, Sydney (353p).
Shulmeister, J., Goodwin, I., Renwick, J., Harle, K., Armand, L., McGlone, M.S., Cook, E., Dodson, J., Hesse, P.P., Mayewski, P., Curran, M., 2004. The Southern Hemisphere westerlies in the Australasian sector over the last glacial cycle: a synthesis. Quat. Int. 118–119, 23–53. https://doi.org/10.1016/S1040-6182(03)00129-0.
Stive, M.J.F., Cowell, P.J., Nicholls, R.J., 2009. Beaches, cliffs and deltas. In: Slaymaker, O., Spencer, T., Embleton-Hamann, C. (Eds.), Geomorphology and Global Environmental Change. Cambridge University Press, pp. 158–179.
TASMARC, 2019. Tasmanian Shoreline Monitoring and Archiving Project. website. www.tasmarc.info (includes all beach profile data used for Ocean Beach). Antarctic Climate and Ecosystems Co-operative Research Centre, Hobart, Tasmania.
Thompson, D.W.J., Solomon, S., 2002. Interpretation of recent Southern Hemisphere climate change. Science 296, 895–899.
Troccoli, A., Muller, K., Coppin, P., Davy, R., Russell, C., Hirsch, A.L., 2012. Long-term wind speed trends over Australia. J. Clim. 25, 170–183. https://doi.org/10.1175/2011JCLI4198.1.
Walford, H., 2011. Assessment of Coastal Erosion at Ocean Beach, Western Tasmania. Unpublished Honours Thesis. School of Geography and Environmental Studies, University of Tasmania (80p).
Walsh, K., White, C.J., McInnes, K., Holmes, J., Schuster, S., Richter, H., Evans, J.P., Di Luca, A., Warren, R.A., 2016. Natural hazards in Australia; storms, wind and hail. Clim. Chang. https://doi.org/10.1007/s10584-016-1737-7.
Watson, C.S., White, N.J., Church, J.A., King, M.A., Burgette, R.J., Legresy, B., 2015. Unabated global mean sea-level rise over the satellite altimeter era. Nat. Clim. Chang. 5 (6), 565–568.
White, N.J., Haigh, I.D., Church, J.A., Koen, T., Watson, C.S., Pritchard, T.R., Watson, P.J., Burgette, R.D., McInnes, K.L., You, Z., Zhang, X., Tregoning, P., 2014. Australian sea levels – trends, regional variability and influencing factors. Earth Sci. Rev. 136, 155–174.
Zhang, K., Douglas, B.C., Leatherman, S.P., 2004. Global warming and coastal erosion. Clim. Chang. 64, 41–58.